PROCEEDINGS of the

18th DOE NUCLEAR AIRBORNE WASTE MANAGEMENT AND AIR CLEANING CONFERENCE

Held in Baltimore, Maryland
12-16 August, 1984

**Sponsors: U.S. Department of Energy
The Harvard Air Cleaning Laboratory**

**Editor
Melvin W. First**

**Published
March, 1985**

with an INDEX to the 17th and 18th CONFERENCES

PROGRAM COMMITTEE

W.L. Anderson

C.B. Bastin

R.R. Bellamy

A.G. Croff

H.L. Ettinger

A.G. Evans

W.P. Gammill

H. Gilbert

R.T. Jubin

M.J. Kabat

J.L. Kovach

W.H. Miller, Jr.

D.W. Moeller

K.S. Murthy

A.C. Richardson

T.R. Thomas

A.K. Williams

CONFERENCE CHAIRMAN

Melvin W. First
Harvard Air Cleaning Laboratory

TABLE OF CONTENTS

VOLUME I

Session 1

OPENING OF THE CONFERENCE

MONDAY: August 13, 1984
CHAIRMAN: M.W. First
           Harvard School of Public Health

Session 2

IODINE ADSORPTION AND ADSORBENTS

MONDAY: August 13, 1984
CHAIRMEN: M.J. Kabat
           Onatrio Hydro
           J.W. Jacox
           Jacox Associates

Session 3

PERFORMANCE OF HVAC AND AIR CLEANING SYSTEMS IN NUCLEAR POWER PLANTS

MONDAY: August 13, 1984
CHAIRMEN: A.G. Evans
E.I. duPont de Nemours
J.P. Pearson
Nuclear Consulting Services

Session 4

SOURCE TERMS AND ENVIRONMENTAL IMPACTS

MONDAY: August 13, 1984
CHAIRMEN: A.G. Evans
E.I. duPont de Nemours
J.P. Pearson
Nuclear Consulting Services

Session 5

FILTERS, FILTRATION, AND FILTER TESTING

TUESDAY: August 14, 1984
CHAIRMEN: W.L. Anderson
              Consultant
              Commission
              R.G. Dorman
              Consultant

Session 6

RECOVERY AND RETENTION OF AIRBORNE WASTES: PROTOTYPE AND OPERATIONAL SYSTEMS

TUESDAY: August 14, 1984
CHAIRMEN: A.G. Croff
              W. S. Groenier
              Oak Ridge National Laboratory

Session 7

WORKING LUNCHEON

TUESDAY: August 14, 1984
CHAIRMAN: D.W. Moeller
           Harvard School of Public Health

Session 8

FIRE, EXPLOSION, EARTHQUAKE, TORNADO

TUESDAY: August 14, 1984
CHAIRMEN: H.J. Ettinger
            S.C. Soderholm
            Los Alamos National Laboratory

Panel 9

SOURCE TERM IN RELATION TO AIR CLEANING

TUESDAY: August 14, 1984
MODERATOR: J.L. Kovach
Nuclear Consulting Services

PANEL
MEMBERS: A.P. Malinauskas
Oak Ridge National Laboratory
J.A. Gieseke
Battelle Columbus Laboratory
P.S. Littlefield
Yankee Atomic Electric
Company
R.M. Bernero
U.S. Nuclear Regulatory
Commission

Session 10

RECOVERY AND RETENTION OF AIRBORNE WASTES:
PREPARATION FOR DISPOSAL

TUESDAY: August 14, 1984
CHAIRMEN: C.B. Bastin
           R. Philippone
           U.S. Department of Energy

Panel 11

BEST AVAILABLE AND MOST READILY AVAILABLE TECHNOLOGY FOR
OFF-GAS TREATMENT AND GASEOUS WASTE RETENTION

TUESDAY: August 14, 1984
ARRANGED BY: R.T. Jubin
               Oak Ridge National
               Laboratory
MODERATOR: A.G. Croff
               Oak Ridge National
               Laboratory
PANEL
MEMBERS: W.S. Groenier
               Oak Ridge National Laboratory
               K. Naruki
               Tokai Works
               W. Hebel
               Commission of the European
               Communities

x

E. Henrich
Kernforschungszentrum
Karlsruhe

VOLUME II

Session 12

AIR AND GAS CLEANING METHODS

WEDNESDAY: August 15, 1984
CHAIRMEN: W.P. Gammill
J. Hayes
U.S. Nuclear Regulatory
Commission

Panel 13

NUCLEAR AIR CLEANING FIELD EXPERIENCES

WEDNESDAY: August 15, 1984
MODERATOR: W.H. Miller, Jr.
Sargent & Lundy

PANEL
MEMBERS: R.R. Bellamy
U.S. Nuclear Regulatory
Commission
D.M. Hubbard
Duke Power Company
J.W. Jacox
Jacox Associates
W.R. Lightfoot
Florida Power & Light

Session 14

RECOVERY AND RETENTION OF AIRBORNE WASTES: NOBLE GASES

WEDNESDAY: August 15, 1984
CHAIRMEN: R.R. Bellamy
U.S. Nuclear Regulatory
Commission
V. Deitz
Naval Research Laboratory

PANEL 15

PROS AND CONS OF STORAGE AND COLLECTION OF RADIO-KRYPTON, -IODINE,
-CARBON AND -HYDROGEN

WEDNESDAY: August 15, 1984
MODERATOR: K.S. Murthy
Pacific Northwest Laboratory

PANEL
MEMBERS: T.R. Thomas
Westinghouse Idaho Nuclear
K. Ebert
Kernforschungszentrum
Karlsruhe
P. Mellinger
Pacific Northwest Laboratory
D.M. Wuschke
Atomic Energy of Canada
Research

Session 16

HEPA FILTER PERFORMANCE UNDER HIGH HEAT AND
HUMIDITY CONDITIONS

WEDNESDAY: August 15, 1984
CHAIRMEN: H. Gilbert
Consultant
J. D'Ambrosia
U.S. Department of Energy

Session 17

SAFETY SYSTEMS PERFORMANCE

WEDNESDAY: August 15, 1984
CHAIRMEN: H. Gilbert
           Consultant
           J. D'Ambrosia
           U.S. Department of Energy

Session 18

RECOVERY AND RETENTION OF AIRBORNE WASTES: RESEARCH

WEDNESDAY: August 15, 1984
CHAIRMEN: T.R. Thomas
            S.J. Fernandez
            Westinghouse Idaho Nuclear
            Company

Session 19

OPEN END

THURSDAY: August 16, 1984
CHAIRMEN: M.W. First
          Harvard School of Public Health
          S. Steinberg
          Air Techniques, Inc.

Session 20

CODES, STANDARDS, REGULATIONS

                THURSDAY: August 16, 1984
                CHAIRMAN: M.W. First
                           Harvard School of Public Health

Session 12

AIR AND GAS CLEANING METHODS

WEDNESDAY: August 15, 1984
CHAIRMEN: W. P. Gammill
J. Hayes
U.S. Nuclear Regulatory
Commission

USE OF ACOUSTIC FIELD IN GAS CLEANING
D. Boulaud, G. Madelaine, C. Malherbe

REMOVAL OF RADON DECAY PRODUCTS WITH ION GENERATORS - COMPARISON OF
EXPERIMENTAL RESULTS WITH THEORY
E. F. Maher, S. N. Rudnick, D.W. Moeller

PROTOTYPE FIRING RANGE AIR CLEANING SYSTEM
J.A. Glissmeyer, J. Mishima, J.A. Bamberger

CALCULATING RELEASED AMOUNTS OF AEROSOLS
R. Nagel, J. Furrer

USE OF ACOUSTIC FIELD IN GAS CLEANING

D. Boulaud G. Madelaine and C. Malherbe
Laboratoire de Physique et de Métrologie des Aérosols
IPSN/DPT/SPIN
Centre d'Etudes Nucléaires de Fontenay-aux-Roses
BP n° 6, 92260 FONTENAY AUX ROSES, France

Abstract

The use of acoustic field in gas cleaning can be done according to two ways : the first, is the conditionning of an aerosol by acoustic agglomeration before filtration by conventional methods (cyclones, granular beds, ...), the second, is the collection efficiency improvement of granular bed filters exposed to an acoustic field.

In a first part, experimental results are given on the acoustic agglomeration of a polydisperse aerosol of mass concentration between 0.5 and 1 g/m^3. An important effect of wall precipitation of particles is described and deposition velocity due to the presence of an acoustic field are measured as a function of particle diameter, sound pressure level and acoustic frequency. A dimensionless relationship between the deposition velocity and particle relaxation time is established from these results. At the end of this part energetic criteria for the use of acoustic agglomeration in a gas cleaning train is given.

In a second part experimental results are given on the influence of acoustic field on the collection efficiency of monodispersed aerosols ranging from 0.1 to 1 μm.

For these both uses of acoustic field in industrial gas cleaning the different alternatives for the acoustic field generation are discussed.

I. Introduction

Acoustic field can be used in two ways for gas cleaning :
- conditionning of aerosols by acoustic agglomeration in order to increase the efficiency of prefiltering systems (cyclones, granular beds, ...)
- increasing filtering collection efficiency by applying acoustic field.

II. Acoustic agglomeration (AA)

II.1. Introduction

The acoustic conditionning of fine particles in an aerosol is a process by which the fraction of particles having the smallest diameters vanishes through agglomeration on large particles ; this phenomenon is induced by an acoustic field. The corresponding variation in the particle size distribution is an important factor as it allows the fraction which is most difficult to filter directly to be eliminated. Conventional equipment located further downstream such as cyclones, granular beds, ... can then be used to eliminated the agglomerates formed.

Increased agglomeration rates leading to these rapid changes in size are due to the increase in particles collision rates through particle and acoustic field interactions.

Acoustic agglomeration has already been successfully used for particle size conditionning. Most of the experiments carried out are summarized in E.P. MEDNIKOV's book (1965) (1). The subject has recently been the object of renewed attention by D.T. SHAW (1976) and K.H. CHOU et al (1981) (2) (3). The latter studies showed the effects of high acoustic intensities of the order of 160 dB (1 W/cm^2) on agglomeration mechanisms.

II.2. Acoustic agglomeration mechanisms

Generally, the agglomeration equation describing variations in the concentration of particles of volume x over time t can be written :

$$\frac{\delta n(x,t)}{\delta t} = \frac{1}{2} \int_0^x K\ (y,x-y,t)\ n\ (x-y,t)\ n\ (y,t)\ dy$$

$$- n\ (x,t) \int_0^\infty K\ (x,y,t)\ n\ (y,t)\ dy$$

The first term of the righthand member of the equation represents the production of particles of volume x through collisions between particles of volume y and (x-y).

The second term represents the vanishing of particles of volume x through collisions with other particles, n (x,t) is the distribution function expressed as a function of the volume of number of particles per unit volume of fluid at time t ; K (x,y,t) is the agglomeration coefficient for particles having volumes x and y.

A knowledge of the coefficient of agglomeration is therefore entirely sufficient to predict n (x,t) behavior when the conditions at the origin are known. Unfortunately, the phenomena intervening in A-A are extremely complex and four types of interactions must be combined :
- orthokinetic,
- hydrodynamic,
- turbulent inertial,
- turbulent diffusional,
in order to define an agglomeration coefficient that can be used in the preceeding integro-differential equation.

II.2.1. Orthokinetic interactions result from collisions between small particles highly influenced by vibrations and large particles which are virtually stationary.

In this case, the coefficient of coagulation has the following form :

$$K_{oc} = \frac{N_1}{N_t} (a_1 + a_2)^2\ E_{oc}\ \mu_{12}\ U_g$$

where N_1 is the large particle concentration, N_t the total concentration, a_1 and a_2 the radii of the large and fine particles, μ_{12} the relative entrainment factor, E_{oc} the collision efficiency and U_g the vibrational velocity of the gas-medium. μ_{12} is a function of the vibrational frequency and the relaxation time of the particles. U_g is a function of the acoustic intensity, velocity of sound and density of the gas-medium.

II.2.2. _Hydrodynamic interaction_. This type of interaction is mainly resulting from mutual distorsion of the flow fields around interacting particles. In this case the agglomeration coefficient has the following form :

$$K_{IH} = \pi \; (a_1 + a_2)^2 \; E_{IH} \; V_{rel}$$

E_{IH} is the colision efficiency and V_{rel} the relative velocities between interacting particles. V_{rel} has a complex analytical form which is a function of the vibrational velocity of the fluid, the relative entrainment factor, the size of the particles and vibrational frequency.

II.2.3. _Turbulent interactions_. When the acoustic intensity increases (I > 160 dB), interactions due to turbulence in the fluid become very important and lead to increased particles agglomeration. This type of interaction can be divided into two categories : turbulent diffusional and turbulent inertial. In these interactions, the agglomeration process occurs in small eddies whose sizes are characterized by the Kolmogorov microscale :

$$d \cong (\nu^3/\varepsilon)^{1/4}$$

where ε is the time rate of energy dissipation of turbulence per unit mass and ν is the kinematic viscosity of the gas-medium.

In the case where particles are completely entrained by the fluid, the agglomeration process can be treated by an approach identical to the diffusional approach of Smoluchowski : In the opposite case the relative velocities of particles must be taken into account as a result of their different inertias ; collision likelihoods are increased in consequence.

II.2.3.1. _Turbulent diffusional interactions_. The hypothesis of particles being completely entrained leads to a coefficient of agglomeration of the following form :

$$K_{DT} \cong \pi \; (a_1 + a_2)^3 \; E_{DT} \; (\varepsilon/\nu)^{1/2}$$

where E_{DT} is the collision efficiency, often taken as unit for particles of the same size.

II.2.3.2. _Turbulent inertial interaction_. The hypothesis of different degrees of entrainment for particles of different size leads to a coefficient of agglomeration of the following form :

$$K \cong \pi \; E_{IT} \; (a_1 + a_2)^2 \; (1 - \frac{\rho_g}{\rho_p}) \; (\tau_1 - \tau_2) \; (\varepsilon^3/\nu)^{1/4}$$

where ρ_g and ρ_p are the respective densities of the gas and particles, τ_i the relaxation time of particles i and E_{IT} the collision efficiency.

A knowledge of the analytical forms of the different agglomeration coefficients enables their variations to be predicted as a function of the conditions imposed. In the K.H. CHOU et al article (1981), a parametric study as a function of particle concentration, aerosol median diameter, standard deviation, acoustic intensity and frequency, temperature and pressure is presented (3).

However, these studies are based on a mainly theoretical approach of particle collisions mechanisms under an acoustic field. Too scarce an amount of exploitable experimental studies are available to confirm theoretical predictions.

This situation led our laboratory to engage in an exprimental study of AA in order to determine the sensitivity of this phenomenon to various parameters (acoustic intensities and frequencies, median diameters and standard deviations associated with size distributions of aerosols, residence times in agglomeration chambers).

During these experiments described in a first part of this article, significant particle deposits were observed on the agglomerator walls ; this phenomenon led us to undertake a specific study, described in the second part of this article, of particles precipitation under the influence of acoustic fields.

II.3. Experimental studies

II.3.1. Acoustic agglomeration

II.3.1.1. Experimental apparatus the experimental device used, sketched on figure 1, consists of the following elements :

- Agglomeration chamber : this is a 4 liter glass cylinder (diameter 7 cm, length 100 cm). The aerosols produced are fed into the top of the tube at a flow rate of 20 to 100 lpm, corresponding to a residence time between 12 and 2.4 seconds.

- Acoustic source : a 100 W compression chamber (Bouyer 2 R 200) is placed at the top of the agglomeration cylinder. This chamber is powered by a low-frequency signal generator (Hewlett Packard 3310 A) combined with a 200 W amplifier (Bouyer AS 240).

- Acoustic intensity measurement : this is performed by a Bruel and Kjaer measurement line comprising a microphone (BK 4136), a preamplifier (BK 2619) and a reading amplifier (BK 2609). The shape of the acoustic waves is monitored by an oscilloscope.

- Aerosol source : a polydisperse aerosol is produced by pneumatic spraying of dioctylphtalate (DOP) solution. Before entering the agglomeration chamber this aerosol passes through a neutralizer, consisting of a krypton 85 source, to bring the electric charge of the aerosol to Boltzmann's equilibrium.

- Measurement of the aerosol size distribution : samples are taken at the bottom of the agglomeration chamber and measured by a cascade impactor (Andersen Mark II). The impactor calibration and data reduction have been described in earlier articles (BOULAUD et al 1981, BOULAUD and DIOURI 1982) (4)(5).
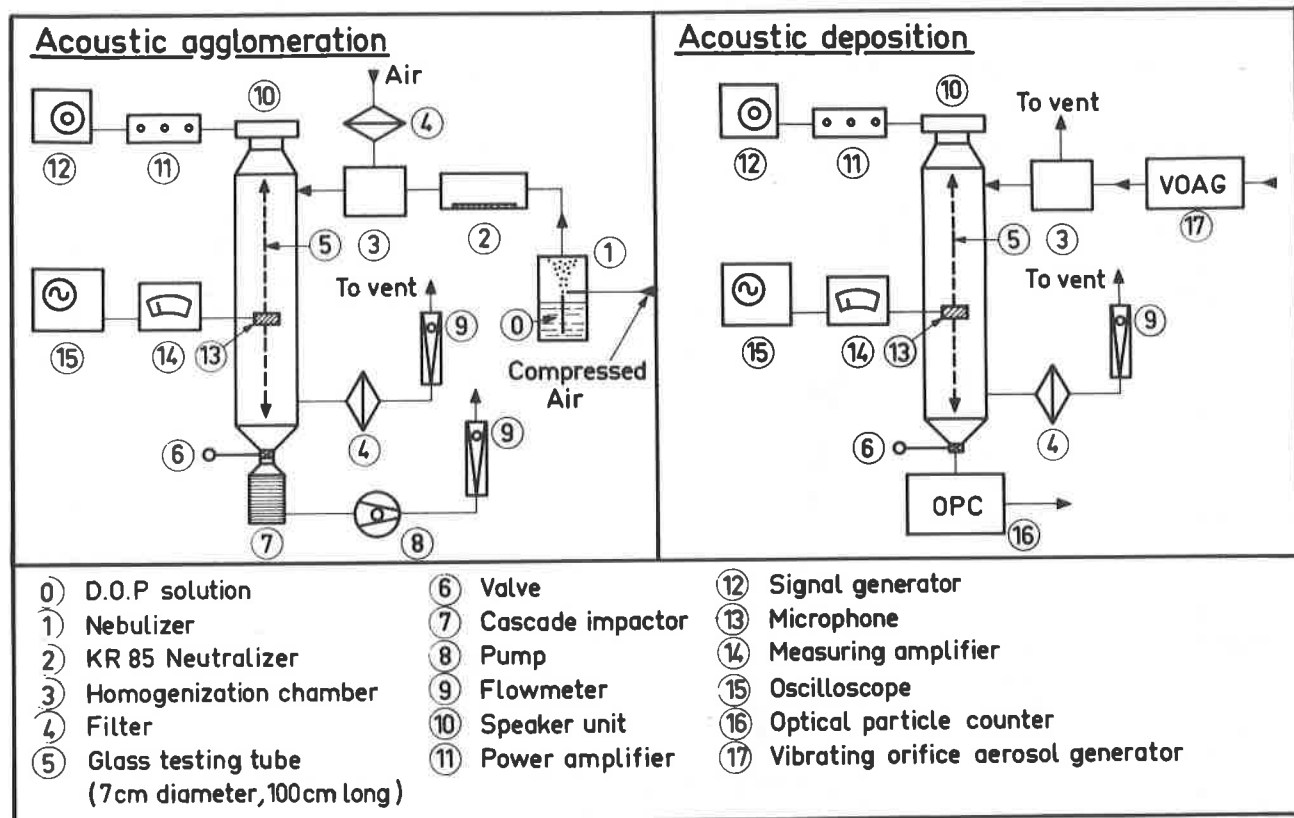
Figure 1 : Experimental set up for acoustic agglomeration and acoustic precipitation experiments

II.3.1.2. Experimental procedure. After measurement of the acoustic field in the tube the DOP solution is atomized and injected into the system. When the stationary state is established a first sampling with the impactor in the absence of acoustic field provides the original size distribution of the aerosol. The measured values of the aerodynamic mass median diameter (AMMD) and standard deviation (σg) are reproducible, 1.5 µm and 1.75 respectively, whatever the residence time chosen (3.8 or 8.6 seconds), which shows that agglomeration phenomena other than acoustic are negligible. The mass concentration value can vary slightly from one experiment to another, remaining within the 0.5 to 1 g/m^3 range.

The above operation is then repeated but in the presence of an acoustic field. This measurement gives the new aerosol size distribution after an agglomeration period corresponding to the residence time in the tube.

807

Figure 2 shows an example of the results obtained. Curve 1 represents the original distribution, curves 2 and 3 the change in this distribution under the effect of an acoustic field of rising intensity, 156.7 and 162.7 respectively, and constant frequency 1020 Hz, the residence time in the agglomerator remaining constant at 8.6 seconds.

Qualitative analysis of these results shows as expected that the AMMD and σg values increase with the sound pressure level. At the same time the mass concentration of the aerosol falls sharply, due to deposition of the particles on the agglomerator walls. This phenomenon, clearly apparent here, is hardly mentioned in the literature except by K.H. CHOU and al (1982) (6).
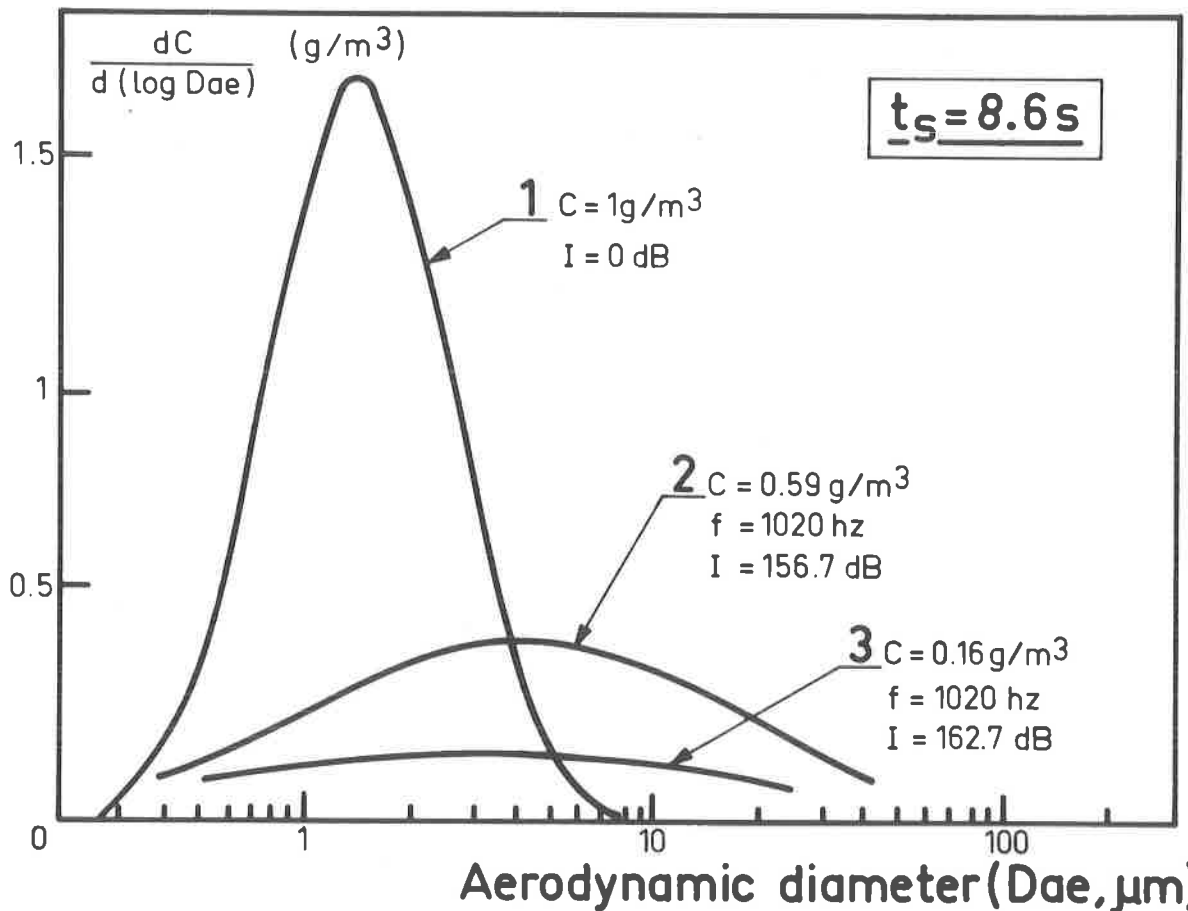
Figure 2 : Variations of the size destributions for different acoustic intensities (residence time t = 8.6 s)

II.3.1.3. Experimental results. Discussion. During these experiments the characteristics of the aerosol introduced in the agglomerator were kept constant at the values given in section II.3.1.2., the variables being the residence time in the agglomeration volume, the sound pressure level and the acoustic frequency.

Figures 3 and 4 show the AMMD and σg variations after agglomeration as a function of acoustic intensity for two different frequencies (540 and 1020 Hz) and the same 8.6 seconds residence time. Figure 5 plots AMMD versus acoustic intensity for two different residence times (8.6 and 3.8 seconds) at the frequency 540 Hz.
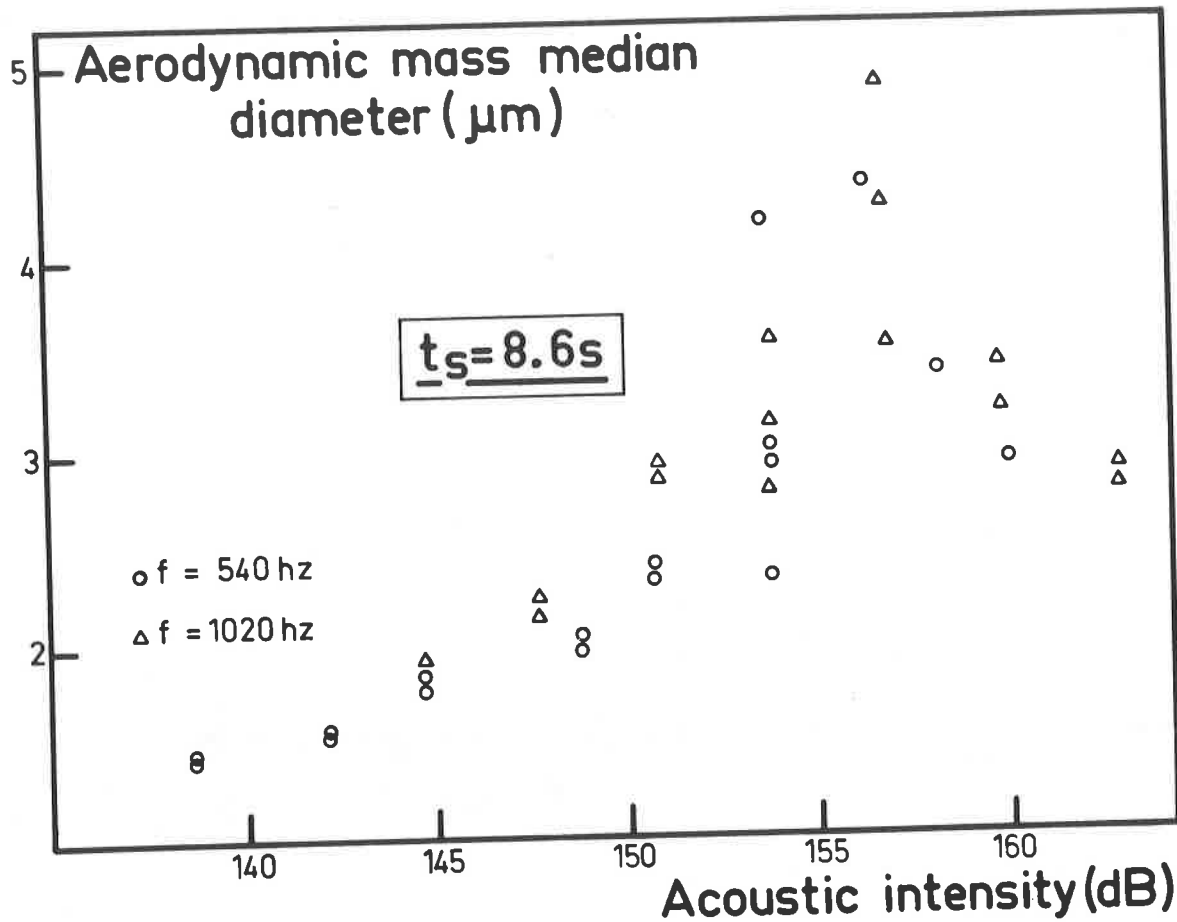
Figure 3 : Aerodynamic mass median diameter after an 8.6 seconds agglomeration time versus acoustic intensity, for two acoustic frequencies (540 and 1020 Hz)
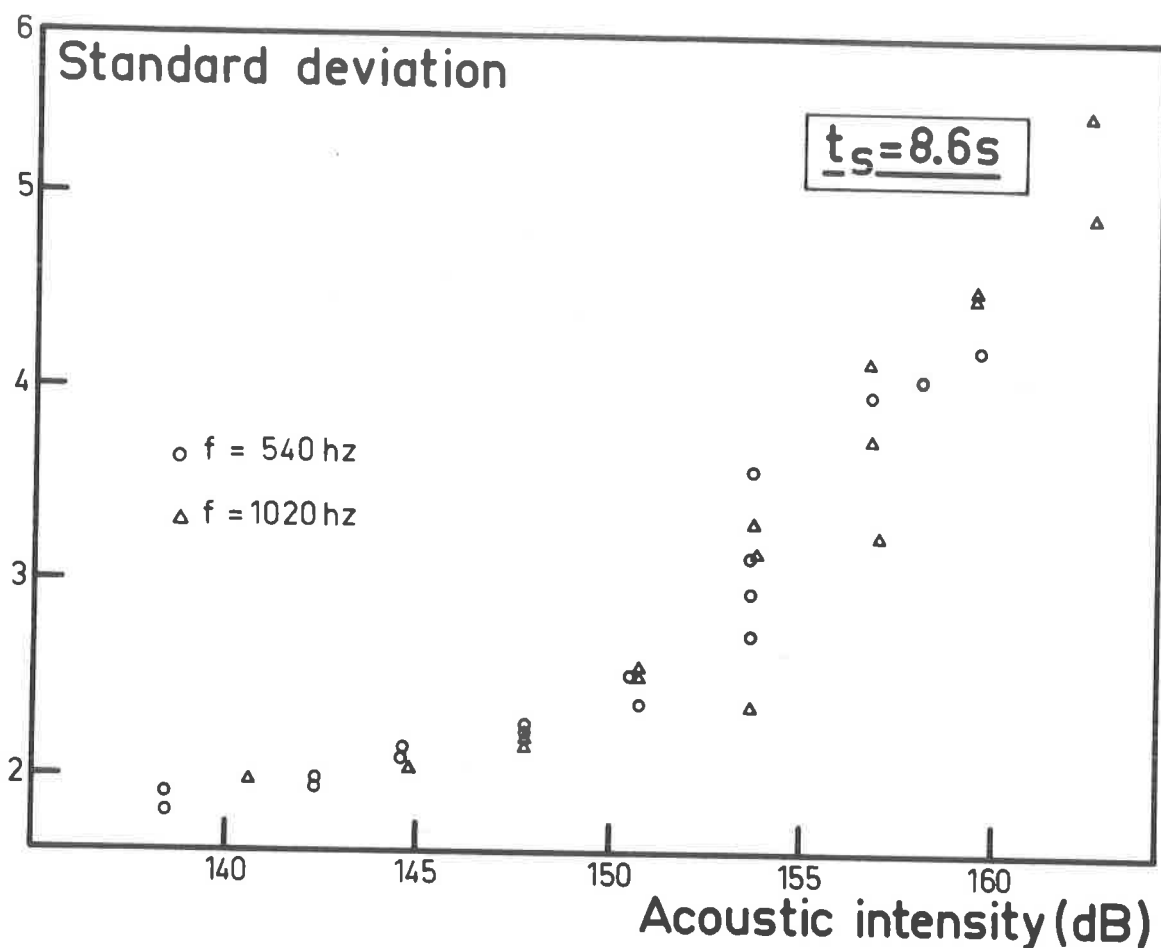
Figure 4 : Standard deviation versus acoustic intensity, for two acoustic frequencies (540 and 1020 Hz)

From these three figures the following conclusions may be drawn :
- little variation in AMMD and σg is observed between 100 and 140 dB,
- AMMD increases from 1.5 to 4.5 μm between 140 and 155 dB, reaches a maximum between 155 and 158 dB then drops suddenly when the acoustic intensity is raised further,
- similarly σg rises from 1.75 to 5 in the 140 to 160 dB range.

The influence of acoustic frequency on the AMMD and σg variations is insignificant in the 500 to 1000 Hz range, while the effect of residence time on AMMD remains negligible except around the maximum. This tends to prove that agglomeration phenomena are effective mainly during the first few seconds, then diminish as the particles collide and their numerical concentration decreases. This effect is enhanced by heavy particle deposits on the walls as shown on figure 6, where the percentage aerosol mass deposition varies from 0 to 85% as the sound pressure rises from 130 to 163 dB.
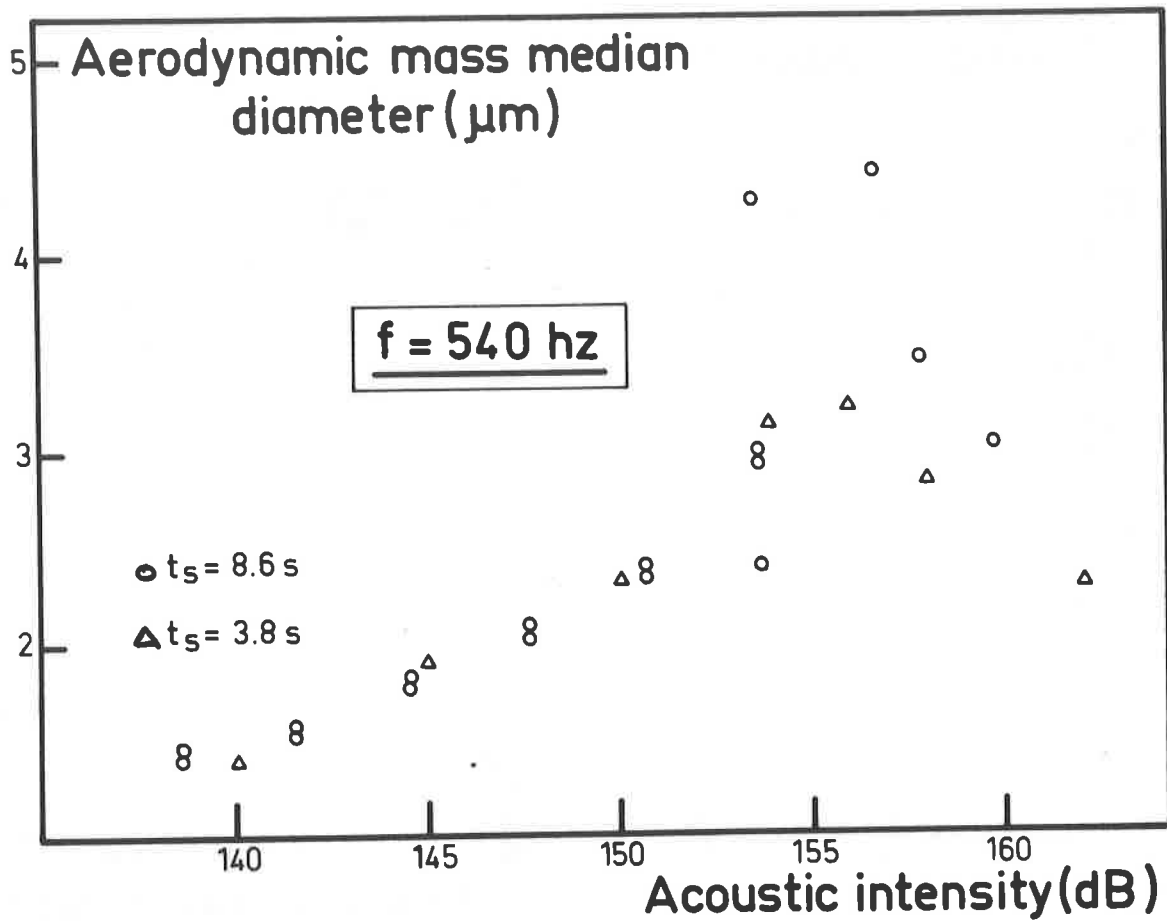
Figure 5 : Aerodynamic mass median diameter versus acoustic intensity for two different residence times (8.6 and 3.8 s) and constant frequency 540 Hz
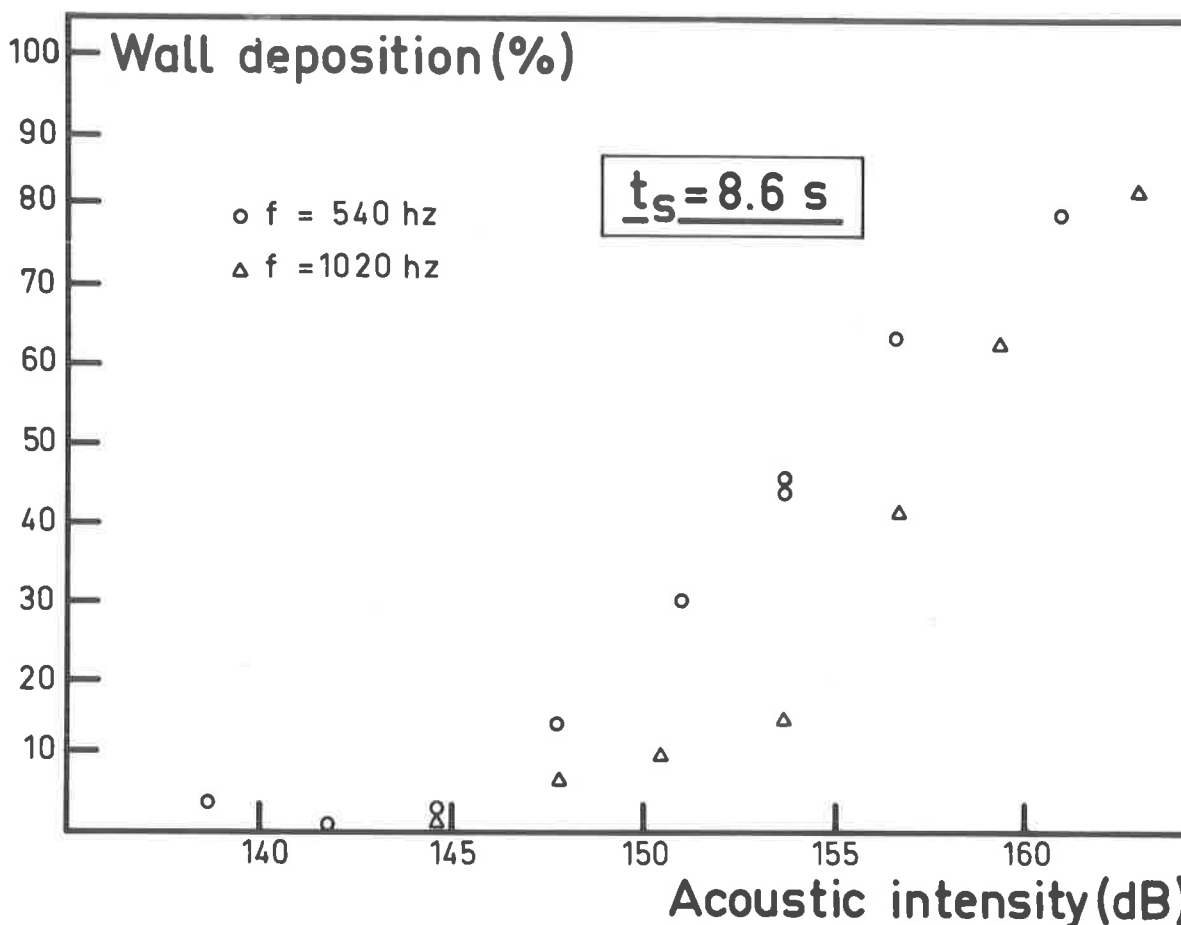
Figure 6 : Wall deposition versus acoustic intensity for two different frequencies (540 and 1020 Hz). Residence time 8.6 seconds.

The maximum of the AMMD versus acoustic intensity curve (figures 3 and 5) may also be due to these deposition mechanisms, as demonstrated in part II.3.2 below.

II.3.2. Acoustic deposition. The aim here is to determine the relations between the establishement of an acoustic field and the precipitation of an aerosol on the walls of a pipe. For these experiments therefore, unlike those described in part one, it was decided to keep the characteristic parameters of the aerosol constant (diameter and standard deviation). For this purpose the aerosol is monodispersed and has a low numerical concentration (under 50 particles/cm^3) to reduce the collision frequency when the acoustic field is applied.

II.3.2.1. Experimental apparatus. The device used is represented on figure 1. The components are the same as those of the previous set-up except for the aerosol source and the numerical particle concentration measurement.

- Aerosol source : a monodispersed DOP aerosol is produced by a vibrating orifice generator (TSI 3050). Before entering the precipitation chamber it passes through a krypton 85 source neutralizer to reach Boltzmann's equilibrium.

- Particles concentration measurement : this is accomplished by a "Kratel model 328" type spectrophotometer on samples taken at the bottom of the precipitation tube.

II.3.2.2. Experimental procedure. Once the acoustic field has been measured in the tube, the DOP aerosol is injected into the system. When the stationary state is established a first concentration measurement is performed at the base of the tube (C_o), after which the operation is repeated but in the presence of the acoustic field. This measurement supplies the new downstream concentration value (C). Assuming that the liquid DOP particles entering into contact with the wall are not carried away again the particle fraction deposited in the tube is given by the following expression :

$$\text{Deposit } (\%) = 100 \ (1 - (C/C_o))$$

In this way, if the different wall precipitation mechanisms are considered to be independent, the measured deposit can only be due to application of the acoustic field.

II.3.2.3. Experimental results. During these experiments the geometry of the precipitation tube and the fluid flow rate inside were kept constant (fluid velocity = 12 cm/s), the variables being the particle diameter, sound pressure level and acoustic frequency.

Figure 7 gives the results obtained for six diameters (0.7, 1, 2, 3, 5 and 7 μm), three acoustic intensities (152, 155 and 158 dB) and two acoustic frequencies (540 and 1020 Hz), representing 36 experiments altogether. From these curves and for our experimental conditions the first conclusions are the following :
- the wall deposition rate increases with particle size, sound pressure level and acoustic frequency,
- for given acoustic intensity and frequency the deposition rate increases abruptly between 0.7 and 2 μm, then slightly between 2 and 7 μm,
- for given particle size the deposition rate increases steadily with acoustic intensity and frequency.

From these wall deposition curves an acoustically induced deposition velocity (K_a) may be deduced, as follows :

$$Ka = \frac{-\ UD}{4\ L} \ Ln \ (C/C_o)$$

where U is the flow rate of the fluid in the tube, D the tube diameter and L its length. On figure 7 the Ka values are also plotted as ordinates.
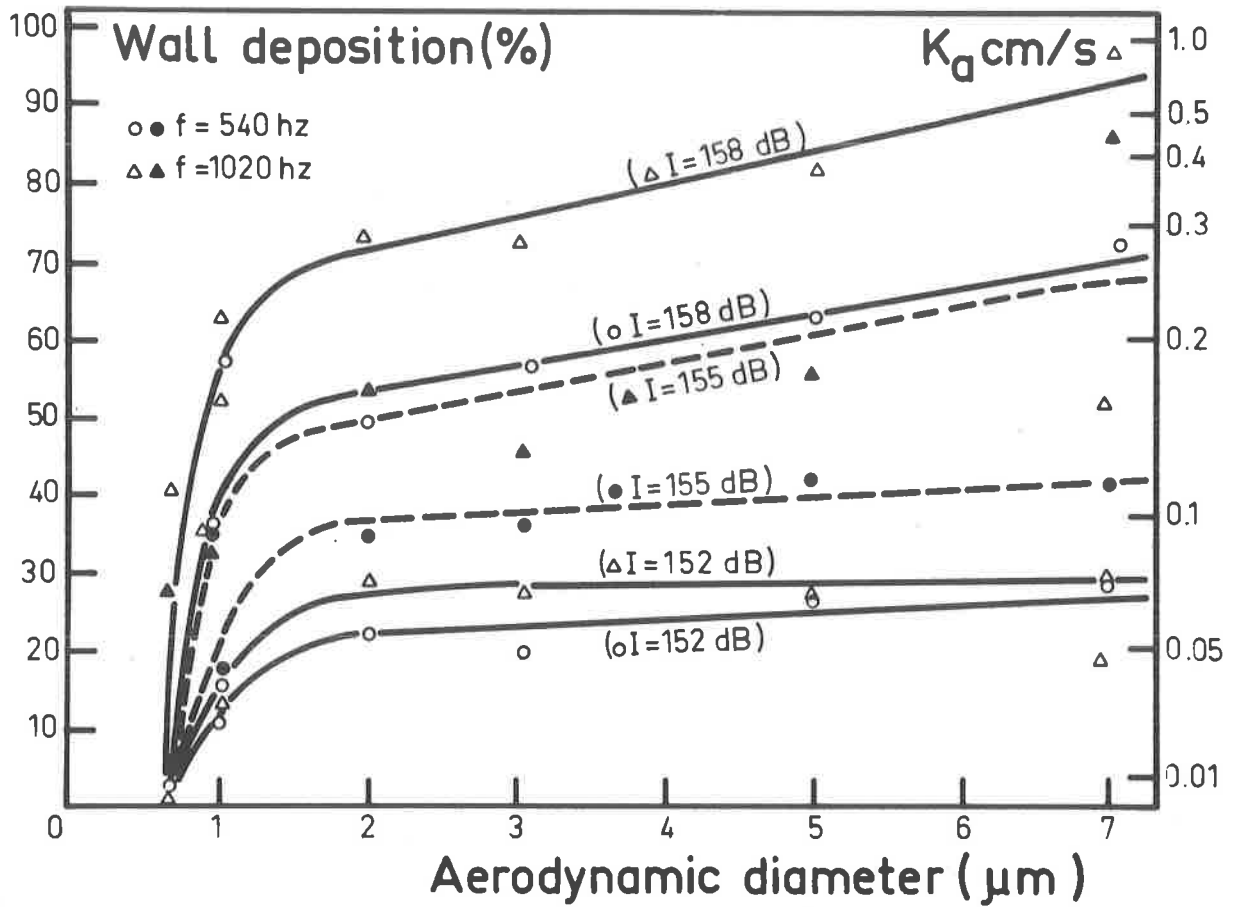
Figure 7 : Percentage wall deposition versus aerodynamic particle diameter, with four acoustic intensities and two frequencies. The residence time being 8.6 s, K_a represents the acoustic deposition velocity.
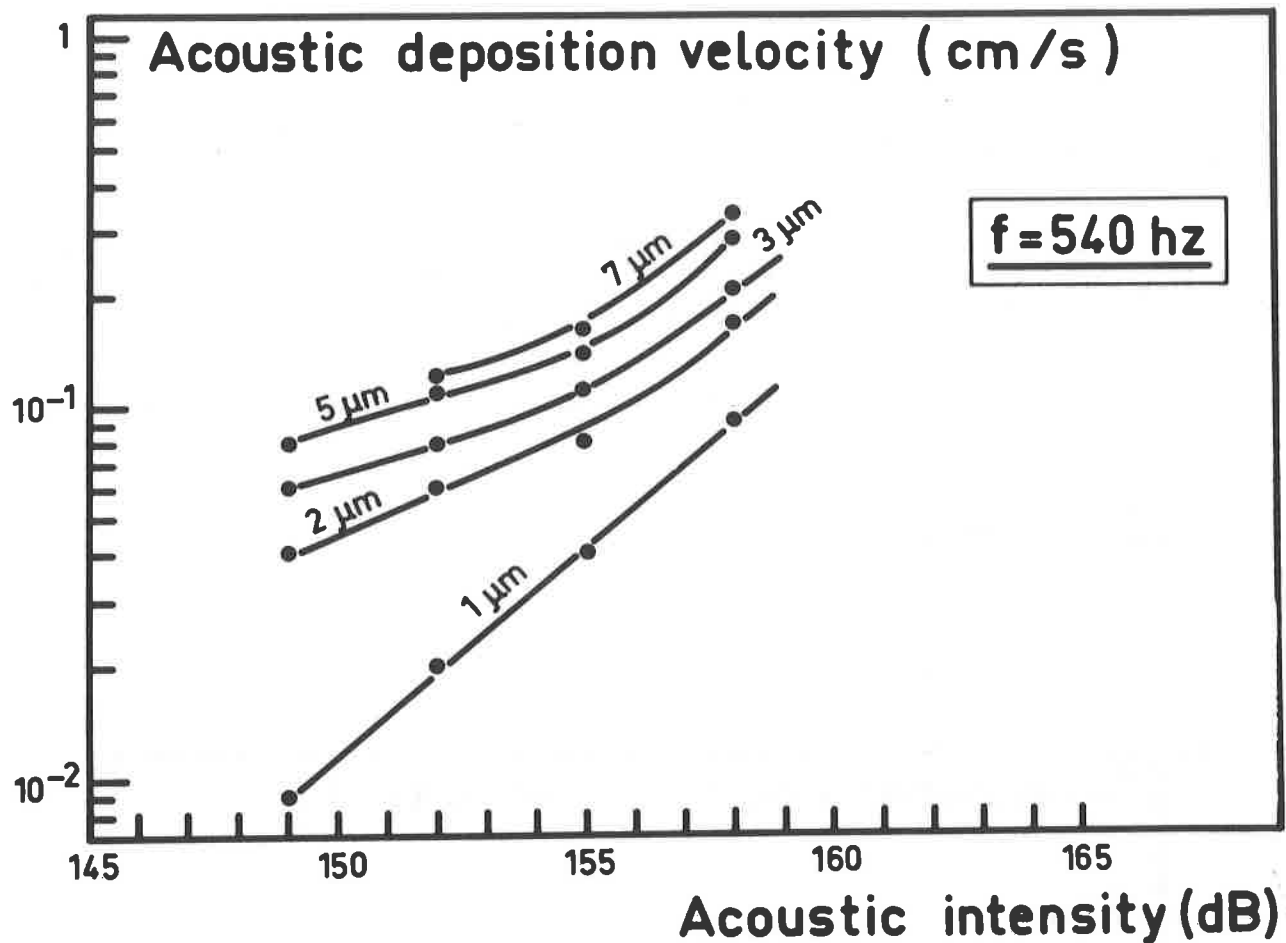
Figure 8 : Acoustic deposition velocity versus acoustic intensity for different particle diameter. Acoustic frequency is constant 540 Hz.

On figure 8 the K_a values are plotted versus the acoustic intensity for different values of particle diameter, in this case the acoustic frequency is maintained constant (540 Hz).

II.3.2.4. Interpretation. More generally it is useful to relate acoustic deposition rate to particles diameter through dimensionless quantities. For this purpose a dimensionless acoustic deposition velocity is introduced, defined by :

$$K_a^+ = K_a / (\varepsilon/\nu)^{1/4}$$

ν being the kinematic viscosity and ε the energy dissipated per unit time and fluid mass due to turbulences induced by the acoustic field.

To describe the inertial behavior of aerosols, caused by acoustically induced turbulences, we introduce a dimensionless relaxation time defined by the expression :

$$\tau^+ = \tau . (\varepsilon/\nu)^{1/2}$$

with τ the particle relaxation time being expressed by :

$$\tau = Cu \, D_p^2 \, \rho_p / 18 \, \mu$$

815

where Cu represents Cunningham's correction slip factor, Dp the particle diameter, ρ_p its mass per unit volume .and μ the dynamic viscosity of the fluid.

By choosing the expression given by MEDNIKOV (1965) for $\epsilon(1)$:

$$\epsilon = (I^{3/2} f)/(\rho_g^{3/2} C_g^{5/2})$$

where I is the acoustic intensity, f the frequency, ρ_g the fluid mass per unit volume and C_g the acoustic wave propagation velocity in the fluid, all the results of figure 7 can be given in dimensionless form as shown on figure 9 where K_a^+ has been plotted against τ^+.

Fitting the points by a power function leads to the following expresssion :

$$K_a^+ = 0.031 \ \tau^{+\ 0.471}$$

for a τ^+ variation range between 10^{-3} and 1.
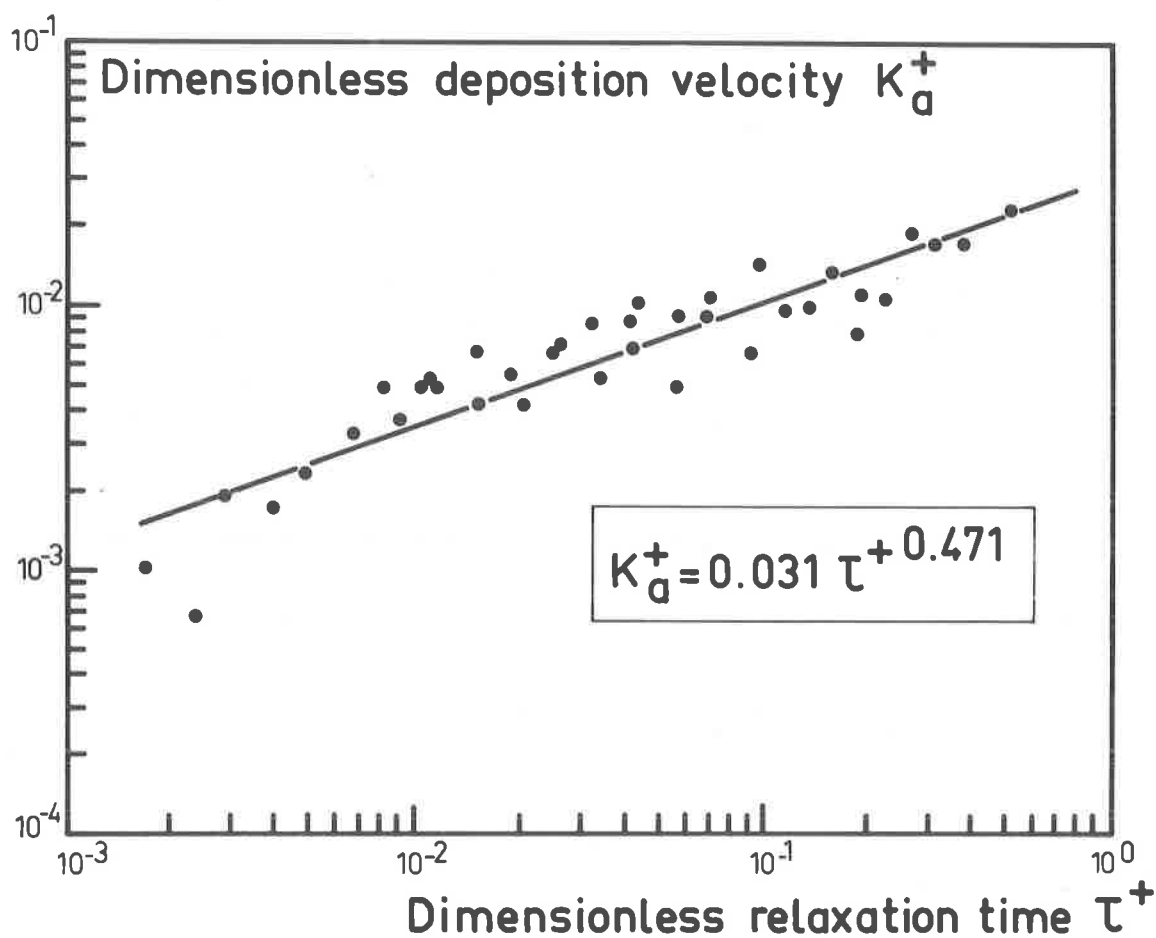
Figure 9 : Dimensionless deposition velocity versus dimensionless relaxation time

This dimensionless relation, obtained under restricted experimental conditions (constant tube geometry and fluid flow rate) remains to be confirmed for different tube geometries (variable diameter) and varying aeraulic conditions (different flow rates) ; after fitting with a correlation coefficient of 0.834 it offers a first empirical approach to acoustic deposition phenomena if we take for ε the expression given by MEDNIKOV (1). In fact an exact knowledge of ε is essential to understand these mechanisms and we have now undertaken a specific experiment to characterize the turbulences induced by an acoustic field (laser doppler velocimetry of small particle).

II.3.3. <u>Summary of experimental studies</u>. Two phenomena occur when an aerosol pass through a volume exposed to an acoustic field :
- a mutual agglomeration of particles resulting in an increase in the median diameter of the aerosol and the corresponding standard deviation. These acoustic field effects begin to occur at around 140 dB but only became significant above 155 dB. The value of the acoustic frequency has little effect in the 500 to 2000 Hz range. Particle should spent a few seconds in the agglomerator (1 to 3 seconds depending on the numerical concentration of the aerosol) ;
- a precipitation of particles on the wall of the volume ; this mechanism depends on, the geometrical characteristics of this volume, fluid flow, level of turbulences induced by the acoustic field and particles inertia.

II.4. <u>Dimensioning an acoustic agglomerator</u>

II.4.1. <u>Main characteristics</u> of an agglomerator are therefore its volume (V) that can be calculated from the flow rate of the gas been treated (Q) and the residence time (t) necessary for an agglomeration

$$V = Q \, t$$

The energy (E) consummed per unit volume of gas treated is written :

$$E = I.S.t/V\eta$$

where I represents the acoustic intensity, S the agglomerator cross section and η the overall yield of the latter. E can also be expressed in the following way :

$$E = I \, t/L\eta$$

where L represents the length or the height of the agglomerator (L = V/S).

II.4.2. <u>Energy criteria for AA</u>. The use of an acoustic agglomerator in conjuction with pre-filtering devices such as cyclones or granular beds should satisfy both technological and energy criteria.

Energy consumption from acoustic agglomerator is an often cited disadvantage weighing against this choice being taken at design level. Although the energy criteria is not always the most important consideration, we shall develop an approach to define a criterion of this type for a project in which a cyclone is or is not used in conjuction with an AA system. A cyclone is designed in such a way as to minimize aerosol penetration with constants such as overall cost and pressure drops being taken into consideration. Penetration is defined as the ratio between the total number of particles leaving the device per unit time and the total number of particles entering per unit time. Optimization is achieved by defining a criterion designated "efficiency factor" or "quality factor" q using the following expression (7) :

$$q = -\ln(Pn)/\Delta P$$

where Pn represents the penetration of a particle of size Dp and ΔP the pressure drop accross the device. This quality factor can be considered to be a measure of the volume of gas cleaned per unit energy.

In our particular case, we therefore should compare the performance of a cyclone used by itself

$$q_1 = -\ln(Pn_1)/\Delta P_1$$

ΔP_1 = pressure drop across cyclone 1
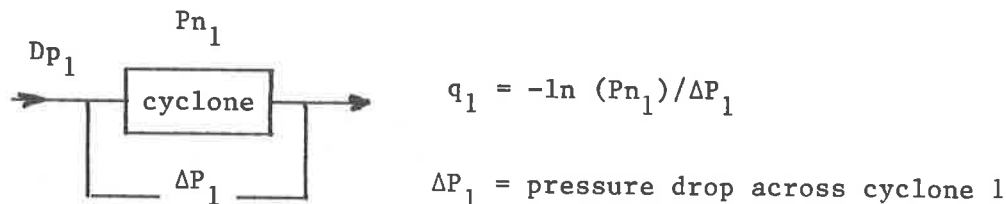
with that of a cyclone when used in conjunction with an acoustic agglomerator.
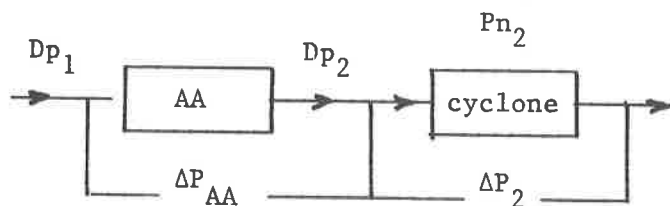
$$q_2 = -\ln(Pn_2)/(\Delta P_2 + \Delta P_{AA})$$

ΔP_{AA} is the equivalent pressure drop associated with the operation of the AA. ΔP_2 is the pressure drop across cyclone 2.

We suppose that the agglomerator only modifies the size of the aerosol $(Dp_1 \rightarrow Dp_2)$ but does not introduce a retention factor. Furthermore, for demonstration purposes only monodispersed aerosols having an initial diameter Dp_1 and a final diameter Dp_2, after passing through the AA have been considered.

The penetration in a cyclone can be expressed by the following formula (8) :

$$Pn = \exp\left[-2\,(C\psi)^{1/(2n+2)}\right]$$

where ψ is an inertial parameter dependant on the particle relaxation time, the fluid velocity at the inlet of the cyclone and on a dimensional characteristic of the cyclone, C is a correction coefficient and n a parameter "Vortex exponent" empirically related to the characteristic dimension of the cyclone.

Under these conditions, our two cases have the following quality factors respectively :

$$q_1 = k_1\,(Dp_1^2)^{1/(2n+2)}/\Delta P_1$$

$$q_2 = k_2\,(Dp_2^2)^{1/(2n+2)}/(\Delta P_2 + \Delta P_{AA})$$

k_1 and k_2 being constants depending on the geometrical characteristics of the cyclone and aeraulic conditions.

The energy criterion for the acoustic agglomerator thus impose that $q_2 > q_1$

i.e. $\dfrac{k_2 \ (Dp_2^2)^{1/(2n+2)}}{k_2 \ (Dp_1^2)^{1/(2n+2)}} > \dfrac{\Delta P_2 + \Delta P_{AA}}{\Delta P_1}$

This shows that the AA must increase the Dp_1 size of the aerosol up to Dp_2 while introducing a pressure drop ΔP_{AA} so that the above defined condition is respected.

In order to make the preceeding relation explicit, the parameters k_1, k_2, ΔP_1, ΔP_2 and ΔP_{AA} must be formulated. For simplification purposes, we illustrated the possible case where the cyclones and gas flow rate to be treated are, in both cases, identical ; this leads to :

$k_1 \cong k_2 \quad \Delta P_1 = \Delta P_2$

Under these conditions (9) :

$\Delta P_1 = 8 \ \sigma_g \ Q^2/abD_c^2$ \quad (SHEPPERD and LAPPLE, 1940) (9)

where Q represents the flow rate in the device, ρ_g the density of the fluid and a, b, and Dc the characteristic dimensions of the cyclone (LEITH and METHA, 1973) (10).

In the case of AA, it is possible to relate the power Pu dissipated at a flow rate Q through the associated pressure drop ΔP_{AA}.

$Pu = Q.\Delta P_{AA}$

The power dissipated is itself related to the acoustic intensity (I) and to the cross section of the agglomerator (S) by the relationship :

$Pu = I.S/\eta$

where η represents the overall yield of the AA, i.e. $\Delta P_{AA} = I.S/Q\eta$.

By introducing a residence time (t) in the AA and the heigh (L), the explicit criterion can be written :

$\left(\dfrac{Dp_2}{Dp_1}\right)^{1/n+1} > \dfrac{It/L\eta}{8 \ \rho_g \ Q^2/abD_c^2} + 1$

Which defines the condition that an acoustic agglomerator must satisfy for the case of monodispersed aerosols.

For polydispersed aerosols, the penetration expression takes the integral form which alters certain details in the calculations but does not modify the reasoning developed previously.

This type of approach thus provides definition of an energy criterion to determine whether or not an AA should be used upstream from a cyclone or other cleaning device. Nevertheless, energy is not always the decisive criterion, in particular for devices operating under accidental conditions.

III. Acoustic filtration

III.1. Introduction

As already mentioned in the preceeding paragraph, in order for acoustic agglomeration effects become appreciable, it is necessary to induce high mass concentrations because coagulation mechanisms are proportional to the square of the numerical concentration of the aerosol. This fact tends to limit AA applications to very dusty gas. The aim of filtration in an acoustic field is to exploit the deposition phenomenon previously observed by increasing the walls surface/volume ratio through interposing a granular bed or a fiber bed exposed to an acoustic field in the path of the fluid charged with particles.

With such an effect, it is possible to increase the collection efficiencies of prefilters (granular beds, fiber beds) for particles with diameter of less than 5 μm without affecting the depth of filtration. This property leads to the advantages of equivalent performances with less bulky equipment and reduced volume of matter requiring treatment (this is particularly true for granular beds where granules are regenerated).

The phenomena of filtering in an acoustic field is still little known and few experiment have been performed in this field. The first studies were carried out in 1969 by BEECKMANS et al on a granular bed (11). These qualitative experiments led to a marked increase in collection efficiency. The same authors renewed their attention to this kind of test in order to apply it to flat filtering media (NGUYEN and BEECKMANS (12). More recently, we performed some experiments on a laboratory scale in order to demonstrate that the filtering efficiency of a granular bed could be significantly improved by exposing it to a high intensity acoustic field (BOULAUD et al 1982) (13). We have also in collaboration with the University of Paris XII engaged a study for investigating the filtration mechanisms involved with granular beds in the presence of acoustic field.

III.2. Acoustic filtration mechanisms

In 1974 NGUYEN and BEECKMANS determined the various mechanisms intervening in fiber media filtration with an acoustic field (12).

* Impaction mechanism is enhanced due to a significant increase in the instantaneous velocity of particles by the acoustic field ; as a result particles in the vicinity of a fiber can be projected on to this latter.

* Interception mechanism is also enhanced because the "apparent" cross section of a particle is increased by vibrations.

* Diffusion mechanism is also enhanced because by inducing turbulences in the gas, the acoustic field increases the diffusion coefficient of the particles.

The results of the studies performed can be expressed in terms of an acoustic efficiency (η_a) defined in accordance with the following relation as a collection efficiency due solely to sound :

$$1 - \eta = (1 - \eta_o)(1 - \eta_a)$$

η is the collection efficiency of the filter in the presence of the acoustic field and η_o the efficiency of the filter under the same conditions but without the acoustic field.

In this case, the variations in η_a as a function of the various parameters involved are the following :
- a reduction due to increased frontal velocity,
- an increase with increasing particle size,
- an increase with increasing acoustic intensity
- the obtaining of a maximum η_a value by placing the filtering medium at a maximum wave amplitude.

More recently, TAVOSSI (1984) has theoretically studied the effect of an acoustic field on the collection efficiency of a granular bed and established a relation applicable to the turbulent diffusion of particles.

III.3. Experimental studies

III.3.1. Preliminary experiments were conducted to demonstrate the feasibility of increasing the collection efficiency of a granular bed by exposure to an acoustic field.

The infrastructure employed is exactly the same as that already described (figure 1). In addition, we have included in the middle of the tube a granular bed, 20 cm high (glass pebble diameter : 0.3 cm).

The pneumatic atomizer enables concentrations of the order of 50 mg/m^3 to be obtained upstream from the granular bed. It is possible, in this way, to perform a direct detection downstream from the filter using a Sinclair Phoenix type photometer (it is recalled that the mass median diameter is of the order of 1.5 µm with a standard deviation of 1.75). Under these concentration conditions, the mutual agglomeration of particles during the residence time in the tube can be considered negligible.

In this demonstration experiment partial results have been obtained. The first column of table 1 indicate the values of the most important experimental parameters (I : acoustic frequency at the face upstream from granular bed ; f : acoustic frequency ; V : frontal velocity). The last column gives the value obtained for the collecion efficiency (E) under these conditions.

Table 1 : Acoustic filtration

I dB	f Hz	V cm/s	E %
0	–	5	62
0	–	10	58
163	550	5	90
163	850	5	90
169	550	5	99.994
169	550	10	99.96

These experimental facts thus suggest that an inefficient filter (E = 60%) can become efficient (E = 99.994%) by applying a very high intensity acoustic field.

III.3.2. Currently conducted experiments. The first experiments carried out gave very promising results. In consequence a theoretical and experimental study of acoustic filtering mechanisms was undertaken in collaboration with the University of Paris XII.

III.3.2.1. Experimental device. The infrastructure of this device is the same as that already described but its size and operating conditions are however different.

The main part of our device consists of a two meter high, 15 cm diameter glass column in which we have installed our granular bed having the following characteristics : glass pebble diameter 0,2 cm ; bed thickness 22 cm ; porosity 0.35.

Experimental conditions and working parameters :
- the flow rate through the bed is in the range of 3 to 40 m^3/h. The superficial velocity is in the range of 4 to 50 cm/s under standard ambient atmospheric conditions ;
- the maximum acoustic intensity attainable upstream of the bed is about 153 dB in the frequency range 400 Hz to 3000 Hz ;
- modonodisperse oil aerosol (DOP) could be generated in the size range 0.05 μm to 15 μm.

The particle concentration is analyzed using a condensation nuclei counter for submicronic aerosols and an optical counter for larger particles.

III.3.2.2. Experimental results. Initially we have determined the collection efficiency of our granular bed, under given experimental conditions, using the theoretical overall collection efficiency reviewed by us (TAVOSSI and al. 1983) (15).

Our main interest in the first step of this study is the minimum collection efficiency. For the size range corresponding to this minimum (0.1 μm to 0.3 μm) and for the superficial velocity of about 5 cm/s the calculated value is 16%.

Our experiments were performed with aerosols in the size range mentioned above. The range of particles concentration was from 50 000 to 100 000 particles per cc.

Preliminary experiments were aimed at measuring collection efficiency without acoustic waves. The results of these investigations are in good agreement with calculated values. For example for an aerosol diameter of 0.3 μm the mean value of the experimental collection efficiency for forty runs was 16.5% with a standard deviation of 3.8%.

The above experimental investigations were repeated in the presence of acoustic waves. The first results demonstrate that there were significant increases in collection efficiency for the size range corresponding to the minimum in efficiency. But this effect was not observed below an acoustic intensity level of about 145 dB which suggest the existence of a threshold intensity. For example, for a diameter of 0.3 μm, (the most penetrating size in this case), an acoustic frequency of 400 Hz and an acoustic intensity level upstream of about 153 dB, the collection efficiency was about 60% under the above described experimental conditions this is more than three times the value obtained in the absence of acoustic waves.

III.4. Conclusions

These significant results have encouraged us to undertake further detailed experimental and theoretical investigations in order to discover the exact relationship between, collection efficiency, acoustic parameters (intensity, frequency, propagation direction etc.), particle size and flow characteristics of the system.

IV. Acoustic sources

Five important methods exist for generating high intensity acoustic waves :
- crystals and piezoelectric ceramics,
- vibrating membranes or vibrating pistons,
- resonant pipes or cavities (statical generators),
- sirens (dynamic generators),
- pulsed jets.

The first two types of device are mainly used in laboratories for relatively low powers. The last three types of generators are used industrially and enable large levels of power to be achieved.

The choice of acoustic source will obviously depend on the thermalhydraulic conditions under which the device with acoustic effects is intended to operate and on the need to introduce or not to introduce supplementary fluids (pulsed jets, sirens, resonant cavities).

As far as this last point is concerned, the systems installed in a cleaning circuit may employ the fluid to be treated as an energy source for the acoustic generator. It is thus possible to design for example : sirens operating with the totality of the fluid to be cleaned ; resonant cavities installed inside the flow of gas to be treated.

V. General conclusions

The various elements grouped together in this study demonstrate the various advantages offered by acoustic field for gas cleaning. Although the technical feasibility and operating conditions associated with the use of acoustic agglomeration are now better know and understood, studies of collection efficiency increase by filtering media in acoustic fields have only been partially completed and many aspects still requise further work.

The economic aspects of these systems in cleaning trains still have to be optimized and criteria determining whether or whether not such systems should be employed remain to be defined (a first approach has been elaborated in this paper). A useful application of these systems, would however be, to employ them in cleaning devices intended to operate under accident conditions (fires, accidental release of aerosols).

References

(1) MEDNIKOV E.P., Acoustic coagulation and precipitation of aerosol a special research report. Trans. from Russian, New York, 1965

(2) SHAW D.T., Recent developments in Aerosol Science, Wiley Interscience, 279, 1978

(3) CHOU K.H., LEE P.S., SHAW D.T., "An investigation of high intensity-acoustic agglomeration", J. Colloid Interface Sci., 83, 335 (1981)

(4) BOULAUD D., DIOURI M., MADELAINE G., "Parameters influencing the collection efficiency of solid aerosols in cascade impactors", in Aerosol in Science, Medicine and Technology, 9th Conference of the Gesellchaft für Aerosol Forschung (1981)

(5) BOULAUD D., DIOURI M., "Methodes de traitement des données experimentales obtenues par impaction et par sedimentation", Rapport CEA-R-5177 (1982)

(6) CHOU K.H., LEE P.S., WEGRZYN J., SHAW D.T., "Aerosol deposition in acoustically induced turbulent flow", Atmospheric Env., 16, 1513-1522 (1982)

(7) COOPER D.W., "Cyclone design : sensitivity, elasticity and error analyses", Atmospheric Environment, 17, 485-489 (1983)

(8) LEITH D., LICHT W., "Collection efficiency of cyclone type particle collectors a new theoretical approach", A.I.Ch.E. Symp. Series : Air (1972)

(9) SHEPPERD C.B., LAPPLE C.E., "Flow pattern and pressure drop in cyclone dust collectors", Ind. Engng. Chem., 32, 1246-1248 (1940)

(10) LEITH D., METHA D., "Cyclone performance and design", Atmospheric Environment, 7, 527-549 (1973)

(11) BEECKMANS J.M., KEILLOR S.A., "Enhanced deposition in a filter in a presence of low frequency sound", J. Colloid Interface Science, 30, 387-390 (1969)

(12) NGUYEN X., BEECKMANS J.M., "Sonically enhanced depth filtration of aerosols" J. Aerosol Science, 5, 133-143 (1974)

(13) BOULAUD D., MADELAINE G., "Utilisation des effets acoustiques dans la filtration des effluents gazeux", FILTRA 82, 383-396 (1982)

(14) TAVOSSI H., "Performance et efficacité de fixation des aérosols par un lit granulaire en présence d'ondes acoustiques", Rapport CEA-R-5259 (1984)

(15) TAVOSSI H., RENOUX A., MADELAINE G., BOULAUD. D., "Influence of an acoustic wave on the aerosol collection efficiency of a granular bed", J. of Hungarian Meteorological Service, 87, 327-342 (1983)

REMOVAL OF RADON DECAY PRODUCTS WITH ION GENERATORS
- COMPARISON OF EXPERIMENTAL RESULTS WITH THEORY

E.F. Maher, S.N. Rudnick, and D.W. Moeller
Harvard Air Cleaning Laboratory
Boston, MA 02115

Abstract

The potential of ion generators to remove radon decay products from the airspace of residences or mines was investigated both experimentally and theoretically. A positive ion generator, producing an air ion current of less than 2 µA and operated in a 78 m^3 chamber with air exchange rates ranging from 0.2 to 0.8-hr^{-1} and relative humidities ranging from 20 to nearly 100%, reduced the concentrations of airborne radon decay products by as much as 85%. A negative ion generator, operated under the same range of conditions, was less effective, producing airborne radon decay product removals up to 67%. Experimental results compared favorably with a simple theoretical model that hypothesizes a three-part process: 1) radon decay products, as well as aerosol particles to which some of these decay products attach, are charged by diffusion of the air ions produced by the generator; 2) the air ions also produce a nonuniform space charge in the chamber that results in an electric field gradient radially outwards from the generator to the chamber surfaces; 3) because of the influence of this electric field, the charged decay products and particles migrate toward nearby surfaces where they plate out. The net benefit of unipolar space charging is a substantial decrease in the steady-state radon decay product concentrations in the airspace with a corresponding reduction in the lung dose equivalent to the occupants.

Introduction

The single greatest source of radiation exposure to the general public is from naturally occurring airborne radionuclides inside residences (1). Inhalation of the short-lived decay products of radon (Rn-222), i.e., Po-218 (RaA), Pb-214 (RaB), and Bi-214 (RaC) account for nearly all of the public's annual lung dose equivalent, which by recent estimates is 3 rem/y (0.2 WLM/y) to the bronchial epithelium of an average adult member of the U.S. population (1,2). Epidemiological investigations on uranium miners have produced convincing evidence that prolonged inhalation of radon decay products is associated with an increased risk of lung cancer. Risk projections reported by the National Council on Radiation Protection and Measurements (NCRP) (2,3) have suggested that radon decay product induced lung cancer may account for as much as one fifth of the spontaneous lung cancers in the nonsmoking population. Higher estimates have been hypothesized by other groups (4,5,6); however, these estimates differ only by a factor of 5 or less.

The current interest in radon in residences is due to the concern that has been expressed by public health officials regarding increased public exposures from all types of indoor air pollutants due primarily to deliberate reductions in the natural air infiltra-

tion rates of US homes for energy conservation purposes (7). A recent NCRP study has concluded that indoor exposures to radon and its decay products are typically several times greater than those outdoors, with extreme differences as much as two orders of magnitude possible in some highly contaminated homes (2). Most often, these high exposures are associated with dwellings built over soils with higher-than-usual radium concentrations resulting from natural geological formations, radon intrusion from ground water sources (8), or through technological enhancement of existing natural radiation. Despite a few isolated instances where mining wastes were improperly utilized (9, 10), the greatest single component of the collective dose equivalent to the US public is due to natural-occurring sources of radon (2,5).

In the past, indoor radon and decay product exposures have been inadvertently low because typical air infiltration rates of homes were generally greater than 1 hr^{-1}. These rates were sufficient to dilute radon gas accummulations. However, increasing energy costs and federally sponsored energy conservation programs have spurred a gradual reduction in residential air infiltration rates. The continuation of these trends in the foreseeable future and because most individuals spend 80-90% of each day indoors will, in all probability, mean increased radon and decay product concentrations indoors and still greater radiation exposures to the general public.

The potential health consequences associated with these trends have emphasized the need for exploring low-cost remedial air treatment for reducing indoor radon decay product exposures. One potential, yet untested, air treatment method is unipolar space charging through air ion generation. Compared to more traditional air cleaners, ion generators are inexpensive to own and operate, produce no noise or air movement, and are simple to install. Their demonstrated effectiveness in reducing radon decay product exposures would represent an attractive alternative to other forms of remedial control technology.

The objectives of this paper are two-fold. The first is to report the results of an experimental study that evaluated the effectiveness of unipolar space charging for removing radon decay products from the airspace within a full-scale simulated residence. The second objective is to compare the experimental results to the predicted results obtained with a analytical room model that describes the decay product removal in terms of the physical processes involved.

Theoretical Considerations

The role of small air ions and charged condensation nuclei in the environment has been studied by aerosol scientists for the past 50 years. Early investigators have shown that uniform concentrations of unipolar air ions inside an enclosed air space will decrease with time owing to the mutual replusion (electrostatic scattering) of the ions and their eventual deposition onto surfaces (11-15). Without a continuous source of ions present, the air ion concentration will ultimately become very small, i.e., less than 200 cm^{-3}; the residual concentration attributable to ion production from natural

background radiation. Unipolar charged condensation nuclei will ex-
hibit similar behavior except that the rate of concentration decrease
will be slower because their electrical mobility is smaller than the
ions.

Particle Removal due to Unipolar Space Charging

In the presence of a continuous point source of unipolar ions,
the concentration of ions at radial distances from the source will
decrease as described by solution of Poisson's equation assuming
conservation of ions and a spherical room geometry. The ion con-
centration at a radial distance, r, from the source has the form
(11-12):

$$N_i(r) = \frac{(3\,Q/2\,Z)^{1/2}\ r^{-3/2}}{4\,\pi\,q} \qquad (1)$$

where:

N_i = Air ion concentration, cm^{-3}.

Q = Ion generation rate, stA.

Z = Ion electrical mobility, $cm^2/stV \cdot s.^{-1}$

r = Radial distance from ion source, cm.

q = Electron charge, 4.80×10^{-10} stC.

The nonuniform space charge distribution creates an electric
field gradient that is also a function of radial distance from the
ion point source. According to Whitby and McFarland (11-12), the
electric field strength, E (stV/cm), at a radial distance, r, from
a point source of ions is:

$$E(r) = (\,2\,Q/3\,Z\,r\,)^{1/2} \qquad (2)$$

Aerosol particles within the enclosed airspace will become
charged to the air ion polarity through diffusion charging by the air
ions (16-19). The number of elemental charges acquired by a particle
can be approximated by White's diffusion charging equation (16);

$$n_p(t) = \frac{d_p\,k\,T}{2\,e^2}\ LN\left(\,EXP(2\,n_0\,e^2/d_p\,k\,T) + e^2\,d_p\,N_i\,v_i\,t/2\,k\,T\,\right) \qquad (3)$$

where:

$n_p(t)$ = number of elemental charges acquired in t seconds.

d_p = particle diameter, micrometers.

e = electron charge, 4.80×10^{-10}, stC.

k = Boltzmann's constant, 1.38×10^{-16} dyn $\star$ cm/ K.

T = absolute temperature, ^{0}K.

n_0 = number and polarity of elemental particle charge at t=0.

N_i = air ion concentration, cm^{-3}.

v_i = thermal speed of air ions, cm $\star$ s^{-1}.

t = charging time, s.

In the presence of a very strong ion source it can be assumed that the concentration of air ions is much greater than the aerosol particle concentration, so that the space charge and electric field contributions from the charged particles are negligible compared to those due to the air ions.

Once charged, the particles will move radially outwards along the electric field gradient towards the boundary of the enclosure and eventually deposit on the inner surface with particule flux, Φ_p. We have assumed for this analysis that particle surface losses due to molecular diffusion, impaction, and gravitational setting are small enough to be ignored. The particle deposition velocity at the inner surface of the boundry, v_p, is related to the particle electrical mobility, Z_p and electric field strength, E, by the familiar relationship: $v_p = Z_p \cdot E$.

The particle electrical mobility and hence the particle deposition velocity are dependent on the number of elemental charges acquired by the particle and the particle diameter. The particle flux at the boundary of the spherical room can be directly related to the aerosol number concentration, N_p, and the deposition velocity, v_p, which in turn, can be related to the particle electrical mobility and electric field intensity at the boundary. For a sperical room of radius, R, the flux is;

$$\Phi_p = v_p N_p = Z_p E(R) N_p \tag{4}$$

The rate of particle deposition can be determined from the flux and surface area, A, of the sphere as follows:

$$\Phi_p A = -4 \pi R^2 Z_p E(R) N_p \qquad (5)$$

Since at any instant, the rate of particle loss from the airspace must equal the deposition rate, then:

$$4/3 \pi R^3 \frac{dN_p}{dt} = -4 \pi R^2 Z_p E(R) N_p \qquad (6)$$

Upon combining equations (2) and (5) and integrating equation (6), the particle removal constant, Γ_p, (analogous to a radiological decay constant) can be expressed:

$$\Gamma_p = -Z_p R^{-3/2} (6Q/Z)^{1/2} \qquad (7)$$

Radon Decay Product Removal Constant

The results of equation (7) can be used to obtain a removal constant for radon decay product activities, however, it is first necessary to make some relational assumptions regarding the decay product activities and the particle size of the host aerosol. Ideally what is needed is a relationship linking some descriptive measure of the aerosol size distribution to the radon decay product activity.

Raabe (20) has reported that the kinetic theory of gases best describes the attachment state of radon decay products to submicrometer aerosols, i.e., the attachment probability is proportional to the aerosol number concentration and the square of the particle diameter. His results are applicable to low radon concentrations where the decay product diffusion gradients about the aerosol particle are negligible. These conditions generally typify indoor environments in that the decay product number concentration is always much smaller than the aerosol number concentration. Several investigators have measured the attachment status of the radon decay products to submicrometer aerosols and have found good agreement with Raabe's conclusions (21, 22, 23).

In accordance with Raabe's work, the descriptive measure for a polydisperse aerosol which would directly relate to the attached radon decay product activity is the diameter of average surface area, $\bar{d}_{sa}$, which for a grouped particle size distribution of n groups is calculated as follows:

$$\bar{d}_{sa} = \left[\sum_{i=1}^{n} N_p^i \, d_p^{i\,2} \, / N_p^o \right]^{1/2} \tag{8}$$

where,

N_p^i = number concentration of the i-th particle size group.

N_p^o = total aerosol number concentration, cm.$^{-3}$

d_p^i = characteristic diameter of the i-th particle size group.

For modeling purposes, we made the assumption that the radon decay product removal constant due to unipolar space charging can be calculated by equation (7), using the diameter of average surface area (DASA) for the chamber aerosol.

Decay Product Concentrations Model

Radon decay product air concentrations inside a well-mixed volume, V, can be modeled by a series of first order, linear differential equations containing rate constants that account for all known sources and sinks for the decay product atoms (24,25). For our purposes, we have included in the room model a removal term for decay products due to unipolar space charging. This term is equivalent to the particle removal constant calculated in equation (7), using the diameter of the average surface area for the host aerosol, and is treated simply as another sink for radon decay products. The steady-state solutions for the n-th decay product airborne concentration can be expressed as follows (26);

$$C_n(\infty) = \frac{Q_o}{V(\lambda_0 + I_v)} \prod_{n=1}^{N} \frac{\lambda_n}{(\lambda_n + I_v + P_n + \Gamma_n)} \tag{9}$$

where;

C_n = Activity air concentration of the n-th decay product, pCi ℓ l^{-1}

λ_0 = Radon (Rn-222) decay constant, min^{-1}

λ_n = Decay constant for the n-th decay product, min^{-1}

$I_{/v}$ = Room air infiltration rate, min^{-1}

Q_s = Radon source emanation rate, pCi ℓ min^{-1}

P_n = Surface plateout constant for the n-th decay product, min^{-1}

V = Room volume, liters

Γ_n = Space charge removal constant for the n-th decay product, min^{-1}.

The term outside the product portion of equation (9) represents the steady-state radon air concentration. The removal rate constant for ventilation or air infiltration, I_v, was assumed the same for each decay product. The plateout rate constant, P_n, denotes the removal rate of airborne decay products by deposition onto room surfaces via diffusion. The plateout constants used in the model were derived from measurements described elsewhere (26).

<div align="center">Experimental Methods</div>

Sampling Chamber Description

Experimental tests were conducted in a 78-m^3 chamber that, except for its painted metal walls, resembled a room in a typical residence. Air infiltration was controlled at 0.2, 0.5, and 0.8 air changes per hour by exhausting air from the chamber through a calibrated venturi flowmeter. The accuracy and repeatability of the air exchange rates were verified by sulphur hexafluoride (SF$_6$) tracer measurements. Makeup air infiltrated from adjoining rooms through pores in the walls, floor, and ceiling and also around door jams and window seals. 1.259 x 10^4 pCi/min of radon was introduced into the chamber through a distribution manifold designed to simulate radon intrusion from soil beneath a home and to facilitate mixing of radon with the chamber air. Concentrations of radon and its decay products in the chamber under no-treatment conditions ranged from 0.05 to 0.40 Working Levels (WL) and are representatives of concentrations in highly contaminated homes where remedial control would be indicated.

The relative humidity of the air in the chamber was selected and controlled by a LiCl humidity sensor that activated two steam vaporizers which could add moisture to the room air. The controllable humidity range was 20-98%. The room air temperature was continuously monitored and varied between 20-26 °C. The aerosol properties of the chamber were not controlled but were measured during testing by an eleven-stage, screen-type diffusion battery in conjunction with a pair of Pollak condensation nuclei counters. A light-scattering particle spectrometer was used to measure the contribution of particles greater than 0.3 µm. The instrumentation permitted particle size distribution measurements throughout the size range of 0.001 to 3.0 µm. Particle size distributions were derived

from a reconstructive linear algorithm (29). The diameter of the average surface area (DASA) was then calculated from the grouped particle size data. The chamber aerosol was approximately bimodally distributed (Figure 1) with mode diameters of 0.006 and 0.04-μm. The diameter of the average surface area (DASA) was 0.065-μm, and the condensation nuclei concentration ranged from 6000 to 110000 cm^{-3}. A detailed description of the experimental apparatus and chamber characteristics is given elsewhere (26).

Radon and Decay Product Measurements

Radon and Radon decay product concentrations were determined from air sampling at two locations from the chamber. These locations are referred to as the exhaust and wall ports in Figure 2. The exhaust port was connected in parallel with the exhaust blower used to establish the chamber air exchange rate, while the wall port was a simple wall entry some 2.5 meters away. Each port consisted of a plastic adapter into which an open-face filter holder could be inserted. A comparison between the decay product concentrations measured at the exhaust and wall sampling ports was made using a simple paired-t-test and showed that the concentrations were identical, thus verifying that the chamber was well-mixed. Radon decay products were sampled at 14-18 lpm onto 50-mm diameter membrane filters (0.8-μm pore size). Sampling times ranged from 5 to 20 minutes depending on the concentration of decay products in the chamber.

The counting and calculative procedures were based on the modified Tsivoglou methods described by Thomas (27). This method consists of counting the sampling filter alpha-activity over three different counting intervals and then solving three simultaneous equations for the airborne RaA, RaB, and RaC concentrations. The three counting intervals chosen were 1-5, 7-27, and 35-55 minutes after the end of sampling. These intervals are longer than those recommended by Thomas and resulted in improved precision estimates when measuring low decay product concentrations. Air samples for radon were collected from the exhaust port through a filter into an evacuated 100-cm^3 scintillation flask and counted using the method of Lucas (28).

Ion Generation System

The ion generator system tested was specifically designed for research applications and was capable of producing both positive and negative air ions (30). The entire device consisted of a control module with output connectors for positive and negative electrodes and 30-ft extension cables. The control module was mounted outside the chamber while the electrodes and cables were passed through the chamber wall and suspended 1 meter down from the center of the chamber ceiling. The ion generator output was continuously variable over its entire voltage range by a rheostat control. Operating parameters and manufacturer specifications are given in Table I:
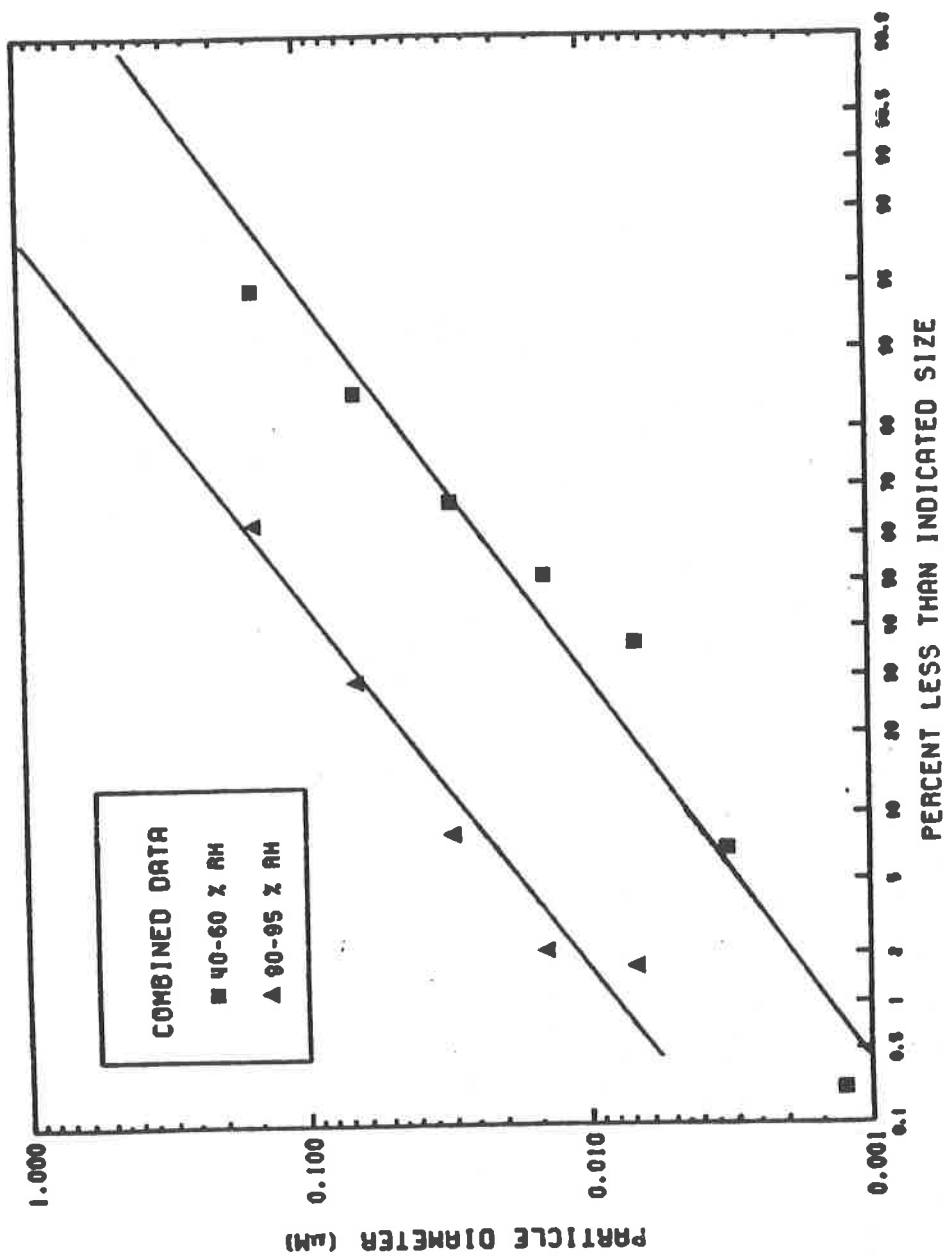
Figure 1: Measured particle size distributions in the chamber for relative humidities, 40-60 and >90%
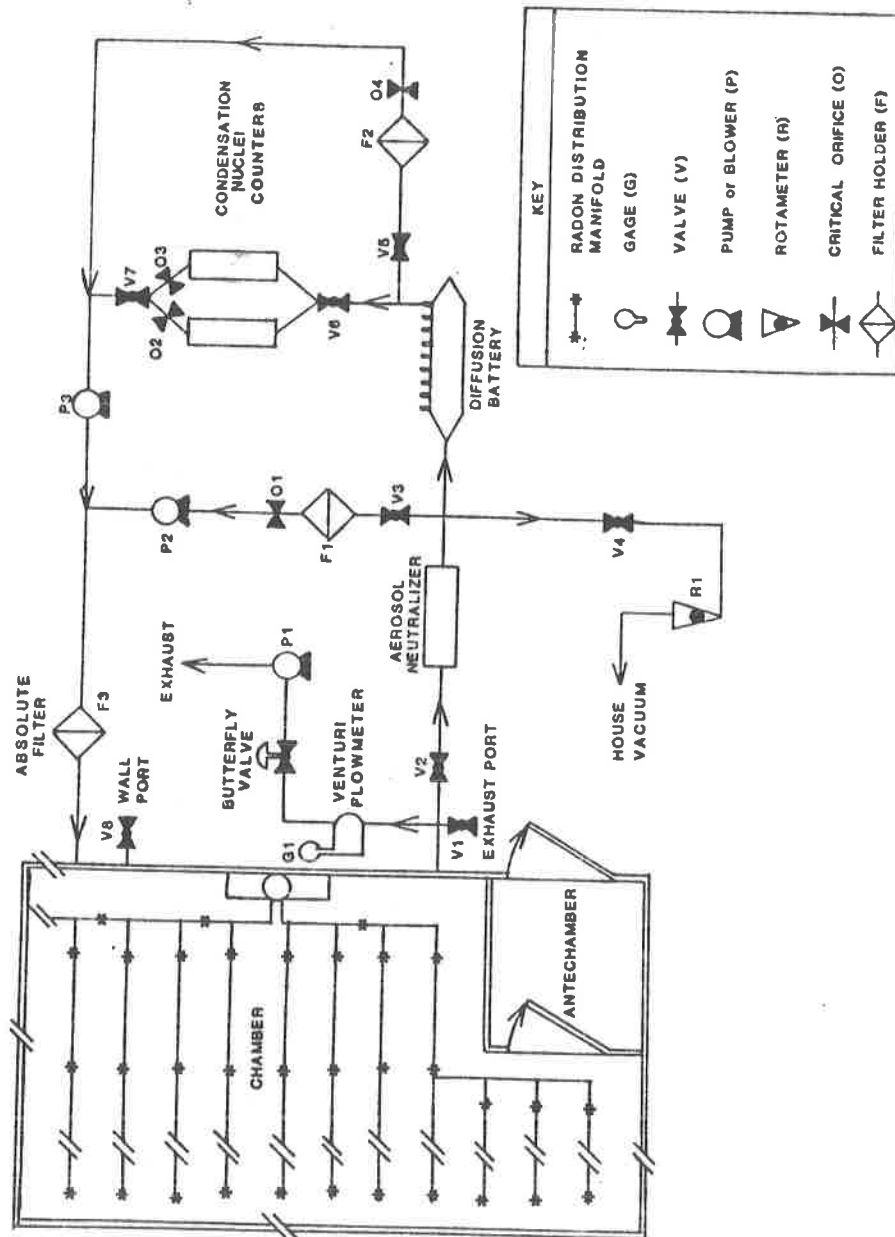
Figure 2: Chamber piping diagram and apparatus

Table I: Ion Generator Specifications.

Ion generator Polarity	Voltage Range(kV)	Ion Output* Rating (cm^{-3})	Power(W) Consumption
Positive	4.15-15.7	8,000-425,000	5-10
Negative	3.85-15.8	11,000-425,000	5-10

* Output at 1 meter and 30% relative humidity.

The specifications in Table I were taken from literature supplied by the manufacturer or through direct communication with a company representative. The actual air ion output was found to vary substantially with relative humidity and, to a lesser extent, the dust concentration in the chamber. Since exact knowledge of the ion generator output was crucial to these investigations, we constructed an air current monitoring circuit as suggested by the ion generator manufacturer (31). The circuit consisted of placing an electrostatically shielded, direct-current microammeter in series with the high-voltage output of the ion generator. Two microammeters, with ranges of 0-10 and 0-50 μA, were alternately used, depending on the generator output and relative humidity, to measure the air current originating from the electrode. The meters were shielded from electrostatic effects by covering them with copper screening and grounding one terminal to the wire screen. Since the impedance of the meter was negligible as compared to that experienced at the output electrode, the performance of the ion generator was unaffected by the current monitoring circuit.

Results

Measured Decay Product Reductions

The effect of unipolar space charging on the airborne concentrations of the radon decay products within the chamber are summarized in Figure 3. The bar graphs represent mean values for percent Working Levels (WL) and airborne concentrations of Po-218 (RaA), Pb-214 (RaB), and Bi-214 (RaC) remaining relative to the no-treatment concentrations following negative and positive ion treatment. (Radon concentrations were not affected by the air ion treatment). All results represent measurements taken after steady-state conditions had been reached. The 95% confidence intervals obtained by radomized replication of experiments are indicated by the lines extending above the bars. The relative humidity in the chamber ranged from 30-65% with no statistical difference discernable in the treatment effectiveness within this range. The air ion output remained stable at 1.4 and 1.2 μA for negative and positive ion production, respectively.
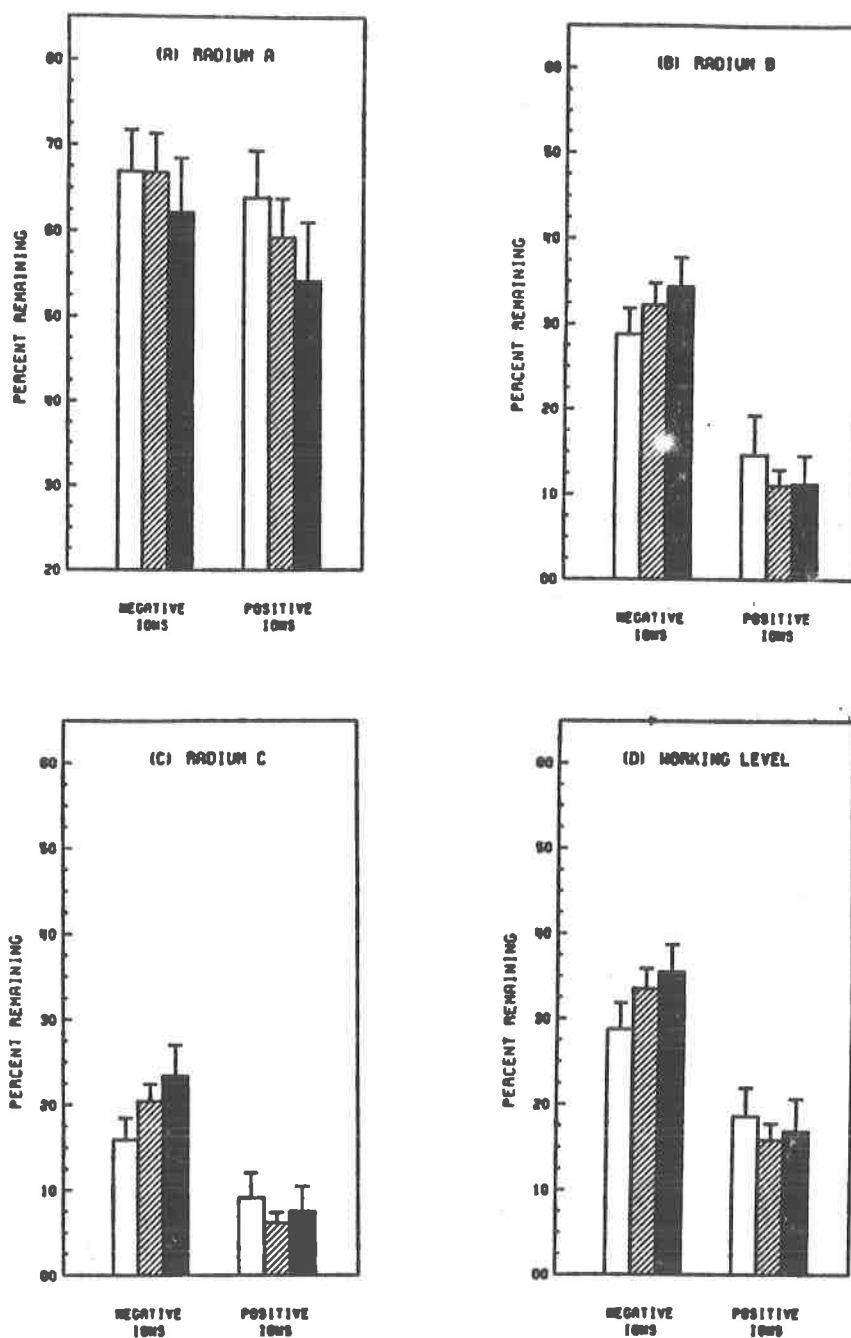
Figure 3: Measured Percent of Radon Decay Products Remaining Following Negative and Positive Air Ion Treatment. (a) Radium A (Po-218), (b) Radium B (Pb-214), (c) Radium C (Bi-214, and (d) Working Level Air Concentration. Ion Current: 1.2 μA (+), 1.4 μA (-). Open bars are for 0.2, cross-hatched bars are for 0.5, and solid bars are for 0.8 air changes/hour.

Positive air ion treatment was decidedly more effective in reducing airborne decay product concentrations than negative ion treatment, despite the fact that the positive ion output was 30% less at the same electrode voltages. We speculate the reason for this difference stems from the charge status of the Po-218 and Pb-214 decay products which tend to be positively charged due to the stripping of orbital electrons upon alpha-decay of their respective radioactive predecessors (32,34). Since these decay products and host aerosol can already possess a single positive charge, they immediately become more conducive to being electrostatically scattered by a positive space charge than uncharged or oppositely charged decay products. With negative air ion treatment, uncharged and positively charged decay products and host aerosol particles must first attain a negative charge by diffusion charging before the space charge electric field can promote their deposition onto chamber surfaces.

The overall enhanced working level reductions with positive, as opposed to negative, air ion treatment were primarily attributed to greater space charge removal of Pb-214 (RaB) as compared with Po-218 (RaA). Although the space charge removal rate constants for RaA and RaB calculated from measured data were approximately equal, the relatively large decay constant for RaA, i.e. short half-life (3.05 minutes), rivals the space charge removal rate. As a result, the latter's influence on the airborne RaA concentration is not as dominant as its effect on the RaB concentration. Consequently, steady-state decay product reductions from air ion treatment depend not only on the magnitude of the space charge removal constant, but also on the comparative magnitude of other mechanisms (sinks) present, e.g. radioactive decay, ventilation, plateout, etc.

Upon discontinuation of ion treatment, the radon decay product concentrations eventually returned to their no-treatment levels. For trials involving negative ion treatment, the time constant for this process was longer than expected from theory (25) or that observed with positive ion treatment. The application of an anti-static spray to the chamber surfaces hastened the return to no-treatment conditions. This phenomenon suggests that ion treatment imparts a residual charge to the chamber surfaces that transiently persists long after the air ion source has been removed. We surmise that the negative surface charge attracted positively charged, unattached decay products that entered the air boundary layer and facilitated their deposition onto the chamber surfaces. Electrical image forces are not believed to play a major role in this process. Conversely, a positive residual surface charge should, in theory, hasten the return of no-treatment conditions; however, we were unable to detect such an effect. Surface charge effects were not observed when the chamber relative humidity was greater than 70%.

Effect of Chamber Relative Humidity

A substantial number of chamber trials were conducted to study the effectiveness of unipolar space charging in reducing radon decay product exposures under a wide range of relative humidities. The experimental protocol was identical to that for the previously reported data. Figure 4 summarizes the percent working level reductions measured as a function of the chamber relative humidity (%) for
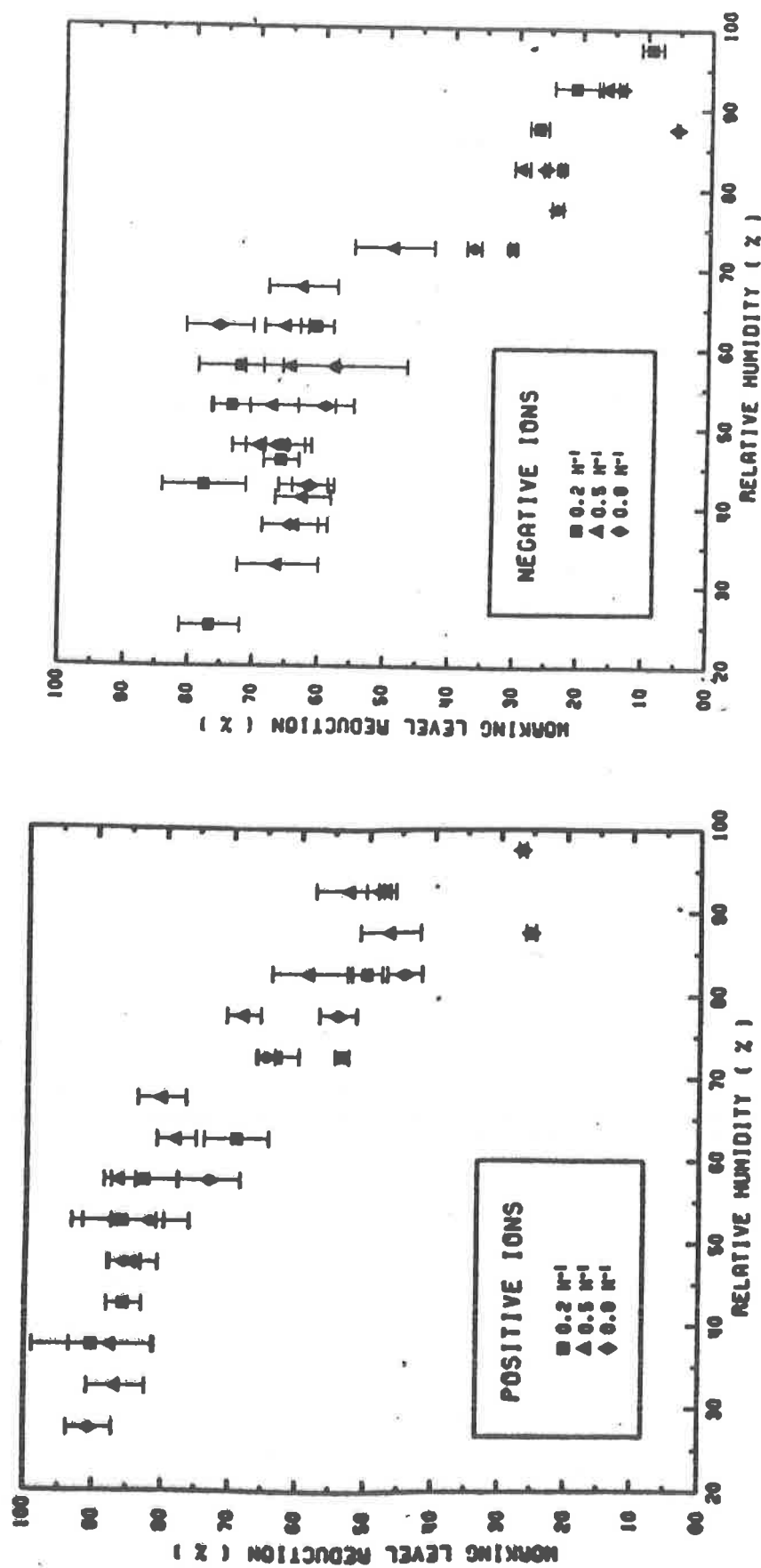
Figure 4: Radon Decay Product Removals Versus Relative Humidity

positive and negative air ion treatment. The statistical un-
certainties (standard errors) associated with these measurements
are also indicated. All reductions are referenced to the no-treat-
ment Working Level under the same relative humidity.

The effect of relative humidity on the Working Level reductions
was the same regardless of the air ion polarity and the air infiltra-
tion rate. In all instances, high relative humidities degraded the
effectiveness of air ion treatment, although the reductions were
still greater with positive air ions. There was no statistical
difference in Working Level reductions up to approximately 60-65%
relative humidity. At chamber relative humidities greater than 65%
the Working Level reductions became progressively less. These re-
sults are in contrast   to Bigu's (33), who found no effect of
increasing relative humidity on decay product reductions with nega-
tive air ion treatment. We are unable to explain our different
findings except to state that the experimental methods used by the
respective studies were too disimilar to permit a valid comparison
of the results.

The reasons for the lower air ion reductions of Working Levels
with increasing relative humidities are not well understood. One
explanation seems to be related to the observed increase in the
particle size distribution. At a chamber relative humidity of
90-95%, the diameter of the average surface area was found to in-
crease greater than a factor 3, from 0.065 to 0.210 μm (Figure 1).

The implications of this have at least two bearings on the air
ion removal rates: lower decay product and host aerosol electrical
mobilities, and a lower unattached fraction of decay products. In
the former case, particle electrical mobility is inversely propor-
tional to the square of the particle's diameter, thus the observed
increase in the DASA would roughly correspond to the 10-fold de-
crease in particle electrical mobility if no additional charges are
acquired. Offsetting this effect is the increased number of
elemental charges that a larger particle would acquire from diffusion
charging (approximately proportional to the increase in diameter.)
The net result is that particle mobility should, to a first approxi-
mation, be inversely related to the increase in particle diameter.
The increased DASA also results in a 10-fold increase in particle
surface area available for decay product attachment. This could
eliminate most if not all of the decay product species with the
highest electrical mobilities. We verified that this occurred in the
chamber measurements. The unattached Po-218 concentration decreased
from 25% to less than 0.5% when relative humidity was increased from
60 to 95%.

Other possible reasons for the decreased effectiveness of air
ion treatment under high humidities may also be related to lower air
ion mobilities due to the clustering of water vapor molecules about
the ions (34) or neutralization of charged decay products by water
molecules (32). These explanations are only speculative since we did
not conduct any experiments that would confirm the physical mechan-
isms that were primarily responsible for lower decay product removals.

Measured vs. Predicted Decay Product Reductions

A comparison of the room model predictions with measured radon decay product reductions from negative and positive air ion treatment is shown in Table II for the three air exchange rates tested. Predicted concentrations for air ion treatment and no-treatment were calculated through application of equations (7) and (9), assuming a spherical room with radius equal to 196 cm. This value for room radius was chosen because it had the same surface area to volume ratio as the rectangular chamber in which the measurements were conducted. Predicted decay product and Working Level reductions were calculated from these theoretical concentrations. The decay products and host aerosol were assumed to be uncharged initially and to have acquired their final charge in accordance with equation (3). The charging parameter, $N_i t$, in equation (3) was determined as follows: N_i, the mean air ion concentration obtained by volume integration of the equivalent 196 cm sphere having an ion density function given by equation (1). The mean ion density corresponded to a 123 cm distance from the ion source. The charging time, t, was taken to be approximately equal to the effective mean-life for the particular radon decay product. The effective mean-life was assumed equal to the reciprocal of the sum of the radiological decay and room ventilation constants, λ_n and I_v, respectively.

The airborne radionuclide reductions predicted using the equivalent room model and space charge effects were in overall good agreement with measured reductions for identical conditions, notable exceptions to this being the comparisons for Po-218 (RaA) removals which tended to be underestimated by the model. These disagreements are due to the fact that the model assumes that all of the RaA and RaB decay products are attached to particles having the DASA, when, in fact, up to 25% of the RaA and 5% of the RaB decay products in the chamber were unattached. For reasons discussed previously, unattached species, because of their much larger electrical mobility, should be more easily removed by the space charge electric field. The current model has no provisions for accounting for unattached decay products because White's diffusion charging equation is not applicable to the unattached size range, i.e. <0.01 μm.

From inspection of Table II it is obvious that the model predictions for negative space charge ions compare more favorably with measured data than do predictions for the positive ions. This is merely reflecting the fact that a significant number of decay products were already positively charged due to alpha-decay. The deficiencies encountered with this aspect of the model were expected and provide a basis for additional work. A more thorough consideration of the polydisperse nature of the room aerosol, including the unattached sizes, will probably be required in order to improve the model's predictive value, particularly when applied to positive ion treatment.

TABLE II: Measured versus Predicted Airborne Radionuclide

Reductions from Unipolar Space Charging

FRACTIONAL REDUCTIONS

Radio-nuclide	Air Exchange Rate (hr^{-1})	Positive Ions		Negative Ions	
		Measured (SE) in chamber*	Predicted by model**	Measured (SE) in chamber*	Predicted by model**
RaA	0.2	0.361 (0.027)	0.126	0.323 (0.024)	0.129
RaB	0.2	0.854 (0.016)	0.752	0.713 (0.015)	0.758
RaC	0.2	0.909 (0.015)	0.912	0.841 (0.013)	0.915
WL	0.2	0.814 (0.016)	0.733	0.712 (0.014)	0.738
RaA	0.5	0.437 (0.022)	0.121	0.332 (0.023)	0.124
RaB	0.5	0.890 (0.010)	0.715	0.678 (0.013)	0.721
RaC	0.5	0.938 (0.006)	0.889	0.796 (0.010)	0.892
WL	0.5	0.841 (0.010)	0.685	0.665 (0.011)	0.690
RaA	0.8	0.458 (0.034)	0.118	0.378 (0.032)	0.121
RaB	0.8	0.888 (0.016)	0.681	0.656 (0.017)	0.688
RaC	0.8	0.924 (0.015)	0.865	0.766 (0.018)	0.870
WL	0.8	0.831 (0.018)	0.641	0.646 (0.016)	0.645

* Standard Error for fractional reductions shown parenthetically.
** Assuming initially uncharged decay products and DASA of 0.065 μm.

Conclusions

Unipolar polar space charging via ion generation was found to cause substantial reductions in radon decay product concentrations inside a simulated residence. A positive space charge (positive ions) proved superior to a negative space charge (negative ions) for air treatment effectiveness. The primary reason appears to be related to the charge status of the decay products. The results of our investigations clearly demonstrate that unipolar space charging is a very effective air treatment method for reducing indoor exposures to naturally-occurring radionuclides. Our data further suggests that space charging may be useful for reducing concentrations of other indoor pollutants that are associated with ultrafine aerosol particles.

Extremely high relative humidites (>65%) tend to inhibit the effectiveness of unipolar space charging air treatment; the mechanisms by which this occurs are not clear, although the growth or size of the room aerosol seems to play a role. This aspect deserves further investigation.

Experimental data obtained within a simulated residence compare favorably with a simple theoretical model that predicts the removal of airborne radon decay products from space charge theory. The model requires some refinements for handling the pre-existing charge status of unattached decay products and ultrafine aerosol particles. Such refinements are necessary for modeling the observed differences in air treatment effectiveness between positive and negative space charges.

References

1. NCRP Report No. 77, "Exposures from the uranium series with emphasis on radon and its daughters", National Council on Radiation Protection and Measurements, Bethesda, MD (March 15, 1984).

2. NCRP Report No. 78, "Evaluation of occupational and environmental exposures to radon and radon daughter in the United States", National Council on Radiation Protection and Measurements, Bethesda, MD (May 31, 1984).

3. Harley, N., "Radon and lung cancer in mines and homes", N. Engl. J. Med. 310:1525 (1984).

4. Radford, E.P. and St. Clair Renard, K.G., "Lung cancer in swedish iron miners exposed to low doses of radon daughters", N. Engl. J. Med. 310:1485 (1984).

5. USRPC, "Report of the task force on radon in structures", U. S. Radiation Policy Council, Washington, D.C. (August 15, 1980).

6. NAS, "Effects on population of exposure to low levels of ionizing radiation", Committee on the Biological Effects of Ionizing Radiation, National Academy of Sciences, National Research Council, Washington D.C. (1980).

7. Budiansky, S., "Indoor air pollution", Envir. Sci. & Tech. 14:1023 (1980).

8. Gesell, T. and Prichard, H.M., "The contribution of radon in tap water to indoor radon concentrations", in National Radiation Environment III, CONF-780422, NTIS, Springfield, VA 22161 (1980).

9. Federal Register, Volume 44, No. 128 (Monday, July 2, 1979).

10. Guimond, R.J. Jr., Ellet, W.H., Fitzgerald, J.E., Windham, S.T. and Cuny, P.A., "Indoor radiation exposure due to radium-226 in Florida phosphate lands", USEPA Report 520/4-78-013, Washington, D.C. (February 1979).

11. Whitby, K.T. and McFarland, A.R., "Decay of unipolar small ions and homogeneous aerosols in closed spaces and flow systems", Proc. Intern. Conf. Air pp. VII-1-30, Franklin Institute (16-17 October 1961).

12. Whitby, K.T., Liu, B.Y.H., and Peterson, C.M., "Charging and decay of monodispersed aerosol in the presence of unipolar ion sources", J. Colloid Sci. 20:585 (1965).

13. Foster, W.W., "Desposition of unipolar charged aerosol particles by mutual repulsion", Brit. J. Appl. Phys. 10:206 (1959).

14. Dunskii, V.F. and Kitzev, A.V., "Precipitation of a unipolarly charged aerosol in an enclosed space", Colloid J. (U.S.S.R.) 22:167 (1960).

15. Kasper, G., "Electrostatic dispersion of homopolar aerosols", J. Colloid Interface Sci. 81:32 (1981).

16. White, H.J., "Particle charging in electrostatic precipitation", Trans. Am. Inst. Elec. Engrs. 70:1186 (1951).

17. Gentry, J.W. and Brock, J.R., "Unipolar diffusion charging of small aerosol particles", J. Chem. Phys. 47:64 (1967).

18. Gentry, J.W., "Charging of aerosol by unipolar diffusion of ions" J. Aerosol Sci. 3:65 (1972).

19. Marlow, W.H. and Brock, J.R., "Unipolar charging of small aerosol particles", J. Colloid Interface Sci. 50:32 (1975).

20. Raabe, O.G., "Concerning the interactions that occur between radon decay products and aerosols", Health Phys. 17:177 (1969).

21. Raabe, O.G., "The adsorption of radon daughters to some poly-disperse submicron polystyrene aerosols", Health Phys. 14:397 (1968).

22. Kruger, J. and Andrews, M., "Measurement of the attachment co-efficient of radon-220 decay products to monodispersed poly-styrene aerosols", J. Aerosol Sci. 7:21 (1976).

23. Ho, W.L. and Hopke, P.K., "The attachment of RaA (Po-218) to monodisperse aerosol", Atmos. Envir. (1982).

24. Jacobi, W., "Activity and potential alpha-energy of Rn-222 and Rn-220 daughters in different air atomospheres", Health Phys. 22:441 (1972).

25. Porstendorfer, J., Wicke, A. and Schraub, A., "The influence of exhalation, ventilation, and deposition processes upon the concentration of radon (Rn-222), thoron (Th-220) and their decay products in room air", Health Phys. 34:465 (1978).

26. Rudnick, S.N., Hinds, W.C., Maher, E.F., Price, J.M., Fujimoto,K, Gu, F. and First, M.W., "Effect of indoor air circulation systems on radon decay product concentrations", Final Report for USEPA Contract No. 68-01-6050, Harvard School of Public Health, Harvard University, Boston, MA 02115 (February 25, 1982).

27. Thomas, J.W., "Measurement of radon daughters in air", Health Phys. 23:783 (1972).

28. Lucas, H.F., "Improved low-level alpha-scintillation counter for radon", Rev. Sci. Instrum. 28:680 (1957).

29. Maher, E.F. and Laird, N.M., "EM algorithm reconstruction of particle size distributions from diffusion battery data", (Submitted to J. Aerosol Sci.), (Nov.,1984).

30. Air Care II, Model R-100, DEV Industries, 5721 Arapahoe Avenue, Boulder, CO 80303

31. Personal communication with Mr. Rex Coppom, President, DEV Industries (April 7, 1983).

32. Busigin, A., van der Vooren, A.E., Babcock, J.C. and Phillips, C.R., "The nature of unattached RaA (Po-218) particles", Health Phys., 40:333 (1981).

33. Bigu, J., "On the effect of a negative ion-generator and a mixing fan on the plate-out of radon decay products in a radon box", Health Phys. 44:259 (1983).

34. Raabe, O.G., "Measurement of the diffusion coefficient of radium A", Nature 217:1143 (1968).

35. Hinds, W.C., Rudnick, S.N., Maher, E.F. and First, M.W., "Control of indoor radon decay products by air treatment devices", J.A.P.C.A. 33:135 (1982).

DISCUSSION

JEFFORD: When the air change rate went from 0.2 to 0.5 air changes per hour, the radon decay product removal rate decreased. Do you have an explanation why the increased air turbulance did not result in increased radon decay product removal?

MOELLER: The decrease is believed due to two factors. The first is the increased steady state aerosol number concentration in the room, which is inherent with higher air exchange rates. The second factor is that higher air exchange rates also tend to enhance natural convection within the room and thus the incremental increase in air turbulence caused by the fan has a lesser effect. The enchanced natural convection also increases the natural wall deposition of un-attached decay products. Both of these factors act to decrease the fraction of unattached decay products in the room. Since the fan is most effective in removing the unattached fraction, a lower unattached fraction in the room will reduce the available radioactive material that the fan can remove, thus reducing the effectiveness of the fan as an air cleaner.

PROTOTYPE FIRING RANGE AIR CLEANING SYSTEM

J. A. Glissmeyer, J. Mishima, and J. A. Bamberger
Pacific Northwest Laboratory
Richland, Washington

Abstract

The Ballistics Research Laboratory, a component of the U.S. Army Research and Development Command, contracted with Pacific Northwest Laboratory (PNL) to provide a prototype air cleaning system for a new large caliber firing range where depleted uranium munitions are test-fired. The existing system consists of two banks of prefilters and a bank of HEPA filters in series at a rated airflow of 24,000 acfm. Experience at similar ranges indicated that the existing filtration system would be too costly to operate because shock waves and rapid particle loading result in short filter life necessitating frequent replacement and disposal as low-level radioactive waste. The rapid particle loading also results in decreased airflow causing an excessive waiting period before personnel can reenter the target area. The project's objectives were to provide a prototype air cleaning system that would substantially reduce operating expense, shorten the delay for personnel reentry and enhance the particle removal performance.

PNL's study proceeded by examining the characteristics of the aerosol challenge to the filtration system and the operating experience at similar firing ranges. Candidate filtration systems were proposed; including baghouses, cartridge houses, electrostatic precipitators, cleanable high efficiency filters, rolling filters and cyclones-- each followed by one or more of the existing filter banks. Methodology was developed to estimate the operating costs of the candidate systems. Costs addressed included the frequency (based on fractional efficiency and loading data) and cost of media replacement, capital investment, maintenance, waste disposal and electrical power consumption. The recommended system will be installed during calendar year 1984.

Introduction

The U. S. Army Materiel Test Directorate (MTD) and the Ballistics Research Laboratory (BRL) both operate two firing ranges (Ranges A, B, and C, D respectively) for the testing of large caliber depleted uranium (DU) penetrators. The targets are housed in enclosures which contain the DU aerosols and fragments produced by the test firings. One of the drawbacks of using a target enclosure is that the airborne DU must be removed by ventilation and air cleaning before personnel can enter the enclosure without respiratory protection.

BRL recently completed construction of Range D, shown in Figure 1. The Army's experience with air cleaning systems at such ranges has shown that the operation of the systems is very costly because of the short life of the filters. Our objective was to recommend an air cleaning system that would meet the requirements for effluent discharge and have substantially lower operating costs.
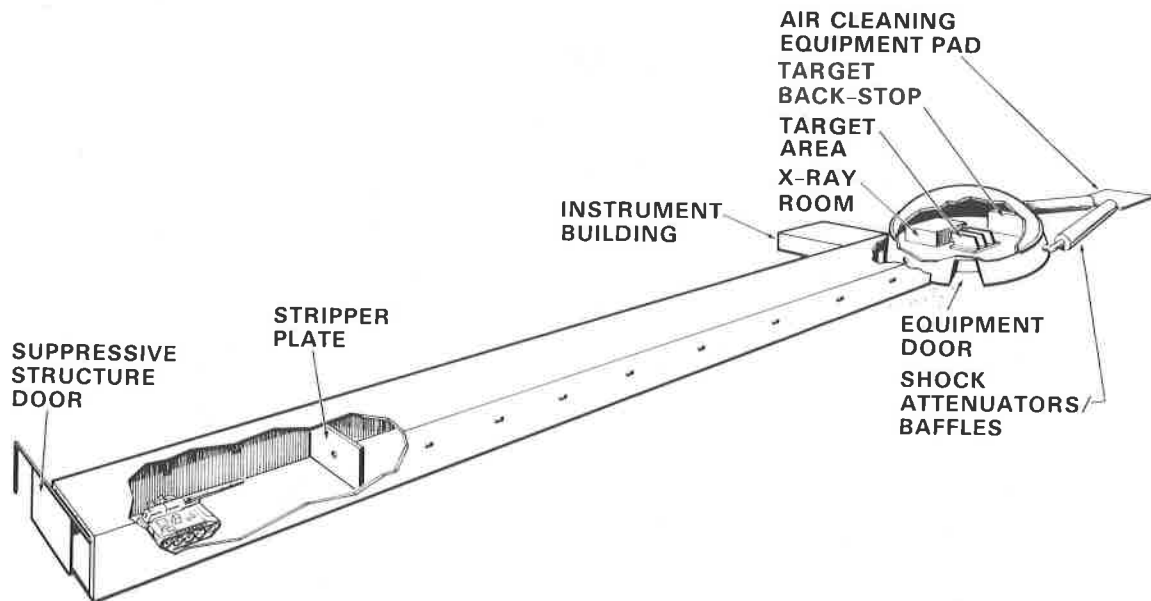
Figure 1. Range D

This paper describes the air cleaning challenge with a brief review of the performance of the air cleaning systems at the earlier ranges and the characteristics of the airborne DU aerosol. The candidates for the prototype air cleaning system are then outlined and the economic evaluation of them is detailed. Finally, the recommended systems and configurations are discussed.

Challenge To The Air Cleaning System

Prior to selecting candidate air cleaning systems to replace or augment the existing system, we investigated the performance of the existing cleaning systems at the ranges described below. In particular, we focused on the filter life, pressure pulses and measurements of aerosol characteristics.

System Descriptions

The existing Range D filtration unit, sized for an airflow of 24,000 cubic feet per minute (cfm), consists of three banks of disposable filters in series. There are twenty-four filters in each bank -- three filters high by eight filters wide. The filters are enclosed in a housing as shown in Figure 2. The double width-double inlet fan, with 60 hp motor, is rated at 24,000 cfm at 11 in. H_2O and is also enclosed in the housing. Electrically driven opposed-blade dampers are located at the inlet and outlet of the housing to provide some measure of isolation when the system is shutdown. The dampers drive to their full-open position when the fan is started. The housing has a 12 gauge wall thickness and the roof has a 20 gauge outside liner.

The first filter bank consists of prefilters which have pleated cotton media with an ASHRAE 52-76[1] dust spot rating of 25%. The dimensions of a single filter are 24 in. x 24 in. x 2 in. The second

847
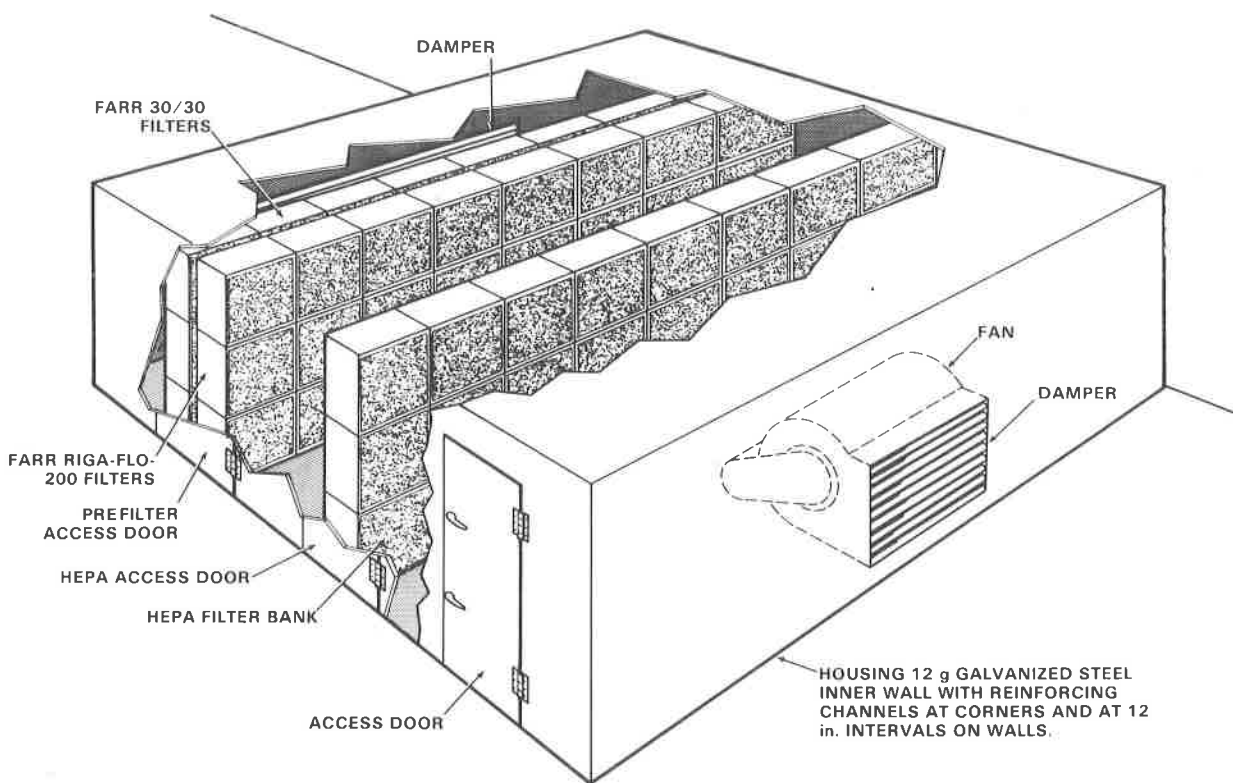
Figure 2. Existing Range D Filter House

filter bank contains filters which have pleated glass-fiber media
reinforced with hardware cloth and cardboard separators. The filter
rating is 95% ASHRAE. The frame enclosing the media is galvanized
steel with dimensions of 24 in. x 24 in. x 12 in. The first two
banks of filters are mounted in commercial side-loading housings.
The third bank consists of HEPA filters with galvanized steel frames
and aluminum separators. The HEPA filter mounting frame permits
individual installation and clamping of the filters with filter gas-
kets on the downstream side of the filters to maintain the seal dur-
ing a pressure pulse. The filter housing was not designed according
to the typical standards for nuclear facilities.

Ranges A, B, and C are functionally the same as Range D, shown
in Figure 1, with a projectile entrance tunnel, target bay and air
cleaning system; however, there are many differences in design and
they are smaller overall. The target bays are box shaped and enclose
15,000 to 28,000 cu. ft as opposed to 54,000 cu. ft at Range D. The
ventilation rates range from 6,000 to 18,000 cfm and the projectile
entry tunnels are cylinders 6-7 ft in diameter and 30 to 150 ft
long. The filter houses contain three banks of filters in series.
The last two filter banks are of the same type as Range D (95% ASHRAE
and HEPA's). At Range C the first prefilter is the same type as
Range D (25% ASHRAE); however, 40-60% ASHRAE prefilters are used at
Ranges A and B. At Ranges A and B, the filter house is located
behind the target bay and connected to it by box shaped baffled shock
attenuators. At Range C, the filter house is located on the roof of
the target bay and connected to it with a duct containing fragment
baffles but no shock attenuator. Ranges A and C use industrial grade

side-loading filter housings of about 16 gauge sheet metal. The
housing at Range B is shop-built to nuclear facility standards using
0.5 in. steel, marine bulkhead access doors, bagout ports, and face
loading filters.

Filter Life

Operating data from Ranges A and C were compiled and the filter
life expectancies are shown in Table 1. Different filter change
philosophies existed at the two ranges. At Range A, the two pre-
filter banks and the HEPA bank were changed at pressure drops of
approximately 1, 4 and 4 in. H_2O respectively. At Range C the second
prefilter and the HEPA were changed at about 4 and 3 in. H_2O. The
first prefilter bank did not have a pressure gauge and was changed
when bank 2 was being changed.

Table 1. Filter Life

Range	Shots Per Year	Number of Filters Per Filter Bank	Range of Filter Life, Rounds/Change		
			1st-,	2nd-Prefilters	HEPAs
A	230	12	1-2	10-20	100-200
B	230	18	No data available, life estimated to be similar to Range A		
C	180	6	1-6	1-6	5-60
D	180	24	No data available, life estimated to be similar to Range C		

Filter damage at Ranges A and B has been mostly limited to con-
densation and subsequent moisture damage to the filter media. At
Range A, inadequate sheet metal seals in the filter housing permitted
water entry. On one occasion, excessive plugging of the media caused
the 1st prefilters to impact the 2nd prefilters and break their
seals. At Range B, condensation was caused by temperature gradients
in the system.

Temperature measurements at Range C showed that a heat front
passes through the exhaust system approximately 1 second after the
pressure shock. The heat front has caused ignition of the prefilter
banks for some target/penetrator combinations, destroying the media
and leaving only the wire support mesh and the cardboard frames. In
one instance, sparks from the prefilters ignited the HEPA filters and
melted the media. Since this incident, temperature sensors were
installed in the exhaust duct and temperatures greater than 212°F
have been recorded. It is unknown whether hot target or penetrator
fragments had a role to play in these incidents. The absence of a
shock attenuator at this range may be the reason that such incidents
have only occurred at this range.

Pressure Pulses

Measurements of pressure pulses generated by static charges and the target/penetrator interactions were made at the ranges prior to the start of routine testing to verify the structural integrity of the target bay and the air cleaning system. During these tests at Ranges A and B no damage to the filters was observed by either visual inspection or standard aerosol penetration tests. At Range C, damage was caused by the temperature effects discussed above.

Range A

Blast overpressure measurements in the target bay and air cleaning system for five test firings are listed in Table 2. The pressures measured at the face of the prefilter banks are listed under Locations 9 and 10. Location 11 was downstream of the HEPA filters. In the filter house, the pressures pulses were of considerably lower magnitude and longer duration than in the target bay.

Range B

An extensive set of static and dynamic tests were performed at Range B. Table 3 gives the results of twelve static charge tests. The highest pressures observed at the two prefilter banks and the HEPA bank were 1.2, 0.6 and 0.7 psig respectively. Pulse durations were not available.

Table 4 presents the dynamic overpressure data for seventeen test shots with two penetrator and three target configurations. The filter bank pressures were significantly lower than in the target enclosure due to the action of the shock attenuator. In these tests the maximum pressures at the two prefilter banks and the HEPA bank were 0.89, 0.61 and 0.59 psig respectively. Maximum reflected pressures would be double these values.

Range C

Table 5 lists representative values of the pressure pulse and duration for the Range C static and dynamic tests. Peak overpressures of 4 psig were measured in the target enclosure. In front of the prefilters the average pressure dropped to 0.6 psig.

Range D

Range D has only been tested with static charges to date. The measured face-on pressures at the first prefilter have ranged from 1.05 to 2.35 psig. No damage was observed to the filters but the wall joints of the housing were severely damaged. No follow-up standard aerosol penetration testing has been performed yet.

Aerosol Characteristics

Quantity and Composition of the Airborne Material

The impact of the DU penetrator upon the target results in aerosolization of a portion of both the penetrator and target. The

Table 2. Range A Pressure Measurements in Exhaust Duct System Using a 3.4 kg DU Round

Pressure Transducer Location
Over Pressure-psi (Duration - ms)

Round Designation	1	2	5	6	8	9	10	11
14	1.0 (5)	0.9 (4)	0.6 (1)	—	0.3 (499)	0.3 (456)	0.2 (479)	0.2 (474)
15	1.8 (4)	2.2 (4)	8.1 (2)	—	0.6 (535)	0.5 (464)	0.4 (477)	0.3 (407)
16	1.9 (4)	2.2 (4)	1.4 (9)	0.6 (11)	0.4 (521)	0.4 (467)	0.3 (479)	0.2 (520)
17	1.8 (2)	2.4 (5)	5.1 (9)	0.5 (35)	0.4 (518)	0.5 (470)	0.4 (480)	—
18	8.9 (3)	—	4.0 (5)	2.2 (10)	—	—	—	—

Pressure Transducer Location

1 Right wall, 4.5 ft from floor, 15.5 ft from rear wall, target enclosure
2 Right wall, 4.5 ft from floor, 17.5 ft from rear wall, target enclosure
5 Left wall, 5 ft from floor, 18 ft from rear wall, target enclosure
6 On air intake louvres, target side, 5 ft from floor
8 Behind baffles in exhaust plenum
9 1st filter, upstream side
10 2nd filter, upstream side
11 Fan compartment

Table 3. Range B Static Tests: Blast Overpressure Data

Type of Explosion	Pentolite Above Plate			C4 Explosive on Plate (New Baffle Installed in Plenum)								
Charge weight, lb	0.50	0.75	1.00	1.00	1.50	1.75	2.00	2.25(a)	2.50(a)	2.50(a)	2.50(a)	2.50(a)
Enclosure Side-wall, PR, psi	12.7	14.4	16.1	17.1	23.9	24.4	41.2	47	48	17	19	28
Enclosure Over-head, PR, psi	5.0	5.5	6.3	6.6	8.5	9.4	11.0	13	15	7.2	8.1	11
Shock Attenuator, PS, psi	–	1.0	1.4	1.2	1.0	0.9	1.5	2.2	2.2	1.3	1.5	1.9
Filters, PS, psi												
First prefilter	–	0.5	0.7	0.4	0.6	0.7	0.7	0.6	1.2	0.4	0.4	0.6
Second prefilter	0.4	0.5	0.6	–	–	–	–	0.3	0.5	0.3	0.3	0.4
HEPA	0.4	0.5	0.7	–	–	–	–	0.5	0.6	0.3	0.3	0.4
Fan, PS, psi	0.4	0.6	0.7	0.4	0.5	0.7	0.7	0.5	0.7	0.3	0.3	0.4

PR: Face-on, normally reflected pressure. For the plenum, filter and fan data PR is double the PS value

PS: Side-on pressure

(a) Exhaust fan running

Table 4.   Range B Dynamic Tests: Peak Overpressure Data

	Target 1, Penetrator A			Target 2, Penetrator A			Target 1, Penetrator B		
Round Number	1	2	3	4	5	6	7	8	9
Sidewall, PR, psi	5.3	5.2	--	7.4	17	23	4.7	4.9	--
Overhead, PR, psi	2.7	2.9	4.2	4.8	6.8	5.5	4.4	--	11
Plenum, PS, psi	0.41	0.56	0.64	0.91	0.84	0.86	0.83	0.68	0.66
Filters, PS, psi									
First	0.16	0.24	--	0.39	0.32	0.37	--	0.36	0.32
Second	0.11	0.20	0.20	0.32	0.24	--	0.18	0.30	0.26
HEPA	0.22	0.25	0.30	0.42	0.46	0.48	0.27	0.31	0.19
Fans, PS, psi	0.10	0.19	0.17	0.24	0.20	0.35	0.17	0.26	0.24

	Target 2, Penetrator B		Target 3, Penetrator B			Target 2, Penetrator B		
Round Number	10	11	13	14	15	16	17	18
Sidewall, PR, psi	--	21	4.0	3.1	4.7	11	--	5.5
Overhead, PR, psi	3.7	--	2.8	2.6	2.7	6.2	5.0	6.3
Plenum, PS, psi	1.3	1.2	0.21	0.22	0.28	1.1	1.3	1.1
Filters, PS, psi								
First	0.52	0.65	0.14	0.15	0.17	0.59	0.89	0.76
Second	0.42	0.54	0.10	0.12	0.13	0.50	0.61	0.53
HEPA	0.25	0.59	0.10	0.12	0.12	0.50	0.53	0.54
Fan, PS, psi	0.17	0.46	0.09	0.10	0.10	0.40	0.41	0.41

PR: Face-on, normally reflected pressure
      For the plenum, filter and fan data PR is double the PS value.
PS: Side-on pressure

Table 5.   Summary of Range C: Blast Overpressure Data

| Test | Center of Roof 21.7 ft Above Target | | Inside Ventilation Duct Between Baffles and Prefilters | | |
| | | | Pressure | | |
	Pressure (psi)	Duration (ms)	Average (psi)	Peak (psi)	Duration (ms)
0.34 kg Pentolite (static)	4.1	2.5	0.17	0.87	1300
2.1 kg Tungsten	1.7	3.0	0.07	0.29	1000
2.0 kg DU	4.1	3.0	0.29	0.58	2200
3.4 kg DU	4.4 (a)	--	0.59	0.87	3000

(a) Maximum pressure recorded for a 3.4 kg round.

fraction of the penetrator made airborne has been measured and ranged from 0.9% to greater than 70% [2,3,4]. The broad range is due to a variety of factors such as penetrator velocity and size, type of target, method of measurement, etc. For the purposes of this study, 100% of the materials generated during test firings were considered to challenge the air cleaning system.

Unfiltered ambient air is drawn into the enclosure during test firings. The median background level for real-time, mass-airborne monitors currently in use onsite is approximately 30 micrograms per cubic meter. Assuming 8 hours per day of operation, as much as 10 g of fugitive dust could be drawn into the facility and challenge the air cleaning system. This does not include water or water vapor concentrations which vary greatly. The chemical composition of the fugitive dust is not known.

Small quantities of soot, unburned propellant grains and vapors (water, nitric acid, potassium hydroxide, sulfuric acid)[5] from the burning of the propellant are found. The vapors could condense upon cold surfaces or be absorbed in water vapors or particles, thereby producing some potential for corrosion. The quantities generated per firing are estimated to be negligible.

Based upon analysis of the airborne particulate material from outdoor test firings, it was estimated that the composition of the airborne material will be 80% to 95% oxides of uranium (75% of which is U_3O_8), 4% to 19% iron oxide with minor amounts of aluminum oxide, titanium oxide, and silicon dioxide plus trace quantities of the products from the combustion of the propellant. If the target material is non-ferrous, most of the iron oxide would be replaced by the new target material. It was further assumed that the total mass of airborne material is equivalent to the mass of the penetrator.

Size Distribution of Airborne Particles

Particle size distributions of the airborne material under pre-
cisely the Range D operating conditions have not been found. Size
distributions of depleted uranium oxide particles under similar
conditions have been reported [2,3,4]. The distribution with the
largest fractions of small particles, Table 6, presents the most
difficult challenge to the air cleaning system and was assumed for
the purposes of this study.

Table 6. Approximate Aerodynamic Equivalent Particle Size
Distribution

Particle Aerodynamic Equivalent Diameter, Micrometers	Mass Percent in Size Range
<0.18	31
0.18 – 0.56	14
0.56 – 1.8	15
1.8 – 5.6	13
5.6 – 18.0	11
18 – 56	7
>56	9

Airborne Mass Concentrations as a Function of Time

Measurements of the aerosol concentrations made 7.5 seconds
after the shot during the unenclosed test firings ranged from 1.5
to 2.6 g/cubic meter[3]. Measurements of the aerosol concentration
made 5 minutes after the shot during the enclosed test firings
ranged from 0.05 to 0.15 g/cubic meter.[4,6] The critical airborne
concentration for this study is that which will challenge the air
cleaning system. If the entire penetrator mass were airborne in
the target enclosure, the airborne mass concentration would be
4.2 g DU/cubic meter. For this study a maximum airborne concen-
tration of 0.5 g DU/cubic meter with the particle size distribution
shown in Table 6 was assumed. This aerosol has a half life of 4.1
minutes in the target enclosure.

Candidate Systems

The basic assumptions for selecting equipment were: 1) particle
collection should not produce a liquid effluent requiring treatment,
and 2) the final control device should be a bank of HEPA filters to
act as a polishing and safety stage. The fifteen candidate systems
are listed in Table 7.

Baghouses, precipitators, common rolling filters and cyclones
are familiar devices in the air cleaning field. The lesser known
devices will be briefly described in the following subsections;
however, because the pulse-jet baghouse will be shown to be one of
the recommended devices, a typical cutaway is shown in Figure 3.

Table 7. Candidate Air Cleaning Systems

1 Existing Disposable Filters

2 Existing Disposable Filters With Extended Surface Filter In Place of Bank 2

3 Rolling Prefilter + Disposable Filters

4 Peeled Roll Filter + Disposable Filters

5,6 Pulse-jet Baghouse + Disposable Filters
     standard felt media
     coated media

7,8 Shaker Baghouse + Disposable Filters
     standard fabric media
     coated felt media

9 Electrostatically Augmented Baghouse + Disposable Filters

10,11 Cartridge House + Disposable Filters
       standard media
       coated media

12 Cyclones + Disposable Filters

13 Electrostatic Precipitator + Disposable Filters

14 Cleanable High Efficiency Filter + Disposable Filters

15 Vaned Inertial Separator + Pulsed Panel Filter + Disposable Filters

Extended Surface Filter

The extended surface filter is a prefilter that fits into the same holding frame as the current second prefilter. The medium is a thick glass-fiber pad shaped into pockets or envelopes that are about 30 in. deep. The efficiency is about the same as the current second prefilter but has greater particle holding capacity.

Peeled Roll Filter

The peeled roll filter is similar to the common rolling filter; both use clean and used media reels. However, the airflow passes radially inward through the layers of media wound on the clean media reel and then out through the end of the reel's core instead of through the media stretched between the reels. Because the air passes through many layers of media the filtration efficiency is greater than for the common rolling filter although the media is essentially the same. When the outer layer becomes loaded with particles the layer is wound onto the other reel. Several media units are contained in a single housing. This filter was originally designed for viscous liquid aerosols.
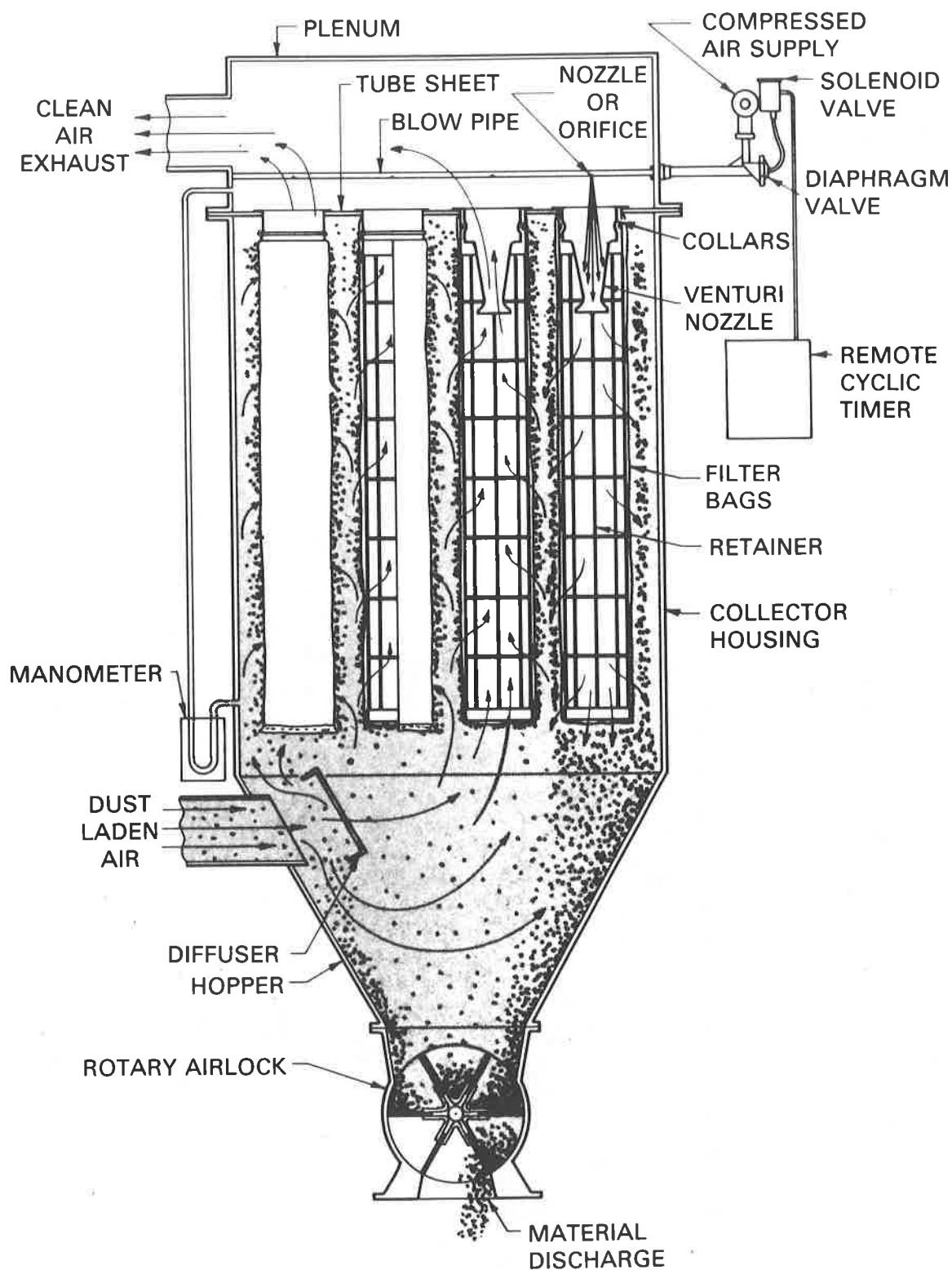
Figure 3.   Cutaway of Pulse-Jet Baghouse (after Mikropul[7])

Cartridge House

A cartridge house collects particles on a filter medium made of a treated cellulose paper which is pleated and formed into a cylindrical cartridge, very similar in appearance to a truck carburetor air-cleaner. The cartridge is about 12 in. diameter by 24 in. high. Figure 4 shows a typical cartridge house with several cartridges mounted below a tube-sheet in a configuration similar to a pulse-jet baghouse. Dirty air enters near the bottom of the hopper and passes upward through the cartridges to be exhausted at the top of the housing. Particles collected on the cartridges are removed by pulses of clean air directed through the cartridge in a direction opposite to the normal airflow. The removed particles that have agglomerated to a sufficiently large size settle into the hopper by gravity. Venturies between the compressed air nozzles and the cartridges amplify the cleaning airflow.
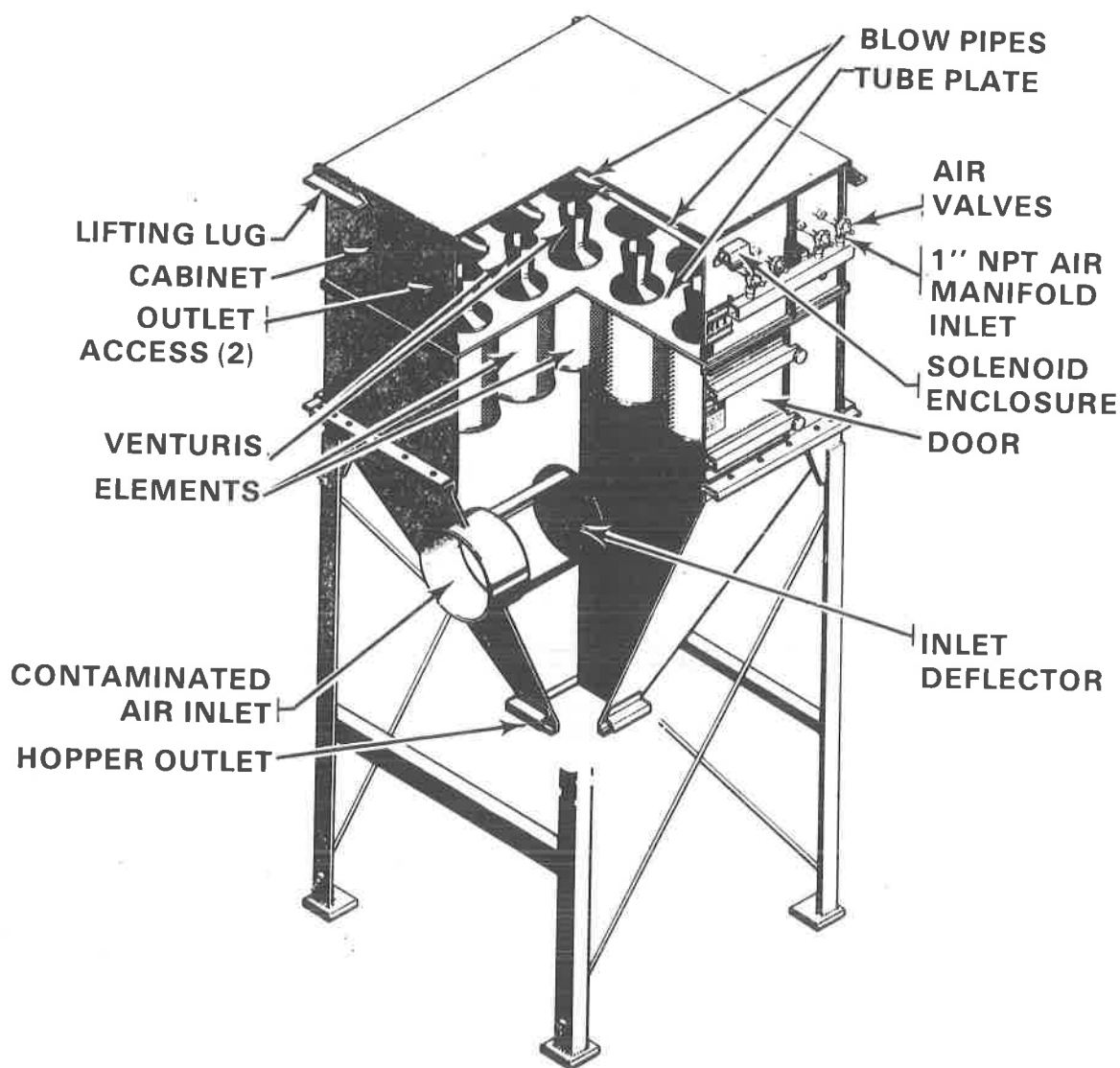
Figure 4. Typical Cartridge House (after Donaldson[8])

A preferable configuration has a walk-in plenum on top of the tube sheet. For filter maintenance a person enters the plenum, which is on the clean side of the cartridges, and the cartridges are removed through the tube sheet. Figure 5 shows another advantageous design where cartridges are mounted on a slight angle to the horizontal plane. The clean air side, tube sheet and pulse cleaning pipes are at the back of the cabinet. Pairs of cartridges are accessed through hatches on the front of the cabinet. This design has several more seals that must be checked for airtightness; however, with a modified hatch design, it lends itself to a type of bagout method for cartridge changes similar to that used in gloveboxes. The dirty airflow is from the top to the back of the cabinet which would enhance the movement of particles to the hopper during pulse cleaning. The cartridges are also compartmentalized in groups of twelve to reduce the tendency to blow particles to adjacent cartridges during cleaning.

Cleanable High Efficiency Filter

The cleanable high efficiency filter, Figure 6, contains one or two banks of high efficiency filters that look very similar to the HEPA filter used in the existing system. The filters differ from
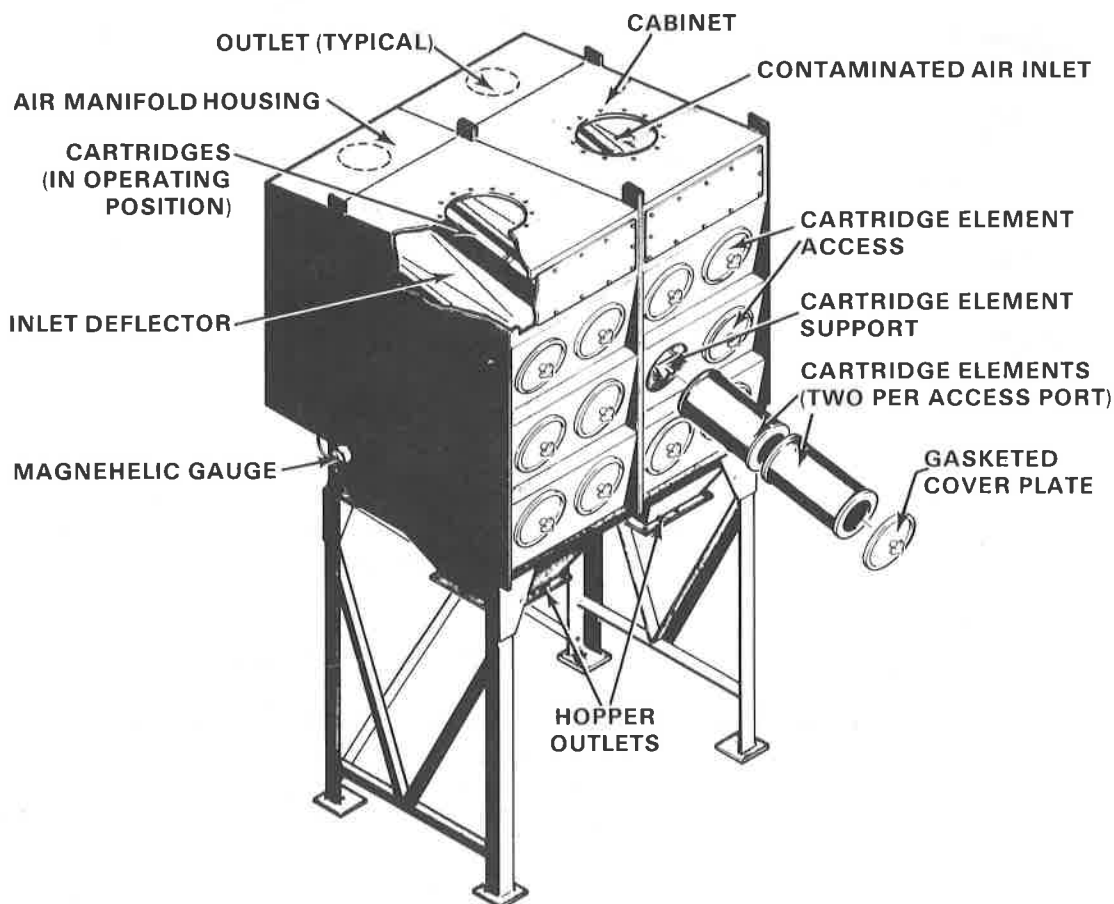
Figure 5. Downflow Cartridge House (after Donaldson[8])
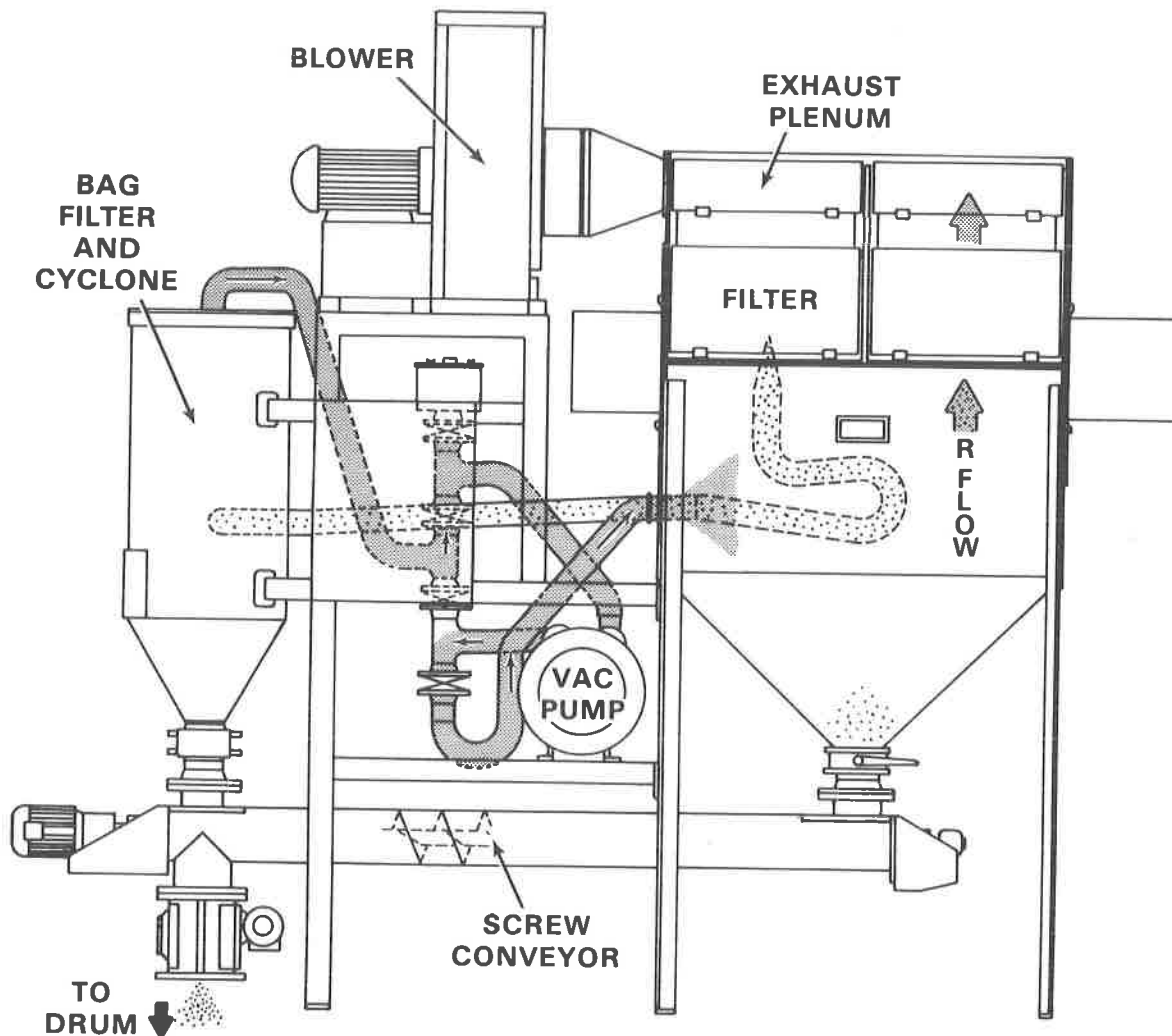
Figure 6. Single Stage Cleanable High Efficiency Filter
(after Kermatrol[9])

HEPA's by a thin coating on the particle collection side so particles do not penetrate into the fibers of the media. The medium acts as a support for the porous coating which does the filtering. The filters are cleaned in-place by either a vacuum system or pulses of compressed air.

Another type of cleanable filter uses 80% ASHRAE dust spot efficiency cleanable filter panels housed in a steel box with hoppers beneath. The filter medium appears similar to that of the the medium efficiency prefilter in Bank 2 of the existing system except the medium is not pleated as deeply, and the individual filter dimensions are 2 ft x 4 ft x 3 in. For the design airflow the device would contain 24 panel filters. The filters are cleaned periodically with pulses of compressed air directed opposite to the airflow. This device will be referred to as the Pulsed Panel filter.

Vaned Inertial Separator

The vaned inertial separator is rated at 80% ASHRAE dust spot efficiency. Ninety percent of the airflow is sharply turned through vanes while 10% of the airflow proceeds in a straight line. Large particles cannot follow the rapid change in direction and follow the 10% airflow in a straight line. The 10% airflow, now more heavily laden with particles, is passed through another dust collector (the manufacturer recommended the Pulsed Panel) which removes 80-90% of the particles. The airflows from the vaned inertial separator and the Pulsed Panel are recombined and passed through a second Pulsed Panel.

Economic Analysis Method

Because this air cleaning application is unusual and applicable data describing the performance of the filtration devices was lacking, costs attributed to the different system configurations were estimates based on several factors with considerable uncertainty. Factors considered in this study were the particle collection efficiency of the devices, individually or in series, and the frequency of mechanical repairs. The former proved to be the most significant because several important items hinge on the question of efficiency, including the life of media, frequency of media replacement, media disposal and the disposal of collected dust. We used the best efficiency data available to us from the literature or vendors; however, in most cases, extrapolations beyond the data were required. Estimates of maintenance and repairs were obtained largely from vendors. Estimating methods were applied uniformly to identify the relative ranking of the candidate systems even though the estimates were inexact. In most cases the candidate systems include all or a part of the existing filter banks as polishing filters. To explore which filter banks should be retained, cost estimates were generated for each practical combination of the existing filters with the candidate devices.

A complete estimate of procurement, operating and maintenance costs of each system was attempted. The cost elements addressed were

- Media Life   -- how long the media lasts
- Media Replacement   -- replacement and disposal of media
- Waste Disposal   -- collected powder
- First Costs   -- initial investment
- Maintenance   -- operation, maintenance, repairs
- Electrical Power   -- power for fan and auxiliaries

The general method of estimating these elements will be explained in the following subsections. Labor costs are assessed under the topics to which the labor is applied. The several assumptions, derived from current operating practice, that provided a starting point for cost estimating are enumerated in Table 8. Others will be introduced as they pertain to specific method elements.

Table 8. Assumptions Used for Cost Estimating

1. Labor rate for BRL personnel: $31/man-hour

2. Power cost: $0.04/kWhr

3. Waste disposal cost including container, shipping fees, labor, burial fees: $25/cu.ft

4. System equipment life: 20 years

5. Test firings during 20 yr life: 6000

6. Average weight of test round: 4.9 kg

7. Average aerosol mass per test: 4.9 kg

8. Bulk density of the collected dust: 1.5 g/cu.cm

9. Annual operating time for system 365 day x (5/7) x 8 hr/day =   2006 hr

10. HEPA filters will be retained as last device in system for a polishing and safety stage

Media life

The media life expectancy is a concern for all of the devices except for cyclones or ESP's. Mechanical media failure which results in particle leakage is the principal factor determining the life of cleanable media. The filtration efficiency of cleanable media affects only the subsequent disposable filters, because it determines the challenge aerosol. For disposable filters, the filtering efficiency and the particle holding capacity are equally important to media life. Therefore the question of media life was approached differently for the two media types.

Disposable Filters

The approach developed was applied to all the types of disposable media investigated: the rolling filters, the existing filters, and extended surface filters. To estimate media life, the filtration efficiency as a function of aerodynamic particle size and the dust holding capacity at the final operating pressure drop must be known; however, data covering the entire range of interest were generally not available and extrapolations were required.

The particle size range of interest was subdivided into seven size brackets equally spaced logarithmically and the mass of particles in each bracket was estimated as was shown in Table 6. All of the particles in a given bracket were assumed to behave as the particle whose size was the bracket midpoint. The collection efficiency of each device was obtained for each size bracket midpoint. The amount of particles collected by and penetrating a device was computed separately for each size bracket. The total amounts collected

and penetrated were computed by summing the bracket values. The size distribution of the penetrating particles was used as the input aerosol of the next stage of filtration. This approach was used to estimate the useful life of a bank of disposable filters in a series of banks.

Table 9 is an example performance calculation for the three existing filter banks in series. The initial mass distribution, fractional efficiency, mass collected and penetrated for each stage and size bracket are shown. Also shown are the overall and cumulative efficiencies for each stage.

Table 9 also illustrates how the cost of filter usage was calculated. The table shows the vendor's estimate for the maximum amount of dust that may be collected on a bank of 24 filters at the pressure drop which requires filter replacement. The mass collected by a filter stage was divided by the dust capacity to estimate the fraction of filter life, or life fraction (LF), used in the test. The inverse of the life fraction, 1/LF, is the number of tests the filter can be exposed to before replacement and is shown in the table as "Shot Life". While this method may be simple and have some theoretical shortcomings, the results shown in the table for "Shot Life" were within the range experienced at BRL and MTD, giving us some confidence in applying the method.

Table 10 shows how we calculated the estimated costs for replacing the banks of existing disposable filters as $267, $1949 and $4291 for stages 1,2 and 3 respectively. The calculations accounted for filter cost, labor cost and disposal cost as low level radioactive waste. The compacted volume fractions used (0.067, 0.088 and 0.25 for banks 1,2 and 3 respectively) were those achieved at BRL. The life fraction times the bank replacement cost was the estimated cost incurred for the test, which was multiplied by the number of tests expected in twenty years to estimate the cost during the facility life. Table 9 shows the results of these calculations for the existing filter system. Similar calculations were made for each candidate system configuration. Table 10 is illustrative of the factors accounted for in computing the replacement costs of filters in the other types of devices.

Cleanable Filters

Estimates of media life for the cleanable media devices were obtained from the equipment manufacturers' experience. The controlling factor for these devices is mechanical wear resulting in filter media failure. Most often these devices are used in harsh industrial ventilation environments where aerosol concentrations are higher and more continuous than expected for the firing range. Most vendors felt that the aerosol loading at the firing range is light compared to their typical applications. The life estimates for each type of device using cleanable media are given in Table 11.

To estimate the characteristics of the aerosol penetrating to the filters downstream and the quantities of dust to be transferred to disposal containers, a calculation method similar to that described above for the disposable filters was applied to most cleanable media devices. For pulse-jet baghouses an alternate method,

Table 9.   Example Efficiency and Cost Calculation
            for Existing Filters

Size Midpoint Dia. Microns	Distribution		Bank One -- 25% ASHRAE Filters		
	Mass %	Initial Grams	Fractional Efficiency	Grams Collected	Grams Penetrated
0.1	31	1519	0.00001	1.519E-02	1.519E+03
0.32	14	686	0.00001	6.860E-03	6.860E+02
1	15	735	0.007	5.145E+00	7.299E+02
3.2	13	637	0.82	5.223E+02	1.147E+02
10	11	539	0.983	5.298E+02	9.163E+00
32	7	343	0.995	3.413E+02	1.715E+00
100	9	441	0.9972	4.398E+02	1.235E+00
Total		4900		1.838E+03	3.062E+03
Cum. Total				1.838E+03	

Stage Efficiency		3.752E-01
Cumulative Efficiency		3.752E-01
Max Load, g		6720
Shot life, shots		3.66
Bank Replacement Cost		$267
20 yr Cost By Bank		$438,260
System 20 yr Cost		
Bank Changes in 20 yr		1641

Size Midpoint Dia. Microns	Bank Two -- 95% ASHRAE Filters			Bank Three -- HEPA Filters		
	Fractional Efficiency	Grams Collected	Grams Penetrated	Fractional Efficiency	Grams Collected	Grams Penetrated
0.1	0.83	1.261E+03	2.582E+02	0.998	2.577E+02	5.165E-01
0.32	0.94	6.448E+02	4.116E+01	0.99968	4.115E+01	1.317E-02
1	0.987	7.204E+02	9.488E+00	0.9999	9.487E+00	9.488E-04
3.2	0.998	1.144E+02	2.293E-01	0.99999	2.293E-01	2.293E-06
10	0.9994	9.158E+00	5.498E-03	1	5.498E-03	0.000E+00
32	0.9996	1.714E+00	6.860E-04	1	6.860E-04	0.000E+00
100	0.9997	1.234E+00	3.704E-04	1	3.704E-04	0.000E+00
Total		2.752E+03	3.091E+02		3.086E+02	5.306E-01
Cum. Total		4.591E+03			4.899E+03	

Stage Efficiency	8.990E-01		9.983E-01
Cumulative Efficiency	9.369E-01		9.999E-01
Max Load, g	9600		9600
Shot life, shots	3.49		31.11
Bank Replacement Cost	$1,949		$4,291
20 yr Cost By Bank	$3,352,883		$827,574
System 20 yr Cost			$4,618,717
Bank Changes in 20 yr	1720		193

Table 10.   Cost of Replacing Banks of Disposable Filters

Bank 1 25% ASHRAE Prefilters

```
New filters = 24 x $6.15 =                              148
Changeout labor = 2 manhr x $31/manhr =                 62
Compactor operator = 1 manhr x $31/manhr =              31
Disposal = 16 cu.ft x 0.067 x $24.26/cu.ft =            26
                                        Total =       $267
```

Bank 2 95% ASHRAE Filters

```
New filters = 24 x $67.50 =                            1620
Changeout labor = 2 manhr x $31/manhr =                 62
Compactor operator = 2 manhr x $31/manhr =              62
Disposal = 96 cu.ft x 0.088 x $24.26/cu.ft =           205
                                        Total =      $1949
```

Bank 3 HEPA's

```
New filters = 24 x $130 =                              3120
Changeout labor = 16 manhr x $31/manhr =               496
Compactor operator = 3 manhr x $31/manhr =              93
Disposal = 96 cu.ft x 0.25 x $24.26/cu.ft =            582
                                        Total =      $4291
```

based on the work of Leith and Ellenbecker[10], was used for esti-
mating particle flux to downstream devices. This alternate method
discards the notion of collection efficiency and relates particle
penetration flux to the media area, dust cake on the media and the
frequency of cleaning.

Maintenance

We accounted for waste disposal, equipment repairs and operating
labor as maintenance costs.

Waste Disposal

The major waste disposal problem, other than disposing of
filters (which was accounted for in previous sections), is disposal
of dust collected in the hoppers of most of the candidate systems.
The dust will be a mixture of about the same composition as the air-
borne particles. The dust collected in the hoppers will be transfer-
red to a container via an airlock valve. To estimate the disposal
cost we made the following assumptions: 1) 55 gal drum, 7.35 cu.ft;
2) 2 hr labor involved in filling each drum; 3) powder bulk density
the same as uranium oxide, 1.5 g/cu.cm, 4) $25/cu.ft disposal cost
includes the container, shipping and burial costs. Allowing some
head-space, each drum will contain about 300 kg of dust. Because the
quantity of dust collected in the hopper varies with the equipment,
individual dust disposal costs were estimated for each system.

Table 11. Media Life

Device	Life Expectancy, Months
Common Rolling Filter	1
Peeled Roll Filter	84
Pulse-jet Baghouse: standard felt	24
coated felt	27
Electrostatically Augmented Baghouse	24
Cartridge House	24
Cleanable High Efficiency Filter	80-120
Pulsed Panels	1

Repairs

The expected repairs included compressor maintenance, pulse valve rebuilds, cleaning cycle control board replacement, blower repair, and a 16 man-hr annual allowance for miscellaneous repairs.

Operation

To estimate the labor cost of operating the systems we estimated the time involved for daily start-up and shutdown, annual inspection and annual housekeeping. For the daily operation we assumed 20 min was required to start and shutdown the existing system. For the candidate systems we added additional time for more complicated equipment. The approach for inspection and housekeeping was similar; one day for housekeeping and a half-day for inspection for the existing system per year. For the other systems additional time was allotted for more complicated equipment as appropriate.

First Costs

The first cost, or initial capital investment, included the costs of fabrication, flowrate controls, upgraded fans for various pressure drop requirements, air compressors, concrete pads, sheds, drum handling equipment, freight, ductwork of various types, installation labor and leak testing in the field as appropriate for each candidate system. The material of construction for most system components was mild steel.

Electrical Power

For BRL, power costs for the range were not part of its direct operating costs; however, power costs were estimated to provide a basis for discriminating between systems with otherwise comparable costs. Included in our estimates were the power for operating the fan, the control device and the auxiliary equipment such as compressors or blowers.

Total Costs

Following the method outlined, the twenty year cost of acquiring, maintaining and operating each candidate system was computed. Total costs were estimated for 294 different combinations of the

15 primary control devices and after-filters. HEPA filters were assumed to be used as the final stage of filtration to serve as a polishing stage and as a final barrier to particle release. It was further assumed that the HEPA stage would require a medium to high efficiency prefilter upstream that would collect the bulk of particles penetrating the first device. This ensures that the HEPA stage can remain functional even when the first filtration device fails catastrophically by explosive overpressurization of the system during a test firing. For the preferred after-filter combination of a particular candidate system there were several vendors which supplied estimated initial acquisition costs. The complete economic analysis was performed for each vendor's equipment and the results for maintenance, power, filter replacement, and etc. were averaged. The averages were then used as the cost estimates representative of the particular candidate system. Intercomparisons between the candidate systems were based on these averages.

Comparisons of Candidate Systems

Summarized cost estimates for candidate systems are shown in Table 12. The first two columns of Table 12 list the configuration recommended for each device. The initial investment values include equipment acquisition, installation, freight, ventilation fans, controls and desireable accessories for waste handling. The filtration penetration estimates are for the device plus the filter banks as a system. Given the uncertainties in filter efficiency data, the penetration estimates are probably accurate to 1-2 orders of magnitude. The totals in the last three columns exclude the cost of power as requested by BRL. The operating cost plus the initial procurement is the total number of constant dollars that would be spent on the system during the 20 yr. facility life. Amortizing the operating costs over 20 years at four percent interest and adding the initial cost yields the life cycle estimate in the last column.

The systems in Table 12 were listed in order of ascending life cycle cost. There were two distinct groupings with about an order of magnitude difference in total cost between the two. The expensive group was characterized by systems where most of the filtration duty is performed using disposable filters. This was true even of the cyclone system because the cyclone's low efficiency for the challenge aerosol puts the filtration burden on the disposable filters. The average life cycle cost for this group was about $6500K. The less expensive group was characterized by performing most of the filtration with a high efficiency device using cleanable filters or no filters at all as was the case for the ESP. The average life cycle cost for this group was $570K. The most important distinction between the two groups was the cost entailed in the useage and disposal of throw-away filters. Another significant difference, but of lesser impact, was the relative average costs of maintenance, $139K and $345K for the first eleven and the last five systems respectively. It should also be noted that none of the expensive group of systems met BRL's efficiency criterion of 99.998%, although they were close to meeting the criterion within the accuracy of the available data. The expensive group was then eliminated from further consideration.

Table 12. Cost Summary by Air Cleaning System

System (Device + Filter Bank)	Filter Bank	Initial Investment, $K	Calculated System Fractional Penetration	Maintenance Total Labor, Man hr	Maintenance Total Parts, $K	Total Maintenance	Power mw hr	Power $K
Cartridge, Coated Media	2,3	129	5.0E-08	3542	8	118	3475	139
Clnbl. Hi-Eff Filtr, 1 Stg	2,3	187	2.0E-07	3884	3	124	5750	230
Clnbl. Hi-Eff Filtr, 2 Stg		197	6.3E-07	4638	2	146	3850	154
Electrostatic Baghouse	2,3	167	6.3E-07	4946	3	157	4000	160
Baghouse, Pulse-jet, Std. Felt	2,3	157	2.0E-09	4748	8	155	4000	160
Baghouse, Shaker, Std. Sateen	2,3	134	1.0E-08	6192	1	192	2950	118
Baghouse, Pulse-jet, Coated Felt	2,3	157	3.8E-10	4434	8	145	4000	160
Cartridge, Standard	2,3	129	5.0E-06	3732	8	123	3475	139
Vaned Inertial Separator	2,3	119	7.0E-06	4158	2	131	4525	181
ESP	2,3	466	1.6E-06	3427	1	107	3100	124
Pulsed Panel	2,3	100	9.0E-06	4096	2	129	3275	131
Peeled Roll Filter	2,3	253	1.1E-04	8047	1	250	4825	193
Cyclone	1,2,3	112	1.1E-04	8447	0	262	6575	263
Standard Rolling Filter	1,2,3	31	1.1E-04	10585	1	329	2950	118
Existing System	1,2,3	20	1.1E-04	12041	0	373	3200	128
Extended Surface @ Bank 2	1,2,3	10	2.5E-04	16470	0	511	2700	108

System	Waste Disposal Replacement Media, $K	Man hr	Vol, cu.ft	Total $K	Operating, $K	Excluding Power Operating + Initial, $K	Life Cycle, $K
Cartridge, Coated Media	40	252	1043	34	191	320	413
Clnbl. Hi-Eff Filtr, 1 Stg	14	204	749	25	163	350	429
Clnbl. Hi-Eff Filtr, 2 Stg	15	205	776	26	186	383	475
Electrostatic Baghouse	20	214	1075	34	210	377	480
Baghouse, Pulse-jet, Std. Felt	60	259	1400	43	257	414	540
Baghouse, Shaker, Std. Sateen	49	221	1247	38	279	413	550
Baghouse, Pulse-jet, Coated Felt	94	208	1100	34	273	430	563
Cartridge, Standard	122	347	1528	49	294	423	567
Vaned Inertial Separator	216	440	1807	59	406	525	724
ESP	51	255	1004	33	191	657	751
Pulsed Panel	249	477	2008	65	443	543	759
Peeled Roll Filter	2649	3138	15345	481	3380	3633	5285
Cyclone	3031	3739	17607	556	3848	3960	5842
Standard Rolling Filter	3482	4814	19633	640	4451	4482	6658
Existing System	3631	5661	20920	698	4703	4723	7023
Extended Surface @ Bank 2	3640	4640	33064	970	5121	5131	7634

Several of the candidate systems in the lesser expensive group were eliminated for operational reasons. The vaned inertial separator and Pulsed Panel systems were eliminated because of the inconvenience and potential inhalation hazard inherent in requiring that the filter panels be changed by entering the contaminated hopper portion of the Pulsed Panels.

The ESP had the lowest estimated maintenance cost ($107K) of the remaining systems; however, the ESP had a significantly higher initial cost which outweighed the maintenance advantage. We also suspected that the ESP would be more susceptible to "puffing", briefly reduced efficiency for the instant of pressurization following a test shot, than would devices using filter media.

The shaker baghouse was eliminated for several reasons. First, it relies entirely on a dust cake for filtration, which would be disrupted during cleaning and probably during each test firing pressure pulse. Smith, Cushing and Carr[11] showed that shaker efficiency declines significantly following cleaning until such time as a dust cake is rebuilt, which would be a long time in the firing range case because the dust concentration is essentially atmospheric. Second, the pressure pulse could severely damage the unsupported filter bags. The filter bags are inflated by the ventilation airflow and the only supports to the fabric are rings sewn into the fabric at intervals. The brief pressurization following a test shot may over-stress an inflated bag. This argument would also apply to the electrostatically augmented baghouse due to its similar fabric support configuration. An additional drawback of the shaker baghouse was the very large number of bags (960) that would eventually require replacement.

The remaining devices, in order of initial cost, were

1. Cartridge house ($129K)
2. Pulse-Jet Baghouse ($157K)
3. Cleanable High Efficiency Filter, 1 Stage ($187K)
4. Cleanable High Efficiency Filter, 2 Stage ($197K)

Table 13 lists the pros and cons for these remaining candidate systems. Any of these three would be suitable air cleaning systems for this application depending on the preferences of the user for the positive aspects of each.

The cartridge house system with walk-in filter access was chosen for the firing range application. A single cartridge filter was adapted to the prefilter bank of Range C for some preliminary testing. After one test shot the filter appeared undamaged from the pressure pulse. Initial static tests in Range D resulted in failure of the original joints in the front and back filter house walls which have since been rebuilt. Because of that failure, the cartridge house will be fabricated of 0.25 in. steel and must pass a leak test at the design pressure of +3 psig. We anticipate that the cartridge house will attenuate the pressure pulse transmitted to the filter house.

Table 13.   Pros and Cons For Remaining Candidate Systems

	PRO	CON
Cartridge House	1. Filter removal from clean side, out of weather, available 2. Extensive user experience 3. Broad vendor support 4. Filters compact, easy to change 5. Lowest initial cost 6. Compact housing	1. Standard high pressure housing unavailable
Pulse-Jet Baghouse	1. Filter removal from clean side, out of weather, available 2. Extensive user experience 3. Broad vendor support 4. Standard high pressure models available 5. Fewest door seals	1. Walk-in filter access requires high-bay 2. Filters awkward to change because of support cage 3. Highest number of filter elements to change
Cleanable High-Efficiency	1. Convenient filter changeout 2. Fewest filter elements 3. Compact housing 4. Bagout system for filters 5. Eliminate existing filters w/2 stage housing 6. Two stages of filters with slightly larger housing	1. No existing systems of comparable capacity 2. Many door seals that could leak 3. Most expensive 4. Single vendor filter supply 5. No standard high pressure models 6. Single stage models had highest pressure drop

References

1. ASHRAE 52-76. 1976. Method of Testing Air Cleaning Devices Used in General Ventilation for Removing Particulate Matter, American Society of Heating, Ventilating, and Air Conditioning Engineers, New York.

2. Glissmeyer, J. A., and J. Mishima. 1979. Characterization of Airborne Uranium from Test Firings of XM774 Ammunition. PNL-2944. Pacific Northwest Laboratory. Richland, Washington.

3. Gilchrist, R. L., and P. W. Nickola. 1979. Characterization of Airborne Depleted Uranium from April 1978 Test Firings of the 105 mm, APFSDS-T, M735El Cartridge. PNL-2881. Pacific Northwest Laboratory. Richland, Washington.

4. Chambers, D. R., R. A. Markland, M. K. Clary and R. L. Bowman. 1982. Aerosolization Characterization of Hard Impact Testing of Depleted Uranium Penetrators, Technical Report ARBRL-TR-02435, U.S. Army Ballistics Research Laboratory, Aberdeen Proving Ground, Maryland.

5. Trinks, H. 1981. "Gun Muzzle Blast Field Research: Multiphase Flow Aspects and Chemistry of Muzzle Flash Including Chemical Flash Suppression." Published in Proceedings from Sixth International Symposium on Ballistics, Joseph E. Backofen, ed. October 27-29, 1981. Orlando, Florida.

6. Hanson, W. C., and J. C. Elder, H. J. Ettinger, L. W. Hantel, J. W. Owens. 1974. Particle Size Distribution of Fragments from Depleted Uranium Penetrators Fired Against Armor Plate Target. LA-5654. Los Alamos Scientific Laboratory. Los Alamos, New Mexico.

7. Mikropul Corporation. Copyright 1982. "Mikro-Pulsaire Dust Collectors," Brochure PC-5, Summit, New Jersey.

8. Donaldson Company, Inc. Copyright 1983. Torit Division, Brochure GB-83, Minneapolis, Minnesota.

9. Kermatrol, Inc. 1980. Drawing No. 1000-1-21-02. Santa Monica, California.

10. Leith, D., and M. J. Ellenbecker. 1983. Dust Emissions from a Pulse-Jet Fabric Filter, Filtration and Separation, July-August 1983, pp. 311-314.

11. Smith, W. B., K. M. Cushing and R. C. Carr. 1981. Measurement Procedures and Supporting Research for Fabric Filters. In Proceedings of First Conference on Fabric Filter Technology for Coal-Fired Power Plants. CS-2238, Electric Power Research Institute.

DISCUSSION

SCRIPSICK: What is the life extension of cleanable filters relative to the filters with no cleaning?   What is the efficiency of the air cleaning system you described?

GLISSMEYER: Assuming effective cleaning action, the life of the cleanable filter is not directly related to particle loading in the same way as a filter with no cleaning. For a cleanable filter, the life is more often related to mechanical wear, which usually occurs during the cleaning cycle. One manufacturer of a cleanable coated filter recommends replacement after 2,000 cleaning cycles. A second manufacturer of a cleanable coated filter suggests a life of 80-120 months. There was no evidence from users of such filters that I contacted to contradict the manufacturers' claims as long as the cleaning was effective for the particles; however, their longest experience was only three years.

Our working criterion for the combined air cleaning system efficiency was 99.998%, to meet the sponsor's requirements. Using the estimating method outlined in the paper, all of the recommended systems, and some of the others, were expected to meet the criterion. The efficiency data, as a function of size, that were used in the study will be included in a report to be published. Except for the rolling filters, cyclones, and vaned inertial separators, all of the cleanable prefilters should have an overall efficiency of around 99% or better for the aerosol distributions in the paper.

BERGMAN: I want to concur with and emphasize one of the findings of your study; namely, that the use of cleanable prefilters may result in significant savings in total filter costs. We had installed an electric prefilter in a Pu process box in Rocky Flats and were able to extend the HEPA life by over 50 times and had 98% recovery of the Pu aerosols.

GLISSMEYER: Most cleanable prefilters have good efficiency and can result in a very significant cost savings over non-cleanable filters in applications with aerosol concentrations greater than ambient outdoor concentrations and may be of value for systems where operability during accidents must be assured.

CADWELL: The components that are referred to as cleanable HEPA filters are not, by definition, HEPA filters because their initial resistance to air flow is substantially greater than the maximum allowed for HEPA filters.

GLISSMEYER: This is correct. These filters are also not DOP tested as required for HEPA filters. We, therefore, do not refer to these filter as HEPA filters but as cleanable high efficiency filters.

CALCULATING RELEASED AMOUNTS OF AEROSOLS

K. Nagel, J. Furrer

Kernforschungszentrum Karlsruhe GmbH

Postfach 3640, D-7500 Karlsruhe

Abstract

PASSAT is a test facility to remove iodine isotopes and aerosols from dissolver off-gas. It is located at the Nuclear Research Center Karlsruhe (LAF II). On the basis of experimental results coming from PASSAT the aerosol retention of the dissolver off-gas has been modelled for a large reprocessing plant.

The experimental performance to get results for the wave-plate droplet separator and packed fiber mist eliminator (PFME) is described in detail. Theoretical considerations about the aerosol retention factor of the droplet separator have to be changed to reconcile these considerations with the experimental results. The decontamination factor of PFME could be approximated as a function of aerosol diameter and gas flow rate. On the assumption of 10 mg/Std.m^3 in total mass of aerosols and three different frequency distributions in the aerosol diameter we calculated the released amount of aerosols.

1. Introduction

The aerosols entrained in the dissolver off-gas of a reprocessing plant play a major role in accident considerations. Their importance lies in the noxious constituents which are present in the off-gas. Noxious constituents include the radioactive fission materials in the solution, but also the toxic fractions such as Pu, Np, Am, Cm.

Aerosol removal from the off-gas is an essential element in a cleaning section. The technical-scale off-gas section for aerosol removal set up at the Karlsruhe Nuclear Research Center (KfK) has been described repeatedly /1/. It consists of a wave-plate droplet separator, a packed fiber mist eliminator, and a HEPA filter. The dependence of the removal efficiency of the wave-plate droplet separator and packed fiber mist eliminator on the aerosol size distribution is known from experiments.

Estimation of the aerosol release in normal operation and under accident conditions calls for the definition of the aerosol source term. However, the source term is not fully known and therefore the attempt will be made in this work to define source terms starting from certain boundary conditions and to estimate the influences exerted by these source terms. These are the boundary conditions:

- The total aerosol mass per $Std.m^3$ off-gas is 10 mg.

- Aerosols having diameters >10 μm plate out at the tube walls due to gravity.

The information about aerosol sizes is introduced into the calculations of releases to be performed by three different assumptions on the distribution of diameters.

2. Experimental and Results

2.1 Sampling

It is a requirement imposed by the licensing authority that before coupling of aerosol retention systems in the dissolver off-gas of a reprocessing plant the behavior of both the individual aerosol filter stages and the aggregate removal efficiency of all filters connected in series are known for an aerosol spectrum to be expected.

The interplay of the two droplet separators (wave-plate droplet separator and cleanable packed fiber mist eliminator) is important for off-gas cleaning because the droplet separators are used as roughing filters. They remove the majority of aerosol generated and return them into the wet process. This prolongs the service life of the downstream HEPA filter.

To be able to determine the removal efficiencies of the droplet separators droplets must be generated whose mass and number upstream and downstream of the separators can be evaluated with the help of analytical equipment and related to each other.

At the inlet of the PASSAT filter section a reproducible droplet spectrum (Fig.1) was generated by spraying salt solutions with a two-component nozzle. The spectrum lies in the range of 1 to 23 μm with the maximum in the number of droplets occurring at 4 μm. Upstream and downstream of the separators isokinetic part streams were extracted from the gas stream.

To obtain validated results several methods were used for determining the removal efficiencies at the individual filter positions:

1. Measurement of the droplet sizes at the droplet separators by use of the particle size measuring instrument HC 15 operating on the light scattering technique.

2. Introduction of the droplets into heated tubes where the droplets evaporate, and collection of the residual salt nuclei at Nuclepore or particulate air filters.
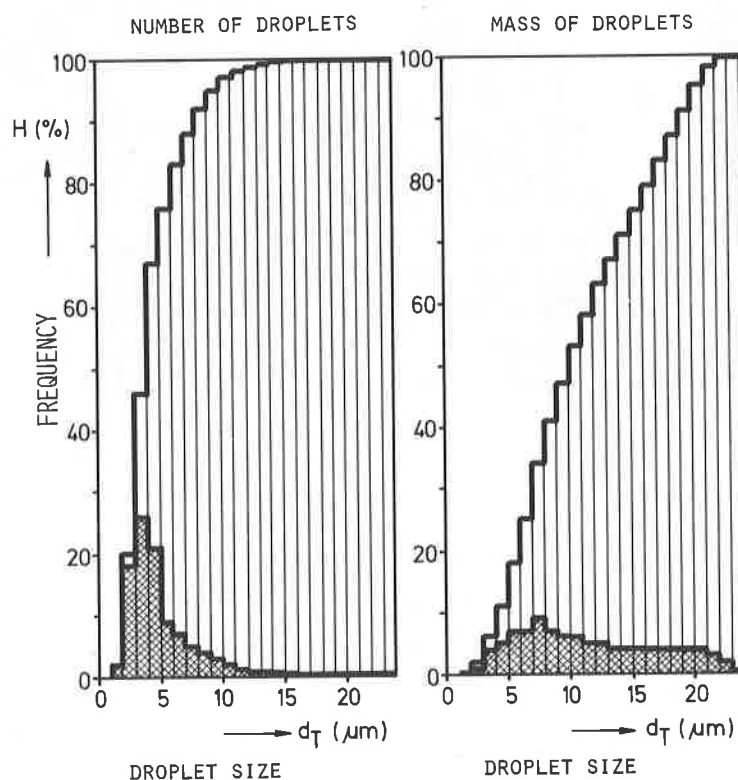
Figure 1: Size distribution of the injected droplets from $Ba^{139}(NO_3)_2$, Na fluorescein and $NaNO_3$ solutions

2.2 Removal of Droplets at the Wave-Plate Droplet Separator

The wave-plate droplet separator (Fig.2) constitutes the first filter barrier in the dissolver off-gas section. In principle, it fulfils the following two functions:

1. Removal of large droplets (>10 µm) in normal operation in order to reduce the exposure of downstream components.

2. Retention of large amounts of liquid and droplets in case of malfunction in the upstream NO_2 absorption columns.
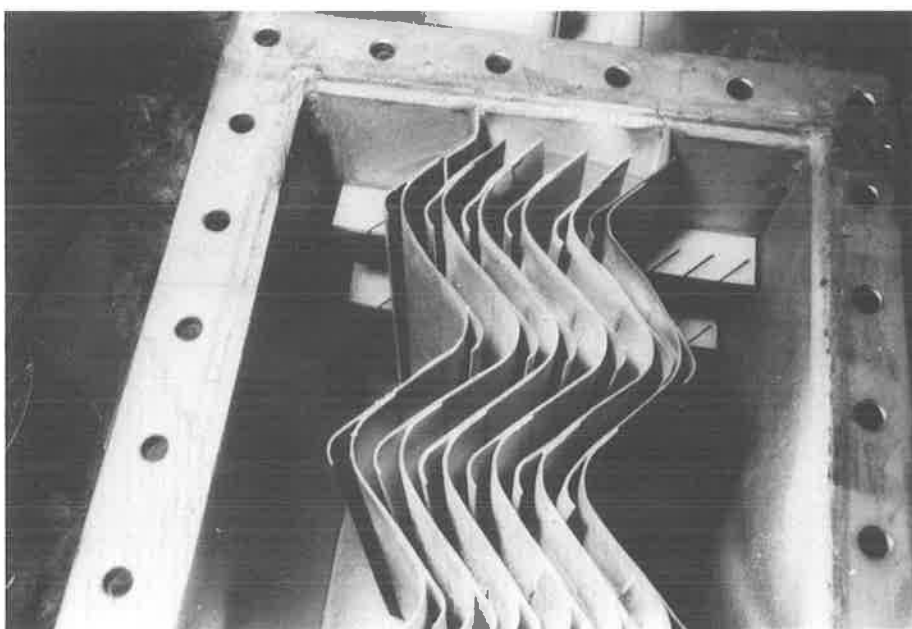
Figure 2: The wave-plate droplet separator.

By scattered light measurements the specific removal efficiencies were determined for single droplet sizes at volumetric flow rates between 75 and 150 Std.m^3/h at 30°C and 100% r.h. (Table 1). With the face velocity increasing from 0.63 to 1.26 m/s removal is shifted towards smaller droplets. The droplet limit sizes for a removal efficiency of 90% are 9, 7.5 and 6.5 µm, the corresponding volumetric flow rates being 75, 125 and 150 Std.m^3/h.

The mass removal efficiencies for the different volumetric flow rates were determined by evaluation of the number of the respective droplet

sizes per unit of volume in the upstream air and downstream air. The mass removal efficiency rose from 30 to 70% between 75 and 150 $Std.m^3/h$.

In further test series the removal efficiency was determined by spraying salt solutions and by collecting samples from filters. The droplet mass was calculated from the amount of salt deposited on the filters and from the given concentrations of the sprayed salt solution. By measurement and counting of the residual salt nuclei on the Nuclepore filters the individual droplet sizes were calculated (Table 1).

Table 1: Measured values of aerosol removal at the wave-plate droplet separator.

Scattered Light Measurements

75 $Std.m^3/h$			125 $Std.m^3/h$			150 $Std.m^3/h$		
$D(\mu m)$	DF	η	$D(\mu m)$	DF	η	$D(\mu m)$	DF	η
8.	0.62	0.62	3.5	1.0	0.0	3.	1.0	0.0
8.5	4.07	0.75	4.	1.06	0.06	3.5	1.16	0.14
9.	17.78	0.94	4.5	1.32	0.24	4.	1.51	0.34
			5.	1.70	0.41	4.5	2.14	0.53
			5.5	2.14	0.53	5.	2.82	0.65
			6.	2.69	0.63	5.5	4.17	0.76
			6.5	3.89	0.74	6.	5.37	0.82
			7.	5.49	0.82	6.5	9.12	0.89
			7.5	9.44	0.89	7.	14.79	0.93
			8.	22.39	0.96	7.5	28.84	0.97
			8.5	109.65	0.99	8.	107.15	0.99

With volumetric flow rate increasing from 50 to 150 $Std.m^3/h$ the mass removal efficiency is enhanced from 24 to 76% while the pressure differential across the wave plate separator increases from 0.5 to 3 mbar (Fig.3).
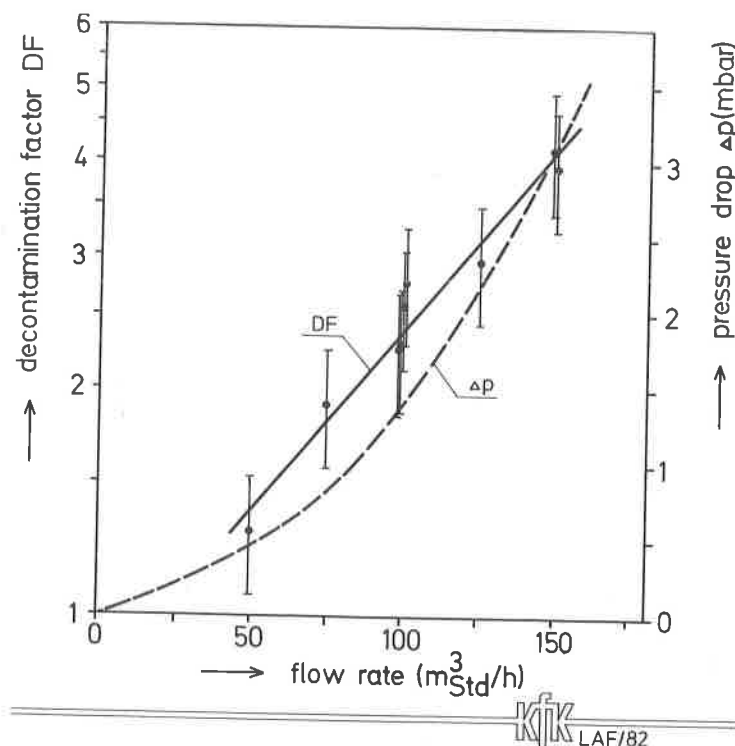
Figure 3: Decontamination factor and pressure
drop as a function of the volumetric
flow rate for droplets (1-25 μm).

2.3 Removal of Droplets at the Packed Fiber Mist Eliminator (PFME)

The PFME (Fig.4) serves as a fine droplet separator for droplets <10 μm (density of packing 300 kg/m^3, thickness 5 cm).

By intermittent spraying it can be cleaned from the salt accumulated. It assumes the function of a preseparator with a view to prolonging the service life of downstream HEPA filter. With the PFME exposed to droplets from a two component nozzle in the upstream air with a droplet spectrum of 1-23 μm and a maximum droplet number of 9-10 μm, scattered light measurements were performed upstream and downstream of PFME.

All the mass removal efficiencies were above 99.999% under this method of measurement for temperatures of the upstream air of 30 and 60°C and volumetric flow rates between 75 and 150 $Std.m^3/h$. However, this value can be used with some reservation only because large droplets are removed much more conveniently than small ones, whereas a few large droplets combine in themselves practically the whole mass and thus
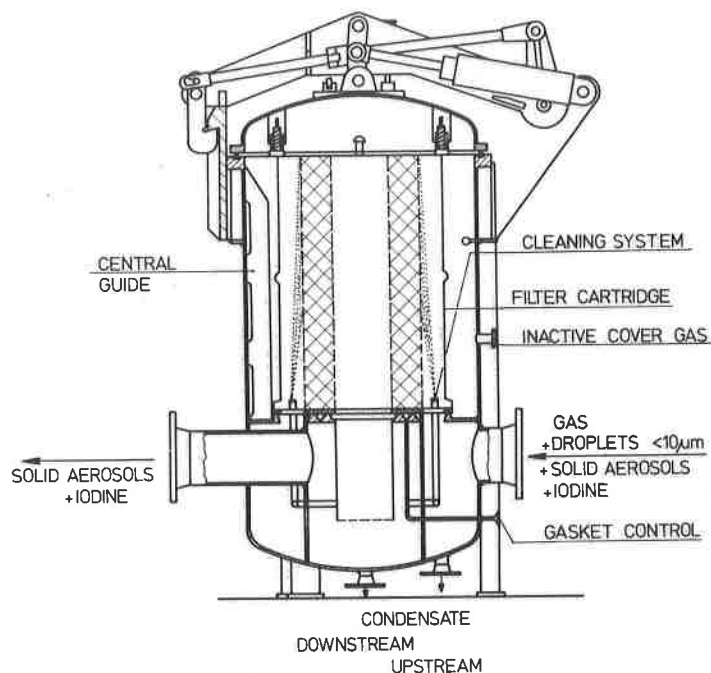
Figure 4: PASSAT packed fiber mist eleminator (PFME) for droplet removal <10 µm.

automatically yield high removal efficiencies. Therefore, the frequencies of occurrence of identical particle sizes in the upstream and downstream air were correlated to each other. For small droplets (<10 µm) the removal efficiency specific of the diameter was between 99.8 and 99.99995% with the corresponding decontamination factors of 500 to 2×10^6 (Table 2).

In additional investigations PFME was exposed to sodium fluorescein particles at volumetric flow rates of 75 to 150 Std.m^3/h, 30°C and 20% r.h. The decontamination factors measured for the particle mass exceeded 1000 for volumetric flow rates of 75, 100, 125 and 150 Std.m^3/h, the decontamination factor decreasing with increasing face velocity at PFME. This is attributed to the smaller influence of the diffusion effect during removal.

3. Wave-Plate Droplet Separator

The droplet separator of the PASSAT test facility is a Euroform wave-plate droplet separator with n = 6 lamellas, a deflection angle $\alpha = 45^\circ$ and spacings s = 2 cm. The aerosols carried by the air stream are

forced to follow curved tracks due to the deflection angles of the lamellas. If these curved tracks are considered as circular arcs with the radius r, centrifugal forces (Z) and friction forces (W) act on the aerosols. The equilibrium of these forces results in a radial velocity v_r /2/:

$$Z = m \bullet v^2/2 = \rho \bullet \pi \bullet D^3 \bullet v^2/6 \bullet r = 3 \bullet \pi \bullet D \bullet \mu \bullet v_r = W$$

or

$$v_r = \pi \bullet v^2 \bullet D^2/18 \bullet \mu \bullet r$$

where ρ ist the density of the areosols (1.007 g/cm^3), v is the flow velocity of the gas, D is the aerosol diameter and μ is the viscosity of the gas (~1.88 x 10^{-6} kg/m$\bullet$s at T_p = 30°C). The removal efficiency η of a lamella is obtained from the ratio of descent path s' to lamella spacing s:

$$\eta = s'/s = v_r \bullet t/s = v_r \bullet \alpha \bullet r/v \bullet s = \rho \bullet v \bullet D^2/18 \bullet \mu = \alpha/s$$

or

$$\mu = \alpha \bullet \Psi.$$

The dimensionless variable Ψ is termed parameter of inertia. The removal efficiency of several lamellas is obtained from

$$\eta(D) = 1 - EXP(- n \bullet \alpha \bullet \Psi).$$

With the numerical values indicated the parameter of inertia reads

$$\Psi = 1.488 \text{x} 10^9 \bullet V \bullet D^2.$$

Comparison of $\eta(D)$ with the following general setup

$$F(D) = 1 - EXP(- A \bullet D^B)$$

yields the coefficients A(1/m^2) and B as

$$A = 7.012 \text{x} 10^9 \bullet V$$
$$B = 2.$$

The following table compares the removal efficiencies, which can be calculated from the theoretical considerations made, with the experimental results given in Table 1:

Volumetric Flow Rate (Std.m^3/h)	Gas Velocity V(m/s)	A(1/m^2)	S
75	2.20	1.542×10^{10}	0.058
125	3.66	2.566×10^{10}	0.260
150	4.39	3.078×10^{10}	0.242

where S is the sum of the quadratic deviations of the calculated values $F(D_i)$ from the experimental removal efficiencies $\eta(D_i)$:

$$S = \sum_{i=1}^{k} (F(D_i) - \eta(D_i))^2$$

k = number of experimental values.

The attempt of approximating the experimental removal efficiencies of the wave-plate droplet separator with the highest accuracy possible, i.e. using a minimum value of S, was undertaken by the following mathematical setup:

$$F(D) = 1 - EXP(- A_1 \cdot D^B 1).$$

The coefficients A_1, B_1 determined separately for each gas velocity, and the respective values of S of the scattered light measurements from Table 1 were obtained as:

Gas Velocity V(m/s)	A_1	B_1	S
2.20	4.53×10^{35}	7.0	0.003
3.66	7.92×10^{21}	4.2	0.016
4.39	3.33×10^{18}	3.5	0.037

The values for S demonstrate a marked improvement of fitting as compared with the previous values. This approximation and the experimental values have been represented in Fig.5.

$$F(D) = 1. - EXP(-A(I)*(D**B(I)))$$
(o) $A(1) = 4.53E+35$, $B(1) = 7.0$
(□) $A(2) = 7.92E+21$, $B(2) = 4.2$
(×) $A(3) = 3.33E+18$, $B(3) = 3.5$
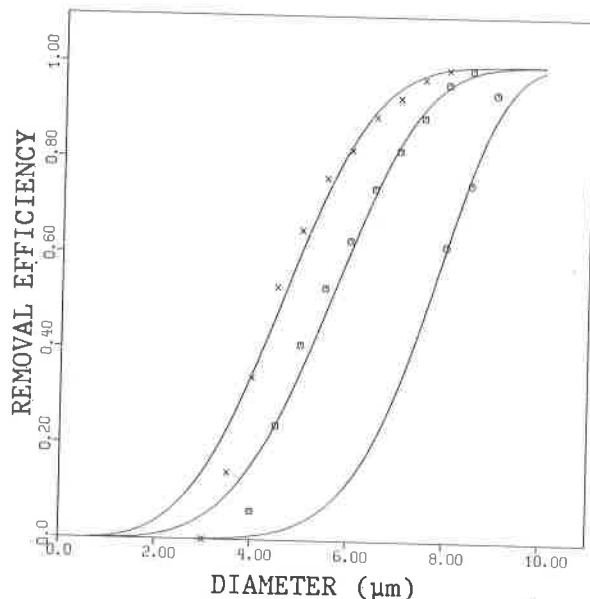
Figure 5: Dependence of removal effi-
ciency on aerosol diameter for
a wave-plate separator at three
different gas velocities.
Representation of the experi-
mental findings and their
individual approximations.

It appears from the figure that the removal plots are shifted with
increasing gas velocity V towards smaller aerosol diameters. This is in
agreement with the previous theoretical considerations because with
increasing velocity also the smaller aerosols find it more difficult
to follow the curved current threads. However, the coefficient B_1
is obviously no constant value but a function of V. This function takes
the following form:

$$B_1(V) = 15.36/V.$$

The other mathematical setups for representation of the aerosol
removal effiencies will be related to the theoretical statements
made; therefore, they are expressed as follows:

$$F(D) = 1 - EXP(- A \cdot D^2)^{B(V)}$$
with
$$B(V) = B_1(V)/2.$$

This gives

V(m/s)	$A(1/m^2)$	B
2.20	1.55×10^{10}	3.5
3.66	2.68×10^{10}	2.1
4.39	3.84×10^{10}	1.75

The representation of the coefficients A as a linear function of the gas velocity V

$$A(V) = A1 \cdot V + A2$$

yields, by application of the least squares method, the following coefficients

$$A1 = 9.3 \times 10^9 \ (s/m^3) \text{ and } A2 = -5 \times 10^9 \ (1/m^2).$$

This two-dimensional approximation produces the following result:

V(m/s)	$A(1/m^2)$	S
2.20	1.54×10^{10}	0.003
3.66	2.90×10^{10}	0.037
4.39	3.58×10^{10}	0.046

The values of S in the preceding table indicate that the two-dimensional approximation of the function

$$F(D,V) = 1 - EXP(- (A(V) \cdot D^2)^{B(V)})$$

is acceptable in the velocity range of 2.2 to 2.4 m/s. Sections of this approximation and the underlying experimental findings have been represented in Fig.6.

F(D,V) = 1. - EXP(-(A(V)*D**2)**B(V))

A(V) = A1*V + A2

A1 = 9.3E+09, A2 =-5.E+09

B(V) = 15.36/2V
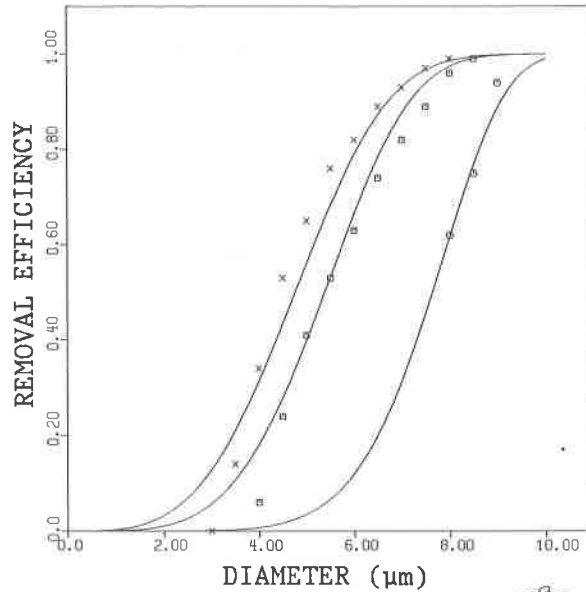
Figure 6: Section of the two-dimensional fitting and the corresponding experimental results. Symbols similar to Fig.5.

The function F(D,V) in the range of 1 to 12 μm of aerosol diameter and 2 to 8 m/s of gas velocity is shown in Fig.7.

F(D,V) = 1. - EXP(-(A(V)*D**2)**B(V))

A(V) = A1*V + A2

A1 = 9.3E+09 A2 =-5.E+09

B(V) = 15.36/2*V
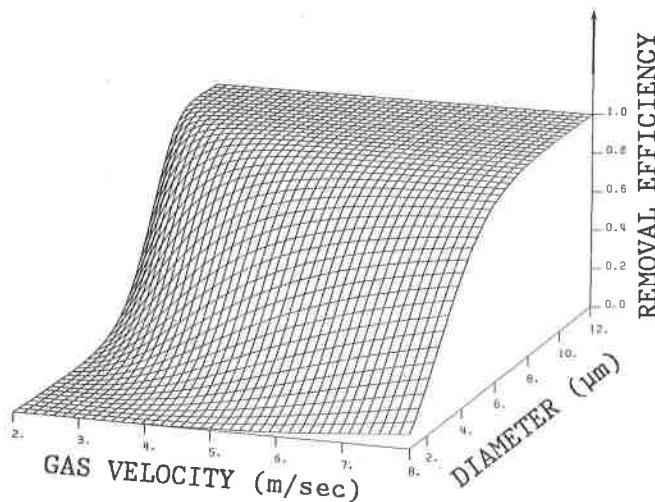
Figure 7: The complete three-dimensional representation.

This approximation give for $B(V) = 1$ a gas velocity $V = 7.68$ m/s and

$$A(7.68) = 6.64 \times 10^{10} \ (1/m^2).$$

For the expression $n \bullet \alpha \bullet \Psi$ one calculates:

$$n \bullet \alpha \bullet \Psi = 5.385 \times 10^{10} \bullet D^2$$

i.e., the linear velocity extrapolation of $A(V)$ gives a higher value compared with the theoretical one. In addition, measured values are available of the removal efficiency of a different Euroform wave-plate droplet separator operated at a gas velocity $V = 8$ m/s /3/. These results can be described by

$$\eta(D) = 1 - EXP(- 3.05 \times 10^{12} \bullet D^2).$$

Consequently, the linear dependence on velocity is not sufficient to describe the results available. Therefore, to represent the dependence of A, we choose the following power setup:

$$A(V) = A1 \bullet EXP(A2 \bullet V^{A3})$$

with $\quad A1 = 1.35 \times 10^{10} \ (1/m^2)$, $A2 = 0.0173$, $A3 = 2.82$

and obtain as a result:

V(m/s)	$A(1/m^2)$	S
2.20	1.58×10^{10}	0.004
3.66	2.64×10^{10}	0.027
4.39	4.14×10^{10}	0.050
7.68	3.08×10^{12}	

This approximation has the advantage that it correlates the theoretical concepts with the experimental results at hand. However, it calls for an exponential dependence on velocity of A, the parameter of inertia. Figure 8 shows the two-dimensional fitting of the experimental results using the exponential dependence on velocity of the coefficient A(v).

$$F(D,V) = 1. - EXP(-(A(V)*D**2)**B(V))$$

$$A(V) = A1*EXP(A2*(V**A3))$$

A1 = 1.35E+10, A2 = 0.0173, A3 = 2.82

$$B(V) = 15.36/2*V$$
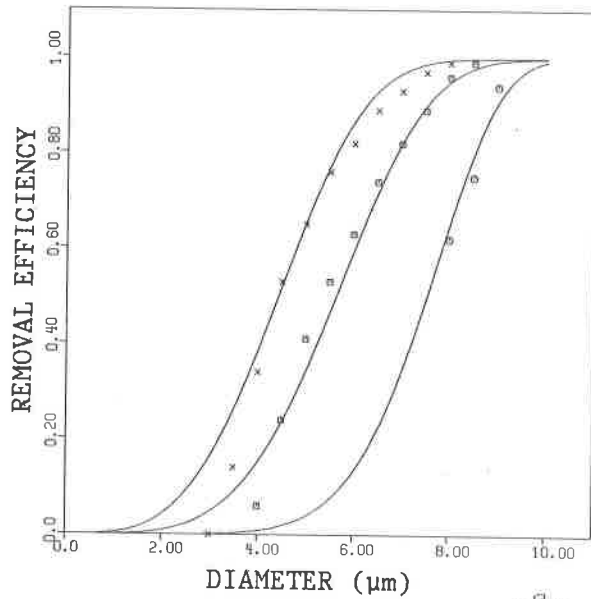
Figure 8: Section of the two-
dimensional fitting
and the corresponding
experimental results.
Symbols similar to Fig.5.

Figure 9 shows the overall approximation of the removal efficiencies of
the wave plate droplet separator.

$$F(D,V) = 1. - EXP(-(A(V)*D**2)**B(V))$$

$$A(V) = A1*EXP(A2*(V**A3))$$

A1 = 1.35E+10 A2 = 0.0173 A3 = 2.82

$$B(V) = 15.36/2*V$$
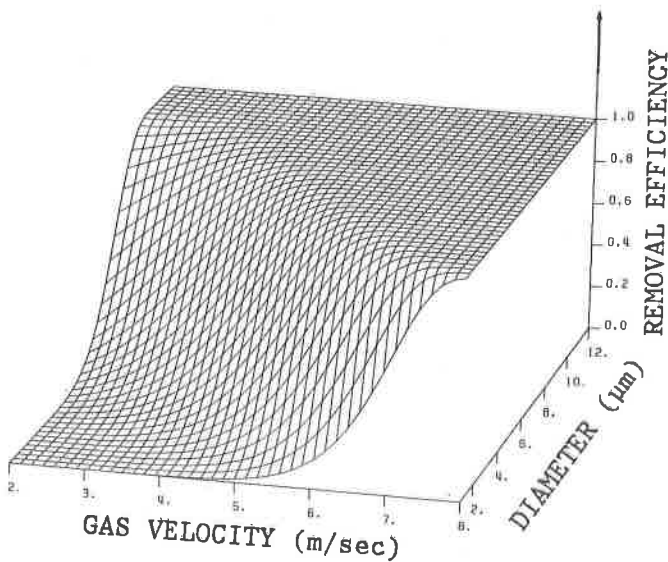
Figure 9: The complete three-
dimensional repre-
sentation.

886

4. Packed Fiber Mist Elminator (PFME)

A PFME acting as a demister is connected in series to the wave-plate droplet separator described in the foregoing chapter. The decontamination factors of the PFME have been listed in Table 2 as a function of the aerosol diameter /4/.

Table 2 Measured values of aerosol removal at PFME

LogD	LogDF	LogD	LogDF
0.143	2.805	0.555	5.000
0.201	2.875	0.602	5.750
0.279	2.911	0.634	5.607
0.322	3.500	0.652	6.089
0.342	3.500	0.690	6.125
0.380	3.964	0.719	5.821
0.477	4.661	0.748	6.107
0.517	4.768	0.778	6.089

In the initial accident computations on aerosol release from PASSAT the following representation of this dependence was used /5/:

$$logDF = 7.4 \cdot logD + 1.11$$

with diameter D = particle diameter in µm.
This corresponds to a straight line in a double logarithmic coordinate system. The sum of quadratic deviations between the results calculated from the equation above and the experimental values is S = 1.74. Application of the least squares method for approximation of these experimental results yields the following linear relation:

$$logDF = 6.2 \cdot logD + 16.0$$

with   S = 0.89.

The similarity of the double logarithimc representaion of the experimental pairs of values (logDF, logD) of the packed fiber mist eliminator to the representation of the pairs of values (η, D) of the wave-plate droplet separator led to the following

mathematical setup:

$$\log(DF) = K \cdot (1 - EXP(-A \cdot (\log D)^B) + M.$$

This selection of suitable initial values followed by application of the least squares method yielded the coefficients:

$$A = 7.814, \ B = 3.0, \ K = 3.75, \ M = 2.5, \ \text{and} \ S = 0.46.$$
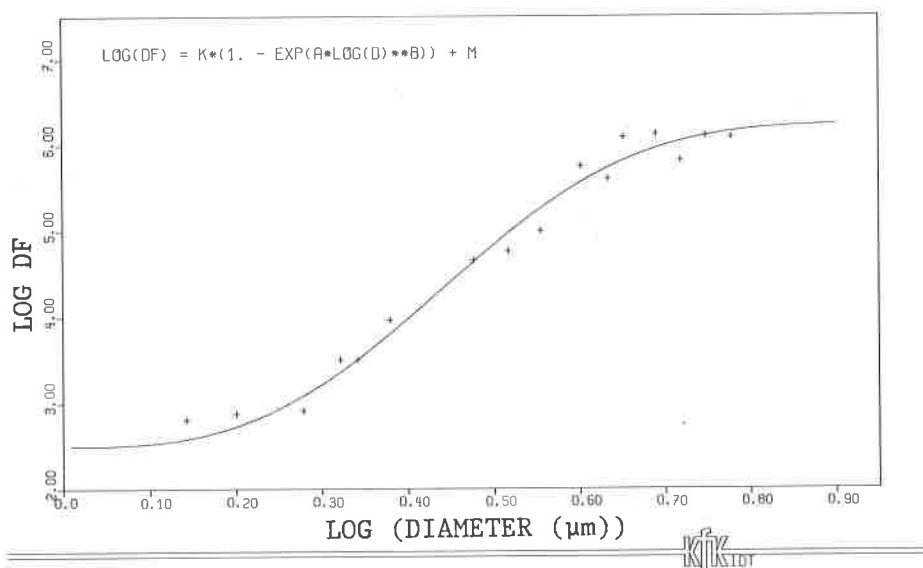
Figure 10: Decontamination factor of the PFME as a function of the aerosol diameter in a double logarithmic scale.

Figure 10 shows both the experimental pairs of values and their approximations. The approximation of the experimental values is good but not suited for description of the overall aerosol removal behaviour of the packed fiber mist eliminator. The decontamination factor of a separator approaches DF = 1 for particle diameters getting smaller. Reasons for this discrepancy might be:

- Either the two smallest values derived from experiments lead to a wrong conclusion, i.e., the values actually decrease further towards logDF = 0;

- or flattening of the function in the range of diameters around D = 1.5 µm is correct and constitutes the superposition of various mechanisms of filter efficiency, such as the removal of aerosols by inertia and diffusion effects, respectively.

This discrepancy can be finally clarified only by additional experiments on aerosol retention at packed fiber mist separators involving smaller aerosol diamters.

The approximation of the dependence of the decontamination factor on the volumetric flow rate is based on the following experimental results:

Volumetric Flow Rate $V(Std.m^3/h)$	DF
75	4583
100	1854
125	1333
150	1166

The aerosol spectrum underlying these experiments covered the range of diameters of 0.1 to 0.4 µm with the maximum number of particles 0.12 µm in diamter. The mathematical functional setup was:

$$F(V) = A/V^3 + B/V^2 + C/V + D.$$

The coefficients of the function are:

$$A = 9.6 \cdot 10^9, \; B = -1.9 \cdot 10^8, \; C = 1.4 \cdot 10^6, \; D = -2.6 \cdot 10^3$$

This approximation actually reflects the experimental values in an exact manner in the range from V = 74 to 300 Std.m^3 but it is not applicable to the range of volumetric flow rates V <75 Std.m^3/h because in this range it tends towards infinity.

5. Aerosol Burden

The removal efficiencies of the aerosol filters described in the preceding chapter allow statements to be made about the spectral aerosol release and their masses provided that the spectral distribution and aggregate mass of aerosols in the dissolver off-gas are known. But this aerosol source term is not available.

Estimates suggest that the total mass of aerosols per $Std.m^3$ off-gas is about 10 mg, also under the present state of knowledge. If one further assumes that all aerosols having diameters >10 μm plate out at the tube walls due to gravity, aerosol spectra can be indicated by making assumptions on size distributions. The following information about the aerosol source term relates to a range of diameters of 0.1 to 10 μm and three different distributions in size. These are:

- Constant number of aerosols over the whole range, i.e., for each diamter 0.1,...,10 μm, $7 \cdot 10^6$ aerosols are present. This gives a total mass of 11 $mg/Std.m^3$.

- An exponential distribution of diameters:
  $A = 3 \cdot 10^9 \cdot e^{-D}$ $D = 0.1, \ldots, 10$ μm
  the total mass is 10.7 $mg/Std.m^3$.

- A Gauss-type distribution of the aerosol diameters:
  $A = 2 \times 10^9 \cdot e^{(D-1)^2/2}$ $D = 0.1, \ldots, 10$ μm
  the total mass is 12.7 $mg/Std.m^3$.

Application of the functions for aerosol removal at wave-plate droplet separators and at packed fiber mist eliminators gives the results in Table 3. It shows the total aerosol mass upstream and downstream of the individual separators.

<u>Table 3:</u> Off-gas flow, distribution of aerosol diameters, and total aerosol mass upstream and downstream of the separators

Flow (Std.m^3/h)	Distribution of Aerosol Diameters	Total Aerosol Mass (mg/Std.m^3)		
		Wave Plates		PFME
		Upstream	Downstream	Downstream
	$A = 7\times10^6$	10.97	3.37	5.75×10^{-5}
75 =	$A = 3\times10^9 \cdot e^{-D}$	10.72	10.06	7.66×10^{-3}
(2.20 m/s)	$A = 2\times10^9 \cdot e^{-(D-1)^2/2}$	12.74	12.72	1.29×10^{-2}
125 =	$A = 7\times10^6$	10.97	1.22	5.58×10^{-5}
(3.66 m/s)	$A = 3\times10^9 \cdot e^{-D}$	10.72	8.53	7.64×10^{-3}
	$A = 2\times10^9 \cdot e^{-(D-1)^2/2}$	12.74	12.37	1.2×10^{-2}
	$A = 7\times10^6$	10.97	0.65	5.45×10^{-5}
150 =	$A = 3\times10^9 \cdot e^{-D}$	10.97	7.36	7.60×10^{-3}
(4.39 m/s)	$A = 2\times10^9 \cdot e^{-(D-1)^2/2}$	12.74	11.71	1.27×10^{-2}

The table makes evident that a very low dependence on velocity exists downstream of the packed fiber mist eliminator although under certain circumstances it must be taken into account to a considerable extent for the wave-plate droplet separator. The distribution of aerosol diameters exerts a noticeable influence on the total mass of aerosols released downstream of the removal system which is particularly obvious at the wave-plate droplet separator. The influence of the wave-plate droplet on the aerosol mass released is negligible if one assumes a Gauss-type distribution of the particle diameters. The three spectral aerosol size distributions at the inlet of the aerosol filter section, downstream of the wave-plate droplet separator and downstream of the packed fiber mist eliminator have been represented in Figs.11, 12 and 13.

Figure 11 shows the constant number of aerosols of 0.1 to 10 µm diameter by the wave-plate droplet separator and, in addition, the conspicuous change of the spectrum downstream of the PFME.
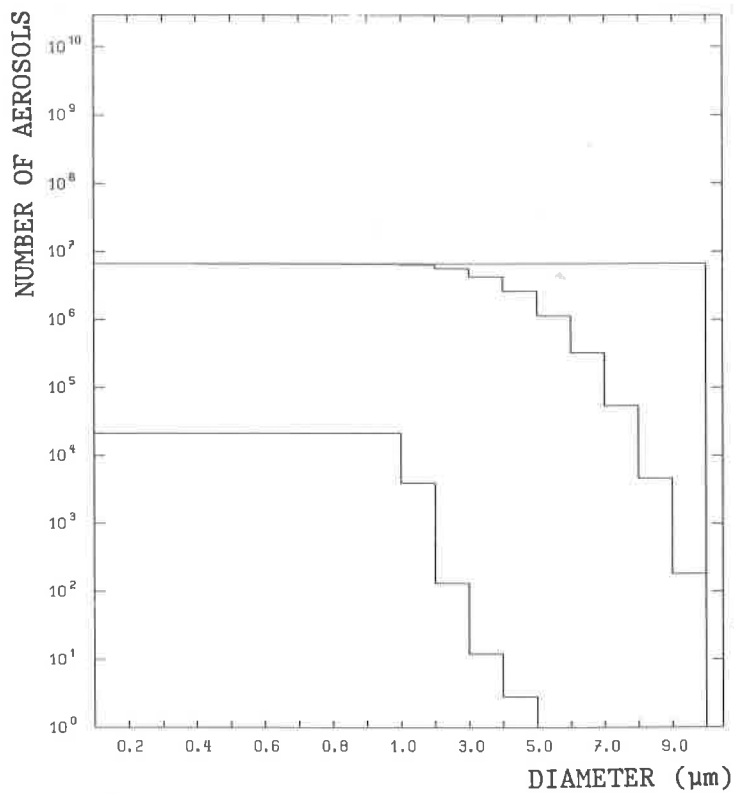
Figure 11: Distribution of aerosol diameters at the inlet, downstream of the waveplate droplet separator, and downstream of the PFME.
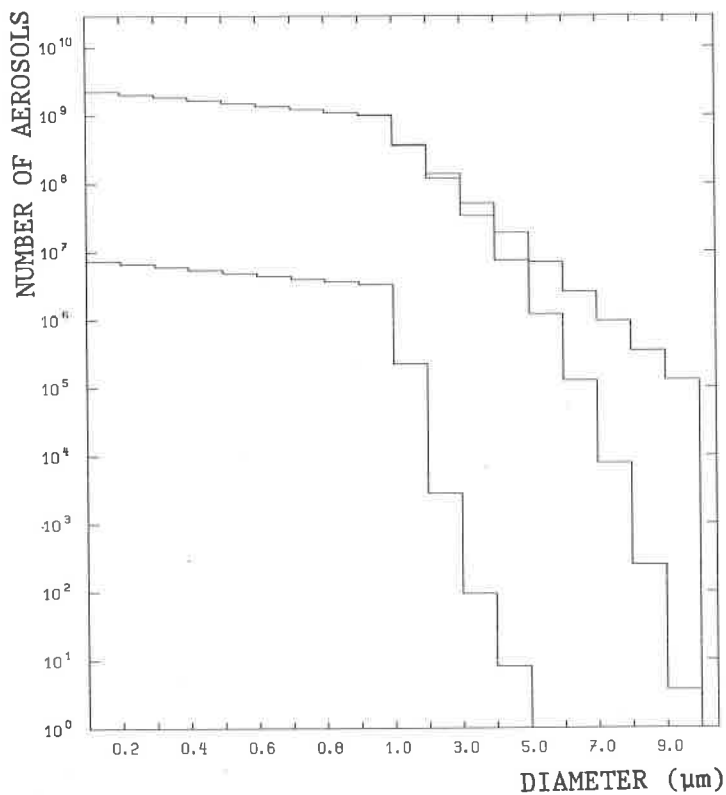
Figure 12: See Fig.11 with exponential distribution at the inlet.

Figure 12 represents the specified exponential distribution of the aerosol diameters and the influence exerted on them by the wet separators.
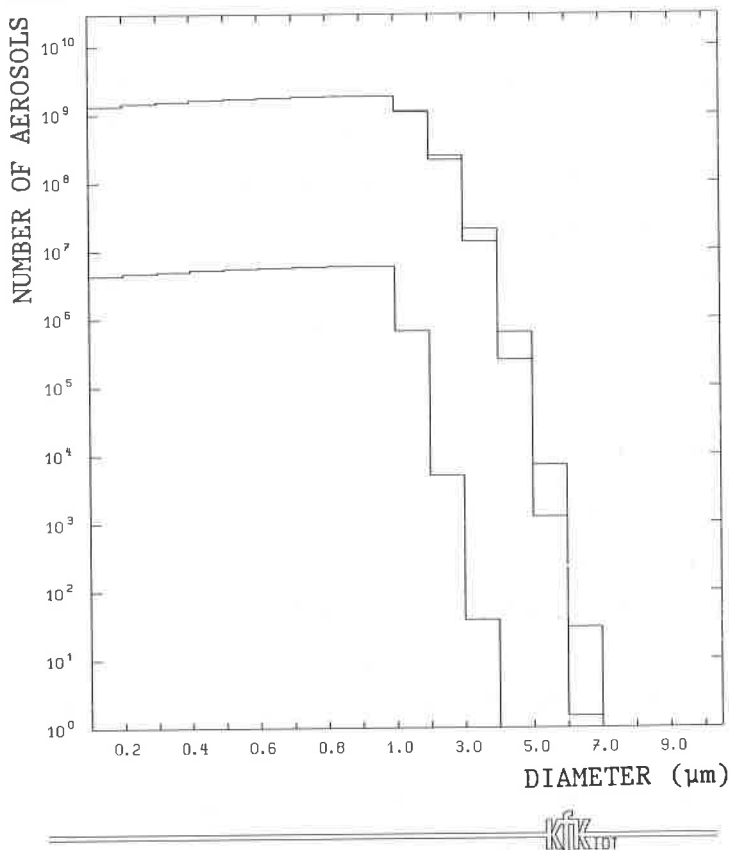
Figure 13: See Fig.11 with Gauss-type distribution at the inlet.

Conclusions

The attempt was made in this work to record the removal efficiency on an overall system for aerosol retention on the basis of the removal efficiency of the individual components and with certain assumptions made on the aerosol source term. The poorest result regarding aerosol release, extracted from Table 3, applies for a 75 Std.m^3/h flow and a Gauss-type distribution of aerosol diameters. The total mass of aerosols downstream of the packed fiber mist eliminator is $1.29 \cdot 10^{-2}$ mg/Std.m^3 which results in a mass of 15.48 mg per dissolution. A constant decontamination factor of DF = 100 gives a release downstream of the HEPA filter of 0.15 mg aerosols/Loading of the HEPA filter with 500 g aerosols is equivalent to approx. 3300 dissolutions or a service life about 10 years. The amount of aerosols released during this period is 495 mg. The assumed decontamination factor (DF = 100) is very small considering that in the PASSAT test facility decontamination factors >10^4

893

have been demonstrated.

As a matter of fact, the calculated service life of a filter of 10 years seems to be highly utopian and will certainly be strongly reduced as a result of other influences such as crack formation in the filter media, ageing of sealing and filter material or uptake of water, specific radiation burden of the workers (supposed service life 3-6 months). The calculation of aerosol release performed on the basis of estimating on the aerosol source term of the dissolver off-gas suggest the following: the release of aerosols via the dissolver off-gas section of a reprocessing plant does hardly play any role as compared to iodine release as long as the system of wet separator remain; intact.

REFERENCES

/1/ Furrer, J., Jannakos, K., Wilhelm, J.G.: "Aerosol- und Jod-
    abscheidung in einer Wiederaufarbeitungsanlage; Konzept der
    Auflöser-Abgasstrecke PASSAT".
    Tagungsbericht V/2266/78 der Kommission der Europäischen Gemeinschaft

/2/ Bürkholz, A., Muschelknautz, E.: "Tropfenabscheider Übersicht
    zum Stand des Wissens".
    Chemie-Ing.-Technik 44, Jhrg. 1972, S. 503

/3/ Hochleistungsabscheider, Typenreihe TS5
    Euroform (Aachen), Produkinformation

/4/ Furrer, J., Kaempffer, R., Linek, A., Maerz, A.: "Results of Cleaning
    Dissolver Off-gas in the PASSAT Prototype Dissolver Off-gas Filter System".
    CONF-801038, p. 566 (1980)

/5/ Nagel, K., Furrer, J., Becker, G., Obrowski, W., Seghal, Y.P.,
    Weymann, J.: "Time-Dependent Analyses of Dissolver Off-gas Cleaning
    Installations in a Reprocessing Plant".
    CONF-820833, p. 51 (1982)

Panel 13

NUCLEAR AIR CLEANING FIELD EXPERIENCES

WEDNESDAY: August 15, 1984
MODERATOR: W.H. Miller, Jr.
Sargent & Lundy

PANEL
MEMBERS: R.R. Bellamy
U.S. Nuclear Regulatory
Commission
D.M. Hubbard
Duke Power Company
J.W. Jacox
Jacox Associates
W.R. Lightfoot
Florida Power & Light

REGULATORY EXPERIENCE WITH NUCLEAR AIR CLEANING
R.R. Bellamy

FIELD TESTING OF NUCLEAR AIR CLEANING SYSTEMS AT DUKE POWER COMPANY
D.M. Hubbard

NATS FIELD TESTING OBSERVATIONS AND RECOMMENDATIONS
J.W. Jacox

IN-PLACE TESTING OF NON ANSI-N509 DESIGNED SYSTEM
W.R. Lightfoot

OPENING REMARKS OF PANEL MODERATOR:

In the organizational meetings for this conference, it was generally agreed that the nuclear air cleaning industry needs a forum to establish dialogue among the various participants in the air cleaning system life cycle: regulators, engineers, designers, contractors, testers, and operators. In selecting the participants for this panel, I have included knowledgeable, experienced representatives from all of these areas. Each of our panel members has prepared remarks on topical air cleaning issues or pertinent field experiences. After each panel member has concluded his prepared remarks, we will ask for members of our audience to step to a microphone and participate with questions, comments, or some of your own related experiences.

Before I introduce our first panel member, I'd like to make some recommendations which should improve this session's benefits:

1. When relating an experience, please refrain from naming specific utilities, stations, manufacturers, contractors, engineers, or regulators.

2. Let's keep the session upbeat by not only concentrating on problems, but mentioning some successes and to what you attribute that success.

3. Let's remember that many of the country's operating air cleaning systems predate current codes and standards. If the problem you're relating would have been precluded by proper use of a current code or standard, please mention this.

4. Since there are many representatives of various codes and standards committees in attendance, feel free to make suggestions for new standards or revisions to old ones which would help you solve your field problems.

It is my hope that we leave this panel session today with a better understanding of our current air cleaning system problems and perhaps some insight into how we can work together better in the future to solve them and avoid their repetition.

I'll reserve a few minutes at the end of this session to solicit your reaction to this session and discuss the possibility of more frequent forums of this type.

REGULATORY EXPERIENCE WITH NUCLEAR AIR CLEANING

Dr. Ronald R. Bellamy
U. S. Nuclear Regulatory Commission
Region I
631 Park Avenue
King of Prussia, PA   19406

Abstract

There are a large number of guidance documents available today that are concerned with nuclear air cleaning. These documents cover a wide range of technical areas, and have varying degrees of importance. From a regulatory viewpoint, there are regulations which all licensees are required to adhere to, there are regulatory guides which present one acceptable means of satisfying the regulations, there are standard review plans to indicate how regulatory reviews are performed, there are industry codes and standards to explain detailed technical guidance, and there are plant technical specifications which are requirements on the licensee.

Even with every conceivable effort to publish guidance that is clear, concise, accurate, and easy to implement, a significant number of questions, comments, concerns, complaints, and criticisms have arisen with respect to the available regulatory guidance. Those that have produced the most controversy are discussed.

I. HEPA Filter Testing

Prior to 1978, all HEPA filters designated for use in engineered-safety-feature (ESF) filter systems in commercial nuclear power stations were required to be visually inspected and dioctyl phthalate (DOP) tested at a DOE Operated Quality Assurance Filter Testing Station prior to shipment to the power station. This practice was based on DOE requirements since the early 1960's to use the QA stations, and was initiated because filter vendors were unable to consistently provide satisfactory HEPA filters.

Regulatory guidance was changed in 1978 (Revision 2 to Regulatory Guide 1.52), and HEPA filters for use in commercial nuclear power facilities no longer need to be tested at DOE QA stations. The reasons for the change in position are numerous: (a) the QA tests are a duplicate of those required to be performed by the manufacturer, and are available for audit by licensee representatives; (b) QA station test data showed only 1.5% of those filters designated for ESF filter installation in commercial nuclear facilities failed; (c) damage occurs in transport from filter manufacturer to QA station; (d) the cost of the filters increases approximately 30% when QA station testing is required; and (e) inplace testing of installed systems is required to verify the leak-tightness of the system prior to use (1).

Although strong industry support for the change in testing requirements was expected, just the opposite occurred. Other analyses of the data (2) and further studies by manufacturers (3), have shown that some technical experts believe HEPA filter quality is degrading, and the QA station test should be re-instated for all HEPA filters. At present, Regulatory Guide 1.52, Revision 2, is still in effect, and testing at QA stations of HEPA filters designated for ESF filter systems at commercial nuclear facilities is not required. It is to be noted that the availability of the DOE QA stations is clearly stated in the Regulatory Guide for those licensees that wish to use its services.

II. Applicable Industry Guidance

The guidance available, and revisions, for design, testing, and maintenance of air cleaning components and systems is almost too voluminous to list. Once a commercial nuclear power station receives a license, the technical specifications contain the controlling guidance. The technical specifications should be given the weight of laws and regulations. Even if an outdated version of a document is referenced, this outdated version can be followed by the plant with no negative legal implications. However, if a newer version of a document is available, the licensee would be updating his technical conformance by using the newer guidance. This cannot be done, however, without approval (by changing technical specifications or resident inspector knowledge).

The bases for criteria for ESF filtration systems is contained in Regulatory Guide 1.52. Revision 2 is the latest issue (July 1978), and there are plans for a future revision. The bases for criteria for non-ESF filtration systems is contained in Regulatory Guide 1.140. Revision 1 is the latest issue (October 1979), and there are no immediate plans for a revision. As much as possible, ANSI/ASME N509-1980 provides the guidance for design criteria, and ANSI/ASME N510-1980 provides the guidance for inplace testing criteria. As revisions to earlier ANSI standards, these versions contain the latest industry-accepted guidelines, and are better technical documents than earlier versions.

Laboratory testing criteria for activated carbon was originally based on RDT M16-1T, which had been referenced in Regulatory Guides and technical specification. Today, ANSI/ASME N509-1980 includes Table 5-1, "Performance Requirements and Physical Properties of (Unused) Activated Carbon." This table indicates both test method and acceptance value. ASTM D3803 (1979) is referenced, and actual acceptance values are tabulated. Further credibility for the acceptance values has been afforded by the publication of ASTM D4069 (1981). When technical specifications do not supply guidance for all necessary test parameters, ASTM D3803 is applicable (ASTM D3803 can also be interpreted as updated guidance based on RDT M16-1T).

NRC Generic Letter 83-13 (March 2, 1983) is entitled "Clarification of Surveillance Requirements for HEPA Filters and Charcoal Adsorber Units in Standard Technical Specifications on ESF Cleanup Systems". This guidance revised technical specifications to indicate that inplace leak-testing acceptance criteria are a function of the credit assigned to the system for accident analyses.

III. Laboratory Testing of Used Carbon

Some of the most difficult data to obtain that would characterize operation of air cleaning systems are results of laboratory testing of used carbon. Even when available, data sheets have proven to be incomplete. Furthermore, it is difficult to compare data from one air cleaning system with another, let alone correlate data from one plant to another.

When one does, however, analyze the existing data and attempt to predict the useful life of carbon, an "average" service life for carbon in continuous service can be predicted of approximately 2100 hours (three months). In order to build a degree of conservatism into plant technical specifications, laboratory testing for iodine removal is presently required after 720 hours (one month).

The results of laboratory testing should be received by the licensee in a timely manner, since carbon that fails a laboratory test puts the air cleaning system into an inadequate operating status. Once an ESF air cleaning system is defined as inoperable, an action statement is entered in the technical specifications, wherein the licensee must return the air cleaning system to operable status, or shut the reactor down (generally in seven to 31 days). A time period of 31 days is considered sufficient and appropriate time for a licensee to obtain a representative sample of carbon, ship the sample to a testing laboratory, have the testing performed, and receive the test data.

IV. Redundant HEPA Filters

The recommendation that ESF air cleaning systems contain two banks of HEPA filters is contained in Regulatory Guide 1.52. One bank should be installed upstream of the absorber bank specifically to remove particulate matter, and the second bank installed downstream to act as a redundant bank and also to collect any carbon fines that are removed from the adsorber bank. This position is supported by ERDA 76-21. For non-ESF air cleaning systems, Regulatory Guide 1.140 indicates that some consideration should be given in the design of the air cleaning system for downstream HEPA filters.

V. Fuel Handling Area Filter Systems

One of the most controversial topics in the time period three-to-eight years ago was the designation of the Fuel Handing Area Filter System as engineered-safety-feature. The characterization as engineered-safety-feature is important, since if the system is non-engineered-safety-feature, it need not be redundant, seismic category I, or have any associated technical specifications. An attempt to make the regulatory position clear is contained in the discussion section of Revision 2 to Regulatory Guide 1.52, where the "... emergency air cleaning system for the fuel handling building ..." is specifically identified as an ESF system. This position is based on General Design Criterion 61 of Appendix A to 10 CFR Part 50 - "The fuel storage and handling, radioactive waste, and other systems which may contain radioactivity shall be designed to assure adequate safety under normal and postulated accident conditions. These systems shall be designed ... with appropriate containment, confinement, and filtering systems..."

Although the issue of designing new plants with ESF air cleaning systems for the fuel handling area is not of great significance at present, potential backfits to existing fuel handling systems, and the question of technical specification applicability are still prevalent. Most operating plants have technical specifications (ESF) for testing of the fuel handling area air cleaning system, even if the system was not originally designed to ESF criteria.

VI. Sizing of Filter Systems

In order to adequately test and maintain ESF filter systems, a maximum volumetric air flow rate of 30,000 cubic feet per minute is recommended. Filter layouts of three HEPA filters high and ten wide is preferred. Apparatus available in the past to uniformly generate sufficient test aerosol to perform an inplace test on systems larger than 30,000 cfm was not available. In addition, component changeout becomes extremely difficult with layouts that are more than three HEPAs high. Recently, a number of entities in the testing area have stated the availability of equipment to uniformly generate test aerosols for large (30,000 - 100,000 cfm) systems, but specific substantive evidence has not been produced. There is some flexibility in the 30,000 cfm guideline (approximately 10%), and consideration is being given to raise the 30,000 cfm guideline, but there is still a good technical basis for limiting the size of systems to 30,000 cfm.

VII. Instrumentation

Guidance for instrumentation required for both ESF and non-ESF air cleaning systems was not originally very specific, but was only specified as signalling, alarming, and recording pertinent pressure drops and flow rates in the control room. The term pertinent meant different things to different people, and many discussions also arose with respect to control room versus local readout, signal alarm versus trip alarm, and status indication. In order to resolve

these concerns, the latest revision of ANSI/ASME N509 has included appropriate guidance agreed to by regulatory agencies, designers, architect/engineers, and utilities. Tables are included for both ESF and non-ESF systems, providing with great specificity the instrumentation, alarms and handswitches that are required (shall) as local and remote controls. Recommended (should) instrumentation is also indicated. It is important to emphasize that these tables in ANSI/ASME N509 specify the minimum instrumentation. All inquiries for guidance on instrumentation are referred to these tables.

VIII. Spacing Between Components

The necessity to provide adequate space inside a filter housing for inspection, maintenance and testing, has resulted in the recommendation that there be a minimum of three linear feet from mounting frame to mounting frame between banks of components. If the filtration components are to be replaced, the spacing to be provided should be the maximum length of the component plus the indicated three feet.

For any access, three feet is the minimum spacing considered adequate without damage to any components, and without severe personnel discomfort. For components to be changed, further space is required to manipulate the component into and out of the bank. For example, if a 24-inch by 24-inch adsorber tray is to be changed out, a total of five feet is necessary as spacing in the direction that the adsorber tray will be replaced. Although the substantial cost of increasing the size of a building at a nuclear power station to accommodate a large filter system is noted, the position is still valid.

IX. What is Significant?

It is well-known that painting, fire or chemical fumes will poison activated carbon and result in degraded performance. In order to verify that unacceptable degradation has not occurred, inplace testing is required via technical specifications following significant painting, fire, or chemical release in any ventilation zone communicating with the system. What is considered significant? Although this may be the most frequently asked question for interpretation of the technical specifications, the answer is not definitive. Significant should be interpreted as implying any release that could affect the performance of the filter system. Some licensees allow this decision to be made by the plant superintendent, others are silent on who makes the decision.

Sketchy numerical guidance has been informally pursued. If an "EXIT" sign is being repainted, then a reasonable person could conclude that this is not significant, and would not affect filter system operation. If the inside of the containment structure is being painted, this is obviously significant. A number of proposals have tried to justify 1000 square feet as a cut-off between significant and non-significant painting in terms of area, but rigid justification for this proposal is not yet available.

On a technical basis, the performance of the carbon is of primary concern after painting, fire or chemical release. HEPA filter performance would only be affected by an inordinately large release. However, if testing of the carbon (inplace or iodine removal) is required, it only makes sense to perform inplace tests on all components.

X. Representative Carbon Samples

There are a number of techniques available to obtain representative samples of service carbon for laboratory iodine testing. These include (1) pulling and dumping an entire tray, (2) pulling and dumping one-eighth tray, (3) grain thief, (4) pipe-stem bypass canisters, and (5) in-line canisters in trays. These are discussed in Appendix A to ANSI/ASME N509 - 1980. The goal is to ensure that the sampler is filled with adsorbent from the same lot and batch as the main bed, and that the carbon in the sample shall have experienced the same exposure to all contaminants as the entire bed it represents. If this goal is achieved, then the results of laboratory testing indicate the status of the carbon adsorbent.

Different technical experts give different opinions as to the best method. Grain thieves (also termed slotted-tube samplers) are becoming more prevalent today. Published data (4) has shown that pipe-stem bypass canisters result in representative sampling. At first glance, individual samples in trays would appear to be the best. The choice is up to the user, with the stipulation that, for whatever choice made, carbon samples are representative.

XI. Spinster Carbon

Because of significant delays in the startup dates for many reactors, qualified carbon has been in storage at some sites for up to five years or more. This carbon, that has yet to be in service, has been given the title "spinster" carbon. Can you assume that the carbon has not aged over the time period, or should it be retested to verify degradation has not occurred? The conditions under which the carbon was stored has much to do with the answer. Was storage in vapor-tight bags, in steel drums? Was the carbon exposed to any contaminants? As a rule of thumb, if the carbon was stored properly, it probably need not be retested if the storage time is one or two years of less. If storage approaches five years, retesting should be performed. As a conservative assumption, if you have any concerns about the performance of the carbon, obtain a sample and send it off to a laboratory for radioiodine testing prior to use. Trying to obtain replacement carbon is much easier and cheaper before startup than six months after startup. When technical specification compliance is a concern, be sure to discuss the matter with the NRC on site resident inspector before a problem occurs.

XII. Reactivation and Reimpregnation

Since spinster carbon has not, by definition, been in service, the argument can be made that if it has degraded, reactivation and/or reimpregnation should be allowed. However, precedent has been established that only virgin carbon is acceptable for installation at nuclear facilities (ASME code sections under development support this). Although there may be some financial benefit, the performance of re-treated carbon has yet to be established in actual service conditions, and the re-treatment is not recommended. The same discussion applies to service carbon, only with a stronger basis.

XIII. Summary

This presentation has attempted to stimulate discussion in some controversial areas pertaining to nuclear air cleaning. It is not realistic to expect a group of technical experts to agree on all technical issues, and this is the case for each of the items discussed above. Some of the items have a firm basis and are hard-and-fast positions, others are simply acceptable ranges and guidelines.

Published guidance is continually changing as our experience base is enlarged, and new questions arise. Consensus standards attempt to address all issues in a clear, concise and accurate manner. However, this is not always the case. When concerns arise, it is prudent to seek guidance and clarification before proceeding down a path that could lead to technical, legal, or philosophical problems at a later time.

REFERENCES

1. Collins, J.T., Bellamy, R.R., Allan, J.R., "Evaluation of Data from HEPA Filter Quality Assurance Testing Stations," Proceedings of the 15th DOE Nuclear Air Cleaning Conference, CONF - 780819, pp. 1159-1175.

2. Burchsted, C.A., "A Review of DOE Filter Test Facility Operations," Proceedings of the 17th DOE Nuclear Air Cleaning Conference, CONF - 820833, pp. 775-787.

3. Allan, Thomas T., and Cramer, Robert V., "Evaluation of HEPA Filters Meeting MIL-F-51068 Purchased on the Open Market. Are They Nuclear Grade?", Proceedings of the 17th DOE Nuclear Air Cleaning Conference, CONF - 820833, pp. 1115-1120.

4. Moore, Charles A., "Use of Installed Test Canisters for Representative Sampling of Ventilation Systems Charcoal Absorbers," Proceedings of the 15th DOE Nuclear Air Cleaning Conference, CONF - 780819, pp. 984-986.

FIELD TESTING OF NUCLEAR AIR
CLEANING SYSTEMS AT DUKE POWER COMPANY

Dean M. Hubbard
Duke Power Company
P. O. Box 33189
Charlotte, North Carolina   28242

ABSTRACT

Duke Power has long been committed to protecting the health and safety of
the public we serve. This commitment is reflected in the design, testing
and operation of our nuclear air filtration systems. Duke Power considers
nuclear air filtration as one of several vital means to protect the quality
of the environment we live in, not as an unnecessary evil that has been
forced upon us by regulatory agencies.

Nuclear air filtration has come a long way at Duke Power Company since the
start-up of our first nuclear unit, Oconee 1 in 1973. Air filtration systems
in all three Oconee units predate Regulatory Guide 1.52 and ANSI N509. In
contrast, our Catawba Nuclear Station has nuclear air filtration systems
built and testable to the latest codes, standards, and Regulatory Guides. It
is in this wide range of filtration systems and experiences that I would like
to discuss our practices and plans for the future.

I.   INTRODUCTION

No one is immune to air filtration problems and Duke Power is certainly no
exception. We share many of the common problems that have plaqued the users
of nuclear air filtration systems. In our "pre ANSI N509" systems we encounter
problems typical of the early systems such as: an uninspectable filter unit,
leaking filter bypasses, drains flooding the filters, high humidity without
heaters and poor air flow distribution. Most of these type problems are well
documented by the work of C. A. Burchsted.

Problems encountered on newer systems can occasionally be traced to design
oversights but are more often attributable to operating and maintenance
practices. Nuclear air filtration cannot be viewed as just another HVAC
system. All personnel involved with nuclear air filtration must be well inform-
ed of proper practices in regard to their contact with these systems.

II.   NUCLEAR AIR FILTRATION PROGRAMS AND PRACTICES

Duke Power has implemented a number of programs and practices to ensure the
availability and efficiency of our nuclear air filtration systems. In February
of 1982 we held our first in-house training for in-place testing of nuclear air

filtration systems. This practical training is now offered biannually to our employees and other utility personnel. The purpose of the training is to train new personnel, upgrade experienced personnel, and to promote the transfer of nuclear air filtration experience between stations. Attendance is not limited to testing personnel but includes Design, Maintenance and Operations personnel. The course format is structured to allow the participants to apply the morning lecture information in afternoon lab sessions. Subject material includes: air filtration theory, design and construction of filter units, inspection of filter systems, field and laboratory testing, regulatory aspects, and troubleshooting. Additional lab time is provided at the end of the course to discuss field testing problems and to practice field testing technique. In 1985 this course will be expanded to include more information on industrial ventilation and air conditioning.

To aid in the resolution of in-place testing problems, we have developed a troubleshooting guide (see Appendix). The guide utilizes a symptom/problem chart where the symptom is identified and a series of possible causes are suggested. The numbering system on the chart indicates the best order to search for the cause. All the suggested problems listed on the chart are discussed in some depth in the back of the guide. This guide has proven useful to our field testing personnel by providing them with a systematic approach to finding solutions to elusive testing problems.

Another program Duke Power has started is replacement carbon verification. This program is in addition to the testing done by the carbon manufacturer or vendor. When replacement carbon is purchased for our nuclear air filtration systems, random samples of carbon are removed as the carbon shipment is received. Care is taken to ensure that samples are collected from each batch if more than one batch is shipped. The samples are testing for: methyl iodide removal efficiency (@ 30°C, 95% RH, with 16 hours pre-equilibration), ignition temperature, screen analysis, and an optional TEDH analysis to determine per cent impregnation. Duke started this program to assure that the quality of the carbon being received for use in our systems meets the requirements of ANSI N509-1980. This provides extra margin for the public health and safety, as well as preventing unexpected replacement of carbon and possibly a forced outage. The information can also be used as a baseline for trending carbon life.

Duke Power has gained significant benefits from the in-house design, construction and operation of our nuclear stations. Feedback information from Operations and Maintenance to Design Engineering has been used to correct problems on existing filter systems and improve new systems being specified. Unique solutions found on existing filtration systems are applied at other stations where similar problems exist. We are interested in further expanding our base of experience and knowledge by promoting increased information exchange with other utilities.

Duke Power is encouraged by the efforts being made to improve laboratory testing of carbon. We support the review of testing technique and the accreditation of the labs providing carbon testing services. These actions will help us insure uniformity in the testing of our carbon samples. We are planning to use carbon testing results for trending the carbon life of all

all systems in service. This information will enable us to predict carbon life and better understand the environment that the filter system serves.

One area where we would like to see additional attention is in fire protection of carbon beds. Perhaps through the misnomer of "charcoal" the insurance industry made sure that our carbon beds have water deluge systems to protect us from the extremely remote prospect of a fire. We have quite a few Type III carbon beds that would be at great risk if such a water deluge were released. We would like to see and would support efforts to prove that fire protection in the form of water is unnecessary.

III.   CONCLUSION

In conclusion, we at Duke Power have seen much progress in nuclear air filtration design, operation, maintenance, and testing of these systems. We are convinced of the value and importance of utilities taking a more active role in the proper operation, maintenance, and testing of nuclear air filtration systems. Utilities should not rely too heavily on consulting services, since we are ultimately responsible for the day-to-day operation of our systems. We look forward to increased contact with other utilities for resolution of problems and to assist in the training of personnel.

APPENDIX

TROUBLE SHOOTING GUIDE FOR THE PERIODIC IN-PLACE
LEAK TESTING OF HEPA FILTERS AND CARBON ABSORBERS

Dean M. Hubbard

GUIDE APPLICATION AND USE

This guide was developed to aide in solving problems that occur during periodic in-place leak testing of HEPA Filters and carbon adsorbers. Due to the wide range of problems that can occur and the differences in test equipment, filter systems, and testing technique, it becomes almost impossible to address every problem. The purpose of this guide is to provide an approach to finding and solving most filter testing problems.

Certain assumptions have been made concerning the types of equipment used and the types of tests performed. The following information is assumed:

a.   The particulate filters are HEPA filters,

b.   gas adsorber filters use impregnated activated carbon as the adsorbant,

c.   the challenge agent for testing the HEPA filters is dioctyl phthalate (DOP) aerosol,

d.   the challenge agent for testing the carbon adsorbers is refrigerant 11 (R-11),

e.   leak detection equipment for the DOP is a forward light scattering photo-meter and,

f.   leak detection equipment for the R-11 is a gas chromatograph.

Deviations from the above assumptions must be taken into account when using this guide.

When problems occur, consult the symptom problem chart and find the column listing the symptom. A number of possible problem areas are circled and numbered. The numbering system suggests the best order to search for the problem not based on the most probable cause but rather the easiest to most difficult problems to verify. This is intended as a time saver.

If more information is desired, a column lists the page of the guide where the information relative to the indicated problem may be found.

FILTER TESTING TROUBLESHOOTING GUIDE

SYMPTOM

See this page for information.

PROBLEM	Ref	No upstream sample peak.	No downstream sample peak.	Immediate high downstream peak after injection.	Upstream/downstream peaks erratic.	Downstream peak remains high.	Additional peaks interfer with R-11 peaks.	Chart not following normal pattern of peaks.	Zero base line shifts on recorder.	Standing current decreasing.	High background.	Leak indicated.	Difficulty in setting 100% upstream base.	Stray light uncontrollable.
1. Other refrigerants in system.	3				②		②	③		④				
2. Equipment out of calibration.	4	⑦	⑦			⑧			④	③				
3. R-11 generator flow	5	②	②	②										
4. Sample lines pinched or reversed.	6	③	③	③		②								
5. Probe not properly positioned in flow.	7	⑤	⑤										①	
6. Carbon adsorbers saturated.	8				④	⑤					②			
7. Room contaminated with R-11.	9					④					③			
8. Carried gas contaminated.	10				④		③		②	②				
9. Weak electron capture tube.	12									⑤	④			
10. Instrument column saturated.	13				③			②	③		⑤			
11. Instrument settings/set up.	14	①	①	①	①	①	①	①	①	①	①	①	①	
12. Vacuum pump malfunction.	15	④	①											
13. Need more DOP in system.	16												②	
14. Mechanical leak.	17			⑤		⑥						②		≈
15. Equipment malfunction.	19	③	③		⑤		④	④	⑥	⑤		③	③	≈
16. Scattering chamber dirty.	20												②	
17. Poor mixing of challenge agents.	21	⑥	⑥		③								③	
18. Expended Carbon	22			⑥	⑦									

I.   Other Refrigerants in System

The gas chromatograph used to detect the R-11 challenge for the carbon adsorbers is also sensitive to similar halocarbons and gases normally found in a nuclear facility. Solvents used in painting and cleaning (e.g., trichloroethylene) also can be detected by the gas chromatograph and result in additional peaks. These peaks may or may not interfere with the R-11 peaks depending on when they occur on the chart. All additional peaks should be marked on the chart and an effort made to identify the source of the peaks.

Contaminates can not only affect the accuracy of test data but can also "load" the carbon adsorber such that the carbon must be purged for a length of time or must be replaced. For this reason it is recommended that the source be identified to avoid future contamination and to avoid confusion in future tests. A technique to identify contaminates is outlined below:

A.   Using the downstream probe on the chromatograph, take samples from the room where the test is being performed and from the filter system. If the sample from the room shows the contaminate then most likely painting is being done, or an air conditioning system is leaking somewhere nearby. If the sample from the filter system shows the contaminate, then the contaminate is located in one or more of the areas served by that ventilation system.

B.   Search the suspected area and look for any of the following listed sources:

      1.   air conditioning equipment leaks,
      2.   refrigerant bottles (empty or full),
      3.   cleaning liquids,
      4.   solvents (in cans or on rags)
      5.   spray lubricants,
      6.   degreasing cleansers,
      7.   dry cleaning solvents, and
      8.   painted areas or paint cans.

      Once the contaminate source is located, remove it from the area if possible or if there are leaks have the leaks sealed. Painted areas will require time to dry thoroughly.

C.   After the source of contaminate release has been eliminated, take another sample from location of contaminant release to confirm that the air is contaminate free. If the contaminate remains in the filters (as shown by "clean" air upstream of the filters and contaminated air downstream of the filters), then run the system 2-8 hours* to purge the filters of remaining gas. In some cases purging for extended lengths of time will not remove the contaminate and the replacement of the carbon adsorbant could become necessary.

*See problem VI "Carbon Adsorbers Saturated With R-11 or Contaminant"

II. Equipment Out of Calibration

When the calibration of the equipment is suspected, first check the calibration date on the equipment. If the equipment calibration has expired or is close to expiration have it recalibrated. If not, the following steps should be taken:

A. Verify that <u>all</u> settings on the instrument used during the test were/are correct. Any equipment interfacing with the equipment in question should also be checked.

B. Produce known conditions to verify calibration.

For Chromatograph

(1) Verify zero readings

    a. close all sample parts with tubing caps
    b. cycle through several readings
    c. instrument should "zero" properly

(2) Field calibrate with calibrated gases

    a. introduce calibration gases according to procedure
    b. cycle through several readings
    c. compare readings with expected readings to confirm calibration

III. R-11 Generator Flow

The primary function of the R-11 generator is to convert R-11 from a liquid to a gas and to meter the amount of R-11 entering the filter system. This process can require frequent monitoring depending on the manufacturer and design. It is very important that the rate of R-11 injection remain constant to achieve an accurate comparison of upstream and downstream concentrations.

Rotometers are built into most R-11 generators to measure flow. Check to see if the rotometer indicator ball moves freely in the full range. If not, the rotometer should be cleaned with alcohol and checked again.

If a rotometer was not included on the R-11 generator or the one provided is in question, then substitute a rotometer or another   flow measuring device to confirm R-11 injection levels and the stability of that level.

Additional checks for the R-11 generators include:

a. Checking all fittings and connections for leak tightness
b. Make sure that the supply of R-11 is adequate
c. Check the heating element and make sure it is operating at the correct temperature.

IV. Sample Lines Pinched or Reversed

To insure the integrity of the sample it is imperative that the sample tubing be completely free of any holes and/or kinks. Due to the sensitivity of the instruments which analyze the samples (the chromatograph can detect 1 particle per billion) every effort must be made to keep this tubing and its respective fittings leak tight and free of constrictions.

Sample lines should be visually inspected frequently for holes and kinks (folds) in the tubing. If holes are suspected they can be confirmed by pressurizing the sample lines with the N^2 actuator gas and applying a soap type leak indicator on the suspected leak. If the bubbles appear indicating a leak then the tubing should be replaced. Leaky fittings should be tightened or repaired if possible and replaced if not.

V. Probe Not Properly Positioned in Flow

The tester should be aware of the problems caused by air flow distribution. Sharp bends in the duct work or filter housing may cause the air flow to separate from the innerwall of the bend forming a "dead" pocket of air. Sudden diverges in the duct work can cause the same separation which usually results in the formation of large eddies.

It is important when establishing test port locations that an equal area velocity profile be taken to assure that the sample is taken from the mainstream of the airflow and not from a "pocket" of stagnate air. A copy of the velocity profile for each sample port should be kept on file and on hand for reference purposes. Section 9 of Industrial Ventilation by the American Conference of Governmental Industrial Hygienist outlines a good technique for taking a velocity profile.

VI. Carbon Adsorbers Saturated With R-11 or Contaminant

The activated charcoal in nuclear air cleaning systems is used primarily to adsorb organic radioiodine compounds. However, activated charcoal is also able to adsorb other gases as well, including the tracer R-11 which is used in testing. A given quantity of activated carbon has a limit to the amount of gas that can be adsorbed. The point at which the carbon adsorbant reaches its capacity is known as its breakthrough capacity.

In testing, if too much R-11 is injected into the system being tested, breakthrough capacity will be reached, and R-11 will be detected downstream of the filter banks in quantities that would seem to indicate a leak in the filters. Breakthrough can be distinguished from a mechanical leak by observing when the apparent leak appears. If the leak appears after several "no-leak" samples are taken and continues to increase, then most likely the filters are saturated with R-11. A mechanical leak will appear at the very beginning of the test immediately after the F-11 is introduced into the filter system.

Contaminates such as, solvents from paint, cleaning solvents, refrigerants from cooling systems (see Problem 1 "Other refrigerants present in system"), and high moisture content can saturate the carbon to the point where R-11 cannot be adsorbed. the result is a loss of adsorption sites and a relatively quick breakthrough of the R-11 when it is injected for a test. The best indication of this problem is a high background, or if water is the contaminate, the humidity of the exit air should be significantly higher than normal.

The best solution to the above contaminate problems is to identify and remove the source of the problem. Once the source is removed it will be necessary to run the system (2-8 hours) and allow the contaminates to desorb from the charcoal. Heaters (if available) should also be run to reduce the time required to desorb the contaminants. If the contamination of the carbon cannot be corrected, the carbon must be replaced.

On some systems, guard beds of carbon are placed upstream of the carbon adsorbers to protect them from contaminates. This bed needs to be checked for contamination and saturation that can affect test results.

VII. Room Contaminated With R-11

When testing the carbon adsorbers, the R-11 gas generator is often located in the same room as the chromatograph or near the duct work that feeds into the system being tested. In the process of gasifying the R-11, a considerable amount of it can escape into the room and enter into the chromatograph through leaks in the fittings. R-11 can also leak into the duct work through cracks and affect test results. Because of the sensitivity of the chromatograph, extremely small quantities of R-11 can have a drastic effect.

It is recommended that the R-11 generator be made as leak tight as possible and that all fittings used with the chromatograph be checked for leak tightness. Some people prefer to remove the R-11 generator from the room and use long injection lines. However, this can make it difficult to monitor the flow of R-11 into the system and is usually not recommended.

VIII. Carrier Gas Contaminated

The chromatograph is an extremely sensitive instrument and must have a carrier stream void of <u>any</u> contamination. Outlined below* are the most common sources of carrier gas contamination:

A. <u>Poor quality carrier gas</u>. You must use chromatographic grade carrier gas for good results. Never let the pressure in the external carrier gas supply bottle get below 500 psig. At this point the bottle should be considered empty. Allowing a nitrogen bottle to become empty (0 psig) can severely contaminate your system.

B. Contaminated carrier gas filter. This filter is an optional molecular sieve-type filter that is placed in-line between the external carrier gas supply cylinder and the instrument. Its purpose is to trap moisture and contaminates.

*Information in part from Valco Instrument Co. Operation Manual for Model 100 Halocarbon Monitor.

This filter quickly becomes "loaded" with contaminates when poor quality carrier gas is used or if you leave it exposed to the atmosphere. It can be cleaned by removing the carrier gas line from the instrument, then heating the filter with a torch to red heat with carrier gas going through it. When heating the filter, always start at the upstream end first (towards the regulator) and work down the filter slowly. After you finish with the filter, heat the stainless tubing. This will boil off any moisture or other contaminants in the filter or tubing. For the best results, this should be done after external carrier gas supply bottle is replaced. Be sure to recap lines after every use. Keeping the system clean is of the upmost importance.

C.   Column "loaded" with contaminant. After heating the filter, check your fittings with a soap like leak detector for leaks. If you suspect the chromatograph has moisture in it, connect the carrier gas and let it run for a day with carrier gas going without running samples. Check the chromatograph for improvement after it has run for a day.

"Loaded" columns often occur if: the carrier gas filter has become contaminated, the unit has been idle without the sample ports being capped, or a large slug of R-11 has entered the unit. The best way to correct a loaded column is to increase the column temperature (if possible) and let it "cook-out" for four to five hours; then return the temperature to normal. On heavily loaded columns it may be necessary to "cook" them for extended lengths of time.

D.   Use of improper carrier gas regulator. The carrier gas regulator must be a new two-stage regulator with a stainless steel diaphragm. Any other type can cause baseline problems due to air diffusion through the diaphragms. Two stages are necessary for good pressure control without drifting.

E.   Improper material for carrier gas line. The carrier gas lines that connect the supply tank to the instrument should be manufactured of stainless steel. Plastics tend to give off contaminates and metals such as brass or carbon steel are too porous to totally eliminate contaminates. When stainless steel tubing is contaminated or new, it must be first flame-cleared before putting into service. All related fittings should be treated in the same manner.

IX.   Weak Electron Capture Tube

The heart of the chromatograph analytical capability is the electron capture tube. In this tube is a radioactive source which ionizes the carrier gas creating free electrons. Gases other than the carrier gas that enter the chamber reduce the free electron density by capturing these free electrons and thus infer the concentration of the gas compound present. The radioactive source can deteriorate through use (and misuse) and need replacement.

If the standing current is low first go through all the checks and corrective actions in the Problem VIII "Carrier Gas Contaminated." If the low standing persists, send the instrument back to the manufacturer to correct the problem. Most likely the electron capture tube is weak and needs replacement which is usually done by the manufacturer.

X. Instrument Column Saturated

The "column" in a chromatograph is used to separate gases in a sample before the gases enter the electron capture tube to be analyzed. The column is a long tube filled with "Chromosorb"* which separates gases by delaying the different gases in the mixture for different lengths of time.

A high concentration of R-11 entering the column will saturate the column and result in the R-11 "bleeding-off" the column for long periods of time. The end results can be unusual peaks, zero base line shifts and a decreased standing current. If a loaded column is suspected, raise the temperature of the column to approximately 150°C (if possible) while purging the column with 99.999% pure carrier gas overnight. Note: Contamination of the column can also occur when the carrier gas filter becomes contaminated or the carrier gas itself is not pure (99.999%).

XI. Instrument Settings/Setup

There is little room for error when setting up filter testing instrumentation, especially for the R-11 test of the carbon adsorbers. When problems occur, the first trouble shooting actions should be to check all aspects of the equipment setup and the settings on the equipment.

A check list should be written for each test procedure that includes all aspects of the equipment setup. It is recommended that the checklist include all the following: tubing connections, electrical connections, instrument settings, gas pressure settings, and sample line connections. Simple mistakes can often result in the most baffling problems which could be easily avoided with a checklist.

XII. Vacuum Pump Malfunction

The vacuum pump is used to pull the sample through the tubing and the instruments. Vacuum pump failure would seem to be an obvious problem, but with the high noise levels found in HVAC rooms it is an easy problem to overlook. A vacuum should be verified each time the pump is operated by moistening your finger and placing it over the end of the sample tubing. If a vacuum is present the tubing will have a slight pull on your finger.

Some vacuum pumps will become "caught" in the middle of a stroke when turned off and "freeze" when turned back on. This can be corrected by loosening the tubing fittings on the pump momentarily "breaking" the vacuum. Care should be taken to retighten the fittings to assure a good seal.

*"Chromosorb" is a registered trademark of Johns-Manville Co.

XIII.   Insufficient DOP In System

Large filter systems require larger amounts of DOP to achieve an adequate concentration for testing. If it becomes difficult to adjust the particulate detector to 100% for the upstream base, then it can be assumed that more DOP needs to be introduced into the system. The manufacturer of the DOP generator should be consulted on the maximum size filter system that can be tested for the model used.

Extremely large filter systems may require larger amounts of DOP than one DOP generator can produce. In this case a second generator may be required, or some manufacturers recommend adjusting the gain control on the detector until a 50% reading is obtained (instead of a 100% upstream base). Testing may then be performed with penetration readings multiplied by 2 for relating the reading to a 100% base. Other smaller bases can also be used as long as the test reading is multiplied by the proper factor to bring the reading to a 100% base. A requirement for this technique is that the particulate detector being used has a linear output scale.

XIV.   Mechanical Leaks

A mechanical leak is a leak that occurs when the contaminate to be filtered (particulate or gaseous) finds a pathway through or around the filters that is large enough to exceed the maximum allowable limit. Mechanical leaks for the HEPA and carbon adsorber will be discussed separately.

HEPA Filters

If the particulate detector indicates a leak in the HEPA filters, the first action should be a visual inspection of the filters for: tears, holes, and welding burns. A large leak of DOP can usually be found visually. Look for any housing or system leaks such as: drains, conduits, bypass dampers, cracks in the housing, cracks in the concrete flooring, welding cracks, and silicone sealant leaks.

If no obvious leaks can be found, scan the filter banks and housing downstream of the filters to locate leaks with a hand-held probe. Gaskets between the filter and housing should be compressed 80% to assure a good seal.

Another technique is to illuminate the upstream side and search for light penetration on the downstream side of the filters. Any light penetrating the filters represents a leak in the filter. This technique is only effective with fairly large leaks. Retest after assumed leak is found and sealed.

Charcoal Adsorber Filters

Leaks are more difficult to determine and more difficult to locate in carbon adsorbers than in the HEPA filters. First it is critical to know the characteristics of a leak as seen on strip chart output of a chromatograph.

The most important characteristic of a mechanical leak is that it rapidly appears in the downstream sample after the R-11 is injected upstream. Likewise, the leak rapidly disappears (the downstream R-11 peak decreases significantly) when R-11 injection stops. Other problems with the filters or equipment do not affect the downstream peak as rapidly over time. Usually, the first downstream sample will raise the peak height after R-11 injection when a mechanical leak is present.

915

In contrast, filters that are saturated with R-11 will begin to allow R-11 to escape downstream and <u>slowly</u> increase the peak height over a longer period of time. If R-11 injection is stopped, the saturated filters will continue to give off R-11 with almost no immediate decrease in the downstream peak height.

Leaks once determined can be found in a similar manner to that described for HEPA filters. Look for any housing or system leaks such as: drains, conduits, bypass dampers, cracks in the housing, cracks in the concrete flooring, welding cracks, and silicone sealant leaks. Gaskets between filter and housing should be compressed to 80%* to assure a good seal. Frequently leaks that occur in tray type filter systems are due to gasket relaxation.

Another frequent cause of mechanical leaks is the settling of the carbon in the trays or beds creating pathways through the charcoal. This problem can often be detected by illuminating one side of the filters and observing the level of the carbon from the other side. However, tray type (Type II) filters usually have to be removed to check for settling therefore, gasket compression between the filter and housing should be checked before removal.

If the leak or leaks cannot be discovered with the above methods, use the downstream sample probable to scan the filter(s) and housing downstream of the filters. When scanning, time must be allowed for the chromatograph to analyze the sample and indicate the R-11 level.

XV. Equipment Malfunction

The best way to ascertain whether or not a testing problem is due to the test instrument malfunctioning is to produce known conditions for the instrument and compare the results. This is in essence a type of calibration where it is assumed that if the instrument operates correctly under known conditions, that it will operate correctly under unknown conditions. The manufacturer's operation and maintenance manual should be consulted for becoming aware of potential problems and to help troubleshoot problems when they do occur.

Before setting up a test for the instrument in question make a preliminary check of the instrument settings and set up, the owner supplied fuse, and the calibration date.

XVI. Scattering Chamber Dirty

The scattering chamber in a particulate detector is the device in which the sample is analyzed for the concentration of particulates. High concentrations of DOP or dust can contaminate the scattering chamber by coating the sides and increasing the "scattering" of the light. The result is that the "straylight" control becomes uncontrollable making it impossible to adjust incidental light.

The only remedy is to have the scattering chamber cleaned by the manufacturer or qualified instrument personnel.

XVII. Poor Mixing of Challenge Agents

Poor mixing of the challenge agents with the system air can cause widely varying concentrations of the challenge across the face of the filters and could leave portions of the filter or filter bank totally unchallenged. This is especially a concern with the DOP aerosol but can be a problem with the R-11 gas as well.

Mixing uniformity of the challenge agent with the system air should have been verified during the initial start up testing according to ANSI/ASME N510-1980 Section 9. If there have been any modifications in the filter unit, duct work servicing the filter unit, test port locations, or challenge injection port locations, then the mixing uniformity of the challenge agent should be verified according to the aforementioned standard.

In the event uniform mixing is not present in the system, a new challenge injection port should be chosen further upstream in the system to allow increased mixing. Another alternative is to add mixing baffles if another injection location is not possible. New injection locations or baffles should then be verified for their effectiveness.

XVII. Expended Carbon

Expended carbon is carbon that no longer has the ability to adsorb gases as specified in Regulatory Guide 1.52 Rev. 2 due to age and environmental factors. This state is evidenced by the test gas (R-11) passing through the carbon almost immediately upon introducing the test gas into the system air. Expended carbon will test very similar to a mechanical leak in the system and for this reason, all efforts should be made to locate possible leaks before concluding that the carbon is expended carbon. The lab test of a carbon sample is the only way to definitely confirm expended carbon. This involves sending the carbon to an independent lab which is expensive and can take up to 30 days or more for an answer. Therefore, it is important to search for any possible leaks in the system first.

Activated carbon has an undefined but limited life which is dependent on the environment to which the carbon is exposed. High humidity and fumes from welding and cleaning can dramatically reduce the life of activated carbon.

"New carbon" is generally expected to have a shelf life (when properly sealed in storage) of 3 to 5 years when it can meet the specifications of new carbon.

Used carbon is any activated carbon which is currently being used in a filter system or has been used in a filter system. Under ideal conditions of low humidity and no fumes, used carbon can last 8-10 years. High humidity and fumes can shorten carbon life to as little as 18 months. This can be prevented by limiting the carbon's exposure to fumes and by running the system's heater coils periodically (if available) to reduce the moisture on the carbon. Consult your station's Technical Specifications for the specification of the test on used carbon.

NATS FIELD TESTING OBSERVATIONS AND RECOMMENDATIONS

John W. Jacox
Jacox Associates
1445 Summit Street
Columbus, Ohio 43201

I. Abstract

In many cases good engineering practice has been forgotten and replaced with blind adherence to meeting the letter of the "nuclear" regulations. There is much too much diversity in the interpretation and implementation of codes, standards, and regulations by both the NRC and utilities. It is not reasonable to design an acceptable system in regard to long-term-operation, maintenance and testing unless designers observe those functions in an actual operating plant.

II. Introduction

Over the past 17 years or so, I have been deeply involved with Nuclear Air Treatment Systems (NATS). Recently, this involvement has focused on startup and ANSI/ASME N510 Acceptance Testing at a variety of plants. These have been BWR and PWR plants owned by single reactor utilities and experienced multisite utilities. My experience includes basic consulting on the startup/test procedures, technical specifications and FSAR's; initial walk-throughs of plants to point out the obvious problems through actual testing of systems to qualify other Field Test Engineers to a utility QA Program.

As you would expect, there is great diversity in the physical systems, level of technical expertise and attitude. Equally important is the great diversity in utility interpretation of 10CRF50 Appendix B and their methods of implementation.

III. Observations

A few general correlations seem to exist. I stress these are purely empirical, and personal observations based on current experience at over half a dozen startup sites. These observations are based on plants that use outside contractors for NATS Acceptance Testing. In all cases there are individual exceptions; excellent people in poorly managed situations and the occasional "bad apple" in the best operations.

1. The greater the involvement of the utility operations personnel, the smoother the startup and testing and the better the final systems.

2. The more education, background and experience the client (utility, A/E, etc.) has in NATS the smoother the startup and testing and the better the final systems.

3. There seems to be <u>no</u> relationship between overall utility experience or number of operating plants and startup and acceptance testing efficiency or system quality.

4. The simpler and more standard the plant QA/QC and Security requirements are, the fewer unnecessary problems we experience. I stress this is over and above the <u>specific</u> added paperwork, it is <u>an all pervasive</u> inefficiency and attitude at a site with excess requirements. Universally accepted QA personnel qualifications, security and medical "certification" would save significant time, money and confusion versus today's situation of each plant having to duplicate everything to allow a contractor to work. This, of course, applies to all work and workers.

5. Prior experience of individual utility or architect-engineers can either be a great benefit or problem, depending on the specific experience. Where the engineer learned general technology and NATS background, the experience is extremely valuable. Unfortunately, in a few cases an individual with only limited prior experience can be under the impression that there is only a single approach and all related work must be tortured into conformance with his experience.

6. There is extreme diversity in the utility and NRC interpretation of the same documents (10CFR50 Appendix B, Regulatory Guides, ANSI Standards, etc.) from Region to Region, and project to project. Uniform training, better understanding and direction and overall better communication by the NRC at all levels and through all Regions would be of great benefit to the industry and country.

7. In general there is very little understanding of the adsorbents used in NATS. The results range from a common lack of caution in storage, testing, QA document control and installation to a few cases of over caution. Actually it is difficult to be over cautious given the great cost, and delay, if the adsorbent does not meet the Technical Specifications requirements when needed for start-up.

8. One almost universal problem is the lack of adequate provision of testing manifolds for series filter banks. The usual "provision for testing" is a nipple with a pipe plug in the door or wall of the housing. This meets neither the letter, nor intent, of current N509/N510 for leak testing series banks. Out of 200 systems, I have seen only two systems with what I consider acceptable sample manifolds. Both N509 and N510 need to be much more specific as to the physical provisions for testing since the industry (and NRC) has not met (or enforced) the intent of the current documents or even used good engineering judgement. N510-80 is currently being revised and will carefully address this area.

9. My final comment is the observation that, contrary to the attitude or position of many people involved in NATS, we are not meeting the letter or intent of the nuclear specifications (A/E Specs/ N509/N510/NRC Regulations, etc.). All the engineering principles and experience for well designed HVAC type systems must <u>also</u> be included. We did not throw out good engineering practice when we <u>added</u> nuclear requirements.

IV. Summary

In summary, the diversity of theoretically identical systems constructed to the same standards and NRC regulations is unnecessary and counter productive. The NRC should improve their consistency in enforcement. The utilities and industry in general must work toward common systems rather than seeming to go out of their way to develop unique systems of QA, Audits, Security, Medical, etc., for each site. The A/E must work toward more common and well conceived specifications and bid review. Long term operation, maintenance and testing seem to be of very low priority in the overall design. The NATS fabricators must be more forceful in responding to inadequate specifications by pointing out weak areas and proposing alternates. In general, we must retain the objective of good engineering judgement as well as simply meeting all the specific "nuclear" requirements.

We all must work more closely and improve our communications at all levels. These conferences are excellent, but not enough of the working level engineers attend and the utilities are usually under represented. I propose we investigate some method to allow the designers and utilities personnel access to actual startup experience and later operational experience.

IN-PLACE TESTING OF NON ANSI-N509 DESIGNED SYSTEM

W. R. Lightfoot
Florida Power & Light
Turkey Point Plant

An immediate problem is trying to test older equipment to tighter regulatory standards. This process involves developing alternative test methods for situations where standard procedures just don't apply.

There are two problems with developing alternative test methods for non-standard situations; first, one is not always sure they will work, and second, change is not readily accepted.

In the first case, most systems have technical specification time limits for being out of service; therefore, the opportunity for experimentation is limited, especially if the results are unsuccessful or inconclusive.

Second, alternative tests, however valid, are more difficult to get reviewed, approved and audited than verbatim compliance because they require evaluation and judgement.

Recent events at an older plant have pointed to some of the problems that can be encountered when trying to get older systems to meet recent standards. For example, the internal cleanup systems located inside the containment have an inaccessible suction and do not mix air and aerosal uniformly. During a recent outage, several attempts were made to achieve uniformity by use of a field fabricated distribution header, all to no avail and multiple sampling had to be employed.

The multiple sampling technique entails its own difficulties in that both the 1975 and 1980 (ANSI N510) standards specify that the maximum reading for each traverse area be used. This is satisfactory for the downstream sampling but will yield a less conservative result when applied to the upstream readings.

The multiple sampling technique can be adopted for the HEPA filter test by manually moving from one area to the next, it just takes a little longer. In the case of the time dependant adsorber test, this becomes impractical especially in a large system with over one hundred trays. Therefore, a manifold was developed to get a representative sample.

In addition when using the multiple sampling technique, the standard specifies that the 95% confidence levels be calculated and reported, but doesn't specify if they should be used for acceptance criterion. Fortunately in our case, the lower limit was also satisfied.

These are some of the problems encountered and alternatives employed to ensure that a valid test was performed on a system not designed to be tested to today's standards.

DISCUSSION

MILLER: Two items come to mind. One, is that utilities don't seem to be anxious to change their technical specifications, I think, because that option opens up the docket and they end up with the intervenors sitting in their backyard trying to reopen a lot of other issues. Is there anything that can be done, or any steps that are being taken, to overcome some of the impediments to revising technical specifications?

BELLAMY: One of the best things that could be done in that area is to make sure that the NRC staff members at headquarters, specifically the licensing and operating reactor project managers, know in advance what your concern is and where you are headed. Make sure you discuss it with them so that you don't get into a big discussion later about what is right and what is wrong, and then find out after you have gone down a path, that the technical specification change that you have requested, for whatever reason, will come up with some road blocks in the future. I think it is also probably worthwhile to indicate that if a licensee takes the initiative and requests a technical specification change, there will be a fee involved with that process.

As a regulatory agency, the NRC is frequently called upon for interpretations, explanations, comments, and also receives its share of concerns, complaints and criticisms. Since Nuclear Regulatory Guide 1.52 was first issued in 1973, many of these discussions have related to air cleaning. In the paper, I have listed what I consider to be the eleven technical areas which have received more than their share of discussion since I have been involved in nuclear air cleaning with the Nuclear Regulatory Commission.

I discussed five of these topics briefly they were HEPA filter testing, applicable industry guidance, spinster carbon, definition of significance, and reactivation and reimpregnation. With respect to HEPA filter testing at quality assurance stations, revision 2 to Regulatory Guide 1.52 makes testing voluntary.

MILLER: Is the NRC doing anything to educate their inspectors to be more familiar with the type of air cleaning systems and some of the specific problems you mentioned today?

BELLAMY: I think that a lot of the problems I discussed today are also a part of the control room habitability study concerns that Mr. Hayes discussed earlier this week. I know for a fact that in Region 1, we have conducted a large number of seminars and everybody in that region knows my personal concerns with nuclear air cleaning. I have discussed them with my counterparts in the other regions and I would hesitate to stand before you and say that each of the other regions places the same emphasis on nuclear air cleaning that I require of my inspectors in Region 1, but I am personally trying to do as much as I can in that area.

KOVACH, J.L.:   The first question is related to painting. In some discussions, a slightly different number was being used, such as 100 sq. ft./1000 cu ft. However, I think when you paint an area, it should always be tied to the cfm of air being moved because that is more relevant. If you paint 1,000 sq. ft. in a control room where you may have 2,000 cu ft/m it may have a very different effect than painting 1,000 sq. ft. in an auxilliary building where you may have 40,000 - 70,000 cu ft/m. As I have stressed in the past, my preference would be to establish a painted area to cfm ratio.

BELLAMY: Or an air change ratio?

KOVACH, J.L.:   Something like that, rather than just an absolute number.

BELLAMY: I have to agree with you. As a matter of fact, the licensee I referred to as having a very detailed procedure to handle painting, does specify a square foot per cfm number.

KOVACH.J.L.:   A second question relates to carbon regeneration. If I find that I have a high Freon background in a particular area, and I strip the Freon off in order to run an in-place test, is that a regeneration?

BELLAMY: I would think not. By reactivation, I mean taking the carbon back and actually going through a high temperature process to reactivate the carbon. I think that any treatment in place that does not involve the use of chemicals, but involves just a flow of air at whatever temperature and humidity that you think is technically correct would not be considered reactivation.

KOVACH, J.L.:   So if I do a bad regeneration at 80 C, that is acceptable, but if I do a good regeneration at maybe 400 C, that is not acceptable?

BELLAMY: I am not sure I understand your point.

MILLER: I think he is asking you a trap question.

KOVACH, J.L.:   If I do it in-place, let's say at 80 C, by cranking up all the heaters and using as much humidity as I can get, and I manage to remove only some of the chemical compounds, which is a bad reactivation, that is acceptable? If I remove the carbon and really do a good job on it, that is not acceptable?

BELLAMY: I think that, if you took a sample of carbon after the reactivation and it passed your technical specifications, I would say that was not a bad reactivation, that it would be a good reactivation. But Bill Miller is right, you put me in a trap.

MILLER: I think what Ron Bellamy has said is that the NRC wants to see technical data and documented evidence to support requests of this type. They would rather not make decisions without some assurance that their decision is going to be conservative. How much conservatism is needed is always going to be open for debate. We have to allow a little leeway in this regeneration area, because we haven't got a lot of evidence.

BELLAMY: After you take a sample of used carbon and it does not pass the test, my preference would be to throw that carbon out, irrespective of whether it is spinster carbon or not, and use new, fresh virgin carbon.

JACOX: That is for ESF systems; how about non-ESF systems? This is another trap question.

BELLAMY: Personally, I hate to make distinctions between ESF and non-ESF carbon. We had a recommendation, in jest, a couple of years ago, that non-ESF carbon be painted blue and ESF carbon be painted red. As a matter of fact, when I first wrote the ASME CONAGT proposed code section on sorbent media I put that statement in it and it stayed there for about three drafts until somebody finally caught it and said, "What is this, a joke or something?" and I said, "Yes", and finally took it out. Technically, I would say that it is a lot easier for the licensee not to have differences in ESF versus non-ESF carbons. Unfortunately, I have to take a little exception and indicate that, as a regulator, I have a very hard time justifying how I could require the same quality of carbon in ESF systems as in non-ESF systems. If the licensee believes they can handle the logistics of keeping the carbons straight, and they think that they can save enough money to make it worth their while, I would have a hard time justifying before a licensing board that I have a technical position that says that I require the same quality of carbon in non-ESF as I do in ESF systems.

KOVACH, J.L.:   My next question is, when is Regulatory Guide 1.52 going to be revised? I have been hearing about a revision for a number of years.

BELLAMY: Let me say what I know about revision of Regulatory Guides. As long as there is, today, guidance available that is adequate to assure that we are protecting the public health and safety, the revision of regulatory guides, although a priority item, is not one of the highest priority items among the NRC staff. When it comes to what to work on, I would rather have people working on certifying that plants are safe than have them back in the office revising regulatory guides. We have gotten a lot of comments on Regulatory Guide 1.52. A staff member, as I recall, did go through it and propose some revisions, but, again, budget constraints and personnel constraints, although not putting it on a back burner, has put it into a status where, I belive , we are not considering trying to obtain a contractor to do it. I discussed this specific question with Bill Gammill a couple of weeks ago, and I believe that he has authorized me to say that you will not see a revision to this regulatory guide this year. It would be nice to see it out in late 1985, but sometime in 1986 is probably a more realistic date.

MILLER: We should also point out that Mr. Landis, earlier this week, mentioned some of the problems you get into when you are revising your codes and standards at the same time that you are writing new or revised regulations. Based on the 70 pages of comments that the ASME Committee on Nuclear Air and Gas Treatment received from Mr. Kovach, we are in the middle of a rather major revision, both editorial and substantive, of N510. We would hope that we could get that pretty near finished before the regulations are re-issued, so that an improved version of N510 could be referenced.

KOVACH, J.L.: It was only 60 pages.

BELLAMY: I hope I have made it very clear in this forum, and in other forums, that it makes our job as regulators much easier to have a consensus standard that we can reference instead of having to generate our own technical positions. So, I look to either ASTM or ASME for further written guidance on the definition of significant painting areas.

HYDER: Concerning the paint question, I have heard rumors that there may be paints that do less damage to carbon than conventional paints. I wonder if anyone knows of these or has any experience with them?

MILLER: Latex paints, those with a water base are much better.

VOGAN: Just a comment regarding reactivation and im-pregnation. At last week's CONAGT meeting, the subcommittee on air cleaning equipment initiated the preparation of a test program designed to find ways to perform the reactivation and reimpregnation that would qualify the carbon in conformance with Regulatory Guide 1.52. We hope that we will have enough evidence in a year or so to show that reactivation is, or is not, an acceptable process.

JACOX: On one of the points that you, Dr. Bellamy, list-ed in your paper and showed on a slide, but didn't address in your talk, is the system size limit of 30,000 cfm. You mentioned something to the effect that you hadn't seen adequate data to prove that DOP gen-erators or halide generators could adequately challenge larger sys-tems. Since 1975, systems in the 60,000 to 90,000 cfm range have been tested regularly. My specific question is, in what format should the data be presented to satisfy you that, in fact, there are genera-tors that can adequately test these much larger systems.

BELLAMY: There are abstracts of one or two papers at the last Air Cleaning Conference that I had hoped would have answered that question but, instead, they headed off into discussions of electronic instrumentation that I am sure was a great benefit to people, but was disappointing to me. To answer your question, I would look for data from an actual installation that would tell me exactly what the concentrations were at various locations upstream of the bed and that these concentrations remained constant at all the locations during the entire course of the in-place leak test in compliance with the ANSI standard. I've heard at meetings such as this that there is no problem, that the data are available and easy to get, but I maintain that I still have not seen such data.

MILLER: You mean that you look to conferences like this as a way to present to peers data of this nature and that you would consider its acceptance by attendees to be a semi-peer review after which you could, maybe, accept it?

JACOX: Would listings of the operating plants and the specific systems, with the flow rates that have been accepted, be something you would consider as adequate in the presentation of data.

BELLAMY: I would consider that totally inadequate. I would want to see the basic data that were used during the running of the tests and have them tell me again exactly what the concentrations were. I thought you implied that all I should need was a document showing that an operating plant has a 70,000 cfm system and that Company A tested it at 70,000 cfm on certain dates for the last four years. That doesn't do me any good. I would want to take a look at all the data. My technical position is that the 30,000 cfm number is as good as any other number, so why change it. I think one of the hardest questions we would have to answer (from the Advisory Committee on Reactor Safeguards and from all other commenters) before a new

Regulatory Guide was issued is, "What is the basis for changing to another number?" If the proposal is to change to 50,000 cfm, why 50,000 instead of 60,000? Or, why 80,000 instead of 50,000? We now have a number that is adequate and acceptable and we are not presently seeing newly designed systems for new operating power plants. Maybe we should put this whole discussion on hold for a couple of years.

MILLER: We wanted to have people on the panel who have done testing in the plants and I think for the most part these are the type of people we have here. I don't believe they realize that there is an opportunity at a technical conference like this for them to make some serious input to important questions and to listen to some speakers relevant areas.

PAPAVRAMIDIS: How often are you doing in-place testing of used carbon filters, and how often are you taking samples of the used carbons?

HUBBARD: It is outlined in the technical specifications for the plant: carbon samples every 720 hours and in-place testing every 720 hours. We don't increase the test frequency above what our technical specifications call for. We have seven units, its different from plant to plant.

MILLER: I want to remind the audience that Duke Power Co. is in the unusual position of having older vintage plants that have pre-N509 filter systems with all the associated testing difficulties, as well as some that have been designed to N509 criteria.

CHOI, S.: You mentioned that insurance companies no longer require fire protection systems on charcoal. Is that position also accepted by NRC?

HUBBARD: I didn't mean to say they no longer require
them; they are still inplace in our plants. I was suggesting that
the industry come up with a conclusive statement that such systems
are not necessary for fire protection. The name charcoal must have
reminded the insurance industry of a backyard grill. Nuclear carbon
does not burn at the same temperature as fireplace charcoal that
contains organics that permit it to burn at much lower temperature.
I am suggesting that the danger of fire protection systems capable
of filling our deep beds with water, and producing the obvious con-
sequences, outweigh any benefits there might be from having such
systems in place. I don't know whether the insurance companies
will accept this view, but I think it is a fair statement.

CHOI, S.:   We hear a lot about the problems associated with
fire protection systems, and we are wondereing if they are really
necessary, recognizing the remote possibility of system usage. I
am curious about your statement.

HUBBARD: It has been suggested by certain people that the
introduction of cool air would be much more beneficial in retarding
fire than water. We support that view.

ORNBERG: I'd like to recommend that your appendix, that is
attached to the paper, be considered for addition to N510 or some
other appropriate standard, as a non-mandatory appendix. It
certainly is geared toward your own plant, but it would be helpful
to other utilities in setting up a similar program. My question con-
cerns the course you are giving at Duke,   is it open to other
utilities and engineers?

HUBBARD: Let me take this opportunity to make some addi-
tional comments about the course at Duke. It is not in competition
with the course offered at Harvard, that, I might mention, is an
excellent one. The main reason for establishing the course is to
address field testing at nuclear utilities. It is open to outside
people and always has been. It is a policy of our management to open
it even more for the benefits of sharing information among utilities
and improving the level of testing and associated work that we do.

VOGAN: I have a question regarding third party inspec-
tion, or testing of carbon. How long have you been doing independent
testing of carbon batches?

HUBBARD: We started the beginning of this year.

VOGAN: Have you a lot of data at this point? Have you
noted any significant differences between the manufacturer's report
of test data and the third party test data?

HUBBARD: We have noted some differences, but it is hard
to know what caused the differences because we are at the early
stages of collecting the information. The results are not yet con-
clusive by any means. When you examine the cost of replacing carbon
before it is time to do so, taking into account the labor cost and
downtime, the cost of verifying the tests on your own carbon is
worthwhile.

VOGAN: Do you expect to continue the practice for the next couple of years to obtain more data for the industry?

HUBBARD: Yes, we do.

JENKINS: What prompted you to start doing independent testing of the carbon? Didn't you believe the results you were getting from your supplier?

HUBBARD: There were multiple reasons. The first one cited is that if carbon, for some reason, did not meet specifications, the cost to replace it can be astronomical. We have some systems where we have to bring the unit down when we have to replace carbon and that has a tremendous impact on us. That is part of it. But is your question, "Did we suspect bad carbon?"

JENKINS: Were you in a situation where you put new carbon in, then did in-place testing, and found it didn't pass? I am trying to find out why you started doing that.

HUBBARD: We have had cases where carbon life has been very short. Not having initial data of the new carbon (since it is not usually transmitted to us by the vendor) and being independent, at that, we felt it would be beneficial to have baseline data. Plus, we are interested in examining the trend in carbon life so that we can understand it better. There have been cases where people have inadvertently shipped carbon that did not meet specifications. I won't go into any reasons why that might have happened, I will assume it was accidental.

MILLER: I can't resist the temptation to assign an action item here and say, we look forward to your report on trends in carbon life at the 19th Air Cleaning Conference.

BELLAMY: On that subject, I would like to make two comments. The first is that we are still getting a big push that every HEPA filter should go to a DOE quality assurance station. If you can justify that for a HEPA filter, you can very easily justify a third party test on carbon. Secondly, I think that Licensee X should be applauded for its efforts because the additional cost for having a third party radioiodine test (unless I am a couple of years behind, and I welcome being corrected) is somewhere in the high hundreds to one thousand dollars. (I have just been informed that it is from low hundreds to the high hundreds for a test, so the cost isn't significant.)

JACOX: Based on some of the discussion that has taken place in the last few days, there are three items I would like to add to my prepared comments. First, when Mr. Landis gave his talk, he prefaced it by saying that nuclear safety standards should include something other than minimum legalistic safety requirements. They should be cognizant of functionality, efficiency, practicality, and some of the requirements of the real world. I applaud this greatly. It is something that I have been trying to push with CONAGCT and is a matter that I will be addressing in some detail in a paper I will be presenting this afternoon. Second, I think the paper presented by Mr. Hayes that was prepared by a number of NRC people, on control room habitability, should be greatly applauded by us all. Not simply for the technical expertise, which I believe is going in the right direction, but perhaps more importantly, at least in my experience with air cleaning, is aimed toward an awareness of real problems, not just looking at very narrow, strictly legalistic approaches. I am extremely encouraged by that, and I feel that we all should be. A third comment is that I have been involved as chairman of the CONAGT sub-committee for field testing, with Dr. First as the subgroup chairman, trying for many years to get a personnel qualification standard approved for those who do N510 testing, but the utilities, including Duke Power Co. have opposed it. If everybody was in the same position as Duke, as far as expertise and training, consistancy in taking care of personnel turnover, etc., we all have agreed internally that we would not need a personnel qualification standard. I think their activities in this area are an example to be applauded and one that other utilities should follow.

MILLER: Wouldn't INPO be a logical group to come up with the standards you recommended since they have most of the utilities chartering them and paying the tab?

JACOX: I certainly think so. They were giving a health physics training program, but I don't know if they still do. When I inquired whether or not it would be possible to attend, I got an equivocal response; yes, it was possible I could attend, but, it was really intended for utility people. I wrote to something like thirty utilities with whom we had open contracts and universally they responded, when we got any response, that they would not accept the INPO course in place of their own internal training procedures. So, obviously, there is a waste.

MILLER: You are only interested in doing away with the generic type of training, not the plants specific training?

JACOX: Absolutely, no question. You do need a couple of hours of plant specific orientation, but not, what is gamma versus beta, i.e., the usual generic thing that you have to sit through.

MILLER: One of the problems our utility representatives
have making committee meetings and attending sessions like this,
is that they are usually on the critical path for a shutdown or
startup and I really appreciate the fact that two were able to be
here today.   Is there an advantage to doing adsorber tray refilling
on site or is it better to send them back to the manufacturer to have
it done?

LIGHTFOOT: We don't have any experience filling trays on
site, our trays have been refilled at the factory. I do not see a
large-scale on-site change out as a practical solution unless the
time available made that the only practical alternative.

EDWARDS: On the impracticality of doing multipoint samp-
ling for carbon, for large carbon banks, not only is it impractical,
it is impossible given the time constraints of carbon breakthrough.
I believe you will peak-out on any detector before you can do multi-
point sampling. Jack Jacox, with regard to Bill Miller's question,
whether anybody agreed with your comments; I think everybody here
agreed with all your comments. Particularly, two points. One, about
sitting through classes that everybody has to attend when they go
into a plant. Second, the fact that after the very fine specifica-
tions that someone like Sargent & Lundy writes for a technical
support center, and the very fine purchasing that is done by the
architect-engineer, or the purchasing division, the piece of equip-
ment that is finally delivered and accepted bears no resemblance to
the specifications, and is therefore not testable. These occurrences
are far more common than even this audience may realize. Now, I
have one comment and one question·for Dr. Bellamy. As a general rule,
a carbon supplier will have carbon on hand that has been tested to
the latest test standards of Table 5.1 in N509-1980. But, most
plant technical specifications call for carbon to meet Regulatory
Guide 1.52, and if the technical specifications have been updated to
the '78 version, that is a very late revision. When someone refers
to Regulatory Guide 1.52-1978, which in turn refers to ANSI N509-1976,
Table 5.1, the table in the 1976 document refers to an RDT test
method, of no date, this is important because RDT test standards are
superseded and, according to Webster's, when something is superseded
it is no longer valid. Because the latest RDT is 1977, we are in a
position where a 1976 document is referring to a 1977 document, which
has exactly the same test conditions as ASTM D3803, which is exactly
what is referenced by N509-1980. So, you have a 1978 document that,
through this trail of reasoning, gets ahead to the 1980 version of
N509, Table 5.1. Do you agree with this, Dr. Bellamy?

BELLAMY: If the RDT is automatically superseded by a new
issue, it is clear to me that the newest issue out is what would be
the applicable reference through the tortuous path that you have
just traced; therefore, the answer is, yes. Let me offer a further
thought that maybe can satisfy your concern. The problem that arises
is that a carbon supplier has carbon on his site that has been fully
tested in accordance with the latest issued guidance, although the
latest guidance is not what is referenced in the technical specifi-
cation. The immediate question is, what does the carbon supplier, and
what does the licensee, do to satisfy the technical specifications.
It is my position that the latest ANSI N509 Table and the ASTM
standard which superceded that table, are the best available guid-
ance around today. If you have carbon on site, whatever site that
is, and it satisfies the criteria, that carbon is acceptable to be
installed in your ESF filter systems. I will go one step further
and say very clearly, specifically in Region I, which is the region
that I have jurisdiction over, there will be no potential enforcement
action or discussion with the NRC if an inspector comes back and says,
the technical specifications that were applied were the 1976 version,
not the 1980 version.

HAYES: We don't have a problem with that interpretation.
I think the problem that Ron Bellamy refers to is a regional one,
that is, the way regional inspectors interpret the technical specifi-
cations when making inspections. Region I is fortunate in having
someone like Dr. Bellamy who is quite familiar with the problem.

ORNBERG: I think an easy way to solve this and get all
the regions together is for the NRC to put out an information notice
advising people of the facts of the case. We are expending a lot of
effort going through arguments on technical specifications. The
three weeks that Jim spent tracing all this through, everyone is
doing over and over again. I am getting calls practically every
month from people who ask this type of question. Can't we find an
easy way to distribute the information so that everybody is together
on it?

HAYES: One of the things we face as regulators is we
really do want to help the licensee and we say, go to the new stand-
ards. But the licensee somehow thinks that the new standard is more
restrictive and says, no, I don't want that; I still want the RDT
161T standard, 1973 version. That is a problem we sometimes run
into.

MILLER: They want the best of both worlds. There are
very few times that, in a standard as complicated as N509, there
won't be somethings that are more restrictive. At the same time,
in other areas, it is more informative.

EDWARDS: In this case, however, N590-1980 is less restric-
tive than the 1976 version. I have another question for Dr. Bellamy.
Suppose a utility sends a carbon sample to a laboratory for testing
and the results come back a failure. Lets say that the cutoff point
is 95% and the results come back 94.5%. They know this carbon
shouldn't have aged that much, so they send another sample off to
the same laboratory, or even to a differnt laboratory that tests
according to the ASTM standard, and it comes back 95.5%, a passing

grade. Which result is acceptable? Is the passing result acceptable because here is a test result that passes, or is the result that failed the one you must abide by because you have positive proof the carbon failed?

BELLAMY: That problem has arisen, it is not a make believe problem, and I guess I have gotten at least a double figure number of calls with that specific question. The licensee's responsibility is to operate the plant so as to adequately protect the public health and safety and it is our job to verify that he does that job. If the licensee came to me with those two sets of test results, I would strongly recommend that he run a third test at an independent laboratory so at least he has a majority vote on which direction to go. I would say that the licensee would do well to justify in an internal memo, I don't think a submittal to anybody would be necessary, why he doesn't like the 94.5% result and why he believes he can operate his plant in accordance with the technical specifications even though he has that one piece of information that says it may be time to change out the carbon. Again, I will make the recommendation that you use the consulting services of the onsight resident inspector. I strongly recommend that he be informed about what is going on up-front and that you make sure he clears it with the regional manager before you go off and decide to ignore a piece of applicable data, which is what you would be doing. I think that the numbers that you used make a very easy case. If it is 94.5%, and 95% is the cut off, that is an easier question to answer than if you said one came back 60% and the next one came back 96%. Then, it would represent a greater quandary.

JACOX: I just have a comment for Mr. Edwards; the latest RDT is October 1981.

BAUM: I have a question for the utility members of the panel. I am interested in how to make specific the point about significant contaminants in charcoal? Do you have procedural guidelines that define in specific terms not only paint, which was covered, but also smoke, solvents, chemicals, etc.?

HUBBARD: Obviously, it hasn't all been defined. Are you asking about our approach to evaluating welding and painting?

BAUM: Exactly. Since it isn't well defined in the technical specifications, I would expect there would be some additional definition in procedures used by a given utility that would address specific cases such as welding, painting, or an accidental spill.

HUBBARD: If at all possible, we avoid bringing anything like that into our systems. If it is possible to shut a system off to do any work of that kind, and let it dissipate for a period of time, we will do so. If there is any question at all, we send a sample for analysis. The procedures are not well defined and we haven't developed guidelines. Therefore, if there is any doubt, we sample to erase any doubt.

MILLER: Bill Lightfoot, didn't you acknowledge in your paper, that different plant operators approach the matter differently?

LIGHTFOOT: I would like to say, as Dean Hubbard did, that the solution to the problem is to avoid it. At our plant, during outages, we wrap our filters in polyethylene. Most of the systems in our plant are standby systems, and our technical specifications define the operational exposure of the systems to these fumes. What we try to do is to avoid the problem, rather than having to take corrective measures.

BELLAMY: First, to my knowledge, there has not been any enforcement action taken against any licensee with respect to the definition of significant. Second, if by the use of the term significant, we have informed the nuclear industry, in both this country and abroad, about our concerns, and they have then taken the appropriate steps, I think all of this discussion, and maybe some of the potential ambiguities in the use of the term, significant, is something that we should live with.

AINSWORTH: Are you suggesting that spinster carbon from one plant may be reimpregnated and supplied to a second plant? And if so, can the second plant use several sources of spinster carbon?

BELLAMY: The point I was trying to make was that, if you have spinster carbon at one station and you reimpregnate it with TEDA or KI, you can then test it, and if it satisfies all the applicable regulations, I am not sure that the NRC would have a legal basis to tell you that you could not install that carbon in another filter system or at another station. If your question is, what if you want to get four or five different amounts of spinster carbon from four or five different stations, I would have to say that each case would have to be evaluated independently. I would also suggest that each separate carbon (I won't use the term lot or batch) that you put into the new station, would have to be individually in-place tested, or a sample of carbon taken out for radioiodine testing, in the future, to verify that weathering has not occurred during the use of that particular carbon. I think the answer to your question is, yes.

AINSWORTH: What would be the objection to reimpregnating a carbon that already has KI on it with KI?

BELLAMY: I can't, technically, tell you what my judgements are. The specific question you proposed was, if the carbon only has had KI on it, what about putting TEDA on it? You heard my response to that. I did not try to imply that there would be a different decision if the carbon has KI on it, and if someone wanted to put KI on it. I think that if you had a KI plus TEDA impregnated carbon, you would be hard pressed to convince me that by adding additional impregnants you could bring it back up to specification. I'd say there is probably something else wrong with the carbon.

934

HAYES: As part of the control room habitability review
that we are doing, we are surveying the as-built control room systems
for three plants. One of the things we wanted to determine was
whether the utilities tested the various filtration systems in the
control room in some sort of an independent manner for the purpose
of determing the functionality of the control room system, versus
testing it for either a preoperational test or for the purpose of
meeting surveillance requirements. We have only done two of the
plants, and that is not a representative sample, but it would appear
that probably the only reason for testing is to meet either pre-oper-
ational test requirements or surveillance tests. I would like to
emphasize Jack Jacox's point, it is your plant, and you should be
doing things to benefit your operations.

WILHELM: I would like to make one remark on testing. We
have made, up to now, roughly 3,000 tests of carbon samples and at
least 500 in-place tests on real filter systems inside a reactor
using methyl iodide-131 as a test medium. I point this out so you
can see there is a background to what I am going to say. Our ex-
perience is, if you get your filter poisoned by solvents, for
instance from paint, you will do better to take the sample eight hours
later because the high volatile fraction will be gone and your carbon
will give satisfactory test figures again. Otherwise, you will
throw carbon away that is still good. Let me give you an example.
After making repairs, including painting, in a PWR, they looked at
their filter and it seemed not to be good. They tested the carbon
and it was down to 60%. Three days later, it was up to 99.5% again.
That is one point. The second point is that, in Germany, the price
for a test is roughly the price for a lot of carbon. I think we
could have new carbon to refill our refillable, they are refillable,
filters at least five times for the price of the tests, so that
really doesn't make sense. I have one question, my standard
question, why don't you use deeper filters? You would get rid of
80-99% of your problems.

MILLER: I think we are very well aware that the European
approach is to use deep bed filters. I have to apologize to Dr.
Wilhelm because, this being our maiden flight for this type of panel,
we have concentrated on US utilities. What I would like to see at
the next Air Cleaning Conference would be a world-wide testing expe-
rience panel where we can hear more of the experience of the European
utilities and the way they solve their problems. I think it doesn't
pay us to be parochial in this area.

                          I want to be sure that everybody understands,
first of all, that there is a process that is available for people
who have questions on the interpretation of standards and codes that
are written under the ANSI consensus standards and codes process.
For both ANSI N509 and N510, your specific questions should be direct-
ed to ASME in New York and they will be answered. That is the good
news. The bad news is the time it takes. Because of the litigious
climate we find ourselves in, there is a very specific consensus
procedure that we have to go through in order to arrive at an answer
and have it approved. I would say that, on average, it will take at
least six to nine months for you to get an approved answer concerning

an interpretation of a standard. That doesn't mean there aren't people in this room, members of CONACT, who could give you an opinion, but I think you have to be aware that when you make a decision based on an opinion, you can not go back to that opinion looking for compensation for a mistake that was made. The reason I make that comment is, not only to inform you that the process can be long, but to expand upon Jack Hayes' remark. I get the feeling within the nuclear power industry that Air Cleaning Conferences are not held often enough to permit us to discuss the types of problems that we have heard about today. For example, the poor fellow who is fighting the eight dogs on the door, that Jack Jacox referred to, isn't interested in waiting for six months for the five extra hands. Therefore, I will take seriously Jack Hayes' recommendation to explore with the Main Committee of CONACT an appropriate vehicle for fostering this type of activity. I would appreciate written comments on any of the standards that CONACT has published, or any of your ideas on holding a workshop to foster improvement in the testing area. I also want to mention that we haven't considered revising the ANSI N509 document up to now. We are developing codes for all the equipment covered in N509. Our hope was to get all of those codes issued, and not have to revise N509. However, the five year period at which time the N509 standard must be reviewed, is coming due next year and we will have to develop a position on revision. If there are people who want us to revise N509 quickly (and it can't be any quicker than a year or a year and a half) we would appreciate hearing from you on that point also.

I became aware today that there is an NUS network. I am familiar with the INPO network, where people can communicate with other utilities with similar problems and get answers to their questions, but two of our speakers mentioned to me that they have used the NUS network. They are not sure who operates the network but it is important for us to understand what network we are putting our questions on so we can help each other. NUS is a private network and there is probably a subscription fee for its use. INPO specifically set up their network to create more communication but we haven't seen many questions on filter testing or air cleaning. Is there any reason why it is not convenient to use the INPO network? Let's all agree that we will go back to our organizations and find out if there is a problem with the INPO network. If so, let me know. Otherwise, let's put some questions on air cleaning on the network so we can help you answer questions.

Session 14

RECOVERY AND RETENTION OF AIRBORNE WASTES: NOBLE GASES

WEDNESDAY: August 15, 1984
CHAIRMEN: R.R. Bellamy
U.S. Nuclear Regulatory
Commission
V. Deitz
Naval Research Laboratory

ALTERNATIVE MODES FOR CRYOGENIC KRYPTON REMOVAL
L.P. Geens, W.R.A. Goossens, G.E.R. Collard

BEHAVIOUR OF IMPURITIES IN A CRYOGENIC KRYPTON REMOVAL SYSTEM
R. von Ammon, W. Bumiller, E. Hutter, G. Knittel, C. Mas, G. Neffe

SELECTIVE ABSORPTION OF NOBLE GASES IN FREON-12 AT LOW TEMPERATURES
AND ATMOSPHERIC PRESSURE
E. Henrich, R. Hufner, F. Weirich, W. Bumiller, A. Wolff

CHROMATOGRAPHIC SEPARATION OF KRYPTON FROM DISSOLVER OFF-GAS AT LOW
TEMPERATURES
H. Ringel, M. Meßler

OPENING REMARKS OF SESSION CHAIRMAN BELLAMY:

Welcome to Session 14, entitled "Recovery and Retention of
Airborne Wastes: Noble Gases". As an introduction, I'd like to
comment that all of the papers in this session are contributed by
foreign authors, from Belgium and West Germany, and all papers
are continuations of work reported at previous Air Cleaning Conferences.
Past Conferences have also had U.S. laboratories' participation, as
well, but the lack of their participation this time is noteworthy.
Perhaps this reflects a lack of support in this country for fuel
reprocessing activities, a large source of noble gases. Some of the
results of the studies that will be described may also be applicable
to offgas streams at electric generating stations.

ALTERNATIVE MODES FOR CRYOGENIC KRYPTON REMOVAL

L.P. Geens, W.R.A. Goossens, G.E.R. Collard
S.C.K./C.E.N., Mol, Belgium

Abstract

In the past, oxygen elimination was considered as a necessary pretreatment before cryogenic krypton removal from reprocessing off-gases. In this view, the catalytical reduction of oxygen with hydrogen was investigated in the DEOXO unit, in which a Pd and a Ru catalyst are used. At a gas flow rate of 30 $Nm^3.h^{-1}$ and an oxygen feed concentration up to 15 % volume, the oxygen content in the feed gas of the cryogenic unit could be reduced to 0.5 ppm volume. For the following experiments, the DEOXO unit was connected in series with an adsorption drier and the cryogenic distillation unit. No technical problems arose during the 80 hours' run. Furthermore no significant build-up of an oxygen rich layer in the cryogenic rectification column was observed.

At present increased attention has been devoted to krypton removal in presence of air. In that perspective the study of the selective catalytical reduction of NO_x with ammonia in the DENITRO unit becomes part of the flowsheet. With the use of a H-mordenite catalyst and an ammonia excess of 30 %, the NO_x concentration in a 25 $Nm^3.h^{-1}$ gas stream could be reduced from more than 1 % volume to lower than 1 ppm volume.

The oxygen behaviour in the cryogenic distillation unit was also investigated. Temperature profiles in the rectification column were recorded for different oxygen feed concentrations. At the same time, oxygen analyses were performed to gain information on the oxygen distribution in the column. Although an oxygen rich layer was built up in the column, the krypton-xenon bottom product contained less than 0.1 ppm volume oxygen, so that no oxygen was transferred to the second column. This favourable oxygen behaviour, combined with the feasibility of the selective catalytical NO_x reduction is promising for the cryogenic krypton retention in the presence of oxygen.

I. Introduction

Cryogenic distillation is one of the most advanced processes for the removal of krypton from reprocessing off-gases [1, 2, 3, 4, 5, 6]. The choice of a cryogenic process implies the preceding elimination of condensable compounds from the feed gas, the most important of which are iodine, nitrogen oxides, water vapour and carbon dioxide. For iodine removal several methods have been developed. Water vapour and carbon dioxide can easily be eliminated by adsorption on silicagel or molecular sieves.

In the past, besides the removal of the above-mentioned compounds, the elimination of oxygen was also considered as a necessary pretreatment step. In fact, it was thought that the presence of oxygen in the cryodistillation unit could give rise to ozone formation and accumulation representing an explosion risk. An obvious method for oxygen elimination is the catalytical reduction with hydrogen because nitrogen oxides can be reduced at the same time. The first part of this paper deals with this item. The cryogenic distillation itself in absence of oxygen, which is the next step in an integrated gas cleaning system, has already been reported earlier [6, 7].

Since a few years, cryogenic krypton removal without preceding oxygen elimination is gaining ground [8, 9]. Indeed, the use of large amounts of hydrogen does not only create a serious hazard problem, but it also increases the cost price of the entire process [9, 10]. Recent research work revealed that the accumulation of ozone in the cryogenic distillation unit can be reduced and even prevented by applying the proper operation mode [11]. The omittance of the oxygen reduction step necessitates a selective nitrogen oxides elimination step. While others study a scrub process with hyperazeotropic nitric acid at low temperatures, the S.C.K./-C.E.N. has chosen the catalytical reduction of NO_x with ammonia for this purpose [12, 13, 14]. The first experience with this process is treated in the second part of this paper.

In the third part, the results of the experiments with oxygen in the feed gas of the cryogenic distillation unit are discussed.

II. Catalytical oxygen reduction with hydrogen

Description of the DEOXO unit

The catalytical reduction of oxygen with hydrogen was investigated in the DEOXO unit, a flow sheet of which is given in Figure 1. This unit was designed to reduce the oxygen content in a 50 $Nm^3.h^{-1}$ air stream down to 1 ppm volume. The main part of this installation is the packed bed reactor, which contains three layers of alumina supported catalysts. The upper layer is a silver layer, which acts as an additional iodine trap. The second, a palladium catalyst, is the most effective for the reduction of oxygen. The lower layer, which contains a ruthenium catalyst, is more effective for NO_x reduction. The exit gas stream is then cooled in a shell and tube heat exchanger. Most of the cooled gas is recycled with the help of a roots type compressor in order to dilute the inlet gas stream in such a way that the hydrogen explosion limit after the hydrogen supply is not exceeded. Another important part of the unit is this hydrogen supply, which is controlled by an hydrogen excess measurement after the reactor. Table 1 summarizes the main design characteristics of this DEOXO unit.

Table 1 : Main characteristics of the DEOXO unit

Maximum gas flow rate	: 50 $Nm^3.h^{-1}$
Operation pressure	: 0.51 MPa
Catalysts	: Pd, Ru (Ag)
Oxygen inlet concentration	: 2-20 % volume
Oxygen outlet concentration	: 1 ppm volume
Inlet temperature	: 283-308 K
Outlet temperature	: 303 K
Maximum reactor temperature	: 723 K

Experimental results in the DEOXO unit

The experimental conditions of the DEOXO unit had in practice to be limited due to the constraints of the hydrogen supply. The suitable electrolyser, initially foreseen as hydrogen source, could not be used for technical reasons. The hydrogen delivery capacity of the replacing bottle racks was limited due to safety reasons, in such a way that the maximum applicable gas flow rate and oxygen inlet concentration were 30 $Nm^3.h^{-1}$ and 15 % volume respectively. During the start-up period, which
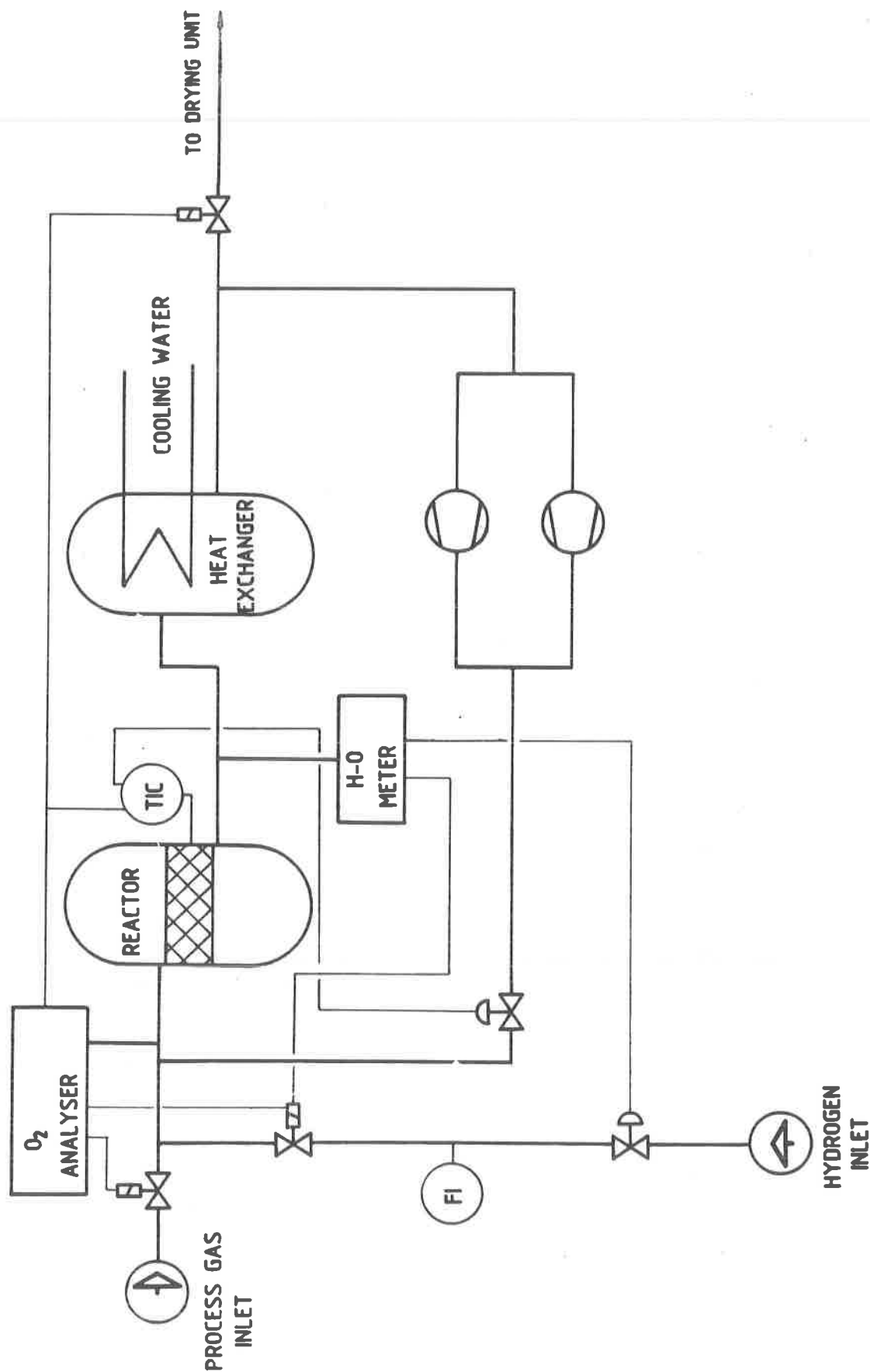
FIG. 1 FLOW SHEET DEOXO UNIT

lasted for about 8 hours, the oxygen inlet concentration was increased gradually to the desired level. At equilibrium, which was reached after two hours more, the oxygen outlet concentration was 0.5 ppm volume, which certainly meets the design value of 1.0 ppm volume. The hydrogen excess in the treated gas at equilibrium amounted to about 2000 ppm volume, a good deal higher than the design value of 500 ppm, but this caused no operation difficulties. Some results of these experiments are summarized in Table 2.

Table 2 : Experimental results in the DEOXO unit

Experiment number	1	2	3	
Gas flow rate	20	25	30	$Nm^3.h^{-1}$
Reactor temperature	673	673	673	K
Oxygen concentration IN	10.0	9.0	15.0	% volume
Oxygen concentration OUT	-	0.5	0.5	ppm volume
Hydrogen concentration OUT	0.22	0.18	0.20	% volume

In a subsequent experiment the DEOXO was connected to an adsorption drier, in which water vapour and carbon dioxide are trapped on molecular sieves. In a membrane type compressor, the dried gases were compressed up to 7 bar and fed to the cryogenic distillation unit. These three units in series were run for 4 days, without any technical problems. No build-up of an oxygen rich layer in the cryogenic rectification column was observed during this relative short run.

These experiments have demonstrated that the catalytical oxygen reduction is a suitable pretreatment step before cryogenic krypton removal. However, before testing it under radioactive conditions, some additional features will remain to be investigated such as : the reduction of nitrogen oxides and the behaviour of methane in the installation, which can be very important for the cryogenic distillation.

III. Selective catalytical NO_x reduction with ammonia

Process chemistry

The selective catalytical reduction of NO_x with ammonia was already studied in earlier times at the S.C.K./C.E.N., on laboratory scale (12). From a screening test of various types of catalysts, the synthetic hydrogen mordenite appeared to be the most active one. The over-all reaction equations which resulted from these experiments, are the following ones :

$$2 NO_2 + 4 NH_3 + O_2 \rightarrow 3 N_2 + 6 H_2O \tag{1}$$

$$4 NO + 4 NH_3 + O_2 \rightarrow 4 N_2 + 6 H_2O \tag{2}$$

$$2 NH_3 + O_2 \rightarrow N_2 + 3 H_2O \tag{3}$$
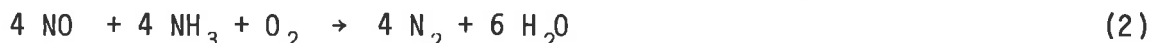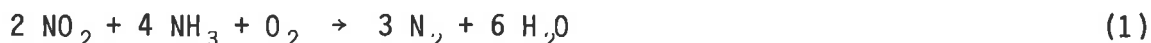
Description of the DENITRO unit

Based on the laboratory results, a pilot installation with a gas through put of 25 $Nm^3.h^{-1}$ was designed. The flow sheet of this DENITRO unit is shown in Figure 2. The incoming process gas is first compressed from a pressure slightly above atmospheric pressure up to 0.5 MPa, in a membrane type compressor. In a compact,
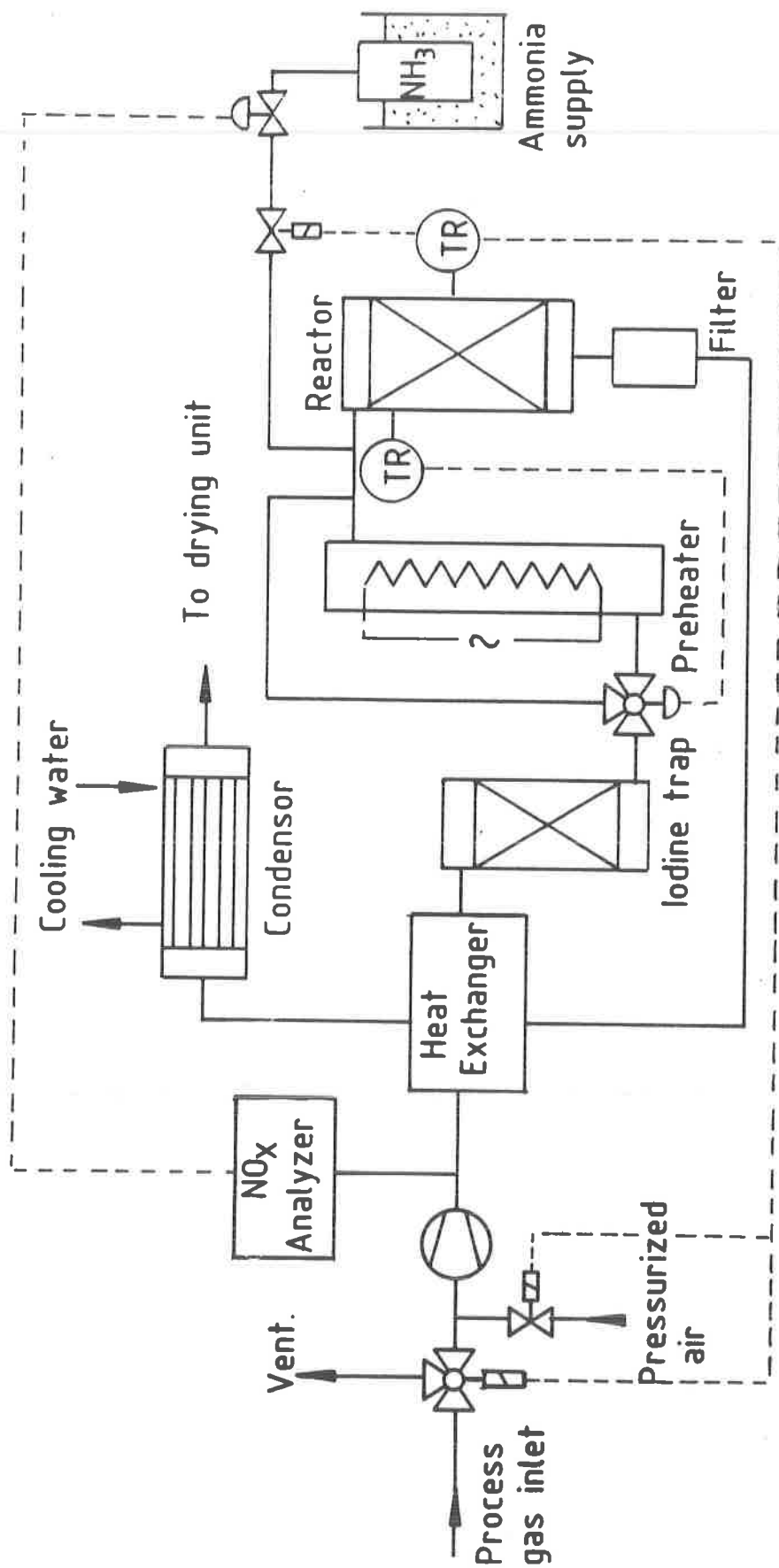
FIG. 2 FLOW SHEET DENITRO UNIT

helicoidal type heat exchanger, the inlet gases are heated by the treated gas stream. After the heat exchanger, an iodine trap is provided to remove any traces of iodine, which might decrease the catalysts lifetime. The iodine trap consists of a fixed bed of silver exchanged zeolites. Before passing to the reactor, the process gas is further heated in an 8500 W electrical preheater. The required amount of ammonia is fed to the main gas stream in top of the reactor. The ammonia is supplied from a bottle rack, which is heated by means of a water bath. The ammonia supply is controlled by the NO_x inlet concentrations. The reactor temperature is kept between 673 and 723 K by electrical heating. As already mentioned, the catalyst used is a synthetic hydrogen mordenite, zeolon 900 H (Norton Chemical Process Products). Catalyst dust particles in the treated gas stream are retained in a 10 μm filter, mounted right after the reactor vessel. Finally the treated gas is cooled, first in the above-mentioned heat exchanger, followed by a water cooled condensor. In Table 3 the main operating characteristics of the DENITRO unit are summarized.

Table 3 : Operational characteristics of the DENITRO unit

Gas flow rate	:	$25 \ Nm^3.h^{-1}$
Operating pressure	:	0.42 MPa
Catalyst	:	H-mordenite, Zeolon 990 H
Reactor volume	:	$20 \ dm^3$
Reactor temperature	:	673 - 723 K
NO_x inlet concentration	:	1 % volume
NO_x outlet concentration	:	1 ppm volume

Experimental results in the DENITRO unit

A first series of experiments in the DENITRO unit was performed with NO in the feed stream up to 1 % volume. Both NO_x inlet and outlet concentrations were measured with a chemiluminescence analyser, the former after dilution, the latter without. Frequently plugging of the tubings in this analyser caused severe operational problems, since the ammonia feed is controlled by the NO_x inlet concentration measurement. As a consequence, the analytical instrumentation had to be completely renewed. At the moment NO and NO_2 inlet concentrations are measured separately by means of I.R. spectrophotometry, without dilution. Also both outlet concentrations are measured separately. For this purpose, two analysers based on a voltametric sensor were purchased, which appear to have a much better operational reliability.

The latest experiments in the DENITRO unit are carried out with an NO_2 containing feed gas. With the new analytical equipment, somewhat higher NO_x outlet concentrations are measured. While the NO_2 outlet concentration still remains lower than 1 ppm volume, the NO content varies between 1 and 3 ppm volume. However by proper adjustment of the ammonia excess, the level of 1 ppm can be sustained. Table 4 gives some results of this second series of experiments.

943

Table 4 : Experimental results in the DENITRO unit

Experiment number	1	2	3	
Gas flow rate	15	20	25	$Nm^3.h^{-1}$
Reactor temperature	673-700	700-730	673	K
NO_2 concentration IN	0.60	0.35	0.95	% volume
NO_2 concentration OUT	< 1.0	< 1.0	< 1.0	ppm volume
NO concentration OUT	1.0-3.0	2.0-3.0	1.0	ppm volume
NH_3 excess IN	30	40	20	% (stoech.)

Although the actual experiments demonstrate the feasibility of the catalytic reduction for selective NO_x removal, long term experiments are needed to study ageing and poisoning behaviour of the catalyst used. Furthermore the use of new zeolitic catalysts with higher activities and lower operating temperatures will be envisaged.

IV. Cryogenic krypton removal in presence of oxygen

Scope

As already was pointed out, the cryogenic distillation in presence of oxygen, as a process for krypton retention, has become more favoured during the last years. In this scope, with the financial support of the E.E.C., the S.C.K./C.E.N. has a research programme running dealing with this item. The aim of the programme is to study the cryodistillation of krypton in presence of oxygen under radioactive conditions.

Since all experimental experience in the past was obtained with nitrogen as carrier gas, the next step was to observe the behaviour of oxygen in the unit under non-radioactive conditions. More particularly temperature profiles had to be recorded in order to establish the necessity for changes in control or alarm set points. Oxygen concentrations in the bottom product were also measured.

Description of the cryogenic distillation unit

Figure 3 shows a flow sheet of the cryogenic distillation unit, as it was developed in Mol. The unit essentially consists of three main parts. In one of two parallel heat exchangers, the feed gas is cooled. Krypton and xenon are separated from the feed gas in a first continuously operating rectification column. Both noble gases are then separated from each other in a batch distillation column. A more elaborate description of the unit and its operation mode has already been given in previous reports [6, 7]. Table 5 summarizes the main characteristics of the principal rectification column.

944
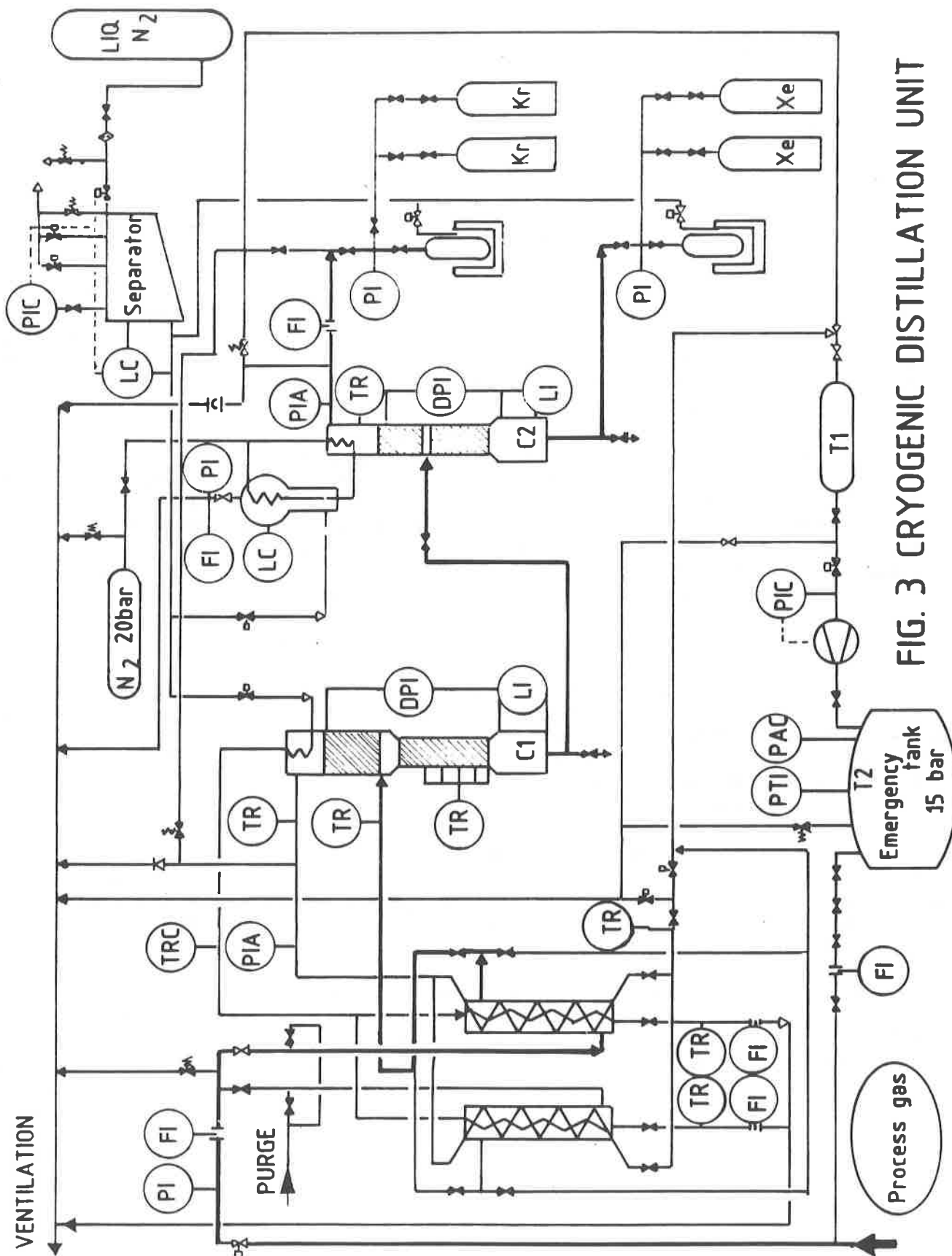
FIG. 3 CRYOGENIC DISTILLATION UNIT

Table 5 : Main characteristics of the rectification column

Gas flow rate	: 25 Nm^3.h^{-1}
Operating pressure	: 0.70 MPa
Inlet temperature	: 124 K
Reflux ratio	: 0.3 - 1.0
Packing	: 3 × 3 × 0.4 spring type Raschig rings
Upper section	: h = 0.80 m, d = 0.10 m
Lower section	: h = 0.72 m, d = 0.07 m

Experiments with oxygen in the cryodistillation unit

Experiments were carried out with three different oxygen concentrations in the feed gas : 6 %, 12 % and 21 % volume, the latter being air. The recording of the temperature profile was in fact limited to the lower packing where we have six thermoresistances with 7.5 cm space between each pair. The thermal balance of the column is controlled in such a manner that the krypton layer always reaches measuring point TR 18 (Figures 4, 5, 6).

Figure 4 gives the equilibrium temperature profile for the experiment with 6 % of oxygen in the feed gas. From TR 20 to TR 18 153 K was measured, which corresponds to a pure krypton layer. In the bottom temperatures greater than or equal to 153 K were measured, depending on the xenon content of the boiling liquid. The 116 K measured at TR 17 corresponds to a very oxygen rich layer. In TR 16 and TR 15 the temperature is decreasing with the oxygen content. In the upper packing where only one temperature measuring point is provided, 103 K was recorded. The equilibrium profile was established in 1.5 to 2 hours.

Figure 5 shows the temperature profile for the 12 % experiment. Obviously the profile is identical below TR 18. However, on the three points above TR 18, the same temperature of 116 K was measured. When lowering the krypton layer it was observed that the oxygen rich layer of 116 K extended over all six measuring points, so that in normal operation it will extend from TR 17 almost up to the inlet section of the column. In the upper packing 105 K was recorded. The profile was established in about 60 minutes.

The temperature profile of the experiment with air as feed gas is shown in Figure 6. In the lower packing the profile corresponds with that in Figure 5. When lowering the krypton layer, an oxygen concentration of 85 % was measured in the 116 K oxygen rich layer. A temperature of 106 K was measured in the upper packing. The time to establish this equilibrium profile was about 30 minutes.

Even more than the temperature measurements, the oxygen analyses were limited to very few points. In Table 6 the oxygen concentrations measured at the different sampling points are summarized. The compositions given are gas phase compositions. In the bottom product the oxygen concentrations were lower than 0.1 ppm volume, the detection limit of the oxygen monitor used. The table also gives the duration of the three experiments.

TEMPERATURE PROFILES IN THE RECTIFICATION COLUMN
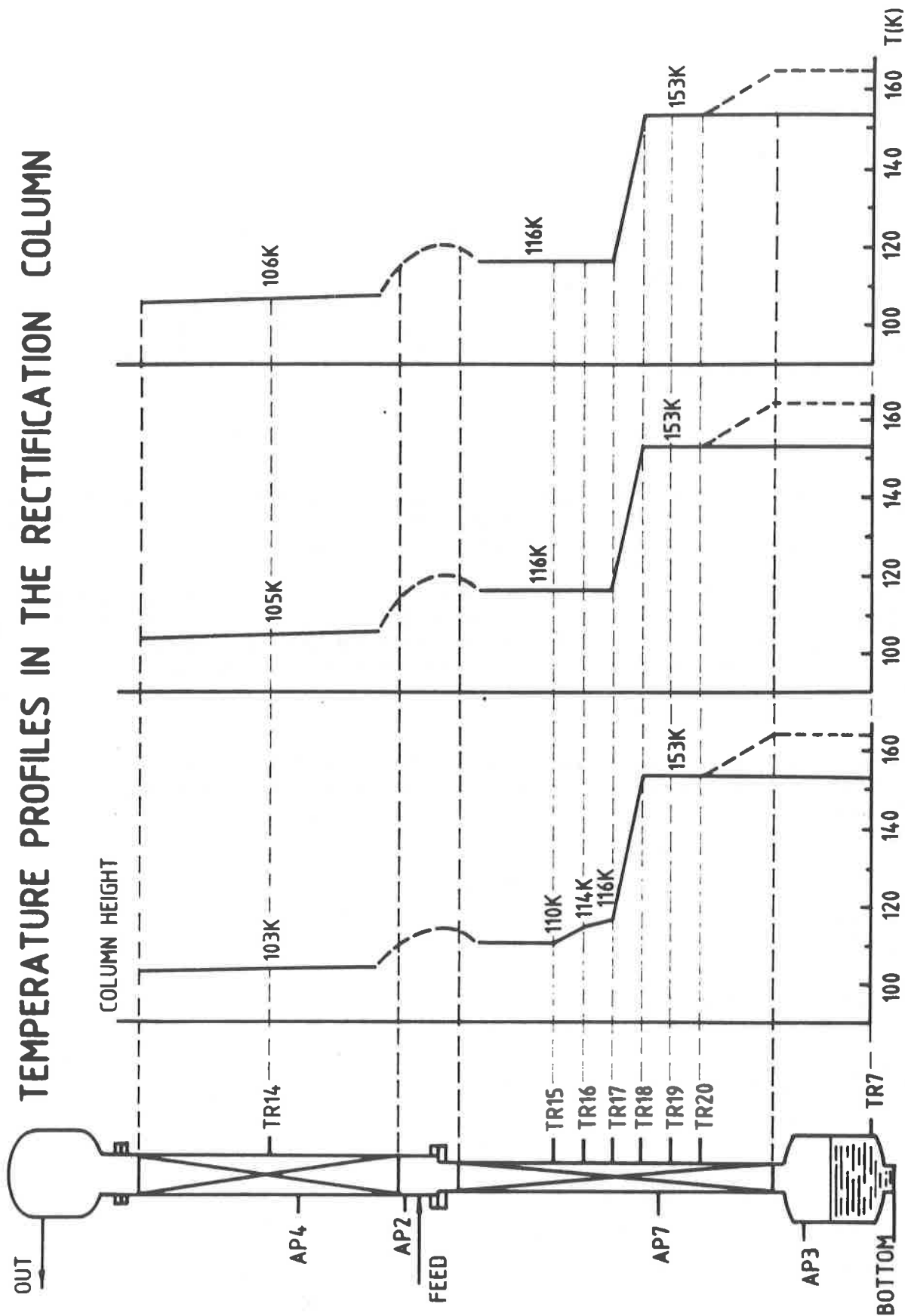
FIG. 4 : 6 %VOL. O₂ IN THE FEED

FIG. 5 : 12 %VOL. O₂ IN THE FEED

FIG. 6 : 21 %VOL. O₂ IN THE FEED

947

Table 6 : Oxygen concentrations in the rectification column

Experiment number	1	2	3	
Feed	6.0	12.0	20.9	% volume
Out	6.2	12.1	20.9	% volume
AP 2	7.0	13.0	22.8	% volume
AP 4	7.9	15.6	25.7	% volume
AP 7	< 0.1	< 0.1	< 0.1	ppm volume
Bottom	< 0.1	< 0.1	< 0.1	ppm volume
Duration	312	528	720	hours

According to the temperature profiles recorded, even with air, no changes in any set point of the different control and alarm systems had to be made. Furthermore, the very low oxygen concentration of 0.1 ppm volume in the bottom product means that, if ozone accumulation can be avoided, no oxygen will be transferred to the second batch distillation column.

Conclusion

It has been shown that the catalytical reduction of oxygen is a feasible pretreatment step for cryogenic krypton removal from reprocessing off-gases. Oxygen feed concentrations of 20 % can be reduced down to 0.5 ppm volume.

However, the use of large amounts of hydrogen remains expensive and potentially hazardous. To avoid this drawback, the selective catalytic reduction of NO_x with ammonia appears to be a valuable alternative to the fore-mentioned process. Further, experimental evidence has been obtained to show that the cryogenic distillation of krypton in presence of oxygen causes no problems under non-radioactive conditions.

In the future, radioactive krypton will be fed to the cryogenic distillation unit to determine experimentally the behaviour of oxygen and ozone under radioactive conditions.

References

[1] BENDIXSEN C.L., OFFUTT G.F., "Rare gas recovery facility at the Idaho Chemical Processing Plant", IN-1221 (1969).

[2] BENDIXSEN C.L., GERMAN F.O., "Operation of the ICPP rare gas recovery facility during fiscal year 1970", ICP-1001 (1981).

[3] BENDIXEN C.L. et al., "1972 Operation of the ICPP rare gas recovery facility", ICP-1023 (1973).

[4] BENDIXSEN C.L., GERMAN F.O., "1974 Operation of the ICPP rare gas recovery facility", ICP-1057 (1975).

[5] von AMMON R. et al., "Auslegung der Tieftemperatur - Rektifikationsanlage KRETA, einschliesslich der Vorreinigungsanlagen ADAMO und REDUKTION und erste Betriebserfahrungen", Seminar "Fuel reprocessing plant effluents", Karlsruhe, 1977, p. 535.

[6] GEENS L. et al., "Experience gained in the cryodistillation unit for krypton removal", BLG 547 (1981).

[7] COLLARD G.E.R., GEENS L.P.M. et al., "Experimental development and design aspects of a krypton-85 removal distillation unit", 16th DOE Nuclear Air Cleaning Conference, San Diego, California, 1980.

[8] COLLARD G.E.R. et al., "Développements récents dans le domaine de la rétention du krypton par distillation cryogénique", CEC Specialists' Meeting on "Methods of Krypton-85 Management", Brussels, 29 June 1982.

[9] von AMMON R. et al., "Considerations on cryogenic krypton separation with or without preceding oxygen removal", CEC Specialists' Meeting on "Methods of Krypton-85 Management", Brussels, 29 June 1982.

[10] BROWN R.A. et al., "Reference facility description for the recovery of iodine, carbon and krypton from gaseous wastes", ICP-1126 (1978).

[11] HUYSKENS P. et al., Personal communications.

[12] BRUGGEMAN A. et al., "Elimination of NO_x by selective reduction with NH_3", 15th DOE Nuclear Air Cleaning Conference, Boston, Massachussets, 7-10 August 1978.

[13] LEIST N.R. et al., "The design of a pilot unit for NO_x destruction with ammonia on a synthetic mordenite catalyst", NLCO-1139 (1976).

[14] HENRICH E. et al., "Removal and conditioning of radiokrypton by pressureless processes and at low gas inventories", CEC Specialists' Meeting on "Methods of Krypton-85 Management", Brussels, 29 June 1982.

DISCUSSION

MONSON: What concentration of ozone do you consider a safety hazard? What is the efficiency of ozone production from oxygen in a Kr-85 field?

GEENS: For our experiments, we will not exceed a concentration of 1% by volume. However, research performed by Mr. Penzhorn in Karlsruhe, Germany indicated that the explosive limits of ozone are about 4% and 7% by volume, respectively, in liquid oxygen and in a liquid Kr-Xe mixture. I do not know the exact figures. At our demand, the University of Louvain, Belgium, investigated the formation and destruction of ozone in à β-γ radiation field. They found that the destruction occurs much faster than the formation. This is logical since ozone is an unstable compound.

von AMMON: With high O_2 concentrations in the Kr-rich section of your column, you undoubtedly have a high formation rate of O_3 which collects in the bottom. Do you have any plans to use destructive methods of this ozone?

GEENS: Yes. In fact, since we have a packed column, we can use destruction catalysts in our packing to limit the accumulation, or even avoid it. At the University of Louvain, there have been studies on the formation and destruction of ozone under the influence of

radioactive radiation and it has been found that destruction goes very much faster than formation. Therefore, if we maintain a radiation level in our bottom product we will destroy the ozone formed in the krypton-oxygen separation layer that trickles down to the bottom.

THOMAS, T.R.:　　　What is the upper allowable limit of oxygen in the fed gas to your cryogenic distillation column?

GEENS:　　　We only went to the concentration in air, which is 21%.

THOMAS, T.R.:　　　What I am asking is, you couldn't operate in an airstream could you?

GEENS:　　　20% is an airstream.

THOMAS, T.R.:　　　Are you considering that a practical operating limit?

GEENS:　　　Yes, it is a maximum for dissolved O_2 in the raw gas stream. It probably won't be as high in a raw dissolver-off gas stream, but we can handle it.

THOMAS, T.R.:　　　The reason I asked this question is because in most of the studies being done today in Germany, France, and elsewhere, they have tried to eliminate oxygen totally. Are you suggesting in your studies that it would be O.K. to use an air stream?

GEENS:　　　Yes, it would be.

THOMAS, T.R.:　　　What are your future plans as far as demonstrating this in a hot mode or on a larger scale?

GEENS:　　　In the European Community, we are planning to feed oxygen in 20% concentration by feeding air to our cryogenic distribution distillation unit together with krypton-85. Since we are limited to our existing unit, we restrict total inventory of krypton to about 100 curies. In order to do something more, we are providing an additional radiation source in the bottom of our column to see if we are forming ozone, and if we are destroying it. We are also planning to feed ozone into our column to see if we can destroy it in the bottom with krypton-85 radiation plus the additional radiation source.

DEITZ:　　　Is there dust formation of the catalyst beads, or pellets, in the operation of the process?

GEENS:　　　We observed some dust, especially during the first experiments, but not much later on.

BEHAVIOUR OF IMPURITIES IN A CRYOGENIC KRYPTON REMOVAL SYSTEM

R. von Ammon, W. Bumiller, E. Hutter, G. Knittel, C. Mas, G. Neffe

Kernforschungszentrum Karlsruhe, Federal Republic of Germany

Abstract

Two radiolytic reactions which may take place in the cryogenic columns of a Kr-85 removal system in the off-gas cleaning system of reprocessing plants were simulated in the inactive test unit KRETA: formation of ozone from O_2 and of nitrogen oxides from O_2 and N_2. The reactions were simulated by adding O_3 and NO + O_2 to the feed gas, respectively.

Whereas accumulation of O_3 in the first column is not critical, it can reach concentrations in the percent range between the krypton and xenon sections of the second column.

NO reacts with O_2 rapidly at low temperatures to N_2O_3 and N_2O_4. The solubility of N_2O_4 in liquid xenon has been determined to be about 1 mole-% at 200 K in a laboratory study. Crystallization of moderate amounts of N_2O_4 in the sump does hot cause column malfunctions. However, if N_2O_4 crystallizes in the feed gas section of the column, plugging of sieve plates may occur.

In a laboratory study and during test runs with the semiscale catalytic unit REDUKTION it was found that CH_4 and other hydrocarbons can be removed from the off-gas by oxidation with H_2O vapor even in an atmosphere containing excess H_2 for the reduction of O_2 and NO_x. For complete removal of CH_4 temperatures of $\geqq 500^\circ$ C must be maintained.

I. Introduction

The main disadvantage of any cryogenic process for the removal of radioactive krypton from the off-gas of reprocessing plants is its sensitivity towards certain impurities which may cause plugging by crystallization or which may create a safety hazard. Therefore a rigorous gas pretreatment including catalytic reduction of O_2 and residual NO_x is usually recommended[1]. The impurities of main concern are O_2, CH_4, and NO, because they accumulate in the krypton-rich sections of the cryogenic columns. In previous publications we had reported studies on the behaviour of each of these compounds in our inactive test unit KRETA[2, 3]. If present simultanously, some of them will react chemically and, in addition, they will radiolyze under irradiation. Products of radiolysis again may undergo chemical reactions.

In lack of hot experiments, we have simulated recently two of the most important radiolytic and chemical reactions by adding trace amounts of O_3 to the feed gas, and NO + O_2 in another experiment. The intention was to gain information about the tolerable concentrations of these impurities in the feed gas from the accumulation of O_3 and the reaction of NO with O_2 to higher nitrogen oxides and their accumulation in the cryogenic columns.

II. Behaviour of Ozone

1. Background of the experiment

In simulating the radiolytic ozone formation in a rectification column one would have to feed ozone formed outside the column into each column stage according to its formation rate. The rate varies strongly depending on the Kr-85 inventory and the G-factor which, in turn, depends on the O_2-concentration. Such an experiment would be very laborious. We simplified it by calculating the O_3 inventory of the first column[2] and adding the cumulated amount to the feed gas. We thus treated O_3 like any other impurity of the off-gas stream[3].

We assumed further that a catalytic O_2 retention unit was implemented in the off-gas cleaning system and that the feed-gas to the first column contained O_2 in a mixing ratio of 10 ppm_v. Under these assumptions an O_3 feed concentration of 3.5 ppm_v is calculated. Therefore we carried out the KRETA experiments with O_3 feed concentrations between 2 and 10 ppm_v.

O_3 was prepared by an electric discharge in an ozonisator (H. Neumayer, Freiburg). The ozonisator was operated with air under normal pressure. The O_3 containing air was then pressurized to 6.5 bar and fed into the feed-gas to the first KRETA column. The desired concentrations of a few ppm_v were obtained by dilution and by control of the discharge voltage. The feed gas also contained fairly large amounts of O_2 (about 90 ppm_v per ppm_v of O_3).

2. Ozone Accumulation in the First Column

A steady state concentration profile of ozone in the liquid phase as calculated for a feed concentration of 10 ppm_v with a plate-to-plate calculation method is shown in fig. 1, where the column height is expressed in terms of theoretical stages.

Feed-gas		
N_2	98.46	Vol.%
Ar	1.00	"
Kr	400	ppm_v
Xe	4000	"
O_2	950	"
O_3	10	"
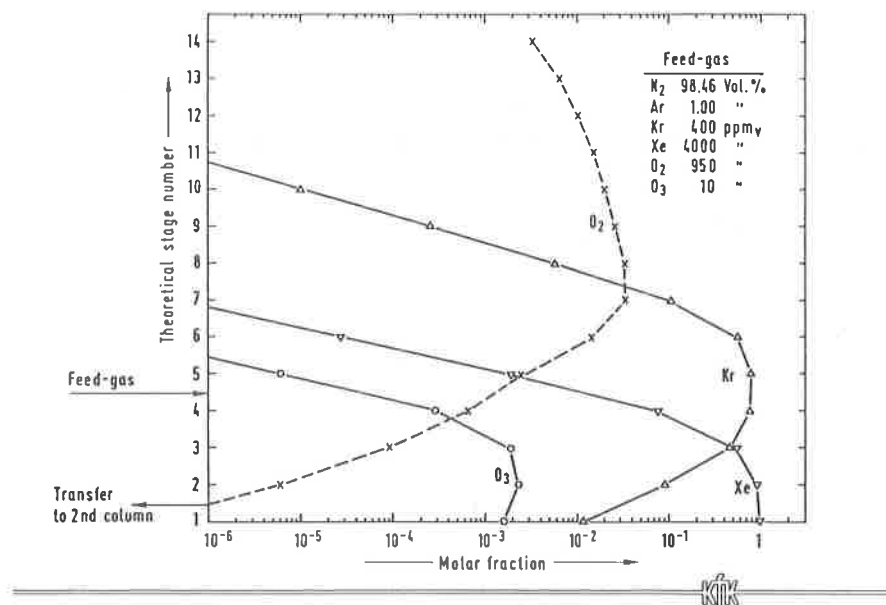
Figure 1   Calculated concentration profiles in first KRETA column

For comparison, the experimental concentration profile is presented in fig. 2 obtained with the same feed concentration.
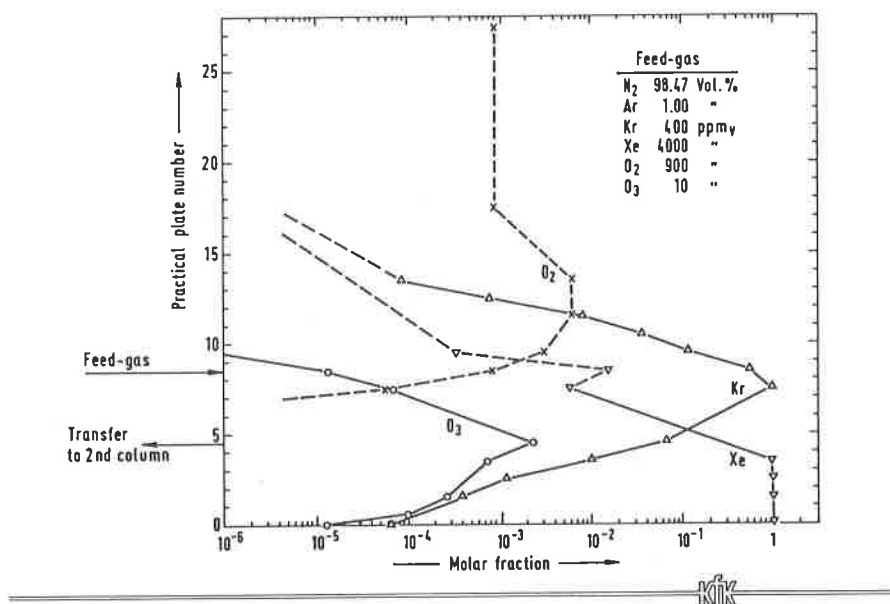
Figure 2   Experimental concentration profiles in first KRETA column

The samples were taken from the gaseous phase except for the points at the abscissa which refer to samples of the sump liquid. The agreement between the calculated and experimental O_3 profiles is good: the maximum calculated concentration in the theoretical stage next to the column bottom and the maximum experimental concentration in the gaseous phase at the fourth practical plate is 0.23 and 0.24 mole-%, respectively. These points coincide approximately because the bottom product was withdrawn from the fourth plate. Although the accumulation with respect to the feed concentration is high, this concentration is far from being critical as far as safety is concerned. The explosive limit of O_3 in Kr/Xe is about 7 mole-%[4].

3. Ozone Accumulation in the Second Column

In order to avoid the relatively high concentration of 0.24 % in the feed gas to the second column we lowered the O_3 feed concentration to the first column from 10 to 3 ppm$_v$. The O_3 concentration in the transfer stream under this condition amounts nominally to 682 ppm$_v$. We have measured 560 ppm$_v$ under steady state conditions (see fig. 3). The difference probably is accounted for by fluctuations in the feed concentration. A feed concentration of 560 ppm$_v$ to the second column still is quite high and it is to be tolerated only if the equivalent amount can be withdrawn from the column together with the xenon product stream. Complete transfer of the ozone to the xenon would result in a nominal concentration of 616 ppm$_v$.

953
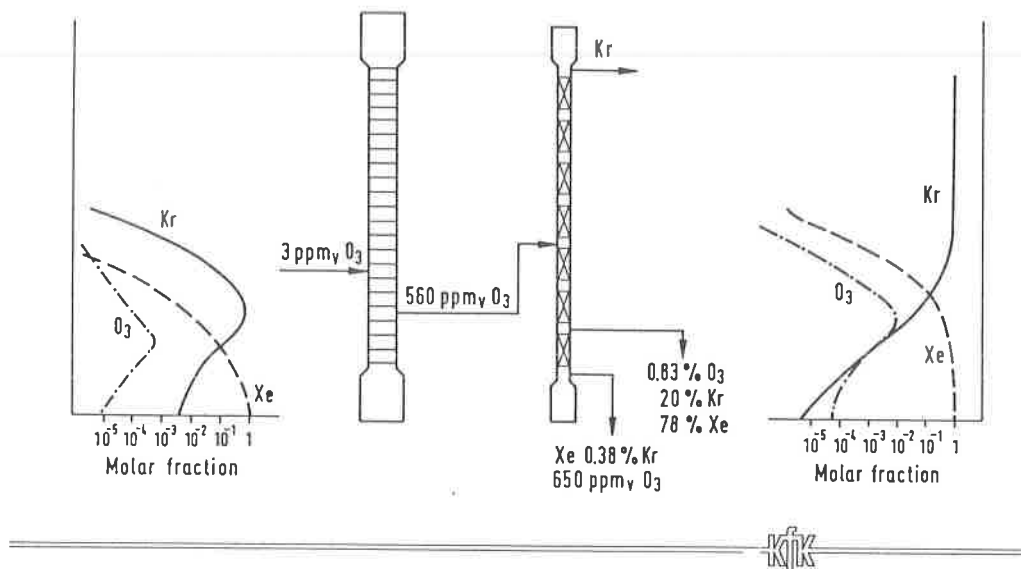
Figure 3   Path of O₃ through the KRETA columns

It turned out, however, that under the operation mode of the second column (reflux ratio approximately 100 and control loops not perfectly optimized) the O_3 concentrations in the xenon consistently were much lower. As a consequence, a strong accumulation took place between the xenon and krypton sections (fig. 3). After a few hours of operation already O_3 concentrations in the percent range were measured. It was clear that safety did not permit further operation in such a manner.

After increasing the cooling power of the column condenser it was possible to condense more O_3 into the xenon thus increasing its concentration into the desired range. But, as it turned out, we also condensed krypton thereby. Its concentration in the xenon product amounted up to 0.38 % instead of 10-100 ppm_v, the usual concentrations measured under routine operation without O_3. In a real plant, such a stream would have to be recycled, of course.

Alternatively, the ozone could be effectively withdrawn with a sidestream from the point of maximum accumulation above the xenon section. We did not test this possibility. Calculations showed, instead, that further increase of the reflux ratio in the column should improve its separation efficiency, so that a satisfactory O_3 concentration in the xenon could be achieved while still keeping it essentially free from krypton. With a reflux ratio of 300 and improved control loops we have achieved residual krypton concentrations of less than 1 ppm_v in the xenon product. A test with ozone will be carried out in the near future.

III. Behaviour of Nitric Oxide

The accumulation of NO in the first column in the absence of O_2 has been studied and reported by us before[2]. NO was found to leave the column via its head because the dimerization equilibrium of NO is shifted to the side of the monomer under high dilution. In the presence of O_2 rapid oxidation occurs to N_2O_3 and N_2O_4. These nitrogen oxides are collected in the column sump and tend to freeze out since their solubility is limited[2].

1. Solubility of N_2O_4

Nevertheless, fairly large amounts of N_2O_4 can be tolerated in the sump without disturbing column operation. One reason is the solubility in liquid xenon which is higher than originally assumed[2]. We have determined the solubility now more exactly in a laboratory cryostat by visual observation of the crystallization limits. The results are presented in fig. 4.
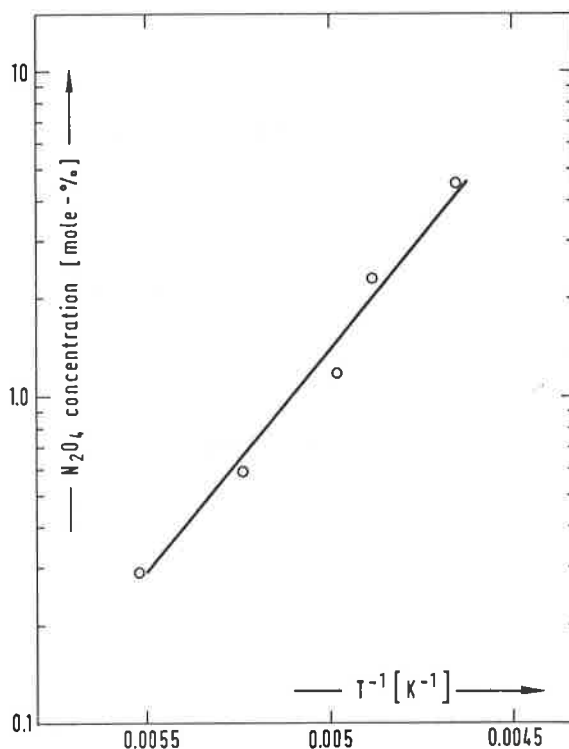
Figure 4   Solubility of N_2O_4 in liquid xenon

At 200 K the solubility limit is approximately 1.2 mole-%. This temperature coincides with the temperature of the sump liquid of the first KRETA column. So in a sump volume of 10 l about 200 g of N_2O_4 can be dissolved before crystallization begins. In order to limit crystallization or avoid it at all, a side stream of the sump liquid would have to be purified from nitric oxides, e.g. by recycling it to the reduction catalyst.

2. Crystallization of N_2O_4 from the Gas Phase

On the other hand, we have noticed that crystallization may take place in the feed entrance region causing plugging of sieve plate holes. This behaviour resembled very much the freezing of xenon which we had experienced during early experiments with the KRETA facility[3]. A slow increase of the differential pressure across the sieve plate just above the feed point, which is an indication for plugging, was observed already with concentrations of 1 ppm_v of NO and 5-10 ppm_v of O_2.

Very likely such a behaviour would not be encountered in a packed column. Nevertheless, a very stringent prepurification of the off-gas from nitric oxides and oxygen has to be postulated in the catalytic reduction unit preceding the cryogenic part. Although some nitric oxides will also be formed in the cryogenic columns by radiolysis from N_2 and O_2[1, 2], it is anticipated that N_2O_4 concentrations arising from this source will remain below the limit to cause plugging. Moreover, the highest radiolytic formation rates will take place in lower parts of the column where the Kr-85 activity is highest[2].

IV. Formation and Removal of Hydrocarbons
at the Reduction Catalyst

The accumulation of CH_4 in the cryogenic columns was described by us before[3]. We also have discussed the possibility of formation of new CH_4 by reduction of CO_2 at the reduction catalyst[5]. CH_4 formation from CO_2 had been found negligible for thermodynamic reasons at temperatures $\geqq 450°C$, because equilibrium reaction 1 is shifted far to the left.

$$CO_2 \quad + \quad 4 \; H_2 \quad \rightleftharpoons \quad CH_4 \quad + \quad 2 \; H_2O \qquad (1)$$

For the same reason it is possible to oxidize CH_4 and other hydrocarbons with H_2O even in the presence of excess H_2. If large concentrations of O_2 and/or NO_x are reduced in the catalytic unit the partial pressure of H_2O in the gas loop will be quite high. For instance, in our semiscale unit REDUKTION (gas throughput in the dilution loop 300-500 m_n^3/h) it is determined by the temperature of the gas cooler behind the catalyst and amounts to almost 3 % by volume. Under these conditions the oxidation yields of hydrocarbons are high. In fig. 5 the dependence of CH_4 oxidation on the H_2O partial pressure at 350° C is shown as determined in a laboratory scale kinetic study. The influence of increasing H_2 concentration was also investigated in this study. The decrease of the oxidation yield with increasing H_2 concentration is not very strong.

In the semiscale tests with the catalytic unit REDUKTION, where the temperature is higher (about 500° C) and the H_2O partial pressure is higher by an order of magnitude, oxidation yields are almost quantitative. Typical results of routine analyses in the effluent gas are $\leqq$ 0.1ppm_v of CH_4 and 2.9 ppm_v of CO, as compared to 1.5 ppm_v of CH_4 and 0.5 ppm_v of CO in the feed gas which partially consisted of air. Obviously CH_4 was effectively oxidized while some of the CO_2 was reduced to CO. The latter result can also be explained by thermodynamic reasons, because formation of CO from CO_2 is an endothermic process being favoured at higher temperatures[5].
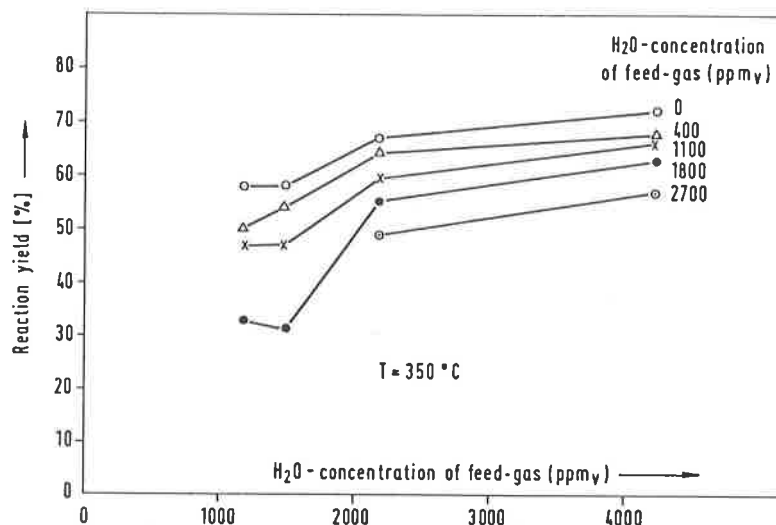
Figure 5   Oxidation of CH_4 by H_2O vapor
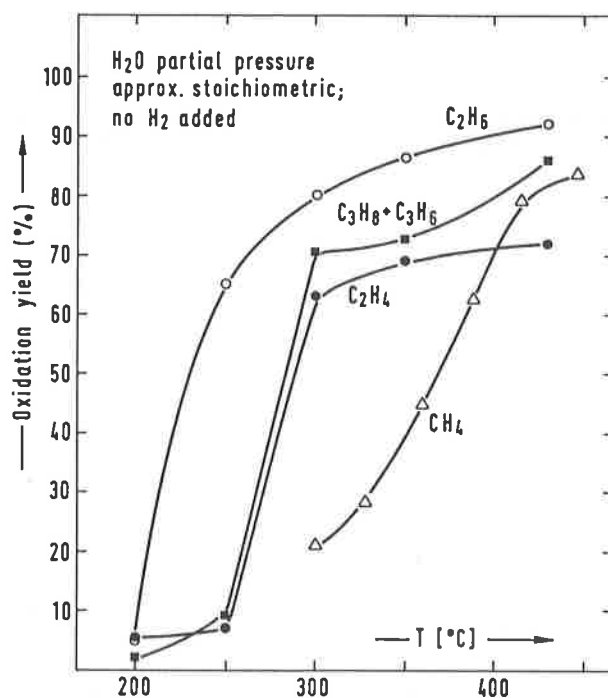
Figure 6 Oxidation of various hydrocarbons by H_2O vapor

957

Higher hydrocarbons are oxidized more easily than CH_4, as the degree of unsaturation and the chain length are increased. From fig. 6 can be deduced that at 300°C only about 20% of the CH_4 have been oxidized whereas the oxidation of C_2H_4, C_2H_6, and a mixture of C_3H_8 and C_3H_6 shows yields between 60 and 80% already. The yields are referred to the amount of CO_2 formed.

Thus, the installation of a catalytic oxidation step for hydrocarbon removal in an off-gas purification system appears unnecessary, if a catalytic reduction step is included [2].

References

1. von Ammon R., Bumiller W., Hauss E., Hutter E., Knittel G., Mas C., Neffe G., in "Methods of Krypton-85 Management" (Hebel W., Cottone G., Eds.) Harwood Academic Publ., New York, p.261, 1983.

2. von Ammon R., Bumiller W., Hauss E., Hutter E., Neffe G., Hammer R.R., "Formation and Behaviour of Nitric Oxides in a Cryogenic Krypton Separation System and Consequences of Using Air as Process Gas", Proceed. 17the DOE Nuclear Air Cleaning Conf.(First M.W. Ed.), CONF-820833, p. 683, 1983

3. von Ammon R., Bumiller W., Hutter E., Neffe G., "Steady State Operation of the First Cryogenic Column in a Krypton Separation System", Proceed. 16the DOE Nuclear Air Cleaning Conf. (First M.W., Ed.), CONF-801038, p. 202, 1981.

4. R.-D. Penzhorn, paper submitted to this conference.

5. Mas C., Knittel G., von Ammon R., "Verhinderung der Methanisierung von CO_2: Ein Problem bei der katalytischen Abgasreinigung in der Kerntechnik", Chem.-Ing.-Techn. 54, 833-836, 1982.

DISCUSSION

DEITZ: When carbon or carbonaceous dust particles are present in ozone mixtures, we have found that ozonides are formed, which are explosive. Are your systems free of dust particles?

von AMMON: We have not observed any formation of carbonaceous dust at the reductive catalyst, although this cannot be excluded for thermodynamic reasons.

SELECTIVE ABSORPTION OF NOBLE GASES IN FREON-12
AT LOW TEMPERATURES AND ATMOSPHERIC PRESSURE

E. Henrich, R. Hüfner, F. Weirich, W. Bumiller, A. Wolff

Kernforschungszentrum Karlsruhe, Institut für Heisse Chemie,
Fed. Rep. Germany

ABSTRACT

A selective absorption process for the removal of noble gases from the dissolver off-gas in a reprocessing plant is under development. The process uses freon-12 as the solvent and operates at low temperatures and atmospheric pressure.

The solubility of various off-gas components (N_2, O_2, Ar, Kr, Xe, CH_4, N_2O, CO_2, NO) has been determined at temperatures between -158° C and -30° C as a basis for modelling the process, which operates with two absorption columns. The inactive Xe plus small amounts of $14-CO_2$, N_2O and traces of Rn are absorbed in the first column at absorption temperatures of about -120° C. The radioactive Kr is removed in the second column at absorption temperatures of about -150° C. The feed-gas to the first absorption column is sub-cooled to prevent the carry-over of impurities.

The process has been tested in a 2.5 cm diameter lab-scale column before an engineering scale column of 10 cm diameter and 12 m height has been constructed and operated. The throughput of the latter column is 25 m³ (STP) off-gas per hour. The essential results of the test runs can be summarized as follows:

- The noble gas decontamination factors are $> 10^3$
- The separation of Kr from Xe is $> 10^5$
- The product gas purity is $> 99\%$ by volume (freon-12 vapour removed)
- The noble gas mean residence time in the column is < 1 h; this indicates a low noble gas inventory and a low radiolytic solvent degradation
- The experimental results are in good agreement with the process model.

Consequences of radiolytic solvent degradation have been estimated, using experimental results obtained under process conditions. Degradation of $< 1\%$ of the solvent inventory per year is expected. The inorganic degradation products, together with any traces of impurities carried over with the feed gas, can be removed continuously from the solvent with solid sorbents. This maintains a pure and dry solvent.

The selective absorption equipment is part of an integrated dissolver off-gas system on an engineering scale. Integrated operation of the selective absorption subsystem is part of the future development program.

1. INTRODUCTION

An about 12 GWe LWR spent fuel reprocessing plant (FRP) is expected to be in operation in Fed. Rep. Germany (FRG) in the mid nineties. In view of the anticipated future increase of the nuclear power economy, experts have recommended the development and demonstration of a control technology for radiokrypton /1/. The recovery of Xe and Kr-85 for commercial use may be an additional incentive.

In a FRP, the fission product (FP) rare gases are routed into the dissolver off-gas (DOG) and can be removed at the end of the DOG purification train. Two alternative processes are being investigated at Karlsruhe KfK on the pilot plant scale: Since 1976 a cryogenic distillation process /2/ and a selective absorption process since the end of 1983, preceded by investigations with a laboratory scale absorption column in 1980-81 /3/.

More than half a dozen different operating modes have been developed for cryodistillation processes in various countries /4/. None of these variants corresponds to the familiar Xe and Kr recovery process in commercial air lique-faction plants. More general characteristics of cryodistillation processes are: a high radiokrypton inventory, high operating pressures and complex precleaning steps, usually requiring H_2 for O_2 removal from the DOG. Such characteristics are not found among the advantages. The high state of development corresponds to the large R+D input.

A selective absorption process was studied at Harwell/UK more than 25 years ago /5/. Xe and Kr are absorbed simultaneously at atmospheric pressure in CCl_4 solvent, at temperatures slightly below ambient. A large solvent flow, comparable to the DOG flow on a volume basis, is required for an efficient Kr recovery.

Extensive development work has been carried out in 3 generations of pilot plants at Oak Ridge/USA for more than 15 years. The final version is a simplified combination column /6/. Xe and Kr are absorbed simultaneously at about 10 bar pressure in CF_2Cl_2 (R12) solvent at temperatures of about -30°C. The operating pressure is not inherent to the process, but helps to reduce the equipment size. The R12 solvent was proposed by Steinberg /7/ in 1958 and has many advantages /8/.

Some more general characteristics of these absorption processes are: a low radiokrypton inventory, preremoval of O_2 is not required and an operation at atmospheric pressure is possible. The small amount of radiolytic solvent degrada-tion products can be removed continuously. A dry system and suitable construction materials serve to prevent potential corrosion.

The selective absorption process developed at Karlsruhe/KfK /3/ can be brief-ly characterized as follows:
-   Xe and Kr are separated from each other using two absorption columns and R12 as solvent. The first column recovers the Xe and the second column revovers the Kr.
-   The process operates slightly below atmospheric pressure
-   Low absorption temperatures reduce the equipment size.
-   Simple and efficient low temperature DOG prepurification steps help to main-tain a pure and dry solvent.
-   The operating mode is especially suited to achieve a low radiokrypton inven-tory and to produce pure product gases, especially a sufficiently Kr-free Xe product for commercial use.

2. SOLUBILITY OF VARIOUS GASES IN LIQUID R12

The basis of the selective absorption process is the good solubility of Xe and Kr and the solubility differences of the various off-gas components in dichlorodifluoromethane CCl_2F_2, (freon-12, refrigerant-12, R12) /8,9/.

2.1. Properties of R12

R12 is the major coolant of industrial and home refrigeration units. It is cheap, non-toxic, non-flammable and chemically stable. Close derivatives are used as fire extinguishers or solvents for ozone. The properties of R12 are well-known and some more important ones are summarized in table 1 /10/.

| CCl_2F_2: | Frigen-12 | Kaltron-12 | Freon-12 | etc. |
| producers: | Hoechst | Kali-Chemie | Du Pont | |

cheap, non-toxic, non-flammable, chemically stable

normal boiling point	-30° C	melting point -158° C
density	1.50 kg/l	1.84 kg/l
heat of vapourization		40 kcal/kg at 1 bar
specific heat		0.2 kcal/kg·K
volume of vapour		160 l/kg at -30° C and 1 bar

PROPERTIES OF R12 (CCl_2F_2, REFRIGERANT-12)
Table 1:

2.2. Method for the gas solubility determination

The experimental procedure is described in the following and the equipment is sketched in fig.1.

A stainless steel vessel of known weight and volume was evacuated, cooled with dry ice and filled with liquid R12 to about half. More volatile impurities were removed in two steps: 1. The vessel was warmed up and about 10% of the R12 were allowed to evaporate. 2. Thereafter, the vessel was cooled down to liquid nitrogen temperatures and evacuated to less than 10^{-3} Torr. The amount of R12 contained in the vessel was determined by the weight difference. At stepwise increasing and decreasing temperatures T, the R12 vapour pressure p between the melting point m.p. at -158°C and the normal boiling point b.p. at -30°C was recorded with a pressure head. The liquid was agitated with a magnetic stirrer. Straight lines were obtained in the log p versus 1/T plot in accordance with literature data, thus indicating the solvent purity.

Then, a known volume of gas was drawn into the vessel at low temperatures. The pressure measurements were repeated within the same temperature range. The existence of equilibrium conditions at a given temperature was confirmed, if the same pressure value was obtained on approaching the equilibrium from the upper and lower temperature sides. Additional volumes of the same gas were added several times to examine the concentration dependence of the gas solubility.

Fig.2 SIMPLIFIED CROSS SECTION
OF EQUIPMENT FOR GAS
SOLUBILITY DETERMINATIONS

Fig.1 SOLUBILITY OF GASES IN LIQUID R12

The temperature dependence of the distribution coefficients can be calculated from these data and is shown in fig.2. On repeated measurements, the standard deviation of the procedure was found to be a few percent in the lower temperature range; it decreases to about $\pm 10\%$ at temperatures near the R12 b.p. at -30°C. The accuracy of the absolute temperature and pressure calibrations was estimated to be $\pm$ 1.5 K and $\pm$ 3% respectively.The individual distribution coefficients are to a first approximation independant from the partial pressure or the presence of additional less soluble gases. The very low mutual influence simplifies the modelling of the process: the data of binary mixtures are sufficient for process calculations.

Within our experimental accuracy the distribution coefficients D can be represented by straight lines in a log D versus 1/T plot, except for O_2 and N_2 at higher temperatures. The solubility of the individual gases increases with the boiling point; the more volatile gases are less soluble. At the absorption temperatures proposed for a process application, the solubilities of the key design components Xe/Kr and Kr/O_2 are about one order of magnitude different. The difference is still half an order of magnitude at the R12 b.p. at -30°C.

In fig.3, the vapour pressure differences of the pure gases are compared to the solubility differences in R12: Both are comparable and sufficiently high. They represent a crude measure for the separation selectivity of a cryogenic distillation and a selective absorption process. The result may be expressed as follows: At atmospheric pressure and temperatures above the boiling point of a gas, a good solvent aids maintaining the gases in a more compact liquid form, without loss of separation selectivity.

2.3. Solubility of solid impurities

The solubility of some trace impurities with higher melting points and lower vapour pressures is of interest in view of low absorber temperatures. The data help to evaluate the sensitivity of the process in case of defective prepurification steps. The consequences of the low radiolytic solvent degradation are treated in a later section.

Water is almost insoluble in R12 (26 ppm at 0°C). A very thorough water vapour removal from the DOG is required in any case, in view of solvent degradation and potential equipment corrosion. A DOG dew point of about -130°C effectively prevents the carry-over of water and other freezing impurities into the solvent. Malfunction of the upstream NO_x recovery system may leave some more volatile NO. Partial NO-oxidation within the absorption columns produces less soluble N_2O_4. Preliminary N_2O_4 solubility data in the absorber temperature range are shown in fig.4 /11/.

3. BRIEF PROCESS DESCRIPTION

The simplified flowsheet of the selective absorption process is shown in fig.5. Xe and Kr are removed from the DOG and are separated from each other using two absorption columns. The first column recovers the more soluble Xe; the second column recovers the less soluble Kr. The operating mode corresponds to a conventional gas absorption process. In the upper absorber zone, the chilled R12 solvent scrubs the rare gases from the off-gas. In the intermediate fractionator zone, the solvent is heated to about boiling point and the coabsorbed carrier gases are flushed back to the absorber. In the lower stripper zone, the rare gases are completely boiled off under reflux. A pump recycles the purified solvent to the absorber via a heat exchanger and a solvent cooler and maintains a constant circulating flow.

Fig. 4 SOLUBILITY OF N_2O_4 IN LIQUID R12

Fig. 3 SEPARATION SELECTIVITY FOR KEY DESIGN COMPONENTS

The process pays special attention to a safe handling of volatile radioactive material: It operates slightly below atmospheric pressure and the Kr-85 inventory is more than two orders of magnitude lower compared to cryodistillation. Moreover, the required prepurification steps are less complex: Neither O_2 nor CO_2 or N_2O must be removed. Only water and nitric acid vapours and NO_x or any other freezing impurities must be removed to the trace level, to prevent plugging or potential corrosion.

An efficient DOG prepurification causes less problems than the consequences connected with a spoiled solvent. A convenient prepurification subsystem consists of a low temperature nitric acid scrubber operated at -30° to -55°C plus a de-frostable feed gas cooler at -130°C or a molecular sieve; a more detailed description is given elsewhere /12/. This combination is also an additional in-line back-up system in case of minor upsets in the upstream NO_x and iodine removal steps. The in-line correction of upsets contributes to the reliability and availability of the total system.
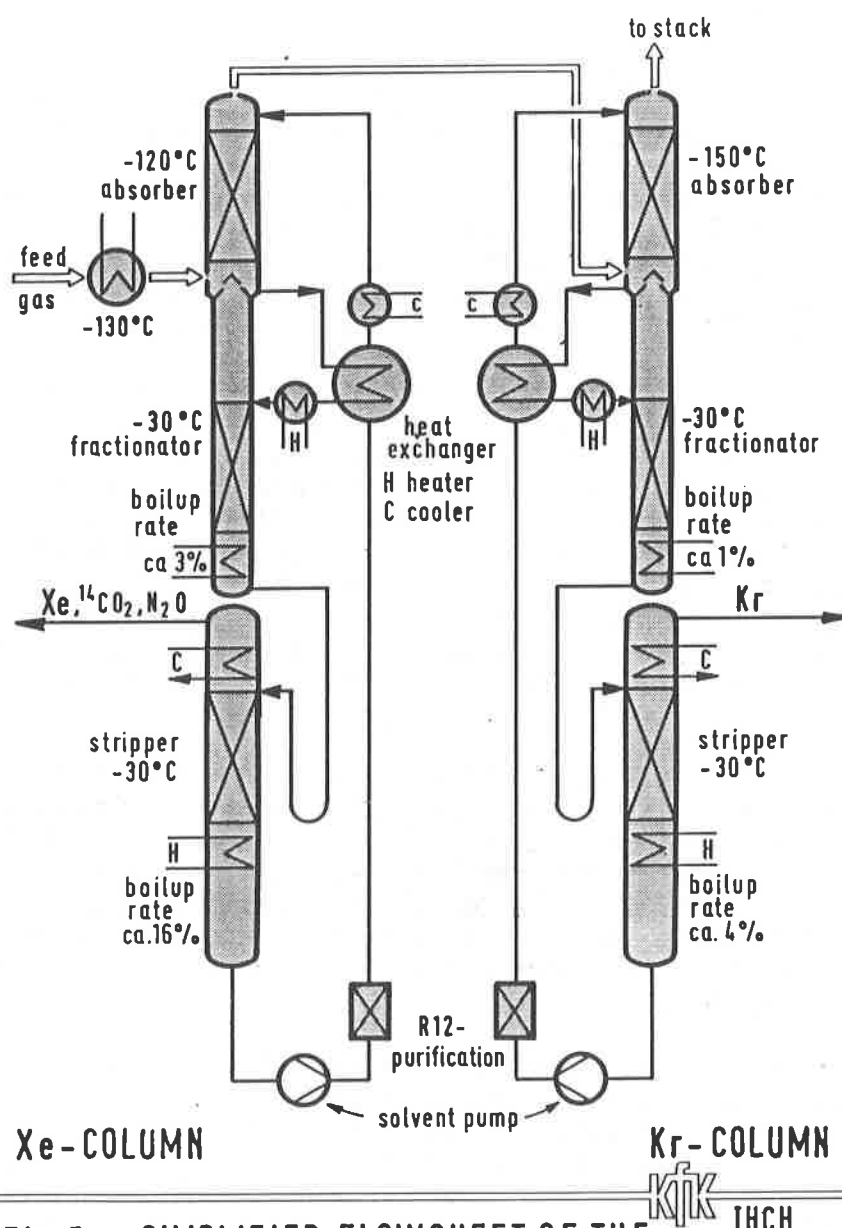
Fig.5 SIMPLIFIED FLOWSHEET OF THE
SELECTIVE ABSORPTION PROCESS

The very low absorber temperatures in the columns are compatible with this prepurification system and have additional advantages:
- The separation selectivity increases at lower operating temperatures
- The R12 solvent flow is reduced considerably; the consequence is a lower energy consumption and a reduction of the equipment size and the required cell space.

The various parts of the Xe scubber are described in more detail:

1. Feed gas cooler: The feed gas cooler includes a deentrainement pad towards the exit and removes the freezing impurities to the trace level. The operating temperature is about -130°C. The small amount of frozen material allows extended defrost cycles and can be recycled upstream without additional treatment. The N_2O should not freeze out and is the key design component. It is a by-product from oxide fuel dissolution. The amount depends on the dissolution conditions and may be close to the Xe concentration.

2. Absorber zone: A subcooled DOG at about -130°C is fed to the Xe absorber zone at about -120°C. The less soluble trace impurities which are carried over into the solvent, can not reach the solubility limit.

   The absorber is responsible for the DOG decontamination. The total Xe and the more soluble N_2O, CO_2 as well as traces of Rn are absorbed in counter-current contact with the chilled solvent. The key design components for suitable operating conditions are Xe and Kr. The Kr is transported with the off-gas into the subsequent Kr absorption column.

3. Fractionator zone: The fractionator is responsible for the final product purity. The coabsorbed carrier gases as well as a fraction of Xe are desorbed from the solvent and recycled into the feed gas. The key design components for suitable operating conditions are Xe and Kr. The cold solvent is first warmed up in the heat exchanger plus an additional controlled heater to a few degrees below the boiling point. A large fraction of coabsorbed gases is already removed during this operation. About 3% of the circulating solvent flow are vapourized in the fractionator sump heater. The small volume of R12 vapour completes the fractional desorption at the boiling point in counter-current flow to the solvent.

   Some product gas is also desorbed in the course of the fractionation operations. The result is a minor product gas accumulation between the absorber and fractionator zones. The increased product gas concentration must be taken into account for the precalculation of the decontamination factor in the absorber. Additionally the coabsorbed carrier gases are flushed back to the feed gas and add to the gas load in the absorber zone. The details of fractionation are the most intricate operations in the selective absorption system.

4. Stripper zone: The stripper is responsible for a complete desorption of the product gases. The key design component is the more soluble CO_2 or the Rn. About 16% of the solvent flow must be vapourized in the stripper heater to completely desorb the product gases. The R12 vapour is separated from the product gases in the reflux condenser. The condensate reflux adds to the solvent load in the stripper zone. The desublimation of CO_2 sets a lower practical limit of about -75° C for the condensation temperature. The R12 vapour fraction in the Xe product is therefore $\geq$ 10% by volume.

5. Solvent tank: The volume difference between the minimum and maximum level of the tank should at least correspond to the R12 inventory in all the other column components during operation.

6. Solvent pump: The solvent pump recirculates the stripped solvent to the top of the absorber and maintains a controlled and constant flow rate. The solvent flow through the absorber, heat exchanger, fractionator and stripper zones into the solvent tank is by gravity. The fractionator and stripper zones are connected directly via a siphon. The closing at the gas side fixes the product gas take-off point to the top of the reflux condensor. The product line is additionally connected to the absorber entrance and allows an automatic short-time recycle of impure product gases.

7. Solid sorbent bed: Solid sorbents continually remove the small amount of impurities from the solvent. A pure and dry solvent may be maintained even in the rare event of an accidental carry-over of impurities with the off-gas. Spent solid sorbent beds may be regenerated or replaced.

8. Solvent heat exchanger: The solvent heat exchanger considerably improves the energy economy of the process. The counter-current heat exchange takes place between the cold and the warm section of the solvent loop. Small and controlled heaters and coolers maintain the suitable solvent operating temperatures for the absorber and fractionator zones and compensate for the incomplete heat exchange.

9. Kr column: The operating mode in the Kr column is comparable to the Xe column. The key design components are Kr and O_2 and the various operating parameters are adjusted correspondingly. The off-gas from the Xe absorber may be fed directly to the Kr absorber, without an additional feed gas cooler, since the heat capacity of the circulating solvent is large compared to the gas. Depending on the operating modes and conditions, more or less of the CH_4 traces in the DOG (air contains about 2 ppmv CH_4) will be found in the Kr product.

10. Raw product purification: The CO_2 in the Xe raw product contains C-14 and can be recovered in a conventional KOH caustic scrubber. For a commercial use of the inactive Xe further purification is required.

    The R12 vapours in the Kr raw product can be removed to less than 100 ppm by refrigeration and to less than 1 ppm by adsorption on Linde 13X molecular sieve /6/.

4. BRIEF DESCRIPTION OF DESIGN AND OPERATION OF THE TEST FACILITY

The design of the test facility is based on previous operating experience with a laboratory scale test column, experimental engineering scale tests of individual components, reported data of the Oak Ridge pilot plants, gas solubility data and a simple model used for process calculations.

The operating temperature and flow ratio on a volume basis in each of the individual column zones are approximately constant over the packed height. The distribution coefficients of the key design components depend to a first approximation only on the temperature. At the low operating pressures, they are sufficiently independent from the partial pressure and the presence of the other gases. Therefore, the FENSKE equation shown in Fig.6 is an acceptable tool for process precalculations.
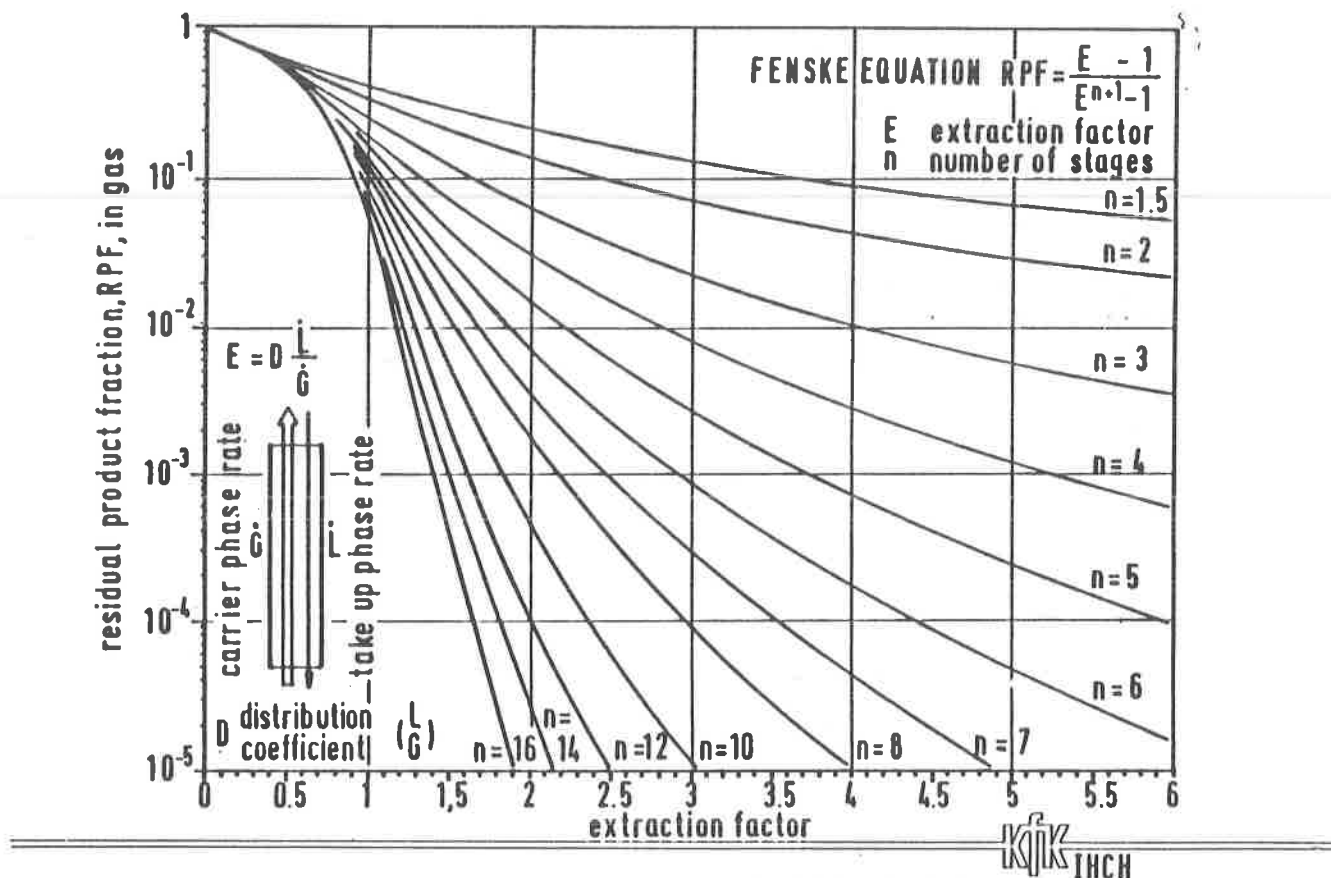
Fig. 6   FENSKE EQUATION, CALCULATED CURVES

The extraction or desorption factor E is the gas distribution coefficient at the operating temperature divided by the volume flow ratio; n is the number of theoretical stages in the packed zone. The packed height equivalent to a theoretical plate (HETP) depends especially on the packing type and somewhat on the operating conditions. A highly efficient wire mesh packing ('Goodloe', Metex corp., USA) has been used. The instructions of the packing manufactorer/13/provided a crude basis for HETP estimates.

Desirable decontamination and separation factors and product purities have been defined and a suitable range of operating conditions has been specified for each individual column zone. The heating and cooling requirements have been calculated from these data and the various packed zone dimensions have been estimated, using the 'Fenske' equation and the HETP estimates.

The test column was designed for efficient Xe recovery and not for Kr however. The essential design data are briefly summarized in table 2.

The pilot plant column is located in a 12 m high cold box on the one half of only 1.4m² inside floor area. The residual half is reserved for the Kr column under construction. The walls of the cold box are made from conventional 0.2 m thick sandwiches of polyurethane foam and steel sheets for thermal insulation. The photo in fig.7 shows the facility with the front wall removed; the cold column parts are thermally insulated.

The cold box is in the immediate vicinity of additional engineering scale facilities for off-gas purification and the start-up of tests with an integrated DOG-purification system is scheduled for next year.
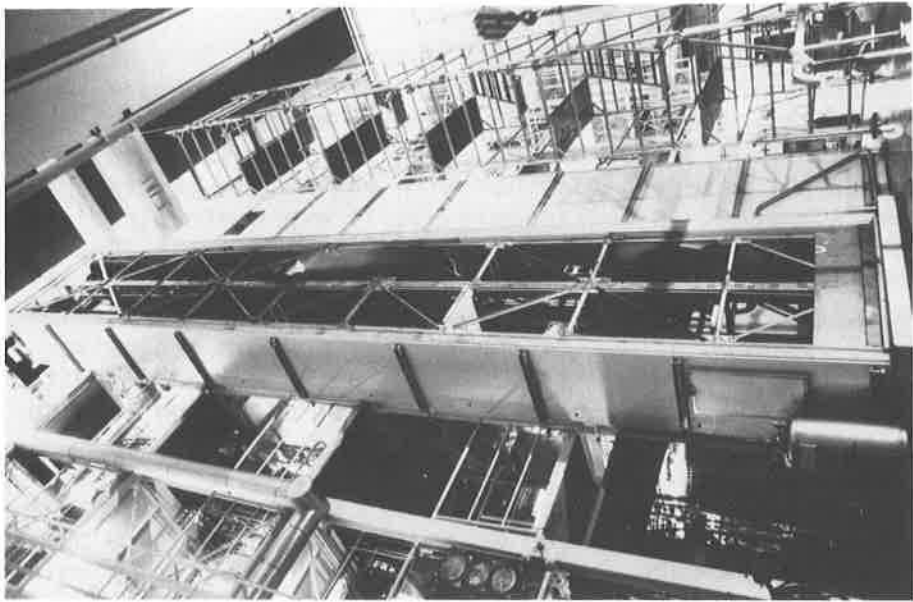
Fig. 7

Photo of the selective absorption facility
(front wall removed from the cold box)

COLUMN DIMENSIONS

	height	diameter
• absorber zone	1.8 m	0.10 m
• fractionator zone	2.7 m	0.075 m
• stripper zone	1.8 m	0.10 m
• total packed height	6.3 m	
• total column height	12.5 m	

CONSTRUCTION MATERIALS   SS 4306 (304 L), 4571

• wire mesh packing   "Goodloe", Metex corp.
  $1.9 \, m^2$ per liter

TYPE OF COMPONENTS

• solvent pump   gear pump
• solvent heat exchanger   plate type, fully welded
• reflux condenser   first stage shell and tube,
  second stage coil in annulus
• heaters   electrical, less than $4 \, Watt/cm^2$
• solvent tank   volume 50 l

REFRIGERATION SYSTEMS

• circulating R11 at $-60°C$ for reflux condenser
• evaporating liquid N_2 for circulating process solvent
• additional option: circulating R12 B1 at $-155°C$

ANALYTICAL EQUIPMENT

• quadrupole mass spectrometer   for purified off-gas
• gas chromatograph   for product and fractionator gas

IHCH

Table 2

DESIGN DATA OF THE XE TEST COLUMN

Analytical equipment

Two gas chromatographs (Perkin Elmer and Hewlett Packard) are used for product and fractionator gas analysis. The detection limits of the instruments are about 10 ppmv for most components; O_2 and N_2 are not separated.

The product gas is continually recycled to the absorber zone in a closed loop equipped with a flow indicator. This mode of operation has several advantages: 1. The product gas analysis and the determination of the feed gas concentrations are made at the same time. Sample volumes of 1 ml are withdrawn from the loop 3 times per hour and are recycled to the absorber together with the helium carrier gas. 2. The loss of the expensive Xe product is negligeable. 3. If a predetermined product gas volume is fed into the column, the circulating flow in the product loop allows a simple determination of the product gas residence time in the column. 4. At extended operating times, the slowly decreasing flow in the product loop allows a simple determination of the decontamination factor even without an expensive instrument. 5. Short-time recycle of impure products is possible , until suitable operating conditions are rearranged. Therefore, this mode of operation is also envisaged for plant application.

The purified off-gas is analysed continually with a calibrated quadrupole mass spectrometer (Balzers). The detection limit for Xe is 10 ppb and about 50 ppb for Kr, even in presence of some R12 vapour. The background spectrum of 1% by volume R12 is negligeable in the Xe mass range. The contribution of R12 fragments in the Kr mass range is considerable and only Kr-83 (11,5% abundancy in natural Kr) is suited for an accurate determination. Spectra in the Kr mass range are shown in Fig.8. The gas sample loop must be heated to prevent memory effects.

Refrigeration equipment

A brine type intermediate temperature refrigeration system cools the reflux condensor during operation and shut-down. A canned motor pump maintains the circulation of the R11 (CCl_3F) heat transfer fluid in a closed loop. Commercial 2-stage refrigeration compressors provide a maximum of 8 kW refrigeration energy at -70° C in the R11 storage tank.

At first, an additional low temperature 'brine' type refrigeration system has been used, to cool the circulating solvent and the feed gas to very low temperatures. The heat transfer fluid is R12B1 ($CClBrF_2$) and has a m.p. of -161° C and b.p. of -3° C. The circulating fluid is cooled down to -155° C by controlled evaporation of liquid N_2 in a special heat exchanger with a large heat capacity.

A considerable simplification of the low temperature refrigeration system has been obtained with an alternative method. The circulating process solvent (R12 m.p. -158° C) is cooled directly by evaporating liquid N_2. The complex refrigeration circuitery and the circulating pump are saved. Though both systems have been operated without much trouble, the reliability and conveniency of the latter proved to be much better.

Start-up and shut down procedures

The start-up operations are as follows: Feed gas and exit pipes are locked and the system is evacuated overnight to less than 10^{-1} Torr, to remove water and any volatile impurities to the trace level. The intermediate temperature refrigeration system is put into operation and about 70 kg of commercial R12 are drawn in via 4A molecular sieve. The gear pump for solvent recirculation is started and then the low temperature refrigeration system and the stripper heater are put into operation. The locks are opened and the fractionator heaters adjusted at a small

gas throughput. After thermal equilibrium is attained at the desired temperatures the column is ready for operation. Some minor readjustment of heaters and coolers is required at normal feed gas throughput to get an optimized performance.

The shut-down operations are as follows. The gas throughput is reduced to a very small value, to prevent the penetration of wet air. Both fractionator heaters are switched off. The coabsorbed air is desorbed in the stripper and the product gas inventory is completely flushed out from the product loop. Otherwise, the product gases are dispersed throughout the column and considerably extend the following start-up procedures. The low temperature refrigeration system is shut down. The stripper heater ist then switched off and the solvent pump some time later. The intermediate temperature refrigeration system keeps running and compensates for the heat input through the insulation. After some time, the solvent from dead volumes (e.g. siphon) has vapourized and is collected in the solvent tank. Start-up from this state takes less than one hour.
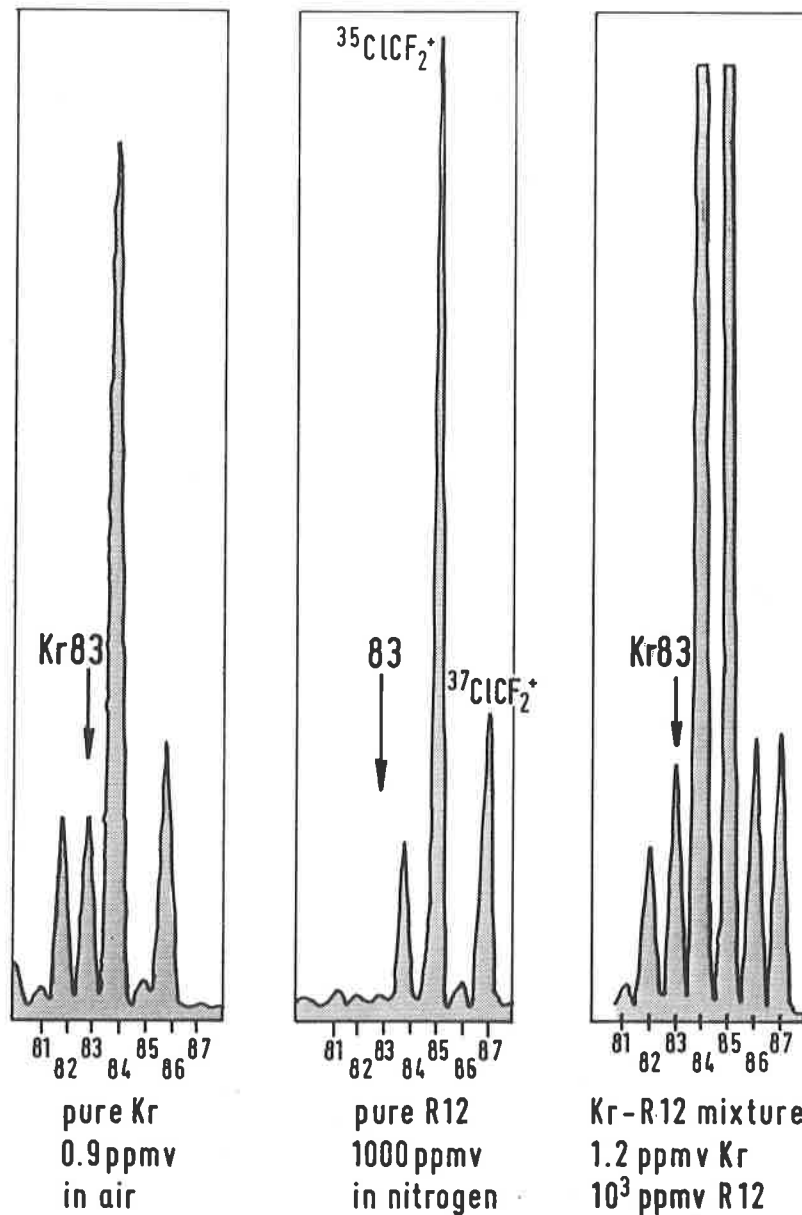
Fig.8 **MASS SPECTRUM IN THE KRYPTON RANGE**

5. EXPERIMENTAL RESULTS

Up to now, about 400 h of test column operation have been accumulated excluding start-up or shut-down time. Of these about 150 h have been employed in short-time testing, requiring frequent start-up and shut-down. The rest of the time was a campaign of 250 h of continuous operation. The plant performance was without serious trouble. Moderate changes of the operating conditions need far less than one hour, until the new steady state conditions are reached. Therefore, more than 60 different operating conditions have been tested.

The major aims of the experimental program are: Verification of the process model and the data basis, evaluation of component type and design and the accumulation of experience in view of process reliability under various conditions. The final objective is the identification of the preferred process modification and the specification of suitable operating parameters and component design details for a demonstration plant.

Essential experimental results are summarized in the following figures and tables:

In fig.9 the dependence of the Xe absorber decontamination factor (DF) from the gas throughput is compared to the results obtained from the "Fenske"-equation. The number of stages decreases somewhat towards the high DF's up to about 10^6. This is a normal behaviour and can be explained by axial backmixing in the gas and solvent phases. In our simple model, axial backmixing has not been included.

Axial backmixing is regarded with the help of stage number versus extraction factor (E) plots, as is shown in fig.10: The slope indicates the backmixing effects. Within this range of operating conditions the dependence of the number of stages on the column load was found to be of minor influence. At the desired operating conditions at about $E = 3$ the HETP can be calculated from these data and corresponds to about 0.2 m. The HETP values in the fractionator and stripper zones are insignificantly lower. The HETP values for the absorption of the less soluble Kr are about 2 times higher. The relatively low stage heights characterize the efficiency of the SS 304 L wire mesh packing. They are expected to be approximately unchanged with increasing column diameters, provided that attention is paid to a smooth solvent distribution at the top of the column zones.

The dependence of the Xe DF from the operating temperature in the absorber zone is shown in fig.11: The data are consistant with the temperature dependence of the Xe solubility in R12. A rather simple liquid N_2 level control system in the solvent cooler was sufficient to maintain the absorber temperature within a range of $\pm 1°$ C.

Fig.12 shows the stepwise decrease of the Xe DF with increasing off-gas flow rates as a function of time. After each change of the gas flow rate, the new steady state conditions are attained in the course of far less than one hour. Even sudden changes from minimum to maximum flow rates, or the other way round, in the course of a few minutes do not cause any trouble of the column performance. During this test run, the fractionator and stripper have been operated under normal conditions. Since they are not in the main off-gas line, the effects of the flow rate variations in the absorber are negligeable.

An efficient operation of the fractionator causes some product gas accumulation between the fractionator and stripper zones. This can be seen in fig.13: The open circles show the experimental DF's for Xe versus the gas rate, obtained under suitable operating conditions in the Xe column. They do not fit with the calculated
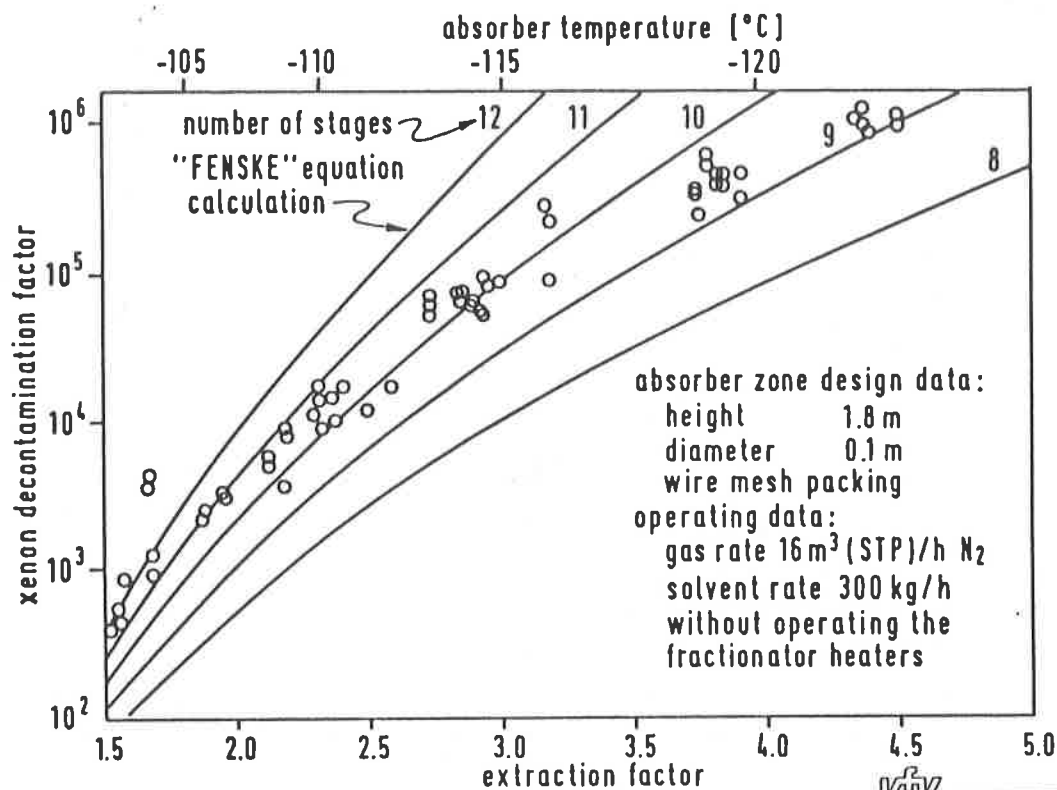
Fig. 9 DECONTAMINATION FACTOR VERSUS EXTRACTION FACTOR
FOR THE XE ABSORBER ZONE
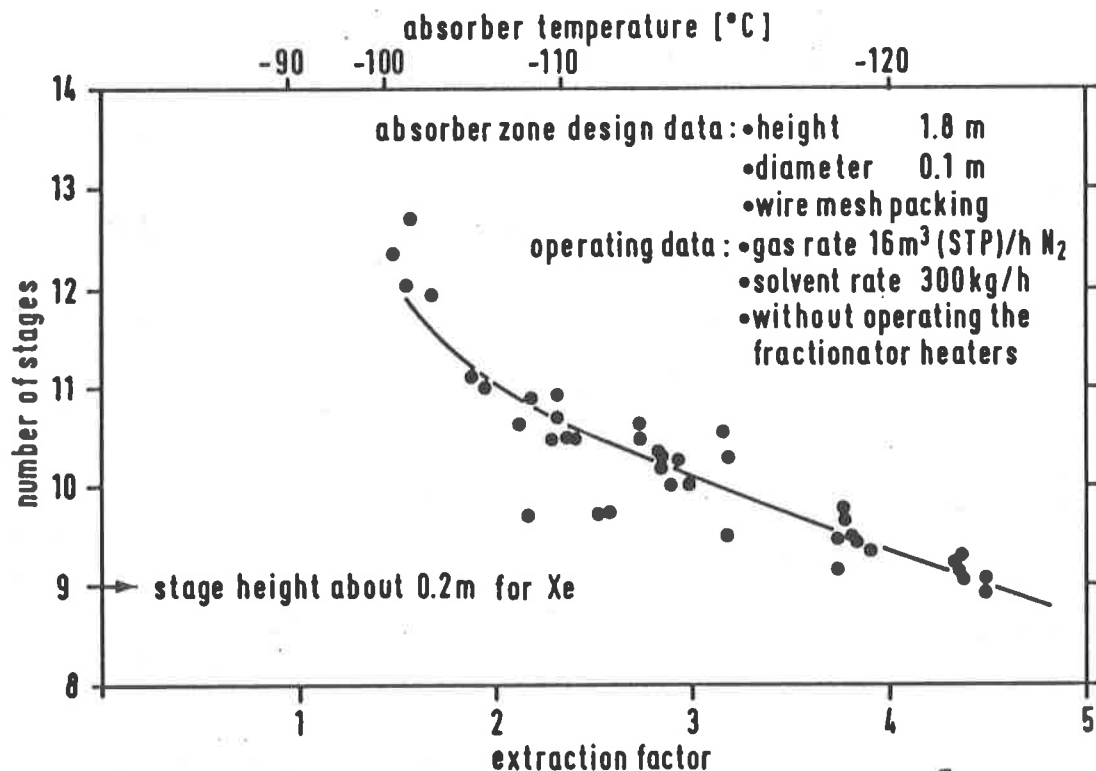
Fig. 10 NUMBER OF STAGES IN THE XE ABSORBER
VERSUS THE EXTRACTION FACTOR

Fig. 12 XE DECONTAMINATION FACTORS
AT STEPWISE CHANGES OF THE GAS RATE

Fig. 11 XENON DECONTAMINATION FACTOR
VERSUS THE ABSORBER TEMPERATURE

curves, as was verified in figs.9 and 10. The decrease of the DF's caused by the product accumulation is allowed for in the upper circles, which are in accordance to the results obtained without fractionation. The accumulation factors obtained experimentally are in agreement with model calculations.

The Fig.14 shows an example of suitable operating conditions for the Xe column. Feed, product and off-gas compositions obtained are also indicated.

A brief summary of all the results obtained up to now is given in table 3. The DF's, separation factors and product purities which have been obtained are comparable to cryodistillation, as was expected from the comparison of the separation selectivity for both alternatives. The results are consistent with the simple process model and the gas solubility data basis. The flexibility of the process is considerable and the desired decontamination and separation factors can be adjusted at will by adaption of the column design and the operating conditions.

Some additional favourable characteristics compared to cryodistillation are worth mentioning: High Xe concentrations in the feed gas up to a few percent by volume do not cause freezing problems or disturbance of the process. This is important in view of the higher fuel burnup's and the somewhat lower DOG dilution with pointless gas volumes from the shear in future plants or variations of the rare gas concentrations.

Operating the columns under standby conditions does not require   rare gases. Steady state conditions may be reached within one hour after startup. The rare gases may be removed in a short time prior to shut-down. Due to the low operating pressure and radiokrypton inventory, an accidental release is expected to be a rare and less serious event.
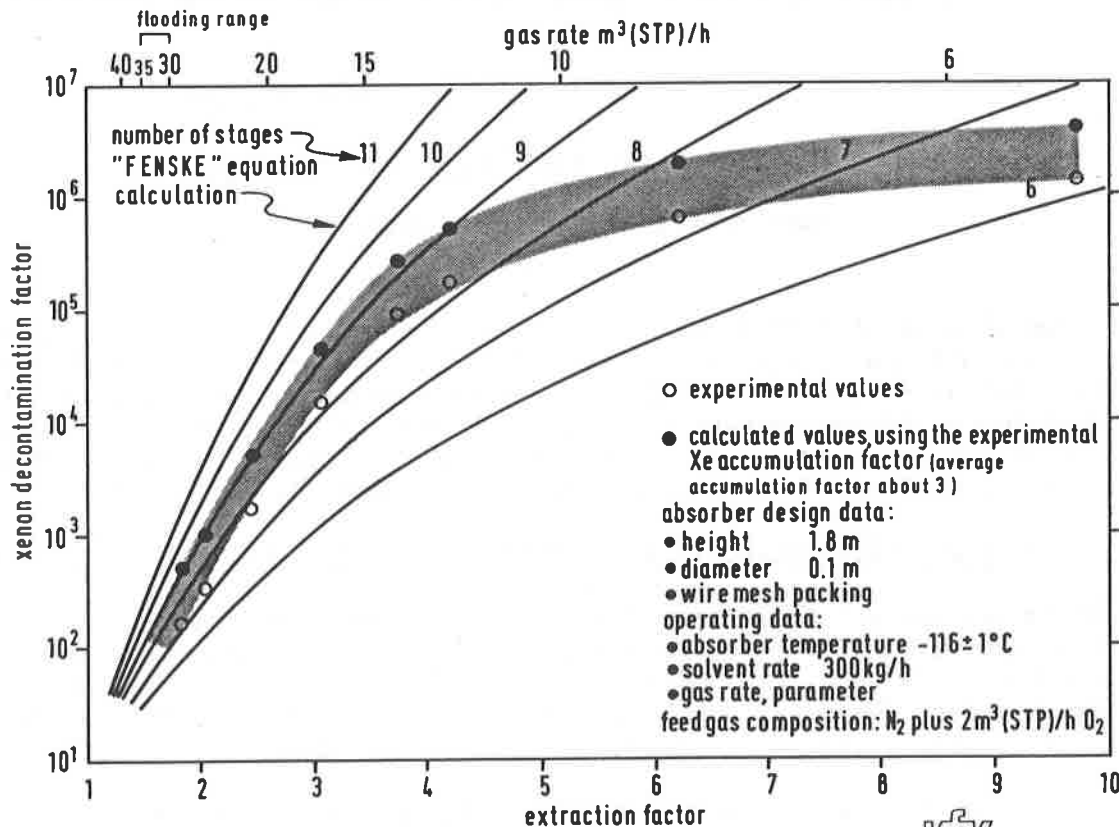
Fig.13   XENON DECONTAMINATION FACTORS
COMPARISON WITH AND WITHOUT FRACTIONATOR OPERATION

OPERATING CONDITIONS

- pressure: 1 bar
- solvent rate: up to 450 kg/h
- gas rate: up to 25m^3(STP)/h
- flooding range: 30 – 35m^3 (STP)/h
- Xe absorber temperature: –100 to –125 °C
  (Kr absorber temperature: about –140 °C)
- feed gas components: carrier gases; N_2, O_2
  product gases; Xe, Kr, N_2O, CO_2
  impurities; $O_3, (NO)$

RESULTS AT SUITABLE CONDITIONS

- consistent with a simple process model
- Xe decontamination factor $> 10^5$
  (Kr decontamination factor $> 10^3$)
- raw product purity $Xe, CO_2, N_2O > 99.9\%$
  without solvent vapours $(Kr > 99.9\%)$
- Kr/Xe separation factor $> 10^5$
- residence time Xe in Xe column $< 0.2h$
  (residence time Kr $< 0.4h$)
- stage height for Xe absorption about 0.2m
  (stage height for Kr absorption about 0.4m)

Table 3:

SUMMARY OF DATA FOR THE XE COLUMN
(preliminary Kr data in brackets)

The selective absorption process is insensitive to the presence of O_3 in the feed gas. About 500 ppm O_3 have been fed to the column. Since the Xe and O_3 b.p.s are similar, the O_3 accompanies the Xe and has been decomposed to O_2 on a small catalyst bed in the Xe raw product stream. The explosion limit of O_3 in R12 vapour is high, about 24% by volume /15/. The O_2 in the Xe raw product does not disturb the subsequent operations to produce a pure Xe for commercial use.

6. RADIOLYTIC DEGRADATION AND PURIFICATION OF THE SOLVENT

A continuous solvent purification is integrated into the process and is above all a preventive measure to maintain a dry solvent and a low impurity level. At normal operating conditions the amount of impurities is very small and does not disturb the process. The small amount can easily be removed from the circulating solvent with a solid sorbent bed. Spent sorbent may be regenerated or replaced.

There are two sources of impurities: 1. Carry-over with the DOG and 2. radiolytic and - probably negligeable - chemical solvent degradation. It is more convenient and economical to purify the feed gas rather than the solvent. Radiolytic solvent degradation is inherent to the process and contributes the bulk of the impurities.

purified off gas

1034 mbar

N_2, O_2 20 m³(STP)/h (10% vol O_2)

N_2O, CO_2 below detection limit

Xe 0.12 ppmv

Kr 300 ppmv

concentrations by volume

0.03 % Kr
0.1 % CO_2
0.4 % N_2O
0.24% Xe

feed gas

N_2, O_2 20 m³(STP)/h
(10% vol O_2)
Kr 300 ppmv

20°C

feed gas cooler

C2

product loop

product take off

-53°C

product gas GC analysis

$O_2, N_2, Kr < 10$ ppm
below GC detection limit

CO₂ 9.3 %
N₂O 37.6 %
Xe 22.4 %
R 12 30.7 %

C1

stripper

-29°C

-26°C

-35°C

-92°C

-105°C

-33°C

-31°C

H

heat exchanger

-119°C

-118°C

C2

-100°C

absorber DP 5 mbar

fractionator

H 0.50 kW
(3.2%)

total height 12 m

3.20 kW H
(16% of reflux)

340 kg/h ±1% solvent rate

solvent tank inventory 70 kg R 12

solvent pump

— unloaded solvent
—·— loaded solvent
⇒ gas
H electrical heater
C1 cooler -60°C loop
C2 cooler (N_2)l evaporation

Fig.14 SUITABLE OPERATING CONDITIONS AND RESULTS
IN THE XE COLUMN

An accumulation of impurities without solvent purification may have disturbing consequences:
1. Scarcely soluble solid impurities may cause plugging (examples are H_2O, N_2O_4)
2. Volatile impurities may contaminate the products (examples are NO, CH_4)
3. Inorganic impurities may be corrosive in the presence of water (examples are Cl_2, HCl, HF)
4. Organic, solvent-like impurities may accumulate to a large extent without causing any trouble (examples are CCl_3F, CF_3Cl, $C_2F_4Cl_2$, $C_2F_3Cl_3$)

Radiolytic solvent degradation: Radiolytic solvent degradation is usually considered to be the major disadvantage of the selective absorption process. Therefore, the consequences have been investigated in some more detail.

Radiolytic R12 solvent degradation is sensitive to the chemical environment and proportional to the Kr-85 inventory. The Kr process inventory is proportional to the Kr residence time, which depends on the operating conditions and the equipment design. The Kr is concentrated in special parts of the columns. The Kr inventory in the first Xe scrubber is very low; a residence time of about 10^{-2} h is estimated. In the second Kr column there are two accumulation zones:
1. The cold feed side in the heat exchanger plus the lower absorber and upper fractionator zone as well as in the space between. 2. The top of the stripper with increasing Kr concentrations toward the product take-off point in the reflux condenser.

Organic and inorganic degradation products are produced: The total amounts are small and do not disturb the process performance. The organic products are solvent-like and inert: CF_3Cl, $CFCl_3$, $C_2F_4Cl_2$, $C_2F_3Cl_3$, $C_2F_2Cl_4$, etc.; they may accumulate without trouble for a very long time. The inorganic products HF, HCl and Cl_2 are potentially corrosive in the presence of water.

The radiation sensivity of the solvent has been determined under process conditions at the Technical University of Munich /16/. The presence of O_2 enhances the production of the inorganic products by about one order of magnitude; additionally, traces of CO_2 are formed by oxidative degradation. The amount of organic products remains approximately unchanged. In the fractionator and absorber zones the degradation occurs in the presence of O_2; normally no O_2 is present in the stripper zone and the reflux condensor. The addition of suitable scavengers to the solvent as for example C_2Cl_4, was found to supress the formation of inorganic products.

A crude estimate of the amounts produced during processing of 1 MTHM in spent LWR fuel has been made. The presence of oxygen and a total Kr residence time of 0.4 h have been assumed. The following values have been calculated: Less than 20g solvent are degraded per MTHM. The production rates of HF, HCl, Cl_2 and CO_2 are less than 2 g for each product per MTHM. Less than 10 g of organic material is formed during processing 1 MTHM. These amounts are rather low. A recheck of these values in a cold pilot plant would be desirable. Since the radiolytic effects of electrons and γ-rays are comparable, an X-ray generator should be a convenient tool for simulation.

7. SOME TECHNICAL ASPECTS

Some important aspects for a technical application are mentioned in the following.

The experimental experience with the test column can be used to develop a crude first idea of approximate design data for 100 m³ (STP)/h absorption columns. This throughput could be compatible with a 6 MTHM per day commercial reprocessing plant. The conceptual design data correspond to a scale up factor of about 6 compared to our test column and are summarized in table 4.

	XE COLUMN		KR COLUMN	
COLUMN DIMENSIONS	height	diameter	height	diameter
ABSORBER	2.4m	0.30m	3m	0.4m
FRACTIONATOR	3.6m	0.22m	3m	0.3m
STRIPPER	2.0m	0.30m	2m	0.4m
total packed height	8 m		8m	
total column height	12 m		12m	
OPERATING CONDITIONS	temperature	pressure	temperature	pressure
ABSORBER	– 120°C	0.8 bar	– 150°C	0.8 bar
FRACTIONATOR,STRIPPER	– 35°C		– 35°C	
CIRCULATING SOLVENT FLOW	1.2m³/h (at R12 b.p.)		3m³/h (at R12 b.p.)	
SOLVENT INVENTORY TANK	0.25m³	″	0.6m³	″
EXPECTED DATA				
DECONTAMINATION FACTOR	> 10^4 Xe		> 10^2 Kr	
SEPARATION FACTOR	> 10^7 Kr from Xe		> 10^6 O_2 from Kr	
RAW PRODUCT PURITY	> 99.9 % Xe,N_2O,CO_2		> 99 % Kr (CH_4,CO_2*)	
exept solvent vapours			*radiolytic solvent degradation	

Table 4:

CONCEPTUAL DESIGN DATA FOR A 100 M³ (STP)/H SELECTIVE ABSORPTION PLANT

The total selective absorption subsystem, including a low temperature nitric acid scrubber for prepurification may be located in a 12 m high cold box with an inner volume of about 200 m³. If the box temperature corresponds to the R12 b.p. -35° C (0.8 bar), large parts of the equipment (fractionator, stripper, solvent vessels, pumps etc.) do not need much individual insulation and are accessible for maintenance and repair even under operation. Access through an air lock chamber maintains a dry atmosphere inside. The Kr-85 inventory and especially the γ-radiation level is low, provided that the two Kr accumulation points are adequately shielded. Short-time access - e.g. to the solvent pumps - might therefore be tolerated even under hot operation. Such characteristics contribute to reliability and availability.

Compared to our test column, the increased packed height, proposed for the Xe fractionator, should produce Xe/Kr separation factors > 10^7. Downstream from 14-CO_2 removal 1 m³ (STP) Xe raw product will contain < 1 m Ci Kr-85. Further purification for commercial use is possible without expensive radiation protection measures. Xe recovery without Kr removal is a simple task and requires only the Xe column.

For the cold box system, a total electric power consumption of about 250 kW has been estimated. This is based on the assumption, that the peripheral equipment outside the cold box, especially the refrigeration equipment, requires about 3 times as much electrical energy as the total energy input into the cold box. The power consumption depends on the efficiency of the solvent heat exchanger and is nearly proportional to the circulating solvent flow.

Both refrigeration systems are located in an inactive area outside the cold box. Heat transfer fluid is R12 at about -60° C, circulating in a closed loop through the reflux condensors. Refrigeration compressors cool the R12 in the storage tank. The second system uses evaporating N_2 at some bar pressure, to cool the process solvent to the absorber temperature. N_2 recondensation machines maintain the liquid level in a N_2 storage tank. Counter-current heat exchange between the feed and the purified off-gas can be used to refrigerate the feed gas cooler. All heat transfer fluids are constituants of the process system and small accidental leaks will not procedure immediate trouble or shut-down.

Redundant on-line equipment is required especially for the moving parts, e.g. for the solvent recirculation pumps, the refrigeration compressors and the N_2 recondensation machines, to achieve a high system availability.

The solvent vapour concentration in the purified off-gas is less than 30 ppm by volume, due to the low Kr absorber temperature at -150° C. This is more than one order of magnitude lower than the 1000 ppm maximum permissible concentration and corresponds to a loss of about 0.3 kg per day, thus obviating additional recovery steps.

8. SUMMARY OF PROCESS CHARACTERISTCS AND CONCLUSIONS

Essential technical and safety characteristics of the selective absorption process under development are briefly summarized in the following:

1. Equipment and operating modes of the process are comparable to many well-known gas absorption processes widely applied on an industrial scale.

2. Xe and Kr are recovered and separated from each other using two absorption columns. Any 14-CO_2 or traces of Rn are recovered simultaneously with the Xe, thus paying attention to potential future release restrictions.

3. The process is flexible: the desired decontamination and separation factors and the product purities can be chosen at will with suitable operating conditions and equipment design. The process accommodates gas rate and concentration variations as well as high Xe concentrations.

4. The operating pressure is slightly below atmospheric pressure; this contributes to safety and reliable process performance. Therefore, an accidental release is expected to be a rare event. Accidental inleakage of small volumes of the dry cold box atmosphere, does not create immediate trouble.

5. The consequences of the low operating temperatures are: an increase of separation selectivity, a decrease of equipment size and energy requirements; solvent recovery from the purified off-gas is not necessary. The solubility of trace impurities is still sufficiently high due to the large solvent volume.

6. The very low rare gas inventory has many favourable aspects:
    -   An accidental release is less serious.
    -   The radiolytic solvent degradation is low. Therefore, only small volumes of spent sorbent beds are produced, in order to maintain a pure and dry solvent.
    -   Steady state operating conditions are reached in a short time.
    -   Stand-by operation is possible without any rare gas inventory.

- Short-time access to the cold box may be acceptable even under hot operation. Such maintenance and repair possibilities improve the reliability and availability.

7. The off-gas prepurification is not complex, as the process is not very sensitive to impurities. Only the freezing DOG constituents, H_2O and HNO_3 vapours and NO_x must be removed to the trace level to prevent plugging or potential corrosion. The sub-cooled feed gas is a very efficient preventive measure. Previous removal of O_2, N_2O and CO_2 or traces of CH_4 and even ozone is not required. In case of defective upstream NO_x or iodine removal steps, the low temperature subsystem in the cold box effects an automatic in-line correction and contributes to the reliability of the entire DOG purification train.

8. Data of simple binary mixtures are a sufficient basis for a process model.

Compared to the cryogenic alternatives, technical as well as safety advantages are expected for the selective absorption process. A final comparison of both variants investigated in Germany, will be made, when the state of development is about comparable. The selective absorption pilot plant (TED) is part of a flexible integrated DOG system (HET facilities) on the engineering scale. Integrated operation of the rare gas absorption subsystem is part of the future development program.

REFERENCES

/1/ Empfehlung der Strahlenschutzkommission vom 24. Febraur 1983 zur Rückhaltung radioaktiver Stoffe bei einer Wiederaufarbeitungsanlage
/2/ Ammon von R., Hutter E., Leichsenring C.H., Weinländer W.; CEC seminar on 'Radioactive Effluents from Nuclear Fuel Reprocessing Plants', Karlsruhe 1977, p.535
/3/ Henrich E., Hüfner R., Weirich F.; KfK-Nachrichten, 14, 3(1982) 172
/4/ Leudet A., Miquel P., Castellani F., Curzio G., Gentili A.; 'Methods of Krypton-85 Management' Radioactive Waste Management Series Vol.10, Hebel W., Cotton G. (CEC editors); Harwood Academic Publishers GmbH, Chur, Switzerland 1983
/5/ Mc Ilroy R.W., Glueckauf E., de Nordwall H.J., Pummery F.C.W.; 2nd Geneva Conference, paper 309 (1958)
/6/ Merriman J.R., Stephenson M.J., Kanak B.E., Little D.K.; IAEA-SM-245/53, February 18-22, 1980, Vienna, Austria
/7/ Steinberg M., Manowitz B. ; Ind. Eng. Chem. 51, 1(1959)
/8/ Merriman J.R.; Paducah Gaseous Diffusion Plant, Kentucky, March 1977, KY-G-400
/9/ Landolt-Börnstein 'Zahlenwerte und Funktionen'; Technik Vol.IV, part 4, Wärmetechnik C, Springer 1976
/10/ Kali-Chemie AG, Hannover, West Germany; 'Kaltron Taschenbuch', 1978
/11/ Ammon von R., Franz G., Henrich E.; unpublished results 1983
/12/ Henrich E., Bauder U., Steinhardt H.J., Bumiller W.; this conference
/13/ Metex Corporation, Edison, New Jersey; Information Bulletin "How to design a Goodloe column"
/14/ Henrich E., Ammon von R., Hutter E.; KfK-PWA status report, march 1984, to be published
/15/ Penzhorn R., KfK, private communication 1983
/16/ Fürst W., Heusinger H.; Technical University Munich, private communication

CHROMATOGRAPHIC SEPARATION OF KRYPTON FROM
DISSOLVER OFF-GAS AT LOW TEMPERATURES

H. Ringel and M. Meßler

Kernforschungsanlage Jülich
Institut für Chemische Technologie
der Nuklearen Entsorgung
Jülich, Germany

Abstract

Separation of krypton from dissolver off-gas by adsorption on solid adsorbers is experimentally investigated. The principle of the developed process consists of adsorption on activated charcoal and separation of the different gas species by purging the charcoal with helium. Different process variations in regard to adsorption pressure and column temperature are compared with each other. For hot cell application a process with gas adsorption at $-150^{\circ}C$ and nominal pressure seems to be most suitable. In this case and for an off-gas flow rate of 100 m^3 STP/h the whole column volume for a continous operating process is about 300 l charcoal and the helium purge flow rate is 8 m^3 STP/h. Among other parameters the influences of the off-gas composition and fluctuations of the noble gas content have been investigated.

I. Introduction

In 1983 the German Radiation Protection Commission (SSK) announced that for a 350 t/a reprocessing plant the retention of Kr-85 would not be necessary; but the Commission did recommend the further development of Kr-85 retention processes (1). The processes which have been investigated so far are typically based on three different principles: low-temperature rectification (2), absorption (3,4), and adsorption (5,6).

This paper reports the further process development of an adsorption process previously described (6). The main principles of the new process are adsorption at low temperature and nominal pressure followed by chromatographic gas separation during temperature rise. It is expected that this process will be very well adapted to the necessary hot cell operation, mainly small hot cell space and simple, as well as reliable, operation.

II. Principle of Dissolver Off-Gas Cleaning

The separation of the noble gas krypton from dissolver off-gas will be the final step in any dissolver off-gas cleaning process. Fig. 1 shows a simplified flow sheet of a dissolver off-gas cleaning process in regard to Kr-85 separation. For the purpose of giving a guideline for
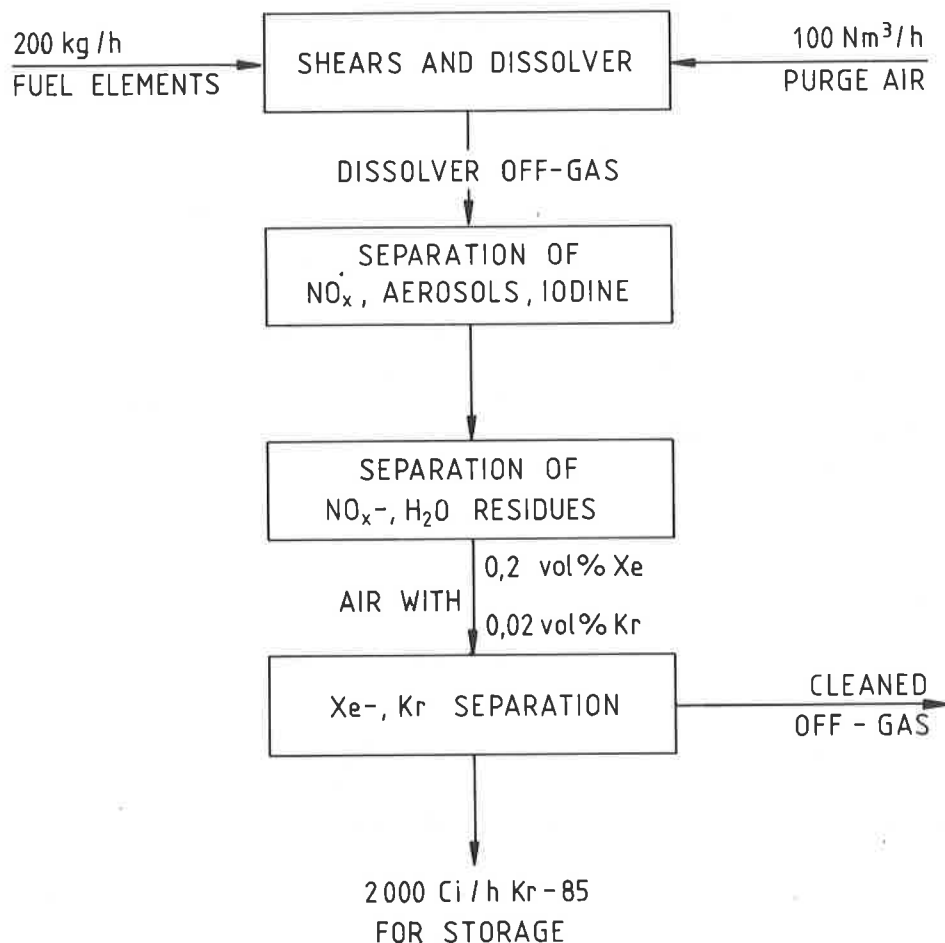
Fig. 1: Basic flow sheet for dissolver off-gas cleaning

the development of a Kr-85 separation process the following overall parameters are assumed:

E.g. shear and dissolver might have a throughput of 200 kg fuel/h and could be purged with 100 Nm^3 air/h. 1 kg of LWR fuel with a typical burn-up and at least 1 a cooling time contains about 0.1 Nl Kr, corresponding to 10 Ci Kr-85. This means that the off-gas will have an average noble gas concentration of 0.02 vol % Kr and 0.2 vol % Xe.

Before noble gas separation the off-gas will be cleaned of NO_x, aerosols and iodine in a main off-gas cleaning process. Residues of

NO_x and H_2O behind this cleaning step can be separated from the off-gas by adsorption on a molecular sieve. A process based on this principle is described in (6).

The CO_2 of the air can either be separated by an additional adsorption column of 5 A molecular sieve or it may be separated in the following Kr separation step, possibly together with Xe and N_2O.

III. Parameters for the Adsorption of Kr, Xe and Air on Activated Charcoal

Charcoal Selection

For the development of a Kr separation process by adsorption, different adsorption characteristics have been measured in the system: Kr, Xe and air on activated charcoal. During the process development several kinds of charcoal were considered. The charcoal with the best characteristics was a "MERCK" activated charcoal. This is a gas chromatography grade charcoal of 0.5 to 0.75 mm particle size, poured density of 440 g/l and a specific surface of 1050 m^2/g. Although this charcoal did not have the highest static adsorption capacity for krypton it showed the best features with respect to dynamic adsorption and desorption. This charcoal was mainly used throughout the experiments.

Adsorption Capacities

The adsorption capacity of charcoal for the noble gases Xe and Kr has been determined for a variety of parameters such as column temperature, noble gas content of the air, pressure and type of charcoal. Fig. 2 gives the most important relationship, which is the dependence of noble gas adsorped versus column temperature. For relatively low partial pressure of the noble gases the increase in the adsorption capacity with decreasing temperature is quite considerable. For instance, the Kr adsorption from an N_2 carrier gas which contains 0.2 vol % Kr increase from 0.04 Nl Kr/l charcoal at R.T. up to 40 Nl Kr/l charcoal at -180°C. This means that at -180°C about 1 l of charcoal has the same Kr retention as 1 m^3 charcoal at R.T.

Breakthrough Curves

The dynamics of the adsorption process in an adsorption column are shown by the measurement of the breakthrough curve. With this curve the length of the mass transfer zone (MTZ) and the adsorption capacity for a specific adsorption column can be determined. For instance, Fig. 3 shows the breakthrough curve for the adsorption of Kr in a column at -130°C. At this low temperature, the breakthrough curve is still symmetrically "S"-shaped, indicating that the Kr adsorption is still in the range where the adsorption capacity is proportional to the partial pressure of Kr. This is not true of Xe as shown by Fig. 4. Compared with the Kr breakthrough, the Xe breakthrough is slowed down in the last part of the breakthrough due to Xe overloading.
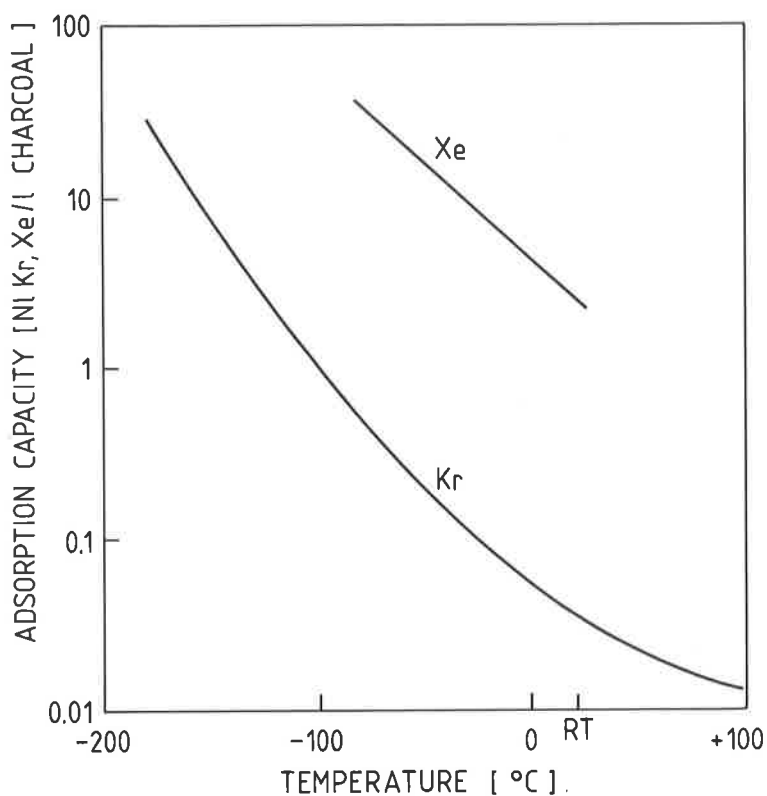
Fig. 2:   Adsorption capacity of activated charcoal for noble gases
          versus temperature
          Dynamic measurement of breakthrough capacity
          Gas composition: N_2 with 2 vol % Xe and 0.2 vol % Kr
          Activated charcoal: MERCK, 0.5 to 0.75 mm particle size
          Pressure: 1 bar
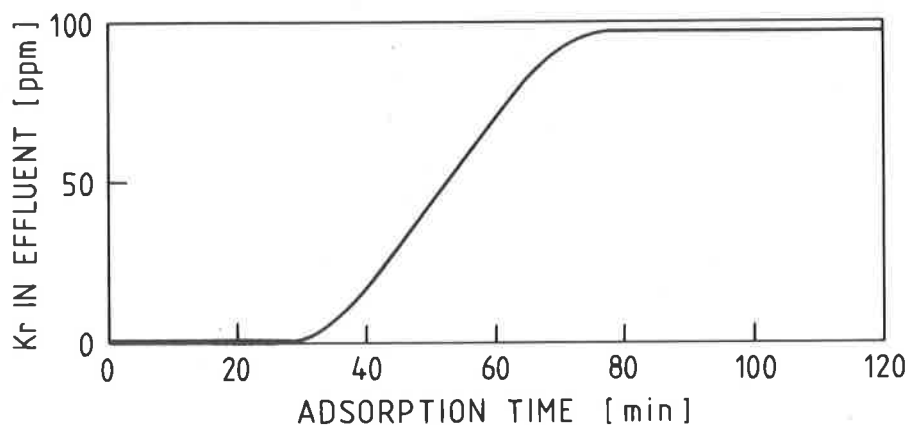
Fig. 3:   Breakthrough curve for Kr on charcoal
          column: 35 mm ID x 520 mm lg., -134°C, 1.2 bar
          gas flow: 1 Nm^3/h, air with 0.01 vol % Kr and 0.1 vol % Xe
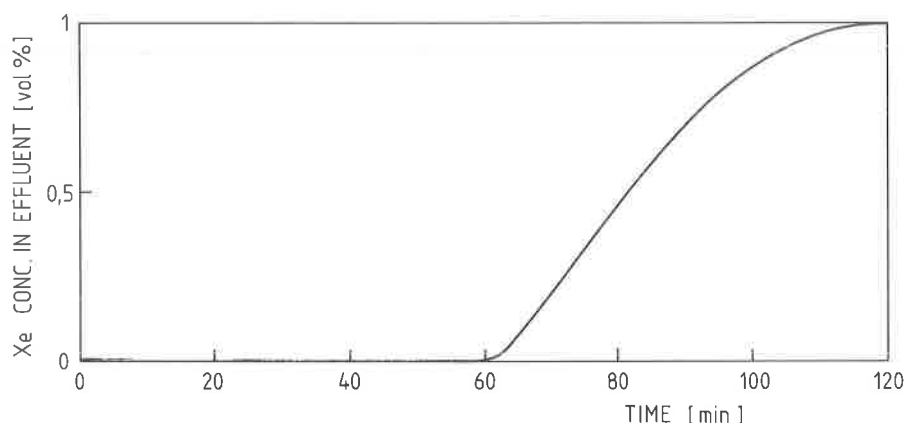
Fig. 4: Breakthrough curve for Xe on charcoal
column: 35 mm ID x 200 mm lg., -108°C, 1 bar
gas flow: 1 Nm^3/h, N$_2$ with 0.1 vol % Kr and 1 vol % Xe

Velocities of Xe, Kr and Air in a Charcoal Column under He Purge

For the separation of e.g. Kr and N$_2$ in a single process step one has to apply the principle of gas chromatography. This means a batch of the Kr-N$_2$ gas mixture is flushed by a carrier gas through an adsorption column, in the course of which Kr and N$_2$ will travel at different velocities through the column and therefore elude at different times.

Fig. 5 gives a chromatogram from a gas chromatograph for the separation of an air-noble gas mixture in a charcoal column at 90°C. Also at temperatures well below 90°C, the air components N$_2$, O$_2$, as well as Ar, will hardly be separated by charcoal, whereas air and Kr separate increasingly more strongly at lower temperatures. The dependence of the separation of an air-Kr-Xe mixture on temperature is demonstrated in Fig. 6. For each gas component the velocity of the peak-beginning (V$_B$) and of the peak-end (V$_E$) was measured for different column temperatures. From the diagram one can read the maximum temperature at which a complete separation of two gas components can be achieved (for the given conditions such as: column length, carrier gas flow and gas batch size). E.g., for the separation of air and Kr the maximum temperature is -30°C; for this temperature the velocity V$_E$(air) = V$_B$(Kr). Of course, this is only true of small batch sizes, such as for analytic measurements. For large batch sizes this maximum temperature is substantially lower and has to be determined experimentally.

986
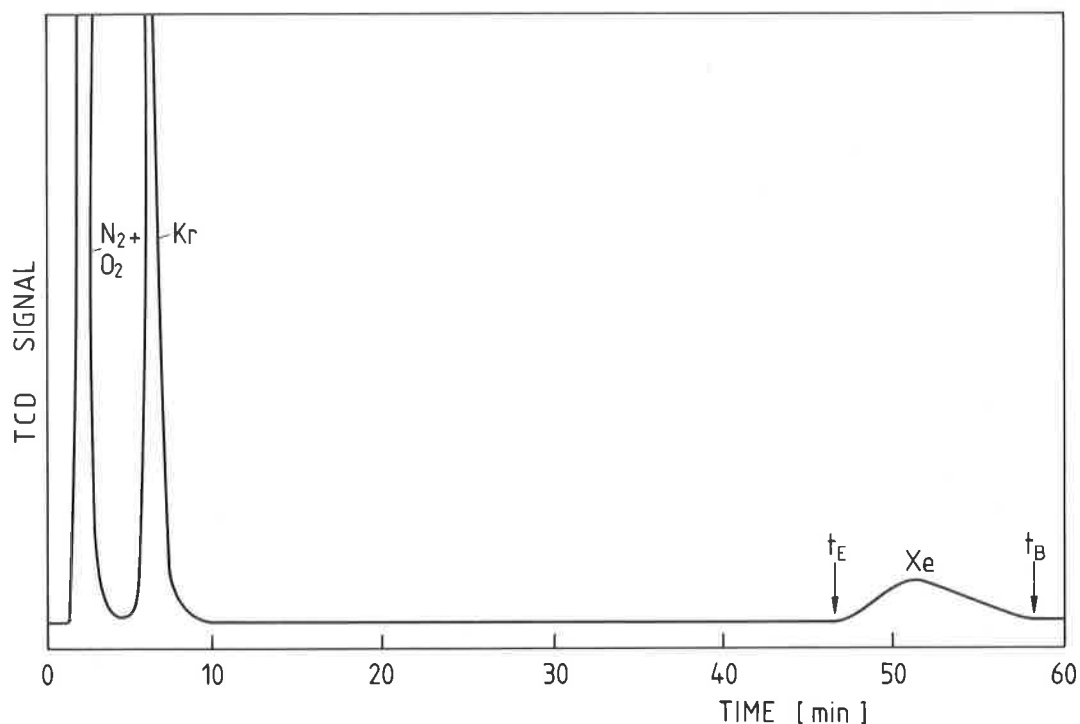
Fig. 5:   Chromatogram of a gas chromatograph for the separation of an
           air-noble gas mixture (5 % Xe and 10 % Kr in air) in a
           charcoal column (4.2 mm ID x 3 m lg.) at 90°C. The He-
           carrier flow was 40 Nml/min. Batch size 10 ml gas

IV.   Kr Separation by Adsorption at RT

The outline of a RT-separating process will be given in this chapter
for a comparison of an adsorption process operating at and above RT
with such processes operating below RT.

A possible process for Kr separation without cooling of the adsorption
column below RT is described in (6). This process consists mainly of
two successive steps:

1.   Xe separation by charcoal columns with simultaneous
     concentration of Kr in the off-gas.

2.   Separation of Kr from the residual off-gas by
     preparative gas chromatography.

In the first process step Xe and Kr are adsorbed in a charcoal column
until Kr breakthrough. At this moment the column is switched into the
regeneration sequence. The regeneration of the loaded column occurs by
heating up to 180°C and by purging the column with a small N_2 flow
under evacuation down to 50 mbar. If a certain part of the desorbed
gas, which has a Kr concentration below and up to the inlet Kr
concentration, is recycled, the main experimental results are as

987
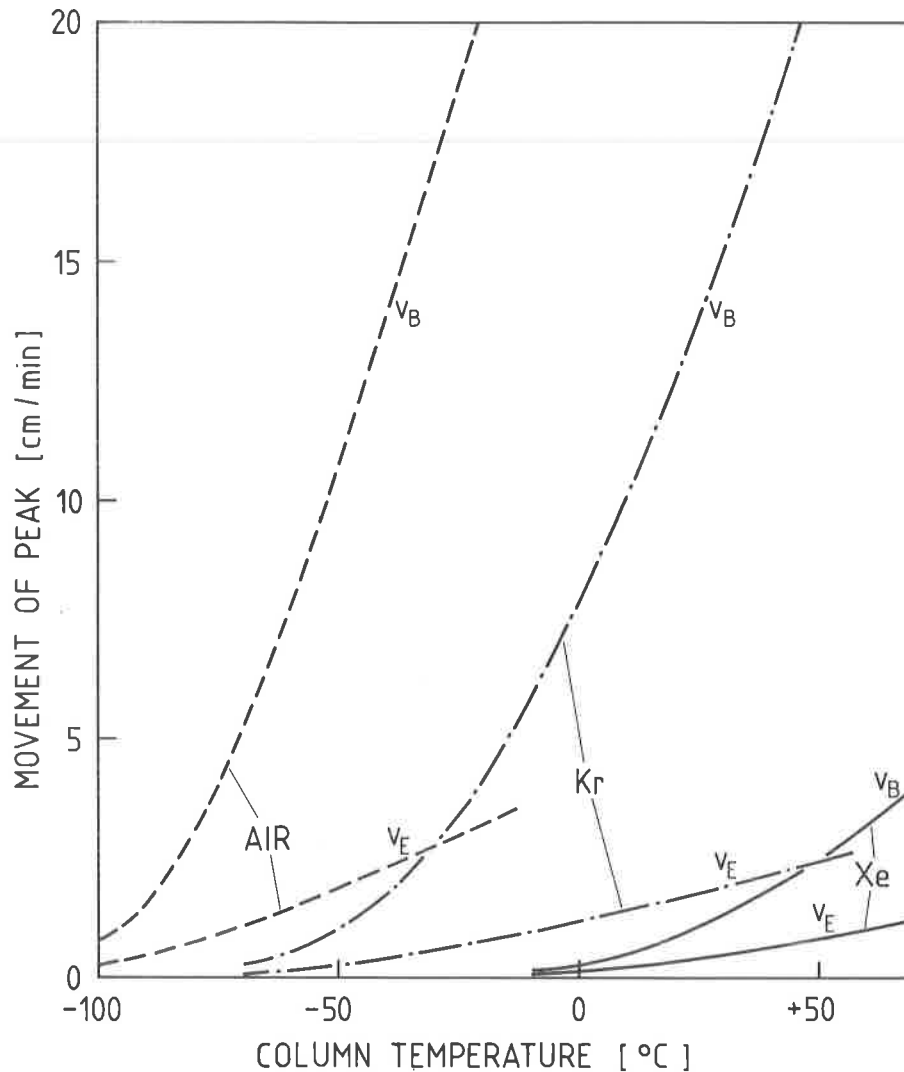
Fig. 6: Movement of peak-beginning (V_B) and peak-end (V_E) for air, Kr and Xe through a charcoal column (3.2 mm ID x 100 mm lg.) in relation to column temperature. He-carrier flow was 30 ml/min, each gas batch size 0.25 ml

follows:

specific off-gas throughput $q = 10 \dfrac{Nl\ gas}{h \cdot l\ charcoal}$

(This specific gas throughput is a value for scale-up approximation and for comparison between different processes. It gives the possible off-gas throughput (Nl/h) per column volume (l) for a continuous operating process. That means for a flow sheet with at least two parallel columns. It is determined by experiment.)

minimum regeneration time: 2 h
off-gas reduction factor: 8
decontamination factor: ≈ 400

988

The main experimental results for the second process step, preparative gas chromatography, were:

specific off-gas throughput: 15 $\dfrac{Nl\ gas}{h \cdot l\ charcoal}$

cycle time: 23 min

quotient of He flow ($\dot{V}_{He}$) to off-gas flow ($\dot{V}_G$) : $\dot{V}_{He}/\dot{V}_G = 4,8$

decontamination factor: ≈ 1000

Kr concentration of the product: 87 vol % Kr

The process operates at off-gas loading at nominal pressure. If one loads the column at elevated pressure, the necessary column volume and He purge flow will be reduced. One example is given in Chapter VI.

V.   Chromatographic Kr Separation at Low Temperatures

Adsorption and Regeneration at Nominal Pressure

A Kr separation process at low temperature and nominal pressure will result in small columns and will not require pumps; that means it should be specially suitable as a hot cell process. Therefore this process scheme was studied in more detail.

The principle of the investigated process consists of adsorption of the noble gases Xe and Kr on charcoal at very low temperatures, followed by gas separation during a specific column regeneration. This regeneration is accomplished by a controlled heating up of the column and purging it with a small He-gas flow.

Fig. 7 gives a flow diagram for the main part of the experimental equipment. In principle, it consisted of two columns which could be cooled by LN_2 to low temperatures and heated by an electric resistance heater. Both columns were of identical design. They consisted of an inner Cu tube of 35 mm I.D. and 520 mm length and an outer Cu tube of 60 mm O.D. and again 520 mm length. Both tubes were connected with Cu fines. The inner tube was filled with charcoal (500 ml) and the annulus between the two tubes served for LN_2-cooling. At the inlet of each adsorption column a countercurrent cooler was placed, by means of which the gas mixture could be cooled to the individual adsorption temperatures.

The composition of the gas mixture could be analysed by a quadripole mass spectrometer at three different locations: at the inlet of the first column (the Xe separation column), between the two columns, and at the outlet of the second column (the Kr separation column).

An operation diagram for the separation of 1.5 Nm^3 gas mixture by the lab facility is shown in Fig. 8. During the adsorption sequence the effluent composition of column 1 was measured. Immediately after beginning loading the air composition N_2, O_2 and Ar will leave the column. After 40 min the Kr starts to break through. CO_2 form the air and Xe remain in the column.
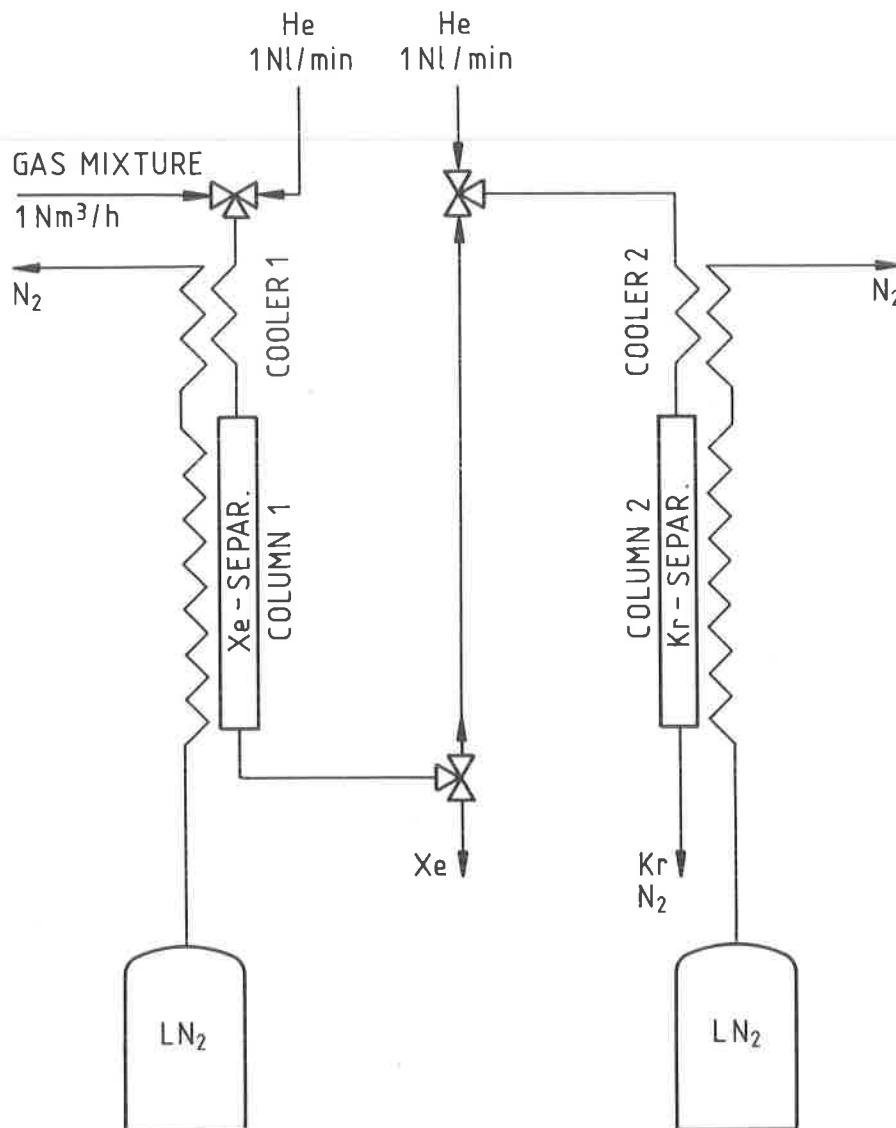
<u>Fig. 7:</u> Flow sheet of the main experimental equipment for chromato-
graphic separation of Xe and Kr from air at low temperatures

The parameters during gas adsorption were:

temperature of column 1: $- 130^{\circ}C$
temperature of column 2: $- 150^{\circ}C$
gas batch loaded: $1.5 \ m^3$ STP
gas flow: $1 \ m^3$ STP/h
gas composition: air with 0.1 vol % Xe and 0.01 vol % Kr

After adsorption for 1.5 h, the columns were regenerated by controlled
heating up to about $+ 120^{\circ}C$ (as indicated in the diagram) and under a
He-purge flow of 1 l STP/h. For the first 70 min of regeneration the
effluent of column 1 was monitored. During this time the residual air
(N_2, O_2 and Ar) as well as the Kr will leave this column; its content
in the He effluent decreases below the detection limit of 1 ppm. At
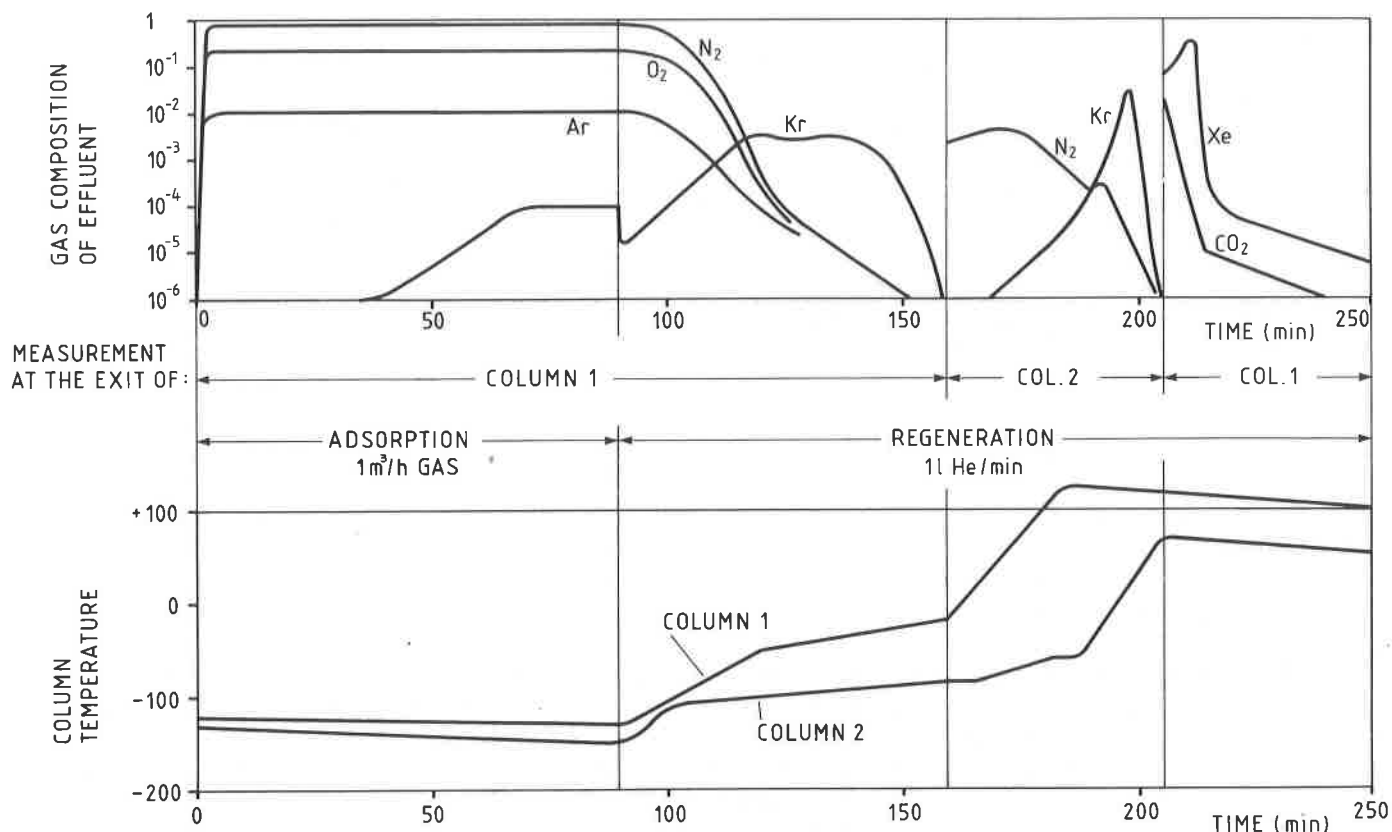
Fig. 8: Operation diagram for chromatographic separation of air containing 0.1 vol % Xe and 0.01 vol % Kr

this time column 1 contains only Xe and CO_2 whereas all the Kr together with some residual N_2 is collected in column 2 and all the O_2 and Ar passed both columns.

For the second part of regeneration, i.e. for the next 46 min only column 2 is purged, whereby at the beginning the residual N_2 eludes from column 2 and then nearly pure Kr can be collected at the column exit.

This collection of the Kr is simply achieved by passing the Kr-He mixture through a bottle which contains charcoal and is cooled with LN_2; a process which is described in (6) in more detail. In the same way any contaminated He leaving the facility may be cleaned before re-use.

The third and last part of the regeneration sequence is the complete regeneration of column 1. The remaining Xe and CO_2 may be purged from column 1 either by an He or an air stream. This can also be performed parallel to the second regeneration part. In case separation of Xe and CO_2 is desired, this can be achieved by a slower heat-up rate and therefore longer regeneration time.

The column regeneration showed the following main results:

regeneration time before N_2-Kr separation: 115 min
whole regeneration time including time
for column cooling: 145 min
He-throughput before N_2-Kr separation: 120 l STP
ratio of He-amount to gas batch: $V_{He}/V_G = 0.08$
decontamination factor: DF $\approx$ 1000
concentration of the separated Kr: γ_{Kr} = 99 %

From these results the specific gas throughput for a continuous
working process can be calculated to

$$q = \frac{V_{gas}}{t_{reg} \cdot V_{column}} = 310 \; \frac{l \; STP \; gas}{h \cdot l \; charcoal}$$

In a series of experiments different influences on chromatographic
Kr separation at low temperatures were investigated:

Composition of Off-Gas

If the average Kr concentration changes from 0.01 % to a few 0.01 %
(for Xe 10 times higher) the separation is hardly influenced. But a
considerable noble gas increase to e.g. 0.2 % Kr and 2 % Xe does
reduce the off-gas batch which can be cleaned in one process cycle
for a given column size. Whereas a considerable fluctuation of the
noble gas concentration about a given average value (in the experiment
fuel element shearing and leaching was simulated) did not influence
the separation process.

The O_2-content in the gas mixture of 20 vol % did have a strong
negative effect. For a gas mixture without O_2 the necessary column
volume to separate a fixed gas batch could be reduced by a factor
of 2. The reason for this is that without O_2 the second column could
be cooled to a lower temperature such as -185°C and therefore the Kr
adsorption capacity could be considerably increased. Whereas with
20 % O_2 in the off-gas the Kr adsorption would not rise if the column
is cooled to below -160°C; it is believed that O_2 condenses in the
pores of the charcoal and therefore changes its adsorption
characteristics.

Temperature during Adsorption

The separation capacity increases e-functionally with decreasing column
temperature. But the mentioned column temperatures have to be
considered as the lower limit temperatures because:

For the 1st column the limit is reached at about -130°C because below
that Xe will freeze out. Even though no plugging will occur, the
separation of Kr and N_2 from Xe is considerably impaired if the
adsorption temperature is below -130°C because the desublimated Xe is
too greatly polluted by Kr and N_2.

For the 2nd column the limit is at about -160°C because problems with
O_2-condensation will occur, as mentioned above.

Temperature Rise and He-Purge Flow during Regeneration

Those two parameters have to be considered together because both determine the movement of the gas species in the column during desorption and depend on each other. By variation of heating rate and He-purge flow rate for different experiments, it was shown that the mentioned values can be considered as "optimum" values for the existing column configuration. It is expected that for different column geometries the optimum values will be different.

VI. Comparison of the Investigated Kr Separation Processes

Besides the two Kr separation processes described - i.e. separation by adsorption at RT and by adsorption at very low column temperatures, in both cases at atmospheric pressure - processes with off-gas loading at elevated pressures have also been investigated. The maximum gas pressure during adsorption was 10 bar, the column being at RT or moderately cooled to -70°C. Table 1 gives the essential parameters for each investigated process for column loading and regeneration. For

Process Flow Sheet

Adsorption at	Regeneration at		Typical Parameters for 100 Nm^3/h Continuous Off-Gas Flow			
Press. Temp.	Purge Gas Press. Temp. 1st Step	2nd Step	V_{Column} [m^3]	$\dot{V}_{He}$ [Nm^3/h]	DF	γ_{Kr} [vol. %]
1 bar RT	N$_2$ 50 mbar + 180°C	He 1 bar RT	10.8	62	400	87
10 bar RT	N$_2$ 50 mbar + 180°C	He 1 bar RT	≈5	≈11	≈400	90
10 bar - 70°C	He 1 bar + 180°C		≈0.3	≈2	≈800	98
1 bar - 150°C	He 1 bar + 120°C		0.32	8	1000	99

Table 1: Comparison of different process flow sheets by the necessary column volume and He-purge for a 100 m^3 STP/h off-gas cleaning plant

purposes of comparison, the necessary column volume and He flow rate for a continuously working off-gas cleaning plant with 100 Nm^3/h off-

gas throughput was calculated for each process. The results for the two processes with gas adsorption at 10 bar contain some uncertainties since only the Kr separation step of the process was investigated experimentally, wheras the Xe-separation step was merely calculated.

The Table shows that by loading the off-gas at 10 bar and RT compared with loading at 1 bar and RT the column volume can be reduced by a factor of 2. The necessary amount of He is reduced even more substantially, but still a relatively high amount of He is needed for column regeneration.

The case for loading at 10 bar and $-70^{\circ}C$ is quite similar with loading at nominal pressure and $-150^{\circ}C$, with respect to column volume and He flow. This latter case requires a relatively high cooling power but is seems to be very suitable as a hot cell process since any pressurizing of radioactive gas is avoided and small column volumes are required.

References

(1)   "Empfehlung der Strahlenschutzkommission zur Rückhaltung radioaktiver Stoffe bei einer Wiederaufarbeitungsanlage", Bundesanzeiger, No. 128, Vol 35, 14. July 1983 p. 7037

(2)   von Ammon, R.; "Formation and Behaviour of Nitric Oxides in a Cryogenic Krypton Separation System and Consequences of Using Air as Process Gas" 17th DOE Nuclear Air Cleaning Conference, CONF-820833, Vol 2, 683-693 (1983)

(3)   Little, D.K. et al.; "Noble Gas Removal and Concentration by Combining Fluorocarbon Absorption and Adsorption Technologies" 17th DOE Nuclear Air Cleaning Conference, CONF-820833, Vol 2, 694-717 (1983)

(4)   Henrich, E.; Huefner, R.; "I-129, Kr-85, C-14 and NO_x Removal from Spent Fuel Dissolver Off-Gas at Atmospheric Pressure and at Reduced Off-Gas Flow", 16th DOE Nuclear Air Cleaning Conference, CONF-801038, Vol 1, 597-611 (1981)

(5)   Pence, D.T.; Paplawsky, W.J.; "Noble Gas Separation from Nuclear Reactor Effluents Using Selective Adsorption with Inorganic Adsorbents", 16th DOE Nuclear Air Cleaning Conference, CONF-801038, Vol 1, 161-176 (1981)

(6)   Ringel, H.; "Experiments on Adsorptive Retention of NO_x and Krypton from Dissolver Off-Gas", 17th DOE Nuclear Air Cleaning Conference, CONF-820833, Vol 2, 664-682 (1983)

DISCUSSION

MONSON: Any problems with ozone?

RINGEL: We did not investigate this question in detail. But
we think that O_3 will be no problem, because we have a small O_3
generation rate (i.e., small Kr-85 inventory) and any generated O_3
will be decomposed in the charcoal column during column regeneration.

Panel 15

PROS AND CONS OF STORAGE AND COLLECTION OF
RADIO-KRYPTON, -IODINE, -CARBON AND -HYDROGEN

WEDNESDAY: August 15, 1984
MODERATOR: K.S. Murthy
Pacific Northwest Laboratory

PANEL
MEMBERS: T.R. Thomas
Westinghouse Idaho Nuclear
K. Ebert
Kernforschungszentrum Karlsruhe
P. Mellinger
Pacific Northwest Laboratory
D.M. Wuschke
Atomic Energy of Canada
Research

CONTROL DECISIONS FOR ^{3}H, ^{14}C, ^{85}Kr, and ^{129}I RELEASED FROM THE
COMMERCIAL FUEL CYCLE
T.R. Thomas, R.A. Brown

KRYPTON CONTROL ALTERNATIVES
E. Henrich, R. von Ammon, K. Ebert

HEALTH RISK ASSESSMENT FOR FUEL REPROCESSING PLANT
P. Mellinger

HOW MUCH DOSE REDUCTION COULD BE ACHIEVED BY COLLECTION AND DISPOSAL
OF ^{129}I and ^{14}C?
D.M. Wuschke

OPENING COMMENTS OF PANEL MODERATOR:

      The panel is concerned with the pros and cons of storage and collection of radio-krypton, -iodone, -carbon and -hydrogen. We have four panelists, each of whom is an expert in his own field.

      In the U.S., the EPA has promulgated regulations that krypton from commercial nuclear power plants should be controlled. There is divided opinion for and against controlling krypton. One opinion is that if the environmental consequences of releasing it or controlling it are only negligibly different, because of the dose consequences to the workers recovering and storing krypton, then, it may not be worth controlling it. Such are the questions that will be addressed by this panel.

CONTROL DECISIONS FOR ^{3}H, ^{14}C, ^{85}Kr, and ^{129}I
RELEASED FROM THE COMMERCIAL FUEL CYCLE

T. R. Thomas and R. A. Brown
Airborne Waste Management Program Office
Westinghouse Idaho Nuclear Company
Idaho Falls, Idaho 83403

Introduction

For the last six years our office has been a lead laboratory for the DOE to provide technical guidance on airborne waste management programs. Besides supporting research and development for recovery, fixation, and disposal of ^{3}H, ^{14}C, ^{85}Kr and ^{129}I, the need for control of these radionuclides in the commercial fuel cycle was also examined(1). It was assumed that the U.S. nuclear fuel cycle would not exceed a 400-GWe capacity in the foreseeable future. The following questions were considered for uncontrolled releases of ^{3}H, ^{14}C, ^{85}Kr and ^{129}I over a 100-year operating period:

- Would the increase in global cancer death rate be significant?

- Would the increase in global inventory in the environment be excessive?

- Would allowable doses to the maximum exposed individual be exceeded?

- Would allowable release rates be exceeded?

- Would the cost of control be reasonable?

Assumptions and Methodology

Source Terms

The following source-term assumptions were used for release of ^{3}H, ^{14}C, ^{85}Kr and ^{129}I from fuel reprocessing plants (FRPs) and light water reactors (LWRs) serving a 400-GWe fuel cycle:

- The fuel would be cooled 1.5 years before reprocessing.

- A 1500 metric ton (MT) FRP would serve a 43 GWe-yr fuel cycle.

- The LWRs would release about 30% of the ^{14}C, 7% of the ^{3}H, and less than 1% of the ^{85}Kr; the FRPs would release the remaining portions of ^{14}C, ^{3}H, and ^{85}Kr and all of the ^{129}I.

- The source terms (full release) for a 1,500 MT FRP would be:

	^{3}H	^{14}C	^{85}Kr	^{129}I
Ci/yr	7.4×10^5	860	1.2×10^7	47
Ci/GWe-yr	1.7×10^4	20	2.8×10^5	1.1

- The source terms (full release) for a 400 GWe-yr fuel cycle would be:

	^{3}H	^{14}C	^{85}Kr	^{129}I
Ci/yr	7.6×10^6	1.1×10^4	1.1×10^8	440

A comparison of the source terms for a 1,500 MT FRP to the 40 CFR 190 release limits of 5×10^4 Ci ^{85}Kr and 0.005 Ci ^{129}I per GWe-yr would indicate a need for about 85% and 99.6% control of ^{85}Kr and ^{129}I, respectively.

Health Effects

The method for estimating accrued health effects (HE) was based on Nuclear Energy Agency (NEA) dose conversion factors (regional + global)(2):

	^{3}H	^{14}C	^{85}Kr	^{129}I
Man-rem/Ci (NEA)	0.012	·262	0.0010	1530
Man-rem/Ci (IAEA)	0.035	346	0.00034	1900

The International Atomic Energy Agency (IAEA) dose conversion factors(3), which were not available at the time of our study, are shown for comparison and indicate that dose models are constantly being revised and refined. The dose conversion factor multiplied times the annual release of the corresponding radionuclide provides an estimate of effective whole-body population dose commitments. The assumptions in the NEA dose model and conversion to HE are:

- A regional dose would be delivered to a steady-state population of 400 million people within 2,000 km of the source over a 500-year period.

- A global dose would be delivered to a steady-state global population of 10 billion people over a 10,000-year period.

- The regional and global doses are additive to give the total population dose.

- The conversion factor to estimate HE from effective whole-body population dose commitments lies between 4,400 and 13,000 man-rem per HE(4); a conservative value of 5,000 was used in this study.

The health effects were calculated by:

$$HE = \frac{(Ci/yr)(years\ of\ operation)(man\text{-}rem/Ci)}{5,000\ man\text{-}rem/HE}$$

Cancer Death Rate

The method for estimating increase in the global cancer death rate was based on the following assumptions:

- A HE is assumed to result in a cancer death.

- The annual cancer death rate in the world would be the same as in the U.S. (176 cancer deaths/100,000 population)(5).

- The total number of cancer deaths in a steady-state population of 10 billion people for 10,000 years would be 176 billion; the accrued HE from ^{14}C, and ^{129}I releases were divided by 176 billion to estimate the fraction of HE that might occur.

- The total number of cancer deaths in a steady-state population of 10 billion people for 200 years would be 3.5 billion; the accrued HE from ^{3}H and ^{85}Kr releases were divided by 3.5 billion to estimate the fraction of HE that might occur. The shorter time span was chosen for comparison because doses and HE from these radionuclides would be accrued within 200 years due to radioactive decay.

Maximum Exposed Individual

The method for estimating annual organ doses to the maximum exposed individual (MEI) was based on dose conversion factors derived from Nuclear Regulatory Commission models used in this country. The model chosen had been developed for the Barnwell Nuclear FRP(6). The dose conversion factors used to estimate the annual dose commitment to the most sensitive organ of the MEI 2.4 km from the FRP were:

	^{3}H	^{14}C	^{85}Kr	^{129}I
Conversion Factors (mrem/Ci)	7.4×10^{-6}	0.0027	5×10^{-8}	45
Sensitive Organ	total body	bone	lung	thyroid
Dose Commitment (mrem/yr)	5.5	2.3	0.6	2115

The dose commitments that would result from the annual releases of a 1,500 MT FRP are also given above. They can be compared to the 40 CFR 190 allowable exposure limits of 25 mrem/yr to the total body or organs and 75 mrem/yr to the thyroid. The sum of the doses from all exposure pathways and radionuclides must not exceed these limits. About 97% retention of ^{129}I would be required to bring the thyroid dose below 75 mrem/yr. The sum of the doses from the remaining radionuclides would be below the 25 mrem/yr limit.

Conclusions

Uncontrolled Releases

The effects of complete release of ^3H, ^{14}C, ^{85}Kr and ^{129}I from operating a 400-GWe fuel cycle for 100 years are shown in Table 1. The postulated accrued HE from ^{14}C and ^{129}I appear large; however, these numbers are insignificant when compared to the 176 billion cancer deaths that would occur from all causes in the 10,000-year reference period. The percent increase in global cancer deaths would be no greater than $5 \times 10^{-5}\%$ for each of the radionuclides. Based on the 1980 inventory of each radionuclide in the environment, complete release for 100 years from a 400-GWe fuel cycle would not increase the ^3H or ^{14}C inventories, however, large increases in ^{85}Kr and ^{129}I inventories would occur. The effects, besides dose impacts, of large increases in inventory are unknown and serve only as "warning flags" that should be taken into consideration. As indicated earlier, only ^{129}I releases from a FRP would exceed the allowable MEI dose limit and ^{85}Kr and ^{129}I would exceed the allowable release limit.

Table 1

Effects of Uncontrolled Releases of ^3H, ^{14}C, ^{85}Kr And ^{129}I From Commercial FRPs

100-Year Operation of a 400-GWe Fuel Cycle	^3H	^{14}C	^{85}Kr	^{129}I
Postulated Accrued Health Effects	1730	60 000	2600	13 400
Increase in Global Cancer Deaths (%)	0.00005	0.00003	0.00005	0.000008
Impact on Global Inventory	Decrease From 1200 to 213 MCi	Increase From 316 to 317 MCi	Increase From 64 to 1800 MCi	Increase From 50 to 44 000 Ci
Maximum Exposed Individual Dose Limit Exceeded	No	No	No	Yes
Maximum Release Limit Exceeded	No	No	Yes	Yes

Controlled Releases

The effects of controlled releases from commercial FRPs serving a 400-GWe fuel cycle for 100 years are shown in Table 2. The assumed degree of recovery from the FRPs is 90, 90, 85 and 99.6% for ^{3}H, ^{14}C, ^{85}Kr and ^{129}I, respectively. The degree of recovery for ^{3}H and ^{14}C from the fuel cycle would only be 85 and 60%, respectively, due to the partial release of these radionuclides from LWRs. The effects of control at the FRPs would reduce postulated accrued HE in Table 1 by the assumed degree of recovery for the fuel cycle. The most significant effect would be a smaller increase in ^{85}Kr and ^{129}I inventories which would occur after 100 years of operation. The cost of control in terms of dollars per man-rem averted, provides a quantitative basis for comparison among the radionuclides. However, the ultimate judgements on costs must be made with reference to other societal costs. Use of 5,000 man-rem/HE converts $100 per man-rem averted to $500,000 per health effect. If we use $1,000,000 as an upper limit value of cost that is acceptable to society to avoid a postulated death, control of ^{129}I and ^{14}C would be recommended while control of ^{3}H and ^{85}Kr would not be recommended.

Table 2

Effects of Controlled Releases of ^{3}H, ^{14}C, ^{85}Kr And ^{129}I From Commercial FRPs

100-Year Operation of a 400-GWe Fuel Cycle	^{3}H	^{14}C	^{85}Kr	^{129}I
Assumed Degree of Recovery (%)	90 (85)	90 (60)	85	99.6
Postulated Accrued Health Effects	266	24 000	390	54
Increase in Global Cancer Deaths (%)	0.000008	0.00001	0.000008	0.00000003
Impact on Global Inventory	Decrease From 1200 to 98 MCi	No Change	Increase From 64 to 310 MCi	Increase From 50 to 226 Ci
Cost of Control (Dollars/man-rem Averted)	1000-4000	10	500-600	100

Overall Assessment

The overall assessment of control decisions for ^{3}H, ^{14}C, ^{85}Kr and ^{129}I releases from commercial FRPs is summarized in Table 3. The overall assessment is based on an accumulation of yes-or-no factors for the radionuclides. Based on these criteria, ^{129}I should be controlled whereas ^{3}H should not be. Even though current regulations mandate control of ^{85}Kr, the need to control should be reconsidered by the regulatory agencies. The small impact of ^{85}Kr releases on population dose commitments, MEI doses, and the large cost per HE averted probably does not justify its control. The only factor that would justify control of ^{14}C is its cheaper cost relative to the other radionuclides. For that reason, it should be considered for control and a more precise cost analysis done. None of the other factors would justify its control.

Table 3

Control Decisions for ^{3}H, ^{14}C, ^{85}Kr and ^{129}I Releases from Commercial FRPs

100-Year Operation of a 400-GWe Fuel Cycle	$\underline{^3H}$	^{14}C	^{85}Kr	$^{129}\underline{I}$
Impact on Global Cancer Death Rate?	No	No	No	No
Impact on Global Inventory?	No	No	SBC*	SBC
Exceed MEI Dose?	No	No	No	Yes
Exceed Release Rate Limit?	No	No	Yes	Yes
Cost of Control Reasonable?	No	Yes	No	SBC
Overall Assessment	No	SBC	SBC	Yes

*SBC = Should be considered.

References

1. Brown, R. A., Christian, J. D., and Thomas, T. R., "Airborne Radionuclide Waste Management Reference Document", ENICO-1133 (July 1983).

2. NEA (Organization for Economic Cooperation and Development, Nuclear Energy Agency Experts Group), "Radiological Significance and Management of Tritium, Carbon-14, Krypton-85, and Iodine-129 Arising from the Nuclear Fuel Cycle", (1980).

3. IAEA (International Atomic Energy Agency, Division of Nuclear Fuel Cycle), Report of the Advisory Group Meeting on "Models and Radiological Basis for Recommendations on Radionuclide Releases of Regional and World-Wide Interest", held in Vienna, (1-4 June 1982).

4. NAS (National Academy of Science, National Research Council), "The Effects on Populations of Exposure to Low Levels of Ionizing Radiation", the BEIR III Report, Washington, D. C., (1980).

5. American Cancer Society, "1981 Cancer Facts and Figures", 777 Third Avenue, New York, NY, 10017, (1982).

6. Finney, B. C., et.al., "Correlation of Radioactive Waste Treatment Costs and the Environmental Impact of Waste Effluents in the Nuclear Fuel Cycle -- Reprocessing Light Water Reactor Fuel", ORNL/NUREG/TM-6, (1977).

KRYPTON CONTROL ALTERNATIVES

E. Henrich, R. von Ammon, K. Ebert
Kernforschungszentrum Karlsruhe, Institut für Heisse Chemie,
Fed. Rep. of Germany

ABSTRACT

A reprocessing plant for 350 metric tons per year LWR spent fuel cooled for at least 7 years is planned in the FRG. A routine Kr-85 retention for radiation protection reasons is not demanded by the German reactor safety and radiation protection commissions, but it has been recommended to develop the Kr-waste management technology for larger plants in the future. The licensing authorities also do not require a routine Kr-85 retention at the plant site. They want a demonstration of a Kr-85 removal technology on a non-routine basis in an additional hot facility.

Technical and safety characteristics of various Kr-85 removal processes will be described and compared, including the precleaning steps in an integrated dissolver off-gas system. The interactions with subsequent conditioning and storage of Kr and with process modifications in the plant headend will also be taken into account. A commercial use of the inactive Xe and part of the Kr-85 may have an influence on a cost-benefit analysis and the selection of a removal process.

Two alternative processes are being developed on an engineering scale at KfK. A cryogenic distillation process using an O_2-free off-gas is under investigation on a pilot plant scale since 1976. A selective absorption process using freon-12 at low temperatures and at atmospheric pressure has been investigated at the laboratory scale since 1980. Test operation on an engineering scale started late in 1983. Essential results and operating experiences with both facilities are summarized.

Technical as well as safety aspects are in favour of the selective absorption process. A final decision what process will be used in the future shall be made as soon as comparable technical experiences from both processes are available.

1. GENERAL ASPECTS OF THE RECOVERY OF FISSION PRODUCT RARE GASES

Krypton is a rare gas and concentrates neither in the food chains nor the human body. The atmosphere contains about 1 ppmv krypton. The present Kr-85 concentration in air is about 21 p Ci/m³ (STP) and about 10^7 times higher than previous natural values. Since the radiotoxicity of Kr-85 is low, an uncontrolled release via the stack from a few fuel reprocessing plants (FRP) is not an extreme radiological hazard on the local or global scale. The present global whole body dose rate due to Kr-85 discharge is only about $3 \cdot 10^{-4}$ mrem per manyear.

Kr is recovered as a by-product in the course of air liquefaction. Today a commercially available 40 l pressurized Kr-cylinder contains about 0.1 mCi Kr-85 at 150 bar. This value may increase by about two orders of magnitude in a few decades with the anticipated increase of nuclear power economy. In that situation 1 m³ (STP) commercially available Kr will contain $2 \cdot 10^{-3}$ Ci Kr-85. There is also some concern in view of the unknown consequences of an increased ionisation density in the atmosphere.

Improvement of public acceptance of nuclear power may be an additional incentive for recovery.

Utilization of Kr-85 /3,4,5/: In view of the low radiotoxicity and the 10.8 y half-life, fission product (FP) krypton may be an ideal nuclide for technical applications either with or without additional enrichment. The present demand is about 1m³ FP krypton or 10^5 Ci Kr-85 per year (corresponding to 10 MTHM LWR spent fuel) and limited by availability and high price. Kr-85 might replace more radiotoxic nuclides in some technical applications and thus indirectly contribute to safety.

Utilization of inactive Xe: The situation for FP xenon is different. LWR spent fuel contains about 1 m³ (STP) Xe per MTHM; it is inactive after 1 y cooling time and the most abundant FP by weight. Xenon is a valuable product, its price is presently about 4000 US-dollars per 1 m³ (STP), due to the low (0.08 ppmv) concentration in air. The demand in the industrialized countries corresponds to about 0.1 kWe nuclear power per man and is limited by the high purchase price. Potential applications are given in the literature /3,6/. Assuming 800 US-dollars for reprocessing and waste treatment per MTHM spent fuel, the Xe value is equivalent to 0.5% of the total cost. Estimates of the total Kr-85 management costs are less than 0.5% /1/. This is a strong incentive for the development of a FP Xe recovery process at least. Without the additional costs for recovery, conditioning, storage or disposal of FP Kr, the recovery of FP Xe would be especially attractive.

Technical consequences are also connected with the low radiotoxicity of radiokrypton. An uncontrolled radiokrypton release and dispersion via the stack does not create an intolerable hazard. A recovery and concentration in the course of the Kr-85 waste management steps, however, creates a new additional hazard for the plant personnel especially in case of a large accidental release. A very careful evaluation of safety-related technical characteristics of candidate processes should guarantee, that the modest radiological benefit to the environment does not occur at the expense of the operating personnel /7/. Technical experience is a valuable, but not the major criterion. It should also be mentioned, that safety and cost-effectiveness do not necessarily exclude each other.

2. BEHAVIOUR OF RARE GASES IN LWR AND FBR SPENT FUEL REPROCESSING PLANTS

LWR spent fuel, cooled for 1 year contains about 0.1 m³ FP krypton and 1 m³ inactive FP xenon per MTHM; the Kr-85 content of krypton is 6% by volume and represents an activity of about 10^4 Curies. Less than 10% of the rare gases escape to the gas plenum of the fuel rods during irradiation. A crude estimate for PWR spent fuel is 1% escape per 1% burnup.

Rare gas production in fast reactor fuel is lower. At a comparable burnup of a core and axial blanket mixture of FBR spent fuel, the volume and activity of FP Kr is about 60% compared to the LWR spent fuel. Up to 90% of the rare gases may escape to the expansion chamber, due to the higher irradiation temperatures and core zone burnups.

In a chop and leach headend the rare gases contained in the plenum space are liberated in the shear. In a bundle shear this fraction is liberated during the first cut and causes a high concentration peak in the shear off-gas. This is not desirable in view of the downstream off-gas purification steps, especially if the entire SBR subassemblies are cut. Prior disassembling of the fuel elements and cutting with a pin row shear results in a more smoothed release and enhances the compatibility with the off-gas treatment.

The off-gas from the shear is usually routed to the dissolver and is the major dissolver off-gas (DOG) diluent. The shear type and the shearing philosophy are important aspects for the design of a DOG purification system. A DOG dilution range of about two orders of magnitude may be found in existing FRP's: A DOG volume of only 100 m³ per MTHM is typical for "fumeless" dissolution conditions. Up to 10^4 m³ per MTHM are usually found in small pilot plants. A pointless DOG dilution is not compatible with a reasonably cost effective recovery of FP rare gases. The consequences would be the following: less efficient recovery, larger and more expensive equipment and more cell space requirements.

In view of further improvements and advanced technologies in a FRP headend, the rare gas recovery processes should be insensititve to high rare gas concentrations and flow fluctuations.

In the following sections 3-7 the successive Kr waste management steps are summarized in some figures and tables. The text is confined to few remarks to aid in understanding and to highlight special and important details.

3. RARE GAS RECOVERY ALTERNATIVES FROM THE OFF-GAS

3.1 Cryogenic distillation process variants:

The rare gas recovery from the dissolver off-gas (DOG) takes place at the end of a relatively complex DOG purification train. The bulk of NO_x, the aerosols and iodine are removed upstream of the rare gas recovery subsystem. More or less complex additional DOG precleaning steps are required prior to the true rare gas separation. In certain alternatives, these adaptation steps may be more complex than the actual recovery procedure and depend on the sensitivity of the process to impurities. It should be borne in mind, that an evaluation of individual process steps is not adequate, since they are only one step in a complex total system. Proper functioning as an integrated part would need to be evaluated and demonstrated.

The intention of fig.1 is to show, that different cryodistillation subsystems are developed in several countries. Fig.1 comprises only the more important processes. Going into more detail, more than twice as many different processes could be identified. For several reasons none of these cryodistillation processes can be identical to the well known Xe and Kr recovery procedures in air lique-faction. This is the major reason for the extensive research and development work in this field.

3.2 Selective absorption process variants:

Various processing modes of selective absorption processes are shown in fig.2. The most extensive development work has been carried out at Oak Ridge. Three different cold pilot plants have been operated since 1967. The combination column shown in fig.2 has emerged as the process of choice.

The selective absorption of rare gases was initiated at HARWELL/UK more than 25 years ago. The aim,then,was to recover the rare gases for utilization.

The most recent process mode is investigated at KfK/FRG at the cold engineering scale since 1984 /8/. The process uses two absorption columns to separate Xe and Kr from each other. It operates at low temperatures and atmospheric pressure for technical and safety reasons.
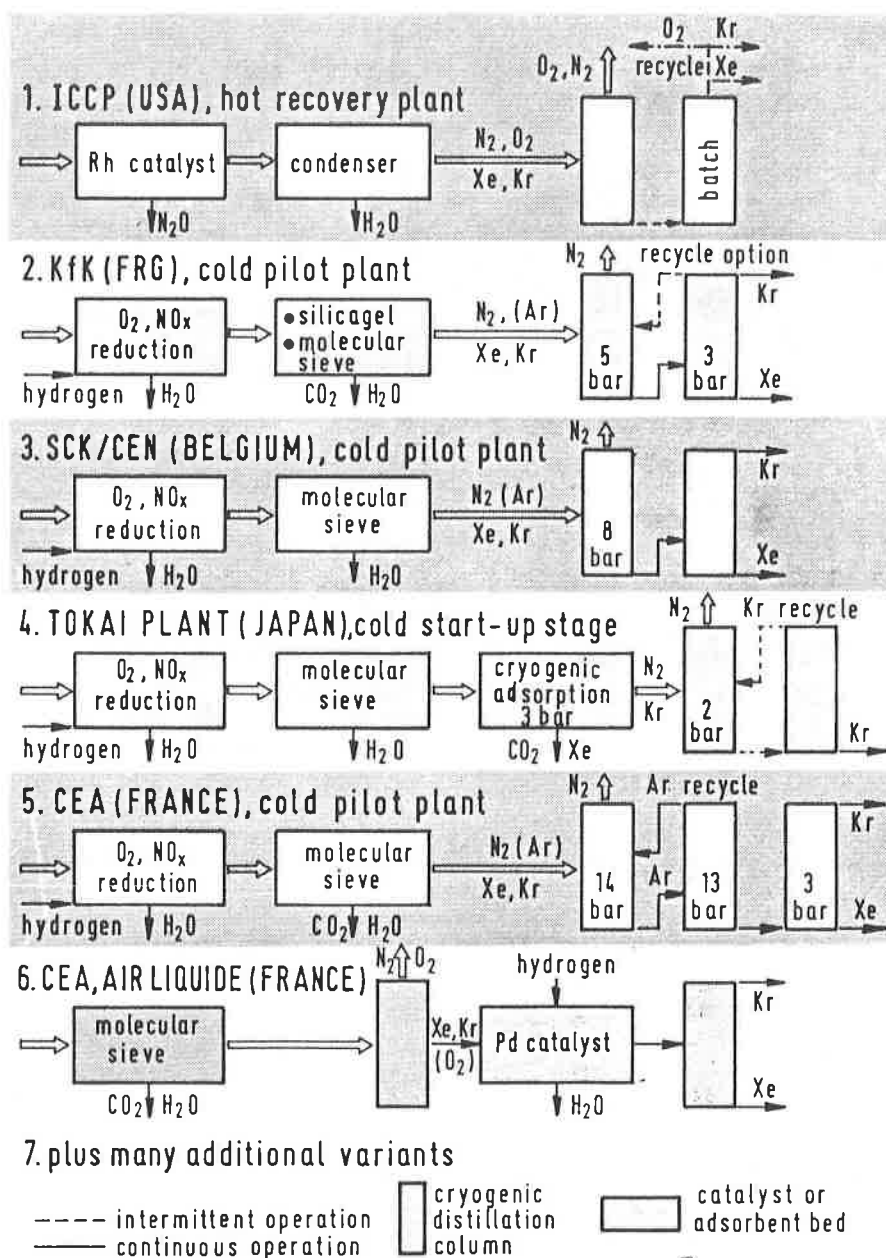
Fig.1

VARIOUS CRYOGENIC DISTILLATION PROCESSES

Compared to cryodistillation, using hydrogen for oxygen removal, the pre-purification steps are less complex. Only NO_x (NO plus NO_2), nitric acid and water vapours have to be removed to the trace level to prevent plugging and potential equipment corrosion in the presence of small amounts of radiolytic solvent degradation products in a wet solvent.

3.3 Selective adsorption process variants:

The use of solid sorbents for off-gas purification is a familiar technology and reference is made to the recent literature /9/. The sequence of operations is very similar to the selective absorption processes: Adsorption corresponds to absorption; purging or partial desorption corresponds to fractionation; desorption of the adsorbed products corresponds to the stripping operation.
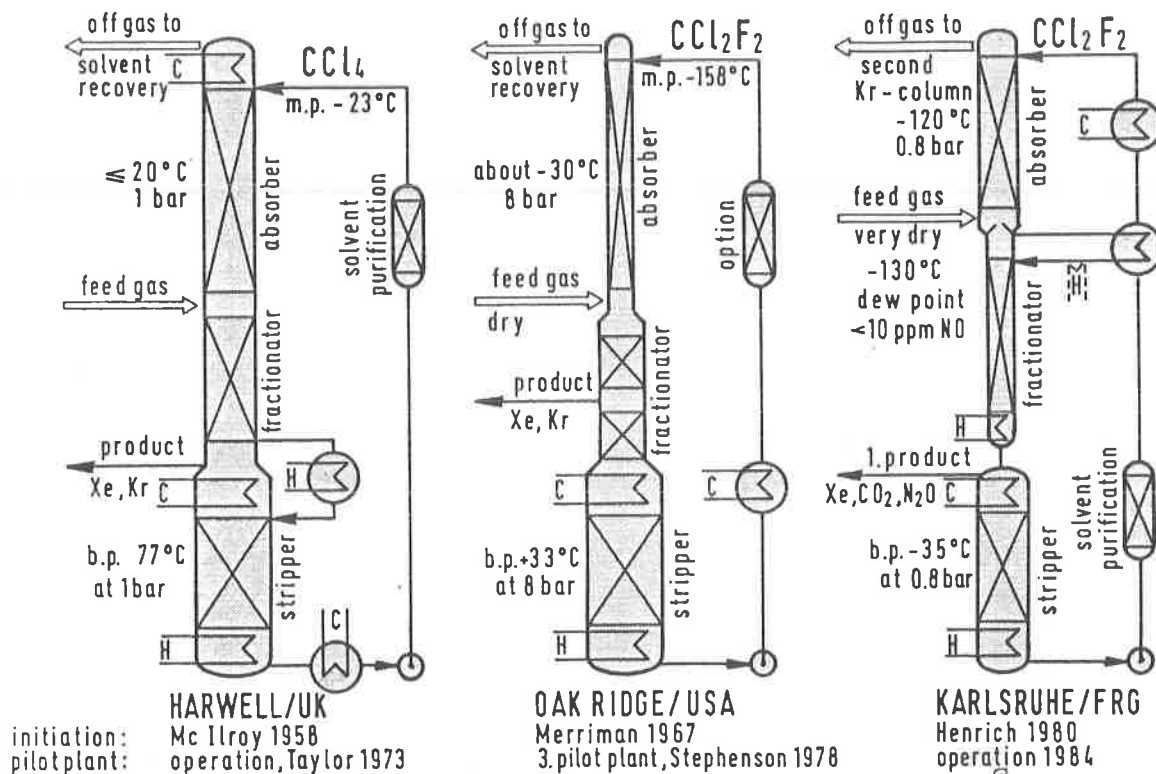
Fig.2

VARIOUS PROCESSING MODES OF SELECTIVE ABSORPTION PROCESS

The solvent of the absorption process may be viewed at as a "liquid molecular sieve", which has sufficient separation selectivity but none of the following disadvantages: discontinuous operation, frequent temperature or pressure swing cycles, frequent actuation of valves, complex heat exchange problems in the large sorbent beds and a less simple purification in case of an accidentally spoiled sorbent.

4. GENERAL CHARACTERISTICS OF RECOVERY PROCESSES

4.1 Separation selectivity of key design components:

The separation selectivity of Kr from O_2 and N_2 carrier gases is a more general aspect for a comparison of the different processes (see Fig.3). The separation selectivity of Xe from Kr is less important (see Fig.4). The lower the temperature, the larger is the separation selectivity but also the sensitivity to impurities and the refrigeration requirements. Though there are some differences between the alternatives, the separation selectivity is sufficient in each case. The decontamination factors, separation factors and product purities depend much more on the number of separation stages, which are usually proportional to the column or bed height. The height equivalent to a theoretical stage (HETP) depends on the type of packing or plates. The diameter of the columns or adsorbers depends on the acceptable superficial velocity of the feed gas. A lower separation selectivity may be compensated for with a few additional stages.

A crude estimate for the equipment volume may be the HETP-value multiplied by the number of stages (column height) and multiplied by the reciprocal superficial gas velocity (cross sectional area). There are no extreme differences among the processes and these considerations do not aid much for an evalution.

Fig.4
SEPARATION OF XE FROM KR BY ADSORPTION
CRYOGENIC AND ABSORPTION PROCESSES

Fig.3
SEPARATION SELECTIVITY OF KR FROM O_2 AND N_2
CARRIER GASES FOR RARE GAS RECOVERY PROCESSES

The melting and normal boiling points of the rare gases are only 5° C different. Pressure is therefore inherent to cryodistillation to extend the temperature range of the liquid state.

4.2 Comparison of the German versions of cryodistillation and selective absorption:

The following comparison is not necessarily representative of cryodistillation and selective absorption in general. A general comparison is a very difficult task, since the interactions of many important details are neglected.

The simplified flowsheets are shown in fig.5 and fig.6; only the cold box part in fig.6 represents the total selective absorption subsystem. The temperature and pressure profiles of the successive operations of both alternatives are shown in fig.7. Technical as well as safety disadvantages in the cryodistillation train are: high temperatures and pressures, large temperature jumps, use of large H_2-volumes in the course of the prepurification steps and complexity induced by many individual operations. The less complex precleaning steps, the stepwise temperature decrease, the low operating pressure and the smaller number of individual operations of the selective absorption subsystem are more attractive.

Additional details not shown in fig.7 are the following: The Kr-85 inventory of the cryodistillation process is about two orders of magnitude higher compared to absorption, therefore an additional emergency tank is required, which could aid to prevent an accidental release of the large Kr-85 inventory in case of process upsets. To prevent Xe freeze-out, the cryocolumn needs a Kr-inventory for start-up; the absorption columns do not. The complex problems connected with the radiolytic degradation of impurities in the cryodistillation process, which may cause plugging, or solvent degradation in the absorption process, which may cause corrosion in a wet system, will not be adressed in this paper.

The KfK selective absorption process pays special attention to the aspect that the wastes of today are the raw materials of tomorrow: The Xe is separated without the Kr in a first absorption column. Moreover, this subsystem provides an additional in-line correction in case of minor malfunctions in the upstream NO_x, iodine or 14-CO_2 removal steps, thus improving the reliability of the total off-gas purification train. A small and constant gaseous stream might be removed from downstream the Xe column to recover some Kr-85. If a preventive "ALARA" Kr recovery is required to obtain the modest radiological benefit, the total off-gas stream may be treated in a larger Kr column.

The state of development of the selective absorption process is still inferior to cryodistillation and a final comparison will only be made if the status of both alternatives is comparable.

4.3 Process comparison including the precleaning steps:

The characteristics of the alternative Kr-recovery processes are compared in table 1. All the processes are technically feasible. An evaluation in terms of cost, reliability, safety, technical complexity would require much more detailed information. The technological basis of the three alternatives is well-known from industrial processes. The state of development is not extremely different and in view of the time available until an uncontrolled Kr-85 release will be an immediate hazard to the environment, it does not seem to be a major selection criterion.

	CRYOGENIC DISTILLATION	SELECTIVE ABSORPTION IN SOLVENTS	SELECTIVE ADSORPTION ON SOLIDS
1. Auxiliary material for separation	liquified DOG component N_2, Ar or O_2	auxiliary solvent CF_2Cl_2, CCl_4 or CO_2	auxiliary solids charcoal, molecular sieves
2. Separation operation	rectification	absorption-stripping	adsorption-desorption
3. Operating mode	continuous	continuous	discontinuous
4. Operating temperature	very low	low - very low	low
5. Operating pressure	more than atmospheric inevitable	$\leqslant$1 bar possible, >1 bar usual for large DOG volumes	$\leqslant$1 bar possible, especially at low temperatures
6. Kr-85 inventory typical residence time	very high, 10^5 Ci 40 h	very low - low, 10^3 Ci 0,4 h (KfK)	low, 10^4 Ci 4 h
7. Xe/Kr separation	yes	possible	yes
8. Kr product purity	high	sufficient-high	sufficient-high
9. DOG purification	complex	moderate	moderate
10. Interfering impurities	H_2O, HNO_3, NO_x, N_2O, CO_2, CH_4, O_2, O_3	H_2O, HNO_3, NO_x	H_2O, HNO_3, NO_x, O_3
11. O_2 removal	combustion using H_2 (except ICPP plant)	not necessary	not necessary
12. State of development	inactive pilot plants Kr-85 recovery at ICPP plant	inactive pilot plants	lab scale facilities (Xe preadsorption step at Tokai plant)
13. Basic technology	conventional	conventional	conventional

Table 1: COMPARISON OF CHARACTERISTICS OF KRYPTON RECOVERY PROCESSES
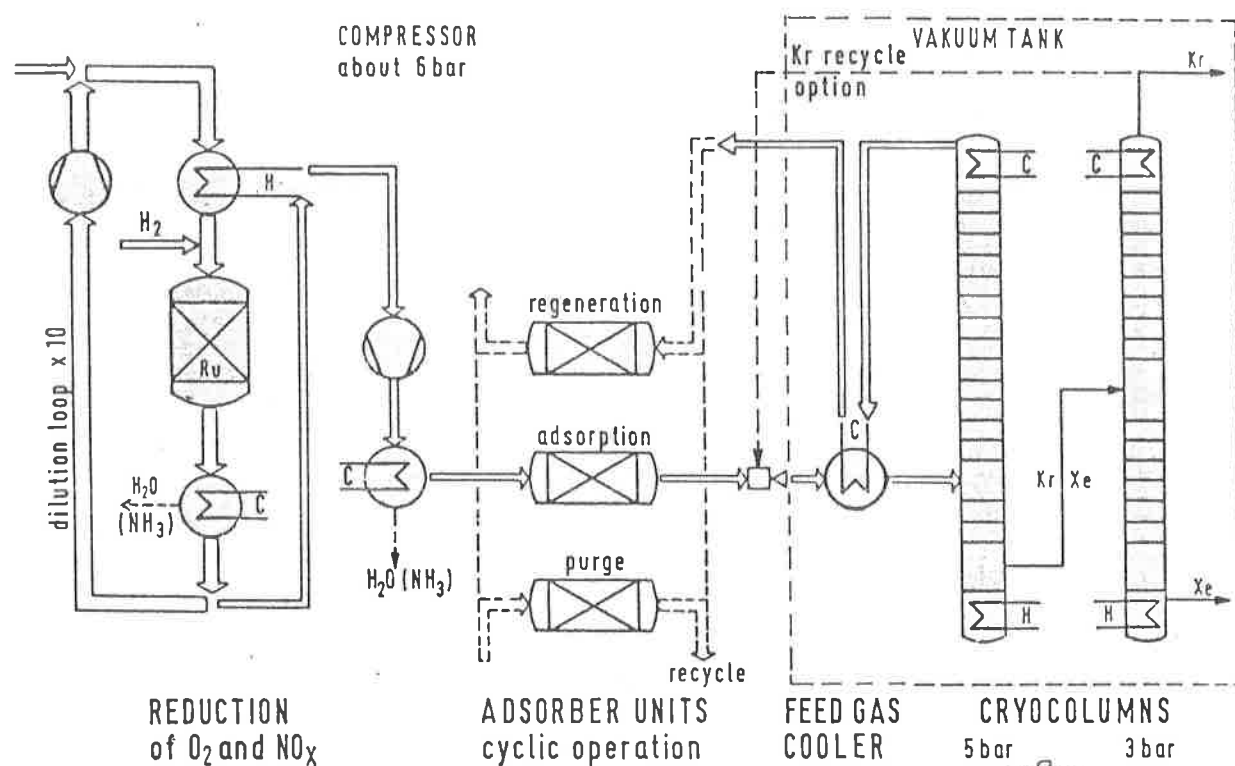
Fig.5 SIMPLIFIED FLOWSHEET OF THE KfK CRYODISTILLATION PROCESS
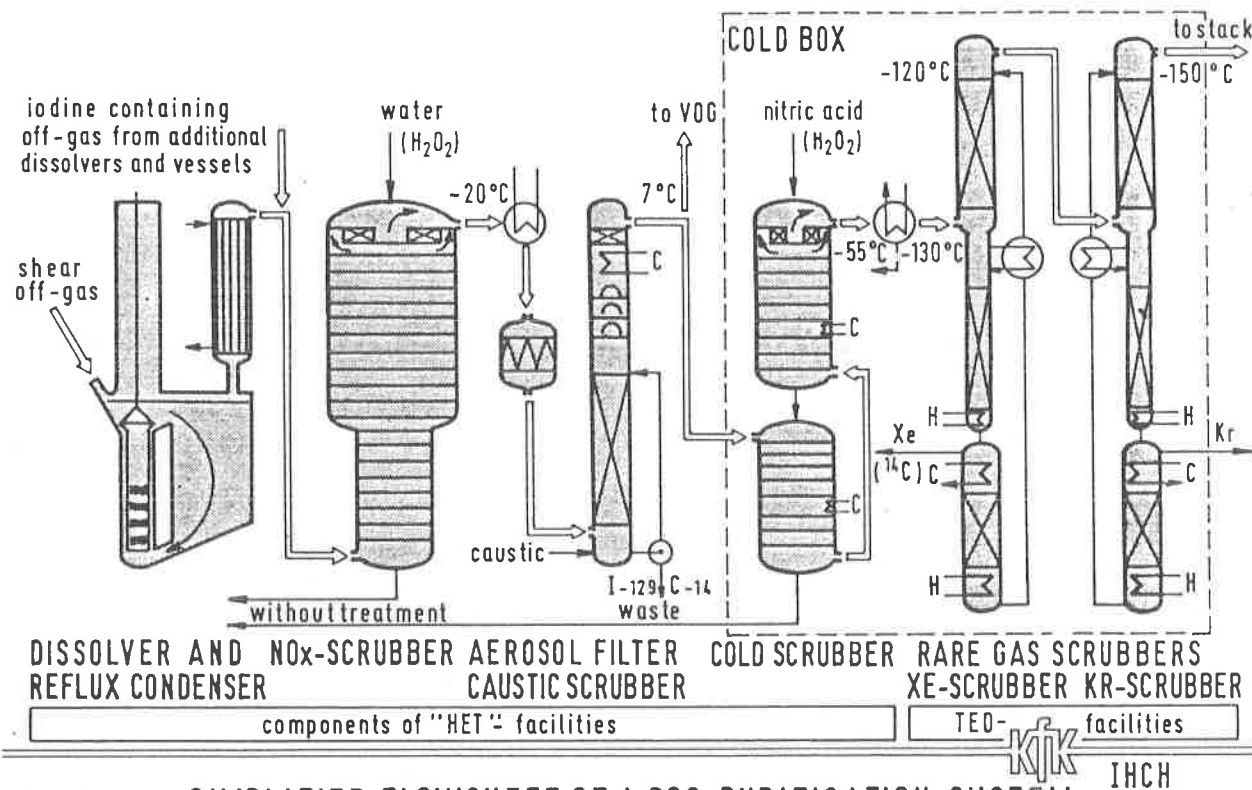
Fig.6 SIMPLIFIED FLOWSHEET OF A DOG PURIFICATION SYSTEM WITH RARE GAS RECOVERY BY SELECTIVE ABSORPTION
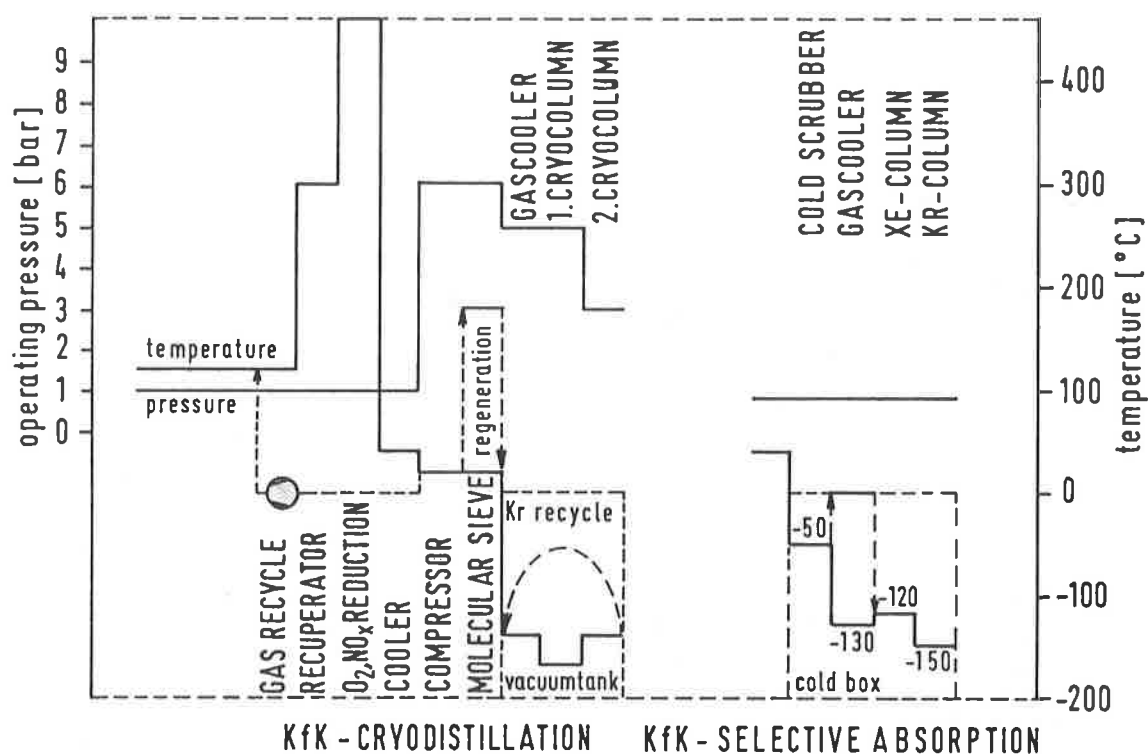
Fig.7   TEMPERATURE AND PRESSURE PROFILES
IN THE COURSE OF RARE GAS RECOVERY PROCESSES

5. RADIOKRYPTON CONDITIONING ALTERNATIVES

5.1 Characteristics of radiokrypton conditioning processes:

Characteristics of various radiokrypton conditioning processes are compared in table 2. Gas storage in pressurized vessels is considered to be an available and less expensive technology. Solid storage forms are under development to improve safety but are more expensive /10/.

5.2 Characteristics of radiokrypton storage products

They are summarized in table 3. A general aspect of gaseous or solid storage forms needs to be mentioned: An accidental dispersion of large volumes of gaseous radiokrypton does not create a tremendous hazard, since the biological half-life is negligeable. An accidental dispersion of the solid products as airborne dust creates a new hazard in view of the much larger biological half-life of the solid material. This hazard is not inherent to the gaseous waste form.

5.3 General comparison of the alternative processes:

The advantages and disadvantages of the alternative radiokrypton conditioning processes are summarized in table 4.

6. COMMERCIAL USE AND STORAGE OR DISPOSAL OPTIONS

Table 5 represents the least well developed aspect of Kr-85 waste management.

1. PROCESS	PRESSURIZED VESSELS	ZEOLITE 5A ENCAPSULATION	KR ION SPUTTER PUMPS
2. DEVELOPING INSTITUTIONS	many	INEL/USA; KfK/FRG	HARWELL/UK PNL/USA; KfK/FRG
3. OPERATING MODE	batch periodic operation of one unit one way Kr flow	batch periodic operation of one unit Kr rework > 50%	continuous parallel operation of a few pumps dead end pumps
4. OPERATING CONDITIONS T P	cryopumping <1 bar	about 400°C about 400 bar	ambient (water cooling) $<10^{-4}$ bar
5. GASEOUS KR INVENTORY	$\geqslant 10^5$ Ci	$\geqslant 10^5$ Ci	< 1 Ci
6. SAFETY ASPECTS DURING OPERATION	high inventory	high inventory high pressure high temperature	low inventory low pressure ambient temperature
7. CAPACITY OF A UNIT	No remarkable differences are expected. A storage unit capacity of 1 m^3 corresponds to about 10 MTHM of spent fuel.		
8. RELIABILITY	depends to a large extent on engineering details		
9. STATE OF DEVELOPMENT	available technology		cold pilot plants
10. COST	moderate	acceptably high and about comparable	

CHARACTERISTICS OF RADIOKRYPTON CONDITIONING PROCESSES   TABLE 2

	PRESSURIZED VESSELS	ZEOLITE 5A ENCAPSULATION	KR ION SPUTTER PUMPS
1 PRODUCT FORM	gas	solid vitrified zeolite 5A	solid compact metal matrix
2 STORAGE TEMPERATURE	The thermal power of 10^5 Ci Kr-85 units is about 0.15 kW and about 1000 C surface temperature are assumed for air cooling. The somewhat higher temperature inside depends on the heat transfer rates in the storage matrices.		
3 STORAGE PRESSURE	about 50 - 100 bar	atmospheric	atmospheric
4 PRODUCT QUALITY:			
- THERMAL AND CHEMICAL	---	good	favourable
- MECHANICAL AND RADIOLYTICAL	---		very good
5 DISPERSIBILITY	extreme	ionic crystal	metal
6 BIOLOGICAL HALF-LIFE OF DISPERSED PRODUCT FORM	negligeable	large	large
	An accidental dispersion of the solid product forms as airborne dust creates a hazard, which is not inherent to the gaseous waste form.		
7 STORAGE DENSITY IN			
- STORAGE MATRIX	20 - 60 bar	corresponds to 20 - 60 bar	corresponds to about 200 bar
- FINAL STORAGE UNIT	Assuming a double containment for pressurized vessels, the forms and dimensions of all waste packages should be comparable to 20 - 60 bar pressurized cylinders.		

CHARACTERISTICS OF KR STORAGE PRODUCTS   TABLE 3

	ADVANTAGES	DISADVANTAGES
KR ION SPUTTER PUMPS	• low Kr gas inventory • continuous operation • low pressure • ambient temperature • solid product from	• high cost • additional development
ZEOLITE 5A ENCAPSULATION	• solid product form	• high Kr gas inventory • discontinuous operation • high temperature and pressure • high cost • additional development
PRESSURIZED VESSELS	• available technology • moderate cost	• high Kr gas inventory • discontinuous operation • gaseous product form

KjK   IHCH

TABLE 4

ADVANTAGES AND DISADVANTAGES OF KR CONDITIONING PROCESSES

• COMMERCIAL USE OF XE AND Kr-85
  - Inactive xenon: better light sources, human anesthesia (20% O_2 mixture), chemistry etc.
  - Kr-85: low-level lighting devices, material tests, leak tests, gas tracers, Kr-85 batteries etc.

• DECAY IN AN ON-SITE STORAGE FACILITY
  - Storage of pressure vessels in storage buildings is an expensive option
  - Cooling may be achieved by air convection or in a water basin
  - The building may be designed to provide a second confinement barrier

• TRANSPORT REGULATIONS
  - Existing regulations and recommendations would not allow shipment of large
    quantities of pressurized radiokrypton.

• DISPOSAL OPTIONS
  - in geological formations, sea disposal is not conform with the "London Convention"

• COST
  - Higher costs for Kr immobilization in solids may be balanced by the
    lower storage, transport or disposal costs.

KjK   IHCH

TABLE 5

COMMERCIAL USE AND STORAGE OR DISPOSAL OPTIONS

7. SUMMARY AND CONCLUSIONS

Fig.8 shows two alternative Kr management trains. The detailed specifications of a total processing train and additional interactions with processing in the plant are required to achieve a reliable comparison and evaluation.

Essential conclusions are briefly summarized in table 8. There are many acceptable solutions to the problem, but probably not an ideal one. International recommendations and national regulations for the release of Kr-85 from FRP's are not fully consistent and may be subject to change.

LIBERATION

shearing and dissolution	cost $\cong$	shearing and dissolution

• Kr inventory operating
• temperature and
• pressure

PREPURIFICATION

$(0.2h)5\cdot10^2Ci$
$500°C$
$<1\,bar$

DOG purification • H_2 for O_2, NO_x removal • adsorber station	cost $>$	DOG purification • cold scrubbing with 90% HNO_3

$5\cdot10^2Ci\,(0.2h)$
$-50°C$
$<1\,bar$

RECOVERY

$(40h)10^5Ci$
$to -175°C$
$5\,bar$

cryogenic distillation without O_2 N_2 (Ar) from Xe/Kr	cost $>$	selective absorption in R12 $N_2(Ar),O_2 / Xe,CO_2,N_2O/Kr$

$10^3\,Ci\,(0.4h)$
$to -150°C$
$<1\,bar$

CONDITIONING

$(40h)10^5Ci$
$about 400°C$
$about 400\,bar$

encapsulation into zeolite 5 A batch process	cost $\cong$	Kr ion sputter pumping 0.4h buffer vessel smoothed Kr rate

$10^3Ci(0.4h)$
$ambient\ T$
$about 10^{-4} bar$

STORAGE

no Kr gas
about $100°C$
atmospheric

building for intermediate storage air-cooled storage units	cost $\cong$	building for intermediate storage air-cooled storage units

no Kr gas
about $100°C$
atmospheric

MANY DISPOSAL OPTIONS

high, about 100 h — KR INVENTORY — low, about 1h

high, considerable jumps — TEMPERATURE — low, stepwise decrease

high — PRESSURE — below atmospheric

(h) average Kr residence time proportional to Kr inventory

KfK   IHCH

Fig.8   ALTERNATIVE KR MANAGEMENT TRAINS
(basis 6 MTHM per day reprocessing plant)

REFERENCES

Most of the material in this paper is compiled in two reviews:

- **COST ESTIMATES FOR KR-85 MANAGEMENT**
  - LESS THAN 0.5% OF REPROCESSING

- **MAJOR INCENTIVES FOR RARE GAS RECOVERY**
  - UTILISATION OF INACTIVE XE AND KR-85
  - PUBLIC ACCEPTANCE OF NUCLEAR POWER
  - INTERNATIONAL AGREEMENTS DESIRABLE FOR ENVIRONMENTAL PROTECTION

- **ALTERNATIVE KR-MANAGEMENT MODES ARE TECHNICALLY FEASIBLE**
  - THE STATE OF DEVELOPMENT IS NOT EXTREMELY DIFFERENT

- **DESIRABLE SAFETY AND TECHNICAL CHARACTERISTICS**
  - LOW KR-85 INVENTORY
  - NO HAZARDOUS CHEMICALS
  - LESS COMPLEX AND EXPENSIVE TOTAL PROCESS TRAIN
  - NO EXTREME TEMPERATURE AND PRESSURE
  - NO CORROSIVE CONDITIONS

- **INTERNATIONAL AGREEMENTS AND COOPERATION**
  - RECOMMENDATIONS IN VARIOUS COUNTRIES ARE NOT CONSISTENT
  - THE VARIOUS COUNTRIES USUALLY PREFER THEIR OWN DEVELOPMENTS
  - THERE IS NO IDEAL PROCESS

Table 6: CONCLUSIONS

/1/ Leudet A., Miquel P.; CEA, Fontenay-aux-Roses, France
     Castellani F., Curzio G., Gentili A.; University of Pisa, Italy
     Hebel W., Cottone G.; CEC editors "Methods of Krypton-85 Management", vol.10
     (1983), 309 pages
     "Radioactive Waste Management", series vol.10
     (editors: Anderson D.R., Platt A.M., Girardi F., Orlowski S.)
/2/ Laser L. (chairman), Report of the Technical Commitee, 23-27 October 1978
     IAEA Technical Report Series No.199, ISBN 92/0/125 180-7, Vienna 1980
     "Separation, Storage and Disposal of Krypton", 64 pages

Additional references /3/ to /6/ in "Proceedings of the Symposium on Waste
Management", Tucson, Arizona Feb.27-March3, 1983.

/3/ Dix G.P.; "An Overview of Byproduct Untilization", vol.2, p.49.
/4/ Remini W.C.; "Application Developed for Byproduct Kr-85 and Tritium", vol.2,
     p.77
/5/ Tingey G.L.; "Potential for Beneficial Use of Krypton-85, vol.2, p.89.
/6/ Rohrmann C.A.; "The Potential for Large Scale Uses for Fission Product
     Xenon", vol.2, p.81.

Additional references /7/ to /10/ refer to this conference.

/7/ Mellinger P.J.; "Kr-85 Health Risk Assessment of a FRP", this conference.
/8/ Henrich E., Huefner R., Weirich F., Bumiller W., Wolff A.; "Selective
     Absorption of Noble Gases in Freon-12 at low Temperatures and Atmospheric
     Pressure", this conference.
/9/ Ringel H., Messler M; "Chromatographic Separation of Krypton from Dissolver
     Off-Gas at Low Temperatures", this conference
/10/ Whitmell D.S.; "Immobilization of Kr-85 in a Metallic Matrix by Combined Ion
     Implantaton and Sputtering", this conference.

HEALTH RISK ASSESSMENT FOR FUEL REPROCESSING PLANT

Peter J. Mellinger
Battelle
Pacific Northwest Laboratories

We have conducted a health risk assessment for ^{85}Kr with a
slightly different prospective than you have heard this morning. The
purpose of our study was to evaluate radiological impacts of the EPA
^{85}Kr legislation as embodied in 40 CFR 190. We did this by conducting
a health risk assessment of the comparative risks involved in a routine
release scenario versus ^{85}Kr capture alternatives at a fuel reproces-
sing plant (FRP). The krypton contained in dissolver offgas, has
historically been released routinely into the environment from FRP
operations. There is an alternative to the routine release and that
is capture, concentrate, and store the gas for long periods of time.
Crypgenic distillation or fluorocarbon absorption are alternative
methods for the capture of krypton. Ion implantation/sputtering is a
method of immobolizing krypton received from the two capture processes.
We evaluated these technologies based on our assumption that, for the
extremely low doses and dose rates involved, the risks to individuals
in the work force can be compared directly to the risks to members of
the general public. We have taken early conceptual facility designs
for the three processes from the literature. Tom Thomas had a hand
in developing this particular one. Generally preconception designs
do not concentrate a great deal on radiation exposure. So we found
it necessary to increase shielding in these three facilities without
taking the step of getting into plant design. Maintenance doses to the
work force cover a range of mr/hr values. The operations we have
looked at, at all three facilities, have shown extremely low dose rates.
This does not represent what a routine, operating facility exposure
situation would look like. It is for routine maintenance. For
example, in a cryogenic distillation facility, Figure 1, the vertical
crosshatching represents a 0.1-1.0 millirem per hour area to maintenance
workers in the oxygen recombiner and hydrogen generator areas of the
facility. Number ten in Figure 1 corresponds to the cold box in the
hot cell. We have assumed that in all of our calculations the areas
that can be purged of krypton prior to maintenance, have been. As you
heard earlier this morning, when using fluorocarbon absorption,
Figure 2, it is not as important to remove oxygen and nitrogen oxides
by feed gas pretreatment as it is for cryogenic distillation. There
is almost no krypton holdup in the top of the column, so we didn't
add significant shielding up there. In the final product purification
step, the two cold traps would give a dose rate of up to 5 mr/hr. In
this particular facility, no single item was the predominant source
of exposure. In the case of the maintenance exposure in the ion
implantation facility, Figure 3, we have increased the exposure range
one level to 1.0-10 mr/hr. in the sputtering cell and in the air lock
areas of the facility. There are eight sputtered assemblies in the
cell shown in Figure 3. Figure 4 shows the maintenance occupational
population dose for cryogenic distillation combined with ion implan-
tation sputtering to be just a little higher than for fluorocarbon

absorption combined with ion implantation sputtering. If we reduce
the maintenance exposure to a man-rem/year, ion implantation combined
with cryogenic or fluorocarbon treatment will be about the same,
i.e., between 450-600 mrem/yr for an individual exposure as shown in
Figure 5. We have also shown in Figure 5 the maximum individual
dose from the second alternative, which is the total release of
krypton to the stack, no capture at all. The maximum individual
dose and the individual in the 50-mile population dose both result
from 100% krypton release. In our study we did something that was a
little different in that we assumed that is the U.S. did resume
reprocessing, the aged fuel would be reprocessed first, and that fuel
less than 30 years old would probably never be reprocessed. Therefore,
we would have about a three million curie/yr release from a 1,500
metric ton/yr FRP.   The lifetime risks to the workers from exposure
to krypton from capture and immobilization of ^{85}Kr are about 10^{-4}
per person per year of exposure. The risk to the public from routine
release of all the ^{85}Kr is down about 5 orders of magnitude, to 10^{-9}.
For radiation induced cancer deaths from 30 years of exposure to ^{85}Kr
we show almost insignificant differences in the actual cancer deaths
expected. From these data we have made the following conclusions:
1) given the uncertainities in the models used to generate lifetime
risks, the differences in total risk between capturing krypton, (and
thereby, exposing the occupational work force) or releasing krypton
(and thereby, exposing the population) are no significant. There is
no reason to conclude from the risks presented here that krypton
released routinely to the environment would give a greater risk than
recovery, immobilization, and storage of the gas. It is possible
that no risks would occur from either situation.

Cryogenic Distillation Facility

Figure 1

1.0-0.1 mrem/hr

0.1-0.01 mrem/hr

<0.01 mrem/hr

Fluorocarbon Absorption Facility

Compressor

F

Heat Exchanger

E

D

Chiller 2

Pump

Cold Trap 1

Cold Trap 2

H

Solvent Removal Beds

C

B

A

Chiller 1

Solvent Pump

Solvent Impurity Removed

G

Kr Column

1.0 - 0.1 mrem/hr

0.1 - 0.01 mrem/hr
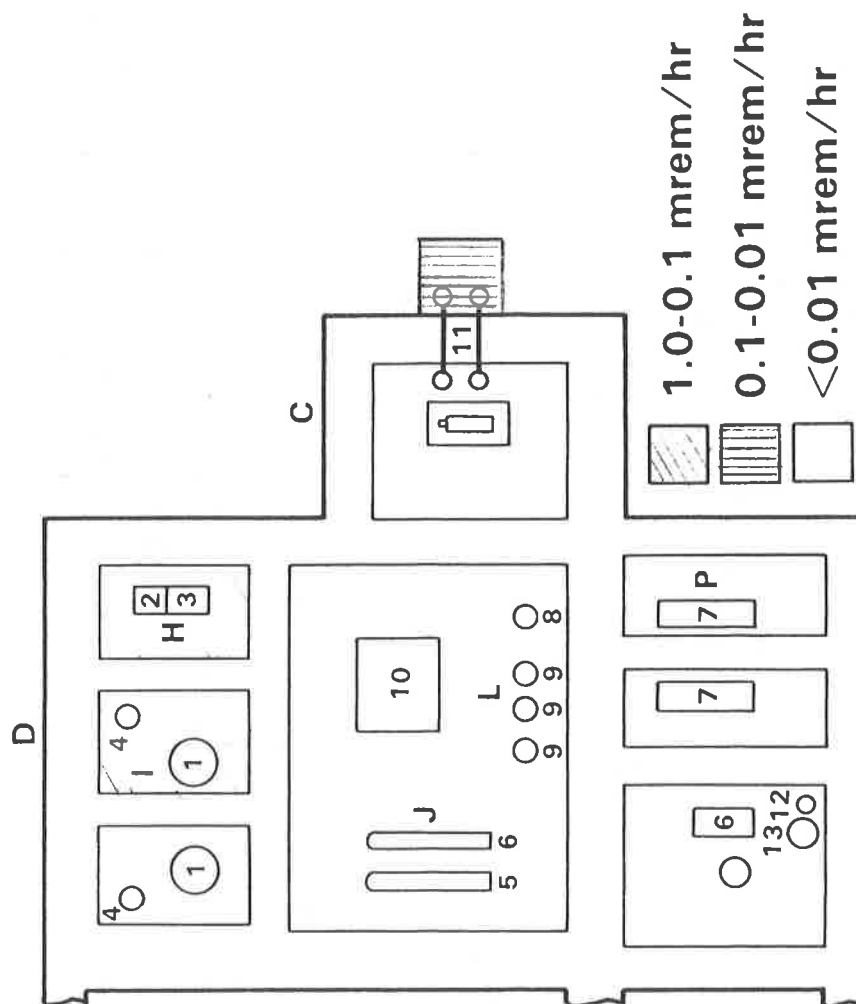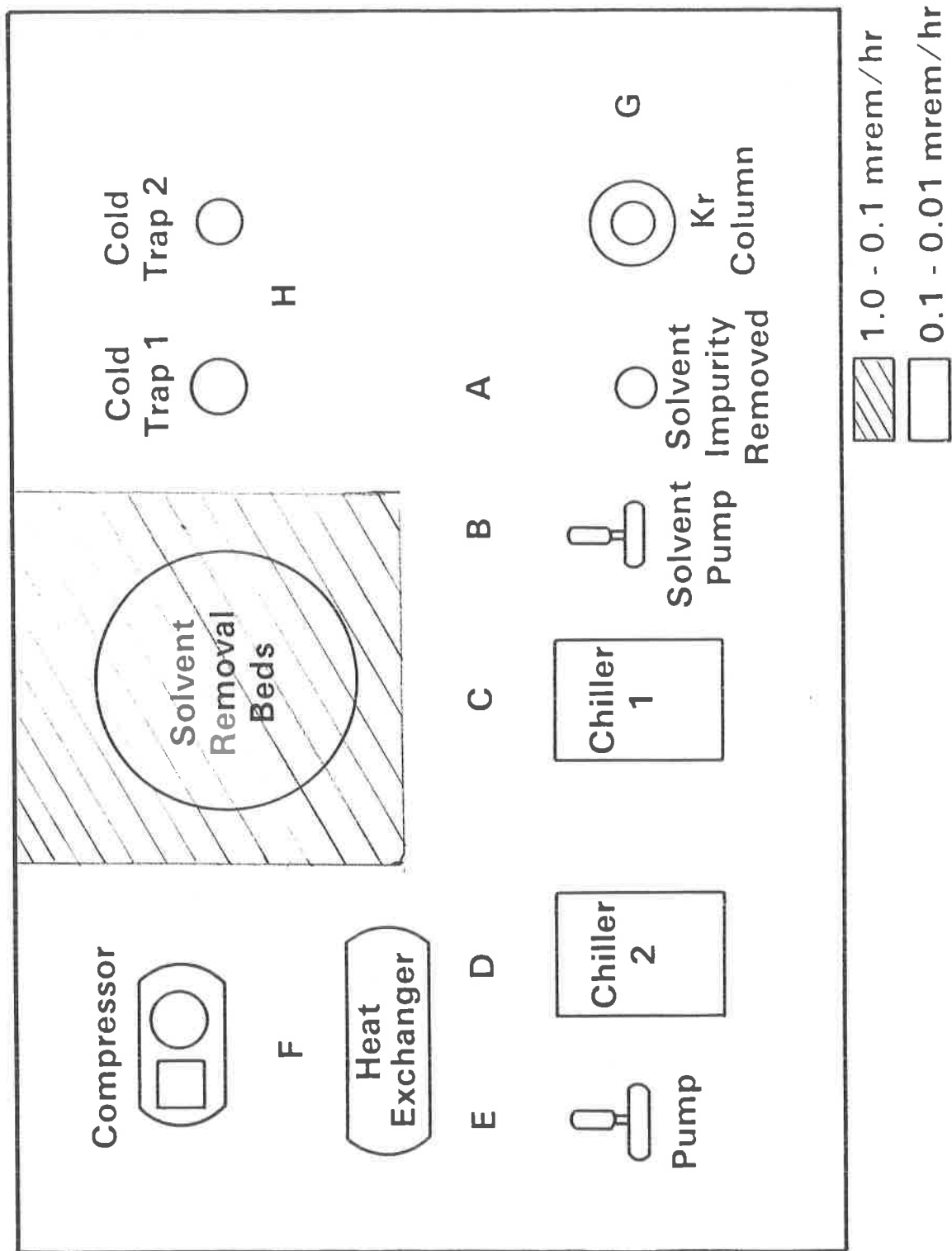
Figure 2

Ion Implantation Sputtering Facility
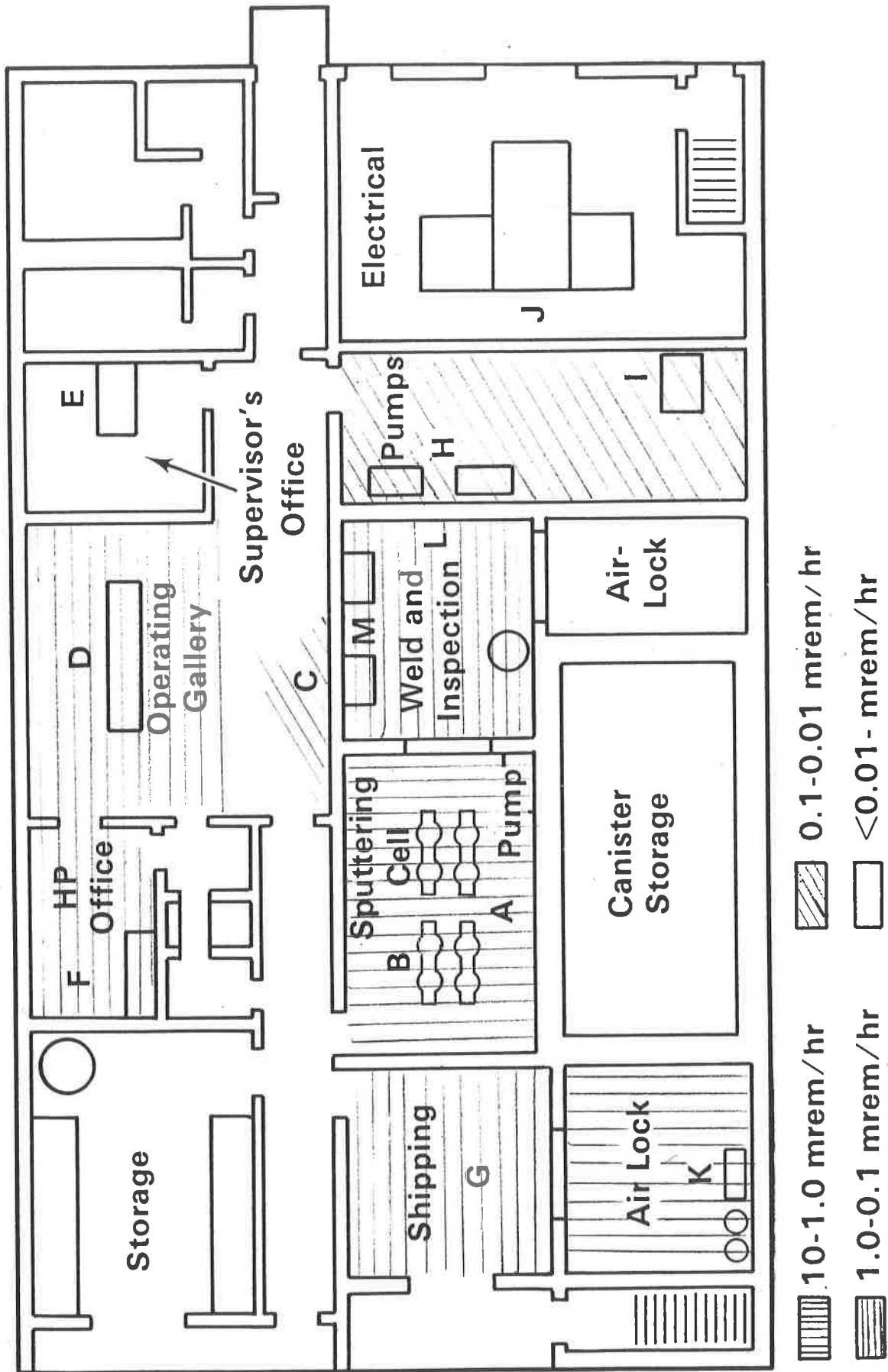
Figure 3
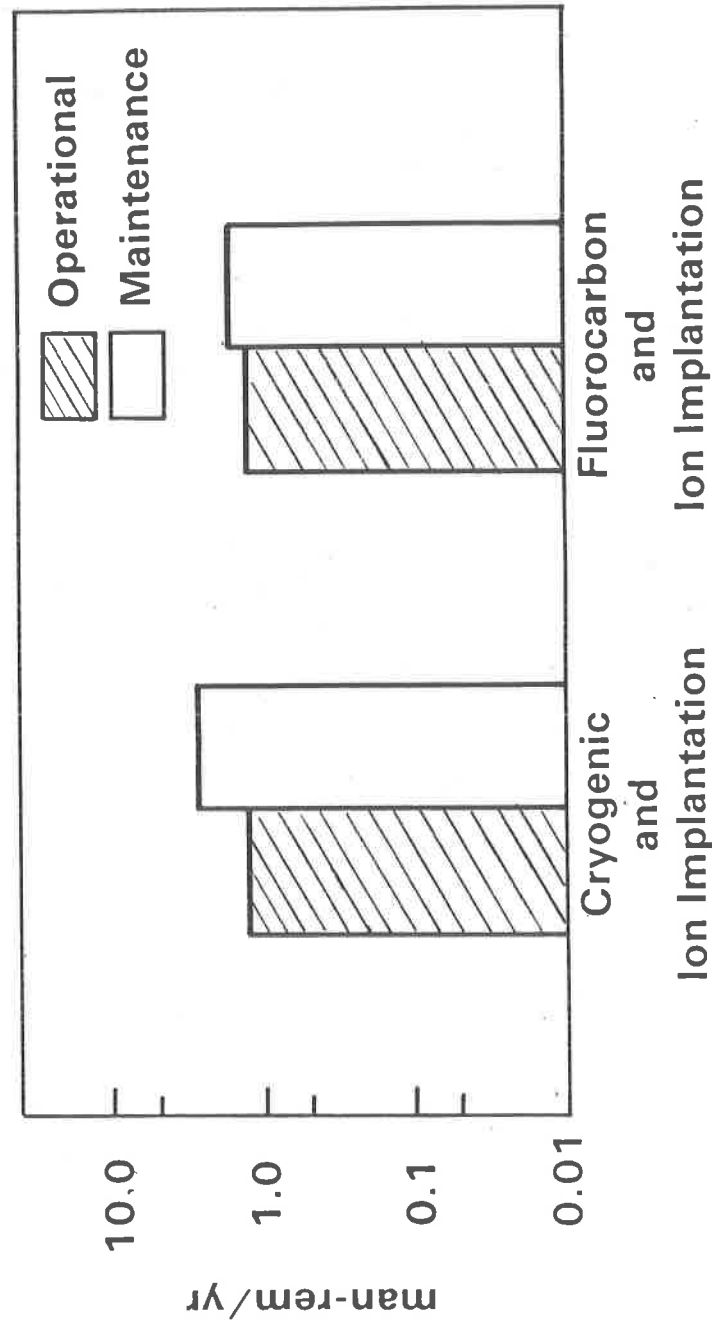
10-1.0 mrem/hr

1.0-0.1 mrem/hr

0.1-0.01 mrem/hr

<0.01- mrem/hr
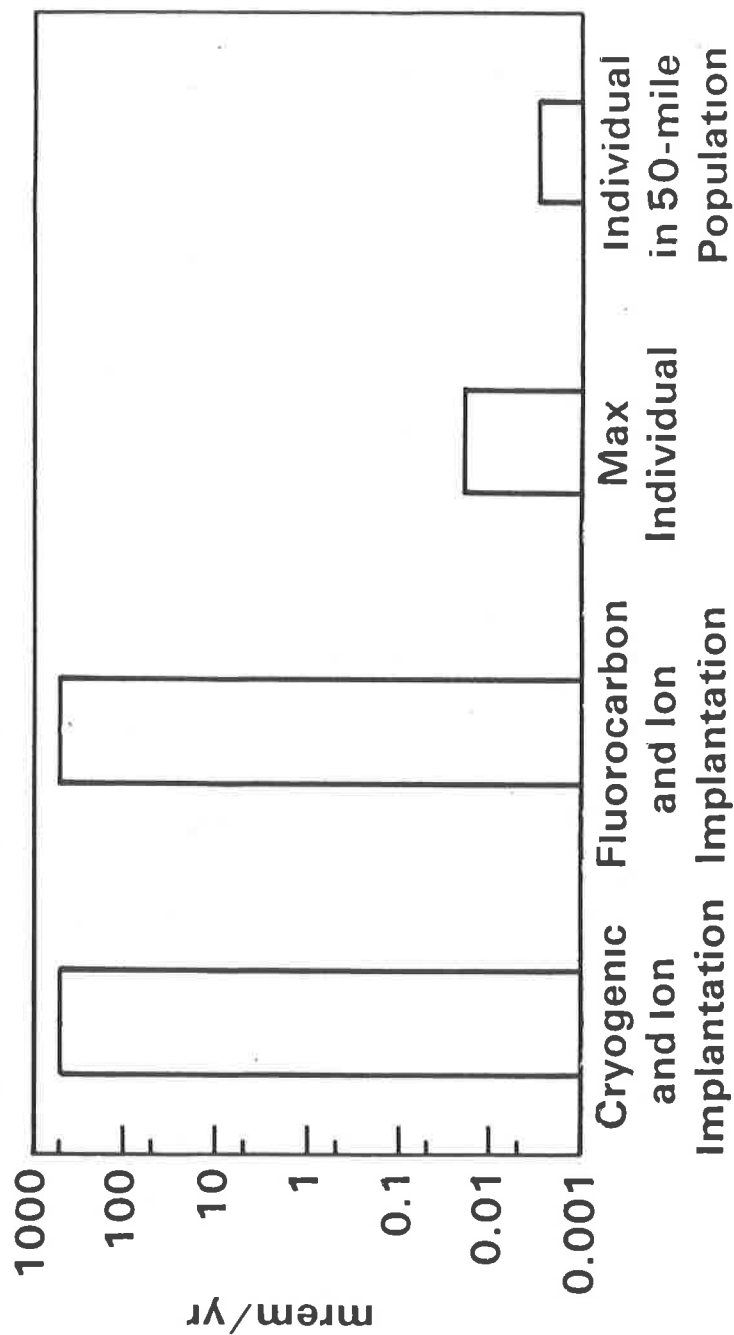
Figure 4

Figure 5

HOW MUCH DOSE REDUCTION COULD BE
ACHIEVED BY COLLECTION AND DISPOSAL
OF ^{129}I AND ^{14}C?

D.M. Wuschke
Atomic Energy of Canada Limited
Environmental and Safety Assessment Branch
Whiteshell Nuclear Research Establishment
Pinawa, Manitoba ROE 1L0

Introduction

Collection of ^{129}I and ^{14}C at fuel reprocessing facilities, followed by geological disposal, has been proposed as a means of reducing potential individual and collective radiation doses from these nuclides. However, assessments of geological disposal have shown that, because of their mobility in the environment, and their long half-lives (16 million and 5700 years for ^{129}I and ^{14}C, respectively), a fraction of these nuclides could return to the environment and become globally distributed. It is of interest therefore to ask, how much dose reduction could be achieved by collection and geological disposal of ^{129}I and ^{14}C, compared to releasing them in effluents from reprocessing plants?

Information for this study was obtained from references 1 to 5, and from an unpublished, preliminary assessment of geological disposal for the Canadian waste management program[7]. It should be noted that many of these analyses, especially for ^{14}C, are based on limited information and are considered preliminary in nature. Doses were normalized to reference inventories of 50 TBq of ^{129}I or 1000 TBq of ^{14}C, which are approximately the amounts that could be released in reprocessing nuclear fuel that had generated 1.0 TW(e).a of electricity, the total production expected in Canada up to about 2040. It was assumed that these amounts would either be released from reprocessing plants in gaseous or liquid effluents at a constant rate over twenty years, or emplaced at one time in a single disposal facility.

Iodine - 129

For ^{129}I, the individual doses compared were maximum annual thyroid dose equivalents for adult members of a critical group living within the region of discharge from the reprocessing, or disposal, facility.

Normalized estimates of thyroid dose rates based on analyses reported in references 1 to 4 are summarized in Figure 1. The line at 5×10^{-4} Sv.a^{-1} represents 1% of the limit recommended by the International Commission on Radiological Protection (ICRP)[6] for thyroid dose rates for members of the public.

The figure illustrates that predicted dose rates from an uncontrolled release of the reference inventory to the atmosphere over 20 years are higher than 1% of the ICRP limit by a factor of about 15 to 250. Predicted dose rates for discharges to a river or

coastal waters are lower than those for atmospheric releases, and are around 1% of the ICRP limit. However, individual dose rates due to disposal in the ocean by dumping, emplacement on a deep ocean bed, or in subseabed sediments are all predicted to be several orders of magnitude lower than dose rates from discharges in gaseous or liquid effluents, and well below 1% of the ICRP limit. For land-based geological disposal, predicted dose rates are generally much lower than 1% of the ICRP limit, but range up to it.
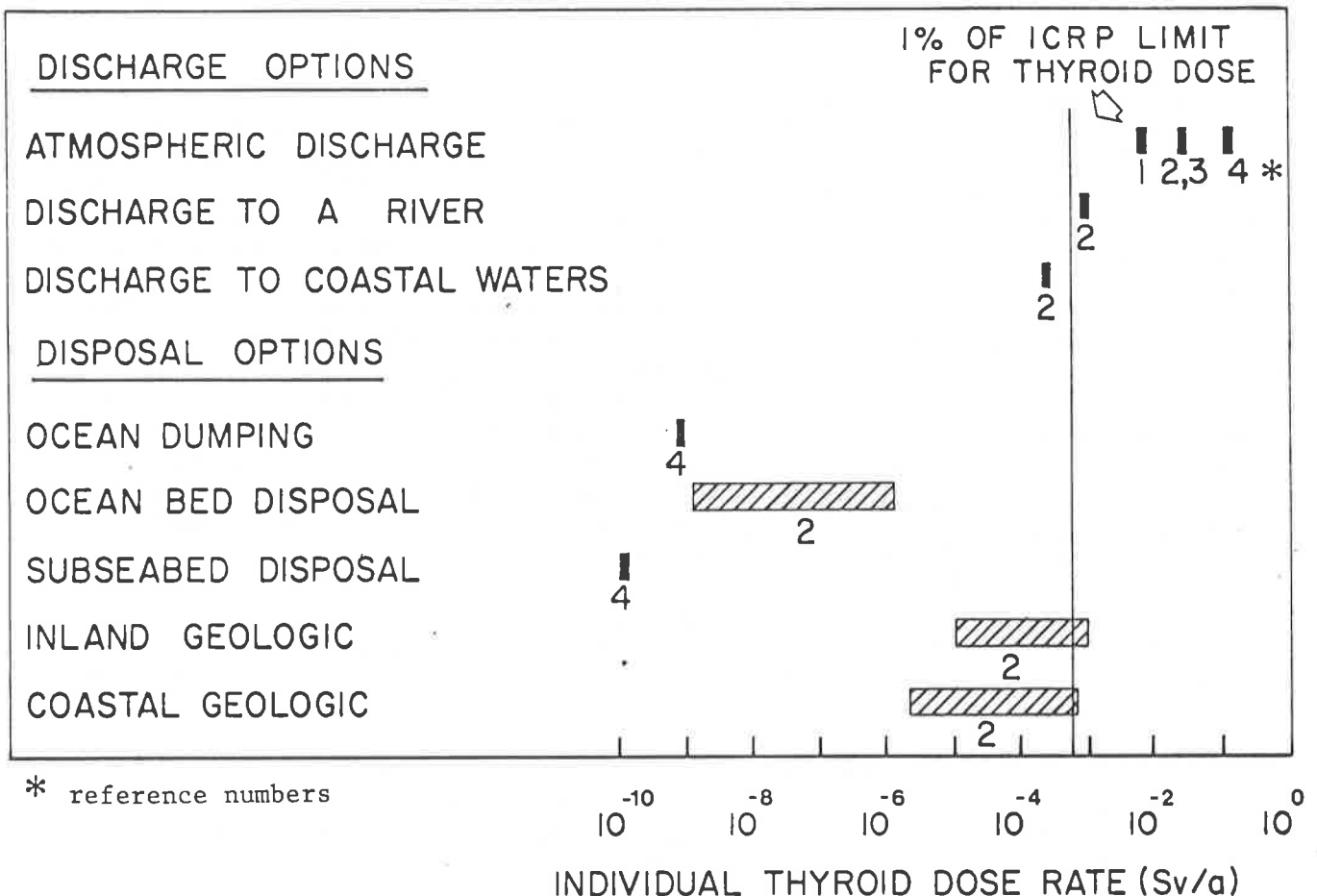
FIGURE 1
ESTIMATED INDIVIDUAL DOSE RATES TO THE HUMAN THYROID
FROM ^{129}I FOR SEVERAL DISCHARGE AND DISPOSAL OPTIONS

Although there are many uncertainties in all these analyses, it is concluded that collection and disposal of ^{129}I would substantially reduce individual dose rates from ^{129}I. The greatest dose reduction would likely be achieved by the ocean disposal options, especially subseabed disposal. However, any geological disposal option that would lead to dilution and dispersion of ^{129}I, before it could be incorporated in man's food chains, would reduce individual dose rates by many orders of magnitude.

In contrast to the substantial reduction in individual dose

rate that may be achieved by geological disposal of [129]I, the re-
duction in "infinite" collective dose commitment (i.e. dose to the
world population, integrated to infinite time) is predicted to be
small [2] [4], as [129]I is expected to become globally distributed
before there would be significant reduction of its inventory by decay
or substantial removal to environmental sinks. However, geological
disposal would postpone the radiological impact, compared to effluent
release.

Carbon-14

The case for collection of ^{14}C at fuel reprocessing plants,
followed by geological disposal, is not as strong as that for [129]I,
since predicted individual doses [3,5] due to uncontrolled atmos-
pheric release would be a substantially lower fraction of the ICRP
dose limit, and the fractional increase in the global inventory would
be much smaller. Furthermore, for most types of nuclear reactors,
the amount of ^{14}C produced in the moderator and coolant is comparable
to or larger than that produced in the fuel. Therefore, for effec-
tive overall control, collection at both reactors and reprocessing
plants is needed. In the present comparison analysis, only the
quantity of ^{14}C that could be released as effluent from fuel repro-
cessing is considered. The reference amount, 1000 TBq, is appro-
priate for heavy water and advanced gas-cooled reactors. For boiling
water or pressurized water reactors, the potential release in repro-
cessing fuel that had generated the same amount of electricity would
be smaller by a factor of 2-3; for Magnox and gas-cooled reactors, it
would be larger by about a factor of three.

For ^{14}C, the individual dose rates compared were maximum annual
effective dose equivalents for adult members of a critical group
living near the discharge zone associated with the reprocessing or
disposal facility.

Normalized estimates of effective dose rates from ^{14}C based on
analyses in references 1, 5 and 7 are summarized in Figure 2. The
line at $5 \times 10^{-5} Sv.a^{-1}$ represents 1% of the limit recommended by the
ICRP for effective dose rates for members of the public.

As illustrated in Figure 2, predicted dose rates from an uncon-
trolled release of the reference inventory of ^{14}C to the atmosphere
over 20 years are below 1% of the ICRP limit. Predicted dose rates
for aqueous discharges to a river, or coastal waters, are approx-
imately an order of magnitude higher. Some dose reduction is predic-
ted for disposal on a deep ocean bed, and for land-based geological
disposal in plutonic rock. However, for land-based disposal in clay,
estimated doses rates range from several orders of magnitude below
the levels predicted for uncontrolled atmospheric releases, to
several orders of magnitude above them, and the higher doses exceed
1% of the ICRP limit, by about three orders of magnitude. This wide
variability is due primarily to differences in the assumed leach
rates of ^{14}C from its waste form, and assumed rates for its transport
through geological media, and reflects a lack of experimental data in
these areas. In the absence of such information, analyses have been
based on assumed leach and transport rates that vary over many orders
of magnitude, and probably include some unrealistic values.

DISCHARGE OPTIONS

ATMOSPHERIC DISCHARGE

DISCHARGE TO A RIVER

DISCHARGE TO COASTAL WATERS

DISPOSAL OPTIONS

OCEAN BED DISPOSAL

INLAND GEOLOGIC IN CLAY

COASTAL GEOLOGIC IN CLAY

SHALLOW PLUTONIC ROCK(50M)

DEEP PLUTONIC ROCK (500M)

1% OF ICRP LIMIT
FOR EFFECTIVE DOSE

+ reference numbers
* 58%} of doses were less
** 78%} than 10^{-10} Sv.a^{-1} in[7]
    a probabilistic analysis[7]

10^{-10} 10^{-8} 10^{-6} 10^{-4} 10^{-2} 10^{0}

INDIVIDUAL EFFECTIVE DOSE RATE (Sv/a)

FIGURE 2
ESTIMATED INDIVIDUAL EFFECTIVE DOSE RATES FROM ^{14}C
FOR SEVERAL DISCHARGE AND DISPOSAL OPTIONS

These preliminary analyses show that collection and disposal of
^{14}C at fuel reprocessing plants is probably not needed to reduce
individual dose rates to an acceptable level, and that disposal in
the ocean would probably result in a substantial reduction in
individual dose rates. However, more information and analysis are
needed before adequate predictions can be made of dose rates from
disposal in land-based geological media.

Predicted "infinite" collective dose commitments[5] are
similar for discharge of ^{14}C as an effluent, for disposal on the
seabed and for land-based geological disposal with unfavourable
hydrogeological conditions. However, land-based geological disposal
could substantially reduce this dose, if there are favorable hydro-
geological conditions that would isolate the ^{14}C from the environment
for times corresponding to several half-lives.

Conclusions

Uncontrolled release of ^{129}I as an effluent from a fuel
reprocessing facility is likely to result in individual doses that
are above 1% of the ICRP limit. Collection and disposal of this
nuclide should substantially reduce individual dose rates, but would

provide little reduction in the "infinite" collective dose commitment.

Uncontrolled atmospheric releases of ^{14}C from a fuel reprocessing facility would probably not produce unacceptable individual doses. Some reduction in individual dose could be achieved by disposal on a deep ocean bed, but if land-based disposal is considered, more information and analysis is needed to demonstrate its effectiveness. The "infinite" collective dose commitment from ^{14}C would not be appreciably reduced by ocean disposal, but could be substantially reduced by land-based geological disposal if hydrogeologic conditions were favourable.

References

(1)   Nuclear Energy Agency, "Radiological significance of and management of tritium, carbon-14, krypton-85, iodine-129 arising from the nuclear fuel cycle, "Nuclear Energy Agency, Organization of Economic Co-operation and Development, report by an NEA Group of Experts, OECD, Paris, France (1980).

(2)   White, I.F. and Smith, G.M., "Management modes for iodine-129." Research Contract 161-81-8-WAS-UK. Work performed under European Community's research program on radioactive waste management, project 8 (1983).

(3)   Brown, R.A., Christian, J.D. and Thomas, T.R., "Airborne radioactive waste management," U.S. Department of Energy Report, ENICO-1132 (1983).

(4)   Wuschke, D.M., Barnard, J.W., O'Connor, P.A., and Johnson, J.R., "Predictions of local, regional and global doses from ^{129}I for four different disposal methods and an all nuclear future," in 18th DOE Nuclear Air Cleaning Conference. Proceedings of a conference held in Baltimore, 1984 August 12-16 (1984).

(5)   Bush, R.P., White, I.F., and Smith, G.M., "Carbon-14 waste management," United Kingdom, Atomic Energy Authority Report, AERE-R 10543 (revised) (1983).

(6)   International Commission on Radiological Protection, "Recommendations of the international commission on radiation protection," ICRP Publication 26, Pergamon, Oxford, 1977.

(7)   Guvanasen, V.M.M., Whiteshell Nuclear Research Establishment, Pinawa, Manitoba, Canada, unpublished information (1984).

DISCUSSION

MURTHY: The common thread of the presentations appear to be that I-129 needs control, not so krypton, but carbon-14, maybe.

EVANS, A.G.:   It is my impression that most of the research that has been done on the carbon cycle in the atmosphere shows that the ocean serves as a sump for most of the CO_2 generated in the normal fossil fuel cycle. I am wondering if you took this into full consideration when you looked at ocean disposal as an option for carbon-14. Since the ocean is, indeed, a sump for CO_2, it would also be so for carbon-14.

WUSCHKE: The analysis of ocean bed disposal was carried out by Bush, White and Smith (reference 5). Dispersion in the ocean was included in the model.

THOMAS: One of the justifications Dr. Henrich mentioned for kr-85 recovery was low inventory. I think he was referring to the operation of his column, where the inventory would be low. I would like to point out that, if you are going to recover krypton from fuel reprocessing plants, you are talking about 10-15 million curies/year, and if you are going to do it for a large fuel economy, you are talking about 110 million curies/year. Somewhere, there is going to be a large inventory and the risks from exposure go up substantially. This is always the argument against taking a low, potential-type risk and concentrating it. If you release the krypton as it forms, the risk is low to everyone, but if you concentrate it, the risk is going to be higher for a small population somewhere.

MELLINGER: Several years ago we looked at the storage of krypton gas in pressurized cylinders. You would have, possibly, 130,000 curies in a cylinder and would be creating a pretty large potential hazard from accidents. I noticed that in some of the slides on the ion implantation pump, there was a low gasous inventory. When you start sputtering this material, however, the metal containers will have about 10^4 curies per container. There could be a high exposure to operational people here also, although, not to the public.

HENRICH: High inventories are dangerous when the risk of a large accidental release is high. If the material is conditioned, the risk for an accidental release is very much lower, otherwise it would make no sense. Low inventories, in any case, would contribute to safety. Concentration in the final storage form is inherent to the process, inevitably, but it should be in such a form that the risk of an accidental release is low.

HEBEL: I would like to make a comment and then ask a question. I think we have heard a very good summary from the speakers of this panel concerning the four famous volatile radionuclides. I think we can say that for I-129, we have to do something to be within the recommendations of the ICRP, although, maybe, we are not now exceeding them and can continue releases to the atmosphere. I think

that in the neighborhood of fuel reprocessing plants, everybody agrees to the need to retain I-129. We have to go ahead with developing techniques for the immobilization of I-129 as long as it can't be disbursed homogeneously into the seas. The sea would be the most convenient method. Concerning Kr-85, I think we can agree that it is really not necessary, according to ICRP recommendations, to remove it and to retain it. It is a question whether according to the ICRP ALARA principle, it is reasonable to retain it. In this case, I think our basis of knowledge might not be adequate, yet, to judge whether it is reasonable or not. We should probably continue to generate knowledge to make this judgment. That means that we should continue to develop retention and removal techniques, and also storage techniques. The question of reasonable retention is, I think, also linked to a systematic study of the entire reprocessing technology. A major problem for krypton retention is the high airflow rate we have at the end of the reprocessing plant. One could ask whether modification of the reprocessing process could help in the future to simplify the retention of krypton and reduce the airflow rate. When we speak about whether it is reasonable to retain krypton, we should make a system analysis to see under what circumstances krypton might be retained in a better way than it is at the moment.

MELLINGER: I would like to make a personal comment. It is very difficult to comprehend the original intention of the man-rem calculation. I think that if you compare an occupational dose from a reactor to that from a reprocessing plant, the concept is probably reasonable. The world dose calculation, to me, is extremely unreasonable. You saw Tom Thomas' calculation of the individual dose to the world population. I didn't even count the zeros to the right of the decimal point. We made such a calculation several years ago for krypton from 180-day-cooled fuel, sixteen million curies were released and the dose was something like 0.405 millirem/yr. Our dose, on the reduced inventory used for this particular discussion today, was 3 microrem/yr and that is for the 50-mile population. In this case, even the U.S. dose is probably what you would get from drinking one beer, probably a light beer, at that. Now, is it worth spending 200 million dollars on a krypton recovery system, and maybe a million or two million dollars per year maintenance on each system you put in?

HENRICH: If krypton need not to be separated because its radiotoxicity is so low, it should be an ideal nuclide for technical use. I know many other nuclides with very much higher radiotoxicity that are used in industry. Present xenon price is about $4,000 per cubic meter. This amount comes from about a ton of spent fuel. There are processes where you can separate xenon without separating krypton. Because you do not have to pay the krypton management costs, recovery of the inactive xenon would make very much sense. In the reprocessing plant, the concentration of xenon is about 10^5 higher compared to the concentration in air. The high price for commercial xenon reflects the low concentration in air, which is only .08 ppm. I might add, the wastes of today are often the raw materials of tommorow.

RINGEL: I would like to comment on krypton retention
and storage but, first, if we retain xenon, I think the price will be-
come very low with respect to the current price. So it may be
questionable whether it would be economic to separate xenon. But for
the krypton, I think we should not retain krypton and then store it
on land someplace in pressurized cylinders, or ion implantations, or
zeolite because it will then create a higher risk than without krypton
retention. We have to put the krypton into a safe formation, such as
in a deep groove in the sea or a deep geographic layer inland. In
that way, it is buffered by a big, geographical water layer or rock
and will not create a bigger problem than without retention. Re-
garding retention of krypton, if we do not retain krypton, it is going
to become the most ionizing isotope in the atmosphere, which will not
be good for the public's acceptance on the nuclear industry.

O'KADA: I have a question for Dr. Henrich. You
mentioned that krypton management costs will be less than 0.5% of the
reprocessing cost. What is the basis for that? Does it include
costs for the disposal of the krypton-85?

HENRICH: The basis for the cost estimates is a group
of experts that Mr. Hebel knows well. "Radioactive Waste Management",
series vol. 10 (editors: D.R. Anderson, A.M. Platt, F. Girardi, S.
Orlowski) "Methods of Krypton-85 Management", vol. 10 (1983), 309
pages (Hebel, ed.). The final statements of this reference give the
total krypton management costs as 0.5% of the total reprocessing costs.
It is a little difficult to translate this into dollars as there are
large differences in reprocessing costs. It is meant to be a crude
number only.

                                 I address a short remark to Mr. Ringel. No-
body knows if increases in the ionization density of the atmosphere
will be a problem or not. But there is a problem at present. In
commercial pressurized cylinders containing 40-50 liters of krypton,
the amount of Kr-85 is more than the permissible limit in Germany.
It is a little bit more than 0.1 millicurie of Kr-85. At present,
that is the Kr-85 concentration where not very much reprocessing is
done. In a few decades, this amount may increase with an increasing
nuclear power economy by at least two orders of magnitude. If so,
you would never again get a Kr-85-free krypton. I don't know if this
will become a problem, but I wanted to mention it.

HEBEL: Concerning the cost-benefit question for
krypton retention, I think the investment cost of retaining gaseous
wastes is relatively low compared to the total costs of the re-
processing plant. It is in the range of 1%, or so. But there is
another aspect, when looking at the cost-benefit relationship.
It is whether an installation such as a krypton retention plant,
could interrupt the operations of the entire reprocessing plant and
produce secondary costs that could be much higher than just the cost
for construction and normal maintenance. Because there are so many
reasons to shut down a reprocessing plant, it makes the product of
the reprocessing plant very expensive. So, we must not only look at
the construction and maintenance costs for a gas retention facility,
but also at the risks that jeopardize the operation of the plant.
If you are recovering only for commercial use, and not because of
licensing conditions, the availability and shut down of a recovery

plant will be no problem. Only if retention is connected with licensing will it become a problem. Not for fuel recovery processes.

ANON: With something like 85% retention required to meet the 50,000 curie per year limit on emissions, you could go above that pretty fast if you have to shut down, or before you catch the fact that you have to shut down. If the cryogenic or other recovery system doesn't work correctly, and you release krypton, you will have to shut down your whole reprocessing plant until you get your krypton capturing system back in running order.

CLOSING REMARKS OF PANEL MODERATOR:

I thank you for participating in the panel. Based on the discussions that have gone on, and the summary and conclusions that we have reached, it was a very useful panel.

Session 16

HEPA FILTER PERFORMANCE UNDER HIGH HEAT AND HUMIDITY CONDITIONS

WEDNESDAY: August 15, 1984
CHAIRMEN: H. Gilbert
             Consultant
             J. D'Ambrosia
             U.S. Department of Energy

A PROCEDURE TO TEST HEPA-FILTER EFFICIENCY UNDER SIMULATED ACCIDENT
CONDITIONS OF HIGH TEMPERATURE AND HIGH HUMIDITY
U. Ensinger, V. Rudinger, J.G. Wilhelm

LIMITS OF HEPA-FILTER APPLICATION UNDER HIGH-HUMIDITY
V. Rudinger, C.I. Ricketts, J.G. Wilhelm

DEVELOPMENT OF A HEPA-FILTER WITH HIGH STRUCTURAL STRENGTH AND HIGH
RESISTANCE TO THE EFFECTS OF HUMIDITY AND ACID
W. Alken, H. Bella, V. Rudinger, J.G. Wilhelm

SIMOUN: HIGH TEMPERATURE DYNAMIC TEST RIG FOR INDUSTRIAL AIR FILTERS
J. DuPoux, Ph. Mulcey, Jl. Rouyer, X. Tarrago

PERFORMANCE TESTING OF HEPA FILTERS UNDER HOT DYNAMIC CONDITIONS
R.P. Pratt, B.L. Green

REPORT OF MINUTES OF GOVERNMENT-INDUSTRY MEETING ON FILTERS, MEDIA,
AND MEDIA TESTING
W.L. Anderson

                  PERTINENT TO QUALITY ASSURANCE FILTER PENETRATION
                  TESTING
                  R.C. Scripsick, S.C. Soderholm, M.I. Tillery

    APPENDIX B.   DEPARTMENT OF ENERGY FILTER TEST PROGRAM-POLICY FOR
                  THE 80's
                  J.F. Bresson

    APPENDIX C.   INTERMEDIATE RESULTS OF A ONE-YEAR STUDY OF A LASER
                  SPECTROMETER IN THE DOE FILTER TEST FACILITIES
                  S.C. Soderholm, M.I. Tillery

    APPENDIX D.   CALIBRATION AND USE OF FILTER TEST FACILITY ORIFICE
                  PLATES
                  D.E. Fain, T.W. Selby

    APPENDIX E.   RESULTS OF CONAGT-SPONSORED NUCLEAR-GRADE CARBON TEST
                  ROUNDROBIN
                  M.W. First

                  CONAGT'S NUCLEAR CARBON ROUNDROBIN TEST PROGRAM
                  R.R. Bellamy

    APPENDIX F.   DEVELOPMENT OF A NEW TECHNIQUE AND INSTRUMENTATION FOR
                  RAPID ASSESSMENT OF FILTER MEDIA
                  Y.W. Kim

A PROCEDURE TO TEST HEPA-FILTER EFFICIENCY UNDER SIMULATED ACCIDENT CONDITIONS OF HIGH TEMPERATURE AND HIGH HUMIDITY*

U. Ensinger, V. Rüdinger, J. G. Wilhelm
Laboratorium für Aerosolphysik und Filtertechnik
Kernforschungszentrum Karlsruhe GmbH
Postfach 3640, D-7500 Karlsruhe 1
Federal Republic of Germany (F.R.G.)

Abstract

In the framework of investigations into air cleaning within nuclear power facilities during accident conditions, a method has been developed to measure the removal efficiency of HEPA filters at high humidity and elevated temperature or at high temperature alone. Tests are performed with condensation aerosols of TiO_2 or MoO_3 generated with the aid of an argon plasma torch. Efficiency measurements are accomplished by the collection of test-aerosol samples onto Nuclepore filters and subsequent atomic absorption analysis. The sensitivity of the method allows decontamination factors as high as 10^4 to be determined. Comparison tests with two different standard procedures at room-air conditions proved the reliability of the newly developed method.

I. Introduction

During accident situations in a light water reactor a release of particulate and gaseous fission products must be expected. In order to protect the environment against an increased amount of particulate radioactivity the reliable performance of the HEPA filters must be ensured.

On account of the heat released, which in general is very high, the air to be filtered may attain high temperature levels. In case of a break of coolant line elevated temperatures and, in addition, high humidities must be anticipated. The activity can be safely contained only if the very high removal efficiency of the HEPA filter elements can be largely maintained in such an adverse case.

In the so-called "Guidelines" the limitation of accident consequences, issued by the Federal Ministry of the Interior /1/, a removal efficiency of 99.9 % is assumed for HEPA filters in all cases where exhaust air filters are used for reduction of the activity release. It must be examined whether the specified filtration efficiency can be guaranteed also under accident conditions.

* Work performed under the auspices of the Federal Ministery of the Interior under Contract No. SR 148/1.

II. Literature Survey

The removal of aerosols at high temperatures and above all at high humidities is influenced by a number of factors. At humidities above 100 % r.h. condensation takes place on particles with diameters greater than a given size. This process is coupled to evaporations so that the spectrum of particle sizes varies with time /2/. Below 100 % r.h. capillary condensation will occur within particle agglomerates. As a consequence of the uptake of water the agglomerated particles will shrink and hence become more difficult to be filtered.

The absorption of humidity by the fiber matrix of the filter medium will enhance the flow velocity between the fibers and increase the effective fiber diameter which could result in a deterioration of the retention capability of the filter. Generally, it can be expected that the removal efficiency will decrease at high humidity /3/.

On the other hand, increased temperatures will probably improve particle removal /4/ which for particles < 0.2 μm in diameter is essentially determined by diffusion. Raising the face velocity in order to maintain the mass flow at its previous level would in turn counteract the influence of increased temperature.

The considerations show that a reliable estimate cannot be made of the removal behavior of aerosol filters under possible accident conditions characterized by increased temperature and elevated humidity. In fact, these data must be elaborated by comprehensive experimental investigations. Only a few relevant experiments have been performed so far in this field, the main reason being the lack of a testing method, which performs in a reliable manner under the conditions indicated before. The standard testing methods as currently used in various countries, e.g., DOP test, NaCl test and uranine test, have been developed for use under ambient conditions. Whereas in the United Kingdom the range of application of the NaCl test has been restricted to temperatures below 300 °C /5/. First measured removal efficiencies of HEPA filters with NaCl as the test aerosol at temperatures up to 540 °C /6/. According to Murphy uranine can only be used up to 120 °C /7/. However, both methods do not seem appropriate for use at high humidities.

Knowledge of the removal behavior under conditions of high humidity essentially results from the investigations performed by Adams et al. /8-10/ on samples of HEPA-grade filter media. The authors used various electric-arc generated radioactive aerosols. It was found that the increase in humidity from ambient air conditions to 100 % r.h. is accompanied by an increase in penetration. Regarding the removal efficiency of full-size HEPA filters exposed to high humidity, measurements have been carried out on only two filter types, using radiotracered noble metal aerosols /11/.

Dennis /29/ reported increasing decontamination factors with increasing humidity for medium efficiency filters. Dorman /3/ cited a private communication with Balieu, who reported the opposite effect with glass-fiber papers used for respirator masks. In other words comprehensive studies on the behavior of 610x610x292 mm HEPA filters are missing. To make possible these investigations, which are important for nuclear safety, an appropriate method of testing the removal efficiency of HEPA filters needed to be developed. The solutions found in this endeavor will be reported in the following sections.

III. Requirements for a Method to Measure the Removal Efficiency under Accident Conditions

A test method suitable for measurement of removal efficiencies under accident conditions must satisfy special requirements. The material from which the test aerosol is to be generated must not undergo changes at elevated temperatures and high humidities. Therefore, it must be very stable both thermally and chemically and also insoluble in water. Together with humidity it must not produce corrosion within the normally expensive test facility even in case of extended use. The mean particle size should be $\leq 0.2~\mu m$, i.e., in the range of maximum penetration. Nonradioactive substances should be preferred because they can be handled more conveniently.

It should be possible to produce mass concentration of $10~mg/m^3$ on the upstream side of the filter and to determine decontamination factors of the order of 10^3–10^4. This means that aerosol concentrations of about $1~\mu g/m^3$ must be reliably detected downstream of the filter.

IV. Plasma Condensation Aerosols

Aerosol Generation

Thermally and chemically stable compounds can be found among the high melting ceramic materials such as oxides, carbides, borides and nitrides of transition metals. Two possibilities are available for generating aerosols of a suitable particle size from these materials.

Firstly, these aerosols can be generated by a physical process, namely evaporation of the appropriate substances in a plasma /12,13/ followed by recondensation in the test air stream. Secondly, such fine particles can also be generated by a chemical process, namely hyrolytic or thermal decomposition of suitable source compounds such as alcoholates or organic chelate complexing agents /14-16/.

The second method depends on the availability of suitable source compounds and is restricted to oxide aerosols. With the first method compounds other than oxides also can be used.

1038

The newly developed technique is based on the first method of aerosol generation, because it offers a wider field of application. To generate the aerosol, a commercially available 20 kW powder spraying plasma device is used. The plasma burner is shown in Fig. 1. It contains a conical tungsten cathode and a hollow cylinder copper anode. The powderous aerosol substances are finely dispersed from a solid particle feeder (Fig. 2) into argon as the carrier gas and fed to the plasma jet through a bore in the anode. For higher volatile material an additional powder feed is provided immediately preceding the anode. Argon is used as the plasma gas to avoid chemical reactions. The amount of substance discharged per unit of time by the powder feeding unit can be adjusted from a few mg/h up to about 50 g/h and kept constant within $\pm$ 10 % over an extended period of time. By variation of the volumetric flow rate of the plasma and carrier gas and by variation of the current intensity, the heat output of the plasma torch can be adjusted to the metered amount and to the thermal properties of the powder used.

To improve the techique, the plasma torch was installed in a filter test rig in which 610x610x292 mm HEPA filters are tested under ambient conditions. The essential features of the test rig are shown in Fig. 3. Figures 4 and 5 show the general view of the test section. The duct is rectangular in cross section. Volumetric flow rates of up to 3000 m^3/h can be set. To homogenize the aerosol concentrations a Stairmand disc has been installed on the upstream and downstream sides of the test filter.

To make easier the setting of the operating parameters of the plasma torch, a sight glass was installed to allow observation of the plasma torch (Fig. 6). The test duct was designed such that investigations can be performed with the DOP, NaCl, and uranine standard test methods without requiring major conversion work. For the NaCl test the test rig was equipped with a forced flow blower and a heater.

Compounds Used

The generation of solid condensation aerosols from high-melting ceramic materials was investigated in detail for the following substances: TiO_2, TiC, ZrO_2, Zr_3C_2, VC, Cr_2O_3, Cr_3C_2, CrB, and MoO_3. ZrO_2 and Cr_2O_3, e.g. may be present during an accident. The aerosol substances were injected into the plasma as fine powders with particle diameters of 2-6 µm. For this purpose, the metering cylinder had to be filled with great care to guarantee uniform powder delivery and to avoid plugging. By drying at 200 $^{\circ}$C the powder was prevented from caking. In some cases Aerosil was added as an anticaking agent. This is a silica made powder with a bulk density of 0.1 g/cm^3. For all compounds the metering rates were 0.5-40 g/h. With a volumetric flow rate of 1700 m^3/h this corresponds to a mass concentration upstream of the filter of 0.3-23.5 mg/m^3. Operating times of one hour and more were easily achieved even at high metering rates.

Characterization of the Aerosols

To determine the shape of the aerosol particles and the particle size distribution, samples of aerosol particles were collected onto Nuclepore filters and subsequently analyzed by scanning electron microscopy. Filters of 0.08 μm pore size were used in these investigations.

Figures 7-9 show examples of VC, Zr_3C_2 and Cr_3C_2 particles. All powders used were transformed into spherical particles with a count median diameter of 0.05-0.06 μm. No significant differences in the particle size distribution were found for the individual substances.

At high aerosol concentrations a great number of particle agglomerations were found. When Nuclepore filters were examined which had been exposed to aerosols at constant mass concentration for various periods of time, it was observed that only negligible agglomeration had taken place for sampling times of < 1 min. The conclusion is, that the particles agglomerate on the filter only.

Figures 10 and 11 show the cumulative and frequency distributions of ZrO_2 and a TiO_2 sample, respectively. For ZrO_2 a count median diameter of 0.064 μm was determined with a relative geometric standard deviation of 1.36. This corresponds to a mass median diameter of 0.077 μm. The count median diameter for the TiO_2 sample was 0.053 μm with a geometric standard deviation of 1.46. The mass median diameter was calculated to be 0.079 μm. Similar values were found for the other aerosol particles.

At high metering rates particles of 1-3 μm diameter were observed in some cases. These are probably powder grains which had been only partly molten and only partly evaporated. An increase in thermal output of the plasma torch and the extention of the residence time of particles in the plasma by reduction of the plasma gas volumetric flow rate led to complete conversion into a largely uniform aerosol of the desired size.

V. Determination of the Aerosol Mass Concentration

Sampling Technique

The aerosol mass concentrations must be measured both upstream and downstream of the filter in order to be able to calculate the removal efficiency. The method selected must be capable of determining ,with a 20 % accuracy, concentrations down to approx. 500 ng/cm³ downstream of the test filter, and also be able to take into account particles down to approx. 0.03 μm diameter. Only proven commercially available equipment should be used.

All optical methods which would offer the advantage of a continuous mode of operation must be ruled out on account of the small particle size of the test aerosol. The same is true for flame-emission-spectroscopy methods because they are sufficiently sensitive only with respect to the elements Na and Ca. The commercially available oscillating quartz monitors are also not sufficiently sensitive. Therefore the mass concentration can only be determined in two stages, i.e., by collection and subsequent analysis of the deposited material.

Among the potential methods of collection involving, e.g., electrostatic removal or use of a low pressure impactor, filtration on Nuclepore filters was selected due to the simplicity and reliability of this method. To minimize the sampling durations, filters of 0.1 μm pore size are used which allow a maximum flow rate of 2 l/min/cm^3. With filters 90 mm in diameter on the downstream side of the test filter about 0.1 m^3 air can be collected per minute.

Despite the relatively large pore size of the sampling filters the particles are practically removed quantitatively. It is known that particles much smaller than the pore size of the Nuclepore filters can be sampled with high removal efficiencies /17,18/. This is more pronounced with decreasing pore radius of the polycarbonate filters /19/. In addition, due to the particle density of about 4 g/cm^3 the aerodynamic diameter of TiO$_2$ particles is about twice the geometric diameter. Hence the fraction of particles removed due to impaction is further increased, thus additionally contributing to quantitative sampling.

Mass Concentration of the Test Aerosol

In the interest of a high sensitivity of the testing method the mass concentration upstream of the filter should be as high as possible. However, given the small diameter of the aerosol particles to be filtered, particle number concentrations are reached in which significant agglomeration takes place. Such agglomerations would shift the particle size distributions towards larger diameters and hence exert an influence on the removal characteristics. In order to maintain clearly defined test conditions such phenomena should be minimized.

Using the approximation equation of Smoluchowski /20/, the admissible mass concentration was estimated by assuming monodisperse aerosol with a particle diameter of 0.05 μm and a solid density of 4 g/cm^3. The premise that the number of individual particles is allowed to decrease, due to agglomeration, to a value of 90 % on the way from the plasma to the test filter results in a maximum mass concentration of about 5 mg/m^3. This value was observed in the tests and only increased to concentrations of approx. 10 mg/m^3 to determine decontamination factors of 10^4.

Analysis

Various specific-element methods are available for analyzing the aerosol samples collected on the Nuclepore filters. Among the eligible spectroscopic techniques, namely NAA, RFA, AAS, ICP, and PIXE /21-23/, the flameless atomic absorption spectroscopy (AAS) was selected because it is the least costly method offering a comparable accuracy.

Upstream and downstream of the filter, sampling flows are passed through Nuclepore filters of 47 mm and 90 mm diameters, respectively. The aerosol samples so collected are first dissolved in a few ml of concentrated mineral acids under pressure at 200 $^{\circ}$C. The solutions are diluted with water to an acid content below 1 mole/l. Then the metal content of the respective compound is determined by Atomic Absorption Spectroscopy by the graphite tube technique. The method is specific for the aerosol substance used and largely intensive to any impurity present in the test duct. The reliability of the method was confirmed by comparisons with gravimetric and spectroscopic measurements. Table I shows for some compounds the mean deviation of the AAS values from the values determined by gravimetry and also the standard deviation for each set of calibration deviations.

Table I: Accuracy of aerosol mass determination using flameless AAS.

Compound	Sample Weight (mg)	Concentration after Dissolution (µg/ml)	Mean Deviation (%)	Standard Deviation (%)
MoO_3	2.2-0.3	0.05-0.4	-1.1	10.2
TiO_2	0.2-2.0	0.2 -1.6	-5.5	6.0
TiC	1.7-4.0	1.4 -3.1	-8.8	5.7
VC	0.3-0.9	0.2 -0.7	-6.5	7.9
Cr_3C_2	0.1-0.8	0.02-0.06	-3.0	3.1
CrB	0.1-0.6	0.02-0.05	+1.5	6.2

The detection limits and element contents of 90 mm Nuclepore filters are summarized in Table II for Ti, V, Cr, and Mo. It can be concluded from these data that Ti, V, and Mo compounds with aerosol concentrations of 1-5 µg/m^3 downstream of the filter can

still be detected with certainty. For Cr compounds, concentrations of about 15-20 $\mu g/m^3$ are necessary. For mass concentrations of about 10 mg/m^3 upstream of the filter decontamination factors of 10^3 can be reliably measured. For Ti, V and Mo compounds decontamination factors of the order of 10^4 can be determined.

Table II: Detection limits and Nuclepore filter 90 mm contents for the elements Ti, V, Cr, and Mo determined by flameless AAS.

Element	Detection Limit (ng/ml)	Trace element content of 90 mm Nuclepore Filters (μg)
Ti	5	< 0.3
V	3	< 0.2
Cr	1	< 4.5
Mo	2	< 0.8

Behavior of the Aerosol Substances in the Plasma

Most of the aerosol substances were examined for changes they might undergo while passing through the plasma. The criteria selected were the solubility behavior and the stoichiometry of the aerosol samples.

The spectroscopic analysis of TiC-aerosol samples yielded a Ti content lower by 40-50 % than the value to be expected from the gravimetric measurements. For VC the solubility in water was found to be unacceptably high. The aerosol samples of the Cr compounds were completely soluble in water. Moreover, the color of the V and Cr samples in some cases differed considerably from the color of the powders used. These phenomena were presumed to be caused by reactions between the hot aerosol material and the ambient air at the plasma-air boundary. Similar phenomena are reported in the literature for plasma spraying /24/. For the Zr compounds, the AAS method of detection is not sufficiently sensitive to allow additional accurate statements to be made. No indications of similar changes were found for TiO_2 and MoO_3. The high detection sensitivity and the extremely low trace-element content of the Nuclepore filters (see Table II) for Ti and Mo allow accurate measurements to be made. These compounds were selected as substances for testing.

Table III: Characteristics of HEPA-filter efficiency test methods

Test Method	Plasma	DOP	Uranine
Aerosol Compound	TiO_2/MoO_3	DOP	Sodium fluoresceine
Aerosol Generation	Vaporization of powders in an argon plasma	Atomization of a liquid	Atomization of a 1% aqueous solution
Shape	Spherical	Spherical	Nearly spherical
Size	0.06 µm	0.7 µm	0.15 µm
Mass Concentration Upstream of Test Filter	5 - 10 mg/m³	approx. 100 mg/m³	12 µg/m³
Sampling Method	Collection on Nuclepore filters	Direct measurement	Collection on Nuclepore filters
Sampling Time	10 - 60 min	1 min	10 - 30 min
Analytical Method	Dissolution and measurement by AAS	Forward light scattering	Dissolution and measurement by fluorometry
Cross Sensitivity	Specific for test compound	Sensitive to contamination	Specific for test compound
Detection Limit	0.5 µg/m³	1 µg/m³	0.001 µg/m³

VI. Proving the Method Under Ambient Conditions

The newly developed method of testing the removal efficiency of HEPA filters under the accident conditions of high humidity and high temperature is represented schematically in Fig. 12. The most important parameters of this method are compiled in Table III and compared with the parameters of the standard techniques, DOP test, and uranine test /25/.

The mass concentrations set for the plasma method upstream of the filter were 5-10 mg/m^3. The sampling times upstream of the filter were 10 minutes, downstream of the filter 10-60 minutes. These time values are comparable to those in the test with uranine. Nuclepore filters 47 mm and 90 mm in diameter and with 0.1 µm pore size were used.

Table IV: Characteristics of the 610x610x292 mm HEPA-filters used for comparative measurements of removal efficiencies

No.	Medium	Frame	Design flow rate (m^3/h)	Pretest history	Particle loading
1	Glass fiber	Metal	1700	Loaded with soot	604 g
2	" "	"	1700	" " "	503 g
3	" "	"	1700	" " "	679 g
4	" "	"	1700	" " "	866 g
5	Polycar-bonat micro fiber	Wood	2000	Humidity tested	Unloaded
6	" "	"	2000	" "	"
7	" "	"	2000	High diff. pressure test	"
8	Glass fiber	Wood	1700	Loaded with plasma aerosol	> 100 g*
9	" "	"	1800	New filter	Unloaded
10	" "	"	1700	New filter	Unloaded

* Estimated value

The test HEPA filters were taken from various test programs and had been previously exposed to various challenges. Four metal-frame glass-fiber filters had been loaded with aerosols from PVC-cable/solvent fires and silicone rubber-cable/solvent fires. In these tests the filters were exposed to temperatures up to 200 $^\circ$C, partly at high humidities. Filter particle loadings varied between 500 g and 870 g, and the pressure differentials at design volumetric flow rate were 1.0-2.2 kPa.

Three prototypical filters with a polycarbonate micro-fiber medium were also investigated. Two of these filters had been exposed to moist air for several hours at 50 $^\circ$C. One filter had been tested at high differential pressure. Finally, three new wood-frame filters with glass-fiber medium were tested. One of them was loaded with plasma aerosols under normal conditions for an extended period of time, and by small artificial leaks the removal efficiency was reduced to about 99.9 %. The other two filters were unloaded. The characteristics of the filters tested are shown in Table IV.

Table V: Plasma, DOP, and uranine decontamination factors (DF) and removal efficiencies (η) of the 610x610x292 mm HEPA-filters used for comparative measurements

Filter/ Method	Plasma		DOP		Uranine	
	DF	η(%)	DF	η(%)	DF	η(%)
1	38.4	97.4	60.6	98.3	39.1	97.4
2	45.1	97.8	164	99.39	89.3	98.9
3	103	99.03	153	99.35	122	99.18
4	527	99.81	440	99.77	530	99.81
5	197	99.49	430	99.77	207	99.52
6	98.1	99.00	500	99.80	340	99.70
7	2000	99.95	2900	99.97	2430	99.96
8	1000	99.90	2500	99.96	1530	99.93
9	10500	99.99	28200	99.996	9780	99.99
10	5700	99.98	25000	99.996	22900	99.996

For each filter at least three efficiency measurements were made and the mean value was calculated in each case. TiO_2 was used as the aerosol substance. For comparison of the plasma technique to other standard methods, the removal efficiencies of these filters were also measured by the DOP test, using polydisperse DOP (mean diameter 0.7 μm) /26/, and by the uranine test (AFNOR NFX 44011) /27/. In Table V the decontamination factors and the removal efficiencies obtained are listed.

By use of the new method, decontamination factors (DF) between 50 and 10^4 were reliably detected. The values were of the same order of magnitude as the values obtained with the other methods. Generally, the highest removal efficiencies were measured with the DOP method, in agreement with Dorman /3/.

Figure 13 is a plot of the decontamination factors determined with the plasma method as a function of the decontamination factors measured with the DOP and uranine tests. It can be seen that the DOP and uranine values show relatively little scatter around a straight line. In the whole range the DOP values are higher by a factor of 2.2, and the uranine values by a factor of about 1.5, compared with the respective values obtained with the plasma method.

The investigations show that with the new plasma method, decontamination factors of up to 10^4 can be accurately measured. This detection limit is considered fully adequate for measurements of filter removal efficiency under accident conditions.

VII. Conclusions

A method has been developed for determination of removal efficiencies of HEPA filters at high temperatures and high humidities. To perform the tests, solid condensation aerosols generated from temperature-resistant and water-insoluble ceramic materials are used. The compounds TiO_2 and MoO_3 are particularly suited because they can be detected with a high accuracy. The decontamination factors which can be determined by this method under ambient conditions are comparable with that obtained by the standard test methods DOP test, and uranine test. On account of the small particle diameter of 0.06 μm (cmd) and 0.08 μm (mmd) the measured values should be considered as conservative estimates of the actual removal behavior of HEPA filters. Regarding sampling time and sensitivity, the technique is still amenable to refinement.

The new method will be used to perform efficiency measurements at temperatures up to 250 °C in the test facility TAIFUN /28/. Efficiency tests at relative humidities up to 100 % as well as with fog conditions, both at temperatures up to 150 °C are also planned. These investigations into the HEPA-filter efficiency at high temperatures and high humidities, relevant to nuclear safety, can be performed with this new test method. Furthermore, it will be possible to increase knowledge of the complex process of particle removal, at high humidities.

References

/1/   Der Bundesminister des Inneren,
"Bekanntmachung der Leitlinien zur Beurteilung der
Auslegung von Kernkraftwerken mit Druckwasserreaktoren
gegen Störfälle im Sinne des § 28 Abs. 3 der
Strahlenschutzverordnung,"
Bundesanzeiger 245, Beilage 59/83/ p. 14 (1983)

/2/   Schöck, W. et al.; "Messungen der Wasserdampfkondensation
an Aerosolen unter LWR-unfalltypischen Bedingungen,"
KfK-Bericht 3153, Karlsruhe 1981

/3/   Dorman, R.G.; "A Comparison of the Methods Used in the
Nuclear Industry to Test High Efficiency Filters,"
Commission of the European Communities, V/3603/83 EN (1981)

/4/   Dorman, R.G.; "Dust Control and Air Cleaning,"
Pergamon Press, Oxford 1974, p. 338

/5/   White, P.A.F., Smith, S.E.; "High Efficiency
Air Filtration,"
Butterworth, London 1964, p. 164

/6/   First, M.W.; "Performance of Absolute Filters
at Temperatures from Ambient to 1000°F,"
CONF-801038, p. 677 (1972)

/7/   Murphy, L.P. et al.; "Comparison of HEPA-Filter Test
Methods in Corrosive Environments,"
CONF-801038, p. 67 (1980)

/8/   Adams, R.E. et al.; "Filtration of Particulate Aerosols
Under Reactor Accident Conditions,"
USAEC Report ORNL TM 1707 (1966)

/9/   Yuille, W.D., Adams, R.E.; "Behavior of Oxide Aerosols
of Uranium and Stainless Steel in Humid Atmospheres,"
USAEC Report ORNL 4198 (1968)

/10/   Davis, R.J. et al.; "Removal of Radioactive Aerosols
on High Efficiency Fibrous Filter Media,"
USAEC Report ORNL 4524 (1970)

/11/   Hirling, J., Gaál, J.; Comparison of Some Particulate
Air Filter Testing Methods Used in Normal and
Unfavorable Conditions,"
IAEA-SR-72/7 (1982)

/12/ Marchandise, H.; "Plasmatechnologie - Grundlagen und
      Anwendung,"
      Deutscher Verlag für Schweißtechnik,
      Düsseldorf 1970, p. 121

/13/ "LMFBR Aerosol Release and Transport,"
      Program Quarterly Progress Reports, Oak Ridge National
      Laboratory 1978 - 82

/14/ Gass, J.L.; "Préparation des aérosols d'oxydes
      metalliques par décomposition thermique des alcoholats
      en phase vapeur et propriétés de ces solides
      II. Préparation des aérosols d'oxyde de titane,
      d'alumine et de silice,"
      Bull. Soc. Chim. France 1970, p. 429

/15/ Kanapilly, G.M.; "A New Method for the Generation
      of Aerosols of Insoluble Particles,"
      Aerosol Sci. 1, p. 313 (1970)

/16/ Kanapilly, G.M. et al.; "Controlled Production of
      Ultrafine Metallic Aerosols by Vaporization of
      an Organic Chelate of the Metal,"
      J. Coll. Interf. Sci. 65, p. 533 (1978)

/17/ Buzzard, G.H., Bell, J.P; "Experimental Filtration
      Efficiencies for Large Pore Nuclepore Filters,"
      J. Aerosol Sci. 11, p. 435 (1980)

/18/ Spurny, K; "Nuclepore Siebfilter-Membranen: Zehn Jahre
      Anwendung für Staub- und Aerosolmessung,"
      Staub-Reinhaltung-Luft 37, p. 28 (1977)

/19/ Spurny, K., Lodge, J.P.; "Die Aerosolfiltration mit
      Hilfe der Kernporenfilter,"
      Staub-Reinhaltung-Luft 28, p. 179 (1968)

/20/ Davies, C.N.; "Aerosol Science,"
      Academic Press, London 1966, p. 37

/21/ Zielkowski, R., Bächmann, K.; "Instrumentelle Multi-
      elementanalyse in biologischen Matrices. Ein Vergleich
      von NAA, RFA und AAS,"
      Z. Anal. Chem. 290, p. 143 (1978)

/22/ Nottrodt, K.H. et al.; "Absolute Element Concentrations
      in Aerosols Analyzed by Atomic Absorption Spectroscopy
      and by Proton-Incuded X-Ray Emission. A Comparison,"
      J. Aerosol Sci. 9, p. 169 (1978)

/23/ Welz, B.; " Bevorzugte Einsatzgebiete von ICP und AAS
      und ihre relativen Vorteile,"
      Chemie-Technik, Sonderdruck 9, p. 161 (1980)

/24/ Meyer, H.; "Über das Schmelzen von Pulvern im
      Plasmastrahl,"
      Ber. Dtsch. Keram. Ges. 41, H2, p. 112 (1964)

/25/ Dorman, R.G., Dyment, J.; "Filter Testing by the
      Manufactures and in the Laboratory,"
      CONF-761145, p. 283 (1977)

/26/ "Testing of Nuclear Air-Cleaning-Systems,"
      American National Standard ANSI/ASME N 510 (1980)

/27/ "Méthode de mesure l'efficacité des filtres au moyen
      d'un aérosol d'uranine (fluorescéine),"
      Norme française homologuees NFX 44011 (1972)

/28/ Wilhelm, J.G. et al.; "Testing of Iodine Filter Systems
      Under Normal and Post-Accident Conditions,"
      CONF-720823, p. 434 (1972)

/29/ Dennis, W.L.; "Effect of Humidity on the Efficiency of
      Particulate Air Filters,"
      Filtration and Separation 10 (1973) pp. 149

Fig. 1:   Spray unit of the plasma generator
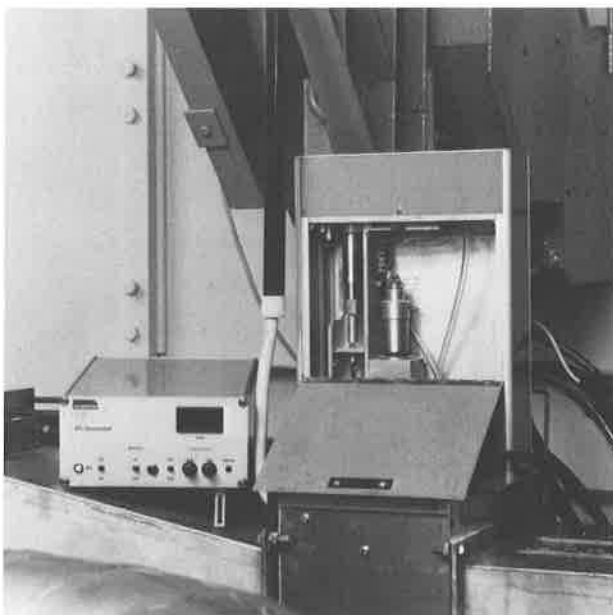
Fig. 2:   Solid particle feeder of the
          plasma generator
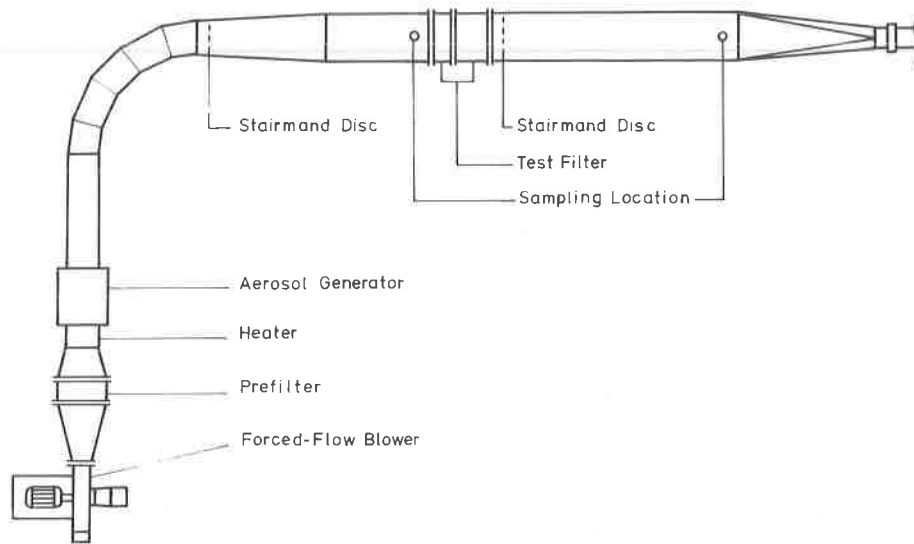
Fig. 3: Schematic of the test rig for HEPA-filter efficiency measurements under ambient conditions
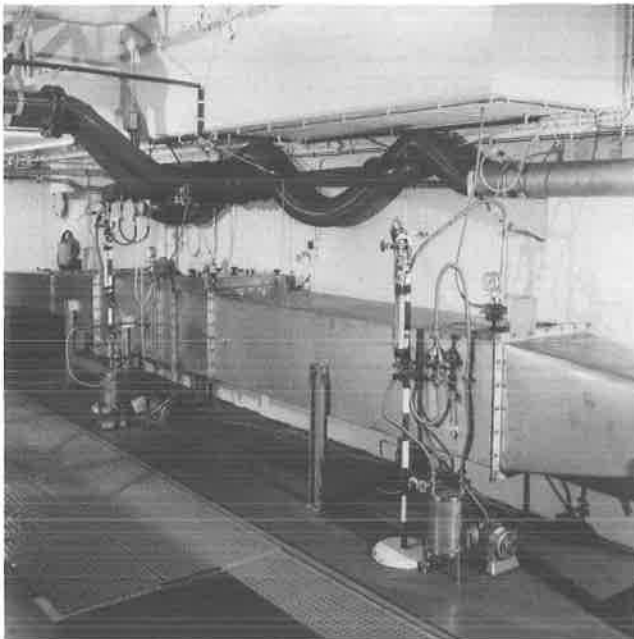
Fig. 4: Photograph of the filter test section and aerosol sampling apparatus of the test rig
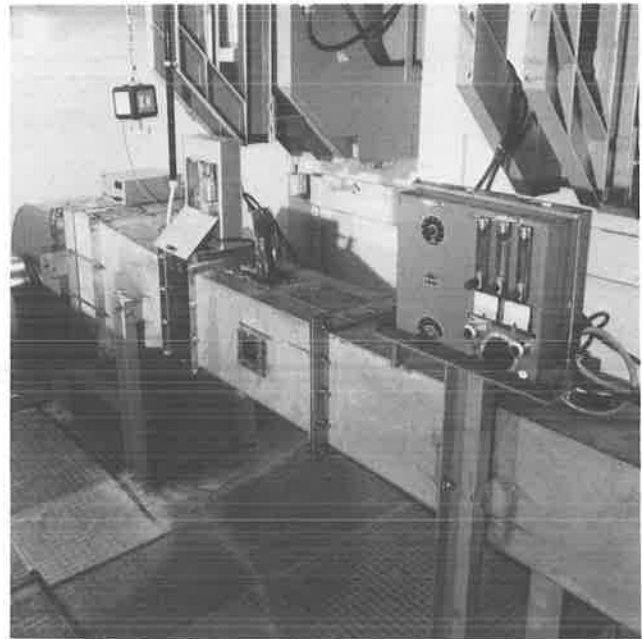
Fig. 5: Photograph of the aerosol generation section of the test rig (with blower, pre-filter, and air heater in background)

Fig. 6: Argon plasma flame with MoO_3 powder
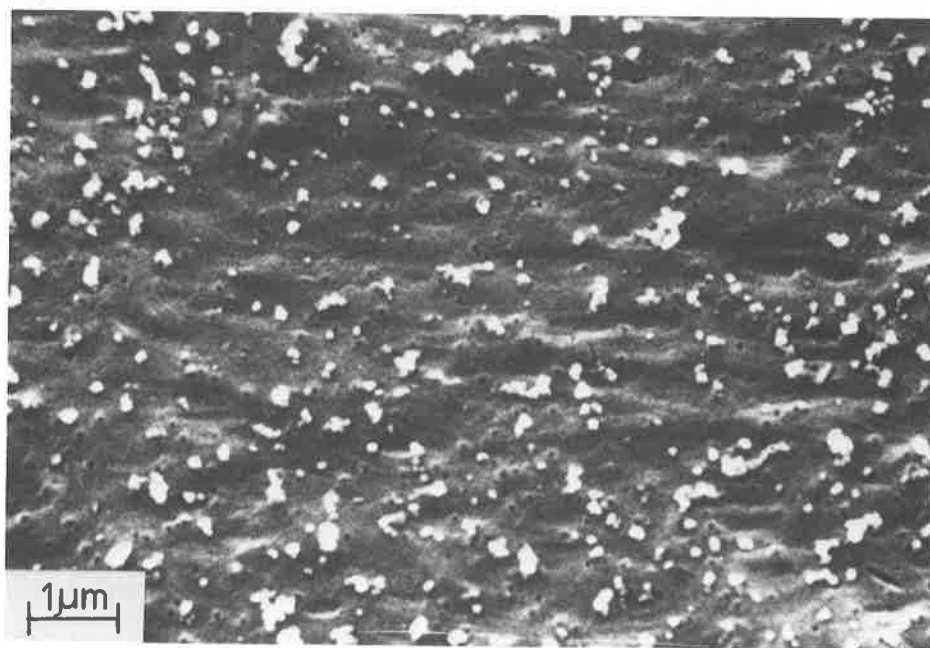
Fig. 7: Scanning electron micrograph of a VC
plasma aerosol
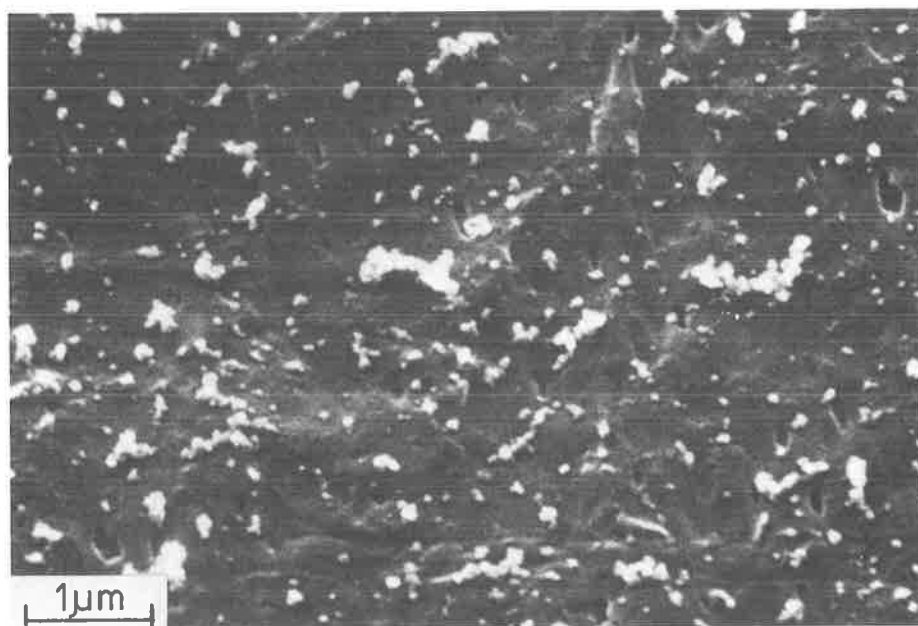
Fig. 8: Scanning electron micrograph of a Zr_3C_2 plasma aerosol
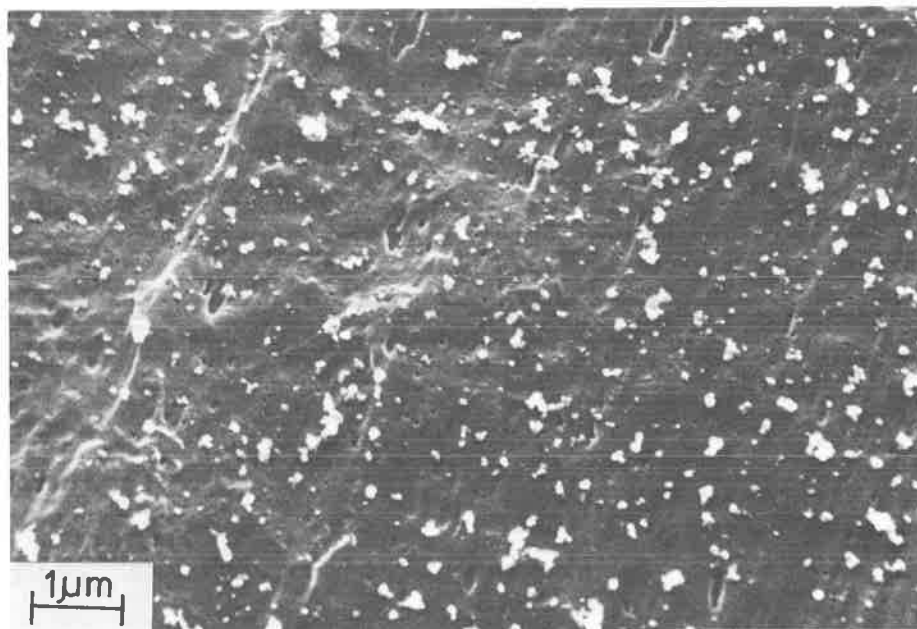
Fig. 9: Scanning electron micrograph of a Cr_3C_2 plasma aerosol
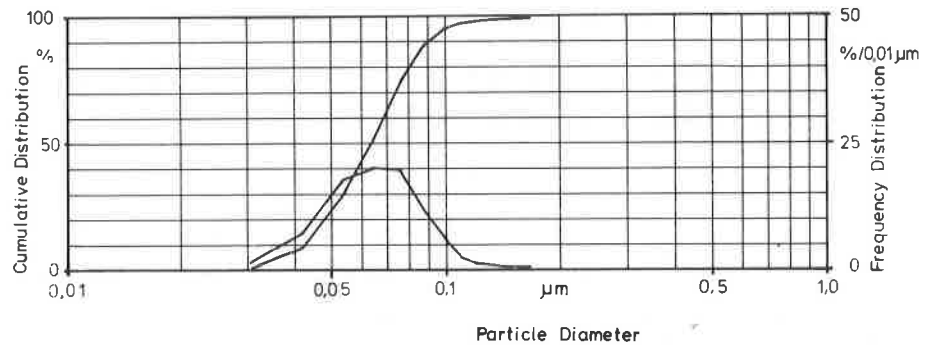
Fig. 10: Cumulative and frequency distribution
of a ZrO_2 plasma aerosol
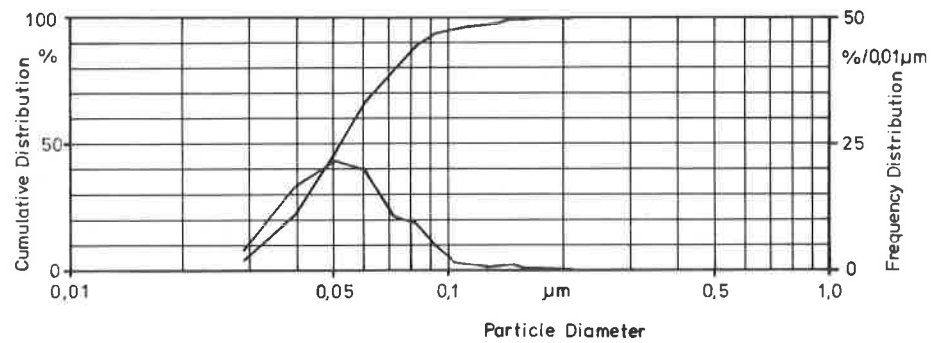
Fig. 11: Cumulative and frequency distribution
of a TiO_2 plasma aerosol
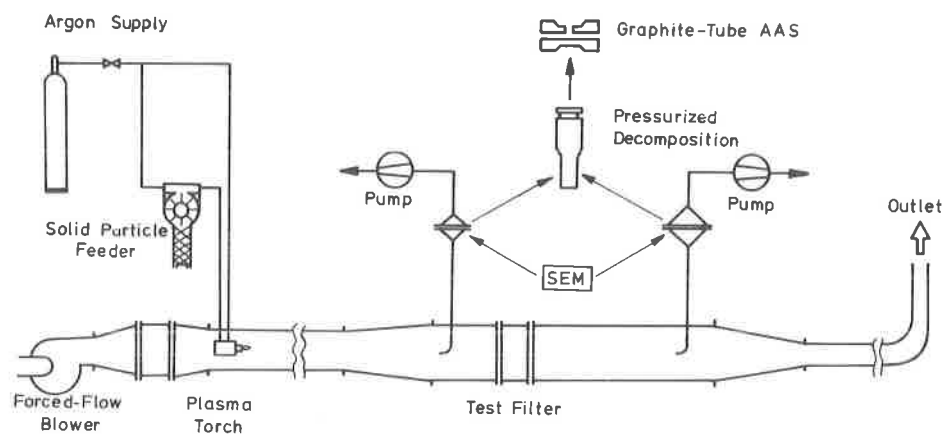
Fig. 12:   Schematic of the plasma-aerosol filter-test method
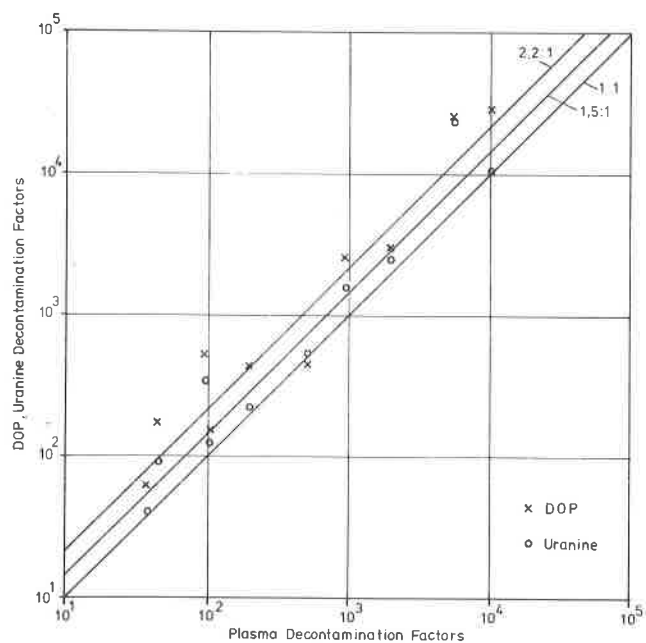
Fig. 13:   Comparison of plasma, DOP and
           uranine decontamination factors

DISCUSSION

<u>BERGMAN</u>:   Is it possible to increase particle size with the plasma aerosol generator?

<u>ENSINGER</u>:   I think it is possible, but we haven't studied it up to now.

<u>BERGMAN</u>:   The reason it would be advantageous is because the present aerosol size measures primarily the diffusional capture capability of the filter. A little bit larger size would, I think, be perfect.

<u>ENSINGER</u>:   We have some possibilities of changing the plasma arc characteristics; therefore, I think we can change the size of the particles.

LIMITS OF HEPA-FILTER APPLICATION UNDER HIGH-HUMIDITY CONDITIONS[+]

V. Rüdinger, C. I. Ricketts, J. G. Wilhelm
Laboratorium für Aerosolphysik und Filtertechnik
Kernforschungszentrum Karlsruhe GmbH
Postfach 3640, D-7500 Karlsruhe 1
Federal Republic of Germany

Abstract

As a result of a loss-of-coolant accident in a water-cooled nuclear reactor, the HEPA filters inside the air-cleaning systems can be exposed to high relative humidity, to condensing water vapor, and even to aerosols of liquid water. The data documented in the literature on the response of HEPA filters to such challenges was judged to be inconclusive and incomplete particularly with respect to filters preloaded with dust during service operation.

Therefore an experimental program was initiated using the test facility TAIFUN, equipped with instrumentation to accurately measure relative humidity. An optical system permitted observation and documentation of the response of the downstream side of the test filter during the tests, which lasted between 6 and 250 hrs.

The 21 filters tested at 50 $^{\circ}$C, constant volumetric air flow rate, and ambient pressure demonstrated that the differential pressure of new clean filters increased significantly only above 95 % r. h., rose up to 0.5 to 2 kPa at 100 % r. h. and reached values between 6 and 9 kPa during filtration of liquid-water aerosols. Extended challenge with liquid-water aerosols caused all new filters to fail structurally. The HEPA filters that were preloaded during prior service exhibited a considerably higher rate and extent of increase in differential pressure. Such filters had already failed under test at 100 % r. h.. The installation of a highly efficient mist eliminator did not prevent failure of the dust loaded filters. The modes and mechanisms of filter failure are discussed.

I. Introduction

The High Efficiency Particulate Air (HEPA) Filters installed in the air-cleaning systems of nuclear power facilities could in the case of an accident be exposed to operating conditions extremely different from those typical for normal operation. One such challenge is high air relative humidity that would result from a loss-of-coolant

---

[+] Work performed under the auspices of the Federal Ministry of the Interior under Contract No. SR 148/1

accident (LOCA). Additional adverse conditions of liquid-water aero-sols and vapor condensation are probable. The challenge of air at high relative humidity also should be taken into account for fires when protective water sprays would be operated.

Detrimental effects of moisture on HEPA filter performance have been long recognized /1,2/. Sensitivity of HEPA filters to moisture continues to be a problem. This is indicated by a recent HEPA filter field performance survey, which revealed that as many as 12 % of the filter elements considered had failed during normal operating condi-tions /3/. One of the most frequent causes of failure was observed to be exposure to high moisture environments. Improvement in filter moisture-resistance characteristics was cited as one of the most important development needs. In the interest of nuclear safety, it should be verified if current commercially available HEPA filters remain effective within the entire range of operating conditions that could be expected during accident situations.

II. Literature Review of Theory and Experiments

Incorporation of Water by the Filter Medium

The glass-fiber matrix of the filter medium represents the fil-tering component and therefore, a study of the interaction between humid air and HEPA filters focuses on the fiber medium. The first step of this interaction is the transfer of water from filtered air to filter medium. The incorporation of water by the medium can occur by any one of three phenomena: sorption /4,5/, condensation, or fil-tration of liquid-water aerosols, depending on the water content of the air.

Sorption. The general term sorption in reference to the inter-action of molecules of a gas with those of a solid or liquid, includes: the effects of physical adsorption and chemical adsorption if an accumulation on the surface takes place; absorption if the gaseous substance is incorporated into a liquid or solid substrate; and capillary condensation if condensation takes place in small diameter pores, due to surface-tension effects /6,7/.

The effects of chemical adsorption and absorption will not occur on an unloaded glass-fiber filter paper. From 0 % up to about 65 % r. h., only physical sorption of water vapor on the fibers' surface will take place. From relative humidities of about 65 % to 100 %, water will be incorporated via capillary condensation. Apart from material properties, the quantity of both phenomena is dependent primarily upon the proportion of the existing partial pressure to the saturation pressure. Since relative humidity is defined by the ratio of the partial and saturation pressures of the water-vapor, the quantity of water incorporated is a function of relative humidity. Therefore this quantity is used here from 0 % r. h. up to saturation, 100 % r.h., to define the extent of air humidity.

The quantity of water incorporated by physical adsorption is relatively low and in general it accounts for less than 1 % of the total weight of the media. At high relative humidity however, capillary condensation can result in moisture contents of an order of magnitude higher, e.g., 8 % at 97 % r.h. in the case of a slightly preloaded filter paper. With increasing relative humidity this value increases exponentially /5/.

During actual service a filter medium becomes loaded with an increasing amount of dust. With the particles deposited on the fibers, the surface available for physical adsorption also increases and, as a consequence, the quantity of water which will be adsorbed at a given relative humidity, increases. Depending on the properties of the dust material, chemical adsorption and absorption may also occur, so that the equilibrium water content would additionally be augmented. Above all, the system of capillaries is altered with growing dust accumulation in such a way, that capillary condensation can begin between the captured aerosol particles at as low as 50 % r.h. /8/. And a steep increase in the uptake of water can be observed beginning with 80 % r.h..

Condensation. In the special case of 100 % r.h. air saturated with water vapor is filtered. If the temperature gradient necessary to remove the heat of condensation exists, condensation will occur and will fill the voids of the filter-medium with water.

Part of the condensed water is held within the filter-fiber matrix by capillary forces. The excess amount will drain due to gravity, and the quantity of water incorporated into the filter medium will result from the equilibrium between condensation and drainage.

Mist filtration. With an increase in the water content of the air above that associated with 100 % r.h., the state of the air-water mixture is shifted into the fog region. The HEPA filter exposed to such conditions is challenged with both saturated air and a fine droplet aerosol of liquid water. In analogy to measurement of the dust content in air filtration processes with units of g/m^3, in this case the liquid moisture content as g liquid water per m^3 vapor-saturated air is used to quantify the moisture content.

Under such operating conditions the actual water content of the filter medium will be the amount needed to establish equilibrium between the quantity of liquid-water aerosol intercepted by the medium and the liquid drainage from the medium.

The Effects of Moisture Incorporation

A number of effects may result from the incorporation of water into the filter medium and from the exposure to moisture of the other construction materials of HEPA filters. Of these, increases in flow resistance and occurrences of filter structural failure have been most frequently reported. Such effects were investigated by different authors, primarily with respect to LOCAs /9-12/ and the use of water

sprays to protect filters during fires /13-15/. A few publications have used filter performance to measure the protective action of mist eliminators /16-19/. A number of these studies were summarized by Burchsted /20/.

Filter Medium. The removal efficiency represents the key performance criterion of any filter medium. In spite of the relevance of this characteristic, only Adams and his coworkers have tested different samples of commercially available filter media /21/. The authors have shown that penetration of a waterproof filter medium increases by a factor of 2.5 if relative humidity is increased from ambient to 100 %. In the case of nonwaterproof papers, penetration increases by approximately one order of magnitude. For a medium-efficiency glass-fiber medium, Hirling observed a 35 % increase in penetration as a result of simultaneous increases in the temperature, superficial velocity, and relative humidity of the test air /22/. Dorman /23/ cited an unpublished work of Balieu who reported an increase in penetration through glass-fiber papers at high humidity. However, an increase by a factor of two in adhesion forces between captured particles and glass-fibers were measured by Loeffler for an increase in relative humidity from 60 % to 80 % /24/.

A few authors have investigated the relationship between flow resistance of HEPA filter media and humidity of the filtered air. Jones /25/ recorded the variation of pressure drop with time at constant relative humidity of 100 % and constant air flow rate. At a temperature of 30 °C a slow increase in pressure drop up to approximately 5 times the initial value was observed with a new filter paper. Filter media with 7 and 48 month service time exhibited increases in differential pressure at a higher rate and to a greater extent.

This type of experiment provides information on the kinetics of the incorporation of water into the fiber matrix. At a test temperature of 60 °C Peters /16/ observed a rather slow process. One comparison test at 90 °C suggests that the rate of sorption of water vapor is strongly increased with temperature.

Treatment of the glass fibers with silicone water-proofing compounds reduces the rate and the extent of the increase in flow resistance caused by humid air flows. This improvement however is more or less compromised by dust accumulation and can be severely degraded by gamma-irradiation doses on the order of 10^7 rad /25/. It is of considerable importance, that the tensile strength of the filter paper can be reduced by as much as 40 % when wet /26/.

Full Size HEPA Filters. For the investigation of full-size HEPA filters a relatively expensive test facility is required to precisely control the relevant test parameters, i.e., air flow, temperature, and relative humidity or liquid-moisture content. The difficulty to fulfil this requirement seems to be one reason why the response of full-scale filter units to the challenge of high moisture has been tested to a very limited extent. Particularly for preloaded filters, only a small number of tests have been carried

out by four authors /4,14,16,19/. It is noteworthy that in many cases of such testing, relative humidity or liquid-moisture content were not precisely determined.

With respect to filtration efficiency of full-size HEPA-filters no data were found in the literature for tests during continuous exposure of filters to high humidity. DOP tests with dry air, performed intermittently for filters with wet medium, during qualification tests which involved high humidity and water spray, generally showed an overall increase in penetration /27/. Dennis found increasing penetration with increasing humidity for medium-efficiency polyurethane foam filters /28/.

In agreement with the results obtained with samples of filter paper, the full-scale filter units also have been shown to exhibit an increase in flow resistance with increasing humidity. Hoffmann /4/ measured equilibrium values and found that a noticeable rise in pressure drop of a clean filter unit only occurred at 85 % r.h.. In the case of a filter unit only slightly loaded with dust, the increase in flow resistance began at lower relative humidity and reached a higher value. Other data refer to experiments with time-dependent pressure drops primarily with constant test-air moisture content /9,11,12,15,16,29/. These data vary between some Pa at constant air flow and several kPa with greatly reduced flow rate. The influence of dust loading and treatment to improve water repellency, that was observed with samples of filter medium, has been quantitatively confirmed with full scale filter elements /16/.

A number of authors /2,9,10,11,15,16,30,31/ have reported on filter failures as a result of challenges with high-moisture air flows. Such failures are accompanied by loss in filtration efficiency, so that proper fission-product confinement is no longer guaranteed. For seven filters, for which the values were known, the differential pressures at structural failure ranged from 0.6 to 2.5 kPa. Whereas Peters /16/ and Durant /31/ found that filter structural failure occurs after a short time of high humidity operation at low differential pressures; slightly preloaded filters tested by Domning /14/ under fog conditions remained undamaged.

Besides ruptures of the filter paper, the exposure of filters to air with a high moisture content may also lead to deterioration of, e.g., the frame or of the adhesive between frame and pack. From the point of view of the investigations reported on here, these effects are of minor importance since they can easily be avoided by proper selection of construction materials.

Protective Action of Moisture Separators

In view of the sensitivity of HEPA filters to high humidities, especially to fog conditions, the effectiveness of mist eliminators as a means of protection has been tested /16-19/. Special emphasis was placed on the collection efficiency of droplets in the size range between 1 and 10 µm. Mist-eliminator performance was primarily evaluated on the basis of the response of a HEPA filter installed

downstream of the separator under test.

For the four test programs reported on in the literature, a total of 24 clean and slightly preloaded filters from at most four HEPA-filter manufacturers were tested. Of these, none of the 8 preloaded filters /16,19/ had been loaded to a $\Delta P > 350$ Pa at design flow rate and 7, actually had pretest ΔP values < 270 Pa. The tests of the other authors /17,18/ included only new filter units.

Conclusions

The survey of the existing literature on the response of HEPA filters to high air humidities revealed that test data for filters in general are not complete, and for loaded filter units in particular, are very limited. Furthermore, information on the increase in flow resistance due to loading with liquid water, and differential pressure at structural failure are not conclusive or complete. This could possibly be attributed to the sometimes limited accuracy of the instrumentation used to measure relative humidity.

Systematic investigations into the influence of relevant air-stream and filter-medium parameters, or into filter-structural failure modes and mechanisms have not been carried out.

Existing knowledge does not permit reliable and precise prediction of HEPA-filter response to various accident situations which involve high air humidities. To fill the need for additional information a filter-test program has been started, and what follows is a documentation of the experiments performed and some of the results obtained as of this time.

III. Experimental

Test Facility TAIFUN

For the investigation of HEPA-filter response to lengthy exposures to moist air, the test facility TAIFUN /32/ was used. It is a closed-loop facility that allows precise control of the relative humidity up to 151 °C. With a spray system, fog conditions can also be simulated. A schematic of the test facility is shown in Fig. 1. The key component is the cylindrical test section, 10 m long and 1 m in diameter. It is designed to accommodate up to six air-cleaning components with respective cross sections of 610 x 610 mm. The auxiliary equipment: heaters, cooler, steam injector, dew point cooler, and two-stage radial blower guarantee precise control of the relative humidity, absolute pressure, and temperature of the test air at flow rates between 400 and 2000 m³/h . The blower is speed controlled in order to maintain the air flow at a set value.

Instrumentation for Humidity Tests

In addition to the measurement and automatic control equipment provided for operation, the facility is equipped with special instrumentation for the humidity tests. This includes accurate temperature sensors and two different models of continuous-output, aspirated, wet and dry bulb psychrometers equipped with aged and calibrated 4-wire platinum resistance thermometers. Relative humidity can be measured with an uncertainty of ± 0.5 % r.h.. Differential pressure across the test filter is measured with variable-capacitance pressure transducers and continuously recorded together with relative humidity. Recently an instrument to determine the liquid-moisture content of the test air was installed but was not used with the tests reported on here.

In order to detect the time and differential pressure at structural failure, an optical system was developed that allows the observation of the downstream side of the filter under test. A schematic of the system is shown in Fig. 2. It consists of an endoscope, to which is mounted the camera of a video recorder system for continuous observation and registration. For precise documentation of the filter during the test, an automatically controlled SLR camera takes photos at regular programmable intervals of 1-60 min.

Filters and Mist Eliminator Tested

All filters tested were of the standard size of 610x610x292 mm and rated at air flows ranging from 1700 to 2000 m^3/h. Included were new clean commercially-available filter units, commercial filters that had been preloaded with dust during service in the exhaust-air filter system of the laboratory building, and prototypical HEPA filters equipped with a polycarbonate micro-fiber medium.

Two tests were performed with a highly-efficient droplet separator and a HEPA filter mounted 1.5 m downstream. The mist eliminator was designed for 1700 m^3/h. It had a cross section of 550x550 mm and was operated at a face velocity of 1.6 m/s. The water mist was intercepted by a fiber mesh with fiber diameters diminishing from the upstream to the downstream side. The removal efficiency for droplets of 1 μm diameter was 50 %. The collection efficiency as a function of the droplet diameters is shown in Fig. 3.

Experimental Procedure

All tests were performed at 50 $^{\circ}$C and a 1700 m^3/h air flow rate. During the test the relative humidity was increased in steps up to 100 % r.h.. Usually a given value of humidity was maintained until the differential pressure across the test filter had stabilized. This was taken to be an indication that the incorporation of water into the medium had reached an equilibrium condition. Exposure to water-saturated air was performed during extended

periods of time in order to investigate the long-term stability of the filters. To simulate conditions of condensing humidity the spray system, fed with deionized water, was operated at test's end. Droplet size was on the order of 5 μm. The liquid-water content was 40 g per m^3 of water-saturated air. Test duration times ranged from several hours up to more than 200 hours.

The variation of humidity and differential pressure across the filter was recorded on a paper chart recorder. In most cases the downstream side of the test filter was continuously monitored and photographed at set time intervals.

After completion of a test, the filter was inspected visually and in those cases where no dammage had occurred, the filtration efficiency was measured with 0.7 μm diameter DOP aerosol.

IV. Results and Discussion

Pressure Drop at Design Volumetric Flow Rate

Unloaded HEPA Filters. An example of the variation of relative humidity with time and the resultant pressure drop of a typical test with a new, clean HEPA filter is shown in Fig. 4. In this case flow resistance remains unaffected up to high values of relative humidity. Only at 98 % r.h. did a 25 % increase in Δp occur. Equilibrium was reached within roughly one hour.

When the air is saturated with water vapor, the differential pressure across the filter increases until, after about 75 h, a relatively stable value of 1 kPa is reached. Tests with other clean filters showed the same results. In some cases during the first phase of operation at 100 % r.h., the rates of increase in differential pressure and final equilibrium values were somewhat higher.

The spray symbol on the abscissa marks the start of the challenge of the filters with water mist. Test-air flow with a liquid-moisture content of 40 g/m^3 caused an increase in differential pressure at an approx. rate of 3 kPa/h. As a consequence of the mechanical load, resulting from the increased differential pressure, the filter failed structurally at 3.3 kPa.

All together 16 new, clean HEPA filters were tested under continuous exposure to moist air. Based on the results obtained, a correlation between filter pressure drop at rated flow and air-flow humidity, as well as liquid moisture content can be illustrated as shown in Fig. 5. The diagram indicates that the differential pressures at 1700 m^3/h fall within a band which broadens with increasing humidity. Up to about 90 % r.h. no significant increase in differential pressure can be observed. Beyond 95 % r.h. the differential pressure rises steeply up to values between 0.5 and 2 kPa. In the case of water-mist filtration at air flows with liquid water contents of 40 g/m^3, differential pressures in the range from 6.3 to 9.0 kPa were obtained. The three additional data points refer to tests of filters that had the polycarbonate microfiber

medium. In these tests no filter failures occurred and these data points can be considered to be equilibrium values. Equilibrium between water-incorporation and drainage rates however, is not fully assured for the two other filters, due to earlier structural failures.

The increase in filter pressure drop with increasing relative humidities up to 100 % is qualitatively consistent with theory and the few data published by Hofmann /4/. Comparison shows that the significant increase in flow resistance began at approx. 85 % r.h. for the results of Hofmann, i.e., a value of 5 % r.h. less than that for the tests reported here. Due to the lack of quantitative data in the literature for tests which involved liquid moisture content in the air flows, comparison with the literature is not possible.

Preloaded HEPA Filters. Seven commercially available HEPA filters that had been utilized in the exhaust air system of the laboratory building were included in the test program. As a result, these filters were preloaded with ambient room-air dust to between 0.7 and 1.3 kPa at 1700 m^3/h. The variation in relative humidity with time and the resultant filter pressure drop during a typical high humidity test is represented in Fig. 6.

In the first phase of all tests with filters preloaded with atmospheric dust, an unexpected decrease in the differential pressure was observed. This is illustrated in detail for this test with the aid of the magnified insert for the first six hours of the test. When the relative humidity was raised to 80 % , the pressure drop increased from 0.8 to 1.8 kPa within a few minutes and then fell to 0.30 kPa within several hours. Exposure of a preloaded filter to a relative humidity of 80 %, thus reduces the pressure drop to approximately the value of a new filter. This phenomenon is attributed to capillary condensation between the dust particles with subsequent contractive migration and final agglomeration of the dust particles, due to surface tension and other forces /33/. Preloaded medium-efficiency sampling filters, exposed to humid air flows, have been observed by Franklin and coworkers /34/ to also exhibit a decrease in differential pressure to a value close to that of the clean filter.

This effect could conceivably be utilized to increase the dust holding capacity of HEPA filters, which find application only under conditions of low relative humidity. For, although the pressure drop has decreased almost to that of a new filter, the response of the particle loaded filter to high humidities remains much more sensitive than that of a clean filter. With the increase of relative humidity up to 93 % the pressure drop rose to 0.36 kPa. Further increase up to 99 % r.h. led to an almost stable differential pressure of 1.5 kPa. Due to a breakdown in one of the facility components, relative humidity decreased to 44 % and, as a result, the pressure drop subsequently fell to 0.30 kPa, i.e., the same value that was measured after the initial pressure drop. This strongly suggests that no additional irreversible effects of moisture on the dust deposited in the fiber medium had occurred as a result of the increase from 80 to 99 % r.h..

After restart of the humidification system and subsequent operation at 100 % r.h. the pressure drop steeply increased to approximately 5 kPa. As a consequence of the mechanical load applied to the filter pack by the relatively high differential pressure, the filter medium broke along the downstream ends of the folds. This structural failure is indicated by the descending steps in the trace of the pressure drop and was additionally observed with the monitoring system. With increasing structural damage the pressure drop fell finally to 2.4 kPa. Exposure to water mist at that stage of damage had only a minor effect on the pressure drop of the filter.

In Fig. 7 the results obtained with HEPA filters preloaded with dust are summarized. The shaded area illustrates that the initial pressure drop of filters preloaded with dust is a characteristic of an unstable condition that shifts to a stable state at a relative humidity of about 70 %. This stable configuration of dust deposited on the fiber matrix begins to incorporate a significant amount of water at about 80 % r.h.. The equilibrium values of pressure drop attained under operation at 100 % r.h. fall within a range from 1 to approx. 7 kPa. This scatter of values is probably due to differences in the amount of dust deposited on the filter paper. It could also possibly be in part attributed to fluctuations of air moisture contents into the range above 100 % r.h.. Since a technique to measure liquid-moisture content was then not yet available, this assumption could not be verified.

The results reported on here are in qualitative agreement with data in the literature with respect to the response of dust-preloaded HEPA-filter units to flows of moist air. Pressure-drop measurements here confirm the results of tests /16/ that demonstrated the higher sensitivity to humid air, of filter units preloaded with dust, as compared to clean units. However, due to the lack of measured values of relative humidity in previously reported work, quantitative comparisons can not be made.

Protective Action of a High-Efficiency Mist Eliminator. From the investigations of different authors it can be concluded /16-19/ that with the installation of a highly-efficient mist eliminator at least clean HEPA filter units can be protected from the detrimental effects of high moisture. However, since only a total of 8 slightly preloaded filters were previously reported as having been tested, the data available in the literature cannot be applied for filters loaded with dust at the end of service time.

To evaluate the protection offered by a mist eliminator, two tests were performed with a highly-efficient mist eliminator located 1.5 m upstream of the HEPA filter under test. One test involved a new filter, and the other test a filter loaded with room-air dust.

In Fig. 8 the pressure drop as a function of time is represented for the test with the clean filter. Within the first phase covering 42 h the spray system was operated to achieve a liquid-moisture content of 40 g/m^3 in the air flow upstream of the mist

eliminator. Pressure drop of the filter increased up to only 0.5 kPa, not enough to endanger the filter. When the test was continued after removal of the mist eliminator, the pressure drop increased immediately and thereby caused the filter to fail. This test demonstrated that the new HEPA filter was protected by the mist eliminator during the test time of 44 h. This result is consistent with the data published by other athors /16-19/.

The record of the pressure drop curve of the test with a HEPA filter preloaded with room-air dust up to 1.3 kPa at design flow rate is represented in Fig.9. During the first few hours of the test, as the relative humidity was increased up to 100 %, the initial increase and subsequent decrease in pressure drop occurred, which is typical for these humidity tests of preloaded filters. The operation of the spray system in air of 100 % r.h. has no significant effect on pressure drop. It can be assumed that water mist is completely removed, and the filter is therefore challenged only by saturated air. However, the mist eliminator was not able to prevent two folds of the filter pack from rupturing. The best a mist eliminator can achieve at saturated conditions is to reduce the liquid-water content to zero, which corresponds to 100 % r.h..

Figure 7 demonstrated that for filters preloaded with room-air dust and exposed to design flow rates of saturated air, resultant differential pressures, high enough to cause filter structural failure , can be expected. And the pressure-drop data obtained both with and without the presence of a mist eliminator suggests that even highly-efficient mist eliminators are not able to fully protect HEPA filters loaded with room-air dust from structural failure due to exposure to high air humidity.

V. HEPA-Filter Structural Failure and Physical Deterioration

Failure Differential Pressure. In order to prevent significant releases of particulate radioactivity into the environment during an accident situation, the structural integrity of the HEPA filters must be guaranteed. For this reason, the structural limits at high air humidity were also determined and the failure modes were investigated. Summarized in Table I are the differential pressures at structural failure for the commercially-available filter elements tested.

The metal-frame, VM-type filter exhibited the lowest average structural limit, 2.5 kPa. This filter type had also been tested under high differential pressure at ambient air conditions /35/ and the corresponding limit was found to have been 7 kPa, i.e., about 3 times that determined during exposure to high-humidity conditions.

The other clean filters had a frame of either plywood or of wood particle board. The filter pack was fixed inside the frame with an elastomeric adhesive/sealant. The DN-type filters broke at an average differential pressure of 7.6 kPa, whereas the AP-type filters failed at 4.7 kPa on the average. The respective values from the low-humidity tests are 22.5 kPa /35: Table I/ and 17.7 kPa /33/.

Table I: Structural limits of commercially available 610x610x292 mm HEPA filters tested under high-humidity or fog conditions (t=50 ^{O}C, $\dot{V}$= 1700 m^3/h).

Test Filter			Exposure Time		Failure Diff.
No.	Frame Material	Test Condition	100 % r.h. (h)	Fog (h)	Pressure (kPa)
VM1	Metal	Clean	69	1.5	3.3
VM2	"	"	0	6	2.1
VM3	"	"	24	0	1.7
DN1	Ply-wood	Clean	43	5	9.0
DN2		"	74	3	6.3
AP1	Wood-particle	Clean	62	0	2.6
AP4		"	0	5	4.8
AP7		"	45	4.5	5.9
AP8	board	"			
CN1	Ply-wood	Dust-loaded	16	0	5.1
AN1	Ply-wood	Dust-loaded	–	1	6.3
AN2			–	2	4.4
AN3	"	"	17	0	5.2
AN4	"	"	25	0	4.1
AN5	"	"	25	0	5.4

In these cases the respective average structural limits after pro-longed exposure to moist air are lower, by factors of 3 and approx. 4, than those measured during tests with dry air.

The filter types CN and AN, were loaded with room-air dust up to a pressure drop of 1.05 kPa at   design flow rate. Some of these filters failed structurally after exposure to only water-saturated air. The differential pressures at failure for these filters are relatively low, as are those of the unloaded filters.

An indication of the influence of dust loading on structural limit can be obtained when the test results of the clean AP-type filters are compared with those of the preloaded AN-type filters. The filters of both groups had been procured from the same manu-facturer and the only difference between them was the frame mate-rial. Because only the filter pack had failed, test results of both types can be directly compared with each other.

The average differential pressure at failure of the clean AP-type filters was calculated to be 4.7 kPa with a standard devia-

tion of 1.3. Since the respective values of the dust-loaded AN-type filters are 5.0 kPa and 0.7, there seems to be no significant influence of dust loading on the structural limits.

The main difference is that failures of clean filters occurred only during mist filtration, whereas four out of six preloaded filters failed when tested only under saturated-air conditions. Hence, dust loading does not influence filter structural strength but endangers filter integrity by promoting incorporation of water into the medium, thus leading to those differential pressures high enough to cause filter structural failure.

The influence of the exposure time as related to possible leaching of the waterproofing agents can be evaluated with the data in Table I. However, with the filters tested so far no such influence, mentioned, e.g., by Peters /16/ has been noted.

Some prototypical HEPA filters with polycarbonate microfiber medium were also included within the test program. Moisture-induced increases in differential pressure as a function of exposure time were the same as those for filters with glass-fiber media. In contrast however , none of the prototypical filters failed. The test results are summarized in Table II where the maximum differential pressure attained during the individual test runs is indicated in the last column.

Table II: Maximum differential pressures attained by 610x610x292 mm prototypical HEPA filters with polycarbonate microfiber media tested under high-humidity and fog conditions (t=50 $^{\circ}$C; $\dot{V}$=1700 m^3/h).

	Test Filter		Exposure Time		Maximum
No.	Frame Material	Test Condition	100 % r.h. (h)	Fog (h)	Differential Pressure (kPa)
E 1	Plywood	ASHRAE dust	73	1.3	7.6
E 3	"	clean	96	20	7.6
E 5	"	"	66	7	8.0
E 9	"	"	24	65	7.1

Modes of Filter Physical Deterioration and Structural Failure.
Three primary types of filter deteriorations and failures were
noted upon completion of the humidity tests. The frames of some fil-
ters, particularly those made from wood particle board, had swollen
and warped. In other instances the elastomeric adhesive/sealant,
used to fix the pack of filter medium and separators within the
frame, had become partially detached from the frame. These observa-
tions indicate that the materials selected for the construction of
the HEPA filters are not always appropriate for operation under
moist-air conditions.

Another important result relates to the filter pack. It was
observed after the humidity tests that the tightness of the pleated
filter packs had significantly decreased. Photographs of the up-
stream sides of two preloaded filter units show this effect in Figs.
10 and 11. Clearly to be recognized on the left side in Fig. 10
and on the right side in Fig. 11 are gaps of approximately 10 mm
width. This is of particular interest because it probably facili-
tates the breaks in the filter folds. The causes responsible for
this effect, need to be carefully investigated before more than a
general hypothesis can be made.

The most important effect of prolonged exposure of filters to
high humidities however, is filter structural failure since this
results directly in the loss of high filtration efficiency.

The typical failure mode of the VM-type filter with a metal
frame is demonstrated in Fig. 12. Due to the mechanical load devel-
oped by the differential pressure, the filter pack was partially
pushed out of the frame. With this particular design in which no
adhesive/sealant is used, the pack is only held within the frame by
friction forces. As a consequence of the exposure to high humidity,
tightness of the pack decreased, the friction forces were reduced,
and thus structural failure occurred at an average differential
pressure of 2.5 kPa.

A failure mode which is typical for those filter units where
the filter pack is satisfactorily fixed within the frame, is shown
in Figs. 13-17. The black spots and stripes in the filter pack
visible in Fig. 13 are due to ruptures in the downstream folds of
the medium. The filter units shown in Figs. 14 and 15 had suffered
the same type of damage during the humidity test. Breaks in the
folds have also occurred for the filters shown in Figs. 16 and 17.
In addition to the rupture of the medium folds, a series of folds
were also sheared horizontally at the bottom of the pack just above
the level to which the adhesive/sealant had been applied to the
filter medium during manufacture.

The rupture of downstream ends of the filter-medium folds
represents the most frequent failure mode as has also been shown in
investigations into the response of HEPA filters to high air velo-
cities and high differential pressures /35/. The breaks probably
occur when the tensile stress in the circumferential direction
exceeds the tensile strength of the filter medium. Fig. 18 shows
the tensile stresses in a downstream fold of the filter medium.

1071

The critical stress is that in the circumferential direction, σ_C, given by:

$$\sigma_C = \Delta p \, \frac{r}{d} , \qquad (1)$$

where Δp is the static differential pressure, r the radius of the fold, and d the thickness of the filter medium. This model explains why the tensile strength of the filter medium is of importance with respect to the structural integrity of the filter pack /36/.

For the DIN norm the tensile strength of glass-fiber medium is usually measured and expressed in terms of the force necessary to rupture a sample strip 5 cm wide. For a new unfolded filter medium a normal value is approximately 50 N. The tensile strength of a glass-fiber medium is less when in a wet condition /37/, less after having been folded, and also less after exposure to humid air flow.

Samples of media were taken from both a new untested filter unit and a clean humidity-tested unit, and the respective values of tensile strength were measured in accordance with DIN 53 857 section B. The results together with the respective standard deviations are listed in Table III.

Table III: Tensile strength of two clean HEPA-filter media, measured dry and wet, with different pretest histories. All samples were taken in the machine direction and tested in accordance with DIN 53 857 Part B.

Filter Type	Pretest History	Tensile Strength/Standard Deviation dry (N/5 cm)		wet (N/5 cm)	
CN	new, unfolded	56.7	2.4	14.8	1.0
	new, folded	29.5	3.9	11.8	1.3
AP 4	humidity-tested, unfolded	20.8	6.4	26.4	5.2
	humidity-tested, folded	6.8	2.7	5.9	1.0

The results obtained show that the tensile strength of new filter paper is reduced by a factor of two due to folding during manufacturing and by a factor of four due to the combination of folding and humidity exposure. Since the weaker areas of the filter paper would be most susceptible to breakage, values somewhat lower than the calculated averages should be considered to be realistic.

In order to check the filter-failure model of Fig. 18 and Eq. 1, the tensile strength of the medium from filter unit AP 4 can

be compared with the stress existing when the first failure occurred. The average tensile strength in the wet condition of 5.9 N/5 cm is reduced by two times the standard deviation in order to estimate the strength at the weakest point of the filter folds, which hence is assumed to be 3.9 N/5 cm. During the humidity test, the filter AP 4 failed at a differential pressure of 4.8 kPa. This failure pressure corresponds to the assumed tensile strength of the paper, if at failure, the radius of the broken fold had been 16 mm. Due to the decrease in tightness of the filter pack this figure is reasonable and therefore lends credence to the proposed model of this failure mechanism.

V. Conclusions

Based on the results reported on here, the most important conclusion is, that HEPA filters preloaded with room-air dust remain endangered by exposure to high humidities even when protected by an upstream high-efficiency mist eliminator.

Prior to any broad generalizations of the results obtained, further tests with different types of filters need to be performed.

The literature survey has revealed that the knowledge in this field is not yet complete or conclusive. In addition to the tests described above, more investigations are needed in order to more precisely establish the relationship between filter pressure drop and high air-stream humidity at constant flow rate, and also to better determine both the kinetics of water incorporation into the filter medium as well as the influence of temperature on the kinetics and the equilibria of water incorporation.

Finally, the failure mechanisms need to be further studied in order to develop HEPA filters with strength sufficient to withstand the effects of exposure to moist air streams.

Acknowledgements

References

/1/   Sapple, C.E.; "Deep Bed Sand and Glass-Fiber Filters";
        WASH 149 (1952) p. 99 ff.

/2/   Palmer, J.H.; "Moisture and Burning Tests of Space Filters";
        TID 7551 (1957) p. 53 ff.

/3/   Carbaugh, E,H.; "A Survey of HEPA-Filter Experience";
        CONF 820833 (1983) p. 790 ff.

/4/   Hofmann, W.M.; "Druckverlust feuchter Schwebstoffilter"; Zeit-
        schrift fuer Heizung, Lueftung, Klimatechnik und Haustechnik
        (HLH) 25 (11) (1974) p. 370.

/5/   Hofmann,W.M.; "Feuchtigkeitsaufnahme von Schwebstoffiltern";
        (HLH) 25 (3) (1974) pp. 77-78.

/6/   Krischner, O. and Kast, W.; "Die wissenschaftlichen Grundlagen
        der Trocknungstechnik"; 3. Auflage, 1. Band; Springer-Verlag,
        Berlin·Heidelberg·New York, 1978, pp. 44-67.

/7/   Lueck, W.; "Feuchtigkeit: Grundlagen · Messen · Regeln";
        R. Oldenbourg, Muenchen·Wien, 1964, pp. 44-59.

/8/   Tierney, G.P. and Conner, W.D.; "Hydroscopic Effects on Weight
        Determinations of Particulates Collected on Glass-Fiber
        Filters"; American Industrial Hygiene Association Journal
        (Aug. 1967) pp. 363-365.

/9/   Hays, J.B.; " Performance of High Efficiency Particulate Air
        Filters Subjected to Steam/Air Mixtures"; TID-7627 (1961)
        p. 549 ff.

/10/   Gunn, C.A. and Eaton, D.M.; "HEPA Filter Performance Study";
        CONF-760822 (1977) p. 630 ff.

/11/   Stratmann, J.; "Bericht eines Grossverbrauchers von Schweb-
        stoffiltern Klasse S"; Proc. Seminar on High Efficiency Aerosol
        Filtration; Comm. European Community,Luxembourg (1977)p.411 ff.

/12/   Nitteberg, L.J. and Smith, R.K.; "Humidity Test Report NPR
        High-Efficiency Filter Bid Evaluation"; TID-7677 (1963)p. 572 ff.

/13/   Gaskill, J.R. and Murrow, J.L.; "Fire Protection of HEPA Fil-
        ters by Using Water Sprays"; CONF-720823 (1973) p. 103 ff.

/14/   Domning, W.E.; "Water Spray Heat Exchangers for HEPA Protection
        in Accidents (Heat Removal Requirements and the Effect of
        Smoke and Water on HEPA Filters)"; CONF-720823 (1973) p. 755 ff

/15/ Murrow, J.; "Plugging of High Efficiency Filters by Water
Spray"; USAEC Report UCRL-50923, Lawrence Radiation Labora-
tory, Livermore CA, NTIS 1970.

/16/ Peters, A.H.; "Application of Moisture Separators and Parti-
cualte Filters in Reactor Containment"; USAEC DP-812,
Savannah River Laboratory, 1962.

/17/ Rivers, R.D. and Trinkle, J.L.; " Moisture Separator Study";
USAEC NYO-3250-6; American Air Filter Co., Inc., Louisville,
Ky., 1966.

/18/ Griwatz, G.H.; Friel, J.V. and Bicehouse, J.L.; "Entrainment
Moisture Separators for Fine (1-10µ) Water-Air-Steam Service:
Their Performance, Development, and Status"; MSAR 71-45;
MSA Research Corp., Evans City, PA, 1971.

/19/ First, M.W. and Leith, D.H.; "ACS Entrainment Separator Per-
formance for Small Droplet-Air-Steam Service"; Harvard Air
Cleaning Laboratory Report 75-1106, Harvard University School
of Public Health, 1975.

/20/ Burchsted, C.A.; Fuller, A.B. and Kahn, J.E.; "Nuclear Air
Cleaning Handbook"; ORNL, Oak Ridge, TN, ERDA 76-21, 1976.

/21/ Adams, R.E. et al.; "Filtration of Stainless Steel-UO_2 Aero-
sols"; pp. 133-148 in Nuclear Safety Program Ann. Progr. Rept.
Dec. 31, 1967, USAEC Report ORNL-4228, Oak Ridge National
Laboratory, p. 137.

/22/ Hirling, J. and Gaál, J.; "Comparisons of Some Particulate
Air Filter Testing Methods Used in Normal and Unfavourable
Conditions"; IAEA-SR-72/23; IAEA Seminar on Testing and Opera-
tion of Off-Gas Cleaning Systems at Nuclear Facilities,
Karlsruhe, Fed. Rep. of Germany, May 1982.

/23/ Dorman, R.G.; "A Comparison of the Methods Used in the Nuclear
Industry to Test High Efficiency Filters"; Comm. European
Community, Luxembourg, V/3603/81, 1981, p. 14.

/24/ Loeffler, F.; "Collection of Particles by Fiber Filters";
pp. 337-375 in "Air Pollution Control" Part I; Edited by
W. Strauss, Wiley-Interscience, New York·London·Sydney·Toronto;
1971, pp. 368 f.

/25/ Jones, L.R.; "Effects of Radiation on Reactor Confinement
System Materials"; CONF-720823 (1972) p. 655 ff.

/26/ Belvin, W.L. et al.; "Development of New Flouride-Resistant
HEPA-Filter Medium"; USERDA TID-26649, Savannah River Opera-
tions Office, 1975, pp. 55-57.

/27/ Burchsted, C.A.; "Environmental Properties and Installation Requirements of HEPA Filters"; in "Treatment of Airborne Radioactive Wastes"; IAEA STT/PUB 195, Vienna (1968), pp. 175-191.

/28/ Dennis, W.L.; "Effect of Humidity on the Efficiency of Particulate Air Filters"; Filtration and Separation 10 (1973), p. 149 f.

/29/ Fenton, D.L. and Dallman, J.J.; " HEPA-Filter Loading by Simulated Combustion Products"; Report submitted by New Mexico State University Mech. Engr. Dept. to Los Alamos National Laboratory, Sept. 1982.

/30/ McCormack, J.D. and Hilliard, R.K.; "Loading Capacity of Various Filters for Sodium Oxide/Hydroxide Aerosols"; CONF-780819 (1979), p. 1018 ff.

/31/ Durant, W.S.; "Performance of Airborne Activity Confinement Systems in Savannah River Plant Reactor Buildings"; CONF-660904 (1966), p. 348 ff.

/32/ Wilhelm, J.G. et al.; "Testing of Iodine-Filter Systems Under Normal and Post-Accident Conditions"; CONF-720823 (1972), p. 434 ff.

/33/ Ruedinger, V. and Ensinger, U.; "Studium des Verhaltens von Schwebstoffiltern unter Stoerfallbedingungen"; in "Projekt Nukleare Sicherheit", Jahresbericht 1982, Kernforschungszentrum Karlsruhe, Bericht 3350 (1983), pp. 4400-4415.

/34/ Franklin, H., Knutson, E.O. and Hinchliffe, L.E.; "A Humidity Effect in the Flow Resistance of Loaded Fibrous Filters"; Atmospheric Environment Vol. 10 (1976), p. 911 f.

/35/ Ruedinger, V. and Wilhelm, J.G.; "HEPA-Filter Response to High Air Flow Velocities"; CONF-820833 (1983), p.1069 f.

/36/ Ricketts, C.I.; "Tornado-Model Testing of HEPA Filters"; Masters Thesis New Mexico State University, Las Cruces, N.M. 1980 p. 93 f.

/37/ Schwalbe, H.C.; "Redevelopment of the Savannah River Laboratory Moisture Resistance Test for Filter Paper";CONF-680821 (1968), p. 86 ff.
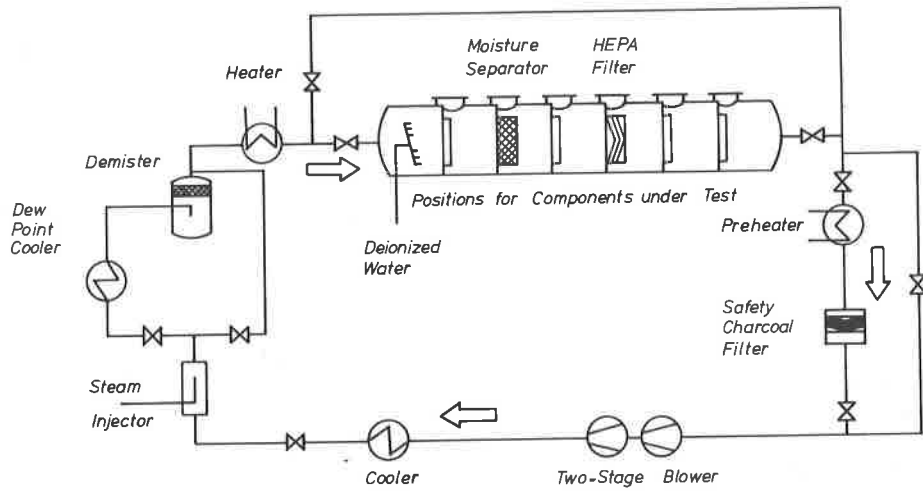
Fig. 1: Schematic of the test facility TAIFUN.
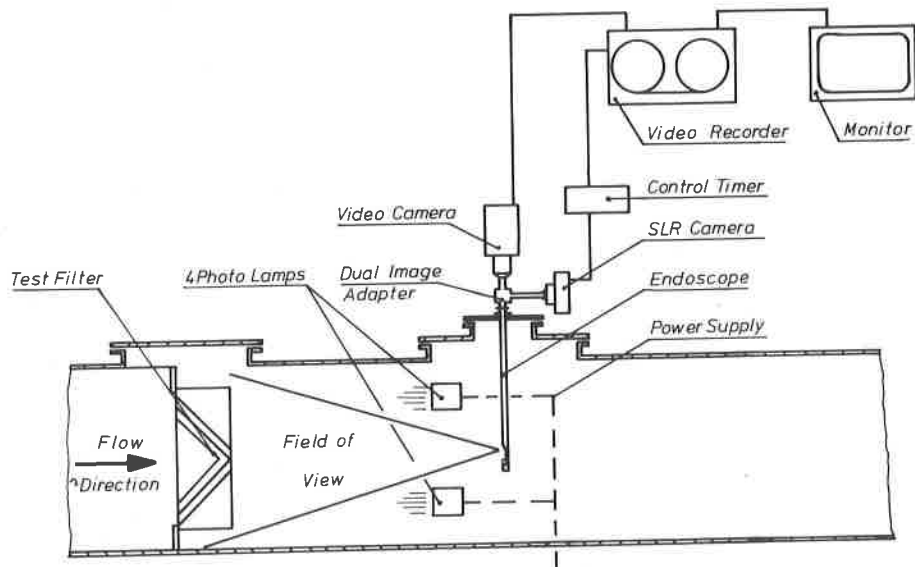
Fig. 2: Optical system for observation and recording
of the HEPA-filter downstream side during
humidity-exposure tests.
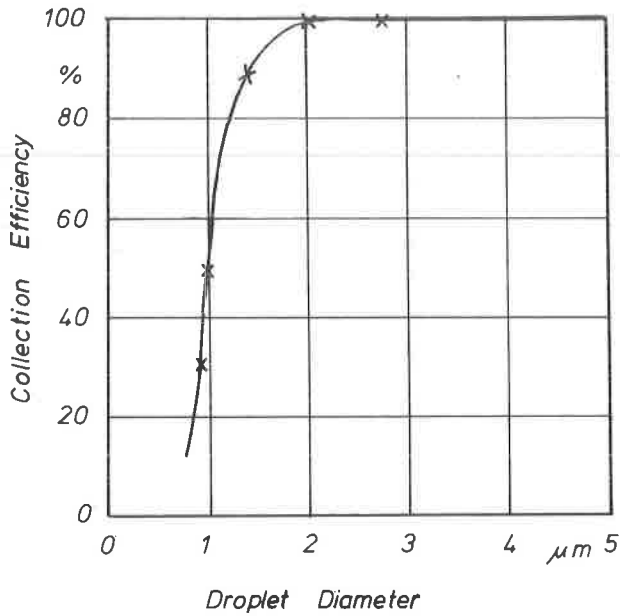
Fig. 3: Collection efficiency
of the mist eliminator
at 1.6 m/s facial air
velocity.
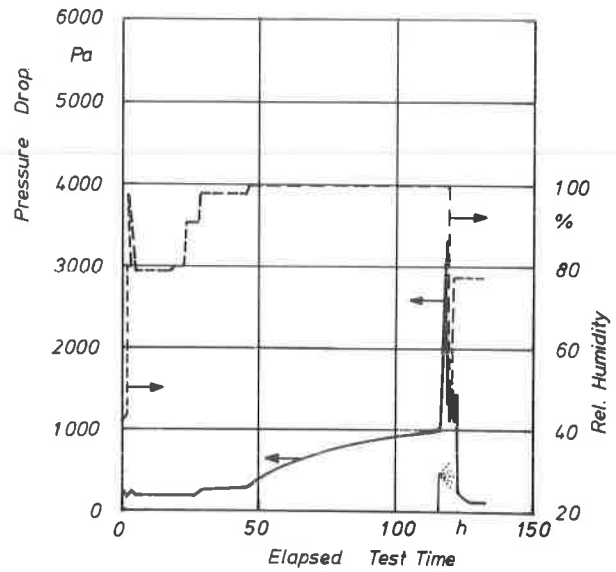
Fig. 4: Air-stream relative hu-
midity and resultant
pressure drop of a clean
HEPA filter as functions
of time (50 ^{O}C; 1700 m^3/h).

Fig. 5: Pressure drop of clean
HEPA filters as a function
of air-stream rel. humidity
and liq. moisture content
(50 ^{O}C; 1700 m^3/h).

Fig. 6: Air-stream relative humidity and resultant pressure drop of a HEPA filter preloaded with room-air dust as functions of time (50 °C; 1700 m³/h).

Fig. 7: Pressure drop of preloaded
HEPA filters as a function
of air-stream rel. humidity
and liq. moisture content
(50 °C; 1700 m³/h).

HEPA Filters Loaded with
Room-Air Aerosol
Glass-Fiber Medium
$\dot{V} = 1700\ m^3 h^{-1}$
$\vartheta = 50°C$

Pressure Drop (kPa)

Rel. Humidity (%)   Liq. Moisture Content (g m⁻³)
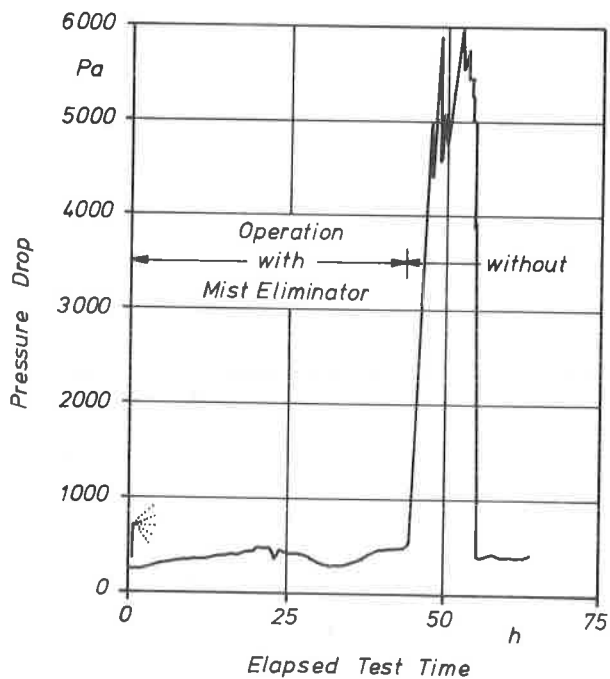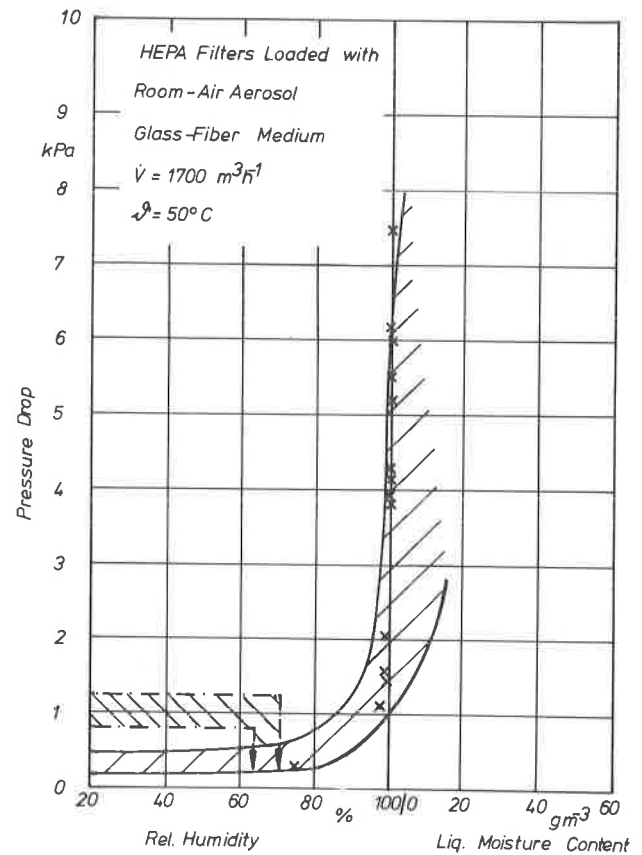
Fig. 8: Pressure drop of a clean
HEPA filter tested with
and without mist elimi-
nator (50 °C; 1700 m³/h).

Operation with Mist Eliminator — without

Pressure Drop (Pa)

Elapsed Test Time (h)
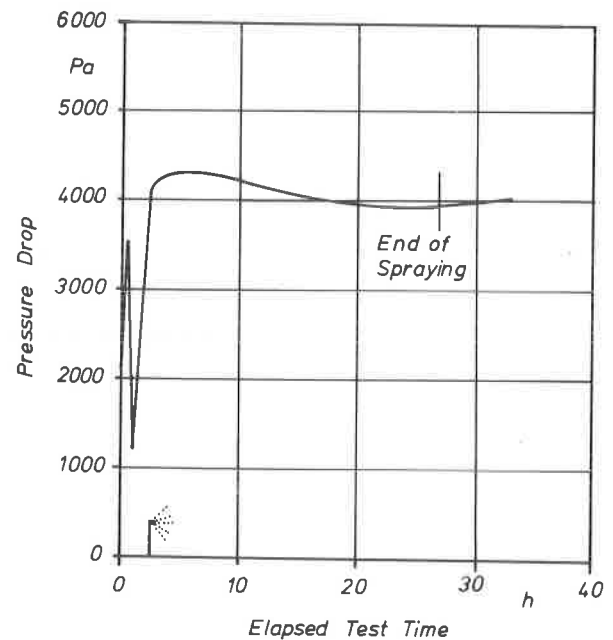
Fig. 9: Pressure drop of a HEPA
filter preloaded with
dust as tested with a
mist eliminator (50 °C;
1700 m³/h).

End of Spraying

Pressure Drop (Pa)

Elapsed Test Time (h)
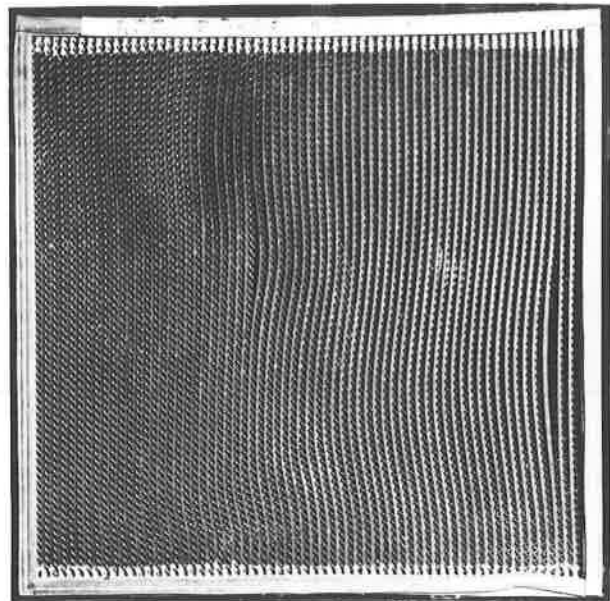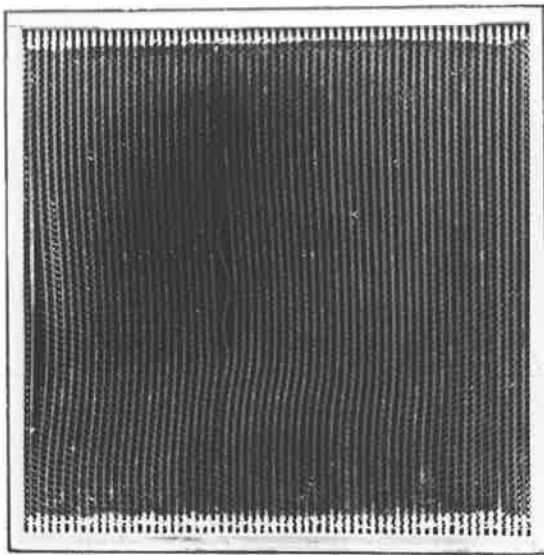
Figs. 10,11: Photos of the upstream side of preloaded HEPA filters after moisture exposure tests.
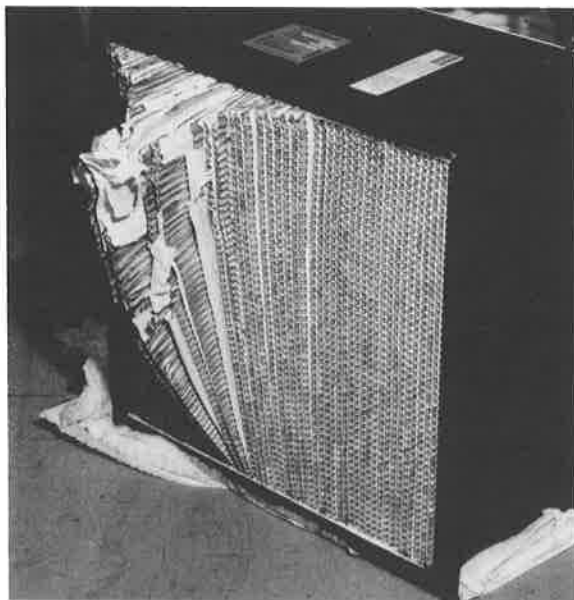
Fig. 12: Extensive structural damage to a metal-frame HEPA filter as a result of exposure to moisture.
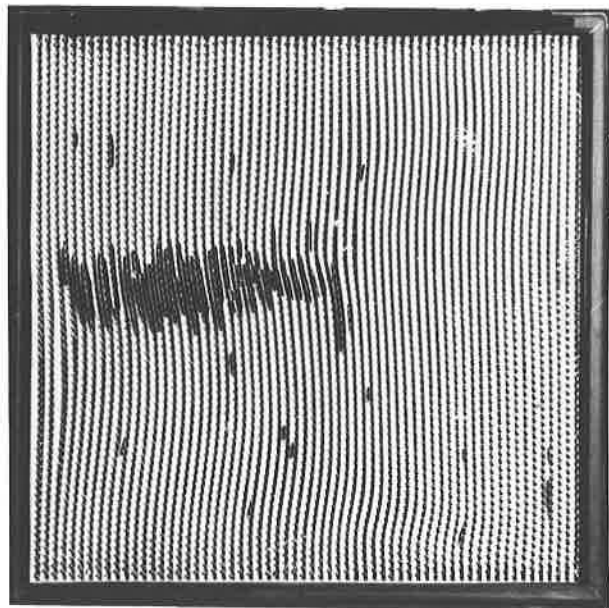
Fig. 13: Ruptured downstream folds and loosened pack of a HEPA filter as a result of exposure to moisture.
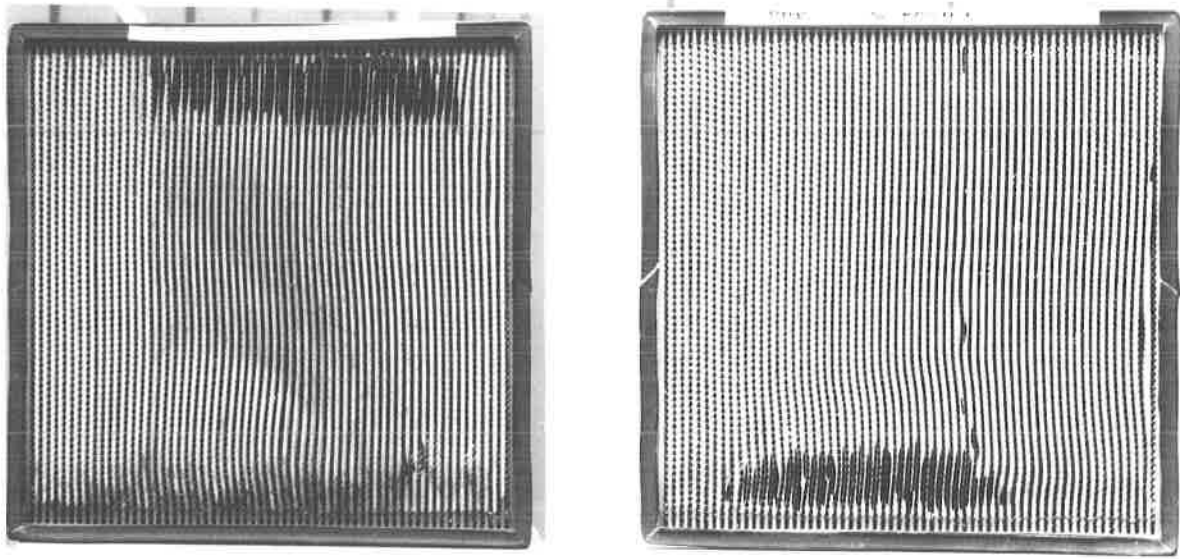
Figs. 14,15: Ruptured downstream folds of 610x610x292 mm HEPA filters as a result of exposure to moisture-laden air flow.
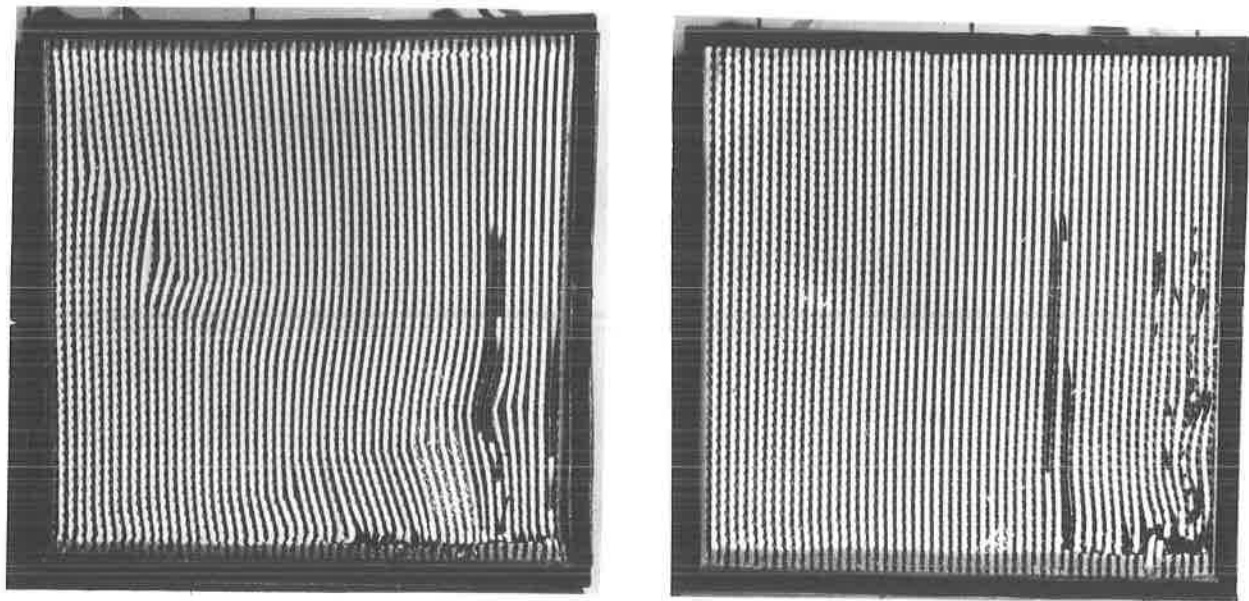
Figs. 16,17: Ruptured as well as sheared, downstream folds of 610x610x292 mm HEPA filters as a result of exposure to moisture-laden air flow.

$$\sigma_c \approx \frac{r \cdot \Delta p}{d}$$
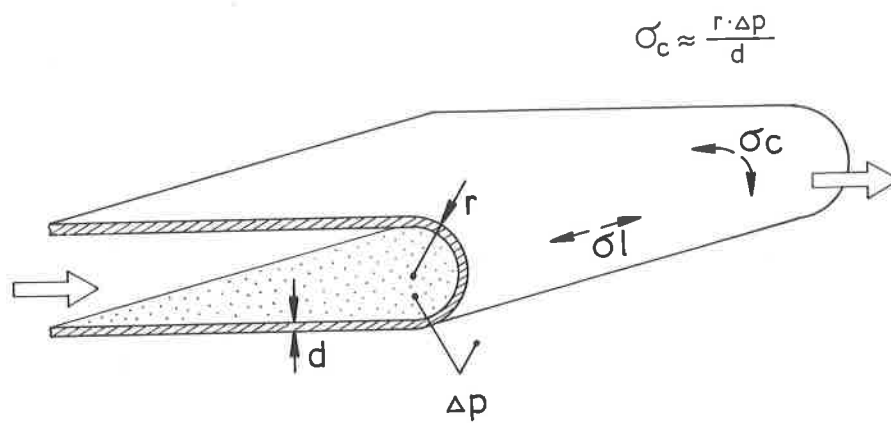
Fig. 18: Tensile stresses in a downstream fold of the filter medium.

DISCUSSION

PRATT: All our conventional filters suffered badly with exposure to high humidity, although they were manufactured with a water-repellent medium. Were your filters constructed from water repellent media?

RUDINGER: All our filters were made with a water-repellent medium.

PRATT: Could you tell us if they were mounted in the test facilities, such that any condensed water was able to drain off?

RUDINGER: The filters were installed in a vertical position so the water could drain off along the ends of the folds.

GILBERT: I am wondering if any of the filters were pre-conditioned with high humidity and at an elevated temperature for 24 hours before you even loaded them or tested them.

RUDINGER: The second part I can answer immediately. The filters were not artifically preloaded. We took the filters from the exhaust air system of our laboratory building. They had been in operation there and, after they were loaded, they were exchanged. We collected them and used them within our test program. For the second question, I am not familiar with this detail of your test procedures. What do you mean by conditioning at higher temperatures?

GILBERT: Ninety five degrees F and 95% relative humidity.

RUDINGER: We mounted the filters inside our test facility and then set the temperature control at 50°C. After it reached that value we increased relative humidity step-wise, starting with 40%, then to 60%, to 80%, and, finally, close to 100%.

DEVELOPMENT OF A HEPA-FILTER WITH HIGH STRUCTURAL STRENGTH
AND HIGH RESISTANCE TO THE EFFECTS OF HUMIDITY AND
ACID

W. Alken*, H. Bella*, V. Rüdinger**, J.G. Wilhelm**

*   Carl Freudenberg, Sparte Vliesstoffe Viledon, Weinheim, F. R. of Germany
** Laboratorium für Aerosolphysik und Filtertechnik, Kernforschungszentrum
     Karlsruhe GmbH, Fed. Rep. of Germany

Abstract

HEPA-filters may be subject to considerable stresses during operation
in nuclear installations, particularly in the case of an accident. The state
of the art of filter media technology presently allows the utilization of
only glass-fiber filter paper in manufacture of HEPA-filters.

This report describes a newly-developed filter medium made of synthetic
micro-fiber nonwoven material, including the production process, the filtra-
tion and the material characteristics, in particular with respect to the
resistance to hydrofluoric acid and high moisture.

The HEPA-filter units manufactured with such filter media have satis-
factorily passed structural tests under both high air velocities and high
differential pressure as well as tests under extended exposure to high
relative humidity and fog conditions.

I. Introduction

The development work was focused on two aims. Improvement should be
achieved both for the resistance to acid, and for the structural integrity
with respect to high mechanical loads, caused by either high air velocities
or high humidity of the air to be filtered. The newly developed filter
elements should withstand differential pressures up to 30 kPa with dry air
and up to 10 kPa with air of high humidity.

Several authors have reported on studies under simulated accident
conditions, with HEPA-filters almost exclusively made with glass-fiber paper.
The structural strength of conventional HEPA-filters is primarily limited by
the low tensile strength of the filter media available. Comparative measure-
ments of material characteristics were therefore made for both glass-fiber
papers and different prototypical synthetic micro-fiber media. Particular
emphasis was put on the tensile strength of the materials, both dry and wet,
on the resistance to chemical attack, and on the manufacturing properties.

The medium to be developed should be as easily workable as glass-fiber
papers. The full-size filter units are required to have the same dimensions
and design flow rate as the conventional filters. During the development
work performed so far, various material combinations were manufactured and
their material properties including the resistance to differential pressure
were determined.

A varity of glass-fiber materials with high filtration efficieny are commercially available. For the tests carried out within the framework of this comparative study, samples were taken of glass-fiber paper procured directly from the manufacturer or directly from HEPA-filter units. Since the results obtained for all glass-fiber media were consistent, hereafter no distinction is made between the two groups of sources.

The results reported refer to the newly-developed filter medium identified here as Microdon S, a special variation of a standard material with the registered trade mark Viledon Microdon. HEPA-filters are required to have a retention efficiency better than 99.97 % for 0.3 µm monodisperse DOB aerosol.

II. Production and Material Characteristics of Micro-Fiber Nonwovens

For years Carl Freudenberg has been producing micro-fiber nonwovens from polycarbonate using an electrostatic spinning process. As filter media these nonwovens are used in respirator masks and high efficiency pocket filters among other applications (1).
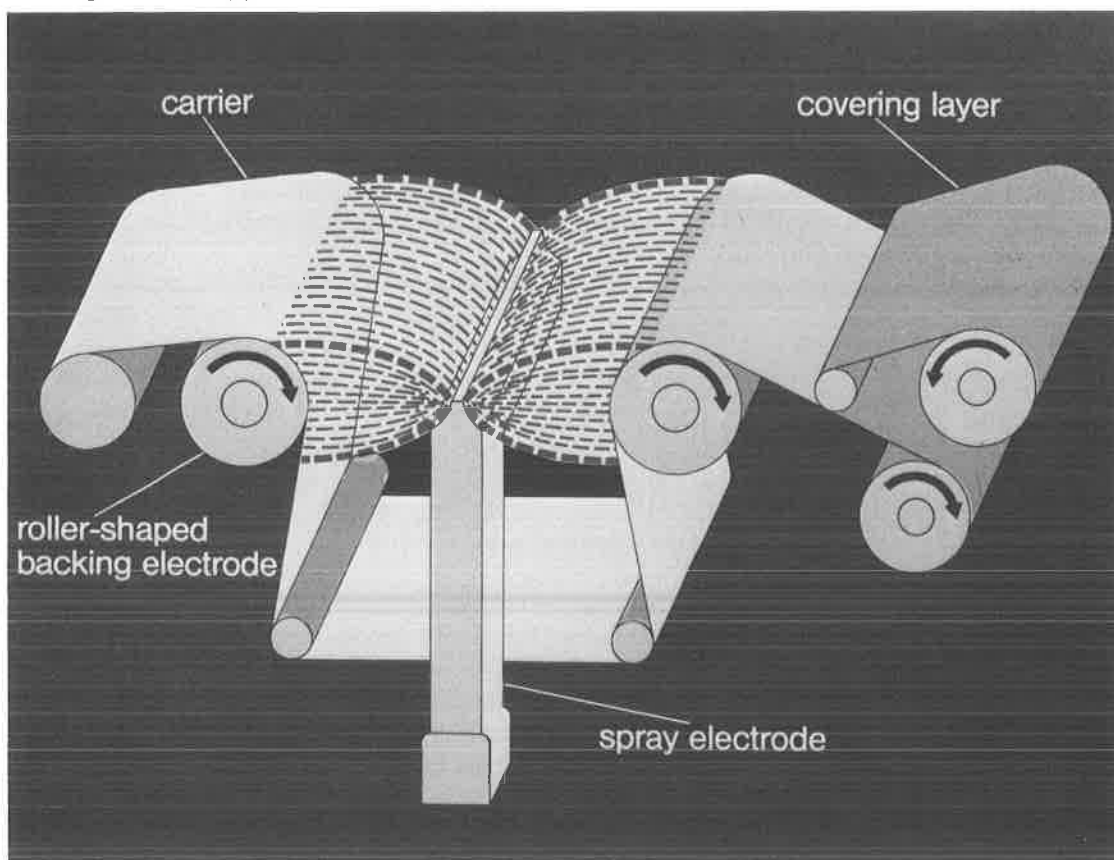
Figure 1:   Schematic of the electrostatic spinning process

Fig. 1 shows the layout of the electrostatic spinning process used. A high-voltage electric field is created between a backing electrode and a spray electrode. The spray electrode is wetted with a polymer solution. The electric forces cause drops to be pulled away from the spray electrode and stretched out to thread-like structures. In route to the backing electrode the

thread of solution solidifies and is deposited onto a carrier which is fed
continuously over the rotating backing electrode. At the end of the production
process the covering layer is added. The diameters of the fibers can be varied
within the range of 1 - 10 μm.
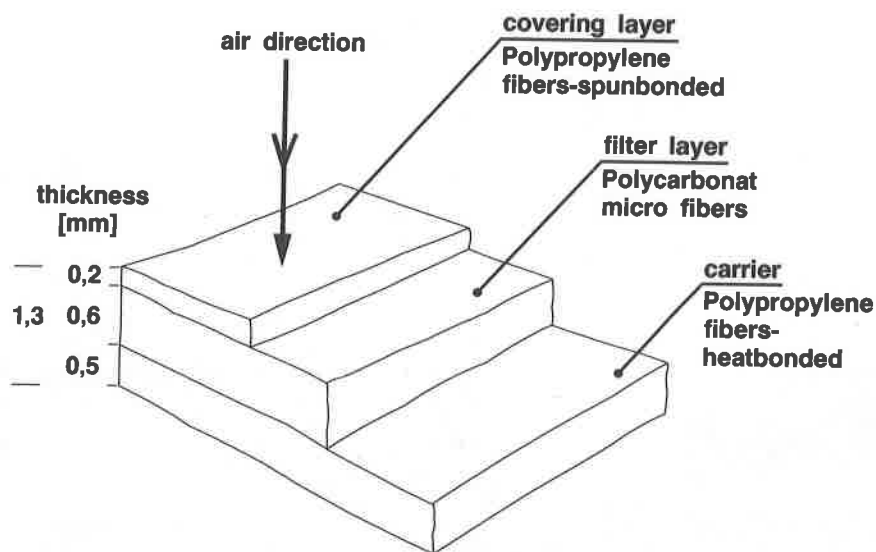
Figure 2:   Sandwich structure of the Microdon S filter medium.

     Fig. 2 shows the typical 3-layer structure of the Microdon S media. The
nonwovens used as carrier material and covering layer for the experimental
media are made from polypropylene fibers. The two outside layers are con-
siderably more porous than the inner micro-fiber layer and their share in
the total flow resistance is negligible. Development was based on the require-
ments for resistance to the expected mechanical and chemical influences.
Total thickness approx. 1.3 mm. The particles are mainly filtered by the inner
micro-fiber layer. The usual practice of applying a binder material was pur-
posely avoided, thereby making the whole fiber surface available for the de-
position of dust.

     Significant differences in comparison to the standard glass-fiber papers
are also apparent in the fibers themselves. The biggest difference, apart from
the geometric shape, lies in the elasticity of the synthetic materials and in
the large elongation prior to rupture of the individual fibers.

     The fiber diameter required for high filtration efficiencies is around
1 μm for glass-fibers in general and was measured to be 1.3 μm for the refer-
ence glass-fiber materials tested here. The round cross-section enables the
diameter to be clearly defined. Polycarbonate fibers on the other hand have
rectangular cross-section with a height/width ratio of approximately 1:3. The
fibers have an average width of 2.2 μm, from which an equivalent diameter of
approx. 1.5 μm can be calculated. Hence the fibers of the experimental media
were slightly coarser than those of comparable filter media made from glass-
fibers. Fig. 3 shows scanning electron micrographs of both types of filter

media, enlarged 4800 X.

Glass   **1 µm**   **Polycarbonat**
scanning electron micrograph (4800 X)
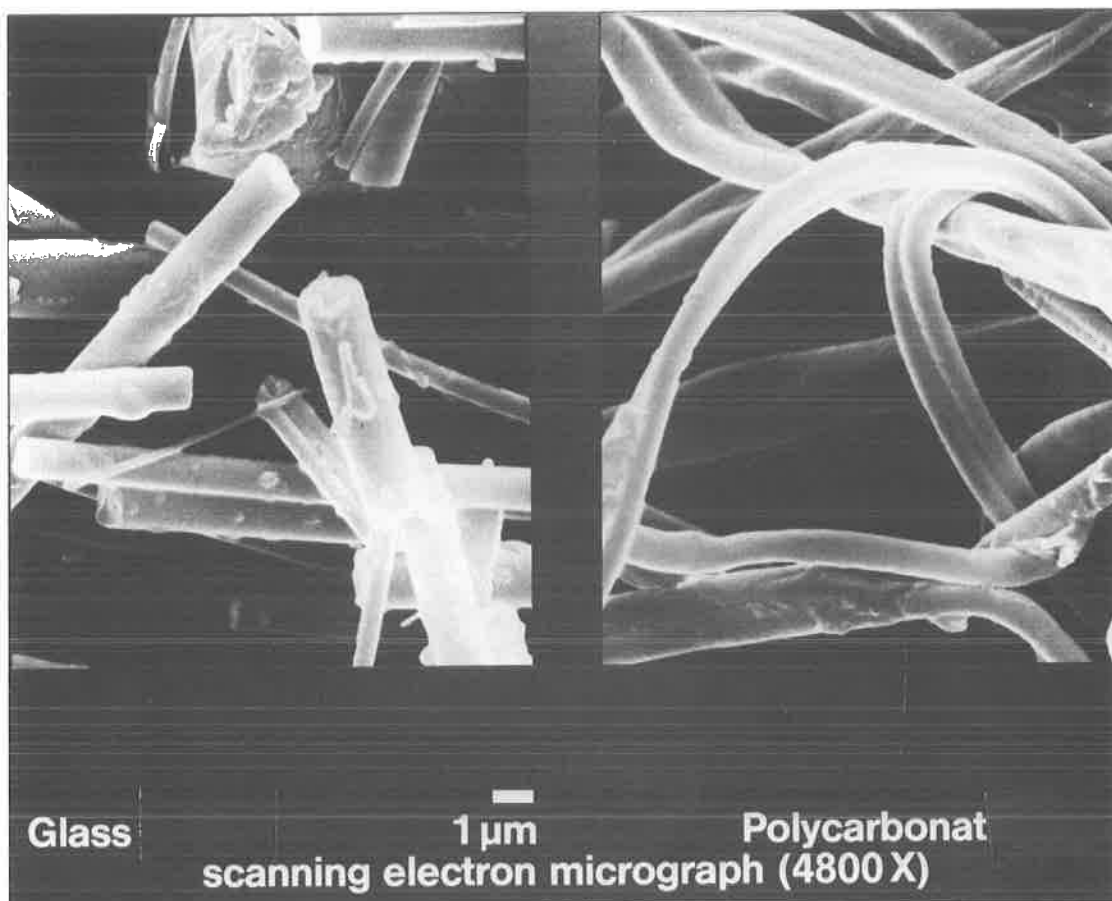
Figure 3:   Fiber diameter and structure

III. Influence of Fiber Charging

The fibers produced by the electrostatic spinning process become electrostatically charged, due to the production process. This "electret" effect has a positive influence on the high efficiency performance (2). As Brown has proved (3) the individual fibers possess positive and negative charges which are stable under normal storage conditions. Long term trials over a period of more than 2 years under ambient atmospheric conditions did not give rise to a significant change in the removal efficiency nor did operation under high relative humidity show any negative effect. However, the presence of liquid aerosols, in particular those containing oils and wetting agents, can, depending on their concentrations, lead to a reduction in the charges. The same decrease also occurs with exposure to elevated temperatures (4). The influence of a temperature increase on the penetration is shown in figure 4.

The samples were stored for 24 hours at a constantly rising temperature. Temperatures above 70° C cause the penetration to increase. At 100° C - 130° C the known filtration mechanisms, such as diffusion and inertia effects, are still effective. At temperatures above 130° C the polypropylene fibers of the
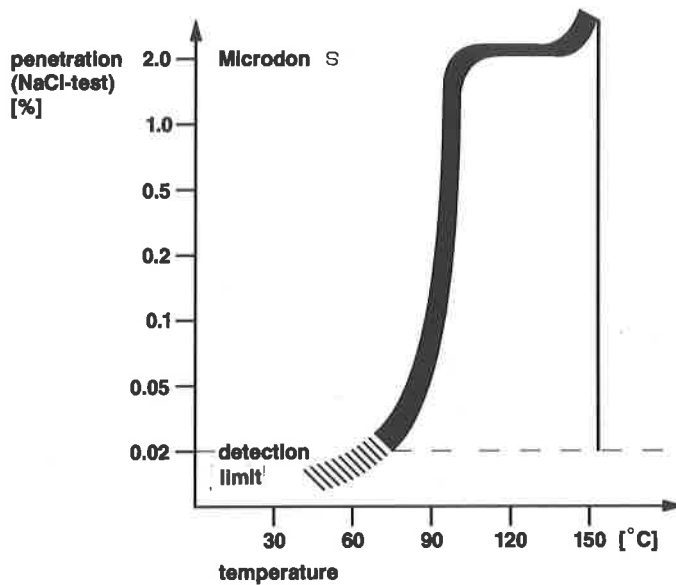
Figure 4:   Influence of temperature on the penetration

nonwovens used as outside layers on this experimental media are damaged or destroyed.

     In extreme cases under particular applications a complete discharge may occur. In order to quantify this phenomenon samples of the media were completely discharged by storage in a solution containing an anionic wetting agent and subsequent drying. Fig. 5 shows the influence on penetration at various linear air velocities.

     Whereas the charged material shows penetrations less than 0.02 %, an increase is apparent with the discharged material. If a maximum efficiency is required for safety reasons even after full discharge has taken place, the amount of micro-fibers used can be increased. This is best demonstrated by the use of two layers of synthetic micro-fibers. This double filtration layer provides the required efficiency at a normal air velocity even in an discharged state. However, the advantage of a lower pressure drop must be sacrificed.

     Future developments are directed at the spinning of even finer fiber laminates. This would mean further positive effects.
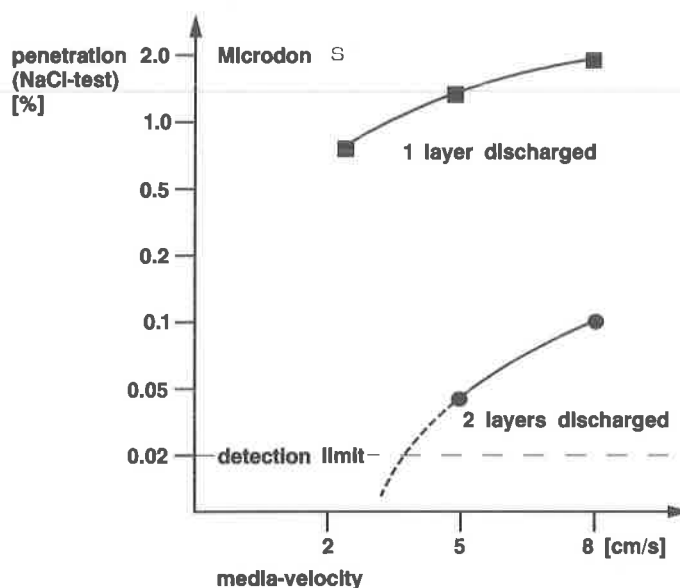
Figure 5:   Influence of fiber charge on penetration

IV.   Performance of Viledon HEPA-Filter Units

Prototypical HEPA-filters with the standard dimensions 610 x 610 x 292 mm were manufactured using the synthetic micro-fiber media. Conventional pleating was applied using the normal aluminium corrugated separators with a plywood frame and polyurethane sealant. Some units were also produced with hard PVC separators in order to achieve resistance to hydrofluoric acid. The HEPA-filters accomodate a medium with a total surface area between 16 and 20 m^2 leading to a pressure drop of 180 to 250 Pa at an air flow of 2000 m^3/h. The "electret" effect of the filter material allows lower pressure drops at a comparable retention efficiency.

Testing the Structural Strength under High Differential Pressure

Gregory and Rüdinger have reported on conditions and results of tests with commercial HEPA-filters made with glass-fiber paper (5, 6). Recent tests were performed with Microdon S fiber media filters. The rapid increase in air velocity in the "blow down" test facility raises the differential pressure across the HEPA-filters to more than 25 kPa, provided the units do not burst. The filter units made from synthetic micro-fiber media suffered no damage after a differential pressure of 28 kPa was applied, whereas the standard glass-fiber HEPA-filters, depending on their construction, were damaged at differential pressures between 4 and 22 kPa.

Fig. 6 shows a print from the high-speed film of the structural test. Despite the swollen pleats the prototype remained undamaged.

In the meantime a new test facility, BORA, has been put into operation
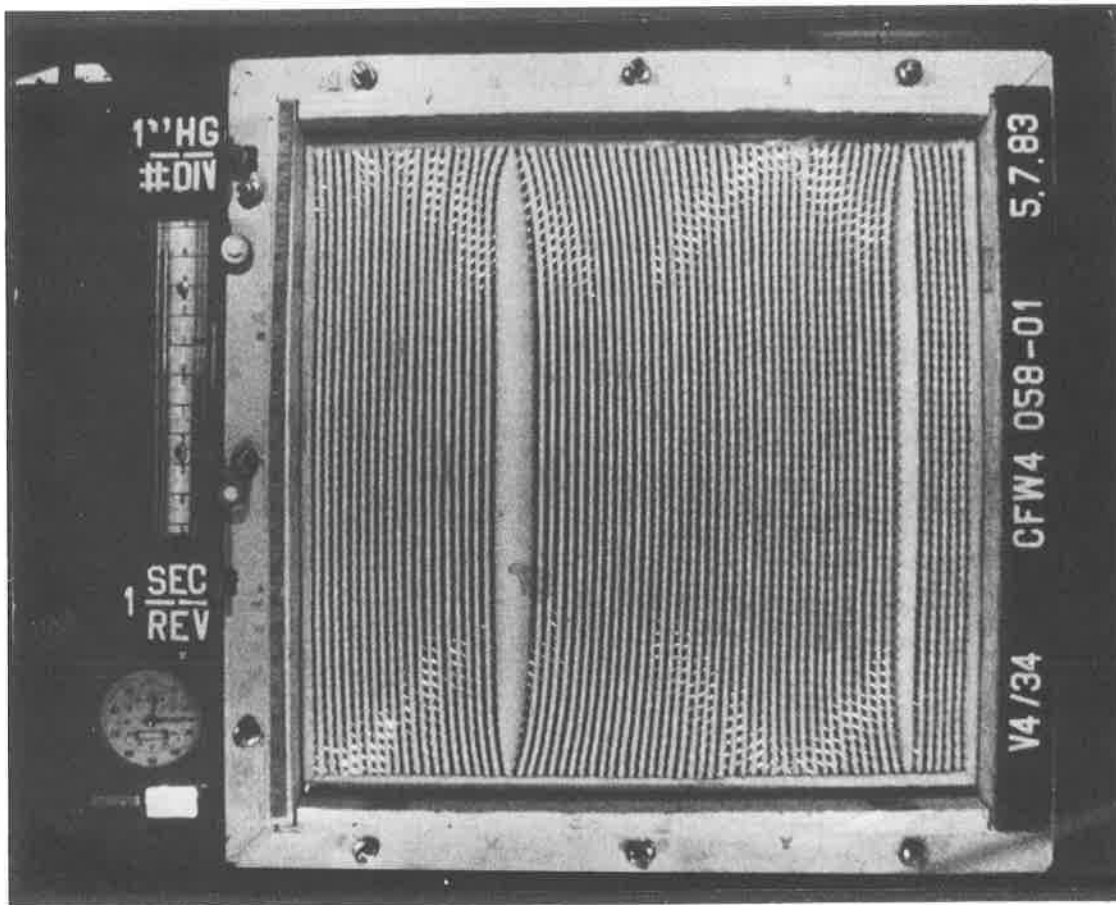
Figure 6:   Swollen folds of the Microdon S filter medium under high
             differential pressure

at the Nuclear Research Center Karlsruhe for testing filters under simulated
accident conditions (7). A prototypical HEPA-filter with the synthetic micro-
fiber medium was subjected to an air flow of approximately 24.000 m³/h for
10 seconds, whereby a differential pressure of 30 kPa was applied. Even
through the exposure time of 2 sec., as tested at the Los Alamos Ntl. Labora-
tory, was increased to 10 sec., no damage was caused to the unit.

Response to High Humidity

        When new HEPA-filters are exposed to increasing relative humidity, the
flow resistance increases. This effect is enhanced on used, dust-loaded fil-
ters. If the filter elements are exposed to liquid moisture the flow resist-
ance rises steeply. These effects are due to the incorporation of water in
liquid form within the filter matrix. The tensile strength of the glass-fiber
media is also reduced (8).

        In order to investigate the response to such operating conditions stand-
ard HEPA-filters and prototypical filters with the polycarbonate micro-fiber
media were tested with the relative humidity increasing up to 100 % at 50° C.
In order to simulate fog conditions, water was sprayed into the test air flow.
During the tests the differential pressure across the filter was measured and

the downstream side was checked visually for damage. All the glass-fiber filters tested so far were damaged as a result of the stress applied. Dust-loaded glass-fiber filters were partially destroyed after exposure to a relative humidity close to 100 %, whereas clean glass-fiber filters performed satisfactorily until exposed to fog. The filters with glass-fiber media failed at differential pressures between 2 and 6 kPa.

The Viledon HEPA Units preloaded with ASHRAE test dust, tested under the same conditions showed no apparent damage even under the maximum differential pressure of approx. 8 kPa possible in the facility. Further details relating to the tests are described in Ref. 9.

V. Strength Characteristics of Microdon S Media

Tensile Strength and Elongation under Ambient Conditions

Fig. 7 shows the stress-elongation diagrams of Microdon S compared to commercial glass-fiber media. The tensile strength of Microdon S is about 5 times greater than that of glass-fiber media, as is the elongation up to rupture. The greater tensile strength represents a significant improvement in the performance of the filter-media material, as the differential pressure required to cause structural failure of a filter unit is thereby increased (10). The influence of elongation on a potential weakness in the filtering media has so far not been tested conclusively.
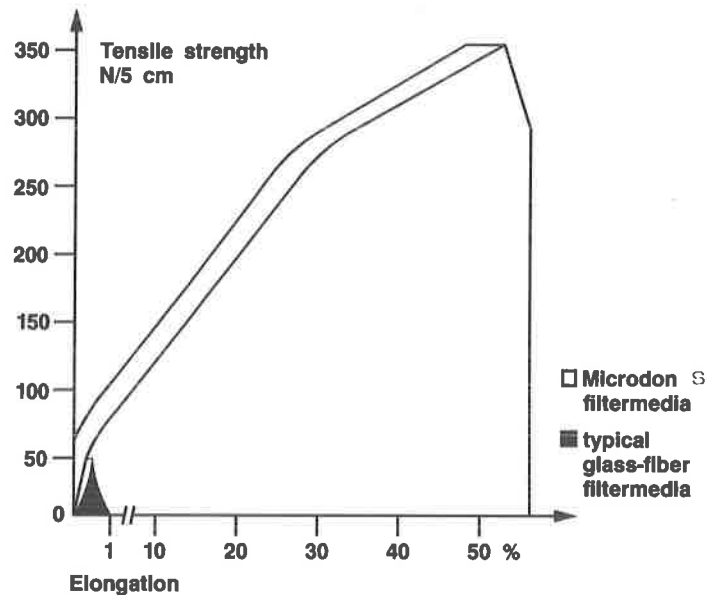
Figure 7:   Tensile test acc. to DIN 53 857

Influences of Humidity Exposure and Folding on Media Strength

Moisture and water have a considerable effect on the strength of filter media. Tensile strength of glass-fiber media is also clearly reduced by pleating during the manufacture of HEPA-filters.

Samples of unused HEPA-Filter-Units		
	Microdon media	glass-fiber media
without any folds		
dry N/5 cm	> 300	< 60
wet N/5 cm	> 300	< 30
containing typical folds		
dry N/5 cm	> 300	< 40
wet N/5 cm	> 300	< 20

Figure 8:   Tensile strength acc. to DIN 53 857

Fig. 8 shows the most important comparative data for the filter-media materials tested. Pleating and exposure to moisture produce no loss in tensile strength for the micro-fiber media. However, the tensile strength of the glass-fiber media drops by 50 % for wet samples. The dry, pleated glass-fiber media show a loss of tensile strength of approx. 33 % and a further 33 % decrease when wet, leaving a residual strength of only 20 N/5 cm. The tensile-strength characteristics of the synthetic micro-fiber media are influenced neither by folding nor by wetness.

Change in Strength after Chemical Attack

An important medium property for nuclear applications is resistance to hydrofluoric acid which destroys glass-fibers within a very short time.

In order to gain some idea of how acids and alkalines affect the strength of filter-media materials, exposure to liquid chemicals was carried out for periods of 24 hours. The selection and concentration was determined by the "Equipment Specification ES 1, Appendix, Page 14", which is applicable to separator materials.

Although the recommended exposure time of only a few minutes already constitutes a considerable stress factor, the prelonged exposure times used, had only a minor influence on the tensile strength of Microdon S as shown in Fig. 9.

However in some cases, the tensile strength of the glass-fiber media dropped to below 10 % of the original value, which is not particularly high to start with. The hydrochloric acid reduced the strength of the glass-fiber media to nil and the hydrofluoric acid entirely destroyed the glass-fiber media after only a few minutes.
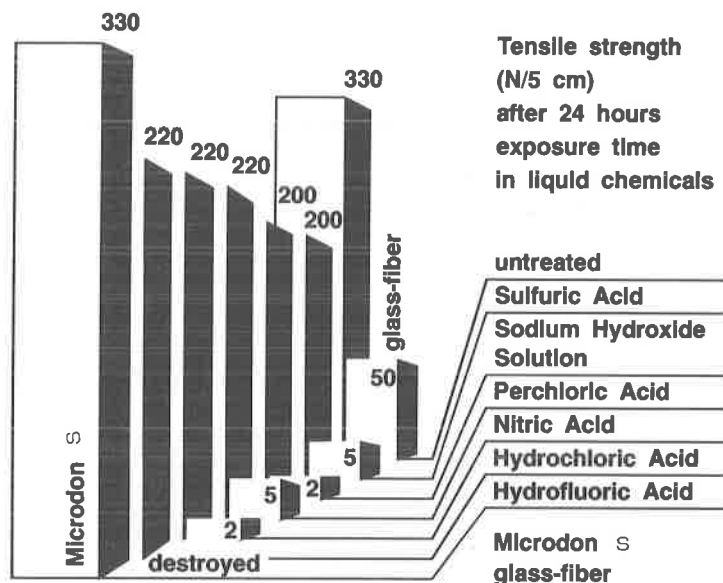
Figure 9:   Corrosion resistance of filter media

VI. Conclusions

Electrostatically charged micro-fiber media with conventional HEPA-filter efficiencies, can be produced from synthetic materials by means of an electrostatic spinning process. The Microdon S medium shows high resistance to acids, in particular hydrofluoric acid, and is not influenced in strength by a high relative humidity or fog. The mechanical and chemical properties of Microdon S can also be adapted to a large extent to other requirements. HEPA-filters made up of Microdon S show excellent resistance to high differential pressure even under difficult conditions such as high relative humidity and liquid moisture.

The electrostatic charge of Microdon S filter material is stable. Performance loss only occurs at temperatures above 70° C or in the presence of aerosols containing oils and ionic wetting agents. This is due to reduced electrostatic charge. The effect can be counteracted by increasing the thickness of the medium or by altering the fiber diameter, whereby the current low pressure drop would be increased.

The synthetic raw material of fibers, carrier and cover layer has different burning properties from the mineral material, thus suggesting advantages in waste disposal. Microdon S is classed as self-extinguishing class F 1 in accordance with DIN 53 438, which is a test method similar to the one described in UL 94.

Another positive characteristic not mentioned so far became clear during the manufacture and testing. The micro-fiber medium is insensitive to rough treatment, thus more or less precluding the appearance of leaks in the medium of finished filters as a result of rough handling during or after assembly.

The polycarbonate micro-fiber medium is particularly suitable for use in the production of HEPA-filters for applications where resistance to high differential pressure and acid are essential criteria. HF-resistant HEPA-filters can provide a vast improvement in the environmental safety of uranium enrichment plants on the other hand in nuclear power reactor facilities, it is the Microdon S filter resistance to fog and high differential pressure which would serve the public interest in nuclear safety.

Further development will be directed towards producing even finer fiber laminate and towards the use of raw materials with greater resistance to heat.

<div align="center">References</div>

(1)   Weghmann, A.; "Production of Electrostatic Spun Synthetic Micro-Fibers and Applications in Filtration", Nonwoven Industry, pp 24 - 32 (November 1982).

(2)   Muhr, W.; Löffler, F.; "Abscheideverhalten von Faserfiltern bei elektrostatischer Aufladung von Staub und Faser", Maschinenmarkt, 82 (1976).

(3)   Brown, R.C.; "Electrical Effects in Dust Filters", World Filtration Congress III, Downingtown (1979).

(4)   Ackley, M.W.; "Degradation of Electrostatic Filters at Elevated Temperature and Humidity", World Filtration Congress III, Downingtown (1979).

(5)   Gregory, W.S.; Martin, R.A.; Smith, P.R.; Fenton, D.E.; "Response of HEPA-Filters to Simulated Accident Conditions", Proc. of the 17th DOE Nuclear Air Cleaning Conference, Denver, Colorado (August 1982).

(6)   Rüdinger, V.; Wilhelm, J.G.; "HEPA-Filter Response to High Air Flow Velocities", Proc. of the 17th DOE Nuclear Air Cleaning Conference, Denver, Colorado (August 1982).

(7)   Ensinger, V.; Rüdinger, V.; Wilhelm, J.G.; "A Procedure to Test HEPA-Filter Efficiency Under Simulated Accident Conditions of High Temperature and High Humidity", Proc. of the 18th DOE Nuclear Air Cleaning Conference, Baltimore, Maryland (1984).

(8)   Rüdinger, V. et al.; "Studium des Verhaltens von Schwebstoffiltern der Klasse S unter simulierten Störfallbedingungen", Projekt Nukleare Sicherheit, Jahresbericht 1983, KfK 3450 (1984).

(9)   Rüdinger, V.; Ricketts, C.I.; Wilhelm, J.G.: "Limite of HEPA-Filter Application Under High Humidity Conditions", Proc. of the 18th DOE Nuclear Air Cleaning Conference, Baltimore, Maryland (1984).

(10) Ricketts, C.I.; "Tornado Model Testing of HEPA-Filters", Thesis New Mexico State University, Las Cruces (1980).

DISCUSSION

WATSON: Have you any figures on the dust loading capacity of your filter, such as pressure drop vs. dust loading?

BELLA: Two tests were made, one with ASHRAE dust and the other one with quartz. For quartz, we had a dust holding capacity of more than 8 kilograms per unit. For the ASHRAE test, we had a dust holding capacity of approximately 2 kilogram per 610 x 610 x 292 mm unit.

WATSON: What sort of pressure drops have you found?

BELLA: In one case, pressure drop was 16 mm w.g. and in the other one, it was more than 80 mm w.g., between 80 and 100.

WHITELY: The material appears to be a composit. From the strength values that you gave, I was curious as to how much was contributed by the outer layers, which do not really participate in the filtration part of it, versus the core material, which is essentially the filter.

BELLA: Tensile strength is mostly influenced by the layers on the both sides. The material does not have high tensile strength, but greater than glass fiber media.

WHITELY: When you have tremendous elongation, what happens to the filtration properties as it is elongated?

BELLA: This we don't know. After we had 50% elongation, I think that we had a lower efficiency, but we haven't measured it up to this time. We know that something happens, that the fibers stretch. After special irrigation, there will be a lower square wave per centimeter and a decrease in efficiency, but I don't know why it occurs.

SIGLI: Just a question concerning efficiency. You mentioned a penetration of 0.02% with NaCl. Can you improve this efficiency? Was it a limit in the sensitivity of your method of measurement? It seems a bit high, can you improve it?

BELLA: Yes, we can improve the efficiency if we use a smaller fiber diameter, but we cannot measure it, because our test rig can only measure to 0.02% penetration.

SIMOUN : HIGH TEMPERATURE DYNAMIC TEST RIG
FOR
INDUSTRIAL AIR FILTERS

J.DUPOUX, Ph.MULCEY, JL.ROUYER and X.TARRAGO
CEN Saclay
CEA - IPSN - DPT
Gif-sur-Yvette

Abstract

The test rig SIMOUN is designed for the testing of air filters (especially particulate filters) under high temperature dynamic conditions. Its operating conditions allow temperatures and flowrates up to respectively 400°C and 4.000 m³/h. The facility is located at the SACLAY NUCLEAR CENTER.

It has been designed to operate fast temperature changes in order to reproduce the typical accidental temperature profiles obtained during simulated fire experiments.

Particular emphasis is given in the paper on the system of control which is a rather sophisticated part of the test rig.

High temperature efficiency measurements are performed during the tests by means of a sodium chloride aerosol. The efficiency test procedure has been developed from the results of a qualification study which included a comparison with the French standardised uranine test method (AFNOR NF-X-44.011).

SIMOUN test rig is operable since October 83. It is being used for the testing of manufactured filter systems and components and for researches on filter behaviour in accident situations, especially fires. Results are given on the behaviour of some manufactured filters.

I. Presentation of SIMOUN

SIMOUN is a high temperature dynamic test rig which has been built in order to evaluate industrial filters capabilities in case of fire.

Till now, no equivalent facility existed in France. Only static test in hot atmosphere were available to appriciate filters resistance under such conditions(1).

A new rig was then necessary to qualify filters (especialy HEPA filters) and filter housings under more realistic conditions. Its thermal and mechanical design features are remembered in Table I.

Table I. Principal features of the SIMOUN test rig

CARRIER GAS

Quality	Filtered atmospheric air
Temperature	Ambient up to 400°C
Flowrate	Up to 4,000 m³/h at 400°C
	Up to 10,000 m³/h at ambient conditions

The tests characteristies (parameters gradients, level and duration of temperature steps, corresponding flowrate, ...) are automaticaly controled by an automaton.

TEST AEROSOLS

Low temperature tests	Soda fluorescein (Uranine) AFNOR standard NFX 44.011
High temperature tests	Sodium chloride (derived from the UK standard) up to 400°C

A continuous efficiency measurement with the NaCl aerosol can be performed during the test.

SAMPLES

HEPA standard cells (610 x 610 x 300 mm) mounted in a SOFILTRA POELMAN stainless steel housing.

The design enables the setting and test of air cleaning componants with different sizes.

SIMOUN is presently in operation and has reached the following performances : 400°C for 4.000 m³/h with temperature gradients till 20°C/min from ambient to 220°C.

It will be possible to upgrade these performances but they appear at this time being sufficient to simulate fire conditions on filters and filter housings.

II. Technical features

Description of the rig itself

A flow pattern of the SIMOUN facility is presented in Figure 1.
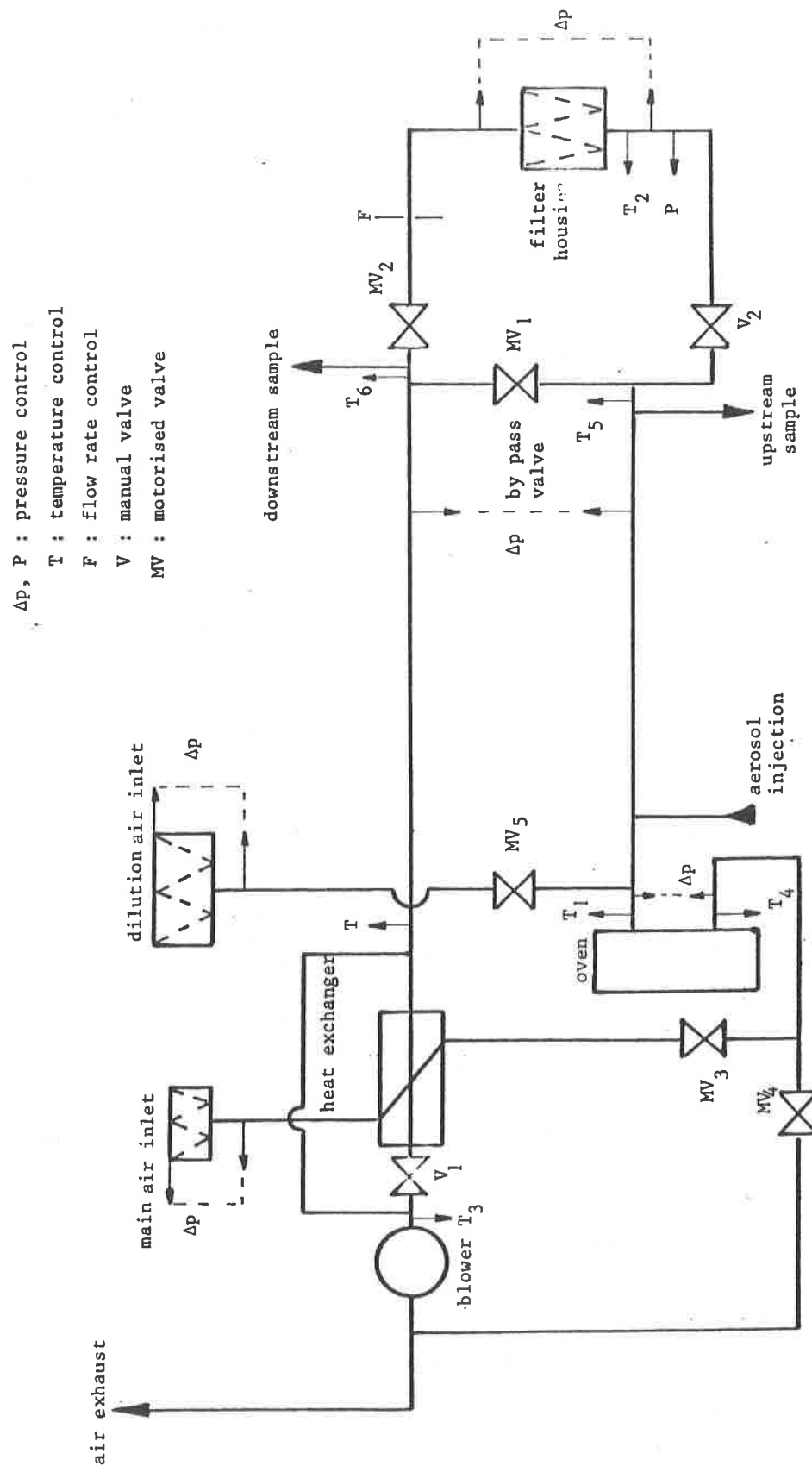
FIGURE   1
SCHEMATIC DIAGRAM OF THE SIMOUN TEST RIG

The various possible flow configurations are the following :

- ambient temperature, flowrates up to 10,000 m³/h. The oven and the heat exchanger are by-passed,
- high temperature with filter by-pass to submit the filter to thermal shockes. Partial by-passing is also necessary for a good oven operation when low flowrates are used in the filter branch,
- without by-pass to obtain progressive temperature rise ; recirculation enables to supply the heat exchanger with hot gases during its temperature setting.

Description of the control system

Particular emphasis will be given in this paper on the system of control which is a rather sophisticated part of this test rig. It is shown in Figure 2.
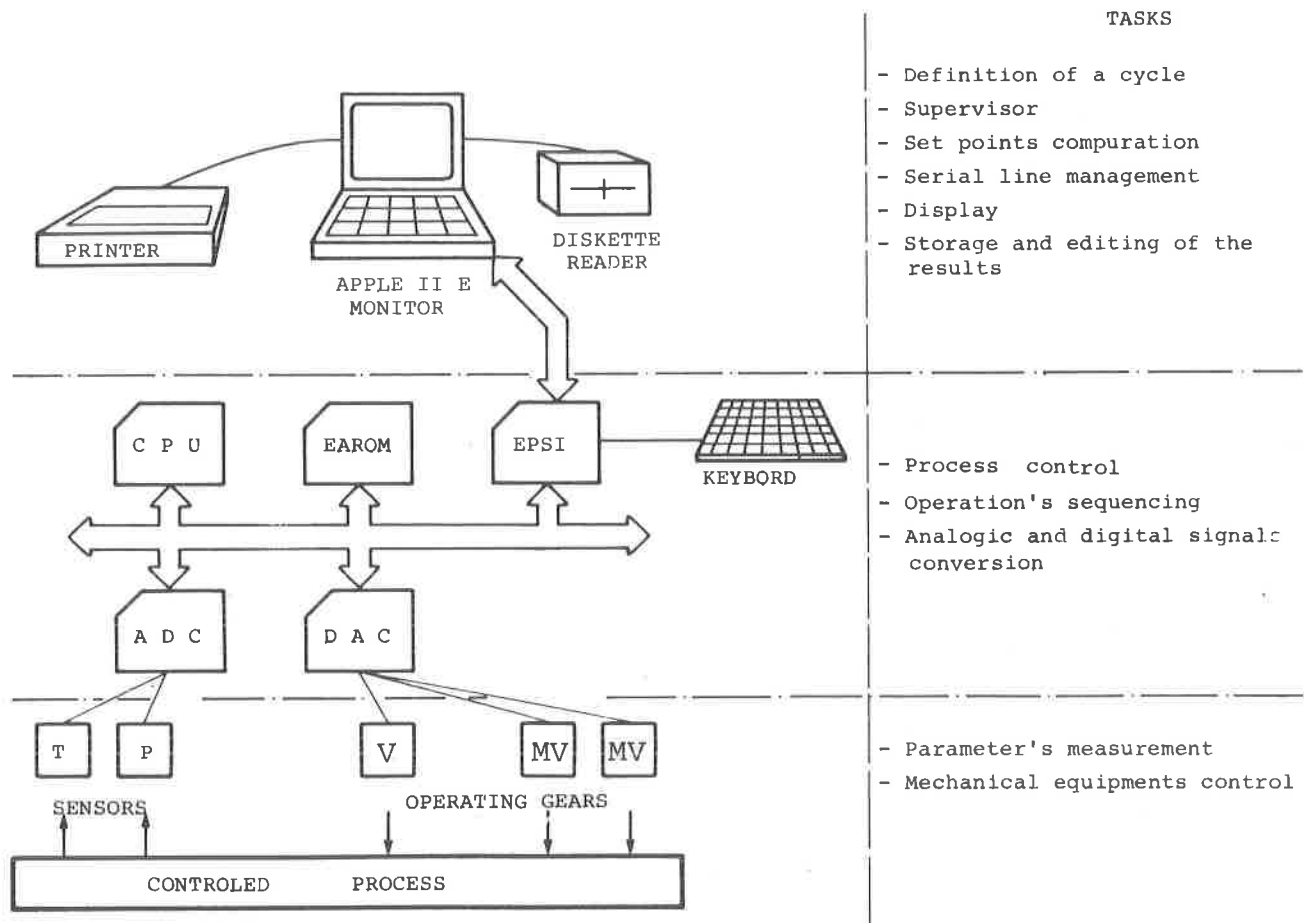
FIGURE 2
CONTROL SYSTEM BLOCK DIAGRAM

Software. It is a hierarchical system which executes the following tasks :

. The so-called regulation. Acquisition of temperature and pressure data ; volumetric and mass flowrates calculation ; control of operating gears (valves and blowers).

. Starting and stopping sequencing of the facility. Starting at low flow rate for power sequencing ; by-pass operation at a medium flow rate for heating sequencing ; course test control ; possible delay of a new test starting ; stopping operations.

. Interactive task with the operator and editing of the results. Instructions input by the operator (definition of a cycle or set points selection) ; test course display, editing of the results, test report typing, storage on diskettes.

Hardware.

. Temperature and pressure sensors (K type thermocouples and 4/20 mA output pressure transducers) ; they allow the measurement of the physical parameters defining the state of the system.

. Control automaton (CRL 2,000 with microprocessor). It is an autonomous system which constitutes a first level control ; it executes the digitalization of the low voltage signals from the thermocouples and of the 4/20 mA signals from the pressure sensors, the calculation of physical parameters of importance for the control operations (volumetric or mass flowrates, temperature corrections, ..) and the control of the operating gears by means of integrated P.I.D. control codes. In other respects, the check - up of starting and stopping operations and the corresponding setting of the control code are executed by a series of sequential codes. The set is managed by a realtime monitor that guarantie a system transparency for the operator. A console enables the operator to select set points and to display the operating conditions of the facility.

. Operating gears. In order to act upon the process one disposes of five motorised valves and variable speed drives for the blowers. Those equipments are controled by 4/20 mA signals. This set of sensors, automaton, operating gears constitutes an autonomous system is able to control constant temperature and flowrate step cycles. When necessary, the operator can execute a manual change of a set point.

. Apple II E system. This system consists in : Apple II E computer and monitor ; printer and interface card ; two diskette readers ; internal clock card ; serial interface card V 24. This classical set is well knowned and acts as a supervisor. The software developped by C.E.A. for this purpose will allow : the definition of a time dependant cycle with respect to flowrate and temperature ; the CRL 2,000 control for the cycle tracking ; the editing and the storage of the results.

IV. Efficiency measurements

The use of the soda fluorescein aerosol is made impossible by temperature conditions. The NaCl aerosol, which is used as a standard test aerosol in the UK (2), is a stable aerosol for high temperature conditions. For these two last reasons the NaCl aerosol was choosen.

Generation and detection apparatus are illustrated in Figure 3.
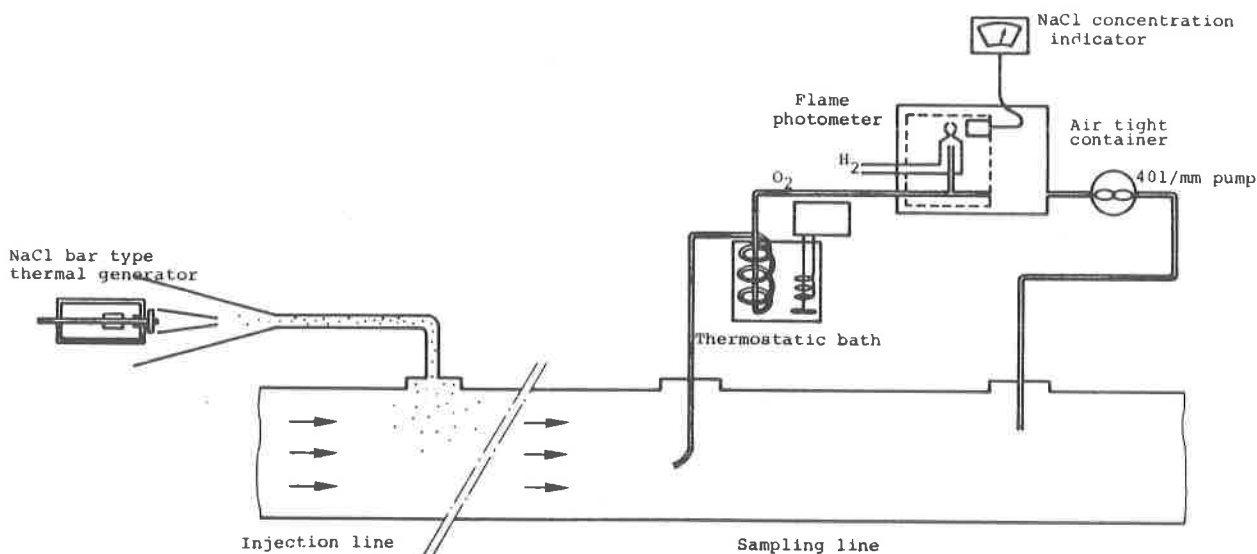
FIGURE 3

NaCl GENERATION AND DETECTION ON THE SIMOUN TEST RIG

Generation

It is operated through a NaCl stick thermal generator (MOORE'S Company Thermal Generator) with an oxy-propane flame.

Detection

The detector is a sodium chloride photometer (portable detector type, MOORE'S Company). It is designed to be supplied by the sampled air under a light overpressure. For this reason it had to be kept in an airtight container operating at equipressure with the duct of the tests rig.

Gas sampling

The gas sampling line includes a thermostatic bath in order to keep constant (about 50°C) the sample temperature. This was done to prevent possible drifts due to temperature variation during NaCl concentration measurements.

1102

A correction is made to take into account a volemetric flowrate variation between the sampling probe and the charber of the detector.

NaCl aerosol characterisation

The granulometry of the aerosol has been established for different temperatures.

The results given in Figures 4 to 7 show a good stability of the aerosol size distribution.

The mass median diameter (main diagonal of the NaCl cube) ranges between 0.10 μm (for about 100°C) to 0.13 μm (for about 400°C) with a standard deviation σ g of about 1.4. The results collected during the setting phase have shown that this aerosol was of a difficult use at ambient temperature when the relative humidity is not controled (3).

As a comparison, an NaCl aerosol generated with the soda fluorescein standard apparatus (solution : 10 % by weight) as a mass median diameter of 0.23 μm with a standard deviation σ g = 1.7.

Conclusions : the NaCl aerosol as a good size distribution stability between 100°C and 400°C, similar to the one of the soda fluorescein aerosol. Its greatest monodispersion, with a maximum located in the region below 0.15 μm, is perhaps not an advantage for efficiency measurements.

V. Hepa filters tests results

A series of experiments was conducted to evaluate the temperature resistance of some hepa filters widely used in France and manufactured by Sofiltra-Poelman company.

For an hepa filter, the critical components, as far as temperature is concerned, are the sealent and the gasket.

The mineral sealent used for these filters shown a very good behaviour till 400°C during several hours. The different gaskets mounted on the galvanized steel behaved differently has shown in the Table II.

Table II. Hepa filters tests under high temperature conditions
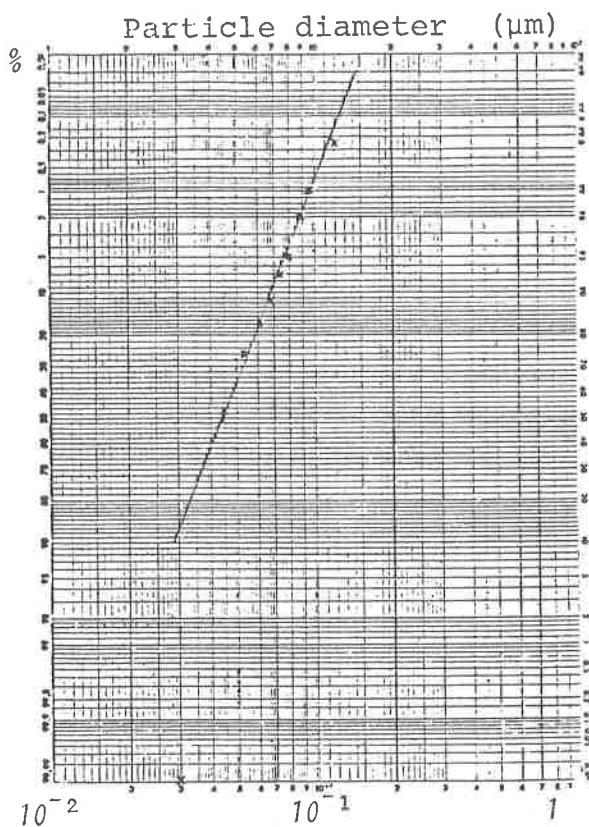
FIGURE 4 : 100°C
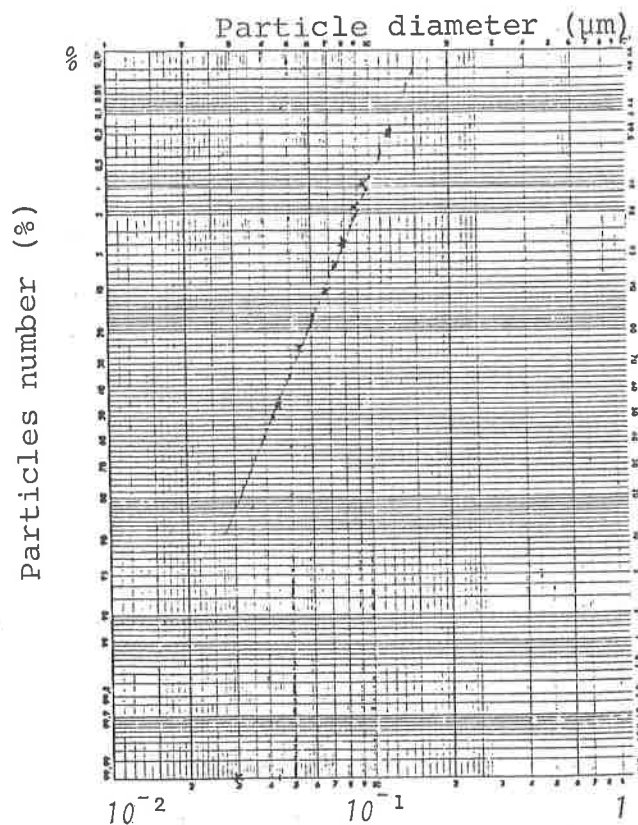
FIGURE 5 : 200°C
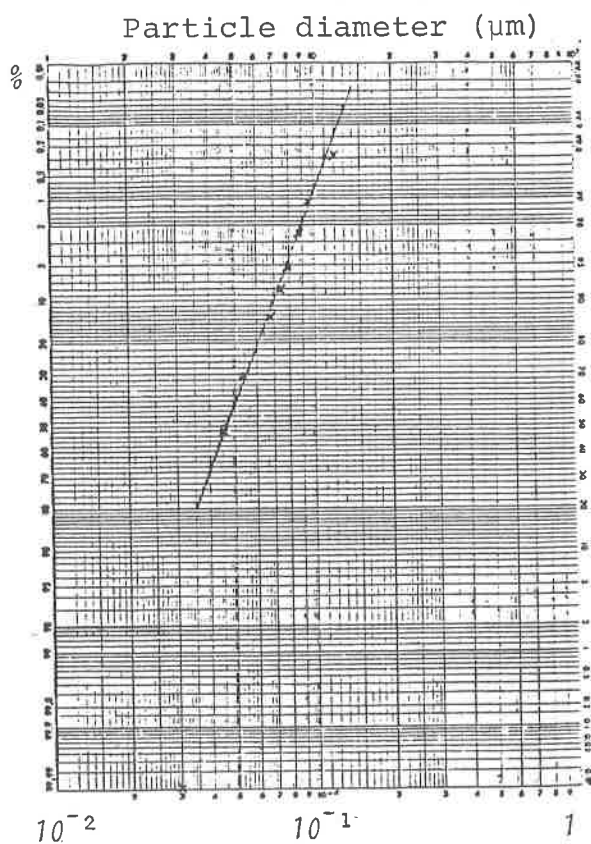
FIGURE 6 : 300°C
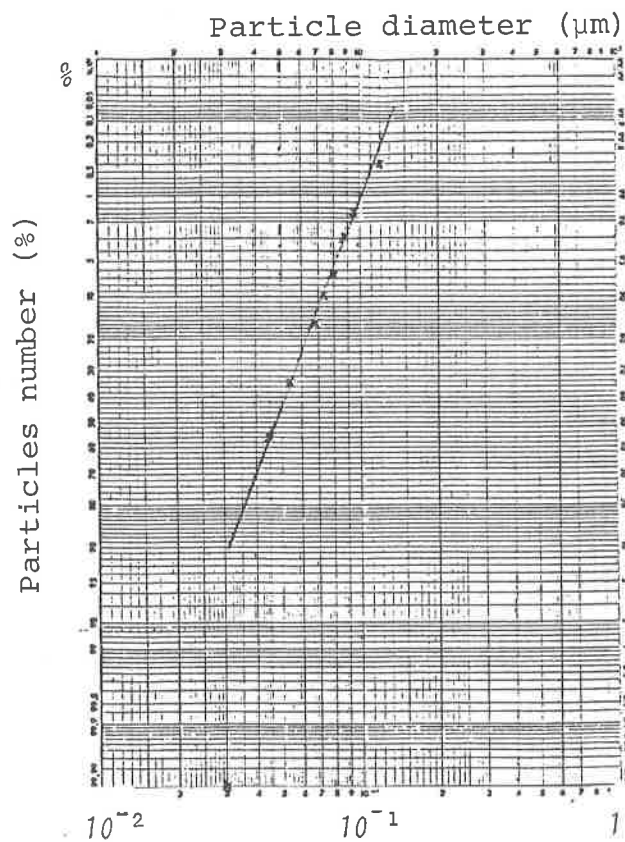
FIGURE 7 : 400°C

Filter reference		1506.40	1506.41	1506.41
Gasket characteristic		one piece molded silicone semi-circular	teflon with a fibrous texture, rectangular	teflon with a fibrous texture, rectangular
Temperature and duration of the test		315°C 2 h	315°C 2 h	400°C 1 h
Soda fluoresceine efficiency measurements at ambient temperature	before	10,700	10,100	6,250
	after	3,000	15,500	275
NaCl efficiency measurements at high temperature	time	8 mm 15 mm 1 l 2 h	> 35,000 (limit sensitivity)	15 mm 2 h
	efficiency	8,000 3,000 6,800 8,000		30,000 8,000

VI. Future work with SIMOUN

A theoretical study is now conducted to derive a model of the efficiency evolution for filter median and hepa filters against temperature.

A comparison with the results obtained with manufactured filters will point out the validity limits of the theoretical approach.

Temperature measurements into filter housings submitted to various temperature cycles. Study of leakage formation due to structural constraints during fast temperature transcients.

A study concerning the response of various fire detectors is also in progress.

VII. References

(1) J.PRADEL, AM.CHAPUIS and J.DUPOUX - Choix et recette des systèmes d'épuration de l'air dans les installations nucléaires, Seminar on High Efficiency Aerosol Filtration, Aix-en-Provence 1976, p 33,

(2) British standard 3928 : 1969,

(3) LP.MURPHY, SJ.FERNANDEZ and BG.MOTES - Comparison of HEPA filters Test Methods in Corrosive Environments - 16th DOE Nuclear Air Cleaning Conference, San Diego, Ca, 1980.

VIII. Acknowledgements

DISCUSSION

DAVIS: What is your heat source?

MULCEY: A propane burner.

DYMENT: The NaCl aerosol generated by the oxypropane
burner described in Part IV of the paper is not the same as the one
used in British Standard 3928, as suggested by the authors.

MULCEY: The BS 3928 aerosol is generated by pneumatic
atomization of 2% aqueous NaCl solution. It has a mass medium
diameter of 0.6 μm and a geometric standard deviation of 2-2.5. The
oxypropane-generated aerosol is used for in-place testing in some UK
installations, but it is not the subject of a British Standard.

PERFORMANCE TESTING OF HEPA FILTERS UNDER HOT DYNAMIC CONDITIONS

R P Pratt and B L Green
United Kingdom Atomic Energy Authority - Harwell

Abstract

A test facility has been designed and built to enable the performance of air filters under conditions of hot air flow to be evaluated. The facility is designed to provide up to 3400 standard m^3/h of air heated to temperatures not exceeding 500°C to the filter and housing under test. Differential pressures up to 400mm water gauge across the test filter can be accommodated. Provision has been made for the measurement of the efficiency of filters at temperatures up to 500°C using thermally generated sodium chloride aerosols and standard photometry techniques.

The associated experimental programme is aimed at determining the safe limiting operating parameters for HEPA filters in terms of air volume flow rate, differential pressure, temperature and time. These data are of relevance in the safety analysis of installed filters associated with fire and explosion accidents.

Preliminary tests have shown that the combination of differential pressure across the filter and hot gas flow significantly reduces the strength of the filter compared with results obtained from the currently specified test procedures of static oven test followed by dust loading to a stated differential pressure across the filter.

Tests have also been carried out to study the temperature gradients generated across the filter and housing associated with the flow of hot air through the test assembly. These show that the temperatures of housing and associated ductwork should not give cause for concern for air temperatures up to 500°C.

The effect of temperature on filtration efficiency is not significant below 300°C, but temperatures in excess of 300°C cause a reduction in the filtration efficiency of glass fibre media.

1. Introduction

High Efficiency Particulate Air (HEPA) filters are installed in nuclear plant ventilation systems as passive containment devices to prevent the discharge of particulate activity under both normal and accident conditions.

It is the policy of the UKAEA and BNFL·to purchase such filters against a specification[1] which prescribes minimum performance criteria for the filters in terms of efficiency, burst pressure and resistance to elevated air temperatures. It also covers requirements such as the materials used and more general aspects of performance.

Tests specified include an evaluation of the filters resistance to exposure to elevated temperatures. They require the filter to be placed in an oven, pre-heated to 500°C and left for 10 minutes. When cool,

following removal from the oven, the filter efficiency to BS 3928[2] must be greater than 98%. The filter is then loaded with a test dust until the differential pressure across the filter at its rated air flow is 305mm water gauge. The filter efficiency is again measured to ensure the filter remains greater than 98% efficient.

This series of tests does not model the circumstances likely to occur under high temperature accident conditions. The filter is likely to be subjected to hot air being passed through it and is also required to remove significant quantitites of aerosol (or smokes) which will tend to block the filter whilst at elevated temperatures. The effect of the hot air passing through the filter and subsequent dynamic loading at elevated temperatures has not been studied to date as no suitable test facilities have been available.

A new test facility has been designed and manufactured at Harwell in order that the performance criteria for filters and other ventilation system components can be evaluated under simulated high temperature accident conditions. The facility has the capability of heating air to temperatures not exceeding 550°C whilst exposing the filter under test to its rated air flow. Provision has been made to allow the filter to be dust loaded with characterised test dusts. The fan provided in the facility can produce differential pressures across the filter and housing of up to 400mm water gauge.

Provision has also been made for the measurement of filter efficiency using sodium chloride techniques whilst the filter is exposed to the hot air flow. Thus the factors affecting the performance of filters under condition of hot air flow, as might be predicted as likely to result from a fire in a nuclear facility, can be evaluated and limiting performance criteria for filters established. These data are necessary if full safety analyses for nuclear plants are to be carried out.

The initial programme of tests described in this paper has been drawn up to examine the general performance under hot dynamic conditions of the three most commonly used types of high temperature HEPA filters in UKAEA and BNFL. The tests are designed to enable the basic weaknesses and modes of failure to be identified. Additionally they aim to provide the basis for the design of further experiments to determine the limiting operating criteria in terms of temperature, differential pressure and time of exposure for high temperature HEPA filters.

II. Rig Description

The flow diagram for the Hot Dynamic Filter Test Rig is given in Fig.1 (see also Fig.2). The rig has been designed as a "once-through" rig, the air from the rig being exhausted to the environment. Air is drawn into the rig through an inlet leg which incorporates flow measurement instrumentation. Thus air flow passing through the filter can be determined in terms of mass flow rate at standard air conditions. From the inlet leg the air passes through a direct heating gas burner rated at 750kW. From the gas burner the air passes through a thermally insulated section of the rig to the filter housing and filter under test. This

Air inlet

Discharge to stack

Principal Features

1 Orifice plate
2 Air heater 750 kW
3 Expansion bellows
4 Aerosol / dust injection port
5 Stairmand mixing disc
6 Filter housing
7 Aerosol sampling pipe
8 Water cooled finned tube heat exchanger.
9 Suction fan (variable speed motor) and acoustic booth
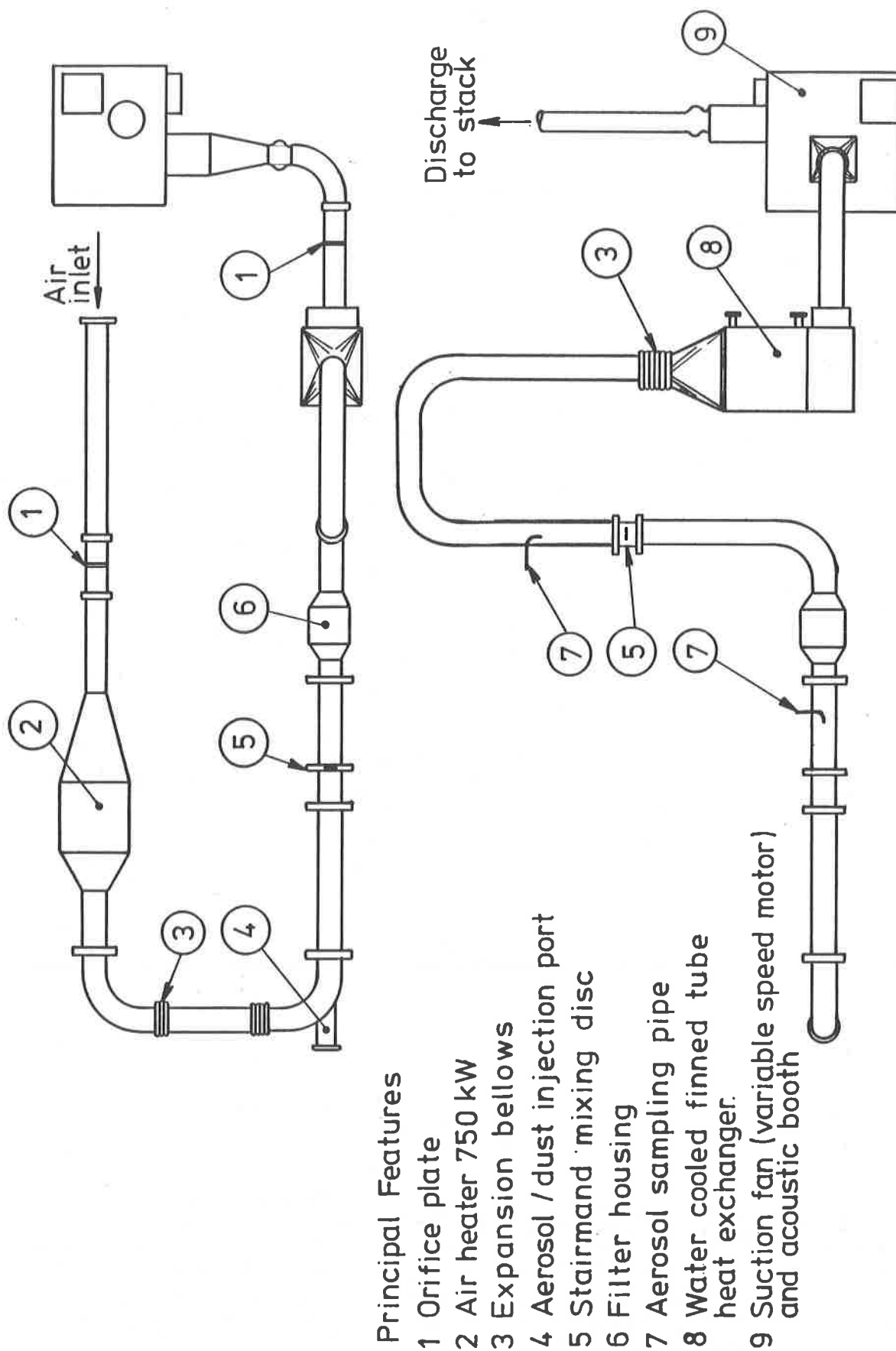
FIG.1 HOT DYNAMIC FILTER TEST FACILITY
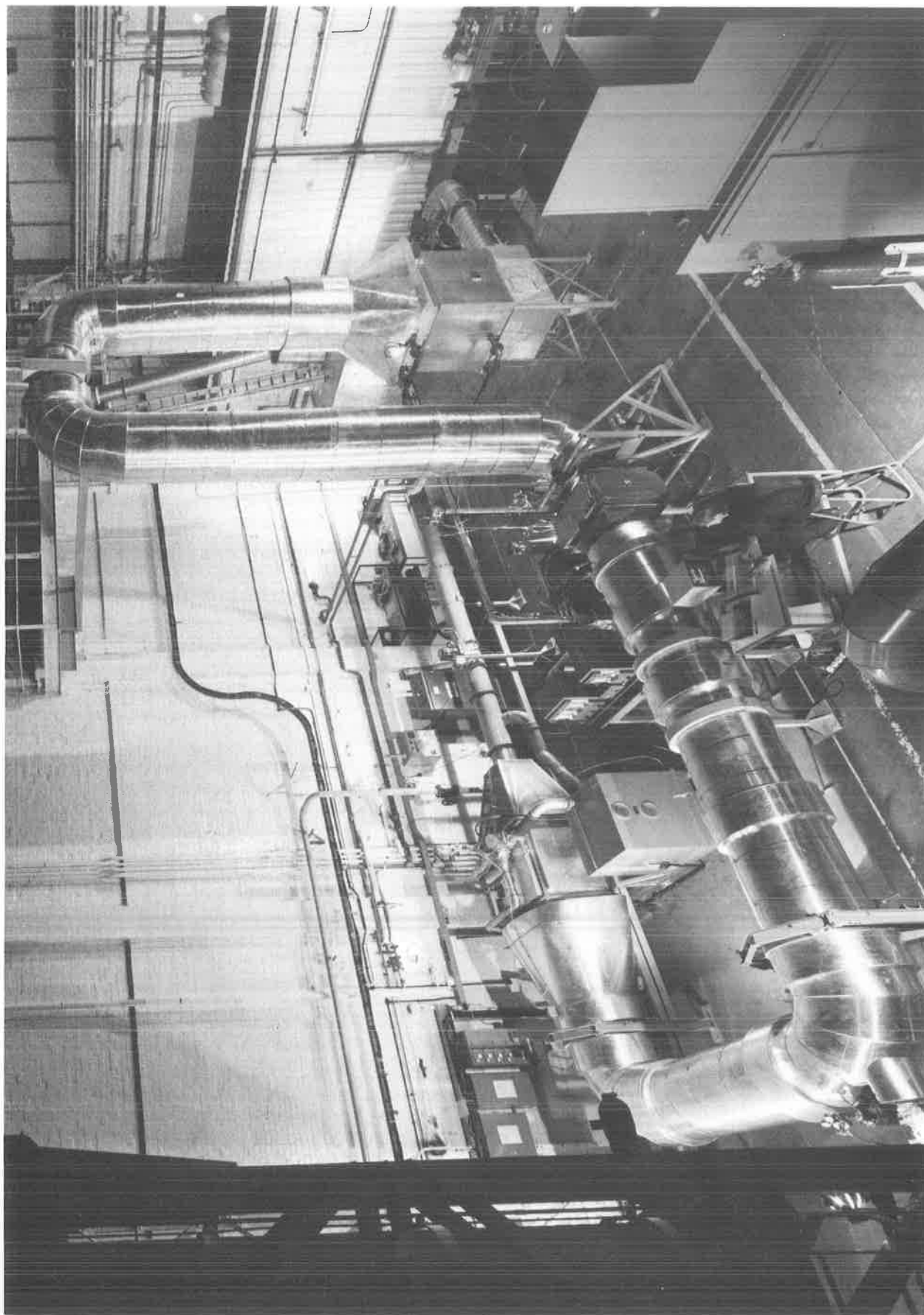
Fig. 2   Hot Dynamic Filter Test Facility

section of the rig is provided with injection and sampling tubes for the sodium chloride aerosol used for filter efficiency measurements. A "Stairmand" disc is included to enable good mixing of the aerosol into the air stream. Thermocouples are provided to monitor air and duct wall temperatures.

The filter housing is of conventional design, incorporating cam-bar clamping of the filter. The housing is deliberately left uninsulated. This enables realistic temperature gradients to be established in the filter and housing. Provision is made for measurement of the filter pressure differential and the housing and filter temperatures. The rig design is such as to allow other types of filter housing to be installed and tested as required.

The vertical ducting downstream of the filter housing includes the downstream sampling tube and a "Stairmand" disc to enable good mixing of the sodium chloride aerosol.

The heated air then passes through a water-cooled finned-tube heat exchanger, where its temperature is reduced to less than 50°C before it enters the fan. Between the heat exchanger and fan further instrumentation is provided to measure air volume flow rates and temperature.

The fan is powered by a d.c. thyristor-controlled variable speed motor. The performance of the fan is such as to enable up to 3400 standard m^3/h to be drawn through the rig against a differential pressure across the filter of up to 400mm water gauge. Finally the air is exhausted to the environment at roof level.

The rig is controlled by a programmable microprocessor control unit, which also acts as a data logger. The unit provides three term control of the gas burner and fan, thus enabling a wide range of experiments to be set up controlling airflow, temperature and pressure differentials.

The filter efficiency is measured using modified sodium chloride techniques. Although the sodium flame photometers and sampling/mixing arrangements conform to BS 3928, the challenge aerosol is generated using the portable sodium chloride aerosol thermal generator developed for in-situ testing. The aerosol is generated by vapourising a stick of sodium chloride in an oxy-propane flame under controlled conditions.

Provision has also been made to allow the test filters to be dust loaded using conventional dust dispensers. This will allow dust loaded filters to be tested. It is unlikely to prove practical to dust load at elevated temperatures, although this option is being evaluated.

III. Test Programme

The test programme has been designed to establish any basic weaknesses and modes of failure of three types of filter commonly used by BNFL and UKAEA. All three types are supplied against the high temperature specification AESS 30/93402, and have been demonstrated to meet its requirements in full.

The filter types used in these tests were:

Type 1 - This filter is of conventional deep-pleat construction, incorporating aluminium spacers between folds of glass fibre media. The seal between the filter pack and the steel case is effected by a compressed matt of glass fibre material or "dry seal". The filter measures 609 x 609 x 292mm and has an efficiency of ⊅99.95% (NaCl) at its rated flow of 1700 m^3/h.

Type 2 - Like the Type 1 filter, this filter is of deep-pleat construction with aluminium spacers. However, the seal between the filter pack and steel case is effected by a high temperature adhesive. The filter measures 609 x 609 x 292mm and has an efficiency of ⊅99.95% (NaCl) at its rated flow of 1700 m^3/h.

Type 3 - This filter is of mini-pleat construction, panels of pleated media being laid up in Vee formation within the steel filter case. The seal betwen the panels and case is effected using the same high temperature adhesive used in the construction of the Type 2 filter. The filter measures 609 x 609 x 292mm and has an efficiency of ⊅99.95% (NaCl) at its rated flow of 3000 m^3/h.

Temperature distribution within the filter and housing

Tests were carried out to determine the temperature distribution within a filter housing and filter when exposed to hot air flows. The tests were carried out at a constant mass air flow rate equivalent to 1700 m^3/h at 20°C through a Type 2 filter. The temperatures of various parts of the unlagged filter housing were recorded in addition to the filter pack bulk temperature and challenge air temperature. The changes in differential pressures generated across the filter housing as a function of air temperature were also measured.

Effect of hot dynamic air flow on HEPA filters

Two types of tests were carried out to investigate the effects of hot air at realistic flow rates on HEPA filters. For the first test, the air flow through the rig is maintained constant at the rated flow for the filter under ambient conditions as the air temperature is raised (Test 1).

For the second test, the air flow through the rig is set at the rated flow for the filter under ambient conditions, but the fan speed is maintained constant as the air temperature is raised (Test 2). Thus in this case mass flow rate falls as the temperature rises.

During these tests the mass air flow, differential pressure across the filter, and challenge air temperature were recorded. All filters were examined visually after the test.

Effect of Temperature on Filter Efficiency

It was considered that sodium chloride would be a more suitable challenge aerosol for efficiency measurements. This consideration was based on a proven technique for aerosol generation, namely controlled vaporising of a salt stick in an oxy-propane flame, which, by definition, involves the use of high temperatures.

The NaCl aerosol so produced was characterised by a LAS-X, laser aerosol spectrometer, for temperatures up to 500°C.

For the filter efficiency measurements, the aerosol was injected into the test rig, and upstream and downstream concentrations measured using conventional photometric techniques.

For the first set of tests the efficiency of the filters was measured at ambient temperature, at 500°C and finally after cooling back to ambient temperature. The associated pressure drops across the filter were also recorded.

A second set of tests were carried out over a range of temperatures up to 350°C.

Effect of hot dynamic testing on filter media strength

In order to quantify any reduction of strength in the filter media, samples were removed from filters after exposure to 500°C for 10 minutes. Tensile strength measurements were taken in the machine and cross machine direction and also in the machine direction across the pleat fold. Similar samples were taken from a new, untested filter for reference.

IV - Results

Temperature distribution within the filter and housing.

The temperatures measured within the filter and housing are given in Table 1.

Table 1 - Temperature distribution in filter and housing

	Temperature °C				
Rig Air	100	200	300	400	500
Filter Pack Centre	80	170	270	360	450
Filter gasket (glass fibre)	40	90	140	200	280
Upstream Transition	50	100	180	250	350
Housing body	20	40	80	120	200
Downstream transition	40	80	140	200	280
Differential Pressure across filter, mm water gauge	43	60	72	86	140

Effect of hot dynamic air flow on HEPA filters

The results for these tests are given in Table 2. In addition a plot of air temperature and differential pressure versus time for a typical run is given in Fig.7. It can be seen that increases in air temperature are followed by proportional increases in differential pressure for constant mass flow rate tests (Test 1). Fig.8, again a plot of temperature and differential pressure versus time, shows the effect of a filter rupture, where at approx 1100 seconds into the run, the differential pressure falls off rapidly during the temperature increase. Further differential pressure transients occur at 1600 seconds and 1900 seconds.

Table 2 – Effect of hot dynamic air flows on HEPA filters

Filter Type	Test Type	Flow s m³/h	Temp °C	Pressure Drop mm H₂0	Comments
Type 1 1700 m³/h dry pack	1	1700	25 100 200 300 400 500	29.2 38.1 51 68.6 84 107	Filter in good condition – centre channel opened up. Paper unbroken Fig.3
Type 1 1700 m³/h dry pack	2	1710 1650 1610 1550 1530 1510	22 100 200 300 400 500	28 35.6 45.7 58.4 71 81	As above
Type 2 1700 m³/h adhesive seal	1	1700	20 100 200 300 400 500	30.5 43.2 58.4 73.7 84 114	Paper torn along top edge of filter Fig.4
Type 2 1700 m³/h adhesive seal	2	1700 1680 1630 1580 1530 1500	20 100 200 300 400 500	30.5 40.1 53.3 60 76.2 120	Paper torn along top edge of filter
Type 3 3000 m³/h adhesive seal	1	3400	20 100 200 300 400 500	35.6 51 Filter pressure rising	Filter failure channels bowed and ruptured. Test terminated at 250mm H₂0 (450°C) Fig.5
Type 3 3000 m³/h adhesive seal	1	3000	20 100 200 300 400 500	33 48.3 66 100 145 250	Filter channels bowed – paper appears to be intact – high pressure drop Fig.6

Fig.3   1700 m^3/h dry pack filter after dynamic test at
500°C showing pack deformation.
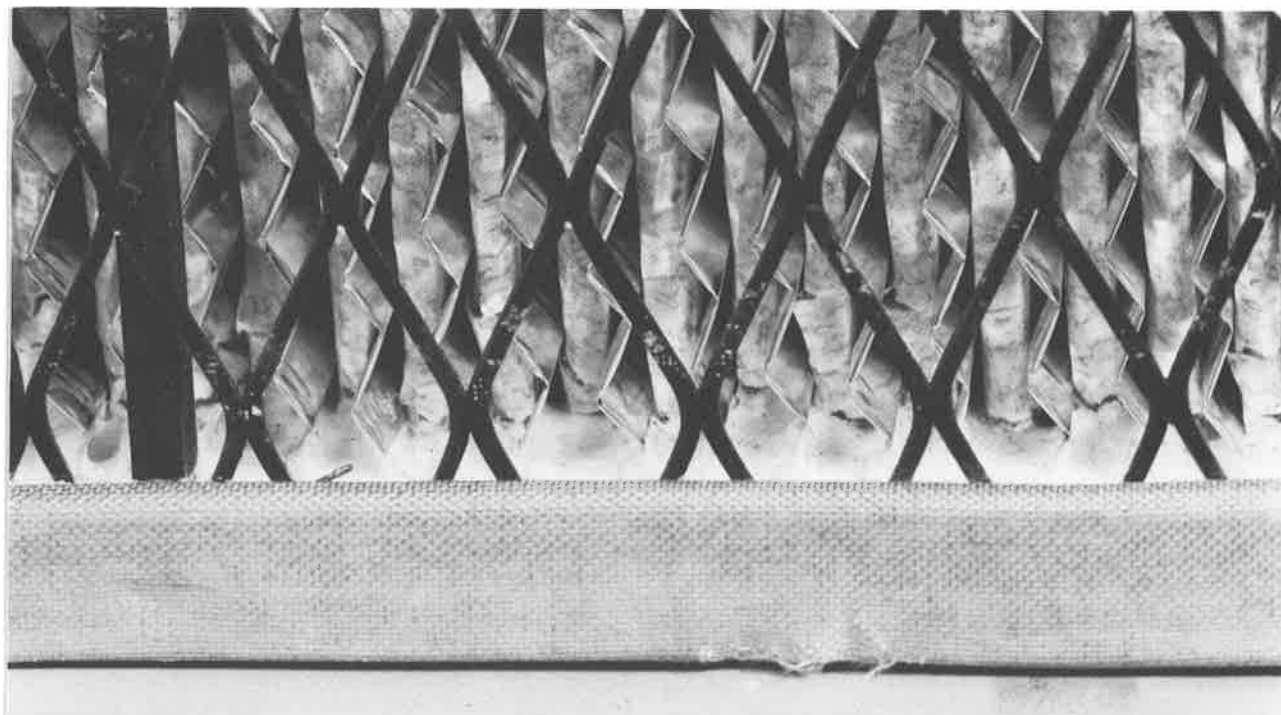
Fig.4   1700 m^3/h adhesive seal filter after dynamic test
at 500°C showing media damage.
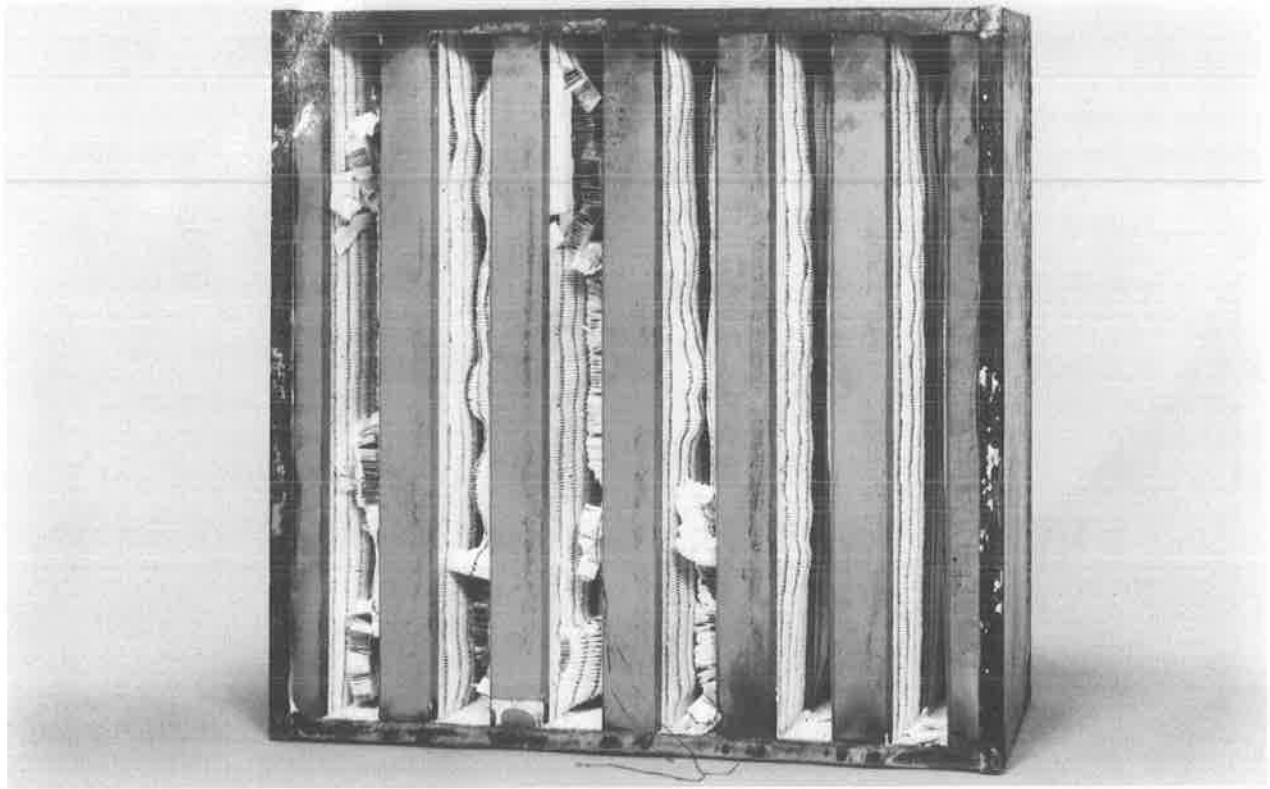
Fig.5   3000 m³/h filter after dynamic test
          at 500°C showing rupture of panels
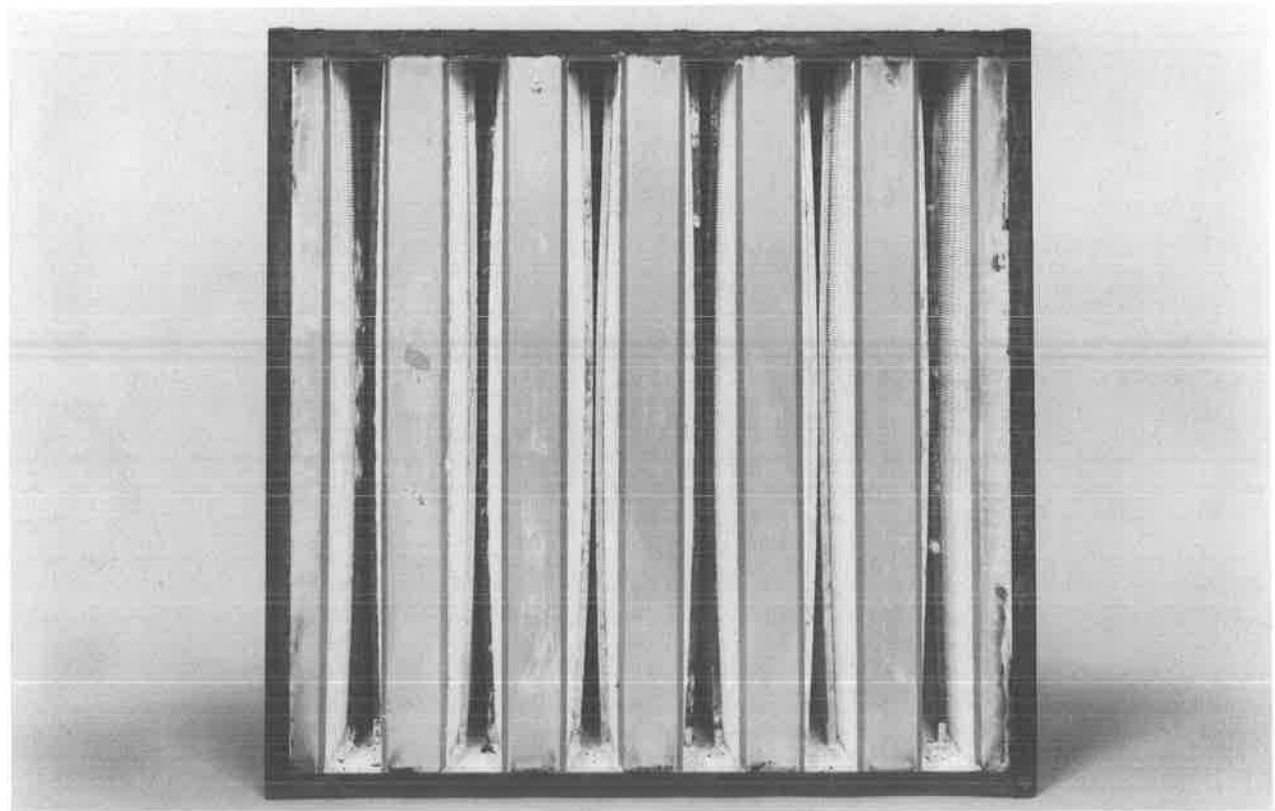
Fig.6   3000 m³/h filter after dynamic test
          at 500°C showing panel deformation.
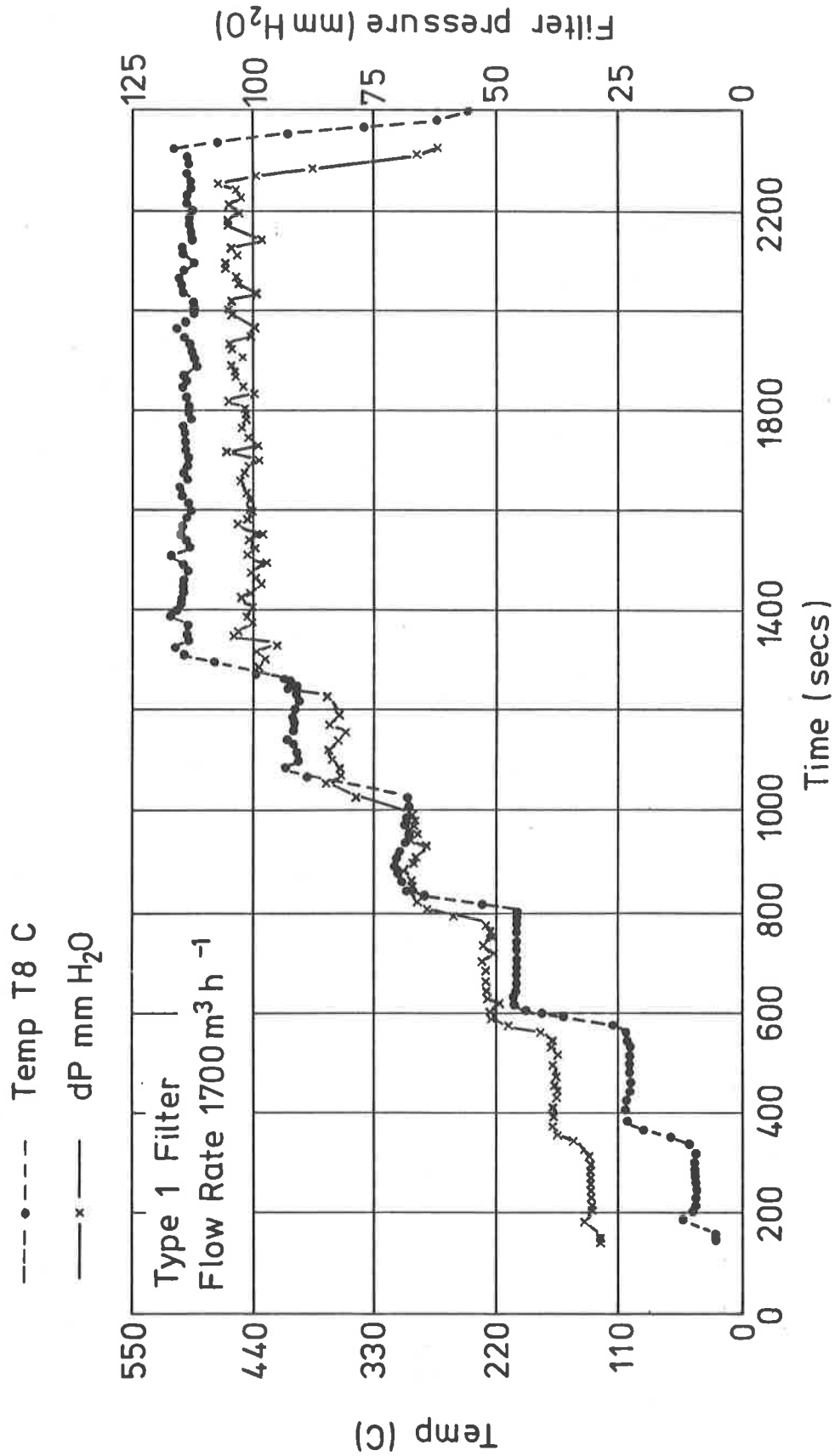
FIG.7. TYPICAL VARIATIONS IN TEMPERATURE AND PRESSURE DIFFERENTIAL ACROSS FILTER AT CONSTANT MASS FLOW RATE
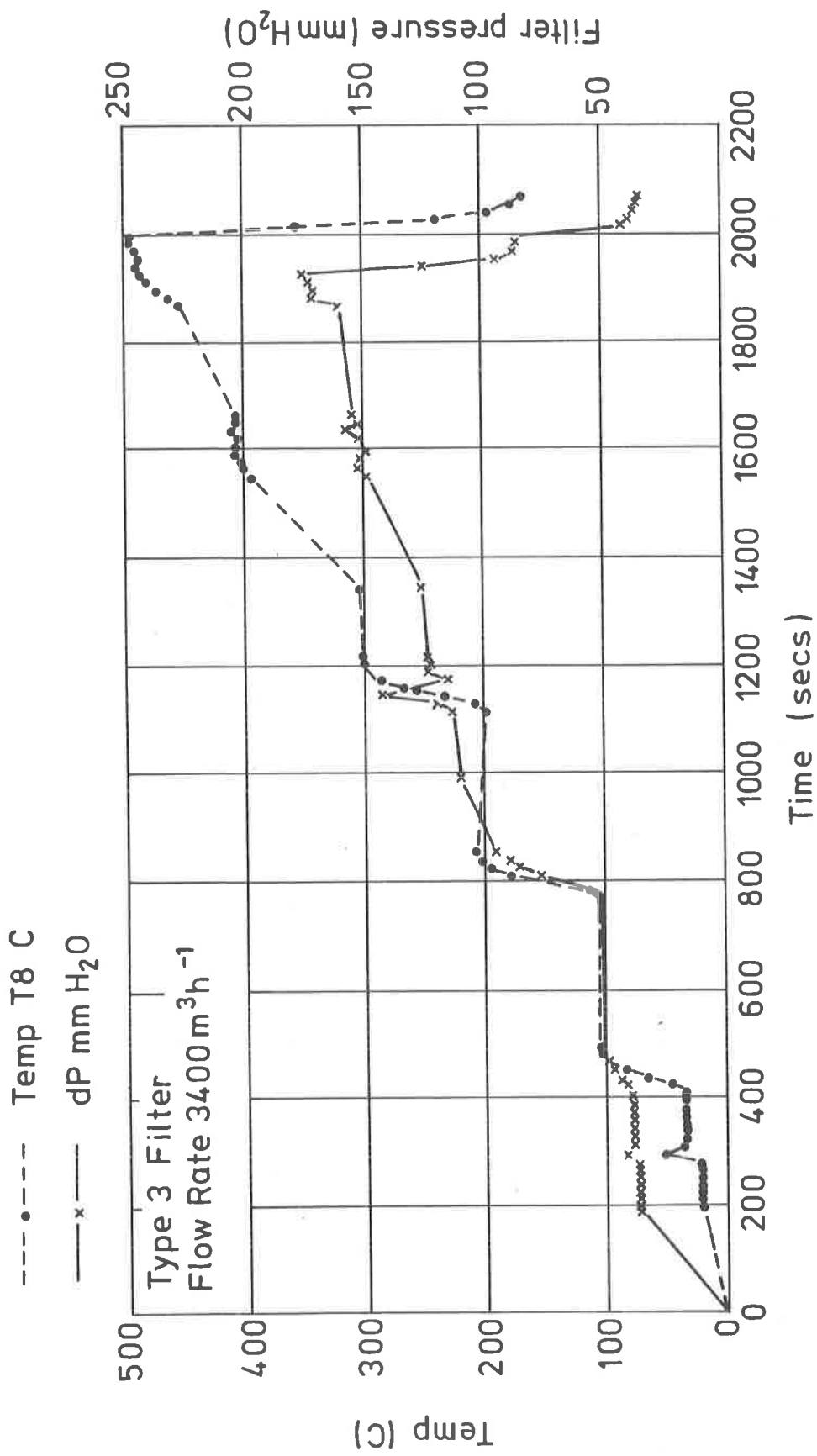
FIG. 8. VARIATIONS IN TEMPERATURE AND PRESSURE DIFFERENTIAL AT CONSTANT MASS FLOW RATE SHOWING EFFECT OF FILTER DAMAGE

All samples of the deep-pleat filters suffered from a relaxation of the pack within the filter case resulting in the pack becoming uneven and flow channels being unsupported.

No media damage was visible on the Type 1 filters. A disturbing feature of the adhesive sealed (Type 2) filter was a tendency for the filter media to split, or tear, along the top and bottom of the pack close to the adhesive seal (Fig.4).

The mini-pleat filters (Type 3) suffered from severe distortion of the panels and support bars and a corresponding increase in differential pressure (Fig.6). In one case this led to rupture of the panels,(Fig.5).

In all the tests, it appeared that the binder was driven off the filter media once temperatures exceeded 300°C. This was evidenced by the presence of "smoke" in the effluent gas and a strong odour.

Effect of temperature on filter efficiency

The size distribution of thermally generated NaCl as measured by a LAS-X spectrometer is given in Table 3. The size distribution for NaCl aerosol to BS3928 (Collison atomisers) is included for reference.

Table 3 - Size distribution of sodium chloride aerosols

Generator	Rig	Temperature (°C)	GMD (μm)	MMD (μm)	GSD (μm)
Collision	BS3928	20 (room)	0.19	0.47	1.75
Salt stick	High temp	20 (room)	0.13	0.14	1.15
		100	0.14	0.15	1.18
		200	0.14	0.15	1.18
		300	0.14	0.15	1.17
		350	0.14	0.15	1.18
		500	0.14	0.15	1.16

These results show that the aerosol is reasonably uniform over the full temperature range considered (20-500°C).

The results of filter efficiency measurements at 500°C are given in Table 4.

The results of measurements over a range of temperatures are given in Table 5.

Table 4 - Efficiency Measurements at 500°C

Filter Type	Test Type	Flow m³/h @500°C	Penetration % @20°C	Penetration % @500°C	Penetration % @20°C	Pressure Drop mm H₂O @20°C	Pressure Drop mm H₂O @500°C max	Pressure Drop mm H₂O @20°C	Comments
Type 1 1700m³/h Dry Pack	1	1700	0.028	0.25	0.25	30	107	-	
Type 1 1700m³/h Dry pack	1	1700	0.031	0.45	0.15	28	109	-	Filter in good condition - centre channel opened up - paper unbroken. Fig.3
Type 1 1700m³/h Dry pack	2	1450	0.05	0.16	0.25	30	86	-	
Type 1 1700m³/h Dry pack	2	1500	0.038	0.2	0.16	28	81	-	
Type 2 1700m³/h Resin adhesive	1	1700	0.003	0.2	0.15	33	-	-	
Type 2 1700m³/h Resin adhesive	1	1500	0.004	0.5	0.6	33	96	1.5	Paper tearing along top and bottom edges of filter. Fig.4
Type 2 1700m³/h Resin adhesive	1	1500	0.013	0.9	1.1	30	147	2.4	

Table 5 - Efficiency Measurements as a function of temperature

Filter No	Test Type	Flow m³/h	Temp °C	Pressure inches H_2O	Penetration %	Comments
Type 2 Resin adhesive	1	1700	20 100 200 300 350	– 2.0 3.1 3.9 4.9	0.02 0.018 0.015 0.01 0.15	No noticeable damage in filter after 500°C excursion
Type 2 Resin adhesive	1	1700	20 200 300 350	– 3.1 4.1 5.1	0.007 0.004 0.004 0.025	No noticeable damage to filter after 500°C excursion
Type 2 Resin adhesive	1	1700	20 100 200 300 350	– 2.3 3.2 3.9 4.7	0.005 0.008 0.03 0.12 0.4	Filter $\triangle \rho$ increasing rapidly from 400°C to 500°C test terminated. Filter failed (Fig.9)

Effect of hot dynamic testing on filter media strength

The results of tensile tests on the filter media removed from tested filters are given in Table 6.

All examples are of the same filter media grade.

Table 6 - Tensile strength of filter media

Tensile Strength (kN/m)

Sample	Filter Type 1	Filter Type 2	Reference Sample
Machine Direction	0.16 – 0.2	0.02 – 0.11	0.94 – 1.16
Cross Machine Direction	0.09	0.05 – 0.09	0.58 – 0.68
Machine Direction across pleat fold	0.02	0.02	0.18 – 0.54

<center>V.   Discussion of Results</center>

Temperature distribution in filter and housing
_____

The heat losses from the surfaces of the filter housing produce
significant reductions in temperature from that of the bulk challenge air
temperature. Of significant importance is the relatively low temperature
of the gasket seal between the filter insert and housing which suggests
that a high temperature elastomer gasket material such as silicon rubber
will have a satisfactory performance under these conditions.

The high differential pressure generated across the filter is due to
increased volumetric flow rate and changes in temperature dependant
properties such as viscosity and density. This increase was calculated to
be between 5 and 6 times the initial pressure drop by Stenhouse[3],
and compares well with the increases measured.

Effect of hot dynamic air flow on HEPA filters
_____

Tests on all filters were accompanied by the production of smoke and
odours in the effluent air stream at temperatures in excess of 300°C.
This was due to the loss of media binder at these temperatures. Binder
loss was anticipated by the media manufacturers, along with a significant
reduction in media strength of perhaps up to 60%[4]. It is also
predictable that there would be some shrinkage of the media and softening
of the aluminium spacers at the elevated temperatures. These factors
combine to cause the relaxation of the filter pack for both Type 1 and Type
2 filters, although this was more noticeable for the Type 1 (dry pack)
filter. Close examination of the Type 1 filters after testing revealed no
noticeable media damage and efficiencies measured give no serious cause for
concern. This type of filter would therefore appear to be satisfactory for
use at temperatures and differential pressures recorded in these tests.

The combination of media shrinkage and softening of the aluminium
spacers is however, less well accommodated by the Type 2, adhesive seal,
filters. The tearing of the media close to the adhesive, noticed on some
50% of samples tested in this programme, gives cause for concern, as it can
rapidly lead to the complete collapse of the filter and subsequent loss of
air flow(Fig.9),

The Type 3 high capacity mini-pleat filters were apparently not
affected by the paper shrinkage effects. With this construction, the
weakness of the filter would appear to derive from the distortion of the
pleated panels resulting ultimately in complete blockage of the vee
formation in the downstream section of the filter. It would therefore be
necessary to increase the degree of support given to the pleated panels to
prevent this distortion if satisfactory performance at these temperatures
is required.

Effect of temperature on filter efficiency
_____

The measurements of particle size distribution of the thermally
generated NaCl aerosol shows it to be substantially uniform over the
temperature range 20-500°C.

<center>1122</center>
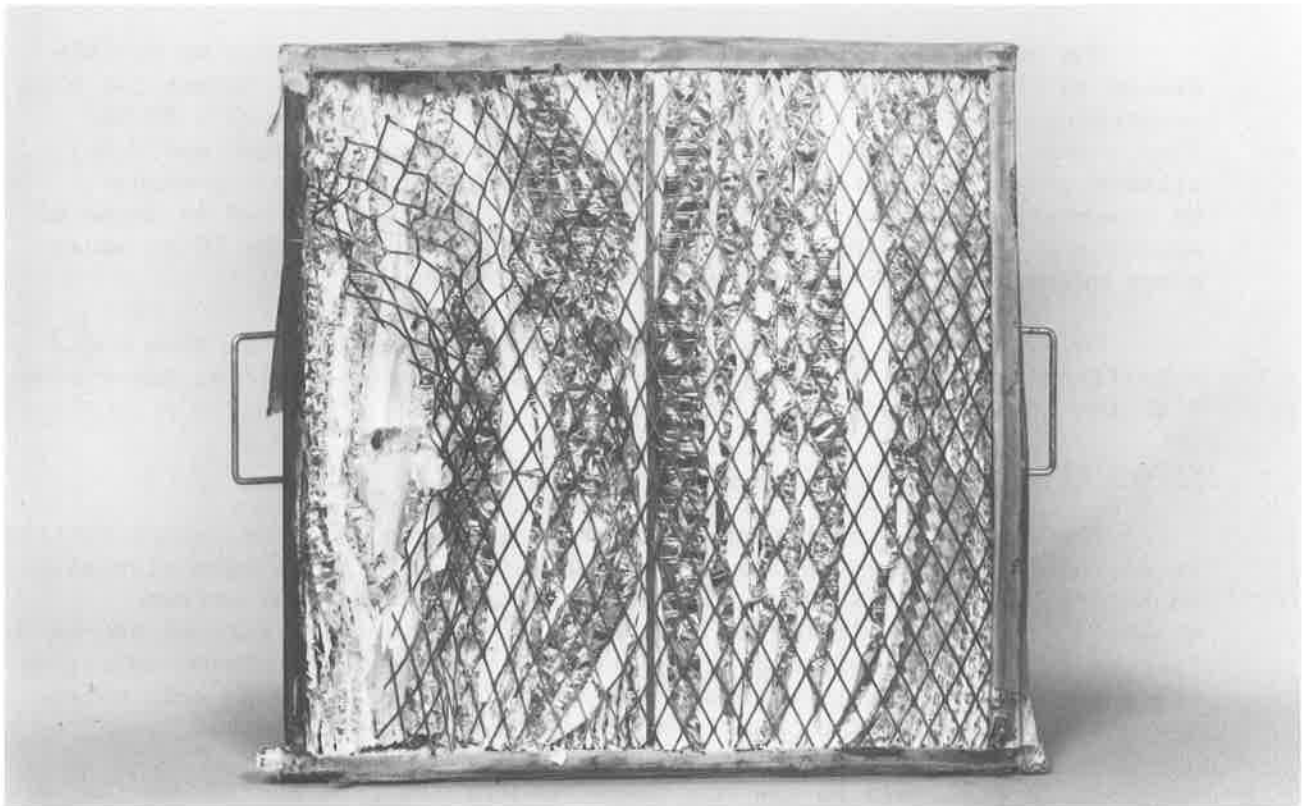
Fig.9   1700 m^3/h adhesive seal filter after dynamic test
to 500°C showing complete failure and blockage.
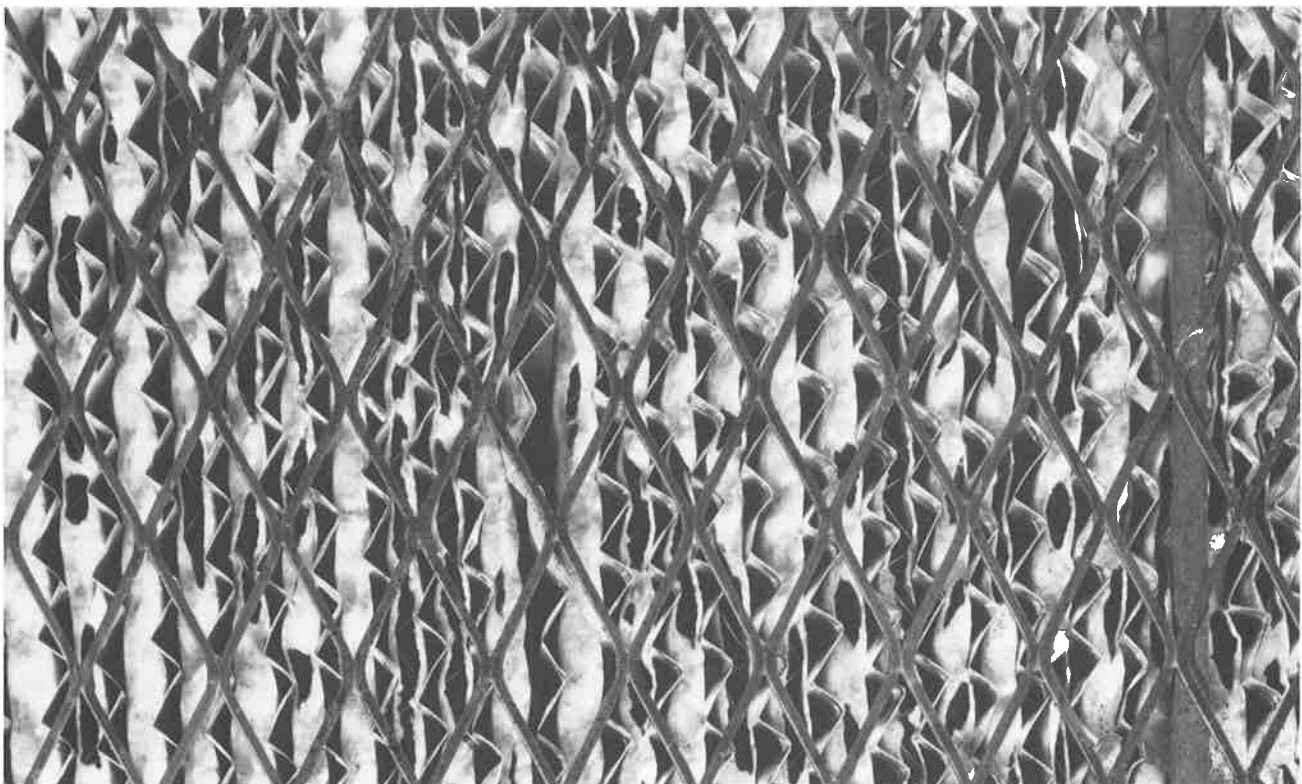
Fig.10   Failure of filter media caused by hot
dynamic testing.

The measured efficiency of filters at 500°C, even where no visible damage to the media occurred, was substantially worse than before the high temperature excursion. Typical values are in the range 99.9% - 99.5%. They should be compared with > 99.95% allowed before the test and > 98% allowed after the test in the purchasing specification[1]. It should be remembered however, that several of the Type 2 filters had evidence of severe media damage at pressure differentials well below the 305mm water gauge required by the specification.

The variations of efficiency with temperature, Table 5, show a significant increase in penetration above 300°C, which could be associated with the loss of binder from the media.

Effect of dynamic testing on filter media strength

The results of the tensile tests of media removed from tested filters is disturbing. Simple handling of the media revealed it to have virtually no strength, which was borne out by the tensile tests. The extreme weakness across the pleat fold was verified by some tests carried out on filters during commissioning of the rig which resulted in random splitting along the pleat folds throughout the filter (Fig.10) although this effect was not reproduced in the more controlled tests reported here.

It is difficult to see how these results can give confidence that a filter can withstand significantly higher differential pressures than those recorded at these temperatures.

VI Conclusions

The high heat loss from the outer surfaces of the filter housing and adjacent ductwork transitions should enable temperature resistant elastomers such as silicon rubber to be used with confidence as gasket and seal materials.

These initial results would indicate that there are significant advantages in the dry pack filter construction over the use of adhesive seals. Although the dry pack filter exhibits a relatively loose media pack in its case after exposure to hot gases no actual damage to the media has been recorded. Provision of a suitable support grille on the downstream face of the pack should be sufficient to prevent complete displacement of the pack from the case.

The use of adhesives, although temperature resistant in their own right, appears likely to result in damage to the filter media, with the attendant possibility of a complete collapse of the filter pack.

The mini-pleat design of filter requires improvements in the method of supporting the panels to prevent gross distortion and damage.

The strength of glass fibre filter media currently specified gives cause for concern when subjected to hot dynamic testing of complete filters. Although the degree of deterioration in efficiency is acceptable, the extremely low tensile strengths measured for media samples is a source of anxiety where accident conditions are likely to give rise to high temperature exhaust gas streams and associated differential pressures.

1124

There would appear to be a significant reduction in the filtering efficiency of HEPA filters after exposure to temperatures in excess of 300°C, even when no visible damage to the media occurs. This deterioration would therefore appear to be a function of the media used rather than the method of construction of the filter.

Further work is required to determine the safe limiting operating parameters for HEPA filters in terms of temperature, time and differential pressure. Such data are essential if full hazard assessment studies are to be carried out.

The present method of specifying filter performance, namely static oven test followed by dust loading, is inadequate in predicting the likely performance of filters under high temperature accident conditions.

Acknowledgements

The authors wish to record their thanks to Dr J I T Stenhouse, Loughborough University, and Mr A Marshall, Frazer Nash Ltd for their assistance in designing the test facility. Also they wish to thank Mr D C Stevens and Mr D J Partridge for their assistance in carrying out this programme of work.

References

1)   AESS 30/93402, November 1982. Filter inserts, high efficiency particulate air (HEPA).

2)   BS 3928:1969. Sodium flame test for air filters.

3)   Dr J Stenhouse, Loughborough University - private communication.

4)   Mr J Holt, Evans Adlard Ltd, verbal communication.

DISCUSSION

DORMAN: Mr. Pratt and I have discussed this paper over lunch and I can assure you that the temperature between us reached well over the 500 Celsius he has been talking about. From Table 4, it appears that, after heating, the filters had a higher penetration than before heating. And they were, therefore, damaged. I am, however, concerned about the results at 500°C. Many years ago, John Dyment and I carried out tests on paper sheets with the Collison-generatored sodium chloride aerosol, and we found that the penetration dropped as the temperature rose to between 300 and 400, and then there was a marked increase, very, very rapid, something like 1%, just over 400. This was due to the vapor pressure of sodium chloride. We checked physical chemistry books on vapor pressure and found that the penetration we were getting on our equipment was exactly what could be predicted from the vapor pressure curve of sodium chloride. In our tests, after we applied heat and found this high penetration, we then cooled the paper and found it was just as good after it had been heated as it was before we started. I see no reason why the thermally-generated sodium chloride aerosol should behave differently from the Collison-generated aerosol. I would like to ask Mr. Pratt these questions. Is he certain that his 500°C results were true aerosol penetrations and not due to vapor? Did he check the vapor pressure data for the sodium chloride? Now I am not questioning the fact that the seals are damaged at 500°C, but I don't think he can quote penetrations at 500°C as due to deterioration of the paper other than by tears and ruined seals. To sum up, sodium chloride is not an aerosol for making tests that match above 300°C. Any figures found above that temperature are just not valid.

PRATT: I fully expected, Richard, that you would make a statement for the record of that sort. And far be it for me to dare to usurp your authority in the field of sodium chloride aerosols and associated equipment. What I will say is this: we did do tests using a particle counter and we did record that the aerosol generated or taken from the rig was of the same size and size distribution throughout the experiment. When you come to the question of vapor pressure, we looked at it and concluded that the time of exposure of the aerosol at the temperatures in the duct, something less than a second, was probably small enough that it would not significantly alter the size of the aerosol. Thirdly, I would like to explain the 500°C limit for the benefit of the USA audience. The 500°C limit comes about, for our experiments, because we are looking into replacing our standard static government test at 500°C with a dynamic test and we felt it would be foolhardy to construct a rig that could not reproduce the same temperature. However, I would suggest that if the UK people in the field were forced into a position, they would say that it is extremely unlikely that temperatures of that sort would be reached in a nuclear facility. And if they were, you would be more worried than just the temperatures that reached the filter. So, I would, perhaps, be prepared to accept that 500°C efficiency measurements could have an error of uncertainity in them. If one talks of more realistic temperatures, and I would

suggest, again, on a personal basis, that it would run about 350°C as a limit of real interest, then we will continue using sodium chloride at that level.

DORMAN: If you limit yourself to 350°C, I am quite in agreement. I object to putting it at 500°C when it is not quite worth above 350°C.

PRATT: No comment.

DYMENT: I comment on Mr. Dorman's statement firstly, in that I believe 440°C to be the upper limit for use of NaCl as a challenge aerosol for testing low penetration HEPA filters. According to Table 5 in the paper, maximum temperature of efficiency measurements appears to be 350°C. Correct me if I am wrong in that reading.

PRATT: You are correct in your reading of Table 5, but there is another table which shows results up to 500°C. There were two sets of tests. The initial tests were all done at ambient, before and after the filters were heated to 500°C. The second set of tests was more detailed, conducted in steps of 100°C, up to 350°C.

DYMENT: Mr. Pratt's Table 4 results, at 500°C, all showed a high penetration, >0.1%, and the high background effect of NaCl vaporization could have been masked. If I can refer to earlier experiments, which the previous speaker mentioned, I recall that the filter paper shrank and, as a result, splits occurred. In order to do experiments at a temperature above about 300-350°C, it was necessary to use pre-heated, pre-shrunk, specimens of paper. Whether this is a hint to manufacturers of high temperature filters, I leave it to them to decide. A final comment on the extreme weakness across the fold in the paper reported by Mr. Pratt in the last section of Part V, I consider that paper shrinkage could cause stress peaks at these positions.

REPORT OF MINUTES OF
GOVERNMENT-INDUSTRY MEETING ON FILTERS,
MEDIA, AND MEDIA TESTING

W.L. Anderson
Technical Consultant
La Plata, MD

Many of the accomplishments of the air filtration programs achieved thus far have been due to the efforts of an informed working group concerned with high efficiency filters. The existence of this group has now spanned eleven conferences and has drawn expanded attendance and technical contributions at each one. From the original handful of participants and their open and often argumentative mode of operation, the sessions have progressed to an invited audience with a permanent chairman and a prepared agenda.

The most recent session of this group was held this past Sunday afternoon, August 11, and was devoted to a series of discussions on current interest subjects. At this, the 18th Conference, over 100 attendees assembled in the meeting room. Although the major portion were from industry, government agencies, academic and contract investigators, over eight international groups were represented. All of the facets of the industrial complex were present, from the basic fiber suppliers, through media producers and, finally, to the filter unit fabricators. Various test facilities and evaluation groups also contributed to the overall process. R & D organizations from government and national laboratories, and academic institutions, all contributed status reports on work currently underway. Users at various levels expressed their problems and actively participated in the discussions.

It is the intent to review, in abstract form, the items of deliberation. Each item will be addressed in the order of their discussion, and not in any priority. At the recent session, the following seven subjects were discussed.

Evaluation of Methods, Instrumentation and Materials in QA Filter Penetration Testing

Ron Scripsick from Los Alamos described their work on alternate equipment and materials for penetration testing of HEPA filters.. He covered a highly diversified field of investigations that included "hot DOP" generators, OWL particle size analyzers, light scattering photometers, Laskin generators, aerosol sizing by both laser spectrometers and condensation nuclei counters, and aerosol diluters. Examples of HEPA testing, together with size and size distrubtion data, were given for the various generators and sizing devices. His presentation indicated that great strides have been made in knowledge accumulation, but futher work is needed before test equipment can be specified and appropriate materials/procedures developed. The complete paper is attached as Appendix A.

DOE Filter Test Programs - Policy for the 80's

Jim Bresson from Albuquerque Operations, DOE, brought us up-to-date on the documentation efforts of the Test Facility Standards Writing Group. He reported that the group had completed their work on documentation related to testing policy, procedures, quality assurance, and filter specifications. Three of the standards are awaiting final approval (expected momentarily) and the fourth has already been issued. He described the total development/review process and copies of all four documents were made available to the group. He discussed the major items involved, and gave the rationale for significant decisions affected by the standards. His group should be commended for completing a job in less than 3 years that formerly

1128

had taken as long as 10. The complete paper is attached as Appendix B.

Intermediate Results of a One-Year Study of a Laser
Spectrometer in the DOE Test Facilities

Sid Soderholm reported on the data accumulated thus far on the use of the LAS-X at the DOE test facilities. This data was intended to acquire aerosol size distributions at each site and to compare the FTF test aerosols to current and proposed test standards. His major conclusions were: (1) LAS-X can operate in the facility environment, (2) backup for the LAS-X will be required for continuous operations, (3) FTF test aerosols are not monodisperse as stated in specifications and standards and (4) aerosols at each FTF were consistent with time but somewhat different between facilities. Final conclusions and recommendations are still to be developed; impact and further action will then be assessed. The complete paper is attached as Appendix C.

Calibration and Use of Filter Test Orifice Plates

Mr. Fain from Martin Marietta Energy Systems, Oak Ridge, described the theory and calibration process of the large orifice plates (CFM) that are used as secondary standards by the test facilities and industry. He showed specific calibration data and reported essential data for orifice calibrations. Comparisons between supposedly identical orifices were also given. Discharge coefficients were also determined to establish measurement validity. He concluded that the results were good and the use of the plates should provide agreement among facilities. He outlined the pitfalls that might be experienced during use and suggested that more modern devices for flow measurement should be considered. He supplied tables to allow temperature and atmospheric pressure corrections for mass/volume flow conditions. The complete paper is attached as Appendix D.

CONAGT's Nuclear Carbon Roundrobin Test Program

Mel First from Harvard described the politics and procedures of the CONAGT carbon test program and reported on the most recent roundrobin test program. He distributed data sheets on the results from the 15 participating organizations. He   analyzed the results in a rigorous manner and after using an elimination process involving three mean calculations and standard deviations, concluded that only two groups were close to the final calculated mean. This data has been referred back to the respective groups and NRC.

Ralph Bellamy from NRC reported that an outside expert has been commissioned to review the data, and procedures by which it was obtained, and recommend corrective methods/procedures to assure uniformity of testing. The combined papers are attached as Appendix E.

Proposed New Techniques for Measurement of
Aerosol Size and Penetration

Dr. Kim from Leigh University described his current work under an Army contract. This investigation involves the use of light scattering spectroscopy followed by extensive computer signal processing at various wave lengths. His earlier work has demonstrated the signal response to both particle size and concentration. He presented a complex theoretical analysis together with experimental data to demonstrate the possibility of useful instruments/techniques for aerosol work. This investigation should be considered preliminary and considerable work needs to be accomplished before comparison with existing laser spectroscopy can be meaningful. It will be interesting to see whether this technique can be used under test conditions that may differ as much as 8 orders of magnitude and with broad complex size distributions. The complete paper is attached as Appendix F.

Army Programs at Los Alamos

Sid Solderholm reported on investigations that Los Alamos is conducting for Edgewood Arsenal. Different concepts of aerosol generation and particle size measurement, together with substitute generator materials, are the Army's major concerns. He described briefly the flash evaporator/condenser and the multiple angle size analyzer used earlier under an Army - Arthur D. Little contract; problems and preliminary results were given. Initial data on PEG (glycol) and oleic acid as a DOP substitute were given and DOP degradation products were mentioned in comparison with them. Since this effort is just beginning, he outlined future plans and project direction. Hopefully, by the next conference, definite procedures/recommendations/instruments will be forthcomming.

In conclusion, it should be re-emphasized that this informal working group, with its diversified representation, provides a means for a comprehensive and expedient solution to the problems of the HEPA industry. The total effort has proven invaluable because it permits the surfacing and exposure of problems that might otherwise be lost in the quagmire of bureaucracy and management. The meetings are intended to be, and actually are, a working level distribution of data and expertise as well as a progress report of ongoing projects in the particle filtration areas. To this end, the group feels that they have been successful and future sessions are contemplated.

Appendix A

EVALUATION OF METHODS, INSTRUMENTATION AND MATERIALS PERTINENT TO QUALITY ASSURANCE FILTER PENETRATION TESTING*

Ronald C. Scripsick, Sidney C. Soderholm and Marvin I. Tillery
Aerosol Sciences Section
Industrial Hygiene Group
Los Alamos National Laboratory
University of California
Los Alamos, New Mexico 87545
USA

Abstract

Every high efficiency aerosol filter used in the United States Department of Energy (DOE) facilities is quality assurance (QA) tested at one of the DOE filter test facilities prior to installation. This testing presently includes measurement of filter penetration at rated airflow using a "hot DOP" aerosol generator, an "Owl" aerosol size analyzer, and a scattered-light photometer aerosol concentration monitor. Alternative penetration measurement methods for testing size 5 high efficiency aerosol filters which have rated airflow capacities of 1000 cubic feet/min (cfm, ~28 m^3/min) are being studied at Los Alamos National Laboratory. These methods are intended to take advantage of commercially available aerosol instrumentation.

A penetration test using a polydisperse aerosol produced with a modified Laskin nozzle aerosol generator was found to have promise as an alternative to the present test method. Such a test eliminates the difficulty in producing a monodisperse challenge aerosol, and takes advantage of state-of-the-art aerosol sizing instruments. Challenge aerosol produced in a modified size 5 filter test system operating at ~1000 cfm (~28 m^3/min) had a concentration of ~5 mg/m^3, a count median diameter of ~0.18 µm and a geometric standard deviation of ~1.4. The aerosol size was measured using an uncalibrated aerosol diluter.

Aerosol sizing and concentration measuring capabilities of a laser aerosol spectrometer (LAS) were evaluated with respect to the needs of QA filter penetration testing. For aerosols with diameters between ~0.15 µm and ~0.4 µm, the size measured by the LAS was within 10 per cent of the size indicated by an electrostatic classifier (EC) and the manufacturer of monodisperse polystyrene spheres (PSS). For aerosols with diameters below ~0.15 µm, the LAS size was within 20 per cent of the EC's size and the PSS manufacturer's size. Aerosol concentration measurements made by the LAS at levels up to ~3000 particles/cm^3 compared well with measurements made by a condensation nucleus counter using both polydisperse and monodisperse test aerosols.

An aerosol diluter was selected and evaluated for use with the LAS in making filter penetration measurements. The coefficient of variation associated with dilution ratio measurements at specific LAS measured aerosol sizes was less than 12 per cent for particles with measured diameters between ~0.1 µm and ~0.4 µm.

An example of filter penetration measurements of size 5 filters operated at ~1000 cfm (~28 m3/min) made using this alternative

filter test system is presented. The size of maximum penetration was observed to be in the vicinity of 0.2 µm diameter. In this example, number penetration, as a function of aerosol size, ranged from ~0.003 per cent to ~0.007 per cent with coefficients of variation associated with these measurements ranging from ~5 per cent to ~11 per cent. Average number penetration of ~0.3 µm diameter particles was ~0.003 per cent.

Potential alternative test materials were scrutinized with respect to certain toxicological and physical criteria. Certain of these alternative materials were selected for further evaluation. Results of this evaluation and findings cited in the literature indicate that the selected materials could be easily adapted for use with the modified Laskin aerosol generator.

I.   Introduction

The method for quality assurance (QA) penetration testing of size 5 high efficiency particulate air filters at Department of Energy (DOE) filter test facilities (FTFs) comes largely from military standard MIL-STD-282.[1] This standard specifies a penetration test using a thermally generated "monodisperse" di-2(ethylhexyl) phthalate (DEHP, also known as DOP) aerosol with a particle size of 0.3 µm diameter. The particle size is determined by an Owl particle size analyzer. A scattered-light photometer (SLP) is used to determine aerosol penetration.

Since the adoption of MIL-STD-282, there have been many advances in aerosol technology. These advances have potential for beneficial application to QA penetration testing in the areas of reproducibility, accuracy, ease of operation, and development of more detailed and meaningful filter performance data. In addition, recent findings by the National Toxicology Program (NTP) have raised some questions about the toxicity of DEHP.[2] For these reasons, an investigation of alternative QA filter penetration test methods, aerosol generators, aerosol monitors and aerosol materials was undertaken at Los Alamos National Laboratory.

Evaluation of Current Test System

In terms of detecting defective filters, indications are that the current test system is performing adequately. Our review of the system suggested certain changes that should improve the defensibility of the method's technical merit and the test system's operability.

Problems with the method's technical merit center around the finding that the FTF tests are being conducted using polydisperse aerosol challenges.[3] This leads to ambiguities in the precise interpretation of penetration results measured by the SLP and aerosol size indicated by the Owl.

Operational problems associated with the current test method include:

1. Precise control of the test aerosol is difficult; hot DEHP can catch fire; and thermal generation of DEHP has been linked to the production of decomposition materials.[4]

2. DEHP has been identified as a carcinogen in laboratory animals.[2]

Alternative Test System

An alternative test system was developed that takes advantage of the commercially available aerosol technology and has the promise of eliminating the problems outlined above. The system uses a modified Laskin nozzle aerosol generator to provide the filter challenge.[5] This generation system is relatively easy to operate, has no potential for causing fires, and is expected to produce no decomposition materials. This unit is also less expensive to manufacture than the currently used thermal generator.

A laser aerosol spectrometer (LAS, model LAS-X, PMS Inc., Boulder CO) has shown the greatest potential for fulfilling the aerosol monitoring needs for the alternative test system. The LAS combines the function of the Owl and SLP. It is capable of measuring penetration at a specific size or over a range of sizes.

All evaluations of the alternative test system conducted thus far have been performed using DEHP. Alternatives to DEHP have been identified in terms of certain toxicological and physical criteria. Enough information has been obtained so that alternatives to DEHP could be readily put into use at the FTF's should DOE decide to eliminate the use of DEHP.

II.   Evaluation of Alternative Test System

Aerosol Generator Evaluation

DOE standard NE-F-3-43 sets system requirements for QA penetration testing of high efficiency filters.[6] This new standard specifies that the challenge aerosol for testing filters must have a count median diameter (CMD) of 0.2 μm $\pm$ 0.04 μm with a geometric standard deviation (σ_g) of 1.4 $\pm$ 0.1. The standard also specifies that the challenge concentration should be <100 mg/m^3. An additional requirement placed on the alternative system generator was that it produce an aerosol challenge sufficient to test size 5 filters using the other components of the alternative test system.

As mentioned above, an air operated Laskin nozzle generator was selected to provide the aerosol challenge in the alternative test system. The generator uses single jet impactors to tailor the aerosol size distribution. The generator produces an aerosol with a CMD = 0.18 μm and a σ_g = 1.4, as measured by the LAS using an uncalibrated aerosol diluter. The aerosol concentration was measured to be ~5 mg/m^3 in a ~1000 cfm (~28 m^3/min) airflow.

The aerosol produced by this generator was found to have a net negative charge. This aerosol charge has been neutralized using [85]Kr aerosol neutralizers. This effectively eliminates the variable of aerosol charge from penetration measurements.

Aerosol Monitor Requirements

The alternative system aerosol monitor is subject to certain aerosol sizing and aerosol concentration measurement requirements. DOE standard NE-F-3-43 requires that the monitor be capable of sizing aerosols with an accuracy and a precision of $\pm$ 10 per cent.[6] In practice, the monitor must be able to perform these size measurements over a range of concentrations of 4 orders of magnitude. The monitor must also be able to make accurate concentration measurements over a range of 4 orders of magnitude.

Aerosol Sizing Evaluation

A comparison of aerosol sizing by the LAS and an electrostatic classifier (EC, model 3071, TSI Inc., Minneapolis, MN) was performed over the range from ~0.1 µm to ~0.4 µm by generating nearly monodisperse DEHP aerosols with the EC with concentrations in the vicinity of 1000 particles/cm^3. The LAS response was corrected for refractive index effects based on Mie theory.[3] Atmospheric pressure and slip factor effects were accounted for in calculating the particle size produced by the EC. Another comparison used monodisperse polystyrene spheres (PSS) with manufacturer's stated diameters of 0.176 µm and 0.261 µm.

Results of this LAS/EC comparison are presented in Figure 1. A linear least squares fit to these data resulted in the equation:

$$Y = -0.019 + 1.016X, \tag{1}$$

where:
   Y = LAS measured size in µm,

   X = EC generated size in µm.

The coefficient of determination, r^2, for this fit was 0.995. The fractional difference between the LAS and EC measurements was also calculated for each measurement set by dividing the difference in the measurements by the EC measurement. The fractional difference in aerosol size indicated by the two instruments was <10 per cent for aerosols with diameters from ~0.15 µm to ~0.4 µm. The difference increased for aerosol diameters below ~0.15 µm until at an EC size of ~0.12 µm this difference was ~20 per cent. Using PSS, similar differences were observed between the manufacturer's size and the LAS size. When a final size standard is established prior to the conclusion of this program, resolution of the size response discrepancy below 0.15 µm may be possible by modifying the operation of the LAS.
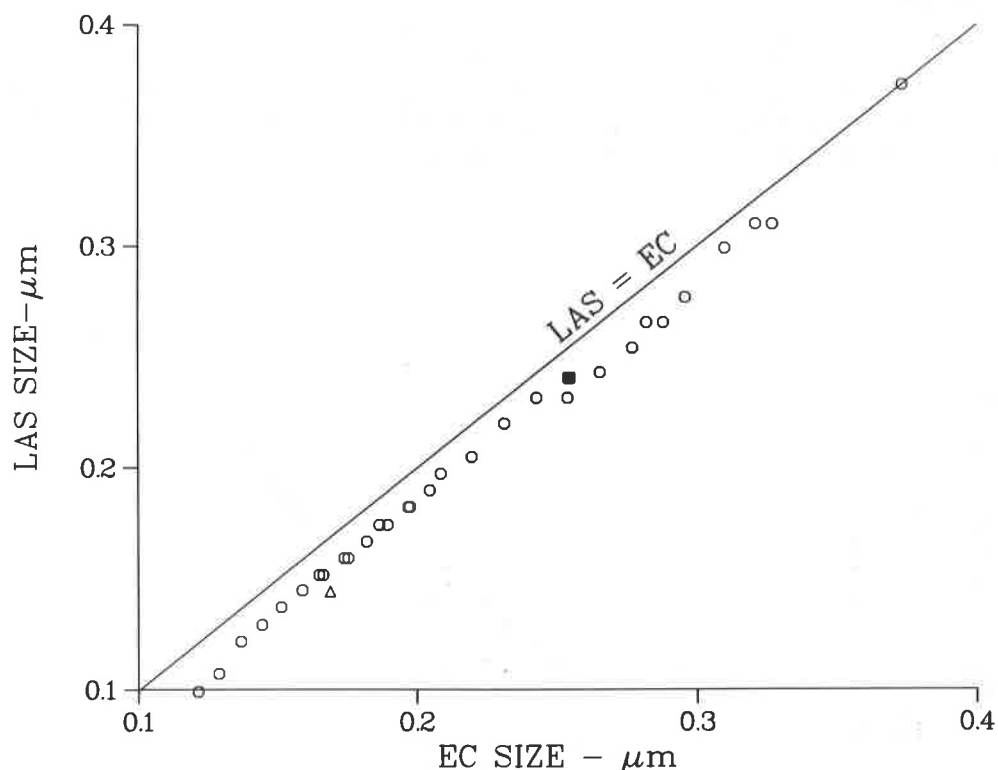
FIGURE 1
OPEN CIRCLES (O) INDICATE RESULTS OF A COMPARISON OF AEROSOL
SIZING BY THE LAS AND THE EC USING A DEHP AEROSOL.   THE LINE
DENOTES EQUAL RESPONSE BY THE INSTRUMENTS.   THE OPEN TRIANGLE
(△) AND THE SOLID SQUARE (■) INDICATE THE RESULTS OBTAINED
FROM THE COMPARISON USING MONODISPERSE POLYSTYRENE AEROSOL WITH
MANUFACTURER'S DIAMETERS OF 0.176 μm AND 0.261 μm, RESPECTIVELY

Aerosol Concentration Measurement Evaluation

    Comparisons of number concentration measurements made by the LAS
and a condensation nucleus counter (CNC, model 3030, TSI Inc.,
Minneapolis, MN) were performed using polydisperse and monodisperse
DEHP aerosols. Sample airflows for each instrument were checked
during the concentration measurements. CNC concentration
measurements made in the count mode were corrected for coincidence
losses.

    A polydisperse aerosol with a CMD of ~0.25 μm and a σ_g of ~1.5
was used in the first concentration comparison. Results of this
comparison for aerosol concentrations from ~50 particles/cm^3 to
~5000 particles/cm^3 are displayed in Figure 2. Comparison data
was collected with the CNC operating in both the count and
photometric modes. The fractional difference between LAS and CNC
measurements was calculated for each measurement set by dividing the

difference in the measurements by the CNC measurement. On the average, the LAS concentration measurements were ~10 per cent lower than those of the CNC with the fractional difference ranging from the LAS measurement being ~27 per cent below the CNC measurement to the LAS measurement being ~15 per cent above the CNC measurement. Some of this bias is thought to be the result of the LAS size range not being broad enough to include aerosol smaller than ~0.1 μm diameter. The degree of bias that was observed is not believed to be significant in terms of the concentration accuracy requirements for QA filter penetration measurements.
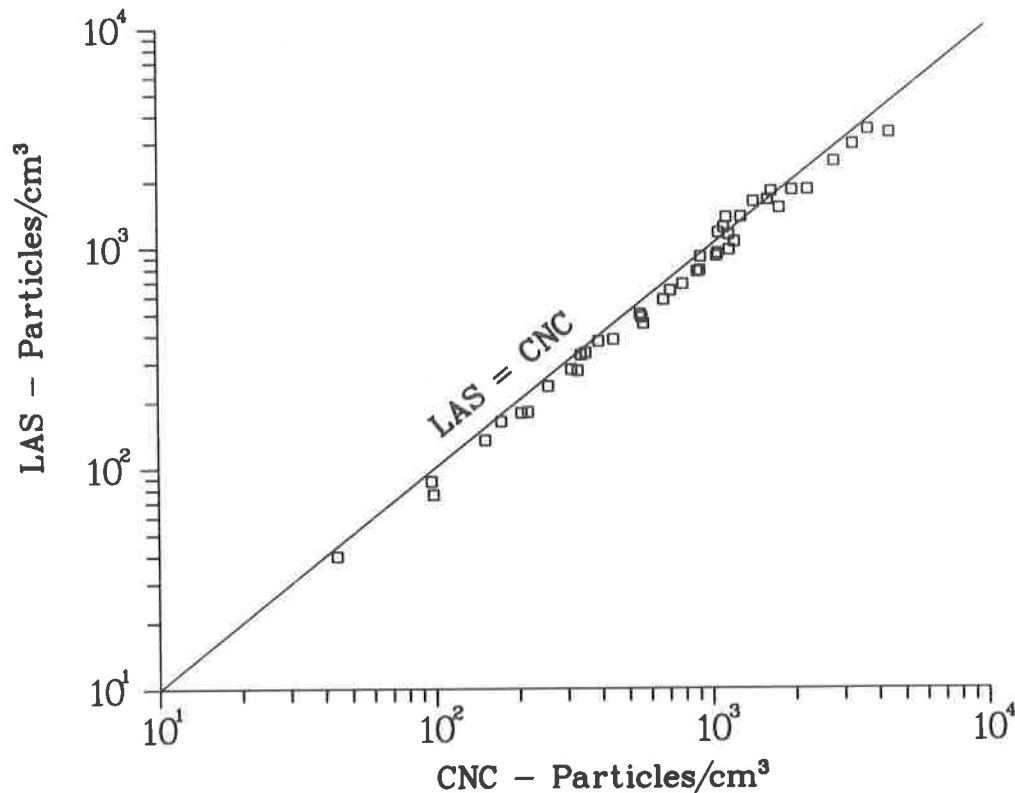
FIGURE 2
DATA POINTS (☐) INDICATE RESULTS OF A COMPARISON OF NUMBER
CONCENTRATION MEASUREMENTS MADE BY THE LAS AND THE CNC USING
A POLYDISPERSE AEROSOL. THE LINE DENOTES EQUAL RESPONSE BY
THE INSTRUMENTS

Monodisperse aerosols for the second concentration measurement comparison were produced by the EC. Comparisons were conducted at seven aerosol sizes with aerosol diameters ranging from ~0.2 μm to ~0.5 μm. Concentration was varied at each size from 10^2 – 10^3 particles/cm^3 up to ~10^4 particles.

A typical example of the results from this set of comparisons is shown in Figure 3. In general, good agreement was observed at each aerosol size. Again, fractional differences between the LAS and CNC
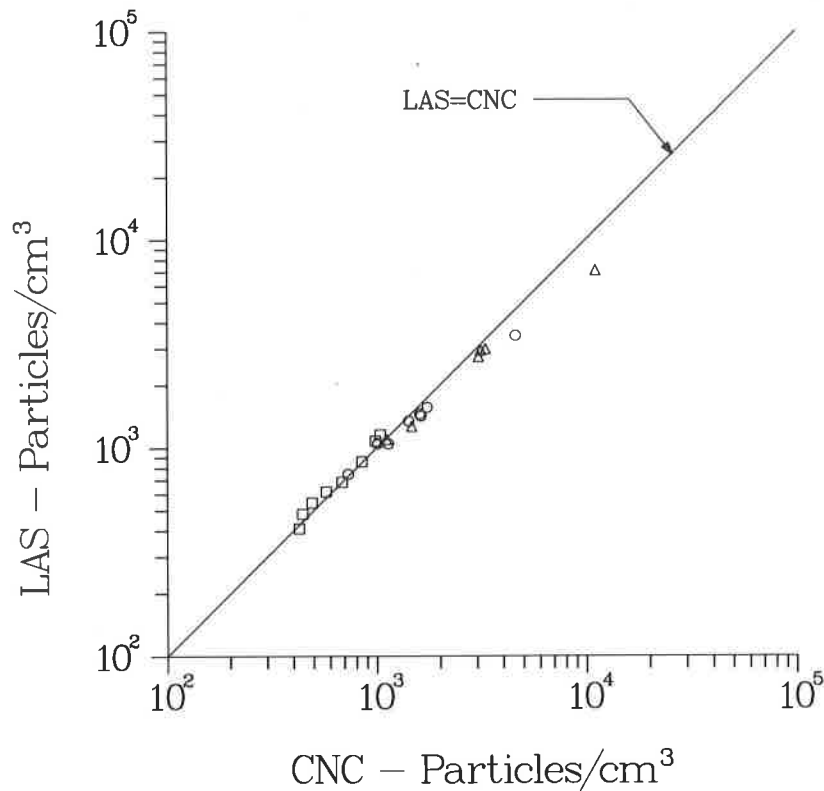
FIGURE 3
EXAMPLE OF TYPICAL RESULTS FROM COMPARISON OF MONODISPERSE
AEROSOL CONCENTRATION MEASUREMENTS MADE BY THE LAS AND
THE CNC.   THE TRIANGLES (△) INDICATE MEASUREMENTS
MADE ON 0.21 μm DIAMETER AEROSOL.   THE SQUARES (▱)
INDICATE MEASUREMENTS MADE ON 0.31 μm DIAMETER AEROSOL.
THE CIRCLES (o) INDICATE MEASUREMENTS MADE ON 0.42 μm
DIAMETER AEROSOL.   THE LINE DENOTES EQUAL RESPONSE BY
THE INSTRUMENTS

measurements were calculated. Over all sizes studied, the LAS
concentration measurement tended to be slightly greater than the CNC
measurement with the CNC operating in the count mode (CNC measured
concentrations below ~1000 particles/cm^3). In this operation
mode, LAS concentration measurements averaged ~6 per cent higher
than the CNC measurements, with the fractional differences ranging
from the LAS measurement being ~6 per cent low to the LAS
measurement being ~17 per cent high.

With the CNC operating in the photometric mode, the LAS
measurement tended to be the lower of the two measurements. The
fractional differences observed in the measurements made with the
CNC operating in the photometric mode tended to be greater than the
differences observed with the CNC operating in the count mode. This
was especially true for CNC measured concentrations greater than
~3000 particles/cm^3 where the fractional difference increased with

increasing concentration until at a CNC measured concentration of ~10^4 particles/cm^3 the LAS measurement ~35 per cent low.

The fractional differences observed for CNC measured concentration between ~1000 particles/cm^3 and ~3000 particles/cm^3 were on the average lower and not as obviously dependent on concentration as were the measurements of higher concentrations. LAS measurements in this range averaged ~13 per cent below the respective CNC measurement with fractional differences ranging from the LAS measurement being 1.6 per cent low to the LAS measurement being ~25 per cent low.

The concentration measurement differences observed with the CNC operating in the photometric mode may be related to LAS coincidence losses as well as inaccuracies associated with the CNC. No aerosol size dependent effect on concentration measurement was observed in these experiments.

Aerosol Diluter Evaluation

In order to make accurate challenge aerosol concentration measurements it was necessary to use an aerosol diluter in conjunction with the LAS. A capillary dilution system was selected for this purpose (see figure 4). Aerosol laden air entering the diluter is split in two streams. The bulk of the flow passes to a
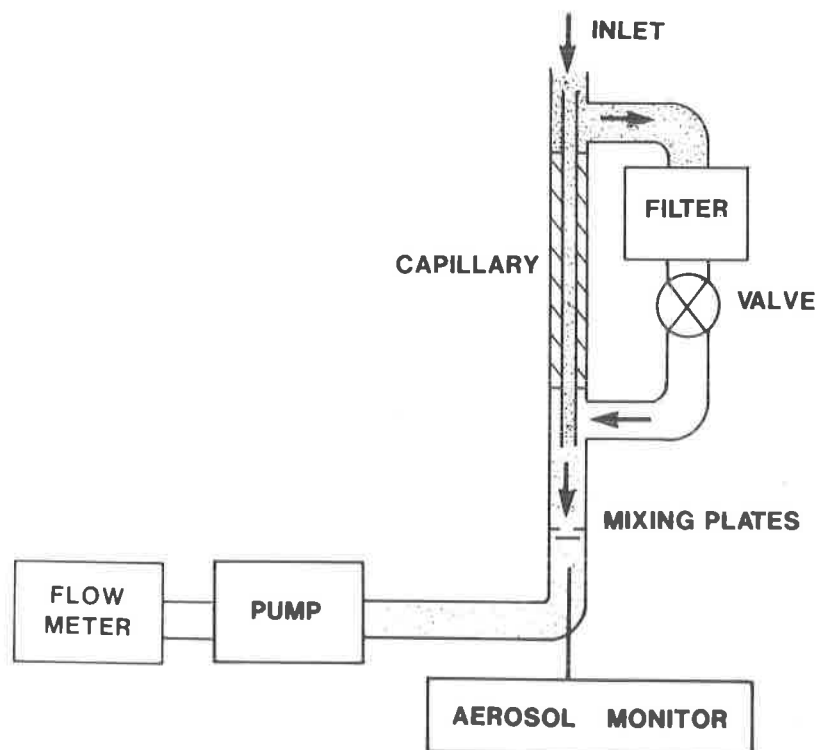
FIGURE 4
DIAGRAM OF CAPILLARY AEROSOL DILUTER SHOWING PLACEMENT
OF AEROSOL MONITOR

filter which removes virtually all aerosol from the stream. The other stream which comprises a know fraction of the original flow passes through a capillary. The two streams recombine producing an aerosol concentration that is a know fraction of the original concentration.

The capillary diluter (model 303, Atmospheric Technology, Calabasas, CA) operation was evaluated at a dilution ratio setting of ~700 and a diluter flow of 5 l/min using a polydisperse DEHP aerosol. The LAS was used to make size distribution measurements upstream and downstream of the diluter. Aerosol concentrations upstream and downstream of the diluter for a given aerosol size between ~0.1 μm and ~0.4 μm were used to calculate dilution ratio for that size.

The dilution ratio averaged over six measurements along with the standard deviation associated with this series of measurements is shown in Figure 5. These average dilution ratios ranged from ~692 to ~768. The coefficient of variation associated with each set of measurements ranged from ~2 per cent to ~11 per cent. In this evaluation, dilution ratio was observed to be largely independent of aerosol size. In some earlier diluter evaluations, a slight increase with dilution ratio with size was noticed.
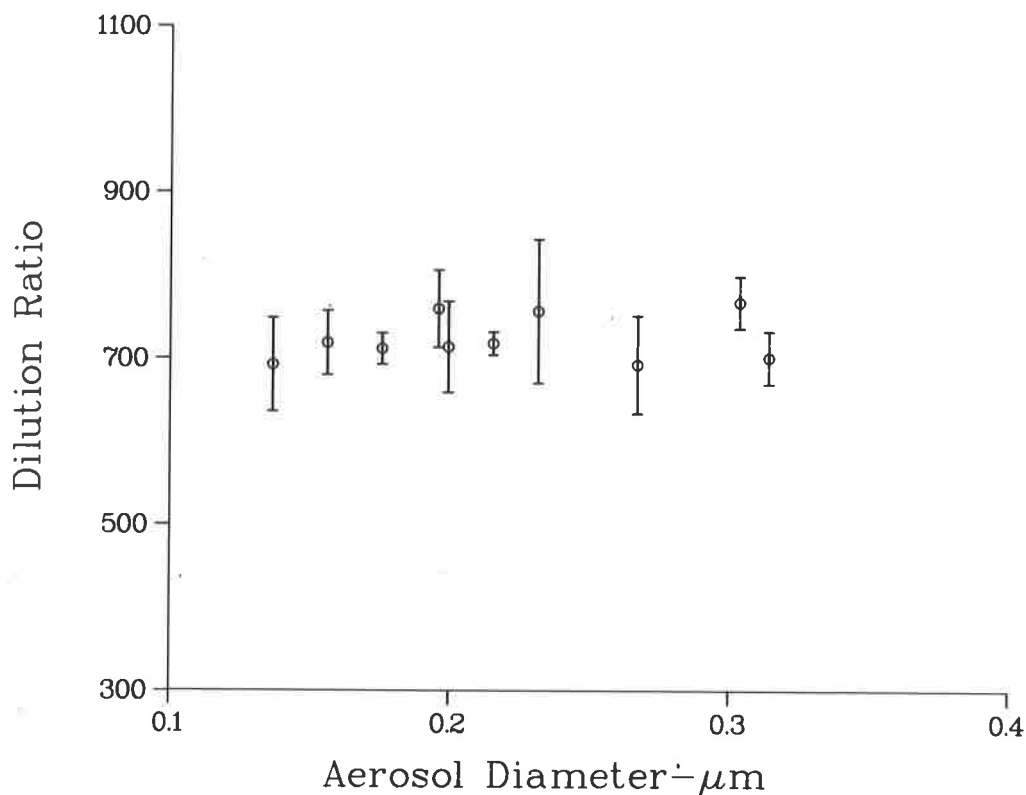
FIGURE 5
RESULTS OF DILUTER EVALUATION DILUTION RATIO SETTING WAS
~700. DILUTER AIRFLOW WAS 5 l/MIN

Alternative Test System Penetration Measurements

Penetration measurements on a series of size 5 high efficiency filters were made with the alternative test system. The test system was adapted to a size 5 filter test system contained in the Flanders Filters Mobile Filter Test Laboratory. The measurements were made at a test filter airflow of ~1000 cfm (~28 m^3/min) using the test stand illustrated in Figure 6. A DEHP aerosol challenge was produced by the modified Laskin nozzle generator. Penetration values were calculated directly by an HP-85 microcomputer interfaced with the LAS using software written at Los Alamos. No allowances for any unbalanced aerosol losses associated with the aerosol sampling system were made.
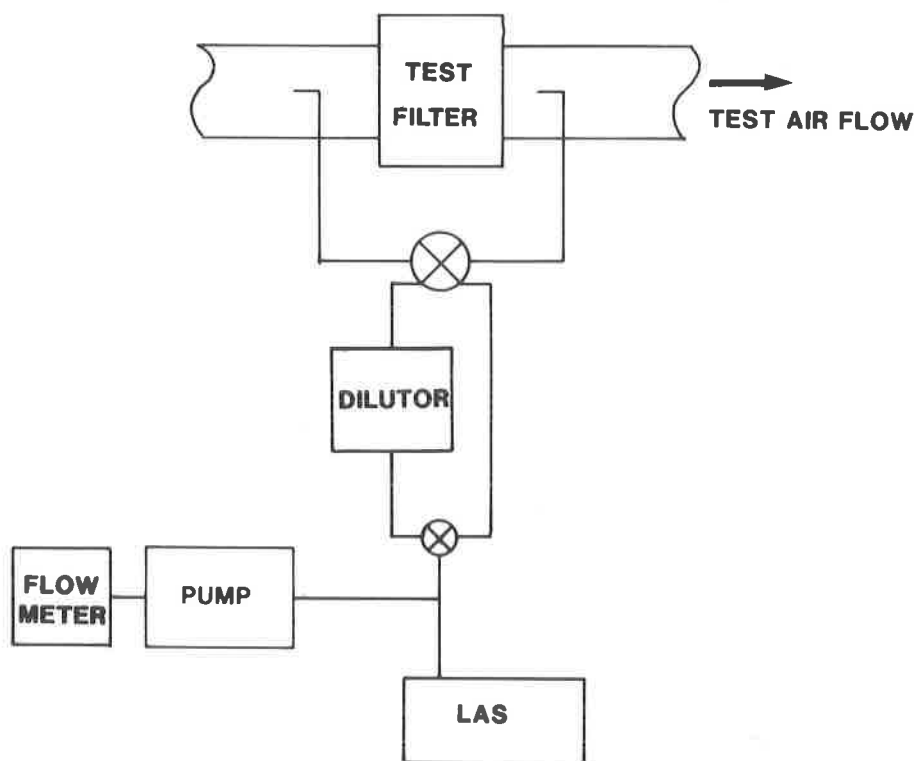
FIGURE 6
TEST STAND FOR FILTER PENETRATION MEASUREMENTS

An example of the penetration measurement results is shown in Figure 7. All penetration measurements displayed a unimodal variation of penetration with particle size. Size of maximum penetration was found to be in the vicinity of 0.2 μm. Number penetration for the example filter averaged over six measurements ranged from ~0.003 per cent to ~0.007 per cent with coefficients of variation associated with these measurements varying from ~5 per cent to ~11 per cent. Average number penetration of ~0.3 μm diameter particles was ~0.003 per cent.
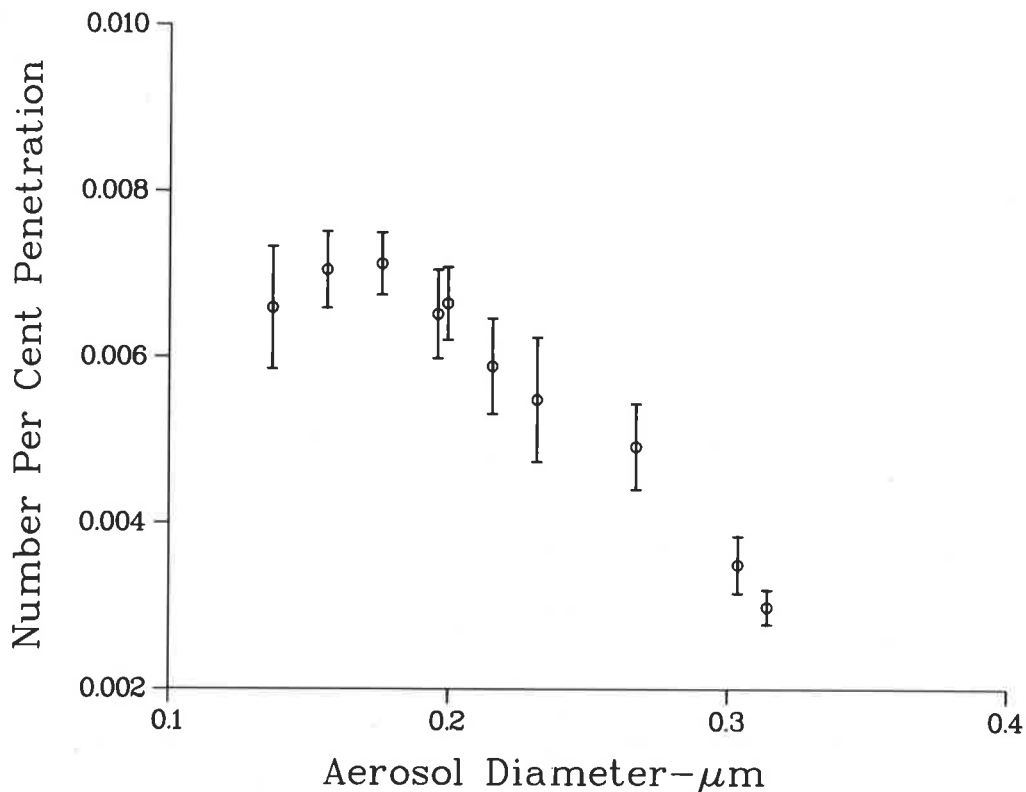
FIGURE 7
EXAMPLE OF SIZE 5 FILTER PENETRATION MEASUREMENT.
FILTER AIRFLOW WAS ~1000 CFM (~28 m^3/MIN)

III.   Evaluation of DEHP Alternatives

    In addition to the experimental work described above, a
literature search was also conducted. Potential alternatives to
DEHP were scrutinized with respect to certain published
toxicological and physical criteria relevant to QA filter
penetration testing. The most promising of these alternative
materials includes oleic acid, PEG-200 and di-2(ethylhexyl) sebacate
(DEHS).

    None of these materials distinguish themselves as obvious
alternatives to DEHP. Oleic acid, even though it is used as an
aerosol carrier in therapeutic inhalants, is characterized as a
"mild irritant".[7,8] Beagle dog inhalation studies performed with
Vanceril, a prescription antiasthmatic that contains oleic acid,
show some tracheal effects.[7] Because of its deliquescent
properties, the stability of a PEG-200 aerosol challenge for filter
testing is suspect. Recently, some questions about the toxicity of
DEHS have been raised.[9]

    All three materials have been generated as an aerosol with a
Laskin nozzle aerosol generator. Oleic acid is being evaluated as a
test agent for respirator filters in a study being conducted at Los

Alamos for the U. S. Army. Hinds has reported on the aerosol size produced by the generator using "PEG" and DEHS.[10] These data indicate that, relative to aerosol generation, little development would be necessary to select a DEHP alternative from among these materials.

If a DEHP alternative material is selected, a comprehensive/ definitive toxicological evaluation of the material should be considered. The evaluation could consist of submission of the material name to NTP for study and/or independent investigation of the inhalation toxicity of the material.

IV. Conclusion

The evaluation completed thus far indicates the alternative test system has potential for making penetration measurements within the constraints of standard NE-F-3-43 and in the setting of the DOE FTF's.[6] Additional evaluation is planned of the individual components and of the complete system. A demonstration of a prototype system is planned during 1985.

Acknowledgments

The authors acknowledge the diligent technical assistance provided by Lloyd Wheat of Los Alamos in conducting this study and the guidance provided by Tom Thomas of the Airborne Waste Management Office and Harry Ettinger of Los Alamos.

Flanders Filters, Inc. of Washington, NC loaned their Mobile Filter Test Laboratory to Los Alamos for this project. This loan has been a great help in conducting the study. We wish to express our appreciation to Mr. Tom Allan and Flanders Filters, Inc. for loaning the mobile laboratory.

References

1. Military Standard, "Filter Units, Protective Clothing, Gas Mask Components and Related Products, Performance Test Methods," MIL-STD-282 (May 28, 1956).

2. National Toxicology Program, "Carcinogenesis Bioassay of Di-2(ethylhexyl) Phthalate (CAS No. 117-81-7) in F344 Rats and B6c3f1 Mice (Feed Study)," US Department of Health and Human Service, Public Health Service, National Institute of Health, NIH Publication No.82-1773.

3. Salzman, G., H. Ettinger, M. Tillery, L. Wheat, and W. Grace, "Potential Application of a Single Particle Aerosol Spectrometer for Monitoring Aerosol Size at the DOE Filter Test Facilities," in proceedings of the 17th DOE Nuclear Air Cleaning Conference, Report CONF-820833, U.S. Department of Energy, Volume 2, pp. 801-820 (1983).

4. Strandberg, S. W., "Chemical Characterization of Challenge Aerosols for HEPA Filter Penetration Testing," Masters Thesis, Department of Microbiology and Environmental Health, Colorado State University, in preparation (July 1984).

5. Echols, W. and J. Young, "Studies of Portable Air-Operated Aerosol Generators," NRL report No. 5929 (1963).

6. Filter Test Facility Standards Writing Group, "Quality Assurance Testing of HEPA Filters and Respirator Canisters," US Department of Energy, February 1984.

7. Huff, B., Ed., Physicians' Desk Reference, 32nd ed., Published by Medical Economics Company, Grandell, New Jersey (1978).

8. Windholz, M., Ed., The Merck Index, 9th ed., Merck and Co., Inc., Rahway, New Jersey (1976).

9. Silverstein, B. D., O. White, Jr., J. E. Bower, and N. M. Bernholc, "Toxic Material Summary Report Di-2-ethylhexyl Sebacate," Draft Brookhaven National Laboratory Report, December 1982.

10. Hinds, W., J. Macher, and M. W. First, "Size Distributions of Aerosols Produced From Substitute Materials by the Laskin Cold DOP Aerosol Generator," in the proceedings 16th DOE Nuclear Air Cleaning Conference, Report CONF-801038, U.S. Department of Energy, Volume 1, pp. 125-138 (1981).

DISCUSSION

GERBER: How long does it take to make a typical measurement?

SCRIPSICK: Downstream sampling is for three minutes, which is the longest amount of time. We make upstream measurements in about 11 seconds, and then there is some data analysis time. We hope to trim time off this at the filter testing facilities. They have to make two penetration measurements; one at 1,000 cfm, and one 200 cfm. They are more interested in the order of magnitude of the reading above 0.03% penetration, so we can reduce the 3 minute time. For a maximum filter penetration value on the order of 0.03%, the downstream counting time for acceptable precision is 30 seconds. An optimum time has to be selected, depending on the standard deviation you want for your measurement.

Appendix B

DEPARTMENT OF ENERGY FILTER TEST PROGRAM - POLICY FOR THE 80'S

James F. Bresson, Physical Scientist
Albuquerque Operations Office, Department of Energy
Albuquerque, New Mexico

Abstract

The first report on this subject was presented at the Government - Industry Committee Meeting on Filters, Media and Media Testing associated with the 17th DOE Nuclear Air Cleaning Conference. The DOE Filter Test Facility Standards Writing Group has completed its task and issued the standards. They apply to testing policy, procedures, quality assurance and filter specifications.

The standards were prepared in consonance with a technical review committee and reflect contributions from the filter manufacturing industry and aerosol physicists from several organizations. Major issues include uniformity of HEPA filter testing methods, characterization of test aerosols, qualification of new instrumentation and test techniques, the Quality Products List (QPL), quality testing, and DOE HEPA filter procurement.

Adopting these standards means that for the first time, the DOE has a formal HEPA filter testing policy, and that the DOE HEPA Test Facilities will all be operating under the same program requirements.

Major items contained in the standards are discussed in some detail, with emphasis on assurance that HEPA filters continue to be of high quality. Rationale for significant decisions reflected in the new standards are also discussed.

Introduction

This report updates a similar report presented at the 17th Air Cleaning Conference, and reflects completion of a writing group task which produced four Department of Energy (DOE) technical standards. Three of these standards are related to HEPA filter test activities conducted at the three DOE funded HEPA Filter Test Facilities (FTFs). The fourth standard is a DOE filter specification standard, to be used when purchasing HEPA filters for use at DOE nuclear facilities.

Establishment of Writing Group

During 1980 and 1981, several items and issues surfaced, all related to HEPA filter manufacturing and testing. The most important of these were:

1. Reports of inconsistant or conflicting test results at the FTFs.
2. Possible toxicology problems with the one accepted HEPA filter test aerosol (DOP).

3. Emerging information on the hot DOP particle size and particle size distribution.
4. Significant increases in HEPA filter rated capacities.

A writing group was established and funded by DOE's Airborne Waste Management Program Office at Idaho. Table 1 depicts the current writing group.

Table 1. HEPA filter test facility standards writing group.

Project Manager

R. C. Hudson
Nuclear Standards Management Center
Oak Ridge National Laboratory

Writing Group

J. F. Bresson, Chairman
Albuquerque Operations Office
U. S. Department of Energy

R. L. Smitherman
Oak Ridge FTF
Oak Ridge Gaseous Diffusion Plant

R. J. Talcott
Rocky Flats FTF
Rockwell International, Rocky Flats Plant

J. A. McIntyre*
Hanford FTF
Hanford Environmental Health Foundation*
*Now associated with Rockwell, Rocky Flats Plant

A Technical Review Committee, (TRC) consisting of well known aerosol technologists and representatives from the filter industry, was established, and the standards are consensus standards, reflecting comments and suggestions from the TRC. All comments submitted by the TRC members were evaluated, and either accepted or rejected with records of comment disposition and reasons for comment rejection recorded on comment resolution sheets. The TRC is as shown in Table 2.

Table 2. Technical review committee.

T. T. Allan, Flanders, Inc.
W. L. Anderson, Consultant
W. Bergman, Lawrence Livermore National Laboratory
M. W. First, Harvard Air Cleaning Laboratory
W. Gammill, Nuclear Regulatory Commission
B. V. Gerber, Aberdeen Proving Grounds
H. Gilbert, Consultant
R. T. Goulet, Cambridge Filters
A. Lieberman, Particle Measuring Systems, Inc.
J. D. McDonough, Mine Safety Appliances Company

The Standards

Operating Policy of DOE Filter Test Program (NE F 3-42)

This standard confirms the DOE policy that all HEPA filters used for radionuclide environmental protection purposes, and all respirator and gas-mask type canisters, meet DOE specification requirements prior to use at DOE installations. Such filters and canisters shall be inspected and tested for compliance with specifications and must successfully pass the inspections and tests at a DOE operated filter test facility. Test services at FTFs are free to DOE prime contractors, and are provided to all others on a cost recovery basis, according to an established fee schedule.

The policy standard allows for certain minor repairs and waivers, but establishes that no waivers shall be granted for excessive penetration or pressure drop across the filter. To identify trends and to help correct possible manufacturing problems, FTFs are required to prepare semiannual reports of testing activities. Review of these reports can lead to early identification of filter quality problems and timely corrective action.

To address the question of consistency among the FTFs, NE F 3-42 has reinstituted a semiannual round robin test program in which the same set of test filters is sent in turn to each FTF for testing, and results are compared. Within the next year, the filter manufacturers will be offered the opportunity to participate in round robin type exercises. The semiannual report and round robin test activities are performed under the supervision, guidance, and review of the Industrial Hygiene Group (H-5) at The Los Alamos National Laboratory. This group, called the Technical Support Group (TSG), has been tasked with providing technical support to FTFs, again in the interest of assuring consistent results by the FTFs.

Quality Assurance Testing of HEPA Filters and Respirator Canisters (NE F 3-43)

This standard covers the basic requirements for the quality assurance inspections and tests conducted at the FTFs, and reaffirms the two most important operating parameters for HEPA filters.

First, penetration of the test aerosol shall not exceed three hundreths of one percent (.03%) at any test airflow. Second, the maximum pressure drop across unencapsulated size 4 (500 CFM) filters and filters of higher capacity shall not exceed one inch water gage (1" wg). The pressure drop limitation helps assure an optimum particle velocity through the filter to enhance collection, but more importantly, establishes an upper limit on filter ratings. The standard 24 inch by 24 inch by 12 inch (24"x24"x12") filter, most often used in exhaust filter plenums, has a nominal capacity of 1000 cubic feet per minute (CFM) and most can accommodate 1200-1500 CFM with pressure drops equal to or less than 1" wg. However, as

additional air is forced through the filter, the resistance increases, and the filter life and integrity can be adversely affected. Further, as filters load-up more quickly, the design capacity of the exhaust handling system may be adversely affected. Therefore it was decided to limit the maximum allowed pressure drop on the large (size 4 and above) filters to 1" wg.

NE F 3-43 also includes qualification requirements for new test aerosols, presents a formal method for approving new aerosols and test measurement techniques, requires calibration of test instruments and secondary measurement equipment, discusses training and other qualifications for test personnel, and requires written operating procedures for filter test activities.

In the standard, di-octyl phthalate (DOP) is defined as the currently approved test aerosol, with use of di-octyl sebacate, (DOS) approved at the Hanford FTF. Neither substance is approved for "man-fit" tests, and this standard covers only evaluation of the respirator canister filter, not respiratory protective devices.

DOE Test Facility Quality Program Plan (NE F 3-44)

This standard requires that each DOE Filter Test Facility be operated under a site specific, documented, and auditable Quality Program Plan (QPP) with implementing procedures. This standard is traceable to DOE Order 5700.6A, "Quality Assurance" and ANSI/ASME NQA-1 "Quality Assurance Program Requirements for Nuclear Power Plants." FTFs perform quality assurance functions on HEPA filters, and must be operated under closely controlled, auditable procedures in order to achieve consistency and credibility. The QPP requirements stress procurement control for measuring and test equipment, calibration with proper traceability for standards, auditable records, training and especially identification of nonconformances with timely corrective action.

Specifications of HEPA Filters Used by DOE Contractors (NE F 3-45)

This standard differs from the others because it presents the minimum specifications for HEPA filters purchased for use in DOE nuclear facilities. These specifications are to help ensure that HEPA filters continue to be of acceptably high quality, because these filters are important in protecting the public health and environment. In general, the specifications incorporate the provisions of the familiar Department of Defense Military Specifications (MIL) MIL-F-51068, "Filter, Particulate, High Efficiency, Fire Resistant" and MIL-F-51079, "Filter Medium, Fire Resistant, High-Efficiency". Prior to sending filters to DOE FTFs, manufacturers are also required to test each filter for penetration and resistance, and provide evidence that each filter has passed the test requirements.

DOE recognizes the Military Quality Products List, (QPL) and a filter model or filter medium type appearing on the QPL is acceptable, provided that tests performed as part of DOE's ongoing

quality program provide no evidence to the contrary. DOE provides other options to filter manufacturers for meeting specification requirements, that is, a filter does not have to be on the QPL to be acceptable for use in DOE nuclear facilities.

The specification standard addresses the subject of qualification testing, e.g., performance of tests related to overpressure resistance, and resistance to fire and heated air. Again, compliance with MIL-F-51068 requirements and QPL listing are considered acceptable, but the manufacturer is given other options for meeting qualification testing requirements, one of which is contracting with the Rockwell Rocky Flats FTF to perform the qualification tests on a reimbursable basis.

Rockwell has recently completed installation and testing on equipment which can perform the qualification tests. DOE now plans to perform qualification tests on HEPA filters from all DOE suppliers on a random and continuing basis.

Conclusions

Writing the DOE standards has been an interesting and rewarding exercise. The writing group and technical review committee members represent a variety of interests and experience, all related to the design, manufacture and testing of HEPA filters. During the time in which the writing group has functioned, we have been made aware of new knowledge and insight into the mechanisms of filtration, particle size analysis, particle distribution analysis, and have watched with interest development of equipment which can measure these parameters.

The filter test program now appears to be aimed at evaluating HEPA filter performance against test aerosols which more closely represent actual challenge aerosols in operating facility air effluent streams. Test methods which can evaluate filter performance for a range of particle sizes are being developed, opening the possibility for use of simpler, less expensive aerosol generating equipment. With these facts in mind, the DOE standards include carefully controlled procedures by which new test aerosols and measurement techniques can be incorporated into the filter test program. General performance standards for these aerosols and test methods are also included.

The above mentioned items have made for lively writing group and review committee meetings, because there are both technical and economic issues to be considered. The interest and support of all participants has been most gratifying. In conclusion, we attempted to keep our main objective firmly in mind, assurance that HEPA filters used in DOE facilities continue to be of the high quality required to aid in providing public health and environmental protection. And although equipment and techniques change with time, the wisdom of the individuals, many of whom are present here today, who first recognized the need for filter testing and developed the initial test methods, should always be acknowledged.

Appendix C

INTERMEDIATE RESULTS OF A ONE-YEAR STUDY OF A LASER SPECTROMETER IN THE DOE FILTER TEST FACILITIES*

S. C. Soderholm and M. I. Tillery
Industrial Hygiene Group
Los Alamos National Laboratory
Los Alamos, New Mexico 87545

Abstract

A 1-year study of the model LAS-X (Particle Measuring Systems, Inc.) laser spectrometer in the Department of Energy (DOE) Filter Test Facilities (FTFs) was begun on August 1, 1983. The principal objectives of the study were to gain operational experience with the LAS-X/diluter/HP-85 particle size measurement system in the FTF environment, acquire size distribution data to quantify the consistency of the Q107 aerosol size distribution at each FTF and among FTFs, and compare the FTF test aerosols to current and proposed standards. Results of the first 9 months of the study are summarized and discussed. Major conclusions based on these data are: 1) the LAS-X system can be operated successfully in the FTF environment, 2) each FTF would require a back-up LAS-X to be able to continue filter testing during the (at least) once each year removal of a LAS-X from service for major recalibration and repair, 3) the FTF test aerosols are not monodisperse, as assumed in the military standard MIL-STD-282, and do not all meet the new DOE Nuclear Standard NE-F-3-43, which a replacement aerosol would be required to meet, 4) the test aerosol at each FTF is quite consistent over time, and 5) the test aerosols at the three FTFs differ consistently. Final conclusions and recommendations from this study will be developed after analysis of the full 12 months of data.

I. Introduction

Los Alamos has undertaken a program "Filter Test Facility Support Laboratory" for DOE. One aspect of this program, a laboratory evaluation of a proposed new filter penetration test system, was discussed elsewhere in this meeting.[1] Another part of this DOE program is to evaluate a laser spectrometer particle size measurement system [consisting of a model LAS-X laser spectrometer (Particle Measuring Systems, Inc.), a diluter, a model HP-85 (Hewlett-Packard) microcomputer, and Los Alamos software] as a possible replacement for the Owl in sizing the aerosols used at the three DOE FTFs for quality assurance testing of size 5 (1000 cfm) high efficiency particulate air (HEPA) filters. Some initial results related to this effort were presented at the 17th DOE Nuclear Air Cleaning Conference.[2]

Based on the initial evaluations, Los Alamos recommended to DOE that the LAS-X particle size measurement system receive an intensive evaluation in the FTFs for 1 year. The 1-year study was begun August 1, 1983. This report presents intermediate results of the study based on data collected during the first nine months.

II. Objectives

The objectives of the 1-year study were to:

1. Evaluate the impact of the LAS-X particle size measurement system on FTF operations including (a) additional costs in time, materials, and equipment, (b) ability of FTF personnel to efficiently operate the system, (c) ability of the equipment to operate reliably in the FTF environment, and (d) benefits due to more complete particle size characterizations.

2. Determine the relationship of the test aerosols at the three FTFs to relevant Standards.[3,4]

3. Provide data on daily variations of the test aerosols produced at each FTF including possible seasonal changes.

4. Compare the test aerosols produced at the three FTFs.

III. Equipment and Procedures

The LAS-X owned by each FTF nominally sizes particles with diameters between 0.09 and 3 μm using four overlapping size ranges. Size is determined by measuring the amount of light scattered into a detector by individual particles. Salzman, et al. have described the operation of the LAS-X, including refractive index corrections.[2] Since it is a single-particle counter, errors occur if the aerosol concentration is as high as that found in the model Q107 penetrometer used at each FTF for testing size 5 (1000 cfm) HEPA filters. During this study, the test aerosol in the Q107 was passed through a capillary diluter prior to entering the LAS-X. A capillary diluter works by passing a small portion of the incoming aerosol stream through a controlled "leak" consisting of a capillary tube and allowing it to mix with the bulk of the incoming stream which was passed through a HEPA filter. The diluter provided by Los Alamos was designed to operate at a flow of approximately 140 L/min (5 cfm).[5] Data acquisition and analysis was accomplished with an HP-85 microcomputer system and software developed at Los Alamos. A detailed description of the equipment and software will be provided in the final report of this study.

Conducting the study at the FTFs did not alter the way in which HEPA filters were tested. All normal procedures were followed, including adjusting the Q107 to obtain an Owl reading of 29°. No Q107 adjustments were made based on the LAS-X size distribution results. Each FTF reviewed its operations prior to the start of the study to ascertain that all normal procedures were being followed and that all equipment was operating properly. Los Alamos provided detailed descriptions of the equipment and procedures associated with the study and visited each FTF prior to the start of the study to help install the equipment and train the operators.

At the start of each day when the Q107 was operated, the LAS-X calibration was checked with an aerosol of polystyrene latex (PSL) spheres using an air-jet nebulizer system supplied by Los Alamos. No LAS-X calibration adjustments could be made in the field, so the PSL measurements served only as a check on the operation of the instrument. Los Alamos provided PSL particles from the same source bottle to each FTF as dilute suspensions which had been prepared at the same time and in the same way. After checking the LAS-X calibration, an FTF operator measured the Q107 aerosol size distribution at the beginning of each day when the Q107 was used to test HEPA filters and at approximately 2-hour intervals thereafter. Size

distributions were obtained only when the Q107 was being operated at a volume flow rate of 28.3 m³/min (1000 cfm) with the filter chuck closed and the Owl reading 29 ± 1°.

Prior to initiating the acquisition of data by the microcomputer, the operator was required to enter or verify the values of several parameters, including the date, aerosol material (di-2(ethylhexyl) phthalate [DEHP] or di-2(ethylhexyl) sebacate [DEHS]), LAS-X sample flow rate, two diluter meter readings (from which an approximate dilution ratio was calculated), and the Owl reading. Data acquisition required approximately 1 minute (11 seconds for each of 4 ranges with a potential initial "dead time" of 11 seconds) after which the filter chuck could be opened and normal operations continued. The microcomputer analyzed the data immediately after acquiring a complete set. The data analysis included index of refraction corrections for DEHP and DEHS. The output of the data analysis system was printed on a paper tape in the form of a graph of the raw data and the calculated lognormal distribution, a table of all entered and calculated parameter values, and a table of the raw data (Figure 1). In addition, the raw data were stored on a cassette tape along with all relevant parameter values.

The operator kept a logbook containing a summary of each calibration and size distribution measurement and a record of comments, costs, and time spent conducting the study. Approximately once a month, the cassette tape and a copy of the relevant logbook pages were sent to Los Alamos for analysis. No preliminary results of the data analyses were provided prior to the end of the 1-year study in order to avoid potential bias of the data.

Each data set recorded on a cassette tape was reanalyzed at Los Alamos to obtain another paper tape copy of the raw data and the results of the data analysis. Initially, the Los Alamos analysis was performed with the same software as had been provided to the FTFs to obtain the principal parameters of the size distribution, the geometric mean diameter (D_g) and the geometric standard deviation (σ_g). The data analysis technique incorporated into that software provided a fast and convenient means of describing the parameters of the measured size distribution by direct calculation of D_g and σ_g from the histogram data. However, one characteristic of that data analysis technique was that it provided an inaccurate description of the size distribution when it was truncated, i.e., a significant fraction of the particles were outside the measurement range of the LAS-X.

It was apparent that truncation was occurring with many of the data sets received from the FTFs, so the data were analyzed with another (much slower) data analysis technique which avoided errors due to truncation of the size distribution. This nonlinear least-squares data analysis technique used a modified simplex search procedure to find the three parameters of a lognormal distribution (number concentration, geometric mean diameter, and geometric standard deviation) which minimized the sum of the squared deviations between the histogram data and the corresponding quantities calculated from the lognormal distribution. All measurements of the Q107 aerosol were analyzed by the nonlinear least-squares technique and those results are presented in this paper. All of the best-fit lognormal distribution found by this technique appeared to fit the data well when checked visually. For data sets in which no significant truncation of the size distribution occurred, the results of the two data analysis techniques agreed well.

ΔNUMCON/Δln(d) (×10^3)

DIAMETER (μm)

DATE 83/11/07   TIME 120153   DEHP
STORED AS LASXDA DATASET   3
MAX CNTS/SEC=   3863   SEC=   11
R 0-3 TRUN   0 BINS   1.00 ML/SEC
DILUTION RATIO   = 1.736E+003
TOT FLOW ΔP (IN H20)= 1.000E+000
DIL FLOW ΔP (IN H20)= 2.100E+000
OWL POL. ANGLE (DEG)= 2.800E+001
TEMPERATURE   (C)= 2.200E+001
ATM PRESSURE (mm Hg)= 6.140E+002
REL HUMIDITY   (%)= 5.000E+001
NUM CONC (NUMB/cm3)= 3.789E+003
GEOM MEAN DIAM   (μm)= 1.626E-001
GEOM STANDARD DEV   = 1.432E+000
MASS CONC   (mg/m3)= 2.819E-002
UNDIL MASSCON(mg/m3)= 4.893E+001
MAX CNTS/SEC   = 3.863E+003
PEAK DIAMETER (μm) = 1.215E-001
FIT NUM CONC (#/cm3)= 4.916E+003
FIT GEOM MN DIA (μm)= 1.347E-001
FIT GEOM STAND DEV = 1.592E+000
FIT UNDIL M0 (mg/m3)= 2.892E+001

PROBE RANGE=2   TOT CNTS=   19682

BIN	DIA	COUNT	DISTN VALUE
0	.160	2887	4.33E+003
1	.170	2310	3.35E+003
2	.181	2257	3.48E+003
3	.192	2032	3.32E+003
4	.203	1612	2.55E+003
5	.215	1466	2.67E+003
6	.226	1246	2.38E+003
7	.237	989	1.82E+003
8	.249	743	1.44E+003
9	.261	610	1.34E+003
10	.272	535	1.13E+003
11	.284	406	9.92E+002
12	.296	326	8.92E+002
13	.306	287	5.83E+002
14	.320	245	7.24E+002
	.330 (	1731=OVERCOUNT)	

PROBE RANGE=1   TOT CNTS=   3848

BIN	DIA	COUNT	DISTN VALUE
0	.260	1768	9.14E+002
1	.310	850	5.17E+002
2	.360	585	4.09E+002
3	.410	399	3.15E+002
4	.460	91	8.02E+001
5	.510	45	4.37E+001
6	.560	19	2.02E+001
7	.610	18	2.08E+001
8	.660	18	2.24E+001
9	.710	14	1.87E+001
10	.760	8	1.14E+001
11	.810	9	1.37E+001
12	.860	8	1.29E+001
13	.910	3	5.10E+000
14	.960	2	3.58E+000
	1.010 (	11=OVERCOUNT)	

PROBE RANGE=3   TOT CNTS=   42492

BIN	DIA	COUNT	DISTN VALUE
0	.095	2803	3.15E+003
1	.103	2943	4.07E+003
2	.110	2724	3.53E+003
3	.118	2891	4.56E+003
4	.125	2596	3.80E+003
5	.133	2478	4.39E+003
6	.140	2339	3.83E+003
7	.148	2277	4.48E+003
8	.155	1893	3.42E+003
9	.163	1733	3.75E+003
10	.170	1770	3.50E+003
11	.178	1642	3.40E+003
12	.186	1405	3.46E+003
13	.193	1478	3.31E+003
14	.201	1322	3.08E+003
	.209 (	10198=OVERCOUNT)	

PROBE RANGE=0   TOT CNTS=   95

BIN	DIA	COUNT	DISTN VALUE
0	.700	47	2.16E+001
1	.853	13	7.16E+000
2	1.006	5	3.21E+000
3	1.159	4	2.93E+000
4	1.312	2	1.65E+000
5	1.465	1	9.15E-001
6	1.618	4	4.02E+000
7	1.771	3	3.29E+000
8	1.924	2	2.38E+000
9	2.077	0	0.00E+000
10	2.230	0	0.00E+000
11	2.383	1	1.46E+000
12	2.536	2	3.10E+000
13	2.689	3	4.93E+000
14	2.842	1	1.73E+000
	2.995 (	7=OVERCOUNT)	

Figure 1.   Example paper tape generated by the HP-85 data analysis system, including graph of histogram data and fitted lognormal distribution, table of all entered and calculated parameters, and table of raw counts and derived histogram values.

The acceptability of each data set for inclusion in the final summaries was judged on three criteria: 1) all data was properly entered (date, aerosol type, Owl reading, and dilution ratio), 2) the count rate was less than 5000 s^{-1}, and 3) there was good overlap in the distribution, i.e., there was good agreement between the two size distribution values obtained at those sizes where adjacent LAS-X ranges overlap. As reported elsewhere in this meeting, the LAS-X count rate must be below 3000 s^{-1} in order to assure accurate counting of particles.[1] However, the less stringent limit on count rate of 5000 s^{-1} was adopted as an upper limit in this study for obtaining valid size measurements. Those data for which the count rate was below 3000 s^{-1} were analyzed separately to determine if the two count rate limits had any significant effect on the results.

IV. Results

Detailed analyses of the costs, manpower requirements, and operational acceptability of the LAS-X will be presented in the final report after all the data are available. The results presented in this interim report are drawn from the calibration data and the measured size distributions of the Q107 aerosols. Table 1 shows the number of days on which data were collected for the study and the number of calibration and Q107 aerosol data sets accepted and rejected for each of the FTFs.

Table 1. Data set census.

	Number of Data Collection Days	Number of Calibration Data Sets		Number of Q107 Aerosol Data Sets	
		Accepted	Rejected	Accepted	Rejected
RF-FTF	109	97	25	128	212
HEHF-FTF	46	55	14	23	60
OR-FTF	45	55	15	58	39

The detailed results of each acceptable data set are graphed in Figure 2 for the Rocky Flats (RF) FTF, in Figure 3 for the Hanford Environmental Health Foundation (HEHF) FTF, and in Figure 4 for the Oak Ridge (OR) FTF as a function of time. The calibration results are presented in the top graph in each of the three figures. The narrow size distribution of each PSL measurement was examined to determine the LAS-X size channel with the maximum height. The central diameter corresponding to that size channel was then plotted on the ordinate as a measure of the size of the PSL spheres as determined by the LAS-X.

The second graph in each of the three figures shows the count rate. All data sets corresponding to count rates greater than 5000 s^{-1} were considered unacceptable for inclusion in the analysis. The count rate was calculated in the data analysis program from the sample duration and the largest of the particle counts recorded in the four LAS-X ranges.
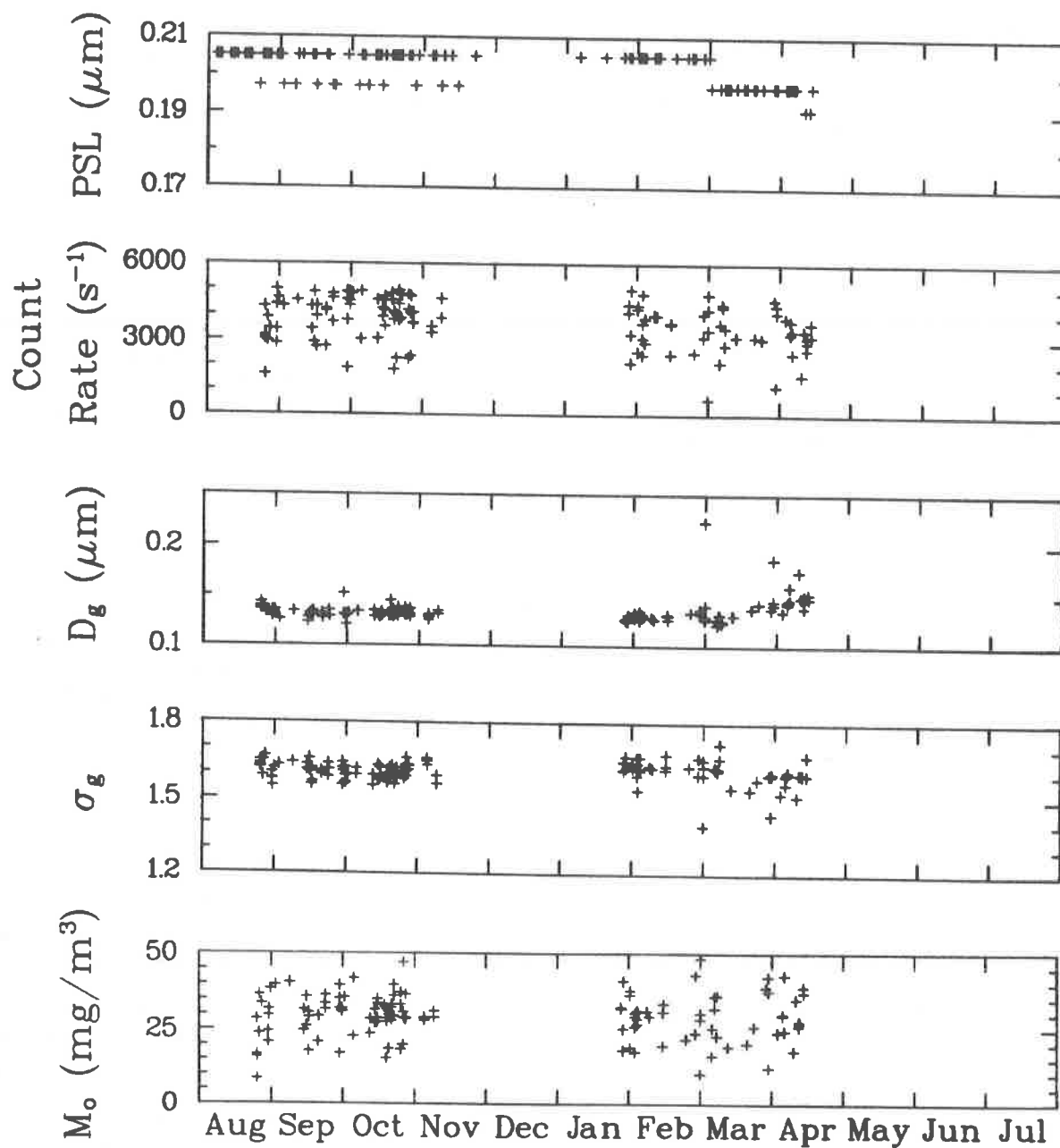
Figure 2.   Summary of first 9 months of data from all acceptable Rocky Flats FTF data sets (having count rate < 5000 s^{-1}), including the central diameter of the LAS-X channel containing the highest peak for PSL, count rate, geometric mean diameter, geometric standard deviation, and estimated mass concentration.
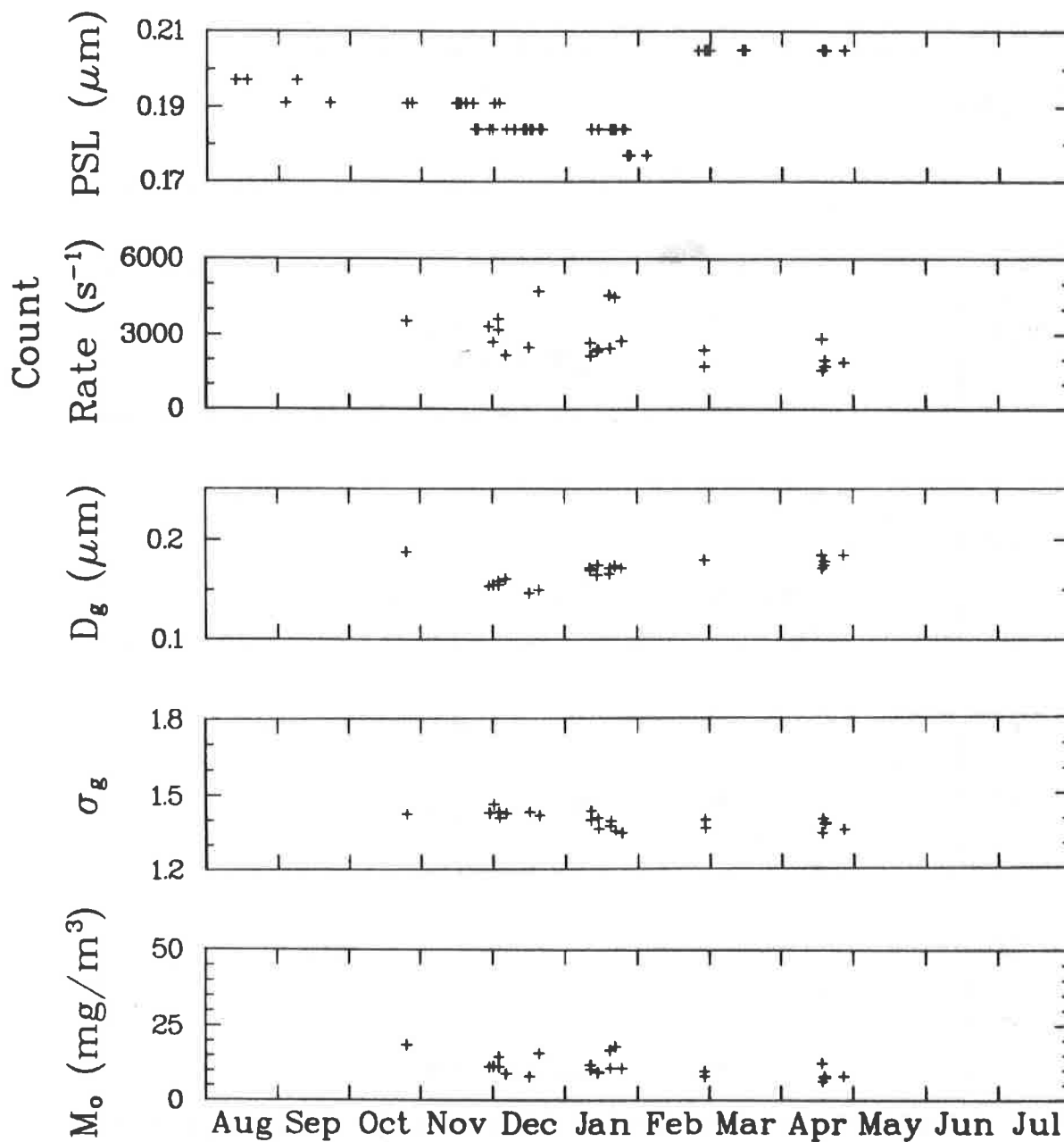
Figure 3.   Summary of first 9 months of data from all acceptable Hanford
Environmental Health Foundation FTF data sets (having count rate
< 5000 s^{-1}), including the central diameter of the LAS-X channel containing
the highest peak for PSL, count rate, geometric mean diameter, geometric
standard deviation, and estimated mass concentration.
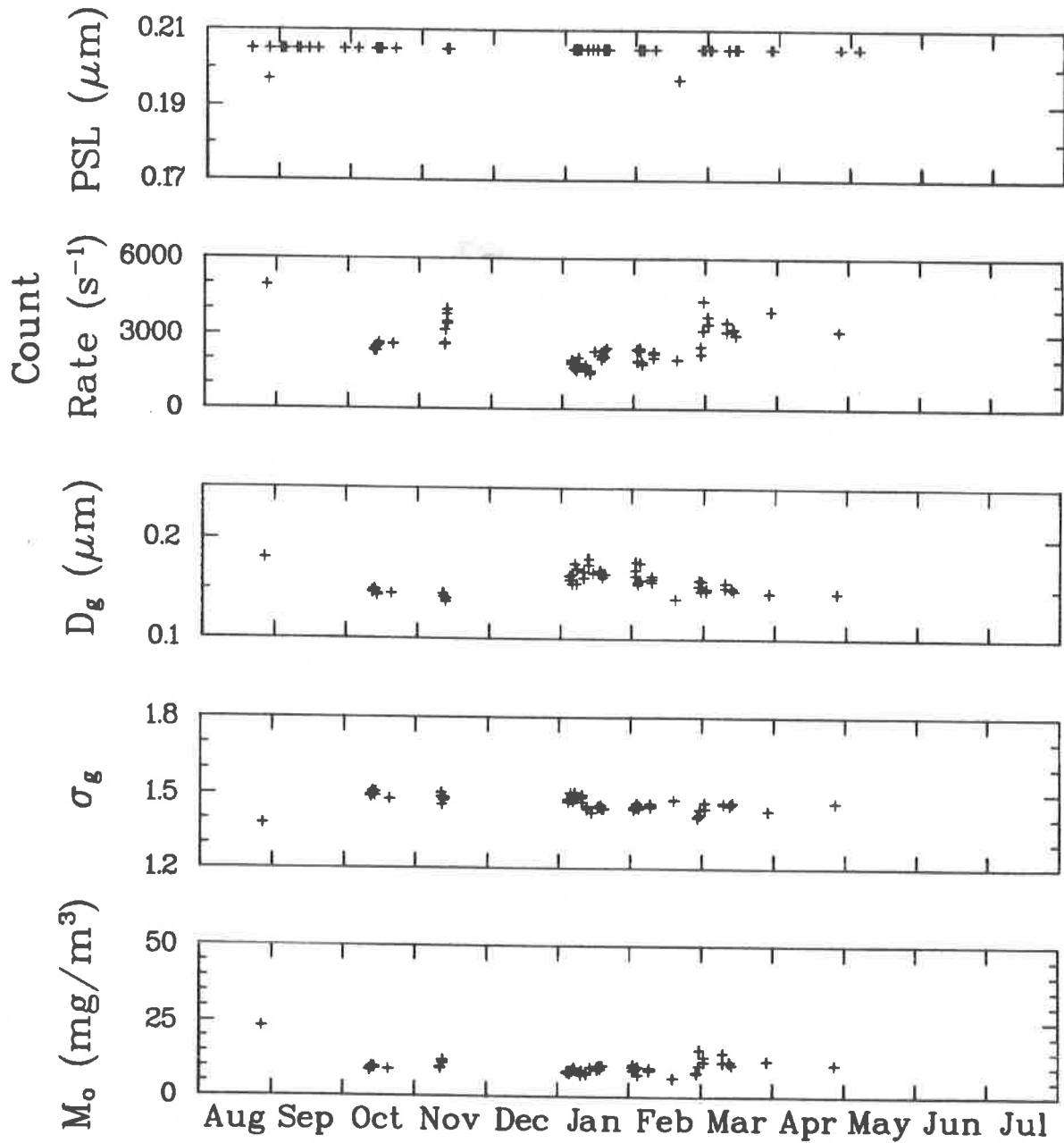
Figure 4.   Summary of first 9 months of data from all acceptable Oak Ridge
FTF data sets (having count rate < 5000 s⁻¹), including the central diameter
of the LAS-X channel containing the highest peak for PSL, count rate,
geometric mean diameter, geometric standard deviation, and estimated mass
concentration.

The bottom three graphs in the three figures show D_g, σ_g, and the calculated mass concentration (M_0) for the best-fit lognormal distribution determined by the nonlinear least-squares analysis of the data. These values provide an accurate description of the raw data, even when the size distribution is truncated.

The means and standard deviations of each of the five quantities graphed in Figures 2-4 are listed in Table 2 for each of the FTFs. The mean values of the geometric mean diameter and geometric standard deviation are essentially unchanged when only the data sets corresponding to a count rate below 3000 s^{-1} are included in the calculations.

Table 2. Summary of numerical results for Count Rate < 5000 s^{-1} (top line) and < 3000 s^{-1} (bottom line).

	RF-FTF	HEHF-FTF	OR-FTF
PSL Peak (μm)	.202±.004 [97][a]	.189±.009 [55]	.205±.002 [55]
Count Rate (s^{-1})	3713±898 [128] 2307±590 [25]	2769±909 [23] 2266±398 [16]	2559±767 [58] 2159±364 [42]
Geometric Mean Diameter (μm)	.14±.01 [128] .14±.02 [25]	.17±.01 [23] .17±.01 [16]	.16±.01 [58] .16±.01 [42]
Geometric Standard Deviation	1.61±.04 [128] 1.60±.06 [25]	1.40±.03 [23] 1.39±.03 [16]	1.46±.03 [58] 1.47±.03 [42]
Mass Concentration (mg/m^3)	29±7 [128] 20±5 [25]	11±3 [23] 10±2 [16]	10±2 [58] 9±1 [42]

[a]Mean±Standard Deviation [Number of Data Sets]

V. Discussion

As described by Scripsick, precise aerosol size, mass concentration, and penetration measurements using a laser spectrometer require a carefully operated and characterized diluter.[1] One important characteristic of a diluter in this application is the amount of variation of dilution ratio with particle size. Such variations might be seen if significant size dependent particle losses occur within the diluter.

The 5 cfm capillary diluters utilized in this study were not originally designed for use with the LAS-X, although they were among the few types available when they were provided to the FTFs during Salzman's early evaluations of the instrument.[2,5] They have not yet been fully characterized with respect to the variation of dilution ratio as a function of particle size. However, the FTFs used identical diluters, so comparisons of size distributions at the FTFs should be valid. Also, the expected particle losses in the capillary due to diffusional losses to the wall are negligible due to the relatively high volume flow rate through it (0.14 L/min at a dilution ratio of 1000). Impaction and sedimentation losses should also be

negligible for the small particle sizes encountered in this study. Thus, it is not expected that the preliminary size distribution measurements summarized in this interim report will differ significantly from those calculated once the diluters are more fully characterized.

The dilution ratios were calculated from the ratio of the volume flow rate through the capillary (calculated from the measured pressure drop across the capillary) and the volume flow rate through the bypass containing HEPA filters (calculated from the measured pressure drop across a metering orifice in the line). Limited validation of dilution ratios calculated by this technique was performed using a submicron oil aerosol and a photometer. The calculated dilution ratios should be considered to be approximate as should the mass concentrations derived using them. Since it was not an objective of this 1-year study to validate the ability of the LAS-X/diluter/HP-85 system to measure mass concentrations precisely, no further effort will be placed on refining the estimated dilution ratios and mass concentrations.

The data set census in Table 1 indicates that 1) the Rocky Flats FTF collected data on a larger number of days during the 9-month study period than did the other two FTFs, 2) approximately one-fifth of the calibration data sets were rejected as unacceptable, and 3) a large fraction of the Q107 aerosol data sets were rejected as unacceptable. Included in the number of data collection days in the first column of Table 1 were all days on which any calibration or Q107 aerosol data sets were recorded.

A "calibration data set" was defined as a data set for which the operator had chosen "PSL" as the value of the aerosol material parameter in the microcomputer program. In almost every case, at least one acceptable calibration data set was obtained by the FTF operators for each day that data was collected. In some cases, more than one calibration data set was obtained on a given day, especially near the beginning of the study when the operators were becoming familiar with the instrumentation and procedures. Common reasons for rejection of a calibration data set were 1) an incorrect date (often entered in an unacceptable format), 2) an incorrect choice of "PSL" for the value of the aerosol material parameter when sampling the Q107 aerosol, and 3) an error in not connecting the LAS-X to the PSL nebulizer output. These errors were relatively infrequent as shown by the 20 per cent rejection rate for the calibration data sets.

A large fraction of the Q107 data sets were rejected as unacceptable. Many of these data sets were rejected because the count rate was larger than 5000 s^{-1}. This was the case for approximately one-half of the rejected Q107 data sets at the RF-FTF, one-third of those at the HEHF-FTF, and three-fourths of those at the OR-FTF. These rejections are mostly due to the inability of the 5 cfm diluter supplied by Los Alamos to provide adequate dilution. During the first month of the study, the attainable dilution ratios were much too low making essentially every Q107 data set unacceptable. By the end of the first month of the study, Los Alamos had supplied a smaller diameter dilution tube to each FTF providing adequate dilution for many measurements, but not for all. Besides high count rates, other common reasons for rejection of Q107 aerosol data sets were 1) incorrect date, 2) incorrect identification of the aerosol material, e. g., DEHS at Rocky Flats where DEHP is used, 3) no dilution ratio entry, 4) no Owl reading entry, and 5) poor agreement in the overlap region of two LAS-X size ranges. Poor overlap is often a symptom of a count rate which is too high but could also be due to a fluctuating aerosol concentration.

Figures 2-4 and Table 2 contain a large amount of information which will be discussed in some detail. Referring to the top plot in each of the three figures, it can be seen that the PSL calibrations were quite consistent over the 9-month period at the RF-FTF (Figure 2), changed systematically with time at the HEHF-FTF (Figure 3), and were very consistent at the OR-FTF (Figure 4). On the highly magnified particle diameter scale of the plots, apparent changes in the size of the PSL spheres are recorded as noticeable jumps in the recorded PSL diameter. Each jump corresponds to the peak of the narrow PSL size distribution changing by one LAS-X size channel. The LAS-X unit at the HEHF-FTF was the only one of the three which may not have adequately corrected for the gradual dirtying of the optics during the many hours of operation. As seen in Figure 3, the apparent PSL size gradually decreased, dropping by three LAS-X bins throughout the first several months of the study. It increased to one bin above the original level after the unit was sent to the factory for maintenance and repair, which included cleaning of the optics. With the exception of the HEHF-FTF unit, the model LAS-X has been found capable of maintaining a consistent calibration in this study and in the laboratory work performed by Los Alamos.

The second plot (labeled Count Rate (s^{-1}) in each of the Figures 2-4 shows that the count rate was quite variable, even among Q107 data sets taken on the same day. The diluter settings were not changed at each of the FTFs after the first several weeks of operation, having been set to give the highest attainable dilution. The variable count rates and nominally constant dilution ratio explain the high variability of the estimated mass concentrations shown in the bottom plot (labeled M_0 (mg/m^3) of each of the Figures 2-4. Highly variable count rates could have arisen either from a highly variable concentration of Q107 aerosol or from a highly variable dilution ratio. If the concentration of the Q107 aerosol concentration varies significantly over 2 hours, the time between LAS-X measurements of the size distribution, it should be detectable as changes in the "100%" setting on the Q107 photometer. If the dilution ratio provided by the Los Alamos 5 cfm diluter varies significantly over 2 hours, it should be detectable as changes in the readings of the two gauges monitoring the two internal volume flow rates in the instrument. Further investigation may reveal the probable source of the high variability of the count rate and the estimated mass concentration. However, no definitive statement of the source of the variability can be made at this time with the available information.

The third plot [(labeled D_g (μm)] and the fourth plot (labeled σ_g) on each of the Figures 2-4 contain information relating to variations of the Q107 aerosol size distribution over time. With few exceptions, the two size distribution parameters are relatively constant at each FTF as shown in Table 2. There are no clear patterns of seasonal or daily variations which can be seen upon visual inspection of the data.

On February 29, the RF-FTF operators measured an unusually large geometric mean diameter (.22 μm) and an unusually small geometric standard deviation (1.40) for the first measurement of the Q107 aerosol of the day even though the Owl reading was constant at 29°. Two hours later the same two aerosol parameters had values of .13 μm and 1.66, which are much closer to the average values for the RF-FTF. A similar occurrence was noted about 4 weeks later when the two aerosol parameters values were D_g = .19 μm and σ_g = 1.44 for the first Q107 aerosol size measurement of the day, when the Owl reading was 28°.

It is a characteristic of the Owl that it cannot distinguish among the many polydisperse size distributions which will give an Owl reading of 29°.[6,7] This is illustrated in a Mie calculation of the Owl reading (polarization ratio) for a variety of lognormal distributions having geometric mean diameters between .1 and .4 μm and geometric standard deviations between 1.0 and 1.5 (Figure 5). In these calculations, the Owl is approximated by a light source which emits a single wavelength at .534 μm and a detector which subtends an negligibly small solid angle at a scattering angle of 90°. The results of the calculations which include these approximations provide a good indication of the trends in Owl response to polydisperse aerosols. As seen in Figure 5, lognormally distributed aerosols having increasingly smaller geometric mean diameters will give the same Owl reading as a .3 μm monodisperse (σ_g = 1.0) aerosol providing the polydisperse aerosol has a sufficiently large geometric standard deviation. This is the same trend seen in the two unusual Q107 aerosol size distribution results obtained at the RF-FTF. It is this ambiguity in measuring the size of a polydisperse aerosol which led to the consideration of the LAS-X as an alternative to the Owl to monitor the size distribution of the test aerosol at each FTF.
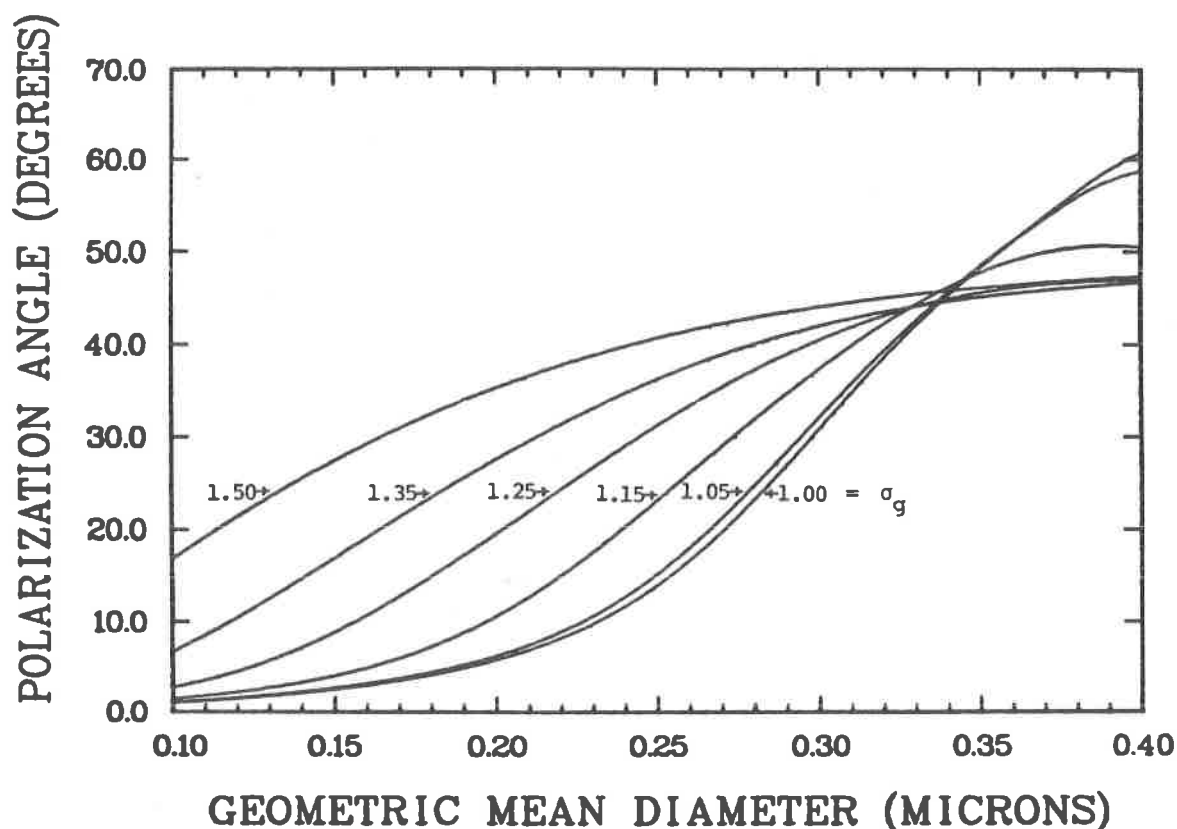
Figure 5.   Results of Mie scattered light calculations providing approximate predictions of the response of the Owl as a function of the geometric mean diameter and geometric standard deviation of lognormally distributed DEHP aerosols. The illuminating wavelength was taken to be .524 μm and the polarization ratio was calculated for 90° scattering.

The summary in Table 2 of the mean geometric mean diameter and geometric standard deviation for each FTF makes it clear that the Q107 aerosol is significantly different from the 0.3 μm monodisperse aerosol which is often associated with the Owl reading of 29° required by MIL-STD-282.[3] This is consistent with previous reports.[2,6] The proposed DOE Nuclear Standard NE-F-3-43 requires that any new penetrometer system which might be proposed to replace the Q107 should test HEPA filters with an aerosol having a geometric mean diameter between .16 and .24 μm and a geometric standard deviation between 1.3 and 1.5.[4] Table 2 indicates that two of the FTFs were testing HEPA filters during the first 9 months of the study with an aerosol which fell within those specifications. The RF-FTF typically had a smaller geometric mean diameter and larger geometric standard deviation.

There is no requirement presently for the FTFs to test HEPA filters with an aerosol meeting the specifications in NE-F-3-43 and no attempt was made to adjust any of the Q107's to match those specifications. It is conceivable that adjustments to the Q107 aerosol size distribution could be made based on the information obtainable from sampling with the LAS-X/diluter/HP-85 system to meet both the aerosol specifications of NE-F-3-43 and the requirement of an Owl reading of 29° in MIL-STD-282.

The RF-FTF proceeded with a planned replacement of the Q107 on which these data were obtained during mid-1984. Approximately 1 month's data should be available at the end of the full study to indicate the typical aerosol size distribution generated by the new Q107 at the RF-FTF.

The mass concentration estimates summarized in Table 2 based on the LAS-X measurements should be considered approximate due to the incomplete characterization of the diluter provided to the FTFs for this study. Accurate mass concentration measurements with a laser spectrometer require accurate sizing, particle counting, and dilution ratios. It was not an objective of this 1-year study to make accurate mass concentration measurements with the LAS-X particle size measurement system.

A complete evaluation of the operation of the LAS-X at each FTF during this study will be given in the final report. Some operational points of interest are: 1) FTF operators typically took only a few minutes to perform the calibration check of the LAS-X each day and a few minutes to make each LAS-X size measurement of the Q107 aerosol, 2) a major repair of the RF-FTF LAS-X was required due to a failure of a circuit involved in data transfer to the HP-85 microcomputer, 3) a major repair of the OR-FTF LAS-X involved replacement of a power supply, and 4) the HEHF-FTF LAS-X was sent to the factory for cleaning and calibration due to the increasing error in measuring the diameter of the PSL calibration aerosol. Loss of the LAS-X due to these repairs accounts for the major data gaps seen in Figures 2-4. Over the period of this program at Los Alamos, it has been found that each LAS-X typically requires replacement of the laser tube approximately once each year. The manufacturer has recently stated that a new laser tube assembly technique may extend the laser lifetime to approximately 5 years. It is clear that if the LAS-X were to be incorporated into the HEPA filter testing system, a back-up LAS-X should be available at each FTF in order to avoid delays in filter testing, since each LAS-X typically has to be removed from service at least once each year for factory calibration and/or repair. Such back-up instrumentation is a normal requirement at any facility requiring uninterrupted operation.

VI.   Summary of Major Conclusions

Several major conclusions have been reached based on the analyses of the first 9 month's data from the 1-year study. Additional detailed conclusions and, perhaps, modifications of the following conclusions will be available in the final report detailing the results of the full study.

1. The LAS-X can be successfully operated in the FTF environment to measure the size distribution of the Q107 test aerosol.

2. Incorporation of the LAS-X into the quality assurance test procedures would require a back-up LAS-X at each FTF and a more convenient and better characterized diluter than the one provided to the FTFs for this study.

3. Either the concentration of the Q107 test aerosol or the dilution ratio of the diluter provided to the FTFs for this study is quite variable over time.

4. The measured Q107 aerosol size distributions are not monodisperse as assumed in the existing MIL-STD-282 and they do not all meet the size distribution specifications which a replacement aerosol would be required to meet by DOE Nuclear Standard NE-F-3-43.

5. The test aerosol at each FTF has a quite consistent size distribution over time.

6. The test aerosols at the three FTFs differ consistently.

The 1-year study is succeeding in providing information to DOE which will be important in deciding whether the LAS-X particle size measurement system should replace the Owl to monitor the aerosol size distributions at the FTFs.

Acknowledgements

The assistance and cooperation of personnel from the three DOE FTFs are greatly appreciated. This study is possible only due to their efforts. Among the many Los Alamos personnel making important contributions to the successful completion of this work are: Harry J. Ettinger, Ronald C. Scripsick, and Lloyd D. Wheat.

References

1.   Scripsick, R. C., Soderholm, S. C., and Tillery, M. I., "Evaluation of Methods, Instrumentation and Materials Pertinent to Quality Assurance Filter Penetration Testing," presented to the 18th DOE Nuclear Airborne Waste Management and Air Cleaning Conference, Baltimore, MD, Los Alamos Report LA-UR-84-2425 (1984).

2.   Salzman, G. C., Ettinger, H. J., Tillery, M. I., Wheat, L. D., and Grace, W. K., "Potential Application of a Single Particle Aerosol Spectrometer for Monitoring Aerosol Size at the DOE Filter Test Facilities," Proceedings of the 17th DOE Nuclear Air Cleaning Conference, CONF-820833, pp. 801-813 (1983).

3. Military Standard, "Filter Units, Protective Clothing, Gas Mask Components and Related Products, Performance Test Methods," MIL-STD-282 (1956).

4. Filter Test Facility Standards Writing Group, "Quality Assurance Testing of HEPA Filters and Respirator Canisters" DOE Nuclear Standard NE-F-3-43, U. S. Department of Energy (1984).

5. Elder, J. C., Kyle, T. G., Tillery, M. I., and Ettinger, H. J., "In-place Testing of Tandem HEPA Filter Stages Using Fluorescent Aerosols," Los Alamos Report LA-8805-MS (1981).

6. Hinds, W., First, M., Gibson, D., and Leith, D., "Size Distributions of the "Hot DOP" Aerosol Produced by ATI-127 Aerosol Generator," _Proceedings of the 15th DOE Nuclear Air Cleaning Conference_, CONF 780819, p. 1130 (1978).

7. Gerber, B. V., "Selected Polyethylene Glycols as "DOP" Substitutes," _Proceedings of the 16th DOE Nuclear Air Cleaning Conference_, CONF 801038, pp. 109-124 (1981).

DISCUSSION

GOULET: What were the effects on filter penetration when you had excusions of CMD and geometric standard deviation at Rocky Flats.

SODERHOLM: We had no information on this point. According to Vern Bergman's arguments, which are probably substantially correct, as long as the OWL reads 29°, the penetration measurements with the photometer will be quite similar.

BERGMAN: I am concerned about potential maintenance problems, if the laser spectrometer is used continuously for filter penetration tests. The reported maintenance represents laser usage over a small fraction of the period anticipated for filter penetration testing. Please comment on anticipated maintenance problems when you use the laser spectrometer for every test.

SODERHOLM: We have gained some experience in the one-year test and will gain more, as needed, before DOE makes any decisions. I am not sure we can extrapolate from that. We found that the technicians at the filter test facility are capable of operating the system, as it exists now, for measuring size distribut   a few. times a day. They are capable of performing a ten minute calibration at the beginning of every day. I think it was important to gain this sort of experience as a basis for having people decide whether this sort of system is too complex and too much trouble to be used in a penetration measuring mode. As we put together the protocol for the penetration test, we will be simplifying many things. We will have

a better diluter system then we had for this test. I think the general operational experience we had will be useful, but there will be sufficient changes that we will have to be careful how we extrapolate the data we have now.

BERGMAN: In a nutshell, my concern is that, if you use the unit every minute of the day, you may find that it is longer at the manufacturer's under repair, than it is in your laboratory. We have had a big problem cleaning the lenses every time I tried to clean them. It's not a simple task. People in the laser field appreciate that it requires a clean room and very sophisticated techniques. That is the question, and it is my primary concern.

SODERHOLM: Did you leave your laser spectrometer on all day, or was it essentially sampling air, or was it turned off and turned on two or three times a day as you needed it.

SMITHERMAN: The LAS-X, HP85 system was turned on only when in use, that is, only when testing 1,000 cfm filters. It was not left turned on all of the time, although it would be turned on throughout each day when testing 1,000 cfm filters.

SODERHOLM: We did not specify, one way or another, on that point in our procedures. Perhaps Ron Scripsick has had more experience than most in making penetration measurements and using

the instrument all day, day after day, with the same type of aerosol as in a spectrometer. We generally found that we needed to clean the lenses infrequently. I think we need more experience, and we will appreciate any additional input you can give us on how often cleaning is necessary.

DAVIS: We use a laser continuously, at least one shift a day, for testing VLSI filters. It is not turned off and on frequently, it is left on all day. We do not have much of a downtime problem.

SODERHOLM: Thank you for that experience.

SCRIPSICK: One of the major components associated with maintenance of the laser spectrometer is the laser tube. It is independent of how long you operate, but is associated with gas leakage from the tube. I know that at least one of the filter test facilities, that conducted the one year study, successfully cleaned the window, which is one of the optical components that Dr. Bergman talked about, and had no difficulty doing that. It demonstrates that it could be accomplished at the filter test facilities.

GERBER: In consideration of a large aerosol-standard deviation, the small mean size, and the lower limit of resolution of the LAS-X, what fraction of the total distribution does the laser see?

SODERHOLM: The latest spectrometers have a cutoff of about 0.095 μm. By the time you make the refractive index correction for DOP, there is a significant fraction of the distribution below 0.095 μm, although the peak of the distribution is well within the range of the laser spectrometer. I think 20-30% of the particles are too small to be sized by the laser. I had to rewrite the data analysis program because the short-form version that we use every day didn't take this into account. I had to go to another form that could handle the truncated distribution to get accurate results. Unfortunately, that takes several minutes per analysis. I was certainly aware that the truncation problem does occur.

GERBER: Might it not be prudent to use another device to check against the laser, such as a cascade impactor, or something of similar range but using a different principle?

SODERHOLM: Based on the work that Ron Scripsick has done, we have a good feel for the calibration of the laser spectrometer. He has mentioned that there are some problems with the calibration below about 0.15 μm. We have two standard, traceable calibration checks for the latest spectrometers. For the part it sees, I think we are measuring it accurately, for the part if doesn't see, we simply use an extrapolation.

ANDERSON: You make an issue of the differences between DOP as measured by the OWL and by the laser. Have you considered that the OWL reports a light scattering mean diameter whereas the LAS-X reports a number mean diameter? If you take the number mean diameter and correct it for standard deviation, and then if you built into it the refractive index difference between calibration with polystryene and with DOP, might there not be agreement? Perhaps you are trying to compare apples and oranges.

SODERHOLM: I have no doubt there probably would be agreement. We certainly are comparing apples and oranges. It seems to be a good source of job security for aerosol physicists. Certainly the OWL is measuring what it is meant to measure. It is looking at the scattered light, analyzing it, and coming up with an effective size which should be much different from the number distributions that are measured with the laser spectrometer. Knowing the theory of the OWL, we could correct the number distributions and come up with a similar light scattering diameter from the laser spectrometer data. I haven't done it, but if it is of enough interest, it can be done. We are not interested in showing whether the OWL works according to theory. I suspect it does. The issue is that the LAS-X gives more information about the size distribution and, thus, might be preferable for assuring that each filter test facility is testing with the same aerosol.

FIRST: It seems to me that it would be important to compare the results from different instruments, even if they don't ultimately agree. At least, we would like to know what the ratio is.

SODERHOLM: I have no doubt the OWL is doing what it is
capable of doing. To me the issue is, is the OWL capable of giving
enough information to the filter test facilities to assure that they
are consistently testing with the same aerosol, month to month and
among different facilities. I place the question in a broader con-
text and say, well, it is interesting to take two size measuring
instruments and see if they are both working right, but what we are
really interested in is testing filters well. One way, is to assure
that we have the same aerosol all the time. I think the laser
spectrometer is capable of giving more information about the aerosol
and, thus, can give us more assurance of testing with the same
aerosol.

FIRST: Let me point out that your slides showed a
great deal of consistency between the results of the laser spectrometer
and OWL. It suggests to me that the OWL was doing equally well in
assuring a uniform aerosol, day by day, at the filter test stations,
even though the specific numbers that were associated with the OWL
may have differed from the numbers that came out of the laser spectr-
ometer. As you have demonstrated, the aerosol characteristics dif-
fered from station to station. Therefore, my first question is,
would you agree that the OWL was giving the same information as the
laser sepctrometer with regard to the uniformity of the aerosol on
a daily basis? My second question is somewhat different, what is
your thought about making the aerosol properties the same for all of
the filter test stations based on the differences which you have
demonstrated in your talk?

SODERHOLM: I couldn't conceive that the OWL and the
laser spectrometer are giving the same information. The laser
spectrometer measures the whole (within truncation problems) dis-
tribution of the aerosol and, as you can see, I can then calculate
and write down a geometric mean diameter and a geometric standard
deviation. Those two numbers are a pretty fair description of the
aerosol since the fitted curves do fit the raw data quite nicely.
The aerosols do seem to be long-normal. So I have two numbers,
geometric mean diameter and geometric standard deviation. In the
case of the OWL, I have one number. It can be stated in different
ways, as an effective size of 0.3 μm, or as a polarization angle of
29°. Simplistically, comparing one number to two numbers, I can't
say I have the same amount of information. Basically, the OWL being
a light scanning instrument, is much more sensitive to the large
particle tail of the distribution. If you are interested in the
large particle tail mainly, that's a very good thing to have a
handle on. Dr. Bergman has made the point, rightfully I think, that
the photometer also looks at the large particle size of the distri-
bution. Therefore, if you have to have an anchor somewhere, some
consistency, that's not a bad place to have it. You certainly wouldn't
want an instrument that is looking only at the small particle tail of
the distribution. However, I think you do have more information from
the laser spectrometer than with the OWL; simply two numbers compared
to one, if you will.

FIRST: 1 don't think you answered the question
I asked. I agree with what you said, but my point was, if the laser
spectrometer gives evidence of a uniform generation of an aerosol, the
size of the aerosol is in fact, being controlled by the OWL. I was
trying to point out that if one instrument is judged to be consistent,
then the other must, likewise, be judged to be consistent since there
was no daily difference in the reading of one or the other. The
point I wish to make is that the OWL was as consistent, on a daily
basis, as the laser spectrometer. Otherwise, I don't see how they
could agree.

SODERHOLM: The data show that the aerosol is con-
sistent at the filter test facilities over months. I think that is
impressive. I would point to those couple of bothersome points at
Rocky Flats which bring out the possibility that two aerosols can
have essentially the same large particle tail and both read 29° on
the OWL but, when measured by the laser spectrometer, differ markedly.
The geometric standard deviation of that February 29 point, was, as
I recall, very close to 1.4, compared to an average of 1.6. I think
that is a noteable difference. The system that is in operation at
the filter test facility now is giving a consistent aerosol. The
aerosol is staying very much the same month after month. I guess
I would question whether, based on an OWL reading only, you can have
confidence on any given day that you have the same aerosol. That is
where I would begin to hedge and draw the line as to the amount of
information you get from the OWL.

FIRST: The other question was whether you are
going to make the aerosols uniform between the filter test facilities?

SODERHOLM: I think there are several questions
there. Perhaps the DOE question is whether they need to be uniform.
Taking a legalistic point of view, I think there is no standard, now,
which requires them to be any more uniform than that they all read
29° on the OWL, and, that, they are doing. It might be nice to bring
all of them closer together, as measured by the laser spectrometer,
and I certainly have no information to say that couldn't be done.
I am far from an expert on operating the Q-107, so I leave it to those
who know more about the operation of the device to say whether it
could be done.

Appendix D

CALIBRATION AND USE OF FILTER TEST FACILITY ORIFICE PLATES

D. E. Fain and T. W. Selby
Oak Ridge Gaseous Diffusion Plant,
operated by Martin Marietta Energy Systems, Inc.
for the U.S. Department of Energy,
under Contract No. DE-AC05-84OR21400

Abstract

Orifice plates used as secondary standards at the three DOE Filter Test Facilities, Edgewood Arsenal and three filter manufacturers, have been calibrated using the gas flow calibration standards at the Oak Ridge Gaseous Diffusion Plant. A description of the flow standards and the automatic data acquisition system used to acquire the calibration data and to achieve usually high precision will be given. The significant variation among the orifice plates made with the same specifications will be discussed. The relative merits of the use of various alternative methods of testing filters for pressure drop and how the results can be expected to compare when acquired at different facilities which are operated at different ambient atmospheric pressure and temperature conditions will be discussed.

I. Introduction

There are three official DOE filter test facilities. These facilities are located at the Oak Ridge Gaseous Diffusion Plant, Martin Marietta Energy Systems, Inc., Oak Ridge, Tennessee; the Rocky Flats Plant, Rockwell International Corporation, Rocky Flats, Colorado; and Rockwell Hanford Operations, Rockwell International Corporation, Richland, Washington. These test facilities are used by the DOE, and others, to test nuclear grade HEPA filters to provide Quality Assurance that the filters meet the required specifications. The filters are tested for both filter efficiency and pressure drop. In the test equipment, standard orifice plates are used to set the specified flow rates for the tests. There has existed a need to calibrate the orifice plates from the three facilities with a common calibration source to assure that the facilities have comparable tests. A project has been undertaken by the Oak Ridge Gaseous Diffusion Plant Flow Calibration Laboratory to calibrate these orifice plates. The Army Test Facility at the Edgewood Arsenal, Aberdeen Proving Grounds in Maryland, Cambridge Filter Corp., Flanders Filters Inc., and Mine Safety Appliances Co. have also chosen to participate in the program. In addition to reporting the results of the calibrations of the orifice plates, the means for using the calibration results will be discussed. A comparison of the orifice discharge coefficients for the orifice plates used at the seven facilities will be given. The pros and cons for the use of mass flow or volume flow rates for testing will be discussed. It is recommended that volume flow rates be used as a more practical and comparable means of testing filters. The rationale for this recommendation will be discussed. In any case, the atmospheric pressure and temperature must be known before either a mass or volume flow can be set up with the existing orifice plates. A recommendation to consider the use of

laminar flowmeters to replace the currently used orifice plates is discussed.

In general, the results of the calibration are quite good. The precision based on the standard deviations from a regression analysis of the discharge coefficients is about 1 1/2% for the small orifice plates and about 1/2% for the large orifice plates. The Oak Ridge large orifice plate was tested first and last. The time lapsed between the two tests was almost three months. The mean value of the discharge coefficient from the two tests was different by only 0.27%. This result clearly shows the quality of the calibrations. There was significant variation in the discharge coefficients for orifice plates from the different facilities. The spread in discharge coefficients for the small plates was 10% and the spread for the large plates was 7%. This variation in discharge coefficients shows the difficulty in making identical orifices and therefore indicates the need for calibration.

II. Discussion

Description of the Orifice Plates

Each of the seven facilities has two standard orifice plates. One of the plates consists of a 3/8-in.-thick metal plate, 24 x 24 in., with 49 holes drilled with a diameter of 3.00 cm on 6.00 cm centers. This plate then has a wooden frame around it with pressure taps located about 3.0 in. on either side of the plate. The wooden frame is about 11 1/2- to 11 7/8-in. thick and the plate is centered in the frame. The other orifice plate is a 1/4-in.-thick metal plate, 12 x 12 in., with 16 holes drilled with a diameter of 1.68 cm on 4 cm centers. These plates have similar wooden frames. Two of the facilities had a third orifice plate. The third orifice plate is similar in size to the larger standard orifice plate except that one had 1.75 in. and the other 2.0-in. diameter holes. The small standard orifice plates have been calibrated in the flow range from 30 to 300 scfm. The large standard orifice plates and the third orifice plates have been calibrated in the flow range from 200 to 2250 scfm.

Calibration Methods and Equipment

The calibrations were made with equipment which was designed to be used to certify and monitor high accuracy flow measurement devices at the three gaseous diffusion plants. Since the three plants are sites remote from each other, the equipment was designed to be portable. The equipment includes a large laminar flowmeter. The laminar flowmeter consists of a Miriam-type 50C2-8 flow element which has been mounted in a specially designed housing to provide flow straightening and fixed pipe runs on both sides of the flow element. This flowmeter was calibrated by the Colorado Engineering Experiment Station, Inc., (CEESI), and is traceable to the National Bureau of Standards. The CEESI calibration data included 27 data points taken at 70°F and 14.7 psia covering a flow range of 600 to 1500 scfm. The quoted accuracy was 0.5%. Through a special correlation method and with considerably more data taken at the ORGDP over a range of pressures from 13 to 20 psia, the useful range of the flowmeter has been increased to a range of 20 to 2500 scfm at operating pressures of

5 to 25 psia. The calibration method, the data, and a description of the equipment have been reported in the proceedings of the Second International Symposium on Flow--Its Measurement and Control in Science and Industry.*

In addition to the flowmeter, two other portable units were constructed. Both units are housed in 5-ft-high instrument cabinets. One of the units contained Datametrics, Inc. capacitance-type pressure transducers. There are three pairs of transducers with ranges of 100, 20, and 1 psid. Duplicate transducers are used, monitored, and compared to provide assurance that the pressure calibrations have not changed. The transducers are calibrated approximately every six months with a Schwein Mercury manometer which uses a laser readout to increase the manometer accuracy. This unit contains two small vacuum pumps, one for vacuum reference for transducers and the other for utility. The unit also contains pressure regulators which, with an adequate supply source, can provide absolute pressures from vacuum to about 100 psi and differential pressures from 0 to 10 psid. This unit has been used as a transfer standard for field calibration and certification of pressure transducers as well as providing the instrumentation for measuring the pressures and pressure differences for the laminar flowmeter and the flowmeter being calibrated.

The other unit contains data acquisition, data processing, data storage, and hardcopy output for graphics and alpha/numerics. These are Hewlett-Packard devices and include an HP-9825 desktop computer, an HP-3790 scanner, an HP-3455 digital voltmeter, an HP-9885 floppy disk drive, and an HP-7245 printer/plotter. This unit is used to acquire, process, store, and hardcopy output both data and graphics.

There is a significant advantage in using automatic data acquisition. The computer can be programed to monitor the instrumentation until steady state is achieved. Then multiple readings of the individual instruments can be made and then averaged to statistically reduce the effect of random variations such as pressure noise. In addition, if a number of readings are made on each individual instrument, then the readings can be correlated with time to assure that the system was close to steady state during the course of the measurement. With the help of the computer it is easy to use analytic expression for the relationship between the instrument output and the variable being measured. The computer then calculates a much more precise value of the variable being measured by using the analytic expression and an averaged instrument output to calculate the variable. The computer also calculates other appropriate parameters, such as flow rates, which may be desired for the particular measurement and outputs any relevant information.

---

*"Flow – Its Measurement and Control in Science and Industry," vol. 2, pp. 707-730, W. W. Durgin ed, Instrument Society of America, Research Triangle Park, NC, 1981.

Discussion of the Results

Twenty measurements were made on each of the orifice plates. Approximately half the measurements were made with increasing flow increments and half with decreasing flow increments. The flow range for the small orifice plates was 30 to 300 scfm and the flow range for the large orifice plates was 200 to 2250 scfm. An example listing of the data, which was obtained with the Oak Ridge large orifice, is given in Table 1.

Table 1.   Experimental data for orifice 63-12

Laminar flowmeter		Orifice plate		
Flow rate scfm	Pressure difference Inches of water	Pressure psia	Temperature °F	Discharge Coefficient
215.9	0.0475	14.455	82.1	0.66552
351.3	0.1261	14.455	82.0	0.66496
518.8	0.2743	14.455	82.0	0.66562
764.6	0.5960	14.456	82.0	0.66549
1011.2	1.0471	14.454	81.9	0.66405
1260.5	1.6305	14.453	81.9	0.66330
1474.2	2.2353	14.451	81.9	0.66260
1652.5	2.8116	14.449	81.9	0.66230
1791.2	3.3163	14.448	81.9	0.66103
1882.5	3.7133	14.447	81.9	0.65653
1944.8	3.9657	14.446	81.9	0.65637
2016.1	4.2085	14.429	82.2	0.66109
2057.5	4.3822	14.426	82.1	0.66120
2155.9	4.8336	14.423	82.2	0.65979
2185.3	4.9671	14.422	82.2	0.65976
2153.1	4.8214	14.417	82.3	0.65996
2029.6	4.2793	14.417	82.2	0.66027
1716.3	3.0480	14.419	82.3	0.66160
1043.2	1.1203	14.422	82.4	0.66325
220.7	0.0490	14.424	82.6	0.67128

Using the measured calibration data, an orifice discharge coefficient was calculated for each measured data point. The discharge coefficient was calculated from the ideal orifice flow equation[1]

$$M = K_m \; C (\frac{P \Delta P}{T})^{1/2} \tag{1}$$

where:

M = mass flow rate in standard cubic feet per minute (scfm)

P = the pressure on the upstream side of the orifice in psi (for all practical purposes, the ambient pressure)

ΔP = the pressure difference across the orifice in inches of water

T = the gas temperature in degree Rankine

K_m = a constant including the area, molecular weight of the gas and unit conversion factors

C = the discharge coefficient,

therefore,

$$C = \left(\frac{T}{P \Delta P}\right)^{1/2} \frac{M}{K_m} \qquad (2)$$

A linear regression of these measured discharge coefficients with mass flow rate was calculated. A graphical presentation of the measured discharge coefficients from Table 1 is shown in Figure 1 where the discharge coefficients are plotted against the mass flow rate in scfm. The Xs are the measured data points and the solid straight line is the linear regression with flow rate. The mean value of the discharge coefficient at 1000 scfm is 0.664. The regression analysis gave a standard deviation for the linear fit of 0.0022 which implies a standard error for the discharge coefficients of only 0.33%.
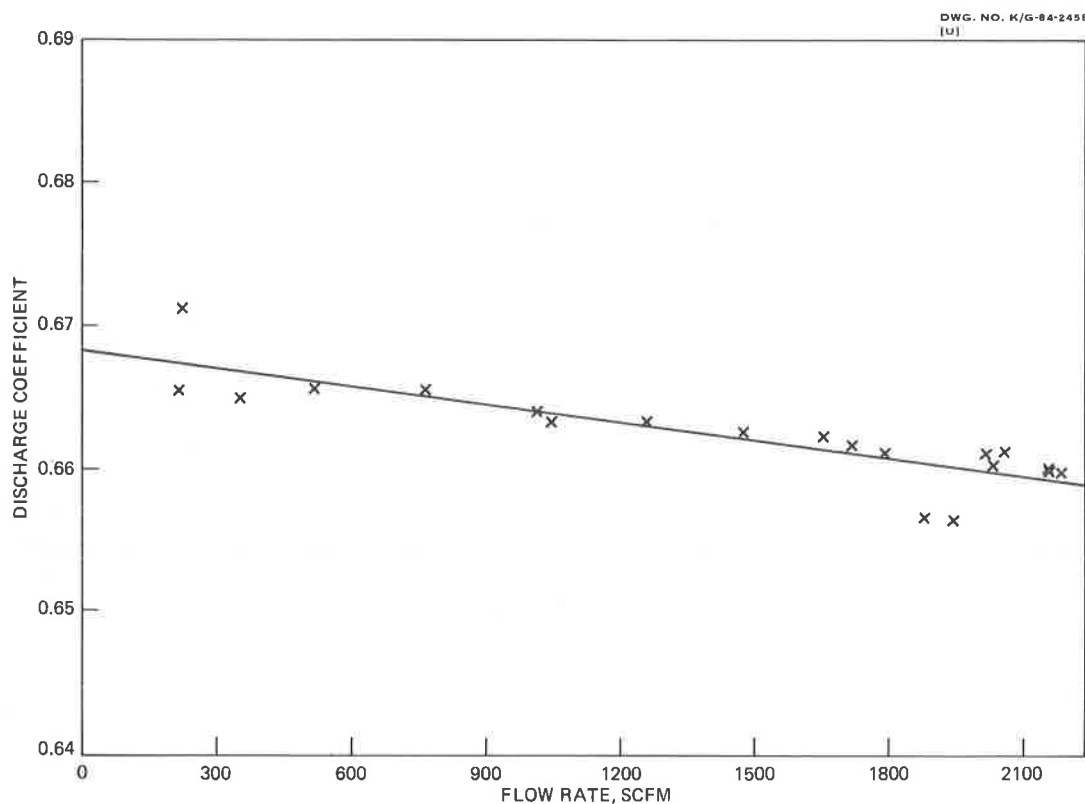
FIGURE 1
ORIFICE PLATE CALIBRATIONS FOR FILTER TEST FACILITIES
ORIFICE PLATE # 63-12

As a measure of control for the overall calibration program this orifice plate, which was the first one calibrated, was recalibrated

again at the end of the program following the same procedures as used in all the other calibrations. The period between the first and second calibration was almost three months. The second calibration was actually better than the first one, in the sense that the standard deviation on the regression analysis was even less than that on the first data set. The standard deviation on the regression analysis for the second set was 0.00083, which implies a standard error of only 0.12%. The difference in the mean value of the discharge coefficients for the first and second calibration was only 0.27%. This excellent agreement between the two results clearly indicates the high quality of the calibrations.

An analysis of the instrument error indicates that essentially all of the uncertainty or random error is associated with the noise or random variation in the measurement of the pressure differences across the orifice plate and the laminar flowmeter. The data did indicate that the pressure drop across the orifice plates was quite noisy. If a low time constant pressure transducer is used for that measurement, then some type of averaging will probably be very desirable. In the case of a water manometer, the inertia of the fluid provides some averaging. The uncertainty or random error of the on-site measurements will depend, primarily, on the type of device used and its error associated with the measurement of the pressure difference across the orifice.

It should be noted that most of the orifice plates tested showed a transition from turbulent to laminar flow at the lower flow rates used in the calibration tests. The transition occurred between 100 and 200 scfm for the larger orifice plates and between 15 and 30 scfm for the small orifice plates. These data points were deleted from the linear regression analyses and, of course, the orifice plates should not be used to measure flows below these values (unless extensive additional calibration data are obtained). In Figure 2, an example of calibration data exhibiting this trend is shown.

The calibration data were obtained over a rather small range of ambient pressures and temperatures. There could well be a question of how much error or uncertainty may be expected in using the discharge coefficients measured under these conditions at other pressures and temperatures. The equation for flow through an orifice is derived from first principles. The pressure drop across an orifice simply represents the force per unit area required to accelerate the gas to the velocity at the throat of the orifice. In terms of the Bernoulli principle, the change in potential energy (pressure) across the orifice is equal to the kinetic energy in the throat of the orifice. The measurement of a discharge coefficient is the classical way of correlating measurements with an orifice. The discharge coefficient represents the ratio of the effective area through which the gas flows to the actual area of the orifice. The effective area of the orifice is smaller than the actual area because the converging effect of the gas flow streamlines tend to cause them to be constricted in the throat of the orifice when the flow is turbulent. One reason the discharge coefficient increases as the flow becomes laminar is that the constricting forces become less as the gas velocity decreases and the flow area then approaches the actual orifice area as the flow rate

DWG. NO. K/G-84-2459
(U)
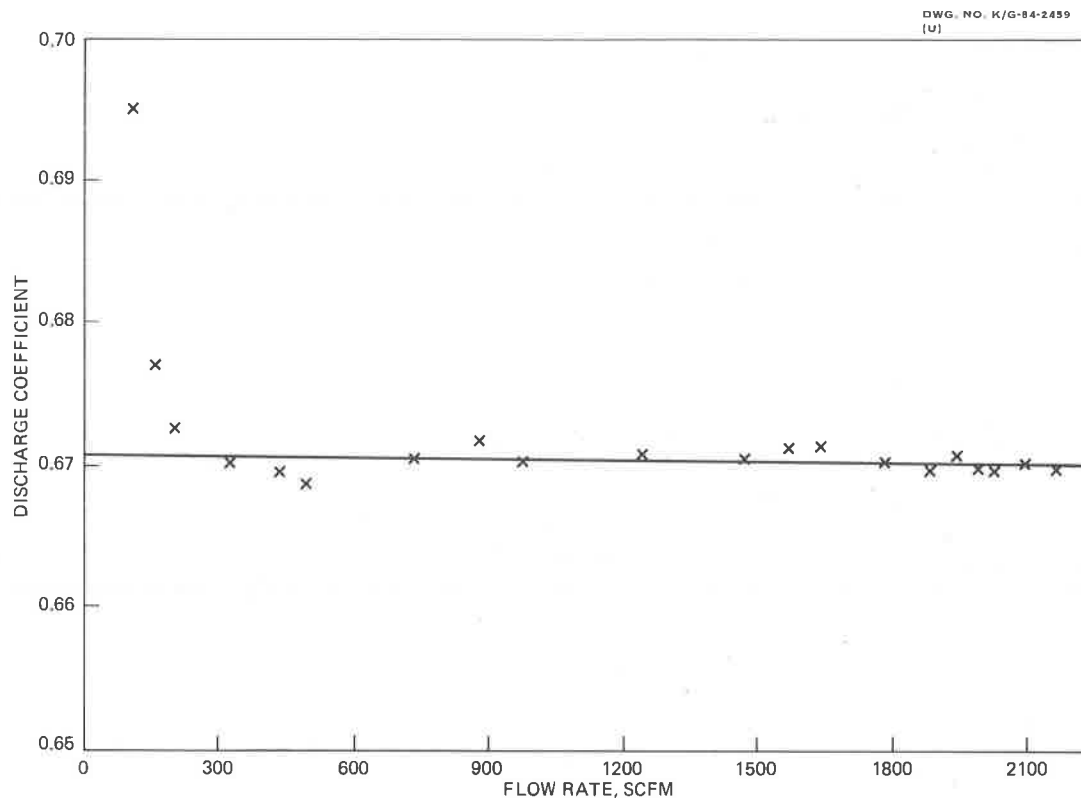
FIGURE 2
ORIFICE PLATE CALIBRATIONS FOR FILTER TEST FACILITIES
ORIFICE PLATE # 63-13

approaches zero. In addition, in the laminar flow range viscous frictional losses become important and even the functional dependence of the flow changes. In the flow range where the discharge coefficient is constant, the effective area is remaining constant and relatively large variations in temperature and pressure should not affect that effective area (except perhaps near the laminar flow range). Usually the correlation or regression analysis of the discharge coefficient is made with the Reynolds Number instead of with the mass flow rate. However, the Reynolds Number is just the mass flow rate divided by the product of the area and the viscosity. Since the variation in the viscosity is rather small compared to the variation of the mass flow rate, a correlation with the mass flow rate is essentially the same as a correlation with the Reynolds Number. This is even more accurately correct since there is very little correlation with the flow rate (the discharge coefficient is nearly constant). Since the discharge coefficients are so nearly constant in the flow range after the flow becomes turbulent, there is a great deal of confidence based on experience that the discharge coefficients will remain constant over a range of pressure and temperature much greater than will be expected for ambient condition variations.

An attempt was made to make some experimental measurements at different pressure levels. This was attempted by trying to throttle the flow (drop the pressure) in front of the orifice plate. The crude means for doing this left the flow somewhat unstable and therefore the precision of the measurements was not nearly as good as the calibration data. However, the result did not indicate that there

1174

should be any concern in using the discharge coefficients in the range of ambient conditions that can be expected to be encountered. In addition it should be noted that during the progress of the calibration testing the ambient conditions did change somewhat. The pressure varied by only 0.25 psia, but the temperature varied by 17°F (from 72 to 89°F). The variation in the discharge coefficients determined on the different orifice plates showed no correlation with either the variation in pressure or temperature. This lack of any correlation tends to indicate that the equations used do properly account for variations in the pressure and temperature.

There may also be questions concerning the affect of various configurations of ducting either upstream or downstream of the orifice plate at the different facilities. This question was a serious concern before calibration testing began. Consideration was given to building a rather elaborate ducting system in the calibration laboratory to try to nearly duplicate the types of arrangements at the various facilities. Prior to the actual calibration test, Oak Ridge's large orifice plate was used to test two different configurations. In one configuration the laminar flowmeter, used as the standard to measure the flow rates, was installed upstream of the orifice plate and a short duct was used to connect the laminar flowmeter and the orifice plate. The outlet from the laminar flowmeter was 10 in. in diameter. In this configuration, there was essentially a 10-in. diameter jet directed at the orifice plate. In the second configuration, nothing was placed in front of the entrance to the orifice plate. The inlet end of the orifice plate was open to ambient atmosphere. The laminar flowmeter was mounted downstream from the orifice plate. The discharge coefficients measured with these two grossly different configurations showed no statistical differences. These data indicate that there should be no difficulty or expectation of error due to variations in the configuration of the various testing facilities.

There may also be some concern about the effect of humidity on the use of the orifice plates. The presence of moisture in the atmosphere should have no effect on the performance of the orifice plates. Even the correction for the gas density at 100% humidity is negligible. While the author has little experience with the types of devices used in the filter test stands to monitor the flows during testing, it is unlikely that the presence of moisture will have a significant affect on the accuracy of the monitoring. There should be no concern that the presence of moisture in the air will adversely affect the flow measurement in the filter test stand. On the other hand, the presence of moisture may have an affect on the performance of the filter which is being tested. If there is any absorption of the moisture into the fibers on the filter, there could be a change in the effective void fraction of the filter which would affect the pressure drop across the filter. An independent study could be performed to determine if moisture has an effect on the test results on the filters.

Using the Calibration Data

The equation[3] for mass flow, M, in standard cubic feet per

minute (scfm)* is

$$M = K_m C \left(\frac{P\Delta P}{T}\right)^{1/2} \tag{3}$$

and the equation[4] for volume flow, V, in actual cubic feet per minute (acfm) is

$$V = K_v C \left(\frac{T\Delta P}{P}\right)^{1/2} \tag{4}$$

In both cases the orifice high-side pressure, P, is in psi, the orifice pressure difference, ΔP, is in inches of water (at 70°F) and the temperature, T, is in degrees Rankine.

   The linear regression equation used for the orifice plate discharge coefficients is

$$C = C_O + SM \tag{5}$$

where:

   C   = the discharge coefficient at the mass flow M

   C_O = the discharge coefficient extrapolate to zero flow

   S   = the slope of the regression line

   In Table 2 the zero flow discharge coefficients, C_O, the slopes, S, and the average value of the discharge coefficients, are given along with the two constants K_W and K_v. The average discharge coefficients, $\overline{C}$, are given for 1000 scfm for the large orifice plates and at 100 scfm for the small orifice plates. Equations (3), (4), and (5) can be used with the appropriate constants to calculate the flow rates for given operating conditions or to calculate the pressure drop needed to achieve a given flow rate at known ambient pressure and temperature.

   The variation of these discharge coefficients is very small and may even be ignored by using the average discharge coefficient $\overline{C}$ for C in Equations (3) and (4). However, the discharge coefficient variation with flow rate can easily be taken into account by using $\overline{C}$, in Equation (3) with the actual pressure, pressure difference, and temperature to estimate an approximate mass flow rate. Using this approximate value for the flow rate, calculate the discharge coefficient. With this discharge coefficient use the appropriate

---

*The standard conditions referred to are one standard atmosphere (i.e. 14.696 psia) and 25°C. The mass flow as indicated is given in standard volume units. The actual mass flow rate is obtained by multiplying this unit by the gas density at the standard conditions.

Table 2.   Flow equation constants for calibrated orifice plates

Orifice No.	Co	S	$\overline{C}$	Km	Kv
Oak Ridge facility					
63-6	0.69189	4.748×10^{-5}	0.69664	926.65	25.374
63-12	0.66825	-4.187×10^{-6}	0.66406	9109.9	249.46
Hanford facility					
63-5	0.71628	1.510×10^{-6}	0.71643	926.65	25.374
63-11	0.66202	-4.202×10^{-6}	0.65782	9109.9	249.46
Rocky Flats facility					
RkyF-2	0.68623	-1.528×10^{-5}	0.68471	926.65	25.374
RkyF-1	0.70887	-5.217×10^{-6}	0.70365	9109.9	249.46
Cambridge facility					
63-7	0.72521	-3.089×10^{-5}	0.72212	926.65	25.374
63-14	0.67041	-3.989×10^{-7}	0.67001	9109.9	249.46
C-2000	0.67821	-7.882×10^{-7}	0.67742	14658.6	401.40
Flanders facility					
63-4	0.67843	4.437×10^{-6}	0.67887	926.65	25.374
63-13	0.67086	-3.031×10^{-7}	0.67055	9109.9	249.46
MSA facility					
63-2	0.68979	6.909×10^{-5}	0.69669	926.65	25.374
63-9	0.67105	-2.318×10^{-6}	0.66873	9109.9	249.46
63-42	0.68943	-1.689×10^{-5}	0.67254	20041.7	548.81
U.S. Army facility					
small	0.65368	4.186×10^{-5}	0.65787	926.65	25.374
large	0.68923	-1.306×10^{-6}	0.68792	9109.9	249.46

equation to calculate either the mass flow rate or the volume flow rate, whichever is desired.

If the operating conditions needed to obtain a specific flow rate are desired, rather than calculation of the flow rate for some set of measured conditions, the procedure would be as follows: Obtain a good measurement of the ambient atmospheric pressure and the temperature.   Then Equations (3) and (4) can be solved for the pressure difference as shown below for a desired mass flow rate, M

$$\Delta P = \frac{T}{P} \frac{M^2}{K_v^2 C^2} \qquad (6)$$

or for desired volume flow rate, V

$$\Delta P = \frac{P}{T} \frac{V^2}{K_v^2 C^2} \qquad (7)$$

As previously given, if orifice high-side pressure, P, is in psi,

temperature is in degrees Rankine and flow rates are standard cubic feet per minute or actual cubic feet per minute respectively, then the pressure difference, ΔP, will be in inches of water. Thus, the pressure difference which should be set up across the orifice to give the desired flow rate can be calculated using Equations (6) and (7).

A less tedious way to use the calibration data is to use the regression equations once to generate tables which can be used by the operating personnel. The tables could show the pressure difference across the orifice plate for various incremental changes in the flow rate at fixed ambient pressures and temperatures. Depending on the individual needs, a large number of tables can be generated with small incremental changes or a smaller number of tables with larger incremental changes. An example of such a data table is shown in Table 3. In the latter case, the following linear interpolation between points given in the table can be helpful for improving accuracy without the complication and tedium of using the full equations.

$$V' = \frac{V}{2}\left(2 + \frac{\Delta(\Delta P)}{\Delta P} + \frac{\Delta(T)}{T+460} - \frac{\Delta(P)}{P}\right) \tag{8}$$

If V, ΔP, T, and P are values of the actual volume flow, pressure difference, temperature, and pressure given in the table, then V' is the volume flow at conditions that are different from those given in the table by a difference in pressure difference of $\Delta(\Delta P)$, a difference in temperature of $\Delta(T)$, and a difference in ambient

Table 3. Pressure difference in inches of water for volume flow rates in acfm orifice plate 63-12 at 750 torr

Flow rate	60	70	80	90	100
200	0.040	0.040	0.039	0.038	0.037
300	0.091	0.089	0.087	0.086	0.084
400	0.161	0.158	0.156	0.153	0.150
500	0.253	0.248	0.243	0.239	0.235
600	0.364	0.357	0.351	0.344	0.338
700	0.496	0.487	0.478	0.469	0.461
800	0.649	0.637	0.625	0.614	0.603
900	0.823	0.807	0.792	0.778	0.764
1000	1.017	0.998	0.979	0.961	0.944
1100	1.232	1.209	1.186	1.165	1.144
1200	1.468	1.440	1.414	1.388	1.363
1300	1.725	1.693	1.661	1.631	1.602
1400	2.003	1.966	1.929	1.894	1.860
1500	2.303	2.259	2.217	2.177	2.138
1600	2.623	2.574	2.526	2.480	2.436
1700	2.965	2.909	2.855	2.803	2.753
1800	3.328	3.266	3.205	3.147	3.901
1900	3.713	3.643	3.576	3.511	3.448
2000	4.120	4.042	3.967	3.895	3.825
2100	4.548	4.462	4.379	4.299	4.223
2200	4.997	4.903	4.812	4.725	4.640

pressure of $\Delta(P)$. Care should be used to assure that the correct algebraic sign is used with these differences. These differences should be the new value minus the table value. If the new value is smaller than the table value then a minus sign should be associated with the value of the difference. If interpolation to a specific flow is desired, then Equation (8) can be solved for the new $\Delta P'$ to give

$$\Delta P' = \Delta P \left(1 + 2\frac{(V' - V)}{V} - \frac{\Delta(T)}{(T+460)} + \frac{\Delta(P)}{P}\right) \qquad . \qquad (9)$$

Although the accuracy of this equation will be best when used to interpolate between adjacent points in the table, the interpolation can extend further. However, the difference in variables probably should not exceed 25%.

The corresponding interpolation equations for mass flow are:

$$M' = \frac{M}{2}\left(2 + \frac{\Delta(P)}{P} + \frac{\Delta(\Delta P)}{\Delta P} - \frac{\Delta(T)}{T + 460}\right) \qquad (10)$$

and

$$\Delta P' = \Delta P\left(1 + 2\frac{(M' - M)}{M} - \frac{\Delta(P)}{P} + \frac{\Delta T}{T + 460}\right) \qquad (11)$$

Comments and Recommendations for Filter Testing Procedures

There might appear to be some controversy over whether one should use mass or volume flow rates in testing filters. The first consideration really should be based on the characteristics of the filter and how it is to be used. Is it most likely to be used in systems that operate with fixed mass flow rates or with fixed volume flow rates? If there is a large majority of one or the other, then that type of flow rate should be used for the filter testing. However, if the flow characteristics of the filters are known, then it really makes no difference because the required parameters can be determined analytically from the measured parameters of either method. It is generally expected that gas flow through HEPA filters is laminar or Poiseuille-Hagen flow.

In order to evaluate the flow characteristics of the HEPA filter, one of the filters was tested over a flow range of 200 to 2000 scfm. The data obtained is shown in Figure 3. The ordinate (Y-axis) is simply the ratio of the variable parameters needed to calculate laminar flow to the measured flow rate. If the filter flow characteristics were ideally laminar, then the ordinate should be a constant and the data should be distributed on a horizontal line in Figure 3. Since the ordinate seems to vary with flow rate, the filter flow characteristics are not ideally laminar. The apparent linear dependence of the ordinate on the flow rate is characteristic of the type of effect caused by entrance and exit pressure losses resulting from the acceleration or deceleration of the gas as it enters or exits the filter. If these data are representative of what can be expected

DWG. NO. K/G-84-2460
(U)
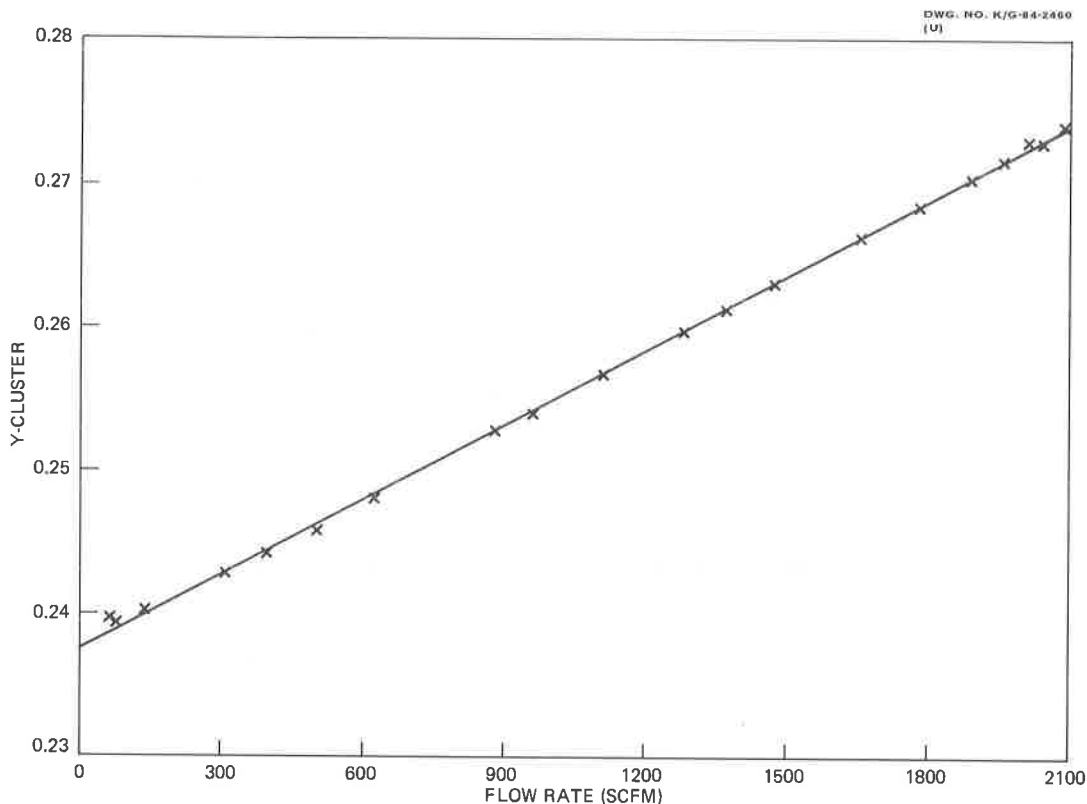
FIGURE 3
FLOW CHARACTERISTICS OF A HEPA FILTER

for all HEPA filters, the deviations from ideal laminar behavior are relatively small; for all practical purposes, the filters may be considered to be essentially ideal laminar flow devices. That being the case, it makes little difference relative to the filter itself which type of flow rate is chosen for the testing. Having the filter characteristics from either type of test, the operating conditions for the filter can be predicted analytically.

The next consideration should be the means that is used to set up the flow rates for the tests. Since laminar flow characteristics are such that for a given volume flow rate the pressure difference across the laminar device is independent of the gas density, it is sometimes assumed that the pressure difference is independent of the pressure and temperature. However, this is not true. The pressure difference still depends on the temperature because of the variation in the gas viscosity with temperature. Neglecting this fact, it would appear that using a given volume flow rate for testing of the filters would be a significant advantage. However, even if this were the case, a device must be available to set up the given known volume flow rate without knowing the gas density or the atmospheric pressure and the temperature. If the reproducible measurement of the pressure difference across a filter were all that is required, a laminar flow device would be ideal for this purpose. It could be used to set up a known pressure difference without knowing or measuring the atmospheric pressure or the temperature. If both the device being tested and the device being used to set up the flow rates are laminar flow devices, then measuring the pressure drop across both devices is all that is needed to describe the device being tested.

Currently the orifice plates are used to set up the known flow rates, the flow characteristics of the orifice plate must be considered. The orifice plate flow characteristics are well determined from the calibration data. These characteristics are described by Equations (3) and (4). As can be seen from these equations, the atmospheric pressure and the temperature must be known for establishing either a mass flow or a volume flow. Since the parameters must be known in either case, it makes little difference whether a given mass flow or a given volume flow is used for the filter tests. The appropriate tables or equations can be used to set up the given flow rate and the appropriate parameter can be related to the filter. The current practice is to rate the filters in terms of pressure difference at a given flow rate. If a mass flow is used, the pressure difference should be related to some standard conditions. This can easily be done by multiplying the measured pressure difference by the ratio of the atmospheric pressure to the standard pressure, dividing by the ratio of the ambient temperature to the standard temperature, and dividing by the ratio of the viscosity at ambient temperature to the viscosity at standard temperature. Both pressure and temperature had to be known to set up a mass flow rate in the first place. If volume flow is used for filter testing, the pressure differences can be used directly without reference to a standard set of conditions with much less error than when mass flow is used. To be correct even with volume flow, the pressure difference should be multiplied by the ratio of viscosity at some standard temperature to the viscosity at the measurement temperature.

Perhaps a better understanding of the relationships can be achieved by using the characteristics of the HEPA filter determined from the flow tests to calculate expected filter test results. In Figure 4 the variation in pressure difference across the filter with pressure level and temperature is shown for a fixed mass flow rate of 1000 scfm. As can be seen, the pressure drop varies 25% over the pressure range calculated and it varies 13% for the temperature range calculated. In Figure 5 the same calculation is made for a fixed volume flow rate of 1000 scfm. Over the same range in pressure and temperature, the variation in the pressure drop across the filter is much smaller, only 5%. There is no variation with pressure. The variation is all with temperature. The reason for that variation is the variation in the value of the viscosity with temperature. If the pressure difference were normalized or corrected to a standard viscosity, most of the variation shown in Figure 5 could be illuminated. However, the same comment also applies to the variation shown in Figure 4. If the pressure drops in Figure 4 were normalized or corrected to a standard condition by multiplying the pressure difference by the ratio of the ambient pressure to a standard pressure, dividing by the ratio of the ambient temperature to a standard temperature, and dividing by the ratio of the viscosity of the gas at the ambient temperature to the viscosity at the standard temperature, essentially all of the variation in the pressure difference would be removed. A small amount of variation will remain because of the non-ideal behavior shown in Figure 3. The results shown in Figure 5 indicate that the use of a fixed volume flow rate produces the best results with the least amount of calculation and correction.

DWG. NO. K/G-84-2461
(U)
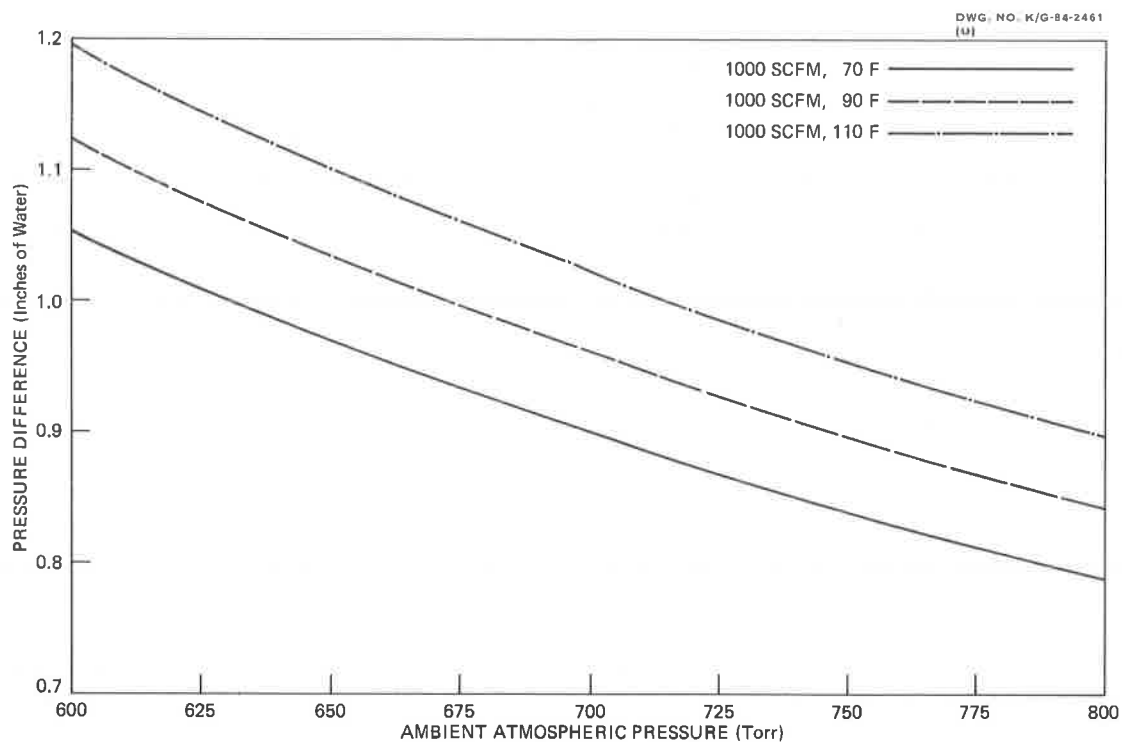
FIGURE 4
PRESSURE DROP ACROSS A HEPA FILTER WITH 1000 SCFM FOR VARIOUS OPERATING CONDITIONS

DWG. NO. K/G-84-2462
(U)
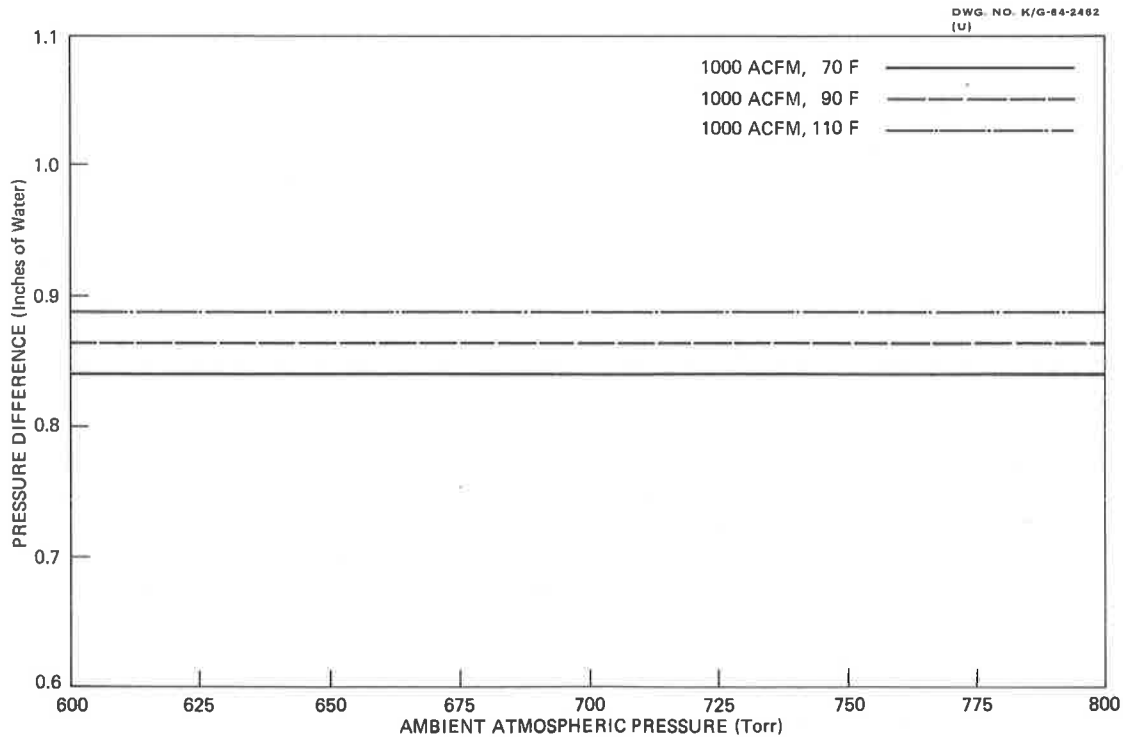
FIGURE 5
PRESSURE DROP ACROSS A HEPA FILTER WITH 1000 ACFM FOR VARIOUS OPERATING CONDITIONS

The use of the mass flow does have some aesthetic value, in that it seems to be a more fundamental parameter. However, using a volume flow does avoid one additional calculation and, therefore, perhaps is a more practical solution. On this practical basis alone, if the error range shown in Figure 5 is acceptable, then it is recommended that specified volume flow rates be used for testing filters.

Perhaps a better recommendation would be for the various facilities to consider using a laminar-flow device in place of the orifice plates.

Comparison of the Orifice Plates From the Various Facilities

A cursory examination was made of the various orifice plates which were calibrated. They were visually inspected and some physical measurements were made. All of the orifice plates were almost identical. Variation in physical measurements were insignificant. With the physical measurements almost the same, the discharge coefficients might be expected to have the same values. A direct comparison of the discharge coefficients is shown in Figures 6 and 7.
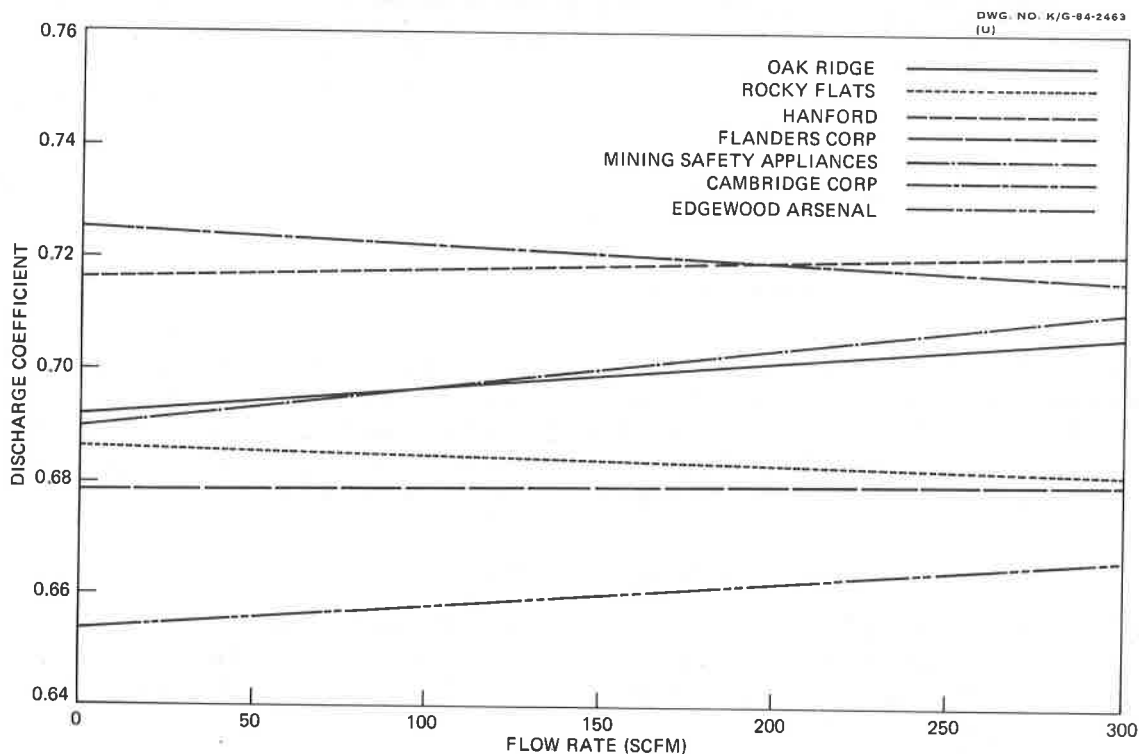
FIGURE 6
COMPARISON OF THE REGRESSION LINES FOR THE
DISCHARGE COEFFICIENTS FOR ALL SMALL ORIFICE PLATES

As can be seen from these figures, the variation in the discharge coefficients is 7% for the large orifice plates and about 10% for the small orifice plates. This is somewhat larger than expected. Since the holes in the plates, which represent the orifices, are simply drilled holes with cylindrical walls either 3/8- to 1/4-in. thick, it is likely that small variations in the roundness of the entrances account for the large differences in the discharge coefficients. This

also dramatically emphasizes the difficulty in manufacturing identical orifice plates, and therefore, the real need to calibrate the orifice plates.
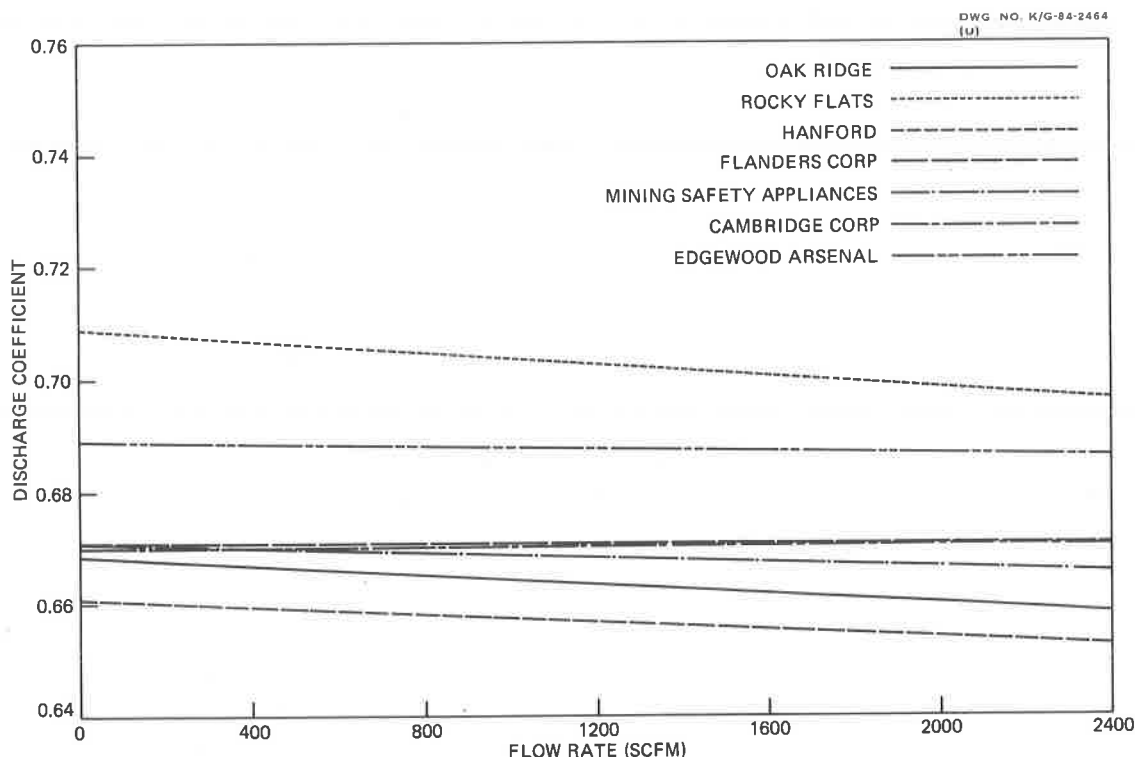
FIGURE 7
COMPARISON OF THE REGRESSION LINES FOR THE
DISCHARGE COEFFICIENTS FOR ALL LARGE ORIFICE PLATES

For all of the orifice plates, the discharge coefficient tends to increase rapidly as the flow changes from turbulent to laminar. This transition limits the low end of the useful flow range for the orifice plates. The flow level where this transition began to take place also varied among the different orifice plates.

III. Conclusion

The results of the calibration measurements made on these orifice plates appear to be quite good. The use of these calibration results and the suggestions regarding the testing of filters should produce good agreement in the results of testing performed at the various facilities.

IV. Acknowledgments

The authors would like to thank Sidney Soderholm and Marvin Tillery of the Los Alamos National Laboratory for their review of the original document. Additional comments and explanations were included in response to their questions and suggestions.

DISCUSSION

GOULET: As a manufacturer, I can only express our pleasure in being able to measure volumetric flow rather than mass flow. This will help us solve some of the problems we have had. I would also like to see this concept applied to the Q127 that measures the penetration of filter media. We still have a problem with it, because it measures mass flow.

ANDERSON: When these orifices were originally supplied, there was an NBS-traceable calibration curve that had been prepared by another individual within your organization. Did you compare the original calibration curve with the one you currently have?

FAIN: I don't have that calibration and I haven't compared it. It would be appropriate to do so. I might add that the laminar flow meters that we are using were calibrated by Colorado Engineering Experiment Station and are traceable to NBS. The accuracy of the laminar flow meter is reported to be $\frac{1}{2}\%$.

Appendix E

RESULTS OF CONAGT-SPONSORED NUCLEAR-GRADE
CARBON TEST ROUNDROBIN

M.W. First
Harvard School of Public Health
Boston, Massachusetts 02115

CONAGT, the ASME-sponsored Committee on Nuclear Air and Gas Treatment Standards and Codes is responsible for ANSI/ASME N509 Nuclear Power Plant Air Cleaning Units and Components, and ANSI/ASME N510, Testing of Nuclear Air Cleaning Systems. Both standards refer to ASTM D3803 as the designated test method for evaluating new nuclear grade activated carbon and to establish adsorbent condition in a previously installed system. However, the test methods for radio-iodine penetration had not been subjected to interlaboratory verification, although the D3803 Committee intended to do so.

Persistent informal and unconfirmed reports that laboratories using the method were arriving at significantly different results, made method verification urgent in the opinion of CONAGT Main Committee because of the test's central position in N509 and N510.

After a number of discussions with the chairman of D3803, who kept his committee informed of the discussions, the D3803 Committee agreed to having CONAGT conduct an interlaboratory roundrobin test of the radioiodine penetration procedure as a first step in the verification program, and agreed that CONAGT had permission to an-nounce that the CONAGT roundrobin test was being conducted with the knowledge and agreement of D3803.

Forty-one companies known or believed to conduct nuclear carbon testing were asked if they wished to participate in a nuclear carbon roundrobin test program in accordance with the ANSI/ASTM D3803 procedure. The arrangement was that all test results would be reported anonymously so there would be no occasion for anyone to suffer embarrassment. From the start, CONAGT wished to shun the responsi-bility of informing official sources that one or more laboratories had performed poorly, should there be such an outcome. Further, CONAGT would have considered withholding such information unethical.

Two samples of new nuclear carbon-source unspecified-and two samples of used, but not radioactive, nuclear carbon were procured by Dr. Ronald Bellamy, a member of NRC, and sent to Dr. Victor Deitz, at the Naval Research Laboratory, for thorough mixing, fractionation into 1 lb samples of each carbon, packaging, and shipping samples of each of the four carbons to the laboratories that volunteered.

Seventeen laboratories agreed to participate in the program, but two later withdrew, leaving 15; 7 from the U.S., 8 from other countries (West Germany, Italy, Japan, Canada, U.K., Finland,

Netherlands, and France).

Two of the four carbon samples were new and two were used. It was not made clear that all four were to be tested as though they were new carbons by ASTM D3803-79, Method A. As a result, eight laboratories analysed each sample twice, once without equilibration (Method B) and once with equilibration (Method A); four laboratories performed only the equilibrated carbon test; and two laboratories performed only the unequilibrated carbon test. One laboratory analysed only one of the four carbon samples, but did it both ways. Some of the reports contained more data on the carbons than was requested. Because there was not enough of this information to treat statistically, it was not reported. The results, converted to percent penetration when reported as efficiency, are shown in the attached Table. The test results are shown precisely as they were reported so that each participating laboratory should have no difficulty identifying their own report. It is recognized that there is diversity in the number of significant figures reported and the presence or absence of reliability figures associated with radioactive counting procedures.

There is considerable spread in each set of results for the same carbon sample, with and without equilibration. The range, mean, and standard deviation of each set is shown at the bottom of the Table. A second and third set of means and standard deviations was calculated for the purpose of trying to define a most probable central range of values for each set of test results. The method used (for which there is no established statistical justification) was the following:(1) values outside $\pm$ two standard deviations of the mean of all the test results (shown in the Table) were eliminated and a new mean and standard deviation (SD) calculated for the retained results. (These values are shown in the Table as recalculated mean and SD ($\pm$ 2 SD).) (2) Next, all values outside $\pm$ one standard deviation of the recalculated mean were eliminated, and a third mean and standard deviation calculated from the remaining test results. (These values are shown in the Table as 2nd recalculated mean and SD ($<\pm$ 1 SD).) The Table then shows the range of results included within $\pm$ 2 and $\pm$ 1 SD of the 2nd recalculated mean. Finally, the Table tabulates the number of test results that fall within $\pm$ one standard deviation of the second recalculated mean as a ratio of the total number of results reported.

The purpose of the statistical exercise that has been described was not to arrive at a "correct answer". In fact, there is no absolute,"correct" penetration for these carbons that has been determined by a recognized reference laboratory; nor was it intended that there should be such a determination, even·if such an agency as a reference laboratory existed. The intended purpose was, simply, to give as many laboratories performing nuclear-grade carbon testing as wished to participate,an anonymous opportunity to compare their analytical results with those of a number of other laboratories performing identical tests. The statistical analysis, therefore, is included only as an aid for evaluating results from a group of laboratories. It will be clear from the Table that fewer than half the analytical results were within the very rigid limits established by $\pm$ one standard deviation of the second derived mean value. The

results that meet this criterion are underlined in the Table. It is believed that they represent the best available concensus values for each carbon sample tested. Some may elect to apply a less rigorous criterion and evaluate acceptable test results on the basis of two standard deviations $\pm$ the mean. Whatever method of comparison is used, test results that deviate greatly from the second derived means should be regarded as a signal for a laboratory to undertake a serious review of the test procedures they are using.

The manufacturer's stated values for the two new carbons, Samples 5288 and 5289, tested according to Method A (equilibrated) are included in the Table. It is not known whether the evaluation of the carbons was conducted for the manufacturers by one or more of the laboratories participating in the CONAGT-sponsored roundrobin, but it is probable that it was, and this provides an additional point of interest when reviewing the equilibrated test results for the new carbons.

Laboratory 3 had the highest, or close to the highest, penetration values in all eight test sets. Laboratories 7, 9, 12, and 13 were close to the mean in all their results.

Inasmuch as there are no "official correct penetration values" for these carbons, it is only possible to assume that the modal test results are likely to be closest to the correct values, as pointed out previously. However the test results are analysed, it remains a matter of concern that not all of the 15 laboratories reported closely identical results when, supposedly, they were using the same standard analytical procedure on identical specimens of carbon.

When the results were transmitted to the ASTM Committee, they analysed the detailed reports of each of the participating laboratories and concluded that many deviations from D3803 had occurred and that this accounted for the dispersion in the results. CONAGT accepted the fact that test method deviations had occurred, but pointed out that this could have resulted from a lack of clarity and specificity in the D3803 standard, itself, and that D3803 should be amended to overcome the problem.

When the roundrobin results came to the attention of the NRC, it was decided that more direct action was called for, and a program was initiated. Dr. Bellamy will discuss the current phase of NRC's activities in resolving this matter.

REPORTED ROUNDROBIN TEST RESULTS

Lab. No.	Penetration % - (Equilibrated)				Penetration % - (Unequilibrated)			
	Sample 5288	Sample 5289	Sample 5290	Sample 5291	Sample 5288	Sample 5289	Sample 5290	Sample 5291
1	0.11	0.17	78.46	39.13	-	-	-	-
2	-	-	-	-	0.05±.003	0.06±.25	83.76±2.05	42.46±1.
3	1.24	9.29	87.62	59.85	0.959	0.74	81.38	31.86
4	0.36+	0.59++	87.82++	54.34++	-	0.36+	-	-
5	-	0.81+	-	-	-	-	-	-
6	1.11	1.63	83.45	50.68	0.27	0.11	68.30	23.54
7	0.29+	0.98+	84.30+	48.98+	0.06+	0.06+	72.04+	19.11+
8	0.46	0.64	88	41	0.06	0.08	77	22
9	0.185	0.201	81.1	43.9	0.0519	0.0299	71.1	15.2
10	0.19+	0.20+	-	-	-	-	67.4+	14.4+
11	0.018	<0.01	78.39	31.68	<0.01	0.03	68.11	21.24
12	0.4	0.5	81.1	46.1	0.1	0.1	68.0	14.0
13	0.6±.03	0.12±.02	83.25±2.21	38.56±1.06	-	-	-	-
14	-	-	-	-	0.09	0.18	26.51	4.01
15	0.27	1.50	66.67	53.52	0.16	0.20	0.37	19.387
Range	0.018-1.24	<0.01-9.29	66.67-88	31.68-59.83	<0.01-0.959	0.03-0.74	0.37-83.76	4.01-42
Mean	0.39	1.3	81.9	46.2	0.18	0.18	62.3	20.7
Std. Dev.	0.39	2.4	6.1	8.3	0.28	0.21	25.5	10.0
Recalc'd Mean-(<± 2SD)	0.31	0.61	83.4	46.2	0.18	0.12	62.5	18.5
Recalc'd SD-(<± 2SD)	0.30	0.54	3.6	8.3	0.28	0.10	15.8	7.3
2nd Recalc'd Mean-(<± 1SD)	0.23	0.38	82.7	46.3	0.095	0.097	73.2	18.6
2nd Recalc'd SD-(<± 1SD)	0.15	0.22	1.4	6.0	0.078	0.062	6.1	3.7
Range of Values = ± 2SD	0-0.53	0-0.82	79.9-85.5	34.3-58.3	0-0.25	0-0.22	61.0-85.4	11.2-26.0
Range of Values = ± 1SD	0.08-0.38	0.16-0.60	81.3-84.1	40.3-52.3	0.017-0.163	0.035-0.159	67.1-79.3	14.9-22.3
No. Results = ± 1SD	7/12	5/13	3/11	5/11	7/10	4/11	7/11	4/11
Carbon Manufacturer's rating	0.1% or less	0.1% or less						

+ Average of two submitted results

++Average of three submitted results

CONAGT'S NUCLEAR CARBON ROUNDROBIN
TEST PROGRAM

Dr. Ronald R. Bellamy
U.S. Nuclear Regulatory Commission
King of Prussia, PA

As a member of both ASME CONAGT and the ASTM D28 committee, I have been actively involved with the Nuclear Carbon Roundrobin Test Program from the beginning. Thus, it is fair to say that the NRC was involved from the beginning. In fact, the NRC was afforded the opportunity to review and comment on each CONAGT submittal: announcements of the program, distribution of samples, compilation of results, and determination of what procedures to specify. The samples of carbon were homogenized and split by an NRC contractor, Dr. Victor Deitz of the Naval Research Laboratory.

With the apparent scatter in results that became obvious in early 1983, the matter was discussed with NRC headquarters staff in Bethesda, MD, whom are present here today and would be happy to answer any questions you might have. The approach decided upon was to obtain outside assistance - get a fresh look at the problem. This contractor has been obtained, and has attended ASTM meetings, reviewed in detail the test procedures, visited labs, witnessed tests, and also set up his own laboratory. This laboratory will be the site of a workshop during the week of August 27, 1984. Although there are many potential reasons for the scatter in results, to include errors and ambiguities in test procedures, differences in laboratory apparatus setups and equipment, and personal idiosyncracies in performing the tests, the workshop should add much to our data base.

In summary, the NRC has been aware of the roundrobin from the beginning, we are aware of the results, concerned about the discrepancies, and are taking active steps to resolve the situation.

DISCUSSION

EDWARDS: Did Dr. Deitz run tests also on the same carbon, and can you reveal the results of his penetration tests?

FIRST: Dr. Deitz very carefully avoided doing so, and I use that language advisedly.

WILHELM: As you know, we had a roundrobin test in Europe years ago, and we also found deviations, but the deviation were not as wide as on this roundrobin test. A funny thing was that the Europeans had found more penetration than the two American laboratories that entered. There was definitely a difference between the European test results and the American test results. As you may know, we studied all the parameters during the past year to determine their importance on the test results. This was done with extra money from the German government and my laboratory. Maybe we will come to Idaho Falls, I am not sure at the moment. Because we compare continuously with other laboratories, it appears to me that the main reason for discrepancies in results may be in the preparation of the methyl iodide. All of us know that the amount of water in the charcoal gives you different results. It is one of the major parameters, the most important parameter perhaps, considering the test conditions themselves. We know that nobody is able to prepare organic compounds of iodine in 100% clean composition. You always get more volatile species. We don't know what they are, but we know they are there, and you know it too. It is well known that it is not HOI although I don't like to mention that at all. There is something there, we found it in a major reactor incident in very large amounts, roughly a year ago. We know that in the preparation of methyl iodide, we get a higher volatile fraction, much more volatile that methyl iodide, and we get a lower volatile fraction, too. We were as clean as possible in our German laboratory. We even performed double distillation of the material, and maybe not everybody is doing this. It could be that this is the major reason for the discrepancies, because, considering the test procedure itself, and the control of the important parameters, I think every laboratory can do the test in a relatively good manner. Therefore, I don't see laboratory incompetence as the reason for the discrepancies. I think the reason is the preparation of the test medium itself.

FIRST: Thank you Dr. Wilhelm. It is really rather mysterious. For example, people tell me that the rate at which the radioiodide is fed to the carbon is very critical whereas others tell me that it makes no differences whatsoever. The people on both sides have a lot of probity, as well as having a lot of experience. It does seem that, if such diametrically opposite opinions are abroad among our experts,   the work that the NRC has proposed is urgently needed. I hope that those responsible for the NRC program will take heed of your comments, because you have introduced still another aspect of the test that is less than well understood. I am delighted that the NRC is moving in a very positive way to resolve this matter, and I look forward to the time when everyone will come up with the same results from their tests.

McDONOUGH: Many investigators have reported that impregnated coal-base charcoal performs as well as shell-base charcoal. The only draw back is the dusting characteristic, which is minor, especially since most systems employ downstream HEPA filters. Coal base charcoal has a cost advantage and shell-base could become difficult to get due to warfare, etc. Please comment on possible use of coal-base in lieu of shell-base charcoal.

BELLAMY: NRC regulations do not dictate the carbon-base material. As long as the carbon satisfies the applicable tests that are listed in the ANSI Standards and Regulatory Guides, it can be used in commercial nuclear power stations. However, it should be noted that in the U.S., over 90% of the carbon in use has a coca-nut shell-base because of its hardness characteristics, and the long record of successful use.

Appendix F

DEVELOPMENT OF A NEW TECHNIQUE AND INSTRUMENTATION FOR RAPID ASSESSMENT OF FILTER MEDIA*

Yong W. Kim
Professor of Physics
Lehigh University, Bethlehem, PA 18015

ABSTRACT

Evaluation of a particulate filter medium for its performance as a function of particle size is of interest from a practical standpoint as well as for studies of mechanisms underlying the particle removal processes. Rapid execution of such evaluation is important in both respects because such filter media undergo changes during any testing activities. A research program has been implemented for development ment of new instrumentation for potentially instantaneous determination of the particle size distribution function both upstream and downstream of a filter medium. The basic technique entails measurement of the continuum light scattering spectrum of a suspension and subsequent analysis of its resonance structures for extraction of the size distribution function. In order to achieve a wide dynamic range of five orders of magnitude in concentration, the technique is implemented in a light scattering loss mode. Design concepts and some early results will be presented.

I. INTRODUCTION

Suspended small particles are of interest from a wide range of viewpoints ranging from chemical processing, extractive and powder metallurgy, controlled dispersal of materials, combustion, industrial hygiene, entrained waste management to flow visualization and fundamental studies of fluid phenomena. The single property central to all of these diverse interests is the particle size distribution function, which determines the mechanical requirements of a filter, chemical reaction rates in a particle-gas mixture, optical transparency of a suspension or coagulation and sedimentation rates of an aerosol, to name a few.

The particle size distribution function is measured by a large number of different methods. Some are based on mechanical techniques, some on microscopy, some on fluid dynamical properties and others on light scattering as well as electrostatic techniques. Light scattering methods, in particular, have gained a considerable popularity in recent years and there are a number of instruments which are in use today. While they are convenient and satisfactory to numerous narrowly defined applications, these light scattering instruments suffer from two major shortfalls: i) The data acquisition time is long so that rapidly evolving phenomena cannot be studied and ii) the applicable range of particle concentration is rather narrow, consequently often requiring dilution of a suspension.

These limitations largely stem from the fact that the size dependence of light scattering as contained in the angular profile of the scattered intensity of light is exploited to deduce the particle size information. The approach which we have recently developed is to obtain the particle size distribution function from the broad continuum resonance structure of the total scattered intensity spectrum from a suspension.[1,2] The total scattered intensity here means the total intensity of the scattered light integrated over all scattering angles and the spectrum is obtained by measuring the total intensity as a function of wavelength of the in-

cident light. This approach of light scattering spectroscopy has been fully imple-
mented into a new technique, resulting in a complete instrument. The spatial inte-
gration of the scattered light is accomplished by means of a large array of fused
silica optical fibres. The incident light is provided by a continuum light source
through a fused silica prism monochromator as a scanned optical filter. The light
scattering volume of the suspension is sharply defined by forming a narrow column
jet of the suspension with the aid of an envelope of clean air flow surrounding the
jet.

The aim of this paper is to describe a new research program aimed at develop-
ment of another new technique for measurement of the size distribution function of
suspended particles based on the basic concept of light scattering spectroscopy.
The emphasis is on rapid measurement and a wide dynamic range of the technique in
particle number density. One major application for the technique is in the area of
evaluation of particle filter media and the associated instrumentation, as will be
discussed later, reflects the specifics of this goal. The idea here is simply to
measure the particle size distribution functions together with the particle number
density at both the upstream and downstream side of a given filter simultaneously.
The particle penetration efficiency is then given by the ratio of the two distribu-
tion functions as a function of particle size. The feature of rapid measurement
allows that the penetration efficiency is determined without the risk of the aging
of the filter media. The wide applicable number density range of the technique
makes it well suited for studies of high efficiency absolute filters.

In order to achieve the dynamic range of at least five orders of magnitude in
number density, measurement is made of the light scattering loss spectrum, i.e.,the
light intensity spectrum shaped by the loss of a continuum light due to scattering
from particles in the long beam path through a suspension. Differently from our
first implementation of the concept in the light scattering spectrum mode where the
scattering volume is small and fixed, the path length of the light beam through the
suspension here becomes an important variable by which widely changing particle
concentration can be counteracted and measurement of statistically significant in-
tensity spectra of the transmitted light can be realized.

It is clear that in the light scattering loss mode the particle suspension
does not have to be sampled, meaning that truly non-invasive in situ measurements
can be carried out.

In the following sections we will first describe the theoretical framework of
the technique as implemented in the light scattering loss mode, followed by a de-
scription of the experimental arrangement. Some discussion will be made of the de-
sign of a tunable particle filter based on a positive corona electrostatic precipi-
tator. The current status of the development will be given in the end.

II. DESCRIPTION OF THE LIGHT SCATTERING LOSS SPECTROSCOPY TECHNIQUE

We will now consider a particle suspension over an extended region of space,
such as in a flow pipe. In order to interrogate the particles for size distribu-
tion, a narrow collimated beam of light is directed into the suspension. The in-
tensity of the beam at the other end of the suspension is attenuated due to scatter-
ing of the light from the particles in the beam path and by absorption of the light
by the bulk of the particles and the host gas.

The absorption by the particles can be analyzed in detail by measuring the
absorption coefficient of the bulk and estimating the total equivalent thickness of
the suspended particles in the beam path from a reasonably assumed size distribu-
tion function. Our analysis based on the data for heavy mineral oil shows that

this contribution is negligible.

The absorption by the gaseous medium which supports the entrained particles can be treated in the manner similar to the above case but it is even more simply disposed of as part of the incident intensity calibration procedure. The incident intensity is measured with a clean gas flow maintained through the light scattering region without the particles.

Under the condition where the beam diameter is very small compared with the path length of the beam, the intensity loss, $dI(x,\lambda)$, due to scattering in a length element dx in the direction of beam propagation is then given by

$$dI(x,\lambda) = - I(x,\lambda)dx \int_0^\infty \pi R^2 Q_s(R,\lambda)f(R)ndR. \tag{1}$$

x and λ denote the position along the beam axis and λ the wavelength of the light. $Q_s(R,\lambda)$ is the total scattering efficiency which is the total scattering crosssection for a particle of radius R at wavelength λ given in units of geometrical crosssection of the particle πR^2.[3] $Q_s(R,\lambda)$, of course, depends on the index of refraction (m) of the bulk material of the particle. The particle number density isdenoted by n and the size distribution function by f(R) which is normalized,i.e.,

$$\int_0^\infty f(R) \, dR = 1. \tag{2}$$

The integral on the right-hand side of eq. (1) gives the total scattering crosssection of all particles in the volume defined by the 1 cm^2 crosssection and thickness dx. The portion of the light scattered from the particles is lost, thus contributing to the attenuation of the beam intensity. We note here that the integral is independent of x, provided that the particle suspension is uniform in space. The uniformity is not a stringent requirement for most practical situations. One can then integrate eq. (1) to obtain

$$I(x,\lambda)= I_o(\lambda) \, e^{-K_f(\lambda)x}, \tag{3}$$

where

$$K_f(\lambda) = \pi n \int_0^\infty R^2 Q_s(R,\lambda)f(R)dR. \tag{4}$$

Eq. (3) gives the intensity of the transmitted light through a particle suspension of thickness x in terms of the incident intensity $I_o(\lambda)$ at x= 0. The attenuation coefficient $K_f(\lambda)$ obviously depends on the specific form of the particle size distribution function and is so indicated by the subscript f. f(R) is in general a multi-parameter function depending on the manner in which particles are generated. We have, however, found that the function with two parameters, one giving the radius at which the function maximizes and another indicative of the width of the distribution, is adequate to describe the liquid drop particles dispersed with an atomizer or Laskin generator.

$K_f(\lambda)$ is at the heart of the light scattering loss technique because it is this quantity which contains the vital information pertaining to the size distribu-

1195

tion function in the form of a convolution of the two functions $Q_s(R,\lambda)R^2$ and $f(R)$. A deconvolution procedure must be devised in order to extract $f(R)$ from $K_f(\lambda)$ and in such activities the uniqueness of resultant $f(R)$ is a question which must be addressed. Simply stated, unambiguous determination of $f(R)$ hinges on the breath of the wavelength range in determining the resonance structure of $K_f(\lambda)$. The resonance structure arises, as alluded to earlier, from the alignment of the maxima in $Q_s(R,\lambda)$ with the maximum of $f(R)$ as λ is varied. The attenuation coefficient $K_f(\lambda)$ then must be measured as a full spectrum covering the major resonance structures.

Accurate determination of the attenuation coefficient spectrum depends on accurate measurement of the ratio $I(x,\lambda)/I_o(\lambda)$. From the standpoint of the wide dynamic range requirement, the ratio must be measured accurately under widely varying conditions in n. The main attractiveness of the light scattering loss mode is found in the fact that the ratio $I(x,\lambda)/I_o(\lambda)$ depends on the product of n and x. The quality of the measured $I(x,\lambda)/I_o(\lambda)$ ratio can be maintained when the particle number density undergoes changes over many orders of magnitude by appropriately changing the path length of the light beam through the suspension so that the product nx is kept in a narrow range of value. In this way, the experimental accuracy of the measured $K_f(\lambda)$ can be kept high even though the absolute magnitude of $K_f(\lambda)$ may decrease with n.

Some sample calculations of the attenuation coefficient spectrum are shown in Figs. 1 and 2, using the zeroth order log-normal distribution function as given by

$$f(R) = \frac{1}{\sqrt{2\pi}\, Z\, R_m}\, e^{-Z^2/2 + (\ln R_m - \ln R)^2/2Z^2} \tag{5}$$

Here R_m denotes the maximal radius of the particle and Z the width parameter. In Fig. 1 three different values of R_m are shown for Z = 0.19: R_m = 0.10, 0.15 and 0.20 μm. In Fig. 2, R_m is fixed at 0.15 μm while Z is varied: Z=0.1, 0.19 and 0.51. It is interesting to see that there emerge certain distinct features in the attenuation coefficient spectrum as the particle size distribution is varied. The principal maximum moves toward longer wavelength as R_m is increased with some influence on this behavior from the Z-variation. The scaling of this nature is extremely valuable in that the measured $K_f(\lambda)$ spectrum rather quickly reveals the range of most likely values of the maximal radius in the particle size distribution function.

The strategy for determination of the particle size distribution is to search for a distribution function, with numerically definite amplitude, width and maximal radius parameters, which gives rise to the calculated $K_f(\lambda)$ that best fits the measured $K_f(\lambda)$. No brute forth deconvolution of the measured $K_f(\lambda)$ is attempted. The search is carried out numerically on a dedicated computer and efficient algorithms have been devised for expeditious execution of the search process.

III. DESIGN OF THE EXPERIMENTAL SETUP

The experimental objective is to measure the incident and transmitted intensities through a particle suspension for rapid, accurate determination of $K_f(\lambda)$ under wide-ranged concentration conditions as found in a filter evaluation environment. The experimental setup is arranged in a single flow train of particle-laden air and its major components are as follows: i) particle source, ii) particle diagnostics station, iii) light scattering loss spectroscopy station-upstream, iv) filter section, v) light scattering loss spectroscopy station-downstream and vi)
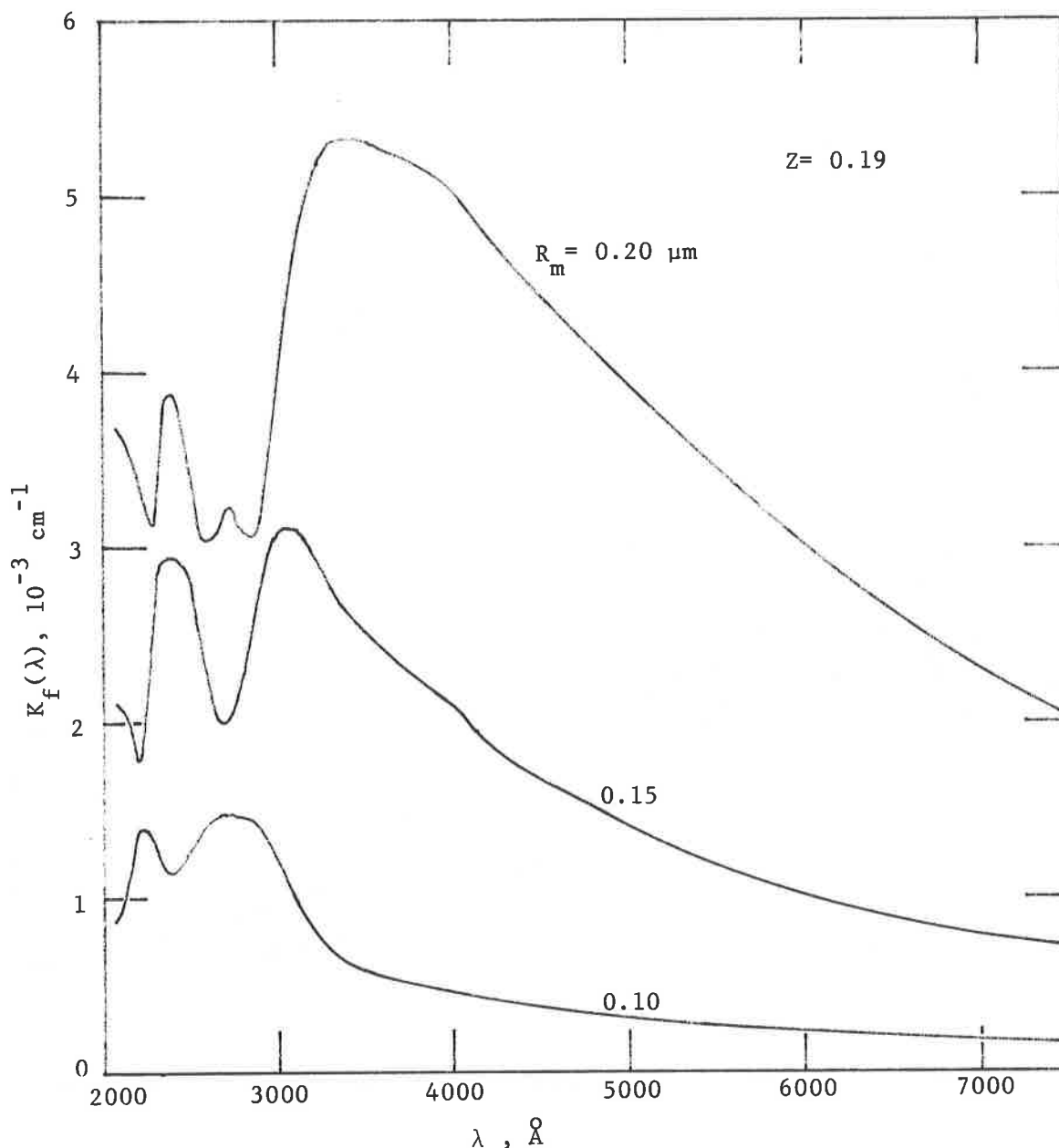
Fig. 1. Calculated attenuation coefficient spectrum $K_f(\lambda)$ for a heavy mineral oil drop suspension. Three spectra are shown, corresponding to the size distribution functions for R_m = 0.10, 0.15 and 0.20 μm with Z= 0.19. The particle number density is set at 10^6 cm^{-3}.

microcomputer for real time analysis.

The particle source consists of a Laskin generator combined with an atomizer and a concentration control tee. The Laskin generator has been modeled after a design provided by Dr. Harry Ettinger of Los Alamos National Laboratories with some modifications to permit observation of the immersed nozzle activities and alternate use of the atomizer. Concentration control is achieved at the tee which permits introduction of fresh air through a 2 μm pore sintered metal wall of the tube carrying the suspension from the particle source. Both the fresh air flow and the flow through the particle source are metered so that the percent dilution of the suspension can be determined. Heavy mineral oil as well as DOP is used to generate the
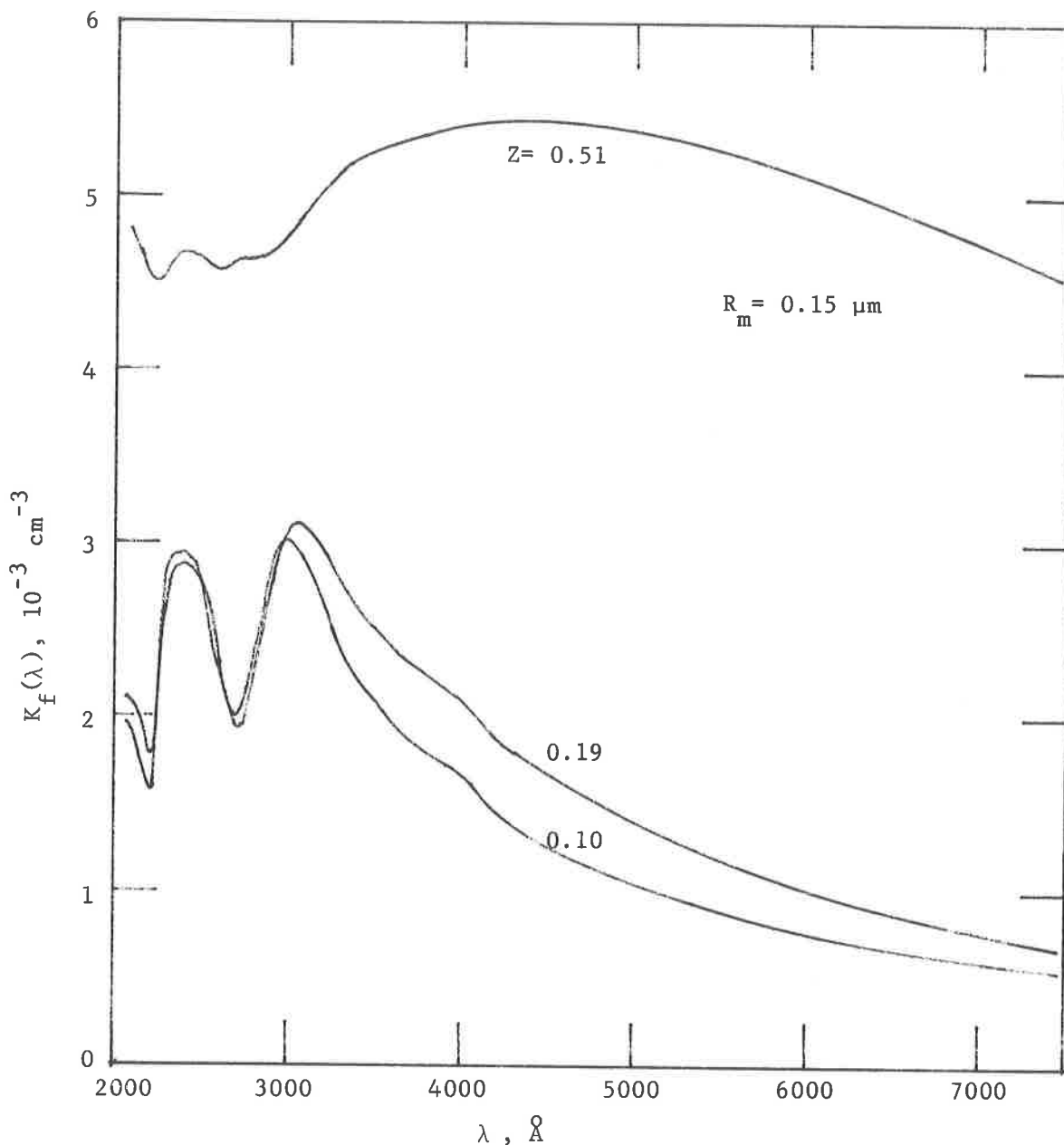
Fig. 2. Calculated attenuation coefficient spectrum $K_f(\lambda)$ for a heavy mineral oil drop suspension. Three spectra are shown, corresponding to the size distribution functions for $Z= 0.10$, 0.19 and 0.51 with $R_m = 0.15$ μm. The particle number density is set at 10^6 cm^{-3}.

suspension.

The suspension flows through the diagnostics station where three different methods of particle size determination are used to generate data for comparison with the size distribution function measured by light scattering loss spectroscopy: electron microscopy, a video ultramicroscope and a California Measurements PC-2 cascade impactor. In cases when electron microscopy is used, particles are first collected onto a microscope grid by placing it flush with the inner wall of a metallic tube section which forms a coaxial electrostatic precipitator. The precipitator is run at the high corona current mode so that entrained particles are collected indiscriminately of different particle sizes.[4] The grid with the particles is then exposed

to the saturated vapor of 4% osmium tetroxide solution of water for several minutes in order to sharply reduce the vapor pressure of the oil of the particle bulk before putting it within the electron microscope column.[5] The video ultramicroscope has been used in our laboratory for some years and it permits measurement of the distribution of sedimentation velocity of particles in the host gas which is brought to rest in an optical cell. The cell is connected through a pair of synchronized valves to the main flow tube carrying the suspension. By means of video recording one can acquire a large number of sedimentation events in a matter of several minutes, free of any sampling activities. This has made it possible to follow the time dependence of the start-up process of the Laskin generator. For instance, we have found that the generator requires about twenty minutes of operation before reaching a steady-state particle size distribution.

The suspension then enters the station for light scattering loss spectroscopy on the upstream side of filter section. The optics, spectroscopic instruments, detectors and data handling electronics for this station are the same as those on the downstream side of the filter section, except that on the upstream side the collimated light beam makes a single pass through the light scattering chamber which offers a path length of up to 85 cm, whereas many passes of the beam are required at the downstream station due to sharply lower particle concentration there. The important requirement here is an intense, highly collimated beam of continuum light so that the beam can travel a large distance and cover a broad spectral range required for unambiguous analysis of a given suspension. A high pressure xenon arc source is used as the light source and all-reflection optics is employed for collimation of the light beam.

The light beam is terminated at a grating spectrograph for analysis of the intensity spectrum. Two different detectors are employed: A photomultiplier and a 1024 element photodiode array detector. The photomultiplier (R955) is used in the scanned monochromator mode of the spectrograph whereas the photodiode array detector is suited for simultaneous detection of the full intensity spectrum as displayed on the image plane of the spectrograph. The advantages of the photomultiplier are its high sensitivity and broad spectral range on the uv-visible side of the spectrum.

The incident intensity spectrum is measured under conditions identical to the case of the transmitted intensity measurement except that the gas flowing through the light scattering chamber has no particles suspended in it. While the experimental arrangement permits simultaneous measurements of both the incident and transmitted intensity spectra, it has been found that both the spectral character of the light source and cleanliness of the optical components can be maintained stable for hours of the measurement activities, thus making the simultaneous measurements unnecessary.

The signal output from either type of detectors are entered into a digital signal processor which is capable of storing a large number of data points with up to 15-bit resolution. In order to improve the signal to noise ratio, signal averaging is performed in one of the three ways: running average of several adjacent data points in a single intensity spectrum, point by point averaging of several sets of consecutively measured intensity spectra, and time integration of the intensity spectrum at the array detector by exposing the detector for a duration significantly longer than the characteristic time associated with noise. The resulting intensity spectrum as stored in the digital memory of the processor is then transferred to a 16-bit CPU microcomputer (Tandy 2000HD) directly through a hard wired link under RS-232C protocol for further processing and analysis. Each intensity spectrum consists of 4096 data points, i.e., the intensity values at 4096 different wavelengths over the typical range of 2000 to 9000Å.

The filter section represents the main object of the development effort of the light scattering loss spectroscopy technique. It may be any one of a large number of filter devices and the experimental arrangement retains the flexibility required to examine all of them. For the purpose of critical evaluation of the technique, we have also incorporated a cylindrical electrostatic precipitator as a tunable particle filter. The precipitator consists of a 60 cm long, 2.54 cm inner diameter tube of stainless steel construction with a 0.25 mm diameter nickel alloy steel wire stretched along the tube axis and is operated in the positive corona discharge mode. The suspension continues to flow from the upstream light scattering chamber into the precipitator through 20 evenly spaced holes (1.6 mm diameter) on the side wall at the upstream end and leaves the precipitator in a similar manner at the downstream end. In this way, the flow field within the precipitator becomes a well-defined laminar field and the collection efficiency as a function of particle size can be predicted from calculations of particle trajectories.

The particles in the precipitator are subjected to two different forces: the hydrodynamic drag which scales with the particle radius and the electrostatic force given by the product of the electrical charge attracted to the particle and the local electrical field strength. It can be shown that the amount of the charge grows as the surface area of the particle and consequently the speed with which the particles can be swept out of the flow grows linearly with particle size. From the kinetics of the positive corona discharge, it is possible to determine the electrostatic force on the particle everywhere in the precipitator. The flow field can be measured in detail by using the tracer particle method. Consequently, the particle trajectories can be calculated for any arbitrary size distribution using a numerical code and the resulting precipitation efficiency has indeed been verified under widely varying flow and discharge conditions.[4,6] The main aspect of the electrostatic precipitator, pertinent to the present application, is that it is possible to change predictably both the particle concentration and size distribution. Such a tunable filter will serve as another valuable check on the technique as applied to rapid evaluation of a filter device.

The downstream station for light scattering loss spectroscopy has a light scattering chamber of 134 cm length. The chamber is placed between a pair of wide area mirrors which can be individually rotated about two mutually orthogonal axis. The collimated light beam can be steered to make multiple traversals through the chamber in order to increase the optical path length x as appearing in eq. (3) in multiples of two chamber lengths. The beam terminates at a second spectrograph. An independent set of detectors and a signal processor is operated in a similar manner to the upstream station and the resulting intensity spectra are transferred to the same computer for analysis.

Fig. 3 shows schematically the fully assembled experimental setup. The particle suspension flows through all of the major components described above in series and is discharged out of the laboratory through an absolute filter. Each experimental run is carried out under a steady state condition for all components. The condition is specified in detail by means of a number of flow meters, pressure gauges and laser light scattering devices. The two arc lamps are operated under a constant current condition with steady state cooling by a forced air flow which also takes out the considerable amount of ozone produced by the lamps. The optical components in the beam collimation optics take considerable heating from the lamp and are therefore cooled by close-loop circulation of refrigerated water. The particle source is operated by air produced by a dedicated oil-less compressor.
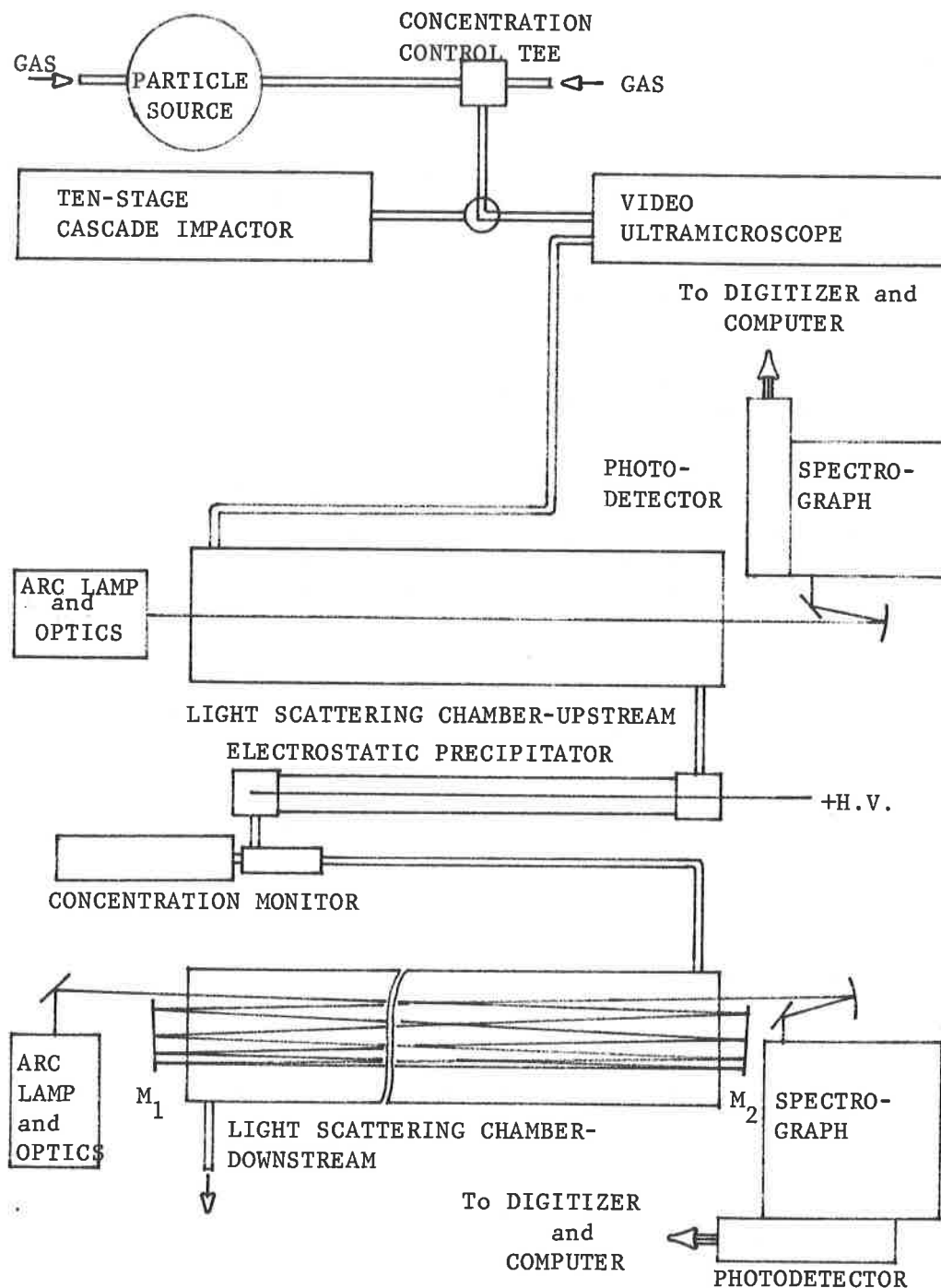
Fig. 3.   Schematic diagram of the experimental arrangement,
consisting of a particle source, diagnostics station,
upstream light scattering station, filter section,
downstream light scattering station and data proces-
sing electronics and computer. Two mirrors M_1 and M_2
are adjusted in order to control the beam path length
in the downstream light scattering chamber.

IV. CURRENT STATUS OF THE DEVELOPMENT

Each of the major components of the experimental setup has been either constructed or assembled and tested for its performance. The experimental setup has been fully assembled and is currently undergoing some preliminary runs.

Fig. 4 shows the measured intensity spectra $I_o(\lambda)$ and $I(x,\lambda)$ where x = 84.5cm, as obtained from the upstream light scattering station for a DOP particle suspension. The spectra are obtained using the photomultiplier with the spectrograph in the scanned mode. In view of the fact that the spectrograph contains a grating as the dispersive element, each spectrum must be corrected for the higher order contribution at wavelengths longer than 4000 Å. It is, however, unnecessary to calibrate them for absolute intensities because we are only interested in obtaining the attenuation coefficient spectrum $K_f(\lambda)$ by evaluating $-[\ln(I(x,\lambda)/I_o(\lambda))]/x$. Fig. 5 shows the resulting $K_f(\lambda)$ spectrum, which clearly shows the features indeed expected of the suspension as produced by the Laskin generator.

The computer algorithm for rapid determination of the particle size distribution for such a measured $K_f(\lambda)$ spectrum has also been developed along the general approach outlined earlier. The index of refraction of DOP has also been measured as a function of wavelength, using a new instrument constructed for such an application. The design of the instrument will be described in a separate article. The measured index of refraction is incorporated into the deconvolution code.

Our estimation of the various time requirements thus far indicates that an under ten minute reduction of the particle size distribution function from the measured $K_f(\lambda)$ spectrum is well within our reach.

We expect that the entire program of rapid evaluation of filter media by light scattering loss spectroscopy will be operational in the very near future.

REFERENCES

* This work has been supported in part by the U. S. Army under contract DAAK11-83-K-005.

1. Y. W. Kim, "Real Time Analysis of Power Plant Flue Gas", Final Report to the Pennsylvania Power and Light Company, Department of Physics, Lehigh University (March 1982).

2. M. C. Reuter, "Development of a New Light Scattering Technique for Particle Size Distribution Measurement and Its Application to Aerosol Coagulation", Ph.D. dissertation (Physics) Lehigh University (1984).

3. M. Kerker, The Scattering of Light and Other Electromagnetic Radiation, Academic Press, New York (1969).

4. Y. W. Kim, "Electrostatic Separation of Pyrometallurgical Particles", Physics of Fluids Technical Report No. 28, Department of Physics, Lehigh University (1983).

5. L. M. Prince, Microemulsions, Theory and Practice, Academic Press, New York (1977), p. 17.

6. Y. W. Kim and E. Samuel, "Electrostatic Precipitators II. The Efficiency and Wire to Plate Spacing Ratio", Physics of Fluids Technical Report No. 27, Department of Physics, Lehigh University (1978).
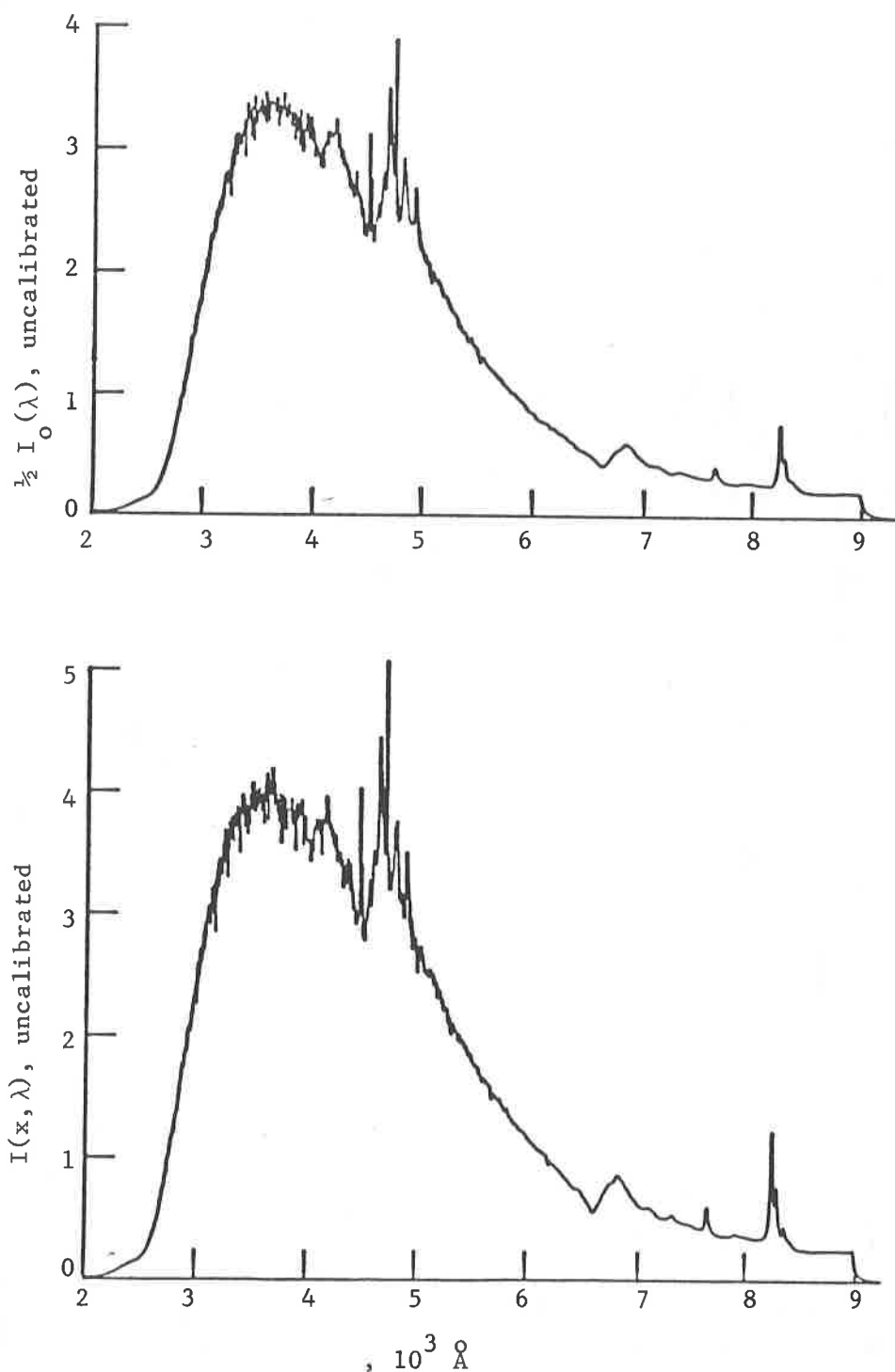
Fig. 4. Measured intensity spectra, a) for the incident
light $I_o(\lambda)$ and b) for the transmitted light $I(x,\lambda)$.
The path length of the light beam through the light
scattering chamber is 84.5 cm. The Laskin generator
was used to produce the suspension of DOP droplets.
Notice that the intensities are uncalibrated but the
two intensities are displayed with a common scale.
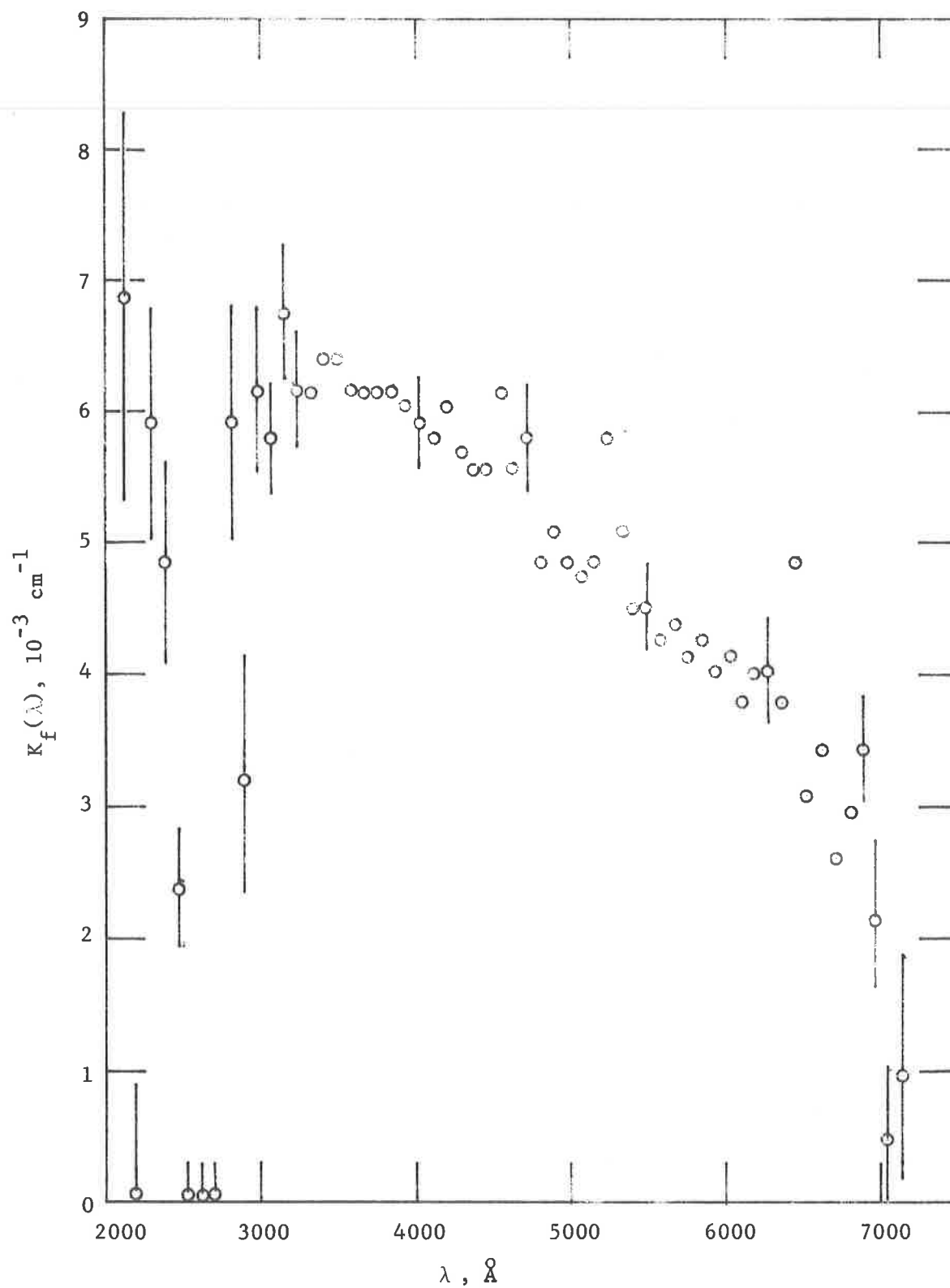
Fig. 5.   Measured attenuation coefficient spectrum $K_f(\lambda)$ as determined from the incident and transmitted intensity spectra of Fig. 4.

DISCUSSION

SCRIPSICK: Have you measured the change in geometric standard deviation with time for Laskin Nozzle operation? Also, how long does it take for the size distribution to stablize?

KIM: As you start the Laskin generator, bubbles begin to form, but it takes a while to saturate the medium with the fine bubbles. In this slowly changing process, the particle size distribution, as well as concentration, is changing. It is not clear how long it takes to stabilize the size distribution function, but it is certainly a useful question to ask.

SCRIPSICK: Did you say that after 23 minutes, you thought the size distribution stabilized?

KIM: That is in the data I have shown you, but it is exponentially approaching a certain asymptomatic behavior, and it is a detailed judgement call by the practitioner as to how long is enough.

SCRIPSICK: Have you documented the change in geometric standard deviation associated with the buildup of saturation?

KIM: I haven't brought the numbers with me, but I think you can tell from the histogram contained in my paper.

SCRIPSICK: We have noticed a decrease in the concentration output of the Laskin generator with a drop in the level of the generating liquid.

KIM: That's right. The level of the generating liquid is very, very important, as well. What we have done is to replace the cylinders with Plexiglass so that we can see the way the atomization process progresses. This is a very clear feature that we saw quite early.

BERGMAN: I did not fully understand the technique you used for filter penetration and particle size distribution measurements. Is the technique a deconvolution of turbidity spectra?

KIM: Filter efficiency measurements would be purely a result of measuring the size distribution function upstream and downstream simultaneously. The ratio of the distribution functions, or the frequency of the particle at a given size upstream divided by that downstream, or a reciprocal of that, would give you efficiency as a function of size. The measurement of the size distribution function is, in this technique, based on the fact that light scattering efficiency depends on both the radius and wave length while the size distribution function is independent of wave length. Considering the convolution integral that gives you the light that is lost or scattered when you change wave lengths while integrating, at one wave length the scattering efficiency function will be compressed with many, many resonancies showing over a small space on the horizontal axis.

You multiply that by the size distribution function and sometimes the distribution function may coincide at a given wave length with one of these peaks in the scattering function. Now, if you do it at another wave length, the maximum in the scattering intensity may not coincide with the maximum in the size distribution function. When you do this continuously, you find a residual structure in the absorption coefficient   that results from the process, and you can reverse the process to give the expected size distribution.

BERGMAN: You are measuring the turbidity experimentally as a function of wave length?

KIM: That is one way of describing it.

BERGMAN: From your experimental set up, it looks like you are making two turbidity measurements, rather than measuring the complete spectrum.

KIM: We are measuring the full spectrum. We are not just measuring turbidity at two or three wave lengths. This is a continuous spectrum over the full spectra range, 2,000 angstroms to whatever wave length you wish to go to.

BERGMAN: Once you have the two spectra, you can then de-convolute?

KIM: That is right, unambiguously. In fact, the process is quite efficient. Just from the signatures I indicated, one can tell quite quickly what the size distribution function is, and one can go through a simple chi square routine.

CLOSING REMARKS OF SESSION CHAIRMAN GILBERT:

Reviewing papers presented earlier in the session, Mr. Ensinger reported a method of Karlsruhe to use aerosols of high density to test filters dynamically under conditions of temperature and humidity. Mr. Rudinger described failures of clean and dust-loaded HEPA filters tested with moisture droplets at rated air flow for varying lengths of time. These efforts contribute directly to support filter improvement. Mr. Bella of Carl Freudenberg reported the availability of polycarbonate and polypropylene fibers and indicated a chemcial resistance that should be helpful in the processing of some nuclear materials.

Mr. Mulcey described Simoun, an automatic rig for dynamic testing of filters at elevated temperatures. Identification of filter gasket and sealant performance from these CEA tests at Saclay will afford a significant basis for filter redevelopment. The sub-jects for future testing with Simoun promise to be beneficial in advancing air cleaning technology. Mr. Pratt of Harwell provided results of dynamic testing of filters at increased temperatures. His efforts isolated prime filter components for improvement and out-lined performance of representative HEPA filter assemblies when tested to 500°C.

Session 17

SAFETY SYSTEMS PERFORMANCE

WEDNESDAY: August 15, 1984
CHAIRMEN: H. Gilbert
            Consultant
            J. D'Ambrosia
            U.S. Department of Energy

EXPERIENCE IN STARTUP, PREOPERATIONAL AND ACCEPTANCE TESTING OF
NUCLEAR AIR TREATMENT SYSTEMS IN NUCLEAR POWER PLANTS
J.W. Jacox

KRYPTON-85 HEALTH RISK ASSESSMENT FOR A NUCLEAR FUEL REPROCESSING
PLANT
P.J. Mellinger, L.W. Brackenbush, J.E. Tanner, E.S. Gilbert

EXPERIENCE IN STARTUP, PREOPERATIONAL AND ACCEPTANCE TESTING OF
NUCLEAR AIR TREATMENT SYSTEMS IN NUCLEAR POWER PLANTS

John W. Jacox
President
JACOX ASSOCIATES
Columbus, Ohio

Abstract

Recent experience in startup and Acceptance Testing of NATS
in nuclear power plants has shown a number of common points of
strength and weakness as well as some direction for methods of
improvement. The consistent areas of common weakness are lack of
technically acceptable provision for leak testing series filter
banks and clear test/acceptance criteria for adsorbents. A
strong correlation has been found between plants operations staff
involvement and startup/testing efficiency.

Perhaps the major point to be considered is the evidence
that in some cases the "nuclear" regulations, codes and standards
are the only requirements used rather than as additional require-
ments to be used along with experience and good engineering
judgement. Closely related to this concept is the lack of field
experience or exposure of the engineers who design the NATS.
Current experience shows that the best systems are designed by
personnel with some plant exposure or experience.

Introduction

While the past few years have had many negative aspects for
the nuclear power industry, the bright side is the fact we have
brought a number of plants on line. Rather than dwell on the
many general problems of the industry, let us benefit from the
startup experience of these plants that are now - or will soon be
putting much needed power into our nations's grid.

An examination of the startup and testing experience of
Nuclear Air Treatment Systems (NATS) brings a wealth of knowledge
in both technical and procedural areas. As with most of life's
experiences, we find there are many problems to be solved and
examples of how to solve them. For essentially every problem
area discussed in this paper, a reference to at least a partial,
if not full, solution will be cited. In only two cases does a
specific problem seem universal and they are being addressed by a
new code currently being prepared and revision to the currently
applicable standard. Since the subject of this paper is NATS the
primary documents of interest are ANSI/ASME 509 (1) and N510 (2),
US NRC Regulatory Guides 1.52 (3) and 1.140 (4), ERDA 76-21 (5),
RDT M16-1T (6), ASTM D4069 (7) D3803 (8) and ANSI N45.2.6 (9).
In all but two cases at least two and as many as eight revisions
of the subject documents exist. Appendix A lists the various
revisions. As most of us are familiar with these documents I
will not discuss them in general. Given that the plants recently

brought online were designed and built over a period spanning more than a decade there is the obvious complication of what edition of a document should be used to perform acceptance testing, what should be used for acceptance criteria and what is the basis to qualify the test personnel. Since basic standards practice requires that when a document is invoked it will be by a specific revision or issue there should be no problem; however, the real world is never that simple. In the case of N510-75 vs. N510-80 the changes were essentially corrections so the technical aspects of the test are greatly simplified if the 80 revision is used. In the case of the Regulatory Guides there are both changes and errors in various revisions. Further, the references to some critical acceptance parameters change in later revisions. Also, the latest revision of 1.52 is over six years old and therefore does not recognize most relevant current industry practice or standards. Many Technical Specifications and PSAR/FSAR documents are incomplete or contain contradictions as far as NATS are concerned. In many cases the details of how personnel are qualified to perform N510 tests by ANSI N45.2.6 are given widely disparate interpretations.

With this introduction on the basic documents it is little wonder that a wide range of physical quality exists and is complicated by an equally wide range of client attitudes.

Discussion

The matter of attitude, or approach, will be the first we will examine. While in all cases the ultimate client is a utility who, as the license holder, has the final legal responsibility, the actual N510 Acceptance Testing may be under contract and/or the direction of the A/E, some other contractor, a utility construction division, a utility startup/test group or the actual utility plant operations division. As a general rule the closer to the plant operating staff the better the attitude. My definition of a "good" attitude is one that has the objective of insuring the NATS not only meet whatever minimum criteria are in the License but are the best systems for operation, maintenance, testing and reliability that good engineering practice and judgement can provide. Conversely a "bad" attitude is one that tries to accept the systems with the bare minimum that can be read into the License documents with little regard for future operations.

It is, in fact, this basic difference that is one of the most important lessons that can be learned from recent startup experience.

From the very first step in preliminary plant design through startup/testing and operation there are two opposite approaches to accomplish the task of providing the required function the NATS are intended to provide. One is to use all the great wealth of historical experience along with the very best engineering practice and judgement to design, fabricate, install, startup, test and operate the system to provide the maximum

performance and cost benefit for the plant. The other is to simply meet the minimum possible interpretation of the specific nuclear standards involved and produce the minimum possible that meets the letter of the legal requirements. I certainly do not intend to accuse anyone of a conscious decision to produce a poor system. There is, however, a common failing in the nuclear industry to ignore the great body of non-nuclear engineering that has been built up by all other industries. There are NATS in new plants today with design and construction features none of us would accept in the HVAC system for our office building. We must always remember that the nuclear standards, codes and regulations are additions to the basic engineering principals required to design a good system. They are not the only requirements. Further, the nuclear aspects create what at times may seem to be contradictions to the usual air handling engineering practice. When such occasions arise, the answer lies in learning from actual experience at operating plants. An engineer, no matter how well educated in theory, can not truly understand the problem of filter changeout of a contaminated system, in full protective clothing, breathing apparatus, ambient temperatures of over 100° F and a tight schedule without at least witnessing such work. I submit that the design of the filter clamping, door size, door dogs and many other details would be designed differently, and far better, by someone who has at least watched such an operation. I stated above that we must not consider the nuclear industry so unique that we ignore other information; rather we must recognize that there are specific, unique aspects and address them to the benefit of the plant operation. Appendix B lists examples of problems found in plants now starting up.

To design and build a good NATS (or indeed any plant system) requires a balance of traditional engineering design theory and practice along with attention to the unique aspects of the nuclear conditions. The only way some of this experience can be gained is in the field, not at a desk, training seminar or even these conferences. In all cases when I have seen exceptionally good systems I know from personal contact that at least some of the people involved had prior field experience.

To move on to a related area of attitude, let us return to the point of operations personnel vs. startup or construction personnel and their involvement with Acceptance Testing. I will use a set of real examples of two real sites currently planning to fuel load in 1984. Both are PWR sites but with little other similarity. The "best" example is a single reactor site operated by a utility with no other nuclear plants. The NATS are all from the same vendor and fabrication is excellent. All but one system was shipped skid mounted with minimum field assembly. The basic specification from the A/E to the manufacturer were good but not exceptional. The manufacturer did a really first-rate job in fabrication and built the systems like the proverbial "battleship." The A/E assigned a man as HVAG site construction supervisor who had been through at least one full startup/acceptance testing series of a PWR so he was fully aware of the possible

problem areas. The utility assigned a team of startup, engineering and operating personnel to work with the A/E on installation and pre-test startup. The A/E startup team was also experienced in N509 and N510 work. The utility went even further and sent the team of utility and A/E personnel to a two-day seminar on NATS startup, Acceptance Testing and operation. This group of engineers had the attitude that they would have the fastest. smoothest startup possible. An outside contractor did the actual N510 testing and while there were the few minor delays which are impossible to avoid on any complex project the testing was performed in textbook fashion.

At the utilities' request, a number of pre-test trips were made by the testing contractor to review the Technical Specifications, FSAR, procedures, physical systems, carbon documentation, etc. When it was pointed out that injection and sample manifolds would be required for series filter banks, the response was rapid understanding and prompt fabrication to the testing contractor's sketches. The basic N510 test series was completed in a few months by a two-man contractor team ably assisted by the knowledgeable utility and A/E personnel. The indepth understanding of the test sequence and good planning allowed maximum efficiency. One very unusual and extremely large system required more attention than the others, but this had been expected from the first, due to a number of unique features.

Most importantly when testing of a system was completed it was not only turned from startup to operations, it was fully testable without any unnecessary problems for operational testing over the life of the plant and there were already utility personnel with test experience at the plant.

While the particular plant just cited was one of the very best examples of utility and A/E involvement more than one-half of the plants in current NATS startup testing have at least similar attitudes and experience. Both the unfortunate examples of Zimmer and Marble Hill had been working with operations personnel deeply involved in the NATS startup and testing and would probably have been in the list of good examples.

On the other extreme there is a two-reactor site (PWR) where the NATS startup is under the direction of a utility construction engineering group with no utility startup, let alone operations, personnel involved. Further, there are many serious design problems with the larger built-in-place systems. Even the package units, which came from three different vendors, are examples of a manufacturer meeting the minimum possible requirements of what are at best minimum specifications.

Again an outside contractor was hired to perform the N510 Acceptance Testing. It took well over a year from the first written reports of gross problems before any serious action was taken to solve these problems. During this period most of the effort by the utility was spent on extreme QA requirements for

qualification of test personnel and continual disagreement over why obvious physical problems need not be addressed. The utility arguments were based on incorrect reading and understanding of the applicable standards and regulations. I hasten to point out I am talking about problems such as holes or gaps in the housing and frames you can see 10 feet away, HEPA Frames bowed 1/4 inch along the two foot filter gasket seating surface, moisture separator drains plumbed to the wrong side of the moisture separator bank, no test manifolds, lack of acceptance criteria for a required test, massive use of RTV caulking on Regulatory Guide 1.52 systems, and missing welds in package systems.

While many of these problems are now being solved, at this writing the test contractor is being told manifolds will probably not be built for most systems. It is possible during startup to perform acceptable N510 leak tests by selective installation of the HEPA filters and carbons filters. This is not practical, or even possible in most systems, during operation. If this decision stands it is simply a case of a construction group passing on known serious problems to an operations group. Obviously during plant operation it will be very much more costly to correct deficiencies. A comparison of the time spent arguing and obtaining useless data on the "worst case" plant (B) shows that this time exceeded the total Acceptance Testing of the "best case" plant (A). To be sure, there are a greater number and some more complex systems in Plant B than A but even on the comparable skid mounted package systems there was a factor of three or four times more effort to complete a test series simply because there was no indepth understanding of what was needed and therefore no advance preparation even when specifically requested. As the testing progressed in Plant B the construction engineer assigned became much more knowledgeable and the testing more efficient, but most overall problems remain due to the large number of people involved not on site who have not learned the problems first hand.

Another interesting correlation is the QA attitude and the overall efficiency of the startup process. At present I have no firm means to know which is the cause and which is the effect but there definitely is a strong correlation between the extent of the QA bureaucracy and the wasted motion getting any productive work performed. Certainly we all realize and agree that QA and QC are critical parts of any complex project and even more so on a nuclear plant. However, perspective must be kept as to the ultimate objective. It is to build and startup a power plant – not simply compile papers forever. The NRC does not help with uneven application of 10CFR50 Appendix B from region to region and project to project. The utilities certainly add greatly to their problems by not providing reasonable alternatives to what are sometimes unreasonable requests. Much worse, the utility may greatly over react to a request with their own unnecessary and burdensome requirements.

To prove this exists today and using the plants A and B previously cited, Plant A had a QA program that accepted the QA personnel qualification documentation (to N45.2.6) the testing contractor had used (with normal upgrading over the years) for a decade. Plant B required a massive additional submission of papers on each man, additional training, written tests and prac- tical tests. Remember we are talking about exactly the same individuals doing the exact same work in the same general period of time (1983-84) and in theory to the same NRC regulations. A similar discrepancy exists in the test procedure and AQ audits required. Furthermore, there exists the extreme situation of QA personnel, who admit they have no idea of the technologies involved (and no need to learn it), down-grading experienced test personnel from Level III to a Level II based on a utility deci- sion to use the N45.2.6 recommended experience periods as an absolute minimum. Probably the worst aspect of the Plant B QA/AC program is the policy on continuous auditing of test procedures. Even after full approval has been given the procedure is audited a number of times in use. I stress the audit is not to ensure that the procedure is being used which is quite proper. The procedure itself is audited and changes often requested. These changes are usually because the auditor does not understand technically what is being done and insists that the procedure be simple enough for a lay person to follow. If that is what is desired why go to the extremes required for such highly qualified personnel to perform the work.

On one hand this is good for the contractor since he is paid by the hour but in my opinion it is a disaster for the industry. It not only runs costs out of sight to no good purpose but breeds a total disrespect for a system gone wild. At times all that seems to matter is piling papers, not performing good technical work. If 10% of the effort that is now going into QA/QC and procedure review and gone into the design, fabrication and installation in Plant B most of the real physical and technical problems would have been caught when they were paper problems, not installed system problems.

There is yet another related QA problem area that has come to light in most startup situations, again to a wide range of severity. At Plant C, a PWR that went on line a couple of years ago, there was a problem with the carbon sample canisters. This plant did the N510 testing itself but required assistance when a bank of Type II carbon adsorbers did not pass the halide leak test. The problem was quickly found to be very poorly designed and filled adsorbent test canisters. You could look right through the canister when holding it in the horizontal operating position. These had passed all the QA/QC requirements and were "blessed." The spares ordered at a later date were on site and had both better design for baffles and better carbon packing. They did not have the required QA papers as yet so could not be used. This was solved only when a high level manager pointed out this problem could delay plant startup unless someone made an engineering decision that would allow the demonstrably better

quality sample canister to be installed so the test could be performed. The paper work did follow so nothing was left undocumented. QA/QC must recognize engineering realities in addition to procedural dogma.

Another common problem found at even the best plants is the lack of definition of what is acceptable adsorbent. As with all these problems it should not exist since the Technical Specifications in theory, define all required parameters. Unfortunately in practice they usually do not. The Technical Specification may reference Regulatory Guide 1.52 (any revision) but may also have been changed to mention N510-80 and perhaps N509-80 which are not recognized in any revision of 1.52. Sometimes they only reference a specific test or two from one of the many RDT M16-1T editions (usually not defined). In any case it is rare that there exists clear, unambiguous acceptance criteria for the carbon. There is also the problem that the carbon, while not used in a system, may be up to 6 or 7 years old. Presumably it should meet all the requirements of new before loading but this is nowhere clearly stated. Then what if it fails the 1.52 requirements but meets the N509-80 (ASTM D4069-81) requirements? This all requires complex negotiations between the utility license personnel and NRC project personnel, neither of whom usually have any idea of the technology involved. This is a current problem.

What can be done to solve all these problems? The answer is both very simple and very difficult. To avoid these and many similar problems the basic requirement is to return to good engineering fundamentals. As previously mentioned, at least in NATS, there seems to be too much attention paid to meeting "nuclear" requirements at the expense of the basic principals of air handling and filtration. We must always remember that the nuclear standards, codes and regulations are additional requirements over and above what our engineering education and experience shows us is a good air handling system. The nuclear aspects of the system may be currently met but at what cost? I propose the conceptual solution is to take the basic system performance parameters and rough out the best possible system based on good general engineering and HVAC practice. Then factor in the additional nuclear standards, codes and regulations. It may take a little more time up front but it is much less costly to upgrade a design deficiency on paper than to make changes when in startup a decade later.

We must also insure that at least the lead designer has had the benefit of some plant experience, not necessarily as a direct utility operations person, but by spending a week or so at a plant during startup and at as operating plant during refueling or maintenance. Yes, this is some added cost, but based on what we find in the field today it would be very cost effective. It is always easy to offer criticism but when one goes through a dozen plants of 1983-1985 startup vintage and finds all the same obvious problems this is strong evidence of a general problem.

Another suggestion to assist in design but which will also assist in installation, startup testing and operation is a detailed list of objectives and requirements for operating, maintenance and testing. In theory this information exists but not in one comprehensive and specific list for each system. Such a list would include all the actual physical operations needed to be performed for startup, operation, maintenance and testing. The designer and later the fabricator, installer, startup group and finally the Acceptance Testing group would go through it at each step. This would eliminate such problems as floor drain check valves installed so the housing door cannot be opened far enough to change out filters or moisture separator floor drains plumbed to the wrong side of the bank as very real examples. Such a check list could start as a generic set for each of the various types of systems such as Standby Gas Treatment, Control Room Emergency, Containment Recirculation or Hydrogen Purge, etc. Equally it could be defined as HEPA only, Prefilter and HEPA, Prefilter + HEPA + Carbon, etc., etc. These generic lists, with appropriate explanation could be written by an existing group such as CONACT, INPO, ANS, etc. Then at the design stage for a new plant (and there will be new plants) and at whatever stage for plants under construction the appropriate list would be customized by an experienced engineer or team for each system in the plant. This list and writeup would be the basis for elimination of the construction generated problem (pipe hangers that prevent a door from being opened, etc.) and allow early modification and correction of design or fabrication deficiencies. While I am the last person to want more checklists and paperwork the problems in the field require solutions and this seem a practical method to investigate.

<div align="center">Summary</div>

In summary, recent continuing plant startups and acceptance tests have shown a number of correlations that exist which should guide us toward improved future work (i.e., better NATS at lower ultimate cost).

1. All "nuclear" requirements are in addition to good engineering practice for air handling systems. They do not replace all we have learned to date from past experience. The nuclear plant may have some unique requirements but experience and good engineering judgement are still the basis for any project.

2. The more involved the plant operations personnel become and the earlier this involvement begins the better. Not only does this greatly decrease the problems during startup and testing, it also trains the operations personnel with indepth, hands-on experience.

3. The converse of the above is also true. When an independent construction group is responsible for startup and testing the realities are such that prompt turnover of the NATS

will have higher priority than insuring long-term maximum ease of operation, maintenance and testing.

4. A few days of formal training of whatever utility or A/E personnel are responsible for startup and testing are extremely beneficial and cost effective. This training provides a good understanding of not only what will be required but why it is necessary. With such a background it is much more likely the proper support will be provided.

5. There are two problems that are nearly universal.
   A. Lack of manifolds for testing series filter banks.
   B. Lack of full definition of acceptance criteria for adsorbent.

6. Beyond an as yet undefined point there is a strong inverse relationship between the bureaucracy required by the utility and the general level of efficiency at the site. After some reasonable level there is a negative return on added paperwork, audits, personnel qualifications and such related nonproductive paper piling.

7. There has been considerable "racheting" of all types of administrative controls from the time the systems were designed and built through startup and testing. This makes correction of original design/construction deficiencies doubly difficult since not only does the technical problem require correction but the process to obtain approval to make corrections is more cumbersome than it was for approval of the original system.

8. The majority of the deficiencies for both basic system design and fabrication details seem to be the result of little, or no field experience by the designer. Some actual plant exposure to NATS during operation testing and maintenance is mandatory.

9. An expanded check list to be used at all stages is recommended as a possible partial solution to the difficulty of designers spending enough time in the field. The Visual Inspection Checklist in N510-80 could be a starting point.

10. Improved uniformity of NRC enforcement and interpretation of regulations in all regions and for all projects would be of great benefit.

11. Improved uniformity of utility procedures for QA/QC, Security, Medical, Audits, etc., will save the industry a great deal of time, money and frustration.

12. Utilities must use great care not to over react to an NRC requirement and/or create procedures so broad that they encompass activities not originally intended to be covered by a given procedure or policy. Since it is impossible to

foresee all contingencies any procedure or policy must have a reasonable method to handle the exceptions that will exist.

Appendix A

1. Regulatory Guide 1.52
   Initial Release, June 1973
   Rev. 1, July 1976
   Rev. 2, March 1978

2. Regulatory Guide 1.140
   Initial Release, March 1978
   Rev. 1, October 1979

3. RDT M16-1T
   Draft, December 1970
   January 1972
   June 1972
   Draft, March 1977
   October 1973
   Draft, December 1976
   December 1977
   October 1981

4. ANSI/ASME N509
   1976
   1980

6. ANSI N45.2.6
   1973
   1978

7. ASTM D3803-79

8. ASTM D 4069-81

Appendix B

1. Missing welds on built-up units and package units field assembled.

2. Lack of provision to block bypass through floor drains.

3. Floor drains plumbed to the wrong compartment in relation to the moisture separator.

4. Moisture separator banks installed so the collected water flows downstream into the prefilter or HEPA banks.

5. Instrument penetrations with no provision for air tight seals.

6. No injection or test manifolds for series filter banks.

7. Door hinges that are grossly too weak for the weight of the door.

8. Door dogs too few in number, incorrectly placed and nearly impossible to tighten.

9. Door gasket assemblies with neither still or knife edge for sealing.

10. Physical obstructions (pipes, hangers, floor drain check valves conduit, braces, etc., etc.) that prevent housing doors from opening fully. In some cases it is not even possible for the filter to fit through the opening.

11. Serious damage to the system due to lack of door locks – or provision for locking.

12. Lost filter clamping hardware.

13. Lost or nonexistent QA papers on filters, carbon and/or the housing.

14. Gross rust or corrosion inside and out.

15. Use of RTV caulking in Regulatory Guide 1.52 systems.

16. Filter clamping systems that require a special filter frame design.

17. Back fit seismic braces that grossly distort a filter frame.

18. Systems made impossible to properly test or service due to location and plant backfit additions.

19. Lack of differential pressure gauges on each bank of filters.

20. Filter housing not accessible in any reasonable manner for testing or service.

21. Conflicting requirements in Technical Specifications, FSAR, Housing Specifications and System Performance documents.

22. Lack of detailed drawings of system for housing leak test (detailed dimensions are necessary).

23. Systems designed and built with inherent problems that make flow uniformity impossible.

Note: Many of these same items have been specifically covered in past conference papers (see bibliography 10, 11).

Bibliography

(1)   ANSI/ASME N509; "Nuclear Power Plant Air Cleaning Units and Components," American Society of Mechanical Engineers, Engineering Center, 345 East 47th St., New York, New York 10017

(2)   ANSI/ASME N510; "Testing of Nuclear Air-Cleaning Systems," American Society of Mechanical Engineers, Engineering Center, 345 East 47th St, New York, New York 10017

(3)   USNRC   Regulatory Guide   1.52;   "Design,   Testing and Maintenance Criteria for Post Accident Engineered-Safety- Feature Atmosphere Cleanup System Air Filtration and Adsorption Units of Light-Water-Cooled Nuclear Plants," USNRC, Washington, DC 20555

(4)   USNRC   Regulatory Guide 1.140;   "Design,   Testing and Maintenance Criteria for Normal Ventilation Exhaust System Air Filtration and Adsorption Units of Light-Water-Cooled Nuclear Power Plants," USNRC WAshington, DC 20555

(5)   ERDA 76-21 (ORNL-NSIC-65); "Nuclear Air Cleaning Handbook," Borchested, C. A., Fuller, A. B., Kahn, J. E., NTIS, US Department of Commerce, 5285 Port Royal Road, Springfield, VA 22161

(6)   RDT M16-1T; "Gas-Phase Adsorbents for Trapping Radioactive Iodine and Iodine Compounds," Nuclear Standards Management Center, ORNL, Building 9204-1, Room 321, M/S 10, P>O> Box Y, Oakridge, TN. 37830

(7)   ASTM D4069; "Impregnated Activated Carbon Used to Remove Gaseous Radio-Iodines from Gas Streams, Specification For," 1916 Race Street, Philadelphia, PA 19103

(8)   ASTM D3803; "Nuclear Grade Gas Phase Adsorbents, Standard Method of Radicicdine Testing of," Part 30, American Society for Testing and Materials, 1916 Race St., Philadelphia, PA 19103   .

(9)   ANSI N45.2.6; "Qualifications of Inspection, Examination, and Testing Personnel for Nuclear Power Plants," American Society of Mechanical Engineers, Engineering Center, 345 East 47th St., New York, New York 10017

(10) Kovach, J. L.; "The Users View of the Reliability of Air Cleaning Systems in Nuclear Facilities," 13th AEC Air Cleaning Conference, Vol. 1, Pages 50-55 (1974)

(11) Graves, C. E., Hunt, J. R., Jacox, J. W., Kovach, J. L.; "Operational Maintenance Problems with Iodine Adsorbers in Nuclear Power Plant Service," 15th DOE Air Cleaning Conference, Vol. 1, Pages 428-436 (1978)

DISCUSSION

MILLER: I couldn't pass up the opportunity to acknowledge your acknowledgement, and to comment that having a paper like this, in what may be considered by the utility industry to be an obscure conference, isn't the best vehicle for communication. What we really need to do is to take this type of information and prepare it so that it is publishable in the magazines and periodicals that the utility management and engineering people read frequently, such as Power Engineering, or Power, or one of the mainline magazines. I think that is a good way to get more of the message across. I intend to follow through by having CONAGT help solve some of the problems. I think that selection of personnel who will be conducting start-up testing is done at a management level at utilities. They are not the people who are here today, and they will never be at an air cleaning conference, unfortunately. So, we have to find a way to get the message to them.

JACOX: I wholeheartedly agree with the intent. Certainly, the suggestion of publishing a similar type of article in a magazine they would read is an excellent one, and one to pursue. I regret that this is considered an obscure conference, this is my nineth, but I agree that it is probably so considered by utility managers. It has been under-attended by utility personnel.

KOVACH, J.L.: In relation to your recommendations and the discussion of the appropriate panel, where constant reference was made to go back to the NRC site inspectors, I have to disagree because it is impossible to have a single NRC inspector who is familiar with all areas and capable of giving standard interpretations for all regulations. I feel that it is the NRC's responsibility to educate their own personnel, it is not the industry's responsibility. I think we already contribute to their education as taxpayers. Therefore, I recommend that CONAGT request the NRC to initiate an internal training program for their own personnel so that when either utility personnel or test personnel go to a particular in-house NRC person, they can get an interpretation that is not based on a legalistic interpretation of the wording, but will be based on the kind of "engineering common sense" that you are recommending.

JACOX: I agree with everything you have said. The only additional comment I would make on what I said, perhaps facetiously, is that CONAGT may try to get a purchase order from NRC or DOE for these workshops.

KRYPTON-85 HEALTH RISK ASSESSMENT FOR A
NUCLEAR FUEL REPROCESSING PLANT*

P. J. Mellinger, L. W. Brackenbush,
J. E. Tanner, and E. S. Gilbert
Pacific Northwest Laboratory
Richland, Washington 99352

Abstract

A health risk assessment was conducted to investigate the impact of implementing regulations from the Environmental Protection Agency's Final Environmental Statement - 40 CFR 190 - Environmental Protection Requirements for Normal Operation of Activities in the Uranium Fuel Cycle. Potential risks involved in the routine release of ^{85}Kr from nuclear fuel reprocessing operations to the environment were compared to those resulting from the capture and storage of ^{85}Kr.

The average occupationally exposed worker was estimated to receive about 400 to 600 mrem/yr from ^{85}Kr recovery and immobilization activities. This dose is a factor of 20,000 to 30,000 higher than the estimated dose to the maximum offsite individual (0.02 mrem/yr), and a factor of 130,000 to 200,000 higher than the dose received by the average member of the 50-mile population (0.003 mrem/yr) from routine release of all ^{85}Kr.

Given the uncertainties in the models used to generate lifetime risk numbers (0.02-0.027 radiation-induced fatal cancers expected in the occupational workforce and 0.017 fatal cancers in the general population), the differences in total risks cannot be considered meaningful. There is certainly no reason to conclude that risks from ^{85}Kr routinely released to the environment are greater than those that would result from recovery, immobilization and storage of the noble gas.

I. Introduction

In the early 1970's, rapid growth of the nuclear power industry was predicted. The Environmental Protection Agency (EPA) projected

---

that there would be 1000 GWe of installed nuclear capacity by the year 2000.[1] In order to minimize public exposure to radiation from the operation of the nuclear fuel cycle, the EPA, in November 1976, issued the Final Environmental Statement - 40 CFR 190 - Environmental Radiation Protection Requirements for Normal Operations of Activities in the Uranium Fuel Cycle.[2] Regulations that apply to radiation doses received by members of the general public and to releases of selected radionuclides that result from operations of the nuclear fuel cycle are specified in 40 CFR 190.

The EPA's regulations limit radiation doses to any member of the public to 25 mrem/yr to the whole body and to any organ except the thyroid gland, which is limited to 75 mrem/yr, from normal routine releases from a fuel cycle site.[2] These regulations also limit the krypton-85 (^{85}Kr) release rate to 50,000 Ci/GWe-yr of electrical energy produced from fuel irradiated after January 1, 1983. In order to comply with these regulations, alternatives to normal release of ^{85}Kr have been developed. Instead of releasing the ^{85}Kr from the fuel reprocessing plant (FRP) dissolver off gas (DOG) directly to the environment, the radionuclide-containing gas can be treated where the ^{85}Kr is captured, concentrated, immobilized, and stored for long periods of time. A health risk assessment was conducted to compare the potential risks to the public from routine releases of ^{85}Kr with the risks to the workforce from capture and immobilization of ^{85}Kr at a reference FRP. We proceeded with the assumption that individuals in the workforce can be compared to members of the public, because, as human and for μrem/yr doses, they have similar risks of dying of cancer from radiation exposures as do the general population.

The predicted growth in the nuclear industry has not occurred, and, in fact, projections are still being revised downward; in the three years from 1980 to 1982,[3,4,5] projections for the year 2000 have dropped from 180 GWe (in 1980) to 165 GWe (in 1981) to 130 GWe (in 1982). Now it is likely that instead of the predicted 18 FRPs operating by the year 2000[1] there could be none. Because there are no FRPs in operation, spent fuel is being stored instead of reprocessed; the longer spent fuel is stored before it is reprocessed, the less ^{85}Kr will be released during reprocessing because of natural radioactive decay. The need to capture and store ^{85}Kr should be reviewed in regard to the actual number of operating FRPs that will contribute to exposing the public to radiation from the nuclear fuel cycle.

For this study, the Barnwell Nuclear Fuel Plant (BNFP) was chosen as a representative FRP. The BNFP has been constructed and cold tested but has never been operated. Two alternative methods of capturing ^{85}Kr (cryogenic distillation and fluorocarbon absorption) and one method of immobilizing the captured radionuclide (ion

implantation/sputtering) were theoretically incorporated into the representative BNFP. The increased radiation dose commitment to the operation and maintenance workforce at the reference FRP due to capturing and immobilizing the [85]Kr was compared to the public radiation dose commitment that would result from the routine release of all the [85]Kr to the atmosphere.

II. The Representative Nuclear Fuel Reprocessing Plant

The BNFP construction permit was granted by the Atomic Energy Commission (AEC) in 1970 to Allied-General Nuclear Services (AGNS), and construction began in 1971. The BNFP is located on the eastern edge of the Department of Energy's (DOE) Savannah River Plant and seven and one-half miles west of the town of Barnwell, South Carolina (Figure 1).

The purpose of the BNFP is to chemically separate and recover uranium and plutonium from spent commercial power reactor fuel. The plant was scheduled for startup in early 1974 at a nominal 5 t/day (1500 tU/yr) throughput. The BNFP incorporated a chop-leach head-end, and used a 3-cycle PUREX solvent extraction system with pulsed column and centrifugal contactors. Both contact and remote maintenance were designed into this plant. The BNFP has been cold tested using uranium, but has not processed any radioactive spent fuel. During cold testing, some desirable minor modifications were identified and some modifications were made. For various reasons, the owner/operator has elected to terminate further activities at the facility.

Historically, the krypton contained in the dissolver off gas has been routinely released to the environment from fuel reprocessing operations. There is an alternative to routine release of all the [85]Kr and that is to capture, concentrate, and store the gas for long periods of time. Several sets of alternative methods to recover and store the radioactive gas were considered by Mellinger et al.[6] for a generic FRP. This effort was refined by theoretically placing a cryogenic distillation or a fluorocarbon absorption system and an ion implantation/sputtering facility at the BNFP site. A defined population distribution and meteorological data are used from the BNFP site environment.

Krypton-85 Releases

Based on calculations using the computer code ORIGEN,[7] the quantities of fission products present in recently discharged spent nuclear fuel have been reported previously.[8,9,10] For [85]Kr, this
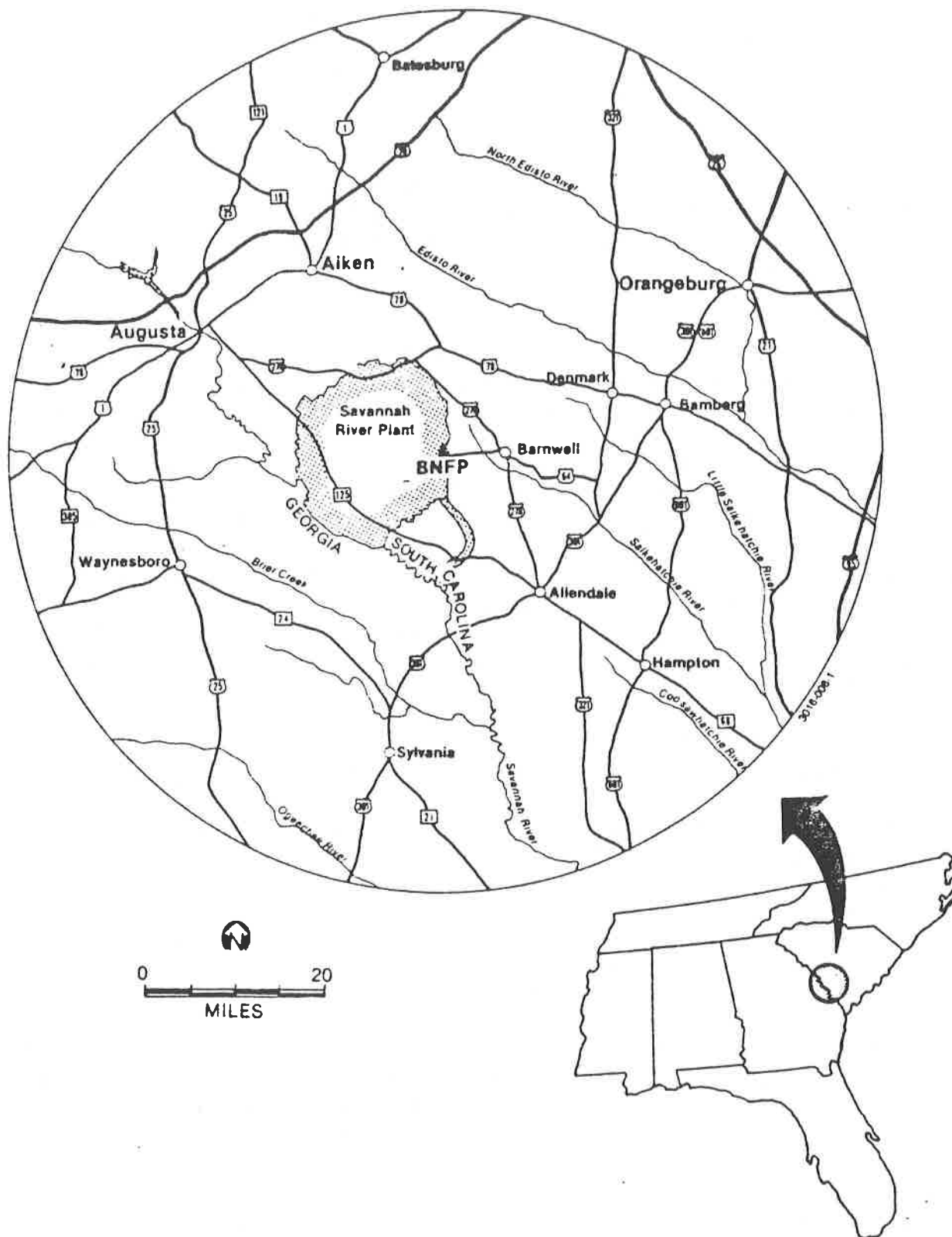
FIGURE 1
BNFP SITE LOCATION

value ranges from 8,500 to 11,200 curies/metric ton of heavy metal (Ci/tHM) in the fuel. For fuel irradiated at a specific power of 30 megawatt/tHM with a total burnup of 33,000 megawatt days/tHM, the calculated ^{85}Kr content 160 days after discharge of the fuel from the reactor is about 10,500 Ci/tHM. A small percentage of fuel elements develop minute leaks in the fuel cladding during irradiation and handling, releasing <1% of the noble gases to the reactor off-gas system. Therefore, the routine releases of ^{85}Kr from commercial LWRs are insignificant when compared to the potential releases from fuel during reprocessing operations. It is also shown that FRP releases can also be insignificant.

As of 1983, the U.S. had accumulated about 9000 metric tons (t) of spent nuclear fuel ranging in age up to more than 12 years old. It is unrealistic to assume that, if a commercial fuel reprocessing plant becomes operational in the U.S., "fresh" fuel will be repro-cessed when such a backlog of aged fuel exists. The earliest real-istic date that a commercial FRP could become operational would be about the year 2000. At that time, if the oldest fuel is always reprocessed first, the facility will never reprocess fuel aged less than about 30 years. Therefore, the routine unperturbed release rate for a 1500 t/yr FRP reprocessing aged fuel is conservatively esti-mated to be about 3×10^6 Ci ^{85}Kr/yr. This is different from what the EPA used as a basis for 40 CFR 190. They assumed 160-day-cooled fuel or about 17×10^6 Ci ^{85}Kr/yr.

III. The Barnwell Nuclear Fuel Plant Environment

The Barnwell Nuclear Fuel Plant (BNFP) site, located on a 1,706-acre tract of land,[11] was selected as the representative site for this study. The land is generally level, with a gently rolling surface, and is heavily wooded with cultivated pines and some native hardwood and softwood trees. About 135 acres of the site were cleared for construction activities. A meteorological tower was located near the southwest corner of the main process area. There are no cities within a 25-mile radius with a population in excess of 5000. The nearest cities of any size are Aiken, South Carolina (population 16,125) which is about 26 miles NW; Augusta, Georgia (population 59,864) located 33 miles WNW; and Orangeburg, South Carolina (population 13,252) located about 39 miles ENE of the BNFP site. The total 1970 population within 25 miles is 65,209. The projected 1980 population estimate is 79,000. The total 1970 popula-tion within a 50-mile radius of the site is 499,000, and the pro-jected 1980 estimate is 658,000. In this scenario, the BNFP is to begin operation in about the year 2000. The projected year-2005 population distribution was selected for calculating the population doses because it was the closest readily available estimate to our operation scenario. The dose from internally deposited ^{85}Kr is

generally small compared to the dose received from direct external radiation and from inhalation.[12]   Therefore, this analysis required only information on regional population distribution and site-specific meteorology. The BNFP release of process gaseous effluents is from a 100-m stack. There are no hills or valleys in the vicinity that would tend to channel air flow or create mechanical turbulence. There are no bodies of water in the vicinity of sufficient size to create atmospheric diffusion problems associated with a water-land transition zone. On the basis of the Gaussian distribution equation and the frequency of wind speed and direction for Pasquill categories A through G for the years 1972, 1975, and 1980, annual average atmospheric dispersion factors for airborne material from the 100-m stack were calculated* and used in our dose calculations.

IV.   Krypton-85 Dose Commitments

Occupational Doses from ^{85}Kr Recovery and Immobilization

There are several ways that workers in the recovery and implantation facilities can be exposed to radiation: 1) the worker can receive an internal dose from air contaminated with ^{85}Kr, and 2) the greatest mechanism is the direct exposure to the gamma rays emitted during the decay of ^{85}Kr.

The majority of the dose to workers from recovery and implantation occurs during maintenance operations on equipment in the hot cells. The type and quantity of equipment used in the krypton recovery facilities was taken from the literature.[10,13,14]   The maintenance requirements (man-hours/yr) used for calculating radiation doses were developed by Pacific Northwest Laboratory's maintenance and craft services organization. The ^{85}Kr inventories in each piece of equipment were determined from data taken from the literature. The resulting dose rates were calculated using a modified version of the computer code PERCS.[15]

The total external integrated doses involved in the capture and implantation of ^{85}Kr each year can be determined by adding together the external doses from the cryogenic distillation facility or the fluorocarbon absorption facility with the external doses from ion

---

*Boone, F. W., Allied-General Nuclear Services, Barnwell, South Carolina. Memorandum to file, Number ENV C.1, SEC/81/205, Revision 1, January 21, 1982.

implantation/sputtering facility. These doses are summarized in Table 1. Since the facility was assumed to operate over a 30-year period, these integrated doses can be multiplied by 30 to calculate the occupational dose over the lifetime of the plant.

Public Exposure to ^{85}Kr Released Routinely from the BNFP

When ^{85}Kr is routinely released to the atmosphere directly from the DOG, the occupational workforce is not generally subjected to its radioactivity in the workplace. However, members of the workforce are exposed about 16 hours a day, and the surrounding population is exposed full-time to the ^{85}Kr released to the environment. There-fore, the total release scenario (no recovery) was used to calculate doses for the maximum individual and the 50-mile regional population. The dosimetry of ^{85}Kr and equations used for these dose calculations were presented by Mellinger et al.[6]

Table 1. Summary of Operational and Contact Maintenance Doses for Each Year of Operation of ^{85}Kr Separation and Encapsulation Facilities

	Integrated Dose (man-rem/yr)		
	Operational	Maintenance	Total
Cryogenic Distillation recovery facility	0.01	2.2 to 0.27	2.2 to 0.28
Fluorocarbon Absorption recovery facility	small	0.16	0.16
Ion Implantation/Sputtering encapsulation facility	1.2	1.4	2.6
Total (Cryogenic + Ion)	1.2	3.6 to 1.8	4.8 to 3.0
Total (Absorption + Ion)	1.2	1.6	2.8

Maximum Individual Dose

The maximum ground-level concentration of ^{85}Kr occurred 1-2 miles east of the site. The 30-year collective radiation dose commitment to a hypothetical individual continually located at this point during continuous routine release was about 0.7 mrem to the total body, about 50 mrem to the skin from immersion in the cloud, and about 1.3 mrem to the lung from inhalation.*

For ^{85}Kr with relatively little penetrating (gamma) radiation, the critical organ will be the skin, even considering its less restrictive dose standard. However, where collective doses are calculated, the total-body dose is preferred for estimating health effects. The annual dose rate to the total body of the maximum individual was about 0.02 mrem. Proposed revisions of 10 CFR 20** include lower (de minimis) limits, below which radiation dose levels need not be considered in dose assessments. The de minimis limit proposed for individuals is 1 mrem/yr. Krypton-85 doses cannot be compared solely to the 1 mrem/yr, because both tritium and ^{14}C, also released by an FRP, would deliver larger radiation doses than ^{85}Kr.(9)

Population Dose

The 30-year cumulative 50-mile population dose commitment was about 70 man-rem. The annual population dose for the 50-mile population (850,000 people) was about 2.35 man-rem/yr. This averages out to be a per capita dose of about 0.003 mrem/yr. The proposed revisions of 10 CFR 20 include lower limits of collective doses to individual members of a general population of 0.1 mrem/yr. However, again, these are not directly comparable.

Summary of Estimated Occupational Doses Vs. Public Radiation Doses

As shown in Table 2, 7 men full-time, or more if part-time, are required if ^{85}Kr is captured by cryogenic distillation and immobilized by ion implantation/sputtering. We assumed a range of 7-9 men for cryogenic distillation and ion implantation/sputtering,

---

* Inhalation dose plus the 0.7 mrem total-body dose.

** An NRC-proposed draft for changes in 10 CFR 20 (Subpart E De Minimis Levels for Doses to Individual Members of the Public) September 26, 1983.

and 5-7 men for fluorocarbon absorption and ion implantation/sputtering. The average annual individual dose to the 7-9 exposed workers was estimated to be about 570-450 mrem (4 man-rem/yr ÷ 7 man). If fluorocarbon absorption is used instead of cryogenic distillation, the average dose to each worker was estimated to be about 600-425 mrem/yr (3 man-rem/yr ÷ 5 men).

Comparing the average occupational exposures of the two recovery options coupled to ion implantation/sputtering and immobilization (about 3.5 man-rem/yr) with the 50-mile population dose resulting from the release of all the ^{85}Kr (2.3 man-rem/yr), the dose commitment to the occupationally exposed workforce was actually slightly higher than for the public. The annual average per capita dose to the occupationally exposed individual was about a factor of 1.7×10^5 greater than to an individual member of the public (500 mrem vs. 0.003 mrem). Therefore, there actually appears to be a possibility of increasing human health effects if ^{85}Kr is captured, concentrated, and stored rather than routinely released to the environment.

Table 2. Comparison of Combined Whole-Body Radiation Dose Rates from Two Krypton-Removal Technologies with Ion Implantation Vs. Public Exposure Resulting from Routine Release of 3×10^6 Ci ^{85}Kr/yr to the Environment

	Man-rem/yr	Number of Individuals Exposed	Average Individual Exposure Rate mrem/yr
^{85}Kr Recovery and Immobilization			
Cryogenic + Ion	4	7-9	570-450
Absorption + Ion	3	5-7	600-425
Routine Total ^{85}Kr Release			
Maximum Individual	0.00002	1	0.02
50-Mile Population	2.3	850,000	0.003

V. Human Health Effects

Health effects likely to result from exposure to low levels of ionizing radiation have been discussed in the Biological Effects of Ionizing Radiation (BEIR) III report issued by the National Academy of Sciences.[16] Cancer mortality due to radiation exposure studies were reviewed, and a model for quantifying risks was developed. The problems that were encountered in relating estimates of risks due to exposure to low levels of radiation are discussed in detail throughout the report. One of the more severe problems is that in populations where the dose and exposure rates are low, extremely large sample sizes are required to reliably quantify the magnitude of effects. In the judgment of the BEIR III Committee, none of the studies involving human populations that have been exposed primarily at low levels provide sufficient information for risk estimation. Thus, it is necessary to extrapolate from estimates based on data from populations that include persons exposed at relatively high dose rates, such as the Japanese atomic bomb survivors and the British ankylosing spondylitis patients who were medically treated with radiation.

Although estimates of risks due to radiation have often been based on a linear extrapolation model,[17,18,19] the BEIR III Committee adopted a linear-quadratic function as the most plausible description of the dose-response relationship in the low-to-intermediate range. The use of such a model as the linear-quadratic function, which provides for a reduction in effects with low Linear Energy Transfer (LET) radiation for small doses and given at low rates, can be justified based on evidence summarized in a National Council on Radiation Protection report.[20] The report states that it is clear from the data obtained from all endpoints examined, from cell death to tumor induction, that a reduction in dose rate in general results in a reduced biological effect.

Another difficulty in obtaining lifetime risk estimates is that none of the populations on which estimates of effects are based have yet been followed to the end of their lifespans. Two approaches were used by the BEIR III Committee to extend risk estimates beyond the observation period where follow-up data have been collected. With the absolute risk model, it was assumed that the number of excess mortalities per unit of population, per unit of time, and per unit of radiation dose will remain constant over a specified time period. With the relative risk model, it was assumed that the excess cancer risk will continue to be a constant ratio to the spontaneous age-specific risk over the specified period. Since spontaneous rates generally increase with age, the relative risk model will yield larger numbers for the years beyond the period where follow-up data

are presently available. The most recent data on the Japanese sur-
vivors[21] as well as the British ankylosing spondylitis patients[22]
indicate that the relative risk projection model is probably more
appropriate than the absolute model.

We compared estimates of cancer mortality based on the results
presented in the last two columns of Table 2. For this purpose, we
used BEIR III estimates for a single exposure to 10 rad.* In all
cases examined in this study, dose rates were lower than those con-
sidered by BEIR III, especially for the situation involving total
^{85}Kr release to the environment. To obtain estimates for the number
of cancers expected in each of these situations, we reduced the BEIR
III 10-rad estimates of risk in proportion to the estimated ^{85}Kr
dose, and then multiplied by the number of individuals at risk to
obtain the expected number of cancer deaths induced by radiation
received in a single year of plant operation. These values were
then multiplied by 30 to estimate the number of cancer mortalities
expected to result from 30 years of plant operation as presented in
Table 3.

It is emphasized that these estimates are based on the assump-
tion that at the levels being compared, risks are assumed to be
proportional to dose. Data from animal experiments indicate that
exposures at low dose rates (in the range of 10 rad per day) produce
less risk per rad than do exposures at high rates (in the range of 50
rad per minute). Unfortunately, there are no adequate data to allow

---

* BEIR III also provides estimates of the effects of exposures of one
  rad per year either persisting throughout a lifetime or for various
  ages intended to reflect occupational exposures. These alternative
  estimates have not been used, because they are based on the assump-
  tion that all persons at risk receive exposure from birth to the
  end of life (or from particular specified ages in the case of
  occupational exposure). In the situation of interest in this
  report, it is expected that persons will begin exposure at diffe-
  rent ages, and that as persons move away or leave their jobs,
  others will replace them. With the linear-quadratic function used
  in BEIR III, the effect (per rad) of 10 rad is not that much
  different from the effect of one rad. The slight per-rad increase
  resulting from using the 10-rad situation, as opposed to using the
  single-rad exposure situation, will be the same for either situa-
  tion (e.g., capture vs. release) being compared in this report.

Table 3.   Comparison of Estimated Cancer Mortality from
the Capture and Immobilization of ^{85}Kr as
Opposed to Routine Release to the Environment

Exposure Situation	Lifetime Risk/Person Per Year Exposure	Total Number of Radiation-Induced Cancer Deaths Expected from 30 Years of Exposure
Occupational (Capture)		
450 mrem/yr 9 people	1.01×10^{-4}	0.027
570 mrem/yr 7 people	1.28×10^{-4}	0.027
425 mrem/yr 7 people	9.58×10^{-5}	0.020
600 mrem/yr 5 people	1.35×10^{-4}	0.020
General Public (Routine Release)		
0.003 mrem/yr 850,000 people	6.76×10^{-10}	0.017

comparing effects of the 500 mrem/year occupational dose to the
0.003 mrem/year population dose developed in this study. It is
possible that no risks would occur from either situation (e.g.,
capture vs. release).

Given the uncertainties in the models used to develop these
estimates, the differences in total risks for the situations con-
sidered here cannot be considered meaningful. Certainly there is
no compelling reason to conclude that risks from ^{85}Kr release are
greater than those from capturing and immobilizing ^{85}Kr.

VI. References

1. U.S. Environmental Protection Agency (EPA). _Environmental Analysis of the Uranium Fuel Cycle, Part III - Nuclear Fuel Reprocessing_. EPA-520/9-73-003-D, Washington, D.C., 1973.

2. U.S. Environmental Protection Agency (EPA). _Final Environmental Statement - 40 CFR 190 - Environmental Radiation Protection Requirements for Normal Operations of Activities in the Uranium Fuel Cycle_. EPA 520/4-76-016, Washington, D.C., 1976.

3. U.S. Department of Energy (DOE). _Spent Fuel Storage Requirements_. DOE/SR-0007, Aiken, South Carolina, 1981.

4. U.S. Department of Energy (DOE). _U.S. Commercial Nuclear Power: Historical Perspective, Current Status, and Outlook_. DOE/EIA-0315, Washington, D.C., 1982.

5. U.S. Department of Energy (DOE). _Spent Fuel Storage Requirements_. DOE/RL-83-1, Richland, Washington, 1983.

6. Mellinger, P. J., G. R. Hoenes, L. W. Brackenbush and J. Greenborg. _^{85}Kr Management Trade-Offs: A Perspective to Total Radiation Dose Commitment_. PNL-3176, Pacific Northwest Laboratory, Richland, Washington, 1980.

7. Bell, M. J. _ORIGEN - The ORNL Isotope Generation and Depletion Code_. ORNL-4628, Oak Ridge National Laboratory, Oak Ridge, Tennessee, 1973.

8. Oak Ridge National Laboratory (ORNL). _Siting of Fuel Reprocessing and Waste Management Facilities_. ORNL-4451, Oak Ridge, Tennessee, 1970.

9. Exxon Nuclear Company. _Nuclear Fuel Recovery and Recycling Center - Environmental Report_. XN-FR-33, NRC Docket No. 50-564. Richland, Washington, 1977.

10. Brown, R. A., D. A. Knecht and T. R. Thomas. _Reference Facility Description for the Recovery of Iodine, Carbon and Krypton from Gaseous Wastes_. ICP-1126, Idaho National Engineering Laboratory, Idaho Falls, Idaho, 1978.

11. Allied-General Nuclear Services (AGNS). _Barnwell Nuclear Fuel Plant - Environmental Report_. NRC Docket No. 50-332, Barnwell, South Carolina, 1971.

12. Soldat, J. K., P. E. Bramson and H. M. Parker. _The Dosimetry of the Radioactive Noble Gases_, BNWL-SA-4813, Rev. 2, Pacific Northwest Laboratory, Richland, Washington, 1976.

13. Waggoner, R. C. _Technical and Economic Evaluation of Processes for Krypton-85 Recovery from Power Fuel Reprocessing Plant Off-Gas_. DP-1637, Savannah River Laboratory, Aiken, South Carolina, 1982.

14. Ralph M. Parsons Company (RMP). _Krypton Encapsulation Preconceptual Design_. Report No. 6154-3-1, prepared for the U.S. Department of Energy, 1981.

15. Reece, W. D., R. T. Hadley, R. Harty, J. Glass, J. E. Tanner and L. F. Munson. _Personnel Exposure from Right Cylindrical Sources (PERCS): The Theory, the Code, and Examples_. NUREG/CR-3573, U.S. Nuclear Regulatory Commission, Washington, D.C., 1984.

16. National Academy of Sciences (NAS). _The Effects on Populations of Exposure to Low Levels of Ionizing Radiation_. (BEIR III). Report of the Advisory Committee on the Biological Effects of Ionizing Radiation, National Academy of Sciences, National Research Council, Washington, D.C., 1980.

17. National Academy of Sciences (NAS). _The Effects on Populations of Exposure to Low Levels of Ionizing Radiation_. (BEIR Report). Report of the Advisory Committee on the Biological Effects of Ionizing Radiation, National Academy of Sciences. National Research Council, Washington, D.C., 1972.

18. United Nations Scientific Committee on the Effects of Atomic Radiation (UNSCEAR). _Sources and Effects of Ionizing Radiation_. United Nations, New York, 1977.

19. International Commission on Radiological Protection (ICRP). _Radiation Protection_. ICRP 26, Pergamon Press, New York, 1977.

20. National Council on Radiation Protection and Measurements (NCRP). _Influence of Dose and its Distribution in Time on Dose-Response Relationships for Low-LET Radiations_. NCRP Report No. 64, Washington, D.C, 1980.

21. Kato, H., and W. J. Schull. "Studies of the mortality of A-bomb survivors 7. Mortality, 1950-1978: Part I. Cancer mortality." _Radiation Research_ 90:395-432 (1982).

22. Smith, P. G., and R. Doll. "Mortality among patients with ankylosing spondylitis after a single treatment course with x-rays." _British Medical Journal_ 284:449-460 (1982).

DISCUSSION

LAMBERGER: If you assume fuel with substantially less cooling than the 30 years you used, does it change you conclusions?

MELLINGER: No. The dose would go up proportionately with the increased source term, proportional to the activity of krypton. In this case, if we used 180 day-cooled fuel, the doses would go up a factor of about 5. The conclusions would remain the same, but the actual magnitude of the doses may be higher. You can also argue that this is for one reprocessing plant. We could put many reprocessing plants in the same area in which case you might not raise the actual exposure of the population work force because, hopefully, they would be working in separate plants, but you would increase the exposure to the population if they had overlaping wind regimens, for example. The significance of this comparison is that you would have to have 100, or 200, or 300 plants in order to really change the conclusions. You won't obtain that kind of density in a given population. So, the conclusions are reasonably straight-forward. Incidentally, we have a full report that we are publishing next week with the details of this study.

WIKTORSSON: Have you made an estimate of the global dose commitment? What will be the resultant collective dose?

MELLINGER: It is considerably more ridiculous than the one we just gave; 0.003 millirem per year. One microrem per year is about the dose you receive from drinking one can of beer a year. If we extended this to the U.S. population, it would drop significantly. The real population dose per measurement would be 0.05 millirems over an 80 year period. So, the annual dose would be about 0.0005 millirem from a younger, 160-day-cooled fuel. The per capita dose is down significantly. I have no problem with the man-rem calculation, comparing two similar populations, such as the exposure of nuclear power plant personnel vs. reprocessing plant personnel, one small community as opposed to another. But, speaking as a radiation biologist, I think that it is pretty absurd to run it up to a world calculation dose.

D'AMBROSIA: My question is, what are you going to do with this information. Will it be made available to EPA?

MELLINGER: We have been asked by DOE to generate some background information if the 40CFR190 law comes back up for its review. We are hoping to be able to have some different considerations for that particular law. One recommendation may be to either postpone the law until the U.S. does have a nuclear fuel reprocessing industry of sufficient magnitude that the law should be brought back up and refiled. Certainly, we shouldn't take one plant and put a 50,000 curie per day electric power generation limit on it.

CLOSING REMARKS OF SESSION CHAIRMAN D'AMBROSIA:

This afternoon, Dr. Anderson spoke of International progress in filter testing and the identification of filtration mechanisms; Mr. Jacox strongly recommended that workers familiar with filtration techniques and operations be involved in the design, construction, check out, and worker training for filtration systems in nuclear facilities; and Dr. Mellinger noted that implementation of the EPA ruling on airborne effluent control could result in greater health effects from the control and immobilization of gaseous radionuclides than from their release.

The common theme of these presentations is that we must respect and provide for the safety of our workers and citizens. The questions during the session indicate that education may be achieved through presenting papers such as these at larger conferences. But without some educational effort, neither our progress, nor our expertise, will be recognized in the construction and operation of filtration systems.

Session 18

RECOVERY AND RETENTION OF AIRBORNE WASTES: RESEARCH

WEDNESDAY: August 15, 1984
CHAIRMEN: T.R. Thomas
S.J. Fernandez
Westinghouse Idaho Nuclear
Company

THE THEORY AND PRACTICE OF NITROGEN OXIDE ABSORPTION
R.M. Counce

NO_x REMOVAL FROM NUCLEAR FUEL REPROCESSING PLANTS OFF-GAS BY CATALYTIC REDUCTION WITH NH_3
S. Hattori, Y. Kobayashi, Y. Katoh, Y. Takimoto, M. Kunikata

REMOVAL OF ^{14}C FROM NITROGEN ANNULUS GAS
C.H. Cheh

DEVELOPMENT OF A WETPROOFED CATALYST RECOMBINER FOR REMOVAL OF AIR-BORNE TRITIUM
K.T. Chuang, R.J. Quaiattini, D.R.P. Thatcher, L.J. Puissant

TRITIUM MANAGEMENT FOR FUSION REACTORS
J.L. Rouyer, H. Djerassi

DEVELOPMENT OF A METHOD TO DETERMINE IODINE SPECIFIC ACTIVITY IN PROCESS OFF-GASES BY GC SEPARATION AND NEGATIVE IONIZATION MASS SPECTROMETRY
S.J. Fernandez, R.A. Rankin, G.J. McManus, R.A. Nielson

REMOVAL OF IODINE FROM OFF-GAS OF NUCLEAR FUEL REPROCESSING PLANTS WITH SILVER IMPREGNATED ADSORBENTS
S. Hattori, Y. Kobayashi, Y. Ozawa, M. Kunikata

VOLATILE RUTHENIUM TRAPPING ON SILICA GEL AND SOLID CATALYSTS
P.W. Cains, K.C. Yewer

RECOVERY AND PURIFICATION OF Xe-133 AS A BY-PRODUCT OF Mo-99 PRODUCTION USING LINDE 5A MOLECULAR SIEVE
N.A. Briden, R.A. Speranzini

OPENING REMARKS OF SESSION CHAIRMAN THOMAS:

Welcome to Session 18 on "Recovery and Retention of Airborne Waste: Research". In the first part of the session we have one American, one Japanese, two Canadian and one French paper covering NO_x, ^{14}C and ^{3}H abatement or recovery. Research in these areas continues to be important because:

NO_x gases may interfere with other recovery processes such as cryogenic distillation for ^{85}Kr recovery and molecular sieve adsorption processes for H_2O and CO_2 removal.

NO_x emissions from some DOE site operations may exceed future State and Federal release or opacity limits.

Uncontrolled ^{3}H releases from future commercial fuel reprocessing plants may exceed allowable dose limits to the maximum exposed individual

Uncontrolled future ^{14}C releases may deliver unacceptable population doese to the world due to its long half-live.

In the second half of Session 18, on reserach activities for the recovery and retention of airborne wastes, we will hear four papers. Each deal with measurement, retention, or recovery of I-129, Ru-106, or noble gases.

THE THEORY AND PRACTICE
OF NITROGEN OXIDE
ABSORPTION

Robert M. Counce
Chemical Engineering Department
The University of Tennessee
Knoxville, Tennessee 37996

I. Introduction

Nitrogen oxide (NO_x) absorbers vary in purpose from bulk nitric acid production to abatement of trace NO_x concentrations from gas streams. Absorbers are typically of plate or packed tower design although some plate/packed combination towers potentially offer some useful advantages. Mathematical models for the design of NO_x absorbers vary from mechanistically based models for absorption into water and dilute HNO_3 to empirically based models for absorption into concentrated HNO_3 solutions.[1-4]

The NO_x content in effluent gas from modern high pressure nitric acid production towers can be reduced to well under 200 ppm.[5] The design of these towers is well established and available from several vendors and other specialists. For many scrubbing applications where the nitric acid content of the product liquid is not the prime concern, atmospheric absorbers offer a lower cost alternative than the standard nitric acid production tower.

The basis for the design of low pressure NO_x absorbers for NO_x recovery or abatement has been established to a sufficient extent to be a reasonable predictive tool although published operating experience is minimal and experimental verification may be necessary for many cases.[1] The availability of high efficiency packing potentially offers significant NO_x removal in minimal sized packed absorbers.[2] An important issue in the design of NO_x abatement systems is the disposition of the effluent scrubber liquid. A partial recycle of this liquid to the absorber normally requires additional processes for regeneration of the scrub solution[2]; if there is an "in plant" use for this effluent stream, then a substantial simplification of the system may be realized.

The focus of this paper is on low pressure NO_x absorbers for the primary purpose of gaseous NO_x recovery and abatement. This design of this type of scrubber is not generally available except from a few specialists in this area.

II. Theory

A summary of important chemical reactions in the modeling of nitrogen oxide scrubbers is shown in Table 1. The form of many of these equations has been chosen to show the effect of nitric acid on the chemical system. The two cases indicated in Table 1 illustrate the important chemistry arising from the contact of gaseous NO_x species with dilute and concentrated aqueous nitric acid. At low nitric acid concentrations there is little effect of nitric acid concentration. For the concentrated nitric acid case the oxidation potential of nitric acid tends to raise the oxidation state of the NO_x species toward the +4 state. At sufficiently high aqueous nitric acid concentrations the hydrolysis of N_2O_4 will not proceed, thus allowing for only its physical

1242

absorption.[7]   The system framework shown in Table 1 provides desorption as well as absorption pathways. For example, the combination of Equations 11,12 and 13 yields

$$3 \ HNO_2(\ell) \leftrightarrow HNO_3(\ell) + H_2O(\ell) + 2 \ NO(\ell), \tag{14}$$
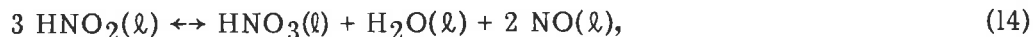
the Abel-Schmid expression for the decomposition of aqueous HNO_2.[8-10]

Multiphase system modeling that considers only the prevailing chemical equilibrium cannot fully represent NO_x absorption/desorption phenomena; the mass transfer characteristics of the two phases must also be considered. This is illustrated by utilizing a combination of Equations 2,6,11,12 and 13,

$$3 \ NO_2(g) + H_2O \leftrightarrow 2 \ HNO_3(\ell) + NO(g). \tag{15}$$
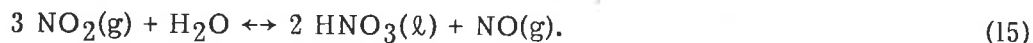
This equation indicates that 1 mole of gaseous NO is produced when 3 moles of NO_2 are removed from the gas phase. However this is not necessarily the case as is shown in some data presented in Figure 1.[12] In this semibatch experiment 1% NO_2* in N_2 was bubbled through water. The resulting concentration profiles and ratios show that the ratio of NO* produced to NO_2* absorbed reaches 1:3 only when a semi-steady state concentration of HNO_2 is established. This is important in scrubber design and results from the kinetic and mass transfer limitations of the aqueous decomposition of HNO_2 requiring a substantial HNO_2 concentration for a driving force.[13] If this concentration driving force is not established during scrubbing the ratio of NO* produced to NO_2* absorbed may be very much less than 1:3.

The role of HNO_2 in the scrubbing of gaseous nitrogen oxides is not clear. There is considerable disagreement as to the gas-phase formation and decomposition reaction rate constants;[14-16] experiments with reactors of small ratios of surface area to reactor volume generally yield the smallest rate constants. This suggests the complication of heterogeneous reactions in this determination. Scrubber results of Counce and Perona[1] for NO_x and NO_2* partial pressures of 0.010 and 0.002 atm, respectively, showed no indication of HNO_2 formation and absorption; this observation is supported by the work of Corriveau.[17] Other work by Andrews and Hanson, covering much lower NO_x partial pressures than Counce and Perona and observations by Carta, and Hoftyzer and Kwanten, indicates the possibility of HNO_2 formation and absorption at lower partial pressures, especially at high NO* to NO_2 ratios.[18-20] Equations for the absorption of NO_x species in a differential section of tower is shown below:

$$-d(GY_{NO_2}*) = [(2R_{N_2O_4} + R_{N_2O_3} + R_{NO_2}) \ a - r_1\varepsilon] \ dz \tag{16}$$

$$-d(GY_{NO}*) = [(R_{N_2O_3} + R_{NO}) \ a + r_1\varepsilon] \ dz \tag{17}$$

where the absorption flux for any component is

$$R_i = k_G(P_i - P_i*) = Ek_L(C_i* - C_i) \tag{18}$$

and

$$C_{NO} = \left[\frac{K_{14} C_{HNO_2}^3}{C_{H^+} C_{NO_3^-}} \right]^{1/2} \qquad (19)$$

This model includes an assumption that the liquid phase HNO_2 decomposition does not proceed significantly in the liquid film.

This scheme of equations does not provide for the gas-phase oxidation of NO by HNO_3. This reaction is not well understood and the reader is referred to articles by Lefers et al, Streit et al, Kaiser and Wu, Carta and Pigford and Abel and Schmid.[7,21,22;23,8-10] One example of reaction (5) is the oxidation of gaseous NO to NO_2 by contact with concentrated aqueous HNO_3 solutions; this has been studied and demonstrated by Lefers et al and Counce and Perona, respectfully.[7,24] The scheme of flux equations is illustrated in Fig. 2 for NO_x absorption into water or dilute HNO_3 solutions. The gas phase portion of this Figure shows the oxidation of NO occurring while N_2O_4 and N_2O_3 are in equilibrium with their respective reactant species.[25-26] In Figure 2 the liquid N_2O_4 and N_2O_3 are shown reacting irreversibly with water in the liquid film (as is usually the case in packed towers when the absorbing solution is water or dilute solutions of aqueous HNO_3), whereas any reaction of NO_2 and water is extremely slow and usually occurs in the bulk phase and may be neglected in many cases.[27]

The desorption of NO may be neglected with little loss of accuracy for many NO_x absorption models involving packed towers with non recycle of the scrub liquid. However for absorption with low liquid-gas ratios as are commonly encountered in plate scrubbers, the ratio of NO produced to NO_2^* absorbed will approach 1:3.

The modeling of NO_x absorption into concentrated HNO_3 solutions is usually modeled empirically based on a plate efficiency concept.[4] In order to help bridge the gap between the mechanistically based models for absorption into dilute HNO_3 and for absorption into concentrated HNO_3, some information exists on the variation of the enhancement factor Ek_L of Equations (16) and (17) with nitric acid concentration for N_2O_4 absorption[7]; similar information is not known for N_2O_3, however one might assume the variation to be similar to that of N_2O_4.

This section has attempted to provide a basis for models of NO_x absorption into aqueous HNO_3 solutions. Some opportunities for further research and development are obvious. However, by using models based on combinations of mechanistically based and empirically based models as well as experience, atmospheric pressure NO_x absorption towers may be designed and some indication as to the uncertainty of the design ascertained.

III. Results and Conclusions

In this section the previously developed mathematical model for NO_x absorption will be compared with experimental data; some mechanistic analysis of these model predictions will be presented, and the model will be used to predict NO_x removal efficiencies for some currently existing "high efficiency" tower packing. The term "high efficiency" is used for structured packings with high surface area per unit volume such as the Koch Sulzer Packing* which will be used in NO_x scrubbing test currently being planned at the University of Tennessee.

1244

The mathematical model is compared with some existing experimental data in Table 2.[1] The equilibrium and kinetic constants, enhancement factors, etc., required by the model for these calculations have been given previously by Counce and Perona.[1] Model predicted and experimental NO_x removal efficiencies are presented in Table 2 for variations of three parameters-superficial gas and liquid velocities and the oxidation state of the feed gas. Over the range of parameter variation of these tests, obviously the most important parameter is the oxidation state of the feed gas.

This effect of the NO_x oxidation state is further investigated in Figure 3 which further shows the importance of this parameter on NO_x removal efficiency. The relative importance of the absorption mechanisms for the prediction of Figure 3 for the lower gas velocity is shown in Figure 4. The parameter ϕ_i is an indicator of the importance of a particular absorption route (i.e. ϕ_{NO_2} is the total molar absorption of NO_2 divided by the total NO_x absorption of the tower for particular parameter settings),

$$\phi_i = \frac{R_{i,T}}{\Sigma R_{i,T}} \tag{20}$$

Inspection of Figure 4 shows that most of the NO_x absorbed at high oxidation levels of the feed gas occurs by the absorption of N_2O_4. At lower oxidation levels in the feed gas the N_2O_3 absorption route becomes more important. The absorption of NO_2 is of negligible importance for these predictions. The mechanistic analysis of Figures 3 and 4 is presented again in Figures 5 and 6 for a feed gas with a higher NO_x concentration. Results indicate higher removal efficiencies, in general, and more dominance of the possible absorption routes by the N_2O_4 route.

A projection of NO_x removal efficiency for very low feed gas concentrations is presented in Figure 7 for a range of gas-liquid interfacial area values. Again these predictions are for an atmospheric pressure water scrubber with no recycle of the scrubber liquid. The ranges of interfacial area from traditional dumped packings is indicated as is the range of interfacial areas from some of the more high efficiency structured packings.[6] As can be seen from this figure, the use of high efficiency packings can improve expected scrubber efficiency for some fairly "hard to scrub" levels of gaseous NO_x concentrations. Further study of projected NO_x removal efficiency with high efficiency packing is shown in Table 3.

Although published experimental case studies are lacking for the projections presented in this paper, these results do indicate that the use of some of the high efficiency packings that are currently available can, potentially, provide substantial NO_x removal efficiencies at very low NO_x concentration levels where the ratio of NO_2^*/NO_x is unity.

*Koch Engineering Company, 161 East 42nd Street, New York, NY 10017

Table 1 Important Reactions in Aqueous NO_x Scrubbing

Dilute HNO_3	Con.HNO_3		
X	X	$2NO(g) + O_2(g) \rightarrow 2NO_2(g)$	(1)
X	X	$2NO_2(g) \leftrightarrow N_2O_4(g)$	(2)
X		$NO_2(g) + NO(g) \leftrightarrow N_2O_3(g)$	(3)
X		$N_2O_3(g) + H_2O(g) \leftrightarrow 2HNO_2(g)$	(4)
	X	$2HNO_3(g) + NO(g) \leftrightarrow 3NO_2(g) + H_2O(g)$	(5)
X	X	$N_2O_4(g) \leftrightarrow N_2O_4(\ell)$	(6)
X		$N_2O_3(g) \leftrightarrow N_2O_3(\ell)$	(7)
X	X	$NO(g) \leftrightarrow NO(\ell)$	(8)
	X	$HNO_3(g) \leftrightarrow HNO_3(\ell)$	(9)
		$HNO_2(g) \leftrightarrow HNO_2(\ell)$	(10)
X	X	$N_2O_4(\ell) + H_2O(\ell) \leftrightarrow HNO_2(\ell) + HNO_3(\ell)$	(11)
X	X	$N_2O_3(\ell) + H_2O(\ell \leftrightarrow 2HNO_2(\ell)$	(12)
X	X	$2N_2O_3(\ell) \leftrightarrow 2NO(\ell) + N_2O_4(\ell)$	(13)

1246

Table 2   Experimental and Calculated Results[a]
for Runs Using an Atmospheric Pressure Water Scrubber
Packed with 13mm Ceramic Intalox Saddles with the NO_x
Feed Partial Pressure at About 0.01 ATM

Variables				-(Low)	+(High)
1. Gas rate ($m \cdot s^{-1}$)				0.35	0.62
2. Liquid rate ($m \cdot s^{-1}$)				2.2×10^{-3}	4.4×10^{-3}
3. Percent of NO_x with N in +IV state				20	100

Run	1	2	3	$(X_{NO_x})_{exp}$	$(X_{NO_x})_{cal}$
10-32-2F	−	+	+	0.64	0.61
10-32-2G	−	−	−	0.10	0.06
10-32-2H	+	+	−	0.00	0.06
10-32-21	+	−	+	0.48	0.43

*Calculated X_{NO_2} is based on ($\sqrt{Dk}/H)_{N_2O_4}$ of 11.0×10^{-5}

Table 3   Projected NO_x removal efficiency of an atmospheric pressure
water scrubber with a gas-liquid interfacial
area of $450 m^{-1}$. Other conditions are: packed
height, 2.74m; total pressure, 1 atm; temperature,
298K; and $P_{NO_2}*/P_{NO_x}$, 1.0.

X_{NO_x} at Varying NO_x Feed Concentrations
and Superficial Gas Velocities

V_G(m/s)	$C_{NO_x,IN}$	X_{NO_x}
0.11	1000	0.86
0.11	500	0.75
0.23	1000	0.75
0.23	500	0.58
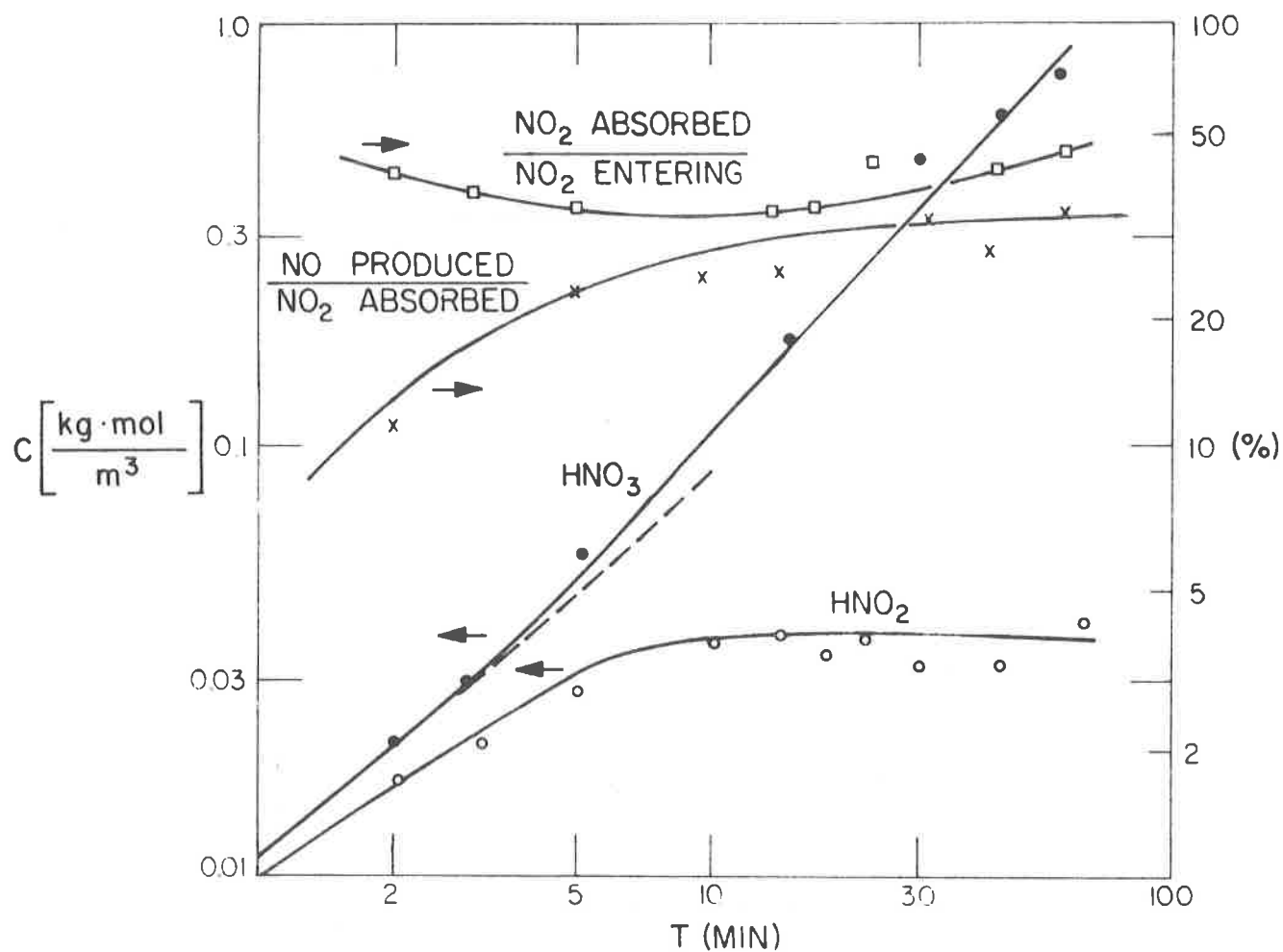
Fig. 1.   Results of semibatch NO_2 absorption studies.

Source: A.F. Makhotkin and A.M. Shamsutidinov,
           Khim.Khim. Takhn. XIX, (1976).
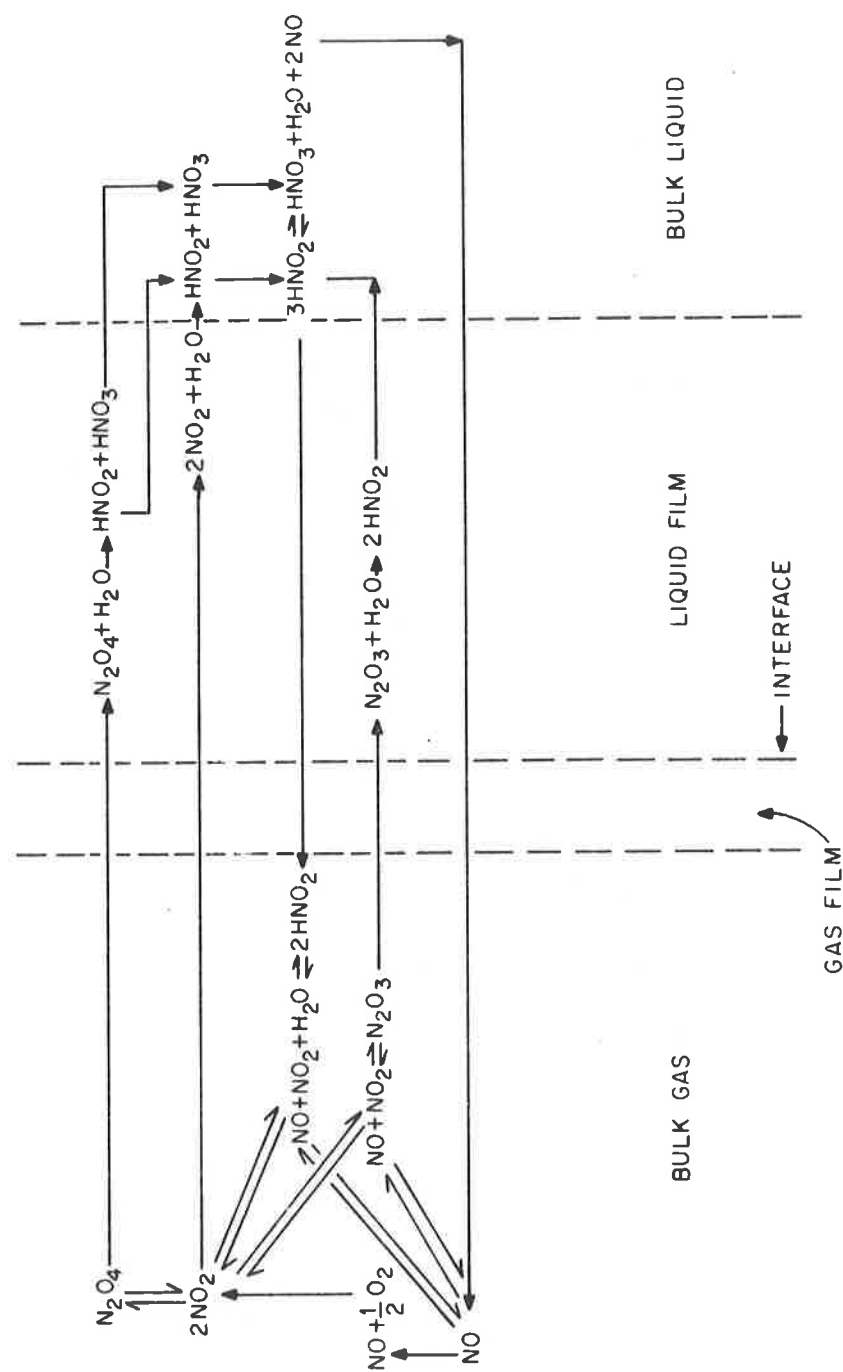
Fig. 2. Model for describing mass-transfer and chemical-reaction phenomena for NO_x absorption into water or dilute HNO_3 solutions.
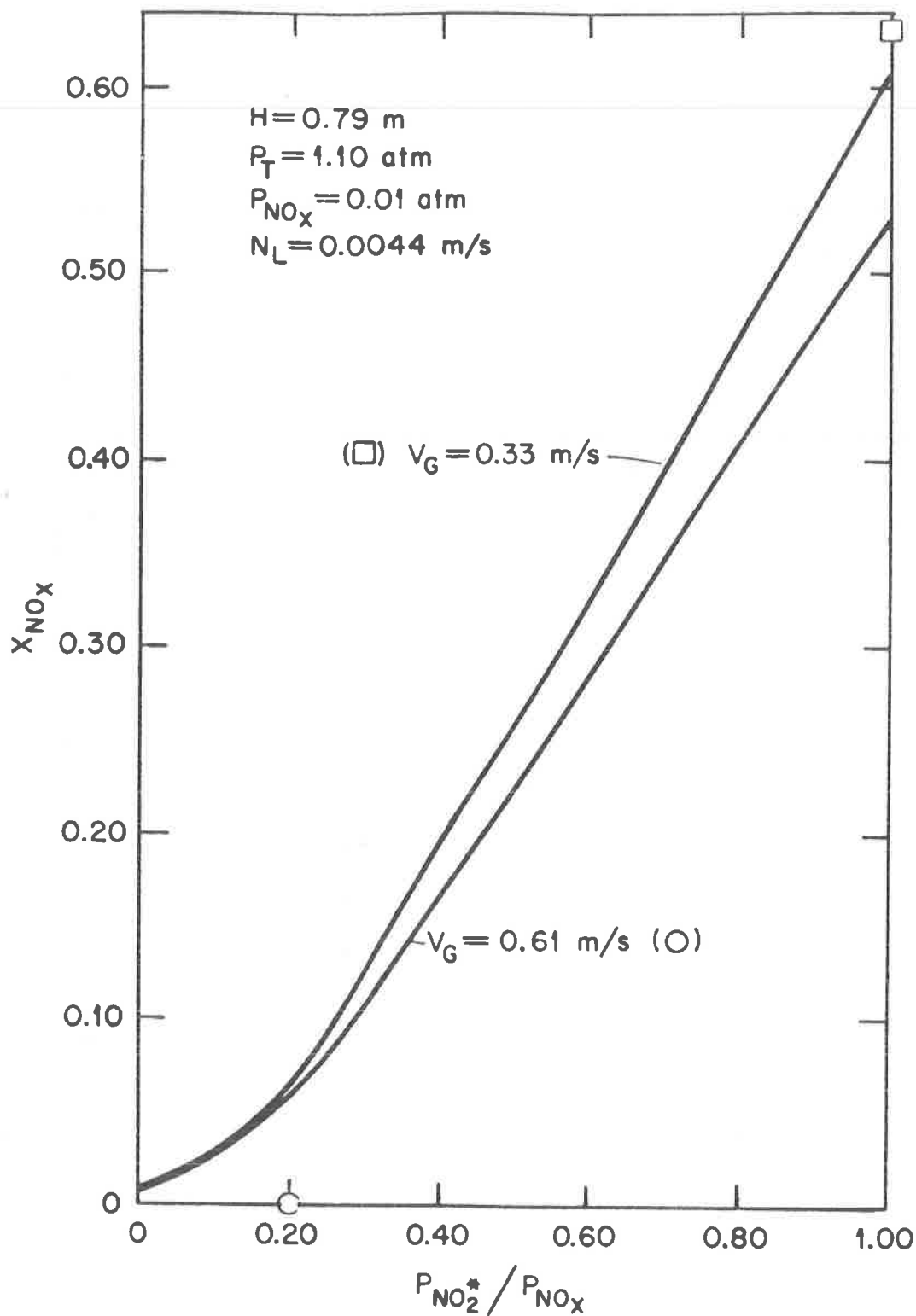
Fig. 3. Model predicted and experimental NO_x removal efficiency in an atmospheric pressure water scrubber packed with 13mm Intalox saddles.
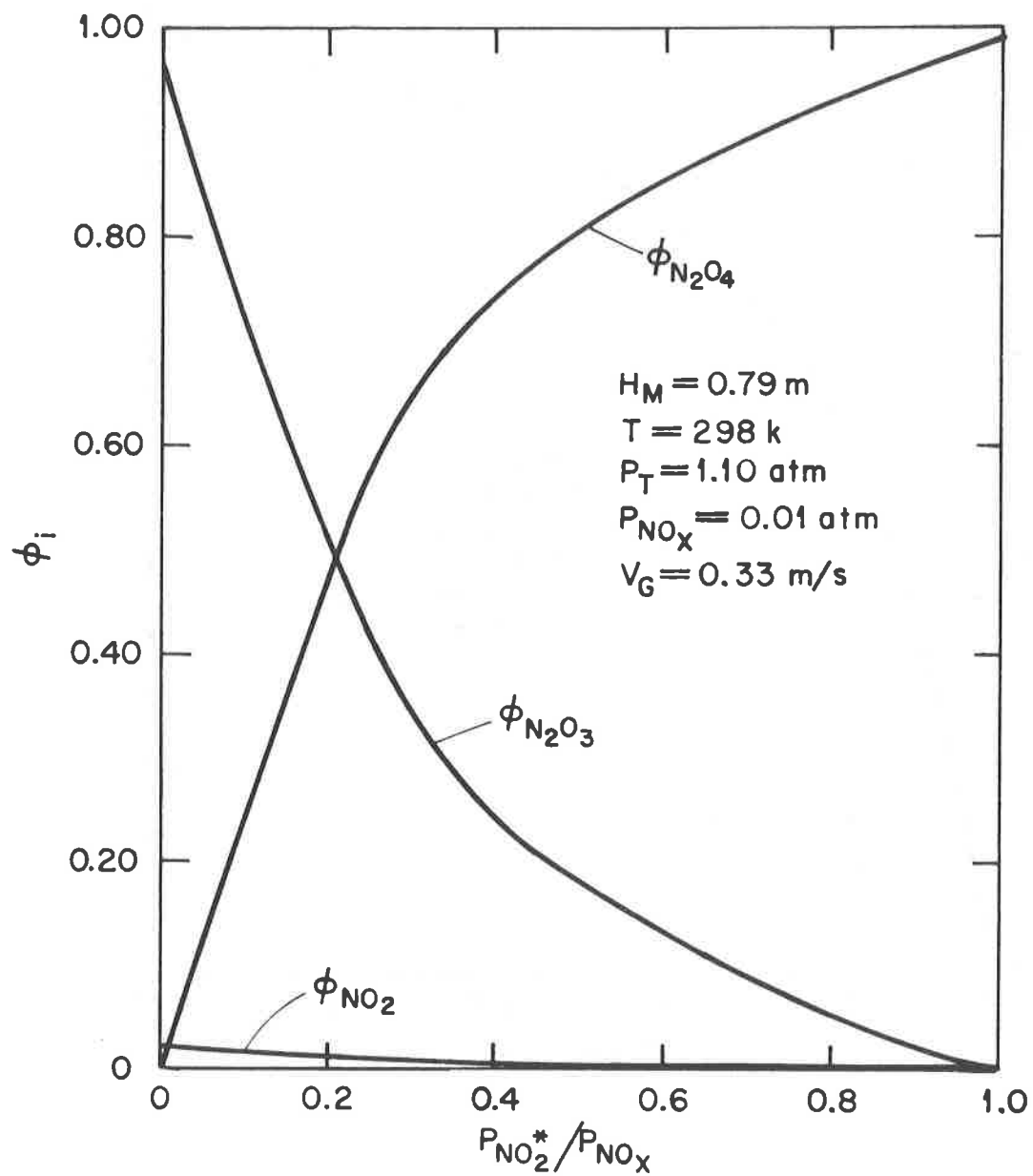
Fig. 4.   Relative importance of removal mechanisms for the indicated conditions. The gas velocity is the lower of the two from Figure 3.
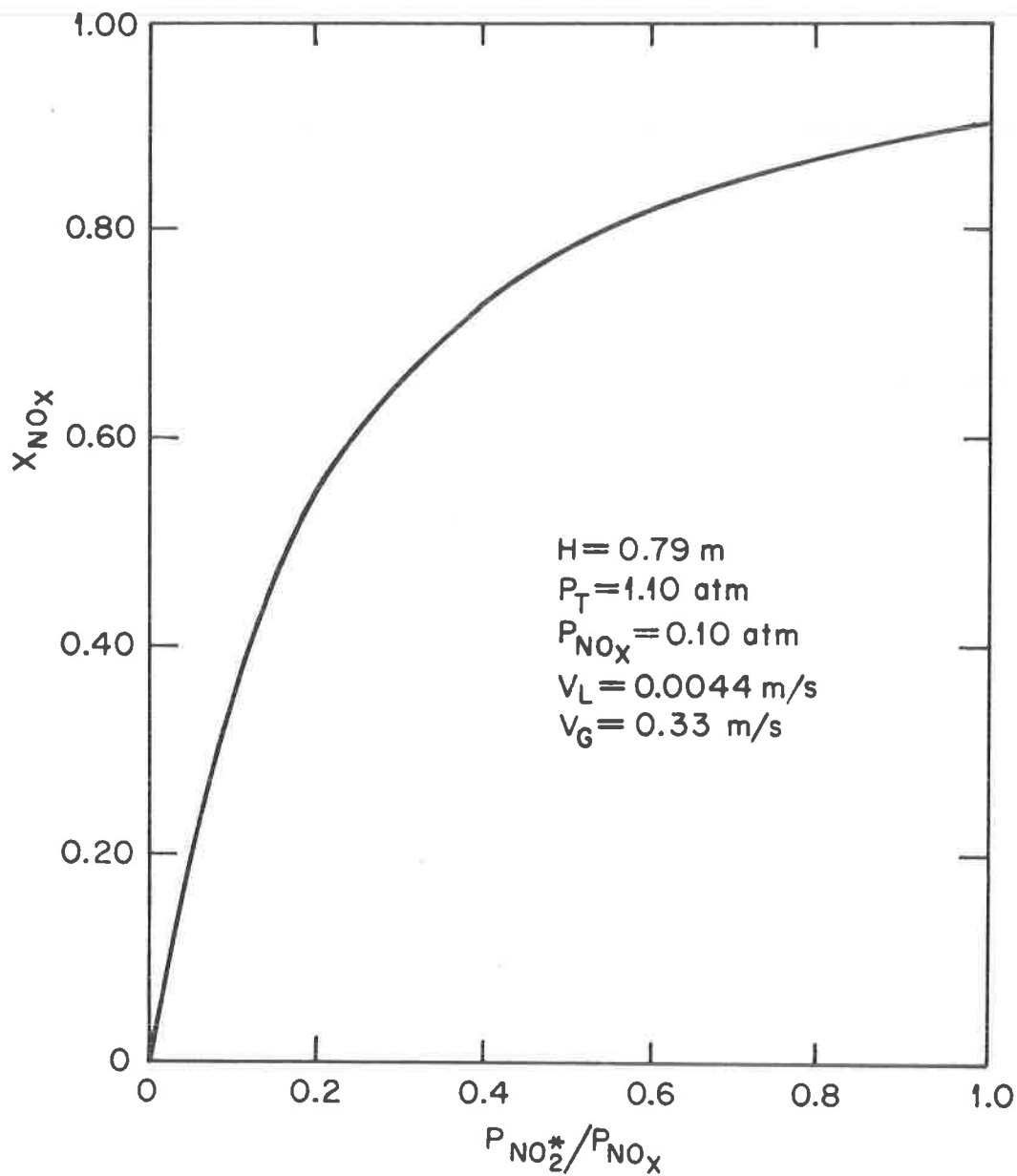
Fig. 5. Model predicted NO_x removal efficiency in a tower packed with 13mm Intalox saddles.
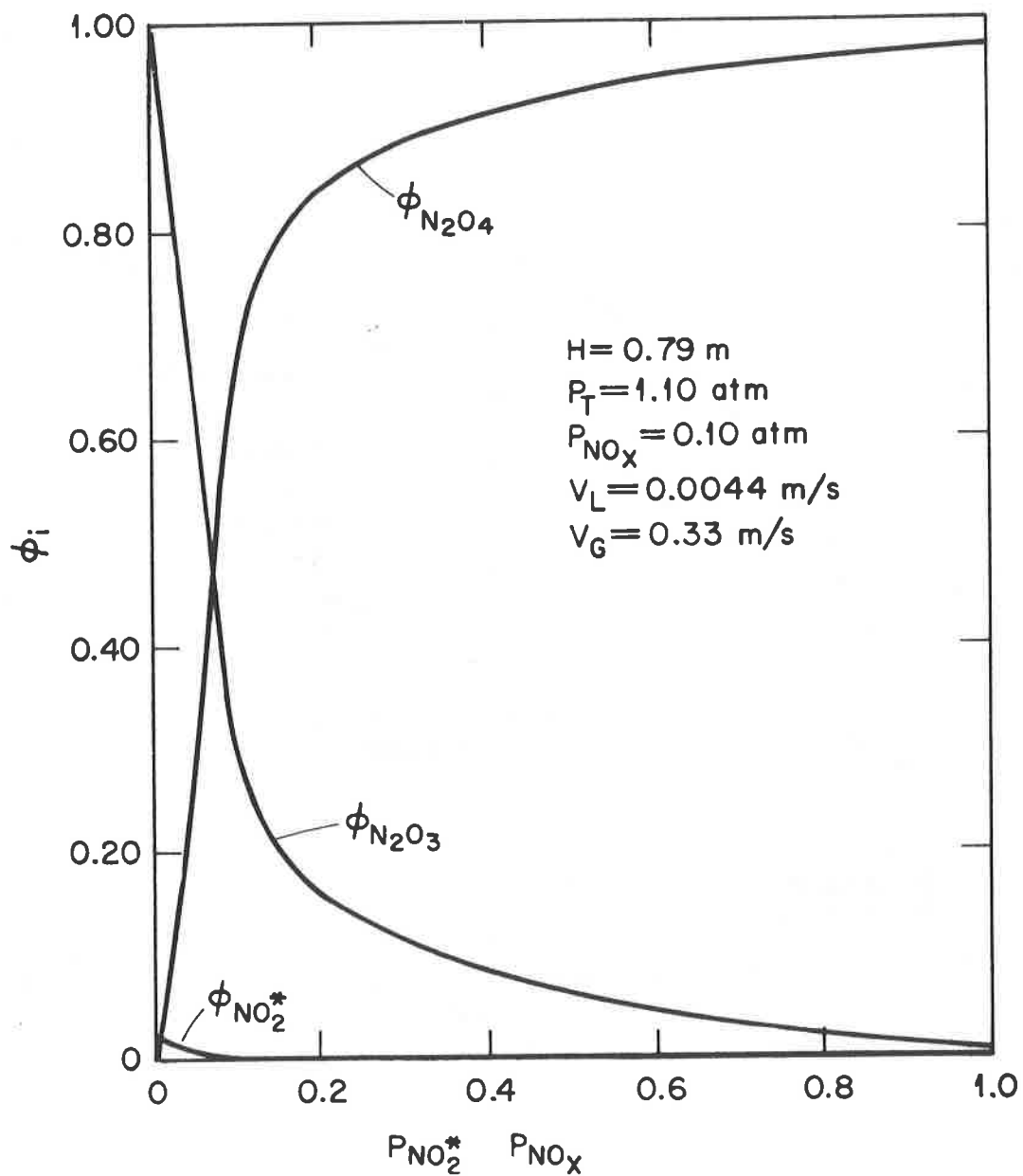
Fig. 6.   Relative importance of removal mechanisms for the
indicated conditions.
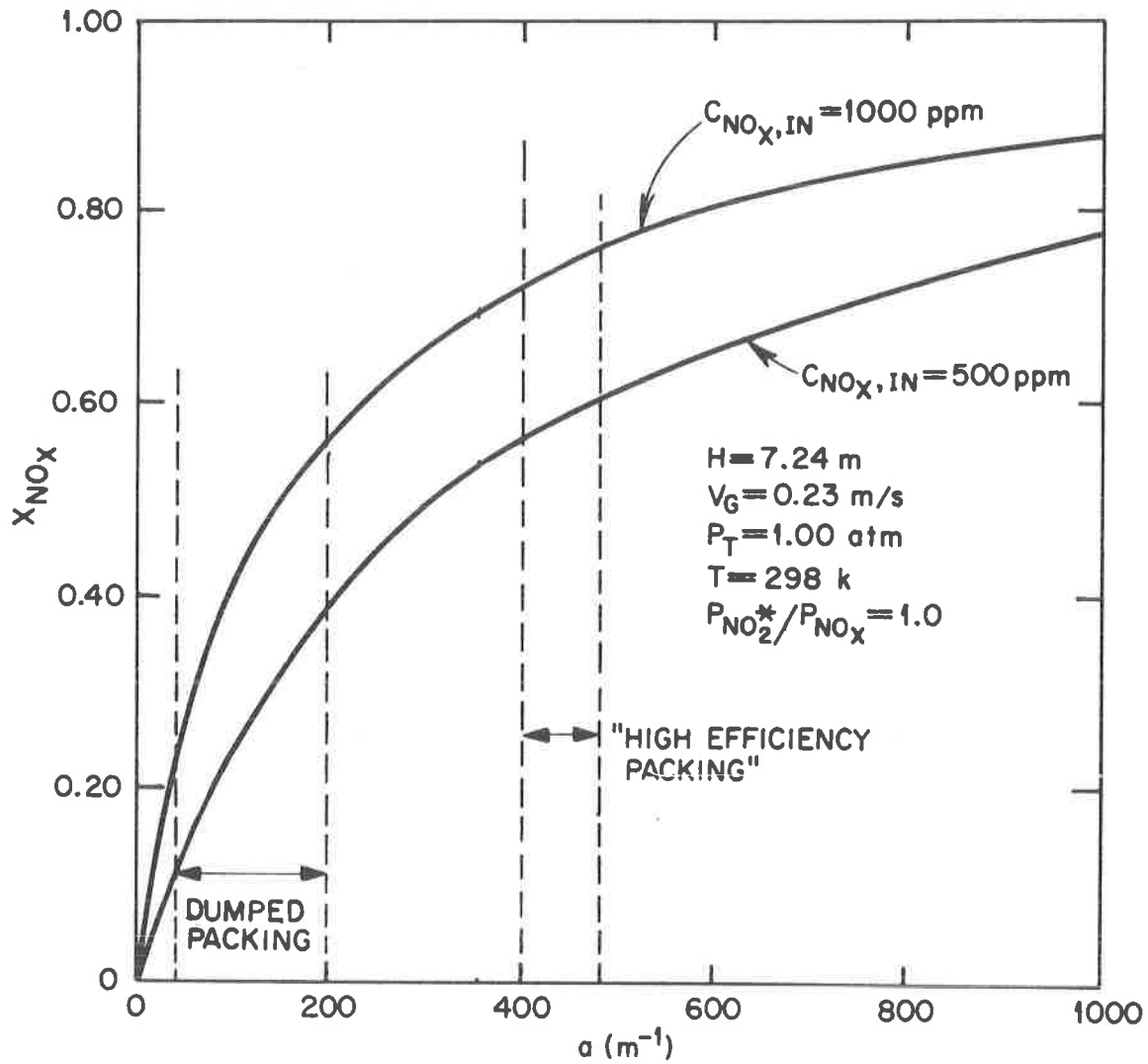
Fig. 7.   A projection of NO_x removal efficiencies at varying
gas-liquid interfacial values.

REFERENCES

1. Counce, R.M., and J.J. Perona; "Scrubbing of gaseous nitrogen oxides in packed towers," AIChE.J., 29; (1983).

2. Counce, R.M., and J.J. Perona, "A mathematical model for nitrogen oxide absorption in a sieve-plate column," Ind.Eng.Chem.Process Des.Dev., 19, 426 (1980).

3. Kongshaug, G., and G.Th. Medgdell, "Modelling of absorption efficiency in nitric acid manufacture," ISMA Technical Conference, Vienna (1980).

4. Zidov, B.A., A.S. Plygunov, V.I. Atrosh Chenko, M.M. Karaveav, G.A. Bochenko, G.A. Skvortson, A.G. Udovenko and A.L. Kontsevoi; "Calculating the efficiency of sieve trays in absorption of nitrogen oxides by aqueous nitric acid solutions;" The Soviet Chem.Ind. 6 (12; 768 (1974).

5. Hopfer, K. and I. Daycisagar, "Manufacture of nitric acid - recent advances in ammonia conversion efficiency and NO_x reduction[2];" Recent Advances in Inorganic Acids Industry (Lecture Series), (1978).

6. Niranjan, K., S.B. Sawant, S.B. Joshi and V.G. Pangarkar, "Counter-current absorption using wire gause packing," Chem.Engr.Sci. 37(3), 367 (1982).

7. Lefers, J.B., F.C. De Boko, C.M. Van den Bleek, and P.J. van den Berg, "The oxidation and absorption of nitrogen oxides in nitric acid in relation to the tail gas problem of nitric acid plants," Sixth International Symposium on Chemical Reaction Engineering (1980).

8. Abel, E., and H. Schmid, "Kinetics of nitrous acid I, introduction and survey," Z. Phys. Chem., 132, 55 (1928a), Translated from German (ORNL-tr-4263).

9. Abel, E., and H. Schmid, "Kinetics of nitrous acid II, orienting experiments," Z. Phys. Chem., 132, 64 (1928b), Translated from German (ORNL-tr-4263).

10. Abel, E., and H. Schmid, "Kinetics of nitrous acid III, kinetics of the decomposition of nitrous acid," Z. Phys. Chem., 134, 279 (1928c), Translated from German (ORNL-tr-4265).

11. Abel, E., and H. Schmid, "Kinetics of nitrous acid IV, equilibrium of nitrous acid-nitric oxide reaction in conjunction with its kinetics," Z. Phys., Chem., 136, 430 (1929, Translated from German (ORNL-tr-4265).

12. Makhotkin, A.F., and A.M. Shamsutdinov, "A study of the kinetics of the absorption of NO_2 and the effect of nitrous acid," Khim. Khim. Tekhn. XIX, 1411 (1976).

13. Komiyama, H., and H. Inoue, "Reaction and transport of nitrogen oxides in nitrous acid solutions," J. Chem. Engr. Japan, 11, 25 (1978).

14. Kaiser, E.W., and C.H. Wu, "A kinetic study of the gas-phase formation and decomposition reactions of nitrous acid," J. Phys. Chem., 81, 1701 (1977).

15. England, C. and W.H. Corcoran, "The rate and mechanism of the air oxidation of parts-per-million concentrations of nitric oxide in the presence of water vapor," Ind. Eng. Chem. Fundam., 14, 55 (1975).

16. Wayne, L. G., and D.M. Yost, "Kinetics of the gas-phase reaction between NO, NO_2 and H_2O," J.Chem. Phys., 19, 41 (1951).

17. Corriveau, C.E., Jr., The Absorption of N_2O_3 into Water, Master's Thesis in Chemical Engineering, University of California, Berkeley (1971).

18. Andrews, S.P., and D.Hanson, "The dynamics of nitrous gas absorption," Chem. Eng. Sci., 14, 105 (1961).

19. Hoftyzer, P.J., and F.J.G. Kwanten, "Absorption of nitrous gases," Processes for Air Pollution Control, CRC Press, Cleveland, Ohio, 165 (1972).

20. Carta, G., "Role of HNO_2 in the absorption of nitrogen oxides in alkaline solutions," Ind. Eng. Chem. Process Des. Dev. 23, 260 (1984).

21. Streit, G.E., and J.S. Wells, F.C. Fehsenfeld, and C.J. Howard, "A tunable diode laser study of the reactions of nitric and nitrous acids: $HNO_3 + NO$ and $HNO_2 + O_3$, J. Chem. Phys., 70, 3439 (1979).

22. Kaiser, E.W., and C.H. Wu, "Measurement of the Rate Constant of the Reaction of Nitrous Acid with Nitric Acid, J. Phys. Chem., 81, 187b (1977).

23. Carta, G., and R.L. Pigford, "Absorption of nitric oxide in nitric acid and water," Ind. Eng. Chem. Fundam., 22, 329 (1983).

24. Counce, R.M. and J.J. Perona, "Designing packed tower wet scrubbers - emphasis on nitrogen oxides," Handbook for Heat and Mass Transfer Operations, Gulf Publishing, West Orange, N.J. (In Press).

25. Bodenstein, M., "Formation and decomposition of higher nitric oxides, Z. Electrochem., 100, 68 (1922).

26. Verhoek, F.H., and F. Daniels, "The dissociation constant of nitrogen tetroxide and nitrogen trioxide," J. Am. Chem. Soc., 53, 1250 (1931).

27. Lee, Y.N., and S.E. Schwartz, "Reaction kinetics of nitrogen dioxide with liquid water at low partial pressure," J. Phys. Chem., 85,840 (1981).

Nomenclature

a gas-liquid interfacial area per unit volume of tower

C_i concentration of component i in bulk liquid

C_i^* concentration of component i at gas-liquid in interface

E enhancement factor

g gas

G superficial mass velocity

k_G gas-phase mass transfer coefficient

k_L liquid-phase mass transfer coefficient

ℓ liquid

P_i partial pressure of component i in bulk gas

P_i^* partial pressure of component i at gas-liquid interface

r_i reaction rate of component i per volume

R_i molar flux of component i

$R_{i,T}$ total molar flux of component i

Z height

ε fractional gas-volume in tower

ϕ as defined by Eqn (20)

NOx REMOVAL FROM NUCLEAR FUEL REPROCESSING PLANTS OFF GAS

BY CATALYTIC REDUCTION WITH NH3

S. Hattori*, Y. Kobayashi**, Y. Katoh***

Y. Takimoto**** and M. Kunikata*****

   * (Central Research Institute of Electric Power Industry)

  ** (Japan Nuclear Fuel Service Company, Ltd.)

 *** (Kure Research Laboratory, Babcock-Hitachi K.K.)

 **** (Kure Works, Babcock-Hitachi K.K.)

***** (Hitachi Works, Hitachi Ltd.)

Abstract

The selective reduction of NOx with NH_3 was investigated, using several kinds of titania catalysts and hydrogenmordenite (Hz, zeolite catalyst), as a basic study of the treatment of off gas generated in nuclear reprocessing plants, which was supposed to contain about 30 % of O_2 and a relatively large amount of NO_2.

N_2O was remarkably formed regardless of the types of catalysts when the NO_2/NOx ratio was higher than 0.5. On the other hand, N_2O was hardly formed when Hz and certain kinds of titania catalysts were used at NO_2/NOx ratios below 0.5. It has been concluded that these kinds of catalysts were suitable and that the NOx should be decomposed according to the following reaction :

$$NO + NO_2 + 2NH_3 \rightarrow 2N_2 + 3H_2O$$
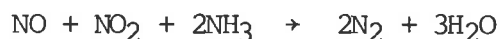
Therefore, it is effective to decompose NO_2 thermally to NO in the first step, to depress the formation of N_2O when the NO_2/NOx ratio of the gas to be treated is higher than 0.5. Hz has catalystic abilities not only to reduce N_2O with NH_3 but also to decompose NH_3, which means that a one reaction system of NOx removal can be carried out for NO_2 rich gases.

I   Introduction

For the past five or six years, some kinds of the dry process have been studied to remove NOx from off gas streams of nuclear fuel reprocessing plants. These systems have some advantages, because of their simplicity and rather small amounts of secondary radioactive wastes, to compare with liquid based methods (e.g. NOx removal by alkaline scrubbing).

This paper is devoted to a study of the elimination of NOx by selective reduction with NH_3, one of the dry process.

The features of the dissolver off gas and the main technical requirements of the NOx removal by selective reduction with NH_3 are as follows :

(1)   high NOx concentration and NO_2 rich in the composition of NOx
(2)   decomposition of the excess NH_3
(3)   no interference of NOx removal efficiency by iodine and moisture in off gas

Several kinds of catalysts were compared in order to elucidate these points under the same experimental conditions of NOx removal.

II   Experimental

1. Catalyst

The catalysts used for this experiment and their physical characteristics are shown in Table 1.   Commercial hydrogenmordenite (Hz : Zeolon 900 H, manufactured by Norton Chemical Company) was used because preferable experiment results were reported at the 15th DOE NUCLEAR AIR CLEANING CONFERENCE[1].   And titania catalysts (HC catalysts) were used because they had the merit of high NO removal efficiency at a lower operation temperature and endurance in the effluent gas treatment equipment of thermal power boiler plants.

2. Experiment equipment

The laboratory loop built to investigate the feasibility of the NOx removal by selective reduction with NH_3 is schematically shown in Figure 1.   The feeding part consists of rotameters and regulating valves for the carrier gas N_2, NO, NH_3 and interfering gas from cylinders.

NO_2 gas was prepared with NO + N_2 gas and O_2 gas at the NO oxidation vessel by the following reaction.

$$2NO + O_2 \rightarrow 2NO_2 \qquad\qquad (1)$$

The test loop has three reactor columns, therefore we are able to get three sets of experimental data at the same time and the same conditions.   The reactor column manufactured for this experiment is shown in Figure 2.

3. Experimental conditions

The outline of the experimental conditions are shown in Table 2.   Detailed conditions are shown in the data of each experimental result.

4. Measurement of catalyst activity

The definitions of the NOx removal efficiency, the NH_3 decomposition rate, the N_2O production rate and N_2O decrease rate are as follows.

$$\text{NOx removal efficiency (\%)} = \frac{(NO + NO_2)_{ent.} - (NO + NO_2)_{ext.}}{(NO + NO_2)_{ent.}} \times 100$$

$$NH_3 \text{ decomposition rate (\%)} = \frac{(NH_3)_{ent.} - (NH_3)_{ext.}}{(NH_3)_{ent.}} \times 100$$

$$N_2O \text{ production rate (\%)} = \frac{(N_2O)_{ext.}}{(NO + NO_2)_{ent.}} \times 100$$

$$N_2O \text{ decrease rate (\%)} = \frac{(N_2O)_{ent.} - (N_2O)_{ext.}}{(N_2O)_{ent.}} \times 100$$

Influent and effluent NOx concentration were measured with a calibrated chemiluminescence monitor and NH_3 with a calibrated infrared spectrometer. Effluent N_2O concentration was analyzed by the infrared spectrometer with a special long gas cell (1 m length).

III   Result and discussion

1.   Preliminary study of NO_2 removal

N_2O was observed as a secondary product when the NO_2 removal experiment was carried out in the condition where the NO_2/NOx ratio was 0.8. The experiment was done to investigate the condition of N_2O production and the results are shown in Figure 3, which gives the relation between the NOx and N_2O production rate and the temperature.
The results are summarized as follows :

(a)   All catalysts produced N_2O as a secondary product.

(b)   The order of N_2O quantity produced in high NOx removal efficiency over 90 % is ;

$$Hz \text{ catalyst} \simeq HC - 103S < HC - 101S$$

On the other hand, Figure 4 also shows the results in the condition where the NO_2/NOx ratio is 0.3. And the results are summarized as follows :

(a)   HC catalysts produced N_2O as a secondary product but the N_2O production rate with HC-103S was low at under 350 °C, as compared with HC-101S catalyst.

(b) N_2O formation was suppressed in the case of the Hz catalyst.

The remarkable formation of N_2O was observed when NO_2 rich gases were treated directly by selective reduction with NH_3, but high efficiency of NOx removal without N_2O remarkable formation could be obtained when using HC-103S catalyst below 300 °C or Hz over 450 °C at a NO_2/NOx ratio of below 0.5.

2. Study of the method of suppression of N_2O formation

(1) Suppression of N_2O formation by the control of NO_2/NOx ratio

The N_2O formation mechanism from experimental results of NOx removal by selective reduction with NH_3 and NH_3 decomposition by oxidation is supposed as the following :

$$2NH_3 + 2NO_2 \rightarrow N_2 + 3H_2O + N_2O \qquad (5)$$
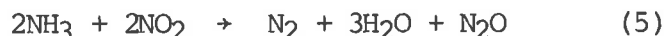
And, the reaction formula is supposed as the following, in a condition of NO and NO_2 coexistence.

$$2NH_3 + NO_2 \rightarrow 2NH_2 + NO + H_2O \qquad (6)$$

$$2NH_2 + 2NO \rightarrow 2N_2 + 2H_2O \qquad (7)$$
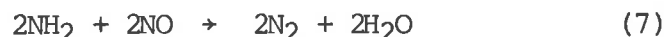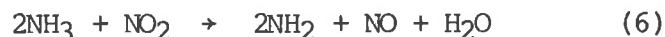
as a summary, the following formula can be derived.

$$2NH_3 + NO_2 + NO \rightarrow 2N_2 + 3H_2O \qquad (8)$$

In the view of the chemical reaction formula described above, it can be suggested, equation (8) shows that NOx can be converted to N_2 under the condition of

$$NO_2 : NO = 1 : 1 \quad (NO_2/NOx = 0.5)$$

Equation (6) can be assumed to progress, because the ability of NH_3 oxidization by NO_2 is stronger than by oxygen.

Also, if NO is exceeded, equation (9) may be predominant. Consequently, N_2O formation can be suppressed if the NO_2/NOx ratio is below 0.5.

$$4NH_3 + 4NO + O_2 \rightarrow 4N_2 + 6H_2O \qquad (9)$$

Figure 5 shows the result of the influence of NO_2/NOx ratio on the NOx removal efficiency and N_2O formation rate. N_2O was formed with a NO_2/NOx ratio over 0.5, but it was not observed where the NO_2/NOx ratio is below 0.5.

(2) Suppression of N_2O formation by the "double step method"

Studies were attempted to investigate the "double step method" where NO_2 is thermally converted into NO in the first step, and then NO is removed in the second step. Because it is clear that N_2O formation is suppressed at a NO_2/NOx ratio of below 0.5.

Equipment used in this experiment is designed so that NO_2 rich gas in feed flows into firstly a convertor, NO_2 is converted into NO, secondly NO rich gas is treated at the reaction of NOx removal by NH_3 addition. Figure 6 shows the result of NOx removal by the double step method. High NOx removal activity could be obtained in the condition of SV 50,000h^{-1} at 250 – 300 °C operated for the HC-103S catalyst, and at over 450 °C for the H_Z catalyst.

It may be suggested that the double step method is effective for NO_2 removal by selective reduction with NH_3.

3. Selection of suitable catalyst

On the basis of the NO_2 removal experiment, it is suggested that there is a capability of NOx removal without N_2O production in case of a NO_2 rich gas. I.e., it is effective to decompose NO_2 thermally to NO in the first step, and to depress the formation of N_2O when the NO_2/NOx ratio of the gas to be treated is higher than 0.5. Therefore, we investigated the catalytic thermal decomposition system of NO_2 firstly, and the influence of the NH_3/NOx mole ratio, moisture concentration and iodine interference.

(1) Catalyst of NO_2 thermal decomposition

Figure 7 shows the NO_2 thermal decomposition activity of catalysts and it can be seen that HC-110S has a higher activity, in case of SV 100,000h^{-1}.

(2) Influence of NH_3/NOx and NO_2/NOx ratio on NOx removal efficiency.

It is important to investigate the relation between the NH_3/NOx and NO_2/NOx ratios and NOx removal efficiency, in order to study the stoichiometry and chemism of this reaction. Setting up of the NH_3/NOx ratio is also important in designing the process system.

Figure 8 and 9 show the relation between the NH_3/NOx ratio removal efficiency and N_2O production rate for each catalyst. It may be concluded that N_2O can be controlled under the condition of NO_2/NOx ratio below 0.5 by using the HC-103S or Hz catalyst, and at the same time, NOx and NH_3 can be reacted by stoichiometry (1 : 1 reation).

(3) Influence of coexistence impurities

Moisture

In case of the NOx removal reaction for HC-103S and Hz catalysts, moisture does not affect the NOx removal efficiency at the condition of NO_2/NOx ratio about 0.5 where the highest NOx removal efficiency can be obtained. On the other hand, NH_3 decomposition rate has a tendency to go down proportionately· as moisture concentration increases.

Iodine

Iodine has no effect on either the NOx removal or NO_2 thermal decomposition activity at the condition where it is fed in 100 ppm for each catalyst. Also 0.01 % or less iodine was measured on and in the catalysts after the experiments, therefore minimal accumulation occurs on the catalysts.

(4) Selection of suitable catalyst

It is concluded that HC-110S was suitable for the single step and the HC-103S or Hz catalyst suitable for the double step, when the NO_2/NOx ratio of the gas to be treated was higher than 0.5.

4. Most suitable operation conditions of the double step method of NOx removal

Experiments were planned in order to survey the most suitable operation conditions of the double step method of NOx removal system. The results obtained are shown in Table 3. If we select the most suitable operation conditions summarized in Table 3, we can get NOx removal efficiency $\geq$ 99 %, effluent NH_3 < 10 ppm and a secondary product N_2O < a few ppm. However, the difference between the HC-103S and Hz catalyst is that the former needs strict control of the NH_3/NOx mole ratio = 1, while the latter needs a less severe 1.4 because the excess NH_3 is oxidized and decomposed by the Hz catalyst.

5. Study of N_2O reduction with NH_3 and the single step method of NOx removal

    (1) N_2O reduction with NH_3

        Experiments were planned to survey the N_2O reduction with NH_3 by HC catalysts and the Hz catalyst. The results are shown in Figure 10. It is clear that the HC catalyst produced much more N_2O than the Hz catalyst, and also the NOx production rate by the former catalyst is higher than the latter.

        It is considered that this is the reason why in the Hz catalyst case, N_2O was reduced with NH_3 in the air by the following formula

$$3N_2O + 2NH_3 \rightarrow 4N_2 + 3H_2O \qquad (10)$$
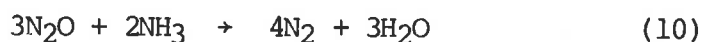
however in the HC catalyst, the NH_3 oxidation by oxygen proceeded preferentialy.

        On the basis of these results, the experiments of the N_2O reduction with NH_3 of the Hz catalyst were carried out in detail

        Figure 11 shows the results that N_2O reduction rate by NH_3 gets to more than 95 % almost no formation of NOx when the NH_3/NOx ratio is over 2.0 and SV is $10{,}000h^{-1}$.

    (2) Single step method of NOx removal

        It is important that the results of the N_2O reduction experiment with NH_3 indicate the applicability of direct elimination of NO_2 by selective reduction with NH_3.

        In other words, the direct elimination mechanism is considered at the Hz catalyst as follows :
        The reaction at the top of the catalyst bed

$$2NH_3 + 2NO_2 \rightarrow N_2 + 3H_2O + N_2O \qquad (5)$$
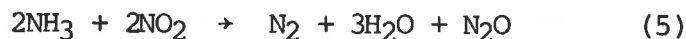
the reaction at the bottom of the catalyst bed

$$3N_2O + 2NH_3 \rightarrow 4N_2 + 3H_2O \qquad (11)$$
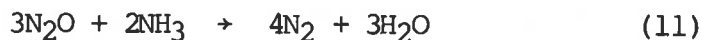
        The experiment was done to confirm the above mechanism with parameters of SV and NH_3/NOx mole ratio.

        The results are shown in Figure 12 and 13 as follows :

(a) Although SV is controlled low, N_2O was detected in the effluent gas in case of NH_3/NOx mole ratio 1.4 and NO_2/NOx 0.95 at the entrance of the catalyst bed, however, no NH_3 was found. This means that more NH_3 is required for the N_2O direct reduction with NH_3.

(b) A secondary product N_2O is decreased in a few ppm and only 5 ppm of NH_3 is contained in the effluent gas in spite of NO_2/NOx 0.95 at the entrance of the catalyst bed, if we select the operation condiitons, SV $3,000h^{-1}$, reaction temperature 475 °C and $NH_3/NOx \geq 1.6$.

<u>IV   Conclusion and summary</u>

From this series of experiments, it may be concluded as follows.

(1) A secondary product, N_2O, was observed when NO_2 was removed by selective reduction with NH_3 in case of a high NO_2 mole ratio in NOx. We find that N_2O production is decreased if we select the NO_2/NOx mole ratio ≤ 0.5 and the catalyst HC-103S or Hz.

(2) In order to set up the NO_2/NOx mole ratio ≤ 0.5 in feed gas before the NOx removal stage, we select a preferable catalyst, HC-110S, which decomposes NO_2 to NO thermally at 475 °C.

(3) Moisture had a almost no effect on either the NOx elimination activity at the condition NO_2/NOx about 0.5 or NO_2 thermal decomposition.

(4) Also iodine had no effect on either the NOx elimination acitivity or NO_2 thermal decomposition, and iodine was not detected in the catalyst used in the experiment.

(5) The most suitable operation conditions selected were : temperature 250 °C, NH_3/NOx ratio 1.0, NO_2/NOx ratio below 0.5 and SV 10,000 h^{-1} for the HC-103S catalyst, and 475 °C, NH_3/NOx 1.4 for the Hz catalyst.

(6) The Hz catalyst had activity of N_2O reduction with NH_3, and of direct elimination of NO_2 by selective reduction with excess NH_3.

Removal efficiency of 99 % and a few ppm of N_2O secondary product were obtained and NH_3 poured within 5 ppm by the single step NOx removal system at the operation conditions of SV 3,000 h^{-1}, temperature 475 °C and NH3/ NOx ≥ 1.6.

Acknowledgement

Authors wish to express their thanks to T. Yamaguchi , S. Yamada and R. Itoh of Japan Nuclear Fuel Service for their continuing guidance and valuable discussions.

References

(1) A. Bruggeman, L. Meynendonckx, W.R.A. Goossens, "ELIMINATION OF NOx BY SELECTIVE REDUCTION WITH NH_3", 15th DOE NUCLAR AIR CLEANING CONFERENCE (1978).

(2) H.D. Ringel, H. Barnet-Wiemer et al, "CONDITIONING OF REPROCESSING DISSOLVER OFFGAS PRIOR TO KR-RETENTION BY CRYOGENIC DISTILLATION", 16th DOE NUCLEAR AIR CLEANING CONFERENCE (1980).

(3) E. Henrich, R. Hufner et al, "I-129, Kr-85, C-14 AND NOx REMOVAL FROM SPENT FUEL DISSOLVER OFF-GAS AT ATOMOSPHERIC PRESSURE AND AT REDUCED OFF-GAS FLOW", 16th DOE NUCLEAR AIR CLEANING CONFERENCE (1980).

(4) D.T. Pence, "CRITICAL REVIEW OF NOBLE GAS TREATMENT SYSTEMS", 16th DOE NUCLEAR AIR CLEANING CONFERENCE (1980).

Table. I   List of catalysts used in experiment

NO.	Catalyst name	a classification of manufacture method		properties of material						Development object			Remark
		Pushing out	Impregnation	grain size (mm)	bulk specific gravity (g/cm³)	packed specific gravity (kg/l)	Pressure strength (kg)	specific surface area (m²/g)	pore surface area (ml/g)	NOx removal	NO₂ decomposition	NH₃ decomposition	
1	Hydrogen-Mordenite	○		1.6	—	0.73	—	36.1	0.234	◎		△	
2	HC-101S		○	5.1	1.65	1.04	6.5	29.4	0.346	◎		△	
3	HC-103S		○	4.9	1.65	1.04	7.5	27.3	0.329	◎		△	
4	HC-106S		○	5.1	1.69	1.04	9.5	28.3	0.320	◎			
5	HC-110S		○	4.9	1.63	1.04	6.8	31.2	0.321		◎		

◎ ; main object

△ ; experiment for other object

Table 2 Experimental Conditions

NO	Experiment item	Experimental conditions
1	NOx removal reaction	1) NOx concentration : 2,500ppm 2) Reaction temp. : 200~500°C 3) S V (space velocity) : ~100,000h^{-1}
2	NO$_2$ decomposition reaction	1) NOx concentration : 2,500ppm 2) NO$_2$/NOx mole ratio : ~0.9 3) Reaction temp. : 300~500°C
3	NH$_3$ decomposition reaction	1) NH$_3$ concentration : 2,500ppm 2) Reaction temp. : 200~250°C
4	N$_2$O decomposition reaction	1) N$_2$O concentration : 1,000ppm 2) Reaction temp. : 300~500°C
5	Influence of moisture	1) Moisture concentration : 0~3%
6	Influence of Iodine	1) Iodine concentration : 100~120 ppm

Table 3. Most suitable operation conditions

conditions	catalysts	
	HC-103S	H z
reaction temperature (°C)	250	475 (400~500)
NH$_3$/NOx ratio	1.0	1.4
S V (h^{-1})	<10,000	<10,000
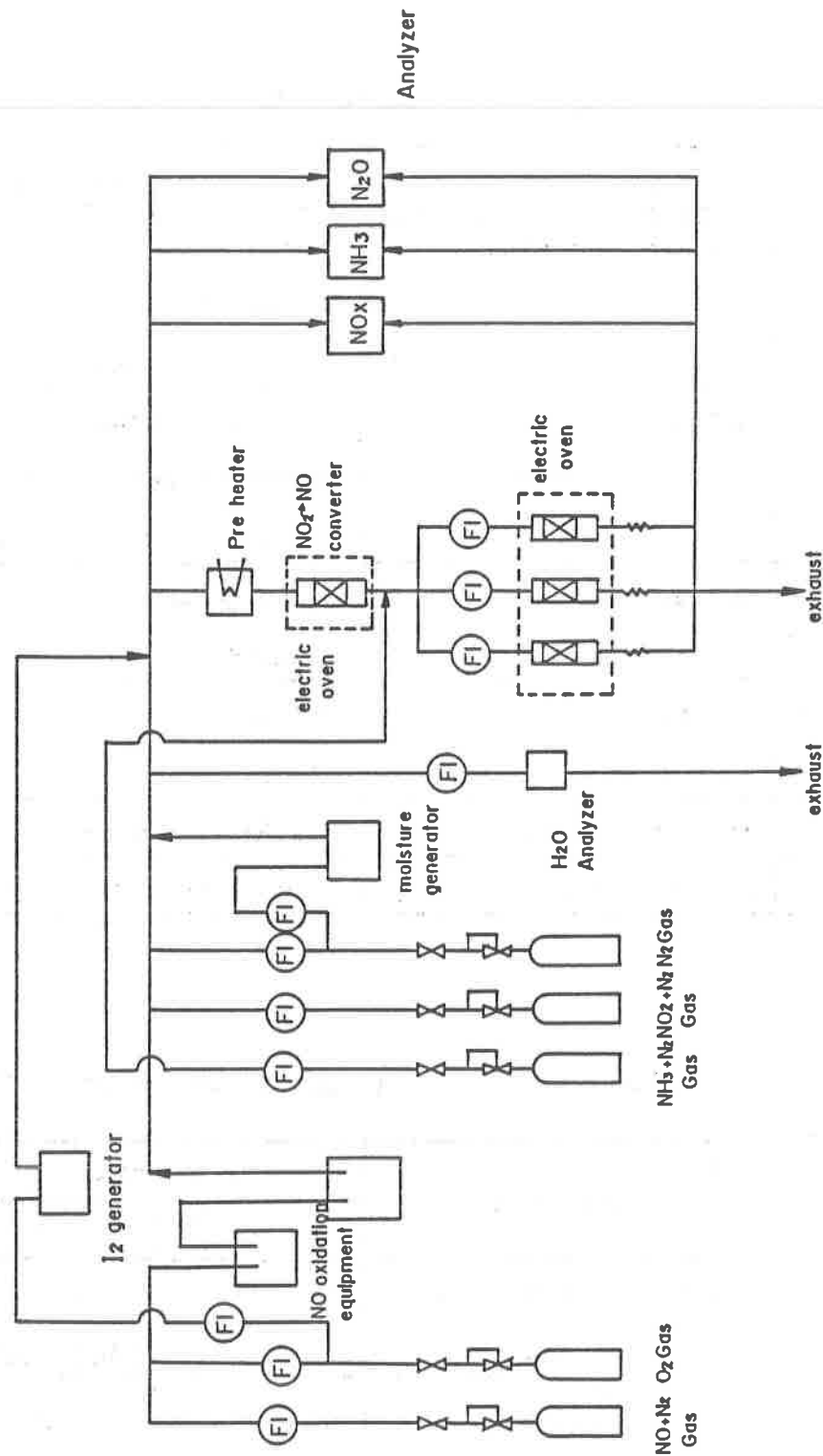
Fig. 1   NOx removal experimental equipment
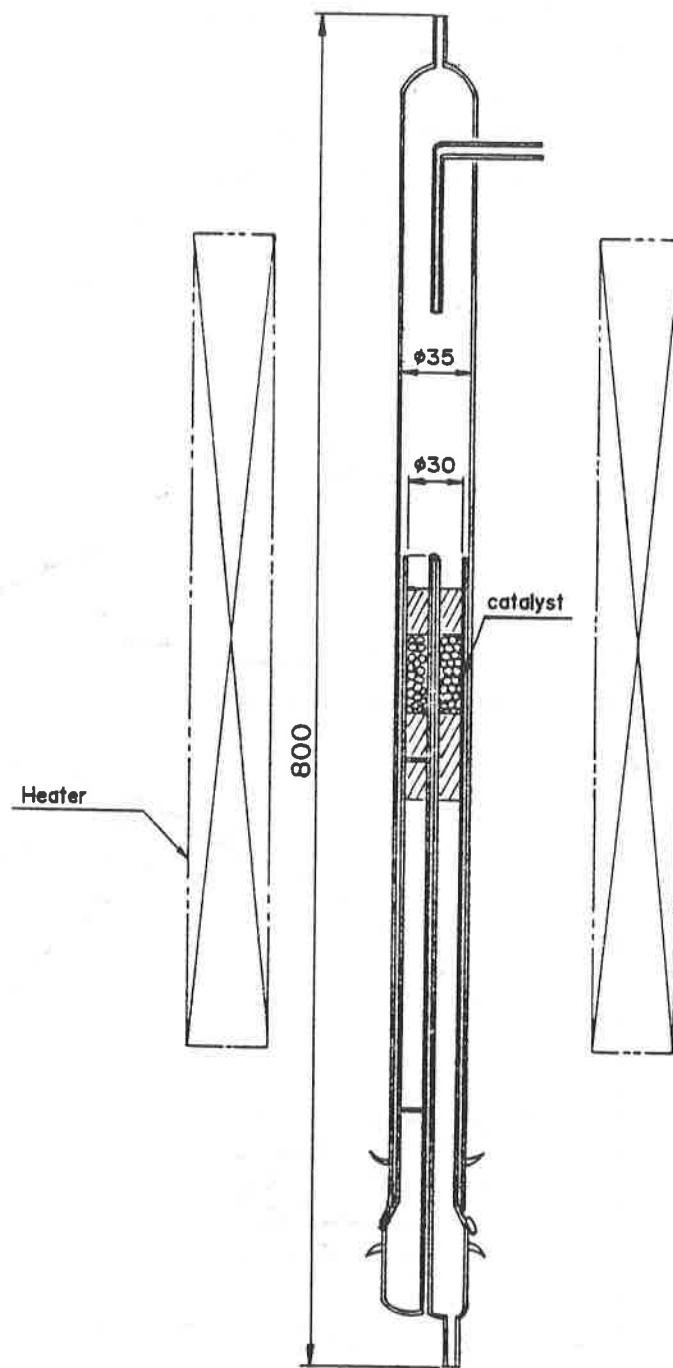
Fig. 2   Reactor column

Experimental condition

(1)	grain size of catalyst	: 10~20mesh	(6)	gas composition
(2)	catalyst volume	: 2.4ml		NOx : 2,500ppm
(3)	diameter of reactor	: 18ϕ		NH$_3$: 3,250ppm
(4)	gas flow rate	: 4ℓ/min		O$_2$: 30%
(5)	S V	: 100,000h^{-1}		H$_2$O : 2%
				N$_2$: balance

Fig. 3   NOx removal efficiency and N$_2$O production rate at NO$_2$-NH$_3$ system   (high NO$_2$ concentration)

Experimental condition

(1) grain size of catalyst : 10~20mesh

(2) catalyst volume   : 2.4ml

(3) diameter of reactor : 18ϕ

(4) gas flow rate   : 4l/min

(5)   S V   : 100,000h^{-1}

(6) gas composition

   NOx : 2,500ppm

   NH$_3$: 3,250ppm

   O$_2$: 30%

   H$_2$O :   2%

   N$_2$: balance
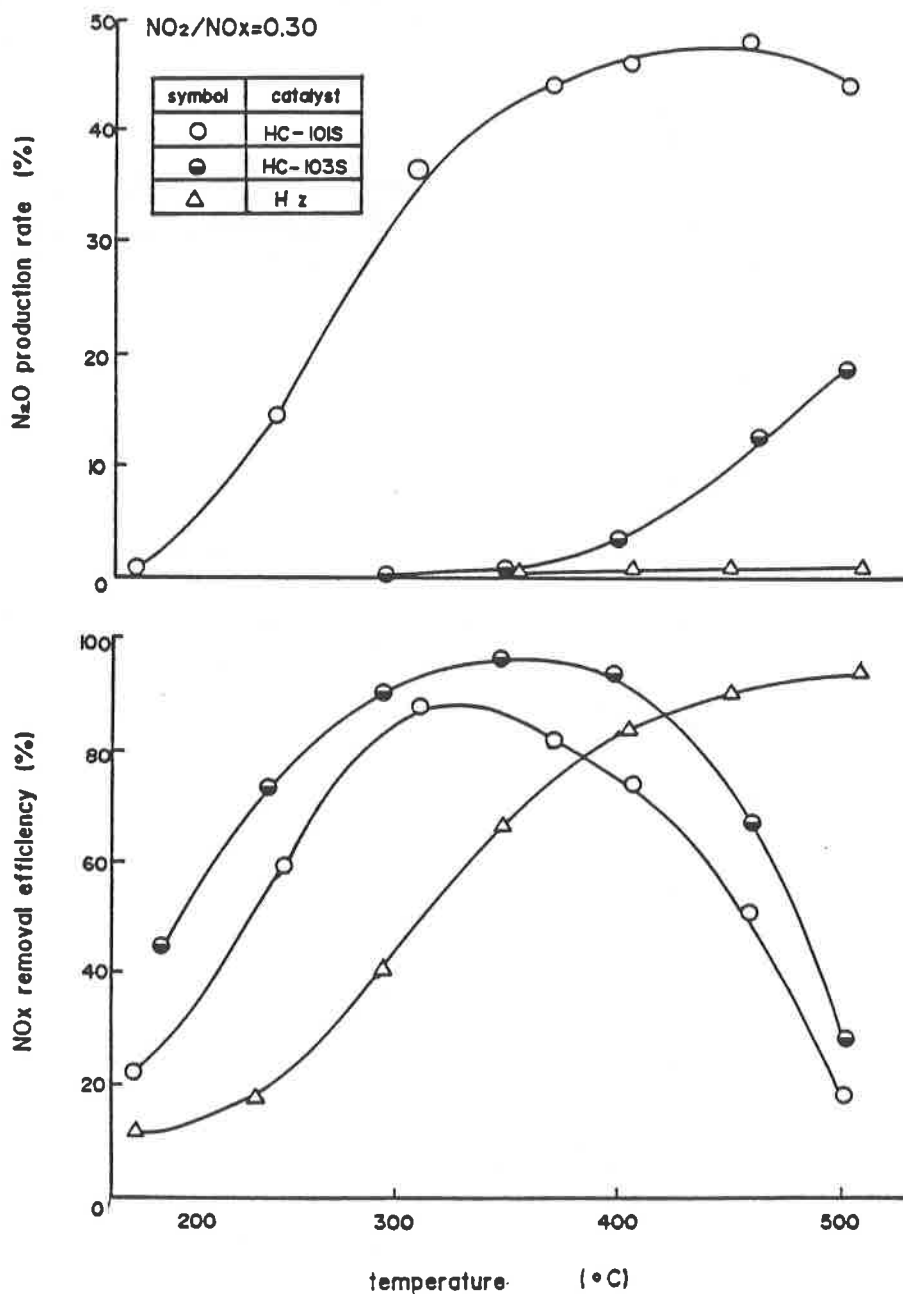
Fig. 4   NOx removal efficiency and N$_2$O production rate at NO$_2$-NH$_3$ system (high NO concentration)

Experimental condition

(1) grain size of catalyst : 10~20mesh
(2) catalyst volume : 4.8ml
(3) diameter of reactor : 18φ
(4) gas flow rate : 4ℓ/min
(5) S V : 50,000h^{-1}

(6) gas composition

NOx : 2,500ppm
NH$_3$: 3,000ppm
O$_2$: 30%
H$_2$O : 2%
N$_2$: balance

symbol	catalyst	experimental temperature (°C)
●	HC–103S	250
△	H z	475
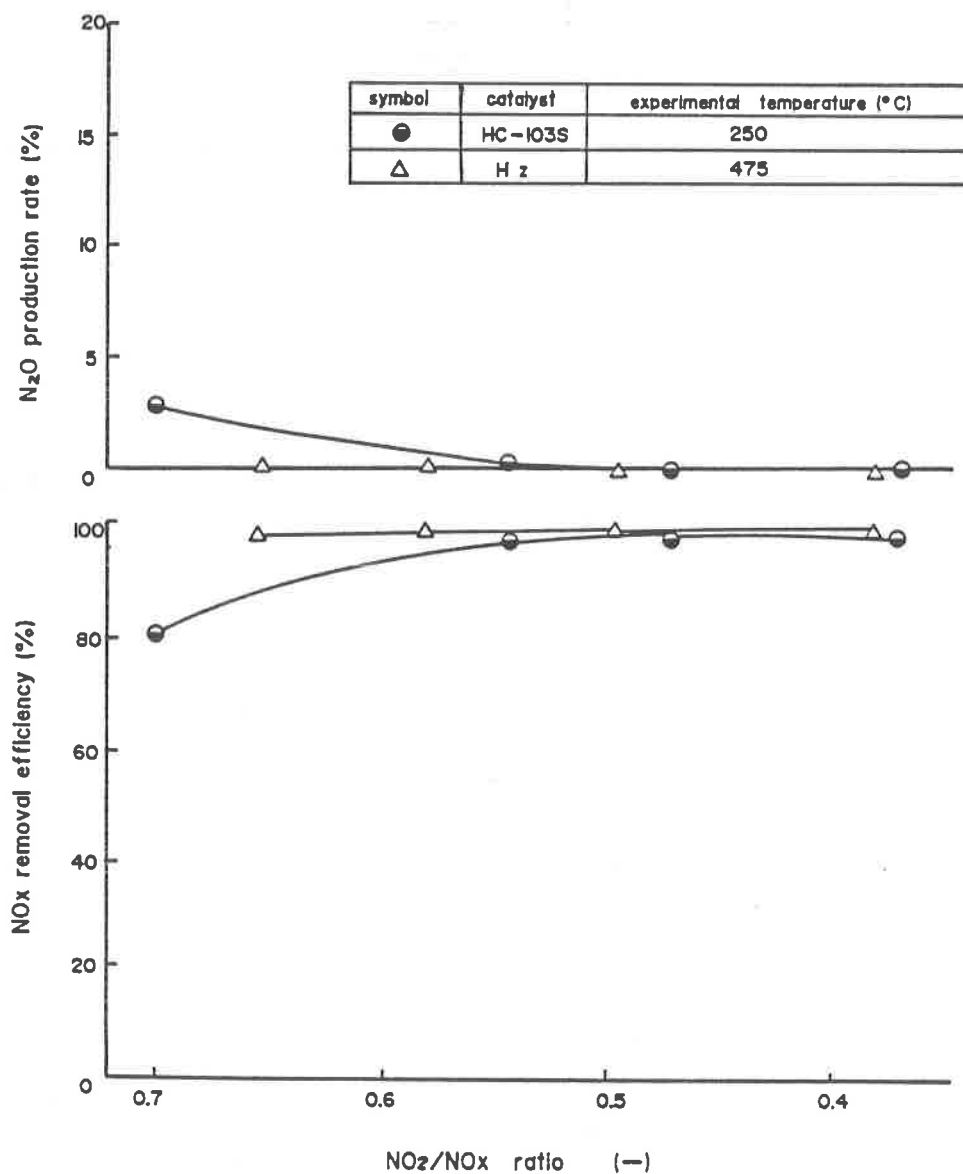
Fig. 5   Relation between NOx removal efficiency, N$_2$O production rate and NO$_2$/NOx ratio
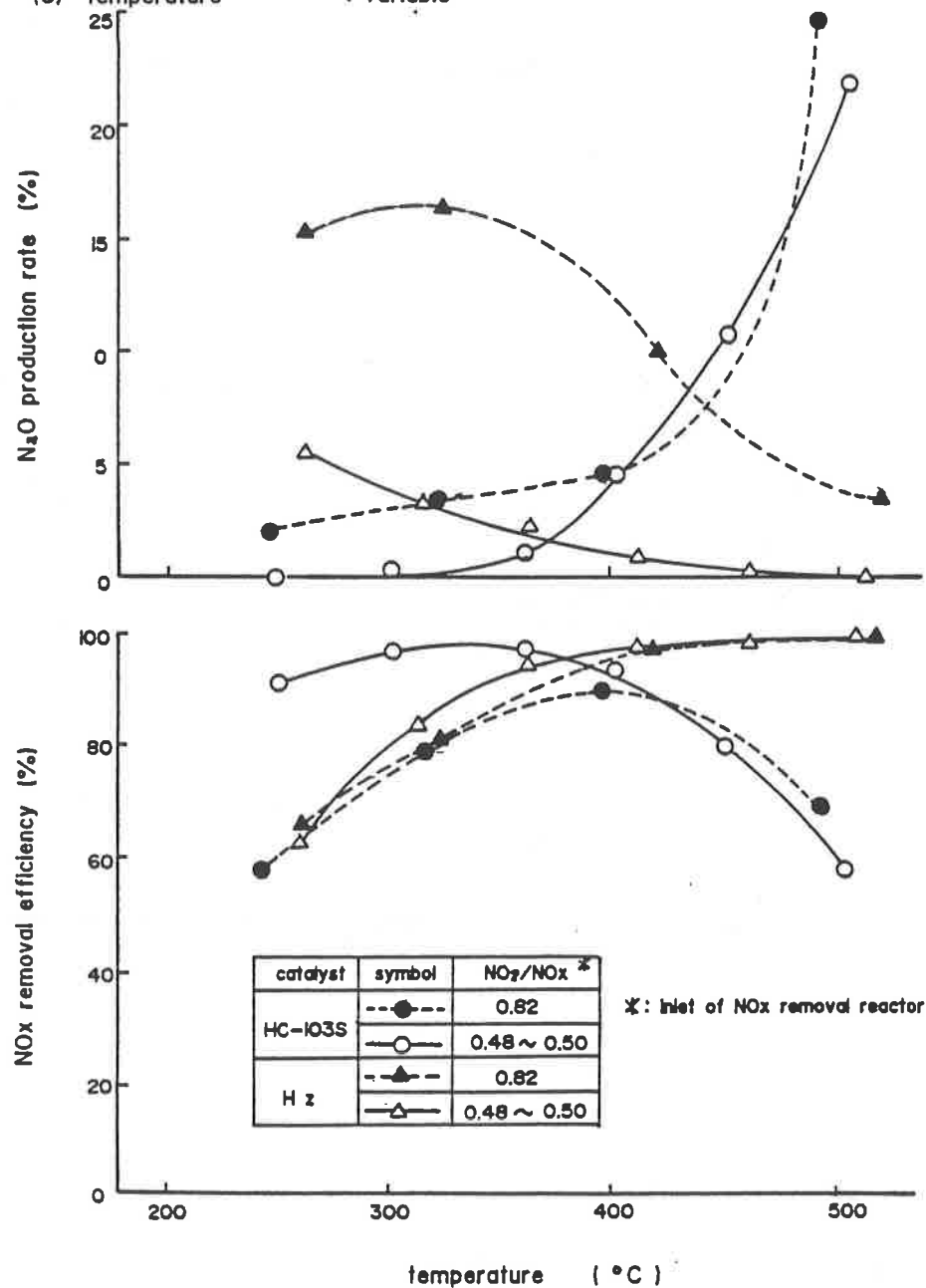
Fig. 6   Experimental result of NOx removal by double step method

Experimental condition

(1) grain size of catalyst: 10~20mesh

(2) catalyst volume : 24ml

(3) gas flow rate : 4ℓ/min

(4) S V : 100,000h^{-1}

(5) gas composition

NOx : 2,500ppm

O_2 : 30%

H_2O : 2%

N_2 : balance
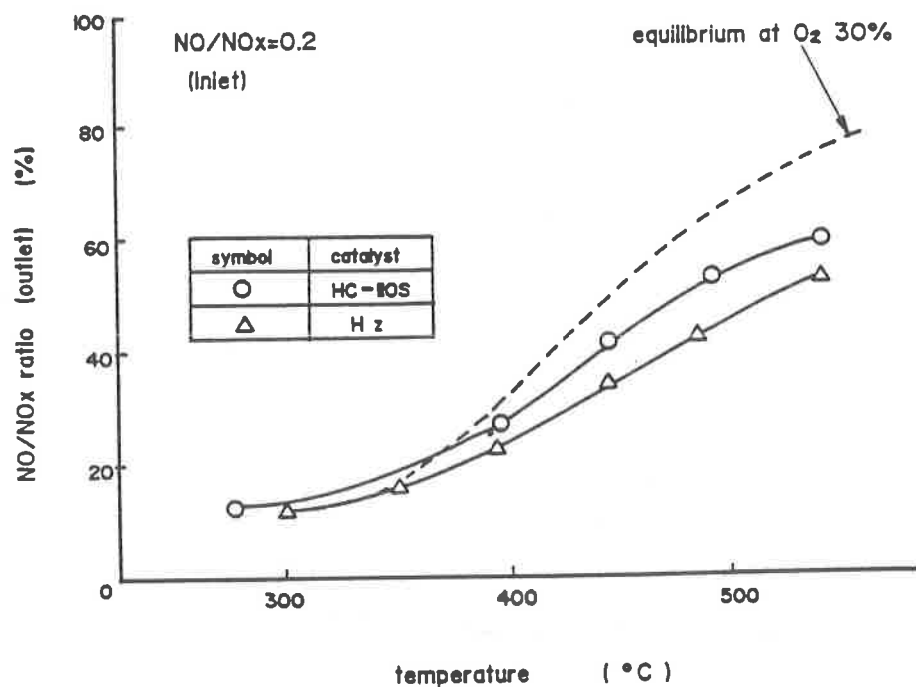
Fig. 7 NO_2 thermal decomposition activity by catalysts

Experimental condition

(1) grain size of catalyst: 10~20mesh
(2) catalyst volume   : 4.8ml
(3) diameter of reactor : 18φ
(4) gas flow rate   : 4ℓ/min
(5)   S   V   : 50,000h⁻
(6) temperature   :   250°C

(7) gas composition
    NOx : 2,500ppm
    NH₃ : variable
    O₂   : 30%
    H₂O : 2%
    N₂   : balance

catalyst	symbol	NO₂/NOx *	*: inlet
	○	0.96 ~ 0.97	
HC 103S	▲	0.75 ~ 0.76	
	□	0.49 ~ 0.51	
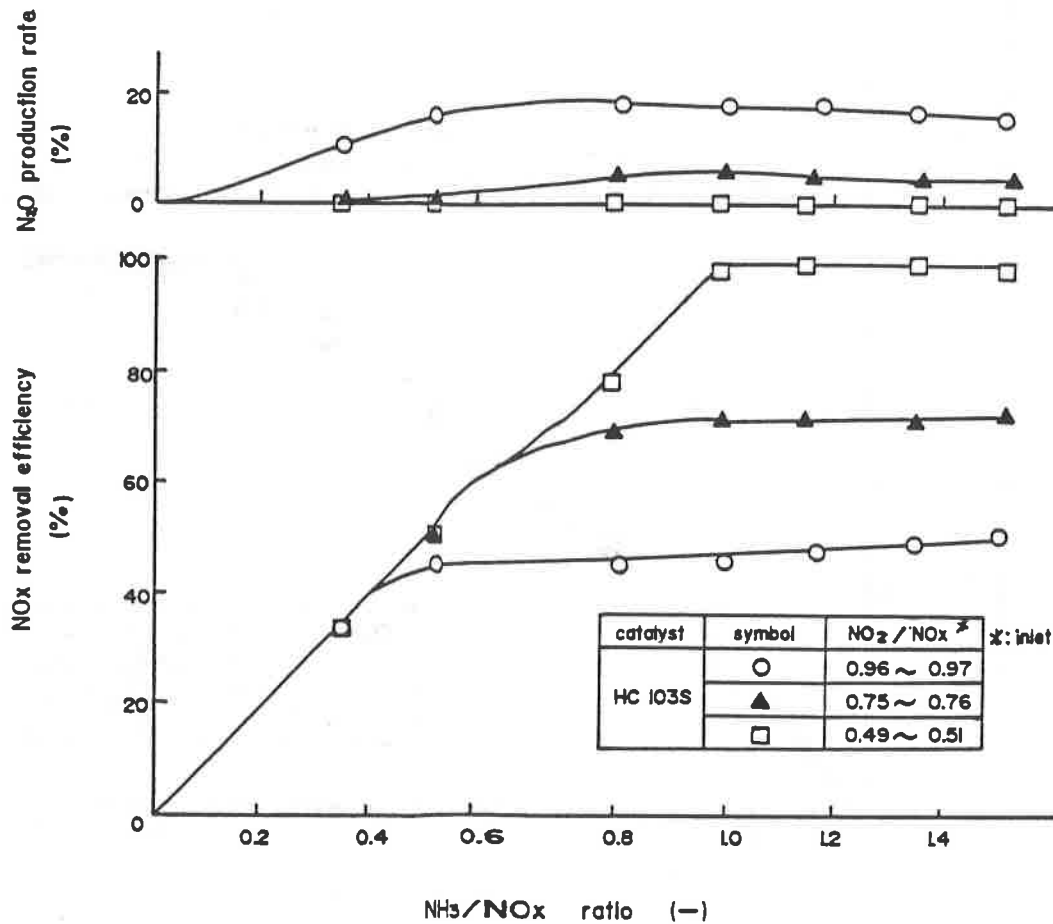
Fig. 8 Relation between NOx removal efficiency, N₂O production rate and NH₃/NOx ratio   (HC-103S)

Experimental condition

(1)	grain size of catalyst:	10~20mesh
(2)	catalyst volume	: 4.8ml
(3)	diameter of reactor	: 18ϕ
(4)	gas flow rate	: 4ℓ/min
(5)	S V	: 50,000h^{-1}
(6)	temperature	: 475°C

(7) gas composition

NOx	:	2,500ppm
NH$_3$	:	variable
O$_2$	:	30%
H$_2$O	:	2%
N$_2$	:	balance

catalyst	symbol	NO$_2$/NOx ^{x}	x: inlet
H z	O	0.96~0.97	
	▲	0.75~0.76	
	□	0.49~0.51	

Fig. 9   Relation between NOx removal efficiency, N$_2$O production
rate and NH$_3$/NOx ratio (Hz catalyst)
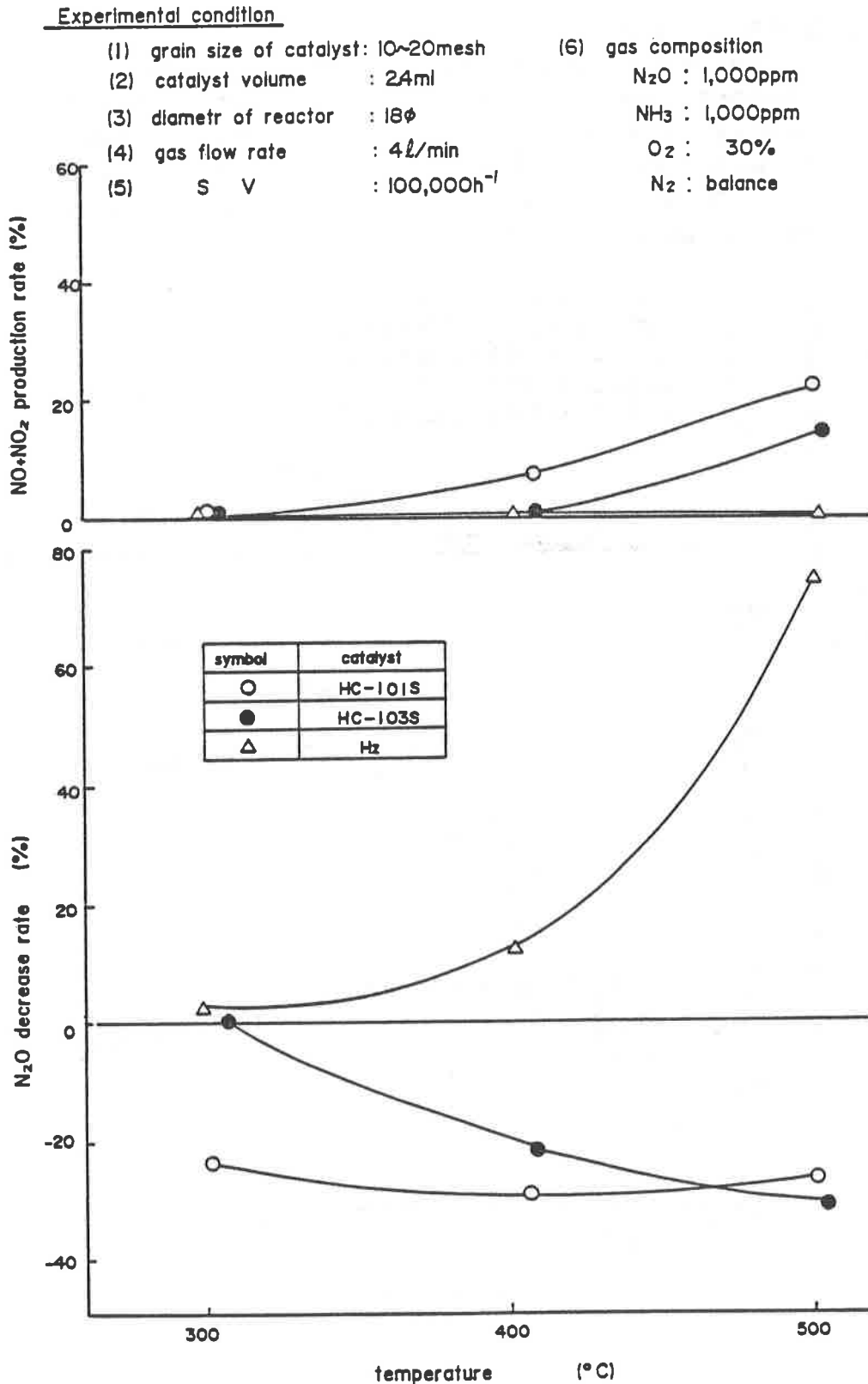
Fig. 10 N₂O reduction activity by NH₃ and NOx production

Experimental condition

(1) grain size of catalyst: 10~20mesh
(2) catalyst volume   : variable
(3) diameter of reactor : 18ϕ
(4) gas flow rate   : 4 ℓ/min
(5)   S V   : variable
(6)   temperature   : 475°C

(7) gas composition

N_2O : 1000ppm
NH_3 : variable
O_2 :   30%
N_2 : balance

symbol	S V	catalyst volume
○	10,000 h⁻¹	24ml
▲	50,000 h⁻¹	4.8ml
□	100,000 h⁻¹	2.4ml
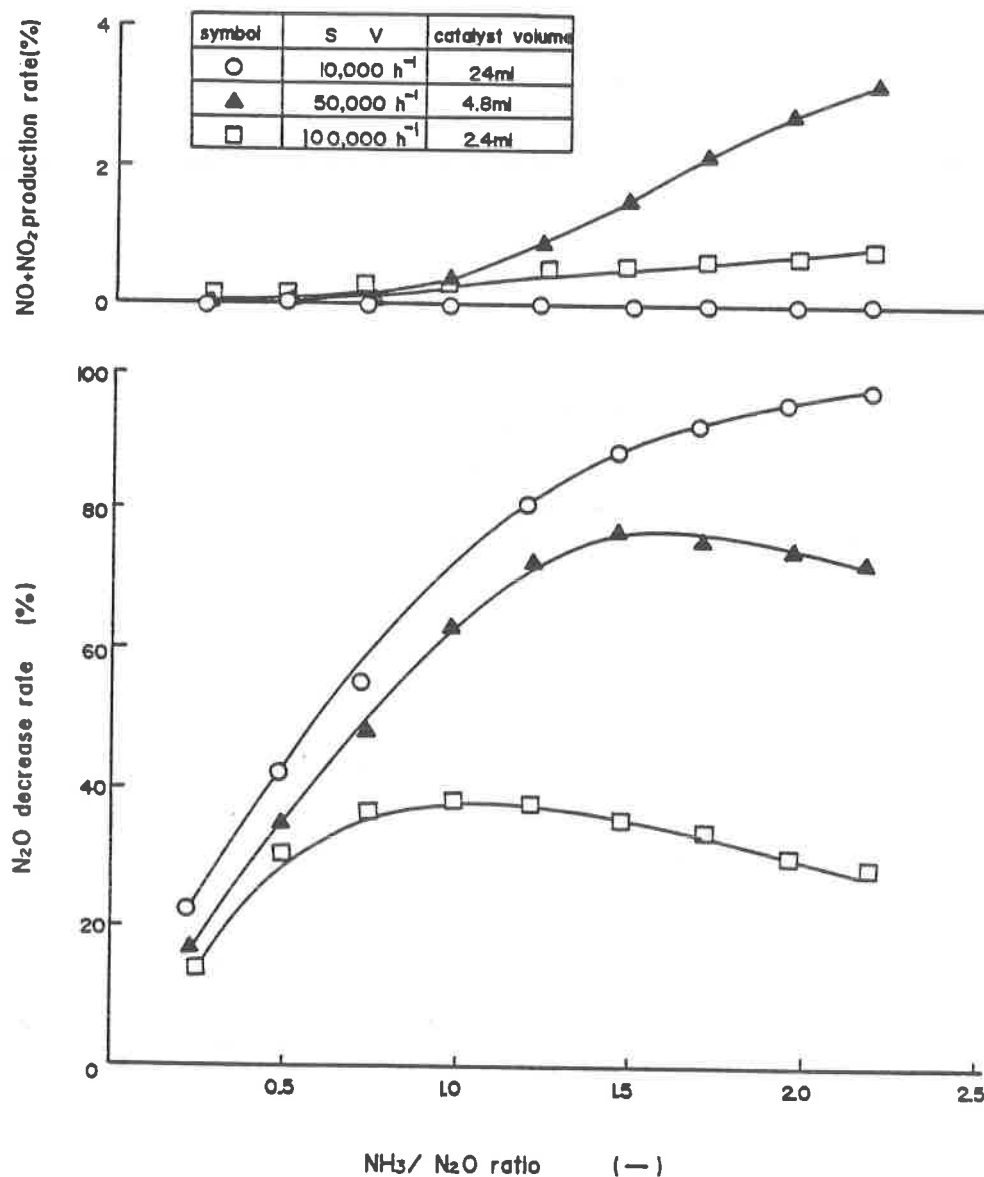
Fig. 11   Influence of NH₃/N₂O ratio on N₂O reduction activity
      (Hz catalyst)

1280

Experimental condition

(1)	grain size of catalyst:	10~20mesh	(6)	gas composition	
(2)	catalyst volume	: variable		NOx :	2,500ppm
(3)	diameter of reactor	: 1830φ		NO_2/NOx :	0.95
(4)	gas flow rate	: 4l/ml		NH_3/NOx :	variable
(5)	temperature	: 475°C		O_2 :	30%
				H_2O :	2%
				N_2 :	balance
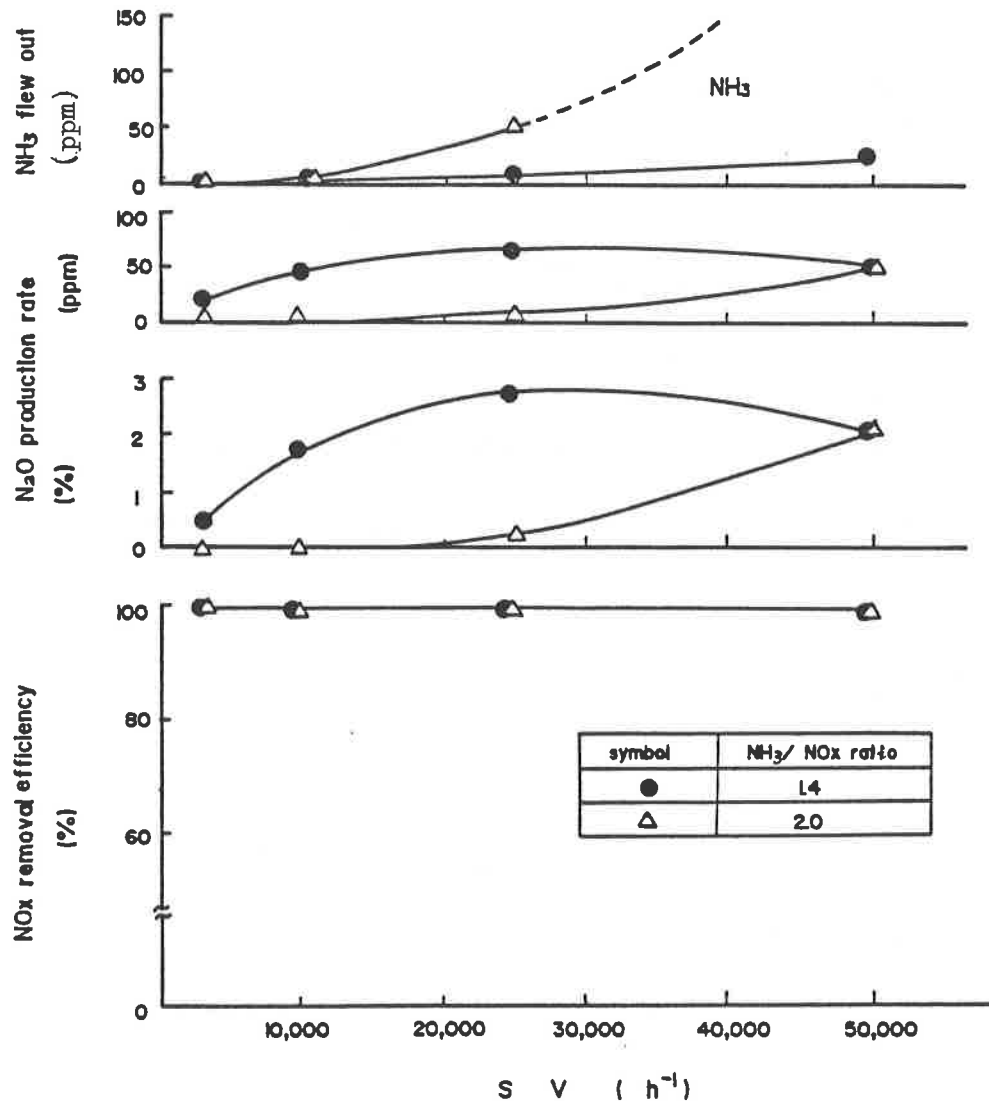
Fig. 12   Relation between NOx removal efficiency and SV
(Hz catalyst, single step method)

Experimental condition

(1) grain size of catalyst: 10~20mesh   (6) gas composition

(2) catalyst volume   : 80ml   NOx   : 2500ppm

(3) gas flow rate   : 4ℓ/min   NO$_2$/NOx : 0.95

(4)   S V   : 3000h^{-1} NH$_3$/NOx : variable

(5)   temperature   : 475°C   O$_2$: 30%

                                       N$_2$: balance
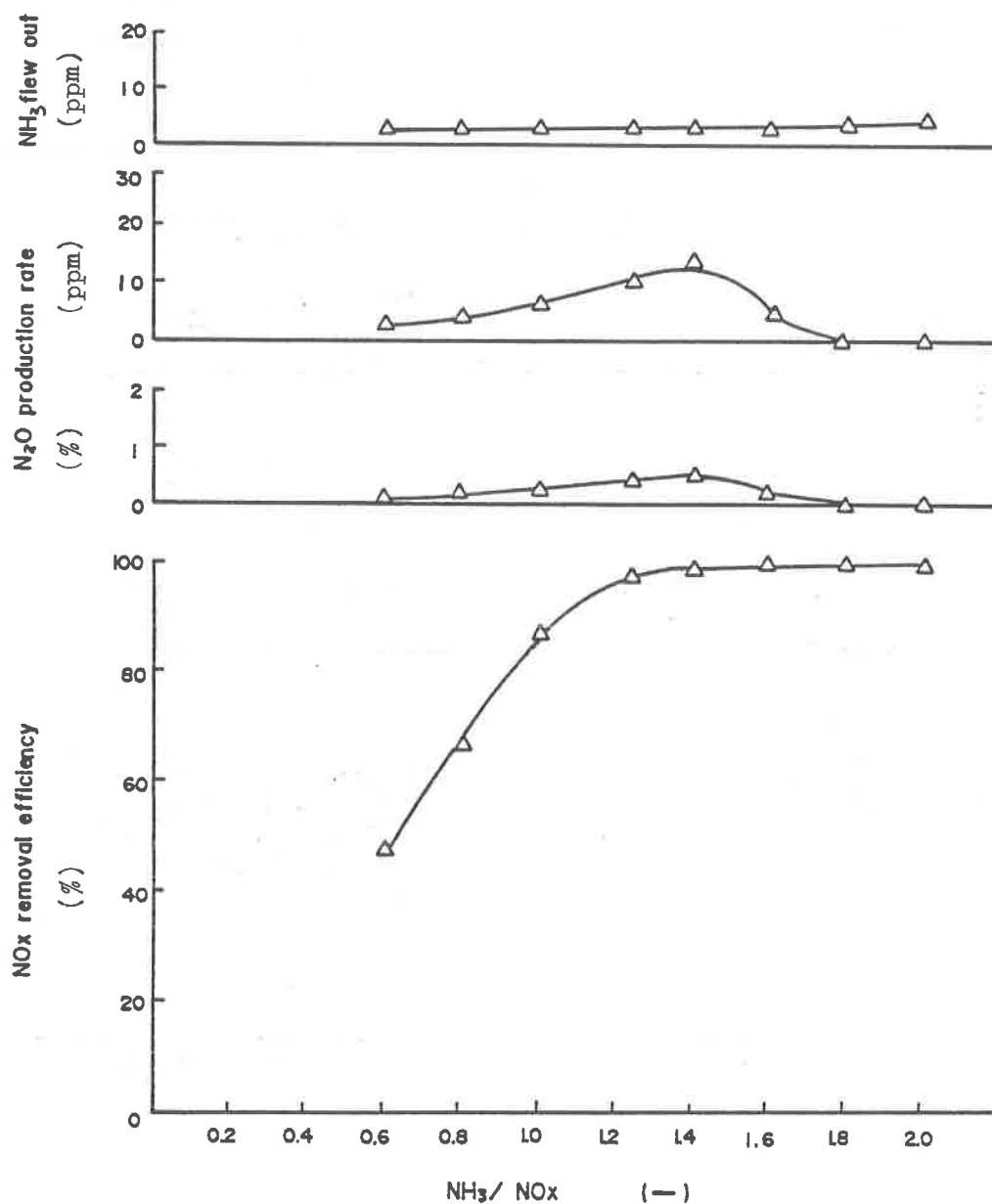
Fig. 13   Relation between NOx removal efficiency and NH$_3$/NOx ratio at single step method (Hz catalyst)

REMOVAL OF ^{14}C FROM NITROGEN ANNULUS GAS

C.H. Cheh
Ontario Hydro Research Division
800 Kipling Avenue
Toronto, Ontario, Canada   M8Z 5S4

Abstract

A dry, ambient temperature process using $Ca(OH)_2$ as the sorbent to remove $^{14}CO_2$ from moderator cover gas was further developed to remove ^{14}C from the extremely dry nitrogen annulus gas. Thermal gravimetric analysis was carried out to study the thermal stability of $Ca(OH)_2$ and the $CO_2-Ca(OH)_2$ reaction at elevated temperatures under extremely low humidity conditions. Results shows that to achieve high utilization and avoid decomposition of $Ca(OH)_2$, humidification of the annulus gas was necessary at high or low temperatures.

Results of the bench scale (1-10 L/min) oxidizer study showed that, with 0.5% Pd or alumina as the catalyst, it was possible to achieve complete oxidation of CO and over 80% oxidation of CH_4 with 1% hydrogen in the nitrogen. The gas superficial velocity should be $\leq$30 cm/s and the residence time $\geq$0.5 s. A pilot scale (up to 160 L/min) system including a catalytic oxidizer, a humidifier/demister, a $Ca(OH)_2$ reactor, a condenser/demister and regenerable molecular sieve dryers, was assembled and tested with simulated nitrogen annulus gas. Results showed that complete oxidation of the CO and 60-100% oxidation of the CH_4 with 0.5% H_2 in the simulated gas were achieved in the pilot plant. The CO_2 concentration was reduced from 30-60 µL/L at the inlet of the $Ca(OH)_2$ reactor to 1 µL/L or less at the outlet. After modifications of the dryer to overcome the problems encountered, the simulated annulus gas was dried to <-40°C dew point before recirculation. Equipment specifications and operating conditions of a ^{14}C removal system for nitrogen annulus gas are summarized.

I.   Introduction

In CANDU reactors, ^{14}C is produced primarily in the moderator (^{17}O (n,α) ^{14}C) and nitrogen annulus gas systems (^{14}N (n,p) ^{14}C), with small amounts of ^{14}C produced in the primary heat transport system and the fuel. Inorganic forms of ^{14}C are removed by the ion exchange columns in the moderator purification circuits. However, ^{14}C in the helium moderator cover gas and annulus gas systems is eventually released to the environment during, for example, pressure relief venting and purging operations.

In a previous study[1], a dry, ambient temperature process using $Ca(OH)_2$ as the sorbent to remove ^{14}CO from moderator cover gas was developed. This process was further developed to remove ^{14}C from the nitrogen annulus gas in this study.

Nitrogen Annulus Gas System

The main purpose of the annulus gas system is to provide thermal insulation between the hot pressure tubes and the relatively cool

calandria tubes and surrounding moderator, to reduce heat losses from the pressure tubes. A simplified flow diagram of the system at Pickering A station is shown in Figure 1. Nitrogen normally at a dew point of <-40°C flows through the annuli between the pressure tubes and the calandria tubes, via inlet and outlet headers through an air-cooled natural convection heat exchanger, HX1. This cools the gas from ~230°C to ~70°C. A water-cooled heat exchanger, HX2, cools the gas further to approximately ambient temperature outside containment. A moisture separator MS1 at the HX2 outlet provides for collection of moisture (leakage) in the system. Two 100% compressors then recirculate the gas through a water cooled heat exchanger, HX3, to remove the heat generated by compression and then into the annuli inlet header.
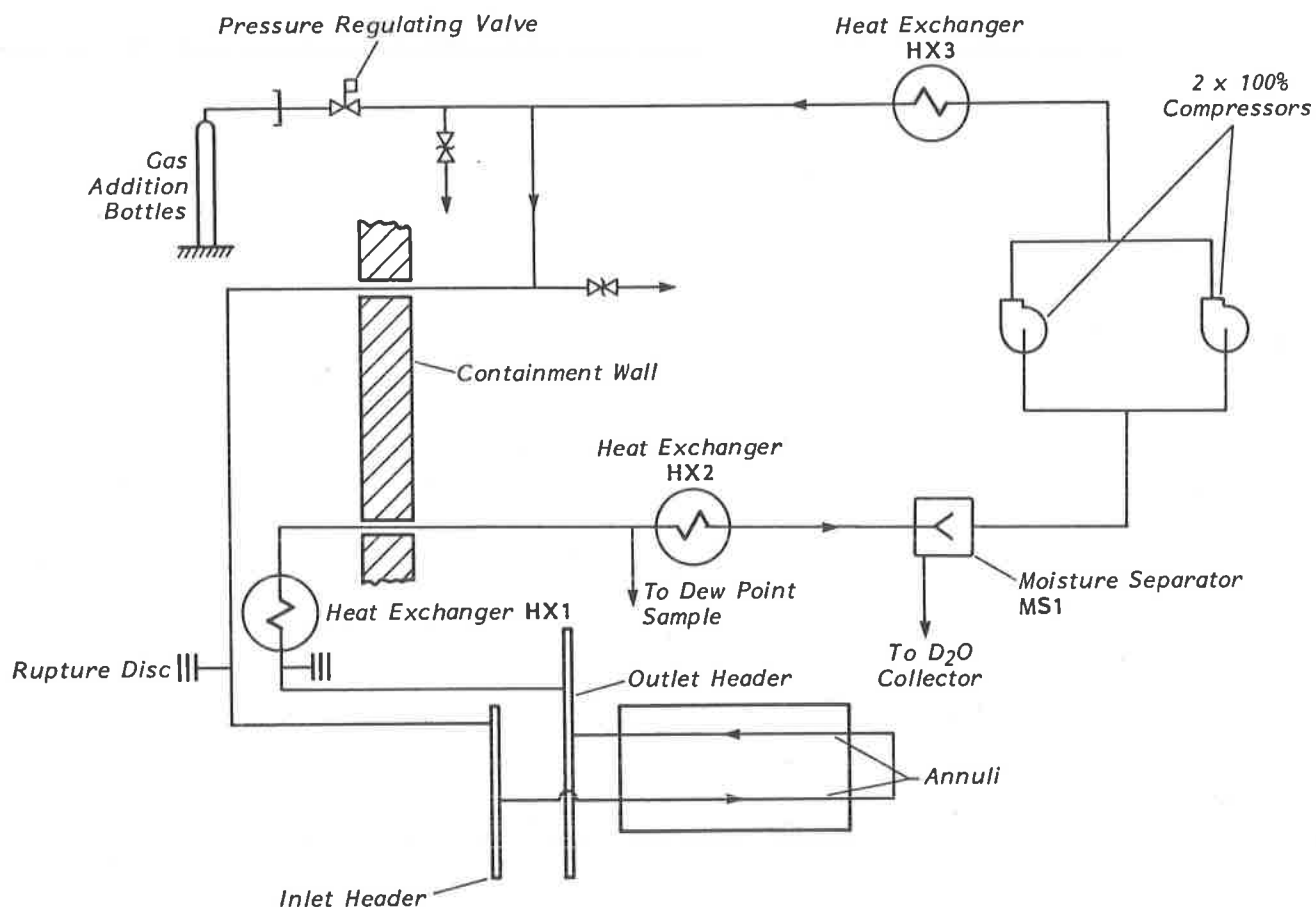
FIGURE 1
SIMPLIFIED ANNULUS GAS SYSTEM

Study Approach

Several CO_2 removal processes have been developed including the double alkali[2], the lime-slurry[3], the $Ba(OH)_2$[4] and the dry $Ca(OH)_2$[1] processes. Both the double alkali and the lime-slurry processes produce a liquid waste whereas the $Ba(OH)_2$ process uses a low melting point, toxic sorbent. The $Ca(OH)_2$ process was, therefore, selected for further development in this study.

The nitrogen annulus gas is extremely dry with a dew point of -40°C and significant amounts of ^{14}C may be in the form of ^{14}CO and hydrocarbons[5]. To remove ^{14}C from the annulus gas as $^{14}CO_2$, it is necessary to oxidize all forms of ^{14}C to $^{14}CO_2$ in a catalytic bed at an elevated temperature (200-400°C). Since it has been shown[6,7] that $Ca(OH)_2$ absorbs CO_2 at high temperatures (400°C) and relatively low humidities (eg, a dew point of 14°C, ie 50% relative humidity at 25°C), it is conceivable that the oxidizer and the $Ca(OH)_2$ absorber could operate at the same elevated temperature to remove CO_2 without humidification of the annulus gas. However, the use of a high temperature $Ca(OH)_2$ bed to absorb CO_2 from an extremely dry gas such as the nitrogen annulus gas has not been tested. The thermal stability of $Ca(OH)_2$ and the CO_2-$Ca(OH)_2$ reaction at elevated temperatures were, therefore, studied under extremely low humidity conditions. Based on the results of the thermal gravimetric study, a pilot scale ^{14}C removal system for the nitrogen annulus gas was assembled and tested.

II. Materials, Equipment and Procedure

Thermal Gravimetric Experiments

$Ca(OH)_2$ samples used in this study were prepared following a technique described in an earlier publication[1]. The thermal stability of $Ca(OH)_2$ and CO_2-$Ca(OH)_2$ reaction at high temperature and low humidity condition were studied using thermal gravimetric analysis (TGA) described in another previous publication[8].

Bench Scale Experiments

Materials and Equipment. A bench scale system (up to 10 L/min) was assembled to develop design information for the pilot scale catalytic oxidizer to convert CO and CH_4 in the annulus gas to CO_2.

A schematic diagram of the bench scale system is shown in Figure 2.

Standardized gases of CO, CH_4, H_2, and O_2 in N_2 and pre-purified N_2 in gas cylinders were fed to the catalytic oxidizer. The flow rates of all gases were controlled by mass flow controllers. The catalytic oxidizer consisted of a 2.7 cm OD, 1.9 cm ID copper pipe with an electric heating sleeve attached to the external surface of the pipe. The upper section of the pipe was filled with stainless steel wool to pre-heat the gases before they reach the catalyst bed. Two catalysts, one with Pd (0.5%) on alumina, the other Pt/Pd on alumina, both supplied by Met-Pro Corp, were tested. The catalysts tested were spherical approximately 2-3 mm diameter and packed in the copper pipe to a depth of 30 cm. Three thermocouples were installed in the reactor, one just above, one in the middle, and the one just below the catalyst bed. The dew point of the gas downstream of the catalyst bed was determined by a dew point hygrometer and the CO and CO_2 concentrations of the gas by infra-red analyzers as shown in Figure 2.
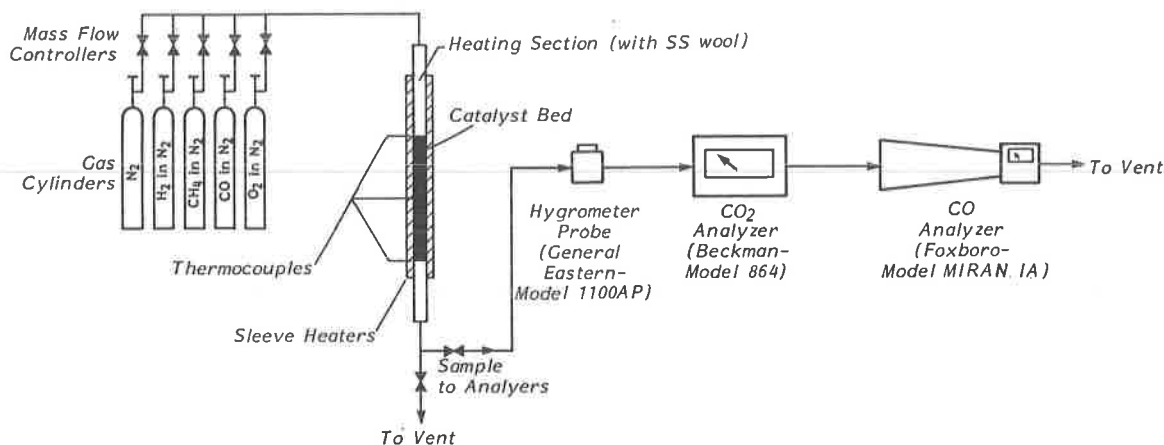
FIGURE 2

SCHEMATIC DIAGRAM OF THE BENCH SCALE OXIDIZER SYSTEM

Procedure. For each experiment, pre-purified nitrogen was passed through the reactor at the desired flow rate. The temperature of the catalyst bed was controlled by adjusting the power to the sleeve heaters; H_2, CH_4, CO and O_2 were added after the temperature of the bed had stabilized. The gas downstream of the catalyst bed was sampled and its dew point and CO_2 and CO concentrations were monitored and recorded continuously during the experiments.

Pilot Scale Experiments

Materials and Equipment. A schematic diagram of the pilot scale system is shown in Figure 3.
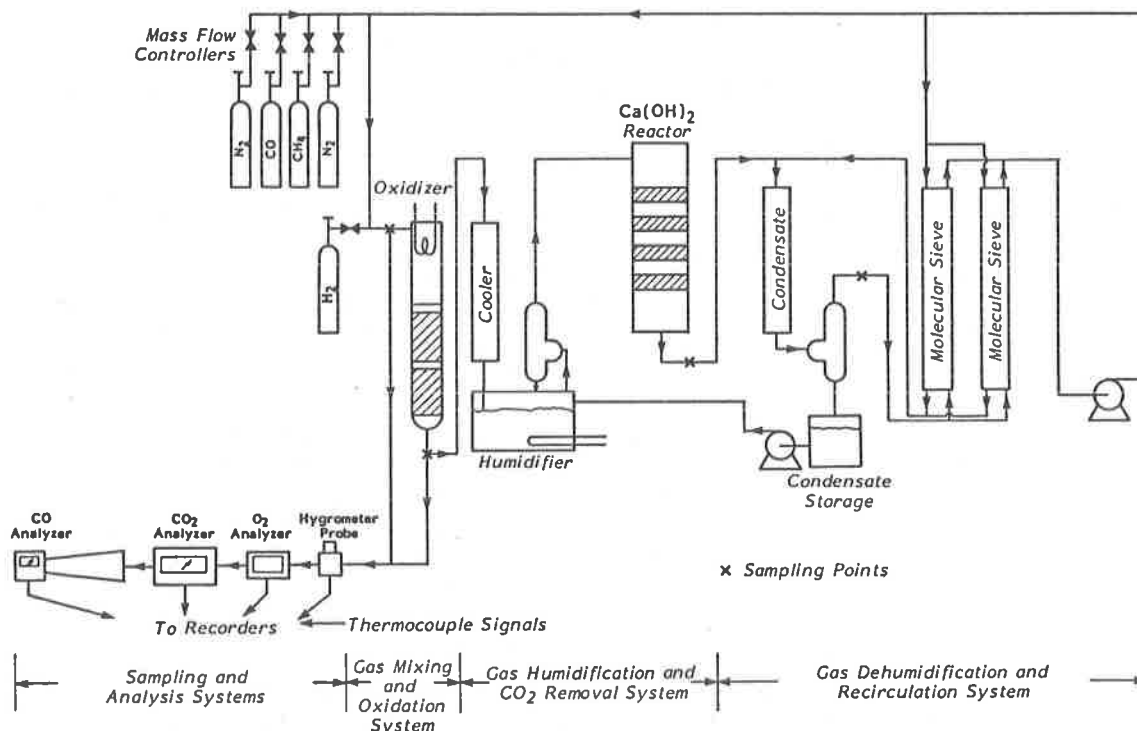
FIGURE 3

SCHEMATIC DIAGRAM OF THE PILOT SCALE ^{14}C REMOVAL SYSTEM
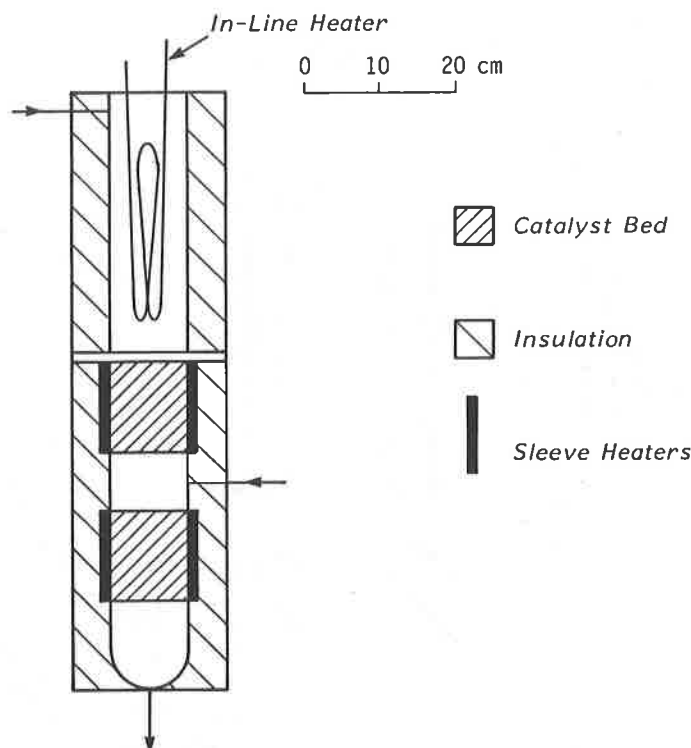
FIGURE 4

SCHEMATIC DIAGRAM OF THE CATALYTIC OXIDIZER

Gas Mixing and Oxidation System. The gases, N_2, CO, CH_4, H_2 and O_2 were supplied by gas cylinders. The gas flow rates from the cylinders were controlled by mass flow controllers. A normally closed solenoid valve was installed in the hydrogen supply line and was activated by the power to the recirculation pump.

The appropriate amount of each gas was added to the recirculating nitrogen just upstream of the oxidizer to simulate the nitrogen annulus gas. A schematic diagram of the oxidizer is shown in Figure 4. It was a 10 cm diameter column with a 40 cm long heating section and two 15 cm deep catalyst beds with a 5 cm space between the two beds.

The catalyst used was 0.5% Pd on alumina spherical particles in the size range of 2-3 mm. The gas entered the top of this heating section tangentially and was heated by a 3 kW in-line heater in the heating section. Two sleeve heaters were also installed around the two catalyst beds to maintain the temperature of the catalyst at ∿400°C.

Gas Humidification and CO_2 Removal System. The gas from the oxidizer was cooled to ambient temperature in a water cooled heat exchanger before entering the humidifier. The water temperature in the humidifier was controlled at 45-55°C by a heater and controller.
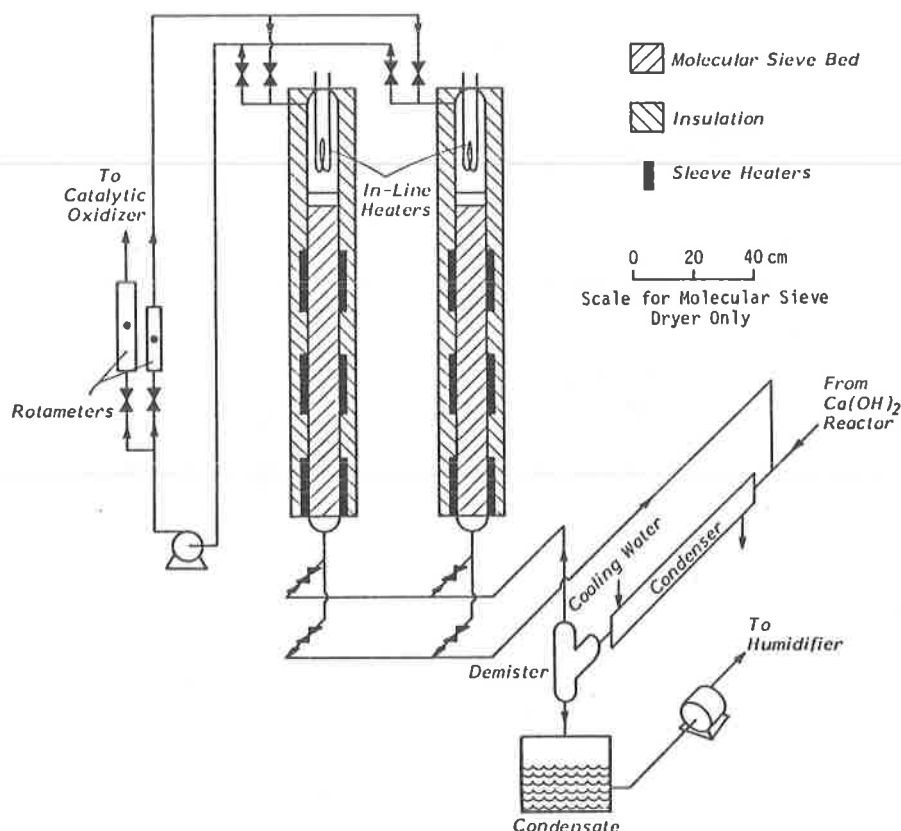
FIGURE 5
SCHEMATIC DIAGRAM OF THE DRYING SYSTEM

The water level was controlled at 2 to 4 cm below the gas inlet by pumping the condensate collected in the gas dehumidification system to the humidifier. A demister at the outlet of the humidifier prevented mist carry-over into the $Ca(OH)_2$ reactor. The $Ca(OH)_2$ reactor contained 2.5 kg of $Ca(OH)_2$ divided into four layers. Detailed dimensions of the reactor were described previously[1]. In this study, the column was made of transparent plastic and the in-line heater was eliminated.

Gas Dehumidification and Recirculation System. A schematic diagram of this system is shown in Figure 5. The gas from the CO_2 removal system entered a condenser and cooled to 4 to 6°C. The condensed moisture was separated from the gas in a mist separator and stored in a 5 L storage tank. The condensate in the storage tank was recirculated to the humidifier by a pump controlled by the level controller for the humidifier. The demisted gas then entered the bottom of one of the two molecular sieve columns and was dried. A carbon-vane pump was used to recirculate the gas to the gas mixing and oxidation system. A small portion of the dried gas (~25%) was recirculated to the top of the other molecular sieve column to regenerate the adsorbent. During regeneration, the in-line and sleeve heaters of that column were turned on and remained on until the outlet gas temperature increased to over 175°C. The column was then cooled with the dried gas for two to three hours before the columns were switched for absorption and regeneration by opening and closing the appropriate valves.

Gas Sampling and Analysis System. Sampling points were installed in the pilot system at the inlet and outlet of the oxidizer, the outlet of the $Ca(OH)_2$ reactor, and the outlet of the demister just downstream of the condenser. These sampling points were connected by two three-way valves to the gas analysis instruments. A General Eastern dew point hygrometer (Model 1100AP) with a cooling jacket on the probe was used to determine the dew point of the gas sample to as low as -40°C. The oxygen contents of the gas samples were determined by a Bendix Model 305 Oxygen Analyzer. A Beckman IR analyzer (Model 864) was calibrated in the range of 0-500 µL of CO_2/L to determine the CO_2 concentration and a Foxboro IR analyzer (Model MIRAN 1A) was calibrated in the range of 0-100 µL of CO/L to determine the CO concentration. All instrumental signals and thermocouple signals were recorded by a multi-point recorder (Esterline Angus Model L1124S Speed Servo II, 12 channels) and a dual pen recorder (Hewlett Packard Model 7132A).

Procedure. To start up the pilot plant, nitrogen was used to pressurize the entire system so that the lowest pressure in the system (at the suction side of the recirculation pump) was about 1 kPa above the atmospheric pressure to prevent any air in-leakage to the system. The heaters in the catalytic oxidizer and in the molecular sieve column that was being regenerated were turned on. After the catalytic oxidizer had reached operating temperature (400°C), H_2, CO, CH_4 and O_2 were then added to the recirculating N_2 to simulate the nitrogen annulus gas with an excess of O_2 added to oxidize H_2, CO and CH_4. Samples at appropriate sampling points were taken to study the performance of the oxidizer, the $Ca(OH)_2$ reactor, the condenser and the molecular sieve dryer.

III. Results and Discussion

Thermal Gravimetric Study

TGA experiments were carried out to study the rate of decomposition of $Ca(OH)_2$ in a -4 to -45°C dew point gas because the dew point of the annulus gas may be <-40°C. It was found that the $Ca(OH)_2$ decomposed at temperatures below 275°C if the gas dew point was about -4°C, but the decomposition temperature decreased to less than 250°C if the gas dew point was less than -35°C. Hence, the operating temperature of the $Ca(OH)_2$ absorber must be less than 275°C to avoid decomposition of the $Ca(OH)_2$ bed unless the gas stream is humidified.

A TGA experiment was carried out to study the reaction of CO_2 and $Ca(OH)_2$ at 250°C in a nitrogen stream with 400 µL CO_2/L and a dew point of -3 to -5°C. The conversion of a $Ca(OH)_2$ (X_B) was calculated from the weight gain curve and X_B, $1/2 - 1/3 X_B - 1/2 (1 - X_B)^{2/3}$ and $1 - (1 - X_B)^{1/3}$ are plotted as functions of time in Figures 6, 7 and 8. The significance of these functions are discussed in the previous study of the mechanism of the CO_2-$Ca(OH)_2$ reaction/8/. Figure 7 shows that there is a linear relationship between $1/2 - 1/3 X_B - 1/2 (1 - X_B)^{2/3}$ and time in the first 10 hours, ie, the reaction was controlled by diffusion through the product layer and the rate constant was estimated to be 0.20 cm/min. The composition of the $Ca(OH)_2$ before and after the experiment is shown in Table 1. The final utilization or conversion of the $Ca(OH)_2$ was
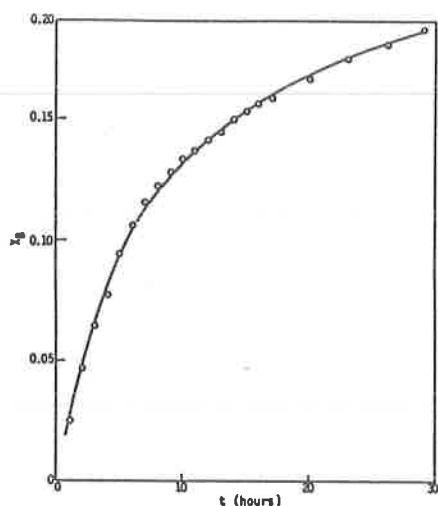
FIGURE 6
DETERMINATION OF RATE CONTROLLING STEP
AT 250°C AND A DEW POINT OF ~-4°C
(ASSUMING GAS DIFFUSION CONTROLLED)

$$\text{Slope} = \frac{2b\,kd\,CA}{\rho_B R} = 2.01 \times 10^{-6}\ \text{min}^{-1}$$

$$kd = \text{Slope} \times \left(\frac{2x\rho_B R}{b\,C_A}\right) = 0.2\text{cm}\ \text{min}^{-1}$$
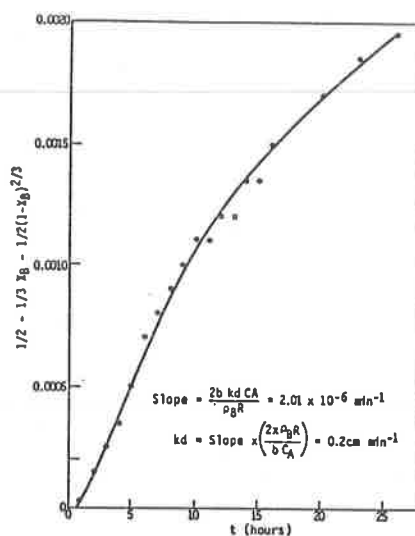
FIGURE 7
DETERMINATION OF RATE CONTROLLING STEP
AT 250°C AND DEW POINT OF ~-4°C
(ASSUMING DIFFUSION THROUGH PRODUCT)
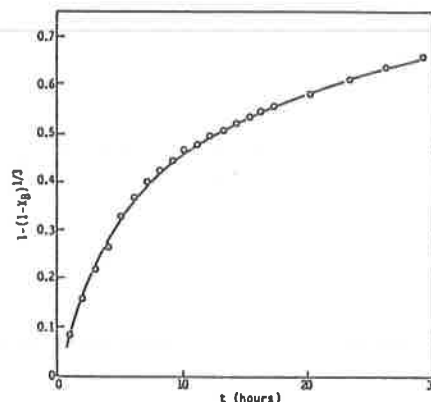
FIGURE 8
DETERMINATION OF RATE CONTROLLING STEP
AT 250°C AND DEW POINT OF ~-4°C
(ASSUMING CHEMICAL REACTION CONTROLLED)

poor and reached about 19% after 30 hours in the 400 μL/L CO_2 gas stream. In the annulus gas with lower dew point and CO_2 concentration, the utilization of the $Ca(OH)_2$ will be even lower.

Based on the above, it can be concluded that to achieve high utilization of $Ca(OH)_2$, humidification of the annulus gas will be necessary whether the absorber is operating at high or low temperature. Since it is safer and easier to operate the absorber at ambient temperature, this option is preferred.

Table 1.   Composition of $Ca(OH)_2$ Samples
Before and After Reacting With
CO_2 at 250°C in Dry Nitrogen
(Dew Point -4°C).

Component	Before Reaction (g/kg)	After Reaction (g/kg)
Moisture	10	6
$Ca(OH)_2$	886	667
$CaCO_3$	57	293
CaO	47	34

Bench Scale Experiments

A total of 28 experiments were carried out to study the effect of catalyst type, temperature (250-400°C) and flow rate (1-10 L/min) on the oxidation of CO, CH_4 and H_2. The experimental conditions and

results are summarized in Tables 2 and 3 for the Pd on alumina and the Pt/Pd on alumina catalysts, respectively.

Table 2. Bench Scale Catalytic Oxidation Experiments with 0.5% Pd on Alumina as the Catalyst

Experiment Equipment No	Bed Temperature (°C)	Total Flow Rate (L/min)	Concentration of Gases				Conversion to CO_2 and H_2O			Comment
			O_2 (µL/L)	CO (µL/L)	CH_4 (µL/L)	H_2 (µL/L)	CO[1] (%)	CH_4[2] (%)	H_2[3] (%)	
8	247	10	6000	–	–	10 000	–	–	96	Low temperature, high flow rate
7	248	10	100	53.5	–	–	87	–	–	
7A	303	10	100	53.5	–	–	87	–	–	Oxidation of CO at ~300°C
4	351	1.0	100*	–	54.5	–	–	82(96)*	–	Effect of flow rate on
3	350	5.0	100*	–	54.5	–	–	88(92)*	–	oxidation at ~350°C
9B	351	5.0	6000	53.5	54.5	10 000	99	88	96	
5	343	10	100*	–	54.5	–	–	80(84)*	–	
5A	355	10	100*	–	54.5	–	–	81(85)*	–	
9A	349	10	6000	53.5	54.5	10 000	99	48	97	
6	400	5.0	100*	–	54.5	–	–	95(100)*	–	
10B	395	5.0	1500*	–	–	10 000	–	–	32(100)	
10D	395	5.0	1500*	–	54.5	10 000	–	42	32(100)	Oxidation with oxygen less than
10C	394	5.0	1500*	53.5	–	10 000	67	–	33(100)	stoichiometric requirement
10A	392	5.0	1500*	53.5	–	10 000	67	–	32(100)	
10	397	5.0	3000*	53.5	–	10 000	95-99	–	57(97)	
10E	399	5.0	6000	–	54.5	10 000	–	99	99	Effect of flow rate at 400°C
9	399	10.0	6000	53.5	54.5	10 000	99	81	96	

[1] Calculated from inlet, outlet CO concentration measurements
[2] Calculated from CO conversion and CO_2 outlet concentrations
[3] Calculated from inlet, outlet dew point measurements
* Insufficient O_2 ()* conversion calculated based on O_2 utilization

Table 3. Bench Scale Catalytic Oxidation Experiments with Pt/Pd on Alumina as the Catalyst

Experiment Equipment No	Bed Temperature (°C)	Total Flow Rate (L/min)	Concentration of Gases				Conversion to CO_2 and H_2O			Comment
			O_2 (µL/L)	CO (µL/L)	CH_4 (µL/L)	H_2 (µL/L)	CO[1] (%)	CH_4[1] (%)	H_2[2] (%)	
1	257	1.0	100	–	58	–	–	50	–	Low temperature
1A	301	1.0	100	–	58	–	–	71	–	Oxidation of methane at 300°C
1B	355	1.0	100	–	58	–	–	85	–	Effect of flow rate at 300°C
2F	379	10.0	100	–	54.5	–		52		
11	367	10.0	6000	53.5	54.5	10 000	52		86	
1C	406	1.0	100	–	58	–	–	90	–	
2C	405	2.5	100	–	54.5	–	–	95	–	
2D	405	5.0	100	–	54.5	–	–	94	–	Effect of flow rate at 400°C
2G	405	5.0	100	–	54.5	–	–	95	–	
11A	390	5.0	6000	53.5	54.5	10 000	70		95	
11B	388	5.0	6000	53.5	54.5	10 000	70		95	

[1] Calculated from outlet CO_2 concentrations
[2] Calculated from inlet, outlet dew point measurements

For the Pd on alumina catalyst, the oxidation of H_2 at low temperature (250°C) and high flow rate (10 L/min) was high (96%) but the CO oxidation was less than 90%. The oxidation of CO became close to 100% only when the temperature was increased to 350°C. The oxidation of CH_4 at 350°C and a gas flow rate of 10 L/min was >80% when hydrogen was not added but decreased to (~48%) with the addition of H_2 and CO even with excess O_2. CH_4 oxidation at 350°C with the addition of H_2 and CO improved to 88% when the gas flow rate was reduced to 5 L/min. At 400°C, the CH_4 oxidation was 81% even at the very high flow rate (10 L/min) and with the addition of H_2 and CO.

It was suggested[9] that reducing condition may adversely affect the performance of the Pd on alumina catalyst. Several experiments (Exp. Nos. 10, 10A,B,C,D) were therefore carried out to study the effect of reducing conditions (insufficient oxygen) on the catalyst. During these experiments, close to complete utilization of oxygen was found. Following these experiments, oxygen concentration was increased to slight excess (O/H_2 stoichiometric ratio of 1.2) in Exp. No. 10E. Close to complete oxidation of H_2 and CH_4 was achieved again indicating that the brief reducing condition did not have any serious adverse effect on the catalyst.

For the Pt/Pd on alumina catalyst, the oxidation of H_2, CO and CH_4 was lower at the same temperature and flow rate when compared with Pd on alumina as the catalyst. At 350°C and gas flow rate of 10 L/min, the oxidation of CO and CH_4 was 52% and H_2 was 80% with Pt/Pd on alumina as the catalyst (Exp. No 11) compared with 74% and 97% respectively with Pd on alumina as the catalyst (Exp. No 9A). At 400°C, the oxidation of H_2 was comparable but the oxidation of CO and CH_4 was significantly lower (70%, Exp. No. 11A,B) for the Pt/Pd catalyst at 5 L/min compared with 90% (Exp. No. 9) for the Pd catalyst at 10 L/min.

The Pd (0.5%) on alumina catalyst was, therefore, selected for testing in the pilot scale experiments. Since the gas flow is about 140 L/min, the pilot scale oxidizer was 10 cm diameter with a superficial gas velocity of 30 cm/s, close to the superficial gas velocity corresponding to 5 L/min in the bench scale oxidizer.

Pilot Scale Experiments

A series of short term experiments (5 to 25 hours) and two long experiments (>100 hours) were carried out to study the performance of the integrated pilot scale system including the catalytic oxidizer, the humidifier and $Ca(OH)_2$ reactor, and the dehumidifier systems.

Catalytic Oxidizer. Experimental conditions, duration of each experiment, and the results of the study of the oxidation of CO, CH_4 and H_2 in the catalytic oxidizer are summarized in Table 4. The oxidizer temperature was controlled at 400°C for all the experiments. The gas flow rate was varied from 129 to 162 standard L/min, the inlet CO, CH_4 and H_2 concentrations varied in the ranges of 15-21, 17-22 and 440-5400 $\mu L/L$, respectively.

The oxidation of CO was determined directly by analyzing the inlet and outlet CO concentrations and found to be consistently at 100%. No CO was detected in the outlet of the oxidizer for all experiments. The degree of CH_4 oxidation was calculated based on the outlet CO_2 concentration due to CO oxidation (see equation in Table 3). In most cases, complete oxidation of the CH_4 was achieved except in five of the experiments during which the oxidation was as low as 60%. To ensure complete oxidation of CH_4 at all times, higher operating temperatures or longer residence times in the oxidizer are required. However, since only a small fraction of the ^{14}C may be in the form of CH_4, complete oxidation of CH_4 may not be necessary to maintain a high ^{14}C removal. The oxidation of H_2 was calculated based on the inlet H_2 concentration and inlet and outlet dew point measurements. The oxidation of H_2 was complete except for two cases where about 90% conversion was obtained. The slightly lower conversion may be due to error in dew point measurements because moisture could be condensed or retained in the sampling line causing difficulties in determing the dew point accurately.

The above results showed that the catalytic oxidizer was capable of oxidizing CO and H_2 completely and consistently and a high degree of CH_4 oxidation was also achieved. If complete oxidation of CH_4 is required at all times, it will be necessary to operate the oxidizer at even higher temperatures, such as 450 to 500°C.

Humidifier and Ca(OH)$_2$ Reactor. The performance of the humidifier and the Ca(OH)$_2$ reactor was investigated previously in the study of the removal of ^{14}C from moderator cover gas[1]. In this study, a simplified demister which did not provide a drain line to return the separated moisture to the humidifier, was installed initially. This demister was used in most of the experiments and led to moisture carry-over into the Ca(OH)$_2$ reactor. Excess condensation in the reactor was observed through the transparent wall of the reactor. However, the Ca(OH)$_2$ reactor was not plugged and the pressure drop increased by about 5 kPa only due to the mist carry-over.

After five months of on-off operation, Ca(OH)$_2$ samples were taken and analyzed for moisture, Ca(OH)$_2$, $CaCO_3$ and CaO contents. All of the samples showed very high moisture contents in the range of 35 to 55% probably due to the mist carry-over from the humidifier. In later experiments a demister in a L-shape with a drain-line to return the mist carry-over to the humidifier was installed to replace the straight demister (see Figure 9). After the installation of the L-shape demister, excess condensation in the Ca(OH)$_2$ reactor was not observed even when the humidifier water temperature was as high as 55°C. The $CaCO_3$ content of the samples on a dry sample basis, which is an indication of the conversion (or utilization) of the Ca(OH)$_2$, is plotted in Figure 6. The $CaCO_3$ content was as high as ∿60% (dry basis) in some of the samples taken from the top layer but significantly lower (<30%) in the samples taken from the lower layers (ie the Ca(OH)$_2$ in the reactor had not been exhausted after five months of on-off operation). The conversion of the Ca(OH)$_2$ was slightly lower near the centre, lower parts of each layer, but somewhat higher at the upper, outer parts of the bed (see Figure 10) as observed in the previous study[1].
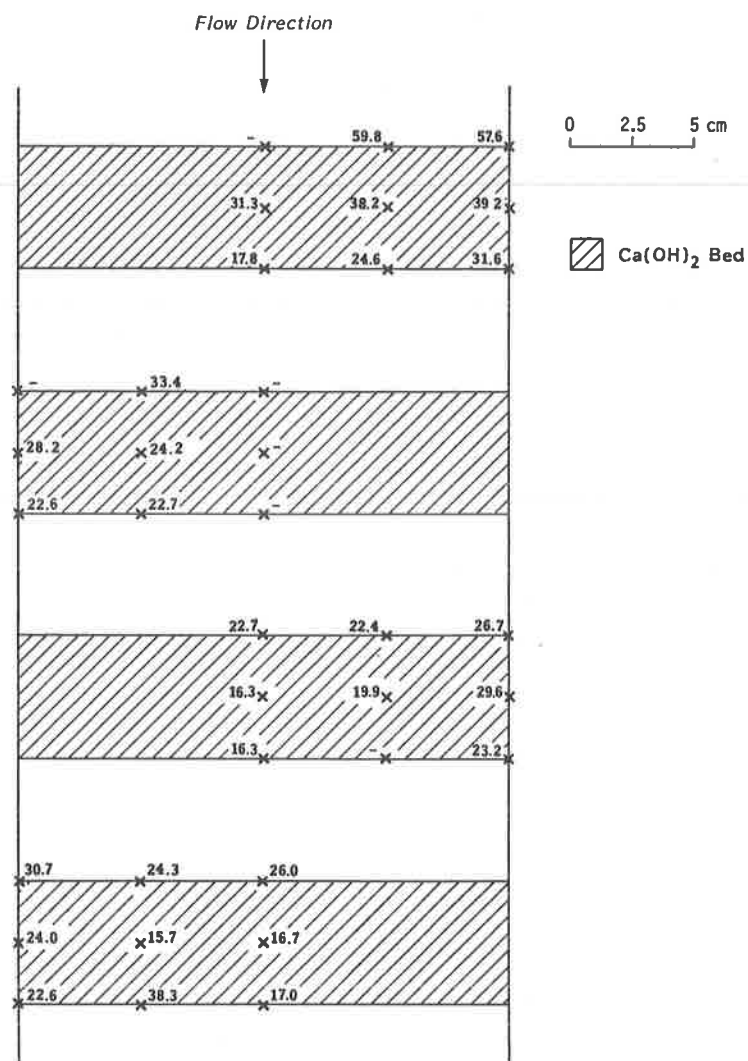
FIGURE 10

CaCO$_3$ CONTENT OF THE BED SAMPLES IN THE Ca(OH)$_2$ REACTOR

(i)
Straight Demister

(ii)
L-Shape Demister
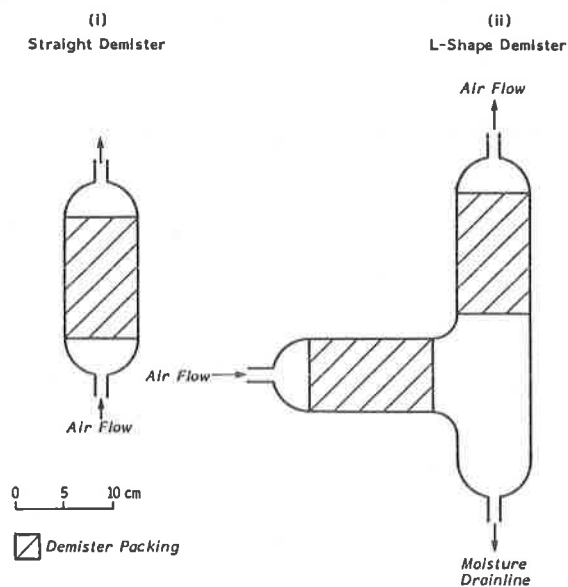
FIGURE 9

SCHEMATIC DIAGRAM OF DEMISTER CONFIGURATIONS

1294

Dehumidification System. The condenser and demister (L-shape with a drain-line to a storage vessel) in this system performed reliably. Cooling water of 3-4°C was used in the condenser to cool the gas from the Ca(OH)$_2$ reactor. At the outlet of the demister, a 4-6°C dew point in the gas stream was achieved consistently. This gas was then further dried in the molecular sieve dryers.

Several difficulties were encountered in the operation of the molecular sieve dryers and the system was modified to overcome these problems.

1. During regeneration, heating the gas by a 2 kW in-line heater just upstream of the molecular sieve bed was not sufficient to heat the molecular sieve quickly because of the low heat capacity of the gas. Furthermore, the heat loss through the column was high even with the column insulated because the column was small in diameter (10 cm) but long (120 cm). With the in-line heater alone, the regeneration gas temperature at the outlet of the column did not reach 175°C after over 10 hours of regeneration. Three 0.5 kW sleeve heaters were added to each of the columns and were turned on during regeneration. The regenration time was reduced to 6 to 8 hours after the installation of the sleeve heaters.

2. The moisture in the gas stream from the regeneration of the column condensed in the piping just downstream of the column. This moisture stayed in the piping and was transferred back to the column when the column was switched to the absorption mode. This led to early breakthroughs. To avoid the condensate remaining in the lines, the piping arrangement was modified so that the pipes in the regenaration line sloped downward to the condenser. The condensate in the system was, therefore, drained through the condenser to the demister and the condensate storage tank.

3. The solenoid valves used failed to operate properly because relatively hot gases were in contact with the valves during regeneration. Instead of purchasing expensive automatic valves that can operate with hot gases for this study, manual valves were added to operate the absorption-regeneration cycle manually to demonstrate the operation of the molecular sieve dryers.

With the above modifications, the molecular sieve dryers performed well and dried the gas to less than -40°C dew point after the column was regenerated properly. During regeneration, heating for about 7 hours was required before the outlet gas temperature reached 175°C. When the column was regenerated for only 5 hours or less before switched to the absorption mode, the outlet dew point was higher in the range of -30 to -20°C. The breakthrough times for both columns were about 16.2 to 16.3 hours for a gas flow rate of 145 L/min and inlet dew point of 6 to 6.5°C. This correspond to a moisture loading of 21.8 g of moixture/100 g of adsorbent, very close to the loading suggested by the manufacturer.

Based on the above results, it is recommended that the molecular sieve dryers be operated in 10 to 12 hour cycles with 8 to 9 hours heating and 2 to 3 hours cooling for regenerating the column before switching to the absorption mode.

TABLE 4

PILOT SCALE STUDY OF THE CATALYTIC OXIDIZER - EXPERIMENTAL CONDITIONS AND RESULTS

Experiment Date	Duration (hr)	Total[1] Flow Rate (L/min)	Inlet of Catalytic Oxidizer										Outlet of Catalytic Oxidizer					
			O_2 rate of addition (mL/min)	O_2 conc (%)	CO rate of addition (mL/min)	CO conc (μL/L)	CH_4 rate of addition (mL/min)	CH_4 conc* (calc) (μL/L)	H_2 rate of addition (mL/min)	H_2 conc (calc) (μL/L)	Dew Point* (°C)	CO_2 conc (μL/L)	CO conc (μL/L)	CO oxidation (%)	CO_2 conc (μL/L)	CH_4 oxidation[2] (calc) (%)	Dew Point (°C)	H_2 oxidation[3] (calc) (%)
2-11-83	7.5	159	-	-	2.8	18*	-	-	-	-	<-26	2-5	0	100	-	-	-	-
7-11-83	2.5	159	-	-	2.8	18*	-	-	-	-	-	2	0	100	-	-	-	-
	4.5	159	-	-	2.8	18*	-	-	-	-	-	2	0	100	43	100	-	-
8-11-83	7.5	159	-	-	2.8	18*	2.8	18	-	-	<-22.5	0	0	100	33-40	83-100	-	-
9-11-83	6.0	159	100	-	2.8	18*	2.8	18	-	-	-	0	?	100	35-40	94-100	-	-
14-11-83	3.0	162	0	0.24-0.32	2.8	17*	2.8	17	-	-	-	0	?	100	33-40	76-100	-	-
	4.0	162	400	0.60-0.92	2.8	17*	2.8	17	700	4300	-	3	0	100	30-38	60-100	-	-
22-11-83	6.5	158	20	-	2.8	15	2.8	18	-	-	-	7-9	0	100	56	100	-	-
24-11-83	3.0	153	20	-	2.8	16	2.8	18	-	-	-	6-7	0	100	53-57	100	-	-
	4.5	153	400	-	2.8	16	2.8	18	700	4600	10.4	6-7	0	100	52	100	158	100
15-12-83	3.0	129	20	0.23	2.8	20	2.8	22	-	-	-	4	0	100	46	100	-	-
	4.5	129	400	0.07-0.12	2.8	20	2.8	22	700	5400	10.0	3	0	100	47-48	100	150-158	87-100
19-12-83	6.3	135	50	0.05-0.19	2.8	21	2.8	21	70	520	12.8	3-5	0	100	50-54	100	13.5	100
20-12-83	25	137	75	0.11-0.16	2.8	20	2.8	20	120	880	-	4-12	0	100	51-63	100	-	-
30-01-84	24 }77	144	20	0.49-0.62	2.5	17*	2.5	17	-	-	-	1	0	100	37-38	100	-	-
01-02-84	53 }	146	45	0.27-0.35	2.5	17*	2.5	17	64	440	-	8-13	0	100	46-54	100	-	-
6-03-84	8.0	147	45	0.03-0.30	2.5	19	2.5	17	64	440	<-38.9	4-6	0	100	34-38	65-76	-24.1	100
12-03-84	8.5	146	45	0.09-0.30	2.5	17-19	2.5	17	64	440	5.5	0-4	0	100	41-44	100	6.3	100
2-04-84	103	145	95-60	0.14-0.48	2.5	18	2.5	17	64	440	<-40	13	0	100	46	88	-26.4	100
3-04-84		145	60	0.38-0.50	2.5	18	2.5	17	64	440	<-40	3	0	100	36-43	90-100	-26	100
4-04-84		145	60	0.43-0.76	2.5	18-19	2.5	17	64	440	-23.5	0-1	0	100	36-37	100	-17.8	90
5-04-84		135	60	0.09-0.37	2.5	17-18	2.5	19	64	470	-24.8	3-4	0	100	33-39	67-90	-18.3	100
6-04-84		135	60	0.24	2.5	16-17	2.5	19	64	470	-19.9	3	0	100	30-33	60-70	-14.7	100

(1) Flow rate = rotameter reading $\times \sqrt{\dfrac{P}{101.3}}$ where P is the pressure at the rotameter in kPa

(2) CH_4 conversion was calculated from the equation = $\dfrac{\text{Total outlet } CO_2 \text{ concentration} - \text{outlet } CO_2 \text{ concentration due to CO oxidation}}{\text{Inlet } CH_4 \text{ concentration}} \times 100\%$

(3) H_2 conversion was calculated based on the inlet H_2 concentration and the inlet and outlet dew point measurements.

* Some of the inlet CO concentrations and all of the inlet CH_4 and H_2 concentrations were calculated by the addition rate divided by the total flow rate

IV. Conclusions and Design Recommendations

In this study an integrated ^{14}C removal system for nitrogen annulus gas including a catalytic oxidizer, a humidifier, a Ca(OH) reactor, and a condenser and molecular sieve dryers was designed, assembled and tested. Based on the experimental results, the equipment specification and operating condition for a 140 L/min nitrogen annulus gas ^{14}C removal system were developed and are summarized below.

Catalytic Oxizider

Catalyst recommended: 0.5% Pd on alumina (2-3 mm particles)
                        suggested manufacturer: Met-Pro Corp

Operating temperature: 400°C

Heaters: 3 kW in-line and 2 - 0.5 kW sleeve heaters, each 15 cm long

Oxidizer diameter: 10 cm (superficial velocity <30 cm/s)

Catalyst bed height: 15 cm (residence time >0.5 s)

Humidifier/Demister

Humidifier diameter: ∿30 cm

Humidifier water operating temperature: 45-55°C (controlled by
                                          immersion heater and
                                          controller)

Water level: controlled at 2 to 4 cm below the gas inlet

Demister configuration: L-shape, 5 to 7.5 cm in diameter with wire
                          packing and drain-line to return the
                          moisture separated to the humidifier.

Ca(OH)$_2$ Reactor

Reactor diameter: 20 cm (superficial velocity <7.5 cm/s)

Thickness of bed: 5-6 cm for each layer with 5 cm space between
                    layers

Number of bed layers: depends on the duration of operation required
                        without changing the bed.

Condenser/Demister

Cooling water temperature: <10°C

Condenser should be lower than the molecular sieve dryers and all piping and the condenser should slope downwards to the demister.

Demister: L-shape, 5 to 7.5 cm in diameter with wire packing and
            drain-line to collect the condensate to the storage tank.

Molecular Sieve Dryers

Type of molecular sieve: 5A acid-resistant

Dryer column: 2, each 10 cm diameter, 105 cm long

Regeneration heaters: one 2 kW in-line heater and three 0.5 kW
                        sleeve heaters (each 20 cm long) for each
                        column

Valves: automatic valves that can operate reliably with hot gases
         (up to 400°C) must be used.

References

1.   Cheh, C.H., Glass, R.W. and Chew, V.S., "Removal of carbon-14 from gaseous streams." Paper presented at the IAEA Seminar on Testing and Operation of Off-Gas Cleaning Systems at Nuclear Facilities, Karlsrueh, FRG. May 3-7, 1982.

2.   Braun, H., Gutowski, H., Bonka, H. and Grundler, D., "Plant for retention of ^{14}C in reprocessing plants for LWR fuel elements." Proc. 17th DOE Nuclear Air Cleaning Conference, Denver, Colorado. August 2-5, 1982.

3.   Holladay, D.W., "Experiments with a lime slurry in a stirred-tank for the fixation of ^{14}C contaminated CO_2 from simulated HTGR fuel reprocessing off-gas." ORNL/TM-5757, (1978).

4.   Haag, G.L., "Application of the carbon dioxide-barium hydroxide hydrate gas-solid reaction for the treatment of dilute carbon dioxide-bearing gas streams." ORNL-5887, (1983).

5.   Kabat, M.J. and Gorman, D.M., "^{14}C in Ontario Hydro's nuclear stations: production, system and effluent levels, dosimetry, environmental data." Ontario Hydro Health and Safety Division Information Report SSD-IR-80-3, (1980).

6.   Kabat, M.M., "Monitoring and removal of gaseous carbon-14 species." Proc. 15th DOE Nuclear Air Cleaning Conference, (1978).

7.   Mozes, M.S., "Evaluation of solid sorbents for the control of $^{14}CO_2$." Ontario Hydro Research Division Report No 80-505-K, December, 1980.

8.   Chew, V.S., Cheh, C.H. and Glass, R.W., "Mechanism of the CO_2 $Ca(OH)_2$ reaction." Proc. 17th DOE Nuclear Air Cleaning Conference, Denver, Colorado. August 2-5, 1982.

9.   Keller, J.H. Met-Pro Corp, Private Communication.

DISCUSSION

THOMAS, T.R.: Are you developing this process to recover C^{14} from CANDU reactors because the generation of C^{14} per giga-watt electrical year is much greater than for light water reactors? Why do you need to do this?

CHEH: If we do not convert C^{14} in the nitrogen annulus gas system to CO_2, our emission is very close to our target. Our target is 1% and if we don't convert CO and CH_4 to CO_2, for some reason, our emission will be very close to 1%. If we do convert and remove them, we have no problem at all. On the other hand, we are looking at another aspect of this. Since the process is so cheap and simple, if we do find a market for C^{14}, which is what we are looking at right now, perhaps it is even economically feasible to recover the C^{14} and market it.

THOMAS, T.R.: How does the release rate of C^{14} from CANDU reactors compare with the release rate from LWRs? Emissions from LWRs are 6-16 Ci/GWe yr.

CHEH: I am sorry I cannot remember the exact numbers, but in our previous publications we have given those numbers. With the nitrogen annulus gas it is much, much higher than in the light water reactor. Even if we use CO_2 as the annulus gas, the moderator cover gas will still release more then from light water reactors.

DEVELOPMENT OF A WETPROOFED CATALYST RECOMBINER FOR
REMOVAL OF AIRBORNE TRITIUM*

K.T. Chuang, R.J. Quaiattini, D.R.P. Thatcher and L.J. Puissant
Atomic Energy of Canada Limited - Research Company
Chalk River Nuclear Laboratories
Chalk River, Ontario   K0J 1J0

Abstract

For cleanup of airborne tritium at tritium handling facilities, it is generally agreed that the most reliable method is to convert the tritium in a recombiner into water vapor followed by adsorption of the vapor in a molecular sieve drier. Decontamination factors of 10^3 to 10^6 have been reported.

Wetproofed catalysts developed at Chalk River Nuclear Laboratories have been shown to maintain their activities when exposed to liquid water or air at 100% relative humidity. When a wetproofed catalyst recombiner is used, operation can be carried out at room temperatures thus greatly simplifying the system.

Two catalysts, Pt/carbon and Pt/silica, were prepared for this study. The activity of Pt/carbon was measured with hydrogen and found to be comparable to the published results for conventional Pt/alumina catalysts at similar conditions. The results were best represented by a rate equation, Rate = 0.045 (Hydrogen Concentration)$^{1.57}$. The activity of the Pt/silica catalyst was similar to the Pt/carbon catalyst; however, it could be increased by a factor of five by exposure to air at 150°C containing 50-200 ppm hydrogen.

Experiments were carried out for the following range of operating conditions: flows from 0.3 to 3.0 m/s, pressure from 100 to 500 kPa. Tritium was added to the air stream at 1-5 MBq.m^{-3} (30 - 140 µCi.m^{-3}). No significant isotope and/or pressure effects were observed. To date lifetime data of greater than four months have been obtained.

I. Introduction

With the expansion of nuclear fusion experiments throughout the world, there is a strong need to develop systems for the recovery of airborne tritium to ensure that environmental releases from tritium-handling facilities are minimized. Oxidation of the tritium on catalyst surfaces followed by adsorption of water vapor in a molecular sieve drier is the widely accepted approach.[1] Existing facilities such as those at Los Alamos-TSTA, Mound Laboratory and Sandia National Laboratories use recombiners packed with precious metal catalysts and operated at 150-200°C. Operating in this temperature range is essential with conventional catalysts to avoid water condensation in catalyst pores and consequent catalyst deactivation. The disadvantage of this approach is the need for heaters and coolers to heat the feed to the recombiner and cool the gas mixture again

before inlet to the driers. For emergency air cleanup systems, it is necessary to heat the gas quickly to the operating temperature and equipment has to be designed to accommodate the warm-up period.

It is clear that significant savings can be realized if the recombiner is operated at ambient temperatures without the need for costly heaters and coolers. This type of recombiner would operate at design efficiency immediately on startup. Therefore, problems associated with the warm-up period no longer exist. It may be necessary to provide substantial emergency power for the heaters.

The advantages of operating a recombiner at ambient temperatures were recognized by several researchers.[1,2] Accordingly, they derived kinetic data for the recombination reaction at room temperatures from experiments using hydrogen/tritium and air mixtures. The catalysts used in their studies were platinum and palladium deposited on alumina, Kaolin and Zeolite. According to Sherwood,[1] catalyst activity declined steadily with exposure time for all catalysts. Although no reason for this was given, it is quite possible that some of the reaction product (water) and additional humidity from the air may be adsorbed by the catalyst supports. As a result the catalyst surface was flooded with water and the rates for further transfer of gaseous reactants to the reaction sites were greatly reduced.

The wetproofed catalysts developed at Chalk River Nuclear Laboratories maintained activity when exposed to liquid water or gases at 100% relative humidity. If this type of catalyst is used in a recombiner operated at ambient conditions, a stable activity can be expected. The objective of this work was to measure the kinetic parameters that are required for the design of a wetproofed catalyst recombiner to make a cost comparison with conventional recombiners possible.

II. Experimental

Apparatus and Procedure

The flowsheet for the reactor system is shown in Figure 1. Compressed air, passing through a 1 μm filter, was mixed with hydrogen and tritium and then fed to the test section. The reactor was 5 cm diameter and 30 cm long, and was operated at ambient temperatures. Hydrogen gas (prepurified grade, Union Carbide) was used as received. Tritium gas was obtained as a 50 μCi/L mixture in nitrogen from Gollob Analytical (Berkeley Heights, N.J) and was used without further purifications. Both hydrogen and tritium could be added independently to the air; typical flows measured with mass flowmeters were: 37-370 L/min air, 3.5-150 mL/min hydrogen and 0-2.2 L/min tritium-nitrogen mixture, all expressed at normal conditions. An ionization chamber (Overhoff and Associates, Cincinatti, Ohio) was used to measure tritium concentrations. It was calibrated against the gas mixture supplied by Gollob Analytical. As shown in Figure 1, the concentrations into and out of the test section were measured after the gases were dried. Hydrogen concentration was measured using a gas chromatograph (Hewlett Packard, model 5700A). The lower detection limit was estimated to be 20 ppm with a thermal conductivity detector.

Catalyst Characterization

Platinum is known to be the most active catalyst for H_2-O_2 reaction at ambient conditions[1,3]. It was decided to use it exclusively in this study. However, the catalyst support, which provided the surface area for platinum deposition, influenced water adsorption and hence catalyst stability. Two different types of catalyst support were found to adsorb very little water when exposed to 100% relative humidity. They were activated carbon and pure crystalline silica. Both were hydrophobic according to the suppliers. The carbon support has been successfully used in the wetproofed catalyst for hydrogen water isotopic exchange reaction. However, carbon was not a suitable material for conditions where the catalyst support might be ignited, say at hydrogen concentrations greater than 0.5%. Under such conditions noncombustible silica would have to be used. The wetproofing agent was polytetrafluoroethylene (Teflon).

The catalyst was prepared by depositing platinum from $(NH_3)_4Pt(NO_3)_2$ onto the catalyst support powder which was calcined at 400°C for one hour and bound to a 28 mesh corrugated metal screen. Teflon was used both as a binder and wetproofing agent. This screen was then rolled to form a cylindrical module of 5 cm diameter with a void fraction of ~90%. Important characteristics of the catalysts are listed in Table 1.

Table 1. Catalyst characterization data

Property	Unit	Catalyst Support Carbon	Silica
Platinum concentration	g/L	1.53	0.89
Surface area of platinum	m²/L	14.7	64.0
Concentration of support	g/L	15.3	49.4
Surface area of support	m²/L	3700	19 000
Packing Density	kg/L	0.40	0.45

An electron micrograph (X7500) of the catalyst surface is given in Figure 2. This shows a surface covered with Teflon but with sufficient opening for the diffusion of gaseous reactants and product to take place. The silica substrate is totally obscured.

Data Interpretation

The reaction rates were calculated assuming a differential reactor. Rates for the average concentration across the reactor were obtained from the analysis of the inlet and outlet hydrogen and tritium concentrations, from the catalyst bed volume and from the total air flow through the reactor. The obtained rate values and

3715E
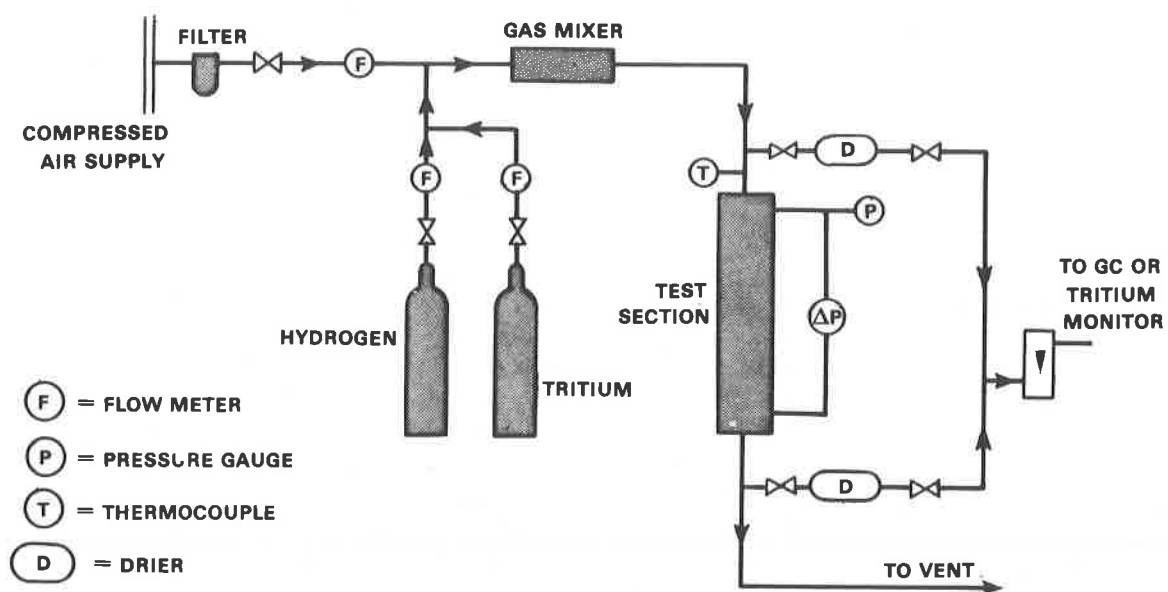
FIGURE 1 EXPERIMENTAL APPARATUS
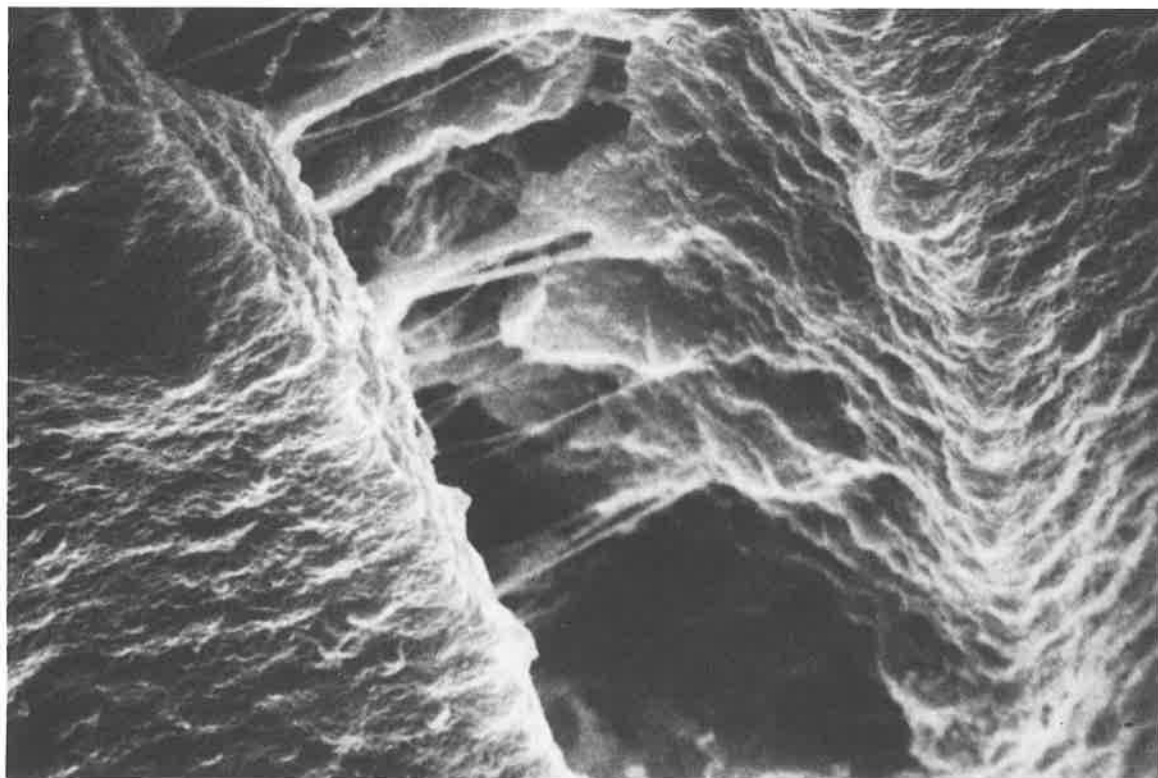
FIGURE 2   Electron micrograph of catalyst surface (X7500)

average concentration were then fitted with a power curve that passed through the origin. When the conversion across the reactor was high (up to 40%) the assumption of a differential reactor was checked by comparing the observed outlet concentration with the outlet concentrations obtained by integrating the rate equation along the catalyst section. The good agreement obtained justified the rate calculation method.

II. Results and Discussion

Although the catalytic reaction between hydrogen and oxygen over a metal surface has been studied extensively, there is still no generally accepted mechanism for this reaction.[4] Proposed rate expressions differ considerably and range from complicated Langmuir-Hinshelwood models to power law equations of orders up to two. In excess oxygen at low temperatures some workers[1,2,8] have observed first order kinetics while others[9] observed second order kinetics. This is in part a result of the considerably diverse conditions employed by various workers. The catalyst activity is influenced by the concentration of the reactants, impurities in the feed, reaction conditions (T, P etc.) and procedures for catalyst preparation and pretreatment. For design purposes it is generally adequate to use the power law expression provided the experiments are carried out under conditions where wide extrapolation is not necessary.

Initial tests were carried out to determine the external mass transfer limitations by varying the gas flow rate and at the same time keeping a constant residence time in the recombiner. Measurement of the feed and effluent concentrations indicated that external mass transfer limitations for the carbon and silica supported catalysts were significant at 37 L/min (or 30 cm/s) and became insignificant at 1 m/s. Calculations based on the method reported by Levenspiel[5] also indicated negligible external mass transfer resistance at 1 m/s.

Additional tests were performed by coating the metal screen with Pt/carbon powder three times thicker than that normally prepared for testing. In this case, the rate of reaction was found to be independent of the thickness of the catalyst layer indicating the effectiveness factor was approaching unity, i.e. pore diffusion was not a rate-limiting step.

Activity of Pt/Carbon Catalyst

The activity of Pt/carbon catalyst was measured with hydrogen at concentrations up to 400 ppm in air. At these low concentrations, heat released from the reaction was small and the reactor was assumed to be under isothermal conditions. Test results are shown in Figure 3 and the data are best represented by the rate equation (1).

$$\text{Rate (ppm } H_2/s) = 0.045 \, C_{H_2}^{1.57} \tag{1}$$

where C_{H_2} is the hydrogen concentration in air, in ppm. The activity is similar to that reported previously for the conventional Pt/alumina catalysts at ambient temperatures[1,2] although the metal surface area is almost forty times lower.
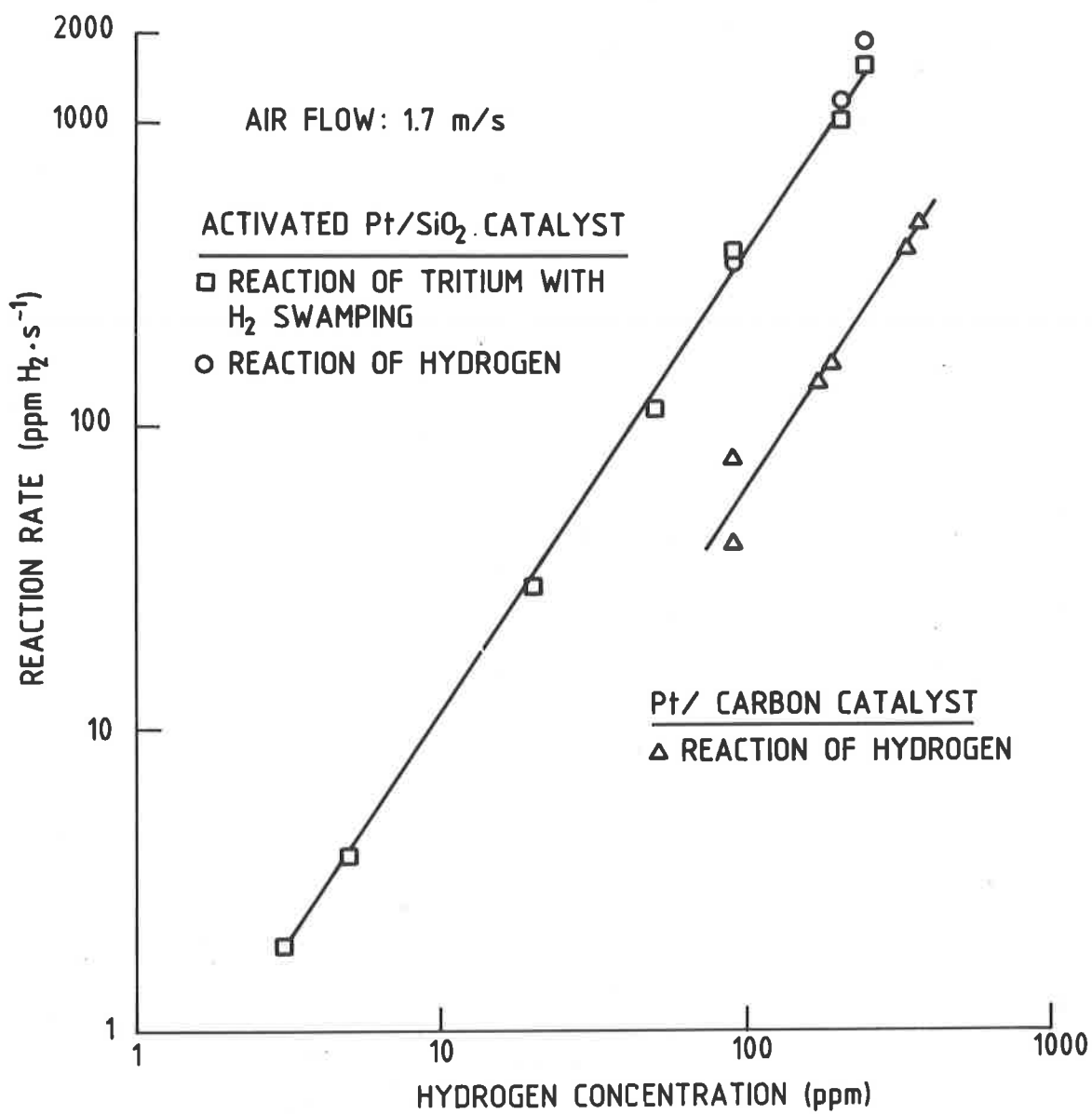
FIGURE 3   ACTIVITY OF PLATINUM CATALYSTS

Activity of Pt/SiO$_2$ Catalyst

The activity of the Pt/SiO$_2$ was first measured with hydrogen containing no tritium. It was found that the activity was similar to that of Pt/carbon catalyst. To determine the activation energy, the catalyst was exposed to an air flow (1.7 m/s) containing 200 ppm H$_2$ at 150°C. However, when reaction rate was remeasured on return to room temperature, it was discovered that the conversion increased from 0.04 to 0.56 as shown in Figure 4. This represents a 10-fold rate increase. Catalyst samples were sent for surface area analysis and the results indicated that the activation did not affect the platinum surface or the support area. However, characterization of the catalyst surfaces by Laser Raman Spectroscopy indicated an impurity peak at 480 cm^{-1} which was not present for the activated sample. The absorption band was attributed to the contaminations of the platinum surface most likely by Pt-N$_2$ which may have originated from the incomplete decomposition of the platinum salt used in the preparation of the catalyst.
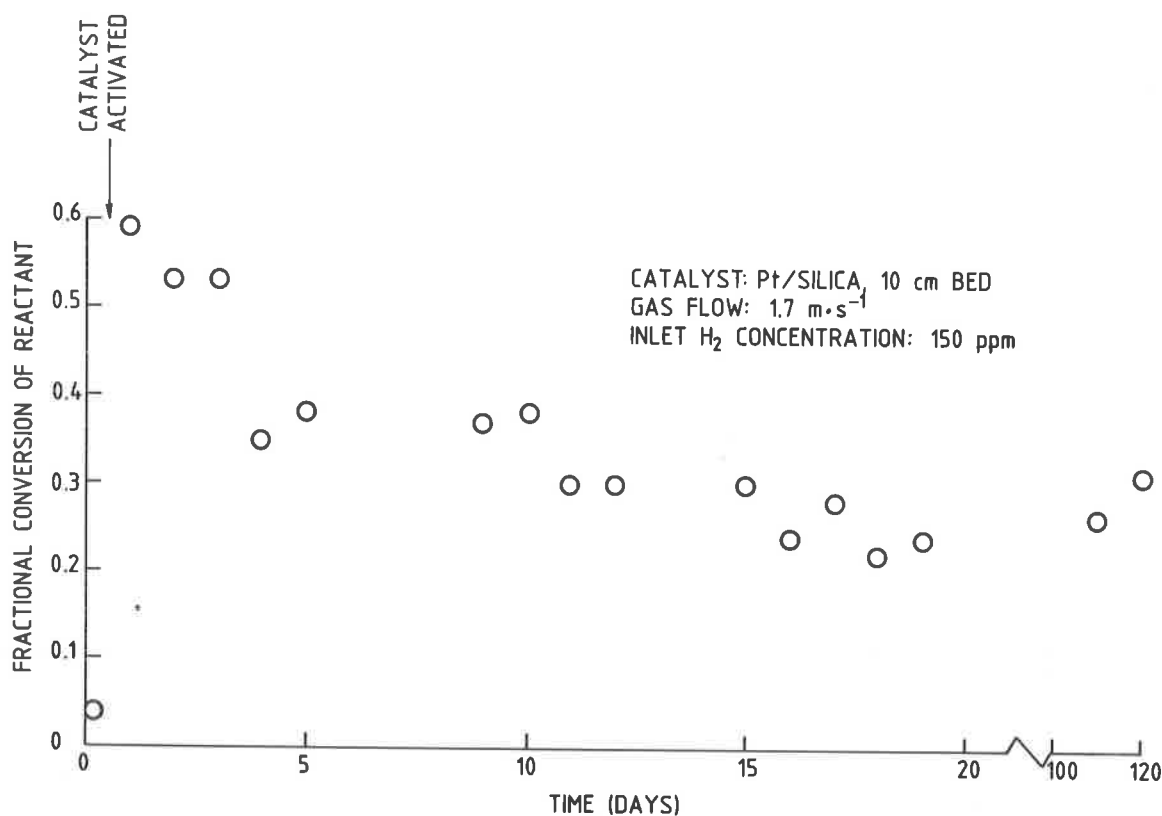
FIGURE 4   CATALYST LIFETIME

Although the activity subsequently decreased somewhat, it seems the conversion was stabilized in the range of 0.2 - 0.4 after four days of operation. The catalyst activity was again measured with hydrogen at various concentrations and the results are shown in Figure 3. The catalyst was then tested with tritium at 1 - 5 MBq/m^3 (30 - 140 µCi/m^3) and found to be inactive toward tritium oxidation. This was similar to that reported by Tanaka and Kiyose[6] who indicate that hydrogen swamping is required for efficient recombination at

very low concentration of hydrogen. With hydrogen swamping the activity of the catalyst for tritium recombination is given in Figure 3. It can be seen that the tritium results follow closely with those of hydrogen and thus isotope effects can be assumed negligible. The data were fitted by the least square method and the most representative rate equation is

$$\text{Rate (ppm TH or } H_2/s) = 0.3069 \ C_{H_2}^{1.57} \tag{2}$$

where C_{H_2} is again concentration in air, in ppm. From Equations (1) and (2), the reaction order with respect to the hydrogen concentration is 1.57 indicating the similarity of the reaction mechanism for the two types of wetproofed catalyst. However, the rate constant for the activated silica is about six times higher than that for carbon. This, together with the fact that silica is a noncombustible material, makes the silica a good choice for future applications.

Additional tests were carried out to determine the effect of pressure and temperature on catalyst activity and pressure drop characteristics for the packed bed. It was found that the reaction rate was independent of pressure which was varied from 100 to 530 kPa. A series of tests were conducted at temperatures between 25 and 150°C and inlet H_2 concentrations between 100 and 300 ppm. From the Arrehenius plot shown in Figure 5, the apparent activation energy was calculated to be 3.96 kcal/mole.

The pressure drop was measured for all test runs and the data can be represented by

$$\Delta P \ (kPa/m) = 0.23 \ F_A^{1.16} \tag{3}$$

where F_A is the F-factor of the air and is defined as linear velocity of air flow times the square root of the gas density, kg/m^3. The equation agrees with the theory developed for packed columns.[7]

Catalyst Stability

A conventional catalyst loses its activity when exposed to humid air. Under these conditions pore condensation takes place until it reaches thermodynamic equilibrium dictated by the Kelvin equation (4).

$$\ln(P/P_o) = -2 \ V\gamma \ \cos\theta/(rRT) \tag{4}$$

where r is the radius of the capillary, V is the molar volume of the liquid and γ the surface tension. Equation (4) indicates that for values of the contact angle θ less than 90°, liquid condenses in the capillary at a pressure P less than the saturated vapour pressure P_o at temperature T. For alumina catalysts the contact angle with water is close to zero. The catalyst deactivation would continue until thermodynamic equilibrium conditions are reached by which time the activity level would be very low. These phenomena have been reported by Sherwood.[1] The equation also implies that increasing contact angle reduces pore condensation. Therefore choosing a

CATALYST: Pt/SILICA, ACTIVATED
AIR FLOW: 1.7 m/s
H_2 CONCENTRATION: 100-300 ppm
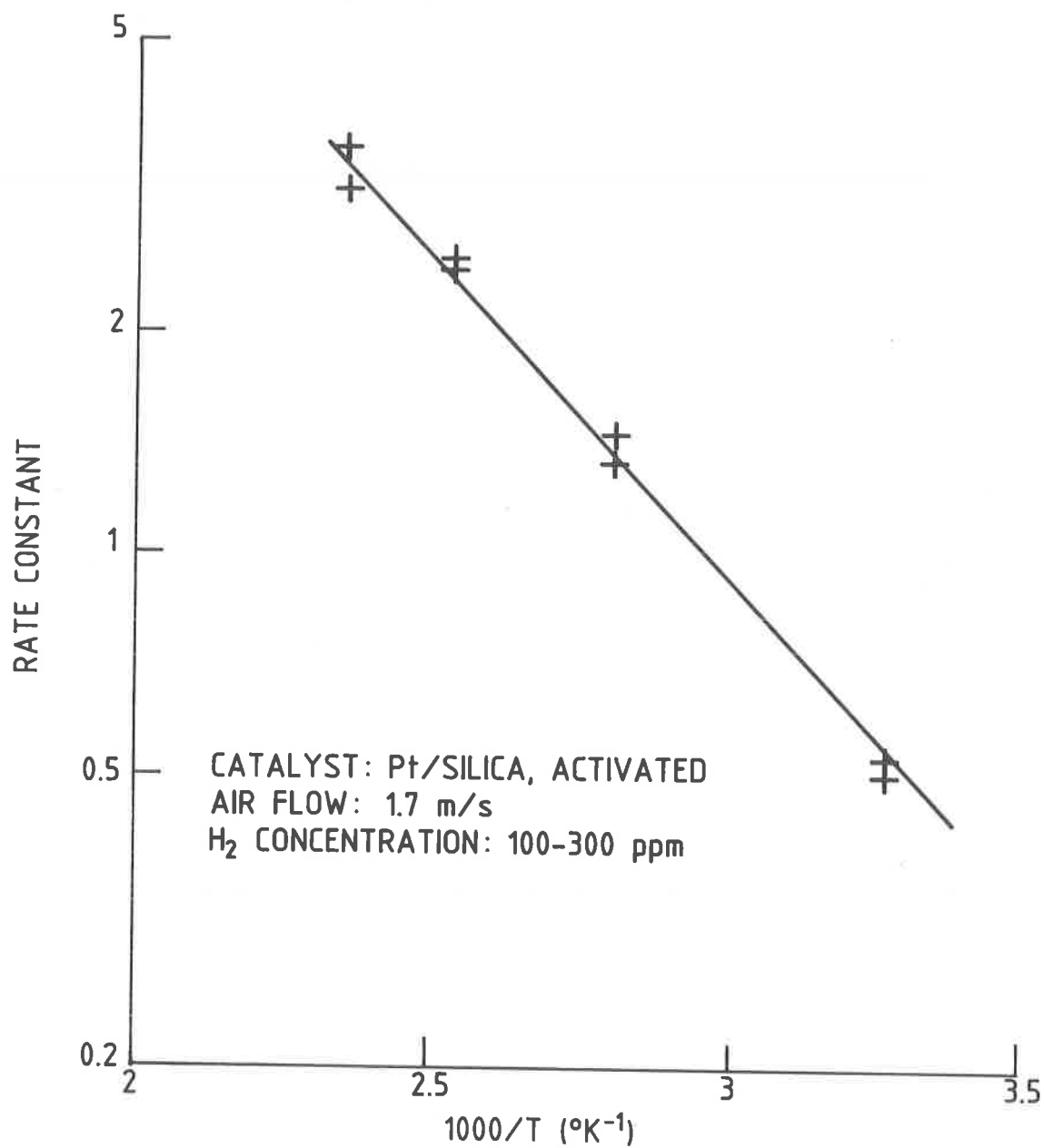
FIGURE 5   TEMPERATURE DEPENDENCE OF REACTION
RATE CONSTANT

hydrophobic catalyst support with high contact angle is the only way to ensure long term catalyst stability. This is confirmed by our study as shown in Figure 4 which indicates stable catalyst activity from the tenth day of operation up to 120 days.

The information presented in this paper is all that is required for the design of a wetproofed catalyst recombiner.

IV. Acknowledgements

The authors wish to thank D.L. Burns for carrying out the experiment, Dr. S. Suppiah for measuring the surface area and Dr. K.J. Monserrat for conducting the LRS studies.

V. References

(1) Sherwood, A.E., "Kinetics of catalysed tritium oxidation in air at ambient temperature", ACS Topical Meeting, Dayton, Ohio, April 29 - May 1 (1981).

(2) Bixel, J.C. and Kershner, C.J., "A study of catalytic oxidation and oxide adsorption for the removal of tritium from air", Proc. 2nd Envir. Prot. Conf., USAEC, WASH-1332 (1974).

(3) Boreskov, G.K., "Catalytic activation of dioxygen", Catalysis - Sci. & Tech., Ed. Anderson, J.R. and Boudart, M., Vol. 3, Springer - Verlag, 72 (1982).

(4) Golodets, G.I., "Heterogeneous catalytic reactions involving molecular oxygen", Elsevier Scientific Publishing Company, Amsterdam, 229-244, 1983.

(5) Levenspiel, O., "Chemical reactor Omnibook", OSU Book Stores, Inc., Corvallis, Oregon, Chapter 22, 1979.

(6) Tanaka, S. and Kiyose, R., "Catalytic oxidation of tritium - effect of isotopic swamping", ACS Topical Meeting, Dayton, Ohio, April 29 - May 1 (1981).

(7) Bird, R.B., Stewart, W.E. and Lightfoot, E.N., "Transport phenomena", John Wiley, New York, p.198-200, 1960.

(8) Hanson, F.V., and Boudart, M., "The reaction between H_2 and O_2 over supported platinum catalysts", J. Catalysis, 53, 56 (1978).

(9) Leder, F. and Butt, J.B., "Surface catalysis of the hydrogen-oxygen reaction on platinum at low temperatures", AIChE, J., 12, 718 (1966).

DISCUSSION

GUEST: Given the fear, that borders on paranoia, that many reactor engineers have for any halogens going into a stainless steel system because they are known to promote stress corrosion cracking, have you considered potential decomposition of the Teflon in the system under radiolysis, etc.?

CHUANG: The tritium in air is assumed to be very, very small in concentration, therefore, the radiation fear is unfounded. We did some tests on the Teflon films under radiation conditions and they can stand up to 10^8 R. Therefore, they can take many, many years of service before you have to do anything.

THOMAS: I am aware of the work that has been going on at Ontario Hydro during the last ten years that Mr. Kabat has been involved in and I am wondering if this is the same hydrophobic catalyst that he developed many years ago. Are you just refining it more for catalytic exchange processes?

CHUANG: I checked with him when we started our development, using similar catalysts for hydrogen isotope separation. Our initial objective was to use the process for production of heavy water by hydrogen isotope exchange. Now, we have changed the catalyst support so that it can react with hydrogen and oxygen. It is a continuation of the prior work, but it is not for quite the same requirement.

TRITIUM MANAGEMENT FOR FUSION REACTORS

JL.ROUYER and H.DJERASSI
CEN Saclay
CEA - IPSN - DPT
Gif-sur-Yvette

I. Introduction

To determine a waste management strategy, one has to identify first the wastes (quantities, activities, ...), then to define options, and to compare these options by appropriate criteria and evaluations.

The work is beginning for fusion wastes. Two European Associations are working together : Studsvik and CEA. CEA deals with waste treatment and tritium problems.

This paper is a contribution to fusion specific tritiated waste management strategy. It demonstrates that best strategy is to retain tritium (outgas and recover, or immobilize it) so that residual tritium releases stand to a minimum.

For that, wastes are identified, actual regulations are described and judged inadequate without amendments for fusion problems. Appropriate criteria are defined. Options for treatment and disposal of tritiated wastes are proposed and evaluated. A Tritium Recovery Solution (TRS) is described and justified.

II. Fusion waste problems

The specific problems of fusion wastes can be seen from their characteristics : heavy metallic pieces, highly tritiated and activated.

As an example, wastes coming from INTOR Torus main components are :

. Semi permanent parts constituting the toroidal vessel
- 12 segments with current breakers
  12 x 70 tonnes= 840 tonnes
- 12 segments with access ports
  12 x 80 tonnes= 960 tonnes
TOTAL : 1,800 tonnes of activated stainless stell (S.S.)

. 12 torus support, including the exhaust ducts of the pumping system
- 12 x 120 tonnes = 1,440 tonnes of activated S.S.

. Renewable blanket segments with breeding blanket
- 12 segments A
  12 x 150 tonnes = 1,800 tonnes of S.S. and
  12 x 2.5 m³   =   30 m³ Li/Pb
TOTAL : 3,000 tonnes of activated stainless steel that may contain some kg of tritium and 60 m³ of eutectic $Li_{17} Pb_{83}$

. 12 renewable divertor cassettes $\longrightarrow$ 12 x 30 tonnes = 360 tonnes of S.S. which is activated and may contain some 100 g of tritium.

Activation of stainless steel is highly dependent of the protection from neutrons flux, but, if unprotected, some pieces main get close to 1 Ci/g in Cobalt 58 and Cobalt 60.

III. Inadequacy of actual regulations and criteria

Regulations and criteria are today inadequate to cope with fusion wastes management.

Wastes should logically be disposed of according to their impact on the environment. Several disposal technologies (shallow land burial, deep seabed, geological, ...) should be adapted to various types of wastes.

But, practically, for political and sociological reasons, a solution with least environmental impact at equal cost may not necessarily be adopted, whereas the one chosen is the one best accepted by the public. Generally, "reversible" solutions are preferred ("if it were a mistake, corrective actions can be realized"), even if radiological consequences of routine operations, accidental situations, or retaking action for further storage operations than for an irreversible solution.

As a result of that situation, regulations and criteria are not homogeneous and often look inadequate for tritium problems. For example :

U.S. regulations

Existing standards that may concern fusion wastes are 40 CFR 190, 10 CFR 20, 40 CFR 141. Proposed standards are 40 CFR 191, 10 CFR 60 and 10 CFR 61.

Franch regulations

Shallow land burial regulations apply to La Hague (Centre de stockage de la Manche : CSM) disposal conditions. Tritiated waste containing more than 0.2 Ci/tonne for non embedded wastes and 2 Ci/tonne for embedded wastes, may not be accepted in similar disposal conditions as CSM.

IV. Tritium inventory and tritium releases impact

Most of the global inventory of tritium is man made and results from weapon testing. It reached a maximum of about $3,100 \times 10^6$ Ci in 1963. It has declined to $1,200 \times 10^6$ Ci around 1980, comprising about 15×10^6 Ci in the atmosphere. If there is no further weapons testing, it will get to a natural level of 70×10^6 Ci in the biosphere by the 2030, accounting for a natural production of 4×10^6 Ci/year.

The annual dose commitment from the 1980 global inventory is

3×10^{-2} mrem/year. This is to be compared to 8×10^{-2} mrem/year that the MEI (Maximum Exposed Individual) receives from 2,000 Ci/year releases of a LWR (1 GWe).

To situate tritium background in biosphere, the following values must be quoted :

Water

- MPC drinking water : 3×10^{-3} Ci/m³
- Detection threshold of tritium in water by liquid scintillation : 1×10^{-6} Ci/m³
- Tritium content in waters of Paris area : $10^{-5}/10^{-6}$ Ci/m³

Air

- MPC public : $2 \cdot 10^{-7}$ Ci/m³
- Tritium content in Paris area : $10^{-9}/10^{-11}$ Ci/m³

V. Choice of a strategy

According to technologies available or which could be developed for NET (Next European Torus) several options are examined with account of all aspects of feasibility, cost, impact on the environment, ...

First, possible operations will be described. Then, options with or without tritium treatment will be evaluated. Last, surface and deep disposal options will be compared.

Description of possible operations

Size reduction. It will be necessary for any option to reduce the size of waste components to pieces of less than 10 tonnes. This will be done, either by dismantling, if design favours this solution, or by cutting ; cutting will raise more problems (costs and pollution) than dismantling. Anyhow, this operation will necessitate a hot cell fully remotly operated. At this stage also, it could be interesting to separate metal parts with different tritium contents (for example by cutting highly tritiated layers if they exist).

Processing. Two management schemes are possible after size reduction : processing of wastes to limit tritium problems afterwards, or not processing. Processing can be done by recovering tritium (heating or fusion) or by immobilizing it (spraying or isotopic process). Both types or operations have similar orders of magnitude of costs (hot cell with robots), though immobilization is probably less costly than recovery, but, when tritium content is high, benefit for tritium recovered renders preferrable this option. Studies and experiments are going on to define the feasibilities and efficiencies of the processing option.

Conditioning (packaging). If processing is applied, waste conditioning will be easier and less costly as will also transportation to an intermediate storage facility.

Intermediate storage. Even if wastes are so activated that surface storage is not possible, there should be intermediate storage where tritium releases and occupational doses must be kept within acceptable limits. This surface storage could be the final disposal, if activation levels permit. Anyhow, also if wastes have not been processed, engineering of that storage facility must be such as to costly when tritium release rate gets high.

Disposal. Size reduction and packaging are necessary for any option, but, after these operations, some straightfoward disposal management schemes are possible, such as deep geological disposal or seabed repositories, these deep disposal anyhow will be necessary if activity levels surpass recommended limits for surface disposal.

Comparison of tritium treatment options

The analysis is made for a chain of management operations concerning 300 tonnes/year of metallic wastes with tritium content varying from 0.1 Ci/g to 1 mCi/g or less.

The options schematized are the following :
- size reduction → tritium recovery → packaging → surface disposal
- size reduction → tritium immobilization → packaging → surface
- size reduction → packaging → surface disposal   disposal

Evaluations are based on a summary design of a facility, prepared by TECHNICATOME, which has quoted investments.

Orders of magnitude of costs give trends for preliminary choices. In the comparison, annual operating costs have been taken as 1/10 of capital costs (2/3 of annual capital costs actualized over about 20 years) for active (processing) operation and 1/20 of capital costs for passive (surveillance) operations.

Table 1. Comparison of tritium treatment options

OPERATIONS OPTI.		SIZE REDUCTION	PROCESSING	PACKAGING	SURFACE DISPOSAL	TOTAL
1	Inv^t	5.0	7.0	2.5	2.5	17.0
	$a = \text{oper. } y^{-1}$	0.5	0.7	0.25	0.12	1.57
	$(a + \text{cap.})\text{cost}$	0.75	1.05	0.37	0.25	2.42
2	Inv^t	5.0	5.0	2.5	2.5	15.0
	$a = \text{oper. } y^{-1}$	0.5	0.5	0.25	0.12	1.37
	$(a + \text{cap.})\text{cost}$	0.75	0.75	0.37	0.25	2.12
3	Inv^t	5.0	0	5.0	2.5 + Det.	12.5 + Det.
	$a = \text{oper. } y^{-1}$	0.5	0	0.5	0.12+ Det.	1.12 + Det.
	$(a + \text{cap.})\text{cost}$	0.75	0	0.75	0.25+ Det.	1.75 + Det.

(Column header: COST (M.\$. 1983))

Some conclusions, which can be drawn from this table, are :

Processing or not processing. The answer to that question depends on cost of detritiation, (if it is necessary), for surface storage must be detritiated, this costs could be a much as 2.5 to 5 M$ (for 2,000 to 10,000 m³/h) in capital costs and 0.25 to 0.5 M$ as operation costs. Option 2 gets then preferable. Further detailed analysis must be performed to estimate design and costs for surface disposal more precisely, but is seems, as a first approximation, that over 100 Ci/tonnes, releases would be too high to avoid expensive atmospheric treatment systems except if storage is of short duration, which means that investments can be amortized on a larger flow of wastes.

Tritium recovery or immobilization. Cost difference between options 1 and 2 is about 0.25 M$. Supposing that price for 1 curie of tritium is 1 $, option.1 would become interesting as soon as about 300,000 Ci are recovered. This situates the economic threshold for tritium recovery at over 1,000 Ci/tonne.

Comparison between surface and deep disposal options

Surface and deep disposal options must be compared on the basis of both criteria of cost and doses to workers and the environment. This should comprise all operations, including mateirals shipment.

For doses, limits are recommended for maximum concentrations of radionuclides in waste for near surface disposal. These limits are based on evaluations of transfer to man, accounting for radioactive decay, confinement of disposal, waste characteristics, atmospheric and aquatic pathways, ...

For USA, regulations from NRC (10 CFR Part 61) give the following maximum concentrations for some fusion relevant radionuclides :

Maximum concentration of radionuclides in waste for near surface disposal

RADIONUCLIDE	CONCENTRATION (Ci/m^3)
H.3	40
Ni 59 in activated metal	700
Nb 94 in activated metal	220
Te 99	0.2
	3

For tritium, the limit expressed in Ci/m^3 does not look appropriate, because it is release rate which is in fact important. If a given maximum release rate can be guaranteed, tritium content is not meaningful (if tritium is well implanted in the metal, releases are small - this is where immobilization technologies are interesting).

If limits are surpassed, deep disposal or better containment should be adopted. Two solutions are possible : underground or cases :

. in countries with dense populations or with scarce appropriate geologic sties

. when tritium leakages are high enough to find pathways to the
surface

A further detailled analysis of costs and pathways for geologic
or seabed disposals is then interesting to perform. A question which
must be raised at this stage of the discussion in whether deep
disposal can be cheaper than surface disposal.

As shown in the table of paragraph "Comparison of tritium
treatment options", the range of costs for 300 tonnes/year is
situated between 1.75 and 2.1 M$. The deep disposal options would
bear anyhow costs of size reduction and packaging, which are about
1.5 M$.

Additional costs for surface disposal are then from 0.25 to
0.75 M$ for 300 tonnes/year, which equals about between 1,000 $ to
2,500 $ per m^3 and per year.

According to estimates which circulate in FRANCE, deep geologic
disposal would cost around 12,500 $/$m^3$. As costs for surface disposal
options have been amortized over 20 years, it is not clear that
surface disposal is cheaper when tritium content of the wastes is of
medium level (However, estimate of 12,500 $/$m^3$ does not include
surveillance costs).

In that case, it may appear that seabed or deep geologic
disposals are cheaper than surface disposals. Here also, more
detailed evaluations would be interesting.

VI. Conclusion

It appears from this first analysis that two types of thresholds
may be defined for the activity in the wastes.

Tritium thresholds

- over a threshold which may be around 1,000 Ci/tonne, it looks
  better to recover tritium
- between 100 Ci/tonne and 1,000 Ci/tonne, immobilization and deep
  disposal could be competitive
- below 100 Ci/tonne, surface storage with some immobilization looks
  acceptable

Activated products thresholds

- over concentrations such as about 1,000 Ci/m^3 of Cobalt 60, which
  will be further analyzed, activated products should be disposed of
  in deep repositories

Aknowledgments

DISCUSSION

LAMBERGER: How will you reduce the size of the large,
heavy components? How will you capture the tritium released during
size reduction? How will you remove the tritium from the large, heavy
pieces?

DJERASSI: When design allows it, large and heavy components
may be dismantled in a hot cell by fully remote operations. When
this solution cannot be used, such components should be cut, either
in ventilated (with a detritiation system) hot cells or in a water
pool. Again, operation must be conducted with help of robots.   The
tritium release will be captured either by the detritiation system,
as a first option, or in tritiated water, for a second one. As I
have said before, to remove tritium out of large pieces, we have to
reduce their weight to a value lower than 10 tons. Then, depending
on tritium content, we must heat or fuse. The efficiency of the
heating process is a function of depth of tritium penetration inside
the metals, and, of course, of the choosen temperature range.
Experiments are being performed by C.E.A. to define what is the
best and the cheapest option.

HEBEL: Is the tritium activity associated with fusion
reactor heavy waste materials the dominant activity which should
determine the route of waste disposal?

DJERASSI: The answer depends strongly on what kind of
components we consider. For pieces close to the neutron flux (for
instance, first wall) it is clear that activated products (Co^{60}, Co^{58},
etc.) give rise to dominant activity. For these, deep disposal will
be necessary. On the other hand, many components have their activity
dominated by their tritium content; for instance, blanket modules.
Depending upon the shielding options choosen, many other components
may be dominated by tritium contamination. However, we have focused
our attention on specific problems raised by fusion reactors, in
addition to the more well-known ones.

DEVELOPMENT OF A METHOD TO DETERMINE
IODINE SPECIFIC ACTIVITY IN PROCESS OFF-GASES
BY GC SEPARATION AND NEGATIVE IONIZATION
MASS SPECTROMETRY

S. J. Fernandez, R. A. Rankin, G. J. McManus, and R. A. Nielson

Westinghouse Idaho Nuclear Co.
Idaho Falls, Idaho

ABSTRACT

This paper documents the development of a method for determining the iodine specific activity emitted from a nuclear fuel reprocessing plant. The technique includes cryogenic sample collection, chemical form separation, quantitation by gas chromatography and specific activity measurement by negative ionization mass spectrometry. The major conclusions were that both organic and elemental iodine can be quantitatively collected without fractionation and that specific activity measurements as low as one atom of ^{129}I per 10^5 atoms of ^{127}I are possible.

I. INTRODUCTION

Receptor models that predict the environmental impacts of ^{129}I releases from fuel reprocessing plants assume the ^{129}I is undiluted with stable iodine and in a chemical form most damaging to the target organism (usually man). Although this assumption will present a conservative limit for ^{129}I releases, it could require unnecessary control equipment.

Thyroid dose calculations for ^{129}I releases from DOE facilities are conservative by several orders of magnitude because the dose rate calculation considers only the actual amounts of the radionuclide in the body instead of an assumed state of equilibrium between stable and radioactive isotopes.[1] The conservativeness of this assumption is apparent when one considers the ^{129}I thyroid burden of 3 µCi (18 mg ^{129}I) exceeds the total iodine inventory for a standard thyroid (8 mg I).[1] Nevertheless, thyroid dose factors based on this assumption are used to assess the thyroid dose from ^{129}I releases. Assuming 1/16 of all ^{129}I inhaled will be incorporated into the thyroid and eliminated from the body with a biological half-life of 138 days,[1] one derives a thyroid dose factor of $1.5 \times 10^{10} \frac{\text{rem} \cdot \text{m}^3}{\text{Ci} \cdot \text{y}}$. This dose factor has been incorporated into the dose factor file of ALLDOS.[2] ALLDOS and the computer codes on which it was based, DACRIN[3] amd PABLM[4], were used extensively for preparing environmental dose estimates for the Low Level Waste Program at Hanford.

Rather than the 8 mrem/Ci released (maximum individual thyroid dose) predicted by the ALLDOS program for the Hanford site, a much lower dose would have been calculated if the uptake of ^{129}I was adjusted to allow for the stable ^{127}I diluting the ^{129}I at the release point. The purpose of the work described in this report was to develop a technique for measuring the specific activity of ^{129}I releases (or the amount by which the ^{129}I has been diluted by ^{127}I).

To date, the measurement of the specific activity of the ^{129}I emitted from fuel reprocessing plants has been limited by several factors:

1) inability to separate ^{129}I chemical species without contamination with stable ^{127}I;

2) inability to measure very low ^{129}I specific activities due to poor mass spectrometric ionization efficiencies (<< 1%);

3) inability to collect and manipulate small ^{129}I samples in the vicinity of ^{129}I sources (such as a nuclear fuel reprocessing plant) without contamination with either stable or radioactive iodine.

This study sought to develop a sampling technique that would allow the quantitative measurement of iodine specific activities. The conceptual design of this technique is shown in Figure 1. As can be seen by Figure 1 the sample is first dried to remove any interference by H_2O before collection. The sample is then split to allow total iodine species and concentration determination by GC and also ^{127}I/^{129}I ratio measurements by mass spectrometry. In order to develop this sampling technique the following approaches had to be evaluated.

1) Demonstration of the accurate measurement of ^{127}I/^{129}I standards by negative surface ionization;

2) Demonstration of a gas chromatographic technique to quantitate and separate the iodine in a form suitable for negative ionization mass spectrometry.

3) Demonstration of the ability to collect an unfractionated ^{129}I sample;

4) Demonstration of an integrated gas chromatography/negative ionization mass spectrometry method to accurately measure specific activities under simulated off-gas conditions.

The results of each step are described in the following sections.

II. MASS SPECTROMETRY DEVELOPMENT

The objectives of the negative ionization mass spectrometry development work were to determine if newly developed ionizers could be used without modification to measure iodine isotopic ratios greater than 10^4, and to determine what types of problems are encountered in the measurement of wide ratio iodine isotopics. Since a complete and detailed discussion of this work has already been published[5], only a brief summary will be presented here.

All mass spectrometric measurements were made on a tandem mass spectrometer, a two-stage instrument equipped with a dual detector system (Figure 2). There are differences between using the tandem mass spectrometer to measure iodine by negative surface ionization, and using the "normal" positive ion mode of operation. Specially prepared porous lanthanum hexaboride (LaB_6) filaments, described elsewhere[6], are used as ionizers. About 3 μg of AgI is dried from the NH_4OH solution on tantalum side filaments and mounted in a standard
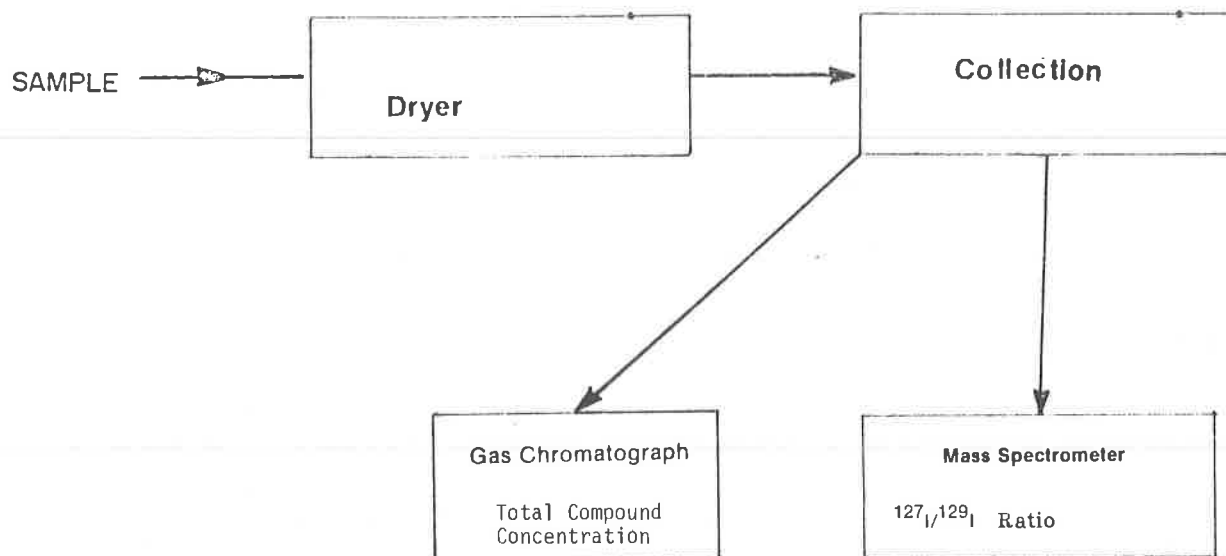
Figure 1. Conceptual Sampling Technique

ICPP-A-9060
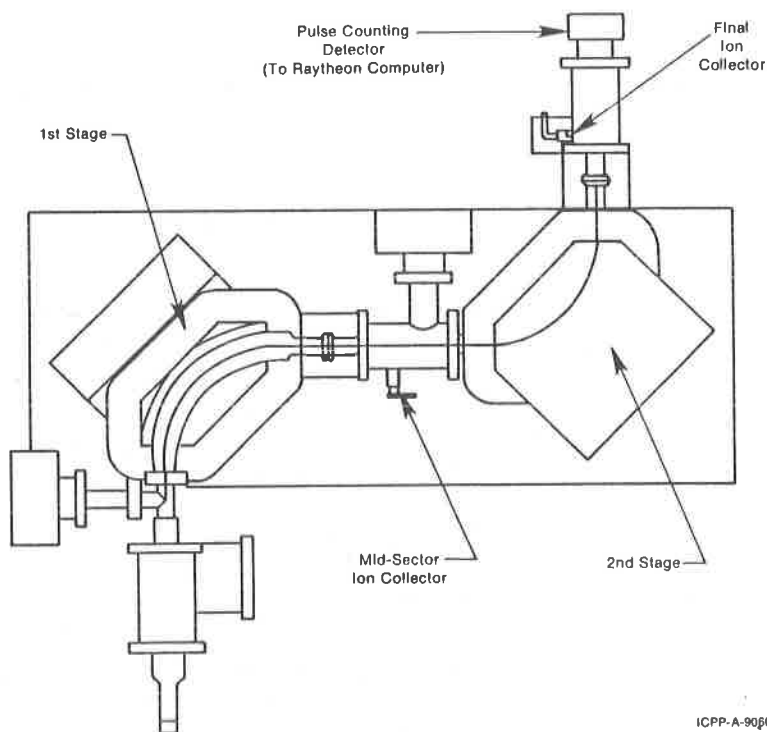
Figure 2. Tandem Mass Spectrometer Magnet and Detector Arrangement

AVCO triple filament arrangement.[7] The ionizing filament is operated at 900-1000°C, or at filament currents from 1.5 to 2.4 amps. With the magnet sectors energized to approximately 5150 gauss, the region was scanned around -9820 volts accelerating potential. This combination of parameters is used to achieve an I⁻ beam strength the equivalent of up to 1.6×10^9 counts in 20 seconds for a 3 microgram sample loading.

Both detectors must be used to make measurements at wide-ratios. The pulse counting detector system consists of an EMI type electron multiplier housed within the mass spectrometer vacuum envelope and connected to an EG&G/Princeton Applied Research amplifier/pulse discriminator unit. The signal from the amplifier/discriminator is fed to a Monsanto 10 MHz counter and then to a 32 KByte Raytheon RDS-500 minicomputer system. This detector system is sensitive to a few thousand atoms of iodine and is used to measure the smaller 129 peaks.

The 127 peaks are measured using a Faraday ion collector located between the two magnetic sectors. The ion collector consists of a collector plate which is within the vacuum envelope and connected to a Keithley 642 FET electrometer. Data are output to a strip chart recorder.

To use both detectors, the relationship between them must be known. This calibration factor was determined by making 12 measurements of a single peak using both detector systems and then equating the output signals to define the relationship. The results of the detector calibration of the pulse counting detector system yielded 2131 ± 263 (1σ) counts per second for each division on the chart produced by the Faraday ion collector system.

To demonstrate the applicability of the measurement technique, the stock solution (127/129 = 590) was analyzed using the pulse counting detector system alone. Subsequently, the 10^5 and 10^7 standard blends were analyzed using both detectors. In making this type of measurement, the 129 mass was measured using the pulse counting detector; the retractable ion collector plate was then inserted, the magnet moved to the 127 mass, and the 127 signal measured with the Faraday ion collection system. The magnet was then returned to the 129 mass, the Faraday system retracted, and the process repeated. This sequence, and the ion collector data processing are done manually. Measurements were made at a number of scale factors, count rates, and percent of scale levels to determine if any effects would be observed from possible differences due to varying counter efficiencies or different ranges.

The stock solution (127/129 ratio of 590), was measured as 590 ± 4.5 using the pulse counting system alone. This demonstrates that iodine at this ratio can be measured accurately and with high precision.

The 10^5 standard, having a makeup value of 4×10^5, was measured as (4.0 ± 0.76) $\times 10^5$ overall, or (3.7 x ± 0.32) $\times 10^5$ with filament 1 deleted. For filament 1, these measurements ranged from 3.3×10^5 to 5.1×10^5. The data presented here clearly demonstrate that ratios on the order of 10^5 can be measured with an accuracy and precision of better than 20%. The 10^5 ratio measurements are summarized in Table I.

TABLE I

10^5 RATIO SUMMARY

Filament	Mean Ratio	Standard Deviation
1	5.1×10^5	2×10^5
2	3.8×10^5	0.45×10^5
3	3.3×10^5	0.19×10^5
4	3.9×10^5	0.64×10^5
Mean of 4 filaments	=	$(4.0 \pm 0.76) \times 10^5$
Mean after deleting filament 1	=	$(3.7 \pm 0.32) \times 10^5$

The results from the measurements of the 2.5×10^7 ratio blend were highly variable and deviated from the nominal value by greater than an order of magnitude. The results from these measurements are summarized in Table II.

The variability of the 10^7 ratio measurements is thought to be a result of two conditions: 1) The ionizing filaments may have been contaminated with a small amount of iodine; 2) Iodine from the analysis was being deposited on the molybdenum ion lens plates inside the mass spectrometer which would then reevaporate during the next analysis, causing an error in the results. A summary of the results of this study is given in Table III.

The conclusions drawn from the first part of this study were:

1) The newly developed ionizers can be used to measure iodine isotopic ratios equal to approximately 10^5 with a precision and accuracy better than 20%.

2) The major problem associated with the measurement of wide isotopic ratios is thought to be due to iodine contamination effects.

After the successful development of a technique to measure isotopic ratios up to 10^5, a study was performed to measure the minimum amount of iodine that must be delivered to the mass spectrometer to accurately measure a $^{127}I/^{129}I$ ratio of 10^4. To determine this amount, a standard blend with a ratio of 8×10^3 was loaded in decreasing amounts and the ratio measured as a function of filament loading. The results are shown in Table IV.

From these results a criteria of 80 ng I delivered to the mass spectrometer was used as the objective of the gas chromatography development described in the next section to assure 10^4 ratios with a precision and accuracy better than 25%.

TABLE II

10^7 RATIO SUMMARY

Filament	Mean Ratio	Standard Deviation
1	0.400×10^7	0.021
2	0.047×10^7	0.046
3	0.20×10^7	0.23

Mean of 3 filaments $= (0.096 \pm 0.090) \times 10^7$

TABLE III

SUMMARY OF MEASUREMENTS

Stock Solution	Nominal Value	=	590
	Measured Value	=	590.6 ± 4.5
Blend 1	Nominal Value	=	4×10^5
	Measured Value	=	$(3.7 \pm 0.32) \times 10^5$
Blend 2	Nominal Value	=	2×10^7
	Measured Value	=	$(0.096 \pm 0.090) \times 10^7$

TABLE IV

ISOTOPIC RATIO MEASUREMENTS AS FUNCTION OF FILAMENT LOADING

Filament Loading (ng l)	Measured Isotopic Ratio
9000	9.3×10^3
2000	9.1×10^3
800	9.5×10^3
80	1.0×10^4
16	1.2×10^4
10	1.9×10^4
8	1.4×10^4
1	2.6×10^4

III. GAS CHROMATOGRAPHY DEVELOPMENT

The development of a gas chromatography (GC) method to measure organic and elemental iodine was done in two phases. The first phase used solutions containing different iodine chemical species and determined the optimum operating conditions. The second phase was performed using representative gaseous forms of iodine species to measure minimum detection limits and response.

3.1   Chromatography of Iodine Solutions

Castello, et al.[8], published the gas chromatographic separation and identification data of several alkyl iodides using glass columns filled with tricresyl phosphate on DMCS-treated Chromosorb W. Castello, et. al.[7] also proposed a homologous series of iodoalkanes as a reference for the calculation of the retention indices of ECD-sensitive substances. Corkill and Giese[9] used fused silica capillary columns coated with either SE52 or SE54 to analyze the iodothyronines. The analysis of I_2 by GC-ECD is more difficult than the analysis of organic iodides because I_2 is less volatile and more reactive than organic iodides.

In this study, the analysis of I_2 by GC-ECD was investigated as a function of detector, injector, and column temperatures. The calculated retention indices were compared to the results of Patte, Echeto, and Laffort[10].

Analysis of iodine compounds were performed with a Varian Model 3700 gas chromatograph equipped with a ^{63}Ni electron capture detector (ECD). Due to the reactivity of I_2 two non-polar liquid phase columns were used: a 30 cm x 0.3 cm stainless steel column of 10% OV-101 on Chromosorb W-HP 80/100 mesh obtained from Varian Instrument Group (Palo Alto, CA); and a 300 cm x 0.3 cm nickel column of 5% SE-30 on Chromosorb W-HP, 80/100 mesh obtained from Alltech Associates (Arlington Heights, Ill.). All experiments were performed using a 30 cm^3/min flow with N_2 or 90% Ar/10% CH_4 carrier gas. The column was operated isothermally at 100° C for the retention index experiments.

Methyl iodide, ethyl iodide, 1-iodopropane, and 2-iodopropane were obtained from Aldrich Chemical (Milwaukee, WI) and were used without further purification. The toluene, benzene, and cyclohexane were distilled-in-glass grade obtained from Burdick and Jackson (Muskegon, MI) and used without further purification.   The elemental iodine used was resublimed grade obtained from Fisher Scientific (Pittsburgh, PA).

Alkyl iodide solutions were prepared by volumetric dilution: the I_2 solutions were prepared by weighing I_2 crystals to better than $\pm$ 0.1 mg, dissolving the crystals in toluene or cyclohexane, and preparing subsequent serial dilutions volumetrically.

3.1.1   Retention Index. The retention index of I_2 was determined in the manner of Castello, et al.[8] and Patte, et al.[10] at 100°C for both OV-101 and SE-30 by comparing the retention time of the I_2 peak with methyl iodide, ethyl iodide, 2-propyl iodide, 1-propyl iodide, benzene, toluene, and cyclohexane on the OV-101 column; with methyl iodide, 1-propyl iodide and cyclohexane on the SE-30 column. The I_2 peak was identified by comparing the chromatograms of blank solvents with serial additions of a 13 mg/L I_2 standard solution. I_2 was then assigned to the peak that increased in area in proportion to the amount of added I_2.

1324

Plots of reduced retention time versus retention index for the two column types are shown in Figures 3 and 4. From these plots, a retention index on OV-101 of 172 ± 14 for the alkyl iodide homologous series and 510 ± 42 for the n-alkane homologous series was calculated. For SE-30, a retention index of 160 ± 16 for the alkyl iodide homologous series and 500 ± 52 for the n-alkane homologous series was calculated.

3.1.2   Resolution. The height equivalent to an effective theoretical plate (HEETP) was calculated using the equation:

$$HETP = \frac{L}{5.54 \left(\frac{t_R'}{W_{1/2}}\right)^2}$$

where: L is the length of the column;

t_R' is the reduced retention time;

$W_{1/2}$ is the full width at half maximum of the I_2 peak.

At 100°C the HEETP for I_2 was 1.1 mm for OV-101 and 39 mm and for SE-30. This was significantly less resolution than reported by Castello, et al.[8] who reported HEETP for alkyl iodides 0.4-0.5 mm. The poorer efficiency may be caused by the greater reactivity of I_2 compared to the alkyl iodides. However, the I_2 peak was sufficiently resolved from CH_3I and CH_3CH_2I for analysis. Despite poorer resolution, the SE-30 column was the column of choice because it was more resistent to degradation by the iodine solutions.

3.1.3   Sensitivity. A plot of ECD response versus quantity of I_2 injected is shown in Figure 5 (column SE-30; temperature 130°C). From this plot, a detection limit of ∿39 ng I_2 was calculated. The ECD response was then studied as a function of injector temperature (Figure 6), column temperature (Figure 7) and detector temperature (Figure 8).

From Figure 5 it appears the sensitivity of the GC-ECD technique is independent of injector temperature in the range of 190 to 220°C; there is no increase in sensitivity above 220°C and sensitivity decreases with decreasing temperature below 190°C. This decrease in sensitivity may be caused by peak broadening from slower vaporization of the solvent in the injector.

The mechanism of the ECD response to I_2 was studied by dividing the I_2 response by the response of a reference compound such as 1-iodopropane[8],[11] or chlorobenzene[12]. The results of simultaneous measurements of the I_2 to 1-iodopropane and I_2 to chlorobenzene ratio are plotted in Figure 8. The I_2 to chlorobenzene ratio first increases (indicating a non-dissociative capture mechanism at high temperatures) and then decreases (indicating a dissociative capture mechanism at low temperatures). Yet, because it is highly unlikely that a dissociative mechanism would be replaced by a non-dissociative mechanism at higher temperatures, there must be another explanation. Corkill and Giese[9] also observed a peak in the response versus reciprocal detector temperature plot for the iodothyronines. They attributed the decreasing response that accompanied increasing temperature to decomposition of the iodine compounds on the narrow
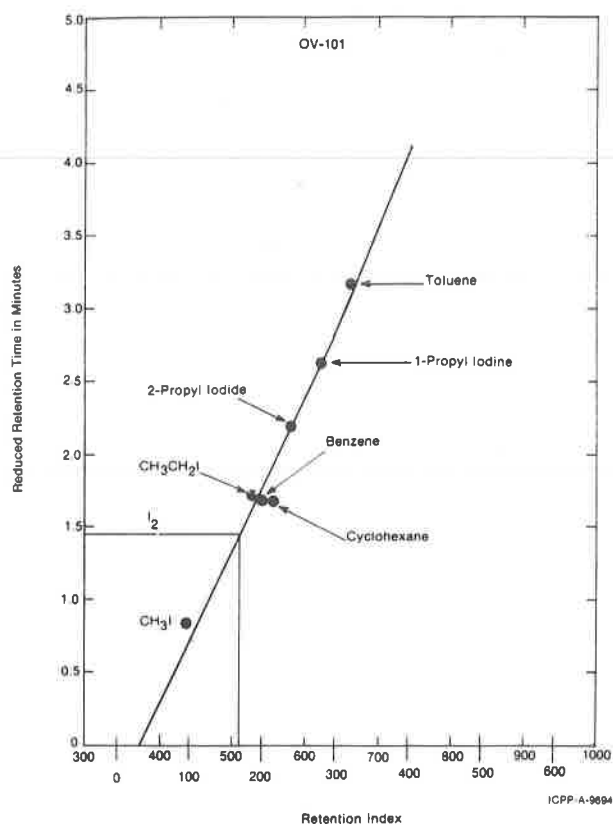
Figure 3. Reduced Retention Time vs. Retention Index for the OV-101 Column
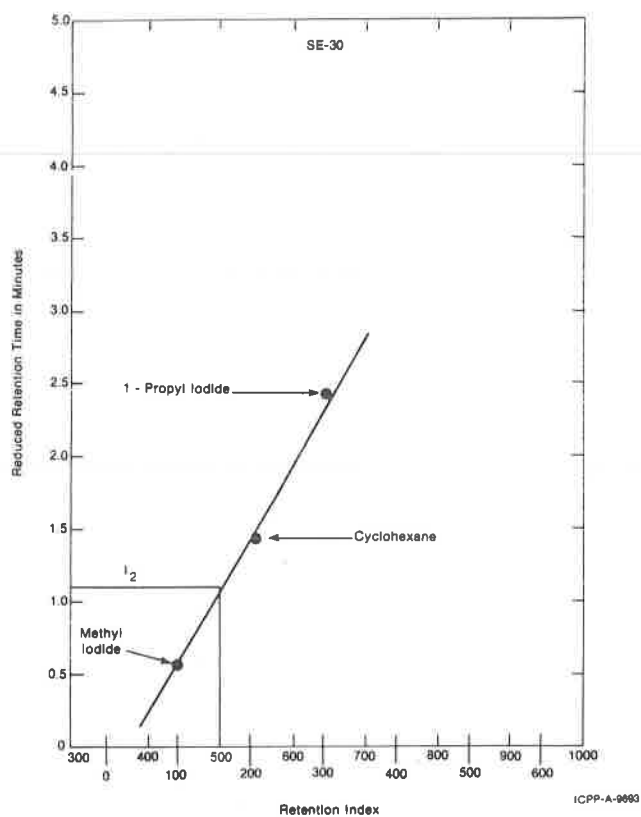
Figure 4. Reduced Retention Time vs. Retention Index for the SE-30 Column
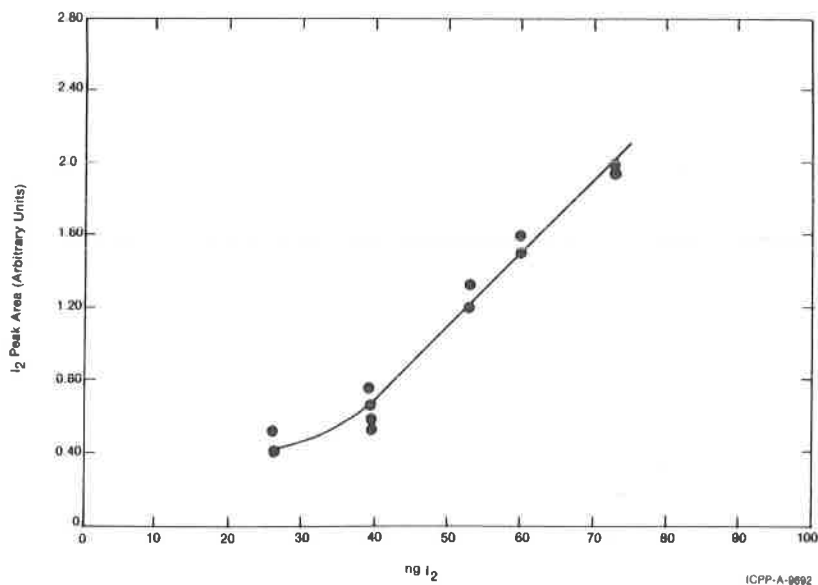
Figure 5. Typical Calibration Curve for I_2 on the SE-30 Column
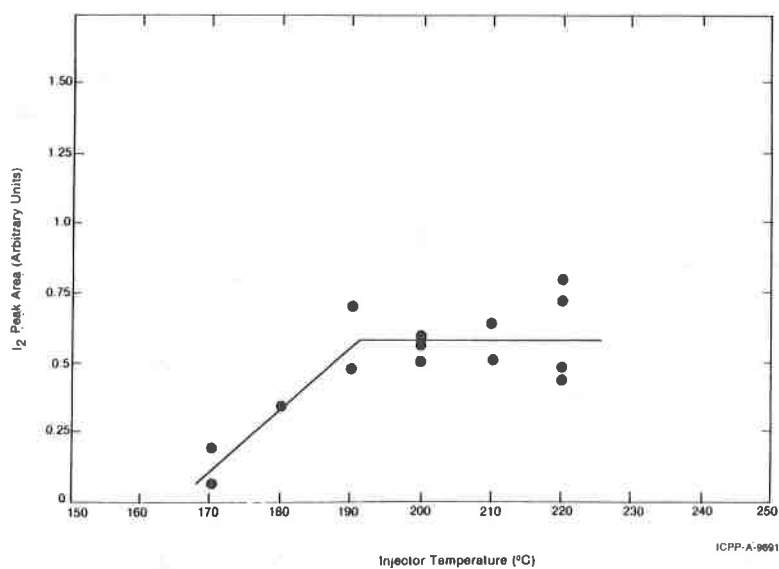
Figure 6. I₂ Response as a Function of Injector Temperature
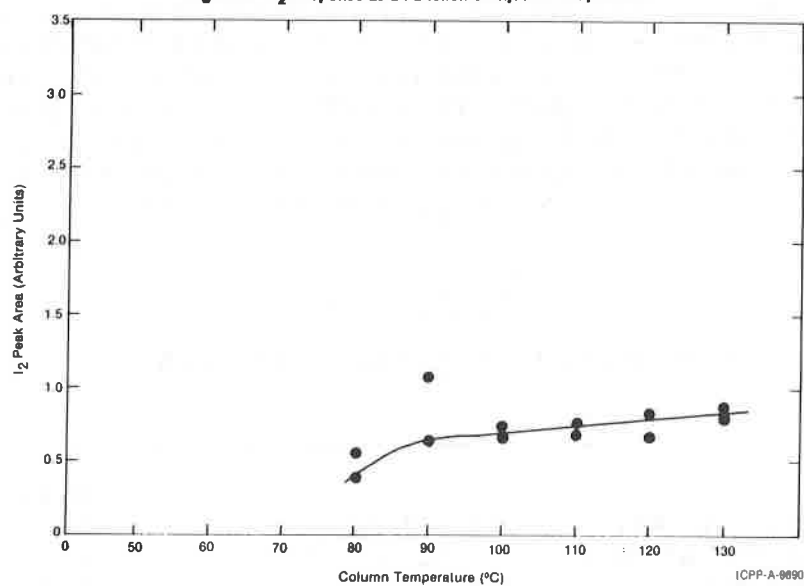
Figure 7. I₂ Response as a Function of Column Temperature
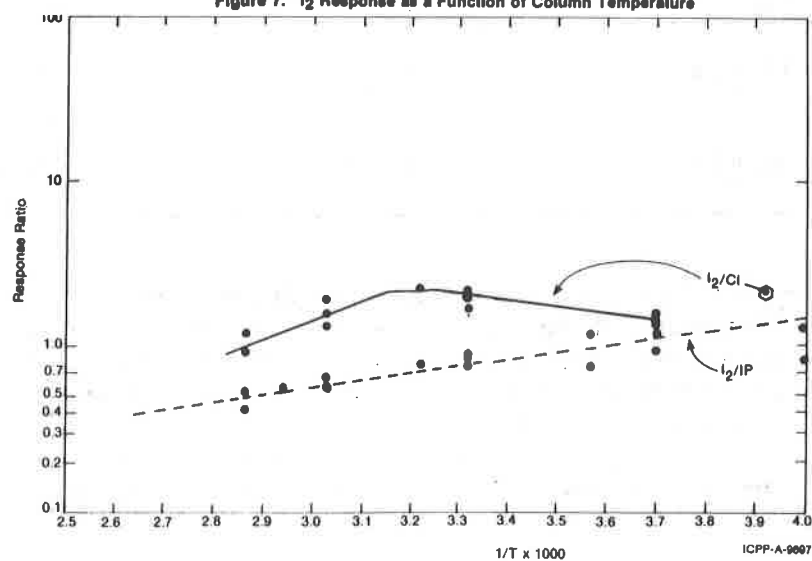
Figure 8. Response Ratio of I₂ to Chlorobenzene and I₂ to Iodopropane as a Function of Reciprocal Detector Temperature

1327

bore glass inlet and on the stainless steel and ceramic in the electron capture detector before the iodine compounds reach the collector region. This effect was also observed by Miller and Grimsrud[13].

This explanation is supported by the I_2 to 1-iodopropane ratio, which decreases monotonically with increasing temperature. Because the 1-iodopropane would also undergo decomposition; one would not expect a maximum in the I_2 to 1-iodopropane ratio. Because I_2 is more reactive than 1-iodopropane, this decomposition would decrease the I_2 to 1-iodopropane ratio as the detector temperature is increased. For these reasons, it appears likely that a dissociative mechanism is responsible for the ECD response to I_2.

A tracer experiment then was performed that confirmed that I_2 was not converted to an organic iodide in the injector or on the column and also measured the transmission efficiency of the column and injector. I_2 in toluene and cyclohexane was traced with ^{125}I. The effluent of the column was routed to an iodine species selective adsorbent sampler in the manner of Keller, et al.[14] The amount of ^{125}I injected and collected by each selected adsorbent was measured by direct x-ray spectrometry of the 27 kev Te Kα x-ray using a hyperpure germanium low energy photon spectrometer. Collection periods corresponded to the time required to produce a chromatogram. The results of these experiments are shown in Table V. From these results, it appears that significant conversion of the I_2 did not occur either in the injector or on the column. In addition, more than 80% of the I_2 injected onto the column eventually reached the detector.

TABLE V

^{125}I TRACER EXPERIMENT RESULTS

Solvent	Fraction of Total Iodine That Reached Detector (%)	Fraction of Transmitted Iodine Found as I_2 (%)	Fraction Transmitted Iodine Found as Organic Iodide (%)
Cyclo-hexane	81 $\pm$ 10	99 $\pm$ 2	1 $\pm$ 2
Toluene	88 $\pm$ 10	90 $\pm$ 2	10 $\pm$ 2

3.1.4 Demonstration. The applicability of the developed GC technique was demonstrated by analyzing an AgI in concentrated NH_4OH mass spectrometric standard. This standard was stored in a stoppered polypropylene test tube. The samples were traced by adding ^{125}I to the samples and allowing the radioiodine to exchange isotopically overnight. Two 1 mL aliquots of the solution were rapidly acidified to pH ∿2 with HNO_3. The nitric acid was covered with a 10 mL layer of toluene at all times to prevent I_2 volatilization losses. One mL of saturated

$NaNO_2$ was added to oxidize any free I^- to I_2; the resulting I_2 was extracted into the toluene. Three microliters of the toluene was injected onto the GC to measure the I_2 formed; while 1 mL of the toluene was counted with a hyperpure germanium low energy photon spectrometer to determine the chemical yield.

Typical gas chromatograms are shown in Figure 9. The results of these analysis are shown in Table VI. The precision of triplicate determinations was 12% at one standard deviation. Although the determinations were within the 95% confidence interval, the analyses were 23% higher than the nominal make up value. The cause of this bias is unknown. However, one possible explanation is the sample was concentrated by permeation through the polypropylene test tube. Based on these results, it appears the technique has an accuracy of less than 23% and precision of 12% at the one standard deviation level.

TABLE VI

AgI ANALYSIS RESULTS

Makeup Value ($\mu g\ I/mL$)[a]	Aliquot 1 ($\mu g\ I/mL$)[a]	Aliquot 2 ($\mu g\ I/mL$)[a]
118	157 ± 38	133 ± 32

[a] $\pm 2\sigma$ as determined by precision of triplicate analysis.

3.2 Chromatography of Gaseous Iodine Compounds

The objectives of the gas chromatography development of gaseous compounds were two fold:

1) Using the determined gas chromatographic conditions, determine detection limits, precision and accuracy of gas phase CH_3I and I_2.

2) Demonstrate the ability to prepare separate CH_3I and I_2 fractions for the mass spectrometric specific activity measurement.

The apparatus used to introduce gaseous samples is shown in Figure 10. Helium carrier gas was directed through a sample bomb or over a permeation tube to generate the required iodine gas phase concentration.

The carrier gas was either directed through a capillary splitter or directly to the eight port valve, depending on the objective of the experiment. The iodine gases were frozen out in a $0.25\ cm^3$ sample loop with liquid N_2 and the He carrier gas exhausted through a vacuum pump. To measure higher levels of CH_3I, syringe
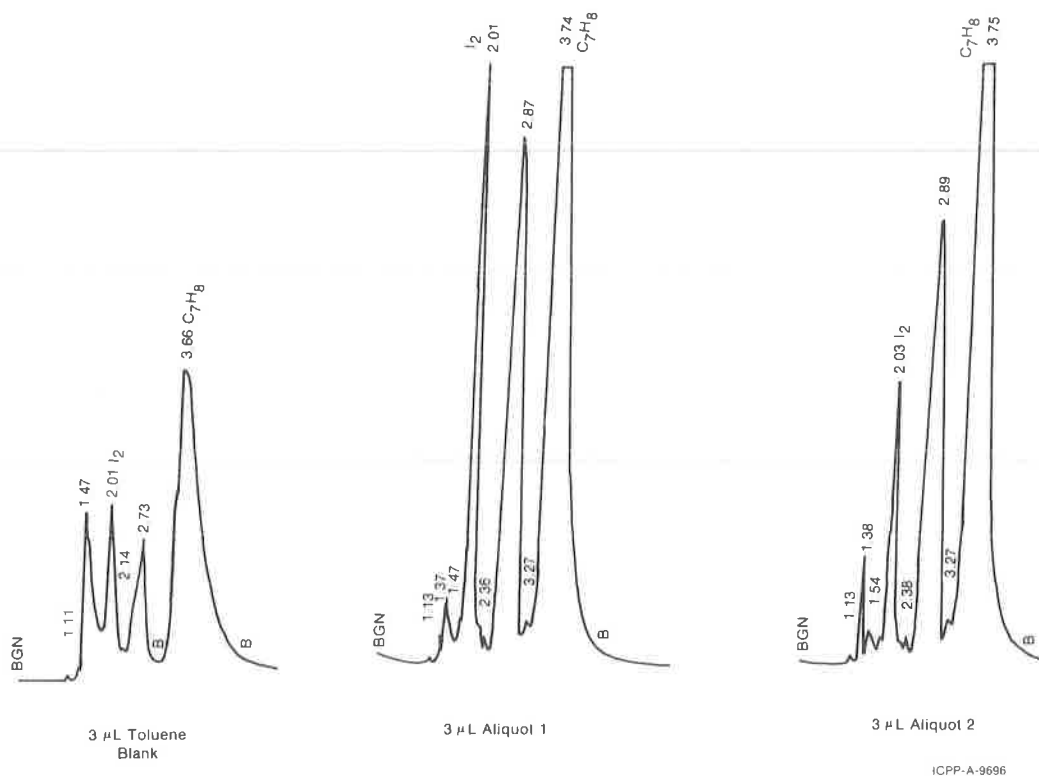
Figure 9. Typical Chromatograms of I_2 Extraction of Mass Spectrometric Standard
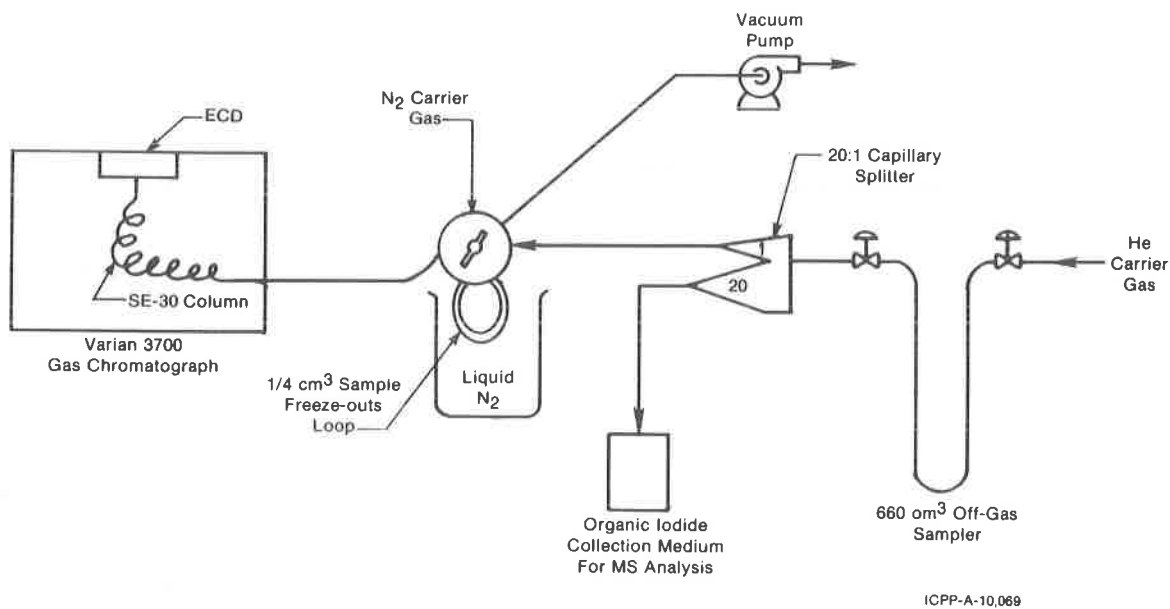
Figure 10. Gas Chromatograph Gas Handling System

1330

samples were injected directly onto the sample loop. After the required sampling time, the eight port valve was used to divert the He stream and introduce the N_2 carrier gas used by the gas chromatograph, to the 0.25 cm^3 sample loop. The liquid N_2 was removed and the sample loop heated with warm water. After 0.5 minutes the GC carrier gas was diverted around the sample loop to continue the chromatogram; the sample loop was then purged with He in preparation of the next sample.

Methyl iodide standards were prepared by volumetric serial dilutions and using permeation tubes. The serial dilutions were prepared by condensing known amounts of CH_3I and CO_2 into a common container. Concentrations were obtained by measuring the partial pressure of each gas within a known volume and assuming ideal gas behavior.

The CH_3I permeation tubes were prepared from 75 mm x 3.2 mm OD Teflon TFE tubing. The tubes were filled with liquid CH_3I and the ends were plugged with 304L stainless steel rods. These tubes had permeation rates on the order of 0.1 μg min^{-1} cm^{-2}. As shown in Figure 11, these permeation tubes required several days before constant permeation rates were achieved.

The I_2 permeation sources were prepared from 25 mm pieces of 6 mm x 8 mm Silastic (Dow Corning) silicone rubber tubing. Each end was plugged with borosilicate glass: one plug was 3 mm rod formed into a hook for easy weighing, the other plug had a test tube end to contain the iodine crystals. All seals were covered with Dow-Corning RTV cement.

The calibration curves determined for CH_3I and I_2 are shown in Figure 12 and 13. Departures from linearity were observed below 0.1 ng for CH_3I and 5 μg for I_2. These may represent the uncertainty associated with significant blank corrections. Typical GC responses to quantities close to the respective detection limits are compared to a typical blank measurement in Figure 14. The higher detection limits than found in the solution measurements for I_2 using the gaseous sample handling system may be related to of the following factors:

1)   Increased wall and surface losses on the gas sample handling system;

2)   Peak boradening due to desorption kinetics of the 0.25 cm^3 sample loop.

The precision and accuracy of the technique as demonstrated by these calibration curves were $\leq 12\%$. Because the I_2 cannot be reliably measured below 5 μg, it is not likely to be detected in fuel reprocessing plant off-gases. However, CH_3I may still be quantitated by GC-ECD. Therefore, an experiment was performed to measure any I_2 interference to the CH_3I determination (perhaps by conversion to CH_3I during sample handling). A mixture of 0.763 ng CH_3I was measured alone and in the presence of 3.62 ng I_2. The results are shown in Figure 15.

The two results agreed within the 12% precision established for the method. Therefore, it was demonstrated that traces of I_2 will not bias the CH_3I measurement.

1331
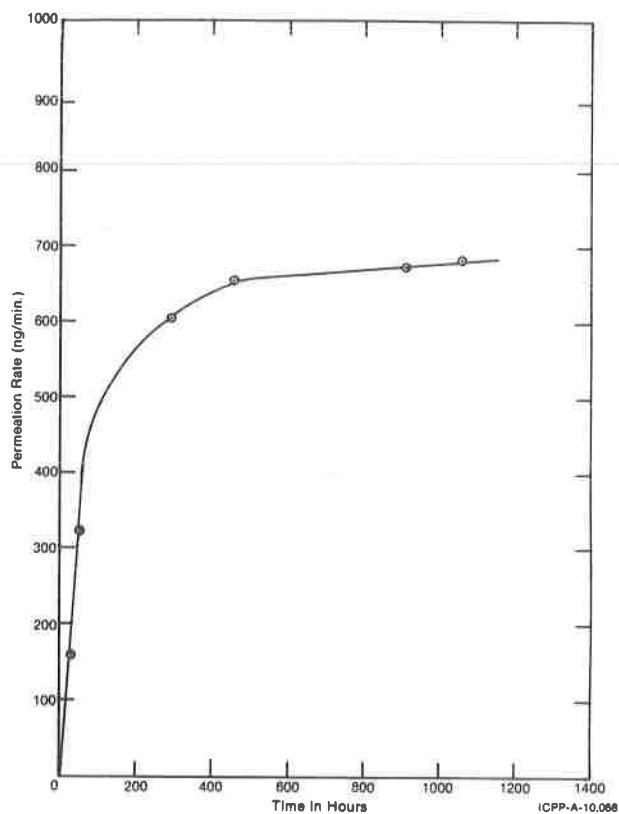
Figure 11.   Permeation Rate as Function of Time After Preparation
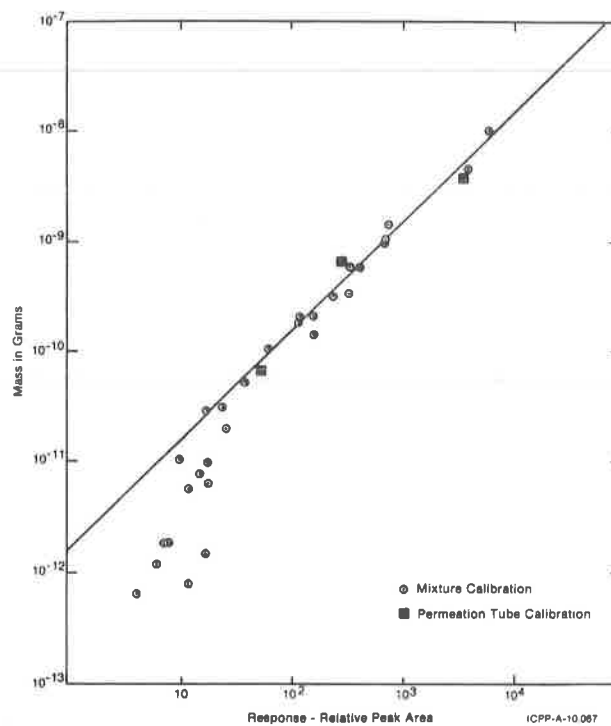
Figure 12.   Methyl Iodide Calibration Curve
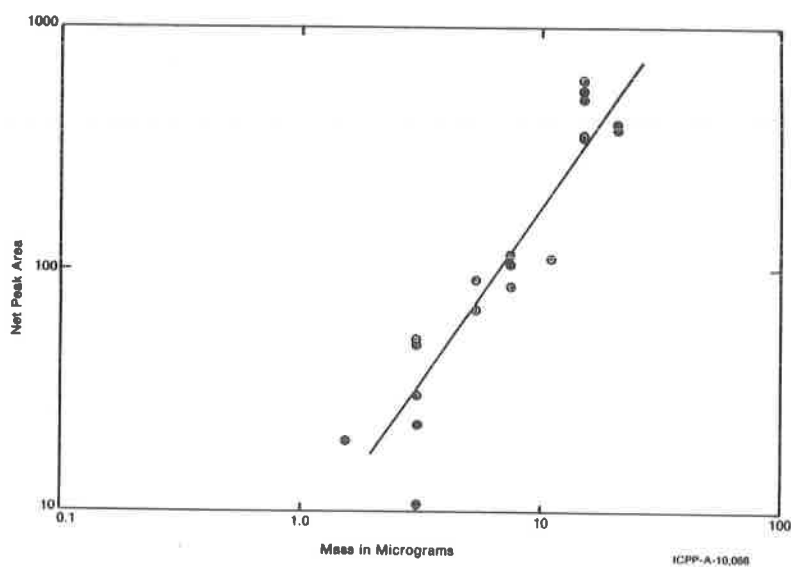
Figure 13.   I₂ Calibration Curve
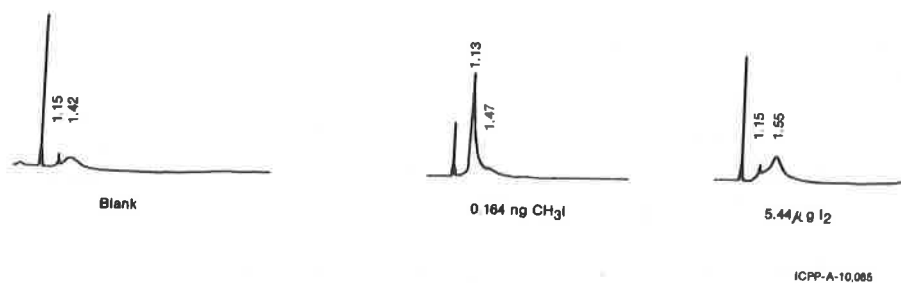
Figure 14. Gas Chromatographic Response to Quantities Approximating the Detection Limit
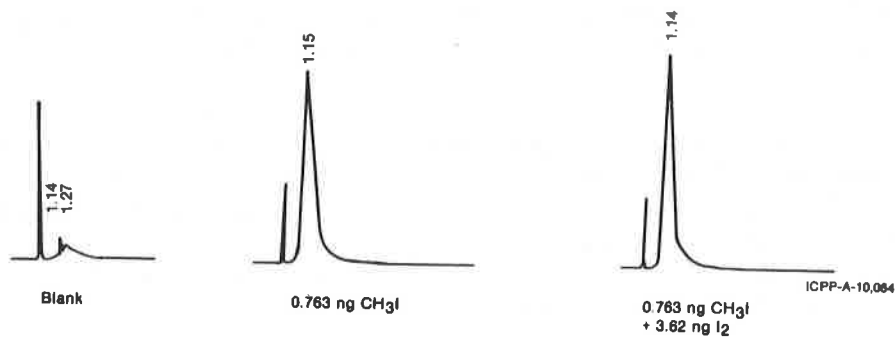
Figure 15. Typical Chromatograms Demonstrating Accuracy of CH_3I Measurement in the Presence of I_2
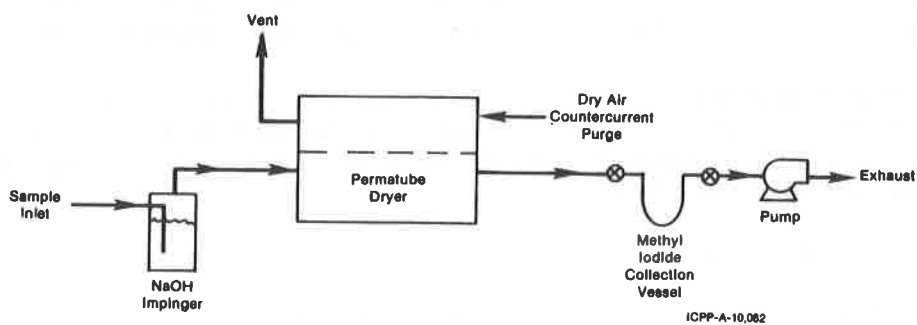
Figure 16. Iodine Sampling Apparatus

In summary, the conclusions drawn from the gas chromatography development were:

1)   The GC technique has sufficient sensitivity to measure CH_3I at the 80 ng level required for the isotopic ratio measurement;

2)   The GC technique does not have sufficient sensitivity to measure I_2 at the 80 ng level required for the isotopic ratio measurement; therefore, another technique for collecting the I_2 fraction must be used;

3)   The presence of I_2 does not bias the CH_3I determination.

IV.   SAMPLING METHODOLOGY

The large difference in GC-ECD detection limits between CH_3I and I_2 required separate I_2 and CH_3I samples be collected and prepared for analysis. The sampling apparatus that was designed is shown in Figure 16. A 250 cm^3 impinger containing 1 M NaOH was used to selectively collect the I_2, allowing the CH_3I to pass through to the permatube dryer. The NaOH also scrubs oxides of nitrogen from the sample stream to prevent any interference with the GC determination of CH_3I.

The I_2 concentration and isotopic ratio were then measured by submitting the solution to isotope dilution mass spectrometry (IDMS). A description of the technique can be found in standard textbooks, such as that by Choppin.[15] In summary the IDMS analysis requires analysis of two aliquots, one before and one after a known amount of ^{129}I is added to the sample. The concentration is calculated from the change in isotopic ratio due to spike addition.

The permatube dryer dried the sample stream to a dew point of –6°C to prevent condensation in the methyl iodide collection vessel. The permatube dryer operates on the principle of diffusion through thin polymeric membranes, thus minimizing the potential for sample losses through surface reactions. These dryers are fabricated by shaping a perfluorosulfonic acid polymeric membrane into thin walled tubes, typically 0.064 cm thick and 60 cm in length, and mounting as many as 200 tubes into common headers. This multiple tube pack is sealed inside a 4 cm diameter stainless steel shell. In principle, the sample enters the sample inlet, wets the inner wall of the polymer tube, and the water continuously diffuses through the polymer into a purge stream which exhausts the removed water vapor.

The methyl iodide collection vessel is a 660 cm^3 glass vessel that can be isolated by a series of valves and inserted into the gas sample handling apparatus shown in Figure 10. The demonstration of each component of the apparatus is described in the following sections.

4.1   Sodium Hydroxide Impinger

The objectives of the sodium hydroxide impinger tests were:

1)   Achieve high collection efficiencies for I_2;

2)   Achieve high transmission efficiencies for CH_3I;

3)   Minimize fractionation of the $^{127}I/^{129}I$ ratio due to sampling.

The recovery efficiency was measured using $^{125}I_2$ generated with a permeation tube containing $^{127}I_2$ crystals traced with ^{125}I. The I_2 concentration was measured before and after a 250 cm^3 impinger containing 0.1 M NaOH; the measurements were conducted by collecting the $^{125}I_2$ on a TEDA impregnated charcoal bed and counting the 27 kev Te X-ray on a hyperpure germanium low energy photon spectrometer (LEPS). The results are shown in Table VII.

TABLE VII

RESULTS OF I_2 COLLECTION BY NaOH

Sampling Period (min)	Flowrate (cm^3/min)	Collection Efficiency (%)
20	250	99.4
20	1900	98.1

As shown in Table VII, quantitative collection of I_2 with a NaOH impinger is achievable.

The absence of exchange between collected $^{125}I^-$ and $CH_3^{127}I$ was then demonstrated by bubbling 0.3 mg/m^3 CH$_3$I sample stream through 200 cm^3 of 1.85 $\mu Ci^{125}I$/L at 2.6 L/min for 4 hours. A TEDA charcoal bed collected the methyl iodide penetrating the NaOH impinger. The charcoal bed was then counted to measure the ^{125}I that had exchanged with the CH$_3$I and penetrated the impinger. After 4 hours, only 9.0 + 3.2% of the ^{125}I was found on the charcoal bed. Although some of the ^{125}I may have been carried onto the charcoal by mechanisms other than exchange (spray from impinger solution, oxidation to I_2) the experiment demonstrated that fractionation was less than the 12% precision of the GC technique.

The high transmission efficiency of the NaOH impinger and permatube dryer was demonstrated by introducing a known concentration of CH$_3$I to the integrated sampler (shown in Figure 16) and comparing the measured concentration (by GC-ECD, Figure 10) to the known concentration. The known concentration of 0.3 mg/m^3 was generated as before. The results are shown in Table VIII. These results demonstrate a recovery of 95.1 + 9.3%, sufficient for the designated purposes. Therefore, the NaOH was deemed suitable as a I_2 sampler.

4.2   Permatube Dryer

The objective of the permatube dryer evaluation was to demonstrate that the CH$_3$I sample could be dried without fractionating the CH$_3$I. As noted in section 4.1 (see Table VIII), high transmission efficiency had already been demonstrated.

TABLE VIII

RESULTS OF CH_3I TRANSMISSION TESTS

Test Number	CH_3I Introduced (ng)	CH_3I Measured (ng)	Recovery (%)
1	235	202	86.0
2	228	202	88.6
3	228	208	92.3
4	228	228	100.0
5	228	248	108.8
		average =	95.1
		standard deviation =	9.3

The fractionation was measured by determining the transmission efficiency of a mixture of $CH_3{}^{127}I$ and $CH_3{}^{125}I$ by both GC-ECD (for $CH_3{}^{127}I$) and by counting the 27 kev X-ray (for $CH_3{}^{125}I$). The $CH_3{}^{127}I/CH_3{}^{125}I$ mixtures were prepared by exchanging ^{125}I with $CH_3{}^{127}I$ and preparing permeation tubes with the tagged CH_3I.

The $CH_3{}^{127}I$ was measured using the apparatus shown in Figure 16 (without the NaOH impinger) followed by GC measurement with the apparatus shown in Figure 10. The $CH_3{}^{125}I$ was measured by replacing the methyl iodide collection vessel with a TEDA charcoal bed and counting the 27 kev X-ray on a hyperpure germanium LEPS. The sample flowrate was maintained at 1 L/min and the purge flow was maintained 5.1 L/min. The results of these experiments are shown in Table IX.

TABLE IX

RESULTS OF DRYER FRACTIONATION EXPERIMENTS

Test Number	$CH_3{}^{127}I$ Transmission Efficiency (%)	$CH_3{}^{125}I$ Transmission Efficiency (%)
1	76	ND[1]
2	85	ND[1]
3	81	ND[1]
4	ND[1]	110
5	ND[1]	75
6	ND[1]	141
average	81 ± 5	109 ± 33

[1] ND = Not Determined

The transmission efficiencies shown in Table IX are not statistically different. Therefore, it can be inferred that the dryer was introducing only negligible changes in the isotopic ratio. The efficiencies measured at 1 L/min (Table IX) are lower than the efficiencies measured at 2.6 L/min (Table VIII). This may be due to the larger residence time in the dryer at the lower flowrate. If quantitative transmission for $CH_3{}^{127}I$ such as shown in Table VIII, can be obtained by operating at 2.6 L/min, then no observable fractionation should occur. From these experiments it was concluded that there were no significant fractionation effects and the sampling apparatus should be operated at 2.6 L/min.

V. INTEGRATED SAMPLE DEMONSTRATION

The integrated sampler was tested to demonstrate its ability to measure:

1) CH_3I concentration and isotopic ratio in the presence of I_2;

2) I_2 concentration and isotopic ratio's in the presence of CH_3I.

The apparatus shown in Figure 17 was used in this demonstration. A CH_3I permeation tube (permeation rate = 0.82 µg/min; $^{127}I/^{129}I = 3.8 \times 10^3$) was connected to an I_2 permeation tube with a different permeation rate (0.42 µg/min) and different $^{127}I/^{129}I$ ratio (2.2×10^3). Both isotopic ratios represent calculated values from mixing standard solutions. A sample flowrate of 0.33 L/min (a worst case lowest flowrate expected for use with the integrated sampler) was maintained over the two permeation tubes. Using this flowrate, CH_3I losses in the permatube dryer are maximized as is the CH_3I contact time with the collected I^- in the NaOH impinger.

Two aliquots of the NaOH impinger solution were taken. One was then spiked with a known amount of ^{129}I. The isotope ratio of unspiked sample represents the I_2 specific activity; the difference in the ratio between the spiked and unspiked sample is used to calculate the I_2 concentration.[15] The methyl iodide concentration was measured by GC-ECD. The specific activity of the CH_3I was not measured directly but calculated by ^{129}I mass balance. This technique is analogous to measuring the total ^{129}I (by collecting a sample on a charcoal bed and determining the total ^{129}I by photon counting) and using this number to calculate the CH_3I specific activity. The accuracy of this technique was tested because mass balance calculations will be used to confirm the accuracy of in-plant measurements.

The results of this demonstration are shown in Table X. The reason the measurement of I_2 concentration was low cannot be attributed to low recovery in the NaOH impinger (as evidenced by Table XI). However, the low concentration measurement and the low isotopic ratio ($^{127}I/^{129}I$) measurement can be simultaneously explained if the unspiked $^{127}I/^{129}I$ measurement of the NaOH solution was low and the spiked isotopic ratio measurement was accurate (or high). The low CH_3I concentration may occur due to losses in the permatube dryer caused by the low sample flowrate.

TABLE X

RESULTS OF INTEGRATED SAMPLER DEMONSTRATION SPECIFIC ACTIVITY MEASUREMENT

Iodine Compound	Ratio ($^{127}I/^{129}I$)		Measured/Actual
	Measured ($\times 10^3$)	Actual ($\times 10^3$)	
CH_3I	4.7	3.8	1.24
I_2	0.9	2.2	0.45

TABLE XI

RESULTS OF INTEGRATED SAMPLER DEMONSTRATION – CONCENTRATION MEASUREMENT

Iodine Compound	Concentration –		Difference (Measured-Actual x 100% Actual)
	Measured (mg/m^3)	Actual (mg/m^3)	
CH_3I	1.46	2.44	–41
I_2	0.83	1.29	–35

From this worst case demonstration it was concluded that concentrations and specific activities of CH_3I and I_2 can be determined with an accuracy of about a factor of two. This accuracy was considered sufficient because:

1) The largest uncertainties in specific activity were conservative, indicating less dilution with stable iodine than is actually present;

2) The uncertainties in concentration were conservative, indicating lower levels of stable iodine (assuming accurate total ^{129}I release measurements);

3) Specific activity measurements may require corrections in dose calculations of up to four orders of magnitude compared to uncertainties on the order of a factor of two.
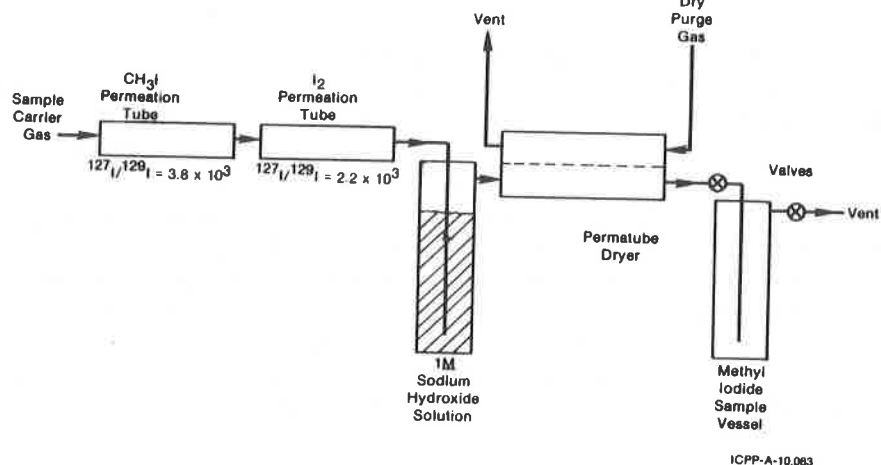
Figure 17. Integrated Sampler Demonstration Apparatus

OFF-GAS SAMPLE COLLECTED DURING PLANT SHUTDOWN

OFF-GAS CHROMATOGRAM DURING NWCF OPERATION
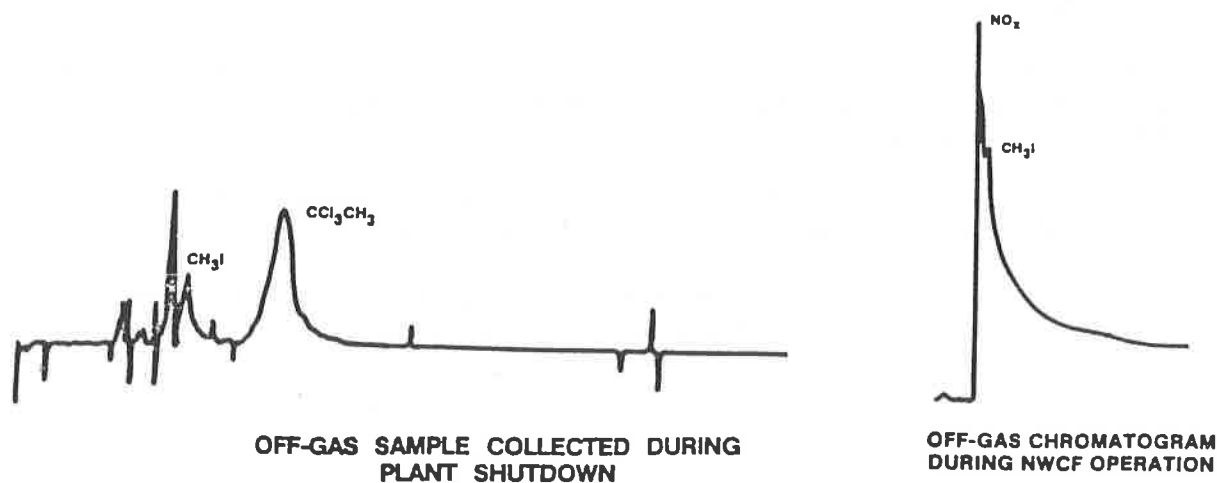
Figure 18.

Therefore, the integrated sampling technique was considered suitable for nuclear fuel reprocessing plant off-gas streams.

VI. IN-PLANT DEMONSTRATION

Since the most probable source of interference to the iodine sampling apparatus is high NO_x concentrations in the off-gas, a number of samples were collected and analyzed for CH_3I during the operation of the New Waste Calcination Facility (NWCF). While the NWCF is operating, NO_x concentrations in the off-gas range from 7000 - 15,000 ppm, mostly as NO_2. Initial results indicated the fraction of NO_2 penetrated the NaOH solutions resulting in a significant gas chromatographic interference. This is illustrated in Figure 18 which shows a typical POG off-gas chromatogram before and after NWCF startup. To remove any residual NO_2 that penetrated the NaOH impinger a packed bed of ascarite was placed in-line before the permatube dryer. The ascarite was found to be effective in removing the NO_x interference while at the same time giving quantitative transport of the CH_3I ($\geq 80\%$).

Therefore, the integrated sampling technique for analyzing CH_3I in actual process off-gas streams containing large NO_x concentrations has been proven effective.

VII. CONCLUSIONS

The major conclusions of this work were:

1) Isotopic ratios of $^{127}I/^{129}I$ as large as 10^5 can be successfully measured on samples as small as 80 ng I.

2) Less than 1 ng CH_3I can be measured by gas chromatography in the presence of I_2, but I_2 must be measured by isotope dilution mass spectrometry using a separately collected sample.

3) The developed integrated sampler can collect separate I_2 and CH_3I samples with high recovery efficiencies and without fractionation provided sample flowrates are maintained above 2.6 L/min.

4) Even under worst case sampling conditions, concentrations can be measured within 40% and isotope ratios can be measured within a factor of two.

Based on these results, the sampling and analysis technique was considered suitable for nuclear fuel reprocessing plant off-gas streams.

VIII. REFERENCES

1. "Report of Committee II on Permissible Dose for Internal Radiation", Health Phys., 3, 1 (1960).

2. D. L. Strenge, et al., ALLDOS - A Computer Program for Calculation of Radiation Doses from Airborne and Waterborne Releases, PNL-3524, October, 1980.

3. D. L. Strenge and E. C. Watson, DACRIN - A Computer Program for Calculating Organ Doses from Acute or Chronic Radionuclide Inhalation, BNWL-B-389 (1976).

4. B. A. Napier, W. E. Kennedy, and J. K. Soldat, PABLM - A Computer Program to Calculate Accumulated Radiation Dose from Radionuclides in the Environment, PNL-3209 (1980).

5. R. A. Rankin, et al., An Integrated Method for the Determination of Iodine Isotopic Ratios Near a Nuclear Facility, ENICO-1142 (1983).

6. J. E. Delmore, "Improved Cataphoretic Deposition Methods for Lathonum Hexaboride," Int. J. Mass Spec. and Ion Phys., 54, 2, 158 (1983).

7. G. W. Snow, et al., "Performance of a New 90° Sector Surface Ionization Mass Spectrometer," Fifteenth Annual Conf. on Mass Spec. and Allied Topics, 467 (1967).

8. G. Castello, G. D'Amato, E. Biagini, "The Gas Chromatography of Alkyl Iodides," J. Chromotogr., 41, 313 (1969).

9. J. A. Corkill and R. W. Giese, "Fused Silica Capillary Column Gas Chromatography of Derivatized Thyroid Hormone Standards with Electron Capture Detection," Anal. Chem., 53, 1667 (1981).

10. F. Patte, M. Echeto, P. Laffort, "Solubility Factors for 240 Solutes and 207 Stationary Phases in Gas - Liquid Chromatography," Anal. Chem., 54, 2239 (1982).

11. G. Castello and G. D'Amato, "Gas Chromatography of Alkyl Iodides II. Influence of Structure on Retention Time and Sensitivity to Electron Capture Detector," J. Chromatogr., 54, (1971).

12. E. Pellizzani, "Electron Capture Detection in Gas Chromatography," J. Chromatogr., 98, 323 (1974).

13. D. A. Miller and E. P. Grimsrud, "Analysis Errors Following Hydrogen Cleaning of an Electron Capture Detector," J. Chromatogr., 190, 133 (1980).

14. J. H. Keller, F. A. Duce, W. J. Maeck, "A Selective Adsorbent Sampling System for Differentiating Airborne Iodine Species," CONF-700816, Eleventh AEC Air Cleaning Conference, 2, 621 (1970).

15. G. R. Choppin, Experimental Nuclear Chemistry, Prentice-Hall, Englewood Cliffs, N.J., 1961.

DISCUSSION

KABAT: What was the concentration of sodium hydroxide in the solution you used for collecting elemental iodine and methyl iodide? For which period were you collecting?

McMANUS: The concentration of sodium hydroxide was 1 molar for the test. Typical collection periods when the calciner was operating, which was when the high NO_x was there, were about 10 min. When the New Waste Calcination Facility (NWCF) was down, we found that we could sample from two to five hours.

THOMAS, T.R.: I want to comment why this work is being done. When modelling, to figure out the I-129 dose to the maximum exposed individual, or to the local population, the isotopic ratio is normally not taken into consideration. I am not aware of any study where the ratio has been used. If we know, for example, that releases from a plant were in the ratio of 10^{-3} for I-129 to I-127, it would mean that the dose to the maximum exposed individual would be 1,000 times less than what our current model shows. This particular aspect has been totally ignored and neglected to this time. It is a very complicated procedure, as you can see, to try to get these ratios, but I think if we ever get to the point in this country where we build reprocessing plants and really have to go out and measure a dose to the individual (not just hypothesize from calcuations) we have to know the specific isotopic ratio. For the few measurements we have made in this country, around the Savannah River Plant and around the West Valley Plant, the highest ratio found, after several years of operation, was 10^{-4}. I cite these figures just to give you a feeling for how important it is to know the isotopic ratio.

Removal of Iodine from Off-Gas of Nuclear Fuel

Reprocessing Plants with Silver Impregnated Adsorbents

S. Hattori

Central Research Institute of Electric Power Industry

Y. Kobayashi

Japan Nuclear Fuel Service Company, Ltd.

Y. Ozawa

Energy Research Laboratory, Hitachi Ltd.

M. Kunikata

Hitachi Works, Hitachi Ltd.

Abstract

Silver impregnated adsorbents such as silver zeolite, silver mordenite, silver alumina and silver silica gel were compared on the basis of their I_2 and CH_3I adsorption characteristics under the simulated dissolver off gas stream conditions.

For silver zeolite and silver mordenite, having carrier pore sizes less than 10 $\overset{\circ}{A}$, the some amounts of adsorbed iodine were found to desorb reversibly and to be affected by the presence of NO_x and H_2O impurities. On the other hand, no effects due to NO_x and H_2O were observed on iodine adsorption for silver alumina and silver silica gel, having carrier pore sizes larger than 100 $\overset{\circ}{A}$

After regeneration by hydrogen gas at 500°C, the amounts of CH_3I adsorbed decreased markedly for silver zeolite, silver alumina, and silver silica gel. This was understood to be due to the formation of metallic silver. Those metallic silver impregnated adsorbents could hardly react with CH_3I. However, NO_x and H_2O had effect to increase adsorption capacity.

Seven cyclic regeneration tests indicated, that both silver

alumina and silver silica gel kept their capacity for I_2 adsorption.

I Introduction

For the past several years, various kinds of silver impregnated adsorbents have been studied[1)2)3)] to remove [129]I from off gas streams of nuclear fuel reprocessing plants. These systems in which adsorbents function as primary filtering of [129]I, have some advantages, because of their simplicity and rather small amounts of secondary radioactive wastes, to compare with liquid based method.

When solid adsorbents are used as primary systems for dissolver off gas streams, the following points should be considered:

(1) Adsorption characteristics of I_2 and CH_3I on silver impregnated adsorbents, and

(2) Effects of NO_x and H_2O impurities on iodine adsorption related on the basis of their chemical forms of silver and carrier pore sizes.

Thus, four different types of adsorbents were compared in order to elucidate these points under the same adsorption conditions.

II Experimental

1. Silver Impregnated Adsorbents

Table 1 compares the specifications of silver impregnated adsorbents used for iodine removal. They were divided into two groups based on carrier pore sizes. Pore sizes of silver zeolite (AgX) and reduced silver mordenite (Ag°Z) were the same order as the diffusion diameter of I_2 molecule (4.6Å)[4)]. On the other hand, those of silver alumina (AgA) and silver silica gel (AgS) were more than 100Å. These adsorbents were all commercially available.

2. Measurement of Iodine Adsorbed on the Adsorbents

The test apparatus for the dynamic adsorption is shown in Fig. 1. N_2 and O_2 were used as carrier gases. The ^{131}I labelled I_2 or CH_3I was prepared by the conventional method[5] using sodium iodide and hydrogen peroxide or sodium iodide and dimethyl sulfate. The specific activity was around $10 \mu Ci/gI_2$. The adsorption column consisted of a 10cm thick cartridge (10mm for each section X 10 sections), in which adsorbent particles were packed. After passing iodine containing gases through the cartridge, radioactivity of each section was detected by a NaI(Tl) scintillation detector to obtain the distribution of iodine adsorbed at different distances from the cartridge inlet.

Table 1　Specifications of Iodine Adsorbents

	Silver Zeolite (AgX)	Silver Mordenite (Ag°Z)	Silver Alumina (AgA)	Silver Silica Gel (AgS)
Carrier	Molecular Sieves 13X	Zeolon 900	Activated Alumina	Silica Gel
Pore Size of Carrier (Å)	10	7	600	100
Impregnated Material	Ag^+	Reduced Ag	$AgNO_3$	$AgNO_3$
Silver Content (wt%)	38	20	10	12
Adsorbent Size (mm)	1 — 2 (Granular)	1 — 2 (Crushed)	1 — 2 (Granular)	1 — 2 (Granular)
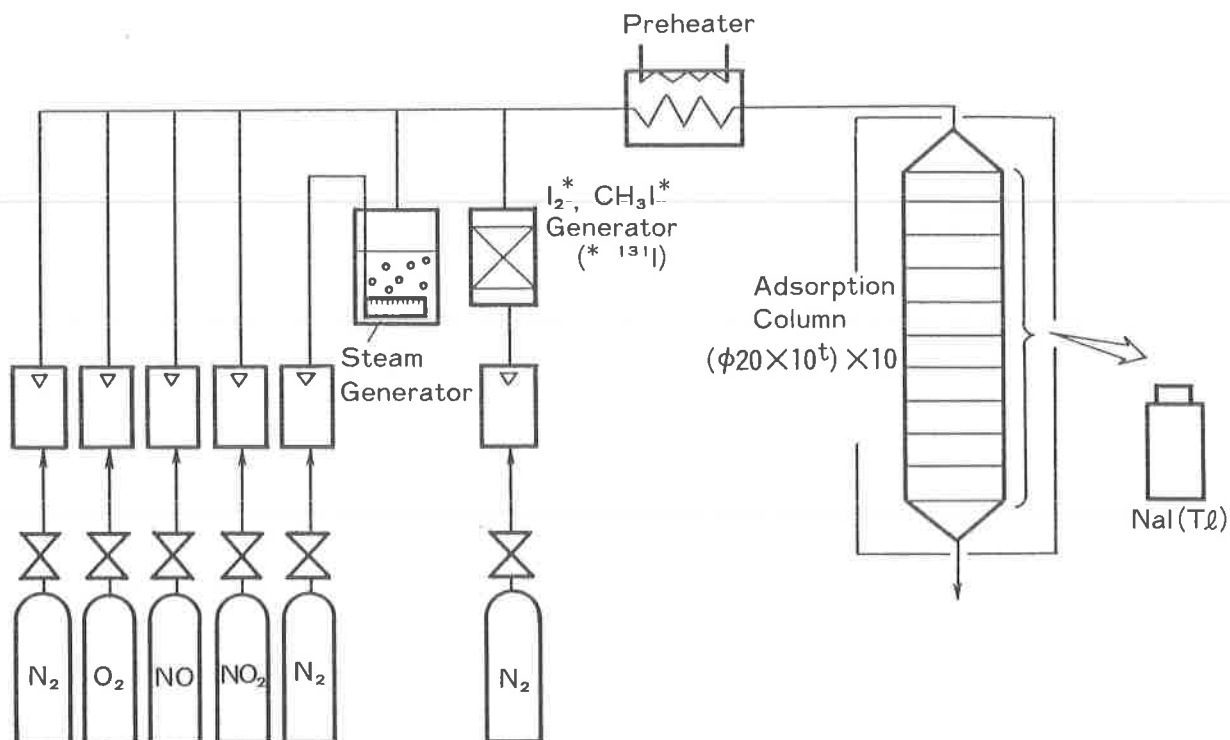
Fig. 1   Flow Diagram of Experimental Apparatus

The main experimental conditions are shown in Table 2. The adsorption temperature of 150°C was selected because of already reported experimental results[1] at about that temperature. The concentration of CH_3I was 1500 vol. ppm, which gave the same iodine feed rate as when I_2 was introduced at 750 vol. ppm. The temperature of regeneration with hydrogen gas was fixed at 500°C, as previously proposed[1,2]. After regeneration of AgA and AgS, their adsorption amounts of I_2 were measured. Regeneration was repeated seven times in these experiments.

When linear velocity was small enough, adsorption zones advanced along the column with time, without changes in the saturated amounts of adsorption, as shown in Fig. 2. The adsorption zone length of about 4cm was negligibly short enough for comparisons with saturated adsorption zones for an actual adsorption bed. Therefore, a large saturated adsorption was one important factor

Table 2   Experimental Conditions

		Adsorption	Regeneration
Temperature (°C)		150	500
Linear Velocity (cm/s)		5	25
Iodine	Concn. of I_2 (vol ppm)	750	—
	Concn. of CH_3I (vol ppm)	1500	—
	Specific Activity (μCi/g-I_2)	~10	
Impurity	Concn. of NOx (vol%)	0 , 1	—
	Concn. of H_2O (vol%)	0 , 1	—
Carrier Gas (vol%)		O_2~30% N_2~70%	H_2 100%

to evaluate the adsorption capacity.   In this report, adsorbents were compared for their capacity mainly in terms of their saturated amounts of adsorption.   NOx or H_2O was introduced into the flow gas to investigate their impurity effects on iodine adsorption.

Adsorbent	AgA
Particle Size	1~2mm
Temp.	150°C
Concn. of I_2	750 vol ppm
Linear Velocity	5 cm/s
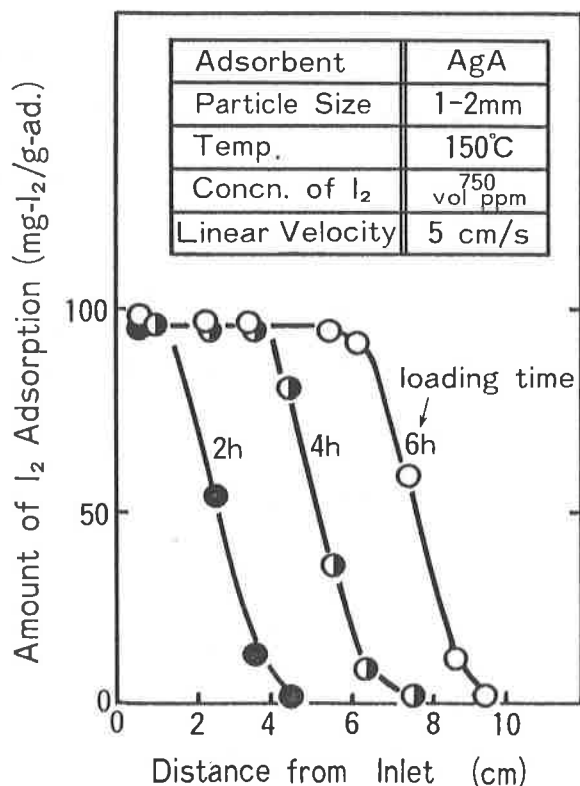
Fig. 2 Adsorption Distribution Changes with Time

A thermobalance was used to determine the stability of iodine adsorbed with increasing temperature. X-ray diffraction and gas chromatography were used for detection of reaction products.

III Results and Discussion

1. Comparison of equilibrium amounts of adsorption for four different types of adsorbents.

Figure 3-1, 3-2, 3-3 and 3-4 show the effects of H_2O and NO_x impurities on I_2 adsorption for AgX, Ag°Z, AgS, and AgA. Saturated amounts of I_2 adsorption for four adsorbents are summarized in Fig. 4.

For AgX and AgŽ, the amounts of adsorbed I_2 decreased in the presence of both NOx and H_2O as shown in Fig. 3-1 and Fig. 3-2. Figure 4 also shows the effects of NO_x and H_2O, respectively, on amounts of I_2 adsorption for Agx and AgŽ. The tendency was more clearly observed for AgX. Each NO_x and H_2O had effects on decresing the amounts of I_2 adsorption. The adsorption of H_2O and NO_x was confirmed by the weight gain measured with a thermobalance. Weight changes by a nitrogen gas purge under the same temperature conditions as iodine adsorption suggested that some amounts of once adsorbed iodine desorbed reversibly.

As for AgS and AgA, no adsorption of H_2O and NO_x at 150°C was observed, and therefore no effects on I_2 adsorption was observed as shown in Fig. 3-3 and 3-4. These facts that AgA and AgS did not adsorb NO_x and H_2O, might be favorable when further treatment of regeneration and fixation of desorbed iodine by a base metal impregnated adsorbent, such as PbX.

In order to compare the stability of adsorbed iodine with temperature for AgX and AgA, the weight loss of both adsorbents
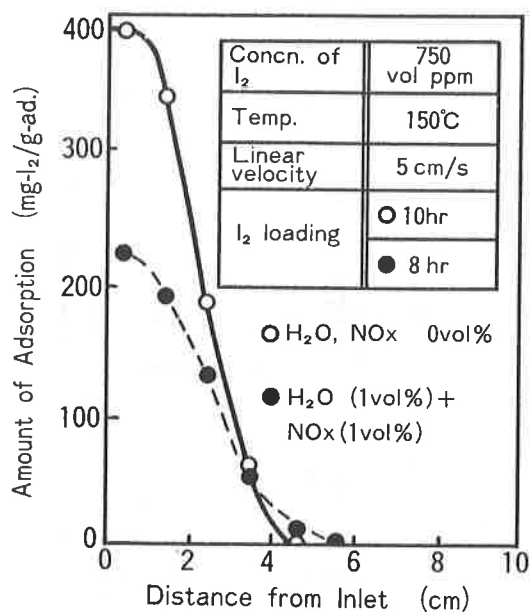
(a) Adsorption Distribution
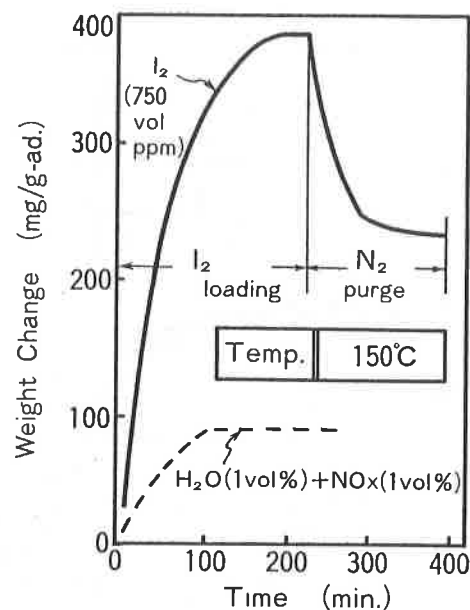
(b) Weight Changes Measured by Thermobalance

Fig. 3-1   Effects of Impurities on I_2 Adsorption (AgX)
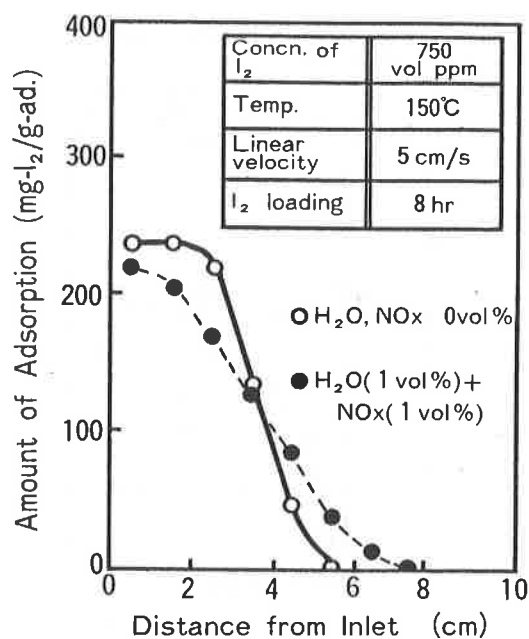
(a) Adsorption Distribution
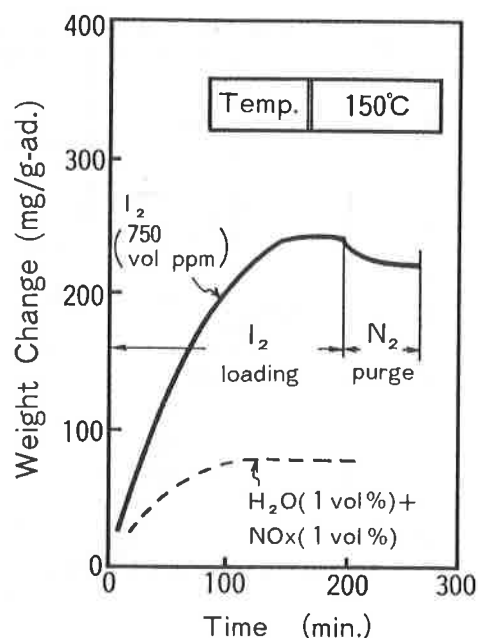
(b) Weight Changes Measured by Thermobalance

Fig. 3-2   Effects of Impurities on I_2 Adsorption (Ag°Z)

(a) Adsorption Distribution

(b) Weight Changes Measured by Thermobalance
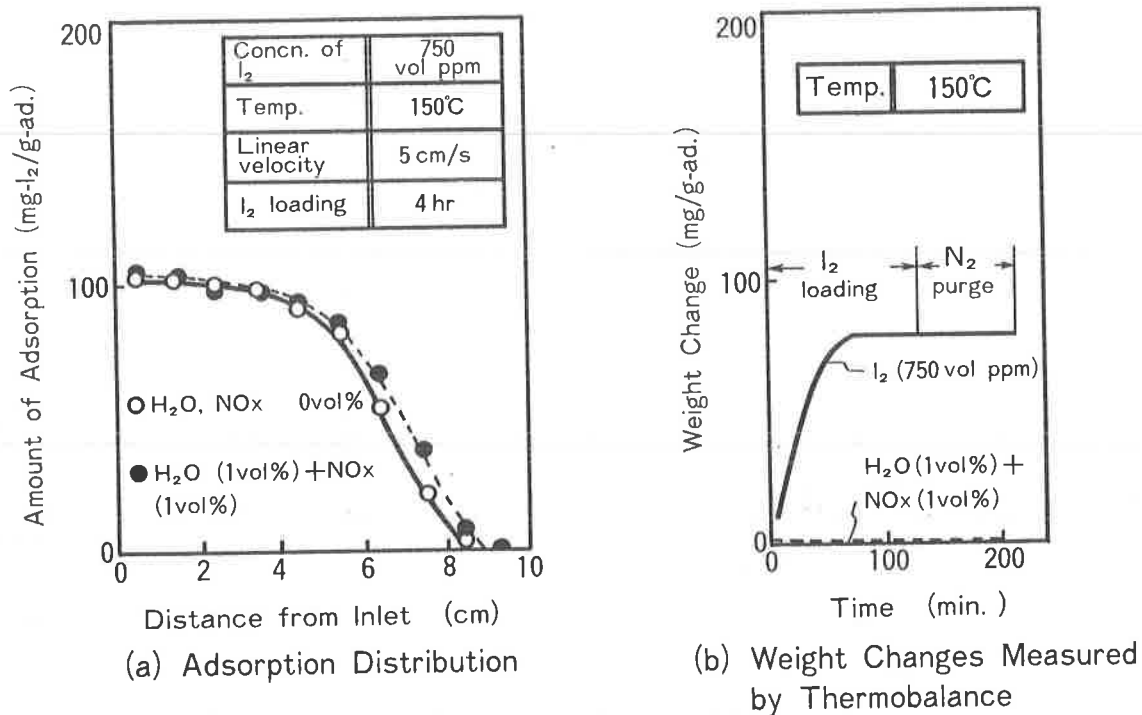
Fig. 3-3   Effects of Impurities on I_2 Adsorption (AgS)

(a) Adsorption Distribution

(b) Weight Changes Measured by Thermobalance
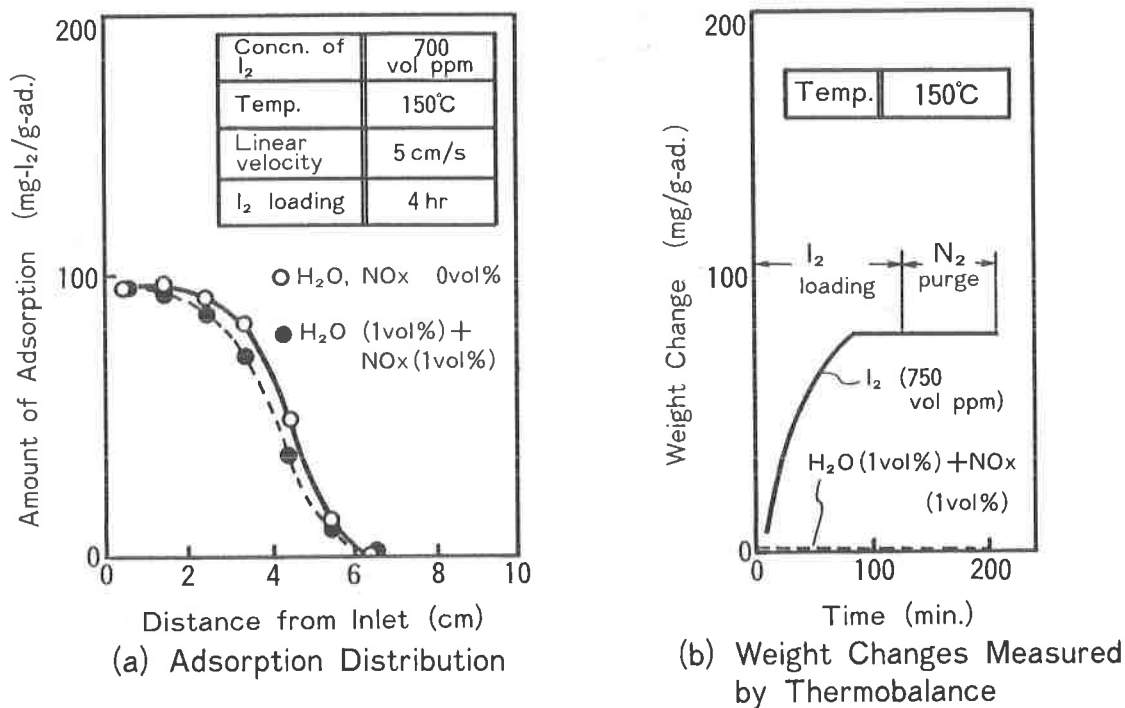
Fig. 3-4   Effects of Impurities on I_2 Adsorption (AgA)
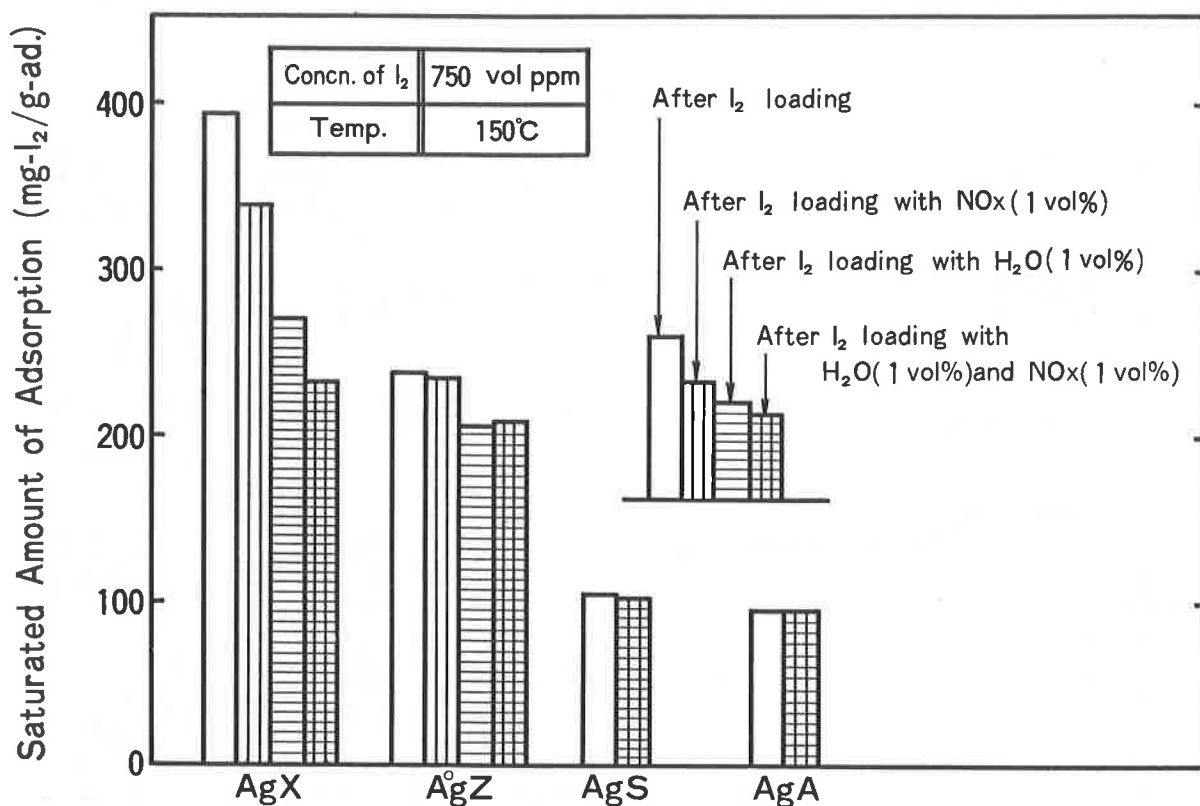
Fig. 4 Comparison of Equilibrium Amount of I_2 Adsorption

with temperature was measured with the thermobalance and results

are shown in Fig. 5. In case of AgX, the main reaction product of

ion exchanged silver with I_2 was recognized as AgI from X-ray

diffraction patterns obtained. Two step weight losses were

observed. The weight loss at lower temperature (150 to 500°C) was

thought to be due to release of reversibly adsorbed iodine, and

that at higher temperatures (around 800°C) was due to evaporation

of AgI. A portion of the AgI remained even at 1200°C. This was

because iodine was trapped on heating in the collapsed crystal

structure of zeolite.

AgA had two step weight losses. The weight loss at lower tem-

peratures (around 400°C) was caused by decomposition of unreacted

$AgNO_3$ or by decomposition[6] of reaction product, $AgIO_3$. Both AgI

and $AgIO_3$ were recognized as reaction products of $AgNO_3$ with I_2

from the X-ray diffraction patterns as shown in Fig. 6. After the
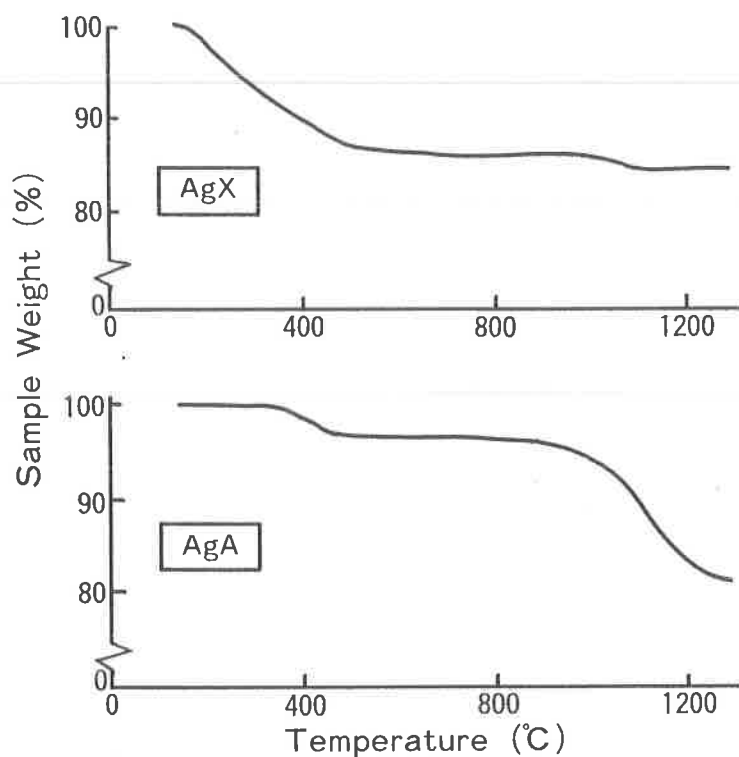
Fig. 5   Thermogravimetric Analysis for AgX and AgA
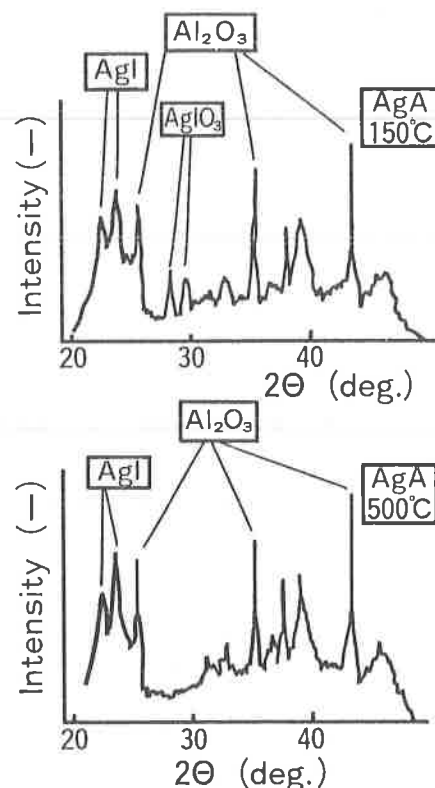
Fig. 6   X-ray Diffraction Pattern Change of AgA

temperature rose to 500°C, peaks for $AgIO_3$ disappeared, and only AgI and $\alpha\text{-}Al_2O_3$ peaks were seen. Almost all the AgI was found to evaporate above 800°C.

These results suggested that those adsorbents like AgA could retain iodine in stabler forms than species like AgX when the materials were stored below 800°C.

2. Changes in Adsorption Characteristics on Regeneration

Figure 7 shows changes of saturated amounts of I_2 and CH_3I adsorption on regeneration. The saturated amounts of I_2 on AgX and AgZ after regeneration decreased by 15 and 10%, respectively, compared to their amounts before regeneration. The same tendency was reported for AgX[1] and Ag°Z[7], which lost some capacity during recycling regeneration with hydrogen gas at 500°C.

1352

On the contrary, the saturated amounts of I_2 for both AgA and AgS did not change before and after regeneration.
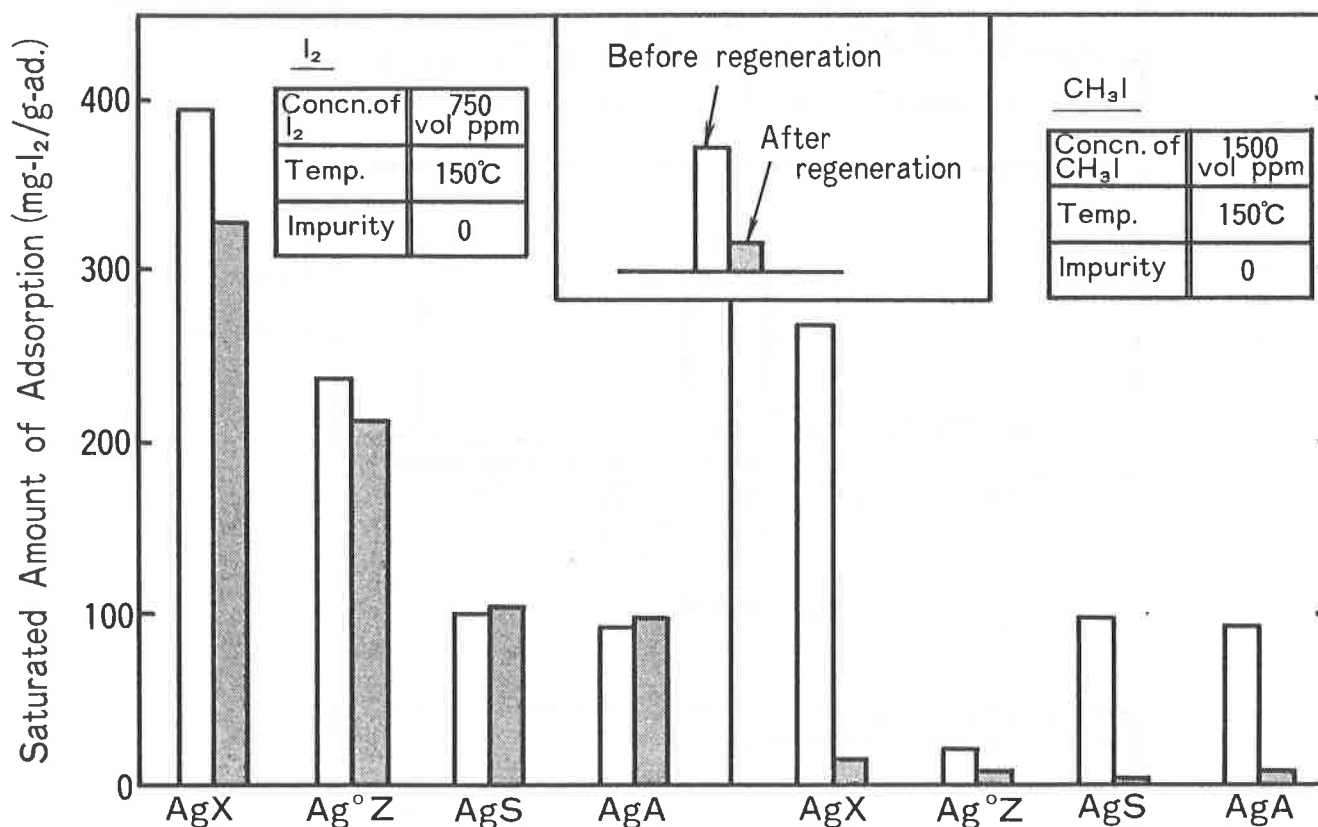
Fig. 7   Changes of I_2 and CH_3I Adsorption on Regeneration

Figure 7 also shows that all adsorbents lost their adsorption capacities for CH_3I after regeneration except Ag°Z, for which CH_3I adsorption capacity was low from the first, when NO_x and H_2O impurities were absent. X-ray diffraction patterns showed the chemical forms of silver changed to a metallic form on regeneration as illustrated in Fig. 8. Therefore, the reason for decreased adsorption capacity of CH_3I on regeneration was thought to be due to the formation of metallic silver, which would hardly react with CH_3I.
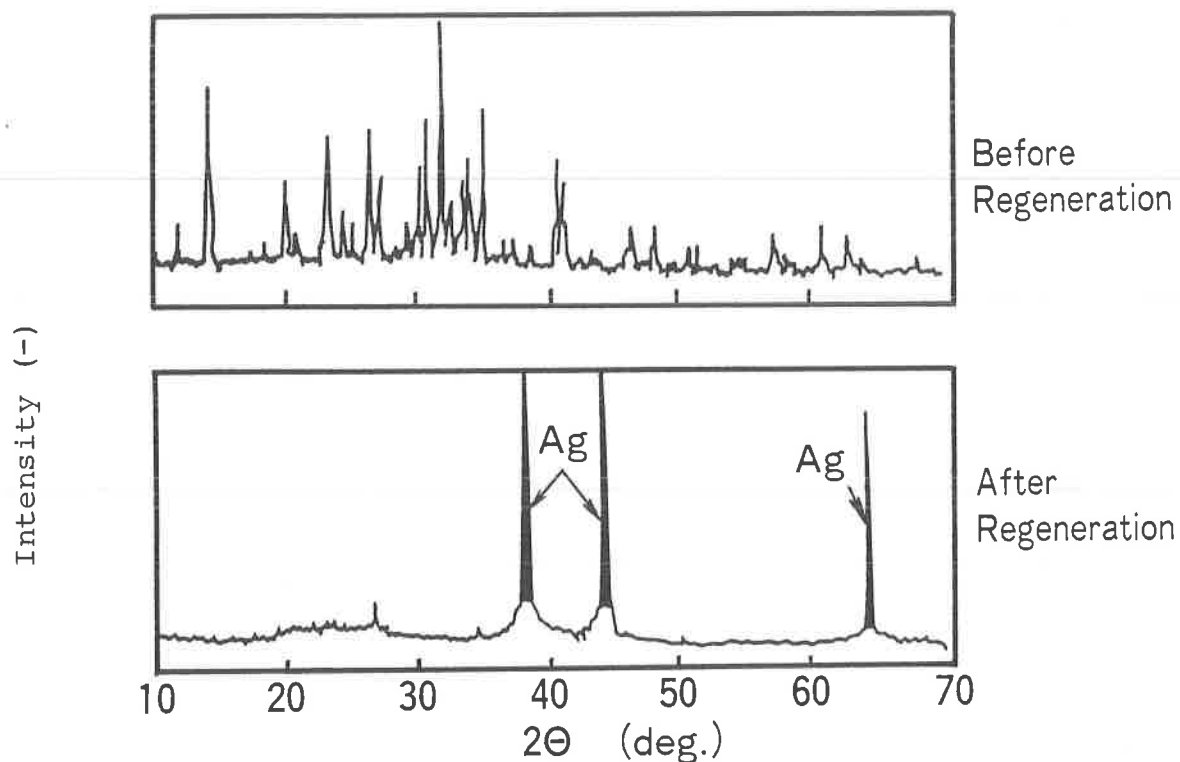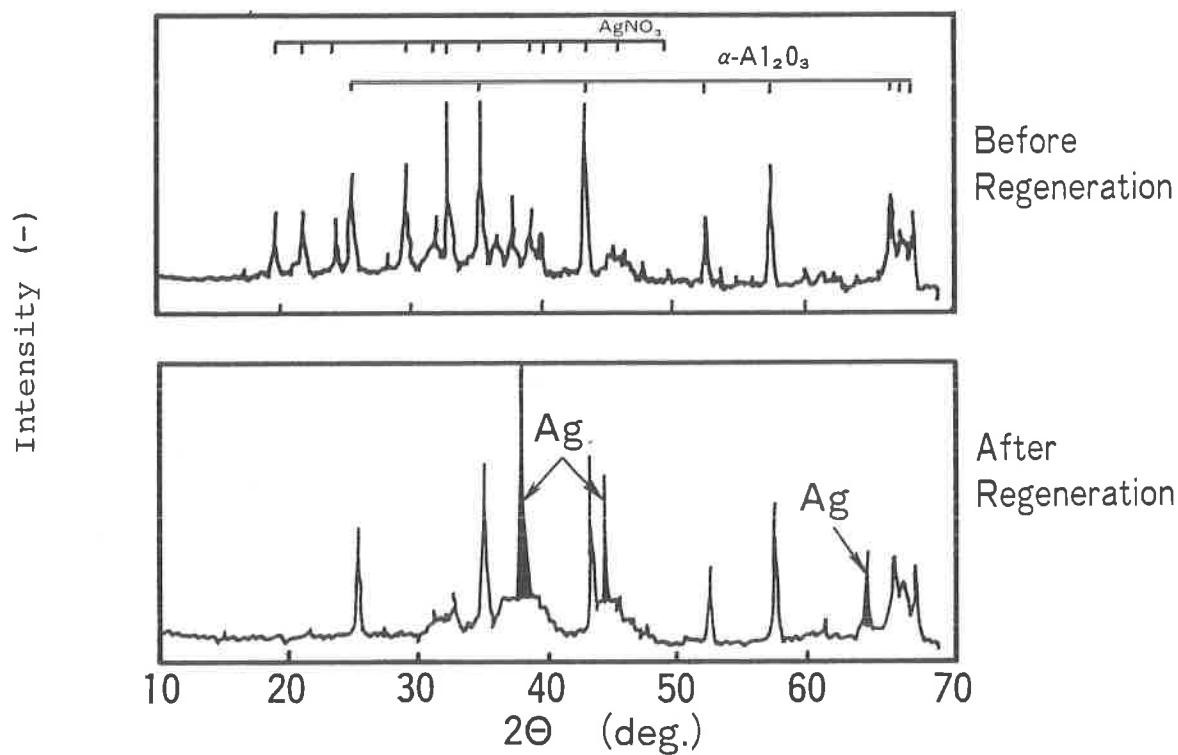
Fig. 8 Chemical Form Changes of Silver on Regeneration

3. Effect of NOx and H_2O Impurities on CH_3I Adsorption of Regenerated Adsorbent

Figure 9 shows the CH_3I adsorption amount increase on regenerated AgA in the presence of NOx and H_2O. These facts correspond to capacity increase for Ag°Z in the presence of H_2O[8] or NO_2[4]. The reaction products of regenerated AgA with CH_3I were clarified in the presence of H_2O and NOx impurities, as summarized in Table 3. The reaction products of CH_4, CH_3OH were found in the presence of H_2O, and those of CH_3ONO_2 in the presence of NOx. Nox had a bigger effect to increase adsorption capacity. The reason could be explained as follows: The reaction product of $AgNO_3$ was detected by X-ray diffraction patterns when regenerated AgA was in contact with the mixed gases of oxygen and nitrogen containing NOx at 1 vol %. This $AgNO_3$ was confirmed to react easily with CH_3I in these experiments, therefore when both CH_3I and NO_2 (a large por- tion of NOx is NO_2 under oxygen rich conditions) existed, the for- med $AgNO_3$ could easily react with CH_3I and produce CH_3ONO_2 and AgI.
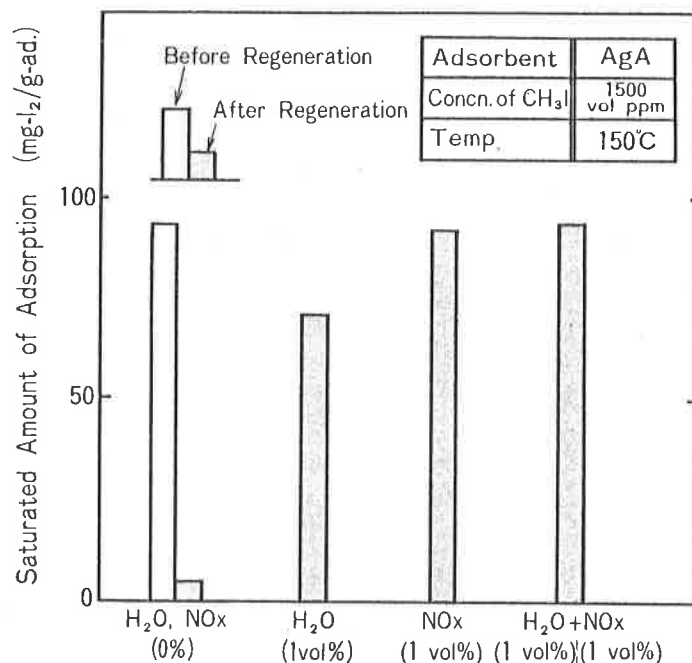
Fig. 9 Effect of Impurity on CH_3I Adsorption

Table 3   Determining of Reaction Products

Impurities	Reaction Product		Possible Reactions
	X-ray Diffraction	Gas Chromatography	
H_2O	AgI	CH_4 CH_3OH	(1) $2Ag + 2CH_3I + H_2O \rightarrow$ $2AgI + CH_4 + CH_3OH$
NOx	AgI	CH_3ONO_2	(2) $2Ag + 2NO_2 + O_2 \rightarrow$ $2AgNO_3$ (3) $AgNO_3 + CH_3I \rightarrow$ $AgI + CH_3ONO_2$
H_2O NOx	AgI	CH_4 CH_3OH CH_3ONO_2	(1) + (2) + (3)

4.   Recycle Tests on AgA and AgS

Figure 10 illustrates changes of I_2 adsorption vs. the number of recycles. The amounts of I_2 for both AgA and AgS did not decrease after seven regeneration cycles, whether NOx and H_2O impurities was present or not. As the pore volume changes did not observed for both adsorbents after seven regeneration cycles, their carriers were found to be proof against heat treatment at 500°C.

Therefore, both adsorbents, AgA and AgS were found to be suitable for regeneration and recycles system to save silver consumption.
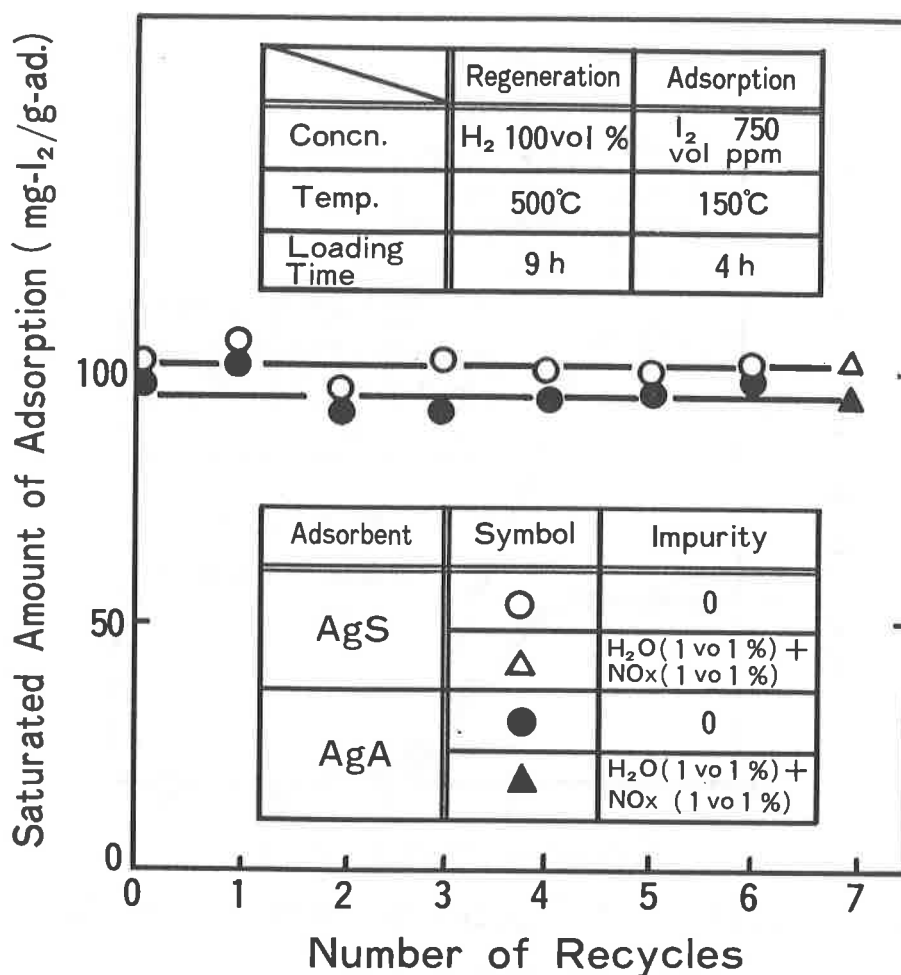
Fig. 10 Changes of I_2 Adsorption of Recycled AgA and AgS

5. Improvement of adsorption capacity on AgA

If these adsorbents, AgA or AgS is used for once through removal system or for recycling system, adsorption capacity of iodine per gram of adsorbents is important to decrease the secondary waste, or to extend recycling period.

Figure 11 shows the capacity increase of I_2 on AgA adsorbent when the content of silver increased from 10 to 24 wt%. It was found that the saturated amount of I_2 adsorption was 235 mgI_2/g-ad for 24 wt% silver content AgA, and which meant over 80 % of silver utilization was achieved. Moreover, no effects due to H_2O and NOx were observed on I_2 adsorption for those adsorbents.

Adsorbent	AgA
Concn. of I_2	750 Vol ppm
Temp.	150°C
Linear Velocity	5 cm/s

Symbol	Ag Content	I_2 loading time
O △	24 wt%	10h
● ▲	10wt%	4h

O ● No impurity

△ ▲ H_2O (1 vol%) + NOx (1 vol%)
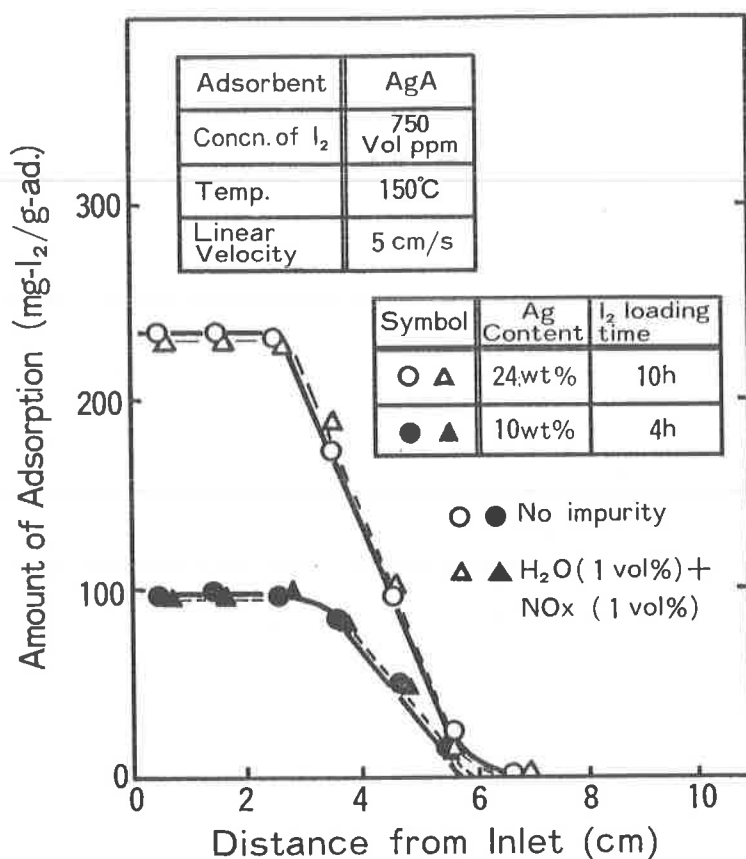
Fig. 11 Improvement of Capacity by Increasing of Ag Content

IV Conclusion

Four different types of silver impregnated adsorbents were compared for their I_2 and CH_3I adsorption characteristics, and following results were obtained.

(1) For AgX and Ag°Z having carrier pore sizes less than 10Å, the amounts of I_2 adsorbed at 150°C were found to desorb at the same temperature reversibly over 10% on a nitrogen gas purge, and to be affected by the presence of H_2O and NOx impurities.

(2) No effects due to H_2O and NOx were observed on I_2 adsorption for AgA and AgS, having carrier pore sizes larger than 100Å.

(3) The amounts of CH_3I adsorption on AgX, AgA and AgS after regeneration by H_2 at 500°C decreased markedly in the absence of H_2O and NOx impurities. This was understood to be due to the formation of metallic silver. Those metallic silver impregnated

1358

adsorbents could hardly react with CH_3I. However, NOx and H_2O impurities had effect to increase adsorption capacity for CH_3I.

(4) Seven cycles regeneration tests indicated that AgA and AgS kept their capacity for I_2 adsorption.

Acknowledgement

Authors wish to express their thanks to T. Yamaguchi, S. Yamada, and R. Itoh of Japan Nuclear Fuel Service and H. Yusa of Energy Research Laboratory of Hitachi Ltd. for their continuing guidance and valuable discussions.

References

1. B.A. Staples et al., "Airborne elemental iodine loading capacities of metal zeolites and a dry method for recycling silver Zeolite." Proc. of 14th ERDA Air cleaning Conf. (1976).

2. T.R. Thomas et al., "The development of Ag°Z for bulk ^{129}I removal from nuclear fuel reprocessing plants and PbX for ^{129}I storage." Proc. of 15th DOE Nuclear Air Cleaning Conf. (1978).

3. J.G. Wilhelm et al., "Head-end iodine removal from a reprocessing plant with a solid adsorbent." Proc. 14th ERDA Air Cleaning Conf. (1976).

4. R.D. Scheele et al., "Methyl iodide sorption by reduced silver mordenite." PNL-4489 (1983).

5. M. Kikuchi et al., "Adsorbent, silver-alumina for radioactive iodine filter." Proc. of 17 th DOE Nuclear Air Cleaning Conf. (1982).

6. L.L. Burger et al., "Selection of a form for fixation of iodine-129." PNL 4045 (1981).

7. L.L. Burger et al., "Recycle of iodine-loading silver mordenite by hydrogen reduction" PNL-4490 (1982).

8. R.T. Jubin et al., "Organic iodine removal from simulated dissolver off-gas streams using partially exchanged silver mordenite." Proc. 17th DOE Nuclear Air Cleaning Conf. (1982).

DISCUSSION

DEITZ: How do hydrocarbons behave as contaminents in silver zeolites? I know you did't use hydrocarbons as contaminents so I am asking how do hydrocarbons influence a silver zeolite in the adsorption of iodine?

HATTORI: I cannot answer your question at this time.

WILHELM: I will try to give an answer to this question. When you have hydrocarbons and you have a material impregnated with silver nitrate and run at a temperature of 150°C, the silver nitrate will be reduced to silver. What will happen then, you have seen from the results of regeneration, the efficiency for methyl iodide drops because methyl iodide doesn't react with silver in AgS and AgR. Therefore, the ability of the material to trap methyl iodide decreases very steeply. We tested the hydrocarbons that give a big effect in the vessel offgas because in the vessel offgas from the extraction process there are a lot of organic as well as the rest of the recycled acids and these can poison the silver nitrate filters. What you can do is quite interesting and goes very easily; if you add NO_2 to the offgas, you will regenerate your filter. We did that and it is a very easy system. You run your filter, anyway, at an elevated temperature, you react, maybe, with 2% NO_2 for some hours, and the poisoned filters are good again. The question is whether you should run them on NO_2 in the first place since NO_2 is not hard to get in a reprocessing plant which dissolves fuel in nitric acid.

VOLATILE RUTHENIUM TRAPPING ON SILICA GEL AND SOLID CATALYSTS

P.W. Cains and K.C. Yewer,
Chemical Technology Division,
AERE Harwell, Oxon. OX11 ORA
UK

Abstract

Packed bed investigations have shown silica gel to be unsuitable as a material for trapping residual volatile ruthenium in high-level waste vitrification off-gas treatment. Desorptive migration of ruthenium trapped on silica gel has been observed with continuing gas flow when the ruthenium concentration is reduced; the nature of this migration suggests that a release from the bed would occur after a very short time.

Subsequent work has concentrated on supported transition metal/oxide catalysts, with the aim of identifying materials that both effectively trap and subsequently retain volatile ruthenium species by promoting their decomposition to stable, solid RuO_2. Four such materials have been shortlisted to undergo further examination.

I   Introduction

During high-level waste calcination and vitrification, some "semi-volatile" fission product elements may volatilise into the off-gas stream. The most important of these is ruthenium; between 1% and 60% of the feed ruthenium may volatilise in the calcination process, depending on process conditions. The presence of volatile ruthenium is an important factor in the design and operation of off-gas treatment plant, because of:-

(a) the tendency of volatile ruthenium to deposit as solid RuO_2 on plant and pipework, and

(b) the requirement to limit environmental releases of the radioisotope ^{106}Ru.

Decontamination of ^{106}Ru is provided by the off-gas condensing and scrubbing units. Under some circumstances, it may also be necessary to install a ruthenium trap. This requirement could be met by a packed column containing a solid sorbent, giving a decontamination factor of the order of 10^2-10^3. This paper outlines the work carried out to date to identify suitable trapping media, and to provide information needed for confidence in the design and satisfactory operation of ruthenium traps.

II Experimental

The packed bed test apparatus used is shown in Figure 1. Volatile ruthenium is generated in the calciner pot, where the ruthenium-containing feed liquor is flash-evaporated at a wall temperature of 400°C. The liquor is fed to the pot by a peristaltic pump at a rate of ~ 0.4 ml min^{-1}. The system is purged

Downstream
samplers

Test
column
(packed,
constructed
in sections)

Upstream
samplers

Carrier/purge gas
(Ar or air)

Calciner
pot
(volatile Ru
generator)

Calciner feed
liquor (containing Ru)
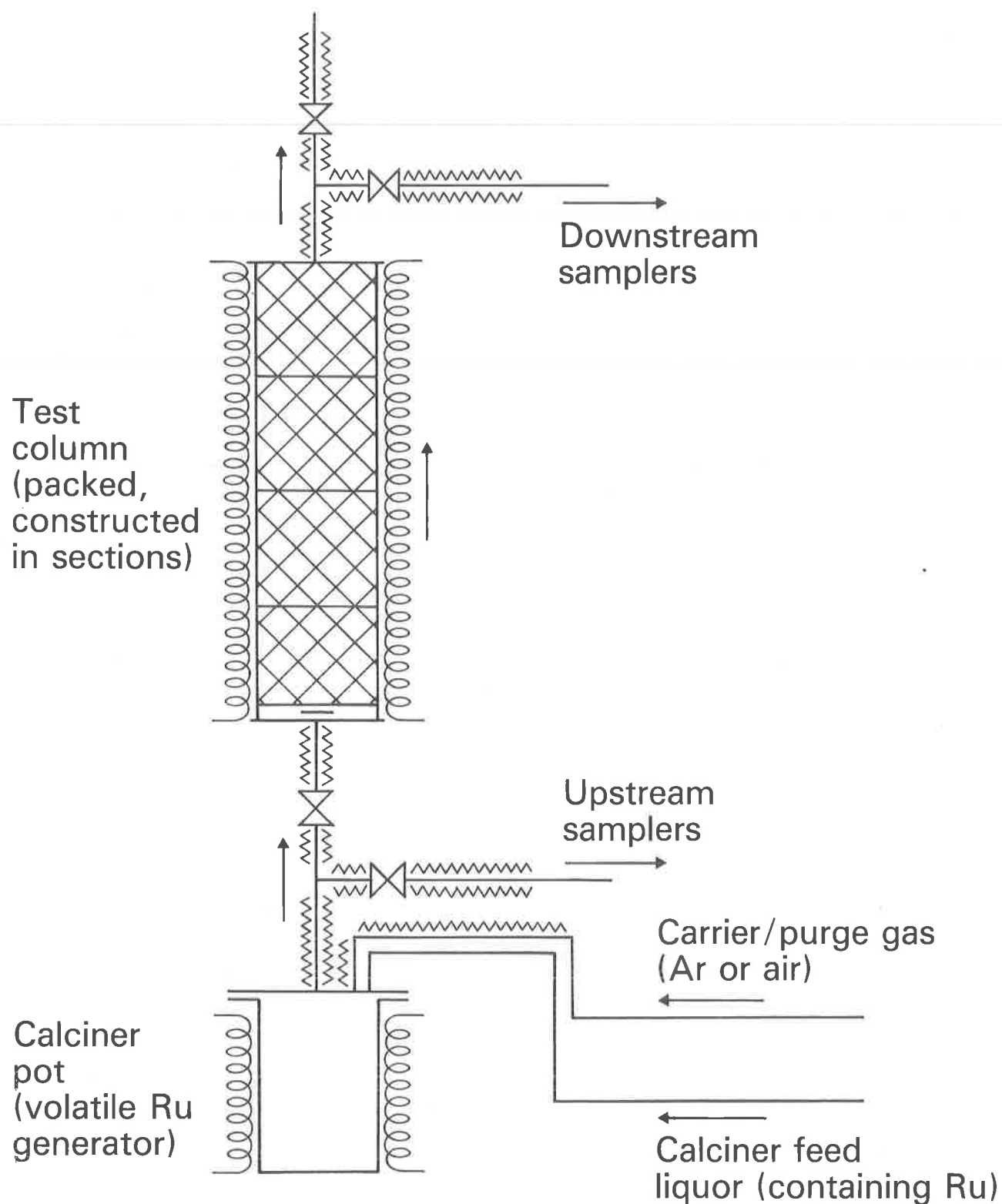
Fig. 1 Packed bed apparatus for ruthenium trapping

by an argon flow of 2 l min^{-1} (at room temperature), which serves as a carrier gas in the test column.

The ruthenium-containing vapours from the pot pass to the test column through a short (100 mm) line held at 350°C. Three different test columns were used, details of which are given in Table 1. A valved diversion is incorporated upstream of the column to allow sampling of the inlet vapours. A similar arrangement is provided down-stream of the column, although in practice the downstream samplers were operational during most of the experimental running time.

In a typical experiment, 15 min periods of 'upstream' sampling are alternated with 2-3 h 'downstream' sampling periods with the vapour passing through the column. 'Downstream' sampling is always preceded by a 20 min stabilisation period to eliminate any perturbations caused by diverting the stream for 'upstream' sampling. The sample lines are led through two Dreschel bottles in series containing ~ 200 ml of 3M HNO$_3$.

Table 1: Details of experimental test columns

Column ref	Diameter (mm)	Superficial velocity (m s^{-1})	Operating temperature range (°C)	Heating 'zones'	No. of Sections (c)
A	82	.01 (a)	up to 200	1	6
B	26	.1 (a)	up to 200	1	2
C	58	.035 (b)	up to 500	3	3

Maximum packing height 0.75m

(a) at 90°C for flowrates specified
(b) at 350°C for flowrates specified
(c) columns are constructed in flanged sections to facilitate assembly, dismantling and profiling.

Early experiments with silica gel were carried out inactively, with column decontamination factors determined from colorimetric analysis of the sampler solutions. The feed solutions to the calciner pot contained nitro/nitrato complexes of nitrosylruthenium (III)[1] (8-10 mg Ru ml^{-1}) in 8M HNO$_3$, to represent the ruthenium in high-level waste solutions[2].

Most of the work has been carried out using the radioisotope ^{103}Ru to measure column profiles and decontamination factors. This is supplied as the chloride in 4M HCl. To ensure satisfactory isotopic dilution, any inactive ruthenium for concentration adjustment is added to the ^{103}Ru preparation as a solution of ruthenium (III) chloride in 4M HCl. The mixed chloride solution is diluted with 8M HNO$_3$ or water as required for the feed liquor.

Where ruthenium is added to 8M HNO_3 as chloride (chloro complex), the fraction volatilised in the calciner pot is significantly lower than for the nitrosyl complexes (at higher concentration) in the inactive work. However, the amounts volatilised were sufficient for trapping measurements in all cases. Although the chemical forms of ruthenium in solution will probably affect the volatilisation process in flash evaporation, it is thought improbable that significant differences will occur in the chemical form(s) of the ruthenium volatilised. In experiments where HNO_3 was absent from the feed liquor, volatilisation was induced by adding $HClO_4$ (to 0.1M).

III   Ruthenium Trapping by Silica Gel

An initial literature survey indicated that silica gel was a leading candidate material for ruthenium trapping. Early work in the USA[3] suggested that decontamination factors of the order required were attainable, and a more recent report[4] recommended silica gel and iron (III) oxide as materials most likely to be suitable. Because of its ready availability, low operating temperature and ease of disposal, silica gel was selected at the start of the programme as the prime contender, and a detailed assessment programme was undertaken.

Gel temperature, particle size and residence time.

This first series of experiments was carried out inactively, with ruthenium vapour concentrations of 100-500 mg m^{-3} (element) at the column inlet. The inlet vapour also contained $\sim$ 3% HNO_3/ nitrogen oxides. Decontamination factors were calculated from the concentrations of the sampler solutions; no bed profiling was undertaken. As will be discussed below, no variation of decontamination factor with inlet concentration may be discerned in the range specified here.

Figure 2 shows decontamination factor (df) versus temperature for a 125 mm packing height of 1.5 - 3.0 mm gel particles in column A. (residence time $\sim$ 4.8s). The highest dfs were recorded at bed temperatures near the dew-point of the vapours in the column (77°-80°C), with decontamination generally decreasing with increasing temperature. A number of points between 85°C and 120°C, with dfs between 100 and 300 show no systematic trends within this range. However, temperature fluctuations may have occurred within the bed owing to the adsorption and desorption of water vapour and the poor heat transfer characteristics of the bed.

The standard pretreatment for the silica gel used was to contact overnight with water vapour at room temperature, followed by drying at 180°C and re-contacting with water vapour. Substituting formaldehyde solution for water in the pretreatment yielded no change in performance (Fig. 2), probably because any residual formaldehyde was driven from the gel surface on heating to the operating temperature. Decontamination performance was also unaffected by the substitution of air for the argon carrier gas.
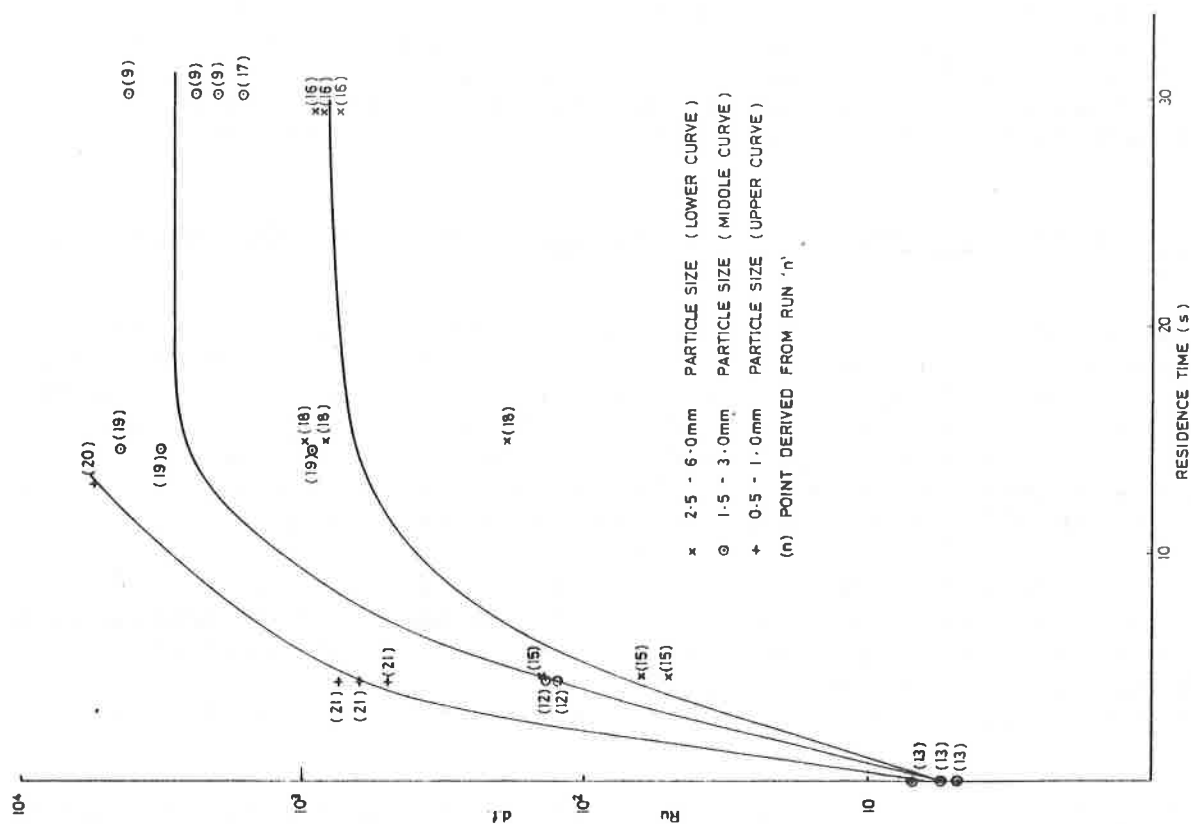
Fig. 3 Ru d.f. vs residence time for gel in various particle size ranges
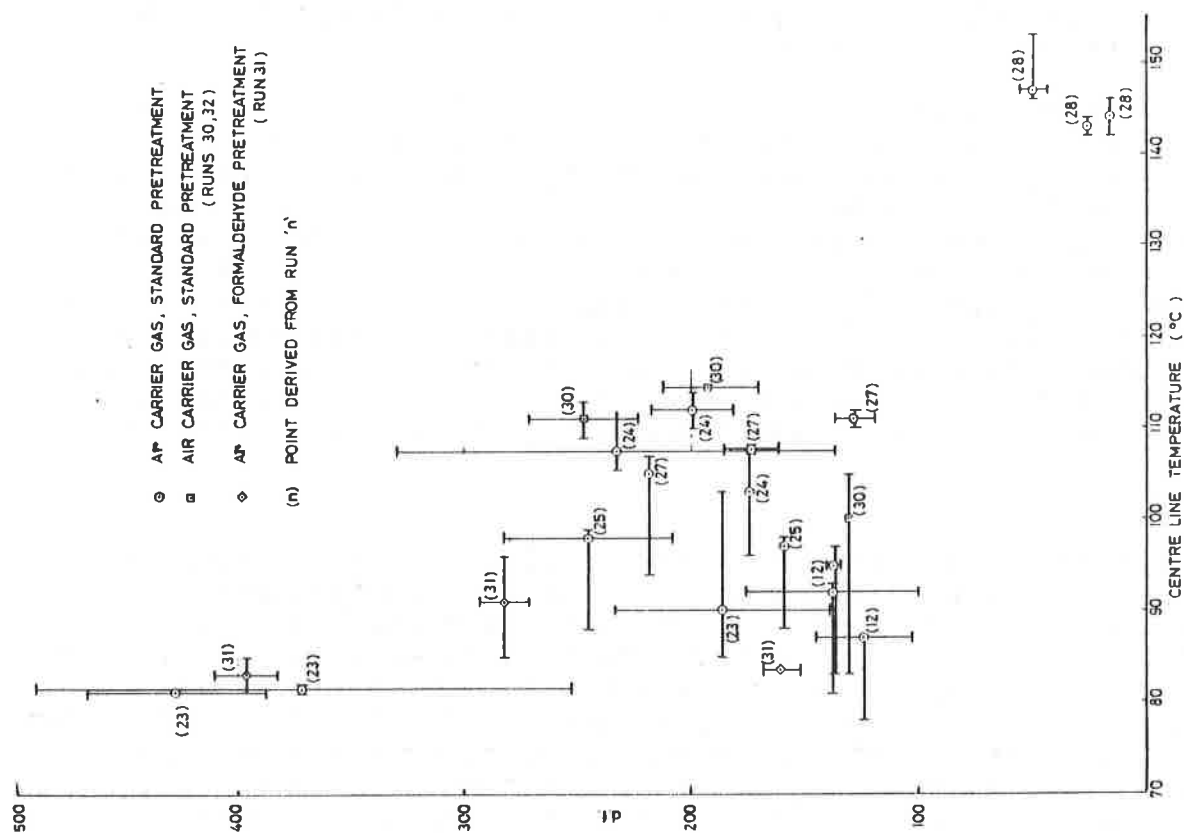
Fig. 2 Ru d.f. vs centre-line temperature for 12.5cm bed silica gel. 1.5-3.0mm

Figure 3 shows decontamination factor as a function of bed height, expressed as residence time, for three different gel particle size ranges. The points on the ordinate refer to the values recorded with the test column A empty, representing the removal of volatile ruthenium by deposition on the equipment. All these experiments were carried out in the gel temperature range 85°-100°C.

Ruthenium inlet concentration and nitric acid vapour/decomposition products

Using the radioisotope ^{103}Ru, decontamination factors have been measured over 4 orders of ruthenium inlet concentration. The circles in Figure 4 represent the results where the feed liquor to the calciner pot is made up to 8M HNO_3, corresponding to a vapour phase nitric acid + nitrogen oxides concentration of 3 mole-%. Column A was employed with a packing height of 125 mm of 1.5-3.0 mm silica gel at 85°-100°C, giving a residence time of 4.8s.

The large error bars on the results at low ruthenium concentrations arise from variations in the measured concentrations of samples taken upstream of the test column. These variations were found in all work at low ruthenium concentrations and are thought to be due to inconsistent volatilisation in the calciner pot.

Despite these potential errors, the circled points in Figure 4 clearly show an increasing df as the ruthenium concentration decreases, and the ratio of nitric acid and decomposition products to volatile ruthenium consequently increases. The points at inlet concentrations above 100 mg.m^{-3} were obtained in the inactive experiments described in the previous section.

In these experiments, the ratio of HNO_3 vapour, NO_2, NO to volatile ruthenium was higher than that expected in practical situations. The introduction and control of small quantities of nitrogen oxides would be difficult in the equipment used here. However, experiments have been carried out where nitric acid is entirely absent from the feed liquor; the results are shown as asterisks in Figure 4. Ruthenium vapour inlet concentrations were in the range 0.1-1 mg m^{-3}, with volatilisation induced by $HClO_4$. Rather lower dfs were recorded compared with the experiments with nitric acid present, and a marked deterioration in decontamination performance is indicated with decreasing ruthenium concentration.

Vapour flow velocity

A single experiment has been carried out using column B to determine the effect of vapour velocity on decontamination performance. The variation of df with residence time was not significantly affected by the ten-fold increase in velocity. The bed profile of adsorbed ^{103}Ru versus residence time was, if anything, slightly steeper in gradient at the higher velocity, but it appears unlikely that ruthenium trapping over the 6-7h periods of these experiments will be greatly affected by superficial velocity in the range 0.01-0.1 m s^{-1}, for any given residence time.
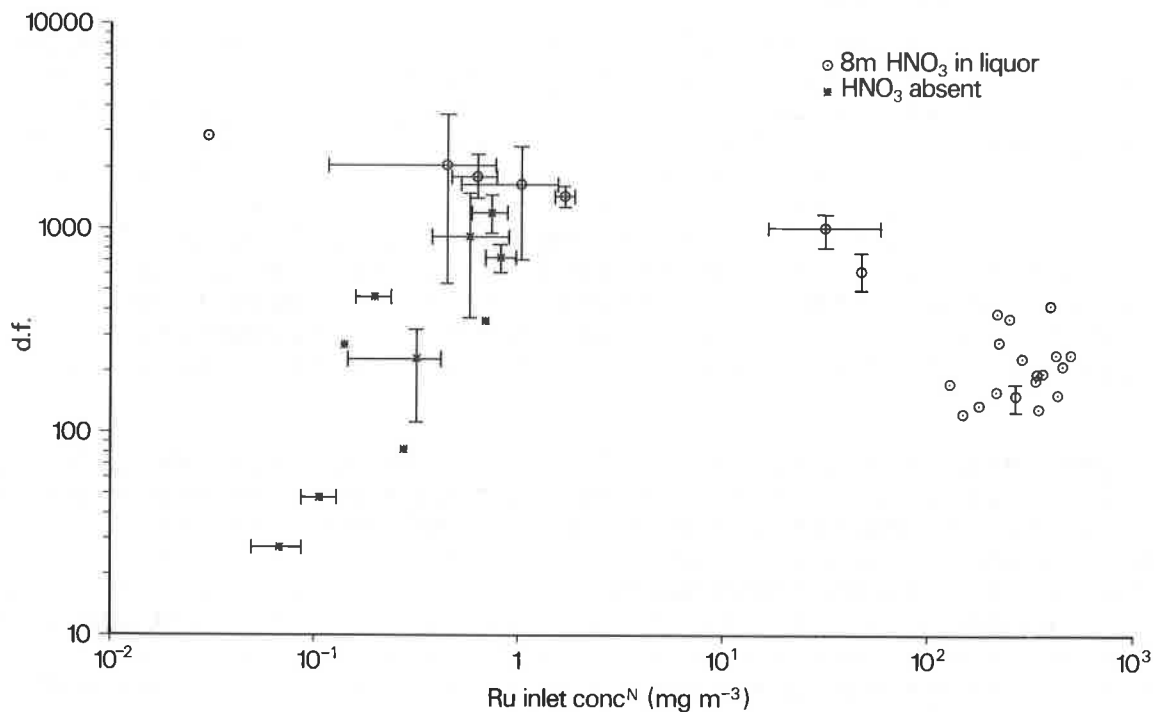
Fig. 4 Plot of d.f. v.s. inlet concentration for adsorption of Ru on a silica gel bed. Bed height 12·5cm. Superficial velocity −1cm S⁻¹
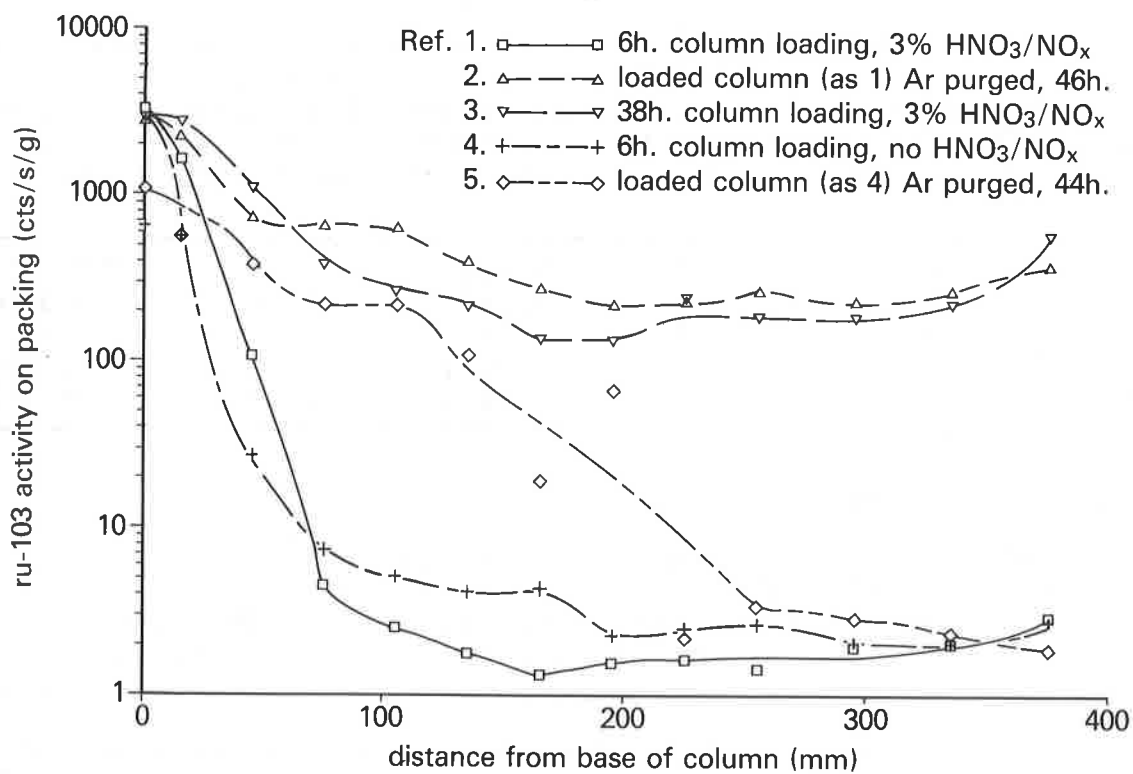
Fig. 5 Profiles of trapped ruthenium on silica gel

Retention of trapped ruthenium

As reported previously[3-5], volatile ruthenium is trapped on silica gel, initially at least, by physisorption. To establish the suitability of silica gel for volatile ruthenium trapping in nuclear plants, it is necessary to demonstrate the retention of the adsorbed ruthenium over realistic operating times, and that a loaded bed will not discharge into the gas stream when the ruthenium vapour concentration is reduced, e.g. in plant 'down' time or fluctuations in process feed rate. Bed profiling experiments to ascertain any desorption effects were therefore undertaken, in which a gel bed was loaded with ruthenium, and subsequently purged at temperature with the carrier gas for up to 48h.

The results are given in Figure 5; experimental details in Table 2. Curves (1) and (2) shows that considerable migration of ruthenium to the downstream part of the bed occurred when the loaded bed was purged with pure argon. This is due to the desorption of trapped (physisorbed) ruthenium into the gas stream, and its re-adsorption in the downstream parts of the bed where the surface concentrations are lower. A qualitatively similar desorption effect was observed where no nitric acid is present, curves (4) and (5), although the extent of the migration appears to be less in this case.

Table 2: Experiments to determine ruthenium retention behaviour on silica gel. Column A.

Curve (Fig 5)	HNO_3 in feed liquor (M)	Total liq feed time (h)	Ru inlet concn* (mg m^{-3})	Gas purge time after feed cessation (h)	DF. across test column*
1	8	6.6	0.3±0.1	−	3900–6600
2	8	6.4	0.3±0.1	46.0	∼ 9000
3	8	37.7	−	−	−
4	−	6.7	∼ 0.1	−	21–27
5	−	6.5	∼ 0.03	43.7	54–181

*during bed loading

Packing height 0.375 m; residence time 15s
Gel temperature 85°–100°C
Dew-point temperatures : curves (1), (2), (3) : 78°–81°C
                          curves (4), (5)   : 64°–67°C

Curve (3) corresponds to continuous bed loading over the 38 h of the experiment. The distribution of trapped ruthenium along the bed suggests that the equilibrium surface concentration of adsorbed ruthenium is low at the vapour concentrations under study. This

indicates that the practical capacity of the bed will be low.

Discussion

The earlier inactive experiments of Figures 2 and 3 suggested that satisfactory decontamination factors for volatile ruthenium may be attained with a silica gel trap. Subsequent radioisotope studies, however, showed that the retention capacity of the gel will in practice be low at the low concentrations of primary interest here. This will severely limit decontamination performance where it is required to trap ruthenium from very dilute streams over long periods. The decontamination and retention behaviour is also affected by nitric acid/nitrogen oxides in the vapour.

The basic physiochemical processes contributing to the mechanism of trapping are thought to include:-

(a) Physisorption of volatile ruthenium species (such as RuO_4) at the gel surface.

(b) Interaction of the adsorbed volatile ruthenium with other adsorbed species, such as NO, NO_2, HNO_3, at the gel surface.

(c) Chemical decomposition of adsorbed volatile ruthenium (and products of (b)) to stable, solid RuO_2.

(d) Intraparticle mass transfer processes (surface diffusion, pore diffusion) removing adsorbed species from (a) and (b) from the active sites of the gel surface.

This mechanism is discussed in some detail elsewhere[8]. In support of processes (b) and (c), early bed loading experiments with HNO_3 present yielded a product gel that was dark red in colour. Backwashing with water removed ~50% of the ruthenium into a red-brown solution, leaving a blackened residue. It is suggested that the insoluble residue arises from step (c), and that the soluble fraction may contain reduced species such as Ru(IV) and Ru(NO)(III). The adsorbed phase interactions in step (b) may account for the apparent enhancement of decontamination performance where HNO_3 and NO_x species are present (Fig 4). Furthermore, the desorption behaviour of curves (1) and (2) in Figure 5 may arise from reversible chemical processes in (b) liberating volatile species.

It has generally been assumed that the chemical form of volatile ruthenium arising in waste calcination is the tetroxide RuO_4. Klein et al[6,7] have suggested that other gaseous forms of ruthenium may exist where nitric acid/nitrogen oxides are present. We feel that interactions in the adsorbed phase are more likely to explain the observed behaviour. Spectroscopic studies of both the gas phase and the adsorbate would be required to further elucidate the underlying trapping mechanism.

Rimshaw and Case[9] observed the conversion of gaseous RuO_4 to particulate RuO_2 aerosol on contact with silica gel. There were

no indications of substantial particulate formation in this work.

IV Ruthenium Trapping by Transition Metal/Oxide Catalysts

More recent work has aimed to identify materials which are suitable for both trapping and subsequently retaining volatile ruthenium. Satisfactory retention of trapped ruthenium would be achieved by promoting the decomposition of adsorbed species to solid RuO_2, following step (c) of the above mechanism.

Iron (III) oxide has been suggested as an alternative to silica gel for ruthenium trapping[4,10]. Laboratory studies[4] reported that trapped ruthenium was not elutable from iron oxide, indicating that conversion to a stable or chemisorbed non-volatile form had taken place. The operating temperatures reported for iron oxide traps are 250°-450°C[4,10].

The rapid conversion of trapped ruthenium to a non-volatile form (and the evidence of RuO_2 deposition on steel surfaces) suggests that iron oxide may catalyse the decomposition of adsorbed RuO_4 (or other volatiles) to RuO_2. At the temperatures specified, this is likely to occur via chemisorption of the volatile species, requiring a trapping medium of high surface area. A commercially produced iron (III) oxide catalyst on a γ-alumina support was therefore selected for evaluation.

Since the conversion of adsorbed ruthenium to RuO_2 involves a redox process (eg $RuO_4 \rightarrow RuO_2$), and the chemisorption of RuO_4 would presumably occur via the oxygen atoms of the tetrahedral molecule[11,12], it is suggested that iron (III) oxide catalyses the process by virtue of its non-stoichiometric "semiconductor" behaviour[13]. This property is exhibited by the oxides of most other transition metals, and arises from their multiple valence states. It seems likely, therefore, that other transition metal oxides will catalyse the formation of stable RuO_2. A range of such catalyst preparations has been tested in an initial screening study to identify the most promising candidates for more extensive ruthenium trapping investigations.

Selection of most promising trapping media

The experiments summarised in Table 3 were carried out with the primary aim of determining the ruthenium retention behaviour of the materials under test. The most important selection criterion was therefore the bed profiles obtained. All experiments except (12) and (13) were carried out in column C at 350°C, with a total bed height of 0.5m. The calciner pot feed solution contained 8M HNO_3.

The vapour samples taken upstream of the column showed wide variations in ruthenium concentration; these variations contribute to the wide ranges of decontamination factors quoted in Table 3. One consistent feature shown in runs (16) to (21) with NiO, V_2O_5 and Ru catalysts, is a marked increase in df after the first 2-3h of running. Two sets of df values are given in each case, corresponding to the earlier and later parts of the experiment.

This effect was not exhibited by the other materials tested.

Although decontamination factors are not the primary objective of this stage of the investigation, the values in Table 3 give some guidance as to whether satisfactory decontamination is likely to be achievable. For example, the silicated iron oxide preparation, run (15), with a df of 7-26, may be rejected. Further work on short-listed materials must include studies of decontamination with respect to Ru inlet concentration, temperature and time. No general correlation of decontamination factor with inlet concentration is apparent.

Of the materials listed in Table 3, the most satisfactory column profiles were exhibited by zinc oxide, ruthenium metal, nickel (II) oxide and chromium (III) oxide. The zinc oxide profile, Figure 6, clearly illustrates the required retention characteristics, with the 'loading' and 'loading + purging' curves coinciding to indicate negligible desorption. However, the ^{103}Ru count rate in the downstream (250-500 mm) part of the column is significantly above the background value. This indicates that some penetration of the bed has occurred, and that the performance of zinc oxide at very low vapour concentrations may not be entirely satisfactory.

The bed profile for the ruthenium metal catalyst, Figure 7, shows the bulk of the ^{103}Ru retained in the upstream 150 mm or so of the bed, suggesting that good decontamination may be attained with as relatively low residence time column. The most significant difference between the two curves is probably at the downstream end of the column, where the 'loading + purging' curve shows slightly, but significantly, higher ^{103}Ru count rates. This may indicate a small amount of migration down the column, but repeat experiments would be required to ascertain that this is not simply experimental error.

The curves for nickel (II) oxide and chromium (III) oxide, Figures 8 and 9, are less satisfactory and suggest that some migration of trapped ^{103}Ru takes place in the 'purging' period. The extension of the 'high-plateau' region of the curves downstream and the occurrence of higher downstream count rates are indicative of migration, but the effect is very much less marked than for silica gel (Fig 5). Figures 6-9 are derived from single experiments, and aim only to provide a first indication of suitability for further experimental investigation. With this in mind, the profiles in Figures 8 and 9 are more satisfactory than those obtained from other materials in Table 3, and their inclusion in the short-list for further investigation is thought to be justified.

Further work

Experiments are now being carried out in which single particles of the short-listed catalyst materials are contacted with vapours containing volatile ruthenium. This should yield fundamental information to assess the performance of these materials with respect to vapour composition (ie Ru and nitrogen

1371

TABLE 3

Packed-Bed Experiments to Determine Ruthenium Retention on Catalysts
(Column C, 350°C)

Ref. no.	Catalyst/support	Surface area (m²)	Total liquor feed time (h)	Ru inlet concentration* (mg·m⁻³)	Gas purge time after feed cessation (h)	DFs recorded across test column*
11	Empty column	–	7.7	0.015–0.63	–	0.5–10
12+	Iron (III) oxide 20% on γ-alumina	40	7.4	0.07–0.16	–	400–850
13+		40	6.7	0.05–0.06	28	700–850
14#		40	7.7	0.35–0.65	–	800–1750
15	'Silicated' iron (III) oxide	–	6.4	0.036–0.069	–	7–26
16	Nickel (II) oxide 11% on γ-alumina	65	6.1	0.028–0.13	–	130–500, 2500
17		65	6.8	0.027–0.14	65.6	115–500, 2500
18	Vanadium (V) oxide 4% on γ-alumina	–	6.0	0.10–0.77	–	100–250, 740
19		–	6.0	0.11–1.3	69.8	150–370, 1450
20	Ruthenium (metal) 0.5% on γ-alumina	100	6.0	0.005–0.085	–	139–170, 110–2500
21		100	5.7	0.15–0.28	48.0	390–750, 1400–2150
22	Chromium (III) oxide 17.5% on γ-alumina	50	5.7	0.06–0.08	–	270–400
23		50	4.4	0.07	48.3	62

Table 3 Continued

24	Copper (II) oxide 12.5-15% on γ-alumina	187	5.8	0.10-0.16	–	340-600
25			5.2	0.37-0.39	48.0	405-1100
26	Zinc (II) oxide (with 3-7% Al$_2$O$_3$, 0.5-3% CaO)	20	5.2	0.56-0.99	–	1400-4500
27			5.3	0.23-0.71	48.0	280-1170
28	Molybdenum (VI) oxide 10-12% on γ-alumina	64	3.2	0.12-0.50	–	360-1400
29			5.5	0.26-0.29	–	>1100
30	Cobalt (II) oxide 3.5% Molybdenum (VI) oxide 10% on γ-alumina	244	5.7	0.11-0.49	–	20-350
31			5.5	0.18-0.42	–	230-920
32	Manganese (IV) oxide 19% on γ-alumina support	70	5.6	0.007-0.014	–	46-73
33			5.3	0.48	–	91
34	γ-alumina support	100-200	5.0	0.26-0.36	–	380-540
35			7.8	0.09-0.18	64.1	580-1500

* during bed loading
+ Column B, 150°-200°C, height 0.7m
‡ bed height 0.32 m
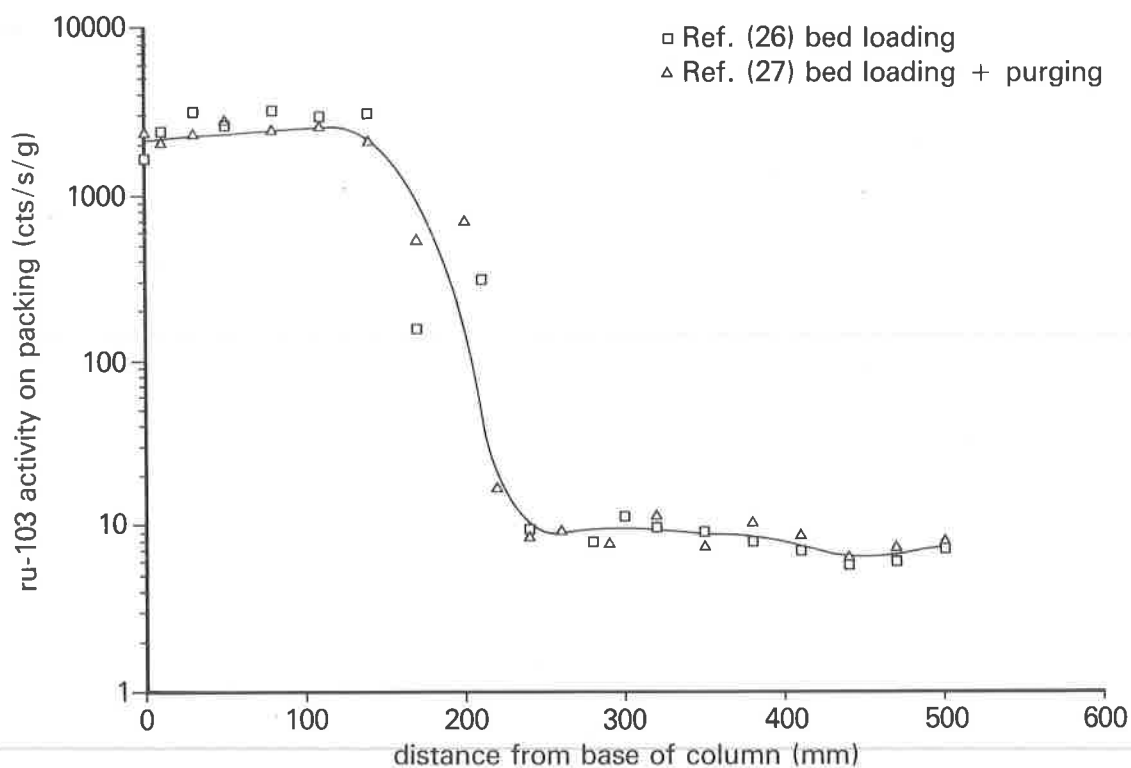
Fig. 6 Profiles of trapped ruthenium on zinc oxide catalyst
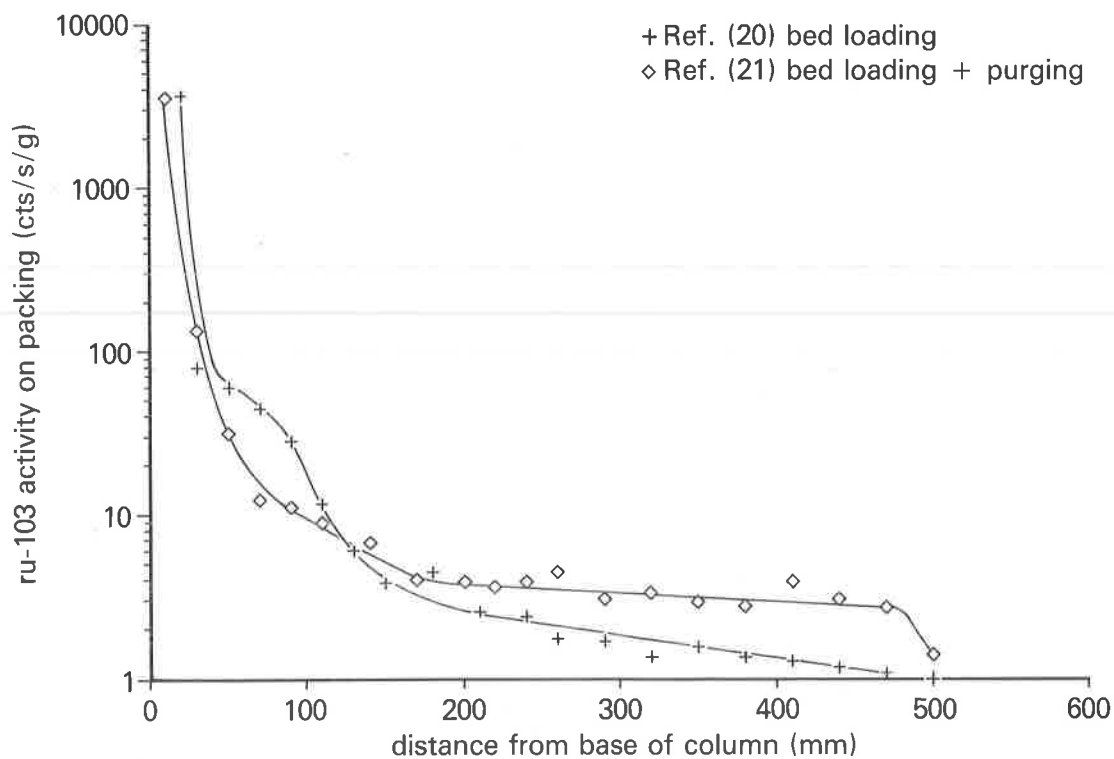
Fig. 7 Profiles of trapped ruthenium on ruthenium metal catalyst
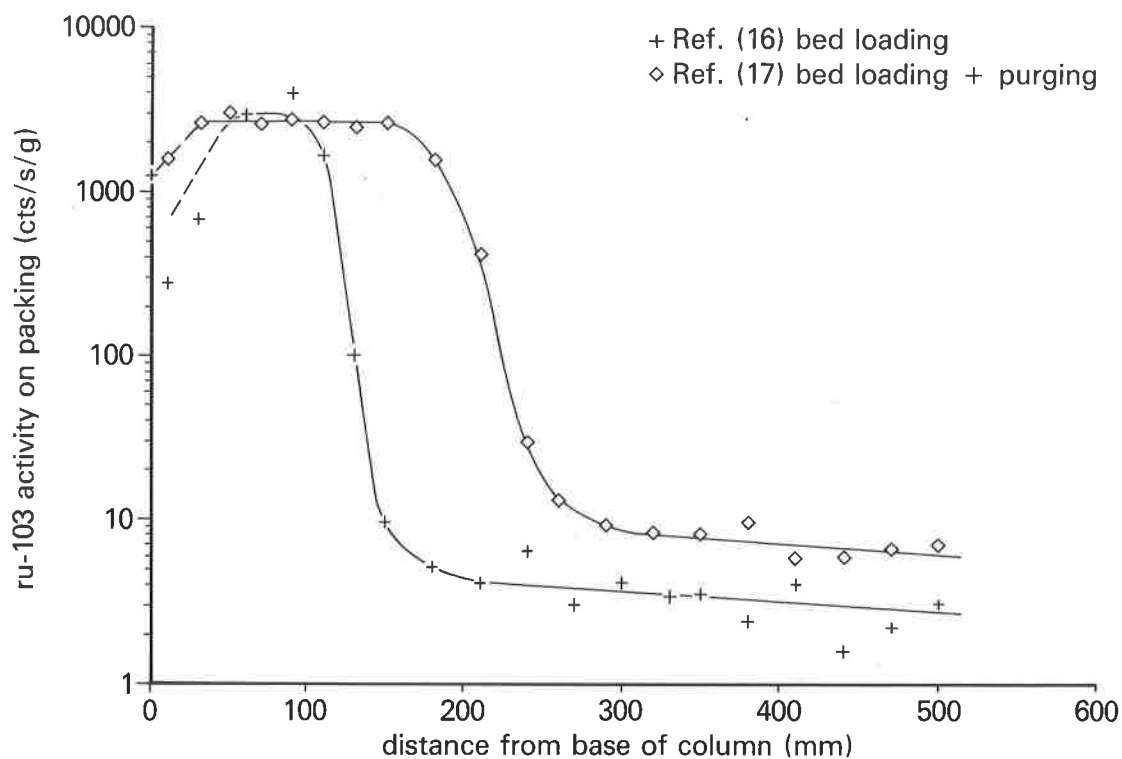
Fig. 8 Profiles of trapped ruthenium on nickel(II) oxide catalyst
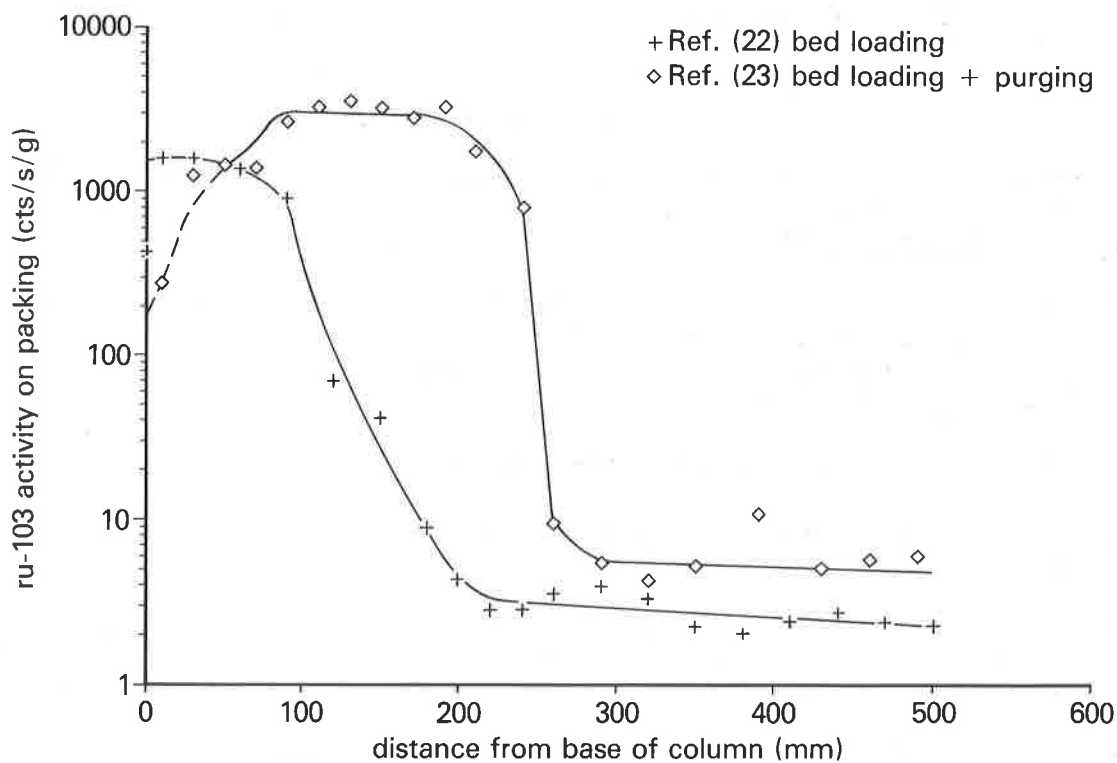
Fig. 9 Profiles of trapped ruthenium on chromium(III) oxide catalyst

oxide concentrations), temperature, and the extent to which the particle is loaded. It is hoped that this work will give some insight into the mechanism of ruthenium trapping on these catalysts.

V Conclusions

1. Silica gel is regarded as unsuitable for trapping residual volatile ruthenium from high-level waste vitrification off-gases. The principal reasons for this are the observed desorption of trapped ruthenium from the gel in a continuing gas flow, and the low effective capacity of the gel under the conditions of interest. The desorption implies that ruthenium could be eluted from a loaded bed into an uncontaminated gas stream during process 'down' time, or when the process feed rate is reduced.

2. An alternative material is being sought which both traps and effectively retains volatile ruthenium. Of the range of 11 catalyst materials that have been examined, a zinc oxide catalyst, and ruthenium metal (0.5%), nickel (II) oxide (11%) and chromium (III) oxide (17.5%) on γ-alumina supports appear to offer most potential, and will be subject to further investigation.

Acknowledgement

References

1. Boswell, G.G.J.; Soentono, S. "Ruthenium nitrosyl complexes in nitric acid solution"
J. Inorg. Nucl. Chem. 43 1625 (1981).

2. Blasius, E.; Glatz, J.P.; Neumann, W. "Ruthenium nitrosyl complexes in radioactive waste solutions of reprocessing plants. I. Cationic ruthenium nitrosyl complexes"
Radiochim. Acta 29 159 (1981).

3. Rhodes, D.W. "The adsorption of volatile ruthenium on silica gel".
paper to 6th USAEC Air Cleaning Conference, July 7th-9th 1959.
Report TID-7593 p.68 et seq.

4. Newby, B.J.; Barnes, V.H. "Volatile ruthenium removal from calciner off-gas using solid sorbents".
INEL Report ICP-1078 (1975).

5. Klein, M.; Desmet, M.; Goossens, W.R.A.; Baetsle, L.H.
"Filtration and capture of semi-volatile nuclides".
Paper IAEA-SM-245/51 to IAEA Symposium on Management of gaseous wastes from nuclear facilities. Feb 18th - 22nd 1980.

6. Klein, M.; Weyers, C.; Goossens, W.R.A. "Volatilization and trapping of ruthenium in high temperature processes". Paper 4-5 to 17th USDOE Air Cleaning Conference Aug 2nd – 5th 1982.

7. Klein, M.; Weyers, C.; Goossens, W.R.A.; Desmet, M.; Trine, J. "Volatilization and trapping of ruthenium during calcination of nitric acid solutions". IAEA Paper IAEA-SR-72/03 (1983).

8. Cains, P.W.; Yewer, K.C. "Volatile ruthenium trapping by adsorption on silica gel" Harwell Report AERE-R 10308 (1982).

9. Rimshaw, S.J.; Case, F.N. "Volatilities of ruthenium, iodine and technetium on calcining fission product nitrate wastes". Paper CONF-801038-4 to 16th USDOE Air Cleaning Conference, 1980.

10. Elliot, M.N.; Gayler, R.; Grover, J.R.; Hardwick, W.H. "Fixation of radioactive waste in glass. Part III. The removal of ruthenium and dust from nitric acid vapours". Harwell Report AERE-R 4098 (Pt III) (1962).

11. Cyvin, S.J.; Brunvoll, J.; Cyvin, B.N.; Meisingeth, E. "Mean amplitudes of vibration and related quantities for XY_4 molecules" Bull. Soc. Chim. Belg. <u>73</u> 5 (1964).

12. Müller, A.; Krebs, B.; Cyvin, S.J.; Diemann, E. "Kraftkonstante, verallgemeinerte mittlere quadratische Schwingungsamplituden, Bastiensen – Morino – Schrumpfeffekt und thermodynamische Funktionen von Rutheniumtetroxid" Z. anorg. allgem. Chem. <u>359</u> 194 (1968).

13. Bond, G.C. "Principles of catalysis" 2nd Ed. Roy. Inst. Chem. monographs for teachers, no. 7, 1968.

DISCUSSION

<u>WICHMANN</u>:   Do you think that you would get the same good results with dissolver offgas from a reprocessing plant?

<u>ROBINSON</u>:   I am not thoroughly familiar with this work, but I think so. The offgases would contain basically the same constituents.

<u>WICHMANN</u>:   Yes, that is what I mean.

<u>ROBINSON</u>:   Intuitively, I say, yes, but you can't say for certain until you try it.

RECOVERY AND PURIFICATION OF Xe-133 AS A BY-PRODUCT
OF Mo-99 PRODUCTION USING LINDE 5A MOLECULAR SIEVE

N.A. Briden and R.A. Speranzini
Atomic Energy of Canada Limited
Research Company
Chalk River Nuclear Laboratories
Chalk River, Ontario, Canada. K0J 1J0

Abstract

The Xe-133 gas from the Mo-99 Production Facility is commercially valuable but is not presently collected for sale because of the NO_x contaminants in the off-gas. The Xe-133 for sale must be produced in a separate cell, where UAl targets are dissolved in NaOH. A procedure has been developed for collecting and purifying the off-gas Xe-133 from the Mo-99 Production Facility. The procedure involves trapping the Xe-133/NO_x gas mixtures released during dissolution of Mo-99 targets on columns containing Linde 5A molecular sieve, then pressurizing the columns with He, and eluting/separating the Xe-133 and NO_xs chromatographically.

During an active demonstration of the procedure using two 2.5 cm i.d. x 2.1 m long columns, an average of 15 TBq of NO_x-free Xe-133, were recovered per gram of U-235 fissioned. The composition and purity of the product compared favourably with the composition and purity of Xe-133 produced by caustic dissolution. In this report, the inactive development work and the procedures and results of the active experiments are described.

Future experiments will be directed at demonstrating that substantial quantities of Xe-133 can be produced on a routine basis and at developing a secondary purification system for cleanup of NO_x-contaminated products.

I. Introduction

The Xe-133 gas from the Mo-99 Production Facility is commercially valuable but is not presently collected for sale because of the NO_x contaminants in the off-gas. The Xe-133 for sale must be produced in a separate cell, where irradiated UAl targets are dissolved in NaOH. Attempts have been made to collect and purify off-gas Xe-133 from the Mo-99 Production Facility. These attempts, using an ammonia reduction system developed by Briggeman et al.[1] to remove NO_xs from the Xe-133, have been unsuccessful to date. Another procedure, in which columns containing Linde 5A molecular sieve are used for trapping, then eluting/purifying the Xe-133 released during dissolution of Mo-99 targets, has recently been successfully developed and demonstrated. These latter experiments are the subject of this report.

Details of the inactive development work, the active experiments and the active demonstration are described in turn following a short summary of the background chemistry.

II. Background Chemistry

Mixed oxides of nitrogen (NO_xs) are produced during dissolution of Al-21 wt% U targets according to the approximate reactions[2] shown below:

$$U + 4.5\ HNO_3 \longrightarrow UO_2(NO_3)_2 + 1.57\ NO + 0.84\ NO_2 + 0.0005\ N_2O + 0.043\ N_2 + 2.25\ H_2O$$

$$Al + 3.75\ HNO_3 \longrightarrow Al(NO_3)_3 + 0.225\ NO + 0.15\ N_2O + 0.1125\ N_2 + 1.875\ H_2O$$
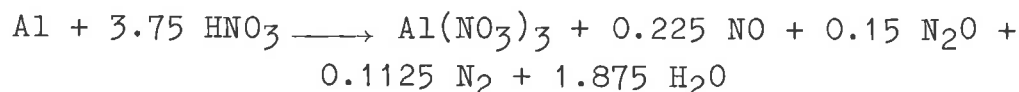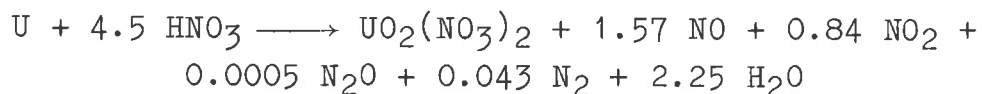
As shown in Table 1, 855 mL of NO, 75 mL of NO_2 and 475 mL of N_2O are produced according to these reactions compared with the 3.5 mL of Xe liberated during the dissolution of a target containing 1 g of U-235 before irradiation.

Table 1   Amounts and physical properties of oxides of nitrogen generated during dissolution of Mo-99 target containing 1 g U.

Description	Compound			
	NO	NO_2	N_2O	Xe
mL from dissolution of 1 g U	145	75	–	–
mL from dissolution of 3.8 g Al	710	–	475	–
Total mL	855	75	475	3.5
Boiling Point	-152°C	21°C	-88°C	-107°C
Colour	clear	brown	clear	clear
Remarks	reacts with O_2 to form NO_2	dimerizes to form N_2O_4	unreactive but decomposes to $N_2 + O_2$ at elevated temp. – used as anasthetic	unreactive

In the Mo-99 production cell, oxygen (O_2) is bubbled through the dissolver solution to oxidize the NO_xs to nitrate (NO_3^-) according to the reactions:

$$2 \; NO + O_2 \rightarrow 2 \; NO_2$$

$$3 \; NO_2 + H_2O \rightarrow 2 \; HNO_3 + NO$$
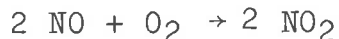
In theory, the overall equation for dissolution of U (for example) becomes[3]:

$$U + 2 \; HNO_3 + \frac{3}{2} \; O_2 \rightarrow UO_2(NO_3)_2 + H_2O$$
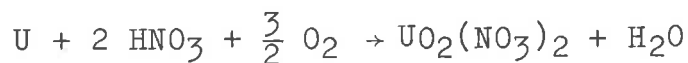
In practice, the reactions of O_2 and NO_xs are incomplete and in the Mo-99 cell, NO_xs are present in the dissolver solution and off-gas. The major fraction of the NO_xs in the off-gas stream are removed in the two off-gas scrubbing solutions. In the first scrubber, containing 0.1 mol/L HNO_3, possible reactions are:

$$2 \; NO + HNO_3 + H_2O \longrightarrow 3 \; HNO_2$$

$$2 \; NO_2 + H_2O \xrightleftharpoons{} HNO_3 + HNO_2$$

$$3 \; NO_2 + H_2O \xrightleftharpoons{} 2 \; HNO_3 + NO$$
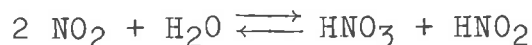
In the second scrubber, containing 5 mol/L NaOH, possible reactions are:

$$NO + NO_2 + 2 \; NaOH \longrightarrow 2 \; NaNO_2 + H_2O$$

$$4 \; NO + 2 \; NaOH \longrightarrow 2 \; NaNO_2 + N_2O + H_2O$$
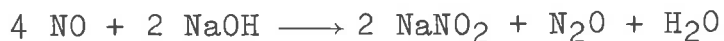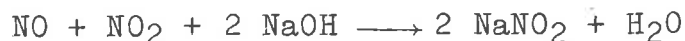
For the purpose of sizing of equipment for experiments, it was assumed that the off-gas treatment system (including O_2 injection) was effective in removing 99% of the NO_xs such that the 1.25 L of off-gases* produced during dissolution of a target containing 1 g of U-235 before irradiation were assumed to contain about 14 mL of NO_xs (10,000 ppm). This compares with about 3 mL of Xe released during dissolution of the target. The assumption was verified by a successful demonstration of the equipment which was designed. Since a product containing less than 100 ppm of NO_xs was required, a decontamination factor of about 100 was required of the NO_x removal system for the treated off-gas.

In the work reported here, samples of gas were analyzed using a Micromass 601 mass spectrometer. The mass 30 peak, which is common to all oxides of nitrogen was used to estimate NO_x content, and so results reported for NO_x contents are composite results which include spectral contributions from NO, NO_2 and N_2O.

---

* includes air leaking into dissolver vessel.

III. Inactive Development Work

Initial inactive studies were directed at identifying an efficient molecular sieve and column geometry for incorporation in a Xe-133 recovery system.

Selection of Most Efficient Molecular Sieve

In the initial experiments, 3 mm diameter extrudates of Linde 3A, Linde 5A and Zeolon-900 molecular sieves were packed into glass columns (2.5 cm i.d. x 30 cm long), and for each type of packing material, the effects of temperature and flow rate of He carrier gas on retention times of Xe were studied. In all experiments, molecular sieves were dried in an oven at 140°C for 5 h. A gas chromatograph with a thermal conductivity detector was used to analyze the effluent gas streams from the packed columns. As shown in Table 2, the retention times of Xe on Linde 5A are about twice those on Zeolon-900 at room temperature and higher at high temperatures, making Linde 5A the more effective molecular sieve for recovery of Xe-133. The retention times of Xe on Linde 3A were all lower than those on Zeolon-900. Flow rates over the range of 25 to 65 mL/min were found to have negligible effects on the retention times.

Table 2   Retention times (s) of Xe on molecular sieves*

Molecular Sieve	Column Dimensions		Retention Times (s) of Xe for Varying Temperatures					
	i.d. (cm)	Length (cm)	0°C	20°C	40°C	60°C	80°C	100°C
Linde 3A	2.5	30	246	228	204	192	177	168
Zeolon-900	2.5	30	–	4020	2130	1260	720	474
Linde 5A	2.5	30	–	7800	5514	3654	2280	1518
Linde 5A	2.5	60	–	23700	10360	6960	4335	2869
Linde 5A	5.0	15	–	10344	5256	2880	2040	1140

* Approximately 1 mL samples of Xe were used. Flow rate of He carrier gas was about 65 mL/min.

i.d. = inside diameter.

Optimum Column Geometry
_____

    Using only Linde 5A, the effect of changing column geometry
on retention time was checked (Table 2). By doubling the column
length, the retention times are longer. It appears, however, that
the retention times are increased by a factor less than two except
at the lowest temperature (20°C) where the retention time for the
longer column is approximately 3 times that of the shorter column.
Changing the column geometry had a dramatic effect on retention
time of Xe; at all temperatures considered, the retention times of
Xe for a 2.5 cm x 60 cm long column were twice the retention times
for the same mass of Linde 5A in a 5 cm i.d. x 15 cm long column.
These latter results suggested that a 2.5 cm i.d. column should
be used for the Xe-133 recovery system in place of a 5 cm i.d.
column.

Chromatographic Separation of Xe and NO_2
_____

    Subsequent studies were directed at developing techniques for
purifying Xe by chromatographic separation. In the preliminary
inactive studies, 3 mm diameter extrudates of Linde 5A molecular
sieves were packed into a glass column (2.5 cm i.d. x 30 cm long)
and the effects of temperature on the elution profiles and separa-
tion of Xe from NO_2 were studied. A gas chromatograph with a
thermal conductivity detector was used to analyze the effluent gas
stream from the packed column. As shown in Table 3, NO_2 can be
effectively separated from Xe using Linde 5A over the range of
temperature from 20°C to 100°C where sample volumes of about 1 mL
were used.

    The apparatus was then scaled up so that experiments with
larger volumes of Xe and NO_2 could be undertaken. The apparatus
used to develop the Xe trapping and elution/purification procedure
is shown below.
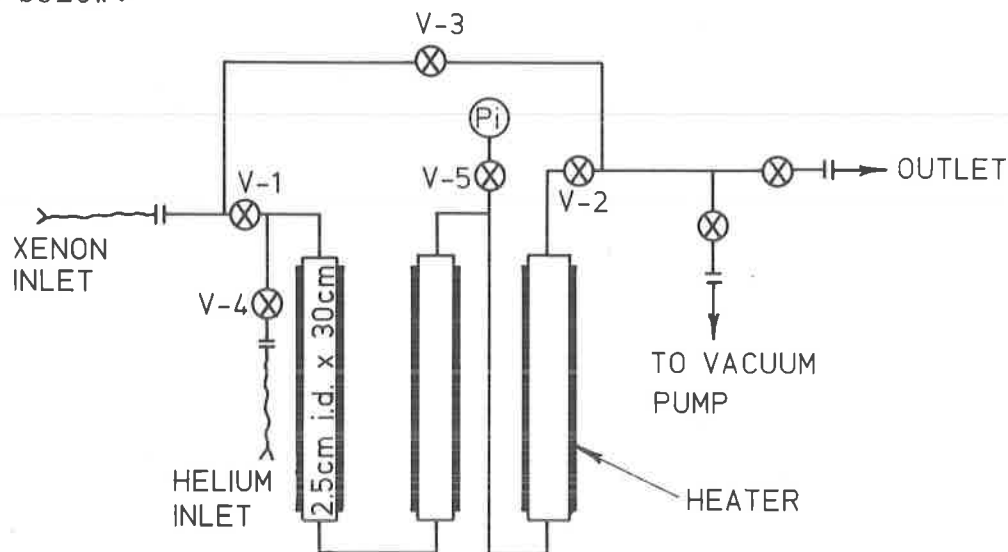
Figure 1   The 0.9 m column containing Linde 5A molecular sieve
            used for Xe-133 recovery and purification.

Table 3   Elution profiles and retention times (s) of Xe and NO_2 on Linde 5A molecular sieve*

Experiment Number	Component	Temperature °C	$t_{initial}$** (s)	Retention† Time	t_{all}†† (s)
1	Xe	100	1740	2869	4297
	NO_2	100	271	465	885
2	Xe	80	3340	4335	5410
	NO_2	80	330	580	630
3	Xe	60	4820	6960	9260
	NO_2	60	430	760	1240
4	Xe	40	6800	10360	3540
	NO_2	40	610	1040	1695
5	Xe (20 mL)	20	17630	23700	35520
	NO_2	20	1280	1800	2700

*   Approximately 1 mL samples of Xe were used unless otherwise stated. Flow rate of He carrier gas was about 65 mL/min. Column dimensions were 2.5 cm i.d. x 30 cm long.

** $t_{initial}$ is time at which peak starts.

† Retention time is the time required for the maximum of a peak to reach the detector.

†† t_{all} is time at which peak ends.

It consists of three 2.5 cm i.d. x 30 cm long stainless steel columns containing 300 g of 3 mm diameter extrudates of Linde 5A molecular sieve. The columns are connected by 3/8" stainless steel tubing using Swagelok fittings. Hoke valves and a vacuum/pressure gauge with a range of -100 kPa to 900 kPa were used. The three columns are wrapped with band heaters.

The development work involved loading the columns with mixtures of Xe and NO_2 under vacuum, then pressurizing the columns with helium to effect a chromatographic separation of the Xe and NO_2. In the development work, loading conditions which simulated those in the Mo-99 cell were used:

(a) It takes 60 minutes to dissolve targets.

(b) The dissolution vessel is evacuated to approximately -20 kPa.

(c) The flow of gas, which is the result of air in-leakage and gases given off during dissolution, averages about 200 mL/min but varies markedly over the 60 minutes.

(d) Cell temperature is 30-35°C.

As shown in Table 4, the mixtures of Xe and NO_2, which were loaded on the columns under vacuum, were effectively separated by passing helium through the columns at 65 mL/min and 140 kPa pressure. The NO_2 is eluted first along with the air during the first 70 to 100 minutes as verified by mass spectrometry analysis of grab samples. The Xe starts to come off the columns after about 130 minutes and continues to be eluted over a period of 10 to 11 hours. A minimum of 30 minutes separates the time at which the NO_2 (air) peak ends and the time at which the Xe peak starts. This observation is the basis of the purification technique: the first 70-100 minutes of eluted gases containing NO_2 and air are not collected and the pure Xe product can be collected after 100 minutes.

IV. Active Experiments

In the active experiments, a 2.5 cm i.d. x 0.9 m long stainless steel column, then a 2.5 cm i.d. x 2.1 m long stainless steel column were used. Experiments done with each column length are described in turn.

Recovery and Purification of Xe-133 Using 0.9 m Columns

The apparatus shown in Figure 2 was used in the first set of active experiments. As well as the Xe recovery traps, a 2.5 cm i.d. x 30 cm long stainless steel column containing 0.3 cm long stainless steel shavings was used. When cooled to dry ice temperatures, this column acts to remove H_2O and some NO_xs, in particular NO_2.

1.   Trapping – The off-gases from the dissolution of targets were passed through the columns at approximately 200 mL/min (-20 kPa) for 60 min. The column containing the SS shavings was cooled with dry ice; the Xe recovery traps were at cell temperature (32°C). After loading, the Xe recovery traps were put aside for two days to allow for decay of short-lived Xe isotopes (Xe-135).

Table 4   Elution profiles and retention times (s) of Xe and NO_2
on Linde 5A molecular sieve*

Expt. No.	Component	Volume (mL)	$t_{initial}$[+] (s)	Retention[++] Time (s)	t_{all}[+++] (s)	Column Used (cm)
1	Xe Air	40** –	3900 0	17580 1800	29520 3600	1 x 90
2	Xe Air	90 –	3900 0	14340 1800	24960 3600	1 x 90
3	Xe Air NO_2	70 – 25	3180 0 –	15120 1500 ***	25200 3180 –	1 x 90
4	Xe Air	70 –	7920 0	24000 2700	45000 5880	3 x 30 Fig. 1
5	Xe Air NO_2	70 – 25	7620 0 –	22920 1800 ***	49200 4080 –	3 x 30 Fig. 1

*   The Xe and NO_2 were injected throughout the 60 minute loading
period under vacuum, –20 kPa, flow rate 200 mL/min. Gases
eluted with helium, 140 kPa, 65 mL/min. Experiments carried
out at 22°C.

**   5 mL injected at t=0, 10 mL at t=15 min, 10 mL at t=30 min,
10 mL at t=45 min and 5 mL at t=50 min. For other experiments,
proportionally larger amounts of Xe were used.

*** Covered by air peak as determined by mass spectrometry.

[+] $t_{initial}$ is time at which peak starts.

[++] Retention time is the time required for the maximum of a peak
to reach the detector.

[+++] t_{all} is time at which peak ends.
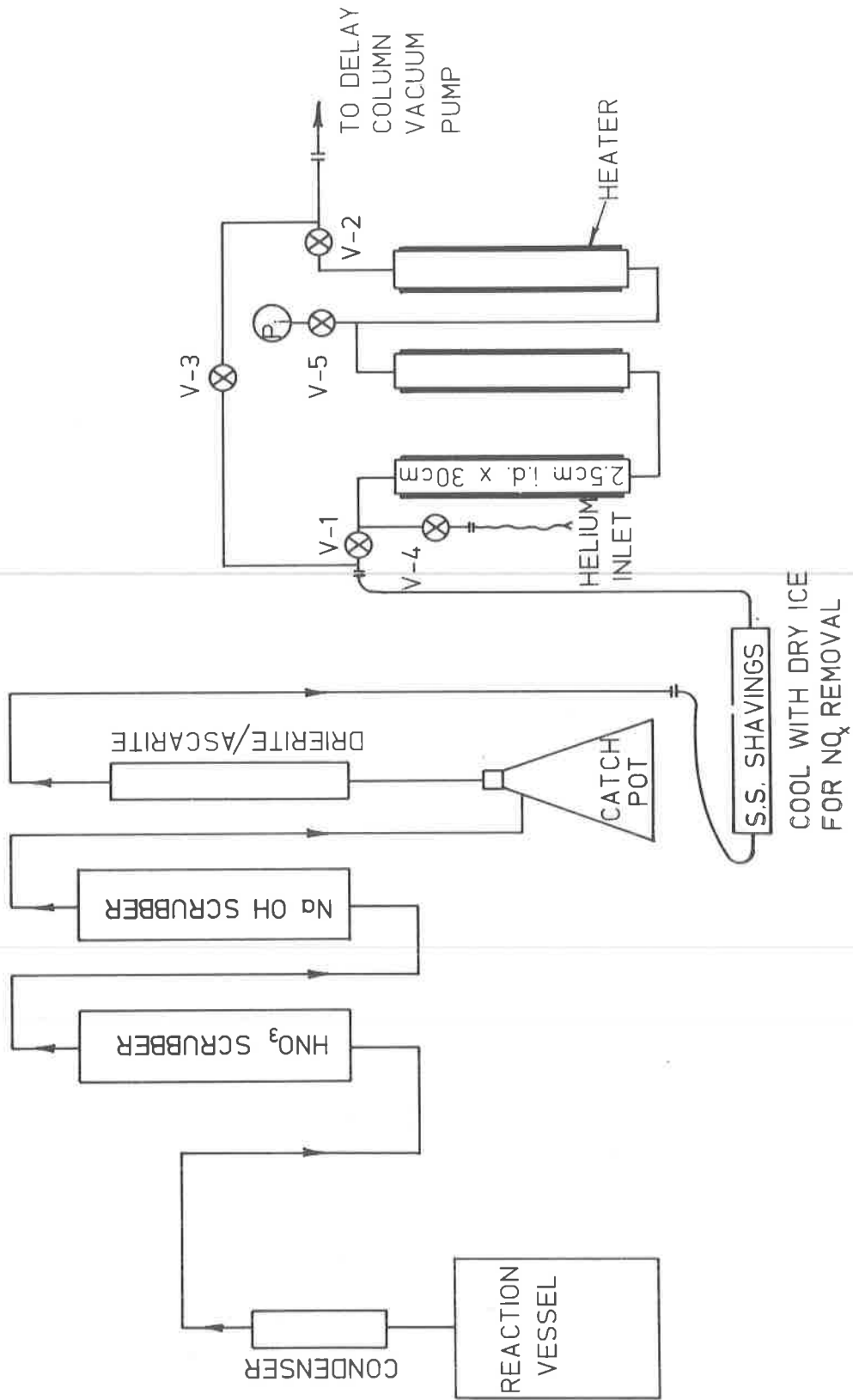
Figure 2   Placement of Linde 5A column in Mo-99 cell for Xe-133 trapping.

2.   <u>Elution/Purification</u> – The Xe recovery traps were pressurized with helium and helium was passed through the columns at 65 mL/min (140 kPa) such that a chromatographic separation of the NO_xs and the Xe was effected. The gases were passed into the Xe dry box illustrated in Figure 3. Details of the experiment are described below.

(a)   The NO_xs were eluted first over a period of 70 minutes and were trapped in the garbage trap of the Xe dry box at liquid N_2 temperature.

(b)   Some Xe was then eluted over a period of 3 hours and collected in Trap #1 of the Xe drybox.

(c)   Heat was then applied to the columns (maximum column temperature of 107°C was reached after 15 minutes) and the remaining Xe was eluted over a period of one hour and collected in Trap #2 of the Xe drybox. In Experiment 2, no heat was applied, so the elution time was increased to two hours.

(d)   Air was removed from the product in Trap #1 by a warming/ freezing cycling procedure and the product was transferred to Trap #3 for radiation and pressure readings and for sampling and analysis by mass spectrometry.

As shown in Table 5, about 18.5 TBq* of NO_x-free Xe-133 was recovered in the first run with the 0.9 m column. This amount of Xe-133 is about 32% of the 58 TBq of Xe-133 that would have been recovered by caustic dissolution of the targets. After reconditioning the column, by heating to 300°C and passing He through the column for 3 h at 65 mL/min, approximately 23 TBq of purified Xe-133 product were recovered from targets in the second run. This is 48% of the 48 TBq of Xe-133 that would have been recovered by caustic dissolution of the targets. Reports in the literature[4,5] that significant amounts of Xe-133 are absorbed and retained on the Linde 5A molecular sieve, even at low pressures, suggest that at least some of the Xe-133 was retained on the columns. It has been assumed in this work that low yields could be tolerated because of the large excess of Xe-133 released during processing of rods for Mo-99 production.

Although the yields were lower, the compositions and purities of the products (Table 5) compared favourably with the composition and purity of Xe-133 produced by caustic dissolution. As shown in Table 6, the isotopic compositions of the Xe-133 products obtained as by-products of Mo-99 production were essentially the same as the composition of Xe-133 product produced by caustic dissolution.

---

* All amounts of recovered Xe-133 in this report are decay corrected to six days after target dissolution and column loadings. The amounts reported are per gram of fissioned U-235.
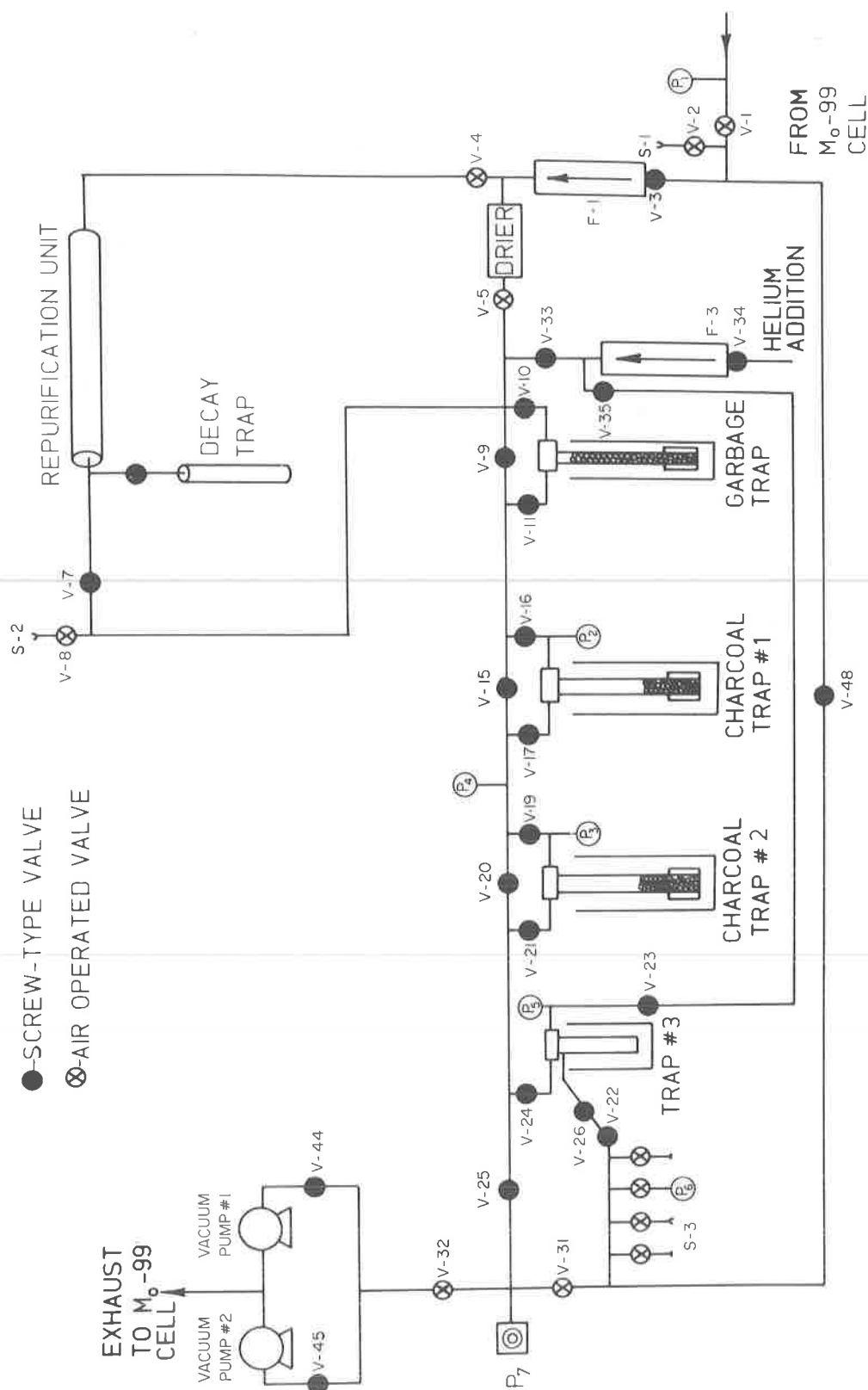
Figure 3   Design of Xe glove box used for collecting and sampling Xe-133 product.

Table 5   Results of Xe-133 recovery experiments using 0.9 m column

Experiment Description	Pressure on Trap #3 kPa	Amount of Xe-133^{+}		Mass Spectrometric Analysis of Product (Volume %)					
		TBq/g	%[++]	H_2	N_2	O_2	CO_2	Xe	NOx
NaOH Dissolution (Sample #82-034) August, 1982	-	-	-	1.4	24.3	3.4	5.9	64.7	0.02
1st run with 1 column	-88	18.5	32	2.8	11.3	0.2	7.7	78.0	<0.01
2nd run with 1 column	-88	22.8	48	1.2	34.6	0.7	2.3	60.8	<0.01
1st run with 2 columns* (Bank A)	-90	10.0	18	<0.1	15.1	1.5	16.3	66.8	<0.01
2nd run with 2 columns (Bank A)	-90	15.3	45	<0.1	2.9	0.7	8.1	87.8	0.57
1st run with 2 columns (Bank B)	-81	14.7	32	<0.1	4.5	2.5	5.7	86.3	1.1
2nd run with 2 columns (Bank B)	-85	9.0	17	<0.1	9.4	4.7	36.5	49.4	>10**

+ Amounts reported are per gram of fissioned U-235, 6 days after columns are loaded.

++ Yield reported is amount of Xe-133 for Linde 5A system compared with amount of Xe-133 that would have been recovered by caustic dissolution.

* Four columns separated into 2 banks of 2 columns were used. Only 1 bank was used in any experiment.

** Other results are given neglecting NO_x.

Table 6 Isotopic composition of Xe-133 products by mass spectrometry.

Sample	Volume %					
	Xe-131	Xe-132	Xe-133	Xe-134	Xe-136
1st run with 1 x 0.9 m column	4.44 (4.87)*	10.74 (11.79)	8.89 (0.0)	29.63 (32.52)	46.30 (50.82)
2nd run with 1 x 0.9 m column	4.56 (4.90)*	12.00 (12.88)	6.86 (0.0)	30.29 (32.52)	46.29 (49.70)
NaOH Dissolution (Sample #82-034) August, 1982	(7.10)	(14.20)	—	(30.18)	(48.52)

* Numbers in brackets correspond to isotopic compositions after decay of all Xe-133.

During the first and second runs with the 0.9 m column, grab samples were taken for analysis by mass spectrometry to obtain an elution profile for the column. The results of the analyses illustrated in Figure 4 highlighted potential problems. As shown in Figure 4, the elution profiles of Xe and NO_xs only approximate the inactive results shown in Table 4. The NO_x peak decreases to a minimum at t = 60 minutes while the Xe peak builds to a maximum starting at t = 70 minutes (first run). This is shorter, by about 50 minutes, than the 130 minutes suggested in inactive tests. In fact, in both experiments, there was some Xe product lost because some Xe (0.1% by volume) was eluted during the first 70 minutes. This suggested that the Xe and NO_xs were being pulled too far down the column as a result of poor vacuum/flow rate control during loading of the column. Because of this, there was not enough column left to separate the NO_xs and Xe completely. This fact was also suggested by the second NO_x peak which appeared after about 150 minutes elution time in both experiments (which may result from erratic dissolution of the targets).

These results suggested that some of the Xe product was being lost along with the impurities during the first 60-70 minutes and also that the Xe product, although acceptable in purity (NO_xs 0.01% by volume), was not as pure as it could be.

Subsequent experiments with 0.9 m columns were directed at increasing the amounts of Xe-133 recovered by loading two 0.9 m columns and eluting them in parallel. As shown in Table 5, while this technique proved successful in increasing amounts of Xe-133 recovered in two of the four runs, the products were NO_x contaminated in three of the four runs. The NO_x contamination was attributed to the short length of column and lack of excess Linde 5A molecular sieve to chromatographically separate the Xe from the NO_xs.

Recovery and Purification of Xe-133 Using 2.1 m Columns

To increase the amounts of Xe-133 recovered and to provide better Xe-133/NO_x separations, the column lengths were increased to 2.1 m. Of the increase in length, 75% allowed the loading of twice as much Xe on one column and 25% provided excess length to separate Xe-133 from the NO_xs.

The results obtained, with one 2.1 m column, containing 700 g of 3 mm diameter extrudates of Linde 5A molecular sieve, are summarized in Table 7 and show that NO_x-free Xe-133 was recovered (7.8 TBq, 9.2 TBq and 18.4 TBq) in three successive runs with the same column. The yields were 19%, 19% and 43%, respectively, of that Xe-133 which would have been recovered had the targets been processed by caustic dissolution for Xe-133 recovery. The 2.1 m column was reconditioned between runs by passing He through the column at 65 mL/min for 4 h. While the yields of Xe-133 were low during the first two runs with the column, the product quality for
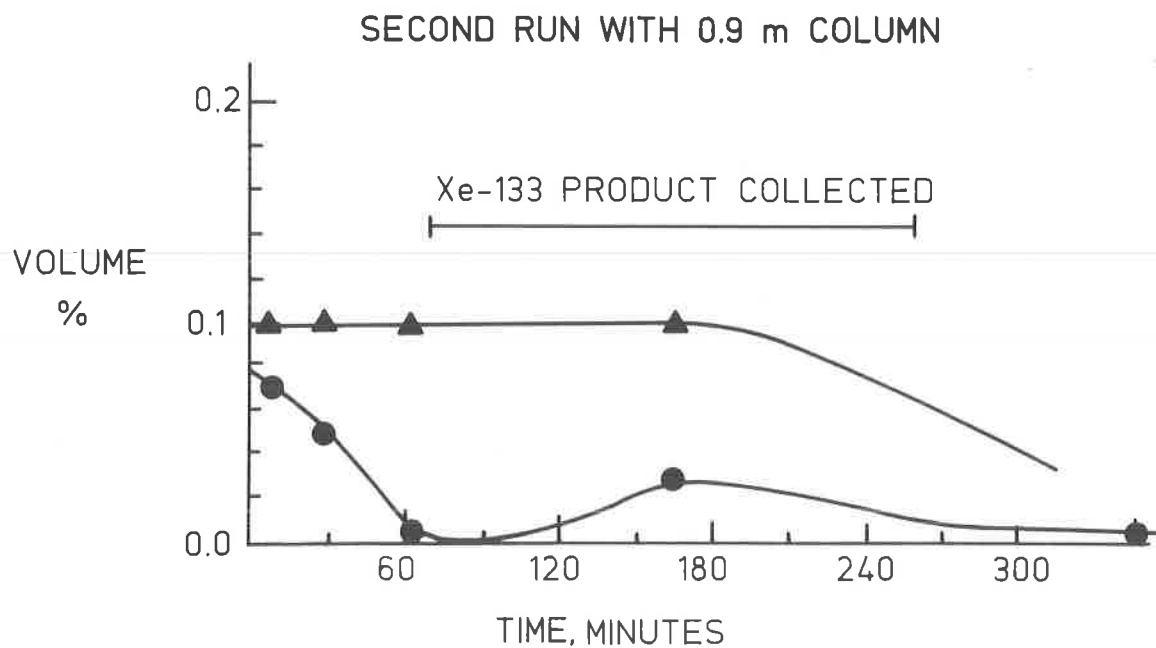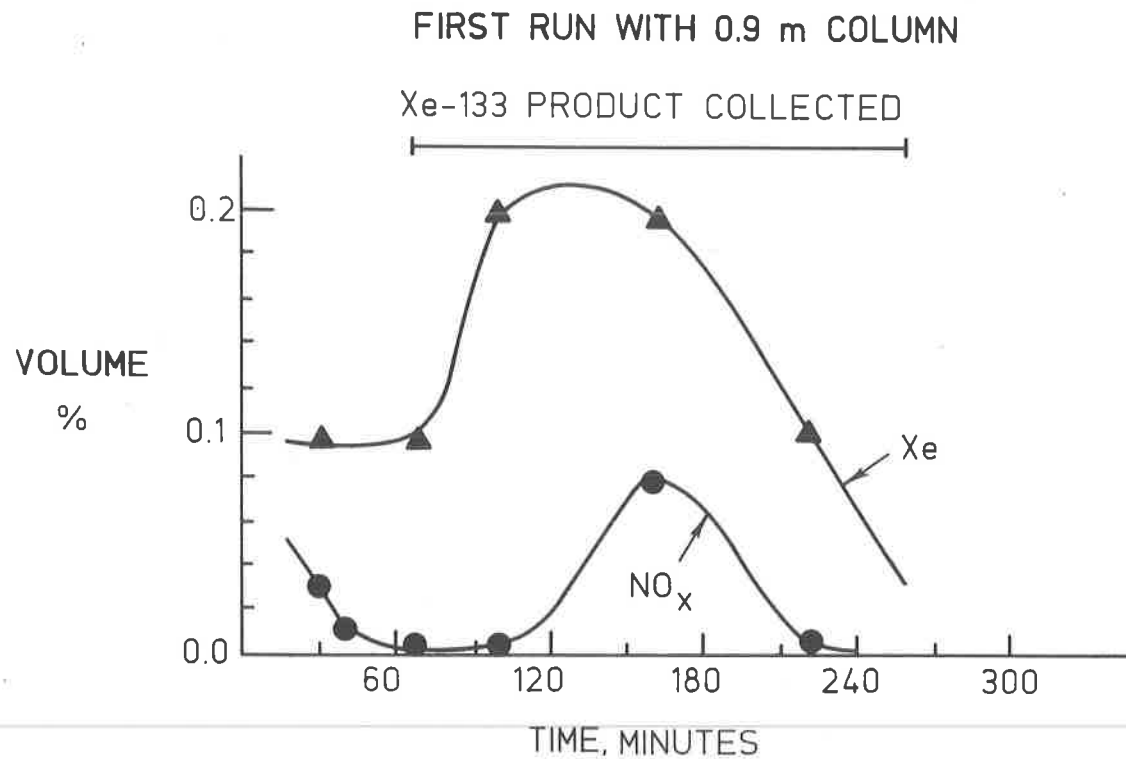
Figure 4   Elution profiles of Xe and NO_xs during two active runs using 0.9 m columns.

Table 7   Results of Xe-133 recovery experiments using 2.1 m column

Run #	Experiment Description	Pressure on Trap #3 kPa	Amount of Xe-133[†]		Mass Sepctrometric Analysis of Product (Volume %)					
			TBq/g	%[††]	H_2	N_2	O_2	CO_2	Xe	NO_x
1	1st run with 1 column	?	7.8	19	3.1	3.5	0.2	10.7	82.5	< 0.01
2	2nd run with 1 column	-86	9.2	19	2.2	8.8	1.0	22.1	65.9	< 0.01
3	3rd run with 1 column	-81	18.4	43	< 0.1	7.4	1.0	23.6	68.1	< 0.01
4	1st run with 2 columns	-70	27.0	46	1.8	1.5	< 0.1	7.5	89.2	< 0.01
5	2nd run with 2 columns	900*	–	–	< 0.1	6.1	0.9	91.1	0.7	> 10***
6	3rd run with 2 columns	300**	–	–	< 0.1	2.1	0.6	96.3	1.0	> 10***
7	4th run with 2 columns	-70	11.1	38	< 0.1	5.3	3.8	10.3	72.5	8.9

†   Amounts reported are per gram of fissioned U-235, 6 days after columns are loaded.

††   Yield reported is amount of Xe-133 for Linde 5A system compared with amount of Xe-133 that would have been recovered by caustic dissolution.

*   Mo-99 cell scrubber plugged just before Xe-133 run. When scrubber solutions were changed and vacuum was applied, the solutions were degassed and loaded columns with air.

**   Columns were deactivated because of degassing incident which occurred in 2nd run.

*** Other results are given neglecting NO_x.

all three runs was good as shown in Table 7. In the fourth run, not shown in Table 7, Xe-133 broke through the column during loading suggesting that the column was spent. This was confirmed by a low yield of contaminated product.

Subsequent experiments with two 2.1 m columns (loaded in sequence but eluted in parallel) were undertaken in attempts to verify that yields of about 40% were attainable and to increase the amounts of Xe-133 which could be recovered. In the first run using the two 2.1 m columns shown in Figure 5, 27.0 TBq of NO_x-free Xe-133 were recovered, where the Xe-133 was collected on two columns. This amount of Xe-133 was 46% of that which would have been recovered by caustic dissolution. Grab samples taken during the run showed that no NO_xs were present in the eluted Xe-133 after 90 min, in contrast to results obtained for 0.9 m columns (illustrated in Fig. 4).
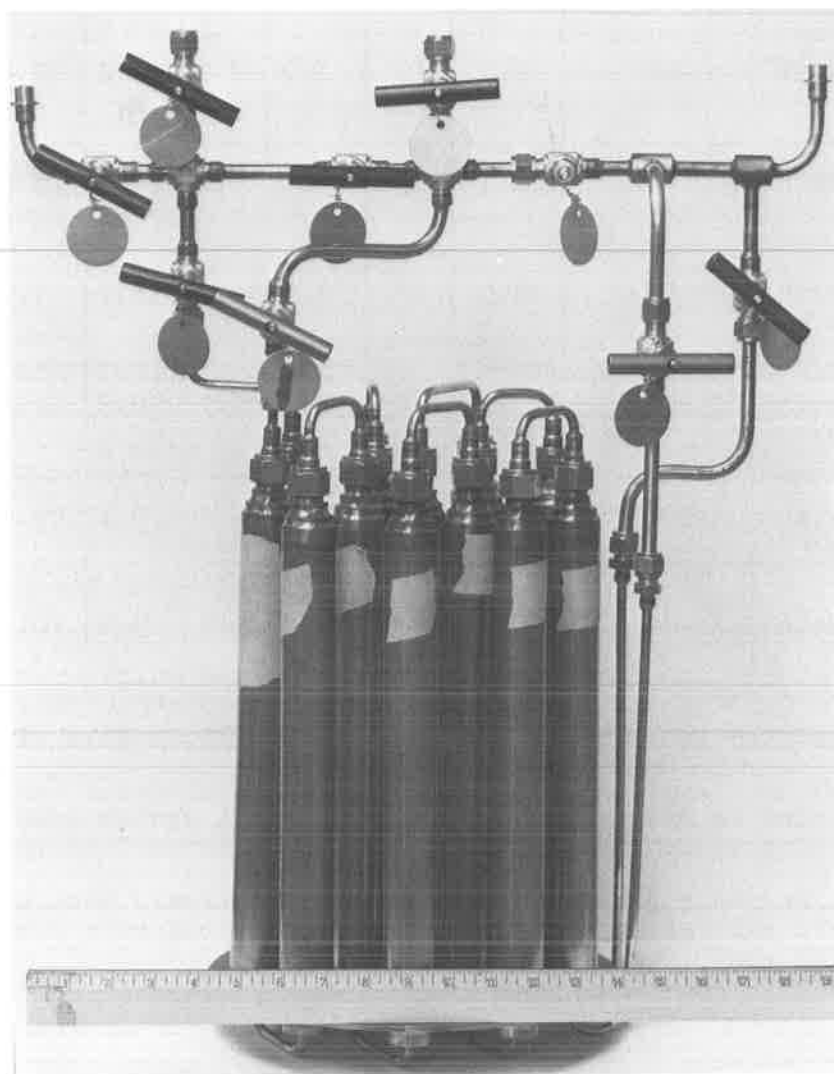
Figure 5   Set of two 2.1 m columns used for Xe-133 recovery and purification (scale in inches; 1 inch = 2.54 cm).

Subsequent experiments were hampered by repeated hardware problems in the Xe glovebox and in the Mo-99 cell. As a result of the hardware problems, attempts to demonstrate the off-gas Xe technique were deferred.

V.   Summary

A procedure has been developed for collecting and purifying the off-gas Xe-133 from the Mo-99 Production Facility. The procedure involves trapping the Xe-133/NO_x gas mixtures released during dissolution of Mo-99 targets on columns containing Linde 5A molecular sieve, then pressurizing the columns with He, and eluting/separating the Xe-133 and NO_xs chromatographically.

Two lengths of columns were tested in active experiments: 2.5 cm i.d. x 0.9 m columns and 2.5 cm i.d. x 2.1 m columns. Neither column length offered an advantage with respect to yield in that the averages of the three best yields for the 0.9 m long and 2.1 m long columns were the same, 42% 8% and 42% 4%, respectively, of the amount of Xe-133 that would have been recovered by caustic dissolution of the same targets. Operationally, 2.1 m long columns offered the advantage of allowing the loading of the Xe on two columns rather than on four columns if 1.05 m columns were used.

VII.   Acknowledgements

VIII.   References

(1)   Bruggeman, A., Meynedonckx, L. and Gossens, W.R.A., "Elimination of NO_x by Selective Reduction with NH_3", in Proceedings of the 15th DOE Nuclear Air Cleaning Conference held in Boston, Massachusetts, 1978 August 7-10, p. 614.

(2)   Wymer, R.G., and Foster, D.L., "Nuclear Reactor Fuel Dissolution", in Progress in Nuclear Energy - Series III Process Chemistry, F.R. Bruce et al., eds., McGraw-Hill Book Co., Inc., New York, 1956, p. 85.

(3)   Miles, G.L., "The Fumeless Dissolving of Uranium", ibid., p. 97.

(4)   Kitani, S., and Takada, J., "Adsorption of Krypton and Xenon on Various Adsorbents", Journal of Nuclear Science and Technology", 2, No. 2, p. 51-56, 1965 February.

(5)   Lloyd, M.H., and McNees, R.A., "Adsorption of Krypton and Xenon by Various Materials", ORNL-3228, 1961.

CLOSING REMARKS OF SESSION CHAIRMAN FERNANDEZ:

I would like to make some brief comments about the papers. Mr. Little spoke about modeling nitrogen oxide scrubbers. The scrubbing technology has had extensive theoretical consideration and practical application. However, its application to NO_x control in fuel reprocessing plants may be somewhat limited if it is impractical to recycle the nitric acid generated. For example, in calcining liquid radioactive waste, the objective is to get rid of NO_x gases generated. Scrubbing could generate secondary low-level radioactive liquid wastes which present additional disposal problems.

Mr. Kobayashi dealt with NO_x removal by abatement with NH_3 over hydrogen mordenite and titanium-based catalyst. I am pleased to see further verification and refinement of a process that I was involved in developing. The main interest of this study was to minimize N_2O production.

Mr. Cheh discussed a method for removal of ^{14}C from the annulus gas of CANDU reactors which generate and release higher levels of ^{14}C than light water reactors. The method consists of passing the gas stream through a packed bed of calcium hydroxide and forming the carbonate. It is similar to a process developed at ORNL which uses barium hydroxide instead.

Mr. Chuang spoke about the development of wet-proofed catalyst for recombination of H_2 and O_2 at ambient temperature and in the presence of water. The catalysts consist of a carbon or silica base impregnated with platinum and coated with Teflon. This technology has a major advantage over high-temperature dry processes which are limited to 4% H_2 in air to avoid the explosion potential; the $H_2 - O_2$ mixtures in this process appear to be unrestricted because the reaction occurs at room temperature and potential gas phase reactions which might lead to explosions are quenched by water being recycled through the column containing the catalyst. The process will be installed in 1985 at the Idaho Chemical Processing Plant to eliminate H_2 generated during the processing of zircaloy-clad fuel; if not removed, the H_2 would interfer with ^{85}Kr recovery in the Rare Gas Plant.

Mr. Djerassi discussed tritium management for fusion reactors. Fusion reactors may contain inventories up to 10 million curies of tritium which will require extensively engineered control, cleanup, and recycle systems. There is considerable effort going on in this country in this subject area but I suspect papers on these efforts will be presented in the 1985 conference on Tritium Control and Waste Management Technologies to be held at Mound Facility.

We heard four papers in the second part of the session that are excellent additions to the literature on the recovery and retention of airborne wastes. A method was described that could produce the measurements necessary to make significant adjustments to I-129 dose receptor models. We have heard new data on the silver-impregnated aluminas and silica gels; in addition to the more thoroughly studied

silver-exchanged zeolites for dissolver offgas. Dr. Robinson reported results that indicate present thinking on Ru-106 trapping should not be limited to silica gels but should include selective catalytic systems. Chromatographic separations have been applied to the difficult separation of Xe-133 from NO_x. Byproduct usage will become more important as effluent regulations become more restrictive. These papers have been ample evidence, if any were needed, that innovative solutions are being developed for the problems of airborne waste management.

Session 19

OPEN END

THURSDAY: August 16, 1984
CHAIRMEN: M.W. First
Harvard School of Public Health
S. Steinberg
Air Techniques, Inc.

TWO-DETECTOR DIOCTYLPHTHALATE (DOP) FILTER TESTING METHOD AND STATIST-
ICAL INTERPRETATION OF DATA
L.L. Dauber, J. Barnes, W. Appel

A FILTER CONCEPT TO CONTROL AIRBORNE PARTICULATE RELEASES DUE TO
SEVERE REACTOR ACCIDENTS AND IMPLEMENTATION USING STAINLESS-STEEL
FIBER FILTERS
H. -G. Dillman, H. Pasler

DUAL AEROSOL DETECTOR BASED ON FORWARD LIGHT SCATTERING WITH A SINGLE
LASER BEAM
B.J. Kovach, R. A. Custer, F.L. Powers, A. Kovach

TEST DATA AND OPERATION DATA FROM CARBON USED IN HIGH VELOCITY SYSTEMS
J.R. Edwards

BORA - A FACILITY FOR EXPERIMENTAL INVESTIGATION OF AIR CLEANING
DURING ACCIDENT SITUATIONS
V. Rudinger, Th. Arnitz, C.I. Ricketts, J.G. Wilhelm

SPRING LOADED HOLD-DOWN FOR MOUNTING HEPA FILTERS AT ROCKY FLATS
K. Terada, C.R. Rose, A.G. Garcia

TWO-DETECTOR DIOCTYLPHTHALATE (DOP) FILTER TESTING
METHOD AND STATISTICAL INTERPRETATION OF DATA

L. Dauber, HQ US Army Armament, Munitions and Chemical Command,
Aberdeen Proving Ground, Maryland
J. Barnes and W. Appel (ret.), Letterkenny Army Depot
Chambersburg, Pennsylvania

Abstract

A two-detector Dioctylphthalate (DOP) testing method has been
field-proven for determining particulate leakage through gas-
particulate filter systems. Two forward light scattering detectors
are electronically tuned to display identical readings over a five-
decade range to ensure duplicatability. One detector is then used
for continuously monitoring the upstream DOP particle concentration
and the second detector is used for continuously monitoring the down-
stream particle concentration. Upstream and downstream data pairs
taken at 10-second intervals over a two minute period are sufficient
to permit both the determination of leak values and the generation
of statistical quality data. Statistical quality data include mean
leakage rate, confidence interval estimates of the mean, and standard
deviation. Computations may be done in the field with a hand-held
calculator. The two-detector method eliminates the more lengthy
detector chamber purging and equilibration time inherent in the one-
detector method. (The one-detector method alternately, rather than
simultaneously, senses upstream and downstream concentrations.) In
consequence, the two-detector method minimizes filter and personnel
exposure to DOP. The collection of many data pairs, even within a
short period, enables one to make statistically sound inferences.
Examples of collected and computed data are presented.

I.   Introduction

Two opposing needs must be met when testing a HEPA filter.
On the one hand, the duration of testing must be kept short to
minimize the degradation of the filter by the challenge compound,
DOP. On the other hand, the downstream and upstream DOP concentra-
tions vary in repetitive tests and, thus, show a need to collect a
sufficient amount of data--and over a sufficient period--to support
any inferences about the filter's efficacy. Traditionally, HEPA
filters have been tested using a single detector for indicating,
sequentially, downstream and upstream concentrations. Once an
upstream sample is taken a minimum of two minutes is required to
purge the detector's forward light scattering chamber before
another pair of downstream and upstream samples can be taken. To
the degree the number of downstream-upstream data pairs is limited,
owing to lengthy sampling time, statistical quality data are sacri-
ficed. The authors perceived that this dilemma could be overcome
through the use of two detectors tuned to give identical readings
whether sampling from the upstream or the downstream probe. Once
tuned together, either could be used for sampling upstream while
the other is sampling downstream. Simultaneous measurements could
be made at 10-second intervals giving a sufficient number of time-
keyed data sets during a single two-minute period to permit statis-
tical quality computations. The following paragraphs describe work

done to prove out the two-detector concept.

II.   Overview of Two-Detector Procedure

The upstream and downstream detectors are coupled in parallel through a tee fitting and shutoff valve to the upstream and downstream probes as shown in Figure 1. NUCON F1000-DG-F thermal DOP generator, and NUCON F1000-DD-SA detectors, are employed. The detectors are checked for electronic linearity over a five-decade range. In order to tune the two detectors to show near-identical values when sampling in either the upstream or the downstream mode, a live challenge is given to the selected filter. If gross leakage is indicated, the filter is repaired or a different one is selected (following an Environmental Safety Check) for the next step, the "tuning", or DOP Detector Duplicatability Check. When tuning is complete and duplicatability is demonstrated, any filter at the site in question may be tested using the equipment arrangement shown in Figure 2. Leak values are computed and quality parameters are determined from the empirical data using a hand-held calculator.
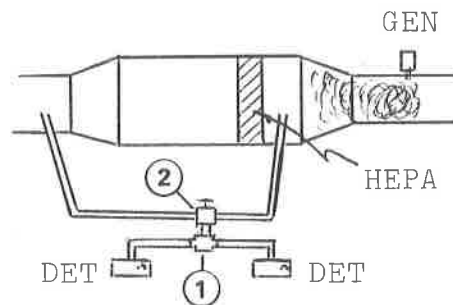
Figure 1.   Equipment arr'gt for DET duplicatability check.
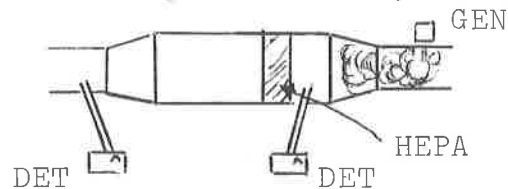
Figure 2.   Equipment arr'gt for testing.

III.   Environmental Safety Check

The purpose of the Environmental Safety Check is to ensure that the filter to be used during the DOP Duplicatability Check is reasonably leak free and adequate to protect personnel areas from high concentrations of DOP. Gross leakage, if it is occuring, will be indicated and corrective measures will be taken. Following are the steps taken during an Environmental Safety Check.

a.   Hook up lines and fittings as shown in Figure 1. Ensure that the generator light is cycling (i.e. that full temperature has been reached).

b.   Set selector valve (2) to <u>downstream</u> positions.

c.   Set TEST/CLEAR switches (3) in CLEAR positions. Set SPAN controls (4) to 0. Set RANGE switches to .01.
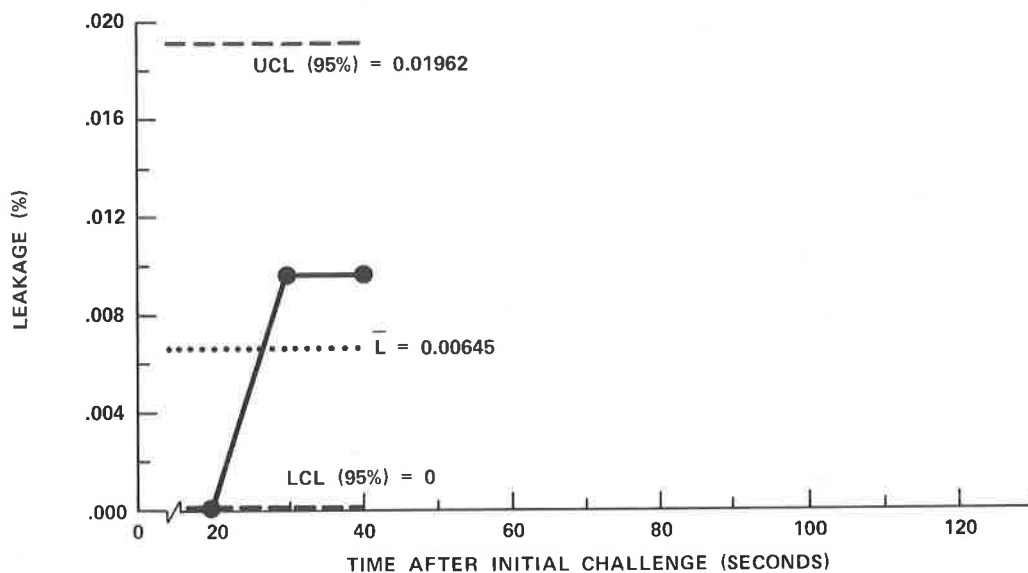
Figure 10. }
Table 7. } DOP LEAK TEST, FILTER C, 3 MEASUREMENTS

	RECORDED DATA					COMPUTED DATA	
RDG. NO. X	TIME AFTER INIT. CHLG. (SECS)	% PEN UPSTR. C_u	RANGE UPSTR. R_u	% PEN DNSTR. C_d	RANGE DNSTR. R_d	LEAKAGE $C_d/C_u \cdot R_d/R_u \cdot 100 = L(\%)$	SAMPLE PARAMETER
1	20	60	100	20	.01	0.000333	$\overline{L}$ = 0.00645
2	30	42		40		0.009524	
3	40	40		38		0.009500	
4	50						
5	60						
6	70						s = 0.00433
7	80						
8	90						
9	100						
10	110						
11	120						m = 0.00458
12	130						
13	140						
14	150						
15	160						

CONFIDENCE INTERVAL ABOUT MEAN:

$$\overline{L} - t_a \hat{\sigma}_{\overline{L}} \leqslant \mu \leqslant \overline{L} + t_a \hat{\sigma}_{\overline{L}} \quad \text{WHERE} \quad \hat{\sigma}_{\overline{L}} = \frac{s}{\sqrt{n-1}} = \frac{0.00433}{\sqrt{3-1}} = 0.00306$$

$$0.00645 - 4.303 \times 0.00306 \leqslant \mu \leqslant 0.00645 + 4.303 \times 0.00306$$

$$0.00645 - 0.01317 \leqslant \mu \leqslant 0.00645 + 4.303 \times 0.01317$$

$$0 \leqslant \mu \leqslant 0.01962$$

Form DOPLE

1412
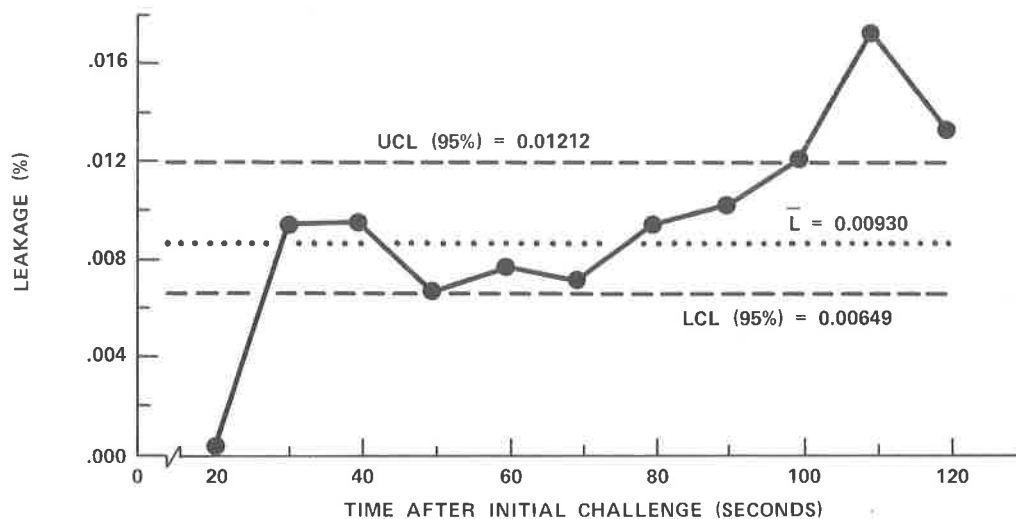
Figure 9. } DOP LEAK TEST, FILTER C, 11 MEASUREMENTS
Table 6. }

	RECORDED DATA					COMPUTED DATA	
RDG. NO. X	TIME AFTER INIT. CHLG. (SECS)	% PEN UPSTR. C_u	RANGE UPSTR. R_u	% PEN DNSTR. C_d	RANGE DNSTR. R_d	LEAKAGE $C_d/C_u \cdot R_d/R_u$ $\cdot 100 = L(\%)$	SAMPLE PARAMETER
1	20	60	100	20	.01	0.000333	$\bar{L}$ = 0.00930
2	30	42		40		0.009524	
3	40	40		38		0.009500	
4	50	32		22		0.006875	
5	60	23		18		0.007826	
6	70	35		25		0.007143	s = 0.00399
7	80	48		45		0.009375	
8	90	72		70		0.009722	
9	100	75		90		0.012000	
10	110	70		12	0.1	0.017143	
11	120	93		12	0.1	0.012903	m = + 0.00098
12	130						
13	140						
14	150						
15	160						

CONFIDENCE INTERVAL ABOUT MEAN:

$$\bar{L} - t_a \hat{\sigma}_{\bar{L}} \leqslant \mu \leqslant \bar{L} + t_a \hat{\sigma}_{\bar{L}} \quad \text{WHERE} \quad \hat{\sigma}_{\bar{L}} = \frac{s}{\sqrt{n-1}} = \frac{0.00399}{\sqrt{11-1}} = 0.00126$$

$$0.00930 - 2.228 \times 0.00126 \leqslant \mu \leqslant 0.00930 + 2.228 \times 0.00126$$

$$0.00930 - 0.00281 \leqslant \mu \leqslant 0.00930 + 0.00281$$

$$0.00649 \leqslant \mu \leqslant 0.01212$$

Form DOPLE
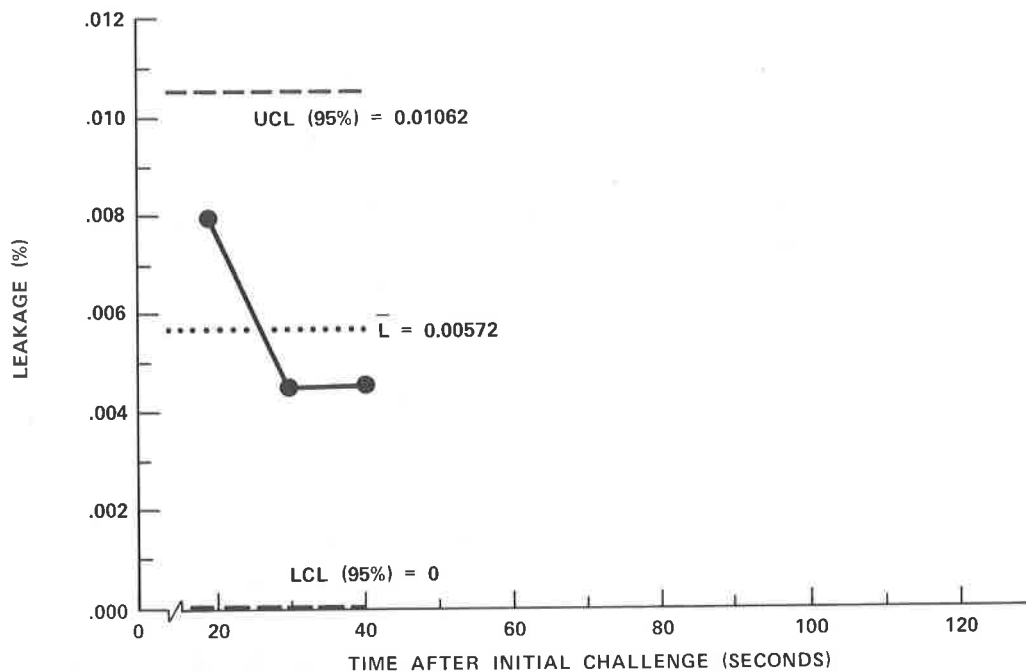
Figure 8.
Table 5. } DOP LEAK TEST, FILTER B, 3 MEASUREMENTS

RDG. NO. X	TIME AFTER INIT. CHLG. (SECS)	% PEN UPSTR. C_u	RANGE UPSTR. R_u	% PEN DNSTR. C_d	RANGE DNSTR. R_d	LEAKAGE $C_d/C_u \cdot R_d/R_u \cdot 100 = L(\%)$	SAMPLE PARAMETER
		RECORDED DATA				COMPUTED DATA	
1	20	50	100	40	.01	0.00800	$\overline{L} = 0.00572$
2	30	100		45		0.00450	
3	40	90		42		0.00467	
4	50						
5	60						
6	70						$s = 0.00161$
7	80						
8	90						
9	100						
10	110						
11	120						$m = -0.00167$
12	130						
13	140						
14	150						
15	160						

CONFIDENCE INTERVAL ABOUT MEAN:

$$\overline{L} - t_a \hat{\sigma}_{\overline{L}} \leq \mu \leq \overline{L} + t_a \hat{\sigma}_{\overline{L}} \quad \text{WHERE} \quad \hat{\sigma}_{\overline{L}} = \frac{s}{\sqrt{n-1}} = \frac{0.00161}{\sqrt{3-1}} = 0.00114$$

$$0.00572 - 4.303 \times 0.00114 \leq \mu \leq 0.00572 + 4.303 \times 0.00114$$

$$0.00572 - 0.00490 \leq \mu \leq 0.00572 + 0.00490$$

$$0 \leq \mu \leq 0.01062$$

Form DOPLE
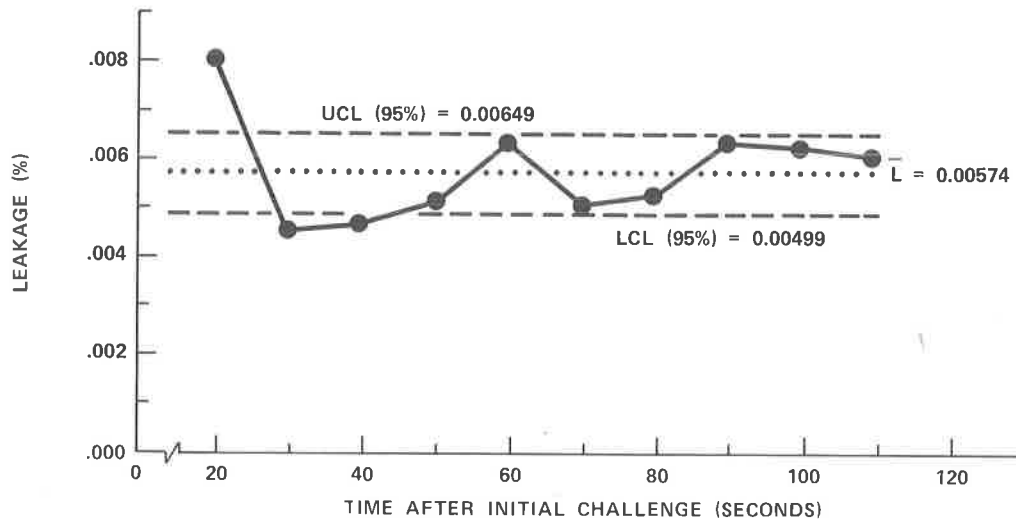
Figure 7. } DOP LEAK TEST, FILTER B, 10 MEASUREMENTS
Table 4.

RDG. NO. X	TIME AFTER INIT. CHLG. (SECS)	% PEN UPSTR. C_u	RANGE UPSTR. R_u	% PEN DNSTR. C_d	RANGE DNSTR. R_d	LEAKAGE $C_d/C_u \cdot R_d/R_u \cdot 100 = L(\%)$	SAMPLE PARAMETER
		RECORDED DATA				COMPUTED DATA	
1	20	50	100	40	.01	0.00800	$\overline{L} = 0.00574$
2	30	100		45		0.00450	
3	40	90		42		0.00467	
4	50	75		38		0.00507	
5	60	60		38		0.00633	
6	70	80		40		0.00500	$s = 0.00100$
7	80	75		40		0.00533	
8	90	60		38		0.00633	
9	100	55		34		0.00618	
10	110	50		30		0.00600	
11	120						$m = 0.00001$
12	130						
13	140						
14	150						
15	160						

CONFIDENCE INTERVAL ABOUT MEAN:

$$\overline{L} - t_a \hat{\sigma}_{\overline{L}} \leqslant \mu \leqslant \overline{L} + t_a \hat{\sigma}_{\overline{L}} \quad \text{WHERE} \quad \hat{\sigma}_{\overline{L}} = \frac{s}{\sqrt{n-1}} = \sqrt{\frac{0.00100}{10-1}} = 0.00033$$

$$0.00574 - 2.262 \times 0.00033 \leqslant \mu \leqslant 0.00574 + 2.262 \times 0.00033$$

$$0.00574 - 0.00075 \leqslant \mu \leqslant 0.00574 + 0.00075$$

$$0.00499 \leqslant \mu \leqslant 0.00649$$

Form DOPLE
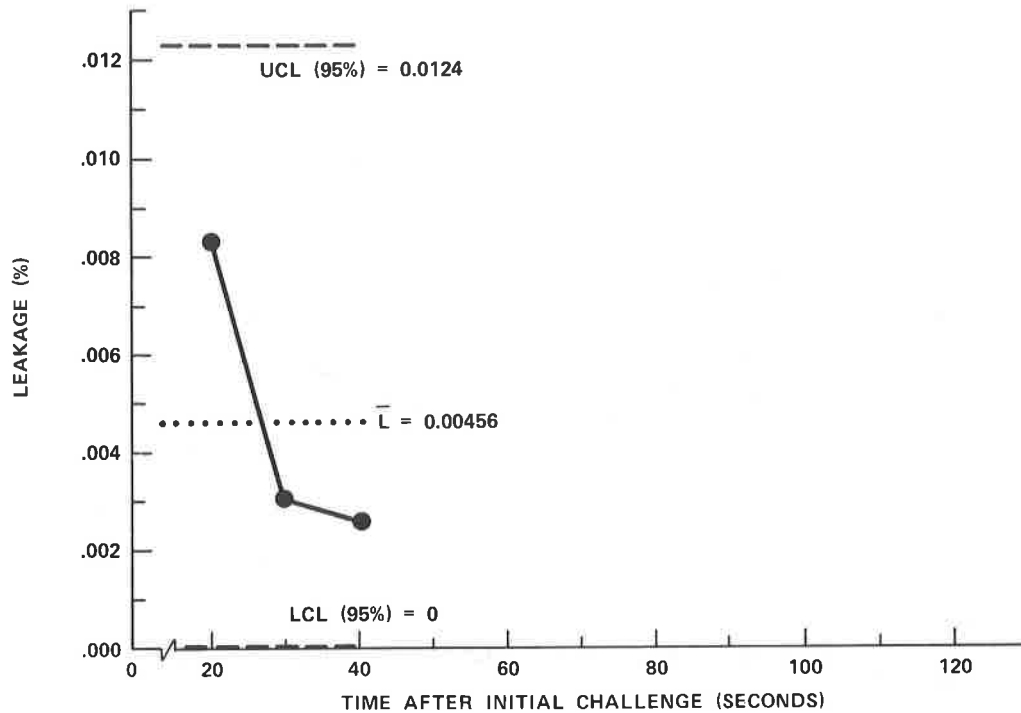
Figure 6.
Table 3. } DOP LEAK TEST, FILTER A, 3 MEASUREMENTS

RDG. NO. X	TIME AFTER INIT. CHLG. (SECS)	% PEN UPSTR. C_u	RANGE UPSTR. R_u	% PEN DNSTR. C_d	RANGE DNSTR. R_d	LEAKAGE $C_d/C_u \cdot R_d/R_u \cdot 100 = L(\%)$	SAMPLE PARAMETER
1	20	22	100	18	.01	0.00818	$\bar{L} = 0.00456$
2	30	60		18		0.00300	
3	40	80		20		0.00250	
4	50						
5	60						
6	70						$s = 0.002568$
7	80						
8	90						
9	100						
10	110						
11	120						$m = -0.00284$
12	130						
13	140						
14	150						
15	160						

CONFIDENCE INTERVAL ABOUT MEAN:

$$\bar{L} - t_a \hat{\sigma}_{\bar{L}} \leqslant \mu \leqslant \bar{L} + t_a \hat{\sigma}_{\bar{L}} \quad \text{WHERE} \quad \hat{\sigma}_{\bar{L}} = \frac{s}{\sqrt{n-1}} = \sqrt{\frac{0.002568}{3-1}} = 0.00182$$

$$0.00456 - 4.303 \times 0.00182 \leqslant \mu \leqslant 0.00456 + 4.303 \times 0.00182$$

$$0.00456 - 0.00781 \leqslant \mu \leqslant 0.00456 + 0.00781$$

$$0 \leqslant \mu \leqslant 0.0124$$

Form DOPLE

Figure 5.
Table 2. } DOP LEAK TEST, FILTER A, 10 MEASUREMENTS

	RECORDED DATA					COMPUTED DATA	
RDG. NO. X	TIME AFTER INIT. CHLG. (SECS)	% PEN UPSTR. C_u	RANGE UPSTR. R_u	% PEN DNSTR. C_d	RANGE DNSTR. R_d	LEAKAGE $C_d/C_u \cdot R_d/R_u \cdot 100 = L(\%)$	SAMPLE PARAMETER
1	20	22	100	18	.01	0.00818	$\bar{L} = 0.00327$
2	30	60		18		0.00300	
3	40	80		20		0.00250	
4	50	100		20		0.00200	
5	60	100		20		0.00200	
6	70	100		20		0.00200	$s = 0.00179$
7	80	100		22		0.00222	
8	90	77		22		0.00286	
9	100	50		21		0.00420	
10	110	56		21		0.00375	
11	120						$m = -0.00021$
12	130						
13	140						
14	150						
15	160						

CONFIDENCE INTERVAL ABOUT MEAN:

$$\bar{L} - t_a \hat{\sigma}_{\bar{L}} \leqslant \mu \leqslant \bar{L} + t_a \hat{\sigma}_{\bar{L}} \quad \text{WHERE} \quad \hat{\sigma}_{\bar{L}} = \frac{s}{\sqrt{n-1}} = \frac{0.00179}{\sqrt{10-1}} = 0.00596$$

$$0.00327 - 2.262 \times 0.00596 \leqslant \mu \leqslant 0.00327 + 2.262 \times 0.00596 = 0.00629$$

$$0.00192 \leqslant \mu \leqslant 0.00462$$

Form DOPLE

1407

c. Reduced exposure time. The five minutes per filter reduction in testing time reduces, ipso facto, the time of exposure to DOP by testing personnel, area occupants, and the filter itself.

d. Improved leakage accuracy. The increased number of data pairs enables one to better estimate the true leakage rate.

e. Confidence data. An easily computed confidence interval about the mean provides goodness-of-data leakage data. An inexpensive hand-held calculator is adequate for computations.

f. Better inferences. The additional data reduce the likelihood of erroneously inferring that a good filter exceeds an established allowable leakage criterion. For example, if maximum allowable leakage were 0.03%, the upper 95% confidence limit (i.e. worst case estimate of the mean) shown in Figure 11 using two detectors is 0.0235%, well below 0.03. However, if the first three values only were to have been used (as if these had had been determined through three independent tests using the one-detector method) the upper confidence limit shown in Figure 12, viz. 0.0352, would apply. It is well above the 0.03 criterion. The additional data also reduce the likelihood of erroneously inferring that a bad filter falls below the established criterion.

REFERENCES

(1)   Clark, C., and Schkade, L., Statistical Analysis for Administrative Decisions, South-Western Publishing Co., Cincinatti, p. 163, 1983.

(2)   Ibid, p. 177.

(3)   Ibid, p. 178.

statistics texts. Example: for 95% confidence, $t_a = t_{.05} = 2.262$[2] for n = 10 measurements (i.e. d.f. = 9).

(3) Determine the confidence interval about the mean using the formula

$$\overline{L} - t_a \hat{\sigma}_{\overline{L}} \leq \mu \leq \overline{L} + t_a \hat{\sigma}_{\overline{L}} \quad (3) \tag{3}$$

(NOTE: the left side of this inequality is the lower confidence limit, LCL (XX%), and the right side is the upper confidence limit, UCL (XX%), around the mean, μ. Stated otherwise, one is XX% confident, based on the number of data pairs (measurements) taken, that the true average leakage lies somewhere between LCL (XX%) and UCL (XX%). UCL (XX%) may be construed as the worst case.)

d. Plot computed L values, $\overline{L}$, and the upper and lower confidence limits. Examples of recorded and computed data are given in the tables listed below and corresponding plotted data are given in the associated figures.

	Table No.	Figure No.
Filter A, 10 meas'mts	2	5
Filter A, 3 meas'mts*	3	6
Filter B, 10 meas'mts	4	7
Filter B, 3 meas'mts*	5	8
Filter C, 11 meas'mts	6	9
Filter C, 3 meas'mts*	7	10
Filter D, 12 meas'mts	8	11
Filter D, 3 meas'mts*	9	12

VII.   Conclusions

a. <u>Increased preparation time</u>. Approximately 15 minutes are required for the Environmental Safety Check and the DOP Detector Duplicatability Check: these steps are not required for a one-detector test. This time loss may be fully recovered when there are three or more filters to be tested.

b. <u>Reduced testing time</u>. By taking upstream and downstream measurements simultaneously rather than sequentially, the time required to collect 10 data pairs using two detectors is less than two minutes. By contrast, the time required to collect only three data pairs using one detector is about seven minutes.

---

*The first three measurements from the 10, 11, or 12-measurement test have been used to illustrate the difference in $\overline{L}$, UCL (95%) and LCL (95%) that would have existed if these measurements had been taken in three independent tests using the one-detector method.

h.   Adjust downstream detector's RANGE switch (5) to lowest possible setting without pegging the meter (7).

i.   Record a minimum of ten meter observations at 10-second intervals beginning 20 seconds after the DOP challenge is first made. Use Form DOPLE. Also record generator flow, air pressure, and generator temperature.

j.   Turn FLOW valve (8) off.

k.   Make computations as described in paragraph VI. If leakage is disclosed in any unit, isolate the fault, correct the deficiency, and repeat the test.

VI.   Computation and Graphing Procedures

Having recorded a minimum of 10 pairs of downstream and upstream meter readings on Form DOPLE, the leakage value and associated confidence data may be obtained using the computational and statistical functions of a TI-55 or similar hand-held calculator: slight alterations may be required for other types.

a.   Compute the leakage, L, for each time-keyed pair of downstream and upstream readings using the formula

$$L(\%) = \frac{C_d}{C_u} \cdot \frac{R_d}{R_u} \cdot 100 \tag{1}$$

b.   For the entire set of computed L values, determine the average, $\bar{L}$; the sample standard deviation, s; and the line slope, m, of the least squares linear regression of L on time, t, as follows:

(1)   Press 2nd key, then press CA key, to clear memory.
(2)   Enter reading number, X; press x ⭧ y; enter value of L; press $\sum$+. Repeat until all points are entered.
(3)   Determine $\bar{L}$ by pressing, in turn, 2nd key and Mean key.
(4)   Determine s by pressing, in turn, 2nd key, Var key and $\sqrt{x}$ key. (5)   Determine m by pressing, in turn, 2nd key and Slope key.
(6)   Record $\bar{L}$, s, and m on Form DOPLE. (NOTE: the slope, m, will be used only to show whether, over repetitive tests, the average value of m approaches zero. When m consistently carries either a + or a - sign, or if it consistently carries a steep slope, a systematic procedural error is suggested.)

c.   Determine the confidence interval about the mean of sample means as follows:

(1)   Compute the estimated universe standard deviation, $\hat{\sigma}_L$:

$$\hat{\sigma}_L = \frac{s}{\sqrt{n-1}} \quad {}^{(1)} \text{ where n is the number of pairs} \tag{2}$$
of readings taken.

(2)   Determine the t_a statistic at a given level of significance and for a given number of degrees of freedom (d.f. = n - 1) using a table of Student's t distribution values found in most

CLEAR positions.

     g.   Turn selector valve (2) to downstream position. Adjust ZERO controls to obtain meter (7) readings of 0. Record ZERO control settings and meter readings on Form DUPLI.

     h.   Turn TEST/CLEAR switches (3) to TEST positions. Turn FLOW valve (8) on. Set RANGE switches (5) to .1 settings. Adjust RANGE settings as necessary. Start stopwatch.

     i.   Record on Form DUPLI 10 downstream meter (7) readings. Take initial reading at 20 seconds and subsequent readings at 10-second intervals. Asterisk any rapidly changing readings.

     j.   Turn FLOW valve (8) off.

     k.   Compare readings between instruments. Discard any rapidly changing readings. If more than 1/3 of stabilized readings from one detector are above or below the readings of the other detector by a factor of 1.2 or greater, repeat the DOP Detector Duplicatability Check. Should the average downstream meter (7) readings have exceeded 50% in the .1 RANGE setting, trouble shoot and correct leakage before conducting further tests.

     l.   This completes the DOP Detector Duplicatability Check.

V.   Testing Procedures

     Testing is done to determine the leakage rate, L, of the HEPA filter. Following are the steps taken using two forward light scattering detectors.

     a.   Position generator, two detectors, lines, and sampling probes as shown in Figure 1.

     b.   Be sure TEST/CLEAR switches (3) are in CLEAR positions. Set upstream detector's RANGE switch (5) to 100 and downstream detector's RANGE switch (5) to .01 setting.

     c.   Adjust ZERO controls (6) to obtain 0 reading on meters (7). Record ZERO control setting on Form DOPLE. (See Figure 13, Forms.)

     d.   If more than approximately four hours have elapsed since the DOP Duplicatability Check, or if the detectors are otherwise suspect (e.g. drift), repeat the DOP Detector Duplicatability Check before proceeding further.

     e.   Change downstream detector's RANGE switch (5) to .1 setting.

     f.   Turn FLOW valve (8) on. Turn TEST/CLEAR switches to TEST.

     g.   Adjust VAPOR ADJUST (10) and FLOW ADJUST (9) valves as needed to obtain a 40% to 90% upstream meter reading. Set stopwatch.

n.   Record SPAN (4) and ZERO control (6) settings on Form ENVIR.

o.   Allow detectors to stabilize. Progressively reduce RANGE switches (5) to 10, 1, .1, and finally .01.

p.   Adjust ZERO controls (6) if needed to again obtain 0 meter readings while TEST/CLEAR switches (3) are in TEST positions. (NOTE: minor adjustment of the ZERO control in .01 RANGE position will have an imperceptible influence on the indicated meter values when in the 100 RANGE setting. Hence, it is not necessary to repeat previous steps following this adjustment.)

q.   Record ZERO control (6) readings on Form ENVIR.

r.   Place RANGE switches (5) in the 1 position.

s.   Turn DOP generator FLOW valve (8) <u>on</u>.

t.   Turn RANGE switches (5) to lowest possible settings. Record downstream readings at time 0:10, 0:20, and 0:30 on Form ENVIR.

u.   Turn DOP generator FLOW valve (8) <u>off</u>.

v.   If gross leak has become evident (i.e. avg $>$ 50% in .1 RANGE setting), trouble shoot and correct leak.

w.   If gross leak has not become evident, proceed to DOP Duplicatability Check. This completes the Environmental Safety Check.

IV.   <u>DOP Detector Duplicatability Check</u>

a.   Place TEST/CLEAR switches (3) in TEST positions. Turn RANGE switches (5) to 100 positions. Place selector valve (2) in <u>upstream</u> position.

b.   Set ZERO controls (6) to give 0 meter (7) readings. Record ZERO control settings on Form DUPLI. (See Figure 13, Forms.)

c.   If necessary, adjust FLOW ADJUST (9) and VAPOR ADJUST (10) valves for meter (7) readings in the 40% - 90% range with RANGE switches (5) set to 100. Start stopwatch.

d.   Take initial readings at 20 seconds and subsequent readings at 10-second intervals until a minimum of 3 readings in the 100 RANGE, and 10 total upstream readings, are obtained. Record meter readings on Form DUPLI. Asterisk any rapidly changing readings.

e.   Turn FLOW valve (8) <u>off</u>. Do not change FLOW ADJUST (9) or VAPOR ADJUST (10) valves.

f.   When meter (7) indications fall below 10%, reduce RANGE switches (5) to next lower setting until sampling line is fully clear in the .01 RANGE settings. Turn TEST/CLEAR switches (3) to

d. Adjust ZERO controls (6) for 0 meter readings (7).

e. Turn TEST/CLEAR switches (3) to TEST positions.

f. Allow meters (7) to stabilize. Adjust ZERO controls (6) for 0 readings on meters. Record initial meter readings and ZERO control settings on Environmental Safety Check, Form ENVIR. (See Figure 13, Forms.)

g. Determine from Table 1 the appropriate target DOP flow scale reading.

h. Turn PRESSURE valve (11) on. Open DOP generator's FLOW valve (8). Slowly open VAPOR ADJUST valve (10) and FLOW ADJUST valve (9). Increase concentration to maximum efficiency (i.e. no dripping) determined visually. Set stopwatch. Should detector meters (7) peg, increase RANGE switch settings (5) as needed.

i. Record meter readings at time 0:10, 0:20, and 0:30 on Form ENVIR.

j. If gross leak becomes evident (i.e. >50% in .1 RANGE setting) turn FLOW valve (8) off, close FLOW ADJUST valve (9) and VAPOR ADJUST valve (10). Trouble shoot the unit under test.

k. If gross leak is not evident, turn RANGE switches (5) to 100. Turn selector valve (2) to upstream position.

l. Adjust SPAN controls (4) for stable 40% to 90% identical (± 1 unit) meter (7) readings at time 0:10, 0:20, and 0:30 on Form ENVIR.

m. Turn generator FLOW valve (8) off. Do not change FLOW ADJUST valve (9) and VAPOR ADJUST valve (10). Turn detectors' TEST/CLEAR switches (3) to CLEAR. Turn selector valve (2) again to downstream position.
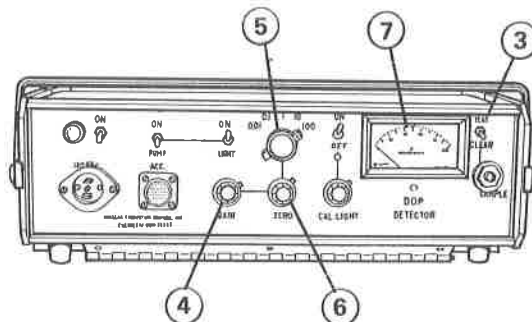
Figure 3. DOP detector.

Table 1. Approximate DOP scale reading.

Filter unit size, cfm	Scale reading (steel ball)
45000	62
30000	48
20000	37
15000	30
10000	24
	(glass ball)
5000	67
2500	48
1200	33
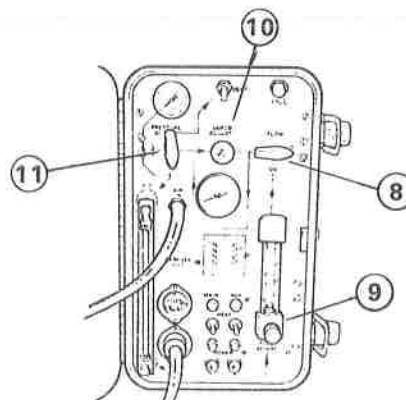
Figure 4. DOP generator.

1401
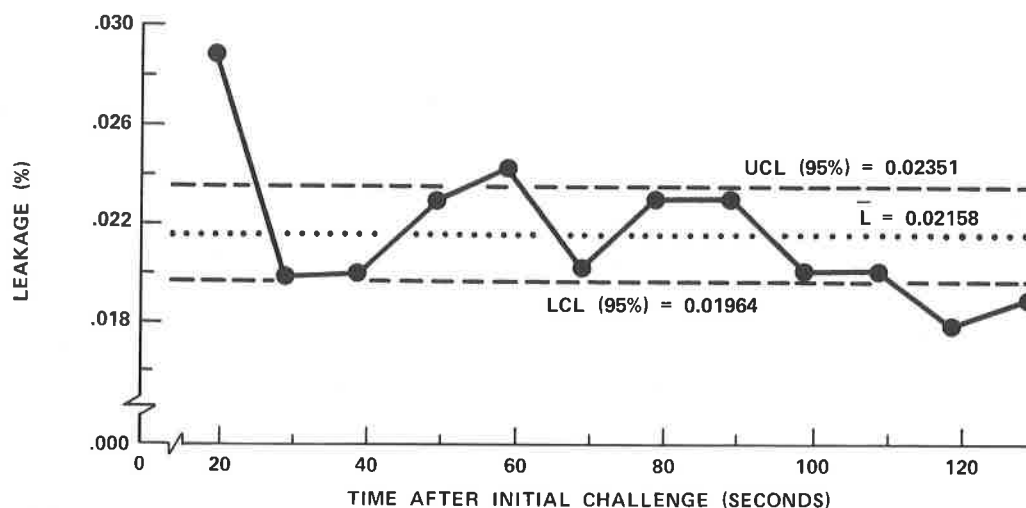
Figure 11. }
Table 8. } DOP LEAK TEST, FILTER D, 12 MEASUREMENTS

RDG. NO. X	TIME AFTER INIT. CHLG. (SECS)	% PEN UPSTR. C_u	RANGE UPSTR. R_u	% PEN DNSTR. C_d	RANGE DNSTR. R_d	LEAKAGE $C_d/C_u \cdot R_d/R_u \cdot 100 = L(\%)$	SAMPLE PARAMETER
			RECORDED DATA			COMPUTED DATA	
1	20	70	100	20	0.1	0.0286	$\overline{L} = 0.02158$
2	30	100		20		0.0200	
3	40	70		14		0.0200	
4	50	85		20		0.0235	
5	60	100		24		0.0240	
6	70	100		20		0.0200	$s = 0.00292$
7	80	90		21		0.0233	
8	90	90		21		0.0233	
9	100	100		20		0.0200	
10	110	100		20		0.0200	
11	120	80		14		0.0175	$m = -0.00052$
12	130	75		14		0.0187	
13	140						
14	150						
15	160						

CONFIDENCE INTERVAL ABOUT MEAN:

$$\overline{L} - t_a \hat{\sigma}_{\overline{L}} \leqslant \mu \leqslant \overline{L} + t_a \hat{\sigma}_{\overline{L}} \quad \text{WHERE} \quad \hat{\sigma}_{\overline{L}} = \frac{s}{\sqrt{n-1}} = \sqrt{\frac{0.0029178}{12-1}} = 0.00088$$

$$0.02158 - 2.201 \times 0.00088 \leqslant \mu \leqslant 0.02158 + 2.201 \times 0.00088$$

$$0.01964 \leqslant \mu \leqslant 0.02351$$

Form DOPLE

1413
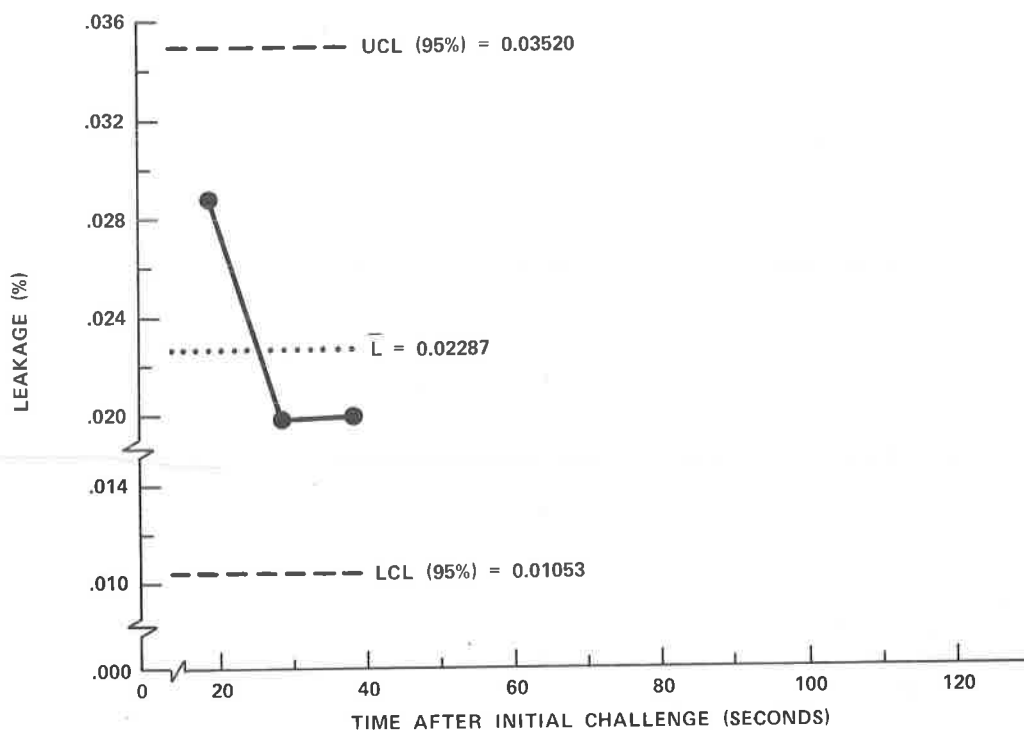
Figure 12.
Table 9.
} DOP LEAK TEST, FILTER D, 3 MEASUREMENTS

RDG. NO. X	RECORDED DATA					COMPUTED DATA	
	TIME AFTER INIT. CHLG. (SECS)	% PEN UPSTR. C_u	RANGE UPSTR. R_u	% PEN DNSTR. C_d	RANGE DNSTR. R_d	LEAKAGE $C_d/C_u \cdot R_d/R_u \cdot 100 = L(\%)$	SAMPLE PARAMETER
1	20	70	100	20	0.1	0.0286	$\bar{L} = 0.02287$
2	30	100		20		0.200	
3	40	70		14		0.200	
4	50						
5	60						
6	70						$s = 0.004054$
7	80						
8	90						
9	100						
10	110						
11	120						$m = -0.0043$
12	130						
13	140						
14	150						
15	160						

CONFIDENCE INTERVAL ABOUT MEAN:

$$\bar{L} - t_a \hat{\sigma}_{\bar{L}} \leqslant \mu \leqslant \bar{L} + t_a \hat{\sigma}_{\bar{L}} \quad \text{WHERE} \quad \hat{\sigma}_{\bar{L}} = \frac{s}{\sqrt{n-1}} = \frac{0.004054}{\sqrt{3-1}} = 0.00287$$

$$0.02287 - 4.303 \times 0.00287 \leqslant \mu \leqslant 0.02287 + 4.303 \times 0.00287$$

$$0.02287 - 0.01234 \leqslant \mu \leqslant 0.02287 + 0.01234$$

$$0.01053 \leqslant \mu \leqslant 0.03520$$

Form DOPLE

1414

ENVIRONMENTAL SAFETY CHECK
DOP DETECTION

A — DETECTOR NO.
B — DETECTOR NO.

DATE/TIME

TIME MIN:SEC	SPAN STG. A	SPAN STG. B	ZERO STG. A	ZERO STG. B	DETECTOR A % PEN R	DETECTOR A % PEN DN	DETECTOR A % PEN UP	DETECTOR B % PEN R	DETECTOR B % PEN DN	DETECTOR B % PEN UP	TEST/CLEAR POSITION
—	0	0			.01	0		.01	0		CLEAR
—	0	0			.01			.01			TEST (BEFORE FLOW STARTS)
0:10	0	0									TEST (AFTER FLOW STARTS)
0:20	0	0									"
0:30	0	0									"
0:10					100			100			"
0:20					100			100			"
0:30					100			100			"
—					.01	0		.01	0		CLEAR
0:10											TEST (AFTER FLOW STARTS)
0:20											"
0:30											"

Form ENVIR

DUPLICATABILITY CHECK
DOP DETECTORS

DATE TIME		DETECTOR NO. SPAN CON. STG.					DETECTOR NO. SPAN CON. STG.				
SET NO.	ELAPSED TIME	UPSTREAM C_u	R_u	ZERO STG.	DOWNSTREAM C_d	R_d	UPSTREAM C_u	R_u	ZERO STG.	DOWNSTREAM C_d	R_d
INIT.											
1											
2											
3											
4											
5											
6											
7											
8											
9											
10											
11											
12											
13											

Form DUPLI

DOP LEAK TEST

RDG. NO. X	TIME AFTER INIT. CHLG. (SECS)	% PEN UPSTR. C_u	RANGE UPSTR. R_u	% PEN DNSTR. C_d	RANGE DNSTR. R_d	LEAKAGE $C_d/C_u \cdot R_d/R_u \cdot 100 = L(\%)$	SAMPLE PARAMETER
1	20						$\bar{\bar{L}} =$
2	30						
3	40						
4	50						
5	60						
6	70						$\mathbf{s} =$
7	80						
8	90						
9	100						
10	110						
11	120						$m =$
12	130						
13	140						
14	150						
15	160						

CONFIDENCE INTERVAL ABOUT MEAN:

$$\bar{L} - t_B \hat{\sigma}_{\bar{L}} \leqslant \mu \leqslant \bar{L} + t_B \hat{\sigma}_{\bar{L}} \quad \text{WHERE} \quad \hat{\sigma}_{\bar{L}} = \frac{s}{\sqrt{n-1}}$$

Form DOPLE

Figure 13. FORMS

DISCUSSION

DAVIS: We at Flanders Filters, Inc, do not find that a two-minute interval between upstream and downstream photometer readings is necessary. Ten seconds is a much more realistic figure. What type of degradation do you anticipate?

DAUBER: Our objective is to obtain additional replicate readings while exposing personnel and filters to the least possible amounts of DOP.

A FILTER CONCEPT TO CONTROL AIRBORNE PARTICULATE RELEASES DUE TO SEVERE REACTOR ACCIDENTS AND IMPLEMENTATION USING STAINLESS-STEEL FIBER FILTERS

H.-G. Dillmann, H. Pasler
Laboratorium für Aerosolphysik und Filtertechnik
Kernforschungszentrum Karlsruhe GmbH
Postfach 3640, D-7500 Karlsruhe 1
Federal Republic of Germany

Abstract

Bursting of the containment of pressurized water reactors as a result of severe reactor accidents can be avoided by installation of accident filter systems which fulfill the function of a safety valve. This greatly reduces contamination of the environment by fission product release. The filter concept and its implementation using stainless-steel fiber filters are described. A comparison is made with other concepts which have been proposed to solve the problem.

1. Introduction

Following severe reactor accidents a reaction between concrete and the melted core could give rise to the buildup of pressures in the reactor containment of LWRs which, depending on the development of the accident and on the types of concrete used, could lead after some days to bursting of the reactor containment /1/. This implies a near-ground release of radioactivity from the containment which, at the time of burst, would be an airborne radioactivity. The process might even be aggravated by a fraction of activity released from the boiling sump as a result of resuspension.

To avoid this release of activity, a number of different solutions are being investigated in several countries, most of them with the objective of causing the steam entraining the radioactivity to condense in a gravel-filled condensation chamber before the reactor will burst.

2. Other Solutions

The studies of Hanford Engineering Development Laboratory /2/ and of Sandia National Laboratory /3/ in the USA should be mentioned here. A similar concept is pursued in Sweden under the FILTRA Project /4/ that proposes condensation systems in which the steam condenses together with the radioactivity. Some of the solutions presented include additional series-connected filter systems in order to enhance safety. These filters are not as highly loaded as filters exposed to direct flow.

The costs of these systems would be on the order of 10-20 million dollars.

A less costly solution is being studied in France where sand bed filters /5/ of about 80 cm layer thickness and about 100 metric tons total weight are planned. We expect that the following problems could be encountered with this accident filter concept: it is not possible to retain iodine. In the initial phase of operation a sand-bed filter shows a low removal efficiency which increases only in the course of filtration due to formation of a filter cake. If the filter is not preheated prior to operation about 2-3 metric tons of water are produced through steam condensation until the dew point temperature is exceeded as a result of condensation heat.

The costs are estimated at about 0.5 million dollars.

3. A German Accident Filter Concept

German PWR power plants are designed for a maximum containment pressure of 6 bar. The burst pressure is assumed to be 8-9 bar. The operating point of an accident filter system should lie in the pressure range of 6-8 bar. The volumetric flow rate of the gas resulting from the reaction of melted core and concrete is known from computations made in /1/ and amounts to about 3000-5000 m^3/h. The demister (Fig. 1) of the venting system is installed within the reactor containment. In this way it is ensured that the outflowing gas stream leaves the reactor containment with a maximum gas relative humidity of 100 % and without the presence of water droplets. The second essential component is a pressure control valve actuated via the internal pressure; it allows only the same volume of gas to escape as is newly generated. In this way, the pressure in the reactor containment is kept at a constant value and the activity confined in the reactor containment for as long as possible. Moreover, by aerosol physical processes the fraction of airborne activity is reduced through agglomeration. Another important function of the valve is to produce an isenthalpic expansion of the containment atmosphere and thus effect a strong drying of the gas, from 160 $^{\circ}$C and 100 % relative humidity to 145 $^{\circ}$C with a 45 $^{\circ}$C distance from the dew point (Fig. 2).

Except for the short start-up phase of about 10 s duration when only about 8 l of condensate are produced in the HEPA filter section, until the 100 ^{O}C limit (dew point 1 bar) is attained, the filter components are exposed exclusively to superheated steam. For safety reasons the valve can be protected by a burst diaphragm connected in parallel which does not open until a pressure of about 8 bar is attained. After the onset of an accident about 4 to 5 days will pass until the filter system is put into operation. During this time interval the filter system can be inertized with N_2, if required, in order to prevent H_2 deflagration.

The first filter stage is a prefilter consisting of stainless-steel fibers and made up of several layers of different fiber diameters for removal of the majority of the coarse aerosols. The measured values will be indicated below. The second stage consists of 2 µm stainless-steel fibers comparable with HEPA glass-fiber media. At this stage, the very fine aerosols of less than 1 µm diameter are removed. The results were presented at the 17th DOE Air Cleaning Conference in Denver /6/. Then follows the iodine filter stage filled with molecular silver sieves. The results of investigations of the iodine filters were reported at the 16th DOE Air Cleaning Conference in San Diego /7/.

It is possible to connect another HEPA filter downstream of the iodine filter in order to remove any contaminated abrasion material from the iodine filter stage. The offgas is subsequently carried via a fan and a flame arrester (on account of the H_2 fraction) to the stack.

In addition, a device will be provided which allows filtration of the air in the annulus, in the case that the latter is contaminated by air leaking from the reactor containment into the annulus.

A bypass of the filter system will be provided to be used during the period after the pressure buildup has come to an end, the pressure in the containment has dropped to values < 6 bar, and the exventing filter system is no longer required for the reactor containment. This bypass allows the removal of the after-decay heat of the plated-out fission products without releasing any more vent air to the outside. And in fact, failure of this bypass cooling would not pose problems since no organic adhesives and sealants are used for the filter components and temperatures up to 500 ^{O}C can be accommodated. At these temperatures, cooling by heat radiation alone should be sufficient.

Another solution consists of a mobile filter system as represented in Fig. 3 because about 4 days will pass until the filter systems would be put into operation. Only installation of the demister, control valve, internal pipework, and appropriate connections will be required. The largest weight to be handled in a mobile system will undoubtedly be the required radiation shield.

4. The Problem of Corrosion

The stainless-steel fibers have been exposed to steam and steam-air mixtures at temperatures between 100 and 180 ^{o}C in endurance tests which lasted for several months. No corrosion whatsoever appeared on the fibers. Therefore, it can be assumed that no critical corrosion phenomena will occur during an estimated service life of 2-4 weeks, not even when the filters are exposed to the offgas of a reactor containment. Repeated use of such a filter system is certainly not to be anticipated.

5. Values Measured at the Prefilters

Prefilters have been investigated with a respect to loading capacity and removal efficiency. The tracer aerosol was a commercial fire-extinguishing powder with an aerosol size distribution between approx. 1 and 10 μm (Fig. 4). Given the long waiting time until the filter is put into operation the fraction of fine aerosols <1 μm should not make a substantial contribution to filter loading because agglomeration takes place. The values are given in Table 1.

Since an exventing filter with an exposure area of about 5 m^2 will be necessary for a volumetric flow rate of 3000-5000 m^3/h in order to realize a HEPA filter section with 2 μm fibers, a theoretical loading of about 50 kg can be expected. However, according to results previously obtained from other investigations such a high aerosol loading is not to be expected so that in this respect also there exists no limit in the application of the filter.

The investigations will be continued at different flow rates in order to cover possible changes in volumetric flow rates as well.

6. Studies with Steam in the HEPA Filter Section

Previous investigations into the HEPA filter section ($\eta = f(T,p,v)$) dealt mainly with filters exposed to air. However, since in a severe accident the major fraction of the containment atmosphere consists of steam, measurements of the removal efficiency under conditions of steam exposure were performed. Superheated steam, 1 bar and 140 ^{o}C, was assumed and the steam temperature was reduced in steps in order to increase the steam moisture until condensation occurred. The values have been entered in Table 2. No significant difference was observed in comparison to tests performed with air. This demonstrates that, at least over several weeks, filtration efficiency can be maintained with the use of stainless-steel fiber filters.

1420

7.Summary

By this demonstration of performance of an accident filter system it can reasonably be supposed that hypothetical accidents in LWRs can also be controlled and the environmental burden reduced by a factor of $\geq$ 1000. Using this filter concept, both aerosol and iodine activities can be contained. Only the noble gases with low radiological impact would be released. The cost of such a filter system should amount to 0.5 to 1 million dollars. This means that, compared with condensation systems, a cost-advantage factor of about 20 could be achieved.

8. References

/1/ M. Reimann,
     The Erosion Behavior of Different Types of Concrete
     Interacting with a Core Melt,
     Proc. Thermal Reactor Safety, April 6-9, 1980
     Knoxville, Tenn. pp. 197-204

/2/ R. K. Owen, A. K. Postma,
     Hanford Engineering Laboratory
     Development of a Passive, Self-Cleaning Scrubber for Containment Venting Applications,
     16th DOE Nuclear Air Cleaning Conference, San Diego 1980,
     Conf.-801038, pp. 335,

/3/ H. C. Walling*, A. S. Benjamin*, P. Cybulskis**,
     * Sandia National Laboratories, ** Battelle Columbus Laboratories,
     16th DOE Nuclear Air Cleaning Conference, San Diego 1980,
     Conf.-801038, pp. 353,

/4/ C. Gräslund, K. Johansson, L. Nilsson, I. Tiren,
     FILTRA, Filtered Atmospheric Venting of LWR Containments,
     A Status Report, IAEA-CN-39/74, 1980-10-20--24,

/5/ Private Information

/6/ H.-G. Dillmann, H. Pasler,
     Theoretical and Experimental Investigations into the Filtration of the Atmosphere within the Containments of Pressurized Water Reactors after Serious Reactor Accidents,
     16th DOE Nuclear Air cleaning Conference, San Diego 1980,
     Conf.-801038, pp. 373,

/7/ H.-G. Dillmann, H. Pasler,
     Experimental Investigations of Aerosol Filtration with Deep Bed Fiber Filters,
     17th DOE Nuclear Air Cleaning Conference, Denver 1982,
     Conf.-820833, pp. 1160,

Table 1 : Loading and removal efficiency of prefilters.

Volumetric flow rate : 200 m^3/h, $^+$400 m^3/h

Exposure area : 0.31 m^2

Tracer aerosol : 1 - 10 µm

Fiber Diameter [µm]	Fiber Loading [g/m^2]	Initial Value of Δp [mbar]	Final Value of Δp [mbar]	Efficiency [%]	Loading [g]	Loading [kg/m^2]
30	2500	0.1	6	78	3243	10.5
22	1500	0.15	7	85	2348	7.6
12	1500	0.25	8.8	96	2288	7.3
8	1500	0.5	13.5	> 99	1080	3.5
4	1500	2.3	17.2	> 99	488	1.56
+8	1500	1.7	24.9	90	1430	4.6
+4	1500	5.1	31	> 99	790	2.5

Table 2: Decontamination factors of stainless-steel fiber filters exposed to steam.

Filter loading	: 1.5 kg/m^2 fibers
Fiber diameter	: 2 μm
Face velocity	: 30 cm/s
Volumetric flow rate	: 350 m^3/h
Pressure differential	: 27 mbar
Pressure	: 1 bar
Test gas	: Superheated steam
Tracer aerosol	: Uranine

Temperature (°C)	Decontamination factor	Removal Efficiency	Decontamination factor with air[+]
140	5650	99.98	
130	4100	99.98	
130	4900	99.95	
120	2050	99.95	
120	3500	99.97	
110	1800	99.94	
110	1400	99.93	
102	1070	99.9	
102	1010	99.9	
140[+]		99.97	4000
100[+]		99.93	1400

FIG. 1

1 Prefilter
2 HEPA Filter
3 Iodine Filter
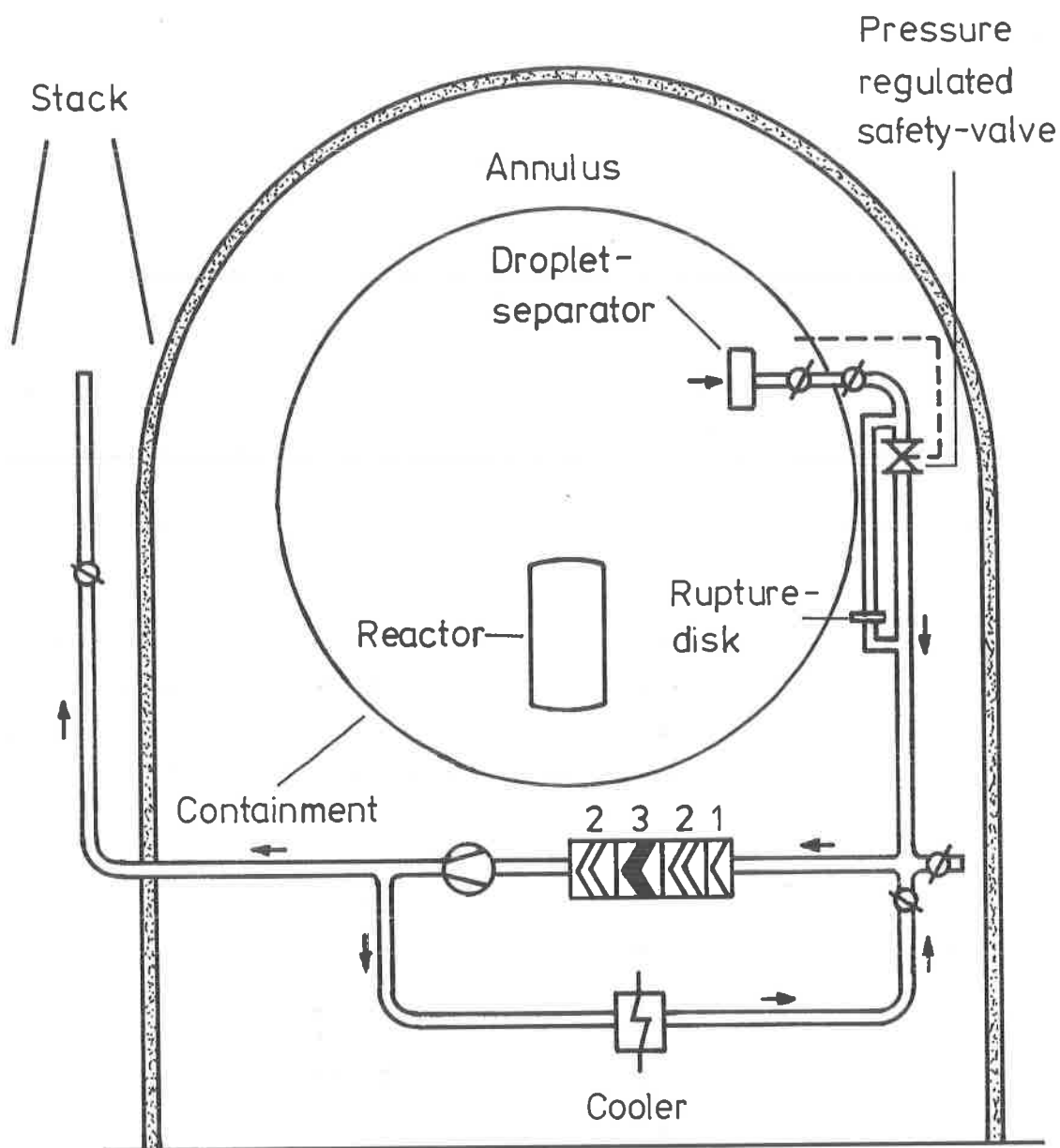
CONCEPT OF AN ACCIDENT FILTER SYSTEM FOR

CONTAINMENT VENTING AGAINST BURSTING
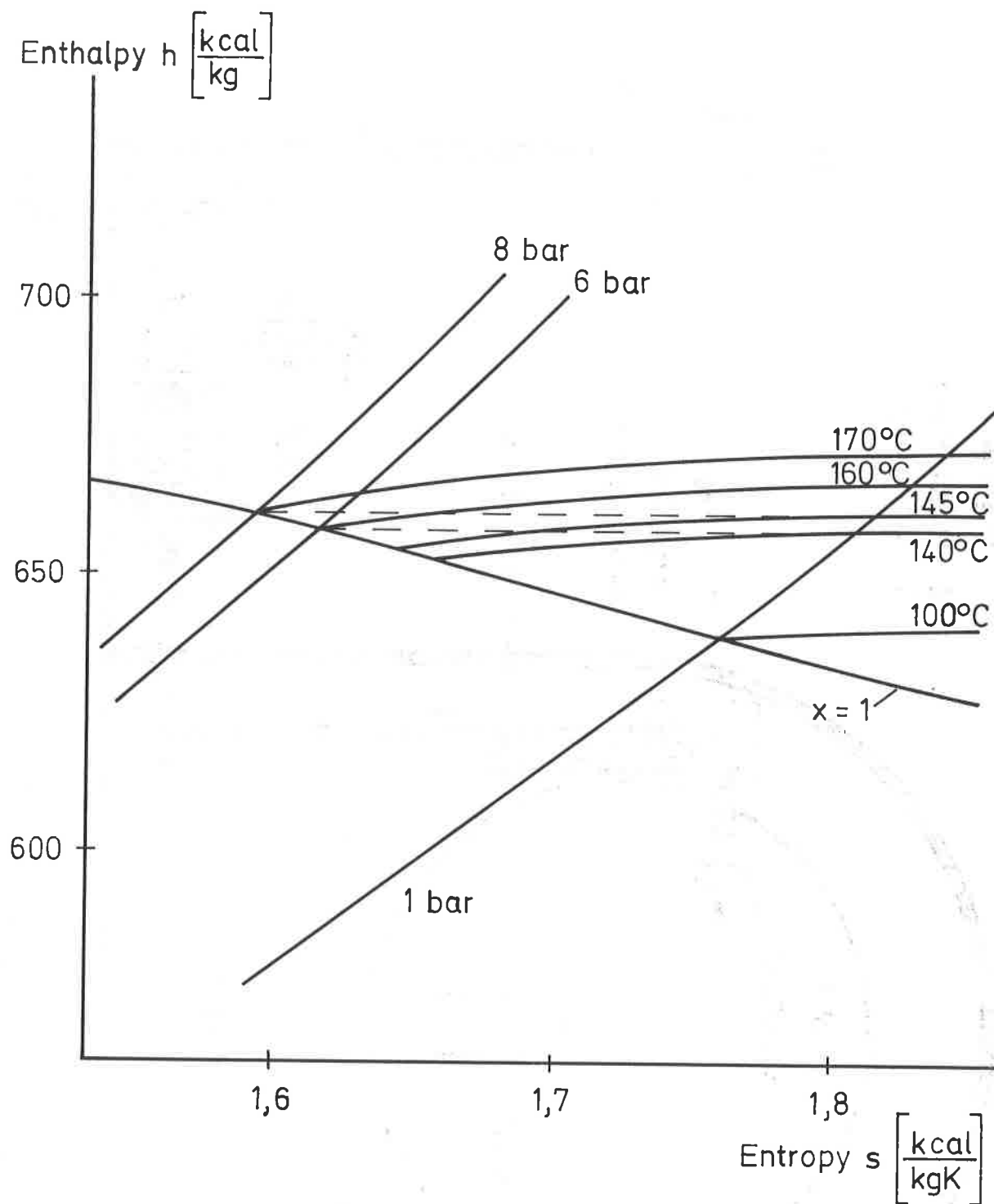
FIG. 2   DRY-EFFECT OF THE SAFETY VALVE BY
ISENTHALPIC PRESSURE DECREASE
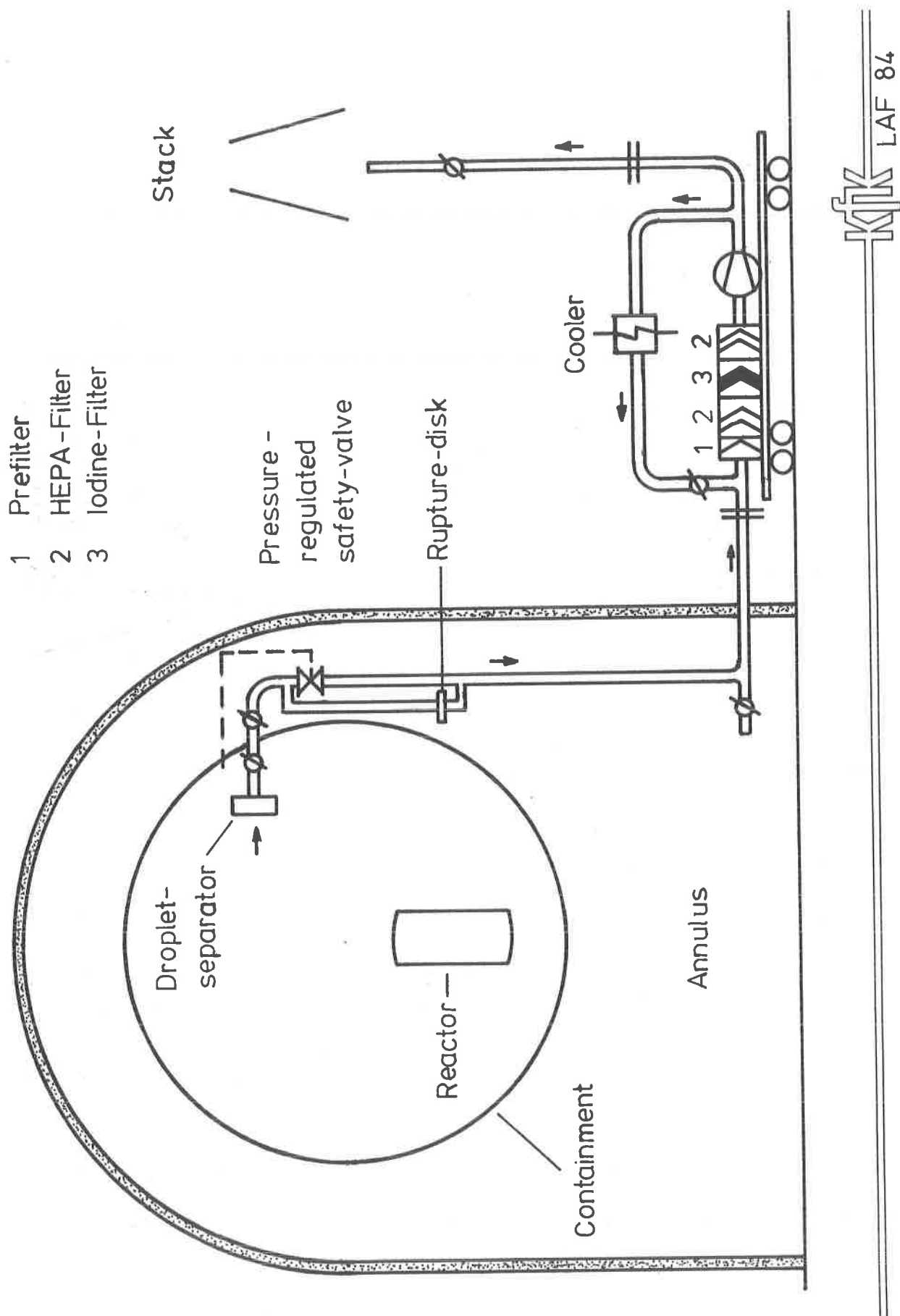
FIG. 3   TRANSPORTABLE FILTER SYSTEM (CONCEPT)
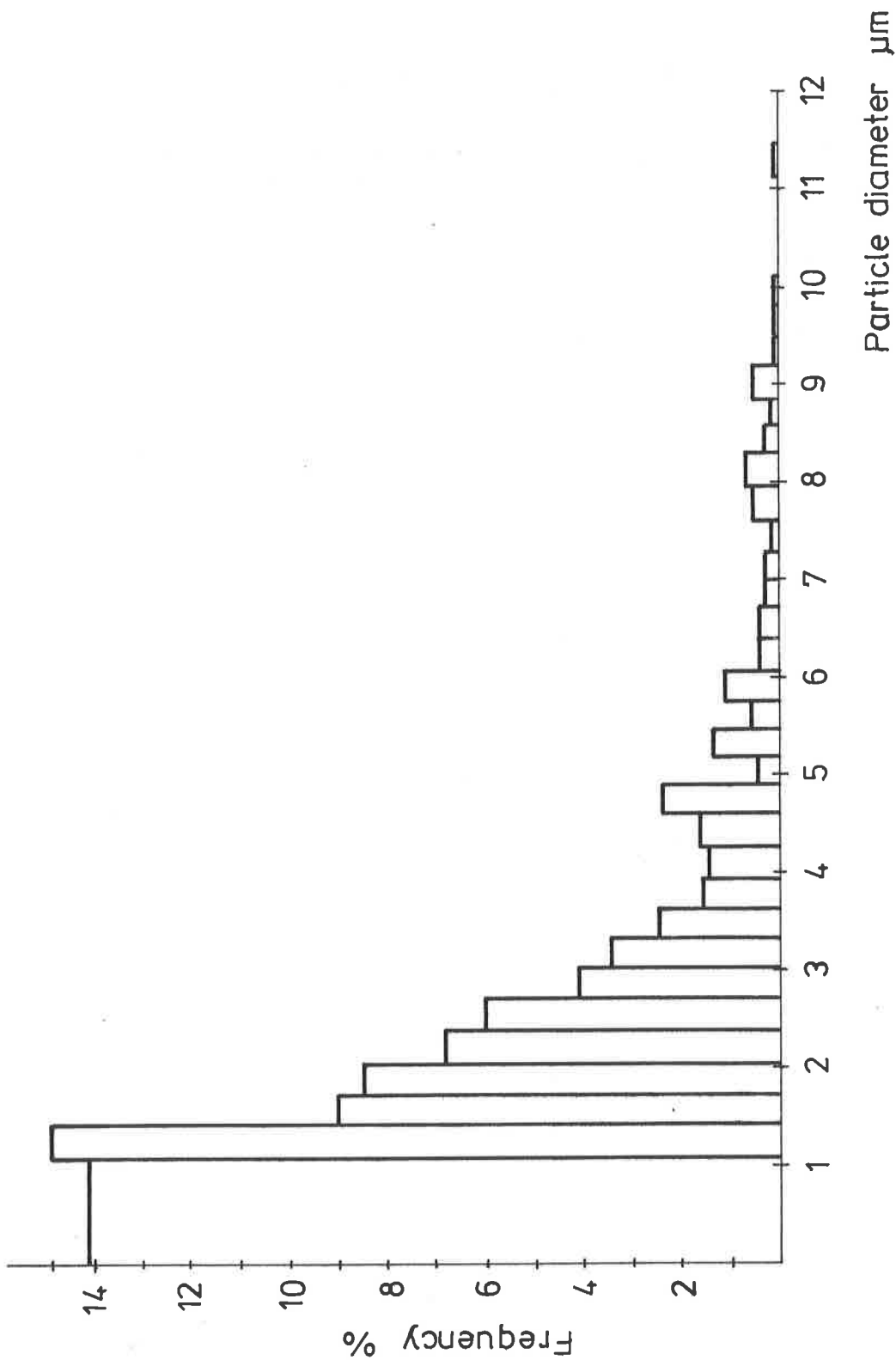
FIG. 4   PARTICLE SPECTRUM OF THE TEST AEROSOL

DISCUSSION

WIKTORSSON: What is the diameter of the outlet pipe to the
filter units?

DILLMAN: I expect airsteam velocities in the pipe to
be 5 to 8 m/s, so you can calculate the diameter from the given
flow rate.

DUAL AEROSOL DETECTOR BASED ON FORWARD LIGHT SCATTERING WITH A SINGLE LASER BEAM

Bela J. Kovach;   Robert A. Custer;   Frank L. Powers; Aram Kovach
Nuclear Consulting Services, Inc
Columbus, Ohio

Abstract

The in place leak testing of HEPA filter banks using a single detector can lead to some error in the measurement due to the fluctuation of the aerosol concentration while the single detector is being switched from the upstream to downstream sampling. The time duration of the test also can cause unnecessarily high DOP loading of the HEPA filters and in some cases higher radiation exposure to the testing personnel.

The new forward light scattering detector uses one 632.8 nm laser beam for aerosol detection in a dual chamber sampling and detecting aerosol concentration simultaneously both upstream and downstream.   This manner of operation eliminates the errors caused by concentration variations between upstream and downstream sample points while the switching takes place.

The new detector uses large area silicone photodiodes with a hole in the center, to permit uninterrupted passage of the laser beam through the downstream sample chamber.

The nonlinearity due to the aerosol over population of the laser beam volume is calculated to be less than 1% using a Poisson distribution method to determine the average distance of the particles.

A   simple   pneumatic   system   prevents mixing of the upstream and downstream samples even in wide pressure variations of the duct system.

Introduction

The widely used forward light scattering detectors are analog rate meters, averaging an analog signal proportional to the light, scattered from the aerosols.   The averaging time, or the meters time constant is, only a fraction of the injection time of the challenging aerosol, which may not represent the concentration of aerosol during a much longer injection time. If samples are taken at different times, the testing personnel are faced with difficulties of maintaining a constant injection flow and near perfect mixing of the challenging aerosol to achieve appropriate precision for good repeatability.

Taking a number of measurements and averaging the results, would be the next logical step in order to decrease the error. This led to the solution of;
1.   Using of double detector for the two sides of the filter simultaneously.
2.   Integrating a long term signal proportional to the aerosol concentration from both the upstream and downstream sides of the filter bank, during most of the injection time.

Extending the time of measurement from the two or three seconds time constant to the 30 to 50 seconds, will increase the repeatability approximately ten times, while maintaining a constant injection flow will be not as critical. The elimination of switching from upstream to downstream of the filterbank (and clearing the detector chamber) reduces the time duration of the test and decreases the "load" on the filters and the testing personnel are shorter time in controlled areas.

The Dual Detector

1. The Light Source . A small 2mW HeNe laser was chosen as a light source, with a 0.65 mm beam diameter and concentrated light intensity equal to 5 MegaWatt per square centimeter. As this light is a narrow beam it scatters from the aerosol particles in all points of interception. The scattered light is therefore proportional to the length of the laser beam, provided that the travel of the light beam is along the air sample filled with aerosols. The limitation on the length of the laser beam used, is the "overpopulation" of the beam with particles causing shaded areas where particles can be hidden without producing scattered light. The shaded area was calculated for 100 microgram per liter concentration and 20 mm laser beam, for different sizes of nonreflective spherical particles, without overlapping shadows. As the shaded area only amounted to 1 % of the laser beam cross section, the possible overlapping of the randomly distributed particles calculated using a Poisson distribution method is negligible.
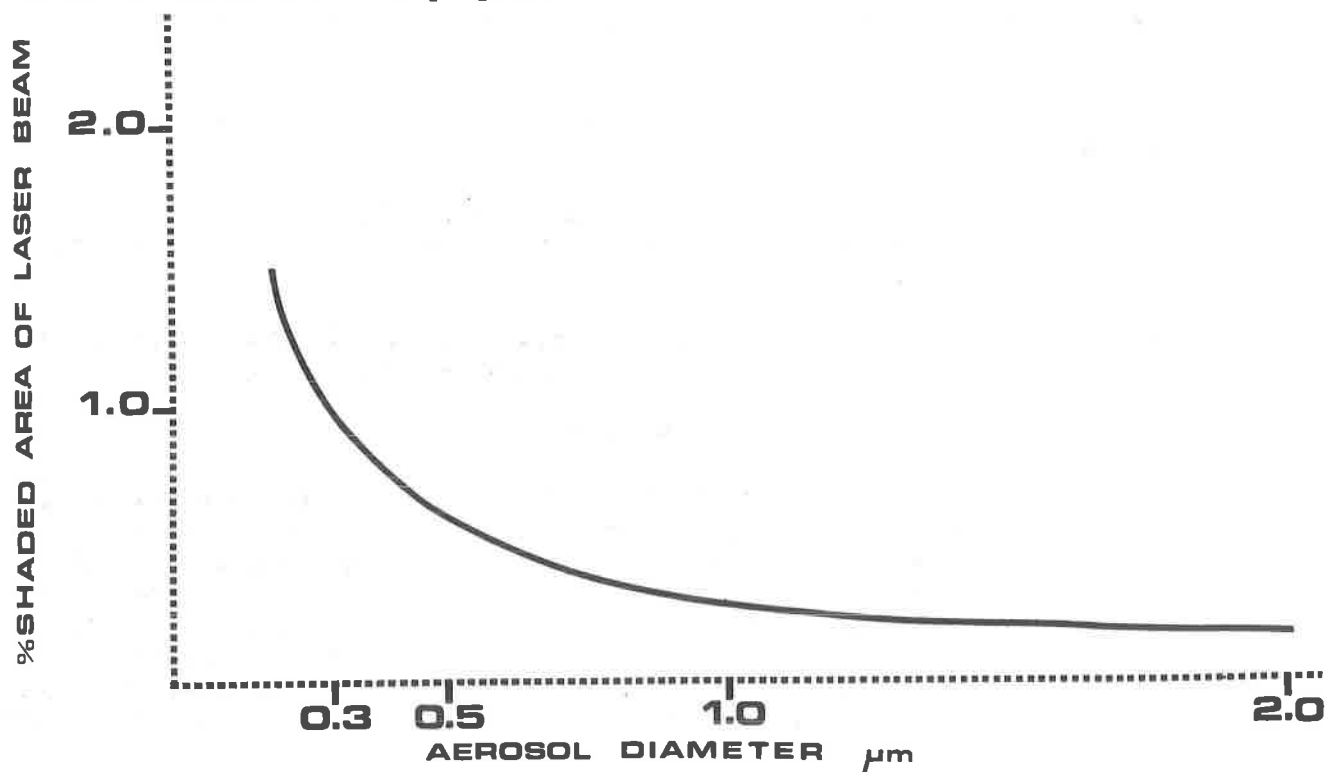
FIG.1

The Shaded Area vs. Particle Diameter

The shaded area was calculated as the cross section to volume ratio of spherical particles in constant weight to volume concentration. (1)

$$\frac{\pi r^2}{\frac{4}{3}\pi r^3} = \frac{3}{2d} \qquad (1)$$

where   r= the radius of the spherical particles
        d= the diameter of the particles

or for 20 mm depth of penetration in 100 microgram/liter air/aerosol concentration the shadow will be (2)

$$\text{Shadow} \quad (\text{in } \%) = 0.3/d \ (\text{in micron}) \qquad (2)$$

In Figure 1, the shaded area vs particle diameter in 20 mm length of laser beam penetrating in 100 micrograms per liter air aerosol concentration is shown.
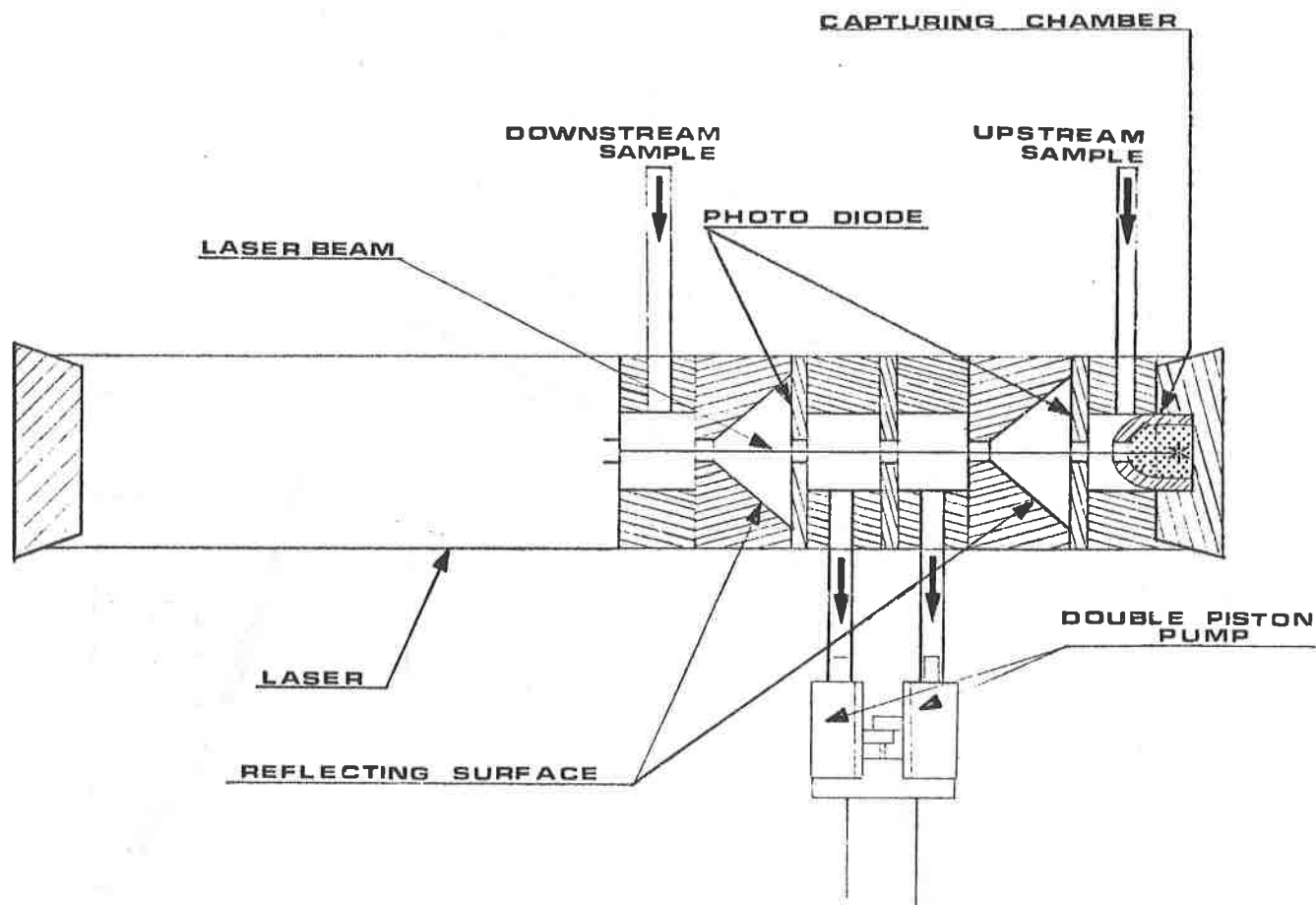
FIG. 2

The Detector Chambers and The Sample Flow

<u>2. The Detector Chambers</u> . Shown in Figure 2, the laser beam enters the first chamber containing the downstream air sample. These chambers are made of black Teflon, resistant to DOP and most other chemicals. The scattered light is collected on a large silicon photodiode. The "unused" portion of the beam then enters in the second chamber where the upstream air sample is pumped through. The last chamber is design to absorb the light from the laser beam, to insure a minimum of light backscattering .

The use of one single laser beam for both the upstream and downstream detection and simultaneously comparing the signal from the scattered light, cancels the drift caused by variations in the light intensity.

<u>3. The Sample Flow.</u> The air/aerosol mixture, from both sides of the filter, (upstream and downstream), simultaneously enters the upstream and downstream detector chambers respectively. The air sample then travels along the laser beam and exits without mixing, insured by the negative pressure in the exit chambers. A double piston diaphragm pump is used for sampling. Both the pump and the detector chambers are solvent resistant and decontamination is possible, (see Figure 2).

<u>4. The Detector</u> is an array of silicon photodiodes of 4 square cm. Its spectral response curve is shown in Figure 3.
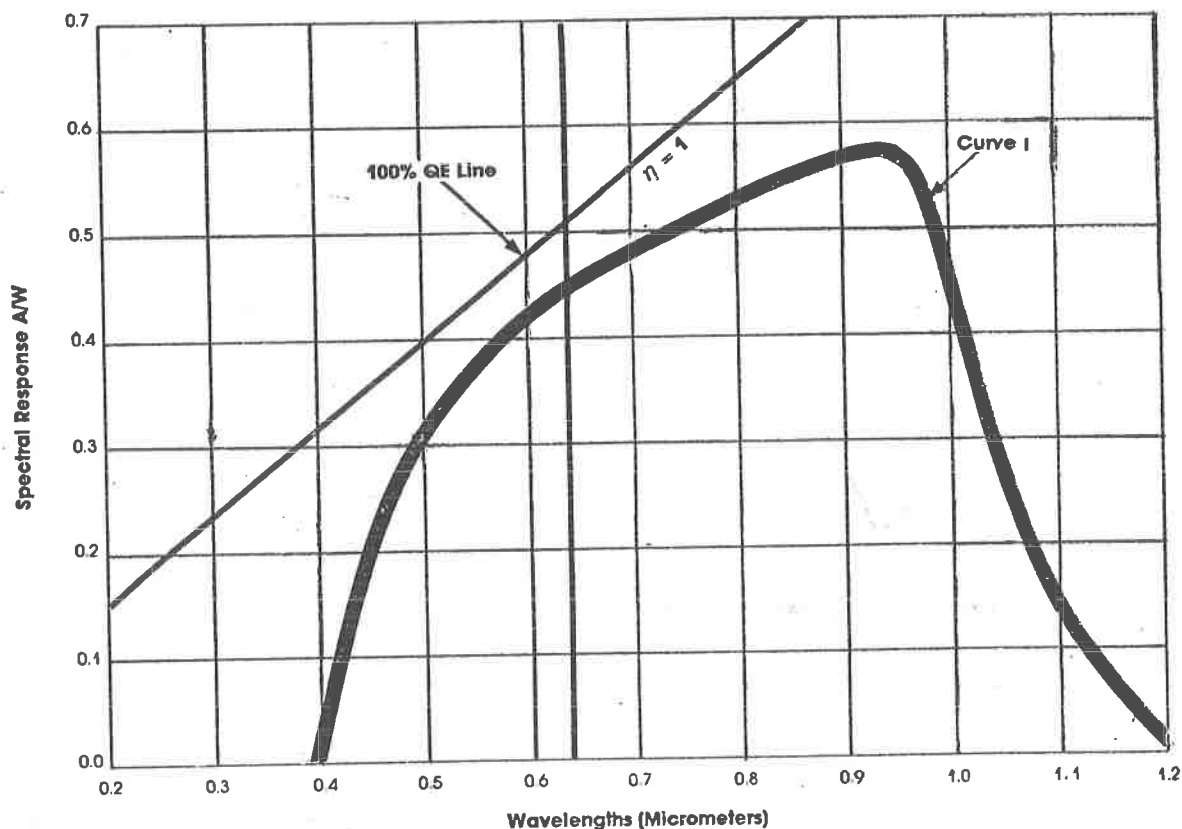
FIG.3

The Photodiode Spectral Response vs. Wavelength.
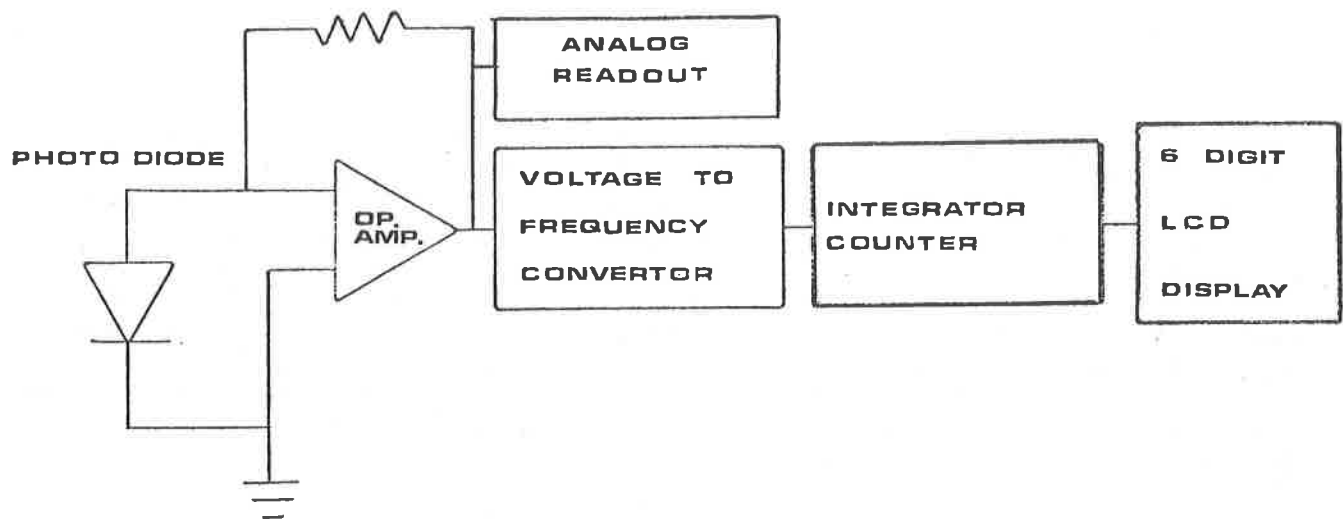
FIG.4

Signal Processing.
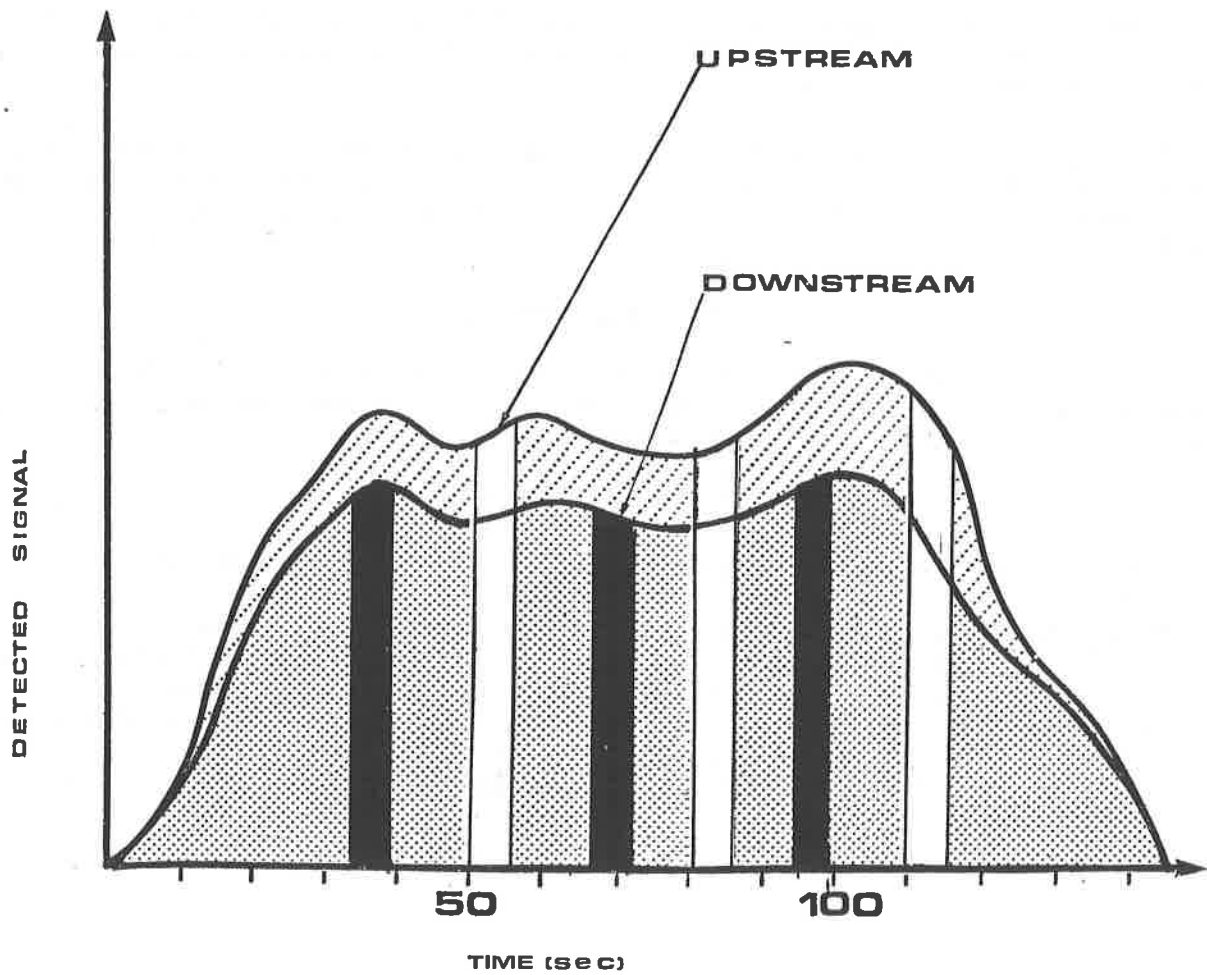
FIG.5

The Integral Method of Measurement vs. Standard Sampling Technique.

5. Signal Processing.   (Figure 4.)   The currents from the photodiode arrays are amplified by low drift chopper amplifiers. The analog signals from the upstream and downstream detectors are then converted by voltage to frequency convertors into a series of electrical pulses. These pulses are accumulated in pulse counters and displayed in digital form. The displayed numbers represent the integral values proportional to the amount of injected/penetrated aerosol passing through the ventilation system during the time of the measurement, regardless of concentration fluctuations during the test period. Dividing these two integrated numbers, (downstream / upstream), the penetration can be instantly displayed. The integral method of measurement vs. standard sampling technique is displayed in Figure 5.

Conclusion

The incorporation of a sturdy, long life, inexpensive, and portable HeNe lasers in an aerosol detector eliminates the need for optical lenses to concentrate the light in a high intensity point. The utilization of a longer path of the laser beam, for the forward light scattering, makes possible the use of the same laser beam for both upstream and downstream detection with very small volume detector chambers.

The simultaneous upstream and downstream sample measurements and the applied integrating technique increased the repeatability, reduced the time of measurement and eliminated the need of maintaining a constant injection flow during the leak test.

Acknowledgement

The authors wish to thank NUCON personnel for their numerous suggestions and Professor R. Bojanic of the Mathematics Dept. at the Ohio State University for helpful discussions.

References

1. Tebo A.R. "Those pesky aerosols" ELECTRO OPTICAL SYSTEM DESIGN pp 23, July 82
2. Dennis R. (Editor) "HANDBOOK ON AEROSOLS" TID-26608,.   1976
3. Salzman G.C., Ettinger H.J., Tillery M.I., at all. "Potential application of a single particle aerosol spectrometer for monitoring aerosol size at the DOE filter test facilities." 17-th DOE Nuclear Air Cleaning Conference LA-UR-82-2090 1982
4. Volz A.F."Results on aerosol light absorption" AFGL-TR-82-0271. 1982

DISCUSSION

PRATT: Can you tell me what the sample flow rate is through the spectrometer?

KOVACH, B.J.:   It is 4 L/m.   This flow rate gave us sufficient sample velocity through the ¼ in. sample line, as well as a fast response time thanks to the very small chamber volume.

TEST DATA AND OPERATION DATA FROM CARBON USED IN HIGH VELOCITY SYSTEMS

James R. Edwards
Charcoal Service Corporation
P. O. Box 3
Bath, N. C.

Abstract

A 10 CFR 100 review required a utility to change the air flow capacity of its Auxilary Building Exhaust Filter systems. Since there was no room to increase the size of the system, the system had to be rated at a higher air flow capacity. This changed the residence time of the air in the carbon bed from 1/4 second to 1/8 second. Carbon to meet these new requirements had to be tested in the new tech spec mode, and the new tech specs implemented.

The results of the testing and the implementation showed that new carbon will meet the requirements, but that the carbon will have a very limited life.

I. Introduction

A 10 CFR 100 regulation review for reactor siting was performed at a utility in August, 1981. The review concluded that the Auxilary Building Exhaust flow was too high to allow the carbon to be used under the existing conditions. Therefore, certain changes were proposed. See Figure 1.

Figure 1   Initial Conditions.

	Bed Velocity	(RT)	BD	Temp	RH
(Existing)	40 ft/min	(1/4 sec)	2"	30°C	80% RH
(Proposed)	80 ft/min	(1/8 sec)	2"	30°C	80% RH

The minimum efficiency for CH_3I^{131} under the proposed criteria would be 96% for used carbon. New carbon was to meet ANSI N509, Table 5-1.

Under these conditions, CH_3I^{131} efficiency for a LOCA was assumed to be 90%, and for a fuel handling accident, 70%.

The change was not immediate. There was time for media sample testing, media evaluation, and program implementation prior to compliance.

II. Test Results

The first step was to initiate a program of what was available, and what results could be expected from new media. See Figure 2.

Figure 2   Some initial test results at proposed conditions.

Bed Velocity	RT	BD	Temp	RH
80 ft/min (24.2 m/min)	1/8 sec	2"	30°C	80% RH

Sample	Penetration	
A	0.04%	(High TEDA Content)
B	1.68%	(KI_3)
C	2.92%	(KI_3)
D	0.40%	(KI and TEDA)
E	0.38%	(KI and TEDA)
F	0.16%	(KI and TEDA)

These results show that the new carbon investigated will meet the tech specs requirements when installed, as well as Table 5-1 of ANSI N509 1980.

The samplers that were already installed in the system would be used to secure media samples for testing. The samplers were connected to the carbon filter frame bulkhead by 3/4" pipes and are pictorially displayed in Figure 3.

Figure 3   Source of carbon samples for media evaluation.
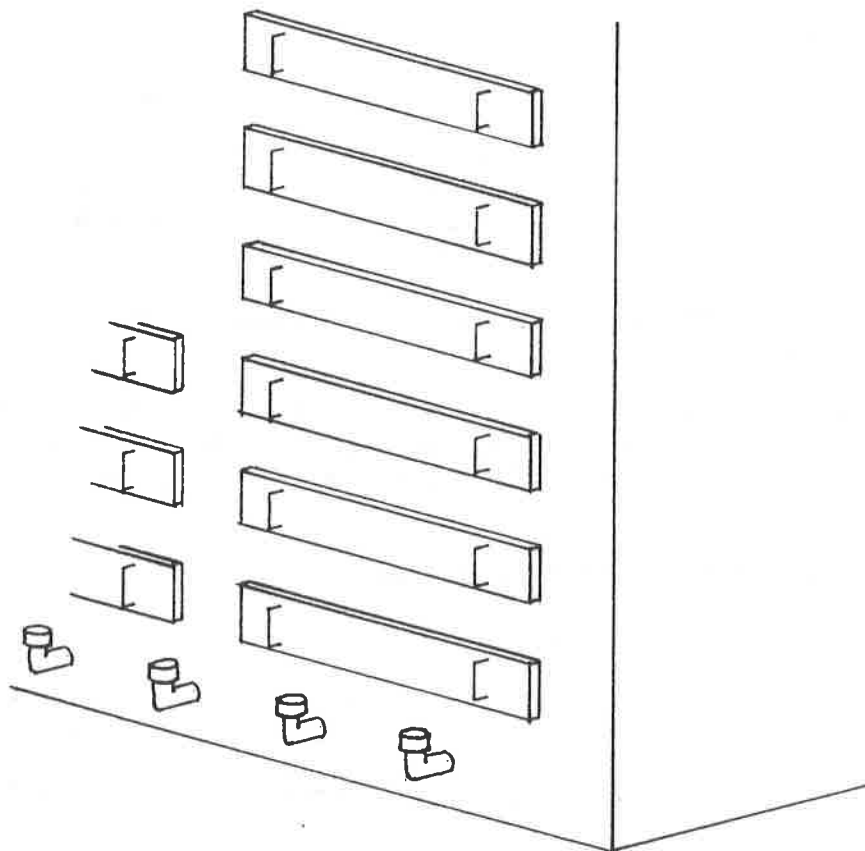
New carbon was installed, and it was decided to treat the new carbon in the filter system as if the tech specs were already invoked ... i.e. a test every 720 hours, under the proposed conditions. The results of this testing caused some consternation.

For example, several tests were conducted after the first 720 hour cycle. Two labs were used. The results for the samples are as follows: See Figure 4.

Figure 4   Test results after 720 hours for Train A.

80 ft/min(1/8 sec)   30°C   80%RH   (720 hrs)

Sample	Penetration	
A	8.12	Lab 1
B	7.96	Lab 1
C	2.30	Lab 1
D	5.25	Lab 2
E	1.21	Lab 2
F	1.45	Lab 2

Samples for the B train were similarly tested. See Figure 5.

Figure 5   Test results after 720 hours for Train B.

80 ft/min (1/8 sec)   30°C 80%RH   (720 hrs)

Sample	Penetration	
A	100%	Lab 2
B	4.14	Lab 2
C	5.88	Lab 2
D	1.47	Lab 2
E	2.24	Lab 3
F	7.86	Lab 3

With these results, there is a question as to whether or not the carbon meets the 96% minimum efficiency criteria.

With the inprecision demonstrated by the sampling method and the test labs, further comparative testing was done on the same carbon samples at both bed velocities, i.e. 40 ft/min and 80 ft/min. Figure 6 shows some typical results for the used carbon.

Figure 6   Test results for used carbon after 720 hours.

Sample	Penetration		
A	1.82	1/8 sec	Lab 1
B	0.34	1/4 sec	Lab 1
C	21.63	1/8 sec	Lab 3
D	4.77	1/4 sec	Lab 3

Note the inconsistency.

As of January, 1984, the test conditions changed to the following: See Figure 7.

Figure 7   Final conditions.

	Bed Velocity	(RT)	BD	Temp	RH
(Existing)	80 ft/min	(1/8 sec)	2"	30°C	80% RH
(Proposed)	80 ft/min	(1/8 sec)	2"	30°C	95% RH

Note that these conditions are much more severe than the 80% RH requirement.

See Figure 8.

Figure 8   Temperature vs. % efficiency as RH changes.
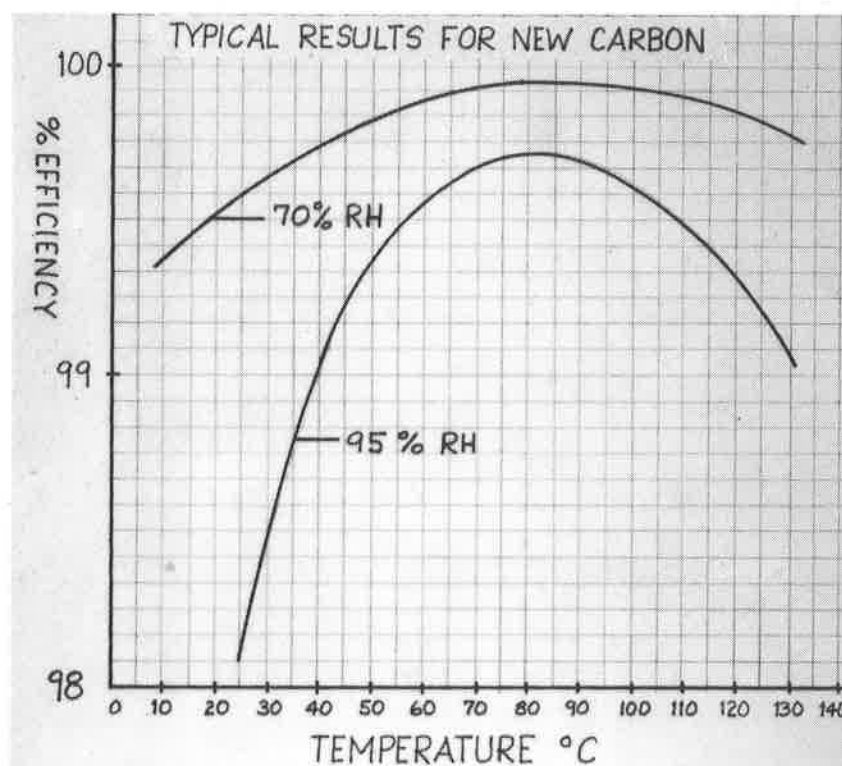
Our experience to date shows that not more than 2 cycles are expected from a batch of carbon.

III. Summary

Figure 9   Summary.

1. NRc mandated certain Tech Spec changes.

2. Labs are not consistent in results.

3. Carbon may be used for perhaps 2 cycles.

4. Management of these Aux Building Exhaust Systems is economically important.

DISCUSSION

KOVACH, J.L.:   Were the results you presented simple tests, or have you submitted blind duplicate samples?

EDWARDS: Duplicate samples were tested. When the test laboratories were aware that these were duplicate samples, results were consistent. When the laboratories did not know of the duplication, results may have been different. However, there was no guarantee that the samples were not subjected to different degradation conditions between the taking of samples and the actual testing. I am not saying however, that the inconsistency is, in fact, the result of faulty laboratory techniques.

BORA - A FACILITY FOR EXPERIMENTAL INVESTIGATION
OF AIR CLEANING DURING ACCIDENT SITUATIONS *

V. Rüdinger, Th. Arnitz, C.I. Ricketts, J.G. Wilhelm

Laboratorium für Aerosolphysik und Filtertechnik
Kernforschungszentrum Karlsruhe GmbH
Postfach 3640, D-7500 Karlsruhe 1
Federal Republic of Germany (F.R.G.)

Abstract

A fluid-dynamic test facility for the experimental study of air-cleaning components and phenomena under simulated nuclear-facility accident conditions has recently been put into operation. With the test facility BORA, test components can be challenged with high differential pressure and flow rate in combination with either high relative humidity and temperature, high relative humidity alone, or high temperature alone.

The test facility was designed to analyze the behavior of air-cleaning system components under extreme test-air conditions at steady and unsteady flows, as well as to help develop and to verify numerical computer codes that can model the response of air-cleaning systems to design-basis and hypothetical accident conditions.

Features of the facility are a recirculating flow of test air, two separate test sections, and a bypass around the test sections for the pretest conditioning of the air stream. Reviewed are the design process, component descriptions, performance characteristics, and first experimental results of the test facility.

I. Introduction

The filter elements within the air-cleaning systems of nuclear power-reactor facilities constitute part of the outermost fission product barrier. Included among the filtration components are activated charcoal filters for the adsorption of radioactive gaseous iodine and High Efficiency Particulate Air (HEPA) filters for the capture of radioactive solid particulates. The performance of these filter elements must be guaranteed not only during normal service but also during accident conditions. Instances of deterioration in performance during normal service have been reported

for HEPA filters /1/. For the more stringent challenges posed during possible accidents, more severe failures can be expected. The risk associated with subsequent discharge of radioactive materials into the environment involves not only those directly released into the containment atmosphere by the accident but those previously captured within the HEPA filters.

In order to be able to prevent contamination of the environment, a thorough understanding of HEPA-filter behavior during possible accident conditions should exist. When justified on the basis of this knowledge, relevant filter-failure mechanisms and their underlying causes can be further investigated, to develop suitable countermeasures.

A number of HEPA-filter test facilities appropriate for such investigations are described in the literature. However, most facilities were designed to challenge filters with only one, and for those exceptions, not more than two, stressing parameter(s). A survey of these facilities will soon be published by OECD /2/. In simulations of fire /3/ and Loss-Of-Coolant Accident (LOCA) conditions, the effects of high temperature /4, 5/ as well as high relative humidity /6, 7/ on filters have been investigated. To determine the effects of explosion generated stresses, filters have been exposed to shock waves /8, 9/. Filter behavior under the influence of high flow velocities and resultant high differential pressures have been extensively studied with a blow-down test facility by Gregory /10/ and Ruedinger /11/. High flow velocities at ambient temperature and relative humidity can be induced by a tornado depressurization which is considered a design-basis accident in the USA.

Combinations of high flow velocities with both high relative humidities and elevated temperatures are possible for LOCAs that also involve a failure in primary containment /11/. Combinations of high flow velocities and high temperatures are conceivable during fire conditions.

Until now no test facility has been available for the realization of these combined challenges to HEPA-filter performance. Consequently, no information exists with regard to the behavior of filter or other air-cleaning-system components under such conditions. In the interest of nuclear safety, this knowledge gap needs to be closed. To make investigations possible which involve these combined challenges together with high flow velocities, the test facility BORA has been constructed and recently put into operation.

II. The design process behind the test facility

The objectives to be fulfilled by the test facility

The development of a conceptual plan was one of the first steps in the realization of the test facility. Bases for this plan were the following two principal objectives.

The improvement of HEPA filter performance. Determination of the modes and characteristics of filter failure can provide relevant information to effectively improve the accident-condition performance of the filter units. The development of a standardized filter-test procedure should ultimately result in the capability to certify HEPA-filter performance under accident conditions.

The development of computer codes for air-cleaning systems under accident conditions. The experimental testing of HEPA filters and other components of air-cleaning systems can provide those empirical data necessary to mathematically model the performance of air-cleaning systems under various accident conditions. With these computer codes, for one example, the actual challenges posed to HEPA-filter units at locations within real systems should be possible to predict. The planned test facility should be able both to aid in the development of and to experimentally verify such computer codes.

The formulation of the performance requirements for the test facility

To realistically define the desired performance requirements for this unconventional facility, a number of philosophical guidelines were followed. Manufacturers' performance specifications for the available individual components were to be considered as nominal and conservatively estimated to be lower than given. The simulations of not only design-basis accidents but also more hypothetical events were to be considered. To determine actual performance limits of components under test situations it was considered necessary to be able to experiment at conditions more extreme than those expected during design-basis accidents. As a net result, it was decided to design the test facility to produce as wide a range of test conditions as economically practical.

On the basis of these considerations, the performance requirements summarized in Table I were roughly formulated. To be able to directly apply all test results to standard-sized HEPA filters, prototypical filters with one-half of the normal cross sectional area, 610 x 305 x 292 mm, were specified for design purposes as the minimum size to be tested, and to perform realistic filter-performance certification tests, required that the test facility also be able to test standard 610 x 610 x 292 mm commercial filters. Foreseen as the maximum differential pressure was a value of 50 kPa. To simulate LOCA conditions, regulation of the relative humidity up to 100 % was a requirement. To model fire conditions, operational temperatures up to 400 ^{o}C were seen as desirable. Finally, test-duration times at steady-flow conditions of at least 1000 s were regarded as necessary to study the effects of exposure time.

Table I: Test-Facility Performance Requirements

Test parameter	Limits
Flow rate with 610x610x292 mm filter	62 kStd m^3/h
Flow rate with 610x305x292 mm filter	39 kStd m^3/h
Differential pressure	50 kPA
Relative humidity	100 $\pm$ 1 %
Temperature	400 $^\circ$C
Test duration time	1000 s

The development of the component schematic for the test facility

During the conceptual planning a number of possible solutions were developed, from which the three illustrated in Fig. 1 were selected for detailed evaluation. The first concept is a once-through or open cycle system, that uses a piston compressor and an air-storage vessel to generate the air stream. This concept employs the same principal of operation as the blowdown test facility of the Los Alamos National Laboratory, (LANL) /12/. Additional components include an air heater to produce the desired temperatures and a steam generator with a steam-air mixer to achieve the desired relative humidities. The principal disadvantage of this concept is the limited time available during the test for the test parameters to stabilize. This is particularly undesirable for tests that involve relative humidity.

In the second concept the piston compressor and the air storage were replaced with a high volume air pump to increase the limited test time. An air cooler with a heat removal capacity of up to 800 kW was added to the air heater, steam generator, and mixer, in order to lower and control the increased air temperatures produced by air compression.

A major drawback common to both open cycle concepts is that a significant total volume of test air must be heated and humidified up to the desired test conditions. This means for example, to produce a relative humidity of 100 % at 90 $^\circ$C for the desired flow rates would require a steam generator with an output of approx. 17 MW. Even with the addition of an intermediate steam-storage volume of 5 Mg capacity, a steam-generator output of 800 kW would still have been needed. And for high temperature tests, an additional supply of 2 MW for the air heater would have been necessary. The equipment costs alone for the steam generator and air heater required by an open cycle facility were thus considered to be excessively high.

1444

A second concern involved accuracy, in particular that associated with the regulation of the relative humidity. Recent studies /13/ have shown that in the range of 90 - 100 % r.h. filter behavior is very sensitive to changes in relative humidity. To be able to examine more closely the causes and resultant effects, it was considered mandatory that the test-air relative humidity and above all the dew-point temperature be regulated to within ±1 %. It was doubted that the necessary regulation accuracy for air-stream mixtures which involved air flow rates up to 70 Mg/h and steam flow rates up to 20 Mg/h would be possible. Thus, two major disadvantages were attributable to concepts with an open cycle.

The third concept considered was a recirculating flow system. This concept had the important advantage that only the system air volume of approx. 50 m^3 would need to be conditioned, i.e., humidified and heated. In addition, a proposal to install a bypass section in parallel to the test section would permit the test-air stream to be preconditioned independently of the test itself. This would be accomplished by a detour of the air stream around the test section until the desired test conditions were attained. As the time available to condition the air stream would not be restricted to less than actual test-duration times, the sizes and power requirements of the air humidifier and heater could be significantly smaller. A reasonable maximum time to condition the test-air stream was considered to be 30 min.

Calculations showed that increases in test-air temperature due to compression were sufficient to attain the desired temperatures within the entire chosen range of test-facility operation. With the concept of recirculating flow it was then possible to eliminate the air heater. Additionally, with a scheme to humidify the test air by a spray of water droplets into the hot air at the discharge of the air pump, the steam generator could also be eliminated. Finally, the technical difficulties in the regulation of test parameters could become greatly minimized due to the longer time available to condition the test air.

The realization of these simplifications permited by a recirculating flow were only possible through the use of a high-volume air pump which could sustain operation at 400 ^{o}C. Roots blowers and rotary screw compressors could produce the required differential pressures but not at the required high operating temperatures. Multistage radial compressors were dropped from consideration due to insufficient flow rates and individual single-stage axial and radial blowers were not considered due to insufficient differential pressures. The only practical alternatives were either a high temperature multistage axial compressor with a rotational speed of 11k rpm or a combination of two radial blowers with rotational speeds of 3k rpm. Both of these two types of machines could have been outfitted for a maximum discharge-air temperature of 350 ^{o}C.

For high temperature operation, an air cooler was added at the inlet of the air pump to permit discharge temperatures up to the maximum of 350 $^{\circ}$C to be attained. For low temperaure operation, an air cooler was added at the discharge of the air pump due to the available cooling water minimum temperature of 18 $^{\circ}$C.

Two identical variable-speed radial blowers which could be operated individually, in series, or in parallel were selected after thorough consideration of the alternatives. Not only is this option the more economical in equipment costs but also the more efficient in partial load operation due to the variable speed and the three modes of blower operation.

From the concept of the recirculating flow system a detailed, schematic diagram was developed, illustrated in Fig. 2. The radial blowers are shown as the heart of the facility, followed by the air-humidifier apparatus, and the low temperature air cooler. At the exit of the low temperature cooler the air stream can take any one of three paths: bypass, structural test section, or model test section. During the conditioning phase the flow is directed through the bypass. Located in the bypass is the control valve, K2, which can simulate the flow resistance of test components for any selected flow rate during the conditioning process. A small radial fan connected to the bypass was added to purge moisture from the test facility after tests.

Installed in the structural test section is the test filter or other test component. A high speed camera records the dynamic structural response of the component under test. The control valve K1 in an open or shut position, respectively, permits or prohibits air flow through the structural test section. In the return duct upstream of the high temperature cooler is a HEPA-filter bank.

Between the filter bank and the inlet to the blowers, the air stream is connected to the ambient atmosphere through an acoustically muffled vent. With the absolute pressure at the inlet of the blowers restricted to 100 kPa, the maximum absolute static pressure at the test filter is limited to approx. 150 kPa. On the basis of the test-facility schematic diagram, the components of the test facility were sized, selected, and assembled.

III. Performance characteristics and components of the test facility BORA

Blower system

The blowers produce the flow and static pressure of the air stream and thus serve as the heart of the facility. The basis for the blower-performance requirements were the flow-resistance curves of three particular test-filter elements as shown in Fig. 3.

The lowest curve is typical for the clean commercial filters /11/ to be certified by performance qualification tests under simulated accident conditions. The middle curve represents the clean prototypical filters to be used for filter-development tests and also approximates typical curves for the loaded commercial filters. The highest curve is that of a deep-bed stainless steel filter /14/ characterized by high resistance and structural strength. The respective maximum differential pressure of 35, 60, and 70 kPa with which the individual filter types are to be tested, determine for design purposes a maximum point of operation on each resistance curve. An arc fitted to these points approx. the performance curve of the required blower and together with the two outer test-filter flow resistance curves bounds the region of desired flow and differential-pressure test conditions. Blowers with backward-curved blades were selected for characteristics of high flow rate and differential pressure, stable operation at low flow rates, and a degressive power curve. The blowers were specially designed for this application and are distinguished by a 1.4 m wheel diameter, a 2980 rpm rated speed, and a 420 kW variable speed DC motor. Fig. 4 shows the installed blower units together with some of the connecting ductwork and one of three pneumatic valves used to select the mode of blower operation.

In Fig. 5 are illustrated the performance curves for the blowers in individual, series, and parallel modes of operation. It can be seen for a dry air density of 1.13 kg/m^3 at 40 $^\circ$C that the blower-performance data fulfill the performance requirements for filter tests from Fig. 3. At lower test-air densities due to higher temperature or water-vapor content, the blower performance will be correspondingly less. As a result of the three modes, the variable speeds, and the 3100 rpm actual maximum speed of blower operation, the desired test conditions of flow rate and pressure can be easily preset for the test component within the given operating region of Fig. 3.

Air humidifier

In order to minimize equipment and operating costs, a fine spray of water at the blower discharge duct rather than a 50 kW steam generator was foreseen to humidify the test air. The water droplets would be vaporized in route to the air cooler by the heat added in compression of the air. The 0.2 s travel time from humidifier to cooler limited the droplet diameter to 20 μm, to assure total evaporation. To generate the desired high relative humidities the amount of air injected into the system with the water droplets was also limited. However, single-phase spray nozzles for fine droplets have the disadvantages of high operating pressures and unstable regulation. Special two-phase air-water spray nozzles with built-in mixing chambers were found to meet the requirements for small droplet diameters, minimal air injection, low operating pressures, and ease in regulation.

The air-humidifier apparatus with two different sizes of these particular spray nozzles is shown schematically in Fig. 6. The three large nozzles with a total constant water flow rate of 9o l/h raise the test-air humidity close to the preset value within 10 min, when the single regulated small nozzle with a variable flow rate of 0-5 l/h takes over to maintain the preset value of relative humidity. These nozzles produce 15 μm droplet diameters, at a 1/5 mass-flow ratio of air/water, with a 600 kPa air-supply pressure, and feature constant droplet diameters with variable water flow-rates adjusted by regulation of the air flow.

Heat exchangers

The task of the high and low temperature air coolers or heat exchangers is to regulate the temperature of the test air-stream by removal of the heat added to the air during compression by the blowers. The challenges faced by the heat exchanger in accomplishing this task were formidable not only in the range of heat removal rates, 100 - 800 kJ/s, but also in the range of temperatures to be regulated, 40 - 350 ^{o}C. When the temperature differentials between air stream and cooling water are considered, heat fluxes of 0.3 - 40 kJ/s-^{o}C suggest the magnitude of the required heat transfer areas. A supplementary factor was the requirement that the low temperature cooler also serve as a dew-point cooler. Foreseen to fulfill these requirements were then a low and a high temperature cooler with respective temperature-regulation ranges of 40 - 200 ^{o}C and 200 - 350 ^{o}C.

The high temperature cooler was installed at the inlet to the blowers to permit blower-discharge air-stream temperatures up to the blowers' maximum rated operating temperature of 350 ^{o}C. The finned tube heat exchanger of galvanized steel is characterized by a flexibility in operation based on three factors. Heat exchange is accomplished in two stages which can be operated either individually or together; the temperature of the inlet cooling water can be regulated by a control valve which meters and mixes fresh cooling water with the partially recirculating flow of water through the unit and the flow rate of cooling water through this heat exchanger can also be regulated by a variable speed pump.

The low temperature cooler is also fabricated from finned tubes of galvanized steel but with six stages of heat exchange. The first four stages are operated in a counter-cross-flow mode to remove practically all the heat while the last two stages are operated in a parallel-cross-flow mode and function as a dew-point cooler. Flexibility in operation is here also accomplished by both the regulation of the temperature and flow rate of the partially recirculating cooling water and the selectable combinations of stages in use. The low temperature cooler is so designed

that at full-load operation of approx. 700 kW and for cooling wa-
ter at 18 $^{\circ}$C, air stream conditions of 40 $^{\circ}$C and 100 % r.h. can
be achieved. Air stream temperatures of less than 30 $^{\circ}$C are
possible for other operating conditions at lower pressures and
relative humidities.

For test-air relative humidities close to and including
100 %, fiber-mesh droplet eliminators are located after the fourth
and the sixth stages to remove any water droplets which remain
from incomplete evaporation after humidication or condense within
the heat exchanger itself. Schematically illustrated in Fig. 7
are the two heat exchangers and relevant control systems.

The duct system and the structural test section

The various individual components of the test facility are
interconnected by a system of stainless steel ductwork that is
dimensioned to minimize friction losses and noise, i.e., the air-
stream velocity at maximum flow in all ducts is less than 40 m/s.
Accordingly, the internal diameters of the low pressure section,
the high pressure section, the bypass, and the model test section
are, respectively, 800, 750, 600, and 300 mm.

Due to the wide range of operating temperatures, compensation
for thermal expansion along the length of the duct system is
provided for with stainless steel bellow-type temperature-
expansion joints installed as part of the ductwork in seven loca-
tions in the facility. Each joint has a support stand which
permits longitudinal movements of up to 9 cm. Also installed in
the ductwork at the two blower inlets and discharges were flexible
vibration-isolation couplings to minimize transfer of mechanical
vibration from the blowers.

Installed around the outside of the high pressure section
ductwork, downstream of the low temperature cooler to include the
bypass and the structural test section, is a regulated electrical
resistance heating system to prevent condensation onto the inner
walls during tests with high humidity.

The outside surface of the test facility is wrapped with a
layer of thermal insulation 18 cm thick, primarily to minimize
unregulated heat transfer out of the system but also to reduce
the ambient noise level.

Particular attention was given to the design of the struc-
tural test section. A long straight duct as well as flow
straighteners were planned for the section upstream of the test
component to provide a uniform and symmetrical air-stream velocity
profile at the upstream face of the test component. Directly down-
stream of the test component, the duct expands into a settling
chamber of 3 m^3 volume to capture larger debris released from the
test component during tests. A wire-mesh screen was mounted at

the chamber exit to protect K1 and downstream instrumentation probes from smaller pieces of debris. Shown in Fig. 8 is an outside view of the end of the settling chamber directly opposite the downstream side of the test component. This end wall is outfitted with six 150 mm diameter glass windows for photo lighting and also photo and video observation of the downstream side of the test component as well as with a hinged man-way cover for removal of debris.

Shock-wave experiments in a scaled model of the ductwork of the low pressure section. During the construction of the test facility a question arose as to what effects the catastrophic failure of a stainless-steel fiber filter under test at a 70 kPa differential pressure would produce on the system components located downstream of the structural test section. Of concern were the possible formation of a shock wave and the subsequent exposure of the ductwork in particular the HEPA-filter bank to shock-wave overpressures. No theoretical or experimental studies which dealt with shock-wave generation by rupture of a porous element in a flow stream or with shock-wave attenuation by the particular physical geometries of interest were found in the literature.

As a result, a model of the test-facility ductwork between structural test section and filter bank, selected 1:1 in length and 1:64 in cross sectional area was built to experimentally investigate shock waves generated by rupture of a porous diaphragm in a flow stream and more importantly, the shock-wave attenuation characteristics of the ductwork geometery. The model shown schematically in Fig. 9 was instrumented with two piezorestive pressure transducers which had a measuring range of $\pm$ 100 kPa, natural frequencies of 150 kHz, and signal amplifiers of 100 kHz brandwith connected to an A/D transient signal recorder that had a sampling rate of 20 kHz.

Illustrated in Fig. 10 are typical test results for a differential pressure of 70 kPa across the diaphragm at rupture. The two principal shock-waves of interest are the initial wave formed by diaphragm rupture and the secondary wave formed by reflection of the initial wave off of the end wall of the test-section settling chamber. The maximum shock-wave amplitude as measured by differential pressure for this worst case situation is seen to be 25 kPa for the ductwork and 5 kPa for the filter bank, well below the design values or allowable differential pressures of 40 and 20 kPa, respectively.

Air stream control valves K1 and K2 and their function during test operations

Several valves in the facility are utilized to direct the air stream and to control some of the test parameters during the different modes of test operation, e.g., during pretest steady

flow through the bypass as well as during tests with steady and unsteady flow through the structural test section. In this, re- gard the pneumatically actuated butterfly-type valves, K1 and K2, function not only as passive individual components to route stea- dy flows but also as a pair of active components to generate the unsteady flows and differential pressures at the test component. Also shown in Fig. 8 is the valve K1 with drive mechanism.

For pretest conditioning of the air stream, valve K1 is com- pletely closed to direct steady recirculating flow via the bypass only. This allows the blower system and then K2, as a partially- open differential-pressure control valve, to be adjusted to set the flow rate and the differential pressure, respectively, to which the test component will be exposed during the subsequent test. To condition the interior walls and the otherwise stagnant test air of the structural test section during the conditioning process, a negligible flow of test air is bled through valve K9.

At the end of a pretest conditioning process, steady flow through the test section can be accomplished after the complete opening of valve K1 followed independently by the complete closure of valve K2. The flow rate can then be set to any desired steady value by the adjustment of blower speed.

To produce an unsteady flow through the structural test sec- tion at the end of a preconditioning process, valves K1 and K2 are actuated as a combination, from fully closed to fully open for the former and from partially open to fully closed for the latter. During the resultant diversion of test-air flow from by- pass to test section, the unsteady differential pressure and flow are generated at the test component.

In this role valves K1 and K2 function as active system com- ponents and the flow-resistance characteristics, timing coordi- nation, and actuating speeds of the valves become parameters which govern the characteristics of the leading edge or "ramp" of the differential pressure pulse. It is desirable to be able to adjust the shape and slope of the ramp as well as to maintain a constant static pressure upstream of the test component during the unsteady flows. To this end the numerical computer code, TVENT, /16/ of LANL was modified /17/ and employed to predict test-facility fluid dynamics during unsteady flow conditions as functions of the valve parameters.

A typical set of predictions as calculated with the modified TVENT code is shown in Fig. 11 for the static pressures at vari- ous locations in the test facility BORA during unsteady-flow con- ditions. Fig. 12 illustrates with a family of "S" shaped curves the differential pressure across a test filter as a function of the opening time of valve K1. For the minimum practical opening time of 3 s a slope of approx. 40 kPa/s is predicted.

Miscellaneous components

In addition to the components discussed above, the filter bank, the acoustically muffled vent and the purge fan of the test facility should be briefly mentioned. Mounted in parallel within the filter bank housing located just upstream of the blowers, are 10 individual 610x610x292 mm nuclear-grade HEPA filters which continuously clean the recirculating test-air stream. Connected to the ductwork between the filter bank and the inlet to the blowers is a 250 mm diameter vent, which maintains the static pressure at the blowers' inlet equal to that of the ambient atmosphere via a straight-through acoustical muffler that helps to minimize ambient noise levels. After tests with high relative humidities, the test facility is purged of moisture with a 1k m^3/h flow of ambient air from a fan which discharges into the bypass duct. The list of facility components is completed with node of the test section for fluid-dynamic and model experiments. This second test section consists of a 300 mm diameter x 4 m long straight duct within which small-scale test components can be mounted.

Instrumentation and control systems

The test facility has two independent systems of measurement instrumentation. One is a part of the automatic control system and the other is a part of the data-acquisition system.

During steady-flow conditions, the automatic control system regulates the air stream parameters of pressure, flow, temperature and relative humidity through regulation or control of such operating parameters as blower speed, cooling water temperature and flow rate and water injection rate. Associated with the automatic control system are probes, transducers displays, and recorders with response times which range from seconds to minutes.

During unsteady-flow conditions, a data acquisition system can measure and record the fluid-dynamic and some thermodynamic air-stream properties, as well as the visible structural dynamic behavior of the test component. This measurement and recording system shown schematically in Fig. 13 as outfitted for filter structural tests is instrumented with probes, transducers and recorders characterized by response times in milliseconds.

This system consists of a number of noteworthy components. Instrumentation probes and sensors include pitot and special T-shaped tubes mounted to variable capacitance and pizeoresistive transducers for pressure measurements, aspirated fine-wire Type-K thermocouples with signal amplifiers to measure temperatures, and the infrared light-beam source and detector together with a signal processor which comprises an instrument for measurement of absolute humidity. The output signals of these transducers are fed into an 8-channel A/D data recorder to register the pressures, temperatures and relative humidity.

A video system, which consists of a camera, monitor and recorder, in addition to a high-speed movie system with a camera, test-data display and image-splicer optics monitor, registers the visible structural-dynamic behavior of the downstream side of the test filter. The optics of the image splicer permit digitally displayed values of test-filter differential pressure and test time to be recorded on each film frame together with the test filter image.

The same control apparatus which controls unsteady flow tests by coordinated actuation of K1 and K2 also simultaneously controls the start, coordination and stop operations of the A/D data recorder, video recorder, and high speed camera of the data aquisition system.

Test facility layout and surrounding physical plant

The test facility is located within the containmment structure of a recently decomissioned research reactor. This choice of location saved the cost of a new-building construction and involved only minor adaptation of the ductwork to conform to required modifications in the existing building structure. These modifications consisted primarily of utility connections and the creation of openings in walls or ceilings.

The components of the test facility are located on three floor levels. The control room and blower system are installed on the first level and the inlet and discharge ducts pass vertically through a ceiling hatch up to the second level where the structural test section, bypass and other major components are located. Inlet and outlet duct continue up to the model test section on the third level. Shown in Fig. 14 is a top view of the facility as layed out on the second level and the manner in which the ductwork conforms to the existing walls, only three of which were cut through during renovation.

Other modification to the surrounding physical plant included the installation of 4 room-air coolers as well as acoustic isolation material and devices to maintain respective acceptable ambient temperatures and sound levels.

After 4 months of building renovation and 4 months of facility erection, the blowers were operated as part of the facility in Jan. 1984.

Performance capabilities and utility requirements of the test facility BORA

The net result of the design, construction and initial performance tests of BORA has been the realization of a test facility with the performance characteristics and utility requirements as shown in Table II. The range of pressure and flow conditions which can be generated at the test filter for 40 $^\circ$C are shown in Fig. 5.

1453

Table II: Performance characteristics and utility requirements
             of the test facility BORA

Performance capabilities	
Test-temperature range:	40 to 350 ^{o}C
max. differential pressure at 40 ^{o}C:	90 kPa
max. differential pressure at 350 ^{o}C:	40 kPa
max. volumetric flow rate at 40 ^{o}C:	110 kStd. m^3/h
max. volumetric flow rate at 350 ^{o}C:	55 kStd. m^3/h
max. test time:	unlimited
max. static pressure ramp (Δ p = 35 kPa):	40 kPa/s
max. temp. for 100 % r.h. at 100 kPa abs. press.:	92 ^{o}C
max. temp. for 100 % r.h. at 170 kPa abs. press.:	105 ^{o}C
Utility requirements	
max. electrical load:	840 kW
max. cooling-water flow rate:	50 m^3/h

IV. First test results

By early April 1984, construction had progressed to the point
where shakedown tests of the test facility as a whole could begin.
At this time the individual performance of the blowers, the air
coolers, the control valves K1 and K2 together with the measure-
ment-instrumentation and test control systems were of particular
interest. With components found to be in good and as-designed op-
erating condition, preliminary HEPA-filter flow-resistance and
structural tests, as well as tests relevant to computer-code
verification, were performed.

HEPA-filter flow-resistance tests

The test data needed to generate filter flow-resistance
curves were taken from four 610x610x292 mm clean HEPA filters with
plywood cases. Three of the filters, RT2 – RT4, were commercial
units with glass-fiber media and the fourth, RT1, was a proto-

typical unit with a polycarbonate-fiber medium. After conditioning to 40 $^\circ$C, the air stream was switched from the bypass to the structural test section and the pressure and temperature data were recorded from digital displays in the control room at a number of steady flows set by blower speed.

The resultant flow-resistance curves are plotted in Fig. 15 and show good similarities with curves obtained for similar filters with the LANL blowdown facility /11/.

HEPA-filter structural tests

Directly after each flow-resistance test, a trial was made to expose individually three of the four filters to a 30 kPa differential pressure pulse as a structural filter test. The first step in the test procedure was to determine the flow rate to be expected for a given filter at 30 kPa by graphical extrapolation of the flow-resistance curves of Fig. 15. With valve K1 closed, the flow rate through the bypass was set to the extrapolated value by adjustment of blower speed and then valve K2 was adjusted to obtain a static pressure of 30 kPa at the test filter. Valve K1 was set for the 3 s minimum opening time and valve K2, for what would have been a closing time of 7.5 s, if the valve had been fully open. The test was peformed by actuation of valves K1 and K2 as described under the heading "Air-stream control valves...". The data-aquisition and associated control system were used during these three structural tests.

Test films showed that one filter, RT1, remained undamaged up to a differential pressure of 30 kPa, one, RT3, failed at 26 kPa, and one filter, RT2, which had been damaged prior to the structural test, failed catastrophically at 15 kPa. Structural limits in each case were comparable to results obtained for similar filters with the LANL test facility /11/.

Static-pressure time histories from two of these structural tests are shown in Fig. 16 for RT1 and, in Fig. 17 for RT2. The increase in static differential pressure across the test filter, as the air stream is diverted from the bypass to the structural test section, is shown for both tests, as are slight variations in the static pressure upstream of the filter.

For test RT2, Figs. 17 and 18 illustrate fluctuations in pressures and flows due to catastrophic failure of the test filter, as well as those due to subsequent blockage of the test-section exit screen by filter debris, followed directly by closure of valve K2. The filter rupture caused a sudden decrease in static pressure upstream of the test filter, a sudden increase in total flow rate and an abrupt flattening in the previously increasing filter flow rate, followed by a sharp increase in filter flow rate, coincident with a sharp decrease in the filter differential pressure to zero. The effects of the flow blockage is most

evident by a sharp decrease in flow rate through the test section while the effects of the closure of valve K2 are most evident by a decrease in total flow rate to almost zero and a final increase in static pressure upstream of the test filter.

These results show that the control valves K1 and K2 can be actuated to produce desired unsteady differential pressures and flow rates at the test filter and also indirectly suggest the importance of the operating parameters of the valves in the generation of the unsteady test conditions.

Computer-code verification tests

To use the test facility for verification of computer codes requires two catagories of experimental data. These include data taken to determine individual component operating characteristics for input into the computer code, as well as data taken during unsteady flow tests for comparison to prediction of the computer code.

Accordingly flow-resistance measurements were made for all passive components in the facility as well as for the active components, e.g., control valves K1 and K2, both of which were additionally measured for: valve position during actuation as a function of time and the air pressure of the pneumatic drive.

Transient test situations were generated by diverting the air stream from the bypass to structural test sections. Four tests were performed with the same initial 23 kPa static pressure at the blower discharge for different combinations of valve actuation times, found in Table III. To demonstrate the influence of the parameters during transient tests, Figs. 19 and 20 shows the time histories of the static pressures at the blower discharge and the slope and shape of the differential pressure ramps across the installed filter in the test section. Interesting is, that the opening speed of the valve K1 influences the slope of the ramp, while the closing speed of valve K2 influences the shape of the ramp.

Table III: Control-valve actuation times

Test (No.)	Valve K1 opening time (s)	Valve K2 closing time (s)
VT1	3	5
VT2	5	8.3
VT3	3	10
VT4	5	15.7

It should be noted that the closing time given for valve K2 is the time to close from a fully-open inital position and not the actual initial position of approx. 33 % of fully open as used for these tests. A comparison of the experiments with calculated results is given in Ref. 17.

V. Conclusions

The realization of the test facility BORA increases the ranges and combinations of the parameters with which HEPA filters and other components of air-cleaning systems can be challanged during experimental tests which simulate accident conditions which could occur within nuclear facilities. The performance capabilities of the facility at steady and unsteady flows fulfill what had been a gap in test conditions of preceding facilities, particularly with respect to high differential pressure and/or flow rate in combination with either high relative humidity alone, high temperature alone, or both high relative humidity and high temperature together. The recirculating flow, the bypass, and the two active-element control valves make the facility also useful for experimental verification of computer codes which model the fluid dynamics and thermodynamics of air-cleaning systems during operation at off-design conditions.

Inital tests of the facility have shown that the design selected to fulfill the performance requirements is viable and successful for dry air at 40 ^{o}C. Performance verification tests are presently in progress for other operating conditions.

Plans for short-, mid-, and long-term future use of the test facility have been laid. The structural limits and failure mechanisms of HEPA filters under combined challenges of high flow rate, relative humidity, and temperature will be investigated. A standard filter-qualification test will be developed in order to be able to certify HEPA-filter performance under accident conditions. To complete the short term plans, further verification experiments for the LANL computer codes TVENT and EVENT are foreseen. Mid-term plans include tests of other air-cleaning system components with combined challenges as well as experiments to verify, yet-to-be-developed, computer codes which account for the presence of high relative humidity. Anticipated for the long term plans are filtration-efficiency tests of HEPA filters under individual and combined, simulated accident conditions of high flow rate, relative humidity, and temperature. For these tests modifications of the test facility are necessary.

It is also anticipated that test time on the facility could be made available for the experimental studies of other interested scientific organizations.

Acknowledgement

The authors wish to express their appreciation to Mr. Steiger, Mr. Wittek and their coworkers from KfK/KTB for their valuable help and support with the construction of the test facility BORA.

References

/1/ Ohlmeyer, M.; "Vor-Ort-Prüfung von Schwebstoffiltern und Entnahme von Sorptionsmaterialproben bei Iod-Sorptionsfiltern," Atomkernenergie-Kerntechnik 40 (1982) p. 259.

/2/ OECD-Report; "Air Cleaning in Accident Situations," to be published 1984.

/3/ Los Alamos National Laboratory; "Proceedings of the CSNI Specialist Meeting on Interaction of Fire and Explosion with Ventialation Systems in Nuclear Facilities," LA - 9911-L (1983).

/4/ First, M.W.; "High Temperature Dust Filtration," Ind. Eng. Chem. 48 (1956) p. 696.

/5/ Hackney, S.; "Fire Testing of HEPA-Filters Installed in Filter Housings," Conf - 820 833 (1983) p. 1030.

/6/ Peters, A.H.; "Application of Moisture Separators and Particulate Filters in Reactor Containment," USAEC DP-812, Savannah River Laboratory (1982).

/7/ Gunn, C.A.; Eaton, D.M.; "HEPA Filter Performance Comparative Study," CONF - 760 822 (1977) p. 630.

/8/ Anderson, W.L.; Anderson, L.; "Effects of Shock Overpressures on High Efficiency Filter Units," CONF - 660 904 (1966) p. 79.

/9/ Gregory, W.S. et al.; "Response of HEPA Filters to Simulate Accident Conditions," CONF - 820 833 (1983) p. 1051.

/10/ Horak, H.L. et al.; "Structural Performance of HEPA Filters Under Simulated Tornado Conditions," LA - 9197-MS NUREG/CR-2565 (1982).

/11/ Ruedinger, V., Wilhelm, J.G.; "Zum Verhalten von Schwebstoffiltern unter hoher Differenzdruckbelastung," 9. Jahreskolloquium des Projektes Nukleare Sicherheit, KfK-Bericht 3470 (1982).

/12/ Gregory, W.S. et al.; "Pressure Transients Across
HEPA Filters,"
Proc. Seminar on High Efficiency Aerosol Filtration
in the Nuclear Industry; Conf. of the European
Communities, Luxemburg (1977) pp. 78.

/13/ Ruedinger, V.; Ricketts, C.J.; Wilhelm, J.G.;
"Limits of HEPA Filter Application Under High Humidity Con-
ditions,"
Proc. 18th DOE Nuclear Airborne Waste Management
and Air Cleaning Conference (1984) to be published.

/14/ Dillmann, H.G.; Pasler, H.; "Experimental Investigations
of Aerosol Filtration with Deep Bed Fiber Filters,"
CONF - 820 833 (1983) p. 1160.

/15/ Reason, J.; "Special Report Fans,"
POWER (Sept. 1983) pp. 53

/16/ Duerre, K.H.; Andrea, R.W.; Gregory, W.S.;
"TVENT - A Computer Porgram for Analysis of
Tornado-Induced Transients in Ventilation Systems,"
LA - 7397-M (1978)

/17/ Hartig, S.H. et al.; "Comparison and Verification
of Two Computer Programs Used to Analyse Ventialtion
Systems Under Accident Conditions,"
Proc. 18th DOE Nuclear Waste Management and Air Cleaning
Conference (1984), to be published.
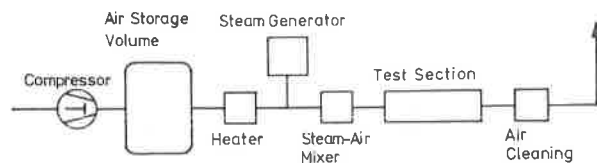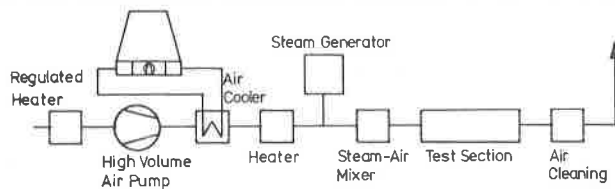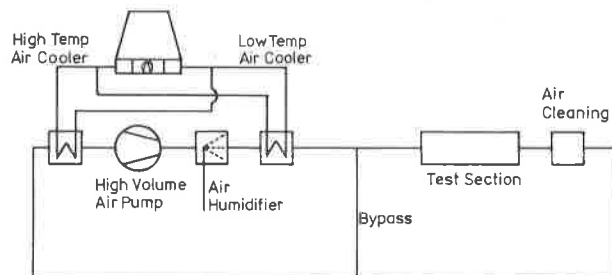
Fig. 1: Fundamental concept for a test facility to study HEPA filters and air-cleaning system components under combined accident-condition challenges
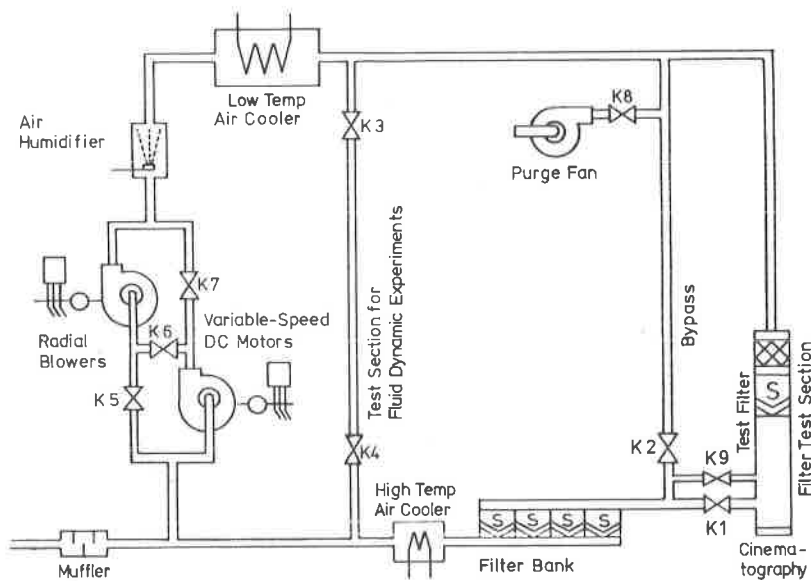
Fig. 2: Schematic of the test facility BORA designed to study HEPA filters and air cleaning system components under combined accident-condition challenges
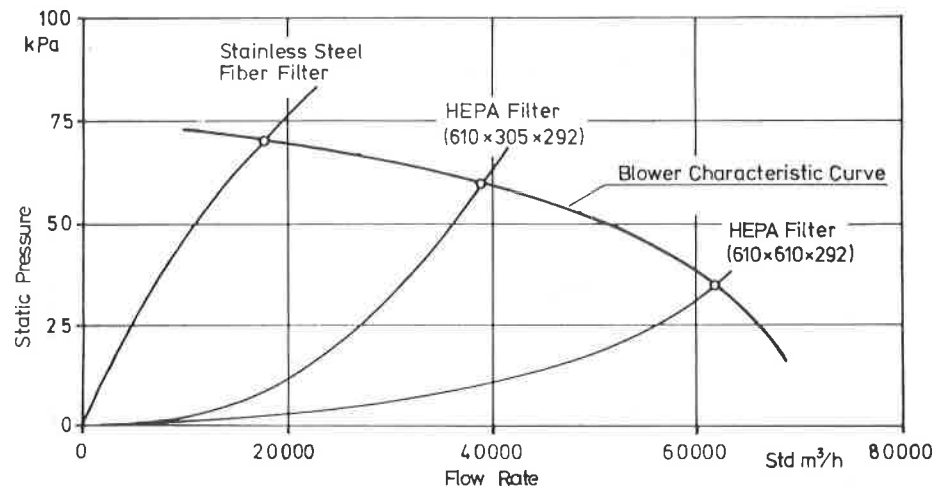
Fig. 3: Performance requirements for the test facility BORA
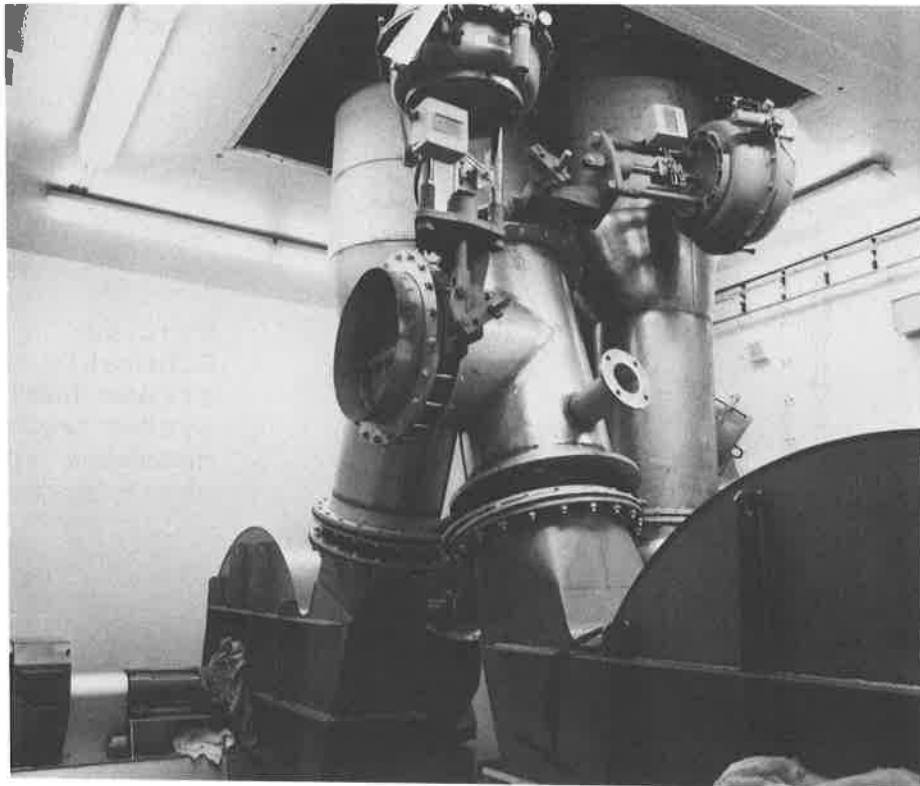
Fig. 4: Photograph of installed blowers and connecting ductwork
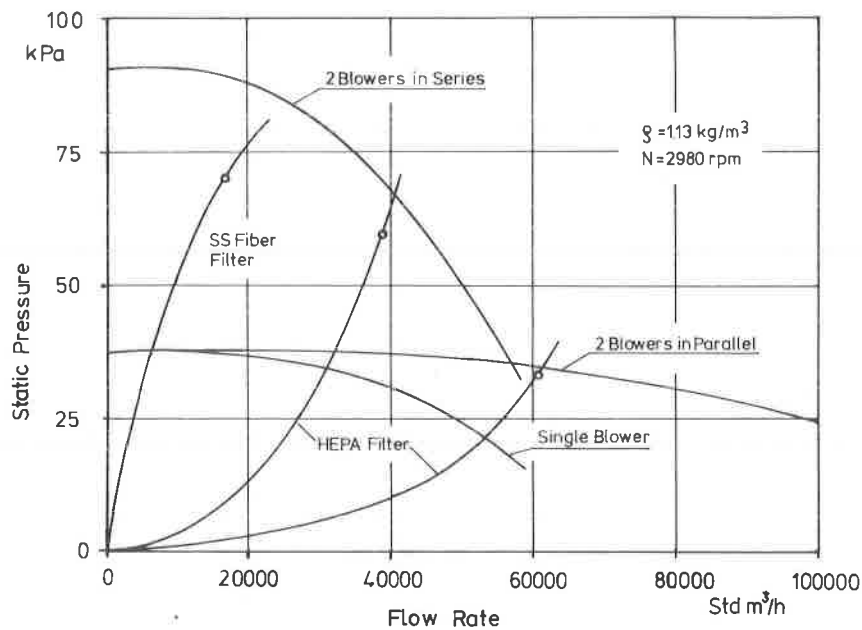
Fig. 5: Blower system performance characteristics at air density of 1.13 kg/m³ and blower speed of 2980 rpm
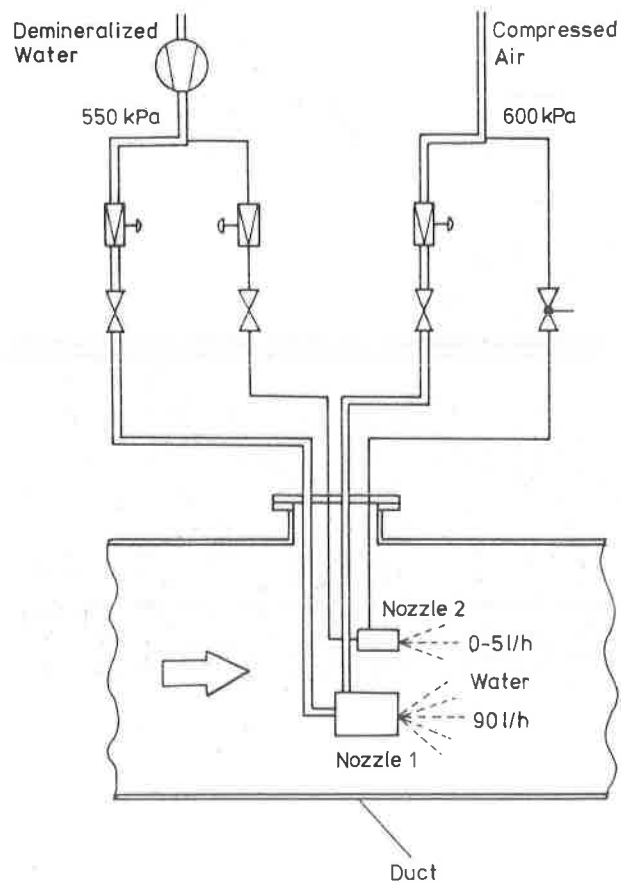
Fig. 6:
Schematic of the air-stream humidifier system with mixing chambers and two-phase spray nozzles
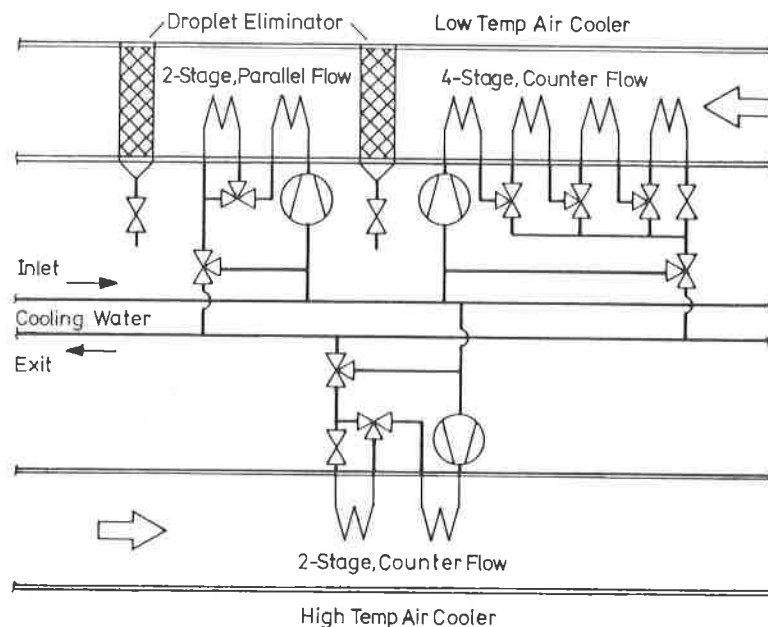
Fig. 7:   The high and low temperature air stream cooling systems
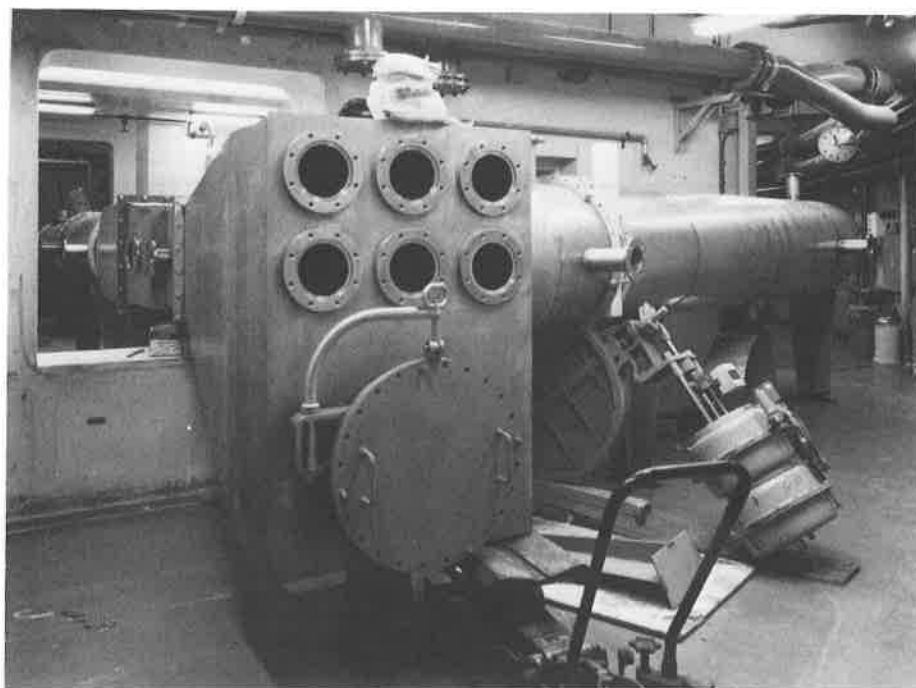
Fig. 8:   Photograph of the end wall of the structural test
section (left) and of the control valve K1 (right)
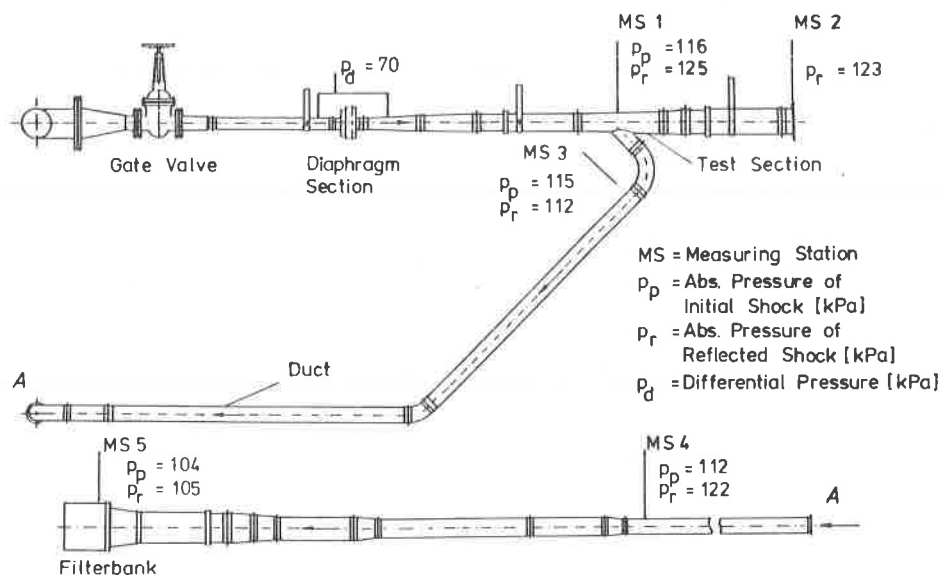
Fig. 9:   Schematic of the model of the test-
          section to filter-bank ductwork from
          BORA used for shock-wave tests
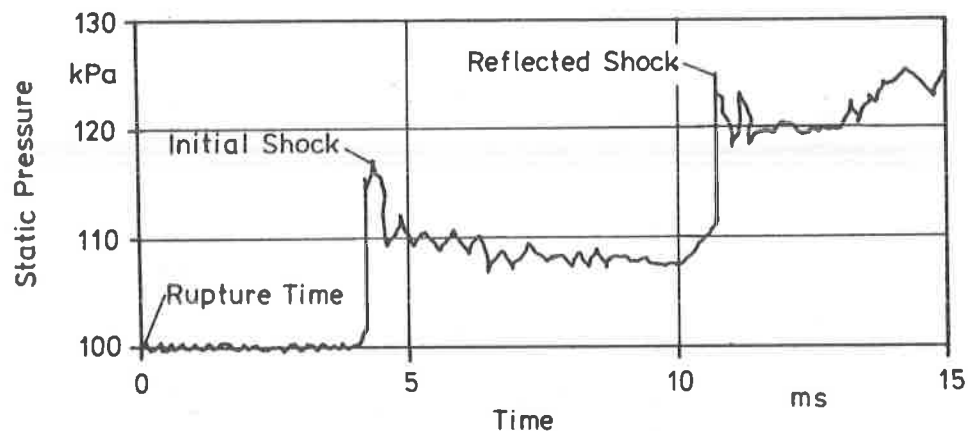
Fig. 10: Initial and reflected shock-waves
          at measuring station 1
          (test apparatus of Fig. 9)

1464
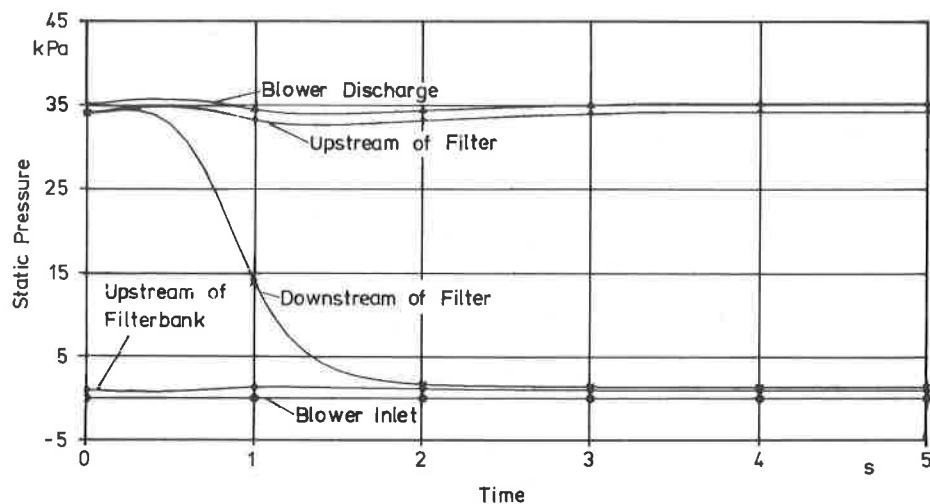
Fig. 11:   Static pressure at various locations of the
           facility BORA calculated with TVENT
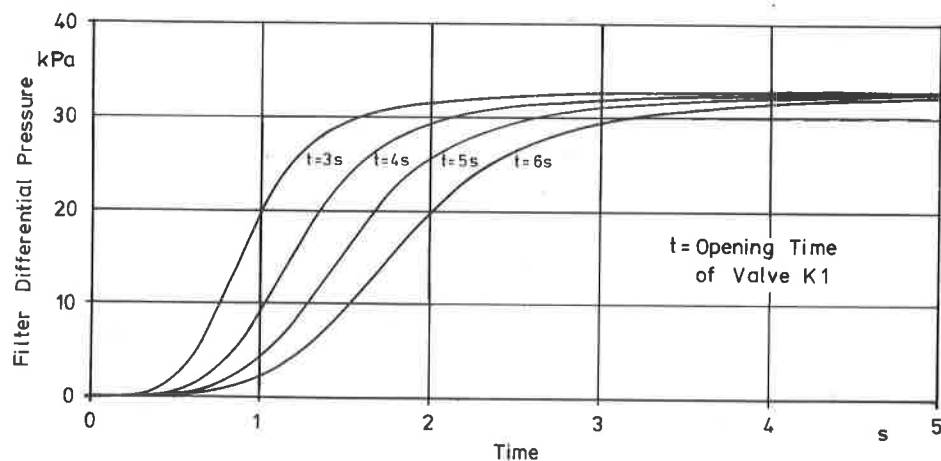
Fig. 12:   TVENT-calculated profiles of the differential
           pressure across the test filter in BORA with
           different valve actuating times

1465
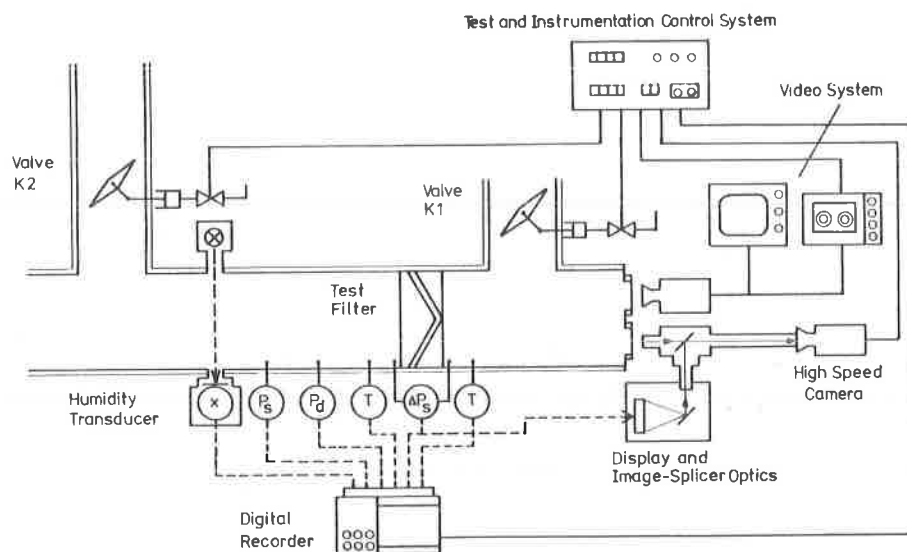
Fig. 13: Schematic of the data-aquisition and control systems for HEPA filter structural tests in BORA
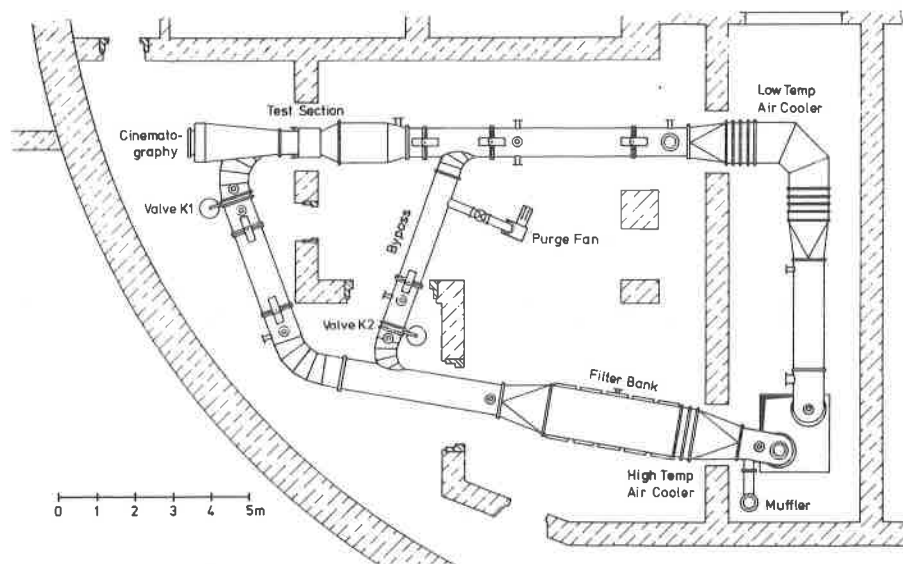
Fig. 14: Plan view of the layout of the facility BORA (second level)
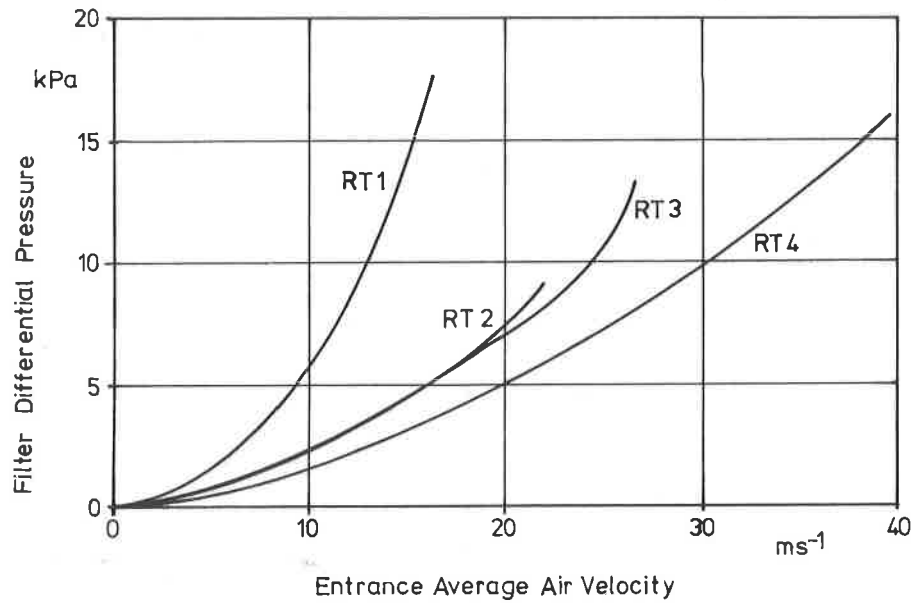
Fig. 15: Flow-resistance curves for four
          HEPA filters tested in BORA
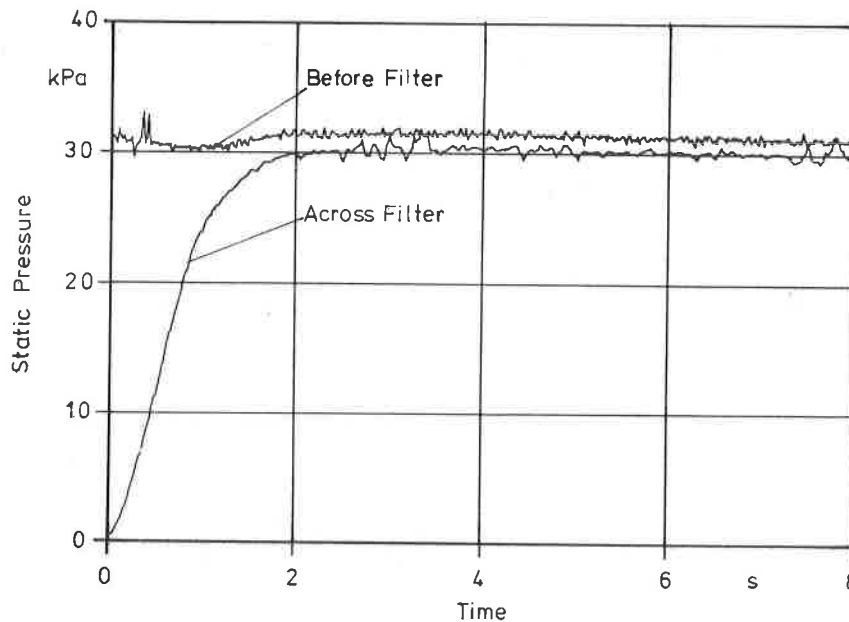
Fig. 16: Time history of the static pressure,
          upstream and across the test filter,
          in BORA during the structural test
          of filter RT1
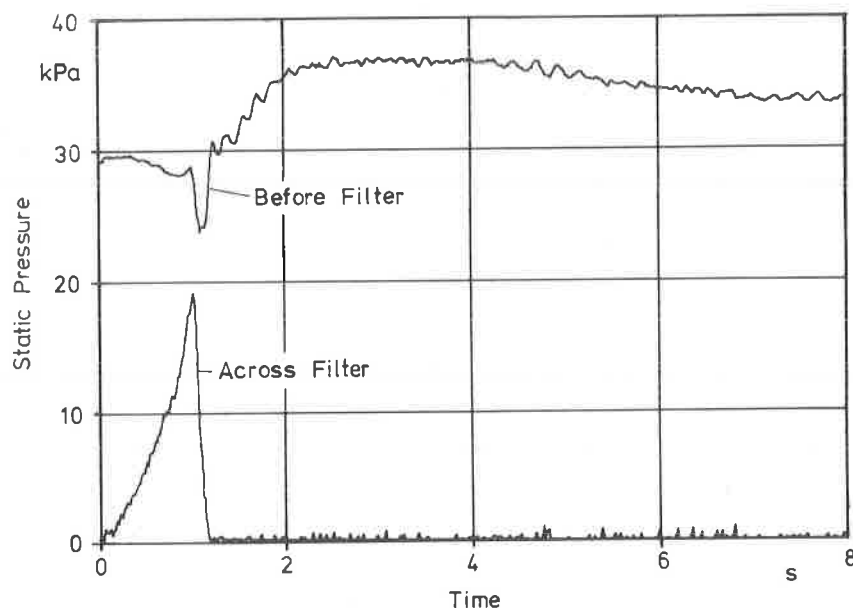
Fig. 17: Time history of the static pressure, upstream and across the test filter, in BORA during the structural test of filter RT2
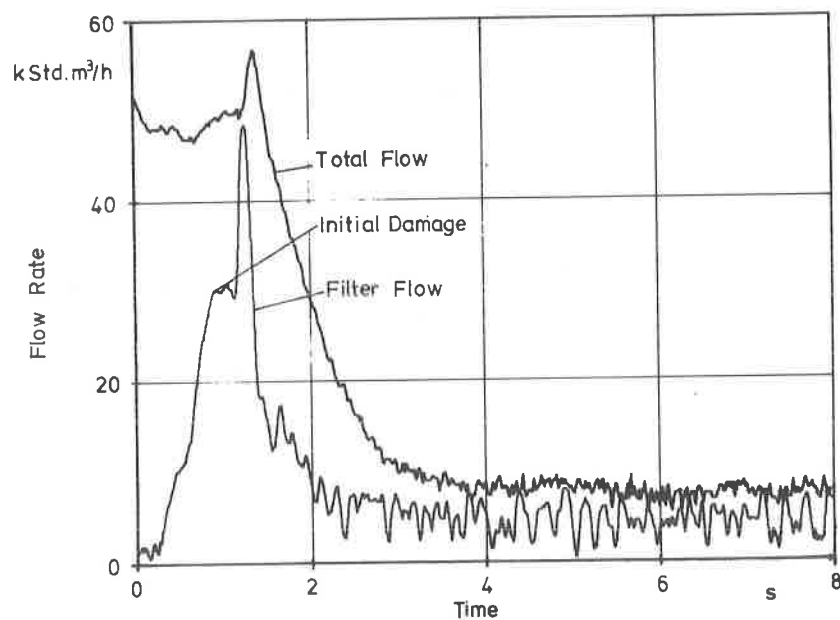
Fig. 18: Time history of blower and filter flow rates during the structural test of filter RT2 in BORA
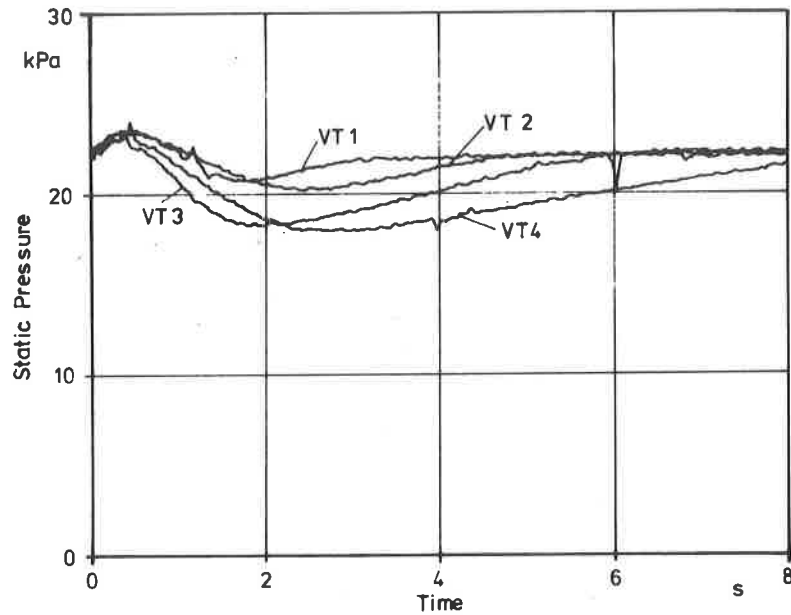
Fig. 19:   Measured profiles of the static pressure at
the blower discharge for different actuating
times of the control valves K1 and K2
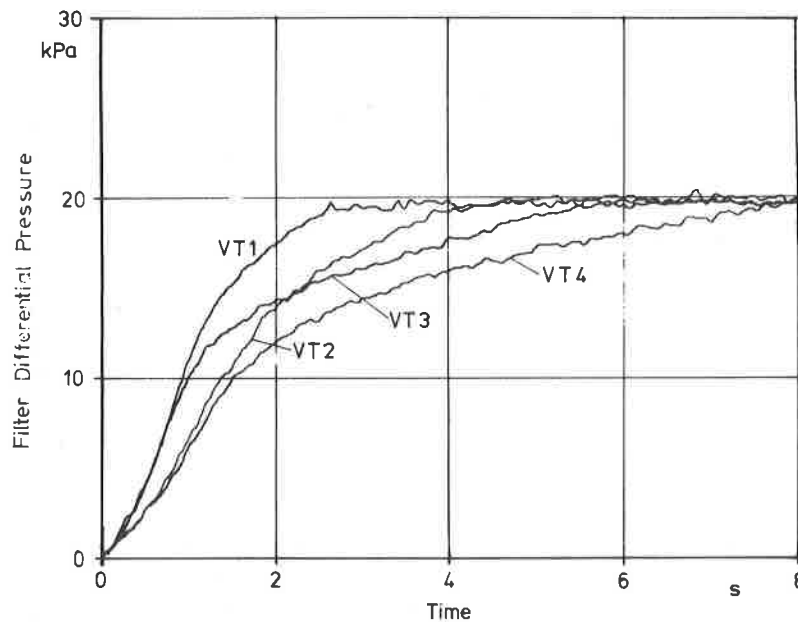
Fig. 20:   Measured profiles of the differential pressure
across the filter in test section of BORA for
different actuating times of the control
valves K1 and K2

SPRING LOADED HOLD-DOWN FOR MOUNTING HEPA
FILTERS AT ROCKY FLATS

K. Terada, C. R. Rose and A. G. Garcia

Rockwell International
Energy Systems Group
Rocky Flats Plant
Golden, Colorado

Abstract

The use of springs to maintain pressure on the gasket to form
air tight seal between HEPA filters and their holders is
described.

I. Introduction

Most HEPA filters in service at Rocky Flats are located in
walk-in plenums where they are mounted for either two or four
stage filtration. The interior of a typical plenum at Rocky
Flats is shown in Figure 1. These plenums vary greatly in size
from those holding 12 filters per stage to about 600 size 5
(2x2x1') filters. After installation, a fraction of the filters
tend to develop leaks at the surface where the gasket is pressed
against the filter mounting frame in the plenum. There are two
reasons for this, one is that leaks develop because the neoprene
gaskets take a "set" with the consequent loss of compressive
seal. The other reason is that the torque wrench or "feel" is
not a very reliable measure of the compressive force on a filter
because of variations in friction as a nut is turned on a
threaded stud. Rust and accumulated debris aggravate this
problem. Visual inspection of the degree of compression of the
gasket is very difficult because when the filters are fully
secured, there is insufficient space to make the observation.

The current remedy to prevent leaks is to reenter the plenum
after a suitable period and retorque the nuts that compress the
filters against the plenum frames. The incorporation of springs
will maintain a steady pressure on the gasket and negates the
effect of its tendency to "set". Minor variations in the
applied torque will be similarly remedied.

II. Loss of Seal Between HEPA Filter and Filter Frame

Closed cell neoprene foam is used as the gasket to seal the
HEPA filter to the plenum frame. Figure 2 shows a steel plenum
frame on which HEPA filters are mounted. Figure 3 shows the
steel plates and nuts which hold the filter in place and
compress the gasket. The nuts are torqued to compress the
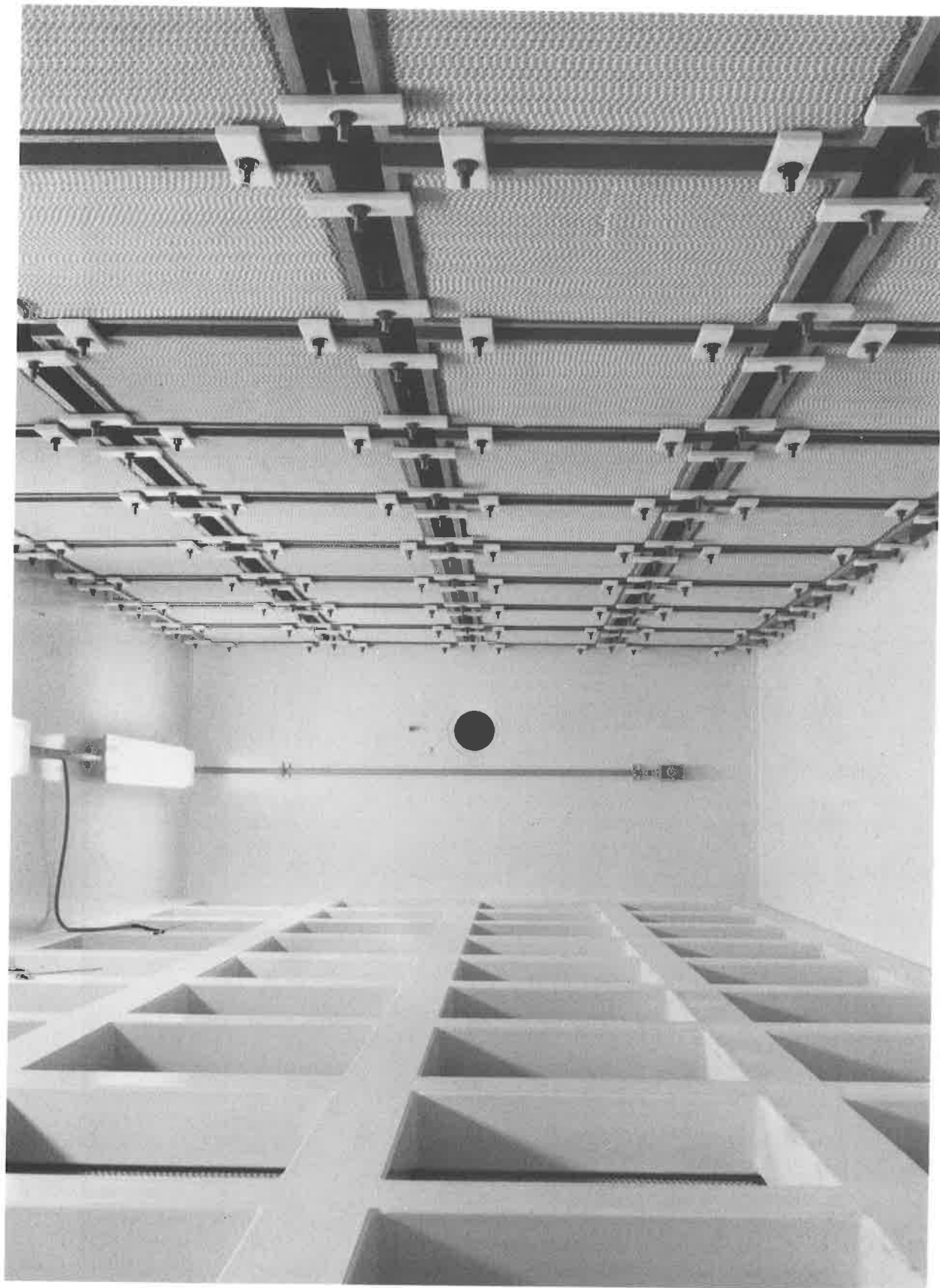
FIGURE 1
INTERIOR OF A TYPICAL PLENUM AT ROCKY FLATS
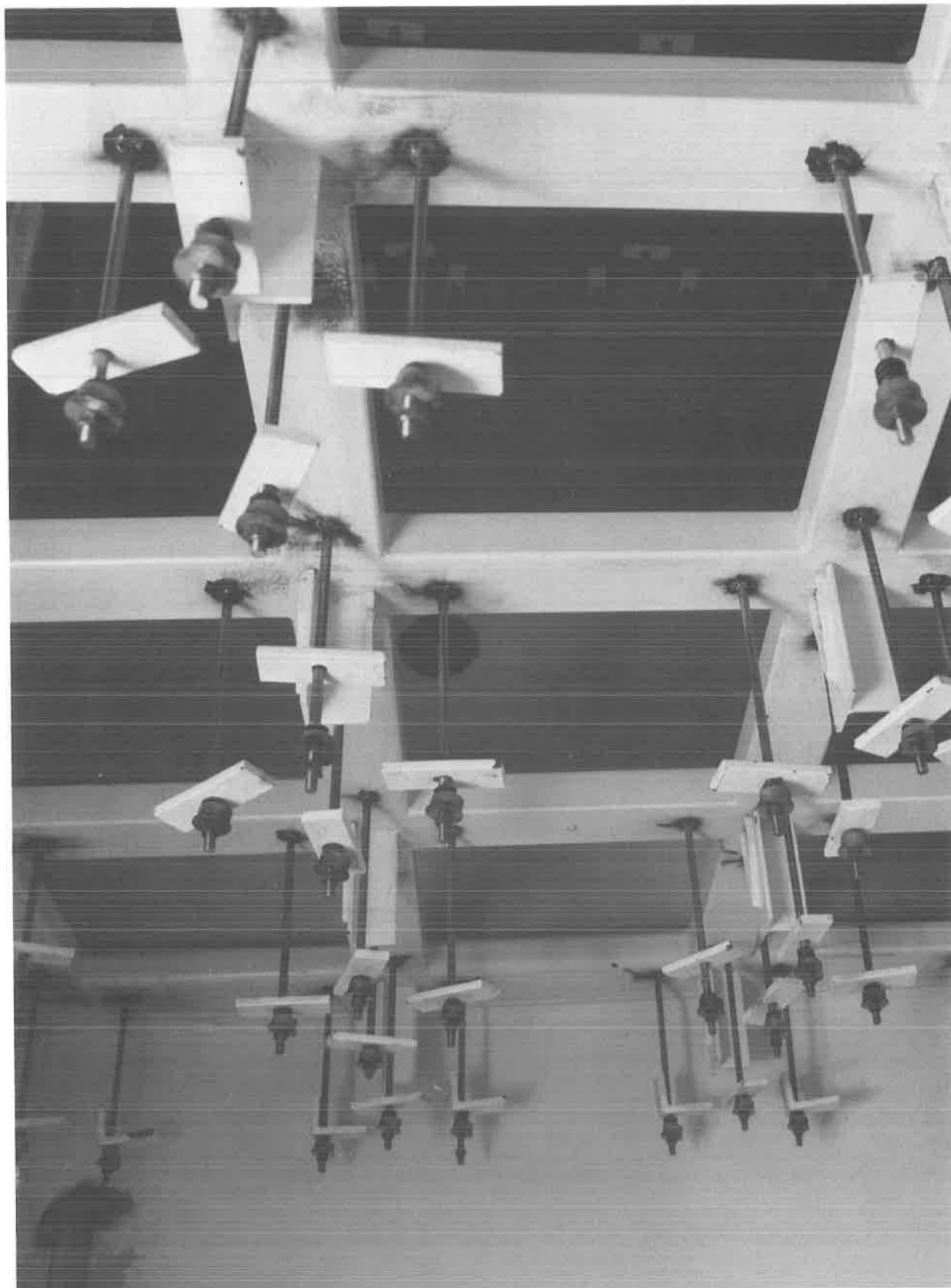
FIGURE 2
PLENUM FRAME FOR MOUNTING HEPA FILTERS
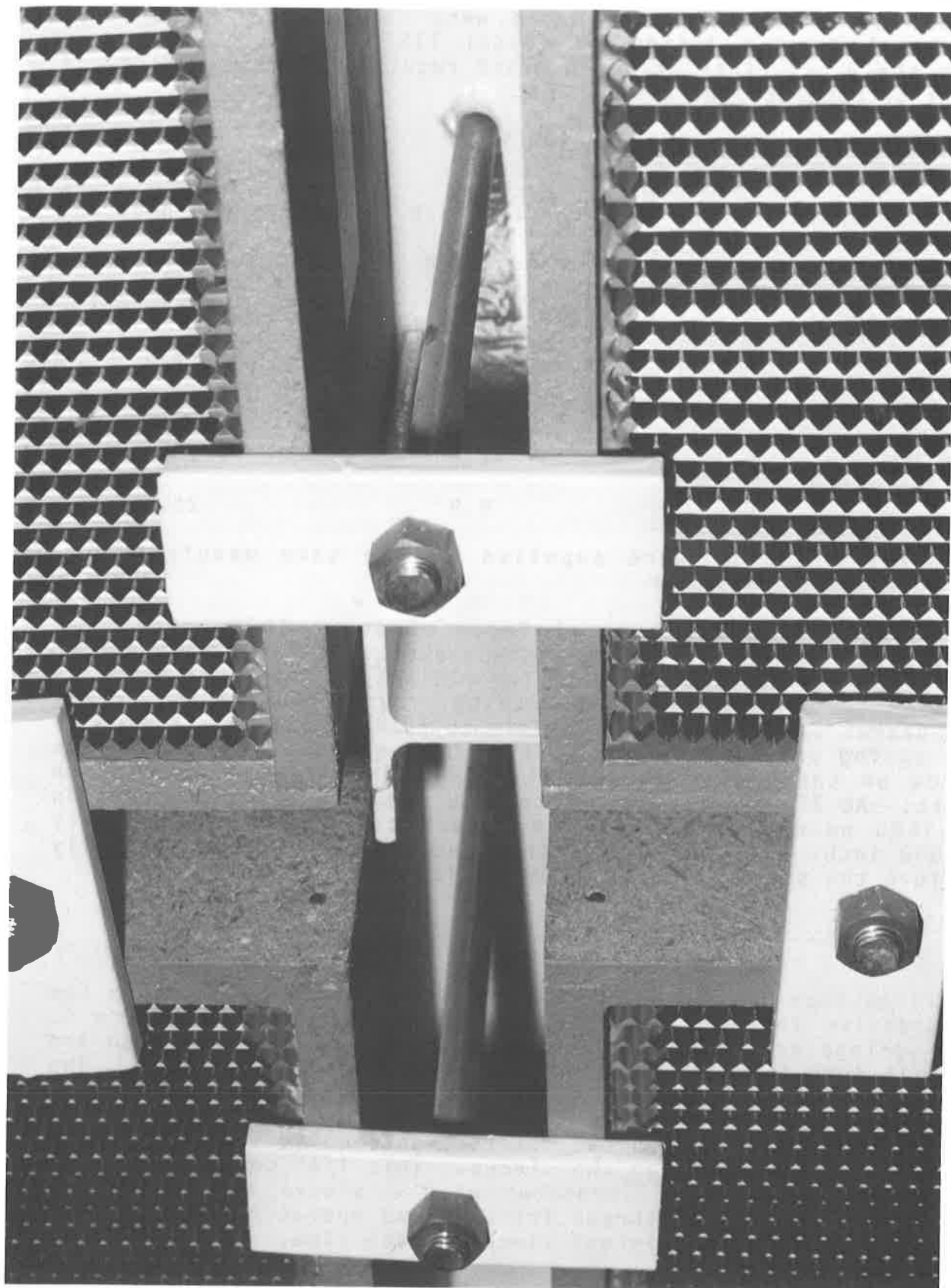
FIGURE 3
CLOSE VIEW OF HOW FILTERS ARE HELD IN PLACE

gasket by approximately 50% of its 1/4" thickness. Table 1 shows some compression data from gasket materials from three filter manufacturers. The tests were conducted on an Instron Universal Testing Instrument (Model 1137). Sample A did not meet the Rocky Flats standard which requires a minimum force of 9 psi to compress the gasket 25%.

TABLE 1

Compression-Deflection Data for 1/4 inch Thick Expanded Neoprene Gaskets

Sample	Average Force at 25% Compression (psi)	Average Force at 50% Compression (psi)
A*	4.8	13.3
A2	10.1	22.6
B	12.5	27.6
C	9.9	25.1

*Samples A and A2 were supplied by the same manufacturer.

The data also shows a total force of about 1500 pounds per filter is required to compress the gasket of a 2x2x1 foot filter to 1/2 of its thickness. With the old setup, the studs acted as springs of very stiff spring rate to provide the tension. When the gasket takes a "set", it tends to relieve all the tension of the spring provided by the studs. Consequently the compressive force on the gasket is greatly diminished resulting in some leaks. At 375 pounds, the force required to exert a compression of 1500 pounds on each filter, each stud is elongated only 0.0008 inch. A "set" of only this small amount will essentially relieve the studs of their clamping force.

III. Use of Springs to Maintain Compressive Force

Springs were placed over each hold-down plate to maintain the compressive force on the gaskets. This is shown in Figure 4. The springs are an off-the-shelf item and are one inch high and 1- 1/16 inch in diameter. The inside diameter is 5/8 inch. The sleeve is made of steel tube and is 3/4 inch high. Since the spring is 1/4" longer that the sleeve a consistent compression of 1/4" is obtained when the nut is tightened to the point where the washer just seats on the sleeve. This 1/4" compression then is controlled by the dimensions of the sleeve and spring and take the variables of thread friction and operator "feel" out of the loop assuring consistent clamping each time.
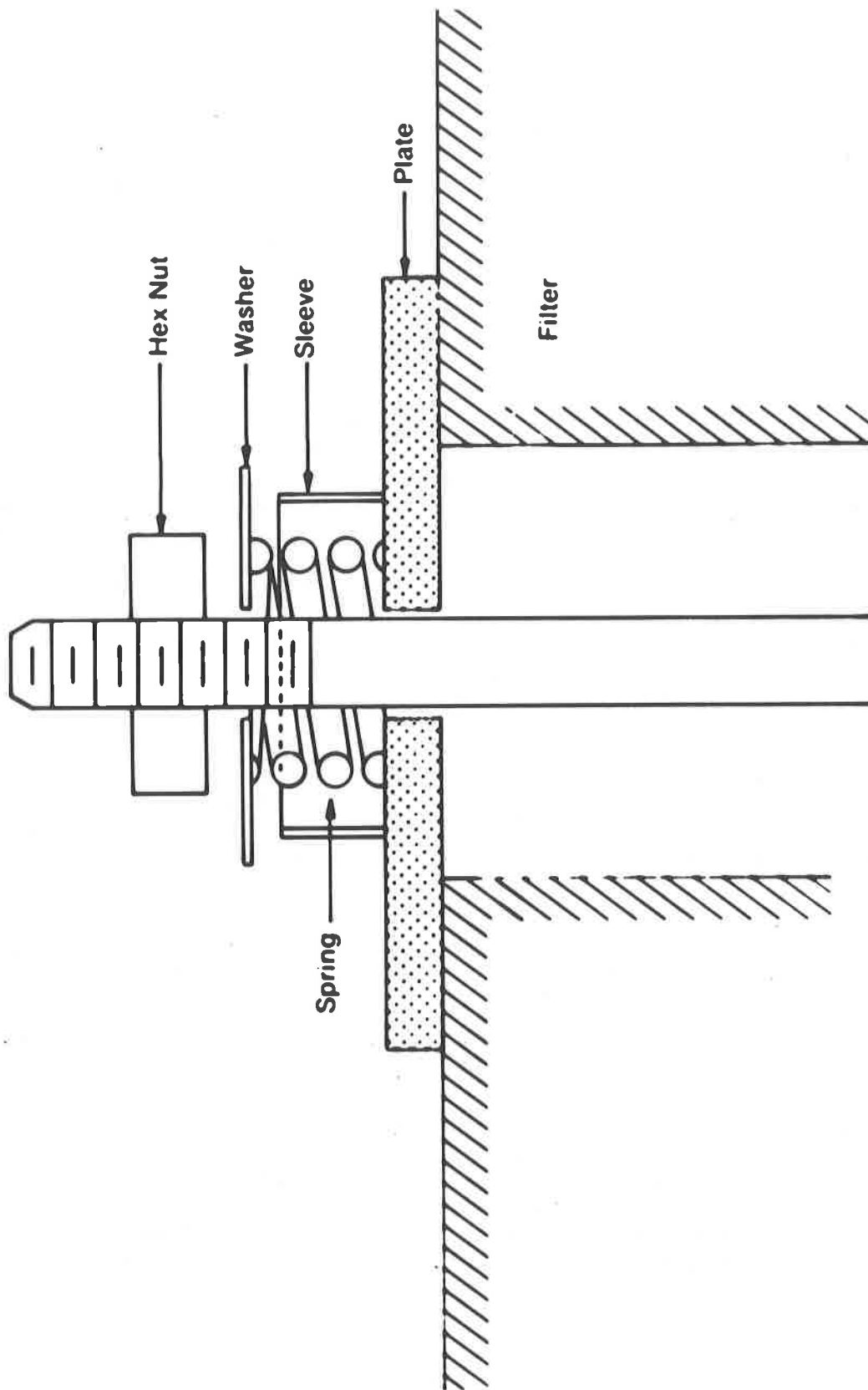
FIGURE 4
SCHEMATIC OF SPRING-LOADED HOLD-DOWN

Table 2 shows the force required to compress three springs 1/4 inch. It shows the compression forces are quite uniform.

TABLE 2

Forces Required to Compress Springs 1/4 Inch

Spring	Full Length (inches)	Length Compressed (inches)	(pounds)
1	1.0	0.25	425
2	1.0	0.25	411
3	1.0	0.25	426

During the past year, these springs have been used in plenums in several locations. Reports on their performance from the filter installation group have been excellent. Filters held down with springs were mounted adjacent to filters without the springs for comparison. Normally 60% of the filter hold-downs require retorquing within a month after installation. Of these, DOP tests show that about 50% leaked around the gaskets. After another month about 25% of the nuts require retorquing but normally there are no leaks. The percentage of nuts that need retorquing rises with the degree of vibration caused by the fans.

Of the approximately 100 filters that are mounted with springs, none has developed leaks or required retorquing. Thus far, the filter installation group has not experienced any difficulty in manipulating the new system.

Currently at Rocky Flats, four new plenums are either in the construction or planning phase where filters will be held in position with these springs. All future plenums will be built with hold-down studs that will accommodate the springs.

IV. Conclusion

In-service tests indicate that the use of springs to hold HEPA filters in position could eliminate the necessity of reentering a plenum to retorque the hold-down nuts of newly installed filters after the sealing gaskets have taken a "set". Also, it decreases the probability of leaks occurring around gaskets that are not in sufficient compression. Filters held in place with these springs will be continued to be monitored to determine whether all HEPA filters at Rocky Flats should use this system.

DISCUSSION

PAPAVRAMIDIS: What material are you using for studs and what material are you using for the frame of the unit stage (not the HEPA cells).

TERADA: For the studs we use carbon steel and then paint it to cut down on corrosion. For the frame, some of the old places use carbon steel, but in the future we will be going to stainless steel.

Session 20

CODES, STANDARDS, REGULATIONS

THURSDAY: August 16, 1984
CHAIRMAN: M.W. First
Harvard School of Public Health

CONAGT'S PLACE IN ASME'S CENTENNIAL YEAR
W.H. Miller, Jr.

AIR CLEANING IN ACCIDENT SITUATIONS
J.L. Kovach

TECHNICAL DEVELOPMENT OF NUCLEAR AIR CLEANING IN THE PEOPLE'S
REPUBLIC OF CHINA
Li Xue Qun, Liu Hui, Wang Tie Shen, Xin Song Niam, Guo Liang Tian

OPENING REMARKS OF SESSION CHAIRMAN:

We have three important papers on the development of standards
for nuclear air and gas cleaning components and systems. One is
concerned with the activities of the Committee of Nuclear Air and
Gas Treatment (CONAGT), sponsored by the American Society of Mechan-
ical Engineers and published by the American National Standards
Institute. A second outlines activities in Western Europe, sponsored
by the Organization for Economic Co-operation and Development (OECD),
and concerned with air cleaning in accident situations. And, finally,
a paper on the technical development of nuclear air cleaning in the
People's Republic of China.

I think these are three very significant presentations to a
meeting such as this because so much of our interest over this week
has been concerned with how to develop regulatory criteria. Much of
the research in our field is motivated by a need to meet regulatory
standards; attention to regulations, standards, and codes is certainly
a primary consideration throughout all our activities. In some prior
Conferences, we have held panel sessions to which have been invited
representatives of each of the countries highly involved with
civilian nuclear power activities. These sessions have always been
of great interest and we have benefitted from having each of the
country representatives tell us a bit about their new air and gas
cleaning and airborne waste disposal activities. Even though
interest is still as keen as ever, we though we would do it a little

differently this year and give fewer people more time and, hence, a better opportunity to develop the significant activities that bear on this subject.

CONAGT'S Place In ASME'S Centennial Year

William H. Miller, Jr.
Sargent & Lundy
Chicago, Illinois

Abstract

The purpose of this paper is to present a status report on ASME's Committee on Nuclear Air and Gas Treatment (CONAGT). This year ASME celebrates its centennial while CONAGT issues its first code sections covering fans, blowers, and refrigeration equipment. Significant code related CONAGT activities are covered as well as an explanation of CONAGT's place in the ASME organization.

Introduction

In 1884, four years after the American Society of Mechanical Engineers was founded, ASME began developing performance test codes for steam boilers to protect our ancestors from frequent boiler explosions which were claiming 50,000 lives and injuring two million people annually. In the 100 years since its inception, ASME has greatly broadened its codes and standards activities to encompass literally hundreds of various mechanical equipment and topics as shown in Table 1. ASME Codes and Standards brought order, stability, and most importantly, safety to the Machine Age and ultimately gave us precious time for travel, cultural enrichment, and play.

ASME's centennial celebration coincides with an important milestone. This year ASME's Committee on Nuclear Air and Gas Treatment (CONAGT) will publish the first equipment code for nuclear power plant HVAC and gas processing systems. The CONAGT code will provide a consistent set of requirements for major components of air and gas treatment systems.

As a resource to the United States and perhaps foreign countries, the CONAGT code will govern design, fabrication, installation, and testing of HVAC and gas processing equipment as follows:

- Fans and blowers
- Refrigeration equipment
- Coils, air washers, humidifiers
- Dampers and louvers
- Moisture separators
- Prefilters, HEPA filters, adsorbers
- Instruments and controls
- Ductwork, housings, accessories
- Process gas equipment
- Field testing procedures

Code Highlights

The CONAGT code is written to be "user friendly." Most sections include a nonmandatory appendix that lists the information exchange requirements and a recommended scope of responsibility among Purchaser, Engineer, and Contractor. Five Nonmandatory Appendixes are provided in the initial issue; to illustrate the appendix format, part of one appendix has been extracted from the Fans and Blowers section and reproduced here in Table 2. These appendixes particularly help the preparer of design and purchase specifications to ensure that all parties understand their responsibilities.

The CONAGT Code consolidates information from many sources. The Structural Design section, for instance, will for the first time provide designers with a consistent set of design rules, analyses, and testing methodologies for the proper structural design of air and gas treatment equipment. Up to now designers relied upon various standards, structural design techniques, and analysis philosophies. Highlights of this code section include the following:

- Definitions of normal and abnormal loads
- Load combination
- Service conditions
- Design and service limits
- Stress criteria
- Deflection criteria
- Design rules for various stress analysis techniques
- Design certification requirements using analytical or testing techniques
- Functionability requirements
- Documentation requirements

The CONAGT Code is one of the first to reference the QA requirements of the recently issued ANSI/ASME NQA-1 - 1984, Quality Assurance Program Requirements for Nuclear Facilities.

Code Organization and Update

CONAGT plans 22 code sections; the first three will be issued within this year. CONAGT organized the code sections into four divisions as shown in Table 3. The initial issue will include Division I, Nuclear Safety Related Common Articles; Division II, Nuclear Safety Related Fans and Blowers; and Division II, Refrigeration Equipment Code Sections. In 1985, CONAGT will publish Nuclear Safety Related Conditioning Equipment, Dampers, Ductwork, Sorbent Media and HEPA Filter Code sections. Each equipment section is organized as shown in Table 4.

All ASME CONAGT Code publications will offer a yearly addenda subscription service to provide code users with code revisions, interpretations, and responses to inquiries. Users need only purchase the particular sections that interest them.

Code-Related Activities

In addition to writing, reviewing, and revising new code sections, CONAGT has undertaken four important projects related to its scope: Program for Developing Structural Design Criteria for Ductwork, the International Round Robin Carbon Adsorbent Testing Program, the Standard on Qualifications of Field Testing, and the second maintenance revision of ANSI N510-80 (originally issued in 1975), Testing of Nuclear Air Cleaning Systems.

Ductwork Qualification

CONAGT prepared the Program for Developing Structural Design Criteria for Ductwork to solicit industry funding for an HVAC Ductwork and Supports dynamic testing program. The program will produce dynamically prequalified ductwork design tables and guidelines. Currently, ductwork design and test data are scarce, and the lack of such data has generally resulted in overdesign. When completed, this test program will provide standard ductwork designs, verification of analytical techniques by actual test data, and a uniform analysis approach for future qualifications, all of which will reduce fabrication and design costs.

CONAGT intends to seek participation and funding from utility companies, the Nuclear Regulatory Commission, and architect-engineering firms.

Round Robin Carbon Testing

CONAGT sponsored a program to check the consistency of carbon adsorbency tests at labs around the world. Test data that does not accurately reflect the radioiodine adsorbency of the air cleaning system could ultimately endanger the public with excessive releases. To ensure acceptable testing results, lab tests must conform with applicable Regulatory Guides, ANSI N-509 and ASTM standards.

CONAGT sent each laboratory adsorbent samples to test in accordance with ANSI N-509 and referenced ASTM standards. Not all labs reported the same results for identical samples.

After being notified by CONAGT of the lab test results, the ASTM committee on Activated Carbon (D28) requested that the federal government establish a national laboratory accreditation program for carbon testing labs. According to the Federal Register (October 27, 1983), the National Bureau of Standards intends to accept responsibility for this accreditation program.

Qualification of Field-Test Personnel

CONAGT is currently finalizing a standard that specifies the skills, experience, and training required of personnel who test nuclear air and cleaning equipment.

This standard follows up on an N45 committee standard, Testing of Nuclear Air Cleaning Systems (ANSI N510-80). The publication describes specific tests for air cleaning systems.

- Air flow distribution
- Air-aerosol mixing
- Dioctyl phthlate (DOP) challenge for leaktesting of high-efficiency particulate air filters
- Fluorocarbon bypass testing of carbon adsorbers

These tests require specialized skills and experience in locating injection and sampling ports or manifolds, calibrating and maintaining sensitive detection equipment, and solving unique system-related problems.

In 1976 CONAGT commissioned experts to prepare a field-testing personnel qualification standard. This standard was initially prepared for issue as a separate standard. However, after considerable review by the utility industry, CONAGT revised it significantly and proposed to issue the standard as a Nonmandatory Appendix to ANSI N510.

Maintenance Revision of ANSI/ASME N510

CONAGT plans to revise the widely used ANSI/ASME N510 standard by 1985. The revision will incorporate recent inquiries and editorial changes.

ASME and CONAGT Organization

In pursuing its worthwhile goals, CONAGT derives its charter, scope, governing procedures, and certain resources from ASME. Since many of this conference's attendees may not be familiar with the ASME organization, Figure 1 illustrates the overall society plan of organization. The ASME Board of Governors delegates the codes and standards activity to a 20-member Council on Codes and Standards which directs all aspects of the program. Under the Council are ten boards, also made up of ASME members and other interested persons. These boards in turn have committees, each responsible for a specific area of standard development. CONAGT reports to the Board on Nuclear Codes and Standards as shown in Figure 2. Over 120 main committees, similar to CONAGT, deal with nearly 600 standards that are under regular review and revision. Forty-five hundred engineers, manufacturers, regulators, and others sit on main committees, subcommittees, subgroups, and working groups.

CONAGT's organization is shown in Figure 3. It is comprised of a 27-member Main Committee, ten-member Executive Committee, and seven subcommittees. A total of 95 dedicated members make up CONAGT's balanced membership, which is a requisite for voluntary consensus codes and standards organizations. Most groups meet quarterly to review code drafts, discuss technical and administrative issues, and ballot on finished publications. Figure 4 illustrates the precautions which are taken to ensure that ASME codes and standards receive broad-based review and are truly consensus documents. On the average, CONAGT finds that it takes approximately 5 years after the first code draft is prepared for it to be fully approved and issued for use.

CONAGT Goals

In 1975 CONAGT was chartered by ASME Nuclear Codes and Standards to "develop, review, maintain and coordinate codes and standards for design, fabrication, installation, testing and inspection of equipment for nuclear power plant air and gas treatment systems." This committee had produced equipment and testing standards under ASME N-45 auspices between 1971 and 1975. Figure 5 depicts major milestones in CONAGT's history. CONAGT owes its productive ten-plus year existence to the hardworking committee members and the farsighted industry sponsors who continue to support this worthwhile development activity despite a period of slow business growth.

CONAGT's future goals are as follows:

- Finish and issue all code sections
- Issue Appendix C to ANSI N510, <u>Testing of Nuclear Air Cleaning Systems</u>
- Revise and issue ANSI N510
- Oversee implementation of the program for developing Structural Design Criteria for Ductwork
- Revise the CONAGT organization as needed to respond to code inquiries and perform periodic updates
- Consider expansion of scope of activities to other nuclear facilities with approval of ASME
- Replenish organization with new members to meet needs.

CONAGT: A Productive Centennial Child

CONAGT is proud to be a part of ASME's rich and rewarding 100-year tradition of codes and standards service to this country. CONAGT trusts that the issue this year of its first code sections will help enhance ASME's already brilliant record of achievements.

CONAGT members are proud to continue their association and support of this Nuclear Airborne Waste Management and Air Cleaning Conference.

Table 1

ASME STANDARDS TOPICS

Acoustic Emission Testing
Abbreviations
Accreditation
Air Heaters
Atmospheric
Automatically Fired Boilers
Automotive Lifting Devices
Beverage Equipment
Boiler Accreditation
Boilers
Boilers, Control and Safety
  (Automatically Fired)
Building Service Piping
Cableways
Calibration of Instruments
Canvass Projects
Care and Operation of Heater Boilers
Care and Operation of Power Boilers
Charts
Chemical Plant Piping
Compressor Systems
Conveyors and Related Equipment
Consumable Tools
Conveyor Backstops
Cooling Tower
Cranes (Nuclear)
Cranes (Safety)
Cryogenic Piping
Decompression Chambers
Definitions
Density Determination
Derricks
Design, Boilers and Pressure Vessels
Digital-Systems Techniques
Dockboards
Drafting
Drug Equipment
Dumbwaiters
Dust Separating Apparatus
Electrical Measurements
Elevators and Associated Equipment
Elevator Inspection and Inspector
  Qualification
Emission Testing, Acoustic
Escalators
Fans
Fastners
Fine Particulate Matter
Fits
Fittings
Flanges
Flue Gas Desulfurization

Flow Measurement
Flue and Exhaust Gas Analysis
Food Equipment
Gaskets
Gas Guide
Gas Turbines
Gauge Blanks
Graphs
Handling Trucks
Heating Boilers
High-Pressure Systems
High-Pressure Vessels
Hoists (Overhead)
Hoists (Safety)
Hooks
Humidity Determination
Hyperbaric Chambers
Identification of Piping Systems
Ignition Systems
Incinerators, Testing
Indicated Power Measurement
Industrial Engines
Industrial Trucks
Instruments and Apparatus
Inspection, Elevators
International Standards
Jacks
Keys
Letter Symbols
Lifting Devices, Portable
  (Automotive)
Limits and Fits
Linear Measurements
Liquid Petroleum
  Transportation Piping Systems
Loading Dock Levelers
Low-Pressure Boilers
Machine Guarding
Manlifts
Material Specification
Measurement Uncertainty
Metrication
Metrology
Model Testing
Moving Walks
Nominal Sizes
Nondestructive Examination
Nuclear
  • Accreditation
  • Air and Gas Treatment
  • Codes and Standards
  • Concrete Construction

- Cranes
- Inservice Inspection
- Mechanical Equipment
  Qualification
- Plant Operations and Maintenance
- Power
- Quality Assurance

Offshore Oil and Gas
  (Pollution Prevention)
Pallets
Petroleum Refinery Piping
Pipe
Piping
- Chemical Plant and Petroleum
  Refinery
- Gas Transmission and Distribution
- Identification Scheme
- Liquid Petroleum
  Transportation
- Power
- Refrigeration
- Slurry

Piston Rings
Pollution Prevention
- Offshore Oil and Gas
- Operations

Portable Lifting Devices
  (Automotive)
Power Boilers
Power Piping
Power Transmission Apparatus
Pressure Gauges
Pressure Measurement
Pressure Piping
Pressure Vessel Accreditation
Pressure Vessels
Pressure Vessels for Human
  Occupancy
Pressure Trip Systems
Properties of Metals
Pumps
Pumps Testing
Quality of Steam
Qualification of Elevator
  Inspectors
Refrigeration Piping
Reinforced Plastic Pressure Vessels
Reinforced Thermoset Plastic
  Corrosion Resistant Equipment
Retaining Rings
Rotary Steam Measurement
Safety Codes and Standards
Safety Device,
  Automatically Fired Boilers
Safety Pollution Prevention
  Equipment

Safety Valves, Performance and
  Terminology
Safety Valve Requirements
Shaft Horsepower
Screw Threads
Slings
Slip Sheets
Slurry Pipelines
Solar Energy
Spray Cooling
Steam Condensing Apparatus
Steam Generators
Steel Smokestacks
Surface Qualities
Symbol Stamps
Temperature Measurement
Thermowells
Time Measurement
Terminologies (Industrial
  Engineering)
Transmission Chains
Transmission Shafting
Trucks
Turbine (Hydraulic) (Steam)
Turbine, Gas
Turbine, Gas Procurement
Turbine, Steam
Turbine Water Damage
Valve Actuators
Valves
Viscosity Determination
Weighing Scales
Welding
Wheelchair Lifts
Wind Turbines
Window Cleaning
Wrenches
Wrought Iron and Steel Piping
  and Tubing

1486

Table 2

ASME — CONAGT Code on Fans
Nonmandatory Appendix B

Division of Responsibility

Section	Item	Responsible Party
3200	Limitations on Materials	Engineer
3400	Certificate of Compliance	Manufacturer
4110	Performance	
	a) Fan type and blade shape	Engineer
	b) Air flow	Engineer
	c) Total pressure	Engineer
	d) Maximum discharge velocity	Engineer
	e) Air density at rating	Engineer
	f) Maximum air density expected	Engineer
	g) Operating temperature	Engineer
	h) Details of intake and discharge transitions	Engineer
	i) Parallel fan operation	Engineer
	j) Peak design temperature	Engineer
4150	Centrifugal Fans/Support Boundary	
	a) Size and type of anchorage	Engineer/Manufacturer
	b) Anchorage loads	Manufacturer
4220	Drivers	
4221.1	Speed Torque Curve	Fan Manufacturer
4221.2	Inertia	Fan Manufacturer
4221.3	External Forces	Fan Manufacturer
4221.4	Power Source	Engineer-Fan Manufacturer

Table 3

Organization of
ASME Code on Nuclear Air and Gas Treatment

Division I—General Requirements
   Section AA—Common Articles

**Division II—Ventilation Air Cleaning and Ventilation
            Air-Conditioning**
   Section BA—Fans and blowers
   Section CA—Conditioning equipment
   Section DA—Dampers and louvers
   Section FA—Moisture separators
   Section FB—Prefilters and frames
   Section FC—HEPA filters and frames
   Section FD—Sorbers and frames
   Section FE—Sorbent media
   Section IA—Instrumentation and control
   Section RA—Refrigeration equipment
   Section SA—Ductwork

Division III—Process Gas Treatment
   Section GA—Pressure vessels, piping, heat exchangers, and valves
   Section GB—Noble gas hold-up equipment
   Section GC—Compressors
   Section GD—Other radionuclide equipment
   Section GE—Hydrogen recombiners
   Section GF—Gas sampling

Division IV—Testing Procedures
   Section TA—Field testing of air treatment systems
   Section TB—Field testing of gas processing systems
   Section TC—Personnel qualification
   Section TD—Laboratory qualification

Table 4

**ASME Code on Nuclear Air and Gas Treatment
Section Organization**

Article Number	Title
1000	Scope
2000	Referenced documents
3000	Materials
4000	Structural design
5000	Inspection and testing
6000	Fabrication, joining, welding, brazing, protective coating, and installation
7000	Packaging, shipping, receiving, and storage and handling
8000	Quality assurance
9000	Nameplates and stamping

Figure 1   ASME Organization

```
                        ┌──────────────────────┐
                        │  Board of Governors  │
                        └──────────┬───────────┘
                ┌──────────────────┴──────────────────┐
    ┌───────────────────────┐              ┌──────────────────────┐
    │   Council on Codes     │              │    Other Councils    │
    │    and Standards       │              └──────────────────────┘
    └───────────┬────────────┘                • Education
        ┌───────┴────────┐                     • Engineering
┌─────────────────┐  ┌─────────────────┐       • Member affairs
│ Supervisory     │  │ Advisory Boards │       • Public affairs
│ Boards          │  └─────────────────┘
└─────────────────┘
```

Supervisory Boards

- Pressure technology
- Safety
- Performance test codes
- Standardization
- Nuclear codes and standards

Advisory Boards

- International standards
- Metrication
- Hearings and appeals
- Accreditation
- Council operations

Other Councils

- Education
- Engineering
- Member affairs
- Public affairs

Figure 2   ASME Board on Nuclear Codes and Standards Organization

Board on Nuclear Codes and Standards

Committee on Nuclear Air and Gas Treatment Equipment

Other Committees

- Authorized nuclear Inspection
- Nuclear quality assurance
- Operation and maintenance of NPP
- Boiler and pressure vessel
- Cranes for nuclear facilities
- Qualification of mechanical equipment in NPP
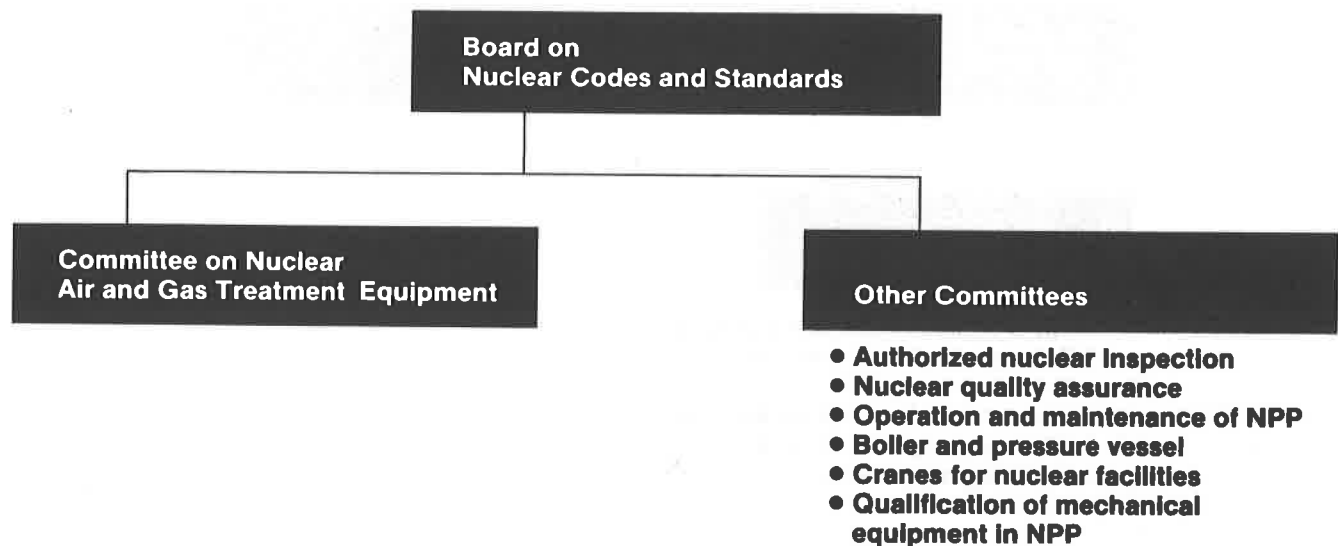
Figure 3   ASME Committee on Nuclear Air and Gas Treatment Equipment Organization

- Ventilation air cleaning equipment
- Process gas treatment equipment
- Common equipment
- Ventilation air conditioning equipment
- General support services
- Field-testing procedures
- Administration
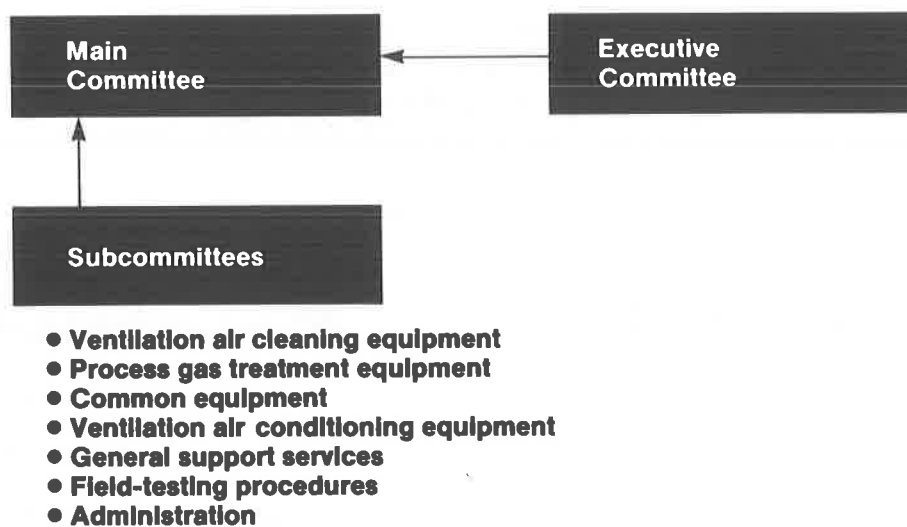
Figure 4   Flowchart of Consensus Process
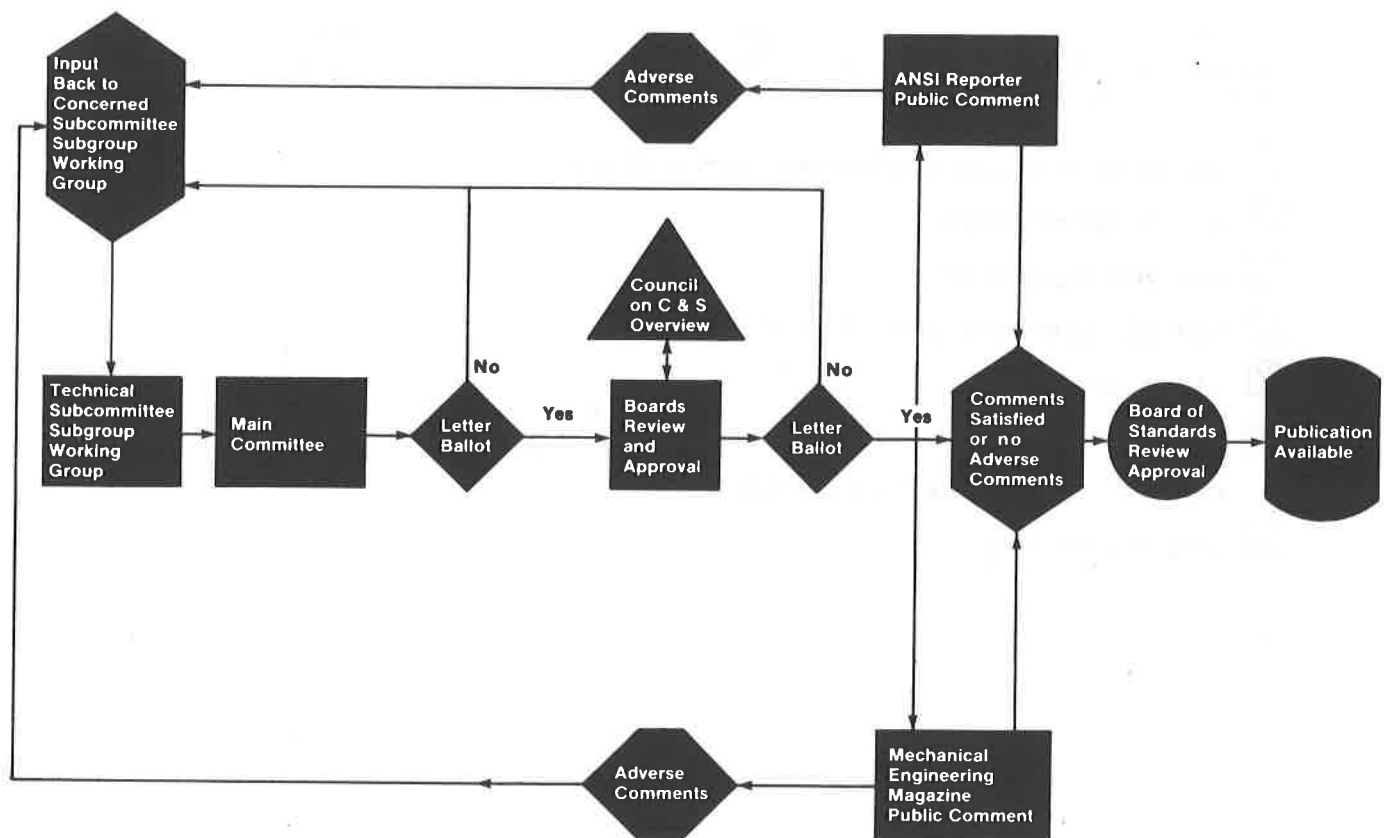
Figure 5   ASME CONAGT History

| 1971 | 1975 | 1976 | 1980 | 1984 | ? | 1990 |

☐ **Committee on Air and Gas Treatment started (N45-8)**

▨ **ANSI N-509 published**

▧ **ANSI N-510 published**

▦ **CONAGT Committee chartered by ASME**

■ **ANSI N-509 revised**

■ **ANSI N-510 revised**

▨ **CONAGT publishes first code sections**

▦ **All code sections published**
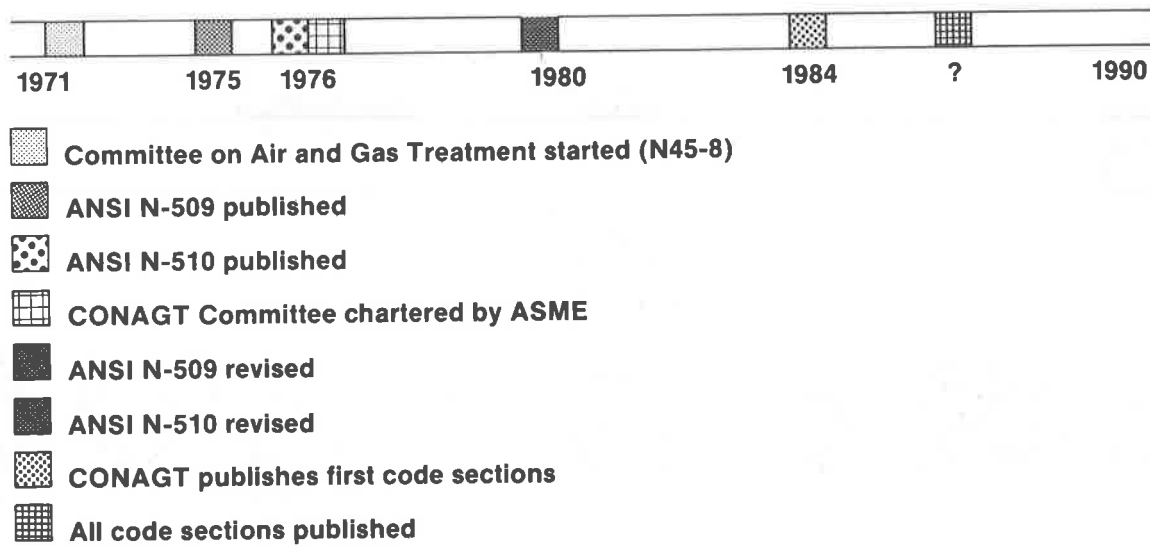
AIR CLEANING IN ACCIDENT SITUATIONS

J. Louis Kovach
Nuclear Consulting Services, Inc.
Columbus, Ohio

Abstract

The Organization for Economic Co-Operation and Development (OECD) through its subsidiaries the Nuclear Energy Agency (NEA) and the Committee on the Safety of Nuclear Installations (CSNI) established in 1979 a "Group of Experts or Air Cleaning in Accident Situations". This group met seven times to establish a draft report based on its Terms of Reference which were:

1) review the performance of off-gas cleaning systems in accident conditions;

2) collect information about operating experience with these systems;

3) seek to establish common principles for the design of off-gas systems;

4) review methods used in the different countries for testing filters from the standpoint of accident conditions;

5) suggest specific mechanisms for improving cooperation, with regard, for example, to filter testing.

In the following the conclusions and recommendations of the Group are summarized.

I. INTRODUCTION

The initial meeting indicated that the manner of thinking and the method of establishing accident scenarios for power reactors are different from those for other fuel cycle facilities. Therefore the Group was divided into two Subgroups for part of the discussions. The power reactor Subgroup was able to start from scenarios of design basis accidents (DBAs) previously established by Member countries, whereas the fuel cycle facilities Subgroup*, not having such pre-established scenarios available, had to develop reference accident conditions (fires and explosions) in order to undertake their work.

It was realized very early in the discussions that a DBA which may have worst effects on the primary loop of a reactor may not be the worst accident challenging the Air Cleaning Systems (ACSs) and the conventional DBA concept is not conservative enough for the establishment of the most serious challenges for ACSs. Similarly, worst accident concepts for ACSs are not identical to worst accidents for overall facilities in the non-power-reactor area.

---

*This Subgroup primarily considered events which may take place in fuel reprocessing plants; however, some of the considerations apply to the other facilities.

While the evaluation proceeded in two different directions, it is significant that both Subgroups identified almost the same problems and arrived at very similar conclusions and recommendations. The arrival at a consensus using two different evaluation methods strengthens the value of the findings.

The report by no means solves the outstanding problems but it identifies areas where additional knowledge has to be obtained and where future cooperation is of paramount interest.

It was also strongly felt that more refined input from other groups is required in a more realistic technical establishment of accident source terms for the further refinement of the conclusions. Such information is available or is being generated in additional testing under a broad range of accident parameters. The report should therefore be revised periodically.

II. OUTSTANDING PROBLEMS AND THEIR SAFETY SIGNIFICANCE

The Group considered accidents primarily to power reactors (more so for LWRs) and to fuel reprocessing facilities. In these two areas, progress was made in defining various anticipated accident modes and consequences. Other than noting that problems can occur in other stages of the nuclear fuel cycle, no indepth analysis was made relating to accidents in those areas.

General

In power reactors the basic consideration was to evaluate air cleaning system (ACS) response to design basis accidents. Several members of the Group felt that this limitation was not realistic; however, it was generally agreed that current conventional ACSs would not be able to operate under severe accident conditions with any realistically predictable efficiency, even though there are currently no clearly defined conditions for severe accidents.

The general conclusion is that in a predictable design basis accident (DBA) the ACSs may withstand the effect of the DBA as long as their protection systems are working. However, in particular, high-efficiency particulate air (HEPA) filters may reach their limit of design capability.

Appropriate design performance of these ACSs, even under DBA conditions, can only be maintained if a number of protective devices are also operational. Such items as isolation valves have to function perfectly, HEPA filters have to be protected from widely changing conditions, iodine adsorbers must not be poisoned, and motor blower packages have to be capable of maintaining design air flow through the ACSs. Thus the operation of the ACSs in a DBA is predicated on the total reliability of the ACSs and of any directly or indirectly affiliated component, including interlocks, which protects the ACSs from the potential harmful effects of the DBA.

In other nuclear facilities, several types of accident have been identified which challenge the ACSs and ACS components (ACSCs) currently used; failure of protective systems seem, as for reactors, to be the most probable accidents, although the consequences may be somewhat less severe; the major accidents appear to be fire and explosion. The source term parameters and their effect on the performance of the ACSs and ACSCs are ill defined. As in the case of power reactor ACSs, the correct funtioning of all the ACSCs and their protective devices is essential.

Such ideal interfacing of all components is rarely attained in practice. As an example, there are many ACSs with ACSCs designed and built to withstand DBA conditions but which have interconnecting ducts incapable of withstanding the predicted accident conditions. The preliminary study recently presented by Moeller and Sun showed hundreds of failures in ACSs on their affiliated components even under normal operating conditions. It is inevitable that such failures would also be present under accident conditions, either because they were not detected and remedied before the accident or they occurred as a result of the accident. The majority of these failures were of affiliated equipment, not direct components of the ACSs, and would have severely limited the design efficiency of the ACSs.

Therefore, one of the major problems is lack of control of the entire design envelope of ACSs. The ACS reliability evaluation should start from the intake point and include all components, even the nonfiltering ones which affect its operation, such as humidity controls, heaters, dampers, fire control, drains, motor blower trains and all affiliated control equipment to the discharge point of the system.

There is a lack of dissemination of information on ACS and component testing performed by military agencies, of previously classified reports and of the descriptions of ACS behaviour in some of the past accidents. Indeed what is required both retrospectively and in the future is a much more widespread effort to identify, collect and disseminate information on relevant experience.

HEPA Filters

While the actual amount of airborne particulate fission products is still under debate it is certainly expected that an operational ACS would give a certain amount of protection from the release of these, mainly by the use of HEPA filter(s). It is apparent that HEPA filters have questionable trapping efficiencies for very small particles, but 0.1 µm particles and larger are trapped with an efficiency of 99.9+%. However, very little is known regarding lower aerosol size ranges where this efficiency decreases to a very low value. It is widely assumed that agglomeration will occur immediately of atomic-size, solid decay products to larger sizes, while the common practice of applying radiation to prevent agglomeration of particles in the evaluation of monodisperse aerosols is completely ignored.

Insufficient attention is paid to possible radiation damage to neoprene filter gaskets and other ACS components under accident conditions.

Moreover, the available information on HEPA filters relates primarily to new filters and virtually no data exist for the normal or accident condition behaviour of aged filters. Many ACS HEPA filters remain in place for more than five years. It is unrealistic to expect that accidents will occur only with freshly installed HEPA filter banks.

The limitations affecting our knowledge of the performance of the HEPA filter itself under various challenge conditions can be divided into three separate areas:

a) Performance of the new unit - i.e., as manufactured capability (test requirements in national standards, where they exist, vary widely).

b) The effects of ageing, as caused by normal operation, which may degrade performance and ability to withstand deviations from the norm.

c) Situations which may be specific to an accident scenario - such as smoke loading, chemical effects, etc.

Current knowledge for HEPA filters can be summarized in tabular form.

	Extent of Knowledge*			
Operational Parameters	New		Aged	
	Normal	Accident	Normal	Accident
Pressure Differential	VG	F	F	NE
Vibration	G	G	NE	NE
High Humidity / Free Water	F	F	NE	NE
Chemicals	P	P	NE	NE
Radiation	G	F	P	NE
Temperature	G	P	NE	NE
Loading Capacity	G	F	P	NE

*VG - Very Good
 G - Good
 F - Fair
 P - Poor
NE - Non-Existent

Little is known on any combination of extreme values of these parameters.

Adequate design ensures that for normal operation the challenge to the HEPA filter is within the known capability of the filter. However, under accident conditions, knowledge of the generated aerosol characteristics, even when available, is insufficient to reliably predict the performance of either the pre-conditioning elements (prefilter, demister, etc., if they are used) or the performance of the HEPA filter.

Defining the precise value of the challenge to the HEPA filter stage presents one of the major problems in deciding how adequately the filter system will perform.

While it can not be claimed that its development was based on foresight, the currently evolved US filter train design using prefilter-demister-HEPA-carbon-HEPA filter components represents good system design, because at least the last HEPA system is well protected by all the preceding components from many of the potential hazards which could result in the failure of a single prefilter-HEPA filter combination.

In the case of reprocessing plant conditions the possibility of fires and explosions has been discussed. The consequence of these events also leads one to conclude that the strength of HEPA filters, even under optimum conditions, is inadequate to protect the environment. It points toward the necessity of further studies of accident behaviour of filters and probably the need to develop new components for aerosol filtration. The fuel cycle facilities Subgroup relied to a greater extent on the development and utilization of computer codes to define accident scenarios, which need to be validated by actual experiments under various conditions. However, again the difficulty of separating DBA and out of DBA conditions causes serious problems in defining HEPA filter behaviour.

Demisters

Extensive testing of demisters has been performed in the United States and in the Federal Republic of Germany. However, all of the test programmes were of a qualification nature and only very sketchy quality control or design/operational criteria are available.

In spite of this very limited information, compared with the extremely voluminous data presented on HEPA filters, the demisters may be the most underrated components of ACSs. In the only evaluation under accident conditions (the Savannah River Plant rod drop accident), the installed demisters removed in excess of 90% of the particulate load. This value would have been probably higher if the installation had been periodically inspected (and/or tested) as is common for HEPA filter and iodine adsorber banks.

By themselves, demisters may not be adequate for the control of the total aerosol load of an accident; however, in combination with HEPA filters, where the HEPA filter is recognized as a secondary polishing component, the combination package can be very important. The use of stainless steel demisters ahead of HEPA filters probably provide significant:

> a) shock attenuation,
> b) fire protection,
> c) overload protection,
> d) free water damage protection.

Currently very few of these probable advantages are quantified. Other than the free water damage protection, no tests have been performed on demister – HEPA combinations to evaluate how much quantitative protection demisters can supply and how they would behave under actual accident conditions.

Iodine Adsorbers

The behaviour, evaluation and performance of iodine adsorbers has been extensively treated in the literature. However, in spite of the very extensive studies, there are still problems to be solved. It is agreed that primary and well analyzed species of iodine forms are elemental iodine and methyl iodide; traces of other forms which have been positively identified are diiodomethane, vinyl iodide and iodobenzene. Several investigations in the past have identified an iodine chemical species as HOI in the vapour phase, whereas other investigators found it only in the liquid phase and could not verify its presence in the vapour phase. Current data indicate that the presence of HOI in the vapour phase under the various postulated accident conditions is very unlikely.

There are virtually no test data on other possible compounds, such as HI or higher oxyacids of iodine.

The evaluation of all accident conditions and their appropriate iodine chemistry resulting in vapour phase components has to be established.

The test methods used by various countries have been evolved to suit particular laboratory conditions and the correlation of results on identical samples has been somewhat dismal. It is difficult to rationally evaluate removal efficiencies for various iodine species within the accuracy claimed by many researchers when the different laboratories obtain orders of magnitude differences in DF on similar geometry and nominally identical conditions. A current round robin initiated by the US ANSI-ASME group indicates there is no improvement in this respect. The

results are as divergent as in the European round robin testing, and a serious credibility problem exists.

Another problem identified by the Group is the applicability of data generated using stable methyl iodide for the evaluation of radioactive methyl iodide removal. Because of the isotope exchange, even in the case of amine-impregnated carbons the correlation between the tests with $CH_3{}^{127}I$ and $CH_3{}^{131}I$ for nuclear applications is not established.

The seriousness of poisoning has been evaluated mainly under nonaccident conditions. Under such conditions it is shown that guard beds or deep beds offer significant protection. However, the only actual accident condition with iodine impregnated carbons has been the TMI-2 Auxiliary Bldg and Fuel Handling Bldg Filter Systems with somewhat dismal results. What happens to the strongly adsorbed high molecular weight organic compounds in the guard bed or in the front of the deep bed under the high-activity, high-concentration iodine load of an accident is not known. Such conditions could foreseeably result in the formation of hitnerto unconsidered organic iodine forms, with unknown retention behaviour.

There is only limited type and quality control testing for some postulated DBA conditions. This may lead to surprises if iodine adsorber systems are used under accident conditions.

Current knowledge regarding carbon-based iodine adsorbers is summarized in the following table:

Extent of Knowledge*

Operational Parameters	New		Aged	
	Normal	Accident	Normal	Accident
Pressure Differential	VG	G	G	G
Vibration	VG(USA) P (Others)	VG(USA) P(Others)	NE	NE
High Humidity/Free Water	VG	VG	F	P
Chemicals (Poisoning)	P	P	P	P
Radiation	VG	VG	VG	F
Temperature	VG	G	F	P
Loading Capacity	VG	F	F	P

*VG - Very Good
 G - Good
 F - Fair
 P - Poor
 NE - Non-Existant

Little is known about combinations of extreme values of these parameters.

Knowledge is more limited for other types of iodine adsorbents such as silver-treated materials.

Major Outstanding Problems

For all systems, whether in power reactor or in other nuclear facilities, the major problems are:

1) Ill-defined accident conditions even where a DBA philosophy is applied. Indeed the DBA may not represent the most severe conditions under which the air cleaning system has to operate.

2) Significant lack of confidence in HEPA filters.

3) Lack of international coordination of accident condition test work, despite the great expense of test rigs to evaluate component behaviour under accident conditions.

4) Limited information exchange, even of the meagre data available for accident conditions.

5) Lack of knowledge on demister and demister-HEPA combinations under accident conditions.

6) Lack of tests and standards on complete ACSs.

7) Lack of tests and standards on some components of the ACSs.

8) Lack of reproducibility in iodine adsorbent testing.

9) Limited information on long-term behaviour of adsorbed iodine on charcoal.

10) Accident environment effects, including hydrogen, on adsorbents.

III. CONCLUSIONS AND RECOMMENDATIONS

The work to date indicates that fire and explosion are the major accidents to be considered. These accidents have the potential to endanger current air cleaning systems and their components, primarily HEPA filters and their housings, which are the major protection in fuel cycle facilities. The fuel cycle facilities Subgroup has therefore evaluated Solvent Fire and Explosive Source Term* parameters. Data were submitted by Japan, France, the Federal Republic of Germany, the United Kingdom and the United States. The data, while useful for preliminary evaluation, are by no means complete at the present time.

The source term tabulation is based on estimates, and very little actual experimental work has been completed to date. The consequences of some of the postulated source terms have been evaluated using computer models. These computer programs have had only limited verification. Based on the submitted data the assumed maximum fire source term parameters were:

Temperature	1000°C
Smoke Production	120 kg
Unburned Flammable	unknown
Hazardous Material	100 kg

---

*In this context source term means not only amounts of radioactivity but also quantities of materials, temperatures, etc.

The main difference between nuclear facilities and most industrial facilities is their confinement. Burning will typically result in excessive smoke; depleted oxygen conditions will cause inefficient combustion and a subsequent release of unburned flammables including combustible gases. This phenomenon, while decreasing the life of the fire, may result in the air cleaning system being filled with unburned flammables, leading to possible reignition at any point where contact with an oxygen-rich atmosphere occurs.

The currently assumed maximum explosive source term parameters based on the tabulations were:

Temperature	3000°C
Pressure	40 bar
Aerosol Concentration	100 mg/m^3 (average in the enclosure)

Processes involving hydrogen, acetylene, zirconium dust and red oil were listed as having explosion potential. The most serious case is hydrogen detonation, where the high speed of pressure wave propagation and the potential pressure doubling caused by reflection of pressure waves far exceeds the structural limits of most air cleaning systems and of their primary component HEPA filters. As an example, in several BWR off-gas systems where hydrogen explosions have taken place, the HEPA filters before the carbon beds were blown to pieces.

The wide divergence of estimates of fire source terms is undoubtedly due in part to insufficient knowledge about the actual source term conditions. Although certain conclusions can be drawn, the modeling is based on inadequate experimental data.

Not only better experimental input is required for the source term but such a critical component as the HEPA filter has not been evaluated under actual accident conditions. As an example, it is presumptuous to assume that, becuase a new clean HEPA filter is capable of being elevated to 385°C then cooled down and still have near its initial efficiency, it will be capable of maintaining the known efficiency under other accident conditions which involve loading, humidity, ageing, potential reignition of unburned combustibles or contact with particles with unknown temperature.

The consequences of the fire source term parameters in underventilated enclosures were analyzed using both the CEA and the Los Alamos models. The results from these calculations are comparable for the temperature.

	CEA Computer Model Estimates	LANL Computer Model Estimates
Temperature	400°C avg.	350°C avg.
Smoke	---------	24 kg
Unburned Flammable	---------	46 kg
Hazardous Material	---------	1 kg
Pressure	0.2 bar	-----

Both models predict that temperatures will be significantly attenuated away from the flame zone, due to heat loss and potential dilution from other branches of the air cleaning system, before reaching active elements of the ACS. Even so, the models predict that temperatures potentially hazardous to filtering elements may be propagated. The models do not discuss the transport of burning or hot particulates within the cell or in the ducts.

Explosion-caused shock waves will also be attenuated a little as they propagate along a duct. Should the shock wave be perturbed, as must of necessity occur at the ventilation system inlet from the cell, or if there are bends in the duct, the reflection phenomena may increase the pressure exerted by the shock wave above its intrinsic value. In the extreme of complete reflection, as occurs when a wave hits the wall of a confinement vessel, it may double the pressure. Conventional ducting, or unprotected HEPA filter banks, will be destroyed by any appreciable explosive shock wave.

Finally, the Subgroup noted that there are insufficient facilities for testing components and systems using realistic accident conditions.

It is concluded that current knowledge is grossly inadequate in many areas. As a consequence it is recommended that further work and cooperation is required to:

1) Establish all accident source term parameters under realistic experimetal conditions.

2) Improve the availability of reports of accidents which have occurred in Member countries.

3) Establish conditions which air cleaning systems must withstand in accidents including explosions and reignition of unburned combustibles.

4) Evaluate the performance of HEPA filters and other components under the combined effects of the various accident parameters.

5) Undertake R&D for HEPA substitutes and/or protrection devices for existing HEPA filters.

6) Investigate methods of retention of radionuclides which are particulate under ambient conditions but may be transformed to volatile species under accident conditions and penetrate the air cleaning components.

7) Verify and/or refine existing computer codes by realistic experiments, and develop additional codes to model the challenges to filter elements and other air cleaning components in the various accident situations.

8) Evaluate handling and reinstatement of air cleaning systems after an accident.

9) Collect and disseminate within the Member countries relevant operational experience in an organized way.

These actions necessitate close collaboration with the experts of other CSNI Groups, especially within Principal Working Groups No. 4*.

---

*i.e., the CSNI Group of Experts on the Source Term (GREST) and the CSNI Group of Experts on Accident Consequences (GRECA); the CSNI Group of Experts on Air Cleaning and Containment Atmospheric Control Systems under Accident Conditions (GENAC) is the third Group under Principal Working Group No. 4

Power Reactors

The Subgroup evaluating the accident consequences on filter systems and their components considered only the design basis accidents, as was originally stated in the terms of reference. However, the Subgroup is not convinced that the DBA philosophy has always been correctly applied in taking full account of the ventilation clean-up system environment. In any case, the DBA does not necessarily represent the worst conditions under which the ventilation system will be required to function.

A tabulation of the environmental conditions which could challenge the air cleaning system was solicited for the various containment, and water reactor types. The conditions are specific to the location of the system; and the types of containment; therefore, only the most severe conditions based on the data collection, not necessarily simultaneous, are summarized here:

Temperature	200°C
Humidity	100% RH + free water
Activity	3kCi
Pressure	equal to containment design pressure
Fire Hazard	potential exists
Chemicals	potential exists
Particulate Loading	potential exists
Hydrogen Reactions	potential exists
External Atmospheric Force	potential exists
Seismic	potential exists
Deterioration (ageing, poisoning, etc.)	potential exists
Excessive Pressure Differential	potential exists

These are not representative of all reactor types, but only worst conditions.

These conditions permit the operation of filter systems only if appropriate protection devices exist to prevent damage to the system. However, information regarding the behaviour of filters under accident conditions, especially aged HEPA filters, is so limited that the performance of these filters cannot be predicted. Particular problems were also identified in that designers of the air cleaning units often include consideration of these maximum conditions; however, connecting ducting and associated equipment, which are equally important for the availability of the units, are not designed to withstand these conditions.

Detailed surveys of HEPA and Iodine Adsorbent test methods were prepared. These tabulations pointed out that, with very few exceptions, routine testing of both HEPA filters and adsorbents (or adsorbent modules) is performed under short-term ambient conditions, and only a limited amount of test data are available for the consideration of all the accident parameters.

A significant problem exists also in the area of source term revision based on the consequences of the TMI accident and on subsequent research. Following the TMI-2 events, both the form and quantity of airborne fission products are being revised and questions regarding hydrogen detonation inclusion in design basis accidents are being raised.

The major areas of concern are the following:

1) Lack of knowledge about ACS conditions in accident situations.
2) HEPA filter reliability.
3) Chemical effects on iodine adsorbents.
4) Reliability of existing test methods.
5) Lack of test methods simulating accident conditions.

It is the opinion of the Group that stainless steel demister – HEPA combinations are superior to prefilter – HEPA combinations in regard to loading and pressure transients, and further work should be carried out in the development of HEPA filters maintaining adequate filtration efficiency under the postulated accident conditions.

Chemical effects on iodine adsorbents can be offset by deep beds or guard beds to protect part of the adsorbent from being poisoned.

To improve the reproducibility of interlaboratory test exercises, reference test conditions have been established. Also, most Member countries participated in the round robin testing arising from the US ASME/ANSI N509 group.

The most significant variations exist in the in-place leak test methods of iodine adsorbents. Work is being performed in the United Kindgom to compare module tests using both CH_3 ^{131}I and Halide 11. The Federal Republic of Germany and the United States are initiating tests of installed systems using both CH_3 ^{131}I and Halide 11.

The Group noted that the claimed existence of iodine forms such as HOI has not been verified, and interpretation of stable methyl iodide removal efficiencies of impregnated carbon beds cannot be correlated with the behaviour of radioactive methyl iodide.

Another concern was raised primarily by the United States regarding the assurance of habitability of control rooms under both in- and off-site accident conditions. Investigations have shown that measures currently considered, such as complete isolation of the control room and self-contained breathing apparatus are not satisfactory solutions.

Finally, the Group again noted that there are insufficient facilities for testing components and systems under simulated accident conditions.

It is concluded that current knowledge is grossly inadequate in many areas. As a consequence it is recommended that further work and cooperation is supported in:

1) Construction and operation of test facilities to evaluate air cleaning system components under the simultaneous effects of an accident, allowing

2) assessment of current components and development of more effective systems, and their testing.

3) Evaluation of radioaerosol filtration behaviour and retention in particle sizes below 0.1 micron.

4) Definition of more realistic source terms and accident scenarios, and the development of test procedures based on these definitions.

5) Verifying and/or refining existing computer codes by realistic experiments, and developing additional codes to model the challenges to filter elements and other air cleaning components in the various accident situations.

6) The establishment of the full extent of air cleaning components, including controls, dampers, interlocks, i.e., all affiliated components required for the safe operation of the system.

7) Adoption of standardized test methods for adsorbents.

8) Prevention and/or limitation of adsorbent degradation.

9) Ensuring protection of control room personnel from both on-site and off-site events by reliable air cleaning systems.

10) Post-accident handling and reinstatement of filter systems.

11) Selection or development of a reference aerosol for accident condition filtration tests.

12) The organized collection and dissemination within the Member countries of relevant operational experience.

TECHNICAL DEVELOPMENT OF NUCLEAR AIR CLEANING
IN THE PEOPLE'S REPUBLIC OF CHINA

Li Xue Qun, Liu Hui, Wang Tie Shen,
Xin Song Niam and Guo Liang Tian

Radiation & Protection Branch of
Chinese Nuclear Society

Introduction

In the past 20 years, with the utilization of nuclear technology
in China, air cleaning techniques were developed persistently to pre-
vent the environment from pollution caused by radioactive materials
and to ensure the safety of occupational personnel. The technical
developments involve many fields including the manufacture of filter
media and adsorbents; the application of filters and iodine adsorbers
and the testing of them; the improvement of instruments and methods
for aerosol concentration measurement; the retention of radioactive
noble gases; and others. As nuclear power stations are to be built in
China, nuclear air cleaning will be advancing more rapidly. Many pro-
grams have been scheduled, such as producing other types of adsorbers,
moisture separators, nuclear grade HEPA filters that have excellent
performance to resist adverse circumstances, and in-place testing for
units of ventilation systems in nuclear facilities.

I. Air Filtration

1. Development of the HEPA Filter and Filter Media

For the high efficiency particulate air filter (HEPA), the fil-
ter media are very important parts. In past years we principally de-
veloped three kinds of media; polyvinyl dichloride (PVDC) fiber,
asbestos-fiber and glass fiber, but asbestos-fiber media have not
been applied extensively in practice because it failed in performance.

At the end of the 1950s, the PVDC fiber media were prepared, by
dissolving ethylene dichloride resin into dichloroethane and then
pressure spinning the solution. It has excellent features - resisting
hydrofluoric acid, water high temp. (above 70° C), radiation, organic
solvents and some strong acids, as shown in Table 1.

Because the PVDC media can be damaged by organic solvents, it
is very difficult to select proper sealing materials. The filters with
this kind of medium are sealed mechanically, that is, the separators
with ⌐ form edges are pressed together with the media by bolts, as
shown in Figure 1. This kind of filter is heavier, more expensive
and more complex of structure, but has longer service life.

In 1960s, glass fiber media started to be produced. Up to now
general glass fiber media, water resistant glass fiber media, and
fungus resistant glass fiber media have been developed. The perfor-
mance of the first kind of media is shown in Table 2.

Table 1 Performance of $_*$PVDC fiber media
(LXGL-25)

Test Condition	Group	Resistance mm w.g.	Penetration %	Tensile Strength g/15 x 180 mm
Temp. 70°C	Test	2.40	3.7×10^{-3}	438
	control	2.40	4.3×10^{-5}	457
Water (1) Soak	Test	2.2	1.7×10^{-4}	403
	control	2.16	1.6×10^{-4}	439
Exposure to 100R	Test	3.56	2.7×10^{-3}	746
	control	3.52	2.3×10^{-5}	741
40% Nitric (2) Acid	Test	2.24	7.6×10^{-3}	369
	control	2.18	8.8×10^{-5}	407
36-38% Hydrochloric Acid (2)	Test	3.20	7.8×10^{-2}	764
	control	3.22	1.6×10^{-4}	763
40% Hydrofluoric Acid (2)	Test	3.44	1.8×10^{-4}	753
	control	3.40	2.6×10^{-4}	766
30% TBP-Kerosene	Test	dissolve	dissolve	dissolve

* LXDL-25 is trademark of this medium.

Note: (1) The media were soaked in water for 3 days at ambient temp., and then dried in the shade and measured.

(2) The media were soaked through in acid and then dried in shade and measured.

At the same time, filters with glass fiber media were studied. Through a model test, the resistance of the filter was found to be a function of separator height and filter depth described by empirical formula (1):

$$H = KV + 1.2967 \frac{L^{1.8}}{h^{3.645}} V^{1+5 \times 10^{-5}L^2} \exp(-7 \times 10^3 L) \quad (1)$$

Table 2 Performance of general glass fiber
media (without adhesive)

Test Conditions	Group	Resistance mm w.g.	Penetration %	Tensile Strength g/15x180 mm
Temp. 500°C	Test	6.88	7.0×10^{-5}	589
	control	6.68	6.1×10^{-5}	429
Water Soak[1]	Test	8.48	2.2×10^{-5}	400
	control	8.45	2.1×10^{-5}	404
Exposure to 10^6 R	Test	6.60	9.5×10^{-5}	367
	control	6.60	4.6×10^{-5}	354
40% Nitric[2] Acid	Test	7.98	2.1×10^{-5}	339
	control	8.04	1.6×10^{-5}	318
36-38% Hydrochloric Acid[3]	Test	9.92	5.2×10^{-5}	187
	control	8.18	1.5×10^{-5}	350

Note: (1) see Table 1 Note (1)
(2) See Table 1 Note (2)
(3) The media were exposed to vapor of 36-38% hydrochloric
acid for 10 days and then measured.

Where:

L = depth of filter core, mm

h = wave peak height of separator, mm

v = filtration velocity, L/cm^2. min

K = ratio showing resistance characteristic of media

H = filter resistance, mm w.g.

Later, two kinds of filters of size 610 x 610 x 290 mm with
metal frame and aluminum separators resistant to heat or water were
manufactured. Rated flow, 1700 M^3/h, penetration < 0.01% (sodium
flame test), resistance ≤ 25 mm w.g. At an environmental test facility
equipped specially (Fig. 2), heat resistant filters were tested after
exposure to hot air flow (250°C) for 30 minutes; water resistant
filters after spraying with water and adding pressure (pressure drop
up to 250 mm w.g.) for 15 min and then drying by air flow. The test

results show that no significant changes in resistance and penetration were observed. The two kinds of filters have been used for some nuclear applications.

In some ventilation systems the filters with PVDC media have been replaced by glass fiber filters because the latter are cheaper. Table 3 gives the performance comparison of the two kinds of filters in the same ventilation system.

Table 3 Filter penetration comparison

	Filter with PVDC Media	Filter with glass Fiber Media
Frame Material	polychloroethene	plywood
Separator Wave Peak Hight, mm	7.5	4
Number of Separators	38	75
Area of Media M^2	14	17
Penetration * %	0.1-0.2	0.1-0.2
Overall Size mm	345x630x750	345x630x420
Weight of Filter unit Kg	55.5--60	13-13.5

* The penetration was calculated from an in-place radioactive measurement.

2. Test of HEPA Filter

Presently testing of filter units is conducted using the oil fog test or the sodium flame test.

At the beginning of the 1960s, oil fog test instruments were made. The aerosols used in this test are turbid oil fogs, which are generated by evaporation and condensation. Concentration is measured by a light-scattering photometer. This test can measure penetration down to 0.0001%, but it affects the penetration and strength of some kinds of media.

In 1965, the first sodium flame test set was built. The flow rate was 1400 M^2/h. Up to now, 20 similar sets have been built (Fig. 3). Most are operated at a flow rate of 2500 M^3/h. For the largest test set, the air flow rate is 7000 M^3/h. Generally, detector sensitivity is in the range of 0.001 - 0.0001%. Compared to the British sodium flame test, there are several differences:

1510

1. A "sleeve: was added onto the atomizer, to stop large liquid drops, so that the aerosol dispersity was modified.

2. When the sodium flame photometer background is measured, burner offgas is drawn from the system pipe and filtered through an absolute filter instead of using outside air, thus avoiding the deviation resulting from a difference in relative humidity between the offgas and the outside air.

3. When measuring concentration, the gas flow upstream of the HEPA filter is diluted by a factor 50-100 prior to entering the detector. This prevents burner contamination from high conc. sodium and makes the measured value within the linear range. It also eliminates the "self-absorption" effect.

The in-place testing of installed filters is being investigated.

In the past, the filters to be tested were gripped on the sealed-end faces and filled with air, and then the pressure drop was measured. It is difficult for this kind of test to be done in practice, because it needs high precision processing. Today, research on the in-place test by the sodium flame method and polydisperse DOP method are under way. Equipment to generate thermally large amounts of NaCl aerosol has been set up. The study of a portable sodium flame photometer has been completed in lab. We are also trying to measure the aerosol concentration by means of a light-scattering particle counter rather than a light-scattering photometer to reduce the amount of DOP used in the in-place test.

On the basis of theoretical derivation and experimental results, a new filter testing procedure was put forward. This procedure is still able to show the influence of pinholes in the media on filter penetration, but it makes a penetration test at 20% of rates flow unnecessary.

3. Mount and Apply of HEPA Filter

For air cleaning in differenct ventilation systems, various forms are adopted to mount the filters, such as bell form (Fig. 4), multi-pit form (Fig. 5), pit form (Fig. 6) and quick-dismantling case form (Fig. 7).

The sealing performance of home-made gum rubber and neoprene closed cell sponge has been investigated in order to improve the efficiency of HEPA filters. The data shown in Fig. 8 and Fig. 9 indicate that the second material can satisfy engineering needs.

II. Removal of Radioactive Iodine and Noble Gases

In this paper we describe mainly some adsorption experimental results although other techniques have been used in practice.

At first, a lot of fruit shell charcoal and coal-based activated carbon were tested in lab. According to their dynamic saturation capacities of adsorption for elemental iodine, the experimental results show that for better adsorbents there are at least three kinds of charcoal: Coconut shell charcoal made in Beijing, oil palm charcoal, and hickory charcoal-201. The experiments also indicate that these charcoals possess larger specific surface areas (about 1000 M^2/g carbon) and high saturation water capacity (about 80%).

Because the beds filled with the charcoal mentioned above were penetrated more quickly by methyl iodide, various impregnated carbons were prepared and examined

for their removal efficiencies under the same conditions. The comparison indicates that when each of the aforesaid three kinds of charcoal was impregnated with TEDA or KI, the impregnated carbon captured the methyl iodide efficiently, and that the impregnated carbons with TEDA are more effective than those impregnated with KI_3. Table 4 summarizes the efficiency test results measured under four groups of test conditions. Furthermore, under another set of conditions, the 5 cm depth beds filled with 5% TEDA impregnated hickory charcoal were continuously challenged with 2 mg/M³ methyl iodide for 240 hours, and penetration still did not exceed 0.06%, Table 5.

Other charcoal properties directly effecting their usage and efficiency for iodine adsorption were examined to evaluate their overall performance. For all the impregnated charcoals listed in Table 4, the ignition temperature was above 396°C, Ball-Pan hardness more than 98, apparent density over 0.4, total ash content less than 3%. They all meet application requirements.

The removal efficiency of charcoals varies with several parameters, that have been extensively investigated, such as relative humidity (R.H.), adsorbate concentration, temperature, superficial velocity, particle size distribution, etc.

Besides activated carbon, some inorganic materials are being studied to remove radioactive iodine from offgases.

At the same time that adsorbers of flow rate 1700 M³/h are being manufactured, other types of adsorbers are being designed for use in even larger ventilation systems.

To guarantee that the manufactured iodine adsorbers have proper efficiency, equipment for nondestructive testing of adsorbers has been built, which can detect leakage to 0.01% in few minutes and the existence of a "thin layer" on the adsorber can be examined. The conditions for leak test are: inlet concentration of freon-112 20 ppm, superficial velocity 1.5 L/cm² min, gas temperature < 40°C, R.H. ≤ 70%, moisture content of carbon ≤ 37%. For "thin layer" examination, inlet concentration of freon-112 120 ppm, R.H. ≤ 50%, moisture content of carbon ≤ 5%.

To retard radioactive noble gases released from some nuclear facilities, adsorption techniques were also studied for application to K_r-air, X-air, X_e-CO_2-air mixtures. The dynamic adsorption coefficients of the gas mixtures on various fruit shell charcoals have been measured. The results show that the coconut shell charcoals with abundant micropores are best in adsorption performance. The adsorption coefficients were investigated as a function of noble gas concentration and temperature. From the experiments, coefficients increasing strongly with decreasing temperature were observed. In some necessary cases a low temperature adsorption technique was adopted to reduce the used carbon volume. It also was noticed that differences in adsorption coefficient exist between xenon and krypton and that the differences get more significant with temperature drop. Based on this fact, we have successfully separated radioactive pure K_r from X_e.

Table 4 Radioiodine/Methyl Iodide Penetration
and Retention Test[1] Results

	Test 1 Methyl Iodide Penetration %	Test 2 Methyl Iodide Penetration %	Test 3 Elemental Iodine Penetration %	Test 4 Elemental Iodine Retention %
5% TEDA + Char. I[2]	0.05	0.2	0.02	99.97
4% KI_3 + Char. I	0.2	0.2	0.06	99.98
4% S_nI_2 + Char. I	1.0	2.7	0.03	99.86
4% S_nI_4 + Char. I	1.3	0.4	0.01	99.90
5% TEDA + Char. II[2]	0.05	0.04	0.01	99.99+
4% KI_3 + Char. II	0.7	0.16	0.01	99.92
4% S_nI_2 + Char. II	4.4	2.0	0.01	99.50
4% S_nI_4 + Char. II	2.3	0.5	0.01	98.00
5% TEDA + Char. III[2]	0.02	0.04	0.04	99.90
4% KI_3 + Char. III	1.7	0.4	0.04	99.84
4% S_nI_2 + Char. III	16.5	0.6	0.8	99.10
4% S_nI_4 + Char. III	8.8	0.9	0.02	99.00

Note (1) The test conditions for Table 4 are as below:

	Test 1	Test 2	Test 3	Test 4
Test Adsorbate	$CH_3^{127}I$ + $CH_3^{125}I$	$CH_3^{127}I$ + $CH_3^{125}I$	^{127}I + ^{125}I	^{127}I + ^{125}I
Test Adsorbate Concentration, mg/M^3	4	4	20	80
Equilibration Period:				
Temp. ^{o}C	30	80	30	30
R.H., %	95	95	95	ambient
Duration, h	16	0	16	0
Feed Period:				
Temp., ^{o}C	30	80	30	30
R.H., %	95	95	95	ambient
Duration, min	120	60	120	10
Elution Period:				
Temp., ^{o}C	30	80	30	180
R.H., %	95	95	95	ambient
Duration, min	240	240	240	240
Absolute Pressure	normal pressure	normal pressure	normal pressure	normal pressure
Gas Velocity, M/min	12	12	12	12
Bed Depth, mm	50	50	50	25
Safety bed Depth mm	30	30	30	30

Note (2): Char. I refers to coconut shell charcoal made in Beijing; char. II, hickory charcoal – 201; char. III, oil palm charcoal.

Table 5 Continuous challenging test

Duration (hour)	20	60	140	180	220	240
Efficiency (%)	100.0	100.0	99.99	99.96	99.96	99.94

Test conditions: temp. 30°C, R.H. 60%, superficial velocity 1.5L/min. cm^2, 5% TEDA+ hickory charcoal, bed depth 5cm.
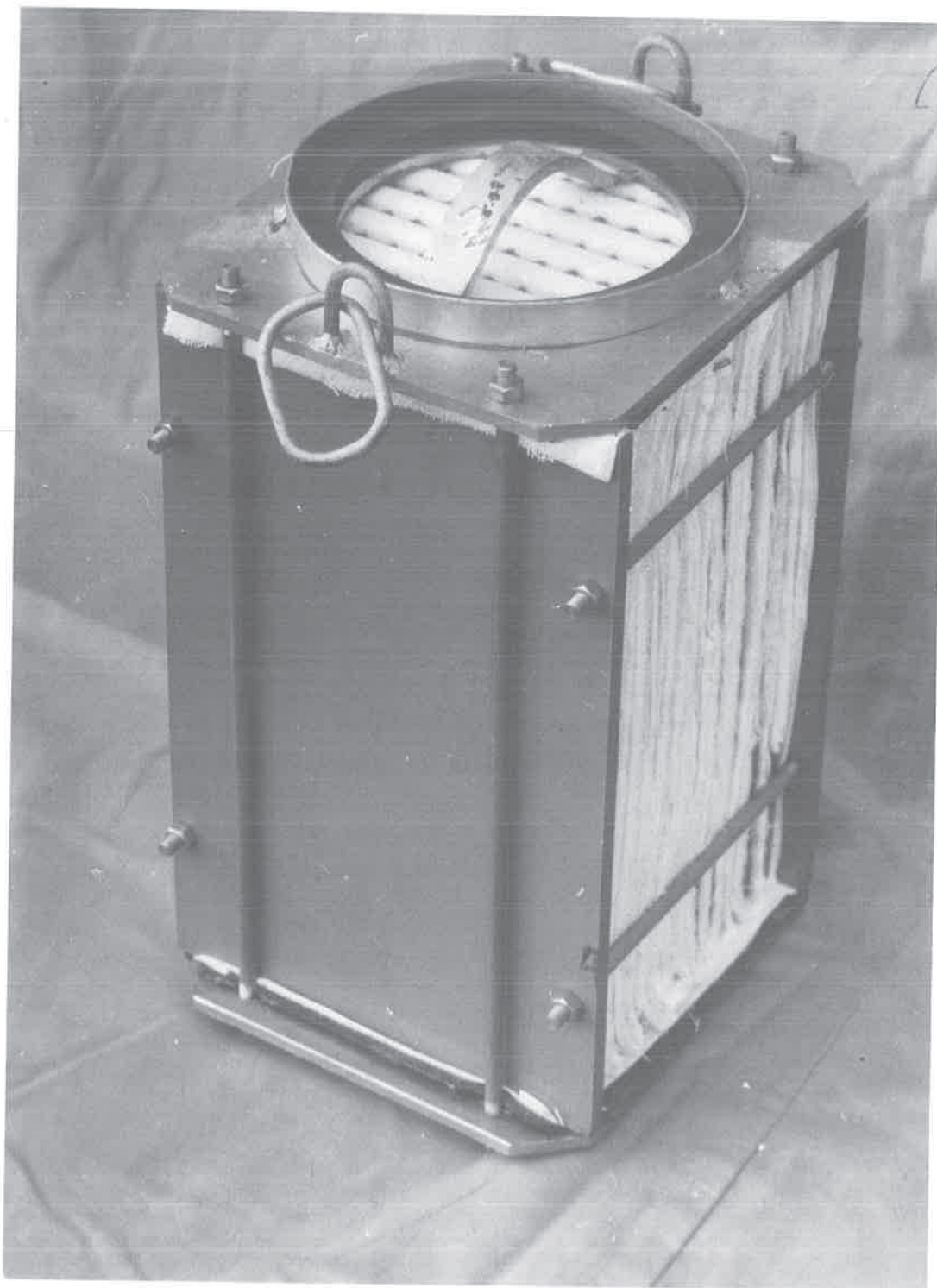
FIGURE 1   PVDC FILTER
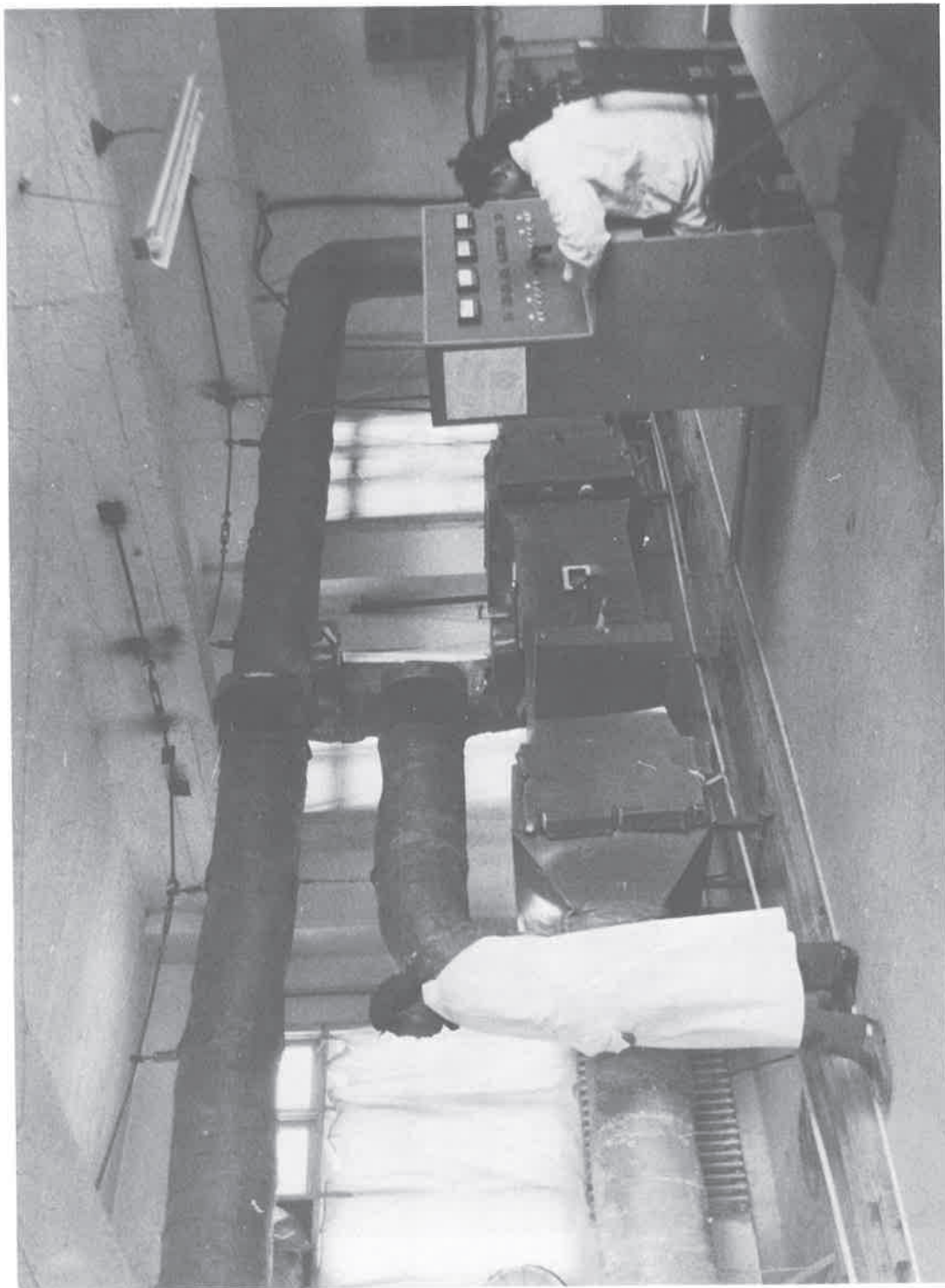
FIGURE 2   ENVIRONMENTAL TEST FACILITY
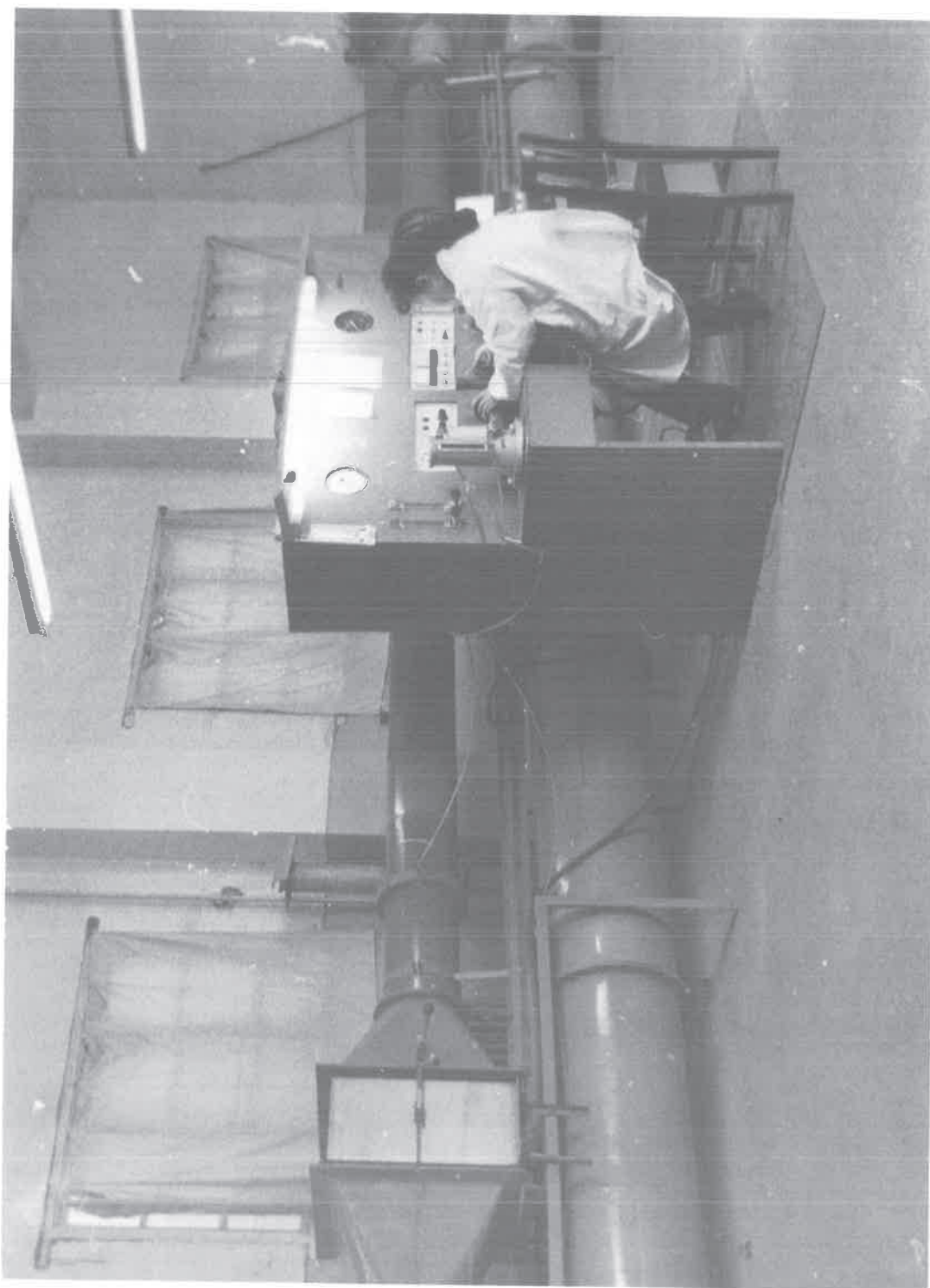
FIGURE 3   A SODIUM FLAME TEST EQUIPMENT
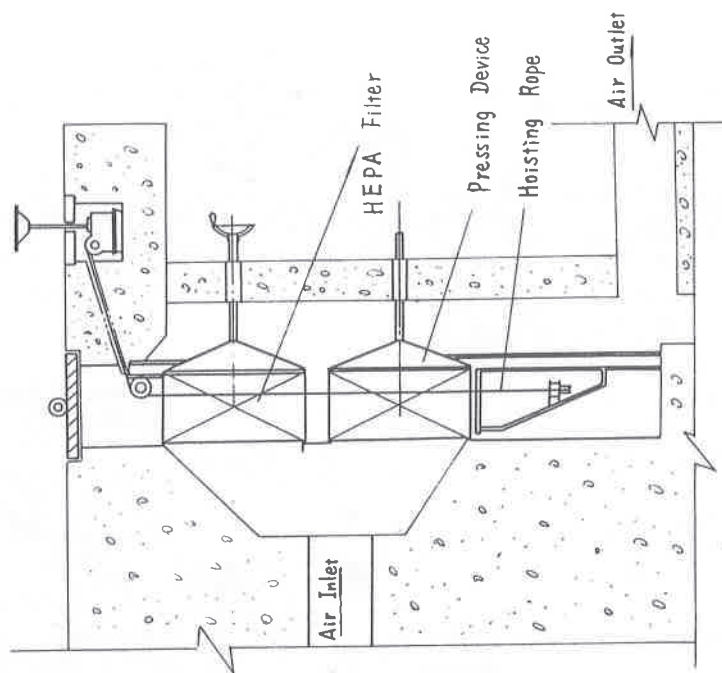
FIGURE 5
MOUNTING SCHEMATIC DIAGRAM
FOR MULTI-PIT FORM
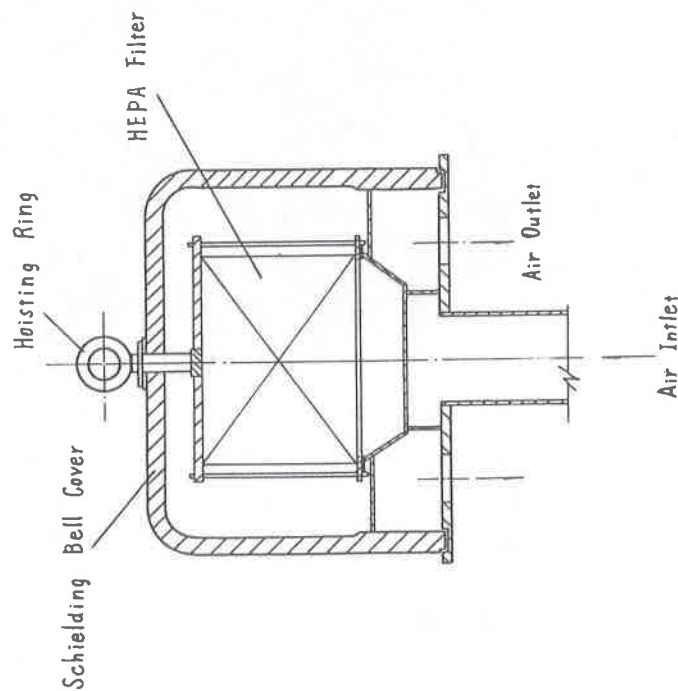
FIGURE 4
MOUNTING SCHEMATIC DIAGRAM FOR BELL FORM

FIGURE 7
MOUNTING SCHEMATIC DIAGRAM FOR
QUICK-DISMALTING CASE FORM

FIGURE 6
MOUNTING SCHEMATIC DIAGRAM
FOR SINGLE PIT FORM
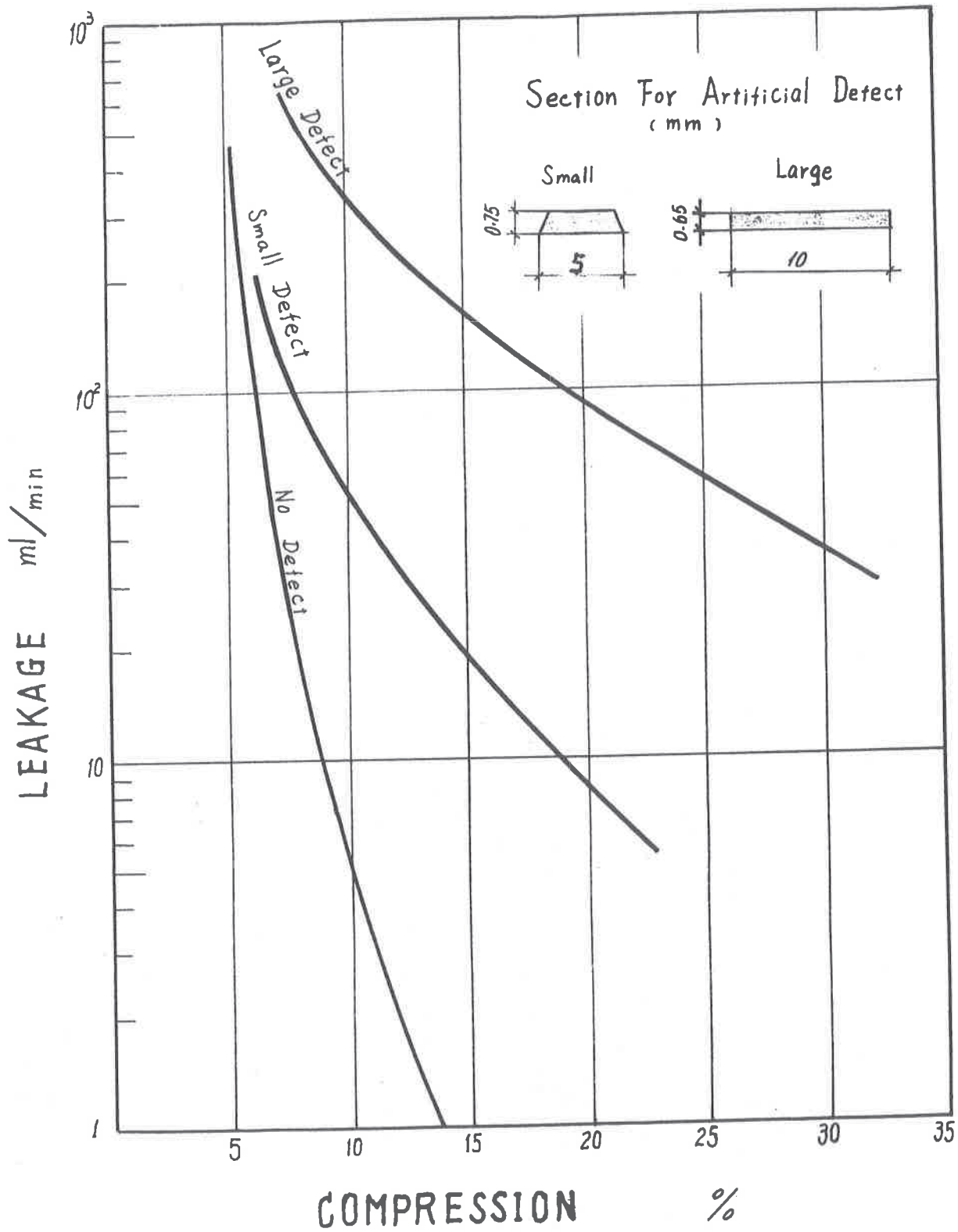
FIGURE 8 CLOSED CELL GUM RUBBER GASKET
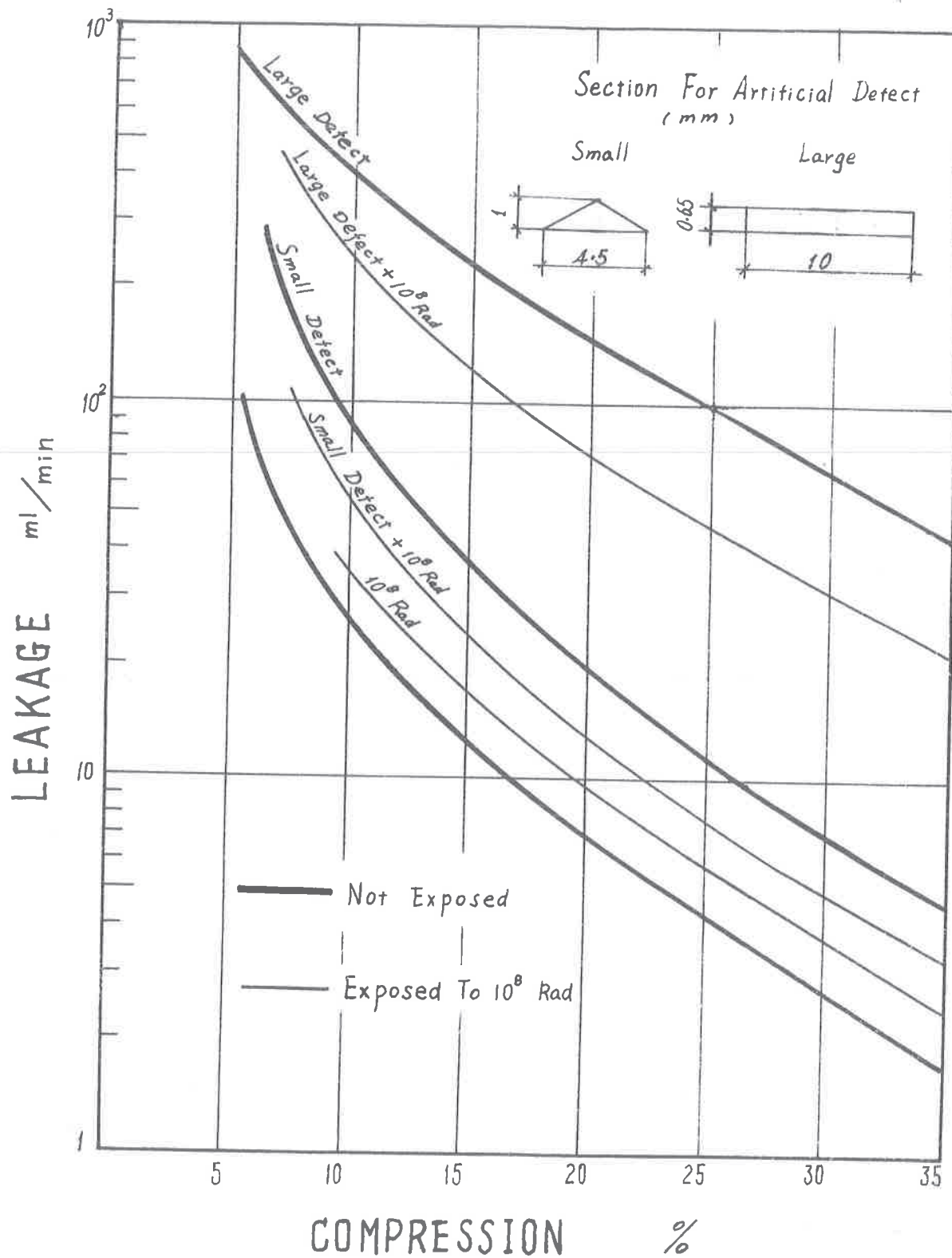
FIGURE 9   CLOSED CELL NEOPRENE GASKET

INDEX OF AUTHORS AND SPEAKERS

LIST OF ATTENDEES

Baltimore, Maryland
August 12-16, 1984

ACIERNO, Thomas
Fluor Engineers, Inc.
3333 Michelson Drive
Irvine, CA   92730

ADAMS, Gregory W.
CRDC
Aberdeen Proving Grounds
MD   21010

AICHELE, Walter
Rockwell Hanford Operations
1306 Cottonwood
Richland, WA   99352

AINSWORTH, David
Sutcliffe Speakman, Inc.
Suite 200
Heaver Plaza
1301 York Road
Lutherville, MD   21093

ALKEN, Werner
Carl Freudenberg, Viledon
Postfach 1369 D-6940
Weinheim
FEDERAL REPUBLIC OF GERMANY

ALLEN, Thomas
Flanders Filters, Inc.
P.O. Box 1708
Washington, NC   27889

AMEND, Juergen
KBT/EA
Kernforschungszentrum
Karlsruhe
Postfach 3640, D-7500
FEDERAL REPUBLIC OF GERMANY

AMIR, Giora
Israel Atomic Energy Comm.
P.O. Box 9001
Beer Sheva S4190
ISRAEL

ANDERSON, Wendell
Technical Consultant
RR #4, Box 4172
La Plata, MD   20646

ARNITZ, Theo
KFK, Karlsruhe
Postfach 2640, D-7500
FEDERAL REPUBLIC OF GERMANY

ARTEAGA, Francisco C.
Techatom, S.A.
SPAIN

ATKINSON, Robert B.
Philadelphia Electric Co.
2301 Market Street
Philadelphia, PA   19101

BARDELL, Timothy W.
UNC Nuclear Industries
P.O. Box 490
Richland, WA   99352

BARNERT-WIEMER, Heidrum
Kernforschungsanlage Julich
Postfach 5170, Julich
FEDERAL REPUBLIC OF GERMANY

BARNES, John B.
Letterkinney Army Depot
SOSLE — QAA
Chambersburg, PA   17201

BARR, James
Westinghouse Idaho Nuclear
P.O. Box 2300
Idaho Falls, ID   83401

BASTIN, Clinton
U.S. Department of Energy
NE 42
Washington, DC   20545

BAUM, Paul W.
P.O. Box 56
Avila Beach, CA   93424

BELLA, Hartmut
Carl Freudenberg, Viledon
Postfach 1369, D-6940
Weinheim
FEDERAL REPUBLIC OF GERMANY

BELLAMY, Ronald
U.S. Nuclear Regulatory Comm.
631 Park Avenue
King of Prussia, PA   19406

BERGMAN, Werner
Lawrence Livermore Labs
L-386
P.O. Box 5505
Livermore, CA   94566

BERNERO, Robert M.
Division of Systems Integration
U.S. Nuclear Regulatory Comm.
Washington, DC 20555

BOARDWAY, John C.
CML, RSCH & DEV. CTR.
Aberdeen Proving Grounds,
    MD   21010

BOHANNON, Michael
BEPA Corporation
3071 E. Colorado Street
Anaheim, CA   92806

BOND, Leroy
Lydall Inc.
P.O. Box 1713
Rochester, NH   03837

BRAUER, Fred
Battelle Northwest
P.O. Box 999
Richland, WA   99352

BRAUN, H.
Federal Ministery of Interior
5300 Bonn
FEDERAL REPUBLIC OF GERMANY

BURNETTI, Armando
Filtra Corporation
104 Wagaraw Road
Hawthorne, NJ   07506

CADWELL, George H.
Flanders Filters, Inc.
P.O. Box 1708
Washington, NC   27889

CAMBELL, Robert
Mine Safety Appliances Co.
R.D. 2
Evans City, PA   16033

CAMBO, Bill
Lydall, Inc.
P.O. Box 1713
Rochester, NH   03837

CAPRIO, Gerald
Vitro Engineering Company
1835 Terminal Drive
Richland, WA   99352

CHEH, Christopher
Ontario Hydro
Chemical Research Division
800 Kipling Avenue
Toronto, Ontario
CANADA M8Z 5S4

CHERRY, John
Charcoal Service Corp.
P.O. Box 3
Bath, NC   27808

CHOI, Eric T.
Ontario Hydro
700 University Avenue
H-18
Toronto, Ontario
CANADA M5G 1X6

CHOI, Seung
Yankee Atomic Electric Co.
1671 Worcester Road
Framingham, MA   01701

CHUANG, K.T.
Atomic Energy of Canada
Chalk River
Ontario
CANADA KOJ 1JO

CHUNG, Kun Mo
Korea Power Engineering
P.O. Box 109
Yeoeuido
Seoul, KOREA

CLIFTON, Frank
Westinghouse Hanford
119 Newport Drive
Oak Ridge, TN   37830

CONLISK, John
Phys. Prot. Div.
CRDC
Aberdeen Proving Ground,
    MD   21010

COSTELLA, George
Lawrence Livermore Labs.
P.O. Box 5505
Livermore, CA   94550

COX, George
Fire Research Station
Dept. of Environment
Building Research Est.
Borehamwood, Hertforshire
ENGLAND WD6 2BL

CROFF, Allen G.
Bldg. 4500N, Rm 233
Oak Ridge National Lab.
P.O. Box X
Oak Ridge, TN   37831

D'AMBROSIA, Julie
U.S. Department of Energy
Office of Waste Operation
    and Technology
Washington, DC   20545

DARR, David B.
U.S. Department of Energy
Savannah River
Aiken, SC   29801

DAUBER, Lyle
U.S. Army Armament, Munition
    and Chemical Command
DRSMC-MAY-MA
Aberdeen Proving Ground,
    MD   21005

DAVIS, Michael
Flanders Filters, Inc.
P.O. Box 1708
Washington, NC   27889

DEITZ, Victor R.
Naval Research Lab.
Code 6170
Washington, DC   20375

DEUBER, Hermann
KFK, Karlsruhe
Postfach 3640, D-7500
FEDERAL REPUBLIC OF GERMANY

DILLMAN, Hans-Georg
KFK, Karlsruhe
Postfach 3640, D-7500
FEDERAL REPUBLIC OF GERMANY

DJERASSI, Henri
Instit de Protection et de
  Surete Nucleaire
91191 Gif-Sur-Yvette
Cedex, FRANCE

DORMAN, R.G.
Consultant
24 Balmoral Road
Salisbury, ENGLAND SP1 3PX

DUNFORD, Gary
Rockwell Hanford Operations
1306 Cottonwood
Richland, WA   99352

DYKES, Maynor
E.I. DuPont
Savannah River Plant
Aiken, SC   29808

DYMENT, John
Atomic Weapons Research Est.
Aldermasten, Reading
ENGLAND RG7   4PR

EDWARDS, James R.
Charcoal Service Corp.
P.O. Box 3
Bath, NC   27808

ELDER, John
Los Alamos National Lab.
P.O. Box 1663
Los Alamos, NM   87545

ELINSKY, Harry C.
Filtech Inc.
215 Bessemer Avenue
East Pittsburgh, PA   15112

ELLIOTT, Robert D.
Flanders Filters, Inc.
P.O. Box 1708
Washington, NC   27889

ELLIOTT, William
Rockwell International Lab.
P.O. Box 464
Golden, CO   80401

ENDLER, Jerry
ANCO Engineers, Inc.
9937 Jefferson Blvd.
Culver City, CA   90232

ENGLISH, David
CML, RSCH & DEV Center
Aberdeen Proving Ground,
   MD   21010

ENSINGER, V.
KFK, Karlsruhe
Postfach 3640, D-7500
FEDERAL REPUBLIC OF GERMANY

ETHERIDGE, E.L.
United Nuclear Industries
P.O. Box 490
Richland, WA   99352

ETTINGER, Harry J.
Los Alamos National Lab.
P.O. Box 1663
Los Alamos, NM   87545

EVANS, Gary
E.I. DuPont
Bldg. 735A
Savannah River Plant
Aiken, SC   29801

EVANS, R. John
Hollingsworth & Vose Co.
112 Washington Street
East Walpole, MA   02032

FAIN, D.E.
Martin Mariette Energy Systems
P.O. Box P
Oak Ridge, TN   37830

FAIRHURST, W.A.
British Nuclear Fuels
Risley, Warrington
Cheshire
ENGLAND WA3 6AS

FEIZOLLAHI, Fred
Bechtel National Lab.
P.O. Box 3965
San Francisco, CA   94119

FERNANDEZ, Jean-Marie
CEA, CEN Valrho
CEZE, FRANCE

FERNANDEZ, Steven
Westinghouse Idaho Nuclear
P.O. Box 2800
Idaho Falls, ID   83408

FIRST, Melvin W.
Harvard School of Public
    Health
665 Huntington Avenue
Boston, MA   02115

FOELIX, Charles
General Electric Co.
Knowlls Atomic Power Lab.
Bldg A3-99, Box 1072
Schenectady, NY   12302

FOLKERS, Charles
Lawrence Livermore Nat. Lab.
Livermore, CA   04550

FORRESTER, D.J.
Atomic Weapons Research Est.
Aldermasten, Reading
ENGLAND RG7 4PR

FRANKENBERG, Ronald
CVI Inc.
P.O. Box 2138
Columbus, OH   43216

FREEMAN, W. Peter
Nuclear Consulting Services
6400 Huntlet Road
Columbus, OH   43229

FRY, Frank
Hollingsworth & Vose Co.
112 Washington Street
East Walpole, MA   02032

GAMMILL, W.P.
U.S. Nuclear Regulatory Comm.
Effluent Treatment System
Washington, DC   20555

GEENS, Ludo
S.C.K./C.E.N.
Boeretang 200, B-2400
Mol, BELGIUM

GEER, John A.
2395 Darthmouth Avenue
Boulder, CO   80303

GEISEKE, James A.
Battelle
Columbus Laboratories
Columbus, OH   43201

GIBBS, Roger L.
Naval Surface Weapons Ctr.
G-51
Dahlgren, VA   22448

GILBERT, Humphrey
P.O. Box 704
McLean, VA   22101

GILL, Charles F.
U.S. Nuclear Regulatory Comm.
Glen Ellyn, IL   60137

GILMIRE, Robert
Hanford Environmental
P.O. Box 490
Richland, WA   99352

GLADDEN, David
Tooele Army Depot
SDSTE-CAME
Tooele, UT   84074

GLISSMEYER, John
Pacific Northwest Lab.
P.O. Box 999
Richland, WA   99352

GORBUNOV, S.
TAEA
Wagramer Ste., 5
Vienna, AUSTRIA

GOULET, Roger T.
Cambridge Filter Corp.
P.O. Box 4906
Syracuse, NY   13221

GRAVES, Curtis E.
Nuclear Consulting Services
P.O. Box 29151
Columbus, OH   43229

GREEN, Frank
Lawrence Livermore Nat. Lab.
P.O. Box 808
Livermore, CA   04550

GREGONIS, Robert A.
Rockwell Hanford Operations
P.O. Box 800
Richland, WA 99352

GREGORY, William
Los Alamos National Lab.
P.O. Box 1663
Los Alamos, NM   87545

GROENIER, William S.
Martin Marietta Energy Systems
Oak Ridge National Lab
P.O. Box X
Oak Ridge, TN   37831

GUEST, Alan
Ontario Hydro
700 University Avenue
Toronto, Ontario
CANADA M5G 1X6

GUEVARA, Frank
Los Alamos National Lab.
1680 N. Sage
Los Alamos, NM   87544

GUNN, Charles
Mine Safety Appliance
R.D. 2
Evans City, PA   16033

GUO, Liang Tian
Institute of Radiation & Protection
  of Ministry of Nuclear Industry
POX 120
Taiyuan, Shanxi
PEOPLE'S REPUBLIC OF CHINA

HALSEY, Tim
Barnabey Cheney
P.O. Box 2526
Columbus, OH   43216

HARTIG, Stefan
Universitaet Karlsruhe
Kaiserstrasse 12
FEDERAL REPUBLIC OF GERMANY

HAYES, John J.
U.S. Nuclear Regulatory Comm.
Washington, DC   20555

HEBEL, W.
European Communities
Rue de la Loi 200
Brussels, BELGIUM

HENRICH, Edmund
KFK, Karlsruhe
Inst. Heisse Chemie
Postfach 3640, D-7500
FEDERAL REPUBLIC OF GERMANY

HERMAN, Ray
Rockwell Hanford
1954 Sheridan Place
Richland, WA   99352

HERRING, Warren M.
Test Equipment Shop
Baltimore Gas & Electric
Calvert Cliffs Nuclear Power
Lusby, MD   20657

HESBOL, Rolf
Sudsvik Energiteknik AB
S-611 82 Nykoeping
SWEDEN

HOLLMAN, Ronald K.
Flanders Filters, Inc.
P.O. Box 1708
Washington, NC   27889

HORN, Hans-Georg
Lergebiel Strahlenschutz
Templegraben 55
D-5100
Aachen
FEDERAL REPUBLIC OF GERMANY

HUBBARD, Dean
Duke Power Company
P.O. Box 33189
Charlotte, NC   28242

HUI, Liu
Bieging Instit. of Nuclear
   Engineering
P.O. Box 840
Beijing, CHINA

HULL, Andrew P.
Step. Div.
Brookhaven National Lab
Upton, NY   11973

HUSSEINI, Ahmed
Consumer & Corporate Affairs
Government of Canada
220 Woodridge Cres.
Apt. 504
Nepean, Ontario
CANADA

HUTTEN, Marshall
James River-Rochester Inc.
340 Mill Street
Rochester, MI   48063

HYDER, M. Lee
E.I. DuPont Company
Savannah River Lab
Aiken, SC   29808

ISHIDA, Seiji
HVAC Consultant
4-14 Yokokawa
Hachioji City
Tokyo, JAPAN

JACKSON, Roger D.
Goodyear Atomic Corp.
P.O. Box 628
Piketon, OH   45661

JACOX, John W.
Jacox Associates
1445 Summit Street
Columbus, OH   43229

JANNAKOS, Konstantin
KFK, Karlsruhe
Postfach 3640, D-7500
FEDERAL REPUBLIC OF GERMANY

JEFFORD, J. David
Ontario Hydro
700 University Avenue, H-10
Toronto, Ontario
CANADA M5G 1X6

JENKINS, Dwayne B.
GPU Nuclear
Three Mile Island
P.O. Box 480
Middletown, PA   17057

JENSEN, Dan D.
GA Technologies Inc.
P.O. Box 85608
San Diego, CA   92138

JENSEN, Richard
Rockwell International
P.O. Box 3450
Golden, CO   80401

JOHNSTON, Stephen
Delta Filter Corp.
14 Arch Street
Watervliet, NY   12189

KABAT, Milo
Ontario Hydro
757 McKay Road
Pickering, Ontario
CANADA   L1W 3C8

KAGAN , Richard J.
National Inst. of Health
Radiation Safety
Building 21
Bethesda, MD   20215

KAISERUDDING, Mohammed
Sargent & Lundy
55 E Monroe Street
Chicago, IL   60603

KAJIWARA, Shigeki
JGC Corporation
1-14-1 Bessho
Takahama
JAPAN 232

KEATING, W. Gregg
Johns-Manville Company
P.O. Box 143
Braintree, MA   02184

KELLEY, Claud
Kaiser Engineers
Hanford
Richland, WA   99352

KIKUCHI, Ko
Power Reactor & Nuclear
Fuel Development Corp.
Ibaraki-ken, Japan

KIM, Prof. Yony W.
Dept. of Physics
Bldg 16
Lehiegh Univ.
Bethlehem, PA· 18015

KIM, You Sun
Korea Advanced Energy
 Research Inst.
P.O. Box 7
Chyungryang, Seoul
Korea

KIRCHNER, K. N.
Rocky Flats Plant
Energy Systems Group
Rockwell International Corp
Golden, CO   80401

KLAES, Leo J.
Tennessee Valley Authority
wllcl06c-k
400 W. Summit Hill Dr.
Knoxville, TN   37902

KOBAYASHI, Yasutoshi
Japan Nuclear Fuel·Service
Fukokuseimei Bldg.
2-2, 2-Chome, Uchisaiwaicho
Chiyado-ku, Tokyo,
Japan

KONDO, Yoshikazu
Hitachi Works
Hitachi Ltd.
1-1 Saiwaicho 3 chome
Hitachi-shi, Ibaraki-ken
Japan 317

KOTRA, Janet
Advisory Committee Reactor
  Safeguard
Mail Stop H-ST-1016
U.S. Nuclear Regulatory Com
Washington, DC 20555

KOVACH, Bela
NUCON
P.O. Box 29151
Columbus, OH 43229

KOVACH, J. Louis
Nuclear Consulting Services
P.O. Box 29151
Columbus, OH 43229

KRATZKE, Robert
Office of Nuclear Safety
U.S. Dept of Energy
PE-221, GTN
Washington, DC 20545

LAHNER, Klaus
BBR-Brown Boveri Reaktor
Dudnestr, 44
6800 Mannheim
FEDERAL REPUBLIC OF GERMANY

LAMBERGER, Paul H.
Monsanto Research Corp.
Mound
P.O. Box 32
Miamisburgh, OH 45342

LANDIS, John W.
4 Whispering Lane
Weston, MA 02193

LANGHORST, Susan
University of Missouri
Research Reactor Facility
Columbia, MO 65211

LECKIE, Fred
Nuclear Containment Systems
4555-41 Groves Road
Columbus, OH 43216

LEINONEN, Paul
Ontario Hydro
700 University Avenue
H10C22
Toronto, Ontario
CANADA M5G 1X6

LEUDET, Alain
Comm. d l'Energie Atomique
Centre d'Etudes Nucleaires
P.O. 6 Font-aux-Roses
92260 Paris
FRANCE

LEVY, M.
Atomic Energy of Canada
P.O./C.P. Box 13500
Kanata, Ontario
CANADA K2K 1X8

LIGHTFOOT, W.R.
Florida Power & Light
P.O. Box 529100
Miami, FL 33152

LITTLE, D.K.
Martin Marietta Energy Systems
P.O. Box P
Oak Ridge, TN 37831

LITTLEFIELD, Peter
Yankee Atomic Electric Co.
1671 Worcester Road
Framingham, MA   01701

MacAULAY, Thomas
E.I. DuPont de Nemours
Engineering Department
Louviers Building Rm. 4327
Wilmington, DE   19898

MACHIELS, Albert J.
EPRI
P.O. Box 10712
Palo Alto, CA   94303

MAIER, Peter
Technischer Ueberwachungs
Verein - Dudenstrk 28
FEDERAL REPUBLIC OF GERMANY

MALINAUSKAS, A.P.
Oak Ridge National Lab.
P.O. Box X
Oak Ridge, TN   37830

MANLEY, Dennis
Mine Safety Appliances
R.D. 2
Evans City, PA   16033

MARCHANT, Ira
Westinghouse Idaho Nuclear
P.O. Box 2800
Idaho Falls, ID   83401

MARTIN, R.A.
Los Alamos National Lab
P.O. Box 1663
Los Alamos, NM   87545

MASON, Allen S.
Los Alamos National Lab
Mail Stop J-514
P.O. Box 1663
Los Alamos, NM   87545

MATHEWES, Wolfgang
Kraftwerk Union
Berliner Strasse 2950299
Postfach 962
D-6050 Offenbach Am Main
FEDERAL REPUBLIC OF GERMANY

McCORMACH, J.D.
Westinghouse Hanford
P.O. Box 1970
Bldg. 22 T-HE
Richland, WA   99352

McDONOUGH, John
Mine Safety Appliances Co.
R.D. 2
Evans City, PA   16033

McGILL, Michael
Philadelphia Electric
2301 Market Street
Philadelphia, PA   19115

McMANUS, Gary
Westinghouse Idaho Nuclear
P.O. Box 2800
Idaho Falls, ID   84301

MELLINGER, Peter
Battelle Northwest Lab
P.O. Box 999
Richland, WA   99352

MILLER, William, Jr.
Sargent & Lundy
55 E. Monroe Street
Chicago, IL   60603

MOELLER, Dade W.
Harvard School of Public
   Health
Continuing Education
677 Huntington Avenue
Boston, MA   02115

MONSON, Paul R.
E.I. DuPont de Nemours Co.
Savannah River Lab
Aiken, SC   29801

MORGAN, Michael G.
North Anna Power Station
P.O. Box 402
Mineral, VA   23117

MORRISON, Robert W.
Physical Protection Division
Chem. Res. & Dev. Center
Aberdeen Proving Grounds,
   MD   21010

MULCEY, Philippe
CEA - Centre de Etudes
   Nucleaire
91191 Gif-Sur-Yvette
Cedex, FRANCE

MURTHY, Kesh
Battelle Pacific Northwest
Richland, WA   99352

NAKAZAWA, Kiyohiko
Shin Nippon Air Conditioning
Engineering Co,, Led.
1-1-34, Nakahara
Isogo-ku, Yokohama
JAPAN

NARUKI, K.
Power Reactor Nuclear
   Fuel Dev. Corp.
Toaka Works
Tokai-Mura 1 Baragi-ken
JAPAN

NORMANN, Bard
Studsvik Energiteknik AB
Reactor Sys/Nuc. Safety
S-611 82 Nykoping
SWEDEN

O'KADA, Takeshi
Kobe Steel, Ltd.
Wakinohama Cho 1-1
Fukiai-ku
Kobe, JAPAN

OMA, Ken H.
Battelle Northwest
P.O. Box 999
Richland, WA   99352

O'NAN, Alex
American Air Filter Co.
215 Central Avenue
Louisville, KY   40277

ORNBERG, Stephen C.
Sargent & Lundy
55 E Monroe St.
Chicago, IL 60603

ORTIZ, John
Los Alamos National Lab.
P.O. Box 1663
Los Alamos, NM   87545

OSLINGER, Arne
Ontario Hydro
700 University Avenue
H-10 C-12
Toronto, Ontario
CANADA   M5G 1X6.

OTUSKA, Kazuhiki
Nitta Industries Corp.
172 Ikezawa-cho
Yamato Koriyama
Nara, JAPAN

OURFALI, Mounir
Sappico-Saudi Arabia
P.O. Box 2828
Rivadh, SAUDI ARABIA

OZAWA, Yoshihiro
Hitachi
1168 Moriyama-cho
Hitachi-shi
Ibaraki-key, 316 JAPAN

PANCHUCK, Fred
Atomic Energy of Canada Ltd.
Chalk River Ontario KOJ IJO
CANADA

PAPAVRAMIDIS, Dimitri
Ontario Hydro
700 University Avenue
Toronto, Ontario
CANADA M5G 1X6

PARSONS, Robert D.
Hollingsworth & Vose Company
112 Washington Street
East Walpole, MA   02032

PEARSON, John
Nuclear Containment Systems
4555-41 Groves Road
Columbus, OH   43216

PENCE, Dallas T.
Science Applications, Inc.
4030 Sorrento Valley Blvd.
San Diego, CA   92124

PERKINS, William
E.I. DuPont de Nemours Co.
Savannah River Lab
Aiken, SC   29801

PHILIPPI, H.M.
Atomic Energy of Canada
Chalk River
Ontario, CANADA KOJ 1P0

PHILIPPONE, Richard L.
U.S. DOE
Oak Ridge Operations
P.O. Box E
Oak Ridge, TN   37830

PHILIPPS, Daniel
Cleveland Electric Illumin.
10 Center Road SB-311
Perry, OH   44081

PIERCE, Mary
Hollingsworth & Vose Co.
Townsen Road
West Groton, MA   01472

PISTRITTO, Joseph
Research Division
U.S. Army CRDC
Aberdeen Proving Grounds,
 MD   21020

PORCO, Richard
Mine Safety Appliance Co.
R.D. 2
Evans City, PA 16033

POREMBSKI, Thaddeus
Westinghouse Electric Co.
955 Tahita Road
Jacksonville, FL 32216

PORREY, Douglas
Ionex Research Corp.
P.O. Box 602
Broomfield, CO   80020

PRATT, Ronald Philip
U.K. Atomic Energy Author.
Bldg. 10 Harwell
Dicot, Oxon
ENGLAND

PYSH, W.A.
620 West 6th Street
Erie, PA 16507

QI-DONG, Li
Fudan University
Dept. of Nuclear Science
Shanghai
PEOPLE'S REPUBLIC OF CHINA

QUANTE, M. John
Particle Measuring System
101 Fairway Drive
Washington, NC 27889

RE, Gary C.
New York Power Authority
123 Main Street
White Plains, NY   10601

REDDICK, Randy
U.S. DOE
P.O. Box 5400
Albuquerque, NM   87115

RINGEL, H.D.
Instit for Chem. Tech.
Kernforschungsanlage Julich
5170 Julich
FEDERAL REPUBLIC OF GERMANY

ROBINSON, Keith
U.K. Atomic Energy Author.
Harwell, Oxforshire
ENGLAND, OXII ORA

ROBERSON, Philip W.
Duke Power Company
McGuire Nuclear Station
P.O. Box 488
Cornelius, NC   28031

RYDER, Christopher
Nuclear Regulatory Comm.
Washington, DC   20555

RYDER, Douglas
Lydall Inc.
1 Wakefield Street
Rochester, NH   03867

RUEDINGER, V.
Kernforschungszentrum
  Karlsruhe
Postfach 3640, D-7500
FEDERAL REPUBLIC OF GERMANY

SALMINE, Olli P.
Finnish Center for Radiation
 & Nuclear Safety PL/PB
P.O. Box 268
SF 00101
Helsinki 19, FINLAND

SCANLAN, T.F.
Oak Ridge National Lab
P.O. Box X
Oak Ridge, TN 37830

SCARPELLINO, C.W.
E.G. & G. Idaho
Idaho National Engineering
  Lab
P.O. Box 1625
Idaho Falls, ID 83415

SCHEFFEL, Norman B.
Manville Products Corp.
P.O. Box 5108
Denver, CO   80217

SCHULZ, Jorge
Bechtel Power Corp.
P.O. Box 3965
San Francisco, CA   94119

SCHWARTZ, Frank, R., Jr.
North American Carbon, Inc.
432 McCormick Blvd.
Columbus, OH   43212

SCRIPSICK, Ronald
Los Alamos National Lab.
P.O. Box 1663
MS-K-486
Los Alamos, NM   87545

SEEL, Richard
General Dynamics Reactor
 Plant Services
285 Eastern Point Road
P.O. Box 1147
Groton, CT   06340

SGALAMBRO, Gaetano
ENEA-DISP/ACO
Via Vitaliano Brancati 48
Rome, ITALY 00144

SIGLI, Paul
Sofiltra-Poelman
71 DB, National
La Garenne Columes
92255 FRANCE

SKAFI, Michael
R-362 KWU
6050 Offenbach Am Main
Berliner Str. 295-29G
Postfach 964
FEDERAL REPUBLIC OF GERMANY

SMITH, George P.
Chemical Research & Dev. Center
Attn: DRSMC-CLW-E (A)
Aberdeen Proving Grounds, MD 21010

SMITH, Phillip P.
New Mexico State University
P.O. Box 3450
Las Cruce, NM 88003

SMITH, Wayne
Mine Safety Appliances
R.S. 2
Evans City, PA 16033

SMITHERMAN, R.L.
Martin Marietta Energy Systems
P.O. Box P
MS-324
Oak Ridge, TN 37831

SNOVER, M.W.
Hollingsworth & Vose Co.
112 Washington Street
East Walpole, MA 02032

SODERHOLM, Sid
Los Alamos National Lab
P.O. Box 1663
Los Alamos, NM 87545

SPEIDEL, Robert W.
NUS Corporation
910 Clooper Road
Gaithersburgh, MD 20878

SPERANZINI, Robert A.
Atomic Energy of Canada
Chalk River Nuclear Lab
Chalk River, Ontario
CANADA JOJ IJO

STEINBERG, Samuel
Air Techniques Inc.
1801 Whitehead Road
Baltimore, MD 21207

SWARTOUT, C.W.
Rockwell International
P.O. Box 464
Golden, Co 80401

TAKIMOTO, Y.
6-9 Takara-Machi
Babcock-Hitachi K.K.
Kure City, Hiroshima
JAPAN

TANAKA, Takeaki
Toshiba
Isogo Engineering Center
8, Shinsugita-cho
Isogo-ku
Yokohama 235, JAPAN

TERADO, Kazuji
Rockwell International
P.O. Box 464
Golden, CO 80401

THOMAS, M.G.
Lydall Inc.
P.O. Box 1713
Rochester, NH 03867

THOMAS, R. Thomas
Westinghouse Idaho Nuclear
P.O. Box 4000
Idaho Falls, ID 83415

TINKLIN, B.
Mitchell Cotts Air Filtration
Kent, England

TOURNAS, Arthur
Lydall Inc.
1 Wakefield Street
Rochester, NH 03867

VIKIS, A.C.
Atomic Energy of Canada
WNRE
Pinawa, Manitoba
CANADA ROE 1L0

VOGAN, Thomas J.
Florida Power & Light Co.
P.O. Box 1400
Juno Beach, FL 33408

VOGELHUBER, Bill
Barnebey-Cheney Co.
P.O. Box 2526
Columbus, OH 43216

VOILLEQUE, Paul
Science Application Inc.
P.O. Box 696
Idaho Falls, ID 83402

von AMMON, Reinhard
Kernforschungszentrum
Instit fu Heisse Chemie
Postfach 3640
D-75 Karlsruhe
FEDERAL REPUBLIC OF GERMANY

WALDEN, Richard
International Filter Co.
P.O. Box MM
Cathedral City, CA 92230

WALKER, R.
Atomic Energy Control Bd.
Government of Canada
Ottawa Centre District
Services Offices Ottawa, Ontairo
CANADA

WAMBACH, Paul
Department of Energy
OOS 1PE-241
Washington, DC 20545

WATCHER, Peter
Air Filter Service
3 Commerce Street
Sumter, SC 29150

WATSON, Brian W.
Safety & Reliability Dir.
U.K. Atomic Energy Author.
Culcheth, Warrington
ENGLAND WA3 4NE

WEISHAPL, Robert
E.I DuPont Company
Engineering Dept L-4323
Wilmington, DE 19898

WHITE, E.R.
E.G. & G. Idaho Inc.
P.O. Box 1625
Idaho Falls, ID 83415

WHITELY, E.F.
Lydall, Inc.
P.O. Box 1713
Rochester, NH 03867

WICHMANN, Hans-Peter
Wiederaufarbeitungsanlage
Karlsruhe
Betriebsges
FEDERAL REPUBLIC OF GERMANY

WIKTORSSON, Christer
National Instit. of Radiat.
  Protection
S-10401, Stockholm
SWEDEN

WILHELM, J.G.
Kernforschungszentrum Karlsruhe
Postfach 3640
D-7500 Karlsruhe
FEDERAL REPUBLIC OF GERMANY

WILLIAMS, John
Letterkenny Army Depot
SDSLE-MEE
Chambersburg, PA 17201

WILLIS, Charles
Nuclear Regulatory Comm.
Bethesda, MD 20014

WOODRING, D.F.
Martin Marietta Energy Systems
MS0324
P.O. Box P
Oak Ridge, TN 37831

WUSCHKE, Donna
Atomic Energy of Canada Res.
Whiteshell Nuclear Res. Est.
Pinawa, Manitoba
CANADA ROE 1L0

YASUDA, Yukio
Shin Nippon Air Conditioning
Engineering Co., Ltd.
1-1-34 Nakahara
Isogo-ku, Yokama
JAPAN

YODER, Robert E.
Rockwell International
P.O. Box 464
Golden, CO 80401

ZACHARIAS, John
Whatman Inc.
9 Bridwell Place
Clifton, NJ 07014

ZIPPLER, Donald
E.I. DuPont de Nemours
Savannah River Plant
Aiken, SC 29801

INDEX TO THE 17th AND 18th AEC/ERDA/DOE

NUCLEAR AIR CLEANING CONFERENCES*

NUCLEAR STANDARDS MANAGEMENT CENTER

Oak Ridge National Laboratory
Oak Ridge, Tennessee 37831

TABLE OF CONTENTS

PART I

Index of Papers by Conference

Conference No.	Title	Author
17-0010	Welcome and Objectives of Conference	First, M. W.
17-0013	Keynote Address	Mattson, R. J.
17-0021	Potential Air Cleaning Problems in Fusion Reactors	Crocker, J. G.
17-0036	Nuclear Standards and Safety Progress in Nuclear Standards Development	Fish, J. F.
17-0040	Balance and Behavior of Gaseous Radionuclides Released During Initial PWR Fuel Reprocessing Operations	Leudet, A. Miguel, P. Goumondy, J. P. Charrier, G.
17-0051	Time-Dependent Analyses of Dissolver Off-Gas Cleaning Installations in a Reprocessing Plant	Nagle, K. Furrer, J. Becker, G. Obrowski, W. Seghal, Y. P. Weymann, J.
17-0075	A Model of Iodine-129 Process Distributions in a Nuclear Fuel Reprocessing Plant	McManus, G. J. Duce, F. A. Fernandez, S. J. Murphy, L. P.
17-0099	Carbon Dioxide-Krypton Separation and Radon Removal from Nuclear Fuel Reprocessing Off-Gas Streams	Hirsch, P. M. Higuchi, K. Y. Abraham, L.
17-0123	Adsorption of Gaseous RuO_4 by Various Sorbents II	Vujisic, Lj. Nikolic, R.

Conference No.	Title	Author
17-0131	Test Results in the Treatment of HTR Reprocessing Off-Gas	Barnert-Wiemer, H. Bendick, B. Juergens, B. Nafissi, A. Vygen, H. Krill, W
17-0151	Surface Deposition of Radon Decay Products with and Without Enhanced Air Motion	Rudnick, S. N. Maher, E. F. Hinds, W. C. First, M. W.
17-0172	Formation and Characterization of Fission-Product Aerosols Under Postulated HTGR Accident Conditions	Tang, I. N. Munkelwitz, H. R.
17-0183	Organic Iodine Removal from Simulated Dissolver Off-Gas Streams Using Partially Exchanged Silver Mordenite	Jubin, R. T.
17-0199	A Parametric Study on Removal Efficiency of Impregnated Activated Charcoal and Silver Zeolite for Radioactive Methyl Iodide	Shiomi, H. Yuasa, Y. Tani, A. Ohki, M. Nakagawa, T.
17-0223	Data Analysis of In-Place Tests of Iodine Filters in the French Nuclear Facilities	Mulcey, P. Trehen, L. Rouyer, J. L.
17-0239	Iodine Filtering for French Reprocessing Plants	Bruzzone, G. Rouyer, J. L. Mulcey, P. Vaudano, A.
17-0248	Retention of Elemental Radioiodine by Deep Bed Carbon Filters Under Accident Conditions	Deuber, H. Wilhelm, J. G.

Conference No.	Title	Author
17-0278	Experiences with a Charcoal Guard Bed in a Nuclear Power Plant	Scholten, L. C.
17-0285	Deposition of Airborne Radioiodine Species on Surfaces of Metals and Plastics	Kabat, M. J.
17-0305	Off-Gas Characteristics of Liquid-Fed Joule-Heated Ceramic Melters	Goles, R. W. Sevigny, G. J.
17-0333	Immobilization of Krypton-85 in Zeolite 5A	Christensen, A. B. Del Debbio, J. A. Knecht, D. A. Tanner, J. E. Cossel, S. C.
17-0358	The Long-Term Storage of Radioactive Krypton by Fixation in Zeolite 5A	Penzhorn, R. D. Leitzig, H. Gunther, K. Schuster, P. Noppel, H. E.
17-0371	Volatilization and Trapping of Ruthenium in High Temperature Processes	Klein, M. Weyers, C. Goossens, W. R. A.
17-0381	Plant for Retention of 14-C in Reprocessing Plants for LWR Fuel Elements	Braun, H. Gutowski, H. Bonka, H. Grundler, D.
17-0400	Mechanism of the $CO_2-Ca(OH)_2$ Reaction	Chew, V. S. Cheh, C. H. Glass, R. W.
17-0414	14-C Release at Light Water Reactors	Kunz, C.
17-0431	Carbon-14 Immobilization Via the $Ba(OH)_2 \cdot 8H_2O$ Process	Haag, G. L. Nehls, Jr., J. W. Young, G. C.

Conference No.	Title	Author
17-0457	Vertical Removable Filters in Shielded Casing for Radioactive Cells and Process Gaseous Wastes	Prinz, M.
17-0482	Development of Filters and Housings for Use on Active Plant	Hackney, S. Pratt, R. P.
17-0504	Aerosol Filtration with Metallic Fibrous Filters	Klein, M. Goossens, W. R. A.
17-0523	Evaluation of Permanently Charged Electrofibrous Filters	Biermann, A. H. Lum, B. Y. Bergman, W.
17-0548	Evaluation of Prototype Electrofibrous Filters for Nuclear Ventilation Ducts	Bergman, W. Kuhl, W. D. Biermann, A. H. Johnson, J. S. Lum, B. Y.
17-0576	A New Method of Determining the Overall Particle Decontamination Factor for Multiple Off-Gas Cleaning Components in Reprocessing Plants	Furrer, J. Linek, A.
17-0591	In-Situ Control of Filtration Systems in France: 5 Years Experience	DuPoux, J.
17-0602	Air Cleaning Philosophy in a Nuclear Materials Fabrication Plant	Ward, F. Y. Yoder, R. E.
17-0612	System Operational Testing of Major Ventilation Systems for a Plutonium Recovery Facility	Linck, Jr., F. J.

Conference No.	Title	Author
17-0626	New Adsorbent, Silver-Alumina for Radioactive Iodine Filter	Kikuchi, M. Funabashi, K. Kawamura, F. Yusa, H. Tsuchiya, H. Takashima, Y.
17-0641	Charcoal Performance Under Simulated Accident Conditions	Deitz, V. R.
17-0652	Teda Vs. Quinuclidine: Evaluation and Comparison of Two Tertiary Amine Impregnants for Methyl Iodide Removal from Flow Air Stream	Kovach, J. L. Grimm, J. J. Freeman, W. P.
17-0664	Experiments on Adsorptive Retention of NOx and Krypton from Dissolver Off-Gas	Ringel, H.
17-0683	Formation and Behaviour of Nitric Oxides in a Cryogenic Krypton Separation System and Consequences of Using Air as Process Gas	Ammon von, R. Bumiller, W. Hauss, E. Hutter, E. Neffe, G. Hammer, R. R.
17-0694	Noble Gas Removal and Concentration by Combining Fluorocarbon Absorption and Adsorption Technologies	Little, D. K. Eby, R. S. Norton, J. L. Patton, J. L. Schultz, R. M. Varagona, J. M.
17-0768	Failures in Air-Cleaning, Air-Monitoring, and Ventilation Systems in Commercial Nuclear Power Plants (1/1/78 - 12/31/81)	Moeller, D. W. Casper Sun, L. S.

Conference No.	Title	Author
17-0771	Report of Minutes of Government-Industry Meeting on Filters, Media, and Media Testing	Anderson, W. L.
17-0775	A Review of DOE Filter Test Facility Operations 1970-1980	Burchsted, C. A.
17-0788	DOE Filter Test Program - Policy for the '80s	Bresson, J. F.
17-0790	A Survey of HEPA Filter Experience	Carbaugh, E. H.
17-0801	Potential Application of a Single Particle Aerosol Spectrometer for Monitoring Aerosol Size at the DOE Filter Test Facilities	Salzman, G. C. Ettinger, H. J. Tillery, M. I. Wheat, L. D. Grace, W. K.
17-0821	Operational Experience Using Diethylhexylsebacate (DEHS) as a Challenge Test Aerosol in Filter Testing	Gilmore, R. D. McIntyre, J. A. Petersen, G. R.
17-0836	The Need for Revising U. S. Nuclear Regulatory Commission Regulatory Guide 1.52 in Light of NRC-Sponsored Research Program Results and Other Developments	Bangart, R. L.
17-0847	In-Place HEPA Filter Aerosol Test System	Herman, R. L.
17-0867	In-Place Realtime HEPA Filter Test Method	Hohorst, F. A. Fernandez, S. J.
17-0882	DOP Testing HEPA Filter Banks in Series	Hanson, W. D.

Conference No.	Title	Author
17-0895	The Effect of Particle Size Variation on Filtration Efficiency Measured by the HEPA Filter Quality Assurance Test	Tillery, M. I. Salzman, G. C. Ettinger, H. J.
17-0909	Performance of 1000- and 1800- CFM HEPA Filters on Long Exposure to Low Atmospheric Dust Loadings, III	First, M. W. Price, J. M.
17-0919	Portable Filter Testing Instrumentation Used for In-Place Leak Testing of Large Air Filters up to 38 m3 sec-1 (80,000 CFM)	Kovach, J. L. Kovach, B. J. Powers, F. L. Johnson, W. A.
17-0937	Polymeric Diffusion as Applied to a Radioiodine Off-Gas Monitor	Fernandez, S. J. Murphy, L. P.
17-0952	Energy and Fear	Specter, H.
17-0990	Methods for Nuclear Air Cleaning System Accident Consequence Assessment	Andrae, R. W. Bolstad, J. W. Gregory, W. S. Krause, F. R. Martin, R. A. Tang, P. K. Ballinger, M. Y. Chan, M. K. Glissmeyer, J. A. Mishima, J. Owczarski, P. C. Sutter, S. L. Compere, E. L. Godbee, H. W. Bernstein, S.
17-1003	HEPA Filter Experience During Three Mile Island Reactor Building Purges	Bellamy, R. R.
17-1011	Simulation of Forced Ventilation Fires	Krause, F. R. Gregory, W. S.

Conference No.	Title	Author
17-1030	Fire Testing of HEPA Filters Installed in Filter Housings	Hackney, S.
17-1051	Response of HEPA Filters to Simulated Accident Conditions	Gregory, W. S. Martin, R. A. Smith, P. R. Fenton, D. E.
17-1069	HEPA Filter Response to High Air Flow Velocities	Ruedinger, V. Wilhelm, J. G.
17-1093	Effects of Shock Waves on High Efficiency Filter Units	Cuccuru, A. Cultrera, S. Marandola, U. Lanza, S.
17-1110	The Development of a Lightweight, Compactible/Disposable HEPA Filter	Allan, T. T.
17-1115	Evaluation of HEPA Filters Meeting MIL-F-51068 Purchased on the Open Market. Are They Nuclear Grade?	Allan, T. T. Cramer, R. V.
17-1121	Recent Changes in MIL-F-51068 Specification	Smith, G. P.
17-1125	Development and Evaluation of Acid-Resistant HEPA Filter Media	Brassell, G. W. Thorvaldson, W. G.
17-1134	A Changeable Bed Activated Carbon Filter with High Accuracy and Efficiency	Stiehl, H. Lippold, H. J. Mathewes, W.
17-1142	Iodine Removal by Silver-Exchanged Zeolite Filters from the Vessel Off-Gas in Tokai Reprocessing Plant	Kawaguchi, A. Fukushima, M. Miyahara, K. Matsumoto, K.

Conference No.	Title	Author
18-0033	Regeneration of the Iodine Isotope-Exchange Efficiency for Nuclear-Grade Activated Carbons	Deitz, V. R.
18-0044	Influence of Aging on the Retention of Elemental Radioiodine by Deep Bed Carbon Filters Under Accident Conditions	Deuber, H.
18-0065	Long-Term Desorption of 131-I from KI-Impregnated Charcoals Loaded with CH3-I, Under Simulated Post-LOCA Conditions	Vikis, A. C. Wren, J. C. Moore, C. J. Fluke, R. J.
18-0078	A Study of Adsorption Properties of Impregnated Charcoal for Airborne Iodine and Methyl Iodide	Qi-dong, L Sui-yuang, H.
18-0093	Evaluation of Quaternary Ammonium Halides for Removal of Methyl Iodide from Flowing Air Streams	Freeman, W. P. Mohacsi, T. G. Kovach, J. L.
18-0098	Investigations on the Extremely Low Retention of 131-I by an Iodine Filter of a Boiling Water Reactor	Deuber, H. Gerlach, K. Wilhelm, J. G.
18-0116	Transmission of Radioiodine Through Sampling Lines	Unrein, P. J. Pelletier, C. A. Cline, J. E. Voilleque, P. G.
18-0127	Analyses of Charcoal Filters Used in Monitoring Radioactive Iodines	Langhorst, S. M.

Conference No.	Title	Author
18-0145	Commentary on Nuclear Power Plant Control Room Habitability - Including a Review of Related LERs (1981-1983)	Moeller, D. W. Kotra, J. P.
18-0162	NRC Study of Control Room Habitability	Hayes, Jr., J. J. Muller, D. R. Gammill, W. P.
18-0184	Ventilation of Nuclear Rooms and Operators' Protection	Vavasseur, C.
18-0188	Performance Evaluation of Control Room HVAC and Air Cleaning Systems Under Accident Conditions	Almerico, F. Machiels, A. J. Ornberg, S. C. Lahti, G. P.
18-0217	Monitoring of Noble Gas Radioisotopes in Nuclear Power Plant Effluents	Kabat, M. J.
18-0233	Noble Gas Confinement for Reactor Fuel Melting Accidents	Monson, P. R.
18-0244	Technical Feasibility and Costs of the Retention of Radionuclides During Accidents in Nuclear Power Plants Demonstrated by the Example of a Pressurized Water Reactor	Braun, H. Grigull, R. Lahner, K. Gutowski, H. Weber, J.
18-0260	Design Experiments for a Vented Containment	Hesbol, R.
18-0277	In-Situ Continuous Scanning High Efficiency Particulate Air (HEPA) Filter Monitoring System	Kirchner, K. N. Johnson, C. M. Lucerna, J. J. Barnett, R. L.

Conference No.	Title	Author
18-0299	In-Place Testing of Multiple Stage Filter Systems Without Disruption of Plant Operations in the Plutonium Facility at Los Alamos	Ortiz, J. P.
18-0311	Projects on Filter Testing in Sweden	Normann, B. Wiktorsson, C.
18-0327	Effect of DOP Heterodispersion on HEPA-Filter Penetration Measurements	Bergman, W. Beirmann, A.
18-0348	A New Procedure for Testing HEPA Filters	Hui, L. Nian Song, X. Tian Liang, G.
18-0357	The Design of Graded Filtration Media in the Diffusion-Sedimentation Regime	Robinson, K. S.
18-0373	A Dispersion Model for Airborne Particulates Inside a Building	Perkins, W. C. Stoddard, D. H.
18-0400	Selected Operating Results of the Passat Prototype Dissolver Off-Gas Cleaning System	Amend, J. Furrer, J. Kaempffer, R.
18-0423	Treatment of the Off-Gas Stream from the HTR Reprocessing Head-End	Barnert-Wiemer, H. Jurgens, B. Vijgen, H.
18-0434	Test Results from the GA Technologies Engineering-Scale Off-Gas Treatment System	Jensen, D. D. Olguin, L. J. Wilbourn, R. G.
18-0451	Experience of Iodine Removal in Tokai Reprocessing Plant	Kikuchi, K. Komori, Y. Takeda, K.

Conference No.	Title	Author
18-0461	Iodine-129 Process Control Monitor for Evaporator Off-Gas Streams	Burr, J. R. McManus, G. J.
18-0472	Continuous Chemical Cold Traps for Reprocessing Off-Gas Purification	Henrich, E. Bauder, U. Steinhardt, H. J. Bumiller, W.
18-0495	Development of the ELEX Process for Tritium Separation at Reprocessing Plants	Bruggeman, A. Meynendonckx, L. Parmentier, C. Goossens, W. R. A. Baetsle, L. H.
18-0513	The Search for Greater Stability in Nuclear Regulation	Asselstine, J. K.
18-0526	Seismic Simulation and Functional Performance Evaluation of a Safety Related, Seismic Category I Control Room Emergency Air Cleaning System	Manley, D. K. Porco, R. D. Choi, S. H.
18-0555	Comparison and Verification of Two Computer Programs Used to Analyze Ventilation Systems Under Accident Conditions	Hartig, S. H. Wurz, D. E. Arnitz, T. Ruedinger, V.
18-0572	Response of Air Cleaning System Dampers and Blowers to Simulated Tornado Transients	Gregory, W. Idar, E. Smith, P. Hensel, E. Smith, E.
18-0597	Fire Simulation in Nuclear Facilities - The FIRAC Code and Supporting Experiments	Burkett, M. W. Martin, R. A. Fenton, D. L. Gunaji, M. V.

Conference No.	Title	Author
18-0629	The Mathematical Modelling of Fire in Forced Ventilated Enclosures	Cox, G. Kumar, S.
18-0644	Fission Product Source Terms and Engineered Safety Features	Malinauskas, A. P.
18-0647	Aerosol Challenges to Air Cleaning Systems During Severe Accidents in Nuclear Plants	Gieseke, J. A.
18-0655	Utility View of the Source Term and Air Cleaning	Littlefield, P. S.
18-0659	Source Terms in Relation to Air Cleaning	Bernero, R. M.
18-0667	Choice of Materials for the Immobilization of 85-Krypton in a Metallic Matrix by Combined Ion Implantation and Sputtering	Whitmell, D. S.
18-0683	Off-Gas Treatment and Characterization for a Radioactive In Situ Vitrification Test	Oma, K. H. Timmerman, C. L.
18-0702	The Behaviour of Ruthenium, Cesium and Antimony During Simulated HLLW Vitrification	Klein, M. Weyers, C. Goossens, W. R. A.
18-0732	Predictions of Local, Regional and Global Radiation Doses from Iodine-129 for Four Different Disposal Methods and an All-Nuclear Future	Wuschke, D. M. Barnard, J. W. O'Connor, P. A. Johnson, J. R.

Conference No.	Title	Author
18-0755	Summary of United States Activities in Commercial Nuclear Airborne Waste Management	Groenier, W. S.
18-0761	Research and Development on Air Cleaning System of Reprocessing Plant in Japan	Naruki, K.
18-0775	Status of R&D in the Field of Nuclear Airborne Waste Sponsored by the European Community	Hebel, W.
18-0780	Development of Technologies for the Waste Management of I-129, Kr-85, C-14 and Tritium in the Federal Republic of Germany	Henrich, E. Ebert, K.
18-0803	Use of Acoustic Field in Gas Cleaning	Bouland, D. Madelaine, G. Malherbe, C.
18-0825	Removal of Radon Decay Products with Ion Generators - Comparison of Experimental Results with Theory	Maher, E. F. Rudnick, S. N. Moeller, D. W.
18-0846	Prototype Firing Range Air Cleaning System	Glissmeyer, J. A. Mishima, J. Bamberger, J. A.
18-0873	Calculating Released Amounts of Aerosols	Nagel, K. Furrer, J.
18-0897	Regulatory Experience with Nuclear Air Cleaning	Bellamy, R. R.
18-0904	Field Testing of Nuclear Air Cleaning Systems at Duke Power Company	Hubbard, D. M.

Conference No.	Title	Author
18-0918	NATS Field Testing Observations and Recommendations	Jacox, J. W.
18-0921	In-Place Testing of Non ANSI-N509 Designed System	Lightfoot, W. R.
18-0938	Alternative Modes for Cryogenic Krypton Removal	Geens, L. P. Goossens, W. R. A. Collard, G. E. R.
18-0951	Behaviour of Impurities in a Cryogenic Krypton Removal System	Ammon von, R. Bumiller, W. Hutter, E. Knittel, G. Mas, C. Neffe, G.
18-0959	Selective Absorption of Noble Gases in Freon-12 at Low Temperatures and Atmospheric Pressure	Henrich, E. Hufner, R. Weirich, F. Bumiller, W. Wolff, A.
18-0982	Chromatographic Separation of Krypton from Dissolver Off-Gas at Low Temperatures	Ringel, H. Mubler, M.
18-0998	Control Decisions for 3-H, 14-C, 85-Kr, and 129-I Released from the Commercial Fuel Cycle	Thomas, T. R. Brown, R. A.
18-1004	Krypton Control Alternatives	Henrich, E. Ammon von, R. Ebert, K.
18-1019	Health Risk Assessment for Fuel Reprocessing Plant	Mellinger, P. J.
18-1026	How Much Dose Reduction Could be Achieved by Collection and Disposal of 129-I and 14-C?	Wuschke, D. M.

Conference No.	Title	Author
18-1036	A Procedure to Test HEPA-Filter Efficiency Under Simulated Accident Conditions of High Temperature and High Humidity	Ensinger, U. Rudinger, V. Wilhelm, J. G.
18-1058	Limits of HEPA-Filter Application Under High-Humidity Conditions	Rudinger, V. Ricketts, C. I. Wilhelm, J. G.
18-1085	Development of a HEPA-Filter with High Structural Strength and High Resistance to the Effects of Humidity and Acid	Alken, W. Bella, H. Werke, C. F. Rudinger, V. Wilhelm, J. G.
18-1097	Simoun: High Temperature Dynamic Test Rig for Industrial Air Filters	DuPoux, J. Mulcey, P. Rouyer, J. L. Tarrago, X.
18-1107	Performance Testing of HEPA Filters Under Hot Dynamic Conditions	Pratt, R. P. Green, B. L.
18-1128	Report of Minutes of Government-Industry Meeting on Filters, Media, and Media Testing	Anderson, W. L.
18-1131	Evaluation of Methods, Instrumentation and Materials Pertinent to Quality Assurance Filter Penetration Testing	Scripsick, R. C. Soderholm, S. C. Tillery, M. I.
18-1144	Department of Energy Filter Test Program Policy for the 80's	Bresson, J. F.
18-1149	Intermediate Results of a One-Year Study of a Laser Spectrometer in the DOE Filter Test Facilities	Soderholm, S. C. Tillery, M. I.

Conference No.	Title	Author
18-1168	Calibration and Use of Filter Test Facility Orifice Plates	Fain, D. E. Selby, T. W.
18-1186	Results of CONAGT-Sponsored Nuclear-Grade Carbon Test Round Robin	First, M. W.
18-1190	CONAGT's Nuclear Carbon Round Robin Test Program	Bellamy, R. R.
18-1193	Development of a New Technique and Instrumentation for Rapid Assessment of Filter Media	Kim, Y. W.
18-1209	Experience in Startup, Preoperational and Acceptance Testing of Nuclear Air Treatment Systems in Nuclear Power Plants	Jacox, J. W.
18-1224	Krypton-85 Health Risk Assessment for a Nuclear Fuel Reprocessing Plant	Mellinger, P. J. Brackenbush, L. W. Tanner, J. E. Gilbert, E. S.
18-1242	The Theory and Practice of Nitrogen Oxide Absorption	Counce, R. M.
18-1258	NOx Removal from Nuclear Fuel Reprocessing Plants Off-Gas by Catalytic Reduction with NH3	Hattori, S. Kobayashi, Y. Katoh, Y. Takimoto, Y. Kunikata, M.
18-1283	Removal of 14-C from Nitrogen Annulus Gas	Cheh, C. H.
18-1300	Development of a Wetproofed Catalyst Recombiner for Removal of Airborne Tritium	Chuang, K. T. Quaiattini, R. J. Thatcher, D. R. P. Puissant, L. J.

Conference No.	Title	Author
18-1311	Tritium Management for Fusion Reactors	Rouyer, J. L. Djerassi, H.
18-1318	Development of a Method to Determine Iodine Specific Activity in Process Off-Gases by GC Separation and Negative Ionization Mass Spectrometry	Fernandez, S. J. Rankin, R. A. McManus, G. J. Nielson, R. A.
18-1343	Removal of Iodine from Off-Gas of Nuclear Fuel Reprocessing Plants with Silver Impregnated Adsorbents	Hattori, S. Kobayashi, Y. Ozawa, Y. Kunikata, M.
18-1361	Volatile Ruthenium Trapping on Silica Gel and Solid Catalysts	Cains, P. W. Yewer, K. C.
18-1378	Recovery and Purification of Xe-135 as a By-Product of Mo-99 Production Using Linde 5A Molecular Sieve	Briden, N. A. Speranzini, R. A.
18-1399	Two-Detector Dioctylphthalate (DOP) Filter Testing Method and Statistical Interpretation of Data	Dauber, L. Barnes, J. Appel, W.
18-1417	A Filter Concept to Control Airborne Particulate Releases Due to Severe Reactor Accidents and Implementation Using Stainless-Steel Fiber Filters	Dillman, H. G. Pasler, H.
18-1429	Dual Aerosol Detector Based on Forward Light Scattering with a Single Laser Beam	Kovach, B. J. Custer, R. A. Powers, F. L. Kovach, A.

Conference No.	Title	Author
18-1436	Test Data and Operation Data from Carbon Used in High Velocity Systems	Edwards, J. R.
18-1441	BORA - A Facility for Experimental Investigation of Air Cleaning During Accident Situations	Rudinger, V. Arnitz, T. Ricketts, C. I. Wilhelm, J. G.
18-1470	Spring Loaded Hold-Down for Mounting HEPA Filters at Rocky Flats	Terada, K. Rose, C. R. Garcia, A. G.
18-1478	Technical Development of Nuclear Air Cleaning in the People's Republic of China	Qun, L. X. Hui, L. Shen, W. T. Niam, X. S. Tian, G. L.
18-1480	CONAGT's Place in ASME's Centennial Year	Miller, Jr., W. H.
18-1495	Air Cleaning in Accident Situations	Kovach, J. L.

P A R T   II

Index of Papers by Author(s)

Author	Title	Conference No.
Abraham, L.	Carbon Dioxide-Krypton Separation and Radon Removal from Nuclear Fuel Reprocessing Off-Gas Streams	17-0099
Alken, W.	Development of a HEPA-Filter with High Structural Strength and High Resistance to the Effects of Humidity and Acid	18-1085
Allan, T. T.	The Development of a Lightweight, Compactible/Disposable HEPA Filter	17-1110
Allan, T. T.	Evaluation of HEPA Filters Meeting MIL-F-51068 Purchased on the Open Market. Are They Nuclear Grade?	17-1115
Almerico, F.	Performance Evaluation of Control Room HVAC and Air Cleaning Systems Under Accident Conditions	18-0188
Amend, J.	Selected Operating Results of the Passat Prototype Dissolver Off-Gas Cleaning System	18-0400
Ammon von, R.	Formation and Behaviour of Nitric Oxides in a Cryogenic Krypton Separation System and Consequences of Using Air as Process Gas	17-0683
Ammon von, R.	Behaviour of Impurities in a Cryogenic Krypton Removal System	18-0951

Author	Title	Conference No.
Ammon von, R.	Krypton Control Alternatives	18-1004
Anderson, W. L.	Report of Minutes of Government-Industry Meeting on Filters, Media, and Media Testing	17-0771
Anderson, W. L.	Report of Minutes of Government-Industry Meeting on Filters, Media, and Media Testing	18-1128
Andrae, R. W.	Methods for Nuclear Air Cleaning System Accident Consequence Assessment	17-0990
Appel, W.	Two-Detector Dioctylphthalate (DOP) Filter Testing Method and Statistical Interpretation of Data	18-1399
Arnitz, T.	Comparison and Verification of Two Computer Programs Used to Analyze Ventilation Systems Under Accident Conditions	18-0555
Arnitz, T.	BORA - A Facility for Experimental Investigation of Air Cleaning During Accident Situations	18-1441
Asselstine, J. K.	The Search for Greater Stability in Nuclear Regulation	18-0513
Baetsle, L. H.	Development of the ELEX Process for Tritium Separation at Reprocessing Plants	18-0495

Author	Title	Conference No.
Ballinger, M. Y.	Methods for Nuclear Air Cleaning System Accident Consequence Assessment	17-0990
Bamberger, J. A.	Prototype Firing Range Air Cleaning System	18-0846
Bangart, R. L.	The Need for Revising U. S. Nuclear Regulatory Commission Regulatory Guide 1.52 in Light of NRC-Sponsored Research Program Results and Other Developments	17-0836
Barnard, J. W.	Predictions of Local, Regional and Global Radiation Doses from Iodine-129 for Four Different Disposal Methods and an All-Nuclear Future	18-0732
Barnert-Wiemer, H.	Test Results in the Treatment of HTR Reprocessing Off-Gas	17-0131
Barnert-Wiemer, H.	Treatment of the Off-Gas Stream from the HTR Reprocessing Head-End	18-0423
Barnes, J.	Two-Detector Dioctylphthalate (DOP) Filter Testing Method and Statistical Interpretation of Data	18-1399
Barnett, R. L.	In-Situ Continuous Scanning High Efficiency Particulate Air (HEPA) Filter Monitoring System	18-0277
Bastin, C. B.	Advancement in Reprocessing Technology	18-0004

Author	Title	Conference No.
Bauder, U.	Continuous Chemical Cold Traps for Reprocessing Off-Gas Purification	18-0472
Becker, G.	Time-Dependent Analyses of Dissolver Off-Gas Cleaning Installations in a Reprocessing Plant	17-0051
Beirmann, A.	Effect of DOP Heterodispersion on HEPA-Filter Penetration Measurements	18-0327
Bella, H.	Development of a HEPA-Filter with High Structural Strength and High Resistance to the Effects of Humidity and Acid	18-1085
Bellamy, R. R.	HEPA Filter Experience During Three Mile Island Reactor Building Purges	17-1003
Bellamy, R. R.	Regulatory Experience with Nuclear Air Cleaning	18-0897
Bellamy, R. R.	CONAGT's Nuclear Carbon Round Robin Test Program	18-1190
Bendick, B.	Test Results in the Treatment of HTR Reprocessing Off-Gas	17-0131
Benjamin, A. S.	Cost-Benefit Considerations for Filtered-Vented Containment Systems	17-1201
Bergman, W.	Evaluation of Permanently Charged Electrofibrous Filters	17-0523

Author	Title	Conference No.
Bergman, W.	Evaluation of Prototype Electrofibrous Filters for Nuclear Ventilation Ducts	17-0548
Bergman, W.	Effect of DOP Heterodispersion on HEPA-Filter Penetration Measurements	18-0327
Bernero, R. M.	New Source Terms: What do They Tell Us About Engineered Safety Feature Performance?	18-0011
Bernero, R. M.	Source Terms in Relation to Air Cleaning	18-0659
Bernstein, S.	Methods for Nuclear Air Cleaning System Accident Consequence Assessment	17-0990
Biermann, A. H.	Evaluation of Permanently Charged Electrofibrous Filters	17-0523
Biermann, A. H.	Evaluation of Prototype Electrofibrous Filters for Nuclear Ventilation Ducts	17-0548
Bolstad, J. W.	Methods for Nuclear Air Cleaning System Accident Consequence Assessment	17-0990
Bonka, H.	Plant for Retention of 14-C in Reprocessing Plants for LWR Fuel Elements	17-0381
Bouland, D.	Use of Acoustic Field in Gas Cleaning	18-0803
Brackenbush, L. W.	Krypton-85 Health Risk Assessment for a Nuclear Fuel Reprocessing Plant	18-1224

Author	Title	Conference No.
Brassell, G. W.	Development and Evaluation of Acid-Resistant HEPA Filter Media	17-1125
Braun, H.	Plant for Retention of 14-C in Reprocessing Plants for LWR Fuel Elements	17-0381
Braun, H.	Technical Feasibility and Costs of the Retention of Radionuclides During Accidents in Nuclear Power Plants Demonstrated by the Example of a Pressurized Water Reactor	18-0244
Bresson, J. F.	DOE Filter Test Program - Policy for the '80s	17-0788
Bresson, J. F.	Department of Energy Filter Test Program Policy for the 80's	18-1144
Briden, N. A.	Recovery and Purification of Xe-135 as a By-Product of Mo-99 Production Using Linde 5A Molecular Sieve	18-1378
Brown, R. A.	Control Decisions for 3-H, 14-C, 85-Kr, and 129-I Released from the Commercial Fuel Cycle	18-0998
Bruggeman, A.	Development of the ELEX Process for Tritium Separation at Reprocessing Plants	18-0495
Bruzzone, G.	Iodine Filtering for French Reprocessing Plants	17-0239

Author	Title	Conference No.
Bumiller, W.	Formation and Behaviour of Nitric Oxides in a Cryogenic Krypton Separation System and Consequences of Using Air as Process Gas	17-0683
Bumiller, W.	Continuous Chemical Cold Traps for Reprocessing Off-Gas Purification	18-0472
Bumiller, W.	Behaviour of Impurities in a Cryogenic Krypton Removal System	18-0951
Bumiller, W.	Selective Absorption of Noble Gases in Freon-12 at Low Temperatures and Atmospheric Pressure	18-0959
Burchsted, C. A.	A Review of DOE Filter Test Facility Operations 1970-1980	17-0775
Burkett, M. W.	Fire Simulation in Nuclear Facilities – The FIRAC Code and Supporting Experiments	18-0597
Burr, J. R.	Iodine-129 Process Control Monitor for Evaporator Off-Gas Streams	18-0461
Cains, P. W.	Volatile Ruthenium Trapping on Silica Gel and Solid Catalysts	18-1361
Carbaugh, E. H.	A Survey of HEPA Filter Experience	17-0790

Author	Title	Conference No.
Casper Sun, L. S.	Failures in Air-Cleaning, Air-Monitoring, and Ventilation Systems in Commercial Nuclear Power Plants (1/1/78 - 12/31/81)	17-0768
Chan, M. K.	Methods for Nuclear Air Cleaning System Accident Consequence Assessment	17-0990
Charrier, G.	Balance and Behavior of Gaseous Radionuclides Released During Initial PWR Fuel Reprocessing Operations	17-0040
Cheh, C. H.	Mechanism of the CO2-Ca(OH)2 Reaction	17-0400
Cheh, C. H.	Removal of 14-C from Nitrogen Annulus Gas	18-1283
Chew, V. S.	Mechanism of the CO2-Ca(OH)2 Reaction	17-0400
Choi, S. H.	Seismic Simulation and Functional Performance Evaluation of a Safety Related, Seismic Category I Control Room Emergency Air Cleaning System	18-0526
Christensen, A. B.	Immobilization of Krypton-85 in Zeolite 5A	17-0333
Chuang, K. T.	Development of a Wetproofed Catalyst Recombiner for Removal of Airborne Tritium	18-1300
Cline, J. E.	Transmission of Radioiodine Through Sampling Lines	18-0116

Author	Title	Conference No.
Collard, G. E. R.	Alternative Modes for Cryogenic Krypton Removal	18-0938
Compere, E. L.	Methods for Nuclear Air Cleaning System Accident Consequence Assessment	17-0990
Cooper, D. W.	Venturi Scrubbing for Filtered Vented Containment	17-1175
Cossel, S. C.	Immobilization of Krypton-85 in Zeolite 5A	17-0333
Counce, R. M.	The Theory and Practice of Nitrogen Oxide Absorption	18-1242
Cox, G.	The Mathematical Modelling of Fire in Forced Ventilated Enclosures	18-0629
Cramer, R. V.	Evaluation of HEPA Filters Meeting MIL-F-51068 Purchased on the Open Market. Are They Nuclear Grade?	17-1115
Crocker, J. G.	Potential Air Cleaning Problems in Fusion Reactors	17-0021
Cuccuru, A.	Effects of Shock Waves on High Efficiency Filter Units	17-1093
Cultrera, S.	Effects of Shock Waves on High Efficiency Filter Units	17-1093
Custer, R. A.	Dual Aerosol Detector Based on Forward Light Scattering with a Single Laser Beam	18-1429

Author	Title	Conference No.
Dauber, L.	Two-Detector Dioctylphthalate (DOP) Filter Testing Method and Statistical Interpretation of Data	18-1399
Deitz, V. R.	Charcoal Performance Under Simulated Accident Conditions	17-0641
Deitz, V. R.	Regeneration of the Iodine Isotope-Exchange Efficiency for Nuclear-Grade Activated Carbons	18-0033
Del Debbio, J. A.	Immobilization of Krypton-85 in Zeolite 5A	17-0333
Deuber, H.	Retention of Elemental Radioiodine by Deep Bed Carbon Filters Under Accident Conditions	17-0248
Deuber, H.	Influence of Aging on the Retention of Elemental Radioiodine by Deep Bed Carbon Filters Under Accident Conditions	18-0044
Deuber, H.	Investigations on the Extremely Low Retention of 131-I by an Iodine Filter of a Boiling Water Reactor	18-0098
Dillman, H. G.	A Filter Concept to Control Airborne Particulate Releases Due to Severe Reactor Accidents and Implementation Using Stainless-Steel Fiber Filters	18-1417

Author	Title	Conference No.
Dillmann, H. G.	Experimental Investigations of Aerosol Filtration with Deep Bed Fiber Filters	17-1160
Djerassi, H.	Tritium Management for Fusion Reactors	18-1311
Duce, F. A.	A Model of Iodine-129 Process Distributions in a Nuclear Fuel Reprocessing Plant	17-0075
DuPoux, J.	In-Situ Control of Filtration Systems in France: 5 Years Experience	17-0591
DuPoux, J.	Simoun: High Temperature Dynamic Test Rig for Industrial Air Filters	18-1097
Dyment, J.	The Development of Mobile Filtration Units for Use in Radioactive Facilities	17-1152
Ebert, K.	Development of Technologies for the Waste Management of I-129, Kr-85, C-14 and Tritium in the Federal Republic of Germany	18-0780
Ebert, K.	Krypton Control Alternatives	18-1004
Eby, R. S.	Noble Gas Removal and Concentration by Combining Fluorocarbon Absorption and Adsorption Technologies	17-0694
Edwards, J. R.	High-Efficiency Charcoal Air Filter with Combustible Frame	17-1157

Author	Title	Conference No.
Edwards, J. R.	Test Data and Operation Data from Carbon Used in High Velocity Systems	18-1436
Ensinger, U.	A Procedure to Test HEPA-Filter Efficiency Under Simulated Accident Conditions of High Temperature and High Humidity	18-1036
Ettinger, H. J.	Potential Application of a Single Particle Aerosol Spectrometer for Monitoring Aerosol Size at the DOE Filter Test Facilities	17-0801
Ettinger, H. J.	The Effect of Particle Size Variation on Filtration Efficiency Measured by the HEPA Filter Quality Assurance Test	17-0895
Fain, D. E.	Calibration and Use of Filter Test Facility Orifice Plates	18-1168
Fenton, D. E.	Response of HEPA Filters to Simulated Accident Conditions	17-1051
Fenton, D. L.	Fire Simulation in Nuclear Facilities - The FIRAC Code and Supporting Experiments	18-0597
Fernandez, S. J.	A Model of Iodine-129 Process Distributions in a Nuclear Fuel Reprocessing Plant	17-0075
Fernandez, S. J.	In-Place Realtime HEPA Filter Test Method	17-0867

Author	Title	Conference No.
Fernandez, S. J.	Polymeric Diffusion as Applied to a Radioiodine Off-Gas Monitor	17-0937
Fernandez, S. J.	Development of a Method to Determine Iodine Specific Activity in Process Off-Gases by GC Separation and Negative Ionization Mass Spectrometry	18-1318
First, M. W.	Welcome and Objectives of Conference	17-0010
First, M. W.	Surface Deposition of Radon Decay Products with and Without Enhanced Air Motion	17-0151
First, M. W.	Performance of 1000- and 1800- CFM HEPA Filters on Long Exposure to Low Atmospheric Dust Loadings, III	17-0909
First, M. W.	Welcome and Objectives of the Conference	18-0002
First, M. W.	Results of CONAGT-Sponsored Nuclear-Grade Carbon Test Round Robin	18-1186
Fish, J. F.	Nuclear Standards and Safety Progress in Nuclear Standards Development	17-0036
Fluke, R. J.	Long-Term Desorption of 131-I from KI-Impregnated Charcoals Loaded with CH3-I, Under Simulated Post-LOCA Conditions	18-0065

Author	Title	Conference No.
Freeman, W. P.	Teda Vs. Quinuclidine: Evaluation and Comparison of Two Tertiary Amine Impregnants for Methyl Iodide Removal from Flow Air Stream	17-0652
Freeman, W. P.	Evaluation of Quaternary Ammonium Halides for Removal of Methyl Iodide from Flowing Air Streams	18-0093
Fukushima, M.	Iodine Removal by Silver-Exchanged Zeolite Filters from the Vessel Off-Gas in Tokai Reprocessing Plant	17-1142
Funabashi, K.	New Adsorbent, Silver-Alumina for Radioactive Iodine Filter	17-0626
Furrer, J.	Time-Dependent Analyses of Dissolver Off-Gas Cleaning Installations in a Reprocessing Plant	17-0051
Furrer, J.	A New Method of Determining the Overall Particle Decontamination Factor for Multiple Off-Gas Cleaning Components in Reprocessing Plants	17-0576
Furrer, J.	Selected Operating Results of the Passat Prototype Dissolver Off-Gas Cleaning System	18-0400
Furrer, J.	Calculating Released Amounts of Aerosols	18-0873
Gammill, W. P.	NRC Study of Control Room Habitability	18-0162

Author	Title	Conference No.
Garcia, A. G.	Spring Loaded Hold-Down for Mounting HEPA Filters at Rocky Flats	18-1470
Geens, L. P.	Alternative Modes for Cryogenic Krypton Removal	18-0938
Gerlach, K.	Investigations on the Extremely Low Retention of 131-I by an Iodine Filter of a Boiling Water Reactor	18-0098
Gieseke, J. A.	Aerosol Challenges to Air Cleaning Systems During Severe Accidents in Nuclear Plants	18-0647
Gilbert, E. S.	Krypton-85 Health Risk Assessment for a Nuclear Fuel Reprocessing Plant	18-1224
Gilbert, H.	A Recollection of Mr. Clifford Burchsted	18-0019
Gilmore, R. D.	Operational Experience Using Diethylhexylsebacate (DEHS) as a Challenge Test Aerosol in Filter Testing	17-0821
Glass, R. W.	Mechanism of the CO_2-$Ca(OH)_2$ Reaction	17-0400
Glissmeyer, J. A.	Methods for Nuclear Air Cleaning System Accident Consequence Assessment	17-0990
Glissmeyer, J. A.	Prototype Firing Range Air Cleaning System	18-0846
Godbee, H. W.	Methods for Nuclear Air Cleaning System Accident Consequence Assessment	17-0990

Author	Title	Conference No.
Goles, R. W.	Off-Gas Characteristics of Liquid-Fed Joule-Heated Ceramic Melters	17-0305
Goossens, W. R. A.	Volatilization and Trapping of Ruthenium in High Temperature Processes	17-0371
Goossens, W. R. A.	Aerosol Filtration with Metallic Fibrous Filters	17-0504
Goossens, W. R. A.	Development of the ELEX Process for Tritium Separation at Reprocessing Plants	18-0495
Goossens, W. R. A.	The Behaviour of Ruthenium, Cesium and Antimony During Simulated HLLW Vitrification	18-0702
Goossens, W. R. A.	Alternative Modes for Cryogenic Krypton Removal	18-0938
Goumondy, J. P.	Balance and Behavior of Gaseous Radionuclides Released During Initial PWR Fuel Reprocessing Operations	17-0040
Grace, W. K.	Potential Application of a Single Particle Aerosol Spectrometer for Monitoring Aerosol Size at the DOE Filter Test Facilities	17-0801
Green, B. L.	Performance Testing of HEPA Filters Under Hot Dynamic Conditions	18-1107

AEC/ERDA/DOE AIR CLEANING CONFERENCES
INDEX OF PAPERS BY AUTHOR

Author	Title	Conference No.
Gregory, W.	Response of Air Cleaning System Dampers and Blowers to Simulated Tornado Transients	18-0572
Gregory, W. S.	Methods for Nuclear Air Cleaning System Accident Consequence Assessment	17-0990
Gregory, W. S.	Simulation of Forced Ventilation Fires	17-1011
Gregory, W. S.	Response of HEPA Filters to Simulated Accident Conditions	17-1051
Grigull, R.	Technical Feasibility and Costs of the Retention of Radionuclides During Accidents in Nuclear Power Plants Demonstrated by the Example of a Pressurized Water Reactor	18-0244
Grimm, J. J.	Teda Vs. Quinuclidine: Evaluation and Comparison of Two Tertiary Amine Impregnants for Methyl Iodide Removal from Flow Air Stream	17-0652
Groenier, W. S.	Summary of United States Activities in Commercial Nuclear Airborne Waste Management	18-0755
Grundler, D.	Plant for Retention of 14-C in Reprocessing Plants for LWR Fuel Elements	17-0381

Author	Title	Conference No.
Gunaji, M. V.	Fire Simulation in Nuclear Facilities - The FIRAC Code and Supporting Experiments	18-0597
Gunther, K.	The Long-Term Storage of Radioactive Krypton by Fixation in Zeolite 5A	17-0358
Gutowski, H.	Plant for Retention of 14-C in Reprocessing Plants for LWR Fuel Elements	17-0381
Gutowski, H.	Technical Feasibility and Costs of the Retention of Radionuclides During Accidents in Nuclear Power Plants Demonstrated by the Example of a Pressurized Water Reactor	18-0244
Haag, G. L.	Carbon-14 Immobilization Via the Ba(OH)2.8H2O Process	17-0431
Hackney, S.	Development of Filters and Housings for Use on Active Plant	17-0482
Hackney, S.	Fire Testing of HEPA Filters Installed in Filter Housings	17-1030
Hammer, R. R.	Formation and Behaviour of Nitric Oxides in a Cryogenic Krypton Separation System and Consequences of Using Air as Process Gas	17-0683
Hanson, W. D.	DOP Testing HEPA Filter Banks in Series	17-0882

Author	Title	Conference No.
Hartig, S. H.	Comparison and Verification of Two Computer Programs Used to Analyze Ventilation Systems Under Accident Conditions	18-0555
Hattori, S.	NOx Removal from Nuclear Fuel Reprocessing Plants Off-Gas by Catalytic Reduction with NH3	18-1258
Hattori, S.	Removal of Iodine from Off-Gas of Nuclear Fuel Reprocessing Plants with Silver Impregnated Adsorbents	18-1343
Hauss, E.	Formation and Behaviour of Nitric Oxides in a Cryogenic Krypton Separation System and Consequences of Using Air as Process Gas	17-0683
Hayes, Jr., J. J.	NRC Study of Control Room Habitability	18-0162
Hebel, W.	Status of R&D in the Field of Nuclear Airborne Waste Sponsored by the European Community	18-0775
Henrich, E.	Continuous Chemical Cold Traps for Reprocessing Off-Gas Purification	18-0472
Henrich, E.	Development of Technologies for the Waste Management of I-129, Kr-85, C-14 and Tritium in the Federal Republic of Germany	18-0780

Author	Title	Conference No.
Henrich, E.	Selective Absorption of Noble Gases in Freon-12 at Low Temperatures and Atmospheric Pressure	18-0959
Henrich, E.	Krypton Control Alternatives	18-1004
Hensel, E.	Response of Air Cleaning System Dampers and Blowers to Simulated Tornado Transients	18-0572
Herman, R. L.	In-Place HEPA Filter Aerosol Test System	17-0847
Hesbol, R.	Design Experiments for a Vented Containment	18-0260
Higuchi, K. Y.	Carbon Dioxide-Krypton Separation and Radon Removal from Nuclear Fuel Reprocessing Off-Gas Streams	17-0099
Hilliard, R. K.	Testing of a Passive Submerged Gravel Scrubber for Containment Venting Applications	17-1183
Hinds, W. C.	Surface Deposition of Radon Decay Products with and Without Enhanced Air Motion	17-0151
Hirsch, P. M.	Carbon Dioxide-Krypton Separation and Radon Removal from Nuclear Fuel Reprocessing Off-Gas Streams	17-0099
Hohorst, F. A.	In-Place Realtime HEPA Filter Test Method	17-0867
Hubbard, D. M.	Field Testing of Nuclear Air Cleaning Systems at Duke Power Company	18-0904

Author	Title	Conference No.
Hufner, R.	Selective Absorption of Noble Gases in Freon-12 at Low Temperatures and Atmospheric Pressure	18-0959
Hui, L.	A New Procedure for Testing HEPA Filters	18-0348
Hui, L.	Technical Development of Nuclear Air Cleaning in the People's Republic of China	18-1478
Hutter, E.	Formation and Behaviour of Nitric Oxides in a Cryogenic Krypton Separation System and Consequences of Using Air as Process Gas	17-0683
Hutter, E.	Behaviour of Impurities in a Cryogenic Krypton Removal System	18-0951
Idar, E.	Response of Air Cleaning System Dampers and Blowers to Simulated Tornado Transients	18-0572
Jacox, J. W.	NATS Field Testing Observations and Recommendations	18-0918
Jacox, J. W.	Experience in Startup, Preoperational and Acceptance Testing of Nuclear Air Treatment Systems in Nuclear Power Plants	18-1209
Jensen, D. D.	Test Results from the GA Technologies Engineering-Scale Off-Gas Treatment System	18-0434

Author	Title	Conference No.
Johnson, C. M.	In-Situ Continuous Scanning High Efficiency Particulate Air (HEPA) Filter Monitoring System	18-0277
Johnson, J. R.	Predictions of Local, Regional and Global Radiation Doses from Iodine-129 for Four Different Disposal Methods and an All-Nuclear Future	18-0732
Johnson, J. S.	Evaluation of Prototype Electrofibrous Filters for Nuclear Ventilation Ducts	17-0548
Johnson, W. A.	Portable Filter Testing Instrumentation Used for In-Place Leak Testing of Large Air Filters up to 38 m3 sec-1 (80,000 CFM)	17-0919
Jubin, R. T.	Organic Iodine Removal from Simulated Dissolver Off-Gas Streams Using Partially Exchanged Silver Mordenite	17-0183
Juergens, B.	Test Results in the Treatment of HTR Reprocessing Off-Gas	17-0131
Jurgens, B.	Treatment of the Off-Gas Stream from the HTR Reprocessing Head-End	18-0423
Kabat, M. J.	Deposition of Airborne Radioiodine Species on Surfaces of Metals and Plastics	17-0285
Kabat, M. J.	Monitoring of Noble Gas Radioisotopes in Nuclear Power Plant Effluents	18-0217

Author	Title	Conference No.
Kaempffer, R.	Selected Operating Results of the Passat Prototype Dissolver Off-Gas Cleaning System	18-0400
Katoh, Y.	NOx Removal from Nuclear Fuel Reprocessing Plants Off-Gas by Catalytic Reduction with NH3	18-1258
Kawaguchi, A.	Iodine Removal by Silver-Exchanged Zeolite Filters from the Vessel Off-Gas in Tokai Reprocessing Plant	17-1142
Kawamura, F.	New Adsorbent, Silver-Alumina for Radioactive Iodine Filter	17-0626
Kikuchi, K.	Experience of Iodine Removal in Tokai Reprocessing Plant	18-0451
Kikuchi, M.	New Adsorbent, Silver-Alumina for Radioactive Iodine Filter	17-0626
Kim, Y. W.	Development of a New Technique and Instrumentation for Rapid Assessment of Filter Media	18-1193
Kirchner, K. N.	In-Situ Continuous Scanning High Efficiency Particulate Air (HEPA) Filter Monitoring System	18-0277
Klein, M.	Volatilization and Trapping of Ruthenium in High Temperature Processes	17-0371

Author	Title	Conference No.
Klein, M.	Aerosol Filtration with Metallic Fibrous Filters	17-0504
Klein, M.	The Behaviour of Ruthenium, Cesium and Antimony During Simulated HLLW Vitrification	18-0702
Knecht, D. A.	Immobilization of Krypton-85 in Zeolite 5A	17-0333
Knittel, G.	Behaviour of Impurities in a Cryogenic Krypton Removal System	18-0951
Kobayashi, Y.	NOx Removal from Nuclear Fuel Reprocessing Plants Off-Gas by Catalytic Reduction with NH3	18-1258
Kobayashi, Y.	Removal of Iodine from Off-Gas of Nuclear Fuel Reprocessing Plants with Silver Impregnated Adsorbents	18-1343
Komori, Y.	Experience of Iodine Removal in Tokai Reprocessing Plant	18-0451
Kotra, J. P.	Commentary on Nuclear Power Plant Control Room Habitability - Including a Review of Related LERs (1981-1983)	18-0145
Kovach, A.	Dual Aerosol Detector Based on Forward Light Scattering with a Single Laser Beam	18-1429
Kovach, B. J.	Portable Filter Testing Instrumentation Used for In-Place Leak Testing of Large Air Filters up to 38 m3 sec-1 (80,000 CFM)	17-0919

Author	Title	Conference No.
Kovach, B. J.	Dual Aerosol Detector Based on Forward Light Scattering with a Single Laser Beam	18-1429
Kovach, J. L.	Teda Vs. Quinuclidine: Evaluation and Comparison of Two Tertiary Amine Impregnants for Methyl Iodide Removal from Flow Air Stream	17-0652
Kovach, J. L.	Portable Filter Testing Instrumentation Used for In-Place Leak Testing of Large Air Filters up to 38 m3 sec-1 (80,000 CFM)	17-0919
Kovach, J. L.	Evaluation of Quaternary Ammonium Halides for Removal of Methyl Iodide from Flowing Air Streams	18-0093
Kovach, J. L.	Air Cleaning in Accident Situations	18-1495
Krause, F. R.	Methods for Nuclear Air Cleaning System Accident Consequence Assessment	17-0990
Krause, F. R.	Simulation of Forced Ventilation Fires	17-1011
Krill, W	Test Results in the Treatment of HTR Reprocessing Off-Gas	17-0131
Kuhl, W. D.	Evaluation of Prototype Electrofibrous Filters for Nuclear Ventilation Ducts	17-0548
Kumar, S.	The Mathematical Modelling of Fire in Forced Ventilated Enclosures	18-0629

Author	Title	Conference No.
Kunikata, M.	NOx Removal from Nuclear Fuel Reprocessing Plants Off-Gas by Catalytic Reduction with NH3	18-1258
Kunikata, M.	Removal of Iodine from Off-Gas of Nuclear Fuel Reprocessing Plants with Silver Impregnated Adsorbents	18-1343
Kunz, C.	14-C Release at Light Water Reactors	17-0414
Lahner, K.	Technical Feasibility and Costs of the Retention of Radionuclides During Accidents in Nuclear Power Plants Demonstrated by the Example of a Pressurized Water Reactor	18-0244
Lahti, G. P.	Performance Evaluation of Control Room HVAC and Air Cleaning Systems Under Accident Conditions	18-0188
Landis, J. W.	Nuclear Standards: Current Issues and Future Trends	18-0023
Langhorst, S. M.	Analyses of Charcoal Filters Used in Monitoring Radioactive Iodines	18-0127
Lanza, S.	Effects of Shock Waves on High Efficiency Filter Units	17-1093
Leitzig, H.	The Long-Term Storage of Radioactive Krypton by Fixation in Zeolite 5A	17-0358

Author	Title	Conference No.
Leudet, A.	Balance and Behavior of Gaseous Radionuclides Released During Initial PWR Fuel Reprocessing Operations	17-0040
Lightfoot, W. R.	In-Place Testing of Non ANSI-N509 Designed System	18-0921
Linck, Jr., F. J.	System Operational Testing of Major Ventilation Systems for a Plutonium Recovery Facility	17-0612
Linek, A.	A New Method of Determining the Overall Particle Decontamination Factor for Multiple Off-Gas Cleaning Components in Reprocessing Plants	17-0576
Lippold, H. J.	A Changeable Bed Activated Carbon Filter with High Accuracy and Efficiency	17-1134
Little, D. K.	Noble Gas Removal and Concentration by Combining Fluorocarbon Absorption and Adsorption Technologies	17-0694
Littlefield, P. S.	Utility View of the Source Term and Air Cleaning	18-0655
Lucerna, J. J.	In-Situ Continuous Scanning High Efficiency Particulate Air (HEPA) Filter Monitoring System	18-0277
Lum, B. Y.	Evaluation of Permanently Charged Electrofibrous Filters	17-0523

Author	Title	Conference No.
Lum, B. Y.	Evaluation of Prototype Electrofibrous Filters for Nuclear Ventilation Ducts	17-0548
Machiels, A. J.	Performance Evaluation of Control Room HVAC and Air Cleaning Systems Under Accident Conditions	18-0188
Madelaine, G.	Use of Acoustic Field in Gas Cleaning	18-0803
Maher, E. F.	Surface Deposition of Radon Decay Products with and Without Enhanced Air Motion	17-0151
Maher, E. F.	Removal of Radon Decay Products with Ion Generators - Comparison of Experimental Results with Theory	18-0825
Malherbe, C.	Use of Acoustic Field in Gas Cleaning	18-0803
Malinauskas, A. P.	Fission Product Source Terms and Engineered Safety Features	18-0644
Manley, D. K.	Seismic Simulation and Functional Performance Evaluation of a Safety Related, Seismic Category I Control Room Emergency Air Cleaning System	18-0526
Marandola, U.	Effects of Shock Waves on High Efficiency Filter Units	17-1093
Martin, R. A.	Methods for Nuclear Air Cleaning System Accident Consequence Assessment	17-0990

Author	Title	Conference No.
Martin, R. A.	Response of HEPA Filters to Simulated Accident Conditions	17-1051
Martin, R. A.	Fire Simulation in Nuclear Facilities - The FIRAC Code and Supporting Experiments	18-0597
Mas, C.	Behaviour of Impurities in a Cryogenic Krypton Removal System	18-0951
Mathewes, W.	A Changeable Bed Activated Carbon Filter with High Accuracy and Efficiency	17-1134
Matsumoto, K.	Iodine Removal by Silver-Exchanged Zeolite Filters from the Vessel Off-Gas in Tokai Reprocessing Plant	17-1142
Mattson, R. J.	Keynote Address	17-0013
McCormack, J. D.	Testing of a Passive Submerged Gravel Scrubber for Containment Venting Applications	17-1183
McIntyre, J. A.	Operational Experience Using Diethylhexylsebacate (DEHS) as a Challenge Test Aerosol in Filter Testing	17-0821
McManus, G. J.	A Model of Iodine-129 Process Distributions in a Nuclear Fuel Reprocessing Plant	17-0075

Author	Title	Conference No.
McManus, G. J.	Iodine-129 Process Control Monitor for Evaporator Off-Gas Streams	18-0461
McManus, G. J.	Development of a Method to Determine Iodine Specific Activity in Process Off-Gases by GC Separation and Negative Ionization Mass Spectrometry	18-1318
Mellinger, P. J.	Health Risk Assessment for Fuel Reprocessing Plant	18-1019
Mellinger, P. J.	Krypton-85 Health Risk Assessment for a Nuclear Fuel Reprocessing Plant	18-1224
Meynendonckx, L.	Development of the ELEX Process for Tritium Separation at Reprocessing Plants	18-0495
Miguel, P.	Balance and Behavior of Gaseous Radionuclides Released During Initial PWR Fuel Reprocessing Operations	17-0040
Miller, Jr., W. H.	CONAGT's Place in ASME's Centennial Year	18-1480
Mishima, J.	Methods for Nuclear Air Cleaning System Accident Consequence Assessment	17-0990
Mishima, J.	Prototype Firing Range Air Cleaning System	18-0846
Miyahara, K.	Iodine Removal by Silver-Exchanged Zeolite Filters from the Vessel Off-Gas in Tokai Reprocessing Plant	17-1142

Author	Title	Conference No.
Moeller, D. W.	Failures in Air-Cleaning, Air-Monitoring, and Ventilation Systems in Commercial Nuclear Power Plants (1/1/78 - 12/31/81)	17-0768
Moeller, D. W.	Commentary on Nuclear Power Plant Control Room Habitability - Including a Review of Related LERs (1981-1983)	18-0145
Moeller, D. W.	Removal of Radon Decay Products with Ion Generators - Comparison of Experimental Results with Theory	18-0825
Mohacsi, T. G.	Evaluation of Quaternary Ammonium Halides for Removal of Methyl Iodide from Flowing Air Streams	18-0093
Monson, P. R.	Noble Gas Confinement for Reactor Fuel Melting Accidents	18-0233
Moore, C. J.	Long-Term Desorption of 131-I from KI-Impregnated Charcoals Loaded with CH3-I, Under Simulated Post-LOCA Conditions	18-0065
Mubler, M.	Chromatographic Separation of Krypton from Dissolver Off-Gas at Low Temperatures	18-0982
Mulcey, P.	Data Analysis of In-Place Tests of Iodine Filters in the French Nuclear Facilities	17-0223

Author	Title	Conference No.
Mulcey, P.	Iodine Filtering for French Reprocessing Plants	17-0239
Mulcey, P.	Simoun: High Temperature Dynamic Test Rig for Industrial Air Filters	18-1097
Muller, D. R.	NRC Study of Control Room Habitability	18-0162
Munkelwitz, H. R.	Formation and Characterization of Fission-Product Aerosols Under Postulated HTGR Accident Conditions	17-0172
Murphy, L. P.	A Model of Iodine-129 Process Distributions in a Nuclear Fuel Reprocessing Plant	17-0075
Murphy, L. P.	Polymeric Diffusion as Applied to a Radioiodine Off-Gas Monitor	17-0937
Nafissi, A.	Test Results in the Treatment of HTR Reprocessing Off-Gas	17-0131
Nagel, K.	Calculating Released Amounts of Aerosols	18-0873
Nagle, K.	Time-Dependent Analyses of Dissolver Off-Gas Cleaning Installations in a Reprocessing Plant	17-0051
Nakagawa, T.	A Parametric Study on Removal Efficiency of Impregnated Activated Charcoal and Silver Zeolite for Radioactive Methyl Iodide	17-0199

Author	Title	Conference No.
Naruki, K.	Research and Development on Air Cleaning System of Reprocessing Plant in Japan	18-0761
Neffe, G.	Formation and Behaviour of Nitric Oxides in a Cryogenic Krypton Separation System and Consequences of Using Air as Process Gas	17-0683
Neffe, G.	Behaviour of Impurities in a Cryogenic Krypton Removal System	18-0951
Nehls, Jr., J. W.	Carbon-14 Immobilization Via the Ba(OH)2.8H2O Process	17-0431
Niam, X. S.	Technical Development of Nuclear Air Cleaning in the People's Republic of China	18-1478
Nian Song, X.	A New Procedure for Testing HEPA Filters	18-0348
Nielson, R. A.	Development of a Method to Determine Iodine Specific Activity in Process Off-Gases by GC Separation and Negative Ionization Mass Spectrometry	18-1318
Nikolic, R.	Adsorption of Gaseous RuO4 by Various Sorbents II	17-0123
Noppel, H. E.	The Long-Term Storage of Radioactive Krypton by Fixation in Zeolite 5A	17-0358
Normann, B.	Projects on Filter Testing in Sweden	18-0311

Author	Title	Conference No.
Norton, J. L.	Noble Gas Removal and Concentration by Combining Fluorocarbon Absorption and Adsorption Technologies	17-0694
O'Connor, P. A.	Predictions of Local, Regional and Global Radiation Doses from Iodine-129 for Four Different Disposal Methods and an All-Nuclear Future	18-0732
Obrowski, W.	Time-Dependent Analyses of Dissolver Off-Gas Cleaning Installations in a Reprocessing Plant	17-0051
Ohki, M.	A Parametric Study on Removal Efficiency of Impregnated Activated Charcoal and Silver Zeolite for Radioactive Methyl Iodide	17-0199
Olguin, L. J.	Test Results from the GA Technologies Engineering-Scale Off-Gas Treatment System	18-0434
Oma, K. H.	Off-Gas Treatment and Characterization for a Radioactive In Situ Vitrification Test	18-0683
Ornberg, S. C.	Performance Evaluation of Control Room HVAC and Air Cleaning Systems Under Accident Conditions	18-0188

Author	Title	Conference No.
Ortiz, J. P.	In-Place Testing of Multiple Stage Filter Systems Without Disruption of Plant Operations in the Plutonium Facility at Los Alamos	18-0299
Owczarski, P. C.	Methods for Nuclear Air Cleaning System Accident Consequence Assessment	17-0990
Ozawa, Y.	Removal of Iodine from Off-Gas of Nuclear Fuel Reprocessing Plants with Silver Impregnated Adsorbents	18-1343
Parmentier, C.	Development of the ELEX Process for Tritium Separation at Reprocessing Plants	18-0495
Pasler, H.	Experimental Investigations of Aerosol Filtration with Deep Bed Fiber Filters	17-1160
Pasler, H.	A Filter Concept to Control Airborne Particulate Releases Due to Severe Reactor Accidents and Implementation Using Stainless-Steel Fiber Filters	18-1417
Patton, J. L.	Noble Gas Removal and Concentration by Combining Fluorocarbon Absorption and Adsorption Technologies	17-0694
Pelletier, C. A.	Transmission of Radioiodine Through Sampling Lines	18-0116

Author	Title	Conference No.
Penzhorn, R. D.	The Long-Term Storage of Radioactive Krypton by Fixation in Zeolite 5A	17-0358
Perkins, W. C.	A Dispersion Model for Airborne Particulates Inside a Building	18-0373
Petersen, G. R.	Operational Experience Using Diethylhexylsebacate (DEHS) as a Challenge Test Aerosol in Filter Testing	17-0821
Porco, R. D.	Seismic Simulation and Functional Performance Evaluation of a Safety Related, Seismic Category I Control Room Emergency Air Cleaning System	18-0526
Postma, A. K.	Testing of a Passive Submerged Gravel Scrubber for Containment Venting Applications	17-1183
Powers, F. L.	Portable Filter Testing Instrumentation Used for In-Place Leak Testing of Large Air Filters up to 38 m3 sec-1 (80,000 CFM)	17-0919
Powers, F. L.	Dual Aerosol Detector Based on Forward Light Scattering with a Single Laser Beam	18-1429
Pratt, R. P.	Development of Filters and Housings for Use on Active Plant	17-0482
Pratt, R. P.	Performance Testing of HEPA Filters Under Hot Dynamic Conditions	18-1107

Author	Title	Conference No.
Price, J. M.	Performance of 1000- and 1800- CFM HEPA Filters on Long Exposure to Low Atmospheric Dust Loadings, III	17-0909
Prinz, M.	Vertical Removable Filters in Shielded Casing for Radioactive Cells and Process Gaseous Wastes	17-0457
Puissant, L. J.	Development of a Wetproofed Catalyst Recombiner for Removal of Airborne Tritium	18-1300
Qi-dong, L	A Study of Adsorption Properties of Impregnated Charcoal for Airborne Iodine and Methyl Iodide	18-0078
Quaiattini, R. J.	Development of a Wetproofed Catalyst Recombiner for Removal of Airborne Tritium	18-1300
Qun, L. X.	Technical Development of Nuclear Air Cleaning in the People's Republic of China	18-1478
Rankin, R. A.	Development of a Method to Determine Iodine Specific Activity in Process Off-Gases by GC Separation and Negative Ionization Mass Spectrometry	18-1318
Ricketts, C. I.	Limits of HEPA-Filter Application Under High-Humidity Conditions	18-1058

Author	Title	Conference No.
Ricketts, C. I.	BORA - A Facility for Experimental Investigation of Air Cleaning During Accident Situations	18-1441
Ringel, H.	Experiments on Adsorptive Retention of NOx and Krypton from Dissolver Off-Gas	17-0664
Ringel, H.	Chromatographic Separation of Krypton from Dissolver Off-Gas at Low Temperatures	18-0982
Robinson, K. S.	The Design of Graded Filtration Media in the Diffusion-Sedimentation Regime	18-0357
Rose, C. R.	Spring Loaded Hold-Down for Mounting HEPA Filters at Rocky Flats	18-1470
Rouyer, J. L.	Data Analysis of In-Place Tests of Iodine Filters in the French Nuclear Facilities	17-0223
Rouyer, J. L.	Iodine Filtering for French Reprocessing Plants	17-0239
Rouyer, J. L.	Simoun: High Temperature Dynamic Test Rig for Industrial Air Filters	18-1097
Rouyer, J. L.	Tritium Management for Fusion Reactors	18-1311

Author	Title	Conference No.
Rudinger, V.	A Procedure to Test HEPA-Filter Efficiency Under Simulated Accident Conditions of High Temperature and High Humidity	18-1036
Rudinger, V.	Limits of HEPA-Filter Application Under High-Humidity Conditions	18-1058
Rudinger, V.	Development of a HEPA-Filter with High Structural Strength and High Resistance to the Effects of Humidity and Acid	18-1085
Rudinger, V.	BORA - A Facility for Experimental Investigation of Air Cleaning During Accident Situations	18-1441
Rudnick, S. N.	Surface Deposition of Radon Decay Products with and Without Enhanced Air Motion	17-0151
Rudnick, S. N.	Removal of Radon Decay Products with Ion Generators - Comparison of Experimental Results with Theory	18-0825
Ruedinger, V.	HEPA Filter Response to High Air Flow Velocities	17-1069
Ruedinger, V.	Comparison and Verification of Two Computer Programs Used to Analyze Ventilation Systems Under Accident Conditions	18-0555

Author	Title	Conference No.
Salzman, G. C.	Potential Application of a Single Particle Aerosol Spectrometer for Monitoring Aerosol Size at the DOE Filter Test Facilities	17-0801
Salzman, G. C.	The Effect of Particle Size Variation on Filtration Efficiency Measured by the HEPA Filter Quality Assurance Test	17-0895
Scholten, L. C.	Experiences with a Charcoal Guard Bed in a Nuclear Power Plant	17-0278
Schultz, R. M.	Noble Gas Removal and Concentration by Combining Fluorocarbon Absorption and Adsorption Technologies	17-0694
Schuster, P.	The Long-Term Storage of Radioactive Krypton by Fixation in Zeolite 5A	17-0358
Scripsick, R. C.	Evaluation of Methods, Instrumentation and Materials Pertinent to Quality Assurance Filter Penetration Testing	18-1131
Seghal, Y. P.	Time-Dependent Analyses of Dissolver Off-Gas Cleaning Installations in a Reprocessing Plant	17-0051
Selby, T. W.	Calibration and Use of Filter Test Facility Orifice Plates	18-1168
Sevigny, G. J.	Off-Gas Characteristics of Liquid-Fed Joule-Heated Ceramic Melters	17-0305

Author	Title	Conference No.
Shen, W. T.	Technical Development of Nuclear Air Cleaning in the People's Republic of China	18-1478
Shiomi, H.	A Parametric Study on Removal Efficiency of Impregnated Activated Charcoal and Silver Zeolite for Radioactive Methyl Iodide	17-0199
Smith, E.	Response of Air Cleaning System Dampers and Blowers to Simulated Tornado Transients	18-0572
Smith, G. P.	Recent Changes in MIL-F-51068 Specification	17-1121
Smith, P.	Response of Air Cleaning System Dampers and Blowers to Simulated Tornado Transients	18-0572
Smith, P. R.	Response of HEPA Filters to Simulated Accident Conditions	17-1051
Soderholm, S. C.	Evaluation of Methods, Instrumentation and Materials Pertinent to Quality Assurance Filter Penetration Testing	18-1131
Soderholm, S. C.	Intermediate Results of a One-Year Study of a Laser Spectrometer in the DOE Filter Test Facilities	18-1149
Specter, H.	Energy and Fear	17-0952

Author	Title	Conference No.
Speranzini, R. A.	Recovery and Purification of Xe-135 as a By-Product of Mo-99 Production Using Linde 5A Molecular Sieve	18-1378
Steinhardt, H. J.	Continuous Chemical Cold Traps for Reprocessing Off-Gas Purification	18-0472
Stiehl, H.	A Changeable Bed Activated Carbon Filter with High Accuracy and Efficiency	17-1134
Stoddard, D. H.	A Dispersion Model for Airborne Particulates Inside a Building	18-0373
Strip, D. R.	Cost-Benefit Considerations for Filtered-Vented Containment Systems	17-1201
Sui-yuang, H.	A Study of Adsorption Properties of Impregnated Charcoal for Airborne Iodine and Methyl Iodide	18-0078
Sutter, S. L.	Methods for Nuclear Air Cleaning System Accident Consequence Assessment	17-0990
Takashima, Y.	New Adsorbent, Silver-Alumina for Radioactive Iodine Filter	17-0626
Takeda, K.	Experience of Iodine Removal in Tokai Reprocessing Plant	18-0451
Takimoto, Y.	NOx Removal from Nuclear Fuel Reprocessing Plants Off-Gas by Catalytic Reduction with NH3	18-1258

Author	Title	Conference No.
Tang, I. N.	Formation and Characterization of Fission-Product Aerosols Under Postulated HTGR Accident Conditions	17-0172
Tang, P. K.	Methods for Nuclear Air Cleaning System Accident Consequence Assessment	17-0990
Tani, A.	A Parametric Study on Removal Efficiency of Impregnated Activated Charcoal and Silver Zeolite for Radioactive Methyl Iodide	17-0199
Tanner, J. E.	Immobilization of Krypton-85 in Zeolite 5A	17-0333
Tanner, J. E.	Krypton-85 Health Risk Assessment for a Nuclear Fuel Reprocessing Plant	18-1224
Tarrago, X.	Simoun: High Temperature Dynamic Test Rig for Industrial Air Filters	18-1097
Terada, K.	Spring Loaded Hold-Down for Mounting HEPA Filters at Rocky Flats	18-1470
Thatcher, D. R. P.	Development of a Wetproofed Catalyst Recombiner for Removal of Airborne Tritium	18-1300
Thomas, T. R.	Control Decisions for 3-H, 14-C, 85-Kr, and 129-I Released from the Commercial Fuel Cycle	18-0998
Thorvaldson, W. G.	Development and Evaluation of Acid-Resistant HEPA Filter Media	17-1125

Author	Title	Conference No.
Tian Liang, G.	A New Procedure for Testing HEPA Filters	18-0348
Tian, G. L.	Technical Development of Nuclear Air Cleaning in the People's Republic of China	18-1478
Tillery, M. I.	Potential Application of a Single Particle Aerosol Spectrometer for Monitoring Aerosol Size at the DOE Filter Test Facilities	17-0801
Tillery, M. I.	The Effect of Particle Size Variation on Filtration Efficiency Measured by the HEPA Filter Quality Assurance Test	17-0895
Tillery, M. I.	Evaluation of Methods, Instrumentation and Materials Pertinent to Quality Assurance Filter Penetration Testing	18-1131
Tillery, M. I.	Intermediate Results of a One-Year Study of a Laser Spectrometer in the DOE Filter Test Facilities	18-1149
Timmerman, C. L.	Off-Gas Treatment and Characterization for a Radioactive In Situ Vitrification Test	18-0683
Trehen, L.	Data Analysis of In-Place Tests of Iodine Filters in the French Nuclear Facilities	17-0223

Author	Title	Conference No.
Tsuchiya, H.	New Adsorbent, Silver-Alumina for Radioactive Iodine Filter	17-0626
Unrein, P. J.	Transmission of Radioiodine Through Sampling Lines	18-0116
Varagona, J. M.	Noble Gas Removal and Concentration by Combining Fluorocarbon Absorption and Adsorption Technologies	17-0694
Vaudano, A.	Iodine Filtering for French Reprocessing Plants	17-0239
Vavasseur, C.	Ventilation of Nuclear Rooms and Operators' Protection	18-0184
Vijgen, H.	Treatment of the Off-Gas Stream from the HTR Reprocessing Head-End	18-0423
Vikis, A. C.	Long-Term Desorption of 131-I from KI-Impregnated Charcoals Loaded with CH3-I, Under Simulated Post-LOCA Conditions	18-0065
Voilleque, P. G.	Transmission of Radioiodine Through Sampling Lines	18-0116
Vujisic, Lj.	Adsorption of Gaseous RuO4 by Various Sorbents II	17-0123
Vygen, H.	Test Results in the Treatment of HTR Reprocessing Off-Gas	17-0131

Author	Title	Conference No.
Ward, F. Y.	Air Cleaning Philosophy in a Nuclear Materials Fabrication Plant	17-0602
Weber, J.	Technical Feasibility and Costs of the Retention of Radionuclides During Accidents in Nuclear Power Plants Demonstrated by the Example of a Pressurized Water Reactor	18-0244
Weirich, F.	Selective Absorption of Noble Gases in Freon-12 at Low Temperatures and Atmospheric Pressure	18-0959
Werke, C. F.	Development of a HEPA-Filter with High Structural Strength and High Resistance to the Effects of Humidity and Acid	18-1085
Weyers, C.	Volatilization and Trapping of Ruthenium in High Temperature Processes	17-0371
Weyers, C.	The Behaviour of Ruthenium, Cesium and Antimony During Simulated HLLW Vitrification	18-0702
Weymann, J.	Time-Dependent Analyses of Dissolver Off-Gas Cleaning Installations in a Reprocessing Plant	17-0051

Author	Title	Conference No.
Wheat, L. D.	Potential Application of a Single Particle Aerosol Spectrometer for Monitoring Aerosol Size at the DOE Filter Test Facilities	17-0801
Whitmell, D. S.	Choice of Materials for the Immobilization of 85-Krypton in a Metallic Matrix by Combined Ion Implantation and Sputtering	18-0667
Wiktorsson, C.	Projects on Filter Testing in Sweden	18-0311
Wilbourn, R. G.	Test Results from the GA Technologies Engineering-Scale Off-Gas Treatment System	18-0434
Wilhelm, J. G.	Retention of Elemental Radioiodine by Deep Bed Carbon Filters Under Accident Conditions	17-0248
Wilhelm, J. G.	HEPA Filter Response to High Air Flow Velocities	17-1069
Wilhelm, J. G.	Investigations on the Extremely Low Retention of 131-I by an Iodine Filter of a Boiling Water Reactor	18-0098
Wilhelm, J. G.	A Procedure to Test HEPA-Filter Efficiency Under Simulated Accident Conditions of High Temperature and High Humidity	18-1036
Wilhelm, J. G.	Limits of HEPA-Filter Application Under High-Humidity Conditions	18-1058

Author	Title	Conference No.
Wilhelm, J. G.	Development of a HEPA-Filter with High Structural Strength and High Resistance to the Effects of Humidity and Acid	18-1085
Wilhelm, J. G.	BORA - A Facility for Experimental Investigation of Air Cleaning During Accident Situations	18-1441
Wolff, A.	Selective Absorption of Noble Gases in Freon-12 at Low Temperatures and Atmospheric Pressure	18-0959
Wren, J. C.	Long-Term Desorption of 131-I from KI-Impregnated Charcoals Loaded with CH3-I, Under Simulated Post-LOCA Conditions	18-0065
Wurz, D. E.	Comparison and Verification of Two Computer Programs Used to Analyze Ventilation Systems Under Accident Conditions	18-0555
Wuschke, D. M.	Predictions of Local, Regional and Global Radiation Doses from Iodine-129 for Four Different Disposal Methods and an All-Nuclear Future	18-0732
Wuschke, D. M.	How Much Dose Reduction Could be Achieved by Collection and Disposal of 129-I and 14-C?	18-1026

Author	Title	Conference No.
Yewer, K. C.	Volatile Ruthenium Trapping on Silica Gel and Solid Catalysts	18-1361
Yoder, R. E.	Air Cleaning Philosophy in a Nuclear Materials Fabrication Plant	17-0602
Young, G. C.	Carbon-14 Immobilization Via the Ba(OH)2.8H2O Process	17-0431
Yuasa, Y.	A Parametric Study on Removal Efficiency of Impregnated Activated Charcoal and Silver Zeolite for Radioactive Methyl Iodide	17-0199
Yusa, H.	New Adsorbent, Silver-Alumina for Radioactive Iodine Filter	17-0626

P A R T   III

Key-Word-In-Context (Subject) Index

KWIC INDEX ON AIR CLEANING CONFERENCE TITLES

KWIC INDEX ON AIR CLEANING CONFERENCE TITLES

KWIC INDEX ON AIR CLEANING CONFERENCE TITLES

Left context	Keyword-aligned title	Ref.
Aging on the Retention of Elemental Radioiodine by Deep	Bed Carbon Filters Under Accident Conditions*	17-024
Investigations of Aerosol Filtration with Deep	Bed Carbon Filters Under Accident Conditions*	18-004
Initial PWR Fuel Reprocessing Operations* #Balance and	Bed Fiber Filters*	17-116
System* #Experimental of	Behaviour of Gaseous Radionuclides Released During	17-004
Separation System and Consequences of #Formation and	Behaviour of Impurities in a Cryogenic Krypton Removal	18-095
#The	Behaviour of Nitric Oxides in a Cryogenic Krypton	17-068
Simulated HLLW Vitrification*	Behaviour of Ruthenium, Cesium and Antimony During	18-070
Systems* #Cost-	Benefit Considerations for Filtered-Vented Containment	17-120
#Response of Air Cleaning System Dampers and	Blowers to Simulated Tornado Transients*	18-057
Low Retention of 131-I by an Iodine Filter of a	Boiling Water Reactor* Investigations on the Extremely	18-009
Cleaning During Accident Situations*	BORA - A Facility for Experimental Investigation of Air #	18-144
HEPA Filter Experience During Three Mile Island Reactor	Building Purges*	17-100
#A Dispersion Model for Airborne Particulates Inside a	Building*	18-037
#A Recollection of Mr. Clifford	Burchsted*	18-001
#Mechanism of the CO2-	Ca(OH)2 Reaction*	18-040
Plates*	Calculating Released Amounts of Aerosols*	18-087
from Nuclear Fuel Reprocessing Off-Gas Streams*	Calibration and Use of Filter Test Facility Orifice	18-116
#A Changeable Bed Activated	Carbon Dioxide-Krypton Separation and Radon Removal	17-009
#Retention of Elemental Radioiodine by Deep Bed	Carbon Filter with High Accuracy and Efficiency*	17-113
on the Retention of Elemental Radioiodine by Deep Bed	Carbon Filters Under Accident Conditions*	17-024
#CONAGT's Nuclear	Carbon Filters Under Accident Conditions* of Aging	18-004
	Carbon Found Robin Test Program*	18-119
#Results of CONAGT-Sponsored Nuclear-Grade	Carbon Test Round Robin*	18-118
#Test Data and Operation Data from	Carbon Used in High Velocity Systems*	18-143
	Carbon-14 Immobilization via the Ba(OH)2.8H2O Process*	17-043
Isotope-Exchange Efficiency for Nuclear-Grade Activated	Carbons* #Regeneration of the Iodine	18-003
#Vertical Removable Filters in Shielded	Casing for Radioactive Cells and Process Gaseous Wastes*	17-045
#Development of a wetproofed	Catalyst Recombiner for Removal of Airborne Tritium*	18-130
	Catalysts*	18-136
#volatile Ruthenium Trapping on Silica Gel and Solid	Catalytic Reduction with NH3* #NOx Removal	18-125
from Nuclear Fuel Reprocessing Plants Off-Gas by	Category I Control Room Emergency Air Cleaning System*	18-052
Performance Evaluation of a Safety Related, Seismic	Cells and Process Gaseous Wastes* #Vertical	17-045
Removable Filters in Shielded Casing for Radioactive	Centennial Year*	18-148
#CONAGT's Place in ASME's	Ceramic Melters*	17-030
#Off-Gas Characteristics of Liquid-Fed Joule-Heated	Cesium and Antimony During Simulated HLLW Vitrification*	18-070
#The Behaviour of Ruthenium,	Challenge Test Aerosol in Filter Testing* #Operational	17-082
Experience Using Diethylhexylsebacate (DEHS) as a	Challenges to Air Cleaning Systems During Severe	18-064
Accidents in Nuclear Plants* #A	Changeable Bed Activated Carbon Filter with High	17-113
Accuracy and Efficiency*	Characterization for a Radioactive In Situ	18-068
Vitrification Test*	Characterization of Fission-Product Aerosols Under	17-017
Postulated HTGR Accident Conditions*	Charcoal and Silver Zeolite for Radioactive Methyl	17-019
Study on Removal Efficiency of Impregnated Activated	Charcoal for Airborne Iodine and Methyl Iodide*	18-007
#A Study of Adsorption Properties of Impregnated	Charcoal Air Filter with Combustible Frame*	17-115
#High-Efficiency	Charcoal Filters Used in Monitoring Radioactive Iodines*	18-012
#Analyses of	Charcoal Guard Bed in a Nuclear Power Plant*	17-027
#Experiences with a	Charcoal Performance Under Simulated Accident Conditions	17-064
#	Charcoals Loaded with CH3-I, Under Simulated Post-LOCA	18-006
#Long-Term Desorption of 131-I from KI-Impregnated	Charged Electrofibrous Filters*	17-052
#Evaluation of Permanently	Chemical Cold Traps for Reprocessing Off-Gas	18-047
Purification* #Continuous	China* #Technical Development	18-147
of Nuclear Air Cleaning in the People's Republic of	Choice of Materials for the Immobilization of 85-	18-066
Krypton in a Metallic Matrix by Combined Ion	Chromatographic Separation of Krypton from Dissolver	18-098
Off-Gas at Low Temperatures* #	CH3-I, Under Simulated Post-LOCA Conditions* Desorption	18-006
of 131-I from KI-Impregnated Charcoals Loaded with	Cleaning in the People's Republic of China*	16-147
#Technical Development of Nuclear Air	Cleaning in Accident Situations*	18-149
Particle Decontamination Factor for Multiple Off-Gas	Cleaning Components in Reprocessing Plants* the Overall	17-057

1619

KWIC INDEX ON AIR CLEANING CONFERENCE TITLES

1621

KWIC INDEX ON AIR CLEANING CONFERENCE TITLES

Context (left)	Keyword entry (center)	Code
#Field Testing of Nuclear Air Cleaning Systems at	Duke Power Company* #Performance of 1000- and 1800-	18-090
CFM HEPA Filters on Long Exposure to Low Atmospheric	Dust Loadings, III*	17-110
#Performance Testing of HEPA Filters Under Hot	Dynamic Conditions*	18-110
#Simoun: High Temperature	Dynamic Test Rig for Industrial Air Filters* #Monitoring	18-109
of Noble Gas Radioisotopes in Nuclear Power Plant	Effluents*	18-021
#Evaluation of Prototype	Electrofibrous Filters for Nuclear Ventilation Ducts*	17-054
#Evaluation of Permanently Charged	Electrofibrous Filters*	17-052
Accident Conditions* #Retention of	Elemental Radioiodine by Deep Bed Carbon Filters Under	17-024
Accident #Influence of Aging on the Retention of	Elemental Radioiodine by Deep Bed Carbon Filters Under	18-004
Plants* #Development of the	ELEX Process for Tritium Separation at Reprocessing	18-049
of a Safety Related, Seismic Category I Control Room	Emergency Air Cleaning System* Performance Evaluation	18-052
The Mathematical Modelling of Fire in Forced Ventilated	Enclosures* #	18-062
#Department of	Energy and Fear*	17-095
#New Source Terms: What do They Tell Us About	Engineered Safety Feature Performance?*	18-114
#Fission Product Source Terms and	Engineered Safety Features*	18-001
#Test Results from the GA Technologies	Engineering-Scale Off-Gas Treatment System*	18-064
Deposition of Radon Decay Products with and Without	Enhanced Air Motion* #Surface	18-043
in the Field of Nuclear Airborne Waste Sponsored by the	European Community* #Status of R&D	17-015
#Iodine-129 Process Control Monitor for	Evaporator Off-Gas Streams*	18-077
Simulated Dissolver Off-Gas Streams Using Partially	Exchanged Silver Mordenite* #Organic Iodine Removal from	18-046
Tokai Reprocessing Plant* #Iodine Removal by Silver-	Exchanged Zeolite Filters from the Vessel Off-Gas in	17-018
Testing of Nuclear Air Treatment Systems in Nuclear	Experience in Startup, Preoperational and Acceptance	17-114
*	Experience of Iodine Removal in Tokai Reprocessing Plant	18-120
*	Experience with Nuclear Air Cleaning*	18-045
#Regulatory	Experience During Three Mile Island Reactor Building	18-089
#HEPA Filter	Experience Using Diethylhexylsebacate (DEHS) as a	17-100
#Operational	Experience*	17-082
Purges*	Experience*	17-079
Challenge Test Aerosol in Filter Testing*	Experience*	17-059
#A Survey of HEPA Filter	Experience*	17-027
Power Plant*	Experiences with a Charcoal Guard Bed in a Nuclear #In-	17-090
Performance of 1000- and 1800- CFM HEPA Filters on Long	Exposure to Low Atmospheric Dust Loadings, III* #	17-060
#Air Cleaning Philosophy in a Nuclear Materials	Fabrication Plant*	18-059
#Fire Simulation in Nuclear	Facilities - The FIRAC Code and Supporting Experiments*	17-115
of Mobile Filtration Units for Use in Radioactive	Facilities* #The Development	17-022
In-Place Tests of Iodine Filters in the French Nuclear	Facilities* #Data Analysis of	18-114
study of a Laser Spectrometer in the DOE Filter Test	Facilities* #Intermediate Results of a One-Year	17-080
for Monitoring Aerosol Size at the DOE Filter Test	Facility at Los Alamos* of a Single Particle Aerosol Spectrometer	18-029
Facility at Los Alamos* #BOFA - A	Facility for Experimental Investigation of Air Cleaning *of Multiple Stage Filter Systems	18-144
Without Disruption of Plant Operations in the Plutonium	Facility Operations 1970-1980*	17-077
During Accident Situations*	Facility Orifice Plates*	18-116
#A Review of DOE Filter Test	Facility* #System Operational Testing	17-061
#Calibration and Use of Filter Test	Failures in Air-Cleaning, Air-Monitoring, and	17-076
of Major Ventilation Systems for a Plutonium Recovery	Fear*	17-095
Ventilation Systems in Commercial Nuclear Power Plants #Energy and	Feasibility and Costs of the Retention of Radionuclides	18-024
During Accidents in Nuclear Power Plants #Technical	Fed Joule-Heated Ceramic Melters*	17-030
#Off-Gas Characteristics of Liquid-	Federal Republic of Germany* Technologies for the Waste	18-078
Management of I-129, Kr-85, C-14 and Tritium in the	Fiber Filters* #Experimental	17-116
Investigations of Aerosol Filtration with Deep Bed	Fiber Filters* Releases Due to Severe Reactor	18-141
Accidents and Implementation Using Stainless-Steel	Fibrous Filters*	17-050
#Aerosol Filtration Using Metallic	Field ir Gas Cleaning*	18-080
#Use of Acoustic	Field of Nuclear Airborne Waste Sponsored by the	18-077
European Community* #Status of R&D in the	Field Testing of Nuclear Air Cleaning Systems at Duke	18-090
Power Company* #NATS	Field Testing Observations and Recommendations*	18-091
on the Extremely Low Retention of 131-I by an Iodine	Filter of a Boiling Water Reactor* #Investigations	16-009
#High-Efficiency Charcoal Air	Filter with Combustible Frame*	17-115

KWIC INDEX ON AIR CLEANING CONFERENCE TITLES

KWIC INDEX ON AIR CLEANING CONFERENCE TITLES

KWIC INDEX ON AIR CLEANING CONFERENCE TITLES

KWIC INDEX ON AIR CLEANING CONFERENCE TITLES

KWIC INDEX ON AIR CLEANING CONFERENCE TITLES

KWIC INDEX ON AIR CLEANING CONFERENCE TITLES

KWIC INDEX ON AIR CLEANING CONFERENCE TITLES

1632

KWIC INDEX ON AIR CLEANING CONFERENCE TITLES

KWIC INDEX ON AIR CLEANING CONFERENCE TITLES

1634

KWIC INDEX ON AIR CLEANING CONFERENCE TITLES

KWIC INDEX ON AIR CLEANING CONFERENCE TITLES

#New Source Feature Performance?*
Teda vs. Quinuclidine: Evaluation and Comparison of Two
Generators - Comparison of Experimental Results with
Meeting MIL-F-51068 Purchased on the Open Market. Are
#New Source Terms: What do #Performance?*
Installations in a Reprocessing Plant* #
#Experience of Iodine Removal in
Exchanged Zeolite Filters from the Vessel Off-Gas in
of Air Cleaning System Dampers and Blowers to Simulated
System Dampers and Blowers to Simulated Tornado #
#Volatilization and
#Volatile Ruthenium
#Continuous Chemical Cold
#Nuclear Standards: Current Issues and Future
for the Waste Management of I-129, Kr-85, C-14 and #
#Development of the ELEX Process for
Wetproofed Catalyst Recombiner for Removal of Airborne
52 in Light of NRC-Sponsored #The Need for Revising
Waste Management* #Summary of
#The Development of Mobile Filtration
#Effects of Shock Waves on High Efficiency Filter
#New Source Terms: What do They Tell
#HEPA Filter Response to High Air Flow
#Test Data and Operation Data from Carbon Used in High
#Cost-Benefit Considerations for Filtered-
#Venturi Scrubbing for Filtered
#Design Experiments for a
#The Mathematical Modelling of Fire in Forced
of Prototype Electrofibrous Filters for Nuclear
#Simulation of Forced
#System Operational Testing of Major
1/1/78 - #Failures in Air-Cleaning, Air-Monitoring, and
Verification of Two Computer Programs Used to Analyze
of a Passive Submerged Gravel Scrubber for Containment #
Ventilation Systems Under Accident #Comparison and
Radioactive Cells and Process Gaseous Wastes* #
Removal by Silver-Exchanged Zeolite Filters from the #Utility
and Characterization for a Radioactive In Situ
of Ruthenium, Cesium and Antimony During Simulated HLLW
Temperature Processes* #
the Federal #Development of Technologies for the
United States Activities in Commercial Nuclear Airborne
#Status of KCD in the Field of Nuclear Airborne
Casing for Radioactive Cells and Process Gaseous
Low Retention of 131-I by an Iodine Filter of a Boiling
Plants Demonstrated by the Example of a Pressurized
#14-C Release at Light
#Effects of Shock

KWIC INDEX ON AIR CLEANING CONFERENCE TITLES